犬の遺伝性疾患における原因遺伝子解析のための遺伝子（DNA）バンク拠点形成

平成 23 年度～平成 27 年度私立大学戦略的研究基盤形成支援事業

研究成果報告書

平成 28 年 3 月

学校法人名　麻布獣医学園

大学名　　麻布大学

研究組織名　麻布大学獣医学部

研究代表者　　阪口　雅弘

平成 23 年度～平成 27 年度私立大学戦略的研究基盤形成支援事業
研究成果報告書

研究プロジェクト名：
犬の遺伝性疾患における原因遺伝子解析のための遺伝子（DNA）バンク拠点形成

目次：

研究プロジェクトの概要

犬の遺伝性疾患における原因遺伝子解析のための遺伝子（DNA）バンク拠点形成

研究代表者　　阪口雅弘

犬も人と同様に多くの遺伝性疾患があり、人と病態が似ている疾患も多く存在する。本研究において犬の遺伝子(DNA)資源の活用と保存のために、獣医系大学附属動物病院等の臨床医を中心に遺伝関連疾患を含む非感染性疾患犬や陰性対照となる健常犬からのDNA収集を行う。収集されたDNAを使用して犬の遺伝関連疾患における原因遺伝子の解析を行うことを本研究の目的とした。

本プロジェクトは８組のクループから構成されている。 括弧内がそれぞれのグループ長である。(1)犬の遺伝性疾患におけるDNA収集・精製・供給および疾患情報のデータベース化（阪口雅弘）(2)犬の緑内障および白内障の遺伝子解析（印牧信行）(3) 犬におけるヒトとの適合性に関する遺伝子解析（菊水健史）(4) 犬の腫瘍壊死因子(TNF-α)遺伝子に関する研究（久末正晴）(5) 犬のアロペシア X（ポメラニアン脱毛症）の遺伝子解析（村上賢）(6) 犬のてんかんの遺伝子解析（齋藤弥代子）(7) 犬のアトピー性皮膚炎の遺伝子解析（村上裕信）平成24年度までは川原井晋平講師が研究クループ長であったが25年度から村上裕信助教に変更した。(8) 犬のIL-13遺伝子の解析（滝沢達也）である。収集されたDNA検体は1のグループで精製・管理されて、このプロジェクトの研究者である各グループに提供されて遺伝子解析を行った。また、平成25年から研究クループ以外の他の研究者へもDNAを供給し、共同研究を行っている。

海外における犬のDNAバンクとしては、米国ではマサチューセッツ工科大学とハバード大学のBroad Instituteと米国国立衛生研究所(NIH)による犬ゲノムプリジェクト、ヨーロッパでは１２か国の獣医大学によるLupaプロジェクトが有名である。日本においては犬の遺伝関連疾患の研究を行っている研究は存在するが、それらの研究者が遺伝関連疾患のDNA検体を共有するような遺伝子バンクはなかった。本プロジェクトにより、今後、犬の遺伝関連疾患を含む非感染性疾患のDNAや一般集団犬のDNAなどが共有でき、日本の犬の遺伝関連疾患の原因遺伝子の解析のための検体提供の中心的な役割を担うことができると考えられる。

平成23年度～平成27年度「私立大学戦略的研究基盤形成支援事業」
研究成果報告書概要

1　学校法人名　麻布獣医学園　　2　大学名　麻布大学

3　研究組織名　麻布大学獣医学部

4　プロジェクト所在地　神奈川県相模原市中央区淵野辺 1-17-71

5　研究プロジェクト名　犬の遺伝性疾患における原因遺伝子解析のための遺伝子（DNA）バンク拠点形成

6　研究観点　研究拠点を形成する研究

7　研究代表者

研究代表者名	所属部局名	職名
阪口　雅弘	獣医学部	教授

8　プロジェクト参加研究者数　11　名

9　該当審査区分　理工・情報　　生物・医歯　　人文・社会

10　研究プロジェクトに参加する主な研究者

研究者名	所属・職名	プロジェクトでの研究課題	プロジェクトでの役割
阪口雅弘	微生物第一・教授	犬の遺伝性疾患における DNA 収集・精製・供給および疾患情報のデータベース化	犬の遺伝性疾患の DNA 管理および情報のデータベース化
印牧信行	附属動物病院・准教授	犬の緑内障および白内障の遺伝子解析	眼疾患症例 DNA サンプルの収集および研究の総括
菊水健史	伴侶動物学・教授	犬におけるヒトとの適合性に関する遺伝子解析	犬におけるヒトとの適合性に関する遺伝子解析
久末正晴	内科第２・准教授	犬の腫瘍壊死因子(TNF-α)遺伝子に関する研究	犬の腫瘍壊死因子(TNF-α)遺伝子に関する研究
村上賢	分子生物学・教授	犬のアロペシア X（ポメラニアン脱毛症）の遺伝子解析	犬のアロペシア X（ポメラニアン脱毛症）の原因遺伝子同定
齋藤弥代子	外科第２・准教授	犬のてんかんの遺伝子解析	犬のてんかんの原因遺伝子同定
村上裕信	衛生第２・助教	犬のアトピー性皮膚炎の遺伝子解析	犬のアトピー性皮膚炎の遺伝子解析

滝沢達也	動物工学・教授	犬の IL-13 遺伝子の解析	犬の IL-13 遺伝子の解析
（共同研究機関等）			
久保充明	理化学研究所統合生命医科学研究センター副センター長	犬の遺伝子解析法の助言	犬の遺伝子解析法の助言
大森啓太郎	東京農工大獣医分子病態治療学・講師	犬の DNA 収集とプロジェクトへの助言	犬の DNA 収集とプロジェクトへの助言
大和　修	鹿児島大学・獣医臨床病理・教授	犬の DNA 収集とプロジェクトへの助言	犬の DNA 収集とプロジェクトへの助言

旧

ﾌﾟﾛｼﾞｪｸﾄでの研究課題	所属・職名	研究者氏名	プロジェクトでの役割
犬のアレルギー疾患の遺伝子解析	小動物臨床・助教	川原井晋平	犬のアレルギー疾患の遺伝子解析

（変更の時期：平成25年　4月　1日）

新

変更前の所属・職名	変更（就任）後の所属・職名	研究者氏名	プロジェクトでの役割
犬のアレルギー疾患の遺伝子解析	衛生第２・助教	村上裕信	犬のアレルギー疾患の遺伝子解析

旧

ﾌﾟﾛｼﾞｪｸﾄでの研究課題	所属・職名	研究者氏名	プロジェクトでの役割
犬のDNA収集と遺伝病の予防・治療法の開発	東京農工大獣医内科・教授	岩崎利郎	犬の DNA 収集と遺伝病の予防・治療法の開発

（変更の時期：平成25年　4月　1日）

新

変更前の所属・職名	変更（就任）後の所属・職名	研究者氏名	プロジェクトでの役割
犬の DNA 収集研究プロジェクトへの助言	東京農工大獣医分子病態治療学・講師	大森啓太郎	犬の DNA 収集とプロジェクトへの助言

旧

ﾌﾟﾛｼﾞｪｸﾄでの研究課題	所属・職名	研究者氏名	プロジェクトでの役割
遺伝性疾患の既知の疾患原因遺伝子頻度の調査	東京大学・獣医臨床病理学・助教	玉原智史	遺伝性疾患の既知の疾患原因遺伝子頻度の調査

（変更の時期：平成26年　4　月　1　日）

新

変更前の所属・職名	変更（就任）後の所属・職名	研究者氏名	プロジェクトでの役割
犬の DNA 収集研究プロジェクトへの助言	鹿児島大学・獣医臨床病理・教授	大和　修	犬の DNA 収集研究プロジェクトへの助言

11　研究の概要(※　項目全体を10枚以内で作成)

(1)研究プロジェクトの目的・意義及び計画の概要

犬も人と同様に多くの遺伝性疾患があり、人と病態が似ている疾患も多く存在する。本研究において犬の遺伝子(DNA)資源の活用と保存のために、獣医系大学附属動物病院等の臨床医を中心に各種遺伝関連疾患を持つ犬の DNA 収集を行う。収集された DNA を使用して犬の遺伝関連疾患における原因遺伝子の解析を行うことを本研究の目的とする。

意義としては、大学の獣医病院において臨床学的に信頼性の高い DNA 検体を収集することができ、将来の犬の遺伝関連疾患研究を推進するための DNA バンクの基盤が形成することができる。さらにその研究成果は犬と同じような遺伝関連疾患が存在する人の遺伝関連疾患の解明にも役立つと考えられる。

計画の概要として上述したように犬の遺伝関連疾患に関する症例情報とゲノム DNA など臨床検体を、全国獣医系大学附属動物病院等と連携して収集・保管する。さらに収集された DNA 検体を用いてこれまでに報告されている人やマウス等の遺伝関連疾患に関する原因遺伝子の情報を元に PCR 法等を用いて解析する。また、これまでに原因遺伝子情報がない疾患に関しては各疾患において同犬種の罹患犬群と健常犬群において、網羅的な SNP(一塩基多型:遺伝子配列中に1つの DNA が変異した多様性が認められ、その変異が集団内で 1%以上の頻度で見られるもの)解析や次世代遺伝子解析装置による解析などで原因遺伝子の同定を実施する。遺伝子解析によって明らかとなった原因遺伝子の機能解析を行い、疾患の発生機序を解明する。その発生機序を元に疾患の予防法および治療法の検討を行ない、その疾患の予防法・治療法を開発する。

(2)研究組織

研究代表者の役割:研究代表者の阪口は、麻布大学および他大学や獣医病院における犬の遺伝関連疾患症例を集め、飼い主の承諾後、その病気の犬から血清と DNA を採取・保存する。また、その比較研究のために、一般犬の DNA を採取・保存する。研究者の要望に沿って必要な DNA を供給する。また、遺伝子解析に必要な技術や情報を各研究者に供給し、分子生学的手法に慣れない臨床獣医師に対しては実際の実験・解析を手伝う。また、各研究者間の検体や情報を仲介して研究者間の連携がスムーズに行うようにする。

各研究者の役割分担や責任体制の明確さ:研究者ごとに研究テーマを持ち、年２回研究結果の発表会を行う。その会議には上記の外部の共同研究機関の先生方も参加し、評価・コメントをいただいた。その進捗状況を研究代表者が判断し、スムーズに研究が進むように助言・サポートを行った。研究の進行に関しては担当の研究者と研究代表者が責任を持って行い、研究費の支出は各研究者の進行に応じて研究代表者が支給した。

研究プロジェクトに参加する研究者の人数:研究プロジェクトに参加している主な研究者は１０に記載したとおり、11 名である。その他の研究協力者が 28 名（内訳として麻布大学 10 名、東京大学 4 名、京都大学３名、横浜市立大学２名、成育医療研究センター2 名、科学警察研究所１名、理化学研究所 1 名、メニコン１名、カホテクノ １名、検診センターキャミック２名、渡辺動物病院１名）で合計 39 名である。

大学院生・PD, RA の人数・活用状況:大学院 9 名、PD4 名、RA3 名が参加している。

研究チーム間の連携状況:研究チーム内での連携はうまく機能している。

・久末は滝沢研究室に DNA 変異部分の DNA 解析を依頼した。

・村上賢は小動物臨床所属の川原井先生と協力して脱毛症の犬からの皮膚組織サンプル採集を依頼している。また、小動物臨床所属の印牧と協力してシーズー犬に見られる原

因不明の先天性網膜剥離の眼疾患における遺伝子異常の情報交換をしている。肥満関連遺伝子多型解析のために、菊水から特定の犬種の DNA サンプルの提供を依頼した。
・齋藤はてんかんの遺伝子解析において阪口に遺伝子解析技術指導を依頼した。
・滝沢は動物工学研究室所属の田中和明准教授と共同で、遺伝子多型の解析を進めた。さらに久末と共同で犬の腫瘍壊死因子(TNF-α)遺伝子の多型解析につい共同で研究を進めた。犬の DNA 検体は久末、阪口から検体の供与を受けた。
　このように研究班内で DNA の検体材料を互いに融通しあい、実験手技やデータ解析も協力して進めた。
研究支援体制:上述したように研究者間で得意な分野を生かして相補的に研究をサポートしている。必要な機器等は研究代表者と分担者が話し合って購入をしている。
共同研究機関等との連携:理化学研究所の久保先生は人の遺伝関連疾患の遺伝子解析の専門家で、犬の遺伝関連疾患の解析の助言を行った。犬の白内障の SNP(一塩基多型)解析は久保先生の協力で理研ジェネシスで行った。東京農工大学獣医学科の岩崎先生は獣医内科教授で犬の遺伝関連疾患の DNA 検体の収集や解析のアドバイスを行った。特に犬のアレルギー疾患の研究の権威者である。個人的都合で平成 25 年 3 月に大学を退官されたので、平成 25 年度から同じ大学の大森先生に依頼した。東京大学獣医学科の玉原先生は犬の遺伝病疾患の研究を行っており、犬の遺伝関連疾患の DNA 検体の収集や解析のアドバイスを依頼した。平成 26 年 4 月東京大学から民間の獣医病院に移られたので、平成 26 年度から鹿児島大学獣医学科の大和先生に代わりをお願いした。大和先生は犬・猫の遺伝関連疾患の研究を行っており、犬の遺伝関連疾患の DNA 検体の収集や解析の助言を行った。
共同研究機関以外との共同研究
・印牧は眼疾患の共同研究者として横浜市立大学・医学部眼科学教室の水木信久教授、目黒明講師に本プロジェクト関連のアドバイスを依頼している。また、メニコン社の今安正樹氏に DNA 解析を依頼している。
・菊水は共同研究者として京都大学の藤田和生先生、村山美穂先生からオオカミの DNA の提供に加え、遺伝子解析技術指導を受けている。国立成育医療研究センターの深見真希先生からは DNA のコピーナンバー変異の解析を共同で実施した。また国立成育医療研究センターの秦健一郎先生とは柴犬の次世代型シークエンサーを用いた網羅的遺伝子解析を実施した。理化学研究所の桃沢幸秀先生には、網羅的 SNP 解析と行動との関連解析に関しての助言を依頼した。
・久末は犬の腫瘍壊死因子(TNF-α)遺伝子に関する研究をカホテクノの共同で行っている。
・村上賢は学外共同研究者としている京都大学大学院農学研究科応用生物学専攻の舟場正幸先生に犬の肥満や脂肪細胞分化に関する遺伝子発現の情報提供や実験の協力を依頼している。また、肥満関連遺伝子多型解析のために、東京大学獣医学科辻本先生から特定の犬種の DNA サンプルの提供を依頼した。
・齋藤は麻布大学5名(神経科研修獣医師)、検診センターキャミック、渡辺動物病院から、検体提供と臨床情報提供を依頼した。

(3)研究施設・設備等

研究に必要な設備はこの予算で購入した。以前に購入した設備も本研究に用いている。
平成23年度:蛍光・発光プレートリーダ 156 時間/1年(1回の使用が20分程度)
平成24年度:リアルタイム PCR 装置 1053 時間/1年
平成25年度:蛍光顕微鏡装置一式 180 時間/1年
本予算で購入した他の設備で主なもの:冷却遠心機1000時間/年、サーマルサイクラー(PCR

装置)260 時間/年、メディカル冷蔵庫 8760 時間/1年 、超低温フリーザー8760 時間/1年、タンパク転写装置 300 時間/1年

(4)研究成果の概要

犬の遺伝性疾患における DNA 収集・精製・供給および疾患情報のデータベース化

麻布大学などの大学所属の獣医師や研究者を中心に遺伝病、遺伝関連疾患を含む非感染性疾患の犬および一般集団犬からDNA収集を行い、1万 5865 検体が収集された。収集検体の目標が 1 万 8000 検体なので、88%の達成度である。犬種は 130 種以上で上位3犬種はウェルシュ・コーギー・ペンブローブ 2236 例、チュアダックス 1827 例、プードル 1567 例であった。オス・メスの比率は 49.8%：50.2%で、平均年令は 8 才であった。

白内障をはじめとする眼疾患、てんかんをはじめとする神経疾患、アレルギー疾患をはじめとする免疫疾患など 7628 症例が収集された。現在、最終的な診断が決定していない症例や疾患情報がまだ来ていないものが多数あり、今後、疾患情報を追加していく。一般開業の獣医師の場合、疾患診断基準や能力にバラツキがあるため、症例検体に関しては獣医大学の教員を中心に診療・診断して採取した。しかし、アトピー性皮膚炎に関してはアレルギー治療法の進歩で獣医大学病院に来院する疾患犬が非常に少なくなったため、開業獣医師でアトピー性皮膚炎の専門医に依頼して国際的な診断基準の基に検体を採取した。

疾患症例が集められ、疾患関連遺伝子を解析するときに、陰性対象となる一般集団から採取した犬の DNA が必要となった。一般集団犬の DNA がないと疾患遺伝子解析が進まないため、本プロジェクトでは、一般集団からの犬の DNA 検体の採取も積極的に行うようになり、収集 DNA 検体数に一般集団犬の検体数も加えた。

収集された DNA 検体はこのプロジェクトの研究者に提供して遺伝関連疾患の解析を行った。また、他の研究者へ DNA を供給し、共同研究を行っている。(*1)科学警察研究所で行っている「マイクロサテライト多型解析を用いた犬の個体識別法の検討」に犬の DNA を提供した。これは犬の DNA は，傷害や血統書偽装など直接動物が関わる事件から，強盗や強姦などの現場に犯人に付着した動物毛が遺留される事件まで，多岐にわたって重要な証拠なるためである(学会発表 6)。また、(*2)東京大学獣医学科坪井先生には「Whole Exome Sequence 法による犬の遺伝性神経疾患の原因遺伝子同定」の研究でパピヨン犬の神経軸索ジストロフィーの陰性対照のパピヨン犬の 56 検体の DNA を遺伝子バンクから提供した(学会発表 17)。遺伝関連疾患の研究者は症例から疾患遺伝子の収集を行うが、同じ犬種で陰性対照となるものの収集がない場合が多いので、このような遺伝子バンクの利用も今後、行っていく予定である。

収集された検体情報はバイオバンクに登録し、疾患情報をデータベース化した。今後、収集された犬種や疾患に関しては研究グループ内外での情報の共有を行っていくとともに、上述したように他の研究者が行う研究にも積極的に協力を行う。

・犬の緑内障および白内障の遺伝子解析

犬の緑内障関連遺伝子については解析を行い、論文化できたが、白内障の遺伝子解析についてはまだ解析中で達成度は 60%である。麻布大学附属動物病院の眼科に紹介された眼疾患症例をもとに眼疾患における原因遺伝子を探求した。DNA サンプルの眼疾患は、獣医眼科専門医による眼科検査によって診断された症例とした。このプロジェクトの原因遺伝子解明の疾患は紹介来院頭数を調査し、犬種依存性が極めて高いものとして解析した。麻布大学附属動物病院の眼科に紹介された 4670 症例から、眼疾患症例の DNA サンプルを収集し、延べ 2655 サンプルを収集した。眼疾患における原因遺伝子を探求する目的で、症例の疾患群を調べた。その結果、4670 症例のうち、白内障が約 21%、緑内障が約7%を示してい

た。この2つの疾患に好発犬種が存在することがわかった。(*3)白内障は眼疾患罹患アメリカン・コッカー・スパニエルの 67.7%で認められ、また緑内障は眼疾患罹患柴犬の 42.9%で認められた(論文 11)。そこで、アメリカン・コッカー・スパニエルでは白内障原因遺伝子を、柴犬では緑内障原因遺伝子の解明を行った。

アメリカン・コッカー・スパニエルの白内障の発症について、すでに報告されているスタッフォードシャー・ブル・テリアとボストン・テリアの白内障関連遺伝子 HSF4 遺伝子の変異について、アメリカン・コッカー・スパニエルの白内障症例 25 頭で遺伝子解析を行ったが HSF4 遺伝子の変異は認められなかった。次にDNAアレーを用いたSNP(一塩基多形:遺伝子配列中に1つの DNA が変異した多様性)の網羅的遺伝子解析を行った。15 番染色体上の rs22428454(エンドセリン受容体タイプ A 遺伝子)と 31 番染色体上の rs23685575 が発症との関連を示唆する結果が得られた。エンドセリン受容体タイプ A 遺伝子は7つのエクソンからなり、rs22428454 はエクソン1とエクソン2の間のイントロン領域に存在する。アメリカン・コッカー・スパニエルの白内障犬陽性例 21 例、陰性例 5 例のエンドセリン受容体タイプ A 遺伝子の全遺伝子配列の解析を行った。しかし、エクソン部分において他の変異は認められなかった。このエンドセリン受容体タイプ A 遺伝子のエクソン部分の遺伝子変異が白内障発症に関与する可能性は低いと考えられた。

(*4)犬の緑内障の遺伝子解析の DNA 検体として、柴犬 47 頭、健常犬 34 頭を用いた。その結果、SRBD1 遺伝子の 2 つの新しい変異 rs22018513 と rs22018514 が犬緑内障の発症関連を示唆する結果が得られた(雑誌論文 46、学会発表 31)。犬緑内障の原因関連遺伝子は、すでにビーグル犬で ADAMTS10 遺伝子の SNP56097065 が報告されているが、この SNP と緑内障柴犬との関連はみられなかった。また、(*5)SRBD1遺伝子の rs22018513 と rs22018514 が柴犬の飼育地に依存している可能性が否定できないことから、より広域に飼育している柴犬を対象とした調査を行った。その結果、柴犬緑内障との関連が SRBD1遺伝子の rs22018513 で特に強く認められ、柴犬緑内障における SRBD1 遺伝子の変異の再現性が確認できた(学会発表 10)。

犬におけるヒトへの適合性に関する遺伝子解析

ヒトとの適応性、すなわち社会性に関する遺伝子同定を試み、1)社会性に関する犬種差を遺伝的推移の中に見出した(達成 100%)、2)犬の家畜化の過程でこのような社会性による選択圧が強かったことを示唆するデータを見出した(達成 100%)、3)ヒトへの社会認知能力に犬種差を見出し、それに関連する遺伝子を複数同定した(達成 90%)、ことからほぼ目的を達した。

日本及び米国における一般の飼い主及びブリーダーを対象とした犬の行動特性に関する調査を実施した。犬種を既に報告されていた遺伝分岐図を元に 8 つのグループに分類し、因子分析及び平行分析を行い、各因子の平均値を因子得点として、行動特性の犬種グループ比較に用いた。その結果、(*6)原始的な犬グループの犬はどの犬種グループよりもヒトへの愛着が低いことが明らかとなった($p<0.05$)(雑誌論文 12)。原始的な犬の愛着はその他のどの犬種グループよりも低く、先行研究で知られている遺伝分岐図と一致した。その他の犬種グループでは、ワーキンググループは、見知らぬ人に対する恐怖反応、見知らぬ犬に対する恐怖反応、非社会的刺激に対する恐怖反応、飼い主に対する攻撃性、活発度が低いことなどが明らかとなった。

様々な犬種の犬を用い、犬の認知能力の犬種差を解決不可能課題及び指差し二者選択課題により評価した。解決不可能課題では、原始的な犬は、最初にヒトを見るまでの時間が長く、ヒトを見ている時間が短く、ヒトを見る回数と交互凝視の回数が少なかった($p<0.01$)。指差し二者選択課題では、原始的な犬の成績はその他の犬種グループと同等であり、犬種グ

ループによる有意な差は見られなかった。

社会性能力に関わる遺伝子として、メラノコルチン2受容体（MC2R）とオキシトシン、オキシトシン受容体の遺伝子を選択した。さらにゲノムワイド解析の結果から WBSCR17（ウィリアムズ症候群関連遺伝子）を選抜し、これらに関連する遺伝子の多型を調べ、犬種差や行動実験の結果との関連性を調べた。犬の進化候補遺伝子である WBSCR17 において、原始的な犬と一般的な犬種とで出現頻度の異なる一塩基多型が検出され、T 型の遺伝子型を持つ個体では、指差し二者選択課題の視線＋指差し＋タッピングの課題の正答数が高い結果となった（$p<0.05$）。MC2R において、原始的な犬と一般的な犬種とで出現頻度の異なる一塩基多型が検出され、A 型の遺伝子型を持つ個体を一般的な犬種内で比較した結果、指差し二者選択課題の視線＋指差し＋タッピング課題、視線＋指差し課題、指差し課題の正答数が低い結果となった（$p<0.05$）。OT（オキシトシン遺伝子）において、原始的な犬と一般的な犬種とで出現頻度の異なる一塩基多型と反復数多型が検出され、A/A 型の一塩基多型を持つ個体では、A/C 型の遺伝子型を持つ個体よりも、解決不可能課題のヒトを見ている時間、ヒトを見る回数、交互凝視の回数においてヒトを見ない結果となった（$p<0.05$）。(*7)（オキシトシン受容体遺伝子）においては、原始的な犬と一般的な犬種とで出現頻度の異なる一塩基多型が検出されたものの(雑誌論文 14)、行動実験の結果とは関連性が見られなかった。

オオカミ、秋田犬、柴犬、原始的な犬グループ以外の犬のアミラーゼコピー数を調査した。オオカミのアミラーゼコピー数は 2 コピー程度であった。また、オオカミへの遺伝的近さから予想したとおり、秋田犬のコピー数はオオカミよりも多いが一般的な犬種より少なかった（$p<0.01$）。(*8)犬と同じく原始的な犬グループに含まれる柴犬のコピー数は、一般的な犬種と同程度であり、柴犬のオオカミへの遺伝的近さと反した結果となった。縄文柴のコピー数は、柴犬より少なく（$p<0.01$）、秋田犬より多かった（$p<0.05$）(雑誌論文 15)。

犬腫瘍壊死因子(TNF-α)遺伝子に関する研究

TNF-αの遺伝子である TNFA 遺伝子においてマイクロサテライト変異（1から5塩基の配列が繰り返す領域）を確認した。犬の免疫介在性血小板減少、リンパ腫、悪性黒色腫でその変異の遺伝子解析を実施したが、特異的な SNP の解析には至らなかった。今後、犬の他の免疫介在性血液疾患および腫瘍性疾患について解析中で達成度は 40%である。

ヒトの医学領域では TNF-αは様々な免疫介在性疾患で、その異常が認められている。本研究では犬の TNF-αの遺伝子である TNFA 遺伝子においてマイクロサテライト変異の解析を試みた。犬の遺伝的リスク因子を特定する目的で、まず正常犬の TNF-αの遺伝子である TNFA 遺伝子の塩基配列を解析することとした。ビーグル、チワワ、ミニチュアダックス、トイプードル、コーギーおよび柴犬、各 20 頭以上からなる合計 139 頭の DNA 試料を用い、PCR 産物は 3130 Genetic analyzer を用いた遺伝子型判定に供した。(*9)第1イントロン内に 4 塩基を単位とするマイクロサテライト(tetra-nucleotide repeats;以後 TNR)変異を見出した(雑誌論文 32)。さらに第1イントロン内の TNR 多型を判定するために、約 120 塩基対の産物が得られるプライマーを設計した。犬 TNFA 遺伝子の第1イントロンに GAAT を反復単位とする TNR が存在し、繰り返し数多型が存在することが明らかになった。調査した 139 個体から 5 回, 6 回, 7 回, 8 回型の 4 対立遺伝子が検出された。ビーグル種からは 5 回型から 8 回型まで全ての対立遺伝子が検出されたが、他の 5 品種からは 8 回型は検出されなかた。ヘテロ接合度の期待値（He）および多型情報量(PIC)は、品種によって、それぞれ 0.389 - 0.749 と 0.333 - 0.682 の間で差異が認められた。このマイクロサテライトマーカーは、多型性に富み同時に型判定が容易であるため、犬 TNFA 遺伝子のランドマークとして、伝達不平衡テストなどの疾患相関解析に利用可能であると予想された。

これらのマイクロサテライトは、犬の免疫介在性血液疾患および腫瘍性疾患の診断応用に

有力と考え探索を行った。免疫介在性疾患では、最終的に 36 例の犬の免疫介在性血小板減少で解析を実施したが、特異的な SNP の解析には至らなかった。さらに、リンパ腫 10 例および悪性黒色腫において TNFA 遺伝子のマイクロサテライト解析を実施していたが、変異は見出だすことは困難で特異的な SNP の解析には至らなかった。この原因として、免疫介在性血液疾患はそもそも母集団が少なく、かつ確定診断要件を満たすものが少なったことが挙げられる。また腫瘍性疾患においては、二次診療施設に来院するリンパ腫および悪性黒色腫の検体数が減少傾向であることも挙げられる。このように解析数がごく少数であるため、変異の有無を確認できないこととプライマーの設計自体に問題があった可能性があり、今後検討する必要があるものと考えられた

犬のアロペシア X(ポメラニアン脱毛症)の遺伝子解析

犬のアロペシア X(ポメラニアン脱毛症)の遺伝子解析において最有力候補遺伝子として、Lef1 及び Dlx3 が得られたが、疾患犬と健常犬における遺伝変異については現在、解析中で達成度は 70%である。

ポメラニアンなど特定の犬種で見られる成年発症型非炎症性非掻痒性で、先天性の脱毛疾患である Alopecia X の疾患関連原因遺伝子を同定することを第一の目的とし、その成果を新たな治療法(治療薬の開発)や健全な発毛・育毛へ応用することを最終目的とする。過去に、健常犬と Alopecia X 症ポメラニアン犬の皮膚から抽出した RNA を用いて、DNA マイクロアレイによる網羅的遺伝子発現比較解析を実施し、Alopecia X 症で有意な発現減少が見られた複数の原因候補遺伝子を推定した。これらの遺伝子の厳密な定量的発現解析を real-time RT-PCR 法を用いて、数多くの個体(疾患犬や健常犬など)について実施した。その結果、最有力候補遺伝子として、Lef1 及び Dlx3 が得られた。Dlx3 遺伝子産物は毛包の分化や毛の周期に関与するタンパク質の 1 つであり、Lef1 遺伝子産物は Dlx3 遺伝子発現を促進する転写因子であることがマウスで知られている。犬 Dlx3 遺伝子の様々な長さのプロモーター領域をもつレポーターベクター及び犬 Lef1 遺伝子の発現系ベクターを作製して、レポーターアッセイ系を構築した。Lef1 遺伝子のプロモーター領域をもつレポーターベクターによるレポーターアッセイ系も構築した。これらの評価系を用いて、発毛・育毛関連遺伝子の発現制御機構に関する分子・細胞生物学的分析をするとともに、遺伝子発現を促進する物質の探索を行っている。Lef1 転写因子が応答する配列以外にも、Dlx3 遺伝子の発現を制御する応答エレメントが Dlx3 遺伝子のプロモーター領域に存在することがわかった。また、疾患犬と健常犬における Dlx3 遺伝子(プロモーター領域を含む)の塩基配列の相違を調べている。

犬のてんかんの遺伝子解析

犬のてんかんの遺伝子解析において網羅的な全ゲノム関連解析を行い、4つの SNP を見出した。達成度としては 40%である。特発性てんかんは、人と同様に犬において最も一般的な神経疾患であるが、病因はほとんど分かっていない。遺伝的要因が疑われている。本疾患は原因が不明なため根治療法がなく、ほとんどの犬で、対症療法としてのてんかんを抑える薬の投与が生涯必要となる。本研究において、犬の特発性てんかんの原因遺伝子を同定し、病態機構を明らかにすることは、原因療法開発の糸口となり、獣医学の発展に大きく寄与できると考える。さらにその情報は、ヒトのてんかん医療に対しても有用性が高いと考える。

麻布大学附属動物病院神経科に来院し、特発性てんかんと診断された犬の血液サンプルの収集と臨床情報の収集を行った。発作時の徴候の詳細な問診とビデオ解析を行うとともに、可能な限り脳波検査も行い、それぞれの症例について、発作型分類(発作の表現型の分類)を行った。様々な犬種のサンプルが収集されたが、その中で、特発性てんかんが好発している単一犬種に着目し、罹患犬と非罹患犬の DNA を用いて、SNP アレーで網羅的な全ゲノム関連解析 (GWAS) を行った。非罹患犬の DNA は遺伝子バンクに保管されている罹患犬種

と同一犬種の検体を用いた。

GWAS によって絞った、てんかん発症と有意な関連性を示す SNP について、新たに検体を収集し確認実験を行った。新たな検体は、麻布大学附属動物病院神経科来院症例に加え、てんかんの診断や診療に長けた他の複数の施設からも収集した。

特発性てんかんと診断した計 143 頭から DNA サンプルが得られた。対象とした犬種の特発性てんかん罹患犬 10 頭と非罹患犬 22 頭のサンプルについて、イルミナ社の Chip array を用いて 17 万個の SNP を網羅的に解析したところ、特発性てんかん罹患犬群で変異の出現頻度の高い4つの SNP を認めた。これらの犬におけるてんかん発作型は、強直・間代発作 3 頭、焦点性運動発作 3 頭、行動発作 3 頭、自律神経発作 1 頭であった。特発性てんかん罹患犬群で変異の出現頻度が高かった SNP の幾つかは同一染色体上の一部の領域に存在し、高いオッズ比を示した。この領域には脳の機能に関わる遺伝子、ヒトのてんかんの原因となる遺伝子、さらに犬の症候性てんかんの関連遺伝子と同じ働きを持つ遺伝子が含まれていた。これら候補遺伝子の一つについては、犬の脳組織から抽出した mRNA を用いて RT-PCR を行い、犬で発現していることを確認した。さらに、同様の GWAS による検索を他犬種のてんかん罹患犬と非罹患犬について行ったが、同じ SNP におけるてんかんとの関連性は他犬種では認められなかった。

GWAS にててんかんとの関連性を持つ SNP が明らかになった犬種において、新規検体の収集を行い、新規罹患犬 9 頭と非罹患犬 13 頭の検体が収集された。検体数がさらに増えたのちに、発作型の解析と、ゲノム DNA をテンプレートとして、候補遺伝子に存在する SNP 領域の PCR を行うことによる確認実験を実施予定である。

犬のアトピー性皮膚炎の遺伝子解析

柴犬において網羅的な全ゲノム関連解析を行ったところ、2つの領域に集中して SNP が認められた。現在、その領域に絞って犬のアトピー性皮膚炎に関連する遺伝子の解析と他の犬種での遺伝子解析を行っており、達成度としては 60%である。

犬のアトピー性皮膚炎(cAD)は環境や食物中に含まれる抗原への過敏反応であり、人のアトピー性皮膚炎と病態が類似している。(*10)そのアレルギーの診断のために原因アレルゲンの検査法の開発を行い、本研究に使用する犬のアレルギーの診断に用いた(雑誌論文 68,84)。また、cAD は家族性素因だけでなく犬種により発生率が異なることから、人と同様、疾病と遺伝的背景が密接に関与していることが疑われる。そこで、cAD の発生率が高い柴犬、フレンチブルドック、ミニチュアダックスフント、トイプードルの 4 犬種であり、同じ地域で室内飼育されている犬に限定してサンプルの収集を行った。cAD の診断については Favrot の診断基準(Veterinary Dermatology, 2009)に準じて同じ獣医師によって診断を行った。また、cAD ではない健常犬は年齢、病状、既往歴をもとに診断を行い、サンプルの収集を行った。その結果、cAD 発症犬は、柴犬 45 頭、ミニチュアダックスフント 33 頭、トイプードル 30 頭、フレンチブルドック 20 頭の計 130 頭から DNA サンプルを得ることができた。また、健常犬は柴犬 20 頭、ミニチュアダックスフント 41 頭、トイプードル 16 頭、フレンチブルドック 2 頭の計 79 頭から DNA サンプルを得ることができた。さらに、cAD 発症犬においてダニアレルゲン特異的 IgE 抗体検査を行ったところ、柴犬では 72.5%と他の犬種より高い抗体保有率(フレンチブルドック:55.6%, ミニチュアダックスフント:50.0%, トイプードル:20%)であった。

cAD の原因遺伝子を網羅的に探索するため、柴犬のサンプルを用いてダニアレルゲン特異的 IgE 陽性の cAD 発症犬 29 頭と IgE 陰性で cAD 未発症犬 19 頭において DNA アレーを用いた SNP の網羅的遺伝子解析を行った。その結果、 cAD 発症犬で高頻度認められた SNP は第 29 番染色体では 600kbp 以内に、第 8 番染色体では 90kbp 以内に限局して認められ、そのうちひとつは第 29 番染色体にコードされている機能不明な RBM12B 遺伝子のエクソン上

の SNP であることが明らかとなった。また、第 8 番染色体の 11 の SNP は細胞死に関与する IPTK1 遺伝子上のイントロン領域に位置していた。本研究ではアレルギーに関連する遺伝子上または近傍の SNP は認められなかったが、 cAD 発症犬で高頻度に認められた SNP の上位 5 つは全て第 29 番染色体の限局した位置に存在することから、第 29 番染色体上に cAD に関連する遺伝子領域が存在することが強く示唆された。また、それらの SNP 近傍には 機能が不明な LOC100685605 も存在することから、cAD に関連する遺伝子である可能性も考えられる。cAD 発症犬に関連する遺伝子の同定には至らなかったが、cAD への関与が疑われるゲノム領域を推定することができると考えられる。

犬のアトピー性皮膚炎に疾患原因遺伝子の解析のための基礎的な研究の1つとして犬の CD14 の遺伝子はクローニングを行い、 CD14 の全長配列を初めて決定した。CD14 は単球の細胞表面に主に発現する、グラム陰性菌の細胞壁構成タンパクであるリポポリサッカライド（LPS）の認識に関わるものである。CD14 のプロモーター領域の変異は喘息、アトピー性皮膚炎、鼻腔ポリープとの関係性が人で明らかとなっている。犬の CD14 は 290 個のアミノ酸からなり、牛と75%、羊と76%、人と72%、ヤギと68%の相同性であった。これにより、今後、遺伝子多型の解析を進めることができる。

犬の IL-13 遺伝子解析

犬の腫瘍発症リスクの候補としてIL-13遺伝子の多型との関連は見出せなかったが、 IL13 遺伝子の 5´隣接領域に存在する SNP とアトピー性皮膚炎との関連が認められ、達成度は70%であった。IL-13 遺伝子をノックアウトしたマウスではDMBA-TPA 誘発系の 2 段階皮膚腫瘍形成モデルにおいて腫瘍形成が亢進すると報告されている（Rothe et al.,2013）。そこで、犬の腫瘍発症リスクの候補として IL-13 遺伝子の多型を検索した。コリー、シェットランド・シープドッグ、ボーダー・コリー 、ラブラドール・レトリーバー 、ゴールデン・レトリーバー、柴犬、シベリアン・ハスキー、シーズー、セッター、ポメラニアン、秋田犬、ビーグル、ミニチュアダックスフント、ジャーマン・シェパー ドおよび甲斐犬からなる合計 34 個体を対象に、IL-13 遺伝子の開始コドンより約 1.5kbp 上流から終始コドンより 1kbp 下流までの、約 5kbp の塩基配列を決定した。その結果、犬 11 番染色体の配列（NC_006593）を基準として、g.20957075 AGGTGGGCA:[1]＞[2]、g.20957380 G>C、g.20957425 A>G、g.20957580 G>A、g.20957626 C>T、g.20957831 A>C、g.20957836 G>C、g.20958170 C>T、g.20958378 G>A、g.20958774 C>T、g.20958830 C>A、g.20958940 G>C、g.20960082 A>G、g.20960989 G>C、および g.20961598 T>C の 15 カ所の多型を検出した。このうち g.20960082 A>G は、第3エクソンに存在し、IL13 の 63 番目のアミノ酸をトレオニンからアラニンに置換させるものであった。Polyphen-2（http://genetics.bwh.harvard.edu/pph2/）を用いた推定からアミノ酸置換によってタンパク質の高次構造が大きく変化することが示された。これらの変異と乳腺腫瘍の関連解析を実施したが有意な相関は認められなかった。

また、IL13 は、ヒトではアレルギー性疾患との関連が報告されていることから、バイオバンクにおいて収集されたアトピー性皮膚炎を持つ柴犬を対象に相関解析を実施した。g.20960082 A>G（p.63 Thr>Ala）多型では、アトピー性皮膚炎の患畜 10 個体では、G 型対立遺伝子の頻度は.0.05、非患畜 10 個体では 0.10 であり、変異型対立遺伝子の頻度が低いため相関解析は実施できなかった。g.20957626 C>T (rs8973298)多型では、患畜（CC 型 4 個体、CT 型 3 個体、TT 型 3 個体）と非患畜 33 個体（CC 型 4 個体、CT 型 21 個体、TT 型 8 個体）であった。患畜と非患畜関の遺伝子型頻度は、カイ二乗値が 3.939（p＝0.047）で有意に異なっていた。この時、遺伝子型 CC 型をアトピー性皮膚炎のリスク型と仮定するとオッズ比は 4.833（95%信頼区間は 1.018－23.455）となった。(*11)これにより柴犬では、IL13 遺伝子の 5´隣接領域に存在する SNP（rs8973298）は、アトピー性皮膚炎の発症率リスクと関連する事が示唆された

(学会発表1)。現在、別の犬種に対しても相関解析を進めている。

＜優れた成果があがった点＞

海外における犬の遺伝子バンクとしては、米国では NIH、ハバード大学と MIT の Broad Institute による犬のゲノムプリジェクト、ヨーロッパでは12か国20の獣医大学による Lupa が有名である。日本においては犬の遺伝関連疾患の研究を行っている研究は存在するがそれらの研究者が疾患遺伝子を共有するような DNA バンクはなかった。本プロジェクトにより、これから犬の遺伝関連疾患犬の DNA や一般集団犬の DNA などが共有でき、今後、日本の犬の遺伝関連疾患の原因遺伝子の解析のための検体提供の中心的な役割を担うことができると考えられる。また、ネコの DNA バンクは国際的にも未発達である。本プロジェクトにより、ネコの DNA バンクの設立のきっかけができた。

犬の緑内障において SRBD1遺伝子との関連性を見出した。この SRBD1遺伝子の変異は人の正常眼圧緑内障の関連遺伝子としても認められており、この犬の緑内障が人のモデルとしても有用である可能性が示唆された。

犬におけるヒトの適合性の観点から、その中で日本犬のもつ遺伝的特性を明らかにした。日本犬の行動特性に関わる遺伝子群を調査したところ、オオカミと同様のものを持つことが示され、社会性から犬の進化を明らかにしつつある。

犬の TFN-αのマイクロサテライトについてはこれまでに報告がなく、この知見が初めての報告であった。

Alopecia X 症に関する原因遺伝子はこれまでに報告されておらず、今回、候補遺伝子を絞り込むことができ、犬由来のその遺伝子の発現を評価するアッセイ系を構築した。

てんかん候補遺伝子を絞り込んだ犬種は、世界的にも一般的な犬種であり、表現型については、犬によく見られるタイプのてんかんであった。これに対し、現在までに報告のある犬のてんかんの関連遺伝子は、2つとも比較的特殊な犬種における特殊なタイプのてんかんである。したがって、我々の成果をもとにしたこれからの研究は、より広く獣医療に貢献するものと考えられる。

候補 SNP 遺伝子から原因遺伝子が特定されれば、cAD 好発犬種となりうる犬を診断し、ブリーディングに用いないように診断すること可能である。

犬の 11 番染色体 IL-13 遺伝子のプロモーター領域 g.20957075 において[AGGTGGGCA]を単位とする反復多型を発見した。1000 個体分の犬 DNA を収集できたことから、多型解析に有効なリソースを得ることができた。

＜問題点＞

犬の疾患の DNA 収集の体制は整い、その十分な疾患情報も得られたが、専門にその検体やデータ管理を行う常勤の職員が未整備である。今後、このプロジェクトの DNA バンクを恒久的な大学の施設として運用することが課題と考えている。また、現在、日本語のホームページしか作成してない。今後、英語のホームページを作成して海外の研究者にも情報を供給し、海外の研究者とも情報や共同研究が行える体制を整えたい。

眼疾患症例の DNA サンプルの収集が、眼科専門医が診断された症例に限定されたことで、より多くのサンプルが収集できなかった。また、その収集に基づく解析が、眼科の専門知識を必要としたことで、眼科学的解析に要する人材確保はほとんどできなかった。

犬におけるヒトの適合性の観点から、日本犬のもつ遺伝的特性を明らかにした。日本犬の行動特性に関わる遺伝子群を調査したところ、オオカミと同様のものを持つことが示され、社会性から犬の進化を明らかにしつつある。

構築したレポーターアッセイ系の反応性は、用いる培養細胞株によって影響を受ける。いくつかの培養細胞株を検討し、比較的反応性の良い細胞を選択したが、十分とは言えず、より

発現応答の優れた細胞株を利用したアッセイ系に改良する必要がある。
　遺伝子変異とてんかん発症の関連性を解析することと、原因遺伝子の機能解析と発症との関連の検討を行うことが、遺伝子同定のために実施すべき項目として残っている。
　候補 SNP 遺伝子が cAD の病態に関与しているか不明であるため、SNP と病態の関連性について解析する必要がある。
＜評価体制＞
　各研究者は年2回の研究会議で半年分の研究成果を発表している。この会議には共同研究機関の理化学研究所の久保充明先生、鹿児島大学の大和先生、東京農工大学の大森先生もご出席いただき評価やコメントをいただいた。さらに他の分担研究者からのコメントも参考にして、研究代表者が評価している。研究費は最低限必要な研究費を分配して、あとはその評価に応じて遺伝子解析など費用に充てる。さらにその評価を客観的、公平にするために外部評価委員として、東京大学獣医学科　辻本　元教授、北海道大学獣医学科　稲葉　睦教授、酪農学園大学獣医学科　北村　浩教授にお願いして中間評価会を行い、本プロジェクトの各研究者が研究成果の発表を行い、評価・コメントをいただいた。
＜研究期間終了後の展望＞
　本プロジェクト終了後も犬の DNA バンクにおける DNA 検体の収集を行う予定である。
　収集した眼疾患症例 DNA サンプルは、未だほとんど手付かずで、品種依存性眼疾患の探求を今後も継続して行う。また、白内障および緑内障の遺伝子の一部を見出したが、その機能的な役割がまだ不明のため、研究を継続してその遺伝子の機能の解析を行う。
　柴犬を材料に、社会性の進化にかかわる遺伝子を、次世代型シークエンサーで抽出しつつある。これらの遺伝子と行動との関連解析を実施する予定である。
　犬のアロペシア X の原因となる候補遺伝子を見出し、その遺伝子発現の評価系も構築した。しかし、機能的役割は不明であり、発症メカニズムの解明や原因遺伝子としての特定には至っておらず、またその遺伝子発現を回復する具体的な物質も見つかっていない。候補遺伝子と疾患との関係について臨床応用が可能となるデータが得られるように今後も研究を継続する。また、マイクロチップ次世代シーケンサーを利用して、さらに多くの犬のアロペシア X 疾患候補遺伝子を発見し、発症機構の解明への貢献と遺伝子診断法の開発に取組む。
　犬の特発性てんかんの候補遺伝子を絞り込んだが、同定までは至っていないため、研究を継続して、遺伝統計学的手法によって遺伝子変異とてんかん発症の関連性を解析し、さらに原因遺伝子の機能解析と発症との関連の検討を行う。発作型と遺伝子変異との関連性も調べる予定である。そのために今後も研究を継続する。
＜研究成果の副次的効果＞
　村上が本研究で構築した細胞レベルでの遺伝子発現評価系は脱毛症を対象とした薬剤開発のための候補物質スクリーニングや作用機序解明に貢献できる可能性がある。企業との共同研究も進めている。さらに本研究を進める中で研究者間での犬の遺伝関連疾患の情報交換が活発になり、シーズ―網膜剥離・硝子体変性症の原因遺伝子探索と遺伝子診断法の開発、犬の肥満体質に関与する遺伝子の多型解析、変性性脊髄症とエーラス・ダンロス症候群の関連候補遺伝子の探索研究にも新たに着手しており、これらを引き続き行う。
　特許申請
　印牧信行（代表）は犬の緑内障を診断する方法及びキット（特願 2011-152745）、海外出願（2012 年、PCT/JP2012/067173）及び（2013 年、第 14/232.107 号、US）
　齋藤弥代子　横森稔「てんかん発作のモニタリングシステム及びモニタリング方法」特許公開 2014-217649

12　キーワード（当該研究内容をよく表していると思われるものを8項目以内で記載してください。）

（1）犬	（2）遺伝病	（3）遺伝子
（4）遺伝子解析	（5）遺伝子多形(SNP)	（6）バイオバンク
（7）遺伝子資源	（8）	

13　研究発表の状況（研究論文等公表状況。印刷中も含む。）

上記、11(4)に記載した研究成果に対応するものには＊を付すこと。

＜雑誌論文＞

1) Ohkita M, Nagasawa M, Kazutaka M, Kikusui T.: Owners' direct gazes increase dogs' attention-getting behaviors. Behav Processes. in press. 査読有
2) Miyaji K, Okamoto N, Saito S, Yasueda H, Takase Y, Shimakura H, Saito S, Sakaguchi M. :Cross-reactivity between major IgE core epitopes on Cry j 2 allergen of Japanese cedar pollen and relevant sequences on Cha o 2 allergen of Japanese cypress pollen. Allergol Int in press. 査読有
3) Shigehisa R, Uchiyama J, Kato S, Takemura-Uchiyama I, Yamaguchi K, Miyata R, Ujihara T, Sakaguchi Y, Okamoto N, Shimakura H, Daibata M, Sakaguchi M, Matsuzaki S.: Characterization of Pseudomonas aeruginosa phage KPP21 belonging to family Podoviridae genus N4-like viruses isolated in Japan. Microbiol Immunol in press. 査読有
4) Kawarai, S, Fujimoto, A, Nozawa, G, Kanemaki, N, Madarame, H, Shida, T, Kiuchi, A. Evaluation of weekly bathing in allergic dogs with methicillin-resistant Staphylococcal colonization. Jpn J Vet Res in press 査読有
5) Katakawa Y, Funaba M, Murakami M.: Smad8/9 is regulated through the BMP pathway. J Cell Biochem [Epub ahead of print] 2016. 査読有
6) Kida R, Yoshida H, Murakami M, Shirai M, Hashimoto O, Kawada T, Matsui T, Funaba M.: Direct action of capsaicin in brown adipogenesis and activation of brown adipocytes. Cell Biochem Funct 34, 34-41, 2016. 査読有
7) Shigehis R, Uchiyama J, Kato S, Takemura-Uchiyama I, Yamaguchi K, Miyata R, Ujihara T, Sakaguchi Y, Okamoto N, Shimakura H, Daibata M, Sakaguchi M, Matsuzaki, S.: Characterization of Pseudomonas aeruginosa phage KPP21 belonging to family Podoviridae genus N4-like viruses isolated in Japan. Microbiol Immunol, in press. 査読有
8) Takai T, Okamoto Y, Okubo K, Nagata M, Sakaguchi M, Fukutomi Y, Saito A, Yasueda H, Masuyama, K.: Japanese Society of Allergology task force report on standardization of house dust mite allergen vaccines. Allergol Int 64,181-186, 2015. 査読有
9) Mineshige T, Kawarai S, Yauchi T, Segawa K, Neo S, Sugahara G, Kamiie J, Hisasue M, Shirota K. Cutaneous epitheliotropic T-cell lymphoma with systemic dissemination in a dog. J Vet Diagn Invest. 2016 Mar 7. 査読有
10) Horimoto T, Gen F, Murakami S, Iwatsuki-Horimoto K, Kato K, Hisasue M, Sakaguchi M, Nidom CA, Kawaoka Y. Cats as a potential source of emerging influenza virus infections. Virologica Sinica 30,221-223,2015. 査読有
11) (*3)印牧信行、市川陽一朗、川原井晋平、落合秀治. 麻布大学眼科に来院した緑内

障症例の随伴症の分類、日本獣医師会雑誌、68,55-58, 2015. 査読有

12) (*6)Tonoike A, Nagasawa M, Mogi K, Serpell J, Ohtsuki H, Kikusui T. Comparison of owner-reported behavioral characteristics among genetically clustered breeds of dog (Canis familiaris). Sci Rep Dec 18;5:17710.査読有
13) Nagasawa M, Mogi K, Serpell J, Kikusui T. Comparison of behavioral characteristics of dogs in the United States and Japan. J Vet Med Sci, in press 査読有
14) (*7)Tonoike A, Terauchi G, Inoue-Murayama M, Nagasawa M, Mogi K, Kikusui T. The Frequency Variations of the Oxytocin Receptor Gene Polymorphisms among Dog Breeds. J Azabu Uni 27,11-18, 2015 査読有
15) (*8)Tonoike A, Hori Y, Inoue-Murayama M, Konno A, Fujita K, Miyado M, Fukami M, Nagasawa M, Mogi K, Kikusui T. Copy number variations in the amylase gene in Japanese native dog breeds. Anim Genet 46:580-3. doi: 10.1111/age.12344,2015 査読有
16) Nagasawa M, Mitsui S, En S, Ohtani N, Ohta M, Sakuma Y, Onaka T, Mogi K, Kikusui T: Oxytocin-gaze positive loop and the coevolution of human-dog bonds. Science 348, 333-6, 2015. 査読有
17) Romero T, Nagasawa M, Mogi K, Hasegawa T, Kikusui T.: Intranasal administration of oxytocin promotes social play in domestic dogs. Commun Integra Biol 112, E311-320, 2015. 査読有
18) Kawarai S, Hisasue M, Matsuura S, Ito T, Inoue Y, Neo S, Fujii Y, Madarame H, Shirota K, Tsuchiya R. Canine pemphigus foliaceus with concurrent immune-mediated thrombocytopenia. Am Anim Hosp Assoc 51,56-63, 2015. 査読有
19) Nishino Y, Murakami M, Funaba M.:Expression and role of the TGF-β family in glial cells infected with Borna disease virus. Microbes Infect [Epub ahead of print] 2015. 査読有
20) Kasai T, Kato Y, Saegusa S, Murakami M.:Distribution of major staphylococcalca cassette chromosome mec types and exfoliative toxin genes in Staphylococcus pseudintermedius strains from dogs with superficial pyoderma. J Azabu Uni [in print] 2015.査読有
21) Yamada A, Kodo Y, Murakami M, Kuroda M, Aoki T, Fujimoto T, Arai K.:Hybrid origin of gynogenetic clones and the introgression of their mitochondrial genome into sexual diploids through meiotic hybridogenesis in the loach, Misgurnus anguillicuadatus. J Exp Zool A Ecol Genet Physiol 323,593-606,2015. 査読有
22) Shirai M, Nomura R, Kato Y, Murakami M, Kondo C, Takahashi S, Yamasaki Y, Matsumoto-Nakano M, Arai N, Yasuda H, Nakano K, Asai F.: Short communication: Distribution of Porphyromonas gulae fimA genotypes in oral specimens from dogs with mitral regurgitation. Res Vet Sci 102,49-52,2015. 査読有
23) Kanamori Y, Murakami M, Matsui T, Funaba M.: Role of TPA-responsive element in hepcidin transcription induced by the bone morphogenetic protein pathway. Biochem Biophys Res Commun 466, 162-6,2015. 査読有
24) Murakami M, Ohi M, Ishikawa S, Shirai M, Horiguchi H, Nishino Y, Funaba M. Adaptive expression of uncoupling protein 1 in the carp liver and kidney in response to changes in ambient temperature. Comp Biochem Physiol Part A, 185, 142-9,2015. 査読有
25) Okubo T, Hayashi D, Yaguchi T, Fujita Y, Sakaue M, Suzuki T, Tsukamoto A, Murayama O, Lynch J, Miyazaki Y, Tanaka K, Takizawa T.: Differentiation of rat adipose tissue-derived stem cells into neuron-like cells by valproic acid, a histone

deacetylase inhibitor. Exp Anim [Epub ahead of print] , PMID: 26411320,2015.査読有

26) Yuan Y, Kitamura-Muramatsu Y, Saito S, Ishizaki H, Nakano M, Haga S, Matoba K, Ohno A, Murakami H, Takeshima SN, Aida Y. Detection of the BLV provirus from nasal secretion and saliva samples using BLV-CoCoMo-qPCR-2: Comparison with blood samples from the same cattle. Virus Res 210:248-54,2015. 査読有

27) 村上裕信、間陽子: HIV-1 アクセサリー蛋白質 Vpr と宿主因子. 臨床免疫・アレルギー科. 63:484-488,2015. 査読無

28) Horimoto T, Gen F, Murakami S, Iwatsuki-Horimoto K, Kato K, Akashi H, Hisasue M, Sakaguchi M, Kawaoka Y, Maeda K: Serological evidence of infection of dogs with human influenza viruses in Japan. Vet Rec 174, 96, 2014. 査読有

29) 高井敏朗, 岡本美孝, 大久保公裕, 永田真, 阪口雅弘, 福冨友馬, 齋藤明美, 安枝浩, 増山敬祐:ダニアレルゲンワクチン標準化に関する日本アレルギー学会タスクフォース報告.アレルギー 63,1229-40,2014. 査読有

30) Romero T, Nagasawa M, Mogi K, Hasegawa T, Kikusui T.: Oxytocin promotes social bonding in dogs. Proc Natl Acad Sci U S A, 111, 9085-90, 2014. 査読有

31) Nagasawa M, Shimozawa A, Mogi K, Kikusui T.: N-acetyl-D-mannosamine treatment alleviates age-related decline in place-learning ability in dogs. J Vet Med Sci 76, 757-61, 2014. 査読有

32) (*9)Watanabe M, Tanaka K, Takizawa T, Segawa K, Neo S, Tsuchiya R, Murata M, Murakami M, Hisasue M.:Characterization of a canine tetranucleotide microsatellite marker located in the first intron of the tumor necrosis factor alpha gene. J Vet Med Sci 76,119-22. 2014. 査読有

33) Kamiie J, Shimoyama N, Aihara N, Hisasue M, Naya Y, Ogihara K, Shirota K Quantitative analysis of CD3ε in a cloned canine lymphoma cell line by selected reaction monitoring assay. Biosci Biotechnol Biochem 78,271-5,2014. 査読有

34) Kawarai S, Matsuura M, Yamamoto S, Kiuchi A, Kanemaki N, Madarame H, Sirota K: A case of cutaneous sterile pyogranuloma/granuloma syndrome in a Maltese. J Am Anim Hosp Assoc, 50:278-283, 2014 査読有

35) Watanabe S, Ito J, Baba T, Hiratsuka T, Kuse K, Ochi H, Anai Y, Hisasue M, Tsujimoto H, Nishigaki K. Notch2 transduction by feline leukemia virus in a naturally infected cat. J Vet Med Sci 76,553-7, 2014. 査読有

36) Kurihara Y, Suzuki T, Sakaue M, Murayama O, Miyazaki Y, Onuki A, Aoki T, Saito M, Fujii Y, Hisasue M, Tanaka K, Takizawa T. Valproic acid, a histone deacetylase inhibitor, decreases proliferation of and induces specific neurogenic differentiation of canine adipose tissue-derived stem cells. J Vet Med Sci 76:15-23, 2014. 査読有

37) Kanamori Y., Murakami M., Matsui T. and Funaba M.: The regulation of hepcidin expression by serum treatment: requirements of the BMP response element and STAT- and AP-1-binding sites. Gene 551, 119-126,2014. 査読有

38) Kanamori Y, Murakami M, Matsui T, Funaba M.:Hepcidin expression in liver cells: evaluation of mRNA levels and transcriptional regulation.Gene 546, 50-5,2014. 査読有

39) Yamaguchi S, Sano A, Hiruma M, Murata M, Kaneshima T, Murata Y, Takahashi H, Takahashi S, Takahashi Y, Chibana H, Touyama H, Nguyen Thi Thanh Ha, Nakazato Y, Uehara Y, Hirakawa M, Imura Y, Terashima Y, Kawamoto Y, Takahashi K,Sugiyama K, Hiruma M, Murakami M, Hosokawa A, Uezato H.: Isolation of Dermatophytes and Related Species from Domestic Fowl (Gallus gallus domesticus). Mycopathologia178, 135-43,2014. 査読有

40) Nishita T, Yatsu J, Murakami M, Kamoshida S, Orito K, Ichihara N, Arishima K, Ochiai H.: Isolation and sequencing of swine carbonic anhydrase VI, an enzyme expressed in the swine kidney. BMC Res Notes 7, 116, 2014.査読有
41) Asai K, Funaba M, Murakami M.:Enhancement of RANKL-induced MITF-E expression and osteoclastogenesis by TGF-β. Cell Biochem Funct 32, 401-9, 2014. 査読有
42) Murata M, Murakami M.:Two distinct mtDNA lineages among captive African penguins in Japan. J Vet Med Sci 76, 559-63,2014. 査読有
43) Ogawa M, Uchida K, Isobe K, Saito M, Harada T, Chambers JK, Nakayama H.: Globoid cell leukodystrophy (Krabbe's disease) in a Japanese domestic cat. Neuropathology 34,190-6, 2014. 査読有
44) Utsugi S, Saito M, Shelton D. Resolution of polyneuropathy in a hypothyroid dog following thyroid supplementation. J Am Anim Hosp Assoc 50,345-9, 2014. 査読有
45) Miyaji K, Yurimoto T, Saito A, Yasueda H, Takase Y, Shimakura H, Okamoto N, Kiuchi A, Saito S, Sakaguchi M: Analysis of conformational and sequential IgE epitopes on the major allergen Cry j 2 of Japanese cedar pollen in humans by using monoclonal antibodies for Cry j 2. J Clin Immunol 33, 977-83, 2013. 査読有
46) (*4)Kanemaki N, Tchedre KT, Imayasu M, Kawarai S, Sakaguchi M, Yoshino A, Itoh N, Meguro A, Mizuki N. Dogs and humans share a common susceptibility gene SRBD1 for glaucoma risk. PLoS One 8, e74372, 2013. 査読有
47) Nagasawa M, Kawai E, Mogi K, Kikusui T.: Dogs show left facial lateralization upon reunion with their owners. Behav Processes 98, 112-6, 2013 査読有
48) Nagasawa M, Shibata Y, Yonezawa A, Morita T, Kanai M, Mogi K, Kikusui T.: The behavioral and endocrinological development of stress response in dogs. Dev Psychobiol 56, 726-33, 2013. 査読有
49) Fujimoto A, Neo S, Ishizuka C, Kato T, Segawa K, Kawarai S, Ogihara K, Hisasue M, Tsuchiya R. Identification of cell surface antigen expression in canine hepatocellular carcinoma cell lines. J Vet Med Sci 75,831-5,2013. 査読有
50) Kato T, Hisasue M, Segawa K, Fujimoto A, Makiishi E, Neo S, Yasuno K, Kobayashi R, Tsuchiya R.: Accumulation of xenotransplanted canine bone marrow cells in NOD/SCID/γc(null) mice with acute hepatitis induced by CCl4. J Vet Med Sci 75,847-55, 2013. 査読有
51) Murata M, Takahashi H, Takahashi S, Takahashi Y, Chibana H, Murata Y, Sugiyama K, Kaneshima T, Yamaguchi S, Miyasato H, Murakami M, Kano R, Hasegawa A, Uezato H, Hosokawa A, Sano A.: Isolation of Microsporum gallinae from a fighting cock (Gallus gallus domesticus) in Japan. Med Mycol 51, 144-9, 2013. 査読有
52) Shibuya E, Murakami M, Kondo M, Kamei Y, Tomonaga S, Matsui T, Funaba M.:Downregulation of Pgc-1α expression by tea leaves and their by-products. Cell Biochem Funct 32,236-40,2013. 査読有
53) Suenaga M, Kurosawa N, Asano H, Kanamori Y, Umemoto T, Yoshida H, Murakami M, Kawachi H, Matsui T, Funaba M.:Bmp4 expressed in preadipocytes is required for the onset of adipocyte differentiation. Cytokine 64, 138-45,2013. 査読有
54) Dong J, Murakami M, Fujimoto T, Yamaha E, Arai K.: Genetic characterization of the progeny of a pair of the tetraploid silver crucian carp Carassius auratus langsdorfii. Fish Sci 79, 935-41,2013.査読有
55) Iida N, Fukushima H, Hiroi M, Yagi M, Kanda T, Murakami M, Sugiyama K.: Development of duplex SYBR green real-time PCR for rapid and simultaneous detection of 16 specific genes of 16 major foodborne bacteria. Jpn J Food Microbiol (日本食品微

生物学会雑誌), 30, 160-4,2013. 査読有

56) Yoshida H, Kanamori Y, Asano H, Hashimoto O, Murakami M, Kawada T, Matsui T, Funaba M.:Regulation of brown adipogenesis by the Tgf-β family: Involvement of Srebp1c in Tgf-β- and Activin-induced inhibition of adipogenesis. Biochim Biophys Acta 1830, 5027–35,2013. 査読有

57) Ohnishi M, Okatani AT, Harada K, Sawada T, Marumo K, Murakami M, Sato R, Esaki H, Shimura K, Kato H, Uchida N, Takahashi T.:Genetic characteristics of CTX-M-Type extended-spectrum-β-lactamase (ESBL)-producing enterobacteriaceae involved in mastitis cases on Japanese dairy farms, 2007 to 2011. J Clin Microbiol 51, 3117-22,2013. 査読有

58) Ohnishi M, Okatani AT, Esaki H, Harada K, Sawada T, Murakami M, Marumo K, Kato Y, Sato R, Shimura K, Hatanaka N, Takahashi T.:Herd prevalence of Enterobacteriaceae producing CTX-M-type and CMY-2 β-lactamases among Japanese dairy farms. J Appl Microbiol 115, 282-9,2013. 査読有

59) Hirai N, Shirai M, Kato Y, Murakami M, Nomura R, Yamasaki Y, Takahashi S, Matsumoto-Nakano M, Nakano K, Asai F.:Correlation of age with distribution of periodontitis-related bacteria in Japanese dogs. J Vet Med Sci 75, 999-1001,2013. 査読有

60) Murakami M, Shirai M, Ooishi R, Tsuburaya A, Asai K, Hashimoto O, Ogawa K, Nishino Y, Funaba M.: Expression of activin receptor-like kinase 7 in adipose tissues. Biochem Genet 51, 202-10,2013. 査読有

61) Tsuboi M, Uchida K, Ide T, Ogawa M , Inagaki T, Tamura S, Saito M, Chambers JK, Nakayama H. Pathological features of polyneuropathy in three dogs. J Vet Med Sci 75,327-35, 2013.査読有

62) Aida Y, Murakami H, Takahashi M, Takeshima S.: Mechanisms of pathogenesis induced by bovine leukemia virus (BLV) as a model for human T-cell leukemia virus (HTLV)" Front. Microbiol 4:328, 2013.査読有

63) 藤村正人,阪口雅弘:犬のアトピー性皮膚炎に対する 8 日間プロトコールを用いた急速減感作療法の安全性. 獣医アトピー・アレルギー・免疫学会誌 2,14-18,2013. 査読有

64) Kubota S, Miyaji K, Shimo Y, Shimakura H, Takase Y, Okamoto N, Kiuchi A., Fujimura M., Fujimura T, DeBoer J D, Tsukui T, Sakaguchi M: IgE reactivity to a Cry j 3, an allergen of Japanese cedar pollen in dogs with canine atopic dermatitis. Vet Immunol Immunopathol 149,132-5, 2012. 査読有

65) Kawakami M, Narumoto O, Mastuo Y, Horiguchi K, Yamashita N, Sakaguchi M, Lipp M, Nagase T, Yamashita N: The role of CCR 7 in allergic airway inflammation induced by house dust mite exposure. Cell Immunol 275:24-32, 2012. 査読有

66) Narumoto O, Matsuo Y, Sakaguchi M, Shoji S, Yamashita N, Shubert D, Abe K, Horiguchi K, Yamashita N: Suppressive effects of a pyrazole derivative of curcumin on airway inflammation and remodeling. Exp Mol Pathol 93, 18-25, 2012. 査読有

67) Miyaji K, Suzuki A, Shimakura H, Takase Y, Kiuchi A, Fujimura M, Kurita G, Tsujimoto H, Sakaguchi M: Large-scale survey of adverse reactions to canine non-rabies combined vaccines in Japan. Vet Immunol Immunopathol 145, 447-52, 2012. 査読有

68) (*10)Tsukui T, Sakaguchi M, Kurata K, Maeda S, Ohmori K, Masuda K, Tsujimoto H, Iwabuchi S: Measurement for canine IgE using canine recombinant high affinity IgE receptor α chain (FcεRIα). J Vet Med Sci 74,851-6, 2012. 査読有

69) Nagasawa M, Mogi K, Kikusui T: Continued Distress among Abandoned Dogs in

Fukushima. Sci Rep 2, 724, 2012. 査読有

70) Nagasawa M, Yatsuzuka A, Mogi K, Kikusui T: A new behavioral test for detecting decline of age-related cognitive ability in dogs. J Vet Behav Clin Appl Res 7, 220-24, 2012. 査読有

71) Nagasawa M, Okabe S, Mogi K, Kikusui T: Oxytocin and mutual communication in mother-infant bonding. Front Hum Neurosci 6, 31, 2012.

72) Segawa K, Kondo T, Kimura S, Fujimoto A, Kato T, Ishikawa T, Neo S, Hisasue M, Yamada T, Tsuchiya R. Effects of prostaglandin E1 on the preparation of platelet concentrates in dogs. J Vet Intern Med 26,370-6,2012. 査読有

73) Haishima A, Murakami M, Ikeda T, Inoue K, Kamiie J, Shirota K.: Detection of Bcl-2 mRNA and its product in the glomerular podocytes of the normal rat kidney. Exp Toxicol Pathol 64, 633-7, 2012. 査読有

74) Tanaka M, Izawa T, Kuwamura M, Nakao T, Maezono Y, Ito S, Murata M, Murakami M, Sano A,Yamate J.: Deep granulomatous dermatitis of the fin caused by fusarium solani in a false killer whale (Pseudorca crassidens). J Vet Med Sci 74, 779-82, 2012. 査読有

75) Nishikawa O, Arishima K, Kobayashi T, Shirai M, Murakami M, Sakaue M,Yamamoto M.: Maternal exposure to low doses of DES altered mRNA expression of hepatic microsomal enzymes in male rat offspring. J Vet Med Sci 74, 247-53, 2012. 査読有

76) Yamasaki Y, Nomura R, Nakanoa K, Inaba H, Kuboniwa M, Hirai N, Shirai M, Kato Y, Murakami M, Naka S, Iwai S, Matsumoto-Nakano M, Ooshima T, Amano A, Asai F.:Distribution and molecular characterization of Porphyromonas gulae carrying a new fimA genotype. Vet Microbiol 161, 196-205,2012. 査読有

77) Nomura R, Shirai M, Kato Y, Murakami M, Nakano K, Hirai N, Mizusawa T, Naka S, Yamasaki Y, Matsumoto-Nakano M, Ooshima T, Asai F.: Diversity of fimbrillin among Porphyromonas gulae clinical isolates from Japanese dogs. J Vet Med Sci 74, 885-91,2012. 査読有

78) Ishii Y, Takizawa T, Iwasaki H, Fujita Y, Murakami M, Groppe JC, Tanaka K.: Nucleotide polymorphisms in the canine Noggin gene and their distribution among dog (Canis lupus familiaris) breeds. Biochem Genet 50, 12-8,2012. 査読有

79) Ooishi R, Shirai M, Funaba M, Murakami M. (2012) Microphthalmia-associated transcription factor is required for mature myotube formation. Biochim Biophys Acta 1820, 76–83,2012. 査読有

80) Mizukami K, Kawamichi T, Koie H, Tamura S, Matsunaga S, Imamoto S, Saito M, Hasegawa D, Matsuki N, Tamahara S, Sato S, Yabuki A, Chang H, Yamato O. Neuronal ceroid lipofuscinosis in border collie dogs in Japan: Clinical and molecular epidemiological study (2000-2011). ScientificWorldJournal Volume 2012 Article ID 383174, 7 pages, 2012. 査読有

81) Kaburaki Y, Fujimura T, Kurata K, Matsuda K, Toda M, Yasueda H, Chida K, Kawarai S, Sakaguchi M: Induction of Th1 immune responses to Japanese cedar pollen allergen in mice immunized with Cry j 1 conjugated with CpG oligodeoxynucleotide. Comp Immunol Microbiol Infect Dis 34,157-61, 2011. 査読有

82) Fujimura T, Yonekura S, Horiguchi S, TaniguchiY, Saito A, Yasueda H, Inamine A, Nakayama T, Takemori T, Taniguchi M, Sakaguchi M, Okamoto Y: Increase of regulatory T cells and the ratio of specific IgE to total IgE are potential therapeutic or prognostic biomarkers in two-year sublingual immunotherapy for Japanese cedar pollinosis. Clin Immunol 139,65-74, 2011. 査読有

83) Kawarai S, Sato K, Horiguchi A, Kurata K, Kiuchi A, Tsujimoto H, Sakaguchi M: Potential immunological adjuvant of 'K'-type CpG- oligodeoxynucleotides enhanced the

cell proliferation and IL-6 mRNA expression in canine B cells. J Vet Med Sci 73, 177-84, 2011. 査読有

84) (*10)Okayama T, Matsuno, Yasuda N, Tsukui T, Suzuta Y, Koyanagi M, Sakaguchi M, Tsujimoto H, Ishii Y, Olivry T, Masuda K.: Establishment of a quantitative ELISA for the measurement of an allergen-specific IgE in dogs using anti-IgE antibody cross-reactive to mouse and dog IgE. Vet Immunol Immunopathol 139, 99-106, 2011. 査読有

85) 阪口雅弘: アレルギー疾患の DNA 免疫療法. アレルギー 60, 1591−1597, 2011. 査読有

86) Nagasawa M, Murai K, Ohta M, Mogi K, Kikusui T.: Dogs can discriminate human smiling faces from blank expressions. Anim Cogn 14, 525-33, 2011 査読有

87) Nagasawa M, Tsujimura A, Tateishi K, Mogi K, Ohta M, Serpell J, Kikusui T.: Assessment of the factorial structures of the C-BARQ in Japan. J Vet Med Sci 73, 869-75, 2011. 査読有

88) Mitsui S, Yamamoto M, Nagasawa M, Mogi K, Kikusui T, Ohtani N, Ohta M.: Urinary oxytocin as a noninvasive biomarker of positive emotion in dogs. Horm Behav. 60, 239-43, 2011. 査読有

89) Shimokawa Miyama T, Umeki S, Baba K, Sada K, Hiraoka H, Endo Y, Inokuma H, Hisasue M, Okuda M, Mizuno T. Neutropenia associated with osteomyelitis due to Hepatozoon canis infection in a dog. J Vet Med Sci 73,1389-93,2011. 査読有

90) Umemoto T, Furutani Y, Murakami M, Matsui T, Funaba M.: Endogenous Bmp4 in myoblasts is required for myotube formation in C2C12 cells. Biochim Biophys Acta 1810, 1127-35, 2011. 査読有

91) Morita H, Nakano A, Onoda H, Toh H, Oshima K, Takami H, Murakami M, Fukuda S, Takizawa T, Kuwahara T, Ohno H, Tanabe S,Hattori M.: Bifidobacterium kashiwanohense sp. nov., isolated from healthy infant faeces. Int J Syst Evol Microbiol 61, 2610-5, 2011. 査読有

92) Kato Y, Shirai M, Murakami M, Mizusawa T, Hagimoto A, Wada K, Nomura R, Nakano K, Ooshima T, Asai F.: Molecular detection of human periodontal pathogens in oral swab specimens from dogs in Japan. J Vet Dent 28, 84-89,2011. 査読有

93) 宇津木真一、齋藤弥代子: ミオキミア/ニューロミオトニアのヨークシャーテリアの 1 例. 日獣会誌、64, 56-60,2011 査読有

共同研究機関
久保充明

94) Okada Y, Momozawa Y, Ashikawa K, Kanai M, Matsuda K, Kamatani Y, Takahashi A, Kubo M.: Construction of a population-specific HLA imputation reference panel and its application to Graves' disease risk in Japanese. Nat Genet 47,798-802,2015. 査読有

95) Nakajima M, Takahashi A, Tsuji T, Karasugi T, Baba H, Uchida K, Kawabata S, Okawa A, Shindo S, Takeuchi K, Taniguchi Y, Maeda S, Kashii M, Seichi A, Nakajima H, Kawaguchi Y, Fujibayashi S, Takahata M, Tanaka T, Watanabe K, Kida K, Kanchiku T, Ito Z, Mori K, Kaito T, Kobayashi S, Yamada K, Takahashi M, Chiba K, Matsumoto M, Furukawa K, Kubo M, Toyama Y; Genetic Study Group of Investigation Committee on Ossification of the Spinal Ligaments, Ikegawa S.: A genome-wide association study identifies susceptibility loci for ossification of the posterior longitudinal ligament of the

spine. Nat Genet 46,1012-6, 2014 査読有

96) Kou I, Takahashi Y, Johnson TA, Takahashi A, Guo L, Dai J, Qiu X, Sharma S, Takimoto A, Ogura Y, Jiang H, Yan H, Kono K, Kawakami N, Uno K, Ito M, Minami S, Yanagida H, Taneichi H, Hosono N, Tsuji T, Suzuki T, Sudo H, Kotani T, Yonezawa I, Londono D, Gordon D, Herring JA, Watanabe K, Chiba K, Kamatani N, Jiang Q, Hiraki Y, Kubo M, Toyama Y, Tsunoda T, Wise CA, Qiu Y, Shukunami C, Matsumoto M, Ikegawa S. Genetic variants in GPR126 are associated with adolescent idiopathic scoliosis. Nat Genet 45,676-9, 2013.査読有

97) Okada Y, Kubo M, Ohmiya H, Takahashi A, Kumasaka N, Hosono N, Maeda S, Wen W, Dorajoo R, Go MJ, Zheng W, Kato N, Wu JY, Lu Q; GIANT consortium, Tsunoda T, Yamamoto K, Nakamura Y, Kamatani N, Tanaka T. Common variants at CDKAL1 and KLF9 are associated with body mass index in east Asian populations. Nat Genet 44,302-6,2012. 査読有

98) Arakawa S, Takahashi A, Ashikawa K, Hosono N, Aoi T, Yasuda M, Oshima Y, Yoshida S, Enaida H, Tsuchihashi T, Mori K, Honda S, Negi A, Arakawa A, Kadonosono K, Kiyohara Y, Kamatani N, Nakamura Y, Ishibashi T, Kubo M. Genome-wide association study identifies two susceptibility loci for exudative age-related macular degeneration in the Japanese population. Nat Genet 43,1001-4,2011. 査読有

大森啓太郎

99) Watanabe SY, Iga J, Ishii K, Numata S, Shimodera S, Fujita H, Ohmori T. Biological tests for major depressive disorder that involve leukocyte gene expression assays. Psychiatr Res 66-67,1-6, 2015. 査読有

100) Ohmori K, Minamide K, Goto S, Nagai M, Shirai J, Oku K. Time-of-day-dependent variations of scratching behavior and transepidermal water loss in mice that developed atopic dermatitis. J Vet Med Sci 76,1501-4, 2014. 査読有

101) Tanaka A, Jung K, Matsuda A, Jang H, Kajiwara N, Amagai Y, Oida K, Ahn G, Ohmori K, Kang KG, Matsuda H.: Daily intake of Jeju groundwater improves the skin condition of the model mouse for human atopic dermatitis. J Dermatol 40,193-200, 2013.

大和　修

102) Kohyama M, Yabuki A, Kawasaki Y, Kawaguchi H, Miura N, Kitano Y, Onitsuka T, Rahman MM, Miyoshi N, Yamato O.: GM2 gangliosidosis variant 0 (Sandhoff disease) in a mixed-breed dog. J Am Anim Hosp Assoc 51,396-400,2015. 査読有

103) Rahman MM, Yabuki A, Kohyama M, Mitani S, Mizukami K, Uddin MM, Chang HS, Kushida K, Kishimoto M, Yamabe R, Yamato O.: Real-time PCR genotyping assay for GM2 gangliosidosis variant 0 in toy poodles and the mutant allele frequency in Japan. J Vet Med Sci 76, 295–9, 2014. 査読有

104) Mizukami K, Yabuki A, Kawamichi T, Chang HS, Rahman MM, Uddin MM, Kohyama M, Yamato O.: Real-time PCR genotyping assay for canine trapped neutrophil syndrome and high frequency of the mutant allele in Border collies. Vet J 195, 260–1, 2013.

＜図書＞

1. 齋藤弥代子：犬と猫の抗てんかん薬の使い方「てんかん治療ガイドブック」 ファームプレス、東京、in press.
2. 長谷川大輔、枝村一弥、齋藤弥代子（監修、共著）：犬と猫の神経病学各論編,緑書房、東京、2015.
3. 阪口雅弘.動物アレルゲン「あなたのまわりに潜む身近なアレルゲン」（谷口正実、福富友馬監修）、メデイカルレビュー社、東京、p14-17,2015.
4. 齋藤弥代子（共著）:獣医内科学第２版「神経疾患の検査と診断」文英堂出版,東京、2014.
5. 阪口雅弘:非特異的生体防御（自然免疫）「獣医微生物検査学」（福所秋雄他監修）近代出版、東京、p41-4,2014.
6. 阪口雅弘：ペット．「吸入性アレルゲンの同定と対策」（谷口正実、福富友馬監修）、メデイカルレビュー社、東京、p34-7,2014.
7. 阪口雅弘:CpG ワクチン．「アレルギー疾患の免疫療法と分子標的治療」（近藤直美編集）診断と治療社、東京、p110-4,2013.
8. 阪口雅弘:環境アレルギーアドバイザー試験 公式テキスト(阪口雅弘他監修)、日本能率協会マネジメントセンター、東京、2013.
9. 阪口雅弘,森田英利、田原口智士：微生物学、講談社、東京、2013.
10. Sakaguchi M, Inouye S.: Gelatin allergies associated with diphtheria-tetanus-acellular pertussis (DTaP) vaccines. "Trends in Diphtheria Research." in Wheeler B.S. (ed). Nova Science Publishers, New York, USA, p63-79, 2011.
11. 阪口雅弘:免疫不全と自己免疫「獣医微生物学」（見上　彪監修）文永堂、東京、p363-366,2011.
12. 小方宗次監修，斑目広郎，川原井晋平（共著）:アレルギーわんこの暮らしとレシピ百科、誠文堂新光社、東京、2011.

＜学会発表＞

1. (*11)　田中和明，滝沢達也，山本未咲，岡本憲明，島倉秀勝，阪口雅弘: イヌ IL-13 遺伝の多型と柴犬におけるアトピー性皮膚炎との関連調査．日本畜産学会第 121 回大会，武蔵野、3 月 2016 年
2. 内山淳平、内山伊代、竹内 啓晃、阪口義彦、阪口雅弘、松崎 茂展: 活性型ピロリ菌ファージ KHP30 の特徴付けとその潜伏感染性の解析.第 89 回日本細菌学会、大阪、3 月 2016 年
3. 那須川忠弥、内山淳平、鈴木仁人、宮田玲奈、山口琴絵、平山隆一郎、内山伊代、氏原隆子、阪口義彦、阪口雅弘、松﨑茂展：緑膿菌 PAO1 株とファージ KPP22 の短期間進化的軍拡競走の解析．第 89 回日本細菌学会、大阪、3 月 2016 年
4. 水谷格之、後藤裕子、蔵田圭吾、藤原亜紀、阪口雅弘、大野耕一、辻本元：イヌのリンパ腫症例における血清中可溶性インターロイキン-2 受容体α鎖の測定．第 12 回日本獣医内科学アカデミー学術大会、横浜、2 月 2016 年
5. 白井秀治、阪口雅弘：ダニアレルゲンに対する家庭内対策の非臨床研究を中心した評価.第 52 回日本小児アレルギー学会、奈良、11 月 2015 年
6. (*1)旭　愛，藤井宏治，岡本憲明，窪田 聡，関口和正，阪口雅弘，武内ゆかり，松田秀明：マイクロサテライト多型解析を用いたイヌの個体識別法の検討．第 21

回日本法科学技術学会，柏、11 月 2015 年

7. 村上裕信、二階堂紗恵、佐藤礼一郎、塚本健司： 牛白血病ウイルス G4 遺伝子欠損株のウイルス産生量．第 63 回日本ウイルス学術集会、福岡、11 月 2015 年
8. 鈴木千裕、戸髙晴菜、二階堂紗恵、佐藤礼一郎、塚本健司、村上裕信: BLV 感染性分子クローンを用いたウイルス産生量とゲノム変異の解析．第 63 回日本ウイルス学術集会、福岡、11 月 2015 年
9. 内山淳平，阪口雅弘，松崎茂展：ピロリ菌ファージの発見とその解析．第 68 回日本細菌学会中国・四国支部総会，岡山，10 月 2015 年
10. (*5)Ota N, Kanemaki N, Tsujita H, Kobayashi Y, Abe M, Takimoto Y, Imayasu M, Meguro A, Mizuki N. Associations of single-nucleotide polymorphisms of SRBD1 gene 64 with glaucoma in Shiba-inu dog: A meta-analysis in six Japanese veterinary hospitals. ACVO Annual meeting, Coeur d'Alene, ID, USA, Oct, 2015.
11. 島倉秀勝、齋藤拓、藤村正人 、岡本憲明、内山淳平、阪口雅弘：食物有害反応を示す犬における卵白抗原に対する IgE 反応性の検討．第 158 回日本獣医学会、十和田、９月 2015 年
12. 平山 隆一郎、鈴木 仁人、内山 淳平、松井 真理、鈴木 里和、柴山 恵吾、阪口 雅弘、木内 明男: イヌにおける新規口腔内常在細菌の同定と全ゲノム配列解析． 第 158 回日本獣医学会、十和田、９月 2015 年
13. 内山淳平、松井秀仁、花木秀明、松崎茂展、阪口雅弘:細菌感染症における診断法と治療法の開発：バクテリオファージの利用．第 158 回日本獣医学会、十和田、９月 2015 年
14. 大久保倫子、赤池かんな、村上賢:国内ケープペンギンの個体識別および父子鑑定におけるマイクロサテライト DNA マーカーの有用性．第 158 回日本獣医学会学術集会、十和田、9 月 2015 年
15. Nomura N, Saito M, Hasegawa D, Watanabe N. Uchida K, Okuno S, Nakai M, Orito K. Clinical efficacy and safety of zonisamide monotherapy in dogs with newly diagnosed idiopathic epilepsy. 2015 ACVIM Forum, Indianapolis, June, 2015.
16. 石井崇史，新倉雄一，細木敬祐，津久井利宏，阪口雅弘，三宅健介，長瀬隆英，山下直美： 喘息病態における気道上皮細胞の活性化と新規クルクミン誘導体による制御についての解析.第 55 回日本呼吸器学会、東京、4 月 2015 年
17. (*2)坪井誠也，渡邊学，二瓶和美，吉見奈津子，加藤明久，阪口雅弘，大和修,櫛田和哉,チェンバーズジェームズ，菅野純夫，内田和幸，中山裕之：Whole Exome Sequence 法によるイヌ遺伝性神経疾患の原因遺伝子同定。第 11 回獣医内科アカデミー、横浜、2 月 19 日 2014 年
18. 外池亜紀子、永澤美保、茂木一孝、菊水健史: 認知能力の犬種間比較と関連遺伝子の探索によるイヌの進化に関する研究.「共感性の進化・神経基盤」第 2 回領域会議、東大寺総合文化センター、1 月 2015 年
19. 大北碧、永澤美保、茂木一孝、菊水健史: イヌにおいてヒトからの視線は報酬になるか？「共感性の進化・神経基盤」第 2 回領域会議、東大寺総合文化センター、1 月 2015 年
20. 永澤美保、菊水健史: 収斂進化がもたらしたヒトーイヌ間の絆形成とオキシトシンの役割．「共感性領域」「自己制御精神領域」合同若手育成シンポジウム、東京医科歯科大学、12 月 2014 年
21. 菊水健史: 人と犬の共生 心のつながり．日本神経消化器病学会、学術総合センター・

一橋講堂、11 月 2014 年
22. 原田晋、白井秀治、越本知大、阪口雅弘,工藤比等志：被毛および唾液の両者への感作が認められたジヤンガリアンハムスターによるアナフィラキシーの 1 例.第４４回日本皮膚アレルギー・接触皮膚炎学会、仙台、11 月 2014 年
23. 佐藤美紀、宮崎陽子、青木卓磨、藤田幸弘、圓尾拓也、齊藤弥代子、藤井洋子、久末正晴、田中和明、滝沢達也:イヌ脂肪組織幹細胞(ASC)の細胞増殖と神経分化に及ぼすバルプロ酸と低酸素の影響. 第 87 回日本生化学会、国立京都国際会館、10 月 2014 年
24. 柴田曜、永澤美保、茂木一孝、菊水健史: イヌにおけるストレス内分泌の発達特性と行動との関連. 第 157 回日本獣医学会学術集会、札幌、9 月 2014 年
25. 秋吉 亮人、久末 正晴、土屋亮：原発性門脈低形成と診断した犬 30 症例における臨床病理学的検査所見の検討. 第 157 回日本獣医学会、札幌、9 月 2014 年
26. 黒田真道、村上賢、藤本貴史、荒井克俊:反復配列をプローブとした FISH による染色体識別とクローンドジョウの雑種起源解明. 平成 26 年度日本水産学会秋季大会、福岡、9 月 2014 年
27. 村田倫子、亀井早紀、村上賢:フンボルトペンギン属 3 種のペンギンの核型分析による特徴付け. 第 157 回日本獣医学会学術集会、札幌、9 月 2014 年
28. 片川優子、舟場正幸、村上賢:BMP による Smad8 発現調節メカニズムの解析. 第 157 回日本獣医学会学術集会、札幌、9 月 2014 年
29. 永澤美保、柴田曜、茂木一孝、菊水健史: The development of endocrine stress response in early socialization period is associated with that in adulthood in dogs. 日本動物心理学会第 74 回大会、犬山国際観光センター“フロイデ”、7 月 2014 年
30. 阪口雅弘、白井秀治：室内環境アレルゲン.第 23 回日本臨床環境医学会、京都、6 月 2014 年
31. (*4)Imayasu M, Kanemaki N, Meguro A, Mizuki N. A novel single nucleotide polymerism asocial woth glaucoma in Shiba-inu and Shih-Tzu dogs, ARVO Annual Meeting, Orlando, FL, USA, May, 2014.
32. 石井崇史, 新倉雄一, 白井秀治, 阪口雅弘, 棚元憲一, 室井正志, 長瀬隆英, 山下直美: IRF3 の好酸球性気道炎症病態における役割.第 26 回日本アレルギー学会春季総会、5 月 2014 年
33. 鈴木 麻里子、黒崎 晃彦、飛田 啓輔、青木 康夫、林野 淳、辻本 元、阪口 雅弘: 犬のアトピー性皮膚炎における新規乳酸菌 Lactobacillus crispatus KT-11 製剤の投与試験.第17回日本獣医皮膚科学会学術大会,さいたま、3 月 2014 年
34. 阪口雅弘, 津久井利広, 大隅尊史, 辻本元:犬のアトピー性皮膚炎のアレルゲンを用いた免疫療法について.第 10 回獣医内科アカデミー、横浜、2 月 2014 年
35. 印牧信行、川原井晋平、阪口雅弘：イヌのバイオバンクプロジェクトにおけるイヌ緑内障感受性遺伝子の研究.第１０回獣医臨床遺伝研究会、天童、12 月 2013 年
36. 野﨑淳夫、鈴木直也、成田泰章、白井秀治、阪口雅弘：市販マスクにおける空気汚染物質の除去特性について その 1 ガス状物質（アンモニア、VOC）. 2013 年度呼吸保護に関する研究発表会、東京、12 月 2013 年
37. 片川優子、堀口昌秀、舟場正幸、村上賢:BMP による Smad8 発現調節. 第 36 回日本分子生物学会年会、神戸、12 月 2013 年
38. 浅井久美子、舟場正幸、村上賢:TGF-β による RANKL 誘導性 Mitf-E の発現と破骨細胞分化への影響. 第 36 回日本分子生物学会年会、神戸、12 月 2013 年
39. Kawarai S, Fujimoto A, Nozawa G, Kanemaki N, Madarame H, Shida T, Kiuchi A:

Decreasing methicillin-resistant Staphylococcal colonization in allergic dog skin by shampoo.The Asian Meeting of Animal Medicine Specialties. Bogor,Indonesia, Dec, 2013.

40. 白井秀治、成田泰章、松本蘭世、柴田彰、野崎淳夫、阪口雅弘:マスク着用によるダニアレルゲン吸入予防効果の検討.第 63 回日本アレルギー学会秋季学術大会,東京、11 月 2013 年
41. 村上裕信、萩原恭二、鈴木健裕、堂前直、間陽子: プロテオミクス法により同定した新規 Vpr 結合因子 PRMT5/7 によるウイルス複製制御機構. 第 27 回日本エイズ学術集会、11 月 2013 年
42. 村上裕信、萩原恭二、鈴木健裕、堂前直、間陽子: 新規 Vpr 結合因子のプロテオミクス法による同定およびウイルス産生への影響. 第 61 回日本ウイルス学会学術集会、神戸、11 月 2013 年
43. 外池亜紀子、永澤美保、茂木一孝、菊水健史: 犬の社会認知に関わる遺伝子の探索. 新学術領域研究「共感性の進化神経基盤」 第 1 回 動物行動とオキシトシン研究会議、熱海、11 月 2013 年
44. Murata M, Murakami M.: Characterization of DNA markers isolated from the African penguin (Spheniscus demersus) by using RDA and MASA techniques., 6th Asian Meeting on Zoo and Wildlife Medicine/Conservation, Singapore, Oct, 2013.
45. 村上弘正、細川聖矢、川原井晋平、斑目広郎:減感作療法を実施した犬アトピー性皮膚炎の 2 例. 日本小動物獣医学会東北地区大会. 福島、10 月 2013 年
46. 島倉秀勝、岡山太郎、増田健一、津久井利広、藤村正人、阪口雅弘 : イヌの血清中アレルゲン特異的IgE 抗体量とアレルギー反応閾値濃度との比較.第 156 回日本獣医学会、岐阜、9 月 2013 年
47. 外池亜紀子、寺内豪、永澤美保、茂木一孝、菊水健史. イヌのヒトとのコミュニケーション能力の品種差, 関連遺伝子の探索. 日本動物心理学会第 73 回大会、筑波大学、9 月 2013 年
48. 片山真希、永澤美保、茂木一孝、菊水健史: 体位や情動の変化がイヌの心拍変動に及ぼす影響. 日本動物心理学会第 73 回大会、筑波大学、9 月 2013 年
49. 寺内豪、永澤美保、外池亜紀子、坂田日香理、茂木一孝、菊水健史: イヌのヒトとの視線コミュニケーションの犬種差. 日本動物心理学会第 73 回大会、筑波大学、9 月 2013 年
50. 小川美里、圓史緒理、永澤美保、茂木一孝、菊水健史、: オキシトシン投与によるヒトへの視線増強の日本犬種と洋犬種の比較. 日本動物心理学会第 73 回大会、筑波大学、9 月 2013 年
51. 渡辺征, 田中和明, 滝沢達也, 瀬川和仁, 根尾櫻子, 土屋亮, 村田倫子,村上賢, 久末正晴:イヌ腫瘍壊死因子(TNFA)遺伝子の第１イントロンに存在する 4 塩基反復マイクロサテライトの特徴. 第 156 回日本獣医学会、岐阜、9 月 2013 年
52. 柴田曜、永澤美保、茂木一孝、菊水健史: イヌにおけるストレス内分泌の発達特性と行動の関連. 日本行動神経内分泌研究会（JSBN）、鹿児島市レインボー桜島、7 月 2013 年
53. 阪口雅弘:実験動物アレルギーと環境因子.第 50 回日本実験動物環境研究会,東京,7 月 2013 年
54. 金森耀平、村上賢、松井徹、舟場正幸:肝細胞培養系とヘプシジン遺伝子発現. 第 30 回日本微量栄養素学会学術集会、京都、6 月 2013 年
55. Kanemaki N, Tchedre KT, Imayasu M, Meguro A, Mizuki N. Identification of S1 RNA binding domain-1 SRBD1 as a major gene determing glaucoma in dogs. ARVO Annual Meeting, Seattle, WA, USA, May, 2013.

56. 阪口雅弘: 犬のバイオバンクプロジェクト. 第 155 回日本獣医学会,東京,3 月 2013 年
57. Kikusui T, Mogi K, Nagasawa M: Sociobehavioral study of human-dog interactions: an approach from neuroendocrinology. IIAS Research Conference 2012 “Evolutionary Origins of Human Mind”, International Institute for Advanced Studies, Kyoto, Japan, December, 2012
58. Nagasawa M, En S, Mogi K, Kikusui T Reciprocal communication and neuroendocrine response in human-dog interaciotns. IIAS Research Conference 2012 “Evolutionary Origins of Human Mind”, International Institute for Advanced Studies, Kyoto, Japan, December, 2012
59. 菊水健史: 人と犬の共生進化 ― なぜ犬は人と共に生きるようになったのか. 第 33 回動物臨床医学会年次大会、大阪国際会議場、11 月 2012 年
60. 神崎美玲, 白井秀治, 皆川恵子 橋本知幸、阪口雅弘、眞壁郁, 飯島茂子:お好み焼き粉に繁殖したチリダニ類による即時型アレルギーの母子例. 第 62 回日本アレルギー学会秋季学術大会. 大阪,11 月 2012 年
61. 白井秀治、成田泰章、松本蘭世、柴田彰、野崎淳夫、阪口雅弘: マスク着用によるダニアレルゲン吸入予防効果の検討. 第 62 回日本アレルギー学会秋季学術大会. 大阪,11 月 2012 年
62. 島倉秀勝、周藤明美、増田健一、木内明男、阪口雅弘:乳酸菌を用いた食物アレルギーの新規治療法の開発 : イヌにおける疾患モデルとしての食物アレルギー犬の検討.第 87 回麻布獣医学会、相模原、11 月 2012 年
63. 岡本憲明、石丸浩靖、木内明男、藤村正人、阪口雅弘 : アトピー性皮膚炎犬における Malassezia pachydermatis の感作状況. 第 87 回麻布獣医学会、相模原、11 月 2012 年
64. 宮地一樹、木内明男、藤村正人、栗田吾郎、阪口雅弘 : 日本における犬混合ワクチン接種後副反応に関する大規模な疫学調査. 第 87 回麻布獣医学会、相模原、11 月 2012 年
65. 杉山和寿、小久保聖子、内田貴大、村上賢:Chaetomium globosum 及び Microsporum canis の PCR による鑑別診断の検討. 第 87 回麻布獣医学会、相模原、11 月 2012 年
66. 阪口雅弘:犬の疾患解析のための遺伝子バンク. 第 6 回家畜ＤＮＡ西郷シンポジューム,福島、10 月 2012 年
67. 寺内豪、永澤美保、外池亜紀子、坂田日香里、茂木一孝、菊水健史: イヌのヒトに対する社会的認知能力の犬種差. 日本哺乳類学会 2012 年度大会、相模原、9 月 2012 年
68. 阪口雅弘:帯電微粒子水「ナノイー」によるペットアレルゲン不活化の検討.日本臨床獣医学フォーラム、東京、9 月 2012 年
69. 堀本泰介、玄文宏、岩附研子、加藤健太郎、久末正晴、阪口雅弘、明石博臣、伊藤壽、河岡義裕、鈴木和男、前田健: わが国の哺乳動物におけるインフルエンザウイルス感染. 第 154 回日本獣医学会,岩手,9 月 2012 年
70. 原康弘、中岡優希、藤井祐輝、藤田雄大、山本未咲、宮崎陽子、田中和明、滝沢達也: イヌ脂肪組織由来間葉系幹細胞の神経分化に及ぼすヒストン脱アセチル化酵素阻害剤の影響. 第 154 回日本獣医学会学術集会, 岩手, 9 月 2012 年
71. 細川聖矢、川原井晋平、津久井利広、久末正晴、印牧信行、斑目広郎、土屋亮、小方宗次:国産コナヒョウヒダニ抗原液の有用性に関する再考. 第 154 回日本獣医学会学術集

会. 岩手、9 月 2012 年

72. 瀬川和仁, 藤本あゆみ, 加藤崇, 根尾櫻子, 久末正晴, 土屋亮:イヌの輸血用血小板製剤冷蔵保存の検討.第 154 回 日本獣医学会、岩手、9 月 2012 年
73. 藤本あゆみ, 石塚ちなつ, 浅野将人, 牧石恵利, 加藤崇, 瀬川和仁, 石川武史, 青木卓磨, 川原井晋平, 根尾櫻子, 久末正晴, 土屋亮:イヌ脂肪組織由来間質細胞から肝細胞様細胞への分化誘導と機能解析. 第 154 回日本獣医学会、岩手、9 月 2012 年
74. 根尾櫻子, 牧石恵利, 藤本あゆみ, 加藤崇, 鈴木大介, 代田欣二, 渡辺征, 久末 正晴, 土屋亮:イヌ骨髄細胞から分化誘導した肝様細胞の長期培養の試.第 154 回 日本獣医学会、岩手、9 月 2012 年
75. 加藤崇, 久末正晴, 瀬川和仁, 藤本あゆみ, 根尾櫻子, 小林亮介, 土屋亮:NOG マウスを利用したイヌ骨髄細胞の障害肝への Homing 作用の解析. 第 154 回 日本獣医学会、岩手、9 月 2012 年
76. Mogi K, Nagasawa M, Shibata Y, Morita T, Yonezawa A, Yabana Y, Kikusui T: The relationship between stress response of guide dogs and their temperament traits in peripubatal period. 3rd Canine Science Forum, Barcelona, Spain, July, 2012.
77. Nagasawa M, En S, Mogi K, Kikusui T: Reciprocal communication and neuroendocrine response in human-dog interactions. 3rd Canine Science Forum, Barcelona, Spain, July, 2012.
78. Tsuchihashi N, Kawai E, Nagasawa M, Mogi K, Kikusui T: Dogs show right facial lateralization to stressful stimuli. 3rd Canine Science Forum, Barcelona, Spain, July, 2012.
79. 永澤美保、圓史緒理、小川美里、茂木一孝、菊水健史: オキシトシン投与によるイヌの飼い主への注視行動の増強. 日本動物心理学大会第 72 回大会、関西学院大学、5 月 2012 年
80. 成本治, 松尾由紀子, 阿部和穂、阪口雅弘、長瀬隆英, 山下直美：好中球浸潤を伴う喘息モデルを用いた気道炎症の制御の解析.第５２回日本呼吸器学会, 神戸、4 月 2012 年
81. 飯野瑞貴、西本優子、藤本あゆみ、野澤源太、川原井晋平、信田卓男、木内明男: 犬のアレルギー性皮膚炎の症状維持におけるマイクロバブルを用いたシャンプー療法の有効性の検討. 日本動物看護学会関西地区第 5 回例会. 大阪、2012 年 3 月
82. 阪口雅弘 ：犬のバイオバンクプロジェクトの試み. 平成 23 年度日本獣医師会獣医学術学会,札幌、2 月 2012 年
83. Fujimura T, Yonekura S, Horiguchi S, Sakaguchi M, Taniguchi M, Okamoto Y. : Candidate for response monitoring or prognostic biomarkers in two-year sublingual immunotherapy for Japanese cedar pollinosis. 22th World Allergy Congress, Cancun, Mexico, Dec, 2011.
84. 原田晋、白井秀治、阪口雅弘：お好み焼き粉、タコ焼き粉に混入したダニによるアレルギー反応の発症機序に関する考察 第 61 回日本アレルギー学会総会、東京、11 月 2011 年.
85. 菊水健史: ペットの問題行動への取り組み「気質（性格）を理解して診察を開始する。～患畜の気質および問題行動の把握に有用な C-barq」. 第 32 回動物臨床医学会年次大会. グランキューブ大阪,11 月 2011 年
86. Nagasawa M, Kikusui T.: Reciprocal communication and endocrine response in human-dog interactions. Workshop on the Biology of Prosocial Behavior. Emory University. Oct, 2011

87. 河合絵美、永澤美保、茂木一孝、菊水健史: イヌの表情における情動表出の側性化．４学会合同大会「Animal 2011」．慶應義塾大学三田キャンパス. 9 月 2011 年
88. 24.寺内豪、永澤美保、坂田日香里、茂木一孝、菊水健史: イヌのヒトの社会的ジェスチャー理解の犬種差．４学会合同大会「Animal 2011」．慶應義塾大学三田キャンパス．9 月 2011 年
89. 永澤美保、菊水健史、茂木一孝、寺内豪、河合絵美: 物体選択課題における柴犬の特性.4学会合同大会「Animal 2011」．慶應義塾大学三田キャンパス. 9 月 2011 年
90. 菊水健史: ヒトと犬を絆ぐ —行動から見た 2 者の関係— 公開シンポジウム「犬を学ぶ、犬に学ぶ」．４学会合同大会「Animal 2011」．慶應義塾大学三田キャンパス. 9 月 2011 年
91. 松浦祐介、高橋亮二、川原井晋平、山口忠義、斑目広郎、代田欣二．犬における無菌性肉芽腫性皮膚炎の一例．関東・東京合同地区獣医師大会.神奈川、9 月 2011 年
92. 原康弘、中岡優希、藤井祐輝、藤田雄大、宮崎陽子、田中和明、滝沢達也 : イヌ脂肪組織由来間葉系幹細胞の細胞増殖および多分化能に及ぼすヒストン脱アセチル化酵素阻害剤の影響． 第 152 回日本獣医学会学術集会, 堺， 9 月 2011 年
93. 島倉秀勝、周藤明美、久保田翔太、宮地一樹、高瀬有加里、木内明男、阪口雅弘: 遺伝性が疑われる食物アレルギー犬における家系の調査． 第 152 回日本獣医学会、堺、9 月 2011 年
94. Tsukui T, Fukui M, Ohsumi T, Maeda S, Chimura N, Sakaguchi M, Tsujimoto, H. Immunotherapy using pullulan-conjugated recombinant house dust mite allergen (Der f 2-P). Asian Meeting of Animal Medicine Specialties, Bangkok, Thailand, May , 2011.
95. Kawarai S, Takahashi R, Madarame H, Shirota K. A case of granulomatous dermatitis in a dog. Asian Meeting of Animal Medicine Specialties. Bangkok , Thailand, May, 2011.
96. 成本治, 松尾由紀子, 阿部和穂, 白井秀治, 阪口雅弘, 長瀬隆英, 山下直美 : 喘息病態における気道上皮細胞の活性化と新規クルクミン誘導体による制御についての解析.第 51 回日本呼吸器学会、東京、4 月 2011 年

＜研究成果の公開状況＞（上記以外）

シンポジウム・学会等の実施状況、インターネットでの公開状況等
＜既に実施しているもの＞
本プロジェクトについては関連した学会・研究会での関連シンポジウム等での招待講演で本プロジェクの紹介や成果の発表を行ってきた（学会発表 50,60,76）。さらにホームページを作成し、本プロジェクトの内容や研究成果について公開してきた（http://www.azabu-u.ac.jp/sgk/02.html）。さらに収集状況については収集犬種等について公開する。
＜これから実施する予定のもの＞
本プロジェクトの成果のまとめとして来年度にこのプロジェクトに参加して研究者の成果を発表するシンポジウムを行う予定である。さらに本プロジェクトのホームページで、今後、収集された疾患リストについても公開する。さらに英文でのホームページも作成、海外への情報公開も行う予定である。これによって、海外との研究も幅広く行いたい。また、柴犬の全ゲノムシークエンスデータの公開を行う予定である。

14 その他の研究成果等

久末はカホテクノ社と、マイクロサテライト解析による犬の腫瘍診断へ応用を研究している
村上は株式会社牛越生理学研究所が動物用健康補助食品として製造・販売している R&U には Alopecia X に対して劇的な発毛育毛効果を示すことがあることが報告されている。当該企業と協力してその作用機序の解明を行っている。
齋藤は中央システム技研/セル・コーポレーションと、犬のてんかん発作探知システムのシステム開発を行っている。また、特許出願を行っている加速度を利用した犬のてんかん判別用アルゴリズムを用いて、スマートフォンなどへリアルタイムでてんかん発作の通知、映像でのモニタリングが可能なシステムの開発と臨床検証へ向けたシステム全体の調整を行っている。
村上賢は犬の肥満に関連する候補遺伝子の変異を調べた。マウスとヒトにおいて肥満と関連する遺伝子として、それぞれ Alk7(Avcvr1c)と ALK3(BMPR1A)の変異が報告されている。これらの遺伝子について、犬種による変異について検索した。イヌの Alk7 と Alk3 遺伝子のそれぞれについて、推定される変異部位を簡便に検出できる PCR―RFLP 法を考案し、51 犬種 161 個体と 40 犬種 93 個体について調べたが配列変異は認められなかった。

15 「選定時」及び「中間評価時」に付された留意事項とそれへの対応

＜「選定時」に付された留意事項＞
該当なし
＜「選定時」に付された留意事項への対応＞
該当なし
＜「中間評価時」に付された留意事項＞
該当なし
＜「中間評価時」に付された留意事項への対応＞
該当なし

法人番号	141001
プロジェクト番号	S1101023

16 施設・装置・設備・研究費の支出状況（実績概要）　（千円）

年度・区分		支出額	内訳						
			法人負担	私学助成	共同研究機関負担	受託研究等	寄付金	その他（　　）	備考
平成23年度	施設	0	0	0	0	0	0	0	
	装置	0	0	0	0	0	0	0	
	設備	5,460	1,820	3,640	0	0	0	0	
	研究費	24,520	12,521	11,999	0	0	0	0	
平成24年度	施設	0	0	0	0	0	0	0	
	装置	0	0	0	0	0	0	0	
	設備	5,880	1,960	3,920	0	0	0	0	
	研究費	24,120	13,143	10,977	0	0	0	0	
平成25年度	施設	0	0	0	0	0	0	0	
	装置	0	0	0	0	0	0	0	
	設備	5,200	1,734	3,466	0	0	0	0	
	研究費	24,800	14,706	10,094	0	0	0	0	
平成26年度	施設	0	0	0	0	0	0	0	
	装置	0	0	0	0	0	0	0	
	設備	0	0	0	0	0	0	0	
	研究費	29,999	15,429	14,570	0	0	0	0	
平成27年度	施設	0	0	0	0	0	0	0	
	装置	0	0	0	0	0	0	0	
	設備	0	0	0	0	0	0	0	
	研究費	30,000	15,269	14,731	0	0	0	0	
総額	施設	0	0	0	0	0	0	0	
	装置	0	0	0	0	0	0	0	
	設備	16,540	5,514	11,026	0	0	0	0	
	研究費	133,439	71,068	62,371	0	0	0	0	
総計		149,979	76,582	73,397	0	0	0	0	

※ 最終年度は予定額。

法人番号	141001

17 施設・装置・設備の整備状況 （私学助成を受けたものはすべて記載してください。）

《施　設》（私学助成を受けていないものも含め、使用している施設をすべて記載してください。）　（千円）

施設の名称	整備年度	研究施設面積	研究室等数	使用者数	事業経費	補助金額	補助主体
なし							

※ 私学助成による補助事業として行った新増築により、整備前と比較して増加した面積

㎡

《装置・設備》（私学助成を受けていないものは、主なもののみを記載してください。）　（千円）

装置・設備の名称	整備年度	型番	台数	稼働時間数/年	事業経費	補助金額	補助主体
（研究装置） なし							
（研究設備）							
冷却遠心機	H23	5430R	1台	1,000 h	620	0	
サーマルサイクラー(PCR用)	H23	TP-600	1台	260 h	523	0	
メディカル冷蔵庫	H23	MPR-514	1台	8,760 h	499	0	
超低温フリーザー	H23	VT-208	1台	8,760 h	528	0	
蛍光・発光プレートリーダー一式	H23	BT-SMATBL パワースキャンMX	1台	156 h	5,460	3,640	私学助成 文部科学省
リアルタイムPCR装置一式	H24	7500-01	1台	1,053 h	5,880	3,920	私学助成 文部科学省
蛍光顕微鏡装置一式	H25	IX83P1-24FL/PH	1台	180 h	5,200	3,466	私学助成 文部科学省
タンパク質転写装置	H26	1704150J1	1台	300 h	249	0	
（情報処理関係設備） なし							

法人番号	141001

18 研究費の支出状況

（千円）

年度	平成 23 年度			
小科目	支出額	積算内訳		
		主な使途	金額	主な内容
教育研究経費支出				
消耗品費	14,081	試薬・実験器具	14,081	カスタムプライマー、注射針、メスシリンダー、遠沈管、薬包紙ほか
光熱水費	0		0	
通信運搬費	50	運送費	50	血液サンプル輸送費ほか
印刷製本費	128	論文投稿料	128	(社)日本獣医学会
旅費交通費	285	学会参加費用	256	米国Chest学会
			29	福島県獣医師会
報酬・委託料	2,803	解析料・英文校正料	2,503	DNAシークエンス解析、イヌサイトカイン測定，英文校正料
		報酬料	300	血液サンプル採集
その他	114	その他	114	学会参加費、大判プリンター使用料
計	17,461			
アルバイト関係支出				
人件費支出（兼務職員）	2,277	研究補助・データ整理	2,277	時給 1,300円，年間時間数 1,752時間 実人数 2人
教育研究経費支出	0		0	
計	2,277			
設備関係支出（1個又は1組の価格が500万円未満のもの）				
教育研究用機器備品	4,782	備品	4,782	BioLogic Coreシステム、フリーズ超低温槽ほか
図書	0		0	
計	4,782			
研究スタッフ関係支出				
リサーチ・アシスタント	0		0	
ポスト・ドクター	0		0	
研究支援推進経費	0		0	
計	0			

（千円）

年度	平成 24 年度			
小科目	支出額	積算内訳		
		主な使途	金額	主な内容
教育研究経費支出				
消耗品費	12,004	試薬・実験器具	12,004	DNA全血セット，マイクロチューブ，ペプチド合成ほか
光熱水費	0		0	
通信運搬費	9	運送費	9	宅配便
印刷製本費	515	印刷製本費	515	バイオバンクリーフレット作成費
旅費交通費	28	旅費	28	シェルター保護動物サンプリング（福島）
報酬・委託料	800	解析料	697	DNAシークエンス解析
		英文校正料	103	英文校閲
その他	204	修繕費	158	リアルタイムPCR装置修理，ピペットマン修理
		その他	46	学会参加費、高速道路通行料、駐車場代
計	13,560			
アルバイト関係支出				
人件費支出（兼務職員）	9,135	研究補助・データ整理	9,135	時給 1,300円，年間時間数 7,027時間 実人数 4人
教育研究経費支出	0		0	
計	9,135			
設備関係支出（1個又は1組の価格が500万円未満のもの）				
教育研究用機器備品	1,399	備品	1,399	全自動電気泳動ステーション
図書	26	図書	26	洋書ほか
計	1,425			
研究スタッフ関係支出				
リサーチ・アシスタント	0		0	
ポスト・ドクター	0		0	
研究支援推進経費	0		0	
計	0			

法人番号	141001

（千円）

年　　度	平成　　25　　年度			
小 科 目	支 出 額	積　算　内　訳		
		主 な 使 途	金　額	主　な　内　容
		教　育　研　究　経　費　支　出		
消 耗 品 費	17,232	試薬・実験器具	17,232	DNA合成，試薬，プラスチック製品，ドックフードほか
光 熱 水 費	0		0	
通信運搬費	10	運送費	10	宅配便，振込手数料
印刷製本費	0		0	
旅費交通費	0		0	
報酬・委託料	1,994	解析料・英文校正料	1,070	DNAシークエンス解析，英文校閲
		バイオバンクHP開設	924	バイオバンクHP開設委託費
その他	108	その他	108	学会参加費
計	19,344			
		ア　ル　バ　イ　ト　関　係　支　出		
人件費支出（兼務職員）	4,878	研究補助・データ整理	4,878	時給　1,300円，年間時間数　3,752時間 実人数　2人
教育研究経費支出	0		0	
計	4,878			
		設 備 関 係 支 出（1個又は1組の価格が500万円未満のもの）		
教育研究用機器備品	537	備品	537	ﾌﾟﾗｲﾐﾝｸﾞｽﾃｰｼｮﾝ，生物顕微鏡ほか
図　　書	41	図書	41	洋書
計	578			
		研　究　ス　タ　ッ　フ　関　係　支　出		
ﾘｻｰﾁ・ｱｼｽﾀﾝﾄ	0		0	
ポスト・ドクター	0		0	
研究支援推進経費	0		0	
計	0			

（千円）

年　　度	平成　　26　　年度			
小 科 目	支 出 額	積　算　内　訳		
		主 な 使 途	金　額	主　な　内　容
		教　育　研　究　経　費　支　出		
消 耗 品 費	20,336	試薬・実験器具	20,336	DNA合成，試薬，プラスチック製品，ドックフードほか
光 熱 水 費	0		0	
通信運搬費	75	運送費	75	宅配便
印刷製本費	0		0	
旅費交通費	865	旅費	865	外部評価委員旅費，サンプル収集のため
報酬・委託料	2,056	報酬料	699	血清採取，データ整理
		解析料・英文校正料	1,357	DNAシークエンス解析，英文校閲，ﾊﾞｲｵﾊﾞﾝｸｻｰﾊﾞｰ管理委託費
その他	60	賃借料	60	施設利用料
計	23,392			
		ア　ル　バ　イ　ト　関　係　支　出		
人件費支出（兼務職員）	4,987	研究補助・データ整理	4,987	時給　870～1,300円，年間時間数　3,844時間 実人数　3人
教育研究経費支出	0		0	
計	4,987			
		設 備 関 係 支 出（1個又は1組の価格が500万円未満のもの）		
教育研究用機器備品	1,603	備品	1,603	ﾊﾞｲｵﾒﾃﾞｨｶﾙﾌﾘｰｻﾞｰ，ﾊﾞｲｵﾏﾙﾁｸｰﾗｰほか
図　　書	18	図書	18	脳と神経の見方ほか
計	1,621			
		研　究　ス　タ　ッ　フ　関　係　支　出		
ﾘｻｰﾁ・ｱｼｽﾀﾝﾄ	0		0	
ポスト・ドクター	0		0	
研究支援推進経費	0		0	
計	0			

法人番号	141001

（千円）

年　度	平成　27　年度			
小科目	支出額	積算内訳		
		主な使途	金額	主な内容
教育研究経費支出				
消耗品費	16,780	試薬・実験器具	16,780	ｶｽﾀﾑﾌﾟﾗｲﾏｰ，試薬，プラスチック製品，ﾍﾟｯﾄｼｰﾂほか
光熱水費	0		0	
通信運搬費	126	運送費	126	宅配便
印刷製本費	184	論文投稿料	184	オープンアクセス出版掲載料
旅費交通費	867	旅費	865	サンプル収集のため，学会参加
報酬・委託料	4,231	報酬料	1,147	血清採取，データ整理
		解析料・英文校正料	3,084	DNAシークエンス解析，英文校閲
その他	99	その他	99	学会参加費，賃借料ほか
計	22,287			
アルバイト関係支出				
人件費支出（兼務職員）	6,478	研究補助・データ整理	6,478	時給　890～1,350円，年間時間数　4,999時間 実人数　14人
教育研究経費支出	0		0	
計	6,478			
設備関係支出（1個又は1組の価格が500万円未満のもの）				
教育研究用機器備品	1,134	備品	1,134	CO2ｲﾝｷｭﾍﾞｰﾀｰ，薬用冷蔵ｼｮｰｹｰｽほか
図書	101	図書	101	洋書
計	1,235			
研究スタッフ関係支出				
リサーチ・アシスタント	0		0	
ポスト・ドクター	0		0	
研究支援推進経費	0		0	
計	0			

犬の遺伝性疾患における DNA 収集・精製・供給および疾患情報のデータベース化

阪口雅弘、岡本憲明、島倉秀勝（麻布大学微生物学第１）印牧信行（麻布大学附属動物病院）村上賢（麻布大学分子生物)、菊水健史（麻布大学伴侶動物)、久末正晴（麻布大学内科第２)、齋藤弥代子（麻布大学外科第２)、滝沢達也、田中和明（麻布大学動物工学)

研究要旨

遺伝病や遺伝関連疾患を含む非感染性疾患犬および一般集団犬から DNA 収集を行い 15865 検体が収集され、それぞれの犬はその基本情報とともに疾患情報も日本獣医学会疾患名用語集に部類に基づいてデータベース化された。これらの収集された DNA 検体はこのプロジェクトの研究者に提供して各課題において遺伝子解析を行った。また、このプロジェクト以外の研究者へ DNA を供給し、様々な共同研究を行った。獣医大学病院での多くの症例検体では血清(血漿)も併せて保存した。血清は遺伝疾患をはじめ、他の様々な疾患の発生機序の解析や感染症における血清疫学などを研究するときに非常に役立つ材料であると考えられる。今後も DNA 収集は継続して行い、この遺伝子バンクは獣医学の臨床研究の発展に大いに寄与すると考えられる。

研究目的

犬も人と同様に多くの遺伝性疾患があり、人と病態が似ている疾患も多く存在する。本研究において犬の遺伝子(DNA)資源の活用と保存のために、獣医系大学附属動物病院等の臨床医を中心に様々な遺伝関連疾患を含む非感染性疾患犬や一般集団としての犬などから DNA 収集を行う。収集された DNA はその犬の疾患情報とともにデータベース化して犬の遺伝関連疾患における原因遺伝子の解析やその他の犬の遺伝子を利用した研究を行うことを本研究の目的とする。

材料と方法

麻布大学、東京大学、東京農工大学、鹿児島大学、日本大学などの所属の獣医師や遺伝病研究者などから遺伝関連疾患を含む非感染性疾患犬および一般集団犬から DNA を収集した。収集された疾患は、明らかな遺伝疾患から何らかの遺伝的な要因が関与する可能性があるも疾患まで幅広く収集した。獣医大学病院では収集困難な疾患においては一般獣医病院から DNA を収集した。その犬の基本情報および疾患情報は麻布大学においてデータベース化された。また、一部の検体においては血漿または血清も-80C に保存された。それぞれの疾患は日本獣医学会の疾患名用語集に基づいて分類した。

結果および考察

遺伝関連疾患を含む非感染性疾患犬および一般集団犬から DNA 収集を行い、１万 5865 検

体が収集された。犬種は 130 種以上で上位３犬種はウェルシュ・コーギー・ペンブローブ 2236 例、ダックス 1827 例、プードル 1567 例であった（表１）。オス・メスの比率は 49.8%：50.2%で、平均年令は８年であった。

疾患症例は日本獣医学会の疾患名用語集の大分類に基づいて大きく分けた（表２）。白内障をはじめとする眼疾患、てんかんをはじめとする神経疾患、アレルギー疾患をはじめとする免疫疾患など非感染性疾患 7628 症例が収集された。それぞれの疾患内訳については表 3 から表 17 までに示した。現在、最終的な診断が決定していない症例や疾患情報がまだ来ていないものが多数あり、今後、疾患情報を追加していく。一般開業の獣医師の場合、疾患診断基準や能力にバラツキがあるため、症例検体に関しては獣医大学の教員を中心に診療・診断して採取した。しかし、アレルギー疾患であるアトピー性皮膚炎に関してはアレルギー治療法の進歩で獣医大学病院に来院する疾患犬が非常に少なくなったため、本プロジェクトでは個人病院の開業獣医師でアトピー性皮膚炎を専門する皮膚科専門医に依頼して国際的な診断基準の基に検体を採取した。

疾患症例が集められ、疾患遺伝子を解析するときに、陰性対象となる一般集団からの採取した犬の DNA が必要となった。一般集団犬の DNA がないと疾患遺伝子解析が進まないため、本プロジェクトでは、一般集団からの犬の DNA 検体の採取も積極的に行うようになり、収集 DNA 検体数に一般集団犬の検体数も加えた。

収集された DNA 検体はこのプロジェクトの研究者に提供して遺伝関連疾患の遺伝子解析を行った。また、プロジェクト研究グループ外の他の研究者へ DNA を供給し、共同研究を行っている。科学警察研究所で行っている「マイクロサテライト多型解析を用いた犬の個体識別法の検討」に犬の DNA を提供した。これは犬の DNA は，傷害や血統書偽装など直接動物が関わる事件から，強盗や強姦などの現場に犯人に付着した動物毛が遺留される事件まで，多岐にわたって重要な証拠なるためである。また、(東京大学獣医学科坪井先生には「Whole Exome Sequence 法による犬の遺伝性神経疾患の原因遺伝子同定」の研究でパピヨン犬の神経軸索ジストロフィーの陰性対照のパピヨン犬の 56 検体の DNA を遺伝子バンクから提供した。遺伝疾患の研究者は症例から疾患遺伝子の収集を行うが、同じ犬種で陰性対照となるものの収集がない場合が多いので、このような遺伝子バンクの利用も今後、行っていく予定である。

獣医大学病院での多くの症例検体では血清(血漿)も併せて保存した。これは将来、遺伝関連疾患等疾患の原因遺伝子が明らかになった時にその遺伝病の原因となる機序を解析するときにこれらの血清は役立つ可能性があるために-80℃で保存を行っている。また、人では国立感染症研究所の血清バンクのように様々な集団の血清を保存するシステムがあるが、日本国内では犬の血清を多数保存するシステムがなかった。これは遺伝病をはじめ、他の様々な疾患の発生機序の解析や感染症における血清疫学などを研究するときに非常に役立つ材料であると考えられる。犬におけるインフルエンザ感染の血清疫学調査を行い、犬も人のインフルエンザの感染が起こっていることを明らかにした。

東京大学動物医療センターからは一般的な症例も含めて疾患症例のネコの DNA と血漿が収集を行っており、現在で 828 例がバイオバンクに集まっている。ネコの遺伝病の研究を行っている鹿児島大学の大和先生からも 3477 検体の DNA 情報の提供を受けている。ネコも多くの遺伝疾患が存在するが、解析に必要な検体数が不十分なため、これまで研究があまり進んでいなかった。また、一般的な疾患の研究も犬に比べ遅れている。そのため、東京大学や鹿児島大学の強い要望もあり、これらの DNA 検体を基にネコの遺伝子バンクも始める予定である。また、東京大学動物医療センターの検体については血漿も採取されており、今後、犬と同様に疾患の発症機序や感染症の血清疫学などのネコの疾患研究に幅広く使用できる可能性がある。

収集された検体情報はバイオバンクに登録し、疾患情報をデータベース化した。今後、収集された犬種や疾患に関しては研究グループ内外での情報の共有を行っていくとともに、上述したように研究グループ外の研究者が行う研究にも積極的に協力を行う。

表１　遺伝子バンクに収集された犬種

犬種	頭数
ウェルシュ・コーギー・ペンブローク	２２３６
ミニチュアダックス	１８２７
トイプードル	１５６７
柴犬	１１７２
ボーダー・コリー	８９４
雑種	７５９
ラブラドール・レトリーバー	６９４
チワワ	６６３
シーズー	６３４
ビーグル	４１７
ヨークシャー・テリア	３５０
ゴールデン・レトリーバー	３１８
珍島	２９４
ポメラニアン	２８８
パピヨン	２５９
マルチーズ	２５７
コッカー・スパニエル	２４４
シェットランド・シープドッグ	２４０
フレンチ・ブルドッグ	２３３
ミニチュア・シュナウザー	２２０
キャバリア・キング・チャールズ・スパニエル	２０１
パグ	１７８
ジャック・ラッセル・テリア	１５１
ジャーマン・シェパード・ドッグ	１４５
ミニチュア・ピンシャー	８７
ハスキー	８５
ボストン・テリア	８５
オーストラリアン・ラブラドゥードル	８１
秋田	６９
ウエスト・ハイランド・ホワイト・テリア	６７
グレーハウンド	５９

サルーキ	５４
バーニーズ・マウンテン・ドッグ	５１
シベリアン・ハスキー	４６
コリー	４５
ペキニーズ	４０
北海道	３９
ワイヤー・フォックス・テリア	３９
グレート・ピレニーズ	３６
ビション・フリーゼ	３３
ポインター	３１
バセンジー	２８
フラットコーテッド・レトリーバー	２７
ボクサー	２７
甲斐	２６
スピッツ	２６
ブルドッグ	２４
ケアン・テリア	２３
チン	２３
ダルメシアン	２２
四国	２１
琉球	２０
ドーベルマン	１８
オールド・イングリッシュ・シープドック	１６
ノーフォーク・テリア	１５
グレート・デーン	１４
アイリッシュ・セッター	１３
アフガン・ハウンド	１３
イングリッシュ・スプリンガー・スパニエル	１２
スコティッシュ・テリア	１２
オオカミ	１２
ウィペット	１１
ウェルシュ・テリア	１１
エアデール・テリア	１１
サモエド	１１

ブリタニー・スパニエル	１１
ブルテリア	１１
ボルゾイ	１１
ロットワイラー	１１
セント・バーナード	9
チャウチャウ	9
イングリッシュ・セッター	8
チャイニーズ・クレステッド・ドック	8
チャールズ・スパニエル	8
トイ・マンチェスター・テリア	8
ボロニーズ	8
紀州	7
ニューファンドランド	7
ジャイアント・シュナウザー	5
バセット・ハウンド	5
ベルジアン・シェパード・ドック・タービュレン	5
その他	１１０

その他：４頭以下のものはその他としてまとめた。

表２　遺伝子バンクにおける疾患（大分類）分類

分類	頭数
眼科疾患	３０９０
神経疾患	８６５
消化器疾患	６５２
皮膚疾患	６０６
肝臓・胆道・膵外分泌疾患	５００
血液・免疫系疾患	３２９
泌尿器疾患	２８７
内分泌・代謝性疾患	２５０
循環器疾患	２４８
生殖器・乳房疾患	２２８
骨関節疾患	２１７
呼吸器疾患	１９９
口腔内疾患	１０９
筋疾患	３３
行動疾患	１５
計	７６２８

表３　循環器疾患における疾患分類

分類	頭数
僧帽弁膜疾患	６９
血管肉腫	２５
僧房弁閉鎖不全	１９
三尖弁閉鎖不全	１７
肺高血圧症	１５
三尖弁逆流	１０
動脈管開存	6
リンパ管拡張	6
血栓塞栓症	5
大動脈弁逆流	3
心室中隔欠損	3
肺動脈弁狭窄	3
心臓タンポナーデ	3
海綿状血管腫	3
中皮腫	3
肥大型心筋症	2
大動脈弁閉鎖不全	2
細菌性心内膜炎	2
動静脈ろう	2
横紋筋肉腫	2
血管腫	2
リンパ管肉腫	2
腎性高血圧	2
右心不全	1
左心不全	1
心不全	1
上室頻拍	1
心室期外収縮	1
多源性心室期外収縮	1
洞停止	1
アミロイド症	1

拡張型心筋症	1
僧帽弁逆流	1
肺動脈弁逆流	1
後大静脈欠損	1
先天性心疾患	1
僧帽弁異形成	1
大動脈弁狭窄	1
大動脈弁下狭窄	1
大静脈症候群	1
心膜炎	1
心膜中皮腫	1
大動脈小体腫瘍	1
血栓症	1
静脈血栓症	1
肉芽腫性リンパ管炎	1
リンパ管腫	1
高血圧	1
その他	１７

その他：疾患名用語集にない疾患や分類が難しいものはその他にまとめた。

表４　口腔内疾患における疾患分類

分類	頭数
歯肉炎	１９
根尖周囲膿瘍	１５
歯周炎	１３
口腔内悪性黒色腫	7
唾液腺嚢胞	5
口腔鼻腔瘻	4
線維腫性エプーリス	3
唾液腺炎	3
エナメル上皮腫	3
口蓋裂	3
唾液粘液嚢胞	2
歯原性嚢胞	2
歯原性腫瘍	2
顎関節炎	1
エプーリス	1
骨形成性エプーリス	1
巨細胞性エプーリス	1
唾液腺腫瘍	1
含歯性嚢胞	1
エナメル上皮線維肉腫	1
線維肉腫	1
その他	２０

表５　呼吸器疾患における疾患分類

分類	頭数
鼻腔内腫瘍	３１
気管虚脱	３１
肺腫瘍	１３
慢性鼻炎	１２
気管支炎	１１
軟口蓋過長症	6
誤嚥性肺炎	6
喉頭麻痺	5
腺癌	5
短頭種気道症候群	4
間質性肺炎	4
鼻腔内異物	3
胸水貯留	3
乳糜胸	3
横隔膜ヘルニア	3
気管支肺炎	3
肺血栓塞栓症	2
喉頭炎	1
喉頭腫瘍	1
気管腫瘍	1
無気肺	1
肺水腫	1
気管支腫瘍	1
肺葉捻転	1
気胸	1
漏斗胸	1
気管支拡張症	1
その他	４４

表６　消化器疾患における疾患分類

分類	頭数
食物アレルギー	１２１
蛋白喪失性腸症	９９
消化器型リンパ腫	６１
慢性腸炎	４３
炎症性腸疾患	３４
慢性胃炎	２３
炎症性結直腸ポリープ	２３
腸リンパ管拡張症	２２
会陰ヘルニア	２２
腸腺癌	１４
鼠径ヘルニア	１２
縫合糸関連肉芽腫	１２
巨大食道症	１０
リンパ球形質細胞性腸炎	8
抗菌剤反応性腸症	8
特発性巨大食道症	7
胃炎	6
ポリープ	6
肉芽腫性腸炎	5
胃腺癌	4
咽頭麻痺	3
結腸炎	3
平滑筋腫	3
平滑筋肉腫	3
食道炎	2
逆流性食道炎	2
食道狭窄	2
食道腫瘍	2
萎縮性胃炎	2
胃排出遅延	2
胃腫瘍	2

カルチノイド腫瘍	2
十二指腸炎	2
カタル性腸炎	2
好酸球性腸炎	2
慢性結腸炎	2
腸閉塞	2
消化管間質腫瘍	2
臍ヘルニア	2
肛門嚢炎	2
肛門周囲瘻	2
腸穿孔	2
咽頭炎	1
食道憩室	1
胆汁嘔吐症候群	1
肉芽腫性胃炎	1
幽門狭窄	1
胃拡張	1
胃拡張捻転症候群	1
好酸球性結腸炎	1
組織球性潰瘍性結腸炎	1
小腸内細菌過剰増殖	1
過敏性腸症候群	1
消化器型肥満細胞腫	1
直腸閉塞	1
直腸脱	1
腹壁ヘルニア	1
腺癌	1
その他	４９

表７　肝臓・胆道・膵外分泌疾患における疾患分類

分類	のべ頭数
膵炎	７５
門脈体循環シャント	５４
肝炎	３５
原発性門脈低形成	３３
胆管炎	２８
胆嚢粘液嚢腫	２４
肝結節性過形成	２３
胆石症	１９
肝細胞腺腫	１８
肝細胞癌	１７
胆嚢炎	１５
空胞性肝障害	１３
肝微小血管異形成	１１
ステロイド誘発性肝症	8
門脈高血圧症	7
膵外分泌不全症	7
中毒性肝傷害	6
肝嚢胞	5
肝外胆管閉塞	4
肝不全	3
肝膿瘍	3
肝硬変	3
肝性脳症	3
肝線維症	2
急性胆嚢炎	2
胆管癌	2
門脈低形成	2
肝カルチノイド	1
膵臓癌	1
膵嚢胞	1
その他	７５

表８　泌尿器疾患における疾患分類

分類	のべ頭数
尿石症	５７
膀胱炎	４８
慢性腎臓病	４５
膀胱移行上皮癌	２４
腎結石症	１７
腎細胞癌	5
水腎症	5
急性腎不全	5
ネフローゼ症候群	4
糸球体腎症	4
腎不全	4
多発性嚢胞腎	3
腎芽腫	3
慢性腎不全	3
腎周囲偽嚢胞	2
異所性尿管	2
シスチン尿症	2
糸球体腎炎	1
腎異形成	1
腎盂腎炎	1
急性腎障害	1
尿管結石症	1
尿道炎	1
尿路閉塞症	1
上位運動ニューロン性排尿障害	1
下部運動ニューロン性排尿障害	1
ホルモン反応性尿失禁	1
腺癌	1
腎梗塞	1
その他	４１

表９　内分泌・代謝性疾患における疾患分類

分類	頭数
糖尿病	４０
クッシング病	３０
甲状腺癌	２５
下垂体性副腎皮質機能亢進症	２３
アジソン病	２１
甲状腺機能低下症	１７
高脂血症	１５
副腎腫瘍	１３
上皮小体機能亢進症	8
下垂体性クッシング症候群	7
インスリノーマ	6
高カルシウム血症	3
上皮小体腺腫	3
低血糖症	3
下垂体腫瘍	2
下垂体巨大腺腫	2
副腎腺癌	2
副腎皮質機能低下症	2
悪性高カルシウム血症	1
低リン血症	1
下垂体腺腫	1
ラトケ嚢胞	1
尿崩症	1
抗利尿ホルモン不適合分泌症候群	1
甲状腺機能亢進症	1
原発性甲状腺機能低下症	1
続発性上皮小体機能亢進症	1
高血糖	1
その他	１８

表１０　神経疾患における疾患分類

分類	頭数
てんかん	２２２
椎間板ヘルニア	９１
変性性脊髄症	７０
脊髄空洞症	３９
水頭症	３２
変形性脊椎症	１５
中耳炎	１５
髄膜腫	１４
椎間板疾患	１４
尾側後頭部奇形症候群	１３
肉芽腫性髄膜脳脊髄炎	１３
馬尾症候群	１３
壊死性白質脳炎	１２
顔面神経麻痺	１２
ＧＭ１ガングリオシドーシス	１１
環椎軸椎不安定症	１１
前庭障害	１１
壊死性髄膜脳炎	１０
ホルネル症候群	9
悪性末梢神経鞘腫	8
全身性振戦症候群	7
認知機能不全症候群	6
脳梗塞	5
難聴	5
キアリ様奇形	4
Ｈａｎｓｅｎ　Ｉ型ＩＶＤＤ	4
椎間板脊椎炎	4
脊髄梗塞	4
四丘体嚢胞	3
壊死性髄膜脳炎	3
脳出血	3

先天性水頭症	2
頭蓋内くも膜嚢胞	2
神経鞘腫	2
ステロイド反応性髄膜炎ー動脈炎	2
ミオクロニーてんかん	2
ラフォラ病	2
ナルコレプシー	2
尾側頚椎脊髄症	2
進行性脊髄軟化症	2
特発性三叉神経麻痺	2
ライソゾーム蓄積病	1
孔脳症	1
神経膠腫	1
部分発作	1
ミオクローヌス	1
頭部外傷	1
脳浮腫	1
脳動静脈奇形	1
Ｈａｎｓｅｎ　ＩＩ型ＩＶＤＤ	1
脊椎腫瘍	1
線維軟骨塞栓症	1
内耳炎	1
その他	１５０

表１１　筋疾患における疾患分類

分類	頭数
重症筋無力症	9
多発性筋炎	5
咀嚼筋炎	3
副腎皮質機能亢進症性筋症	1
筋緊張症	1
その他	１４

表１２　骨関節疾患における疾患分類

分類	頭数
関節炎	６０
レッグ・ペルテス病	２２
股異形成	１７
骨肉腫	１６
組織球肉腫	１６
汎骨炎	9
関節リウマチ	8
変形性関節症	5
滑膜細胞肉腫	4
骨炎	3
前十字靭帯部分断裂	3
関節症	3
免疫介在性関節疾患	3
肘関節形成異常	3
成長板早期閉鎖	2
内側上顆癒合不全	2
軟骨肉腫	2
骨形成不全症	2
変形癒合	1
骨髄炎	1
骨腫	1
多葉状骨軟骨肉腫	1
骨軟骨腫	1
その他	３２

表１３　血液・免疫系疾患における疾患分類

分類	頭数
リンパ腫	１００
免疫介在性血小板減少症	４７
骨髄異形成症候群	４６
免疫介在性溶血性貧血	４２
播種性血管内凝固	8
骨髄線維症	8
再生不良性貧血	6
血友病	6
真性赤血球増加症	5
全身性エリテマトーデス	5
鉄欠乏性貧血	4
赤芽球癆	4
白血病	4
慢性リンパ性白血病	4
多発性骨髄腫	4
慢性疾患に伴う貧血	3
ハインツ小体性溶血性貧血	2
フォンヴィレブランド病	2
溶血性輸血反応	1
タマネギ中毒	1
大動脈血栓塞栓症	1
骨髄壊死	1
本態性血小板血症	1
血小板無力症	1
免疫介在性好中球減少症	1
非再生性貧血	1
慢性骨髄性白血病	1
その他	２０

表１４　皮膚疾患における疾患分類

分類	のべ頭数
アトピー性皮膚炎	２１４
肥満細胞腫	８４
悪性黒色腫	８３
扁平上皮癌	２１
血管周皮腫	１９
脂肪腫症	１７
特発性無菌性結節性脂肪織炎	１６
医原性クッシング症候群	１４
肛門周囲腺腫	5
耳垢腺癌	5
皮膚形質細胞腫	5
肥満細胞腫瘍	5
皮膚石灰沈着症	4
脱毛症Ｘ	4
肛門周囲腺癌	4
皮膚肥満細胞症	4
犬皮膚組織球腫	3
脂腺腫	3
脂腺上皮腫	3
多形紅斑	2
表皮過誤腫	2
落葉状天疱瘡	2
脂腺癌	2
表皮向性リンパ腫	2
毛芽腫	2
毛包上皮腫	2
アレルギー性接触皮膚炎	1
アポクリン嚢腫	1
淡色被毛脱毛症	1
間擦疹	1
狂犬病ワクチン接種後脂肪織炎	1

クリオフィブリノーゲン血症	1
脂腺炎	1
尋常性天疱瘡	1
蕁麻疹	1
パターン脱毛症	1
鼻趾角化症	1
ビタミンA反応性皮膚症	1
表在性壊死性皮膚炎	1
表皮嚢胞	1
類表皮嚢腫	1
皮膚血管炎	1
リンパ腫症	1
リンパ腫様肉芽腫症	1
その他	61

表１５　眼科疾患における疾患分類

分類	頭数
白内障	７６３
網膜変性	２５３
ブドウ膜炎	２３７
緑内障	２２１
角膜炎	１５２
水晶体脱臼	１１７
網膜剥離	１１１
虹彩萎縮	８６
角膜ジストロフィー	６３
角結膜炎	５９
硝子体ヘルニア	３８
デスメ瘤	３２
瞳孔膜遺残	２８
眼瞼内反	２６
脈絡網膜炎	２６
角膜潰瘍	２２
前房出血	２１
結膜炎	１９
網膜萎縮	１９
虹彩癒着	１８
核硬化症	１７
角膜穿孔	１６
眼球癆	１６
虹彩後癒着	１６
角膜分離症	１４
乾性角結膜炎	１４
強膜炎	１４
硝子体混濁	１３
視神経炎	１２
網膜症	１１
虹彩炎	１０

星状硝子体症	１０
角膜変性	9
流涙症	9
異所性睫毛	8
角膜浮腫	8
眼瞼下垂	8
眼内出血	8
眼球突出	7
視神経乳頭低形成	7
網膜炎	7
角膜内皮ジストロフィー	6
虹彩異色症	6
上強膜炎	6
睫毛重生	6
睫毛乱生	6
アレルギー性結膜炎	5
結晶性実質性ジストロフィー	5
斜視	5
硝子体炎	5
突発性後天性網膜変性	5
小眼球	4
硝子体出血	4
水晶体偏位	4
瞬膜突出	3
眼瞼欠損	2
虹彩前癒着	2
虹彩嚢腫	2
コリー眼異常	2
色素性角膜炎	2
第三眼瞼腺脱出	2
ぶどう膜皮膚症候群	2
輪部黒色腫	2
類皮腫	2
角膜壊死	1

眼振	1
牛眼	1
球後膿瘍	1
結節性上強膜炎	1
虹彩血管新生	1
虹彩色素沈着	1
好酸球性筋炎	1
視神経萎縮	1
小眼瞼裂	1
硝子体動脈遺残	1
錐体変性	1
色素性ぶどう膜炎	1
第一次硝子体過形成遺残	1
パンヌス	1
表在性点状角膜炎	1
無孔涙点	1
無水晶体眼	1
網膜異形成	1
網膜色素上皮ジストロフィー	1
融解性角膜潰瘍	1
涙小管閉塞	1
涙嚢炎	1
その他	４３４

表１６　生殖器・乳房疾患における疾患分類

分類	のべ頭数
乳腺腫瘍	６５
乳腺癌	２５
前立腺肥大症	１９
前立腺癌	１２
潜在精巣	１１
子宮水症	１１
前立腺嚢胞	9
前立腺炎	6
前立線膿瘍	5
子宮平滑筋腫	5
卵胞嚢腫	5
セルトリ細胞腫	4
乳腺炎	4
前立腺腫瘍	3
黄体遺残	3
精巣炎	2
精上皮腫	2
複合型乳腺腫	2
乳腺腺腫	2
傍前立腺嚢胞	1
卵巣網嚢胞	1
偽妊娠	1
その他	３０

表１７　行動疾患における疾患分類

分類	頭数
所有性攻撃行動	3
恐怖性攻撃行動	2
分離不安	2
肢端舐性皮膚炎	1
尾追い行動	1
その他	6

研究発表

１．論文発表

1) Miyaji K, Okamoto N, Saito S, Yasueda H, Takase Y, Shimakura H, Saito S, Sakaguchi M.: Cross-reactivity between major IgE core epitopes on Cry j 2 allergen of Japanese cedar pollen and relevant sequences on Cha o 2 allergen of Japanese cypress pollen. Allergol Int in press.

2) Shigehisa R, Uchiyama J, Kato S, Takemura-Uchiyama I, Yamaguchi K, Miyata R, Ujihara T, Sakaguchi Y, Okamoto N, Shimakura H, Daibata M, Sakaguchi M, Matsuzaki S.: Characterization of Pseudomonas aeruginosa phage KPP21 belonging to family Podoviridae genus N4-like viruses isolated in Japan. Microbiol Immunol in press.

3) Takai T, Okamoto Y, Okubo K, Nagata M, Sakaguchi M, Fukutomi Y, Saito A, Yasueda H, Masuyama K.: Japanese Society of Allergology task force report on standardization of house dust mite allergen vaccines. Allergol Int 64,181-186, 2015

4) Horimoto T, Gen F, Murakami S, Iwatsuki-Horimoto K, Kato K, Hisasue M, Sakaguchi M, Nidom CA, Kawaoka Y.: Cats as a potential source of emerging influenza virus infections. Virologica Sinica 30,221-223, 2015

5) Horimoto T, Gen F, Murakami S, Iwatsuki-Horimoto K, Kato K, Akashi H, Hisasue M, Sakaguchi M, Kawaoka Y, Maeda K.: Serological evidence of infection of dogs with human influenza viruses in Japan. Vet Rec 174, 96, 2014

6) 高井敏朗, 岡本美孝, 大久保公裕, 永田真, 阪口雅弘, 福冨友馬, 齋藤明美, 安枝浩, 増山敬祐:ダニアレルゲンワクチン標準化に関する日本アレルギー学会タスクフォース報告.アレルギー 63,1229-1240,2014.

7) 阪口雅弘:アレルギーに対する免疫療法：減感作療法と新しい免疫療法の開発. J-Vet 27, 8-14, 2014

8) Kanemaki N, Tchedre KT, Imayasu M, Kawarai S, Sakaguchi M, Yoshino A, Itoh N, Meguro A, Mizuki N. Dogs and humans share a common susceptibility gene SRBD1 for glaucoma risk. PLoS One 8, e74372, 2013.

9) Miyaji K, Yurimoto T, Saito A, Yasueda H, Takase Y, Shimakura H, Okamoto N, Kiuchi A, Saito S, Sakaguchi M.: Analysis of conformational and sequential IgE epitopes on the major allergen Cry j 2 of Japanese cedar pollen in humans by using monoclonal antibodies for Cry j 2. J Clin Immunol 33, 977-983, 2013.

10) 原田晋, 白井秀治, 阪口雅弘： お好み焼き粉, タコ焼き粉に混入したダニによるアレルギーによる眼瞼血管性浮腫の１例. 皮膚臨床 55,1127-1133, 2013.

11) 藤村正人,阪口雅弘:犬のアトピー性皮膚炎に対する 8 日間プロトコールを用いた急速

減感作療法の安全性. 獣医アトピー・アレルギー・免疫学会誌 2,14-18,2013.
12) 白井秀治、阪口雅弘：室内環境アレルゲンの評価.アレルギーの臨床 33,51-56, 2013.
13) Kubota S, Miyaji K, Shimo Y, Shimakura H, Takase Y, Okamoto N, Kiuchi A., Fujimura M., Fujimura T, DeBoer J D, Tsukui T, Sakaguchi M: IgE reactivity to a Cry j 3, an allergen of Japanese cedar pollen in dogs with canine atopic dermatitis. Vet Immunol Immunopathol 149:132-135, 2012.
14) Kawakami M, Narumoto O, Mastuo Y, Horiguchi K, Yamashita N, Sakaguchi M, Lipp M, Nagase T, Yamashita N: The role of CCR 7 in allergic airway inflammation induced by house dust mite exposure. Cell Immunol 275:24-32, 2012.
15) Narumoto O, Matsuo Y, Sakaguchi M, Shoji S, Yamashita N, Shubert D, Abe K, Horiguchi K, Yamashita N: Suppressive effects of a pyrazole derivative of curcumin on airway inflammation and remodeling. Exp Mol Pathol 93, 18-25, 2012.
16) Miyaji K, Suzuki A, Shimakura H, Takase Y, Kiuchi A, Fujimura M, Kurita G, Tsujimoto H, Sakaguchi M: Large-scale survey of adverse reactions to canine non-rabies combined vaccines in Japan. Vet Immunol Immunopathol 145: 447-452, 2012
17) Tsukui T, Sakaguchi M, Kurata K, Maeda S, Ohmori K, Masuda K, Tsujimoto H, Iwabuchi S: Measurement for canine IgE using canine recombinant high affinity IgE receptor α chain (FcεRIα). J Vet Med Sci 74, 851-856, 2012
18) Kaburaki Y, Fujimura T, Kurata K, Matsuda K, Toda M, Yasueda H, Chida K, Kawarai S, Sakaguchi M: Induction of Th1 immune responses to Japanese cedar pollen allergen in mice immunized with Cry j 1 conjugated with CpG oligodeoxynucleotide. Comp Immunol Microbiol Infect Dis 34,157-161, 2011
19) Fujimura T, Yonekura S, Horiguchi S, TaniguchiY , Saito A, Yasueda H, Inamine A, Nakayama T, Takemori T, Taniguchi M, Sakaguchi M, Okamoto Y.: Increase of regulatory T cells and the ratio of specific IgE to total IgE are potential therapeutic or prognostic biomarkers in two-year sublingual immunotherapy for Japanese cedar pollinosis. Clin Immunol 139,65-74, 2011.
20) Kawarai S, Sato K, Horiguchi A, Kurata K, Kiuchi A, Tsujimoto H, Sakaguchi M.: Potential immunological adjuvant of 'K'-type CpG- oligodeoxynucleotides enhanced the cell proliferation and IL-6 mRNA expression in canine B cells. J Vet Med Sci 73, 177-184, 2011.
21) Okayama T, Matsuno Y, Yasuda N, Tsukui T, Suzuta Y, Koyanagi M, Sakaguchi M, Tsujimoto H, Ishii Y, Olivry T, Masuda K.: Establishment of a quantitative ELISA for the measurement of an allergen-specific IgE in dogs using anti-IgE antibody cross-reactive to mouse and dog IgE. Vet Immunol Immunopathol 139,

99-106, 2011.
22) 阪口雅弘：アレルギー疾患に対する根治的免疫療法におけるアジュバントを用いたアレルゲンワクチン. 喘息 24,58-62, 2011
23) 白井秀治、阪口雅弘：室内アレルゲンの測定.空気清浄 48, 17-23, 2011
24) 阪口雅弘:スギ花粉症における自然発症動物と犬のバイオバンクプロジェクト. 関西実験動物研究会会報 33, 64-67, 2011
25) 阪口雅弘: アレルギー疾患の DNA 免疫療法. アレルギー 60, 1591-1597, 2011

２. 学会発表

1) 内山淳平、内山伊代、竹内 啓晃、阪口義彦、阪口雅弘、松崎 茂展: 活性型ピロリ菌ファージ KHP30 の特徴付けとその潜伏感染性の解析.第 89 回日本細菌学会、大阪、3 月 2016 年
2) 那須川忠弥、内山淳平、鈴木仁人、宮田玲奈、山口琴絵、平山隆一郎、内山伊代、氏原隆子、阪口義彦、阪口雅弘、松﨑茂展：緑膿菌 PAO1 株とファージ KPP22 の短期間進化的軍拡競走の解析. 第 89 回日本細菌学会、大阪、3 月 2016 年
3) 水谷格之、後藤裕子、蔵田圭吾、藤原亜紀、阪口雅弘、大野耕一、辻本元：イヌのリンパ腫症例における血清中可溶性インターロイキン-2 受容体α鎖の測定. 第 12 回日本獣医内科学アカデミー学術大会、横浜、2 月 2016 年
4) 白井秀治、阪口雅弘：ダニアレルゲンに対する家庭内対策の非臨床研究を中心した評価. 第 52 回日本小児アレルギー学会、奈良、11 月 2015 年
5) 旭 愛，藤井宏治，岡本憲明，窪田 聡，関口和正，阪口雅弘，武内ゆかり，松田秀明：マイクロサテライト多型解析を用いたイヌの個体識別法の検討. 第 21 回日本法科学技術学会，柏、11 月 2015 年
6) 内山淳平，阪口雅弘，松崎茂展：ピロリ菌ファージの発見とその解析. 第 68 回の日本細菌学会中国・四国支部総会，岡山，10 月 2015 年
7) 島倉秀勝、齋藤拓、藤村正人 、岡本憲明、内山淳平、阪口雅弘：食物有害反応を示す犬における卵白抗原に対する IgE 反応性の検討. 第 158 回日本獣医学会、十和田、9 月 2015 年
8) 平山 隆一郎、鈴木 仁人、内山 淳平、松井 真理、鈴木 里和、柴山 恵吾、阪口 雅弘、木内 明男: イヌにおける新規口腔内常在細菌の同定と全ゲノム配列解析. 第 158 回日本獣医学会、十和田、9 月 2015 年
9) 内山淳平、松井秀仁、花木秀明、松崎茂展、阪口雅弘:細菌感染症における診断法と治療法の開発：バクテリオファージの利用. 第 158 回日本獣医学会、十和田、9 月 2015 年
10) 石井崇史，新倉雄一，細木敬祐，津久井利宏，阪口雅弘，三宅健介，長瀬隆英，山下直美： 喘息病態における気道上皮細胞の活性化と新規クルクミン誘導体による制御につ

いての解析. 第 55 回日本呼吸器学会、東京、4 月 2015 年

11) 坪井誠也, 渡邊学, 二瓶和美, 吉見奈津子, 加藤明久, 阪口雅弘, 大和修,櫛田和哉,チェンバーズジェームズ, 菅野純夫, 内田和幸, 中山裕之：Whole Exome Sequence 法によるイヌ遺伝性神経疾患の原因遺伝子同定. 第 11 回獣医内科アカデミー、横浜、2 月 2014 年

12) 原田 晋、白井 秀治、越本 知大、阪口 雅弘,工藤 比等志：被毛および唾液の両者への感作が認められたジヤンガリアンハムスターによるアナフィラキシーの 1 例. 第 44 回日本皮膚アレルギー・接触皮膚炎学会、仙台、11 月 2024 年

13) 阪口　雅弘、白井　秀治：室内環境アレルゲン.第 23 回日本臨床環境医学会、京都、6 月 2014 年

14) 石井崇史, 新倉雄一, 白井秀治, 阪口雅弘, 棚元憲一, 室井正志, 長瀬隆英, 山下直美: IRF3 の好酸球性気道炎症病態における役割. 第 26 回日本アレルギー学会春季総会、5 月 2014 年

15) 鈴木麻里子、黒崎晃彦、飛田啓輔、青木康夫、林野淳、辻本元、阪口雅弘：犬のアトピー性皮膚炎における新規乳酸菌 Lactobacillus crispatus KT-11 製剤の投与試験. 第１７回日本獣医皮膚科学会学術大会, さいたま、3 月 2014 年

16) 阪口 雅弘, 津久井 利広, 大隅 尊史, 辻本 元:犬のアトピー性皮膚炎のアレルゲンを用いた免疫療法について.第１０回獣医内科アカデミー、横浜、2 月 2014 年

17) 印牧信行、川原井晋平、阪口雅弘：イヌのバイオバンクプロジェクトにおけるイヌ緑内障感受性遺伝子の研究.第１０回獣医臨床遺伝研究会、天童、12 月 2013 年

18) 野﨑淳夫、鈴木直也、成田泰章、白井秀治、阪口雅弘：市販マスクにおける空気汚染物質の除去特性について その 1　ガス状物質（アンモニア、ＶＯＣ）.2013 年度呼吸保護に関する研究発表会、東京、12 月 2013 年

19) 白井秀治、成田泰章、松本蘭世、柴田彰、野崎淳夫、阪口雅弘：マスク着用によるダニアレルゲン吸入予防効果の検討.　第 63 回日本アレルギー学会秋季学術大会、東京、11 月 2013 年

20) 島倉秀勝、岡山太郎、増田健一、津久井利広、藤村正人、阪口雅弘：イヌの血清中アレルゲン特異的 IgE 抗体量とアレルギー反応閾値濃度との比較.第１５６回日本獣医学会、岐阜、9 月 2013 年

21) 阪口 雅弘:実験動物アレルギーと環境因子.第 50 回日本実験動物環境研究会,東京,7 月 27 日 2013 年

22) 阪口雅弘: 犬のバイオバンクプロジェクト. 第 155 回日本獣医学会、 東京、3 月 2013 年

23) 神崎美玲, 白井秀治, 皆川恵子 橘本知幸、阪口雅弘、眞壁郁, 飯島茂子:お好み焼き粉に繁殖したチリダニ類による即時型アレルギーの母子例. 第 62 回日本アレルギー学会秋季学術大会. 大阪、11 月 2012 年

24) 白井秀治、成田泰章、松本蘭世、柴田彰、野崎淳夫、阪口雅弘: マスク着用によるダニアレルゲン吸入予防効果の検討. 第62回日本アレルギー学会秋季学術大会. 大阪,11月2012年

25) 島倉秀勝、周藤明美、増田健一、木内明男、阪口雅弘：乳酸菌を用いた食物アレルギーの新規治療法の開発：イヌにおける疾患モデルとしての食物アレルギー犬の検討.第87回麻布獣医学会、相模原、11月2012年

26) 岡本憲明、石丸浩靖、木内　明男、藤村　正人、阪口　雅弘：アトピー性皮膚炎犬における　Malassezia pachydermatis　の感作状況. 第87回麻布獣医学会、相模原、11月2012年

27) 宮地一樹、木内　明男、藤村　正人、栗田　吾郎、阪口　雅弘：日本における犬混合ワクチン接種後副反応に関する大規模な疫学調査. 第87回麻布獣医学会、相模原、11月2012年

28) 阪口雅弘:犬の疾患解析のための遺伝子バンク. 第6回家畜ＤＮＡ西郷シンポジューム, 福島、10月2012年

29) 阪口雅弘:帯電微粒子水「ナノイー」によるペットアレルゲン不活化の検討.日本臨床獣医学フォーラム、東京、9月2012年

30) 堀本泰介、玄文宏、岩附研子、加藤健太郎、久末正晴、阪口雅弘、明石博臣、伊藤壽、河岡義裕、鈴木和男、前田健: わが国の哺乳動物におけるインフルエンザウイルス感染. 第154回日本獣医学会、岩手、9月2012年

31) 成本治，松尾由紀子，阿部和穂、阪口雅弘、長瀬隆英，山下直美：好中球浸潤を伴う喘息モデルを用いた気道炎症の制御の解析.第 52 回日本呼吸器学会, 神戸、4 月 2012 年

32) 阪口雅弘　：犬のバイオバンクプロジェクトの試み 平成23年度日本獣医師会獣医学術学会,札幌、2月2012年

33) 原田　晋、白井秀治、阪口雅弘：お好み焼き粉、タコ焼き粉に混入したダニによるアレルギー反応の発症機序に関する考察 第61回日本アレルギー学会総会、東京、11月2011年

34) 島倉秀勝、周藤明美、久保田翔太、宮地一樹、高瀬有加里、木内明男、阪口雅弘:遺伝性が疑われる食物アレルギー犬における家系の調査.　第 152 回日本獣医学会、堺、9月2011年

35) Fujimura T,　Yonekura S, Horiguchi S, Sakaguchi M, Taniguchi M, Okamoto Y. : Candidate for response monitoring or prognostic biomarkers in two-year sublingual immunotherapy for Japanese cedar pollinosis. 22th World Allergy Congress, Cancun, Mexico, Decmeber, 2011.

36) Tsukui　T, Fukui M, Ohsumi T, Maeda S, Chimura N, Sakaguchi M, Tsujimoto, H. Immunotherapy Using Pullulan-conjugated Recombinant House Dust Mite

Allergen (Der f 2-P). Asian Meeting of Animal Medicine Specialties、Bangkok, Thailand, May, 2011.

37) 成本治、松尾由紀子、阿部和穂、白井秀治、阪口雅弘、長瀬隆英、山下直美：喘息病態における気道上皮細胞の活性化と新規クルクミン誘導体による制御についての解析. 第 51 回日本呼吸器学会、東京、4 月 2011 年

Allergology International xxx (2016) 1–7

Contents lists available at ScienceDirect

Allergology International

journal homepage: http://www.elsevier.com/locate/alit

Original article

Cross-reactivity between major IgE core epitopes on Cry j 2 allergen of Japanese cedar pollen and relevant sequences on Cha o 2 allergen of Japanese cypress pollen

Kazuki Miyaji [a], Noriaki Okamoto [a], Akemi Saito [b], Hiroshi Yasueda [b], Yukari Takase [a], Hidekatsu Shimakura [a], Saburo Saito [c], Masahiro Sakaguchi [a,*]

[a] Laboratory of Veterinary Microbiology I, School of Veterinary Medicine, Azabu University, Kanagawa, Japan
[b] Clinical Research Center for Allergy and Rheumatology, National Sagamihara Hospital, Kanagawa, Japan
[c] Department of Molecular Immunology, Institute of DNA Medicine, Jikei University School of Medicine, Tokyo, Japan

ARTICLE INFO

Article history:
Received 29 June 2015
Received in revised form
27 December 2015
Accepted 13 January 2016
Available online xxx

Keywords:
Allergen
Cross-reactivity
Epitope
IgE
Pollen

Abbreviations:
CO, *Chamaecyparis obtusa*; CJ, *Cryptomeria japonica*; ELISA, enzyme-linked immunosorbent assay; FU, fluorescence units; mAb, monoclonal antibody; OD, optical density

ABSTRACT

Background: Cry j 2 and Cha o 2 are major allergens in Japanese cedar (*Cryptomeria japonica*; CJ) and Japanese cypress (*Chamaecyparis obtusa*; CO) pollen, respectively. Here, we assessed the epitopes related to the cross-reactivity between Cry j 2 and Cha o 2 using *in vitro* analyses.
Methods: Peptides were synthesized based on Cry j 2 sequential epitopes and relevant Cha o 2 amino acid sequences. Four representative monoclonal antibodies (mAbs) against Cry j 2 were used according to their epitope recognitions. Serum samples were collected from 31 patients with CJ pollinosis. To investigate cross-reactivity between Cry j 2 and Cha o 2, ELISA and inhibition ELISA were performed with mAbs and sera from patients with CJ pollinosis.
Results: Two of four mAbs had reactivity to both Cry j 2 and Cha o 2. Of these two mAbs, one mAb (T27) recognized the amino acid sequence ^{169}KVVNGRTV^{176} on Cha o 2. This is related to the core epitope ^{169}KWVNGREI^{176} on Cry j 2, which is an important IgE epitope. In addition, we found that these correlative sequences and purified allergens showed cross-reactivity between Cry j 2 and Cha o 2 in IgE of CJ patients.
Conclusions: We demonstrated the importance of ^{169}KVVNGRTV^{176} in Cha o 2 for cross-reactivity with the Cry j 2 epitope ^{169}KWVNGREI^{176}, which plays an important role in allergenicity in CJ pollinosis. Our results are useful for the development of safer and more efficient therapeutic strategies for the treatment of CJ and CO pollen allergies.

Introduction

Seasonal allergic diseases including allergic rhinitis and asthma occur worldwide, particularly in developed countries. Pollinosis is a commonly-noted seasonal allergic disease induced by pollen allergens. The pollinosis induced by Japanese cedar (*Cryptomeria japonica*; CJ) pollen is one of the most common allergic diseases in Japan.[1] According to a survey conducted in the central Hokuriku area of Japan in May and June of both 2006 and 2007, 36.7% of study participants (566 of the 1540 subjects) had allergic rhinitis to CJ pollen.[2] Japanese cypress (*Chamaecyparis obtusa*; CO) pollen is one of the most important aeroallergens relevant to allergic symptoms in Japan.[3] The social impact and economic loss related to pollinosis are estimated to be tremendous because of the impaired performance of the patients, often accompanied by a self-imposed ban on leaving home.

Allergen cross-reactivity has been reported at the immunochemical and clinical levels. The cloning and sequencing of allergen genes have provided a better understanding of their cross-reactivity. The first evidence for the existence of clinically relevant cross-reactive IgE antibodies was reported in pollen-food cross-reactive allergens.[4] Other cross-reactive allergenic systems have been induced by aeroallergens and food antigens.[5,6] Many efforts have been made to correlate the serological cross-reactivity with elicitation of symptoms in susceptible patients, because not all cross-reactive IgE antibodies give rise to clinical signs. Therefore, it

* Corresponding author. Department of Veterinary Microbiology, School of Veterinary Medicine, Azabu University, 1-17-71 Fuchinobe, Chuo-ku, Sagamihara, Kanagawa 252-5201, Japan.
E-mail address: sakagum@azabu-u.ac.jp (M. Sakaguchi).
Peer review under responsibility of Japanese Society of Allergology.

http://dx.doi.org/10.1016/j.alit.2016.01.003

has been accepted that serological cross-reactivity may be broader than clinical cross-allergenicity.[7]

Three major allergens, named Cry j 1, Cry j 2, and Cry j 3, have been isolated from CJ pollen. Cry j 1 was isolated as a 41–46 kDa allergen with pectate lyase enzyme activity,[8,9] whereas Cry j 2 is a 45 kDa allergen with polymethylgalacturonase enzyme activity.[10,11] Cry j 3 is a 27 kDa protein that has relatively high homology with thaumatin-like proteins in the pathogenesis-related-5 family proteins.[12] On the other hand, Cha o 1 and Cha o 2 were identified as major allergens of CO with a high degree of homology with Cry j 1 and Cry j 2, respectively.[3,13,14] Amino acid sequence homology between major allergens from CJ and CO results in cross-allergenicity.

Cross-allergenicity is observed between CJ and CO pollen allergens.[15] In our previous studies, animal models of Japanese monkeys and dogs sensitized to CJ pollen demonstrated IgE reactivity to CO pollen.[16,17] Cry j 2 was characterized as a major allergen in CJ pollinosis,[10] and more than 90% of patients (139/145 subjects) had the anti-Cry j 2 IgE.[18] It was demonstrated that the IgE antibody levels to Cry j 2 and Cha o 2 were strongly correlated,[14] suggesting that there are one or more epitopes with high similarity between Cry j 2 and Cha o 2.

Six sequential and one conformational epitopes on Cry j 2 were identified in our previous studies.[19,20] Conformational epitopes on allergens play an important role in initiating human IgE-mediated allergic reactions.[21–23] In fact, the conformational epitopes on Cry j 1 are considered dominant in IgE reactivity as compared to the sequential epitopes.[24] However, we suggested the importance of sequential epitopes on Cry j 2, especially ^{169}KWVNGREI^{176}, for allergenicity at variance with other well-known allergens.[20] To our knowledge, it has yet to be demonstrated whether monoclonal antibodies (mAbs) and patients' IgE to sequential epitopes on Cry j 2 can cross-react with the relevant epitopes on Cha o 2. This is the first report to indicate the cross-reactivity between sequential epitopes on Cry j 2 and relevant sequences on Cha o 2 by mAbs and patients' IgE. Here, we also analyze the cross-reactivity between the Cry j 2 core epitope, ^{169}KWVNGREI^{176}, reported in our previous studies[19] and the related epitope on Cha o 2 by inhibition ELISA. We used ^{169}KWVNGREI^{176} because it was the only core epitope reported in previous studies, and it is known to be a major epitope recognized by patients' IgE.

Table 1
Synthetic peptides and allergenic similarities between Cry j 2 linear epitopes (upper sequences) and relevant Cha o 2 amino acid sequences (lower sequences).

Peptide (No[†])	Position[‡]	mAb to a peptide[§]	Amino acid sequence
P1-1 (13)	166–186	T27	GQC**KWVNGREI**CNDRDRPTA
P1-2	166–186		----V----TV---------
P2-1 (25)	286–305	9E7	GRENSRAEVSYVHVNGAKFI
P2-2	286–305		--D-------H----R----
P3-1 (33)	366–385	J2A01	TYKNIRGTSATAAAIQLKCS
P3-2	366–385		-----H----------M--

The core determinant of P1-1 is shown in bold.
[†] Peptide numbers shown in brackets were linked to the study of Tamura *et al.*[19]
[‡] Amino acid positions were described as complete sequences.
[§] The mAb reactivity to each peptide was determined in our previous study.[20]

Methods

Antigens and mAbs

Cry j 2 in CJ pollen and Cha o 2 in CO pollen were purified as previously described.[10,14] Table 1 shows six peptides that were synthesized based on Cry j 2 sequential epitopes recognized by mAbs for Cry j 2 and relevant Cha o 2 amino acid sequences (Hokkaido System Science Co., Ltd., Sapporo, Japan). We also synthesized the core epitope on Cry j 2 (^{169}KWVNGREI^{176}) and the relevant Cha o 2 amino acid sequence (^{169}KVVNGRTV^{176}). Four representative mAbs for Cry j 2 (S1, T27, 9E7, and J2A01) were used according to their epitope recognitions.[20]

Subjects

Informed consent was obtained from all subjects. The study protocol was approved by the ethical committee at the Jikei University School of Medicine. Serum samples were collected from 31 patients with CJ pollinosis. The patients were selected based on clinical symptoms of seasonal allergic rhinitis and positive CAP (Phadia AB, Uppsala, Sweden) to CJ pollen. Their IgE were preliminarily confirmed to react with Cry j 2. To determine the cut-off value, serum samples obtained from 10 non-allergic subjects, who had been previously confirmed as negative for the crude pollen allergen were used as negative controls.

Colorimetric ELISA for Cry j 2, Cha o 2, and synthetic peptides with mAbs

As previously described, the reactions of the mAbs were measured using a colorimetric ELISA.[19] Briefly, Cry j 2, Cha o 2 (1 μg/ml), P1-1, P1-2, P3-1, and P3-2 (10 μg/ml) were immobilized in the wells of a microplate (F96 Maxisorp® NUNC-Immuno™ Plate, ThermoFisher Scientific, Waltham, MA, USA) overnight at 4°C. The microplate was then washed with phosphate-buffered saline containing 0.05% Tween 20 (PBST) and incubated with biotin-labeled mAbs (1 μg/ml) for 1 h at room temperature. Next, streptavidin-peroxidase polymer (Sigma–Aldrich, MO, USA) was added to the wells. After a 1 h incubation period at room temperature, a substrate solution of o-phenylenediamine dihydrochloride was added. After the enzyme reaction was terminated with 2 M H_2SO_4, the optical density (OD) was measured using a multi-mode microplate reader (Powerscan MX, DS Pharma Biomedical, Osaka, Japan).

Colorimetric ELISA inhibition for Cry j 2 and Cha o 2 epitopes with mAbs

It was difficult to immobilize short peptides on the wells of the microplate. Thus, to evaluate the reactivity of the T27 mAb with ^{169}KWVNGREI^{176} (Cry j 2 core epitope) and ^{169}KVVNGRTV^{176} (relevant sequence within Cha o 2), an inhibition ELISA was conducted using these synthetic peptides as inhibitors.[25] Briefly, P1-1 and P1-2 (10 μg/ml) were immobilized in the wells of a microplate overnight at 4°C. The synthetic peptide inhibitors (final concentrations, 0–100 μg/ml) were incubated with equal volumes of T27 mAb (final concentration, 10 ng/ml) for 1 h at room temperature. Subsequent procedures were the same as described above. The inhibition ratio (%) was calculated as follows:

$$\left(1-\frac{\text{OD in presence of inhibitor}}{\text{OD in absence of inhibitor}}\right)\times 100$$

Fluorometric ELISA for Cry j 2 and Cha o 2 peptides

As previously described, specific IgE against synthetic peptides were measured in the sera of patients using fluorometric ELISA.[20] Briefly, synthetic peptides (20 μg/ml) were immobilized in the wells of a microplate (FLUOTRAC™ 600, Greiner Bio-One GmbH, Frickenhausen, Germany) overnight at 4°C. The microplate was then washed with PBST buffer and incubated with diluted (1:10) serum samples for 3 h at room temperature. The plates were washed, and anti-human IgE antibodies conjugated to β-D-galactosidase (diluted 1:10; Phadia AB) were added to each well. The enzyme reaction substrate, 0.2 mM 4-methylumbelliferyl-β-D-galactoside (Sigma–Aldrich) was added to the wells, and the plates were incubated at 37°C for 2 h. After quenching the reaction, fluorescence units (FU) were measured using a multi-mode microplate reader. Cut-off values were determined using sera from subjects without pollinosis as negative controls.

Fluorometric ELISA inhibition for Cry j 2 and Cha o 2 with human IgE

To evaluate cross-reactivity between Cry j 2 and Cha o 2, we used a fluorometric ELISA inhibition for Cry j 2 and Cha o 2 with human IgE.[20] Briefly, Cry j 2 or Cha o 2 (0.5 μg/ml) were immobilized in the wells of a microplate (FLUOTRAC™ 600) overnight at 4°C. Cry j 2 or Cha o 2 inhibitors (final concentrations, 0–10 μg/ml) were incubated with equal volumes of human sera (final dilution, 1:50) for 3 h at room temperature. The microplate was then washed with PBST buffer and incubated with diluted (1:10) serum samples for 3 h at room temperature. Subsequent procedures were the same as described above.

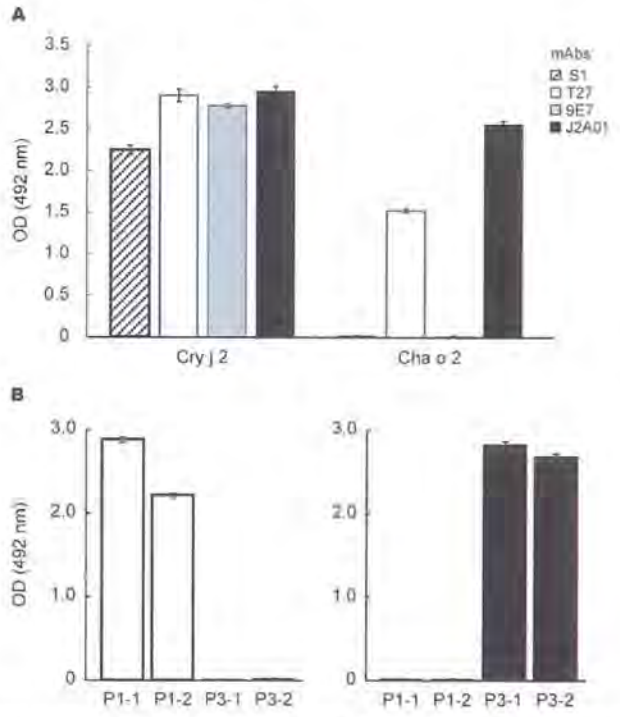

Fig. 1. Reactivity of Cry j 2 mAbs. Cry j 2 and Cha o 2 were immobilized on a microplate **(A)**. The peptides P1-1, P1-2, P3-1, and P3-2 were coated on a microplate **(B)**. Biotin-labeled S1, T27, 9E7, and J2A01 mAbs were reacted with each peptide. The binding activity of each mAb is expressed as optical density (OD). Experiments were performed in triplicate, and data are expressed as mean values ± SD from triplicate determinations. S1 and J2A01 mAbs share the same epitopes as bound by J2A07 and J2A03, respectively.[14]

Fluorometric ELISA inhibition for Cry j 2 and Cha o 2 peptides with human IgE

It was difficult to immobilize short peptides on the wells of the microplate. Therefore, to evaluate the reactivity of human IgE to ^{169}KWVNGREI^{176} (Cry j 2 core epitope) and ^{169}KVVNGRTV^{176} (relevant sequence within Cha o 2), an inhibition ELISA was conducted using these synthetic peptides as inhibitors. Briefly, P1-1 and P1-2 (10 μg/ml) were immobilized in the wells of a microplate (Nunc® Immobilizer™ Amino Plate, ThermoFisher Scientific) overnight at 4°C. The synthetic peptide inhibitors (final concentrations, 0–100 μg/ml) were incubated with equal volumes of human sera (final dilution, 1:100) for 3 h at room temperature. Subsequent procedures were performed as described above.

Results

Reactivity of Cry j 2 mAbs to Cry j 2 and Cha o 2 peptides

To examine the reactivity of four mAbs to Cry j 2 and Cha o 2 peptides, the binding of mAbs to each allergen was measured by ELISA. We found that T27 and J2A01 mAbs reacted with both Cry j 2 and Cha o 2 (Fig. 1A). These two mAbs have cross-reactivity to Cha o 2. However, the S1 mAb against a conformational epitope and 9E7 mAb against P2-1 reacted with Cry j 2, but not with Cha o 2 (Fig. 1A). These two mAbs have Cry j 2-specific binding. T27 mAb reacted with both Cry j 2-related peptide (P1-1) and Cha o 2-related

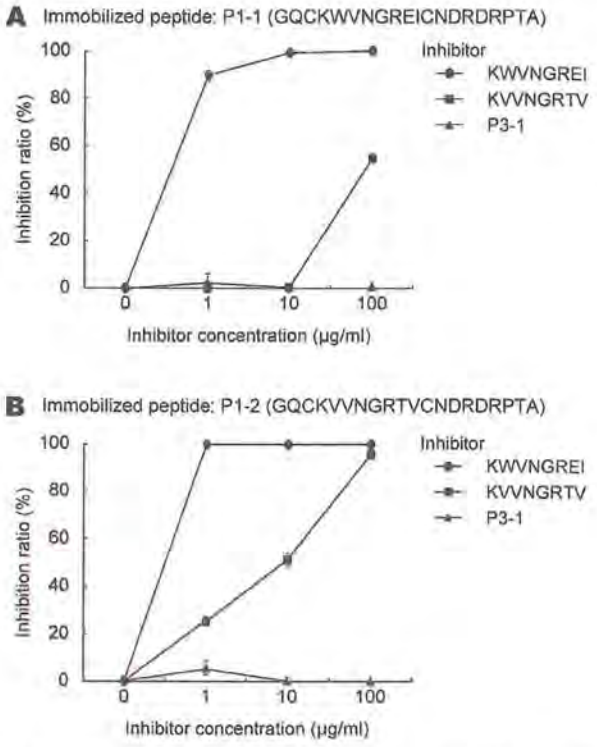

Fig. 2. Colorimetric ELISA inhibition using mAb against epitopes. Cry j 2 **(A)** or Cha o 2 **(B)** peptides (P1-1 or P1-2) were immobilized in the wells of a microplate. The Cry j 2 peptide ^{169}KWVNGREI^{176} (closed circles) and the Cha o 2 peptide ^{169}KVVNGRTV^{176} (closed squares) were incubated as inhibitors with equal volumes of T27 mAb. Unrelated peptide P3-1 was used as a negative control (closed triangles). Inhibition ratios were calculated as a percentage in the presence of homozygous or heterozygous inhibitors. Experiments were performed in triplicate, and data are expressed as mean values ± SD from triplicate determinations.

peptide (P1-2) (Fig. 1B). J2A01 mAb reacted with both Cry j 2-related peptide (P3-1) and Cha o 2-related peptide (P3-2) (Fig. 1B).

Cross-reactivity of T27 mAb between Cry j 2 and Cha o 2 peptides

To further evaluate the mAb reactivity with Cry j 2 and Cha o 2 peptides, we conducted ELISA inhibition using these peptides. The T27 mAb binding to Cry j 2 peptide (P1-1) was concentration-dependently inhibited by both ^{169}KWVNGREI^{176} (Cry j 2 core epitope peptide) and ^{169}KVVNGRTV^{176} (relevant Cha o 2 peptide) (Fig. 2A). In addition, the binding of this mAb to Cha o 2 peptide (P1-2) was inhibited by both Cry j 2 and Cha o 2 peptides (Fig. 2B). We found that this mAb exhibits cross-reactivity between the Cry j 2 core epitope in P1-1 and the relevant Cha o 2 peptide. In T27 mAb for Cry j 2, the inhibitory efficiency of the Cry j 2 peptide ^{169}KWVNGREI^{176} was higher than that of the Cha o 2 peptide ^{169}KVVNGRTV^{176}.

Reactivity of human IgE to Cry j 2 and Cha o 2 peptides in patients with Cry j 2-specific IgE

To evaluate IgE reactivity to Cry j 2 and Cha o 2 peptides, specific IgE to these peptides were measured in the sera of 31 human patients with Cry j 2-specific IgE. We summarize the FU titers of patients' IgE to each peptide in Table 2. The cut-off values used for each peptide were set as the mean value + 3SD of 10 negative controls. Of 31 patients, 10 patients had specific IgE to both P1-1 and P1-2, 13 patients had specific IgE to only P1-1, and 8 patients had no specific IgE to either peptide (Fig. 3A). Of 31 patients, 5 patients had specific IgE to both P2-1 and P2-2, 7 patients had specific IgE to only P2-1, 2 patients had specific IgE to only P2-2, and 17 patients had no specific IgE to either peptide (Fig. 3B). Of 31 patients, 10 patients had specific IgE to both P3-1 and P3-2, 10 patients had specific IgE to only P3-1, 1 patient had specific IgE to only P3-2, and 10 patients had no specific IgE to either peptide (Fig. 3C). Specific IgE to Cry j 2 showed the strongest reactivity to P1-1 and P1-2 among these peptides.

Cross-reactivity of human IgE between Cry j 2 and Cha o 2

In a representative patient with specific IgE to both P1-1 and P1-2 (Fig. 4A), allergenic cross-reactivity of Cry j 2 and Cha o 2 was investigated by ELISA inhibition. Incubation of the serum with the homologous Cry j 2 or Cha o 2 greatly inhibited binding (Fig. 4B). IgE binding to the solid-phase Cha o 2 was greatly inhibited by Cry j 2, but IgE binding to the solid-phase Cry j 2 was not greatly inhibited by Cha o 2 (Fig. 4B). We found cross-reactivity between Cry j 2 and Cha o 2, and Cry j 2 has a trend of greater inhibition than Cha o 2.

Cross-reactivity of human IgE between Cry j 2 and Cha o 2 peptides

To evaluate IgE cross-reactivity with the Cry j 2 peptide ^{169}KWVNGREI^{176} in P1-1 and the Cha o 2 peptide ^{169}KVVNGRTV^{176}

Table 2
Summarized results of total IgE fluorescence units of 31 patients.

Coated peptide	Minimum	Maximum	Median
P1-1	0	31,026	916
P1-2	11	10,242	79
P2-1	1	293	88
P2-2	0	399	62
P3-1	0	822	94
P3-2	0	1268	41

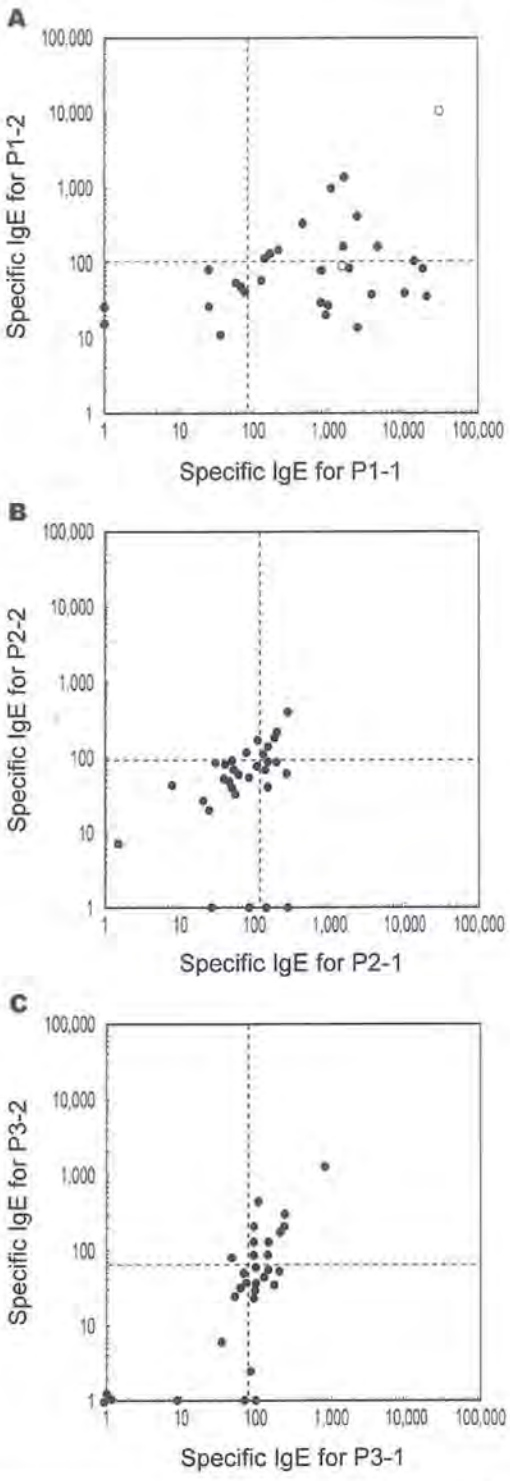

Fig. 3. IgE reactivity between Cry j 2 and Cha o 2 synthetic peptides. Binding activity is expressed in fluorescence units (FU). The x-axis is for Cry j 2-related peptides and the y-axis is for Cha o 2-related peptides. Serum samples from 31 patients were used to examine their IgE reactivity against P1-1 and P1-2 **(A)**, against P2-1 and P2-2 **(B)**, and against P3-1 and P3-2 **(C)**. The cut-off values (dashed lines) were determined as the mean + 3SD FU in negative controls. Open circles in **(A)** indicate representative patients in Fig. 4. Experiments were repeated at least three times.

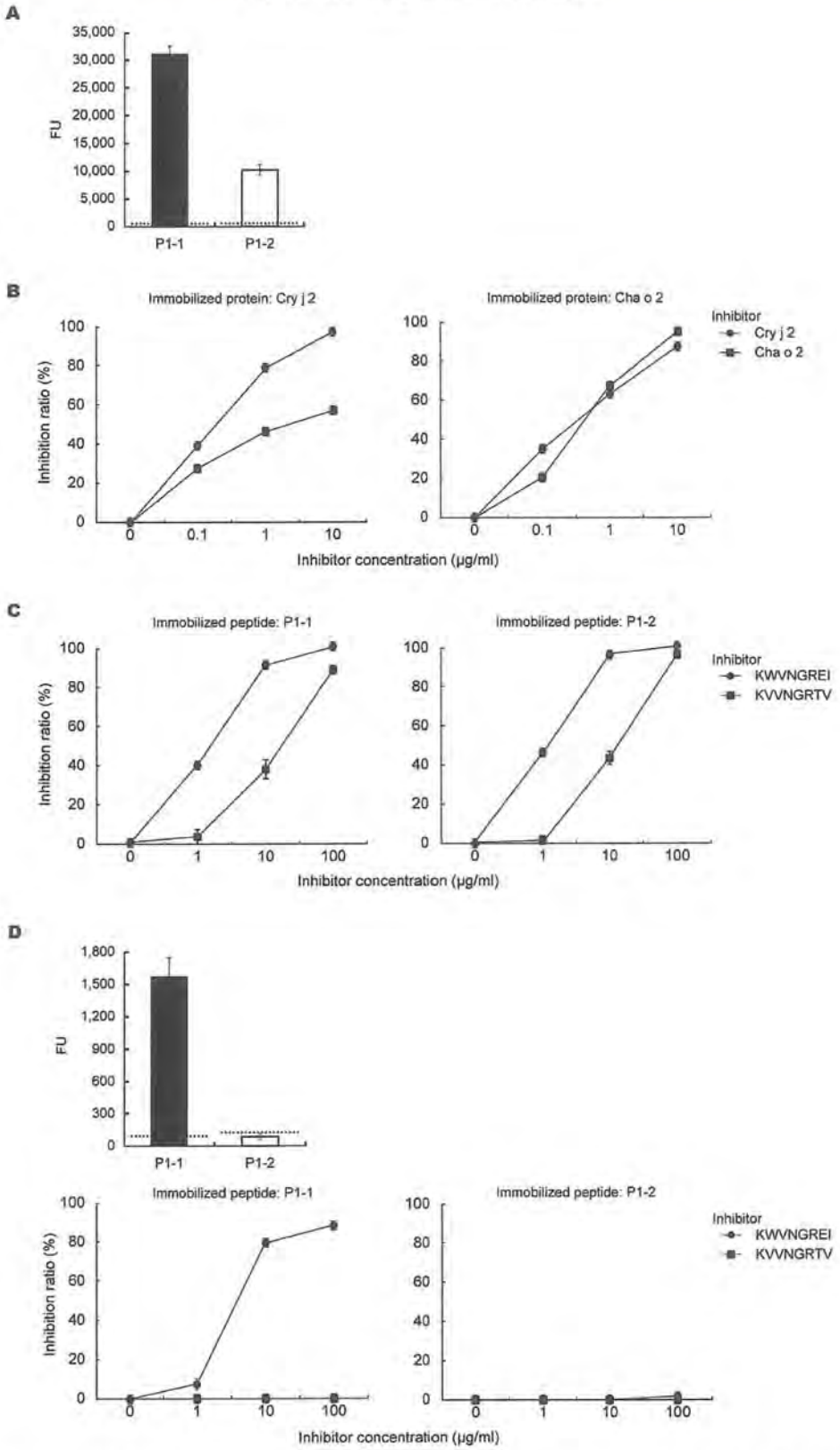

Fig. 4. Reactivity and inhibition ratios of IgE binding in representative patients. Binding activities of IgE from representative patients with double-positive reactivity to P1-1 and P1-2 **(A, patient no. 1)** and single positive reactivity to P1-1 **(D, patient no. 2)** are expressed in fluorescence units (FU). The dashed line represents the cut-off value which was determined as the mean + 3SD FU in negative controls. The cut-off values are 85.9 FU for the Cry j 2 peptide P1-1 and 110.0 FU for the Cha o 2 peptide P1-2. The inhibitory effects of the Cry j 2 (closed circles) and Cha o 2 (closed squares) on IgE binding to Cry j 2 and Cha o 2 were observed in patient no. 1 **(B)**. The inhibitory effects of the Cry j 2 peptide ^{169}KWVNGREI^{176} (closed circles) and Cha o 2 peptide ^{169}KVVNGRTV^{176} (closed squares) on IgE binding to P1-1 and P1-2 were observed in patient no. 1 **(C)**. In contrast, the inhibitory effect of Cha o 2 peptide ^{169}KVVNGRTV^{176} was not observed in patient no. 2 **(D)**. Inhibition ratios were calculated as a percentage under the presence of homozygous or heterozygous inhibitors. Experiments were performed in triplicate, and data are expressed as mean values ± SD from triplicate determinations.

in P1-2, we examined cross-reactivity by ELISA inhibition with human IgE. The binding of IgE from a representative patient was strongly inhibited by ^{169}KWVNGREI^{176} peptide and moderately inhibited by ^{169}KVVNGRTV^{176} peptide (Fig. 4C). We found that the IgE from a representative patient displayed cross-reactivity between the Cry j 2 core epitope in P1-1 and the relevant Cha o 2 peptide. In contrast, an inhibitory effect of ^{169}KWVNGREI^{176} was observed in a patient with single positive reactivity to P1-1, but this was not the case with ^{169}KVVNGRTV^{176} (Fig. 4D).

Discussion

Allergic symptoms such as rhinoconjunctivitis are induced by CJ and CO pollen allergens. The major causal allergen of pollinosis in Japan is CJ pollen because of the abundant pollination and widespread distribution of CJ. CO is the second most common pollinosis-inducing conifer in Japan. Cry j 2 is one of the major allergens in CJ pollen, and its homologue is isolated from CO as Cha o 2.[14] IgE levels between Cry j 2 and Cha o 2 were highly correlated in the sera of patients with pollinosis.[14] Moreover, bioinformatics tools such as the BLASTP (Protein Basic Local Alignment Search Tool; http://www.ncbi.nih.gov/blast) and SDAP (Structural Database of Allergenic Proteins; http://fermi.utmb.edu/SDAP/)[26,27] also suggest the existence of cross-reactive epitopes between Cry j 2 and Cha o 2. Until now, however, the contributing epitopes had not been identified on Cry j 2 and Cha o 2.

The T27 mAb reacted to P1-1 of Cry j 2 and P1-2 of Cha o 2 (Fig. 1B), and both the Cry j 2 core epitope peptide ^{169}KWVNGREI^{176} and the Cha o 2 relevant peptide ^{169}KVVNGRTV^{176} efficiently inhibited the binding of T27 mAb to P1-1 and P1-2 (Fig. 2). ^{169}KWVNGREI^{176} and ^{169}KVVNGRTV^{176} also blocked the binding of IgE from the patient with double-positive IgE to P1-1 and P1-2 (Fig. 4C). These results indicate that the ^{169}KVVNGRTV^{176} sequence in Cha o 2 is cross-reactive with the Cry j 2 epitope ^{169}KWVNGREI^{176} for mAb and patient IgE. This is another example indicating that antibodies can not only bind to the original epitope but also to sequences that may have a few different amino acids. This raises the intriguing possibility of cross-reactivity to non-homologous amino acids, which may have a large contribution to allergic diseases. On the other hand, in a patient with single positive reactivity to P1-1, the IgE binding to P1-1 was inhibited by ^{169}KWVNGREI^{176}, but not ^{169}KVVNGRTV^{176}. This result suggests the presence of another core epitope which partially overlaps with ^{169}KWVNGREI^{176}.

As shown in Fig. 1B, the J2A01 mAb reacted to both the Cry j 2 peptide (P3-1) and the Cha o 2 peptide (P3-2). Therefore, we tried to identify the core determinants for this antibody by using synthetic peptides with 10–20 residues but failed to do so (data not shown). This J2A01 mAb shares the same epitope as bound by J2A03 mAb used in our previous study.[14] In our previous study, it was suggested that the core determinants result from discontinuous amino acids within the synthetic peptides.[20] The present results may support the previous suggestion. The 9E7 mAb against P2-1 did not cross-react with the Cha o 2 peptide (Fig. 1A). However, of the 31 patients, IgE from the sera of 5 patients reacted with both P2-1 and P2-2 peptides, and there seemed to be a good correlation between these peptides (Fig. 3B). Our results suggest that the core determinant for the 9E7 mAb in P2-1 had fewer or no overlaps with P2-2. We did not determine the core epitope of P2-1, because we did not have a sufficient volume of sera from patients whose IgE reacted with this peptide. Further studies are needed to identify the core sequences for J2A01 and 9E7 mAbs by *in vitro* analysis.

We demonstrated IgE responses to Cry j 2 peptides in our previous studies,[19,20] and the cross-reactivity between the sequence epitopes on Cry j 2 and Cha o 2 in the present study. In addition to Cry j 2 and Cha o 2, other group 2 conifer allergens are some of the main pollen allergens: Jun a 2 for *Juniperus ashei* (Mountain cedar),[28] Jun o 2 (also known as Jun o 4) for *Juniperus oxycedrus* (Prickly juniper),[29] Tax d 2 for *Taxodium distichum* (Bald cypress), and Cup a 2 for *Cupressus arizonica* (Arizona cypress). They belong to the family *Cupressaceae* and cause pollinosis in areas such as North America[30,31] and the Mediterranean region.[32,33] In addition to *in vitro* analyses, we suggest the possibility that cross-reactive epitopes exist among some group 2 conifer allergens by *in silico* analyses (data not shown). The *in silico* analysis also estimated that ^{170}KTINGRTV^{177} for Jun a 2 [property distance index (PD) = 6.55], ^{139}KWINGREI^{146} for Tax d 2 (0.68), and ^{117}KTINGRTV^{124} for Cup a 2 (5.87) were epitopes relevant to the Cry j 2 epitope ^{169}KWVNGREI^{176}. The results suggest that cross-reactivity between the Cry j 2 core epitope and the related Tax d 2 and Cup a 2, but not Jun a 2, sequences, will be observed according to the threshold proposed by Ivanciuc *et al.*,[34] which may lie between 5 and 6.5. Conversely, sera from patients with CJ pollinosis demonstrated binding to Jun a 2,[28] suggesting that epitopes rather than P1-1 are important for cross-reactivity between Cry j 2 and Jun a 2. Our findings provide useful information for the development of therapeutic strategies for pollinosis.

IgE antibodies to CJ have also been found in monkeys with pollinosis[15,24] and dogs with atopic dermatitis.[35] Monkeys with CJ pollinosis have symptoms similar to those of human patients. Dogs live in the same environment as humans and naturally develop a pruritic dermatitis that is extremely similar to human atopic dermatitis. Moreover, monkeys[16] and dogs[17] sensitized to CJ pollen were reported to have cross-reactive IgE to CO pollen. Although allergenic cross-reactivity between Cry j 1 and Cha o 1 was demonstrated in those studies, cross-reactivity between Cry j 2 and Cha o 2 remains to be elucidated. Because of the remarkable similarity with the human diseases, monkeys and dogs are considered prime animal models for allergic diseases. Further *in vivo* studies using such animal models will provide a better understanding of cross-reactivity of CJ and CO.

In summary, we showed that the amino acid sequences in Cha o 2 cross-react with Cry j 2 epitopes at the mAb and human IgE levels. We also provided evidence of the importance of ^{169}KVVNGRTV^{176} in Cha o 2 cross-reactivity with the Cry j 2 epitope ^{169}KWVNGREI^{176}, which plays an important role in allergenicity in CJ pollinosis. Induction of blocking IgG4 that can recognize IgE epitopes is responsible for clinically successful allergen-specific immunotherapy.[36] Therefore, targeting epitopes related to cross-reactivity may help in the development of immunotherapy against multiple allergic diseases. Our results are useful for the development of safer and more efficient therapeutic strategies for treating CJ and CO pollen allergies.

Acknowledgments

We are grateful to Dr. Reiko Homma (Torii Pharmaceutical Co., Ltd., Tokyo, Japan) for kindly giving us monoclonal antibodies. This research was partially supported by Program for the Strategic Research Foundation at Private Universities (S1101023), and by a Research Project Grant awarded by Azabu University.

Conflicts of interest

The authors have no conflict of interest to declare.

Authors' contributions

KM conceived and designed the experiments. KM analyzed the data and drafted the manuscript. NO helped KM to conduct the experiments. AS and HY helped to design the experiments and analyze the data. NO, YT, and HS assisted in data

analysis. SS and MS assisted in the study design, sample preparation, and editing of the manuscript. All authors have read and approved the final manuscript.

References

1. Ishizaki T, Koizumi K, Ikemori R, Ishiyama Y, Kushibiki E. Studies of prevalence of Japanese cedar pollinosis among the residents in a densely cultivated area. *Ann Allergy* 1987;**58**:265–70.
2. Sakashita M, Hirota T, Harada M, Nakamichi R, Tsunoda T, Osawa Y, et al. Prevalence of allergic rhinitis and sensitization to common aeroallergens in a Japanese population. *Int Arch Allergy Immunol* 2010;**151**:255–61.
3. Mori T, Yokoyama M, Komiyama N, Okano M, Kino K. Purification, identification, and cDNA cloning of Cha o 2, the second major allergen of Japanese cypress pollen. *Biochem Biophys Res Commun* 1999;**263**:166–71.
4. Anderson Jr LB, Dreyfuss EM, Logan J, Johnstone DE, Glaser J. Melon and banana sensitivity coincident with ragweed pollinosis. *J Allergy* 1970;**45**:310–9.
5. Hirschwehr R, Valenta R, Ebner C, Ferreira F, Sperr WR, Valent P, et al. Identification of common allergenic structures in hazel pollen and hazelnuts: a possible explanation for sensitivity to hazelnuts in patients allergic to tree pollen. *J Allergy Clin Immunol* 1992;**90**:927–36.
6. Valenta R, Duchene M, Ebner C, Valent P, Sillaber C, Deviller P, et al. Profilins constitute a novel family of functional plant pan-allergens. *J Exp Med* 1992;**175**:377–85.
7. van Ree R. Clinical importance of cross-reactivity in food allergy. *Curr Opin Allergy Clin Immunol* 2004;**4**:235–40.
8. Yasueda H, Yui Y, Shimizu T, Shida T. Isolation and partial characterization of the major allergen from Japanese cedar (*Cryptomeria japonica*) pollen. *J Allergy Clin Immunol* 1983;**71**:77–86.
9. Taniguchi Y, Ono A, Sawatani M, Nanba M, Kohno K, Usui M, et al. Cry j I, a major allergen of Japanese cedar pollen, has pectate lyase enzyme activity. *Allergy* 1995;**50**:90–3.
10. Sakaguchi M, Inouye S, Taniai M, Ando S, Usui M, Matuhasi T. Identification of the second major allergen of Japanese cedar pollen. *Allergy* 1990;**45**:309–12.
11. Ohtsuki T, Taniguchi Y, Kohno K, Fukuda S, Usui M, Kurimoto M. Cry j 2, a major allergen of Japanese cedar pollen, shows polymethylgalacturonase activity. *Allergy* 1995;**50**:483–8.
12. Fujimura T, Futamura N, Togawa A, Goldblum RM, Yasueda H, Saito A, et al. Isolation and characterization of native Cry j 3 from Japanese cedar (*Cryptomeria japonica*) pollen. *Allergy* 2007;**62**:547–53.
13. Suzuki M, Komiyama N, Itoh M, Itoh H, Sone T, Kino K, et al. Purification, characterization and molecular cloning of Cha o 1, a major allergen of *Chamaecyparis obtusa* (Japanese cypress) pollen. *Mol Immunol* 1996;**33**:451–60.
14. Yasueda H, Saito A, Sakaguchi M, Ide T, Saito S, Taniguchi Y, et al. Identification and characterization of a group 2 conifer pollen allergen from *Chamaecyparis obtusa*, a homologue of Cry j 2 from *Cryptomeria japonica*. *Clin Exp Allergy* 2000;**30**:546–50.
15. Ito H, Ssuzuki M, Mamiya S, Takagi I, Baba S, Tomita K, et al. Analysis of the allergenic components of Hinoki cypress (*Chamaecyparis obtusa*) pollen by immunoblotting with the sera from patients with Japanese cedar pollinosis. *Allergol Int* 1996;**45**:181–6.
16. Kobayashi C, Nigi H, Saito S, Ide T, Taniguchi Y, Inouye S, et al. IgE reactivity and cross-reactivity of Japanese monkeys (*Macaca fuscata*) to Japanese cedar (*Cryptomeria japonica*) and cypress (*Chamaecyparis obtusa*) pollen allergens. *Clin Exp Allergy* 1999;**29**:856–61.
17. Sakaguchi M, Masuda K, Yasueda H, Saito S, DeBoer DJ, Tsujimoto H. IgE reactivity and cross-reactivity to Japanese cedar (*Cryptomeria japonica*) and cypress (*Chamaecyparis obtusa*) pollen allergens in dogs with atopic dermatitis. *Vet Immunol Immunopathol* 2001;**83**:69–77.
18. Hashimoto M, Nigi H, Sakaguchi M, Inouye S, Imaoka K, Miyazawa H, et al. Sensitivity to two major allergens (Cry j I and Cry j II) in patients with Japanese cedar (*Cryptomeria japonica*) pollinosis. *Clin Exp Allergy* 1995;**25**:848–52.
19. Tamura Y, Kawaguchi J, Serizawa N, Hirahara K, Shiraishi A, Nigi H, et al. Analysis of sequential immunoglobulin E-binding epitope of Japanese cedar pollen allergen (Cry j 2) in humans, monkeys and mice. *Clin Exp Allergy* 2003;**33**:211–7.
20. Miyaji K, Yurimoto T, Saito A, Yasueda H, Takase Y, Shimakura H, et al. Analysis of conformational and sequential IgE epitopes on the major allergen Cry j 2 of Japanese cedar (*Cryptomeria japonica*) pollen in humans by using monoclonal antibodies for Cry j 2. *J Clin Immunol* 2013;**33**:977–83.
21. Varshney S, Goldblum RM, Kearney C, Watanabe M, Midoro-Horiuti T. Major mountain cedar allergen, Jun a 1, contains conformational as well as linear IgE epitopes. *Mol Immunol* 2007;**44**:2781–5.
22. Padavattan S, Flicker S, Schirmer T, Madritsch C, Randow S, Reese G, et al. High-affinity IgE recognition of a conformational epitope of the major respiratory allergen Phl p 2 as revealed by X-ray crystallography. *J Immunol* 2009;**182**:2141–51.
23. Tiwari R, Negi S, Braun B. Validation of a phage display and computational algorithm by mapping a conformational epitope of Bla g 2. *Int Arch Allergy Immunol* 2011;**157**:323–30.
24. Sakaguchi M, Hashimoto M, Nigi H, Yasueda H, Takahashi Y, Watanabe M, et al. Epitope specificity of IgE antibodies to a major allergen (Cry j 1) of Japanese cedar pollen in sera of humans and monkeys with pollinosis. *Immunology* 1997;**91**:161–6.
25. Tamura Y, Sasaki R, Inouye S, Kawaguchi J, Serizawa N, Toda M, et al. Identification of a sequential B-cell epitope on major allergen (Cry j 1) of Japanese cedar (*Cryptomeria japonica*) pollen in mice. *Int Arch Allergy Immunol* 2000;**123**:228–35.
26. Ivanciuc O, Schein CH, Braun W. Data mining of sequences and 3D structures of allergenic proteins. *Bioinformatics* 2002;**18**:1358–64.
27. Ivanciuc O, Schein CH, Braun W. SDAP: database and computational tools for allergenic proteins. *Nucleic Acids Res* 2003;**31**:359–62.
28. Yokoyama M, Miyahara M, Shimizu K, Kino K, Tsunoo H. Purification, identification, and cDNA cloning of Jun a 2, the second major allergen of mountain cedar pollen. *Biochem Biophys Res Commun* 2000;**275**:195–202.
29. Tinghino R, Barletta B, Palumbo S, Afferni C, Iacovacci P, Mari A, et al. Molecular characterization of a cross-reactive *Juniperus oxycedrus* pollen allergen, Jun o 2: a novel calcium-binding allergen. *J Allergy Clin Immunol* 1998;**101**:772–7.
30. Pence HL, Mitchell DQ, Greely RL, Updegraff BR, Selfridge HA. Immunotherapy for mountain cedar pollinosis: a double-blind controlled study. *J Allergy Clin Immunol* 1976;**58**:39–50.
31. Ramirez DA. The natural history of mountain cedar pollinosis. *J Allergy Clin Immunol* 1984;**73**:88–93.
32. Tas J. Hayfever due to the pollen of *Cupressus sempervirens*, Italian or Mediterranean cypress. *Acta Allergol* 1965;**20**:405–7.
33. Panzani R, Centanni G, Brunel M. Increase of respiratory allergy to the pollens of cypresses in the South of France. *Ann Allergy* 1986;**56**:460–3.
34. Ivanciuc O, Midoro-Horiuti T, Schein CH, Xie L, Hillman GR, Goldblum RM, et al. The property distance index PD predicts peptides that cross-react with IgE antibodies. *Mol Immunol* 2009;**46**:873–83.
35. Masuda K, Tsujimoto H, Fujiwara S, Kurata K, Hasegawa A, Taniguchi Y, et al. IgE-reactivity to major Japanese cedar (*Cryptomeria japonica*) pollen allergens (Cry j 1 and Cry j 2) by ELISA in dogs with atopic dermatitis. *Vet Immunol Immunopathol* 2000;**74**:263–70.
36. Fujimura T, Kawamoto S. Spectrum of allergens for Japanese cedar pollinosis and impact of component-resolved diagnosis on allergen-specific immunotherapy. *Allergol Int* 2015;**64**:312–20.

Allergology International 64 (2015) 181–186

Contents lists available at ScienceDirect

Allergology International

journal homepage: http://www.elsevier.com/locate/alit

Original article

Japanese Society of Allergology task force report on standardization of house dust mite allergen vaccines – Secondary publication☆

Toshiro Takai [a, b], Yoshitaka Okamoto [a, c], Kimihiro Okubo [a, d], Makoto Nagata [a, e, f], Masahiro Sakaguchi [a, g], Yuma Fukutomi [a, h], Akemi Saito [h], Hiroshi Yasueda [a, h], Keisuke Masuyama [a, i, *]

[a] *Task Force for House Dust Mite Allergen Standardization of the Committee for Allergens and Immunotherapy of the Japanese Society of Allergology, Tokyo, Japan*
[b] *Atopy (Allergy) Research Center, Juntendo University Graduate School of Medicine, Tokyo, Japan*
[c] *Department of Otorhinolaryngology-Head and Neck Surgery, Graduate School of Medicine, Chiba University, Chiba, Japan*
[d] *Department of Head and Neck Sensory Organ Science (Otolaryngology), Graduate School of Medicine, Nippon Medical School, Tokyo, Japan*
[e] *Department of Respiratory Medicine, Saitama Medical University, Saitama, Japan*
[f] *Allergy Center, Saitama Medical University, Saitama, Japan*
[g] *Laboratory of Microbiology I, School of Veterinary Medicine, Azabu University, Kanagawa, Japan*
[h] *Clinical Research Center for Allergy and Rheumatology, Sagamihara National Hospital, Kanagawa, Japan*
[i] *Department of Otorhinolaryngology-Head and Neck Surgery, Interdisciplinary Graduate School of Medicine and Engineering, University of Yamanashi, Yamanashi, Japan*

ARTICLE INFO

Article history:
Received 13 November 2014
Received in revised form
21 December 2014
Accepted 6 January 2015
Available online 4 March 2015

Keywords:
House dust mite allergen standardization
Intradermal testing
In vivo allergenic potency
Major allergen content
Surrogate *in vitro* assay

Abbreviations:
AU, allergy unit; BAU, bioequivalent allergy unit; CBER, Center for Biologics Evaluation and Research; Der 1, Der p 1 and Der f 1; Der 2, Der p 2 and Der f 2; DF, *Dermatophagoides farinae*; DP, *Dermatophagoides pteronyssinus*; FDA, Food and Drug Administration; HDM, house dust mite; JAU, Japanese allergy unit; JCP, Japanese cedar pollen; JSA, Japanese Society of Allergology; UAS, universal allergen standard

ABSTRACT

Background: In the 1990s, the Japanese Society of Allergology (JSA) standardized Japanese cedar pollen allergen vaccines. In the present study, the task force for house dust mite (HDM) allergen standardization of the Committee for Allergens and Immunotherapy of JSA reports the standardization of HDM allergen vaccines in Japan.
Methods: In vivo allergenic potency was determined by intradermal testing of 51 Japanese adults with positive serum specific IgE to HDM allergens. *In vitro* total IgE binding potency was analyzed by competition ELISA using a pooled serum, with sera obtained from 10 allergic patients. The amounts of HDM group 1 (Der 1) and group 2 major allergens in eight HDM allergen extracts were measured by sandwich ELISAs. Correlation between the *in vitro* total IgE binding potency and major allergen levels was analyzed.
Results: We selected a JSA reference HDM extract and determined its *in vivo* allergenic potency. The *in vitro* total IgE binding potency significantly correlated with Der 1 content, group 2 allergen content, and their combined amount, indicating that measurement of major allergen contents can be used as a surrogate *in vitro* assay.
Conclusions: The task force determined the *in vivo* allergenic potency (100,000 JAU/ml) and Der 1 content (38.5 μg/ml) of the JSA reference HDM extract, selected the measurement of Der 1 content as the surrogate *in vitro* assay, and decided that manufacturers can label a HDM allergen extract as having a titer of 100,000 JAU/ml if it contains 22.2–66.7 μg/ml of Der 1.

☆ This article is a secondary publication of "Japanese Society of Allergology task force report on standardization of house dust mite allergen vaccines" published in *Arerugi [Japanese Journal of Allergology]* 2014; 63: 1229-40 (in Japanese).

* Corresponding author. Department of Otorhinolaryngology-Head and Neck Surgery, Interdisciplinary Graduate School of Medicine and Engineering, University of Yamanashi, Yamanashi 409-3898, Japan.
E-mail address: mkeisuke@yamanashi.ac.jp (K. Masuyama).
Peer review under responsibility of Japanese Society of Allergology.

http://dx.doi.org/10.1016/j.alit.2015.01.005

Introduction

Allergen-specific immunotherapy has been performed in general medical practice since it was first described by Noon in 1911.[1–7] Standardization of allergen vaccines/extracts used for therapy and diagnosis is necessary because their qualities are variable depending on production methods and manufactured lots.[3–5,8–10] In the United States, allergen standardization is based on intradermal testing of allergic patients and the potencies of lots are determined by appropriate surrogate *in vitro* assays, which are based on inhibition of binding of IgE from pooled allergic sera to solid phase reference allergen extracts, or measurement of specific allergen contents in the allergen vaccines.[8] In the European Union, products are standardized using manufacturers' in-house references and labeled in manufacturer-specific units.[9] In Japan, the Japanese Society of Allergology (JSA) standardized Japanese cedar pollen (JCP) allergen vaccines.[11,12] *In vivo* allergenic potency of the JSA reference JCP extract was determined by intradermal testing and measurement of the content of the major allergen Cry j 1 was selected as the surrogate *in vitro* assay.

House dust mites (HDMs) are a major allergen source that provokes allergic rhinitis, asthma, conjunctivitis, and atopic dermatitis.[13,14] However, standardization of HDM allergen vaccines/extracts based on intradermal testing in Japanese subjects with positive serum specific IgE to HDM allergens has not been performed. This report, produced by the task force for HDM allergen standardization of the Committee for Allergens and Immunotherapy of JSA, selected a JSA reference HDM extract, determined its *in vivo* allergenic potency in Japanese allergy units (JAU) by intradermal testing of HDM-sensitized Japanese adults, and determined a surrogate *in vitro* assay that is suitable for HDM allergen standardization in Japan.

Methods

HDM allergen extracts

Each HDM extract was prepared as a mixture of equivalent volumes of extracts from two mite species, *Dermatophagoides pteronyssinus* (DP) and *Dermatophagoides farinae* (DF). United States Food and Drug Administration (FDA) reference extracts, E11-DP (10,000 AU/ml) and E10-DF (10,000 AU/ml), were acquired from the Laboratory of Immunobiochemistry, Division of Bacterial, Parasitic and Allergenic Products, Office of Vaccines Research and Review, Center for Biologics Evaluation and Research (CBER), FDA. Commercial extracts for subcutaneous immunotherapy (DP: lot#B3117094 and DF: lot#F21G6279, 10,000 AU/ml) were purchased from Hollister-Stier (Spokane, WA, USA). Five extracts identified by alphabet letters (Extracts A–E) were obtained from ALK-Abelló AS (Hørsholm, Denmark) and Stallergenes SA (Antony, France). JSA chose an extract other than those described above as the JSA reference HDM extract. Measurement of group 1 allergens and *in vitro* relative IgE binding potency testing took place in the laboratories of Sagamihara National Hospital (Laboratory 1) and Azabu University (Laboratory 2). Measurement of the combined total content of group 2 allergens was conducted only in Laboratory 1.

HDM-sensitized subjects

Inclusion criteria for the HDM-sensitized subjects enrolled in this study were: Japanese adults between the age of 20 and 50 years who were positive for DP or DF-specific IgE, showing ≥0.70 Ua/ml (class 2) in ImmunoCAP assay (ThermoFisher Scientific, Uppsala, Sweden). Subjects were excluded from the study if they had (a) skin disease on the forearm that affects intradermal injection reactions; (b) used (1) external application of medication within one day of study initiation, (2) oral antihistamine, oral α- or β-adrenergic agonists, and topical corticosteroid or immunosuppressive medicine for external application to the injection site within one week of study initiation, (3) tricyclic antidepressants and phenothiazines with an antihistamine effect within 2 weeks of study initiation, (4) non-selective β-adrenergic blockers within 3 weeks of study initiation, (5) systemic immunosuppressive drugs within 30 days of study initiation, (6) specific antibodies within 90 days of study initiation; or if they were (c) pregnant or were possibly pregnancy on the study day; were under (d) HDM-specific immunotherapy; or had (e) severe bronchial asthma; (f) anaphylaxis to adrenaline; (g) concomitant systemic diseases such as cardiac, hepatic, renal, and hematologic disorders or infection that could affect the study trial; or (h) were judged by the examiners as being inappropriate for study enrollment.

Intradermal testing and collection of sera were conducted at the Department of Otorhinolaryngology—Head and Neck Surgery of Chiba University Graduate School of Medicine, Department of Otorhinolaryngology of Nippon Medical School, Graduate School of Medicine, Department of Respiratory Medicine of Saitama Medical University, and Department of Otorhinolaryngology—Head and Neck Surgery of the University of Yamanashi Interdisciplinary Graduate School of Medicine and Engineering. The ethical review committee of each institution approved the protocol of this study. Written informed consent was obtained from all patients before study enrollment and anonymity was preserved using documents and methods approved by the ethical review committees.

Intradermal testing

First, we selected a candidate HDM extract as the JSA reference HDM extract to be used for intradermal testing. The candidate extract was diluted using the 0.005% Polysorbate 80-added control solution for intradermal skin testing, "TORI-I", which contained 0.9% (w/v) NaCl and 0.5% (w/v) phenol (Torii Pharmaceutical, Tokyo, Japan). The dilution factors were from 3^7 to 3^{19} ($2187–1.162 \times 10^9$). Control solution for intradermal skin testing, "TORI-I", was used as the negative control.

Intradermal testing was performed according to a previously described method.[11,12] The protocol for intradermal testing was largely based on the FDA protocol except for criteria for determining the threshold concentration. Briefly, 20 μl of each diluted HDM extract was administered intradermally into the forearm from low to high concentrations using 1-ml tuberculin syringes. Fifteen minutes after the injection, the diameters of the wheal or erythema were measured based on Ishizaki's criteria[15–17] (*i.e.* positive reaction is defined as presence of a wheal or erythematous skin reaction with a diameter of more than 9 mm or 20 mm, respectively). The threshold dilution factor was defined as the maximum dilution factor of diluted extract that can induce a positive reaction.

With respect to the determination of *in vivo* allergenic potency, threshold values of all patients were represented as logarithms that have 3 as the base of the threshold dilution factors, and then an average value for them was calculated. Values, which were from 9 to 11, 11 to 13, and 13 to 15, were assigned the *in vivo* allergenic potencies of 1000 JAU/ml, 10,000 JAU/ml, and 100,000 JAU/ml, respectively, based on the plan used in the standardization of JCP allergen vaccines.[11,12] With this method, the same titer could be assigned to extracts with, at the most, a 3^2-fold (9-fold) difference in allergenic potencies.

Measurement of HDM group 1 major allergens

The group 1 allergens, Der p 1 and Der f 1, in the HDM extracts were measured by a previously described method.[18] Briefly,

sandwich ELISAs for Der p 1 or Der f 1 were performed using murine monoclonal antibodies and 92-*Dp* or 92-*Df* extract,[18,19] respectively, as the standard antigen for ELISA. Previously, the 92-*Dp* and 92-*Df* extracts were prepared from HDM bodies and the contents of group 1 and group 2 allergens in 92-*Dp* and 92-*Df* were determined.[18,19] For validation of the measurement obtained by this method, group 1 allergen content was also determined using other ELISA kits purchased from Indoor Biotechnologies (Charlottesville, VA, USA) and Nichinichi Pharmaceutical (Mie, Japan).

Measurement of the total amount of HDM group 2 major allergens

The total amount of group 2 allergens (Der 2), Der p 2 and Der f 2, was measured using a previously described method.[20,21] Briefly, a sandwich ELISA for Der 2 was performed using rabbit polyclonal antibodies and a mixture of 92-*Dp* and 92-*Df* extracts[18,19] as the standard antigen for ELISA.

Sera for in vitro relative IgE binding potency testing

A total of 20 ml of blood sample was taken from 10 randomly selected patients out of 19 who had ≥17.5 Ua/ml (class 4) for DP- or DF-specific IgE in the ImmunoCAP assay (ThermoFisher). Blood samples were centrifuged and sera were separated and stored at −80 °C. A pooled serum was prepared as a mixture of equivalent volumes of the 10 sera.

In vitro relative IgE binding potency testing

Competition ELISA was used to evaluate the inhibition of allergen-specific IgE binding as described previously.[22] Briefly, the plates were coated with the JSA reference HDM extract or another extract (Extract C). The pooled serum (dilution factor: 50) was mixed with an equivalent volume of each serially diluted inhibitor extract (final serum dilution factor: 100), and after incubation for 30 min at room temperature, the mixtures were added to the wells of the plates. The allergen-specific IgE binding to plate wells were detected with enzyme-conjugated anti-human IgE and a fluorogenic substrate. Relative potencies of extracts were calculated as ratios of the dilution factors of the extracts that gave half the maximum (50%) fluorescence relative to that of the JSA reference HDM extract.

Statistical analysis

Pearson correlation coefficients for the association between major allergen content and *in vitro* relative IgE binding potency were calculated after logarithmic transformation. $P < 0.05$ was regarded as statistically significant.

Results

Selection of a HDM allergen extract as the JSA reference HDM extract

We selected one extract, which can be used for intradermal testing and would be approved for allergen-specific immunotherapy in Japan, as a candidate for the JSA reference HDM extract. The candidate extract showed appropriate values in terms of *in vivo* allergenic potency and HDM group 1 and 2 major allergen contents, as described below. Accordingly, we selected the candidate extract as the JSA reference HDM extract.

Measurement of in vivo allergenic potency of the JSA reference HDM extract

Fifty-two adults (24 men and 28 women) were enrolled in this study. Their mean age (±SD) was 32.9 (±6.5) years. Of the 52 participants, 42 (80.7%) were diagnosed with persistent allergic rhinitis and among them, 5 and 4 also had bronchial asthma and allergic rhinitis provoked by JCP, respectively. Another 4 participants had bronchial asthma and 1 had cough variant asthma. One person was excluded from study analysis because the threshold concentration in intradermal testing could not be examined. Fig. 1 shows the frequency and distribution of threshold values of intradermal testing of the 51 subjects. The average (±SD) threshold value was 13.22 (±1.43), which corresponded to 100,000 JAU/ml.

Major allergen contents in the JSA reference HDM extract

The concentrations of HDM group 1 and group 2 allergens in HDM extracts designated as 92-*Dp* and 92-*Df* had been already determined.[18,19] The group 1 and group 2 allergen contents in the JSA reference HDM extract were measured by sandwich ELISAs using the 92-*Dp* and/or 92-*Df* extract as the standard antigen for ELISA (Table 1). Measurement of the group 1 allergens produced similar results in the two laboratories. The concentrations of Der p 1, Der f 1, and total concentration of Der p 1 and Der f 1 (Der 1) in the JSA reference HDM extract were (as the geometric means of the values obtained in the two laboratories) 25.6, 12.9, and 38.5 μg/ml, respectively. The total concentration of Der p 2 and Der f 2 (Der 2) measured in Laboratory 1 was 55.5 μg/ml.

Validation of measurement of Der p 1 and Der f 1

Other ELISA systems were used to validate the measurement of Der p 1 and Der f 1 in this study (Table 2). Similar results were obtained using two commercially available ELISA kits. Lower values (approximately 20% less) were obtained with the kit purchased from Indoor Biotechnologies. The standard used in the kit is designated as an "universal" allergen standard (UAS), which was developed in the CREATE project funded through the European Union.[23,24] Regardless of whether the monoclonal antibodies were in the kit from Indoor Biotechnologies or developed in Laboratory 1, use of UAS as the standard antigen for ELISA resulted in lower

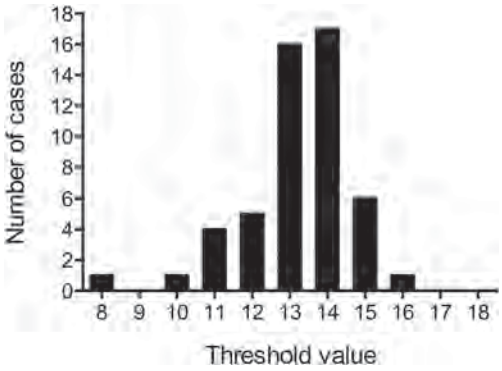

Figure 1. Distribution of the threshold values that induced positive reactions in the intradermal testing of 51 Japanese adults with positive serum specific IgE to house dust mite allergens. Prepared dilution factors of the Japanese Society of Allergology reference house dust mite extract were from 3^7 (2187) to 3^{19} (1.162×10^9). A total of 20 μl of each diluted extract was administered intradermally into the forearm from low to high concentrations. The diameters of the wheal or erythematous skin reaction were measured 15 min after the injection. *Threshold value*: the exponent of the maximum dilution factor that can induce a positive reaction in each subject.

Table 1
House dust mite major allergen content in the Japanese Society of Allergology reference house dust mite extract.

	Concentration (μg/ml)			
	Group 1 allergens			Group 2 allergens
Institute	Der p 1	Der f 1	Der 1	Der 2
Laboratory 1	28.2	14.1	42.3	55.5
Laboratory 2	23.2	11.8	35.0	N.D.
Geometric mean	25.6	12.9	38.5	

Der p 1, Der f 1, and Der 2 were measured by sandwich ELISA in two institutes. Der 1, combined total of Der p 1 and Der f 1; Der 2, combined total of Der p 2 and Der f 2; Laboratory 1, Sagamihara National Hospital; Laboratory 2, Azabu University; N.D., not determined.

values compared with the use of 92-*Dp* or 92-*Df*. This suggests that the small discrepancy was caused by the difference in the defined concentrations of Der p 1 and Der f 1 between 92-*Dp*/92-*Df* and UAS and was not due to the detection system, such as specificity of monoclonal antibodies. The results indicated that the ELISA system for Der p 1 and Der f 1 developed in Laboratory 1 was valid.

Major allergen contents in the HDM extracts tested

Major allergen contents in the seven HDM extracts other than the JSA reference HDM extract were measured (Table 3). Five extracts were from ALK or Stallergenes (Extract A–E) and two were from CBER/FDA and Hollister-Stier. Similar results were obtained in the two laboratories (Tables 3, 4, concentration).

Correlation between the major allergen contents and in vitro relative IgE binding potencies

Competition ELISA was used to evaluate the inhibition of allergen-specific IgE binding to plates coated with the JSA reference HDM extract or Extract C. A pooled serum was prepared as a mixture of equivalent volumes of sera from 10 of 19 patients who had ≥17.5 Ua/ml (class 4) for DP- or DF-specific IgE in the ImmunoCAP assay. The *in vitro* total IgE binding potencies of the HDM extracts relative to the JSA reference HDM extract were determined (Tables 3, 4, *in vitro* relative potency). Similar results were obtained using JSA reference HDM extract-coated plates and Extract C-coated plates. Similar results were obtained in the two laboratories.

Correlation between major allergen contents and the relative IgE binding potency was analyzed. The relative IgE binding potency correlated well with each of the concentrations of Der 1 (Figs. 2, 3), Der 2, and combined total of Der 1 and Der 2 (Der 1 + Der 2) (Fig. 2). Pearson correlation coefficients were greater than 0.9 and were statistically significant.

Table 2
Comparison of house dust mite group 1 allergen contents in the Japanese Society of Allergology reference house dust mite extract determined by sandwich ELISAs using different antibodies and standards.

Institute	ELISA		Concentration (μg/ml)		
	Antibodies[†]	Standard[‡]	Der p 1	Der f 1	Der 1
Lab1	Lab1	92-*Dp*/92-*Df*	28.2	14.1	42.3
	Lab1	UAS	22.1	9.69	31.8
	Indoor	92-*Dp*/92-*Df*	27.4	14.6	42.0
	Indoor	UAS	22.3	11.7	34.0
	Nichinichi	Nichinichi	24.3	13.6	37.9
Lab2	Lab1	92-*Dp*/92-*Df*	23.2	11.8	35.0
	Indoor	92-*Dp*/92-*Df*	22.1	14.0	36.1

Der p 1 and Der f 1 were measured by sandwich ELISA in two institutes.
Der 1, combined total of Der p 1 and Der f 1; Lab1, Sagamihara National Hospital; Lab2, Azabu University; UAS, universal allergen standard; Indoor, Indoor Biotechnologies; Nichinichi, Nichinichi Pharmaceutical.
[†] Capture and detection antibodies used in ELISA.
[‡] Standards with defined concentrations used in ELISA.

Discussion

In the 1990s, JSA standardized the JCP allergen vaccines/extracts.[11,12] The JSA standard JCP extract showed an *in vivo* allergenic potency of 10,000 JAU/ml. The unit JAU[11,12] was determined by intradermal testing, similar to the bioequivalent allergy unit (BAU) and the allergy unit (AU) defined by FDA,[8,25–27] but criteria for the reaction threshold are different between JAU and BAU/AU, and the injection volume is 20 μl for JAU and 50 μl for BAU/AU. JSA selected measurement of Cry j 1 content as the surrogate *in vitro* assay for determining the potencies of other JCP extracts, with the concentration of 12.5 μg/ml of Cry j 1 corresponding to 10,000 JAU/ml. JSA decided that manufacturers can label JCP extracts as having a titer of 10,000 JAU/ml if they contain 7.3–21 μg/ml of Cry j 1 *i.e.*, within a range that is approximately three times the lowest value, the geometric center of which is 12.5 μg/ml.[11,12] In the present study, the task force selected a JSA reference HDM extract, determined its *in vivo* allergic potency in JAU using the same method for JCP allergen standardization, and analyzed the correlation between the *in vitro* total potency determined by IgE binding inhibition ELISA and the major allergen contents in eight HDM extracts.

Through intradermal testing of 51 Japanese HDM-sensitized adults, the *in vivo* allergenic potency of the candidate for the JSA reference HDM extract was determined as 100,000 JAU/ml. As the candidate extract showed an appropriate *in vivo* allergenic potency (Fig. 1) and major allergen contents (Table 1), we decided to use it as the JSA reference HDM extract. Surrogate *in vitro* assay to determine the potencies of extracts from different manufacturers and lots can be based on inhibition of binding of IgE from pooled allergic sera to a reference allergen extract, or measurement of specific allergen contents in the allergen vaccines/extracts. In the United States, FDA adopted relative IgE binding potency determined by IgE binding inhibition assay for HDM and mold allergen vaccines; specific allergen contents for short ragweed pollen and cat allergen vaccines (Amb a 1 and Fel d 1, respectively); and enzymatic activity (hyaluronidase and phospholipases) for Hymenoptera venom allergen vaccines.[8] It has been reported that the major allergen content correlates with the relative IgE binding potency.[28–30] Among more than 20 groups of HDM allergens, group 1 and 2 allergens are considered the major allergens, although some reports showed that other HDM allergens were also important, albeit less so than the major allergens.[13,14] We judged that measurement of HDM major allergens is appropriate as a surrogate assay because the relative IgE binding potency correlated well with each of the major allergen contents (Figs. 2, 3).

The *in vitro* measurement of major allergen content has some advantages as the surrogate assay for allergen standardization *i.e.*, it can determine absolute and not relative values, and does not need sera in which differing individual titers are seen. Species-specific ELISAs using monoclonal antibodies to measure each HDM group 1 allergen, Der p 1 and Der f 1, with high accuracy are available commercially (see the Methods section). However, those for each group 2 allergen, Der p 2 and Der f 2, are not widely available, and the total contents of Der p 2 and Der f 2 (Der 2) determined by ELISA using polyclonal antibodies in the present study are approximate values. Therefore, we selected measurement of the total content of Der p 1 and Der f 1 (Der 1) as the surrogate *in vitro* assay. We determined that the *in vivo* allergenic potency and Der 1 content of the JSA reference HDM extract were 100,000 JAU/ml and 38.5 μg/ml, respectively. Similar to the previous JCP allergen standardization,[11,12] we decided that manufacturers can label an HDM allergen

Table 3
House dust mite major allergen contents and *in vitro* total IgE binding potencies of the eight house dust mite extracts determined in Laboratory 1.

Sample	Concentration (μg/ml)[†]					*In vitro* relative potency[‡]	
	Der p 1	Der f 1	Der 1	Der 2	Der 1 + Der 2	JSA coating	Extract C coating
JSA	28.2	14.1	42.3	55.5	97.8	1.00	1.00
CBER/FDA	16.7	16.3	33.0	19.6	52.6	0.56	0.51
Hollister-Stier	10.1	2.54	12.6	11.3	23.9	0.35	0.33
Extract A	80.0	54.2	134	254	388	4.89	4.85
Extract B	2.69	0.98	3.67	6.76	10.4	0.14	0.13
Extract C	30.9	52.7	83.6	45.8	129	1.83	2.54
Extract D	3.59	2.50	6.09	2.38	8.47	0.08	0.16
Extract E	2.27	5.45	7.72	3.28	11.0	0.15	0.26

Der 1, combined total of Der p 1 and Der f 1; Der 2, combined total of Der p 2 and Der f 2; JSA, JSA reference house dust mite extract.
[†] Der p 1, Der f 1, and Der 2 were measured by sandwich ELISA.
[‡] *In vitro* total IgE binding potency relative to the Japanese Society of Allergology (JSA) reference house dust mite extract was determined on the basis of the results of a competition ELISA that measures the inhibition of allergen-specific IgE binding to plates coated with the JSA reference house dust mite extract (JSA coating) or Extract C (Extract C coating).

extract as having a titer of 100,000 JAU/ml if it contains 22.2–66.7 μg/ml of Der 1 *i.e.*, within a range that is approximately three times the lowest value, the geometric center of which is 38.5 μg/ml.

We validated the measurement of Der p 1 and Der f 1 (Table 2). The amounts of group 1 and group 2 allergens in 92-*Dp* and 92-*Df* extracts were determined previously in Laboratory 1[18, 19]. The measurement of the concentrations of purified group 1 and group 2 allergens previously used as the standard antigens for the ELISA that determine the major allergen contents in 92-*Dp* and 92-*Df* were based on absorbance at 280 nm. UAS is composed of eight purified allergens (Der p 1, Der f 1, Der p 2, Fel d 1, Can f 1, Rat n 1, Mus m 1, and Bla g 2) and the concentrations of the allergens were determined by amino acid analysis.[23,24] The difference in the original methods for determining the concentrations of the standard antigens for ELISA might have caused the lower values (approximately 20% less) obtained by the Indoor Biotechnologies kit compared with the ELISA developed in Laboratory 1 (Table 2).

In conclusion, the task force (1) selected the JSA reference HDM extract and determined its *in vivo* allergenic potency via intradermal testing, (2) showed the correlation between *in vitro* IgE binding potency and major allergen contents, and selected measurement of Der 1 content as the surrogate *in vitro* assay for determining the potencies of other HDM extracts by defining 38.5 μg/ml of Der 1 as 100,000 JAU/ml. Furthermore, (3) the task force decided that manufacturers can label a HDM allergen extract as having a titer of 100,000 JAU/ml if it contains 22.2–66.7 μg/ml of Der 1 *i.e.*, within a range that is approximately three times the lowest value. Der 1 contents can be measured by appropriate methods such as commercially available sandwich ELISAs (see the Methods section). JSA is planning to store and distribute the JSA reference HDM extract. The manufacturers of HDM allergen vaccines would find

Table 4
House dust mite group 1 allergen contents and *in vitro* total IgE binding potencies of the eight house dust mite extracts determined in Laboratory 2.

Sample	Concentration (μg/ml)			*In vivo* relative potency	
	Der p 1	Der f 1	Der 1	JSA coating[†]	Extract C coating[‡]
JSA	23.2	11.8	35.0	1.00	1.00
CBER/FDA	17.6	13.2	30.8	0.71	0.75
Hollister-Stier	9.25	1.79	11.0	0.34	0.34
Extract A	80.5	49.5	130	5.75	5.71
Extract B	2.28	0.93	3.21	0.14	0.14
Extract C	38.8	54.2	93.0	1.47	2.11
Extract D	3.40	4.08	7.48	0.11	0.16
Extract E	2.24	6.87	9.11	0.12	0.20

Der 1, combined total of Der p 1 and Der f 1; Der 2, combined total of Der p 2 and Der f 2; JSA, JSA reference house dust mite extract.
[†] Der p 1, Der f 1, and Der 2 were measured by sandwich ELISA.
[‡] *In vitro* total IgE binding potency relative to the Japanese Society of Allergology (JSA) reference house dust mite extract was determined on the basis of the results of a competition ELISA that measures the inhibition of allergen-specific IgE binding to plates coated with the JSA reference house dust mite extract (JSA coating) or Extract C (Extract C coating).

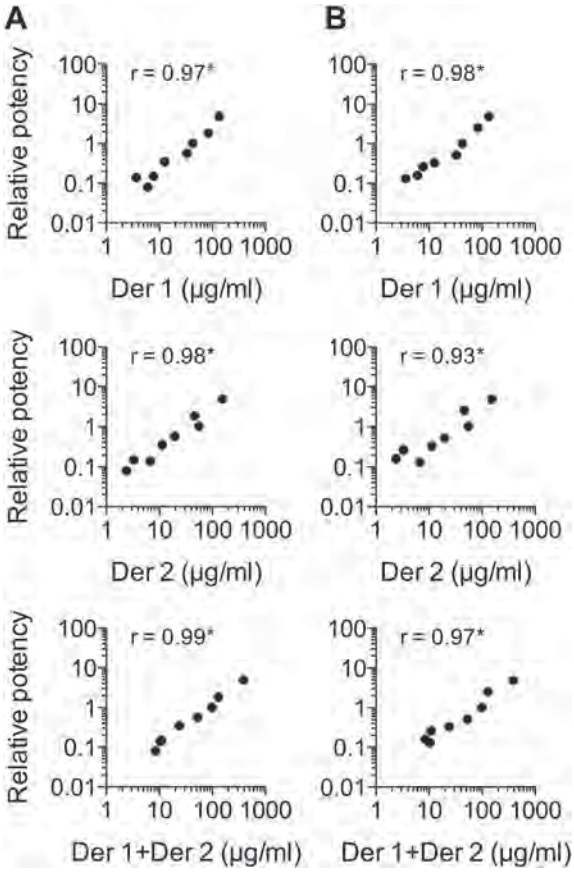

Figure 2. Correlation between house dust mite major allergen contents and *in vitro* total IgE binding potencies of the eight house dust mite extracts determined in Laboratory 1. The values in Table 3 were used for the analysis. *In vitro* total IgE binding potency relative to the Japanese Society of Allergology (JSA) reference house dust mite extract was determined based on the results of the competition ELISA that measured the inhibition of allergen-specific IgE binding to plates coated with the JSA reference house dust mite extract (A) or Extract C (B). r: Pearson correlation coefficient. *$p < 0.01$.

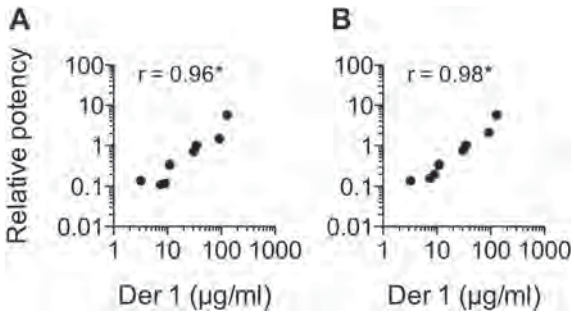

Figure 3. Correlation between house dust mite group 1 allergen contents and *in vitro* total IgE binding potencies of the eight house dust mite extracts determined in Laboratory 2. The values in Table 4 were used for the analysis. *In vitro* total allergenic potency relative to the Japanese Society of Allergology (JSA) reference house dust mite extract was determined based on the results of the competition ELISA that measured the inhibition of allergen-specific IgE binding to plates coated with the JSA reference house dust mite extract (A) or Extract C (B). r: Pearson correlation coefficient. $^{*}p < 0.01$.

the HDM extract useful as the standard antigen for ELISAs that measure the amounts of Der p 1 and Der f 1.

Acknowledgments

The authors thank CBER/FDA for supplying FDA reference HDM extracts and FDA reference HDM-allergic serum; ALK-Abelló AS and Stallergenes SA for supplying HDM allergen extracts; and Torii Pharmaceutical Co., Ltd. and Shionogi & Co., Ltd. for their communication with ALK-Abelló AS and Stallergenes SA, respectively.

This work was financially supported by a Grant-in-Aid for Scientific Research from the Ministry of Heath, Labour, and Welfare of Japan (Immunologic and Allergic Diseases Prevention and Treatment Research Enterprise, Immunology and Allergy Research Field, H25-General-007) (Group Leader: Kimihiro Okubo) and the Japanese Society of Allergology.

Conflict of interest

YO received lecture fees from Torii, Shionogi, Kyowa Kirin, MSD, GlaxoSmithKline (GSK), and Kyorin, and research funding from the Japanese Rhinologic Society and GSK. KO received lecture fees from Torii, GSK, MSD, Mitsubishi Tanabe, Ono, and Kyowa Kirin, and research funding from GSK. MN received lecture fees from MSD and AstraZeneca. KM received lecture fees from GSK, MSD, and Torii, and research funding from GSK.

Authors' contributions

TT: study design and interpretation of the *in vitro* study, and drafting and revision of the manuscript; YO, KO, MN, and KM: study design, data acquisition, analysis and interpretation of intradermal testing, and drafting and revision of the manuscript; MS, YF, and HY: study design, data acquisition, analysis and interpretation of the *in vitro* study, and drafting and revision of the manuscript; AS: data acquisition and analysis of the *in vitro* study.

References

1 Noon L. Prophylactic inoculation against hayfever. *Lancet* 1911:1572–3.
2 Okamoto Y, Ohta N, Okano M, Kamijo A, Gotoh M, Suzuki M, et al. Guiding principles of subcutaneous immunotherapy for allergic rhinitis in Japan. *Auris Nasus Larynx* 2014;**41**:1–5.
3 [WHO position paper. "Allergen immunotherapy: therapeutic vaccines for allergic diseases"]. *Arerugi [Jpn J Allergol]* 1998; **47**:698–704 (in Japanese).
4 Bousquet J, Lockey R, Malling HJ. Allergen immunotherapy: therapeutic vaccines for allergic diseases. A WHO position paper. *J Allergy Clin Immunol* 1998;**102**:558–62.
5 WHO position paper. Allergen immunotherapy: therapeutic vaccines for allergic diseases. Geneva: January 27-29 1997. *Allergy* 1998; **53**:1–42.
6 Nelson HS. Allergen immunotherapy: where is it now? *J Allergy Clin Immunol* 2007;**119**:769–79.
7 Burks AW, Calderon MA, Casale T, Cox L, Demoly P, Jutel M, et al. Update on allergy immunotherapy: American Academy of Allergy, Asthma & Immunology/European Academy of Allergy and Clinical Immunology/PRACTALL consensus report. *J Allergy Clin Immunol* 2013;**131**:1288–96.
8 Slater JE. Standardized allergen vaccines in the United States. *Clin Allergy Immunol* 2008;**21**:273–81. e3.
9 Larsen JN, Houghton CG, Vega ML, Lowenstein H. Manufacturing and standardizing allergen extracts in Europe. *Clin Allergy Immunol* 2008;**21**:283–301.
10 Esch RE, Plunkett GA. Immunotherapy preparation guidelines, rules, and regulation. *Curr Allergy Asthma Rep* 2013;**13**:406–13.
11 Yasueda H, Okuda M, Yoshida H, Ito K, Baba M, Iikura Y, et al. [Guidelines for standardization of allergens and cedar pollen allergen extract in Japan]. *Arerugi [Jpn J Allergol]* 1996;**45**:416–21 (in Japanese).
12 Yasueda H, Okuda M, Yoshida H, Ito K, Baba M, Iikura Y, et al. A basic policy for allergen standardization in our country and standardization of Japanese cedar (*Cryptomeria japonica*) pollen extracts). *Allergol Int* 1997;**46**:135–40.
13 Fernandez-Caldas E, Puerta L, Caraballo L, Lockey RF. Mite allergens. *Clin Allergy Immunol* 2008;**21**:161–82.
14 Thomas WR, Hales BJ, Smith WA. House dust mite allergens in asthma and allergy. *Trends Mol Med* 2010;**16**:321–8.
15 Ishizaki T. [Studies on the immediate intracutaneous reaction, with special reference to positive standards of judgment]. *Arerugi [Jpn J Allergol]* 1963;**12**:14–30 (in Japanese).
16 Fujieda S, Kurono Y, Okubo K, Ichimura K, Enomoto T, Kawauchi H, et al. Examination, diagnosis and classification for Japanese allergic rhinitis: Japanese guideline. *Auris Nasus Larynx* 2012;**39**:553–6.
17 Okubo K, Kurono Y, Fujieda S, Ogino S, Uchio E, Odajima H, et al. Japanese guideline for allergic rhinitis 2014. *Allergol Int* 2014;**63**:357–75.
18 Yasueda H, Saito A, Akiyama K, Maeda Y, Shida T, Sakaguchi M, et al. Estimation of *Der p* and *Der f* I quantities in the reference preparations of *Dermatophagoides* mite extracts. *Clin Exp Allergy* 1994;**24**:1030–5.
19 Yasueda H, Saito A, Yanagihara Y, Akiyama K, Takaoka M. Species-specific measurement of the second group of *Dermatophagoides* mite allergens, Der p 2 and Der f 2, using a monoclonal antibody-based ELISA. *Clin Exp Allergy* 1996;**26**:171–7.
20 Yasueda H, Mita H, Yui Y, Shida T. Measurement of allergens associated with dust mite allergy. I. Development of sensitive radioimmunoassays for the two groups of *Dermatophagoides* mite allergens, *Der* I and *Der* II. *Int Arch Allergy Appl Immunol* 1989;**90**:182–9.
21 Yasueda H, Akiyama K, Maeda Y, Hayakawa T, Kaneko F, Hasegawa M, et al. [An enzyme-linked immunosorbent assay (ELISA) for the quantitation of sugi pollen and *Dermatophagoides* mite allergens and its application for standardization of allergen extracts]. *Arerugi [Jpn J Allergol]* 1991;**40**:1218–25 (in Japanese).
22 Sakaguchi M, Hashimoto M, Nigi H, Yasueda H, Takahashi Y, Watanabe M, et al. Epitope specificity of IgE antibodies to a major allergen (Cry j 1) of Japanese cedar pollen in sera of humans and monkeys with pollinosis. *Immunology* 1997;**91**:161–6.
23 Filep S, Tsay A, Vailes LD, Gadermaier G, Ferreira F, Matsui E, et al. Specific allergen concentration of WHO and FDA reference preparations measured using a multiple allergen standard. *J Allergy Clin Immunol* 2012;**129**:1408–10.
24 Filep S, Tsay A, Vailes L, Gadermaier G, Ferreira F, Matsui E, et al. A multiallergen standard for the calibration of immunoassays: CREATE principles applied to eight purified allergens. *Allergy* 2012;**67**:235–41.
25 Liu D. Regulation of allergenic products in the USA: CBER initiatives. In: Kurth R, Haustein D, editors. *Regulatory Control and Standardization of Allergic Extracts (Seventh Paul Ehlich Seminar)*, 4th ed. Stuttgart: Gustav Fischer Verlag, 1994;7–12.
26 Turkeltaub PC. Allergen extracts. II. In vivo standardization. In: Middleton E, Reed CE, Ellis EF, Adkinson NF, Yunginger JW, editors. *Allergy: Principles and Practice*, 3rd ed. St. Louis: Mosby, 1988;388–401.
27 Turkeltaub PC, Rastogi SC, Baer H. *Office of Biologics Research and Review Skin Test Method for Evaluation of Subject Sensitivity to Standardized Allergenic Extracts and for Assignment of Allergy Units to Reference Preparations Using the ID50EAL Method (Intradermal Dilution for 50 mm Sum of Erythema Determines the Allergy Unit)*, 3rd ed. Bethesda: FDA Publication, 1986;1–12.
28 Baer H, Godfrey H, Maloney CJ, Norman PS, Lichtenstein LM. The potency and antigen E content of commercially prepared ragweed extracts. *J Allergy* 1970;**45**:347–54.
29 van Ree R. Analytic aspects of the standardization of allergenic extracts. *Allergy* 1997;**52**:795–805.
30 Larenas-Linnemann D, Esch R, Plunkett G, Brown S, Maddox D, Barnes C, et al. Maintenance dosing for sublingual immunotherapy by prominent European allergen manufacturers expressed in bioequivalent allergy units. *Ann Allergy Asthma Immunol* 2011;**107**:448–58. e3.

VIROLOGICA SINICA
DOI 10.1007/s12250-015-3580-9

LETTER

Cats as a potential source of emerging influenza virus infections

Dear Editor,

Historically, the influenza virus has not been regarded as a major pathogen of cats. However, since 2003, natural infections of domestic cats with highly pathogenic H5N1 avian virus causing fatal cases have been reported (Songserm et al., 2006; Yingst et al., 2006; Klopfleisch et al., 2007). Furthermore, infections of this animal with A (H1N1) pdm09 virus, causing respiratory illness with some fatal cases, have also been reported in various parts of the world (Fiorentini et al., 2011; Campagnolo et al., 2011; Pigott et al., 2014). These reports revealed that cats are susceptible to influenza A viruses, resulting from bird-to-cat or human-to-cat transmission, and were supported by the detection of several virus subtypes in domestic cats through serological studies (McCullers et al., 2011; Ali et al., 2011; Zhao et al., 2014; Su et al., 2013). In other reports, the H3N2 dog virus was also transmitted to cats in Korea and China, causing respiratory illness (Song et al., 2011; Lei et al., 2012). These findings provide further evidence that cats should be included among the animals that are responsible for interspecies transmission of influenza A virus. Moreover, the findings of these reports suggest that cats may play a role as an intermediate host in which a mutant virus with pandemic potential could emerge. To validate this possibility, here we conducted a serological survey of human and avian influenza virus infections in cats, from either H5N1 virus-endemic or non-endemic areas.

We used a total of 15 serum samples, which were collected from stray cats between April 2010 and February 2012, most of which roamed in the markets where birds are sold on Java Island, Indonesia, which has been an H5N1 virus-endemic area since 2005. Additionally, we tested sera from another group of cats (26 samples), collected from in-door, domestic cats at animal hospital in Kanagawa Prefecture, Japan between April 2009 and July 2010. H5N1 viruses have never been detected before in wild birds, poultry, and mammals including human in this prefecture. The cats were brought to the hospital with various symptoms, and their serum samples were randomly collected for the study with the pet owner's permission. To detect antibodies specific to influenza viruses in the sera, we performed a standard virus-neutralization (VN) test (Horimoto et al., 2011) with human viruses (former seasonal H1N1 virus, seasonal H3N2 virus, A (H1N1) pdm09 virus, and influenza B virus) and H5N1 highly pathogenic avian viruses, after receptor-destroying enzyme treatment (RDEII: Denka) and heat-inactivation (56 °C, 30 min) of the sera to remove non-specific inhibitors. VN antibody titers ≥ 16 were considered positive reactions, because sera with these titers could specifically react to the same viral antigens in an immunoblot assay, confirming the reaction specificity (Horimoto et al., 2011).

In these VN assays, 2 sera (#CP1 and #CP2) of Indonesian cats were positive for the H5N1 virus-specific VN antibody, representing 13.3% positivity (Table 1), although the number of cats tested in the present study may be statistically insufficient to show the exact seroprevalence. VN cross-reactivities to a panel of H5N1 viruses belonging to different clades or subclades revealed that both sera reacted with the highest titers to clade 2.1.3 viruses isolated in Indonesia in 2010, confirming that these stray cats must be infected with the H5N1 virus that spreads endemically in this country. Two H5N1 virus-seropositive cats were found to be roaming in the same market in Jakarta, suggesting that the virus was transmitted to them from the infected poultry, brought into the market from backyard farm, and also that cat-to-cat transmission could occur. Although previous studies including experimentally induced infection (Küiken et al., 2004; Vahlenkamp et al., 2010) showed that H5N1 is a highly pathogenic virus causing systematic infection in cats, asymptomatic or disease-recovered infection was also suggested in another report (Leschnik et al., 2007). The 2 seropositive cats identified in this study fell into the latter category. Notably, another serum sample (#GD7) was positive for VN antibody to A (H1N1) pdm09 virus, albeit a weak reaction, which suggested a human-to-cat transmission of the human virus.

In contrast, sera obtained from Japanese cats were not positive for the VN antibody specific to H5N1 virus; however, 2 sera (#210 and #213) were positive for VN antibody specific to human viruses; one positive for the seasonal H3N2 virus and the other positive for A (H1N1) pdm09 virus. However, none of these seropositive cats showed any typical signs of acute respiratory illness according to the clinical records, suggesting that they were asymptomatic or had minor infections. Nevertheless,

Table 1. Cats seropositive of VN antibodies to influenza viruses.

Country	Sample #	Collection time	Location	Virus										
				H1N1	H1N1 pdm	H3N2	H5N1 cl.1	H5N1/05 cl.2.1.3	H5N1/10 cl.2.1.3	H5N1 cl.2.2	H5N1 cl.2.3.2.1	H5N1 cl.2.3.4	H5N1 cl.2.5	B
Indonesia	GD7	March 2010	Bandung	< 16	16	< 16	ND	< 16	< 16	ND	< 16	ND	< 16	< 16
	CP1	April 2010	Jakarta	< 16	< 16	< 16	< 16	256	512	128	16	128	256	< 16
	CP2	April 2010	Jakarta	< 16	< 16	< 16	< 16	32	64	32	< 16	16	64	< 16
Japan	210	June 2009	Kanagawa	< 16	< 16	32	ND	ND	ND	< 16	ND	ND	ND	< 16
	213	August 2009	Kanagawa	< 16	16	< 16	ND	ND	ND	< 16	ND	ND	ND	< 16

Following influenza virus strains were used for VN test; H1N1, A/Kawasaki/UTK4/09; H1N1pdm, A/Osaka/364/09; H3N2, A/Kawasaki/UTK20/08; H5N1 clade 1, A/Vietnam/1194/04; H5N1 clade 2.1.3, A/Indonesia/3006/05 and A/chicken/East Java/UT551/10; H5N1 clade 2.2, A/whooper swan/Mongolia/4/05; H5N1 clade 2.3.2.1, A/Tundra swan/Tottori/12-002/10; H5N1 clade 2.3.4, A/Hanoi/30850/05; H5N1 clade 2.5, A/chicken/Yamaguchi/8/04; and influenza B virus, B/Tokyo/UT-E2/08. ND: not determined.

human-to-cat transmission of the human virus likely occurred in these in-door pet cats, as reported in other countries (Campagnolo et al., 2011; Pigott et al., 2014).

Based on the findings of the present study, we conclude that cats can be infected with human influenza viruses as well as avian influenza viruses. Actually, the recent study has shown that both human-type (α2,6-linked sialic acid) and avian-type (α2,3-linked sialic acid) influenza virus receptors were extensively detected in the respiratory organs such as trachea, bronchus, and lung of the domestic cats (Wang et al., 2013). Therefore, cats may act as a vector for human influenza virus transmission within households, posing a potential public health concern. Furthermore, we detected both H5N1 and human virus-seropositive cats in neighboring areas at similar sampling times, suggesting that cats can be simultaneously infected with both avian and human viruses in H5N1 virus-endemic areas. Thus, cats, like pigs, may act as an intermediate host for the emergence of new, potentially pandemic viruses. Although our study was a small-scale surveillance of influenza virus infections in cats, these findings evidence the need for continued and large-scale surveillance of influenza viruses in cat populations will be important to achieve the "One Health" concept for this zoonotic disease.

FOOTNOTES

We thank veterinarians at Azabu University for collecting the samples. This work was supported by grants-in-aid for Scientific Research, from the Ministry of Education, Culture, Sports, Science, and Technology, Japan. The authors declare that they have no conflict of interest. Cat serum samples for the study were collected with the pet owner's approval, and the experiments were conducted under the guidelines of the University of Tokyo for animal experiments.

Taisuke Horimoto[1]✉, Fumihiro Gen[1], Shin Murakami[1], Kiyoko Iwatsuki-Horimoto[2], Kentaro Kato[3], Masaharu Hisasue[4], Masahiro Sakaguchi[5], Chairul A. Nidom[6], Yoshihiro Kawaoka[2]

1. Department of Veterinary Microbiology, University of Tokyo, Tokyo 113-8657, Japan
2. Division of Virology, Institute of Medical Science, University of Tokyo, Tokyo 108-8639, Japan
3. National Research Center for Protozoan Diseases, Obihiro University of Agriculture and Veterinary Medicine, Obihiro 080-8555, Japan
4. Department of Internal Medicine II, Azabu University, Sagamihara 252-5201, Japan
5. Department of Veterinary Microbiology I, Azabu University, Sagamihara 252-5201, Japan
6. Avian Influenza Research Center, Airlangga University, Surabaya 60115, Indonesia

✉Correspondence:
Phone: +81-3-5841-5397,
Email: ahorimo@mail.ecc.u-tokyo.ac.jp
ORCID: 0000-0002-9201-9424

Published online: 5 May 2015

REFERENCES

Ali A, Daniels JB, Zhang Y, et al. 2011. J Clin Microbiol, 49:4101–4105.
Campagnolo ER, Rankin JT, Daverio SA, et al. 2011. Zoonoses Public Health, 58:500–507.
Fiorentini L, Taddei R, Moreno A, et al. 2011. Zoonoses Public Health, 58:573–581.
Horimoto T, Maeda K, Murakami S, et al. 2011. Emerg Infect Dis, 17:714–717.
Klopfleisch R, Wolf PU, Uhl W, et al. 2007. Vet Pathol, 44:261–268.
Küiken T, Rimmelzwaan G, van Riel D, et al. 2004. Science, 306:241.
Lei N, Yuan Z, Huang S, et al. 2012. Vet Microbiol, 160:481–483.

Leschnik M, Weikel J, Mostl K, et al. 2007. Emerg Infect Dis, 13:243–247.
McCullers JA, Van De Velde LA, Schultz RD, et al. 2011. Arch Virol, 156:117–120.
Pigott AM, Haak CE, Breshears MA, et al. 2014. J Vet Emerg Crit Care, 24:715–723.
Song DS, An DJ, Moon HJ, et al. 2011. J Gen Virol, 92:2350–2355.
Songserm T, Amonsin A, Jam-on R, et al. 2006. Emerg Infect Dis, 12:681–683.
Su S, Yuan L, Li H, et al. 2013. Clin Vaccine Immunol, 20:115–117.
Vahlenkamp TW, Teifke JP, Harder TC, et al. 2010. Influenza Other Respir Viruses, 4:379–386.
Wang H, Wu X, Cheng Y, et al. 2013. Acta Vet Hung, 61:537–546.
Yingst SL, Saad MD, Felt SA. 2006. Emerg Infect Dis, 12:1295–1297.
Zhao F, Liu C, Yin X, et al. 2014. Virol J, 11:49–52.

Short Communication

Serological evidence of infection of dogs with human influenza viruses in Japan

T. Horimoto, F. Gen, S. Murakami, K. Iwatsuki-Horimoto, K. Kato, H. Akashi, M. Hisasue, M. Sakaguchi, Y. Kawaoka, K. Maeda

HISTORICALLY, influenza virus has not been regarded as a major pathogen of dogs. However, recent infections of racing and pet dogs with H3N8 virus of equine origin in the USA after 2004 (Crawford and others 2005) and retrospectively in the UK in 2002 (Daly and others 2008), as well as with highly pathogenic H5N1 avian virus in Thailand in 2004 (Songserm and others 2006), revealed that dogs are susceptible to influenza A viruses. These infections caused respiratory disease in the dogs and several proved fatal. Moreover, H3N2 virus of avian origin infected pet dogs in Korea in 2007 (Song and others 2008) and China in 2010 (Li and others 2010), supporting the belief that dogs should be included among the animals that are responsible for interspecies transmission of influenza A virus (Kim and others 2013). Furthermore, there were reports in various parts of the world (Dundon and others 2010, Lin and others 2012) of dogs infected with A(H1N1)pdm09 virus of swine origin, possibly due to contact with people infected with this H1N1 virus, suggesting human-to-dog transmission. Together, these reports suggest that dogs may play a role as an intermediate host in which a mutant virus with pandemic potential could emerge. To partially address this possibility, we conducted a serological survey of human influenza virus infection in domestic dogs in Japan.

A total of 366 serum samples were collected from mostly indoor domestic dogs between January 2009 and February 2010 at animal hospitals in the prefectures of Yamaguchi (162 samples) and Kanagawa (204 samples), which are located in western and eastern Japan, respectively. The dogs came to the hospitals with various symptoms, and their serum samples were randomly collected for the study with the pet owners' permission. To detect antibodies specific to human influenza viruses in the sera, we performed a virus-neutralisation (VN) test (Itoh and others 2009) with a former seasonal H1N1 virus (A/Kawasaki/UTK4/09), seasonal H3N2 virus (A/Kawasaki/UTK20/08), A(H1N1)pdm09 virus, and influenza B virus (B/Tokyo/UT-E2/08), after receptor-destroying enzyme treatment and heat-inactivation of the sera to remove non-specific inhibitors. The VN antibody-positive sera (titres ≥10) were then further tested in an immunoblot assay using the same virus antigens to confirm reaction specificity.

In these assays, 14 sera were positive for VN antibody to A(H1N1) pdm09 virus, representing 3.8 per cent positivity (Table 1). One serum sample was also positive for VN antibody to the former seasonal H1N1 virus, but the reaction was weak, suggesting it may have been due to cross-reactivity. Eight other samples were seropositive to seasonal H3N2 virus, representing 2.2 per cent positivity; however, these sera did not react with dog H3N8 virus (A/canine/NE/52-14/06) or avian H3N2 virus (A/duck/Mongolia/301/01), suggesting human-to-dog transmission of the human virus. Notably, six sera were positive for VN antibody to type B virus, representing 1.6 per cent positivity. None of the sera was antibody-positive for both type A and B viruses. Moreover, all samples were negative for VN antibody to highly pathogenic H5N1 avian virus (A/whooper swan/Mongolia/4/05; clade 2.2.). None of the seropositive dogs showed any typical signs of acute respiratory illness according to the clinical records, suggesting that they were asymptomatic or had very minor infections, as supported by the low VN titres for the positive cases.

We conclude that dogs can be infected with human influenza viruses, including type B virus. To our knowledge, there is only one previous report of a possible natural influenza B virus infection of a dog (Chang and others 1976), and even in this case, the infection was not proven with established criteria. There has also been a report of influenza C virus infection of dogs (Ohwada and others 1987). Thus, domestic dogs may act as a vector for human influenza virus transmission within households, posing a potential public health concern. Previous reports that dogs are susceptible to avian viruses, such as H3N2 and H5N1, raise the possibility that dogs, like pigs, may act as an intermediate host for the emergence of new, potentially pandemic viruses. Continued surveillance of influenza viruses in dog populations will be important to achieve the "one health" concept for this zoonotic disease.

Acknowledgements

We thank Sue Watson for editing the manuscript, Ryoko Yamao for technical assistance, and veterinarians in Yamaguchi University and Azabu University for collecting the samples. This work was supported by grants-in-aid for Scientific Research (B), from the Ministry of Education, Culture, Sports, Science, and Technology, Japan.

References

CHANG, C. P., NEW, A. E., TAYLOR, J. F. & CHIANG, H. S. (1976) Influenza virus isolations from dogs during a human epidemic in Taiwan. *International Journal of Zoonoses* **3**, 61–64

CRAWFORD, P. C., DUBOVI, E. J., CASTLEMAN, W. L., STEPHENSON, I., GIBBS, E. P., CHEN, L., SMITH, C., HILL, R. C., FERRO, P., POMPEY, J., BRIGHT, R. A., MEDINA, M. J., JOHNSON, C. M., OLSEN, C. W., COX, N. J., KLIMOV, A. I., KATZ, J. M. & DONIS, R. O. (2005) Transmission of equine influenza virus to dogs. *Science* **310**, 482–485

DALY, J. M., BLUNDEN, A. S., MACRAE, S., MILLER, J., BOWMAN, S. J., KOLODZIEJEK, J., NOWOTNY, N. & SMITH, K. C. (2008) Transmission of influenza virus to English foxhounds. *Emerging Infectious Diseases* **14**, 461–464

DUNDON, W. G., DE BENEDICTIS, P., VIALE, E. & CAPUA, I. (2010) Serological evidence of pandemic (H1N1) 2009 infection in dogs, Italy. *Emerging Infectious Diseases* **16**, 2019–2021

ITOH, Y., SHINYA, K., KISO, M., WATANABE, T., SAKODA, Y., HATTA, M., MURAMOTO, Y., TAMURA, D., SAKAI-TAGAWA, Y., NODA, T., SAKABE, S., IMAI, M., HATTA, Y., WATANABE, S., LI, C., YAMADA, S., FUJII, K., MURAKAMI, S., IMAI, H., KAKUGAWA, S., ITO, M., TAKANO, R., IWATSUKI-HORIMOTO, K., SHIMOJIMA, M., HORIMOTO, T., GOTO, H., TAKAHASHI, K., MAKINO, A., ISHIGAKI, H., NAKAYAMA, M., OKAMATSU, M.,

Veterinary Record (2013) doi: 10.1136/vr.101929

T. Horimoto, DVM, MSc, PhD,
F. Gen, MSc, PhD,
S. Murakami, MSc, PhD,
K. Kato, DVM, PhD,
H. Akashi, DVM, MSc, PhD,
Department of Veterinary Microbiology,
The University of Tokyo,
Tokyo 113-8657, Japan
K. Iwatsuki-Horimoto, DVM, PhD,
Y. Kawaoka, DVM, MSc, PhD,
Division of Virology, Institute of Medical Science, The University of Tokyo,
Tokyo 108-8639, Japan
M. Hisasue, DVM, PhD,
Department of Internal Medicine II,
M. Sakaguchi, DVM, MSc, PhD,
Department of Veterinary Microbiology I,
Azabu University, Kanagawa, Japan
K. Maeda, DVM, PhD,
Department of Veterinary Microbiology,
Yamaguchi University, Yamaguchi,
Japan

E-mail for correspondence:
ahorimo@mail.ecc.u-tokyo.ac.jp

Provenance: not commissioned; externally peer reviewed

Accepted November 24, 2013

TABLE 1: Dogs in the study that were seropositive to human influenza viruses

Prefecture	Number of samples	Virus	Number of positive samples (%)	VN titres (number)	Species (number)
Yamaguchi	162	A(H1N1)pdm09	4 (2.5)	10 (3), 20 (1*)	Miniature dachshund (1), Chihuahua (1), toy poodle (1*), shih tzu (1)
		H1N1	1 (0.6)	10 (1*)	Toy poodle (1*)
		H3N2	1 (0.6)	40 (1)	Miniature dachshund (1)
		B	4 (2.5)	10 (2), 20 (2)	Mongrel (2), toy poodle (1), miniature dachshund (1)
Kanagawa	204	A(H1N1)pdm09	10 (4.9)	10 (4), 20 (5), 80 (1)	Miniature dachshund (3), papillon (2), toy poodle (1), mongrel (1), shiba (1), springer spaniel (1), long coat Chihuahua (1)
		H1N1	0 (0)	–	–
		H3N2	7 (3.4)	10 (4), 40 (3)	Miniature dachshund (3), toy poodle (2), Welsh corgi (1), Yorkshire terrier (1)
		B	2 (1.0)	10 (1), 20 (1)	Miniature dachshund (1), Maltese (1)

*The same dog
VN, virus-neutralisation

TAKAHASHI, K., WARSHAUER, D., SHULT, P. A., SAITO, R., SUZUKI, H., FURUTA, Y., YAMASHITA, M., MITAMURA, K., NAKANO, K., NAKAMURA, M., BROCKMAN-SCHNEIDER, R., MITAMURA, H., YAMAZAKI, M., SUGAYA, N., SURESH, M., OZAWA, M., NEUMANN, G., GEM, J., KIDA, H., OGASAWARA, K., & KAWAOKA, Y. (2009) In vitro and in vivo characterization of new swine-origin H1N1 influenza viruses. *Nature* **460**, 1021–1025

KIM, H., SONG, D., MOON, H., YEOM, M., PARK, S., HONG, M., NA, W., WEBBY, R. J., WEBSTER, R. G., PARK, B., KIM, J.-K., & KANG, B. (2013) Inter- and intraspecies transmission of canine influenza virus (H3N2) in dogs, cats, and ferrets. *Influenza and Other Respiratory Viruses* **7**, 265–270

LI, S., SHI, Z., JIAO, P., ZHANG, G., ZHONG, Z., TIAN, W., LONG, L. P., CAI, Z., ZHU, X., LIAO, M., & WAN, X. F. (2010) Avian-origin H3N2 canine influenza A viruses in Southern China. *Infection Genetics and Evolution* **10**, 1286–1288

LIN, D., SUN, S., DU, L., MA, J., FAN, L., PU, J., SUN, Y., ZHAO, J., SUN, H., & LIU, J. (2012) Natural and experimental infection of dogs with pandemic H1N1/2009 influenza virus. *Journal of General Virology* **93**, 119–123

OHWADA, K., KITAME, F., SUGAWARA, K., NISHIMURA, H., HONMA, M. & NAKAMURA, K. (1987) Distribution of the antibody to influenza C virus in dogs and pigs in Yamagata Prefecture, Japan. *Microbiology & Immunology* **31**, 1173–1180

SONG, D., KANG, B., LEE, C., JUNG, K., HA, G., KANG, D., PARK, S., PARK, B., & OH, J. (2008) Transmission of avian influenza virus (H3N2) to dogs. *Emerging Infectious Diseases* **14**, 741–746

SONGSERM, T., AMONSIN, A., JAM-ON, R., SAE-HENG, N., PRIYOTHORN, N., PAYUNGPORN, S., THEAMBOONLERS, A., CHUTINIMITKUL, S., THANAWONGNUWECH, R., & POOYORAWAN, Y. (2006) Fatal avian influenza A H5N1 in a dog. *Emerging Infectious Diseases* **12**, 1744–1747

J Clin Immunol (2013) 33:977–983
DOI 10.1007/s10875-013-9880-7

ORIGINAL RESEARCH

Analysis of Conformational and Sequential IgE Epitopes on the Major Allergen Cry j 2 of Japanese Cedar (*Cryptomeria japonica*) Pollen in Humans by Using Monoclonal Antibodies for Cry j 2

Kazuki Miyaji · Terumi Yurimoto · Akemi Saito · Hiroshi Yasueda · Yukari Takase · Hidekatsu Shimakura · Noriaki Okamoto · Akio Kiuchi · Saburo Saito · Masahiro Sakaguchi

Received: 18 November 2012 / Accepted: 25 February 2013 / Published online: 16 March 2013

Abstract
Purpose Japanese cedar (*Cryptomeria japonica*; CJ) pollinosis is a type I allergy induced by CJ pollen, and Cry j 2 is one of the major allergens in this pollen. In a previous study, we analyzed IgE epitopes on Cry j 2 in humans by using synthetic peptides. The main purpose of this study was to identify B-cell epitopes on Cry j 2 in patients with CJ pollinosis by using monoclonal antibodies (mAbs) for Cry j 2.
Methods We used ELISA with mAbs for the epitope analysis. Sera samples were collected from 80 patients with CJ pollinosis, and allergenic epitopes for mAbs and human IgE were identified using ELISA with synthetic peptides. The importance of the epitopes for human IgE was analyzed using an inhibition ELISA.
Results Four independent epitopes (epitope #1, #2, #3, and #4) were identified on Cry j 2 with the use of mAbs. Epitope #3 and #4, corresponding to peptides No. 25 and No. 33, respectively, were newly determined as epitopes for mAbs and human IgE. Inhibition ELISA showed that not only epitope #2 (sequential) but epitope #1 (conformational) may play an important role in the CJ pollinosis.
Conclusions Our results revealed 4 epitopes, including two new ones, on Cry j 2. We also found that inhibition ELISA with appropriate mAbs could be a viable method of evaluating the importance of the conformational and sequential epitopes for human IgE. These results are beneficial for the development of safer and more efficient therapeutic strategies for treating CJ pollinosis.

Keywords Japanese cedar pollen · pollinosis · Cry j 2 · IgE · epitope

Electronic supplementary material The online version of this article (doi:10.1007/s10875-013-9880-7) contains supplementary material, which is available to authorized users.

K. Miyaji · T. Yurimoto · Y. Takase · H. Shimakura · N. Okamoto · A. Kiuchi · M. Sakaguchi (✉)
Department of Veterinary Microbiology,
School of Veterinary Medicine, Azabu University,
1-17-71 Fuchinobe, Chuo-ku, Sagamihara,
Kanagawa 252-5201, Japan
e-mail: sakagum@azabu-u.ac.jp

A. Saito · H. Yasueda
Clinical Research Center for Allergy
and Rheumatology, National Sagamihara Hospital,
18-1 Sakuradai, Minami-ku, Sagamihara,
Kanagawa 252-0392, Japan

S. Saito
Department of Molecular Immunology,
Institute of DNA Medicine, Jikei University
School of Medicine, 3-25-8 Nishi-Shinbashi,
Minato-ku, Tokyo 105-8461, Japan

Introduction

Pollinosis is a typical type I allergy induced by pollens, and is defined as the appearance of respiratory symptoms such as rhinoconjunctivitis. Japanese cedar (*Cryptomeria japonica*; CJ) pollinosis is one of the most common allergic diseases in Japan [1]. In an epidemiological study conducted

in the central Hokuriku area of Japan in May and June of both 2006 and 2007 [2], 36.7 % of the study participants (566 of the 1,540 subjects) had allergic rhinitis to CJ pollen. Impaired performance and a voluntary ban on leaving home for patients with CJ pollinosis comprise the tremendous social impact and economic loss associated with this disease. Therefore, CJ pollinosis is one of the most serious public health problems in Japan.

Yasueda et al. [3] purified Cry j 1 as a major allergen from CJ pollen, and we isolated Cry j 2 as another major allergen [4]. Of 145 patients with CJ pollinosis tested for specific IgE levels, 134 (92 %) had specific IgE antibodies to both Cry j 1 and Cry j 2 [5]. Cry j 2 is completely different from Cry j 1 in terms of its chemical and immunophysical properties, N-terminal amino acid sequence, and its molecular mass of 37 kDa under non-reducing conditions [4]. Furthermore, we also recently isolated Cry j 3 as a causative allergen of CJ pollinosis [6].

The identification and characterization of allergenic epitopes are important for establishing safer and more efficient immunotherapy protocols [7, 8]. Previously, we used monoclonal antibodies (mAbs) to characterize the allergenic epitopes of Cry j 1 in CJ pollens, and identified five independent epitopes on Cry j 1 [9]. In our preliminary study [10], in which epitopes on Cry j 2 were analyzed using a synthetic peptide of Cry j 2, we found that ^{124}KWVNGREI^{131} is an important major linear epitope. However, we had not classified IgE epitopes on Cry j 2 with mAbs for the allergen, and the significance of a previously identified epitopes remains to be evaluated.

In the present study, we identified four independent epitopes on Cry j 2 by using mAbs for Cry j 2; two are new epitopes. Analysis of a large number of sera samples obtained from patients with CJ pollinosis has confirmed that they are also new epitopes for human IgE. We additionally predicted whether amino acids that made synthetic peptides recognizable by mAbs and human IgE could be exposed on Cry j 2 by means of bioinformatics tools. Finally, fluorometric and inhibition ELISA assays were used to evaluate the importance of conformational and sequential epitopes recognized by mAbs and human IgE.

Methods

The Cry j 2 Antigen and Monoclonal Antibodies

Cry j 2 was purified as previously described [4]. A library of peptides, consisting of 18, 20, 21, or 25 amino acids overlapping by 10 to 12, was commercially synthesized (Hokkaido System Science Co., Ltd., Sapporo, Japan) [10, 11]. The eight mAbs (S1, S2, S3, N26, T27, 24, 9E7, and J2A01) against Cry j 2 used in our laboratory were categorized according to cross-inhibition ELISA. These mAbs were kindly provided or generated by immunizing mice with Cry j 2 [10, 12–14].

ELISA Cross-Inhibition for Epitopes of Cry j 2 Recognized by mAbs

Epitopes recognized by the mAbs were grouped using the ELISA cross-inhibition test. This test is based on the ability of a mAb to inhibit the binding of a coexisting biotin-labeled mAb to solid-phase Cry j 2. Briefly, Cry j 2 (0.5 μg/mL) was adsorbed onto a microplate (F96 Maxisorp® NUNC-Immuno™ Plate, ThermoFisher Scientific, Waltham, MA, USA). Biotin-labeled mAbs (0.5 μg/mL) were then reacted with the solid-phase antigen in the presence or absence of unlabeled mAbs (5 μg/mL) for 1 h at room temperature. Next, a streptavidin-peroxidase polymer (streptavidin-HRP, Sigma-Aldrich, St. Louis, MO, USA) was added to the wells. After a 1-h incubation period at room temperature, a substrate solution of *o*-phenylenediamine dihydrochloride was added. After the enzyme reaction was quenched with 2 M H_2SO_4, the optical density (OD) was measured using a multi-mode microplate reader (Powerscan MX, DS Pharma Biomedical, Osaka, Japan).

Patient Sera Samples

Informed consent was obtained from all subjects. The study protocol was approved by the ethics committee at the Jikei University School of Medicine. Sera samples from 80 patients with CJ pollinosis. The patents were selected on the bases of clinical symptoms of seasonal allergic rhinitis and positive CAP (Phadia AB, Uppsala, Sweden) to CJ pollen. For the negative control, sera samples were obtained from 25 non-allergic subjects who had previously been confirmed to be negative for the CJ pollen allergen.

Colorimetric ELISA for Overlapping Synthetic Peptides with mAbs

As previously described, the reaction of mAbs to Cry j 2 peptides was measured using a colorimetric ELISA [10]. Briefly, Cry j 2 protein (1 μg/mL) or synthetic peptides (10 μg/mL) were immobilized in the wells of a microplate (F96 MaxiSorp® NUNC-Immuno™ Plate) overnight at 4 °C. The microplate was then washed with phosphate-buffered saline containing 0.05 % Tween 20 (PBST buffer) and incubated with biotin-labeled mAbs (0.1 μg/mL) for 1 h at room temperature. The subsequent procedures were the same as those for the cross-inhibition ELISA described above.

Fluorometric ELISA for Overlapping Synthetic Peptides with Human IgE in Patient Sera

As previously described, specific IgE in the sera of patients with pollinosis for Cry j 2 peptides was measured using fluorometric ELISA [5]. Briefly, Cry j 2 protein (1 μg/mL)

or synthetic peptides (10 μg/mL) were immobilized in the wells of a microplate (FLUOTRAC™ 600, Greiner Bio-One GmbH, Frickenhausen, Germany) overnight at 4 °C. The microplate was then washed with PBST buffer and finally incubated with diluted (1:10) sera samples for 3 h at room temperature. The plates were washed, and anti-human IgE antibodies conjugated to β-D-galactosidase (diluted 1:10; Phadia AB) were added to each well. As the enzyme reaction substrate, 0.2 mM 4-methylumbelliferyl-β-D-galactoside (Sigma-Aldrich) was added to the wells, and the plates were incubated at 37 °C for 2 h. After quenching the reaction, fluorescence units (FU) were measured on a multi-mode microplate reader. Cutoff values were determined using sera from pollinosis-negative patients as controls.

Inhibition ELISA for the Conformational and Sequential Epitopes with the Use of mAbs

To evaluate the importance of the conformational and sequential epitopes, inhibition ELISA was conducted using mAbs as inhibitors [9]. Briefly, Cry j 2 protein (1 μg/mL) was immobilized in the wells of a microplate overnight at 4 °C. Non-labeled mAbs S1 or N26 (20 μg/mL) were reacted with the immobilized protein for 1 h at room temperature. Plates were then washed with PBST buffer and subsequently incubated with diluted (1:10) sera samples for 3 h at room temperature. Sera samples from 50 patients were used for conducting the assay because of their sufficient volume (>100 μL). Subsequent procedures were the same as those of the fluorometric ELISA described above. The inhibition ratio (%) was calculated as follows:

$$\left(1-\frac{\text{FU in presence of inhibitor}}{\text{FU in absence of inhibitor}}\right)\times 100$$

Bioinformatics Tool

The surface exposure of the Cry j 2 amino acids was predicted using NetSurfP (http://www.cbs.dtu.dk/services/NetSurfP/) [15, 16].

Results

Epitope Specificity of Anti-Cry j 2 mAbs and Their Binding to Synthetic Peptides of Cry j 2

Four independent epitopes were identified on the Cry j 2 molecule by using the ELISA cross-inhibition test with mAbs. An inhibition reaction was not observed with a non-labeled mAb that recognized different epitopes. In the present study, the epitope on the Cry j 2 molecule related to mAbs S1, S2, and S3 was defined as epitope #1, mAbs N26, T27, and 24 as epitope #2, mAb 9E7 as epitope #3, and mAb J2A01 as epitope #4 (Table I).

We examined the binding of these mAbs to synthetic peptides of Cry j 2. Our observations were similar to those of a previous report [10]; we reconfirmed that mouse Cry j 2-specific mAb S1 did not react with any of the peptides, and mAbs N26 and 24 reacted with peptide No. 13 (^{121}GQCKWVNGREICNDRDRPTA^{140}). We found that the mAbs 9E7 and J2A01 reacted with peptides No. 25 (^{241}GRENSRAEVSYVHVNGAKFI^{260}) and No. 33 (^{321}TYKNIRGTSATAAAIQLKCS^{340}), respectively. It was determined that epitope # 2 is relevant to peptide No. 13, epitope #3 to peptide No. 25, and epitope #4 to peptide No. 33. We found that epitope #3 and epitope #4 were new epitopes recognized by mAbs.

Binding of IgE in Sera of Human Patients to Synthetic Peptides of Cry j 2

Figure 1 shows the reactivity of human IgE obtained from 80 patients with anti-Cry j 2 IgE to synthetic peptides. The cutoff values for Cry j 2 and peptides were obtained in the maximal FU values of 25 negative controls, because the values were higher than mean value+3SD. We reconfirmed that IgE from 61 patients (76 %) reacted with peptide No. 13 (relevant to epitope #2). We also found that IgE from 11 (14 %) patients reacted with peptide No. 25 (relevant to epitope #3), and IgE from 19 (24 %) patients reacted with peptide No. 33 (relevant to epitope #4). In our previous study, none of the samples obtained from 20 patients reacted with these peptides [10].

Exposed Amino Acids of Sequential Epitopes on Cry j 2

The solvent-accessible amino acids of epitopes epitope #2, epitope #3, and epitope #4 were predicted using NetSurfP (Table II). Core amino acids for epitope #2 (^{124}KWVNGREI^{131}), which were identified using small peptides of peptide No. 13 in the previous study [10], all seemed to be exposed on the Cry j 2 surface. The exposed regions of epitope #3 were predicted to be ^{242}R^{243}E^{244}N^{245}S^{246}R^{247}A^{248}E^{250}S^{256}G^{258}K^{260}I, and those of epitope #4 to be ^{323}Y^{324}N^{326}R^{328}T^{330}A^{331}T^{332}A. All computed results are shown in the Supplementary Table.

Evaluating the Significance of the Epitopes, Epitope #1 and #2, for Human IgE

We determined the inhibition rates of mAbs S1 (for epitope #1) and N26 (for epitope #2) against human IgE for comparison of their importance. Table III indicated FU value of human IgE to

Table I Classification of anti-Cry j 2 mAbs by inhibition ELISA

Unlabeled mAb[a]	Biotin-labeled mAb to							
	epitope #1			epitope #2			epitope #3	epitope #4
	S1	S2	S3	N26	T27	24	9E7	J2A01
S1	+	+	+	−	−	−	−	−
S2	+	+	+	−	−	−	−	−
S3	+	+	+	−	−	−	−	−
N26	−	−	−	+	+	+	−	−
T27	−	−	−	+	+	+	−	−
24	−	−	−	+	+	+	−	−
9E7	−	−	−	−	−	−	+	−
J2A01	−	−	−	−	−	−	−	+

[a]Inhibitor. +, >30 % inhibition. Experiments were repeated at least three times.

peptide No. 13 (relevant to epitope #2), and inhibition ratio of mAbs to epitope # 1 and #2 against human IgE for each subject. We found that their patterns were substantially different. Of the 10 sera samples that showed >50 % inhibition rates for mAb to epitope #1, eight sera samples had negative FU value for IgE to epitope #2 relative peptide.

Discussion

The bioinformatics tool NetSurfP can predict solvent-accessible regions on proteins. Using this tool, we predicted exposed amino acids in Cry j 2 epitopes (epitope #2, #3, and #4). A review article relevant to food allergies discussed that the majority of IgE epitopes are eight amino acids or longer [17]. However, it has been suggested that five to six amino acids play an important role in the binding between antibody and epitope [18], and pentapeptides have been reported as IgE epitopes in wheat gliadin [19]. All core amino acids of epitope #2 determined in our previous study [10] were predicted to be exposed, indicating that ^{124}KWVNGREI^{131} was a completely sequential epitope. Epitope #3 was predicted to contain seven consecutive amino acids, ^{242}RENSRAE^{248}, exposed on Cry j 2, suggesting that these amino acids may contribute as the epitope. Meanwhile, epitope #4 was not expected to contain three or more consecutive amino acids. Our result raises the possibility that the core determinants may result from discontinuous amino acids within epitope #4. Further study is needed to identify the core determinants of those epitopes.

The mAb S1 did not react with any of the synthetic peptides. This result coincides with that from our previous

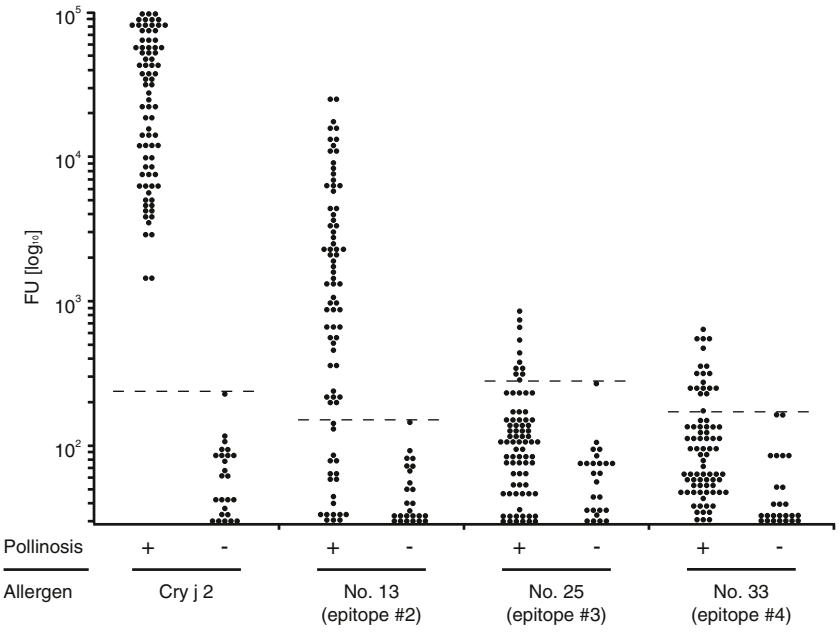

Fig. 1 Binding of human IgE to Cry j 2 and synthetic peptides. Related epitope numbers are indicated within parentheses below to the synthetic peptide numbers. Binding activity is expressed in fluorescence units (FU). The dashed line represents cutoff values, which were determined as highest FU in negative control. The cutoff values are 233.5, 156.0, and 185.5 from the left column. Sera samples from 50 patients were used to provide adequate amounts, and experiments were repeated at least three times

Table II Prediction of solvent-accessible regions of Cry j 2 amino acids using NetSurfP

Epitope	Position	Amino acids
epitope #2[a]	124–131	KWVNGREI ********
epitope #3	241–260	GRENSRAEVSYVHVNGAKFI -*******-*-----*-*-*
epitope #4	321–340	TYKNIRGTSATAAAIQLKCS --**-*-*--**--------

[a] Core sequence for epitope #2 was identified by Tamura et al. [10]

Surface exposure of Cry j 2 amino acids was predicted by NetSurfP, and each amino acid was assigned to "Exposed (*)" or "Buried (-)". See also supplementary table

study, in which the mAb S1 also did not bind to any synthetic peptides [10]. Along with decreasing reaction of S1 to heat treated Cry j 2 [20], these findings indicate that epitope #1 could be a conformational epitope. Although it has been shown that a number of patient IgE reacted to peptide No. 13 (relevant to epitope #2), the importance of a conformational epitope on Cry j 2 for human IgE had not been previously reported. Therefore, the responsiveness of human IgE to epitope #1 (a conformational epitope) and epitope #2 (a sequential epitope) was compared by inhibition ELISA. The reaction of mAb with the epitope #1 inhibited the binding of human IgE to Cry j 2 in a different manner in the reaction of mAb with epitope #2. Eighty percent of the tested sera samples showing >50 % inhibition rates for mAb to epitope #1 were negative for epitope #2. Conformational epitopes on allergens are considered to play an important role in initiating human IgE-mediated allergic reactions [21–23]. Our results suggested that not only conformational but also sequential epitope may play an important role in the CJ pollinosis. Variations in responsiveness to Cry j 2 epitopes could have been influenced by unknown factors such as an individual's genetic background and/or clinical history. It may be worthwhile to analyze IgE-binding epitopes to understand the etiology of this allergy and develop safer and more efficient therapeutic strategies for treating CJ pollinosis.

Table III Inhibition rates of mAbs binding to epitope #1 and #2 for evaluating the importance of the conformational epitope (epitope #1) on Cry j 2 for human IgE

Inhibition rate (%)				Inhibition rate (%)			
Subject	FU value	epitope #1	epitope #2	Subject	FU value	epitope #1	epitope #2
1	0	27.1	0.0	26	1038	47.0	**50.6**
2	0	46.3	21.2	27	1214	32.4	**80.7**
3	0	**50.5**	40.5	28	1229	23.3	**71.0**
4	0	**57.2**	8.5	29	1317	29.0	**50.9**
5	1	34.5	16.5	30	1719	20.0	20.9
6	7	**50.1**	39.8	31	1885	42.3	**59.0**
7	8	**58.0**	41.6	32	2061	21.1	39.4
8	30	46.5	30.8	33	2071	31.2	**72.6**
9	47	36.6	28.4	34	2207	25.9	34.8
10	52	**63.4**	27.4	35	2257	35.7	**54.4**
11	56	34.6	16.9	36	2303	23.1	48.5
12	80	**61.0**	28.4	37	2322	**62.3**	44.8
13	93	41.7	25.6	38	2371	19.3	**54.4**
14	135	**50.6**	25.6	39	2670	3.2	44.2
15	219	26.4	19.7	40	2953	12.4	**72.7**
16	226	**50.1**	44.7	41	3306	34.5	**79.2**
17	230	44.0	26.9	42	3857	37.0	**67.4**
18	235	**54.7**	36.3	43	4214	19.6	**75.2**
19	464	31.5	**68.2**	44	6490	29.1	**54.5**
20	576	37.3	**50.3**	45	6686	22.7	**59.6**
21	670	17.9	35.8	46	7944	9.4	**57.1**
22	676	47.6	28.9	47	9159	24.6	**71.7**
23	815	43.2	41.5	48	11372	12.2	**65.6**
24	849	20.4	42.5	49	13088	6.4	35.7
25	983	45.0	44.6	50	26236	7.5	22.2

FU values of human IgE were calculated based on the activity to epitope #2 relative peptide No. 13, and the cutoff value is 233.5 (see also Fig. 1). The epitope #2 was chosen as a target for comparison, since the affinity of human IgE to peptide No. 13 was higher than to other peptides. Sera samples from 50 patients were used to have enough volume (>100 μL) to conduct inhibition ELISA. Inhibition rate over 50 % is shown in bold. The experiments were repeated at least three times.

A previous study reported that no patients' sera included reactive IgE to the synthetic peptides No. 25 and No. 33 [10]. Our present results show that these peptides were recognized by the mAbs and human IgE (Fig. 1), suggesting that the determinants are newly detected epitopes. The lack of detection in our previous analysis is probably because those sites are minor epitopes and were thus incidentally not recognized in the small sample size. In fact, we tested 80 patients with CJ pollinosis, and only 11 (14 %) patients for peptide No. 25 (relevant to epitope #3) and 19 (24 %) patients for peptide No. 33 (relevant to epitope #4) were detected as being epitope-specific IgE-positive at low FU compared to peptide No. 13 (relevant to epitope #2). Moreover, differences between the methodologies used in previous studies and our study, especially with regard to the detection procedures, may have contributed to the fact that those epitopes were not detected by the other investigators.

Many studies have analyzed IgE epitopes of group 1 conifer pollen allergens, such as Cry j 1 and Jun a 1 [9, 21, 24–26]. Using mAbs for Cry j 1, a major allergen of the CJ pollen, we identified five independent epitopes on Cry j 1 in human patients [9]. Major mountain cedar allergen, Jun a 1, contains conformational and sequential IgE epitopes [26]. Other group 2 conifer pollen allergens, such as Jun a 2 and Cha o 2 from cypress pollen, have also been identified [27–29]. However, few studies have analyzed IgE epitopes in group 2 conifer pollen allergens [10]. In our previous study, we identified important sequential IgE epitopes of Cry j 2 by using synthetic peptides on this allergen [10]. In the present study, we have identified two new IgE epitopes by using mAbs for Cry j 2. These studies concerning IgE epitopes on Cry j 2 will help in developing new allergen vaccines against cedar and cypress pollinosis [30].

Conclusion

Four epitopes, including two new epitopes, were identified on Cry j 2 by using mAbs, and IgE from patients with pollinosis also reacted to the epitopes. The bioinformatics tool NetSurfP could predict the candidate amino acids that accounted for the core determinants in one of the two new epitopes. Our study also demonstrated that inhibition ELISA using mAbs is a viable method to evaluate the importance of the conformational and sequential epitopes for human IgE. These results are useful for the development of safer and more efficient therapeutic strategies for treating CJ pollinosis.

Acknowledgments We are grateful to Dr. Reiko Homma (Torii Pharmaceutical Co., Ltd., Tokyo, Japan) for kindly giving us monoclonal antibodies. This research was partially supported by the Promotion and Mutual Aid Corporation for Private Schools of Japan, Grant-in-Aid for Matching Fund Subsidy for Private University, and by a Project Grant awarded by the Azabu University Research Services Division.

References

1. Ishizaki T, Koizumi K, Ikemori R, Ishiyama Y, Kushibiki E. Studies of prevalence of Japanese cedar pollinosis among the residents in a densely cultivated area. Ann Allergy. 1987;58:265–70.
2. Sakashita M, Hirota T, Harada M, Nakamichi R, Tsunoda T, Osawa Y, et al. Prevalence of allergic rhinitis and sensitization to common aeroallergens in a Japanese population. Int Arch Allergy Immunol. 2010;151:255–61.
3. Yasueda H, Yui Y, Shimizu T, Shida T. Isolation and partial characterization of the major allergen from Japanese cedar (*Cryptomeria japonica*) pollen. J Allergy Clin Immunol. 1983;71:77–86.
4. Sakaguchi M, Inouye S, Taniai M, Ando S, Usui M, Matuhasi T. Identification of the second major allergen of Japanese cedar pollen. Allergy. 1990;45:309–12.
5. Hashimoto M, Nigi H, Sakaguchi M, Inouye S, Imaoka K, Miyazawa H, et al. Sensitivity to two major allergens (*Cry j* I and *Cry j* II) in patients with Japanese cedar (*Cryptomeria japonica*) pollinosis. Clin Exp Allergy. 1995;25:848–52.
6. Fujimura T, Futamura N, Midoro-Horiuti T, Tgawa A, Goldblum RM, Yasueda H, et al. Isolation and characterization of native Cry j 3 from Japanese cedar (*Cryptomeria japonica*) pollen. Allergy. 2007;62:547–53.
7. Kahn CR, Marsh DG. Monoclonal antibodies to the major *Lolium perenne* (rye grass) pollen allergen *Lol p* I (Rye I). Mol Immunol. 1986;23:1281–8.
8. Olson JR, Klapper DG. Two major human allergenic sites on ragweed pollen allergen antigen E identified by using monoclonal antibodies. J Immunol. 1986;136:2109–15.
9. Sakaguchi M, Hashimoto M, Nigi H, Yasueda H, Takahashi Y, Watanabe M, et al. Epitope specificity of IgE antibodies to a major allergen (Cry j 1) of Japanese cedar pollen in sera of humans and monkeys with pollinosis. Immunology. 1997;91:161–6.
10. Tamura Y, Kawaguchi J, Serizawa N, Hirahara K, Shiraishi A, Nigi H, et al. Analysis of sequential immunoglobulin E-binding epitope of Japanese cedar pollen allergen (Cry j 2) in humans, monkeys and mice. Clin Exp Allergy. 2003;33:211–7.
11. Namba M, Kurose M, Torigoe K, Hino K, Taniguchi Y, Fukuda S, et al. Molecular cloning of the second major allergen, *Cry j* II, from Japanese cedar pollen. FEBS Lett. 1994;353:124–8.
12. Taniai M, Kayano T, Takakura R, Yamamoto S, Usui M, Ando S, et al. Epitopes on *Cry j* I and *Cry j* II for the human IgE antibodies cross-reactive between *Cupressus sempervirens* and *Cryptomeria japonica* pollen. Mol Immunol. 1993;30:183–9.
13. Homma R, Uesato N, Miyahara A, Kimura H, Hantani Y, Ito G, et al. Production of a monoclonal antibody against Cry j 2. Arerugi. 1995;44:461–6 (in Japanese with English abstract).
14. Yasueda H, Saito A, Sakaguchi M, Ide T, Saito S, Tniguchi Y, et al. Identification and characterization of a group 2 conifer pollen allergen from *Chamaecyparis obtusa*, a homologue of Cry j 2 from *Cryptomeria japonica*. Clin Exp Allergy. 2000;30:546–50.
15. Petersen B, Petersen TN, Andersen P, Nielsen M, Lundegaard C. A generic method for assignment of reliability scores applied to solvent accessibility predictions. BMC Struct Biol. 2009;9:51.
16. Ingale AG. Antigenic epitopes prediction and MHC binder of a paralytic insecticidal toxin (ITX-1) of *Tegenaria agrestis* (hobo spider). Open Access Bioinforma. 2010;2:97–103.
17. Bannon GA, Ogawa T. Evaluation of available IgE-binding epitope data and its utility in bioinformatics. Mol Nutr Food Res. 2006;50:638–44.
18. Laver WG, Air GM, Webster RG, Smith-Gill SJ. Epitopes on protein antigens: misconceptions and realities. Cell. 1990;61:553–6.
19. Tanabe S. IgE-binding abilities of pentapeptides, QQPFP and PQQPF, in wheat gliadin. J Nutr Sci Vitaminol. 2004;50:367–70.
20. Sawatani M, Yasueda H, Akiyama K, Shida T, Taniguchi Y, Usui M, et al. Immunological and physicochemical properties of Cry j II, the

second major allergen of Japanese cedar pollen (*Cryptomeria japonica*). Arerugi. 1993;42:738–47 (in Japanese with English abstract).
21. Varshney S, Goldblum RM, Kearney C, Watanabe M, Midoro-Horiuti T. Major mountain cedar allergen, Jun a 1, contains conformational as well as linear IgE epitopes. Mol Immunol. 2007;44:2781–5.
22. Padavattan S, Flicker S, Schirmer T, Madritsch C, Randow S, Reese G, et al. High-affinity IgE recognition of a conformational epitope of the major respiratory allergen Phl p 2 as revealed by X-ray crystallography. J Immunol. 2009;182:2141–51.
23. Tiwari R, Negi S, Braun B. Validation of a phage display and computational algorithm by mapping a conformational epitope of Bla g 2. Int Arch Allergy Immunol. 2011;157:323–30.
24. Tamura Y, Sasaki R, Inouye S, Kawaguchi J, Serizawa N, Toda M, et al. Identification of a sequential B-cell epitope on major allergen (Cry j 1) of Japanese cedar (*Cryptomeria japonica*) pollen in mice. Int Arch Allergy Immunol. 2000;123:228–35.
25. Midoro-Horiuti T, Mathura V, Schein CH, Braun W, Yu S, Watanabe M, et al. Major linear IgE epitopes of mountain cedar pollen allergen Jun a 1 map to the pectate lyase catalytic site. Mol Immunol. 2003;40:555–62.
26. Midoro-Horiuti T, Schein CH, Mathura V, Braun W, Czerwinski EW, Togawa A, et al. Structural basis for epitope sharing between group 1 allergens of cedar pollen. Mol Immunol. 2006;43:509–18.
27. Mori T, Yokoyama M, Komiyama N, Okano M, Kino K. Purification, identification, and cDNA cloning of Cha o 2, the second major allergen of Japanese cypress pollen. Biochem Biophys Res Commun. 1999;263:166–71.
28. Yasueda H, Saito A, Sakaguchi M, Ide T, Saito S, Taniguchi Y, et al. Identification and characterization of a group 2 conifer pollen allergen from *Chamaecyparis obtusa*, a homologue of Cry j 2 from *Cryptomeria japonica*. Clin Exp Allergy. 2000;30:546–50.
29. Yokoyama M, Miyahara M, Shimizu K, Kino K, Tsunoo H. Purification, identification, and cDNA cloning of Jun a 2, the second major allergen of mountain cedar pollen. Biochem Biophys Res Commun. 2000;275:195–202.
30. Sakaguchi M, Hirahara K, Fujimura T, Toda M. Approaches to immunotherapies for Japanese cedar pollinosis. Auris Nasus Larynx. 2011;38:431–8.

Veterinary Immunology and Immunopathology 149 (2012) 132–135

Contents lists available at SciVerse ScienceDirect

Veterinary Immunology and Immunopathology

journal homepage: www.elsevier.com/locate/vetimm

Short communication

IgE reactivity to a Cry j 3, an allergen of Japanese cedar (*Cryptomeria japonica*) pollen in dogs with canine atopic dermatitis

Shota Kubota[a], Kazuki Miyaji[a], Yusaku Shimo[a], Hidekatsu Shimakura[a], Yukari Takase[a], Noriaki Okamoto[a], Akio Kiuchi[a], Masato Fujimura[b], Takashi Fujimura[c], Douglas J. DeBoer[d], Toshihiro Tsukui[e], Masahiro Sakaguchi[a,*]

[a] *Department of Veterinary Microbiology, School of Veterinary Medicine, Azabu University, 1-17-71 Fuchinobe, Chuo-ku, Sagamihara, Kanagawa 252-5201, Japan*
[b] *Fujimura Animal Hospital, 5-10-26 Aomatanihigashi, Minou, Osaka 652-0022, Japan*
[c] *Research Center for Allergy and Immunology, RIEKN, 1-7-22 Suehiro-cho, Tsurumi-ku, Yokohama, Kanagawa 230-0045, Japan*
[d] *Department of Medical Sciences, School of Veterinary Medicine, University of Wisconsin, Madison, WI, USA*
[e] *Nippon Zenyaku Kogyo Co., Ltd, 1-1 Tairanoue Sasagawa, Asaka-machi, Koriyama, Fukushima 963-0196, Japan*

ARTICLE INFO

Article history:
Received 17 April 2012
Received in revised form 24 May 2012
Accepted 6 June 2012

Keywords:
Allergen
Canine atopic dermatitis
IgE
Japanese cedar pollen

ABSTRACT

The present study investigated IgE reactivity to a new *Cryptomeria japonica* pollen allergen (Cry j 3) in dogs with atopic dermatitis by using a fluorometric ELISA. Serum samples from 15 dogs that showed IgE sensitivity to crude *C. japonica* pollen allergen by ELISA were tested for specific IgE to each allergen, individually. All 15 dogs had anti-Cry j 1 IgE, 6 (40%) had anti-Cry j 2 IgE, and 11 (73%) had anti-Cry j 3 IgE. Further, we found that these anti-Cry j 3 IgE reacted to Cry j 3 with immunoblotting analysis. These findings indicate that Cry j 3 may be a major allergen in dogs.

1. Introduction

Japanese cedar (*Cryptomeria japonica*) pollinosis is one of the most common immediate-type allergic diseases in Japan (Yasueda et al., 1983), which has been also reported in dogs (Sasaki et al., 1995) as well as in humans. The dogs sensitive to *C. japonica* pollen showed clinical symptoms of canine atopic dermatitis (CAD) and positive immune reactions to the pollen allergen in Prausnitz–Küstner test (Rupa et al., 2008). CAD is a common dermatitis in dogs and defined as an inflammatory and pruritic skin disease with IgE antibodies, most commonly directed against environmental allergens (Halliwell, 2006). Our epidemiological study in Japan reported that approximately 20% of atopic dogs had specific IgE to crude *C. japonica* pollen allergen (Masuda et al., 2000a). These findings suggested that *C. japonica* pollen allergen might be associated with the pathogenesis of CAD.

Two major allergens have been previously isolated from *C. japonica* pollen and characterized as Cry j 1 (Yasueda et al., 1983) and Cry j 2 (Sakaguchi et al., 1990). Cry j 1 was identified as a 41–46 kDa allergen with pectate lyase enzyme activity (Yasueda et al., 1983; Taniguchi et al., 1995), while Cry j 2 was identified as a 45 kDa allergen with polymethylgalacturonase enzyme activity (Sakaguchi et al., 1990; Ohtsuki et al., 1995). We previously showed that humans (Sakaguchi et al., 1990; Hashimoto et al., 1995), Japanese monkeys (*Macaca fuscata*) (Sakaguchi et al., 1992; Hashimoto et al., 1994), and dogs (Masuda et al., 2000b) had specific IgE to Cry j 1 and Cry j 2.

Of the 100 human patients with *C. japonica* pollinosis, 27 serum samples contained IgE against the recently isolated Cry j 3, suggesting that Cry j 3 is an important allergen in some patients (Fujimura et al., 2007). Further, we

* Corresponding author. Tel.: +81 42 850 2481; fax: +81 42 850 2481.
E-mail address: sakagum@azabu-u.ac.jp (M. Sakaguchi).

0165-2427/$ – see front matter © 2012 Elsevier B.V. All rights reserved.
http://dx.doi.org/10.1016/j.vetimm.2012.06.007

found that Cry j 3 is 27 kDa protein and has relatively high homology with thaumatin-like protein categorized in the pathogenesis-related-5 (PR-5) family protein which may act as causative allergens of oral allergy syndrome (OAS) in human patients (Fujimura et al., 2007). OAS is a condition characterized by IgE-mediated immediate allergic symptoms restricted to the oral mucosa, which may involve itching, and vascular edema of the lips, tongue, and pharynx with a sudden onset (Kondo and Urisu, 2009). OAS symptoms occur in association with IgE cross-reactivity arising from structural homologies between pollen allergens and food proteins. A typical manifestation of OAS would be the oral mucosal symptoms that appear when a patient with birch pollen allergy has eaten some foods associated with the family *Rosaceae* such as an apple, cherry, or peach. However, to date, there have been no studies to investigate the allergic responses to Cry j 3 in dogs.

In the present study, we investigated IgE reactivity to Cry j 3 in atopic dogs sensitive to crude *C. japonica* pollen allergen by a fluorometric ELISA.

2. Materials and methods

2.1. Crude and major C. japonica pollen allergens

Crude *C. japonica* pollen allergen was prepared as described previously (Yasueda et al., 1983). Cry j 1 and Cry j 2 as major allergens were purified as described previously (Sakaguchi et al., 1990). Cry j 3 was purified as described previously (Fujimura et al., 2007).

2.2. Sera

CAD was diagnosed based on Willemse's criteria (Willemse, 1986) and Prélaud's major criteria (Prélaud et al., 1998). The sera were obtained from 100 dogs with AD visiting to Fujimura Animal Hospital owed by one of the authors (M.F.) (Osaka, Japan). The sera used as negative controls in the pollen-specific IgE assay were obtained from 19 dogs that had been kept indoors as experimental laboratory animals and had never been exposed to *C. japonica* pollen. They had shown no signs of AD and demonstrated no specific reaction to crude *C. japonica* allergen by intradermal skin testing (IDST).

2.3. Fluorometric ELISA for specific IgE to crude and major C. japonica pollen allergens

Specific IgE to crude and major *C. japonica* pollen allergens were measured by a fluorometric ELISA. A microplate (NUNC-Immuno Plate Maxisorp F96; NalgeNunc International, Roskilde, Denmark) was coated with crude *C. japonica* pollen allergen (4 μg/ml) or the purified allergens, Cry j 1, Cry j 2, or Cry j 3 allergens (1 μg/ml), at 4 °C overnight. After washing, the plate was incubated with diluted sera (1:10) at room temperature for 3 h. The plate was then washed and incubated with a mouse monoclonal anti-dog IgE antibody (0.5 μg/ml) (DeBoer et al., 1993) was then added. The plate was incubated at 4 °C overnight. After washing, the plate was then incubated with biotinylated rat monoclonal anti-mouse IgG_1 (Zymed Laboratories, San Francisco, CA, USA) at room temperature for 1 h. After washing, the plate was incubated with β-D-galactosidase-conjugated streptavidin (Zymed Laboratories) at room temperature for 1 h. After final washing, the plate was incubated with 0.1 mM 4-methylumbelliferyl-β-D-galactopyranoside (Sigma, St. Louis, MO, USA) at 37 °C for 2 h. The enzyme reaction was stopped with 0.1 M glycine–NaOH (pH10.2), and the fluorescence intensity was read as fluorescence units (FU) on a microplate fluorescence reader (Fluoroskan; Flow Laboratories, McLean, VA, USA). The fluorometric ELISA for specific IgE in each sample was repeated more than three times. The cut-off value was determined as the average + 3SD FU in serum samples of 19 dogs as negative control.

2.4. Detection of allergen-specific IgE by immunoblotting analysis

Cry j 1 and Cry j 3 were electrophoresed by SDS-PAGE and then electrotransferred to PVDF membrane (GE Healthcare, Piscataway, NJ, USA). The three sera showing higher FU values of anti-Cry j 1 or anti-Cry j 3 IgE had been respectively pooled for immunoblotting analysis. After blocking with PBS containing 5% skimmed milk, the membrane was incubated with pooled sera diluted 1:10 in PBS containing 0.1% Tween-20 and 5% non-fat dried milk for 2 h. After washing, horseradish peroxidase (HRP)-conjugated goat anti-dog IgE (0.1 μg/ml) (Bethyl Laboratories, Montgomery, TX, USA) was added on the membrane and incubated for 2 h. After washing, the membrane was incubated with ECL reagent (GE Healthcare) for 5 min and exposed to a radiograph film for 5–30 s.

3. Results and discussion

Specific IgE to crude *C. japonica* pollen allergen was measured in the sera of the 100 dogs with AD by ELISA (Fig. 1). The cut-off value calculated from negative control samples was 55 FU. Of the 100 dogs with AD, 15 had IgE sensitivity to crude *C. japonica* pollen allergen similar to the results of our previous epidemiological study (Masuda et al., 2000a). Next, IgE reactivity to Cry j 1 and Cry j 2 was examined in these 15 dogs sensitive with crude *C. japonica* pollen allergen by ELISA (Fig. 2A and B). The cut-off values of specific IgE levels to Cry j 1 and Cry j 2 calculated from the negative control samples were found to be 114 and 96 FU, respectively. Of the 15 serum samples which included specific IgE to crude *C. japonica* pollen allergen, all had specific IgE to Cry j 1, and 6 (40%) had specific IgE to Cry j 2. In humans, more than 90% of the patients with *C. japonica* pollinosis had specific IgE to Cry j 1 and Cry j 2 (Hashimoto et al., 1995). Further, in wild Japanese monkeys, we found that of the 45 monkeys sensitive to crude *C. japonica* pollen allergen, 23 (51%) had specific IgE to both Cry j 1 and Cry j 2, 21 (47%) had specific IgE only to Cry j 1, and 1 (2%) had specific IgE only to Cry j 2 (Hashimoto et al., 1994). In humans and monkeys, Cry j 1 and Cry j 2 are major pollen allergens. In the present study, however, 40% of the dog sera that had specific IgE to crude pollen had anti-Cry j 2 IgE. This result was similar to that of our previous study (Masuda

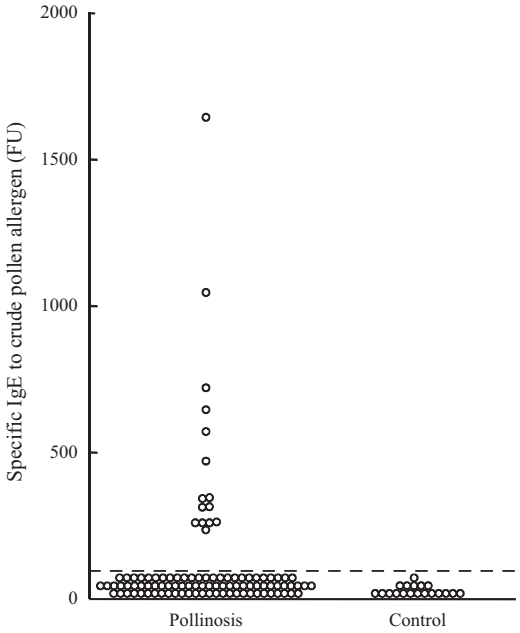

Fig. 1. IgE reactivity to crude *C. japonica* pollen allergen in dogs. The data were obtained by using diluted sera (1:10). The dashed line shows the cut-off value. The cut-off value calculated from negative control samples was 55 FU.

et al., 2000b). These findings indicate that Cry j 1 is a major allergen in dogs as well as humans and Japanese monkeys.

IgE reactivity to Cry j 3 was examined in these 15 dogs sensitive to crude pollen allergen (Fig. 2C). The cut-off values of specific IgE to Cry j 3 calculated from negative control samples were 126 FU. Of the 15 sera which contained specific IgE to crude *C. japonica* pollen allergen, 11 (73%) had specific IgE to Cry j 3. Of 11 sera samples, five also reacted with Cry j 1, and six with both Cry j 1 and 2. The IgE-binding frequency of Cry j 3 in the human patients with *C. japonica* pollinosis was estimated as 27% (Fujimura et al., 2007). More than 70% of CAD with specific IgE to crude *C. japonica* pollen allergen had anti-Cry j 3 IgE. These findings suggest that Cry j 3 may be a more important allergen in dogs than in humans.

To further evaluate anti-Cry j 3 IgE in dogs reactivity with Cry j 3, we conducted immunoblotting analysis. Cry j 1 and Cry j 3 were electrophoresed by SDS-PAGE and then electrotransferred to PVDF membrane. The pooled serum of 3 dogs with anti-Cry j 1 IgE was added to the membrane, and Cry j 1 was detected with anti-Cry j 1 IgE (Fig. 3, lane 1). Similarly, the pooled serum of 3 dogs with anti-Cry j 3 IgE was added to the membrane, and Cry j 3 was detected with anti-Cry j 3 IgE (Fig. 3, lane 3). In contrast, the pooled serum of 3 dogs as negative controls with no anti-Cry j 1 and Cry j 3 IgE was added to the membrane, and Cry j 1

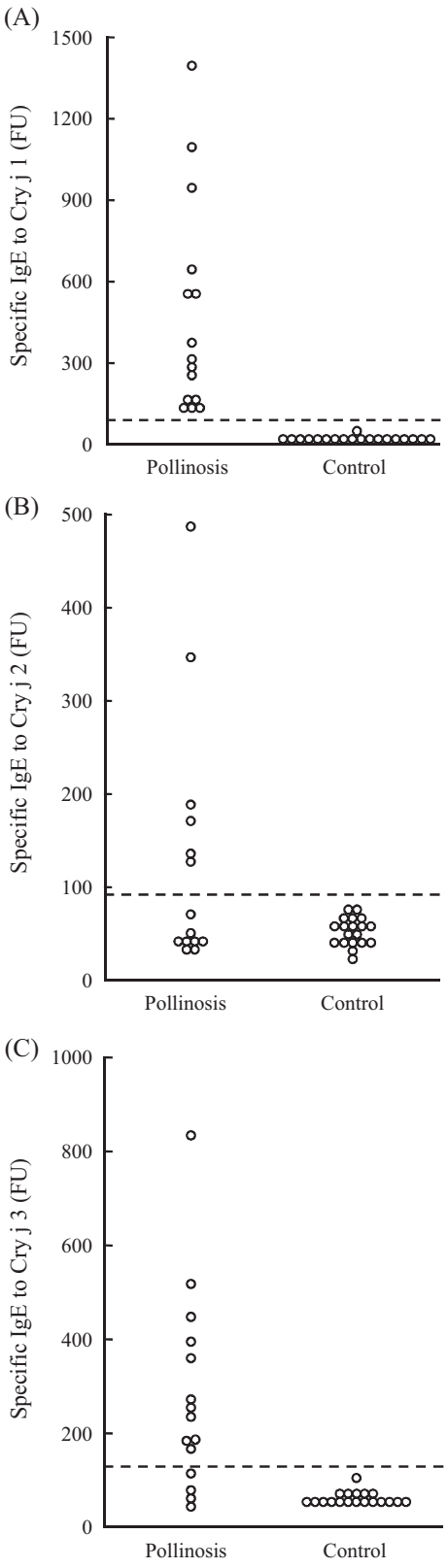

Fig. 2. IgE reactivity to (A) Cry j 1, (B) Cry j 2, and (C) Cry j 3 in atopic dogs sensitive to crude *C. japonica* pollen allergen. The data were obtained by using diluted sera (1:10). The dashed line shows the cut-off value. The cut-off values calculated from negative control samples were 114, 96 and 121 FU, respectively.

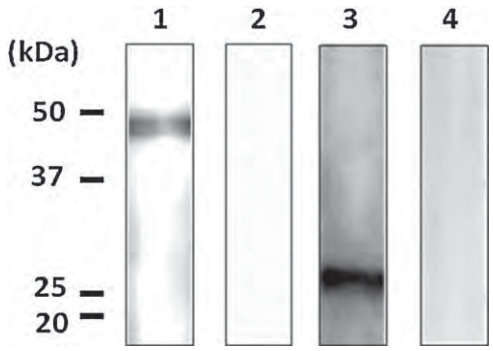

Fig. 3. Immunoblotting analysis of Cry j 1 and Cry j 3. Cry j 1 (lanes 1 and 2) or Cry j 3 (lanes 3 and 4) was electrophoresed by SDS-PAGE and then electrotransferred to PVDF membrane. Lane 1: pooled serum of 3 dogs with anti-Cry j 1 IgE (FU values: 1410, 1090, and 925), lanes 2 and 4: pooled serum of 3 dogs as negative controls with no anti-Cry j 1 and Cry j 3, lane 3: pooled serum of 3 dogs with anti-Cry j 3 IgE (FU values: 812, 507, and 412).

and Cry j 3 were not detected (Fig. 3, lanes 2 and 4). These results reconfirmed that sera of dogs with anti-Cry j 3 IgE reacted to Cry j 3 with immunoblotting analysis.

We found that Cry j 3 has significant homology with the thaumatin-like protein categorized in PR-5 family protein which might act as a causative allergen in OAS (Fujimura et al., 2007). Cross-reactivity between allergens from *C. japonica* pollen and tomato has been reported in dogs and humans (Fujimura et al., 2002; Kondo et al., 2002). PR-5 protein, which was considered as one of the important pollen allergens responsible for pollinosis and OAS, have been identified as Jun a 3 from mountain cedar (*Juniperus ashei*), Jun v 3 from eastern red cedar (*Juniperus virginiana*), and Cup a 3 from Arizona cypress (*Cupressus arizonica*) (Midoro-Horiuti et al., 2000, 2001; Cortegano et al., 2004). Fujimura et al. (2007) revealed that Cry j 3 has significant homology with the thaumatin-like protein and suggested that Cry j 3 might act as a causative allergen for OAS in human patients. Unfortunately, we could not evaluate the presence of OAS in the dogs with IgE to Cry j 3. The present results, however, suggest that Cry j 3 is an important allergen in dogs and might play an important role in the etiology of OAS in dogs.

In conclusion, we found that many dogs with specific IgE to crude *C. japonica* pollen had anti-Cry j 3 IgE. Our results indicate that Cry j 3 can be considered as one of the major allergens in CAD. Further studies are needed to reveal the role of cross-reactivity to other allergens in the etiology of OAS in CAD.

Conflicts of interest

The authors declare no conflicts of interest.

Acknowledgments

This research was partially supported by Grant-in-Aid Matching Fund Subsidy for Private University and by a project grant awarded by the Azabu University Research Services Division.

References

Cortegano, I., Civantos, E., Aceituno, E., Del Moral, A., Lopez, E., Lombardero, M., Del Pozo, V., Lahoz, C., 2004. Cloning and expression of a major allergen from *Cupressus arizonica* pollen Cup a 3, a PR-5 protein expressed under polluted environment. Allergy 59, 485–490.

DeBoer, D.J., Ewing, K.M., Schultz, K.T., 1993. Production and characterization of mouse monoclonal antibodies directed against canine IgE and IgG. Vet. Immunol. Immunopathol. 37, 183–199.

Fujimura, M., Ohmori, K., Masuda, K., Tsujimoto, H., Sakaguchi, M., 2002. Oral allergy syndrome induced by tomato in a dog with Japanese cedar (*Cryptomeria japonica*) pollinosis. J. Vet. Med. Sci. 64, 1069–1070.

Fujimura, T., Futamura, N., Midoro-Horiuti, T., Togawa, A., Goldblum, R.M., Yasueda, H., Saito, A., Shinohara, K., Masuda, K., Kurata, K., Sakaguchi, M., 2007. Isolation and characterization of native Cry j 3 from Japanese cedar (*Cryptomeria japonica*) pollen. Allergy 62, 547–553.

Halliwell, R., 2006. Revised nomenclature for veterinary allergy. Vet. Immunol. Immunopathol. 114, 2007–2008.

Hashimoto, M., Sakaguchi, M., Inouye, S., Imaoka, K., Nigi, H., Fujimoto, K., Honjo, S., Taniguchi, Y., Kurimoto, M., Gotoh, S., Minezawa, M., Yokota, A., Nakamura, S., 1994. Prevalence of IgE antibody to crude and purified allergens of Japanese cedar pollen among different troops of Japanese monkeys (*Macaca fuscata*). J. Med. Primatol. 23, 393–396.

Hashimoto, M., Nigi, H., Sakaguchi, M., Inouye, S., Imaoka, K., Miyazawa, H., Taniguchi, Y., Kurimoto, M., Yasueda, H., Ogawa, T., 1995. Sensitivity to two major allergens (Cry j I and Cry j II) in patients with Japanese cedar (*Cryptomeria japonica*) pollinosis. Clin. Exp. Allergy 25, 848–852.

Kondo, Y., Tokuda, R., Urisu, A., Matsuda, T., 2002. Assessment of cross-reactivity between Japanese cedar (*Cryptomeria japonica*) pollen and tomato fruit extracts by RAST inhibition and immunoblot inhibition. Clin. Exp. Allergy 32, 590–594.

Kondo, Y., Urisu, A., 2009. Oral Allergy Syndrome. Allergol. Int. 58, 485–491.

Masuda, K., Sakaguchi, M., Fujiwara, S., Kurata, K., Yamashita, K., Odagiri, T., Nakao, Y., Matsuki, N., Ono, K., Watari, T., Hasegawa, A., Tsujimoto, H., 2000a. Positive reactions to common allergens in 42 atopic dogs in Japan. Vet. Immunol. Immunopathol. 73, 193–204.

Masuda, K., Tsujimoto, H., Fujiwara, S., Kurata, K., Hasegawa, A., Taniguchi, Y., Yamashita, K., Yasueda, H., DeBoer, D.J., de Weck, A.L., Sakaguchi, M., 2000b. IgE-reactivity to major Japanese cedar (*Cryptomeria japonica*) pollen allergens (Cry j 1 and Cry j 2) by ELISA in dogs with atopic dermatitis. Vet. Immunol. Immunopathol. 74, 263–270.

Midoro-Horiuti, T., Goldblum, R.M., Kurosky, A., Wood, T.G., Brooks, E.G., 2000. Variable expression of pathogenesis-related protein allergen in mountain cedar (*Juniperus ashei*) pollen. J. Immunol. 164, 2188–2192.

Midoro-Horiuti, T., Brooks, E.G., Goldblum, R.M., 2001. Pathogenesis-related proteins of plants as allergens. Ann. Allergy Asthma Immunol. 87, 261–271.

Ohtsuki, T., Taniguchi, Y., Kohno, K., Fukuda, S., Usui, M., Kurimoto, M., 1995. Cry j 2, a major allergen of Japanese cedar pollen, shows polymethylgalacturonase activity. Allergy 50, 483–488.

Prélaud, P., Guaguère, E., Alhaidari, Z., Faivre, N., Héripret, D., Gayerie, A., 1998. Reevaluation of diagnostic criteria of canine atopic dermatitis. Rev. Med. Vet. 149, 1057–1064.

Rupa, P., Hamilton, K., Cirinna, M., Wilkie, B.N., 2008. Porcine IgE in the context of experimental food allergy: purification and isotype-specific antibodies. Vet. Immunol. Immunopathol. 125, 303–314.

Sakaguchi, M., Inouye, S., Taniai, M., Ando, S., Usui, M., Matsuhashi, T., 1990. Identification of the second major allergen of Japanese cedar pollen. Allergy 45, 309–312.

Sakaguchi, M., Inouye, S., Imaoka, K., Miyazawa, H., Hashimoto, M., Nigi, H., Nakamura, S., Gotoh, S., Minezawa, M., Fujimoto, K., Honjo, S., Taniguchi, Y., Ando, S., 1992. Measurement of serum IgE antibodies against Japanese cedar pollen (*Cryptomeria japonica*) pollen in Japanese monkeys (*Macaca fuscata*) with pollinosis. J. Med. Primatol. 21, 323–327.

Sasaki, Y., Kitagawa, H., Fujioka, T., Kitoh, K., Iwasaki, T., Sakaguchi, M., Inouye, S., 1995. Hypersensitivity to Japanese cedar (*Cryptomeria japonica*) pollen in dogs. J. Vet. Med. Sci. 57, 683–685.

Taniguchi, Y., Ono, A., Sawatani, M., Nanba, M., Kohno, K., Usui, M., Kurimoto, T., Matuhasi, T., 1995. Cry j I, a major allergen of Japanese cedar pollen, has pectate lyase enzyme activity. Allergy 50, 90–93.

Willemse, T., 1986. Atopic skin disease: a review and a reconsideration of diagnostic criteria. J. Small Anim. Pract. 27, 771–778.

Yasueda, H., Yui, Y., Shimazu, T., Shida, T., 1983. Isolation and characterization of the major allergen from Japanese cedar (*Cryptomeria japonica*) pollen. J. Allergy Clin. Immunol. 71, 77–86.

Cellular Immunology 275 (2012) 24–32

Contents lists available at SciVerse ScienceDirect

Cellular Immunology

journal homepage: www.elsevier.com/locate/ycimm

The role of CCR7 in allergic airway inflammation induced by house dust mite exposure

Masaki Kawakami [a,b], Osamu Narumoto [a,b], Yukiko Matsuo [a], Kazuhide Horiguchi [c], Satomi Horiguchi [c], Naohide Yamashita [d], Masahiro Sakaguchi [e], Martin Lipp [f], Takahide Nagase [b], Naomi Yamashita [a,*]

[a] Department of Pharmacotherapy, Research Institute of Pharmaceutical Sciences, Musashino University, Tokyo, Japan
[b] Department of Pulmonary Medicine, Faculty of Medicine, University of Tokyo, Tokyo, Japan
[c] Department of Anatomy, Faculty of Medical Science, University of Fukui, Fukui, Japan
[d] Department of Advanced Medical Science, Institute of Medical Science, University of Tokyo, Japan
[e] Department of Veterinary Microbiology, School of Veterinary Medicine, Azabu University, Kanagawa, Japan
[f] Tumorgenetics and Immunogenetics, Max-Delbrück-Center for Molecular Medicine, Berlin, Germany

ARTICLE INFO

Article history:
Received 13 December 2011
Accepted 29 March 2012
Available online 5 April 2012

Keywords:
Asthma
Airway hyperresponsiveness
CCR7
CCL21
House dust mite
Airway inflammation

ABSTRACT

House dust mite (HDM), the most common allergen, activate both the IgE-associated and innate immune responses. To clarify the process of sensitization, we investigated the role of the CCL21, CCL19, and CCR7 axis in a mouse model of HDM-induced allergic asthma. HDM inhalation without systemic immunization resulted in a HDM-specific IgE response. CCR7-knockout (CCR7KO) mice exhibited greater airway inflammation and IgE responses compared to wild-type mice. We examined FoxP3 expression in these mice to clarify the contribution of regulatory cells to the responses. FoxP3 expression was higher in the lungs but not in the lymph nodes of CCR7KO mice compared to wild-type mice. In CCR7KO mice, FoxP3-positive cells were found in lung, but we observed higher release of IL-13, IL-5, TGF-β, IL-17, and HMGB1 in bronchoalveolar lavage fluid. We demonstrate here that immuno-regulation through CCR7 expression in T cells plays a role in HDM-specific sensitization in the airway.

1. Introduction

The inhalation of allergens induces airway inflammation, which is a prominent feature of asthma [1–4]. Dendritic cells are antigen-presenting cells that initiate several immune responses [5]. After dendritic cells take up allergens, they enter afferent lymphatic vessels through a process promoted by CCL21 [6,7]. Antigen-laden antigen-presenting cells then induce activation, expansion, and differentiation of antigen-specific T cells within the draining lymph nodes. We previously showed that paucity of lymph node T cells (plt) mice, which are deficient in CCL21ser and CCL19, resulted in reduced but still substantial airway inflammation, suggesting that allergen sensitization and airway inflammation can be induced without secondary lymph nodes [8]. In contrast, CCL21 and CCL19 play a critical role in the resolution phase of airway inflammation, which is similar to their role in the mucosal immune system [8–10].

In animal asthmatic models, systemic immunization using allergens formulated with alum is used to induce IgE. In plt mice we used ovalbumin in alum to clarify the role of CCL21 [8]. Administration of house dust mite (HDM) by inhalation was recently shown to induce airway inflammation without systemic immunization [11,12]. In many countries, HDM is one of the most common allergens triggering asthma [13–15]. HDM allergens have proteinase activity, which is critical for sensitization [16,17]. HDM allergens react with toll-like receptor 4 (TLR4), which is a receptor for lipopolysaccharide (LPS) [18,19]. In addition, *Derf* 2, a major HDM allergen, possesses structural homology to myeloid differentiation factor (MD) 2, the LPS-binding component of the TLR4 signaling complex [20,21]. Taken together, these findings indicate that allergen sensitization involves complex interactions between antigen-specific and innate immune responses that have not yet been clarified.

CCR7 is the receptor for CCL19 and CCL21, and CCR7-knockout (CCR7KO) mice possess similar impairment of the secondary lymph nodes as plt mice [22]. The impairment of contact sensitivity in CCR7KO mice is greater than that in plt mice [22].

Abbreviations: HDM, house dust mite; CCR7KO, CCR7-knockout; LPS, lipopolysaccharide; BALF, bronchoalveolar lavage fluid; HE, haematoxylin-eosin; PAS, periodic acid-Schiff; iBALT, inducible bronchus-associated lymphoid tissue; HMGB, high-mobility group box; Treg, regulatory T; ACh, acetylcholine; Raw, airway resistance.

* Corresponding author. Address: Department of Pharmacotherapy, Research Institute of Pharmaceutical Sciences, Musashino University, 1-1-20 Shinmachi Nishitokyo-shi, Tokyo 202-8585, Japan. Fax: +81 424 68 8647.
E-mail address: naoyama@musashino-u.ac.jp (N. Yamashita).

0008-8749/$ - see front matter © 2012 Elsevier Inc. All rights reserved.
http://dx.doi.org/10.1016/j.cellimm.2012.03.009

Furthermore, CCR7 is important in maintaining immune responses and immune tolerance [23]. CCR7 is also essential to migrate and exhibit regulatory function of regulatory T (Treg) cells [24–26]. To clarify the process of allergen sensitization and the role of CCR7 expression in this process, we investigated the ability of CCR7KO mice to exhibit HDM-specific airway inflammation. We found that airway inflammation was significantly augmented and lymphocyte accumulation was prominent in CCR7KO mice. Although FoxP3-positive cells were present in the lung, they did not function effectively in CCR7KO mice. This finding suggests that allergen sensitization is controlled by the expression of CCR7. The targeted control of CCR7 expression has potential as an immunotherapy for asthma.

2. Methods

2.1. Animals

C57BL/6. mice were purchased from SLC (Shizuoka, Japan). *CCR7−/−* C57BL/6 mice were established as previously reported [22] and bred in the animal facilities of Musashino University School of Medicine under specific pathogen-free conditions under approval of Institutional Animal experiments Committee of Musashino University. Care and use of the animals followed the guidelines of the "Principles of Laboratory Animal Care" formulated by the National Society for Medical Research. To genotype the pups, tail DNA was extracted by using a DNA Isolation Kit (GENTRA, Minneapolis, MN, USA) and examined by PCR analysis to detect the wild-type and knockout alleles. The sense and antisense primers to amplify the 600-bp CCR7 wild-type allele were 5′-CCCCGGGCAATGTCCTGA-3′ and 5′-CGTGTCCTCGCCGCTGTT-3′, respectively. The sense and antisense alleles to amplify the 400-bp knockout allele were 5′-CTCTCGTGGGATCATTGTTTTTCT-3′ and 5′-GTCTCCGCCTCCATGCTTCACC-3′, respectively.

2.2. Treatment

Mice were treated by intranasal administration with 40 μg of HDM extract dissolved in saline once per day for 7–10 days. The HDM extract was kindly provided by ITEA Inc., Tokyo, Japan. Mice treated with saline were used as controls.

2.3. Measurements of serum and HDM-specific IgE levels

For total IgE detection, total IgE ELISA kits (Morinaga Institute of Biological Science, Yokohama, Japan) were used following the manufacturer's instructions. For mite-specific IgE detection, plates were coated with 20 μg/ml HDM extract in 50 mM carbonate buffer (pH 9.0). After blocking the coated plates with SuperBlock (Pierce, Rockford, In.), samples were diluted 20-fold and added to the plates. Antibodies were detected with rat anti-mouse IgE specific monoclonal antibody (YAMASA, Chiba, Japan), followed by the addition of Streptavidin-HRP (Dako, Corp., Glodtrup, Denmark). The color was developed with tetramethylbenzidine + substrate (BioFx Labo., MD, USA) and the reaction stopped by addition of 1 N H_2SO_4. Optical density at 450 nm (OD450) was measured using a microplate reader. Antibody titers were calculated by comparison with internal standards.

2.4. Bronchoalveolar lavage fluid (BALF) cell analysis

BALF cell analysis was performed 24 h after the last HDM administration, as previously reported [27]. BALF was obtained by incubating and repeatedly washing the lung with 1 ml of saline until the recovered volume was 2 ml. The isolated BALF was centrifuged at 1500 rpm for 10 min at 4 °C. Pellets were dissolved in 1 ml PBS and the number of cells counted. Cytospin preparations were obtained by spinning at 640 rpm for 2 min, stained with Diff Quik (International Reagents Corporation, Osaka, Japan), and then examined by microscopy.

The content of cytokine in the BALF was measured using the ELISA kits; IL-13, IL-5 and TGF-β by Quantising kit (R&D System, Inc. (Minneapolis, MN), IL-35 by specific ELISA kit (Cusabio Biotec, P.R., China). HMGB1 was measured by using an HMGB1 ELISA Kit II (Shino-test Co., Tokyo, Japan), which specifically detects HMGB1 [28].

2.5. Assessment of airway responsiveness

The assessment of airway responsiveness was undertaken 24 h after the last mite administration, as previously reported [27]. Briefly, the anesthetized mice were tracheostomized and injected with pancuronium bromide. The animals were connected to a Harvard ventilator with 0.25 ml tidal volume and a respiratory frequency of 150/min. Next, they were placed in the whole-body plethysmograph (Buxco Electronics) to measure airway resistance (Raw). To assess airway responsiveness, increasing dose of acetylcholine (ACh) (3.12–25 mg/mL) was administered by nebulization. Data are expressed as [Raw after inhalation of ACh/Raw before inhalation) × 100 (%)].

2.6. Histological examination

Mice were perfused transcardially with PBS and then 4% paraformaldehyde in 100 mM phosphate buffer (pH 7.4). The lungs were removed and then immersed in 4% paraformaldehyde for 2 h at 4 °C. After washing with PBS, the specimens were soaked overnight in 30% sucrose in PBS, embedded in optimal cutting temperature (OCT) compound (Miles, Elkhart, IN, USA), and then quickly frozen. Cryostat sections were cut at a thickness of 10 μm by using a Leica CM3050 cryostat (Leica Microsystems, Wetzlar, Germany), and thaw-mounted on poly-L-lysine-coated glass slides (Matsunami Glass, Osaka, Japan). The samples were analyzed by Haematoxylin-eosin (HE) and periodic acid-Schiff (PAS) staining.

For immunohistological analysis, lung sections were preincubated overnight with anti-FoxP3 (1:1000; eBioscience, San Diego, CA) and then incubated with Alexa Fluor 488-coupled donkey anti-IgG (Molecular Probes, Eugene, OR, USA). Rat anti-mouse CD4, CD8 and CD3 antibodies (BD Pharmigen) were used for CD4, CD8and CD3 positive cell detection. Goat anti-mouse CD4 antibody (R&D Systems) was used for double staining experiments. Sections were counterstained with 4′,6′-diamidino-2-phenylindole (DAPI; Roche Diagnostics, GmbH, Mannheim, Germany) and mounted with Vectashield Mounting Medium (Vector Laboratories, Burlingame, CA). Control tissues were prepared by omitting primary antibodies from the incubation solutions; no specific immunoreactivity was observed. Immunofluorescence images were examined with a Leica TCS-SP2 confocal microscope (Leica Microsystems) with excitation wavelengths of 350, 488, and 543 nm. Images were collected and analyzed in Leica Confocal Software (Leica Microsystems).

2.7. CD4+CD25+ and dendritic cell isolation

Lung was homogenized in 1% penicillin/streptomycin/RPMI1640 using cell strainers with 70 μm pores (BD Falcon, NJ, USA). Specimens were then centrifuged at 1500 rpm for 10 min at 4 °C, and the cell pellets were washed twice. Lung cells were purified using NycoPrep (AXIS-SHIELD plc, Dundee, Scotland) followed by separation using CD4+CD25+ regulatory T cell isolation kits (Miltenyi Biotech GmbH, Nordrhein-Westfalen, Germany). In the

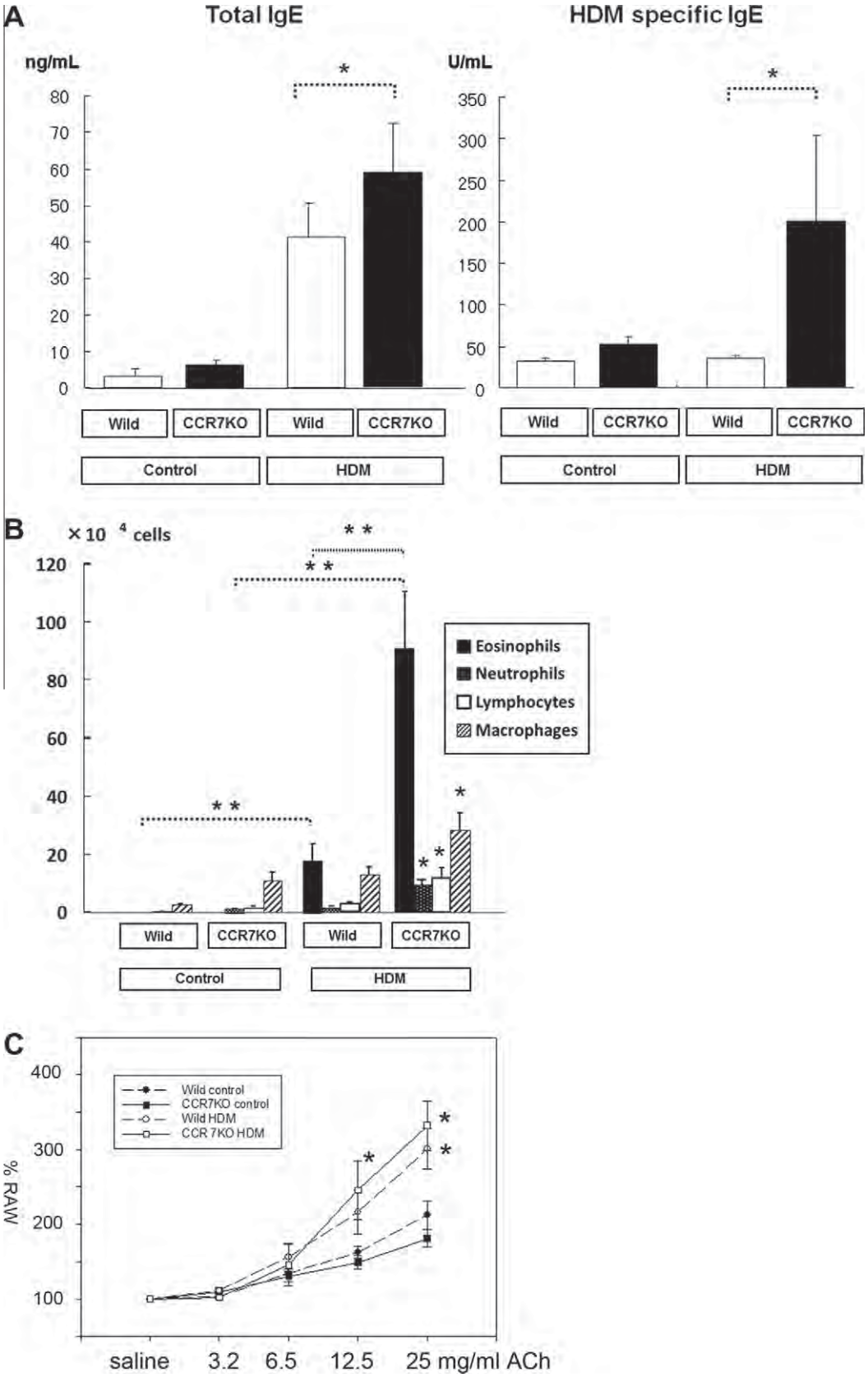

Fig. 1. Airway inflammation and airway response. (A) IgE and HDM-specific IgE synthesis. Each bar represents the mean ± SEM of values obtained from 10–12 different mice. Control indicated mice treated with saline. HDM indicated mice treated with house dust mite (HDM).*$p < 0.05$. (B) BALF cell analysis BALF cells were placed on glass slides using Cytospin. Slides were then stained with Diff Quik, and cell differentiation was assessed microscopically. Control indicated mice treated with saline. HDM indicated mice treated with HDM. The *Y* axis shows the number of cells in total BALF (2 mL). Each bar indicates mean ± SEM of 5–7 different mice. **$p < 0.01$. *$p < 0.05$, CCR7KO compared with wild type mice. (C) Airway response to acetylcholine. The indicated concentrations of ACh were inhaled for 3 min. Airway resistance (Raw) was measured using whole body plethysmographs as described in the Methods. ACh-evoked changes in Raw are expressed as a percentage of the Raw observed before ACh inhalation (100%). The data shown are means ± SEM for six mice.*$p < 0.05$, HDM-treated vs control mice.

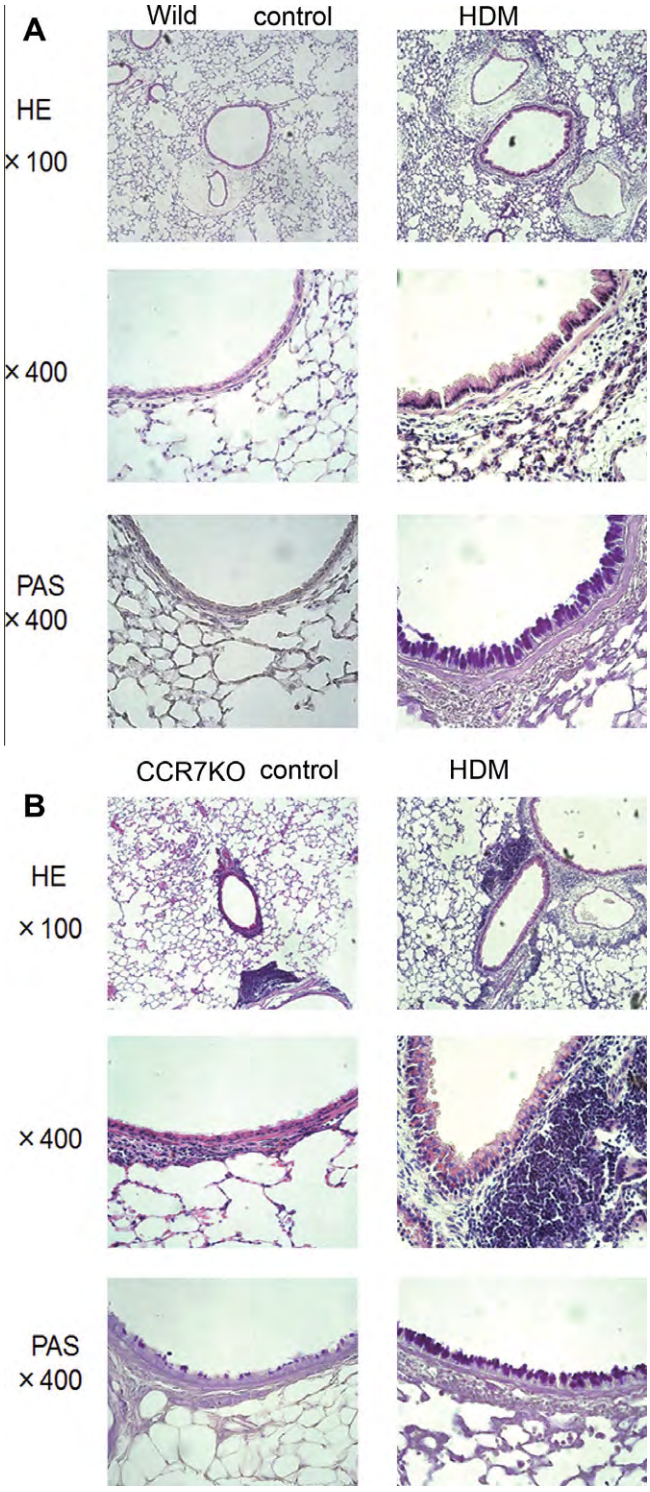

Fig. 2. Histological analysis. Histological analysis was performed with HE and PAS staining. (A) Wild type mice and (B) CCR7KO mice. Control indicated mice treated with saline. HDM indicated mice treated with house dust mite (HDM). Figures are representative data from histological examination of five mice.

first step, CD4+ cells were separated from all non-CD4 cells, and in the second step CD25+ cells were positively selected by using mAb-coated microbeads and magnetic separation columns. The purity of the resultant CD4+CD25+ cell populations was 95% (data not shown). After 2 days of culture, the supernatant was harvested.

For dendritic cells isolation, the lung cells were purified using NycoPrep (AXIS-SHIELD), followed by incubation with anti-CD11c

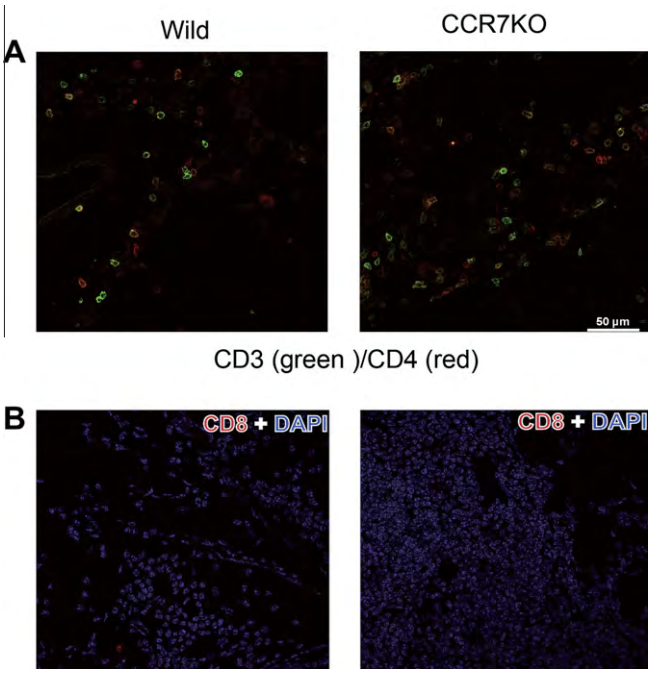

Fig. 3. Confocal micrographs. CD3 (green) and CD4 (red) (A) or CD8 (red) (B) were stained using the specific antibodies. DNA was counterstained with DAPI (blue). original magnification, 400×. (For interpretation of the references to color in this figure legend, the reader is referred to the web version of this article.)

mAb-coated microbeads (Miltenyi Biotech). Bead-bound cells were then isolated using magnetic separation columns. The purities of the $CD11c^+$ cell populations were 90% as shown in Fig. 4.

For flow cytometric analysis, anti-mouse CD16/CD32(Fc block), CD11c, CD40, CD80, CD86, CD83 antibodies (BD Pharmigen) were used. Data were collected using FACSAria (B D Biosciences).

2.8. Examination of mRNA expression using real-time PCR

Total RNA was extracted with ISOGEN (Nippon Gene Co., Ltd., Tokyo, Japan) by a modified acid–guanidium thiocyanate–phenol–chloroform method. RNA purity was established by means of a NanoDrop ND-1000 spectrophotometer (NanoDrop Technologies, Wilmington, DE). The RNA had an OD260/280 ratio of 1.8 indicating high purity. After measuring the amount of total RNA, cDNA synthesis was performed with a cDNA Synthesis Kit (Bio-Rad Laboratories Inc., Hercules, California, USA). The levels of mRNA were examined by real-time PCR using a Light Cycler-Fast Start DNA Master Syber Green I kit (Roche Diagnostics, Mannheim, Germany). In this system, double-stranded DNA labeled with Syber Green I is detected by real-time PCR. Quantification was performed by comparison to a standard curve generated from a serial dilution of specific PCR products. mRNA levels were standardized according to β-actin mRNA levels and were expressed as ratios of control values. The primers used were as follows: β−actin, 5′-CCTGTATGCCTCTGGTCGTA-3′ (sense) and 5′-CCATCTCCTGCTCGAAGTCT-3′ (antisense) to amplify a 260 bp product; FoxP3, 5′-TCTTCGAGGAGCCAGAAGAG-3′ and 5′-TACTGGTGGCTACGATGCAG-3 to amplify a 240 bp product.

2.9. Statistics

For comparisons of multiple parameters, we used multiple analysis of variance (MANOVA). The level of statistical significance was set at $p < 0.05$. Data were expressed as the mean ± SEM.

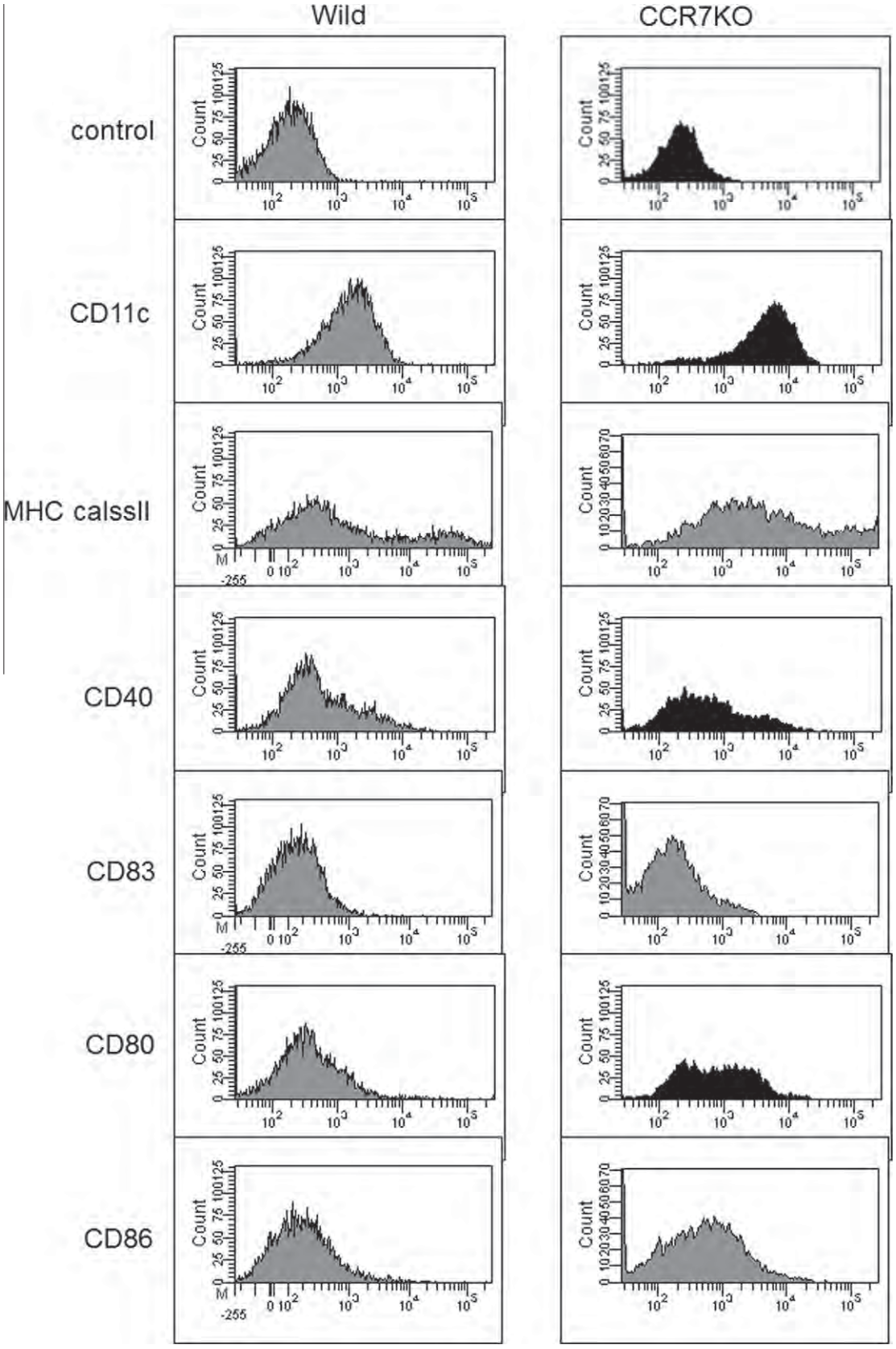

Fig. 4. Flow cytometric analysis of dendritic cells. Dendritic cells positively separated from lung were analyzed for activation marker and co-stimulatory molecules.

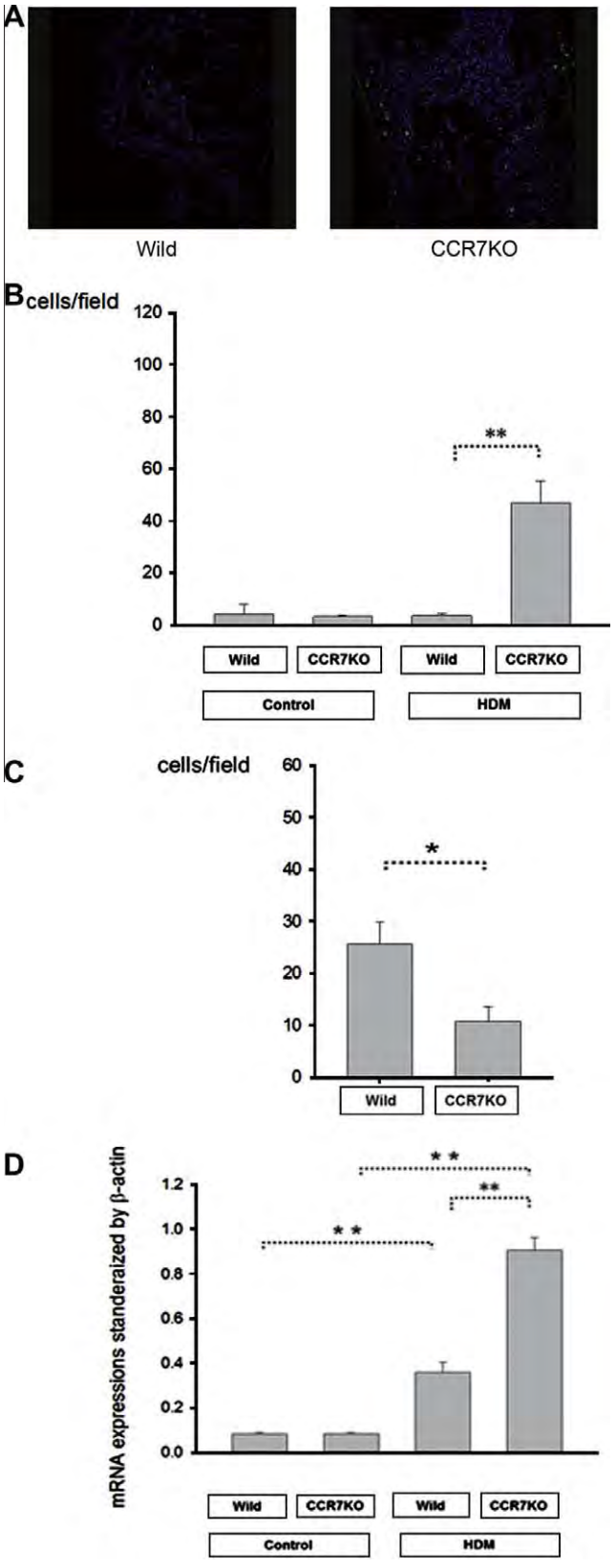

Fig. 5. FoxP3 expression. (A) Confocal micrographs. FoxP3 (green) was stained using the specific antibodies. DNA was counterstained with DAPI (blue). (B) Number of FoxP3 positive cells in lung sections examined by confocal microscopy. (C) Number of FoxP3 positive cells in lymph node. (D) FoxP3 mRNA expression in the lung. $^{*}p < 0.05$, $^{**}p < 0.01$. (For interpretation of the references to color in this figure legend, the reader is referred to the web version of this article.)

Table 1
Characteristics of CD11c positive dendritic cells in the lung.

Percentage of positive cells(%)	Wild type	CCR7KO	
MHC class II positive	43.8 (8.9)	42.1(13.9)	NS
CD40	12.6 (4.9)	11.5 (8,1)	NS
CD83	4.7 (2.3)	5.8 (3.3)	NS
CD80	15.4 (6.5)	16.4 (11.4)	NS
CD86	7.3 (4.0)	17.1 (14.1)	NS

NS: not statistically significant. The number is mean (SE), $n = 3–4$.

Table 2
Characteristics of CD4+CD25+ cells in the lung.

	Wild type	CCR7KO	
Number of cells ($\times 10^5$)	3.4 (1.3)	11.9 (3.4)	$p < 0.001$
IL-10 production (pg/ml)	1453 (134)	1714 (6)	NS
IL-35 production (pg/ml)	190 (23)	256 (24)	NS

Number of cells was number of CD4+CD25+ cells separated from one lung. Cytokine production was from 1×10^4 cells. NS: not statistically significant. The number is Mean (SE), $n = 3–4$.

3. Results

3.1. Total and HDM-specific IgE synthesis after HDM exposure

Total and HDM-specific IgE levels were measured in serum by ELISA to assess the allergic sensitization induced by inhalation of HDM. Inhaled HDM induced IgE synthesis ($p < 0.01$ compared to control) and that IgE synthesis was significantly augmented in CCR7KO mice compared to the wild type ($p < 0.01$) (Fig. 1A). HDM-specific IgE was also elevated in CCR7KO mice treated with HDM. These results indicate that continuous HDM inhalation induced systemic allergic sensitization in both the wild type and CCR7KO mice and that the level of sensitization was higher in CCR7KO mice.

3.2. Role of CCR7 in HDM-induced airway inflammation

We analyzed the infiltration of inflammatory cells into the BALF to examine the role of CCR7 in HDM-induced airway inflammation (Fig. 1B). Significant infiltration of eosinophils and macrophages was observed in mice exposed to HDM compared to controls a (Fig. 1B, $p < 0.01$). The number of eosinophils, neutrophils, lymphocytes and macrophages were significantly higher in CCR7KO mice than in the wild type ($p < 0.01$ for eosinophils, $p < 0.05$ for neutrophils, lymphocytes and macrophages).

Airway responsiveness was also analyzed. CCR7KO mice exhibited significant higher response compared with untreated mice at 12.5 and 25 mg/ml ACh. Wild type mice showed significant response at 25 mg/ml ACh (Fig. 1C).

Histological analysis by HE staining revealed that HDM exposure caused more severe airway inflammation in CCR7KO mice than in the wild type (Fig. 2). As shown by PAS staining, there were significantly more mucus-producing cells in the airways of CCR7KO mice than in the wild type (Fig. 2). These data indicate that HDM induced severe airway inflammation in CCR7KO mice. We also observed prominent lymphoid aggregates in the bronchioles of CCR7KO mice (Fig. 2). Immuno-histochemical examination revealed that these aggregates were composed predominantly of CD4+CD3+ cells and contained a few CD4 single positive cells and few CD8+ cells (Fig. 3).

Dendritic cells play a key role for cell differentiation and antigen presentation [5]. When dendritic cell immobilize antigen, their phenotype changes to mature type and express CCR7 to migrate secondary lymph node [23,29,30]. We examined the mature status of dendritic cells in the lung by flow cytometric analysis. As shown in the Fig. 4, dendritic cells with wild type and those from CCR7KO mice expressed some amount of MHC class II, CD40, CD80, CD83 and CD86 molecules. The amount of expression varied but there were no significant difference between dendritic cells with wild type and those from CCR7KO mice (Table 1). These data suggested that dendritic cells acquired some activation without CCR7 expression.

CCR7 expression is critical for T cells to exit peripheral tissues [31,32]. FoxP3 positive T cells, which are known to suppress airway inflammation, express CCR7 and are activated by pulmonary dendritic cells within secondary lymph nodes [26,33]. We next examined FoxP3 expression in the lung. The results from immuno-histochemical analyses using Foxp3 antibodies are shown in Fig. 5A. In lung sections, we observed significantly more FoxP3-positive cells in CCR7KO mice than in the wild type (Fig. 5B). In the lymph node, however, there were significantly more FoxP3-positive cells in the wild type than in CCR7KO mice (Fig. 5C). FoxP3 mRNA expression was also significantly higher in CCR7KO mice than in the wild type in the lung (Fig. 5D).

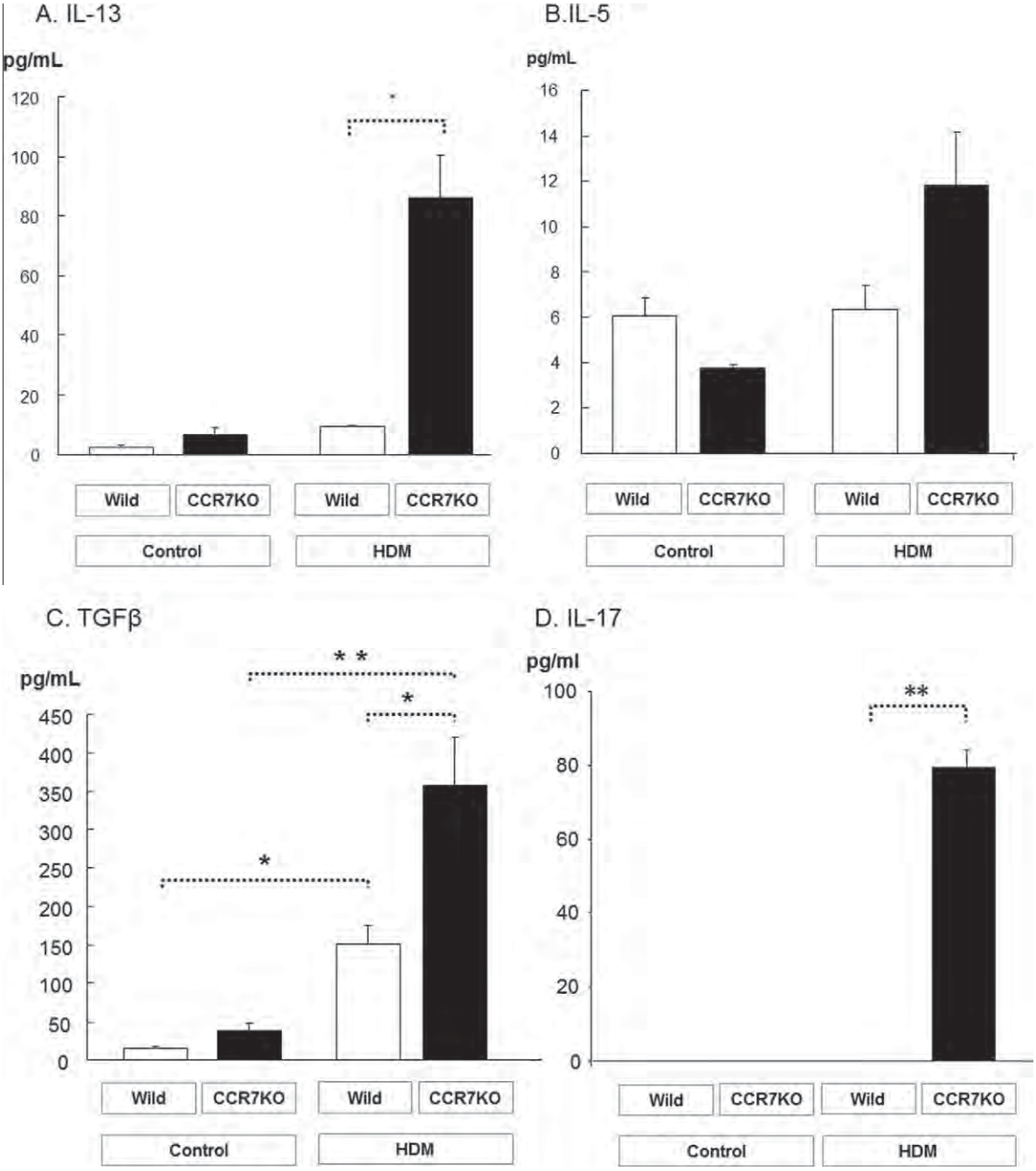

Fig. 6. Analysis of cytokine production in the BALF. BALF supernatants were analyzed for cytokine production by cytokine-specific ELISA. Each bar indicates mean ± SEM of 5–8 different mice. $^{*}p < 0.05$, $^{**}p < 0.01$.

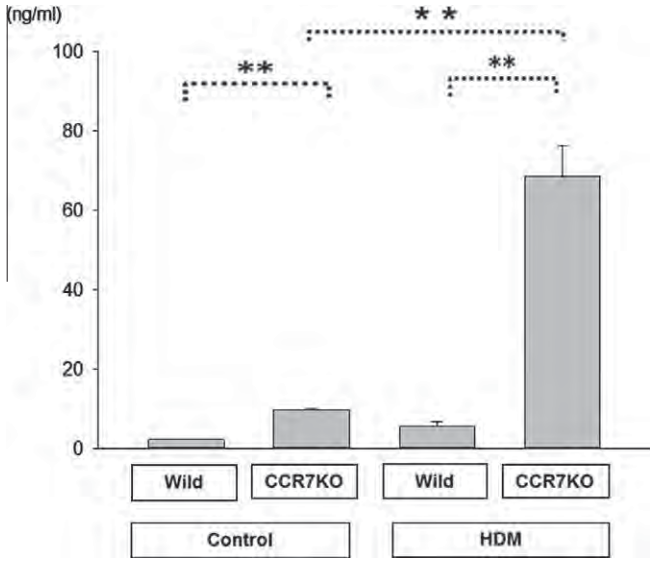

Fig. 7. HMGB1 production in the BALF. BALF supernatants were analyzed for HMGB1 production by specific ELISA. Each bar indicates mean ± SEM of four different mice. $^{**}p < 0.01$.

To further examine the Treg cell function in the lung, we separated Treg cell using CD4+CD25+ cell selection kits. The number of CD4+CD25+ cells was significantly increased in CCR7KO mice compared to wild type mice (Table 2). To examine the regulatory function of CD4+CD25+ cells, we examined the synthesis of IL-10 and IL-35, which is reported the one of the key cytokine of regulatory function [34,35]. When we examined the cytokine production, CD4+CD25+ cells produced equal amount of IL-10 and IL-35 in wild type and CCR7KO mice (Table 2).

3.3. Role of CCR7 in HDM-induced cytokine production

We examined cytokine production in BALF in CCR7KO and wild-type mice to explore the type of airway inflammation induced by HDM in the absence of CCR7. Levels of the Th2 cytokines, IL-13 and IL-5, were significantly higher in CCR7KO mice than in the wild type (Fig. 6A and B). By comparison, levels of the Th1 cytokine, IFN-γ, were below the detection limit (9.4 pg/ml, $n = 6$ for each group), suggesting that the inflammation in CCR7KO mice is Th2-dominant allergic inflammation. We also analyzed the expression levels of the regulatory cytokines TGF-β and IL-17 [36] and found that both were expressed at higher levels in CCR7KO mice than in the wild type (Fig. 6C and D). The formation of lymphocyte aggregates in the CCR7KO mice is consistent with the increased expression of IL-17 in these mice compared to the wild type and with the role of IL-17 in the development of inducible bronchus-associated lymphoid tissue (iBALT) [37].

Next, we examined HMGB1 production in the BALF of CCR7KO and wild-type mice. HMGB1 is a critical mediator of the innate immune response to inflammation and infection [38–40]. HMGB1 is also a regulator of Treg cells [41,42]. We found that HMGB1 production is significantly higher in CCR7KO mice than in the wild type, suggesting that innate immune response is augmented and Treg cell function is depressed in CCR7KO mice ($p < 0.01$, Fig. 7).

4. Discussion

In the present study, we showed that continuous HDM exposure induced allergic airway inflammation, which was augmented in CCR7KO mice. The prominent lymphoid aggregates observed in the bronchioles of CCR7 KO mice were predominantly composed of CD4+ cells, but also contained a few CD8+ cells. We also observed FoxP3-positive cells. Although there was an increased number of FoxP3-positive cells in the lung of CCR7KO mice compared to wild-type mice, the levels of Th2 cytokines as well as IL-17 and TGF-β were also increased. In addition, HMGB1 production was also increased in CCR7KO mice. These results suggest that CCR7-deficient FoxP3-positive cells, which down-regulate allergic airway inflammation [43,44], did not function efficiently in CCR7KO mice.

Intra-tracheal continuous HDM exposure to mice induces the asthmatic phenotype [11,12,45]. In the current study, we also found that HDM exposure by inhalation induced IgE responses. These responses were increased in CCR7KO mice, which was consistent with the increase in systemic immunization seen in CCR7KO and plt mice [8,23,46]. CCR7 is a receptor of CCL21 and CCL19 that plays a critical role in the development of secondary lymph nodes [22,47]. CCR7, which is expressed by dendritic cells and T cells, plays a critical role in the movement of lymphocyte and dendritic cells from peripheral tissue into afferent lymphatics [32,47]. Disruption of this process in CCR7KO mice causes lymphocytes to accumulate in the tissue of these mice [32] and is the reason why HDM exposure caused lymphoid aggregates to form in their bronchioles.

Another reason for T cell accumulation in CCR7KO mice may be related to an impairment of Treg cells in these mice [33]. CCR7KO mice accumulate BALT from day 5 after birth [33]. Treg cells suppress effector T cell function by homing to lymphoid organs, which is confirmed by the fact that Treg cells from wild-type mice work perfectly in CCR7KO mice [33]. Consistent with the previous report that CCR7-deficient T reg cells work normally in vitro [10], we found that Treg cells, present in the BALT, produced IL-10 and IL-35 in vitro. We also found that dendritic cells in the lung of CCR7KO mice expressed activation makers such as MHC class II and co-stimulatory molecules. It is possible that the structure of BALT may not be sufficient for FoxP3 positive cell to possess suppressive function with CCR7 deficient condition. In the case of influenza infection, iBALT, which is essential for local immunity to influenza, is not efficiently formed in the absence of CCL21 and CCL19 [48]. Recently, Ishimaru et al. have reported that CCR7 negative FoxP3-positive cells have defects in the c-Jun and FoxP3 interaction [24]. Thus, it is also possible that FoxP3-positive cells in CCR7KO mice possess defects in local migration to exhibit regulatory function in iBALT. To confirm the Treg function of CCR7KO mice in allergen sensitization, we should precede the experiments by transfusion of Treg cells in vivo and precise functional analysis in vitro, which is continuing subject to be solved.

HDM is known to accelerate not only antigen-specific immunity but also innate immunity through the TLRs [19,20]. TLR, TLR2, and TLR4 are thought to be required to induce allergic inflammation [19,20]. A recent finding of homology between Derf2 and MD2, the relation to TLR4 has been stressed, because MD2 is critical for signal transduction through TLR4 [20]. HMGB1 was produced in CCR7KO mice as an accelerated innate immune response. Beyond its role in maintaining chromosomal integrity, HMGB1 is secreted as a cytokine and is considered an alarmin [40].

In conclusion, we provide results here to highlight CCR7 expression as a promising target for regulation of HDM-induced innate immunity and antigen responses. Further studies are needed to develop the targeted control of CCR7 expression as immunotherapy for asthma.

Acknowledgments

This study was supported in part by grants-in-aid for Scientific Research from the Ministry of Education, Culture, Sports, Science and Technology, Japan; a grant for Allergic Disease and Intractable Diseases from the Ministry of Health, Labor and Welfare, Japan;

and a grant to the Respiratory Failure Research Group from Health and Labor Sciences, Japan.

References

[1] D.B. Corry, H.G. Folkesson, M.L. Warnock, D.J. Erle, M.A. Matthay, J.P. Wiener-Kronish, R.M. Locksley, Interleukin 4, but not interleukin 5 or eosinophils, is required in a murine model of acute airway hyperreactivity, J. Exp. Med. 183 (1996) 109–117.

[2] P.S. Foster, S.P. Hogan, A.J. Ramsay, K.I. Matthaei, I.G. Young, Interleukin 5 deficiency abolishes eosinophilia, airways hyperreactivity, and lung damage in a mouse asthma model, J. Exp. Med. 183 (1996) 195–201.

[3] G. Vogel, Interleukin-13's key role in asthma shown, Science 282 (1998) 2168.

[4] M. Wills-Karp, J. Luyimbazi, X. Xu, B. Schofield, T.Y. Neben, C.L. Karp, D.D. Donaldson, Interleukin-13: central mediator of allergic asthma, Science 282 (1998) 2258–2261.

[5] B.N. Lambrecht, Allergen uptake and presentation by dendritic cells, Curr. Opin. Allergy Clin. Immunol. 1 (2001) 51–59.

[6] J.G. Cyster, Chemokines and cell migration in secondary lymphoid organs, Science 286 (1999) 2098–2102.

[7] J.N. Samsom, F. Hauet-Broere, W.W. Unger, V.A.N.B. La, G. Kraal, Early events in antigen-specific regulatory T cell induction via nasal and oral mucosa, Ann. NY Acad. Sci. 1029 (2004) 385–389.

[8] N. Yamashita, H. Tashimo, Y. Matsuo, H. Ishida, K. Yoshiura, K. Sato, T. Kakiuchi, K. Ohta, Role of CCL21 and CCL19 in allergic inflammation in the ovalbumin-specific murine asthmatic model, J. Allergy Clin. Immunol. 117 (2006) 1040–1046.

[9] M.H. Jang, N. Sougawa, T. Tanaka, T. Hirata, T. Hiroi, K. Tohya, Z. Guo, E. Umemoto, Y. Ebisuno, B.G. Yang, J.Y. Seoh, M. Lipp, H. Kiyono, M. Miyasaka, CCR7 is critically important for migration of dendritic cells in intestinal lamina propria to mesenteric lymph nodes, J. Immunol. 176 (2006) 803–810.

[10] M.A. Schneider, J.G. Meingassner, M. Lipp, H.D. Moore, A. Rot, CCR7 is required for the in vivo function of CD4+ CD25+ regulatory T cells, J. Exp. Med. 204 (2007) 735–745.

[11] J.R. Johnson, R.E. Wiley, R. Fattouh, F.K. Swirski, B.U. Gajewska, A.J. Coyle, J.C. Gutierrez-Ramos, R. Ellis, M.D. Inman, M. Jordana, Continuous exposure to house dust mite elicits chronic airway inflammation and structural remodeling, Am. J. Respir. Crit. Care Med. 169 (2004) 378–385.

[12] J.R. Johnson, F.K. Swirski, B.U. Gajewska, R.E. Wiley, R. Fattouh, S.R. Pacitto, J.K. Wong, M.R. Stampfli, M. Jordana, Divergent immune responses to house dust mite lead to distinct structural-functional phenotypes, Am. J. Physiol. Lung Cell Mol. Physiol. 293 (2007) L730–739.

[13] T. Miyamoto, S. Oshima, A. Domae, K. Takahashi, M. Izeki, Allergenic potency of different house dusts in relation to contained mites, Ann. Allergy 28 (1970) 405–412.

[14] T.A. Platts-Mills, M.D. Chapman, Dust mites: immunology, allergic disease, and environmental control, J. Allergy Clin. Immunol. 80 (1987) 755–775.

[15] N. Yamashita, M. Haida, M. Suko, H. Okudaira, T. Miyamoto, Allergens of the house dust mite *Dermatophagoides farinae*. II. Immunological characterization of four allergenic molecules, Int. Arch. Allergy Appl. Immunol. 88 (1989) 173–175.

[16] L. Gough, E. Campbell, D. Bayley, G. Van Heeke, F. Shakib, Proteolytic activity of the house dust mite allergen Der p 1 enhances allergenicity in a mouse inhalation model, Clin. Exp. Allergy 33 (2003) 1159–1163.

[17] G.H. Caughey, Of mites and men: trypsin-like proteases in the lungs, Am. J. Respir. Cell Mol. Biol. 16 (1997) 621–628.

[18] S. Phipps, C.E. Lam, G.E. Kaiko, S.Y. Foo, A. Collison, J. Mattes, J. Barry, S. Davidson, K. Oreo, L. Smith, A. Mansell, K.I. Matthaei, P.S. Foster, Toll/IL-1 signaling is critical for house dust mite-specific helper T cell type 2 and type 17 [corrected] responses, Am. J. Respir. Crit. Care Med. 179 (2009) 883–893.

[19] H. Hammad, M. Chieppa, F. Perros, M.A. Willart, R.N. Germain, B.N. Lambrecht, House dust mite allergen induces asthma via Toll-like receptor 4 triggering of airway structural cells, Nat. Med. 15 (2009) 410–416.

[20] A. Trompette, S. Divanovic, A. Visintin, C. Blanchard, R.S. Hegde, R. Madan, P.S. Thorne, M. Wills-Karp, T.L. Gioannini, J.P. Weiss, C.L. Karp, Allergenicity resulting from functional mimicry of a Toll-like receptor complex protein, Nature 457 (2009) 585–588.

[21] S. Ichikawa, T. Takai, T. Yashiki, S. Takahashi, K. Okumura, H. Ogawa, D. Kohda, H. Hatanaka, Lipopolysaccharide binding of the mite allergen Der f 2, Genes Cells 14 (2009) 1055–1065.

[22] R. Forster, A. Schubel, D. Breitfeld, E. Kremmer, I. Renner-Muller, E. Wolf, M. Lipp, CCR7 coordinates the primary immune response by establishing functional microenvironments in secondary lymphoid organs, Cell 99 (1999) 23–33.

[23] R. Forster, A.C. Davalos-Misslitz, A. Rot, CCR7 and its ligands: balancing immunity and tolerance, Nat. Rev. Immunol. 8 (2008) 362–371.

[24] N. Ishimaru, A. Yamada, T. Nitta, R. Arakaki, M. Lipp, Y. Takahama, Y. Hayashi, CCR7 with S1P1 signaling through AP-1 for migration of Foxp3+ regulatory T-cells controls autoimmune exocrinopathy, Am. J. Pathol. 180 (2012) 199–208.

[25] C.H. Kim, Migration and function of FoxP3+ regulatory T cells in the hematolymphoid system, Exp. Hematol. 34 (2006) 1033–1040.

[26] J.H. Lee, S.G. Kang, C.H. Kim, FoxP3+ T cells undergo conventional first switch to lymphoid tissue homing receptors in thymus but accelerated second switch to nonlymphoid tissue homing receptors in secondary lymphoid tissues, J. Immunol. 178 (2007) 301–311.

[27] N. Yamashita, H. Tashimo, H. Ishida, F. Kaneko, J. Nakano, H. Kato, K. Hirai, T. Horiuchi, K. Ohta, Attenuation of airway hyperresponsiveness in a murine asthma model by neutralization of granulocyte-macrophage colony-stimulating factor (GM-CSF), Cell. Immunol. 219 (2002) 92–97.

[28] S. Yamada, I. Maruyama, HMGB1, a novel inflammatory cytokine, Clin. Chim. Acta. 375 (2007) 36–42.

[29] G. Hintzen, L. Ohl, M.L. del Rio, J.I. Rodriguez-Barbosa, O. Pabst, J.R. Kocks, J. Krege, S. Hardtke, R. Forster, Induction of tolerance to innocuous inhaled antigen relies on a CCR7-dependent dendritic cell-mediated antigen transport to the bronchial lymph node, J. Immunol. 177 (2006) 7346–7354.

[30] A. MartIn-Fontecha, S. Sebastiani, U.E. Hopken, M. Uguccioni, M. Lipp, A. Lanzavecchia, F. Sallusto, Regulation of dendritic cell migration to the draining lymph node: impact on T lymphocyte traffic and priming, J. Exp. Med. 198 (2003) 615–621.

[31] S.K. Bromley, S.Y. Thomas, A.D. Luster, Chemokine receptor CCR7 guides T cell exit from peripheral tissues and entry into afferent lymphatics, Nat. Immunol. 6 (2005) 895–901.

[32] G.F. Debes, C.N. Arnold, A.J. Young, S. Krautwald, M. Lipp, J.B. Hay, E.C. Butcher, Chemokine receptor CCR7 required for T lymphocyte exit from peripheral tissues, Nat. Immunol. 6 (2005) 889–894.

[33] J.R. Kocks, A.C. Davalos-Misslitz, G. Hintzen, L. Ohl, R. Forster, Regulatory T cells interfere with the development of bronchus-associated lymphoid tissue, J. Exp. Med. 204 (2007) 723–734.

[34] L.W. Collison, V. Chaturvedi, A.L. Henderson, P.R. Giacomin, C. Guy, J. Bankoti, D. Finkelstein, K. Forbes, C.J. Workman, S.A. Brown, J.E. Rehg, M.L. Jones, H.T. Ni, D. Artis, M.J. Turk, D.A. Vignali, IL-35-mediated induction of a potent regulatory T cell population, Nat. Immunol. 11 (2010) 1093–1101.

[35] V. Chaturvedi, L.W. Collison, C.S. Guy, C.J. Workman, D.A. Vignali, Cutting edge: Human regulatory T cells require IL-35 to mediate suppression and infectious tolerance, J. Immunol. 186 (2011) 6661–6666.

[36] L. Yang, D.E. Anderson, C. Baecher-Allan, W.D. Hastings, E. Bettelli, M. Oukka, V.K. Kuchroo, D.A. Hafler, IL-21 and TGF-beta are required for differentiation of human T(H)17 cells, Nature 454 (2008) 350–352.

[37] J. Rangel-Moreno, D.M. Carragher, M. de la Luz Garcia-Hernandez, J.Y. Hwang, K. Kusser, L. Hartson, J.K. Kolls, S.A. Khader, T.D. Randall, The development of inducible bronchus-associated lymphoid tissue depends on IL-17, Nat. Immunol. 12 (2011) 639–646.

[38] H. Yanai, S. Chiba, T. Ban, Y. Nakaima, T. Onoe, K. Honda, H. Ohdan, T. Taniguchi, Suppression of immune responses by nonimmunogenic oligodeoxynucleotides with high affinity for high-mobility group box proteins (HMGBs), Proc. Natl. Acad. Sci. USA 108 (2011) 11542–11547.

[39] H. Yang, H.S. Hreggvidsdottir, K. Palmblad, H. Wang, M. Ochani, J. Li, B. Lu, S. Chavan, M. Rosas-Ballina, Y. Al-Abed, S. Akira, A. Bierhaus, H. Erlandsson-Harris, U. Andersson, K.J. Tracey, A critical cysteine is required for HMGB1 binding to Toll-like receptor 4 and activation of macrophage cytokine release, Proc. Natl. Acad. Sci. USA 107 (2010) 11942–11947.

[40] G.P. Sims, D.C. Rowe, S.T. Rietdijk, R. Herbst, A.J. Coyle, HMGB1 and RAGE in inflammation and cancer, Annu. Rev. Immunol. 28 (2010) 367–388.

[41] Z. Liu, L.D. Falo Jr., Z. You, Knockdown of HMGB1 in tumor cells attenuates their ability to induce regulatory T cells and uncovers naturally acquired CD8 T cell-dependent antitumor immunity, J. Immunol. 187 (2011) 118–125.

[42] X.M. Zhu, Y.M. Yao, H.P. Liang, C.T. Xu, N. Dong, Y. Yu, Z.Y. Sheng, High mobility group box-1 protein regulate immunosuppression of regulatory T cells through toll-like receptor 4, Cytokine 54 (2011) 296–304.

[43] J.R. Grainger, K.A. Smith, J.P. Hewitson, H.J. McSorley, Y. Harcus, K.J. Filbey, C.A. Finney, E.J. Greenwood, D.P. Knox, M.S. Wilson, Y. Belkaid, A.Y. Rudensky, R.M. Maizels, Helminth secretions induce de novo T cell Foxp3 expression and regulatory function through the TGF-beta pathway, J. Exp. Med. 207 (2010) 2331–2341.

[44] M.D. Leech, R.A. Benson, A. De Vries, P.M. Fitch, S.E. Howie, Resolution of Der p1-induced allergic airway inflammation is dependent on CD4+CD25+Foxp3+ regulatory cells, J. Immunol. 179 (2007) 7050–7058.

[45] M. Kashyap, Y. Rochman, R. Spolski, L. Samsel, W.J. Leonard, Thymic stromal lymphopoietin is produced by dendritic cells, J. Immunol. 187 (2011) 1207–1211.

[46] B. Xu, K. Aoyama, M. Kusumoto, A. Matsuzawa, E.C. Butcher, S.A. Michie, T. Matsuyama, T. Takeuchi, Lack of lymphoid chemokines CCL19 and CCL21 enhances allergic airway inflammation in mice, Int. Immunol. 19 (2007) 775–784.

[47] A. Braun, T. Worbs, G.L. Moschovakis, S. Halle, K. Hoffmann, J. Bolter, A. Munk, R. Forster, Afferent lymph-derived T cells and DCs use different chemokine receptor CCR7-dependent routes for entry into the lymph node and intranodal migration, Nat. Immunol. 12 (2011) 879–887.

[48] J. Rangel-Moreno, J.E. Moyron-Quiroz, L. Hartson, K. Kusser, T.D. Randall, Pulmonary expression of CXC chemokine ligand 13, CC chemokine ligand 19, and CC chemokine ligand 21 is essential for local immunity to influenza, Proc. Natl. Acad. Sci. USA 104 (2007) 10577–10582.

Experimental and Molecular Pathology 93 (2012) 18–25

Contents lists available at SciVerse ScienceDirect

Experimental and Molecular Pathology

journal homepage: www.elsevier.com/locate/yexmp

Suppressive effects of a pyrazole derivative of curcumin on airway inflammation and remodeling

Osamu Narumoto [a,b], Yukiko Matsuo [a], Masahiro Sakaguchi [c], Shunsuke Shoji [d], Naohide Yamashita [e], David Schubert [f], Kazuho Abe [g], Kazuhide Horiguchi [h], Takahide Nagase [b], Naomi Yamashita [a,*]

[a] Department of Pharmacotherapy, Research Institute of Pharmaceutical Sciences Musashino University, Tokyo, Japan
[b] Department of Pulmonary Medicine, Faculty of Medicine University of Tokyo, Tokyo, Japan
[c] Department of Veterinary Microbiology, School of Veterinary Medicine, Azabu University, Kanagawa, Japan
[d] Division of Clinical Research, National Hospital Organization Tokyo National Hospital, Tokyo, Japan
[e] Department of Advanced Medical Science, Institute of Medical Science University of Tokyo, Tokyo, Japan
[f] The Salk Institute, Laboratories for Cellular Neurobiology, La Jolla, CA, USA
[g] Department of Pharmacology, Research Institute of Pharmaceutical Sciences Musashino University, Tokyo, Japan
[h] Department of Anatomy, Faculty of Medical Science, University of Fukui, Fukui, Japan

ARTICLE INFO

Article history:
Received 27 December 2011
and in revised form 22 March 2012
Available online 19 April 2012

Keywords:
Asthma
Curcumin derivative
Airway remodeling
EMT

ABSTRACT

To advance the control of airway epithelial cell function and asthma, we investigated the effects of a new curcumin derivative, CNB001, which possesses improved pharmacological properties. Normal human bronchial epithelial (NHBE) cells were stimulated with synthetic double-stranded RNA, Poly(I:C). CNB001 significantly suppressed IL-6, TNF-α, and GM-CSF production by NHBE cells, and did so more effectively than did curcumin or dexamethasone (DEX). CNB001 significantly inhibited the decrease of E-cadherin mRNA expression and increase of vimentin mRNA expression observed in NHBE cells induced by a combination of TGF-β1 and TNF-α, which are markers of airway remodeling. In NHBE cells stimulated by TGF-β1, CNB001 significantly downregulated the level of active serine peptidase inhibitor clade E member (SERPINE) 1, which is also reported to be related to airway remodeling. Whereas DEX alone significantly increased the active SERPINE1 level, the combination of DEX and CNB001 significantly suppressed active SERPINE1. In addition, CNB001 significantly suppressed neutrophil infiltration, IL-6, TNF-α, IL-13 and active SERPINE1 production in bronchoalveolar lavage fluid of the murine asthma model, which was not observed in the case of DEX. In conclusion, the curcumin derivative, CNB001, is a promising candidate to treat asthma associated with neutrophilic airway inflammation and remodeling.

Introduction

Although various effector cells reside within asthmatic airways, airway epithelial cells actively involved in airway inflammation and remodeling, by producing inflammatory cytokines and influencing other cells (Holgate, 2010; Holgate et al., 2000; Lee et al., 2009). Airway epithelial cells are the first cells that encounter various stimulants in the airway and produce cytokines such as IL-6 and TNF-α, which are closely related to the pathophysiology of asthma (Ather et al., 2011; Takizawa et al., 1996; Vieira et al., 2011; Yadav et al., 2011). Viral infection of the respiratory tract is the most frequent factor involved in asthmatic exacerbations and may trigger neutrophilic inflammation in asthmatic airways (Fahy et al., 1995; Wark et al., 2002).

Airway remodeling, which is known to induce irreversible airflow limitation, as in the case of chronic obstructive pulmonary disease is another problem to be solved (Gizycki et al., 1997). Airway remodeling is characterized by structural changes within the airway wall, including smooth muscle hypertrophy, basement membrane thickening, submucosal fibrosis, mucus cell metaplasia, epithelial shedding, and angiogenesis (Gizycki et al., 1997). Among the various factors involved in the pathogenesis of remodeling, we focused on serine peptidase inhibitor clade E member 1 (SERPINE1, also known as plasminogen activator inhibitor-1, PAI-1) and the process of epithelial–mesenchymal transition (EMT) in epithelial cells (Hackett et al., 2009; Kowal et al., 2008; Kucharewicz et al., 2003; Kuramoto et al., 2009; Miyamoto et al., 2011). SERPINE1 regulates

Abbreviations: NHBE cells, normal human bronchial epithelial cells; SERPINE1, serine peptidase inhibitor clade E member 1; EMT, epithelial–mesenchymal transitions; ECM, extracellular matrix; TNF, tumor necrosis factor; DEX, dexamethasone; Poly(I:C), polyinosinic:polycytidylic acid; GM-CSF, granulocyte-macrophage colony stimulating factor; BALF, bronchoalveolar lavage fluid; TLR3, Toll-like receptor 3; MAPK, mitogen-activated protein kinases; CUR, curcumin; OPM, OVA + Poly(I:C) + house dust mite.

* Corresponding author at: Department of Pharmacotherapy, Research Institute of Pharmaceutical Sciences, Musashino University, 1-1-20 Shinmachi Nishitokyo-shi, Tokyo 202-8585, Japan. Fax: +81 424 68 8647.
E-mail address: naoyama@musashino-u.ac.jp (N. Yamashita).

0014-4800/$ – see front matter © 2012 Elsevier Inc. All rights reserved.
doi:10.1016/j.yexmp.2012.04.011

extracellular matrix (ECM) proteolysis (Kowal et al., 2008; Kucharewicz et al., 2003), and the attenuation of SERPINE1 has been reported to exhibit therapeutic properties for airway remodeling (Kuramoto et al., 2009; Miyamoto et al., 2011). Although EMT is a complex process involving various cells, the airway epithelial cells are one of the main targets related to airway remodeling (Hackett et al., 2009; Holgate et al., 2000; Lee et al., 2009).

Here, we explored the effects of a new curcumin derivative on epithelial cell function. Curcumin is a polyphenol derived from turmeric (*Curcuma longa*), a plant that has been reported to possess anticancer, antioxidant, and anti-inflammatory properties (Aggarwal and Harikumar, 2009; Fang et al., 2005; Ray et al., 2003; Santel et al., 2008; Weber et al., 2005; Wong et al., 2010). Although curcumin possesses good pharmacological properties, the utility of curcumin as a potential therapeutic drug is limited because of its poor bioavailability (Anand et al., 2007). Curcumin blocks multiple sites of transforming growth factor beta (TGF-β) signaling (Gaedeke et al., 2004), which plays a key role in the production of SERPINE1 (Dennler et al., 1998) and induction of EMT (Zavadil and Bottinger, 2005). Therefore, we hypothesized that a new curcumin derivative might control not only airway inflammation but also EMT in asthmatic conditions that currently cannot be satisfactorily controlled by any other drugs, including steroids.

We used a curcumin derivative called CNB001, which is more stable and shows stronger cell-protecting effects than curcumin (Liu et al., 2008; Maher et al., 2010). We first compared the anti-inflammatory effect of CNB001 with that of dexamethasone (DEX) and curcumin. We then evaluated the effects of CNB001 on pathways that are thought to be involved in remodeling.

Materials and methods

Chemicals

Curcumin, dexamethasone (DEX), polyinosinic:polycystidylic acid (Poly(I:C)), human recombinant tumor necrosis factor (TNF)-α, and human TGF-β1 were purchased from Sigma-Aldrich (St. Louis, MO, USA). House dust mite allergen (HDM) derived from *Dermatophagoides farinae* (Derf) was provided by Dr. Shirai (Itea Inc., Tokyo, Japan), and contained 8 μg/mg major allergen Derf1. Ovalbumin (OVA) was purchased from Sigma (St. Louis, MO, USA).

CNB001

CNB001 was synthesized as a hybrid molecule between cyclohexyl bisphenol A and curcumin, both of which have a proven neuroprotective effect (Liu et al., 2008). The purity of CNB001 was more than 98%. CNB001 is reported to be superior to curcumin in neuroprotective effects in cell-culture assays for trophic factor withdrawal, oxidative stress, and glucose starvation, as well as amyloid-induced toxicity (Liu et al., 2008).

Cell culture and treatment

Normal human bronchial epithelial (NHBE) cells were purchased from Lonza (Walkersville, MD, USA). The cells were cultured in bronchial epithelial growth medium (BEGM) supplemented with BulletKit (Lonza Walkersville, Inc. MD, USA) on collagen type I-coated dishes at 37 °C in a 5% CO_2/95% air incubator. BulletKit contains human recombinant epidermal growth factor, hydrocortisone, transferrin, insulin, bovine pituitary extract, retinoic acid, triiodothyronine, gentamicin, and amphotericin (concentrations not stated). Cells were used on passage 3 for experiments pertaining to EMT, and on passages 4 to 6 for other experiments.

After the NHBE cells reached 80% to 100% confluency, the cells were incubated overnight in BEGM without BulletKit. Stock solutions of CNB001, curcumin, and DEX (10 mmol/L) were prepared in ethanol and diluted to the appropriate concentration with culture medium. CNB001, curcumin, or DEX was added to the medium at the concentrations described in each experiment. One hour later, Poly(I:C) was added at a concentration of 10 μmol/L. Cells and supernatants were collected 18 h after treatment of Poly:IC. Preliminary experiments showed that CNB001 was not toxic at the dose of 10 μmol/L. A trypan-blue exclusion test of viability showed no significant difference between the control and the CNB001 group (trypan-blue positive cells, 4.6% ± 0.6%, 3.2% ± 1.7%, respectively, $P > 0.05$ NS, $n = 6$). Initial control experiments included solvent (ethanol) at doses of up to 1 μL/mL, which did not significantly affect cell viability or production of cytokines.

To induce EMT, cells were grown on 10-cm dishes until 80% to 100% confluency. They were then incubated with TGF-β1 (5 ng/mL) with or without TNF-α (10 ng/mL).

Real-time PCR and immunoassay

Total RNA was extracted by using Trizol Reagent (Invitrogen Corporation, Carlsbad, CA, USA) and then reverse transcribed by using a cDNA Synthesis Kit (Bio-Rad Laboratories Inc., Hercules, CA, USA). A Light Cycler-Fast Start DNA Master SYBR Green I kit (Roche Diagnostics, Mannheim, Germany) was used for real-time PCR. Primers are listed in Table 1.

Interleukin-6 (IL-6), granulocyte-macrophage colony stimulating factor (GM-CSF), and TNF-α levels were measured by using a Quantikine Immunoassay kit (R&D systems, Minneapolis, MN, USA). Active human SERPINE1 (PAI-1) was measured by using a specific ELISA Quantifying kit (Molecular Innovations, MI, USA).

Animals

Specific-pathogen-free female BALB/c mice (8 weeks old) were purchased from SLC (Shizuoka, Japan). The animals were housed in a specific pathogen-free environment and allowed free access to food and water. All experimental protocols were approved by the Musashino University Animal Care Committee and were in accordance with the NIH Guide for the care and use of laboratory animals. Mice were initially intraperitoneally immunized with 10 μg OVA and 2 mg aluminum hydroxide gel on days 0 and 14, as previously reported (Matsuo et al., 2009; Yamashita et al., 2006). From day 16 onwards, the animals were treated every other day for 2 weeks as follows. Mice were intraperitoneally injected with 25 mg/kg CNB001, 25 mg/kg curcumin, 1 mg/kg DEX, or solvent alone. CNB001 and curcumin were dissolved in 100% ethanol (40 μL for 1 mg) and then diluted 10 fold with 1% (v/v) Tween80/Saline (Sigma). DEX was dissolved in 100% ethanol to a concentration of 0.1% w/v and then diluted 10 fold with 1% Tween80/Saline. Thirty minutes after intraperitoneal injection, the mice were subjected to inhalation of OVA, followed by intranasal administration of Poly(I:C) (500 μg/kg) and HDM (8 μg/kg) dissolved in 80 μL of saline. Saline alone was used for control mice. Inhalation of OVA (20 mg/mL) was conducted at a

Table 1
Primers used for real-time PCR.

Target gene	Primer sequences		Amplicon size (bp)
GAPDH	Forward	5′-TGCACCACCAACTGCTTAGC-3′	87
	Reverse	5′-GGCATGGACTGTGGTCATGAG-3′	
E-cadherin	Forward	5′-TGAAGGTGACAGAGCCTCTGGAT-3′	151
	Reverse	5′-TGGGTGAATTCGGGCTTGTT-3′	
Vimentin	Forward	5′-CCTTGAACGCAAAGTGGAATC-3′	106
	Reverse	5′-CTGAGTTTCCGAATAGCCTG-3′	

flow rate of 0.3 mL/min for 10 min by using a micromist nebulizer (Devilbiss, Somerset, PA, USA).

Twenty-four hours after the last treatment, the mice were sacrificed and bronchoalveolar lavage fluid (BALF) was obtained by instilling and aspirating 3 times with 1 mL aliquots of PBS (recovery >85%). BALF was centrifuged at 540 *g* for 10 min (at 4 °C) and the supernatants were stored at −80 °C for ELISA. The cell pellets were resuspended in 1 mL PBS. After total BALF cell counts were obtained, the resuspended cells were adhered onto glass slides at 640 rpm for 2 min by using a Shandon Cytospin 4 (Thermo Electron Corp., Waltham, MA, USA). The BALF cells on glass slides were stained with Diff-Quik (International Reagents Corp, Osaka, Japan) and were differentially counted at 200 cells per slide (one slide per animal).

For histological examination, mice were perfused transcardially with PBS and then 4% paraformaldehyde in 100 mM phosphate buffer (pH 7.4). The lungs were removed and then immersed in 4% paraformaldehyde. After washing with PBS, the specimens were soaked overnight in 30% sucrose in PBS, embedded in optimal cutting temperature (OCT) compound (Miles, Elkhart, IN, USA), and then quickly frozen. Cryostat sections were cut and thaw-mounted on poly-L-lysine-coated glass slides (Matsunami Glass, Osaka, Japan). The samples were analyzed by haematoxylin–eosin (HE) staining.

Concentrations of IL-6, TNF-α, IL-13, and active murine SERPINE1 (PAI-1) in BALF were measured by using a specific ELISA Quantifying kit (R&D systems, MN, USA and Molecular Innovations, MI, USA, respectively) according to the manufacturers' instructions.

Statistical analysis

The significance of the difference between groups was assessed by using the Wilcoxon/Kruskal–Wallis nonparametric test as implemented in JMP8.0.2 (SAS Institute, Cary, NC, USA). The test was conducted as two sided. *P* values less than 0.05 were considered to be significant. The data were expressed as mean ± SEM.

Results

Comparing the effects of CNB001, curcumin, and DEX on Poly(I:C)-induced expression of inflammatory cytokines

Poly(I:C), a synthetic analog of viral double-stranded RNA and a Toll-like receptor (TLR) 3 ligand, acts as a potent proinflammatory stimulus for lung epithelial cells by inducing the secretion of cytokines, which are important for allergic airway inflammation (Bachar et al., 2004; Groskreutz et al., 2006). As shown in Fig. 1A, and later in Fig. 2, stimulation of NHBE cells with 10 μg/mL Poly(I:C) caused a significant increase in expression of inflammatory cytokines, IL-6, GM-CSF, and TNF-α. We first tested whether CNB001, DEX, or curcumin could suppress the expression of inflammatory cytokines. Pretreatment with either CNB001 or curcumin for 1 h significantly blocked the expression of IL-6 in a dose-dependent manner (Figs. 1A, B). DEX significantly inhibited the expression of IL-6 in a dose-dependent manner up to a concentration of 0.1 μmol/L; however, higher concentrations of DEX did not further reduce the expression of IL-6 (Fig. 1C). The maximum suppression was 94% at the dose of 10 μmol/L for CNB001, 88% at the dose of 10 μmol/L for curcumin, and 73% at the dose of 0.1 μmol/L for DEX. In all further experiments, we used CNB001 and curcumin at a concentration of 10 μmol/L, and DEX at a concentration of 0.1 μmol/L.

We next compared the anti-inflammatory effects of CNB001 with those of DEX and curcumin. CNB001 inhibited Poly(I:C)-induced production of IL-6, GM-CSF, and TNF-α to a significantly greater extent than did DEX or curcumin (Fig. 2). Addition of CNB001 to DEX suppressed inflammatory cytokines significantly more effectively than did DEX alone; however, the levels of inflammatory cytokines observed were almost the same as those obtained with CNB001 alone.

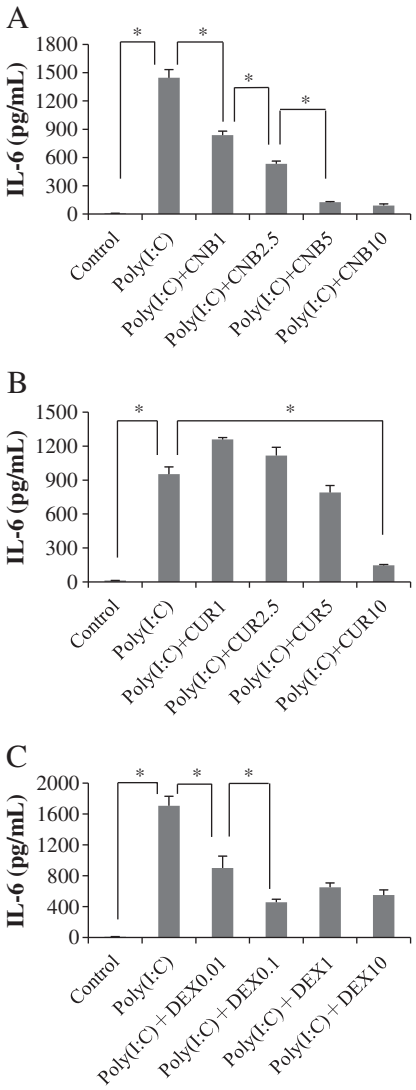

Fig. 1. Dose-dependent effects of CNB001, dexamethasone, and curcumin on Poly(I:C)-induced expression of IL-6. NHBE cells were treated with CNB001 (panel A), curcumin (panel B), or dexamethasone (DEX) (panel C) at the concentrations indicated for 1 h prior to stimulation by Poly(I:C). Cell supernatants and cells were harvested 18 h after the addition of Poly(I:C). Definition of abbreviations: CNB1, 1 μmol/L CNB001; CNB2.5, 2.5 μmol/L CNB001; CNB5, 5 μmol/L CNB001; CNB10, 10 μmol/L CNB001; CUR1, 1 μmol/L curcumin; CUR2.5, 2.5 μmol/L curcumin; CUR5, 5 μmol/L curcumin; CUR10, 10 μmol/L curcumin; DEX0.01, 0.01 μmol/L DEX; DEX0.1, 0.1 μmol/L DEX; DEX1, 1 μmol/L DEX; DEX10, 10 μmol/L DEX. Data represent means ± SD, $^{*}P<0.05$, n = 3 for each group. Similar experiments were conducted 3 times, and one representative experiment is shown.

CNB001 reduces EMT induced by TGF-β1 plus TNF-α

Next, we examined the effect of CNB001 on EMT, which is related to airway remodeling. TGF-β1 is the best-known inducer of EMT in airway epithelial cells, and induction of EMT is enhanced by combining TGF-β1 with TNF-α (Doerner and Zuraw, 2009; Takahashi et al., 2010). To examine the suppressive effects of CNB001, we used TGF-β1 and TNF-α together as stimulants to induce EMT in NHBE cells. We examined the expression of E-cadherin and vimentin, which are markers of EMT (Zavadil and Bottinger, 2005). After 72 h, the cells were harvested, and the expression levels of E-cadherin and vimentin were analyzed by performing real-time PCR. Co-stimulation by TGF-β1 and TNF-α significantly decreased the expression of E-cadherin and significantly increased the expression of vimentin (Fig. 3). Treatment with CNB001 significantly suppressed the decrease in E-cadherin expression and the increase of vimentin

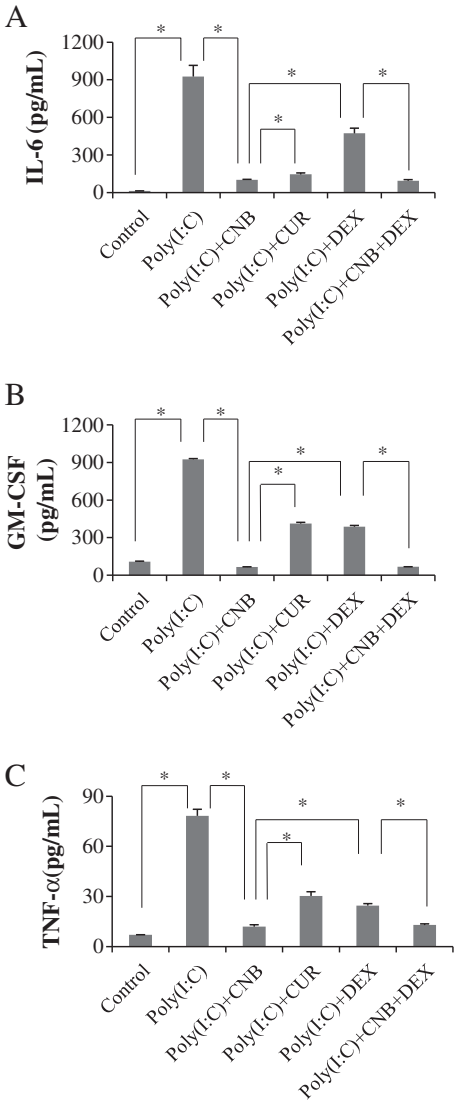

Fig. 2. Anti-inflammatory effects of CNB001, curcumin, and dexamethasone. NHBE cells were treated with CNB001, curcumin, or dexamethasone (DEX) for 1 h prior to stimulation by Poly(I:C). Control cells were not treated or stimulated. Eighteen hours after the addition of Poly(I:C), cell supernatants and cells were harvested. Protein expression of IL-6 (panel A), GM-CSF (panel B), and TNF-α (panel C) was compared between cell supernatants obtained from control cells, Poly(I:C)-stimulated cells, and Poly(I:C)-stimulated cells treated with CNB001, curcumin, DEX, or CNB plus DEX. Definition of abbreviations: CNB, 10 μmol/L CNB001; DEX, 0.1 μmol/L DEX; CUR, 10 μmol/L curcumin. Data represent means ± SD, $^*P<0.05$, n = 3 for each group. Similar experiments were conducted 3 times, and one representative experiment is shown.

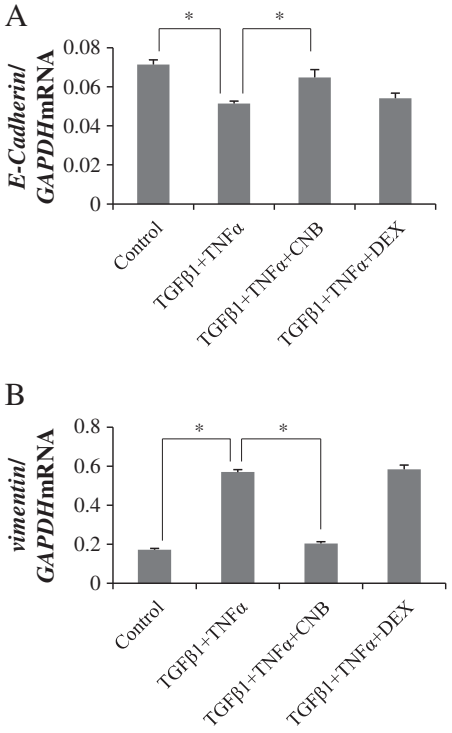

Fig.3. Effects of CNB001 and dexamethasone on the expression of E-cadherin and vimentin. EMT was induced in NHBE cells by 72-h treatment with TGF-β1 (2 ng/mL) plus TNF-α (4 ng/mL). The cells were either treated with TGF-β1 plus TNF-α, or TGF-β1 plus TNF-α in combination with CNB001 (10 μmol/L) or dexamethasone (DEX; 0.1 μmol/L). At the end of the induction period, the E-cadherin (panel A) and vimentin (panel B) mRNA expression levels in the cells were measured and normalized to levels of GAPDH mRNA. Data represent means ± SD, $^*P<0.05$, n = 3 for each group. Similar experiments were conducted 3 times, and one representative experiment is shown.

expression, suggesting that CNB001 efficiently suppresses EMT. In contrast, DEX caused no significant change either in E-cadherin or vimentin expression.

CNB001 inhibits active SERPINE1 synthesis

We next evaluated active SERPINE1 (PAI-1), which plays an important role in airway remodeling by regulating ECM proteolysis. SERPINE1 acts directly through plasmin formation and indirectly through plasmin-mediated activation of matrix metalloproteinases (Kowal et al., 2008; Kucharewicz et al., 2003). For the stimulant, we used TGF-β1 (2 ng/mL), which is an inducer of SERPINE1 and is related to airway remodeling (Dennler et al., 1998; Kowal et al., 2008; Miyamoto et al., 2011). Both CNB001 and curcumin suppressed TGF-β1-induced active SERPINE1 (Fig. 4). CNB001 showed a significantly stronger effect than that of curcumin. In contrast to CNB001, DEX significantly augmented the production of active SERPINE1. When CNB001 was added to the DEX, the induction of active SERPINE1 was significantly and greatly suppressed (Fig. 4).

Comparing the in vivo effects of CNB001, DEX, and curcumin by using a murine model of asthma

We next evaluated the effect of CNB001 on the prevention of airway inflammation *in vivo*. An OVA-specific IgE induced mouse model has been commonly used to examine allergic inflammation, which can be efficiently suppressed by treatment of the model with DEX alone (Brusselle et al., 1995; Chi et al., 2011; Wills-Karp et al., 1998). Intra-tracheal administration of HDM, which is a common allergen in humans, is recently shown to be a new asthmatic model

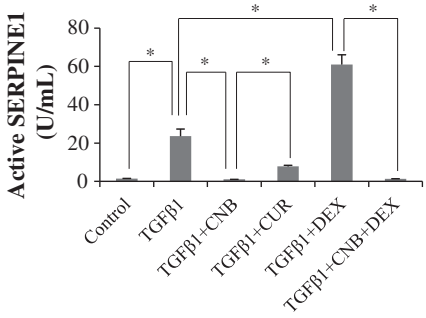

Fig. 4. Effect of CNB001 and dexamethasone on levels of active human SERPINE1. NHBE cells were treated with CNB001 (10 μmol/L) or dexamethasone (DEX; 0.1 μmol/L) for 1 h prior to stimulation by TGF-β1 (2 ng/mL). $^*P<0.05$, n = 3 for each group. Similar experiments were conducted 3 times, and one representative experiment is shown.

without systemic immunization (Fattouh et al., 2005; Gough et al., 2003; Phipps et al., 2009; Trompette et al., 2009). In addition, combining Poly(I:C) stimulation with the OVA-specific IgE induced model represents exacerbation of asthma induced by respiratory viral infections and induced neutrophil accumulation in the BALF (Kim et al., 2007; Takayama et al., 2011). To examine the effects of various treatments on the control of severe airway inflammation, we used the mouse model exposed to OVA plus HDM plus Poly(I:C).

In these mice, the total cell counts in BALF, especially neutrophil counts, were significantly suppressed by CNB001 treatment (Figs. 5A, B), but not by curcumin treatment. In addition, adding CNB001 to DEX significantly increased the suppressive effects compared with those of DEX alone. Eosinophil counts were not significantly suppressed by CNB001 alone, but were significantly suppressed when CNB001 was used in combination with DEX (Fig. 5C). Histological analysis also demonstrated that CNB001 suppressed airway inflammation beneath airway epithelial cells (Fig. 6C).

We then measured cytokine production in the BALF of the mouse model exposed to OVA plus HDM plus Poly(I:C). CNB001 significantly suppressed IL-6, TNF-α, and IL-13 expression in these mice (Figs. 7A–C). We chose IL-6 and TNF-α in order to compare effects of CNB001 *in vivo* with that *in vitro*. We also examined IL-13 to analyze the effects of CNB001 on Th2 allergic inflammation *in vivo*. Furthermore, the concentration of active murine SERPINE1 in BALF was significantly suppressed by CNB001, and significantly enhanced by DEX (Fig. 7D). Addition of CNB001 plus DEX tended to suppress the level of active SERPINE1 when compared with that observed after addition of DEX alone, though the difference was not statistically significant (Fig. 7D).

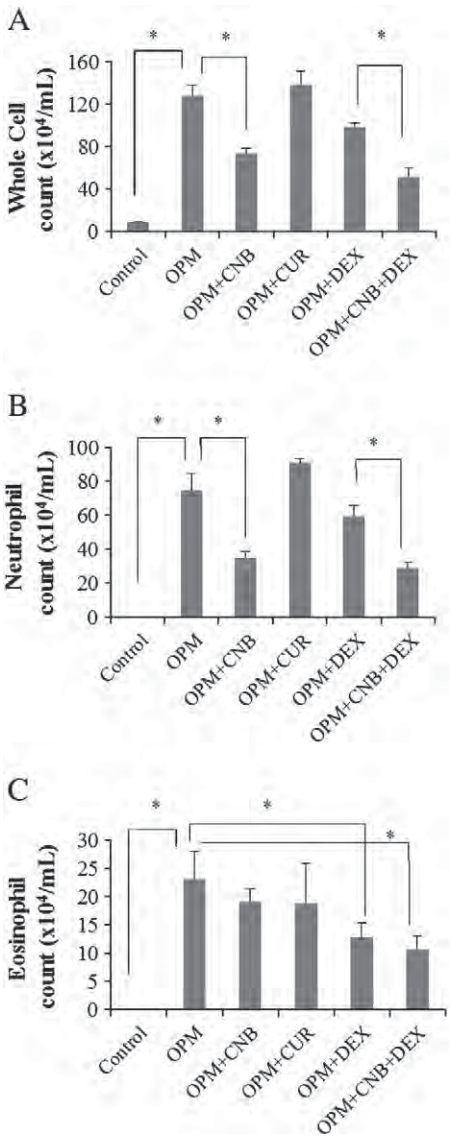

Fig. 5. *In vivo* effect of CNB001, curcumin, and dexamethasone on blood cell counts in bronchoalveolar lavage fluid of a murine asthmatic model. OVA-sensitized BALB/c mice were intraperitoneally injected with 25 mg/kg CNB001 (CNB), 25 mg/kg curcumin (CUR), 1 mg/kg dexamethasone (DEX), or solvent alone. Thirty minutes after, the mice were intranasally administered house dust mite and Poly(I:C), and OVA-immunized by inhalation of ovalbumin (OVA) (indicated as OPM in the figure). Control mice were treated with saline alone. Total cell numbers (A), neutrophil (B) and eosinophil numbers (C) in bronchoalveolar lavage fluid are shown. Data represent means ± SD, $^{*}P<0.05$, n = 7–8 for each group.

Discussion

We studied the effects of a new curcumin derivative, CNB001, as a therapeutic agent for airway inflammation and remodeling. By using epithelial cells stimulated by Poly(I:C) *in vitro*, we showed that CNB001 suppressed the cytokines IL-6, TNF-α, and GM-CSF, which are produced by epithelial cells during the inflammation and play important roles in the pathogenesis of asthma (Doherty and Croft, 2011; Morjaria et al., 2011; Saha et al., 2009). Moreover, CNB001 suppressed these cytokines more effectively than did DEX or curcumin. Our *in vivo* study of a mouse model of asthma showed that CNB001 suppressed IL-6, TNF-α, and IL-13 production, and reduced the number of inflammatory cells, especially neutrophils, in BALF. Furthermore, CNB001 prevented EMT *in vitro*, and suppressed the activity of SERPINE1, a protein that is associated with airway remodeling both *in vitro* and *in vivo*. In addition, combining CNB001 with DEX suppressed the activity of SERPINE1, which was augmented by DEX alone. Our results showed the promising effects of CNB001, in combination with DEX, on airway inflammation and remodeling.

The anti-inflammatory effects of curcumin are mediated through inhibition of the activation of NF-κB and p38MAPK (mitogen-activated protein kinases) (Camacho-Barquero et al., 2007; Jang et al., 2007; Song et al., 2010; Sugimoto et al., 2002; Venugopal et al., 2007). Curcumin inhibits the phosphorylation of I-κB (inhibitor of NF-κB) and prevents translocation of NF-κB into the nucleus (Oh et al., 2011; Song et al., 2010). NF-κB is activated by Poly(I:C), which we used here for stimulation. NF-κB plays a central role in the production of inflammatory cytokines such as TNF-α, IL-6, and IL-8 (Bruewer et al., 2003; Wong and Tergaonkar, 2009). In our *in vitro* and *in vivo* study, CNB001 suppressed the synthesis of inflammatory cytokines to a significantly greater extent than did curcumin. By using the *in vivo* model, we also showed significant inhibition of IL-13, which is a critical cytokine for asthma pathogenesis (Wills-Karp et al., 1998).

Airway remodeling, which is a cause of decreased respiratory function in asthma and cannot be effectively treated by standard therapies, has become one of the major targets of therapies for asthma. In airway remodeling, epithelial cells produce inflammatory cytokines that induce smooth muscle cell hyperplasia and an increase in activated fibroblasts and myofibroblasts that deposit excessive extracellular matrix (Skold, 2010; Westergren-Thorsson et al., 2010). Recent evidence suggests that epithelial cells play an active role in initiating this process (Hackett et al., 2009; Holgate et al., 2000; Willis et al., 2006). Because there is no generally accepted methods to define airway remodeling yet, the evidence of reduced EMT is acceptable to explain the prevent airway remodeling, we examined the effect of CNB001 on EMT. Loss of E-cadherin defines epithelial dedifferentiation, and an increase in vimentin represents differentiation to mesenchymal cells, which represents EMT (Willis et al., 2006; Zavadil and Bottinger, 2005). EMT can be induced by TGF-β1 and enhanced by TNF-α, IL-1β, and fibronectins (Dennler et al., 1998; Takahashi et al., 2010). Here, we confirmed the loss of E-cadherin expression and the increase in vimentin expression in epithelial cells

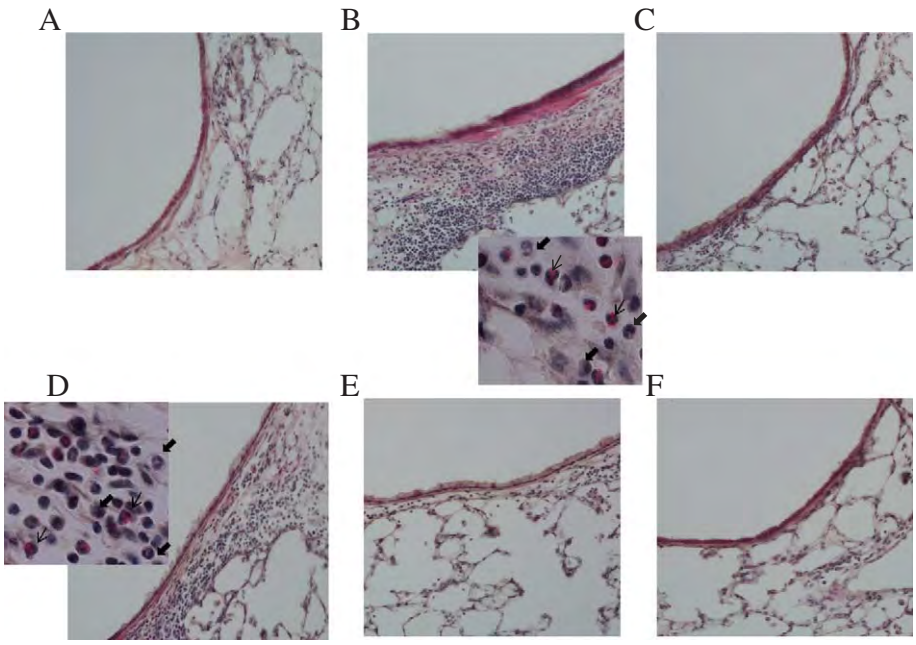

Fig. 6. Histological analysis by hematoxylin and eosin staining. OVA-sensitized BALB/c mice, treated as described in the legend of Fig. 5, were subjected to histological examination. The mice were perfused transcardially with PBS and then 4% paraformaldehyde in 100 mM phosphate buffer (pH 7.4). A, control; B, OVA + Poly(I:C) + house dust mite (OPM); C, OPM plus CNB001; D; OPM plus curcumin; E; OPM plus dexamethasone (DEX), F; OPM plus CNB001 plus DEX. → eosinophils ➡ neutrophils (arrows indicated some of typical cells, original magnification ×1000).

treated with TGF-β1 and TNF-α *in vitro*, suggesting the occurrence of EMT.

We also focused on the production of active SERPINE1, which is reported to play an essential role in tissue remodeling of lung, kidney, and cardiovascular systems after inflammation (Ha et al., 2009; Huang et al., 2008; Kuramoto et al., 2009; Shetty et al., 2008; Sisson et al., 2009). Kuramoto et al. reported increased expression of SERPINE1 in BALF of murine asthma models compared with that of healthy mice (Kuramoto et al., 2009). In addition, they showed that inhalation of urokinase-type plasminogen activator reduces the level of active SERPINE1 and suppresses airway remodeling in these mice (Kuramoto et al., 2009). Miyamoto et al. report that airway remodeling is suppressed in *Serpine1*-deficient mice compared to wild-type mice, and following intra-airway administration of *Serpine1*

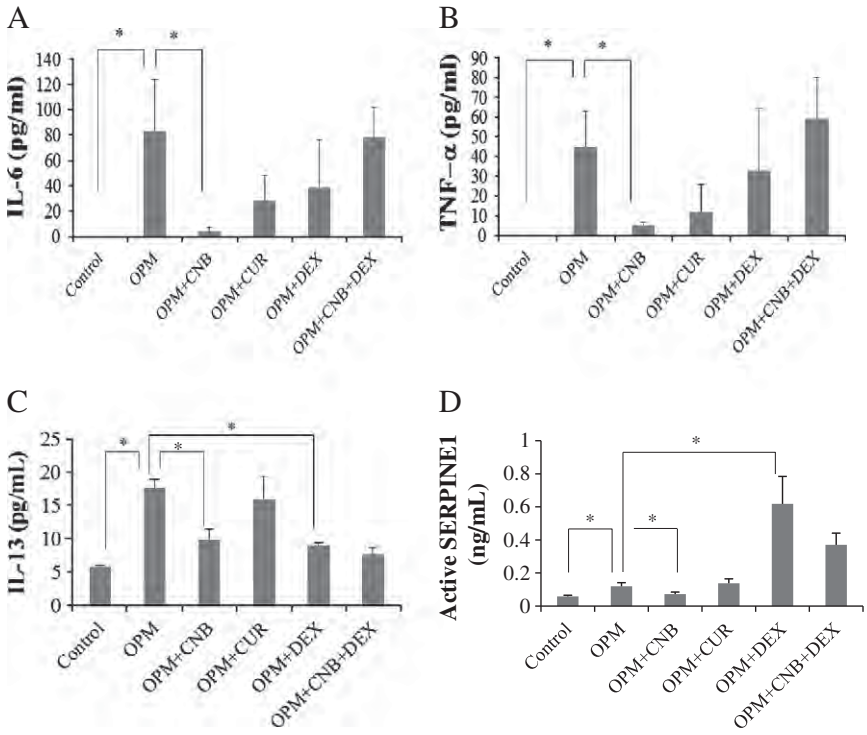

Fig. 7. *In vivo* effect of CNB001, curcumin, and dexamethasone on cytokine synthesis in a murine asthma model. IL-6 (A), TNF-α (B), IL-13 (C), and active murine SERPINE1 (D) levels were measured in bronchoalveolar lavage fluid obtained from OVA-sensitized BALB/c mice that were treated as described in the legend of Fig. 5. OPM indicates OVA + Poly(I:C) + house dust mite. Data represent means ± SD, $^*P<0.05$, n = 5–6 for each group.

siRNA in wild-type mice (Miyamoto et al., 2011). Although DEX possesses strong anti-inflammatory effects, DEX and its receptor complex promote the expression of *Serpine1* by affecting the promoter region of the *Serpine1* gene (Kimura et al., 2009; Wickert et al., 2007; Yamamoto et al., 2004). This may be one of the reasons that glucocorticoids cannot prevent airway remodeling (Kuramoto et al., 2009). Here, we observed that DEX increased the level of active SERPINE1 both *in vivo* and *in vitro*, but, when combined with CNB001, it suppressed the level of active SERPINE1. These results suggest that a combination of glucocorticoids and CNB001 might prevent increased expression of SERPINE1, and thereby suppress airway remodeling.

Our results suggest that a new curcumin derivative, CNB001, could potentially be used for controlling the function of airway epithelial cells by reducing inflammation and airway remodeling in asthma. We focused on epithelial cells in this study, and further studies are needed to determine the effects of this derivative on other cell types involved in EMT and airway remodeling.

Conflict of interest statement

No conflicts of interests are declared by the authors.

Acknowledgments

This study was supported in part by Grants-in-Aid for Scientific Research from the Ministry of Education, Science, Sports and Culture, Japan; a grant for Allergic Disease and Intractable Diseases from the Ministry of Health, Labor and Welfare; a grant from the Respiratory Failure Research Group from the Health and Labor Sciences; and Yamazaki Spice Promotion Foundation. We also thank Michiko Tachibana for her excellent technical assistance.

References

Aggarwal, B.B., Harikumar, K.B., 2009. Potential therapeutic effects of curcumin, the anti-inflammatory agent, against neurodegenerative, cardiovascular, pulmonary, metabolic, autoimmune and neoplastic diseases. The International Journal of Biochemistry & Cell Biology 41, 40–59.

Anand, P., Kunnumakkara, A.B., Newman, R.A., Aggarwal, B.B., 2007. Bioavailability of curcumin: problems and promises. Molecular Pharmaceutics 4, 807–818.

Ather, J.L., Ckless, K., Martin, R., Foley, K.L., Suratt, B.T., Boyson, J.E., Fitzgerald, K.A., Flavell, R.A., Eisenbarth, S.C., Poynter, M.E., 2011. Serum amyloid A activates the NLRP3 inflammasome and promotes Th17 allergic asthma in mice. Journal of Immunology 187, 64–73.

Bachar, O., Adner, M., Uddman, R., Cardell, L.O., 2004. Toll-like receptor stimulation induces airway hyper-responsiveness to bradykinin, an effect mediated by JNK and NF-kappa B signaling pathways. European Journal of Immunology 34, 1196–1207.

Bruewer, M., Luegering, A., Kucharzik, T., Parkos, C.A., Madara, J.L., Hopkins, A.M., Nusrat, A., 2003. Proinflammatory cytokines disrupt epithelial barrier function by apoptosis-independent mechanisms. Journal of Immunology 171, 6164–6172.

Brusselle, G., Kips, J., Joos, G., Bluethmann, H., Pauwels, R., 1995. Allergen-induced airway inflammation and bronchial responsiveness in wild-type and interleukin-4-deficient mice. American Journal of Respiratory Cell and Molecular Biology 12, 254–259.

Camacho-Barquero, L., Villegas, I., Sanchez-Calvo, J.M., Talero, E., Sanchez-Fidalgo, S., Motilva, V., Alarcon de la Lastra, C., 2007. Curcumin, a *Curcuma longa* constituent, acts on MAPK p38 pathway modulating COX-2 and iNOS expression in chronic experimental colitis. International Immunopharmacology 7, 333–342.

Chi, X.Y., Jiang, S.J., Wang, J., Wang, J.P., 2011. Effect of glucocorticoid in mice of asthma induced by ovalbumin sensitisation and RSV infection. Asian Pacific Journal of Allergy and Immunology 29, 176–180.

Dennler, S., Itoh, S., Vivien, D., ten Dijke, P., Huet, S., Gauthier, J.M., 1998. Direct binding of Smad3 and Smad4 to critical TGF beta-inducible elements in the promoter of human plasminogen activator inhibitor-type 1 gene. EMBO Journal 17, 3091–3100.

Doerner, A.M., Zuraw, B.L., 2009. TGF-beta1 induced epithelial to mesenchymal transition (EMT) in human bronchial epithelial cells is enhanced by IL-1beta but not abrogated by corticosteroids. Respiratory Research 10, 100.

Doherty, T.A., Croft, M., 2011. Therapeutic potential of targeting TNF/TNFR family members in asthma. Immunotherapy 3, 919–921.

Fahy, J.V., Kim, K.W., Liu, J., Boushey, H.A., 1995. Prominent neutrophilic inflammation in sputum from subjects with asthma exacerbation. The Journal of Allergy and Clinical Immunology 95, 843–852.

Fang, J., Lu, J., Holmgren, A., 2005. Thioredoxin reductase is irreversibly modified by curcumin: a novel molecular mechanism for its anticancer activity. Journal of Biological Chemistry 280, 25284–25290.

Fattouh, R., Pouladi, M.A., Alvarez, D., Johnson, J.R., Walker, T.D., Goncharova, S., Inman, M.D., Jordana, M., 2005. House dust mite facilitates ovalbumin-specific allergic sensitization and airway inflammation. American Journal of Respiratory and Critical Care Medicine 172, 314–321.

Gaedeke, J., Noble, N.A., Border, W.A., 2004. Curcumin blocks multiple sites of the TGF-beta signaling cascade in renal cells. Kidney International 66, 112–120.

Gizycki, M.J., Adelroth, E., Rogers, A.V., O'Byrne, P.M., Jeffery, P.K., 1997. Myofibroblast involvement in the allergen-induced late response in mild atopic asthma. American Journal of Respiratory Cell and Molecular Biology 16, 664–673.

Gough, L., Campbell, E., Bayley, D., Van Heeke, G., Shakib, F., 2003. Proteolytic activity of the house dust mite allergen Der p 1 enhances allergenicity in a mouse inhalation model. Clinical and Experimental Allergy 33, 1159–1163.

Groskreutz, D.J., Monick, M.M., Powers, L.S., Yarovinsky, T.O., Look, D.C., Hunninghake, G.W., 2006. Respiratory syncytial virus induces TLR3 protein and protein kinase R, leading to increased double-stranded RNA responsiveness in airway epithelial cells. Journal of Immunology 176, 1733–1740.

Ha, H., Oh, E.Y., Lee, H.B., 2009. The role of plasminogen activator inhibitor 1 in renal and cardiovascular diseases. Nature Reviews Nephrology 5, 203–211.

Hackett, T.L., Warner, S.M., Stefanowicz, D., Shaheen, F., Pechkovsky, D.V., Murray, L.A., Argentieri, R., Kicic, A., Stick, S.M., Bai, T.R., Knight, D.A., 2009. Induction of epithelial–mesenchymal transition in primary airway epithelial cells from patients with asthma by transforming growth factor-beta1. American Journal of Respiratory and Critical Care Medicine 180, 122–133.

Holgate, S.T., 2010. A look at the pathogenesis of asthma: the need for a change in direction. Discovery Medicine 9, 439–447.

Holgate, S.T., Davies, D.E., Lackie, P.M., Wilson, S.J., Puddicombe, S.M., Lordan, J.L., 2000. Epithelial–mesenchymal interactions in the pathogenesis of asthma. The Journal of Allergy and Clinical Immunology 105, 193–204.

Huang, W., Xu, C., Kahng, K.W., Noble, N.A., Border, W.A., Huang, Y., 2008. Aldosterone and TGF-beta1 synergistically increase PAI-1 and decrease matrix degradation in rat renal mesangial and fibroblast cells. American Journal of Physiology. Renal Physiology 294, F1287–F1295.

Jang, B.C., Lim, K.J., Suh, M.H., Park, J.G., Suh, S.I., 2007. Dexamethasone suppresses interleukin-1beta-induced human beta-defensin 2 mRNA expression: involvement of p38 MAPK, JNK, MKP-1, and NF-kappaB transcriptional factor in A549 cells. FEMS Immunology and Medical Microbiology 51, 171–184.

Kim, T.B., Kim, S.Y., Moon, K.A., Park, C.S., Jang, M.K., Yun, E.S., Cho, Y.S., Moon, H.B., Lee, K.Y., 2007. Five-aminoimidazole-4-carboxamide-1-beta-4-ribofuranoside attenuates poly (I:C)-induced airway inflammation in a murine model of asthma. Clinical and Experimental Allergy 37, 1709–1719.

Kimura, H., Li, X., Torii, K., Okada, T., Kamiyama, K., Mikami, D., Takahashi, N., Yoshida, H., 2009. Dexamethasone enhances basal and TNF-alpha-stimulated production of PAI-1 *via* the glucocorticoid receptor regardless of 11beta-hydroxysteroid dehydrogenase 2 status in human proximal renal tubular cells. Nephrology, Dialysis, Transplantation 24, 1759–1765.

Kowal, K., Zukowski, S., Moniuszko, M., Bodzenta-Lukaszyk, A., 2008. Plasminogen activator inhibitor-1 (PAI-1) and urokinase plasminogen activator (uPA) in sputum of allergic asthma patients. Folia Histochemica et Cytobiologica 46, 193–198.

Kucharewicz, I., Kowal, K., Buczko, W., Bodzenta-Lukaszyk, A., 2003. The plasmin system in airway remodeling. Thrombosis Research 112, 1–7.

Kuramoto, E., Nishiuma, T., Kobayashi, K., Yamamoto, M., Kono, Y., Funada, Y., Kotani, Y., Sisson, T.H., Simon, R.H., Nishimura, Y., 2009. Inhalation of urokinase-type plasminogen activator reduces airway remodeling in a murine asthma model. American Journal of Physiology. Lung Cellular and Molecular Physiology 296, L337–L346.

Lee, G., Walser, T.C., Dubinett, S.M., 2009. Chronic inflammation, chronic obstructive pulmonary disease, and lung cancer. Current Opinion in Pulmonary Medicine 15, 303–307.

Liu, Y., Dargusch, R., Maher, P., Schubert, D., 2008. A broadly neuroprotective derivative of curcumin. Journal of Neurochemistry 105, 1336–1345.

Maher, P., Akaishi, T., Schubert, D., Abe, K., 2010. A pyrazole derivative of curcumin enhances memory. Neurobiology of Aging 31, 706–709.

Matsuo, Y., Ishihara, T., Ishizaki, J., Miyamoto, K., Higaki, M., Yamashita, N., 2009. Effect of betamethasone phosphate loaded polymeric nanoparticles on a murine asthma model. Cellular Immunology 260, 33–38.

Miyamoto, S., Hattori, N., Senoo, T., Onari, Y., Iwamoto, H., Kanehara, M., Ishikawa, N., Fujitaka, K., Haruta, Y., Murai, H., Yokoyama, A., Kohno, N., 2011. Intra-airway administration of small interfering RNA targeting plasminogen activator inhibitor-1 attenuates allergic asthma in mice. American Journal of Physiology. Lung Cellular and Molecular Physiology 301, L908–L916.

Morjaria, J.B., Babu, K.S., Vijayanand, P., Chauhan, A.J., Davies, D.E., Holgate, S.T., 2011. Sputum IL-6 concentrations in severe asthma and its relationship with FEV1. Thorax 66, 537.

Oh, S.W., Cha, J.Y., Jung, J.E., Chang, B.C., Kwon, H.J., Lee, B.R., Kim, D.Y., 2011. Curcumin attenuates allergic airway inflammation and hyper-responsiveness in mice through NF-kappaB inhibition. Journal of Ethnopharmacology 136, 414–421.

Phipps, S., Lam, C.E., Kaiko, G.E., Foo, S.Y., Collison, A., Mattes, J., Barry, J., Davidson, S., Oreo, K., Smith, L., Mansell, A., Matthaei, K.I., Foster, P.S., 2009. Toll/IL-1 signaling is critical for house dust mite-specific helper T cell type 2 and type 17 [corrected] responses. American Journal of Respiratory and Critical Care Medicine 179, 883–893.

Ray, S., Chattopadhyay, N., Mitra, A., Siddiqi, M., Chatterjee, A., 2003. Curcumin exhibits antimetastatic properties by modulating integrin receptors, collagenase activity, and expression of Nm23 and E-cadherin. Journal of Environmental Pathology, Toxicology and

Oncology: Official Organ of the International Society for Environmental Toxicology and Cancer 22, 49–58.
Saha, S., Doe, C., Mistry, V., Siddiqui, S., Parker, D., Sleeman, M., Cohen, E.S., Brightling, C.E., 2009. Granulocyte-macrophage colony-stimulating factor expression in induced sputum and bronchial mucosa in asthma and COPD. Thorax 64, 671–676.
Santel, T., Pflug, G., Hemdan, N.Y., Schafer, A., Hollenbach, M., Buchold, M., Hintersdorf, A., Lindner, I., Otto, A., Bigl, M., Oerlecke, I., Hutschenreuther, A., Sack, U., Huse, K., Groth, M., Birkemeyer, C., Schellenberger, W., Gebhardt, R., Platzer, M., Weiss, T., Vijayalakshmi, M.A., Kruger, M., Birkenmeier, G., 2008. Curcumin inhibits glyoxalase 1: a possible link to its anti-inflammatory and anti-tumor activity. PloS One 3, e3508.
Shetty, S., Padijnayayveetil, J., Tucker, T., Stankowska, D., Idell, S., 2008. The fibrinolytic system and the regulation of lung epithelial cell proteolysis, signaling, and cellular viability. American Journal of Physiology. Lung Cellular and Molecular Physiology 295, L967–L975.
Sisson, T.H., Nguyen, M.H., Yu, B., Novak, M.L., Simon, R.H., Koh, T.J., 2009. Urokinase-type plasminogen activator increases hepatocyte growth factor activity required for skeletal muscle regeneration. Blood 114, 5052–5061.
Skold, C.M., 2010. Remodeling in asthma and COPD—differences and similarities. The Clinical Respiratory Journal 4 (Suppl. 1), 20–27.
Song, W.B., Wang, Y.Y., Meng, F.S., Zhang, Q.H., Zeng, J.Y., Xiao, L.P., Yu, X.P., Peng, D.D., Su, L., Xiao, B., Zhang, Z.S., 2010. Curcumin protects intestinal mucosal barrier function of rat enteritis *via* activation of MKP-1 and attenuation of p38 and NF-kappaB activation. PloS One 5, e12969.
Sugimoto, K., Hanai, H., Tozawa, K., Aoshi, T., Uchijima, M., Nagata, T., Koide, Y., 2002. Curcumin prevents and ameliorates trinitrobenzene sulfonic acid-induced colitis in mice. Gastroenterology 123, 1912–1922.
Takahashi, E., Nagano, O., Ishimoto, T., Yae, T., Suzuki, Y., Shinoda, T., Nakamura, S., Niwa, S., Ikeda, S., Koga, H., Tanihara, H., Saya, H., 2010. Tumor necrosis factor-alpha regulates transforming growth factor-beta-dependent epithelial–mesenchymal transition by promoting hyaluronan–CD44–moesin interaction. Journal of Biological Chemistry 285, 4060–4073.
Takayama, S., Tamaoka, M., Takayama, K., Okayasu, K., Tsuchiya, K., Miyazaki, Y., Sumi, Y., Martin, J.G., Inase, N., 2011. Synthetic double-stranded RNA enhances airway inflammation and remodelling in a rat model of asthma. Immunology 134, 140–150.
Takizawa, H., Ohtoshi, T., Yamashita, N., Oka, T., Ito, K., 1996. Interleukin 6-receptor expression on human bronchial epithelial cells: regulation by IL-1 and IL-6. The American Journal of Physiology 270, L346–L352.
Trompette, A., Divanovic, S., Visintin, A., Blanchard, C., Hegde, R.S., Madan, R., Thorne, P.S., Wills-Karp, M., Gioannini, T.L., Weiss, J.P., Karp, C.L., 2009. Allergenicity resulting from functional mimicry of a Toll-like receptor complex protein. Nature 457, 585–588.
Venugopal, S.K., Chen, J., Zhang, Y., Clemens, D., Follenzi, A., Zern, M.A., 2007. Role of MAPK phosphatase-1 in sustained activation of JNK during ethanol-induced apoptosis in hepatocyte-like VL-17A cells. Journal of Biological Chemistry 282, 31900–31908.
Vieira, R.P., Muller, T., Grimm, M., von Gernler, V., Vetter, B., Durk, T., Cicko, S., Ayata, C.K., Sorichter, S., Robaye, B., Zeiser, R., Ferrari, D., Kirschbaum, A., Zissel, G., Virchow, J.C., Boeynaems, J.M., Idzko, M., 2011. Purinergic receptor type 6 contributes to airway inflammation and remodeling in experimental allergic airway inflammation. American Journal of Respiratory and Critical Care Medicine 184, 215–223.
Wark, P.A., Johnston, S.L., Moric, I., Simpson, J.L., Hensley, M.J., Gibson, P.G., 2002. Neutrophil degranulation and cell lysis is associated with clinical severity in virus-induced asthma. European Respiratory Journal 19, 68–75.
Weber, W.M., Hunsaker, L.A., Abcouwer, S.F., Deck, L.M., Vander Jagt, D.L., 2005. Anti-oxidant activities of curcumin and related enones. Bioorganic & Medicinal Chemistry 13, 3811–3820.
Westergren-Thorsson, G., Larsen, K., Nihlberg, K., Andersson-Sjoland, A., Hallgren, O., Marko-Varga, G., Bjermer, L., 2010. Pathological airway remodelling in inflammation. The Clinical Respiratory Journal 4 (Suppl. 1), 1–8.
Wickert, L., Chatain, N., Kruschinsky, K., Gressner, A.M., 2007. Glucocorticoids activate TGF-beta induced PAI-1 and CTGF expression in rat hepatocytes. Comparative Hepatology 6, 5.
Willis, B.C., duBois, R.M., Borok, Z., 2006. Epithelial origin of myofibroblasts during fibrosis in the lung. Proceedings of the American Thoracic Society 3, 377–382.
Wills-Karp, M., Luyimbazi, J., Xu, X., Schofield, B., Neben, T.Y., Karp, C.L., Donaldson, D.D., 1998. Interleukin-13: central mediator of allergic asthma. Science 282, 2258–2261.
Wong, E.T., Tergaonkar, V., 2009. Roles of NF-kappaB in health and disease: mechanisms and therapeutic potential. Clinical Science (London, England) 116, 451–465.
Wong, T.S., Chan, W.S., Li, C.H., Liu, R.W., Tang, W.W., Tsao, S.W., Tsang, R.K., Ho, W.K., Wei, W.I., Chan, J.Y., 2010. Curcumin alters the migratory phenotype of nasopharyngeal carcinoma cells through up-regulation of E-cadherin. Anticancer Research 30, 2851–2856.
Yadav, U.C., Ramana, K.V., Srivastava, S.K., 2011. Aldose reductase inhibition suppresses airway inflammation. Chemico-Biological Interactions 191, 339–345.
Yamamoto, Y., Ishizu, A., Ikeda, H., Otsuka, N., Yoshiki, T., 2004. Dexamethasone increased plasminogen activator inhibitor-1 expression on human umbilical vein endothelial cells: an additive effect to tumor necrosis factor-alpha. Pathobiology 71, 295–301.
Yamashita, N., Tashimo, H., Matsuo, Y., Ishida, H., Yoshiura, K., Sato, K., Kakiuchi, T., Ohta, K., 2006. Role of CCL21 and CCL19 in allergic inflammation in the ovalbumin-specific murine asthmatic model. The Journal of Allergy and Clinical Immunology 117, 1040–1046.
Zavadil, J., Bottinger, E.P., 2005. TGF-beta and epithelial-to-mesenchymal transitions. Oncogene 24, 5764–5774.

Veterinary Immunology and Immunopathology 145 (2012) 447–452

Contents lists available at SciVerse ScienceDirect

Veterinary Immunology and Immunopathology

journal homepage: www.elsevier.com/locate/vetimm

Research paper

Large-scale survey of adverse reactions to canine non-rabies combined vaccines in Japan

Kazuki Miyaji[a], Aki Suzuki[a], Hidekatsu Shimakura[a], Yukari Takase[a], Akio Kiuchi[a], Masato Fujimura[b], Goro Kurita[c], Hajime Tsujimoto[d], Masahiro Sakaguchi[a,*]

[a] Department of Veterinary Microbiology, School of Veterinary Medicine, Azabu University, 1-17-71 Fuchinobe, Chuo-ku, Sagamihara, Kanagawa 252-5201, Japan
[b] Fujimura Animal Hospital, 5-10-26, Aomatanihigashi, Minou, Osaka 652-0022, Japan
[c] Kurita Animal Hospital, Furukawa, Furukawa, Ibaraki 306-0016, Japan
[d] Department of Veterinary Internal Medicine, Graduate School of Agricultural and Life Sciences, The University of Tokyo, 1-1-1 Yayoi, Bunkyo-ku, Tokyo 113-8657, Japan

ARTICLE INFO

Article history:
Received 1 December 2011
Received in revised form
27 December 2011
Accepted 29 December 2011

Keywords:
Canine non-rabies combined vaccine
Adverse event
Anaphylaxis

ABSTRACT

Canine non-rabies combined vaccines are widely used to protect animals from infectious agents, and also play an important role in public health. We performed a large-scale survey to investigate vaccine-associated adverse events (VAAEs), including anaphylaxis, in Japan by distributing questionnaires on VAAEs to veterinary hospitals from April 1, 2006 through May 31, 2007. Valid responses were obtained for 57,300 vaccinated dogs at 573 animal hospitals; we obtained VAAEs information for last 100 vaccinated dogs in each veterinary hospital. We found that of the 57,300, 359 dogs showed VAAEs. Of the 359 dogs, death was observed in 1, anaphylaxis in 41, dermatological signs in 244, gastrointestinal signs in 160, and other signs in 106. Onset of VAAEs was mostly observed within 12 h after vaccination (n = 299, 83.3%). In this study, anaphylaxis events occurred within 60 min after vaccination, and about half of these events occurred within 5 min (n = 19, 46.3%). Furthermore, where anaphylaxis was reported, additional information to support the diagnosis was obtained by reinvestigation. Our resurvey of dogs with anaphylaxis yielded responses on 31 dogs; 27 of these demonstrated collapse (87.1%), 24 demonstrated cyanosis (77.4%), and both signs occurred in 22 (71.0%). Higher rates of animal VAAEs, anaphylaxis, and death were found in Japan than in other countries. Further investigations, including survey studies, will be necessary to elucidate the interaction between death and vaccination and the risk factors for VAAEs, and thus develop safer vaccines. Moreover, it may also be necessary to continually update the data of VAAEs.

1. Introduction

Canine non-rabies combined vaccines, containing zoonotic pathogen leptospira, are widely used in small animal veterinary medicine. Vaccination is aimed at protecting animals from infectious agents and plays an important role in public health. No vaccine, however, is completely effective or without adverse reactions, and vaccine-associated adverse events (VAAEs) do occur, albeit infrequently, after vaccinations. Epidemiological surveys in the United Kingdom (Gaskell et al., 2002) and the United States (Moore et al., 2005) identified the rates for VAAEs as 0.093 and 38.2/10,000 vaccinated dogs, respectively.

VAAEs can include anaphylaxis, which is an acute multi-system, severe type I hypersensitivity reaction (Sakaguchi

* Corresponding author. Tel.: +81 42 754 7111x705; fax: +81 42 754 7661.
E-mail address: sakagum@azabu-u.ac.jp (M. Sakaguchi).

0165-2427/$ – see front matter © 2012 Elsevier B.V. All rights reserved.
doi:10.1016/j.vetimm.2011.12.023

Report of Adverse Reactions to Canine Mixed Vaccines

Breed: Gender: □ Male □ Female □ Castrated □ Spayed
Date of Birth: Body Weight:
Date of Vaccination: Number of Vaccination:
Vaccine Used:
Time of Onset after Vaccination
Signs
□ Death □ Anaphylaxis *
Dermatologic signs (□ Facial edema □ Pruritus □ Erythema/Urticaria)
Gastrointestinal signs (□ Vomiting □ Diarrhea □ Anorexia)
□ Others
( )

* The definition of anaphylaxis is the following: collapse, cyanosis, hypothermia, dyspnea, and/or hyperpnea is (are) observed within minutes after vaccination.

Handling of Adverse Reaction(s):
Outcome:

Fig. 1. The questionnaire form used for the investigation of vaccine-associated adverse events (VAAEs). The questionnaire was distributed by the Japan Small Animal Veterinary Association to veterinary hospitals in Japan from April 1, 2006 through May 31, 2007.

et al., 1995; Roth, 1999) occasionally observed in humans and dogs after vaccination, and which sometimes causes death (Brooks, 1991; Sakaguchi et al., 2000). According to large epidemiological studies on canine VAAEs, the incidences of anaphylaxis were 0.018/10,000 vaccinated dogs in the United Kingdom (Gaskell et al., 2002) and 0.65/10,000 vaccinated dogs in the United States (Moore et al., 2005). Based on a survey of a small number (35) of Japanese veterinary hospitals, the anaphylaxis rate in Japan appeared to be somewhat higher, at 0.17% (6/3477 vaccinated dogs) (Fujimura, 2006). However, to date, no large-scale investigation had been carried out on VAAEs associated with canine non-rabies combined vaccine in Japan. Moreover, although incidences of anaphylaxis were provided, none of the previous studies (Gaskell et al., 2002; Moore et al., 2005; Fujimura, 2006) considered important details, such as concurrent symptomatic states.

Here, we report the results of a large-scale survey of VAAEs in Japan, based on diagnosis made by experienced veterinarians in their practices. Our results reveal useful information on VAAEs, including critical detail on anaphylaxis and death caused by canine non-rabies combined vaccines. It is useful to record vaccine reactions routinely, and report VAAEs to specific agents such as local governments in veterinary medicine as well as human medicine.

2. Materials and methods

2.1. Experimental design and questionnaire for study of canine vaccine associated adverse events

The questionnaires about adverse reactions to canine non-rabies combined vaccines were distributed by the Japan Small Animal Veterinary Association to veterinary hospitals in Japan from April 1, 2006 through May 31, 2007. The questionnaires not only recorded standard information: date of birth, breed, sex and neuter status, weight, and date of vaccination, but also included important factors associated with adverse reactions, such as type of vaccination, signs, and time of their onset since vaccination (Fig. 1). Practicing veterinarians diagnosed adverse reactions and classified them into 5 groups according to clinical signs: death, anaphylaxis, dermatological signs (swelling of face, pruritus, urticaria, flush, and erythema), gastro-intestinal signs (vomiting and diarrhea), and other signs (including hypodynamia and anorexia). In cases of anaphylaxis, additional information was obtained by reinvestigation to support the diagnoses. To define the population, each responding veterinarian also stated the number of affected cases per last 100 vaccinated dogs.

2.2. Vaccines

The following non-rabies combined vaccines for dogs are commonly used in Japan: combined live vaccines composed of canine parvovirus, canine distemper virus, canine adenovirus type 2, and canine parainfluenza virus (group 1); adding live or inactivated coronavirus to group 1 (group 2); adding inactivated leptospira to group 1 (group 3); adding inactivated coronavirus and leptospira to group 1 (group 4); adding live coronavirus and inactivated leptospira to group 1 (group 5). Duramune MX5 (Kyoritsu Seiyaku Corporation, Tokyo, Japan; Fort Dodge Animal Health, Iowa, USA), Eurican 5 (Merial Animal Health, Lyon, France), and Nobivac DHPPi (Intervet, Boxmeer, Netherlands) were classified as group 1; Canine-6II (Kyoto Biken Laboratories, Kyoto, Japan), Duramune DX6, and Vanguard Plus 5/CV (Pfizer Animal Health, New York, USA)

Table 1
Number and incidence of clinical signs of vaccine-associated adverse events (VAAEs) in 57,300 vaccinated dogs.

Clinical signs	Numbers of VAAEs[a] (per 10,000 dogs)
Anaphylaxis	41 (7.2)
Death	1 (0.2)
Dermatological signs	244 (42.6)
Gastrointestinal signs	160 (27.9)
Others	106 (18.5)

[a] Total number was over 359 because multiple signs were present in some dogs.

were classified as group 2; Canine-8, Eurican 7, and Nobivac DHPPi+L as group 3; Duramune DX8 and Vanguard Plus 5/CV-L as group 4; and Canine-9 (II) as group 5.

2.3. Statistical analyses

Sex and neuter status were analyzed as categorical data. Continuous variables of age and weight were converted to categorical variables because nonlinear trends were detected in the model-fitting process. Dogs were grouped on the basis of age at date of vaccination as follows: 2–9 months, 9 months to 1.5 years, 1.5–2.5 years, 2.5–3.5 years, 3.5–5.5 years, 5.5–8.5 years, and >8.5 years. Weight was converted from continuous to categorical data of 0–5 kg, 5–10 kg, and > 10 kg. The *P* values for anaphylaxis in total VAAEs were evaluated using a multivariate unconditional logistic regression model. The variants included sex and neuter status, weight, age, and vaccine group. The model was assessed for significance by use of the le Cessie–van Houwelingen test. A value of $P < 0.05$ was considered significant. Statistical analysis was performed with R version 2.11.1 (www.r-project.org/).

3. Results

3.1. Total adverse reactions

Valid responses were obtained for 57,300 vaccinated dogs, from 573 animal hospitals; of these, 359 dogs were diagnosed with VAAE (62.7/10,000 vaccinated dogs). Unfortunately, the detailed information regarding dogs with no adverse events could not be obtained in the present study. Of the 359 dogs, anaphylaxis was observed in 41, dermatological signs in 244, gastrointestinal signs in 160, and other signs in 106 (Table 1). A single death (0.2/10,000 vaccinated dogs) was reported within a few days after vaccination.

In decreasing order of frequency, 181 (50.4%) Miniature Dachshunds, 37 (10.3%) Chihuahuas, 18 (5.0%) Mixed-breeds, and 17 (4.7%) Toy Poodles were reported to have VAAEs in the present survey; other breeds were involved less frequently. The population with VAAEs included 145 (40.4%) sexually intact males, 156 (43.5%) sexually intact females, 24 (6.7%) castrated males, 24 (6.7%) spayed females, and 10 (2.8%) unknown. Almost half these dogs ($n = 164$, 45.7%) were between the ages of 2 and 9 months. Dogs in the weight category of 0–5 kg had the highest frequency of adverse reactions ($n = 249$, 69.4%). Most adverse events ($n = 299$, 83.3%) were observed within 12 h after vaccination (Fig. 2).

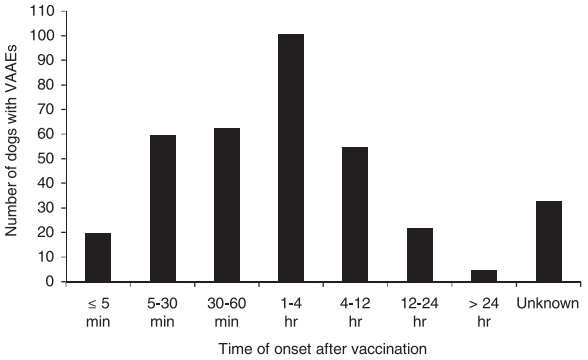

Fig. 2. Numbers of dogs with vaccine-associated adverse events (VAAEs), grouped by time of onset of signs. A total of 359 dogs exhibited VAAEs, including one death. Signs manifested within 12 h of vaccination in 299 cases.

3.2. Anaphylaxis and death

More detailed information about vaccine-associated anaphylaxis is provided in Tables 2 and 3, as well as Fig. 3. Miniature Dachshunds ($n = 13$) accounted for approximately 30% of the anaphylaxis cases. Anaphylaxis occurred in four Miniature Schnauzers out of a population of the eight with VAAEs. Of 41 dogs diagnosed with anaphylaxis, 17 (41.5%) were sexually intact males, 18 (43.9%) were intact females, 3 (7.3%) were castrated males, and 3 (7.3%) were spayed females. According to age and weight, the greatest frequency of anaphylaxis was recorded among dogs aged 2–9 months ($n = 20$, 48.8%) and among dogs weighting less than 5 kg ($n = 27$, 65.9%), respectively. A multivariate logistic regression model, including sex and neuter status, weight, and age satisfied requirements for goodness of fit ($P = 0.12$). In the final model, there was no significant relationship between anaphylaxis and the factors of sex and neuter status ($P = 0.58$), weight ($P = 0.15$), age ($P = 0.24$), or vaccine group ($P = 0.96$). All cases of anaphylaxis occurred within 60 min after vaccinations, and about half occurred within 5 min ($n = 19$, 46.3%) (Fig. 3).

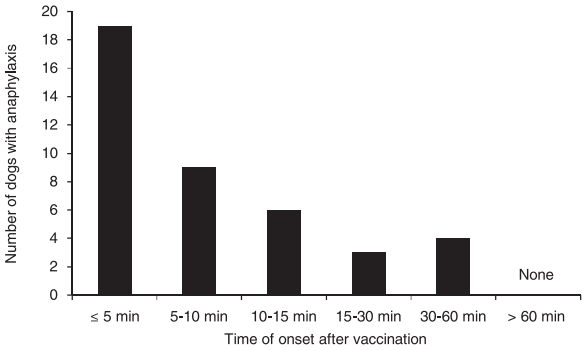

Fig. 3. Numbers of dogs with anaphylaxis, grouped by time of onset. A total of 41 dogs exhibited anaphylaxis signs; anaphylaxis set in within 60 min of vaccination, and within 5 min for 19 cases.

Table 2
Data obtained for 41 cases, where anaphylaxis followed vaccination.

Breed[a]	Sex[b]	Age (years)	Weight (kg)	Onset time (min)	Diagnostic reason[c]
Beagle	M	3.4	8.0	10	ND
C.K.C. Spaniel	F	0.2	2.2	1	Collapse, Cyanosis, Hyperpnea
Chihuahua	F	0.2	0.8	3	ND
J.R. Terrier	M	1.8	4.4	2	Collapse, Cyanosis
M. Dachshund	F	0.2	1.7	5	Collapse, Cyanosis, Hyperpnea
	F	0.2	1.7	10	Collapse, Cyanosis
	F	0.2	2.4	5	Collapse, Cyanosis
	F	0.2	2.6	10	Collapse, Cyanosis
	F	0.3	1.5	5	ND
	M	0.4	1.7	30–40	Collapse, Cyanosis
	S	1.4	4.9	15	ND
	M	2.1	4.4	30	Cyanosis
	C	3.3	5.6	30	Collapse, Cyanosis, Hypothermia
	S	3.5	6.8	40	Collapse, Cyanosis
	M	4.7	5.6	<5	Collapse, Cyanosis
	C	5.3	4.4	30	Collapse, Cyanosis
	M	6.8	4.6	15	ND
M. Schnauzer	M	0.2	0.6	1	Collapse, Hyperpnea
	M	0.4	3.7	15	Collapse, Cyanosis
	F	2.2	6.2	10	ND
	F	2.4	9.5	10	Collapse, Cyanosis, Hypothermia, Dyspnea
Mix	M	0.2	2.0	10	Collapse, Cyanosis
	M	4.2	11.0	<10	ND
	F	7.1	3.7	15	ND
Newfoundland	M	0.3	16.1	11	Collapse, Cyanosis
Pekingese	M	2.6	5.9	1	ND
Pomeranian	M	0.3	1.0	15	Collapse
Pug	F	3.0	7.2	5	Collapse, Cyanosis
Shiba	M	0.2	10.5	10	Collapse, Cyanosis
	F	NA	9.0	5	Collapse, Cyanosis
S. Sheepdog	F	9.6	11.5	5	Collapse, Cyanosis
Shih Tzu	F	0.2	1.6	<5	ND
	M	0.3	1.9	1	Collapse, Hyperpnea
	F	0.3	2.2	60	Cyanosis, Hyperpnea
Toy Poodle	F	0.2	1.3	<5	Collapse
	F	0.2	2.4	<5	Collapse, Cyanosis
	S	1.4	2.5	5–10	Collapse, Cyanosis, Hyperpnea
	M	1.4	2.6	5	Collapse, Cyanosis
	M	13.3	3.8	5	ND
Welsh Corgi	F	0.2	1.7	1	Collapse
	C	1.3	14.8	60	ND

ND: no data.
[a] C.K.C. Spaniel: Cavalier King Charles Spaniel, J.R. Terrier: Jack Russell Terrier, M. Dachshund; Miniature Dachshund, M. Schnauzer: Miniature Schnauzer, S. Sheepdog: Shetland Sheepdog.
[b] M: sexually intact male, F: sexually intact female, C: castrated male, S: spayed female.
[c] Diagnostic reasons were obtained from reinvestigation.

When we attempted to resurvey the 41 dogs that experienced anaphylaxis, responses were received for 31 of these dogs (recovery ratio = 75.6%). As shown in Table 3, collapse and cyanosis were observed in almost all 31 of the dogs, with 27 (87.1%) demonstrating collapse, 24 (77.4%) demonstrating cyanosis, and 22 (71.0%) showing both signs. A single death (Chihuahua, intact female, 2 months, 0.9 kg), occurring 38 h after vaccination, was reported in our questionnaire.

Table 3
Number of signs exhibited by anaphylactic dogs ($n = 31$).

Anaphylactic signs	n[a]	%
Collapse	27	87.1
Cyanosis	24	77.4
Hyperpnea	6	19.4
Hypothermia	2	6.5
Dyspnea	1	3.2

[a] Total number was over 31 because multiple signs were present in some dogs.

4. Discussion

The risks involved in vaccination of dogs were highlighted by previous large epidemiological studies (Gaskell et al., 2002; Moore et al., 2005); however, surveys on VAAEs had only been performed on a small scale in Japan (Ohmori et al., 2002, 2005a; Fujimura, 2006). Here, we present the results of a large-scale investigation of VAAEs at Japanese veterinary hospitals. We found a VAAE rate of 62.7/10,000 vaccinated dogs, which is much higher than the rates reported in the United Kingdom (0.093/10,000 vaccinated dogs) (Gaskell et al., 2002) and the United States (38.2/10,000 vaccinated dogs) (Moore et al., 2005). Previous reports suggested that small breed dogs (<10 kg), especially Dachshunds, were more prone to VAAEs than

larger dogs (Gaskell et al., 2002; Moore et al., 2005; Moore and Hogenesch, 2010). According to the Japan Kennel Club (http://www.jkc.or.jp), Miniature Dachshund, Chihuahua, and Toy Poodle are the most popular breeds in this country, and account for just over half of the total registrations in the Club (50.3%). This popular breed bias and the proposed breed susceptibility may contribute to higher VAAEs rate in Japan than in other countries.

Factors known to cause vaccine reactions include the primary vaccine agent or antigen, adjuvants, preservatives, stabilizers, and residues from tissue culture used in vaccine production (Hogenesch et al., 1999; Roth, 1999; Georgitis and Fasano, 2001). Our previous study reported large amounts of bovine serum albumin (BSA) and bovine IgG contents in canine vaccines (Ohmori et al., 2005b). Furthermore, we found IgE reactivity against fetal calf serum (FCS) components in dogs with allergic reactions after vaccination, suggesting that most of these reactions might be caused by FCS components derived from the culture media used to produce vaccines (Ohmori et al., 2005b, 2007). Many vaccines that are commonly used in Japan are imported from abroad, although a few are made in Japan. Multilateral studies are necessary to clarify the relationship between VAAEs and vaccine by-products, and to ascertain whether certain vaccines are more likely to give rise to VAAEs.

Among the many clinical signs of adverse reactions to vaccines, anaphylaxis is the most dramatic (Roth, 1999). In the present investigation, the incidence of anaphylaxis (7.2/10,000 vaccinated dogs) in dogs was remarkably higher than those reported in previous studies (Gaskell et al., 2002; Moore et al., 2005; Moore and Hogenesch, 2010). The dogs showing anaphylaxis in the present study included many small breeds such as Miniature Dachshund and Miniature Schnauzer. This implies that a breed predisposition may play a key role in anaphylaxis after vaccination of dogs, just as in total VAAEs, and that genetic factors may be involved in these clinical signs.

Moore et al. (2005) have indicated that the risk of VAAEs was significantly increased for small and neutered dogs, highest for dogs approximately 1–3 years old, and least for dogs $\geq$6 years of age. Unfortunately, as the information regarding dogs with no adverse events could not be obtained in the present study, the odds ratios of VAAEs could not be estimated; however, we did estimate the *P* values for anaphylaxis according to adverse reactions after vaccine administrations using a logistic regression model. Additionally, we were not able to analyze the relationship between breed and anaphylaxis due to small sample numbers for many breeds. However, no significant differences were observed in the anaphylaxis risk by sex and neuter status, weight, and age; thus, our data seem to show the same tendency of potential risk factors for VAAEs in the results of Moore et al. (2005). The results of the present study suggest that various factors such as weight and age could predict the potential risk of adverse reactions, including anaphylaxis after vaccination, which may allow practicing veterinarians to allay the anxiety of at least a few owners regarding vaccination.

As only a single death was reported in this investigation, a direct association between death and vaccine administration was not clear; however, as an incidence of 0.02/10,000 vaccinated dogs was reported in the United State (Moore et al., 2005), the mortality rate also appeared to be increased in Japan. This case did not show anaphylactic signs, although other clinical sign was observed. Further extensive surveys are needed to uncover the predictive factors and clinical signs that precede such outcomes, in order to prevent such unfortunate events. Moreover, to clarify the interaction between death and vaccination, comparison with randomized unvaccinated dogs may be effective.

5. Conclusions

We present data regarding VAAEs, and in particular, on anaphylaxis, based on a large-scale study in Japanese veterinary hospitals. Higher rates of VAAEs, anaphylaxis, and death were observed in Japan compared to other countries. Further international studies aimed at obtaining similar information will be necessary to elucidate the risk factors, including breed predisposition, the quality of vaccine products, and prior sensitization with variable allergens, for VAAEs, with a view to developing safer vaccines. In addition, as our study was not current, it may be also be necessary to continually update the data of VAAEs.

Conflict of interest statement

None of the authors of this paper has a financial or personal relationship with other people or organizations that could inappropriately influence or bias the content of the paper.

Acknowledgments

The authors would like to thank all staff of participating veterinary hospitals for their kind assistance in responding to the questionnaires. We also thank the Japan Small Animal Veterinary Association for its support. We thank Dr. Sakae Inouye in Otsuma Women's University for critical review of this manuscript. This research was partially supported by the Promotion and Mutual Aid Corporation for Private Schools of Japan, Grant-in-Aid for Matching Fund Subsidy for Private University, and by a Project Grant awarded by the Azabu University Research Services Division.

References

Brooks, R., 1991. Adverse reactions to canine and feline vaccines. Aust. Vet. J. 68, 342–344.

Fujimura, M., 2006. A survey on the adverse reactions to combined vaccines in a small group of veterinary hospitals (35 hospitals). J. Jap. Vet. Med. Assoc. 46, 17–21 (in Japanese).

Gaskell, R.M., Gettinby, G., Graham, S.J., Skilton, D., 2002. Veterinary Products Committee working group report on feline and canine vaccination. Vet. Rec. 150, 126–134.

Georgitis, J.W., Fasano, M.B., 2001. Allergenic components of vaccines and avoidance of vaccination-related adverse events. Curr. Allergy Asthma Rep. 1, 11–17.

Hogenesch, H., Azcona-Olivera, J., Scott-Moncrieff, C., Snyder, P.W., Glickman, L.T., 1999. Vaccine-induced autoimmunity in the dog. Adv. Vet. Med. 41, 733–747.

Moore, G.E., Guptill, L.F., Ward, M.P., Glickman, N.W., Faunt, K.K., Lewis, H.B., Glickman, L.T., 2005. Adverse events diagnosed within three days of vaccine administration in dogs. J. Am. Vet. Med. Assoc. 227, 1102–1108.

Moore, G.E., Hogenesch, H., 2010. Adverse vaccinal events in dogs and cats. Vet. Clin. North Am. Small Anim. Pract. 40, 393–407.
Ohmori, K., Masuda, K., Sakaguchi, M., Kaburagi, Y., Ohno, K., Tsujimoto, H., 2002. A retrospective study on adverse reactions to canine vaccines in Japan. J. Vet. Med. Sci. 64, 851–853.
Ohmori, K., Sakaguchi, M., Kaburagi, Y., Maeda, S., Masuda, K., Ohno, K., Tsujimoto, H., 2005a. Suspected allergic reactions after vaccination in 85 dogs in Japan. Vet. Rec. 156, 87–88.
Ohmori, K., Masuda, K., Maeda, S., Kaburagi, Y., Kurata, K., Ohno, K., Deboer, D.J., Tsujimoto, H., Sakaguchi, M., 2005b. IgE reactivity to vaccine components in dogs that developed immediate-type allergic reactions after vaccination. Vet. Immunol. Immunopathol. 104, 249–256.
Ohmori, K., Masuda, K., DeBoer, D.J., Sakaguchi, M., Tsujimoto, H., 2007. Immunoblot analysis for IgE-reactive components of fetal calf serum in dogs that developed allergic reactions after non-rabies vaccination. Vet. Immunol. Immunopathol. 115, 166–171.
Roth, J.A., 1999. Mechanistic bases for adverse vaccine reactions and vaccine failures. Adv. Vet. Med. 41, 681–700.
Sakaguchi, M., Ogura, H., Inouye, S., 1995. IgE antibody to gelatin in children with immediate-type reactions to measles and mumps vaccines. J. Allergy Clin. Immunol. 96, 563–565.
Sakaguchi, M., Nakayama, T., Fujita, H., Toda, M., Inouye, S., 2000. Minimum estimated incidence in Japan of anaphylaxis to live virus vaccines including gelatin. Vaccine 19, 431–436.

FULL PAPER *Internal Medicine*

Measurement for Canine IgE Using Canine Recombinant High Affinity IgE Receptor α Chain (FcεRIα)

Toshihiro TSUKUI[1)], Masahiro SAKAGUCHI[2)]*, Keigo KURATA[3)], Sadatoshi MAEDA[4)], Keitaro OHMORI[5)], Kenichi MASUDA[6)], Hajime TSUJIMOTO[7)] and Shigehiro IWABUCHI[1)]

[1)]*Nippon Zenyaku Kogyo Co., Ltd., 1–1 Tairanoue Sasagawa, Asaka-machi, Koriyama, Fukushima 963–0196, Japan*
[2)]*Department of Veterinary Microbiology, School of Veterinary Medicine, Azabu University, 1–17–71 Fuchinobe, Chuo-ku, Sagamihara, Kanagawa 252–5201, Japan*
[3)]*Institute of Tokyo Environmental Allergy, 2–2–4 Yushima, Bunkyo-ku, Tokyo 113–0034, Japan*
[4)]*Department of Veterinary Medicine, Faculty of Applied Biological Sciences, Gifu University, 1–1 Yanagido, Gifu, 501–1193, Japan*
[5)]*Laboratory of Veterinary Molecular Pathology and Therapeutics, Division of Animal Life Science, Graduate School, Institute of Symbiotic Science and Technology, Tokyo University of Agriculture and Technology, 3–5–8 Saiwai-cho, Fuchu, Tokyo 183–8509, Japan*
[6)]*Animal Allergy Clinical Laboratories, Inc., 5–4–30 Nishihashimoto, Midori-ku, Sagamihara Kanagawa 252–0131, Japan*
[7)]*Department of Veterinary Internal Medicine, Graduate School of Agricultural and Life Sciences, The University of Tokyo, 1–1–1 Yayoi, Bunkyo-ku, Tokyo 113–8657, Japan*

(Received 22 November 2010/Accepted 26 January 2012/Published online in J-STAGE 9 February 2012)

ABSTRACT. To detect allergen-specific IgE in dogs with allergic diseases, we developed a recombinant canine high affinity IgE receptor α chain (FcεRIα)-based IgE detection system. Using the recombinant protein of canine FcεRIα expressed by an *Escherichia coli* expression system, we could detect house dust mite (*Dermatophagoides farinae*) allergen-specific IgE in sera from dogs naturally and experimentally sensitized to this allergen with ELISA and western blotting. The IgE binding activity of recombinant canine FcεRIα on ELISA was impaired by heat treatment of these sera. The specificity of this recombinant canine FcεRIα-based IgE detection system was confirmed by inhibition assays with canine IgE. The recombinant canine FcεRIα-based IgE detection system established in this study offers an alternative tool to measure allergen-specific IgE in dogs.
KEY WORDS: atopic dermatitis, canine, FcεRIα, IgE, mite.

doi: 10.1292/jvms.10-0520; *J. Vet. Med. Sci.* 74(7): 851–856, 2012

Canine atopic dermatitis (CAD) is well-recognized as a chronic inflammatory skin disease in dogs [11]. The disease is characterized by pruritis and skin lesions that include erythema, hair loss, hyperpigmentation, and lichenification which are primarily localized on the ventral abdomen, thigh, and/or axillary regions [22]. Previous investigations concerning the etiology of allergy in animals provide evidence for a pathogenesis that closely parallels human allergic disease, the major difference being the ultimate manifestation of disease symptoms [13, 14]. CAD is known to be an immediate type hypersensitivity disease caused by sensitization to various environmental allergens and subsequent exposure to the allergens [2, 4]. Allergens responsible for provoking CAD can be derived from a multitude of sources which include house dust mites, plants, arthropods, epithelia, foods and molds [11, 15, 18].

In vitro assays for allergen specific IgE are a convenient and reproducible alternative to intradermal skin testing (IDST) in dogs and the results of such tests can be used to support a diagnosis of atopic dermatitis and to define appropriate allergens for inclusion in an immunotherapeutic regime [4, 5, 22]. Multiple *in vitro* assays for detection of allergen-specific IgE are available in the veterinary arena [9, 12, 16, 17, 20, 23, 26], yet there is a paucity of useful data describing the assays and comparing the available tests. The best characterized assays for detection of allergen-specific IgE in dogs are a monoclonal antibody cocktail-based ELISA for dog specific IgE [17] and a human high affinity IgE receptor based assay for dog IgE [6, 27]. When directly compared, the concordance of results for these 2 assays was demonstrated to be approximately 92% which is similar to the intra-ELISA/inter-laboratory concordance of results [17]. Generation of high affinity IgE receptor specific for dogs might represent an improvement in reagents available for detection of antigen-specific IgE in dogs.

In the present study we describe the expression, purification, and biotinylation of canine high affinity IgE receptor and provided preliminary information on its utility in an allergen-specific IgE ELISA as well as immunoblotting techniques.

MATERIALS AND METHODS

Dogs naturally sensitized with mite allergen: All dogs used in this study were confirmed to be free of ectoparasite

*CORRESPONDENCE TO: SAKAGUCHI, M., Department of Veterinary Microbiology, School of Veterinary Medicine, Azabu University, 1–17–71 Fuchinobe, Chuo-ku, Sagamihara, Kanagawa 252–5201, Japan.
e-mail: sakagum@azabu-u.ac.jp

infestations and cutaneous bacterial infections. This study included 19 dogs that were diagnosed as having historical and clinical findings consistent with CAD [29] and 10 dogs that were known to be negative for CAD and subsequently shown to be to be non-reactive to mite allergens when evaluated using IDST procedures [19].

Laboratory dogs artificially immunized with mite allergen: Five 6-month old beagles were immunized subcutaneously with 100 μg of crude *Dermatophagoides farinae* allergen extract (Greer Laboratories, Lenoir, NC, U.S.A.) admixed with 50 mg of alum. The subcutaneous injection was carried out twice with a 2-week interval. After immunization, IDST was performed to confirm sensitization to *D. farinae* allergen extract and recombinant Der f 2 (Seikagaku Corporation, Tokyo, Japan).

Purification of recombinant canine FcεRIα: A cDNA clone encoding canine FcεRIα was kindly provided by Dr. Ryo Goitsuka (Science University of Tokyo, Noda, Japan) [8]. The canine FcεRIα cDNA was ligated into EcoRI-XhoI sites of pGEX-4T-1 (GE Healthcare, Piscataway, NJ, U.S.A.) to express canine FcεRIα as a fusion protein with glutathione S-transferase (GST), using a commercially available kit (DNA Ligation kit Ver.2, Takara-Bio, Shiga, Japan). The expression vector, pGEX-cFcεRIα, was prepared in *Escherichia coli* competent cells (Top10: Invitrogen Corp, Carlsbad, CA, U.S.A.) and purified using a commercially available kit (Qiagen Endotoxin Maxi kit, Qiagen, Chatsworth, CA, U.S.A.). The plasmid was then introduced into *E.coli* strain BL21 (Novagen, Madison, WI, U.S.A.). The expression of fusion protein was induced by adding 5 m*l* of 100 mM isopropyl-β-D-thiogalactopyranoside (final concentration=1.0 mM). The incubation of culture was continued for an additional 3 hr. Cells pellets were sonicated in phosphate-buffered saline (PBS). Solubilized bacterial suspensions were centrifuged at 10,000 g at 4°C for 10 min, and the supernatant was rotated with glutathione Sepharose 4B (GE Healthcare) at 4°C overnight. The fusion protein combined with glutathione Sepharose 4B was then separated from the supernatant by the addition of reduced glutathione buffer (10 mM glutathione, 50 mM Tris-HCl; pH 8.0). Biotinylation of FcεRIα was performed as described by Nerurker *et al.* [21].

Detection of canine IgE by ELISA using canine FcεRIα: The binding activity of recombinant canine FcεRIα to canine IgE was assayed by ELISA. Briefly, microtitre plates (MaxiSorp F96; Nunc, Roskilde, Denmark) were coated with monoclonal canine IgE and purified canine IgG (Bethyl Laboratories, Montgomery, TX, U.S.A.) at concentrations ranging from 0.625 to 1,000 *n*g/m*l* in carbonate buffer (pH 9.6), and then blocked with 1% bovine serum albumin (BSA) in PBS at 37°C for 1 hr. For evaluation of binding, biotinylated FcεRIα (1 μg/m*l*) was added to each well and incubated for 2 hr. After washing, peroxidase-conjugated streptavidin (2 μg/m*l*) (Jackson ImmunoResearch Laboratories, West Grove, PA, U.S.A.) was added to each well and incubated for 1 hr. Following final washing, the plate was developed with the use of 2, 2'-azino-bis-(3-ethylbenz-thiazoline-6-sulfonic acid) (ABTS; Sigma Chemical Co., Ltd., St. Louis, MO, U.S.A.) in 0.1 M sodium citrate (pH 4.5). The optical density (OD) of each well of plates was read at 415 nm with a microplate reader (model 3550; Bio-Rad Laboratories, Hercules, CA, U.S.A.).

Detection of allergen-specific IgE by ELISA: Microtiter plates were coated with *D. farinae* allergen extract (Greer Laboratories) (400 *n*g/m*l*) in carbonate buffer (pH 9.6), then blocked with 1% BSA in PBS at 37°C for 1 hr. After washing, the individual serum samples of naturally sensitized or healthy dogs were added to each well and incubated for 2 hr. After washing, diluted biotinylated FcεRIα was added to each well and incubated for 2 hr. The remaining allergen-specific IgE ELISA procedures were the same as described above.

Heat inactivation of IgE in dog sera: To assess the heat lability of the binding activity of canine IgE for FcεRIα, the sera of 5 naturally *D. farinae*-sensitized dogs and 5 artificially *D. farinae*-immunized dogs were heated at 56°C for 1 hr. Dilutions of the unheated and heat-treated sera were then added to plates coated with *D. farinae* extract (2 μg/m*l*). Mite allergen-specific IgE in the intact and heat-inactivated sera were assayed by ELISA in the above-mentioned ELISA.

Detection of allergen-specific IgE by western blotting analysis: Reduced recombinant Der f 2 (1 μg/m*l*) (Asahi Breweries, Tokyo, Japan) was electrophoresed by SDS-PAGE and then electrotransferred to PVDF membrane (GE Healthcare). After blocking with PBS containing 5% non-fat dried milk, the membrane was incubated for 2 hr with naturally Der f 2-sensitized dog sera diluted 1:10 in PBS containing 0.1% Tween-20 and 5% non-fat dried milk. After washing, biotinylated recombinant canine FcεRIα (2 μg/m*l*) was added to the membrane and incubation was continued for 2 hr. Following an additional wash, appropriately diluted streptavidin-HRP was added to the membrane and incubation was continued for an additional 1 hr. Following a final wash, the membrane was incubated with ECL reagent (GE Healthcare) for 5 min and exposed to a radiographic film for 5–30 sec.

For inhibition analysis, recombinant Der f 2 was electrophoresed by SDS-PAGE and then electrotransferred to PVDF membrane. The membrane was incubated with sera of naturally Der f 2-sensitized dogs. After the incubation of Der f 2-sensitized serum with the membrane, admixtures of biotinylated recombinant canine FcεRIα with canine IgE (1 μg/m*l*) or with canine IgG (10 μg/m*l*) were added on the membrane. Detection of canine IgE by recombinant canine FcεRIα was performed using the same method as described for western blotting.

Statistical analysis: Statistical analysis was performed using the Student's *t*-test; *P*-values of less than 0.05 were considered significant.

RESULTS

Purification of recombinant canine FcεRIα: The *E. coli* strain BL 21 transformed with the pGEX-cRcεRIα produced an extracellular domain of canine FcεRIα (1–172 a.a.) as a fusion protein with GST, and it was isolated by glutathione affinity chromatography. The molecular weight of canine

FcεRIα fused with GST was approximately 40 kDa. The total cell lysate of *E. coli* BL21 transformant and the purified recombinant protein were electrophoresed by SDS-PAGE. A single band at a molecular weight of approximately 40 kDa was detected in the lane of purified recombinant canine FcεRIα (Fig. 1).

Analysis of binding activity of recombinant canine FcεRIα to canine IgE: The results presented in Fig. 2 demonstrate the immunoglobulin specificity of the affinity purified recombinant canine FcεRIα. When excess biotinylated recombinant canine FcεRIα was incubated with wells coated with varying concentrations of dog IgE the signal that was observed deceased in an antigen dose dependent fashion. However, when varying concentrations of dog IgG were evaluated, no signal was evident at any of the concentrations tested thereby demonstrating that recombinant canine FcεRIα does not react with IgG immunoglobulins.

Detection of D. farinae allergen-specific IgE by using of recombinant canine FcεRIα on ELISA: To evaluate the utility of recombinant canine FcεRIα-based ELISA for specific IgE to *D. farinae*, we measured the specific IgE in the sera of 19 dogs with CAD. Using a recombinant canine FcεRIα based ELISA, *D. farinae* allergen-specific IgE was detected in the sera of all the dogs diagnosed with CAD and subsequently shown to be IDST-positive (Fig. 3). In contrast, no *D. farinae*-specific IgE was detectable in the sera of IDST-negative dogs.

Heat inactivation of IgE in dog sera: To examine further the specificity of canine FcεRIα binding to canine IgE, serum samples from naturally sensitized (Fig. 4A) as well as artificially (Fig. 4B) immunized dogs were evaluated using our canine FcεRIα based direct bind ELISA specific for mite allergens. The results presented in Fig. 4 document that all dog sera contained *D. farinae*-specific IgE. Although the

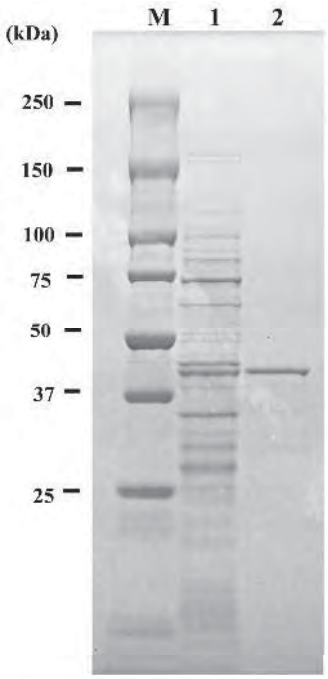

Fig. 1. Expression and purification of recombinant canine FcεRIα in *E. coli*: The DNA encoding extracellular domain of canine FcεRIα was expressed as a fusion protein with GST in pGEX-cFcεRIα. The fusion protein was purified by glutathione affinity chromatography. Molecular weight markers (M), Lane 1: total cell lysate of *E. coli* BL21 transformant (equivalent to 100 μl of the culture), Lane 2: recombinant canine FcεRIα fusion protein purified as a fusion with GST.

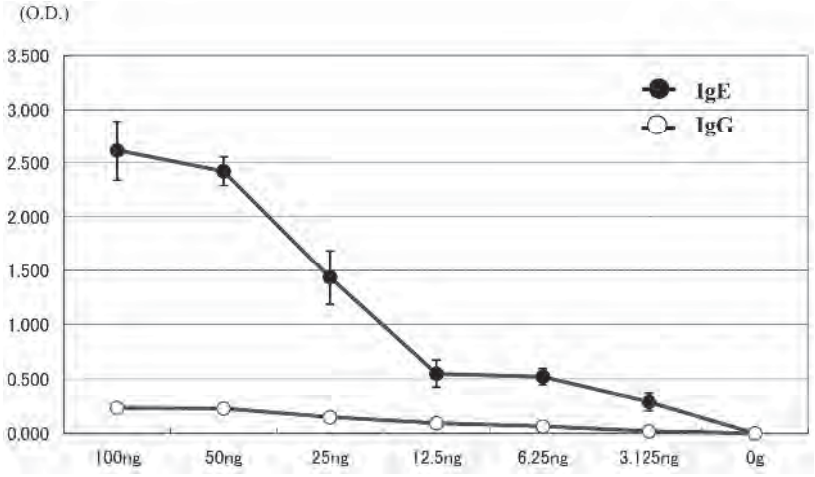

Fig.2. Measurement of binding activity to recombinant canine IgE and IgG by use of recombinant canine FcεRIα. Both canine IgE (Bethyl Laboratories, Montogomery TX, U.S.A.) and IgG were diluted to concentrations ranging from 31.2 to 1,000 *n*g/m*l*. The binding activity of recombinant canine FcεRIα was assayed by ELISA. OD: optical density.

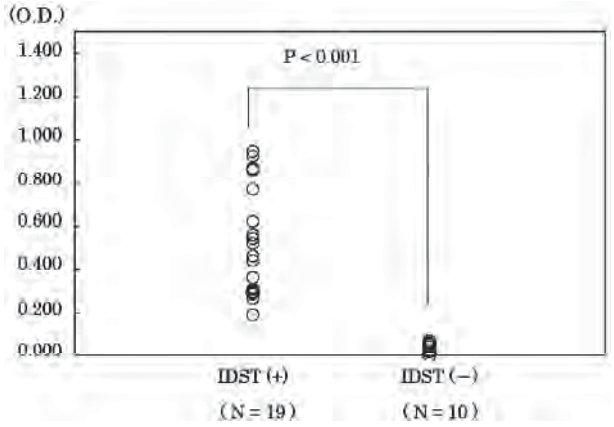

Fig. 3. Measurement of *D. farinae* allergen-specific IgE by ELISA. Sera of dogs with AD (N=19) and healthy dogs (N=10) were assayed by recombinant canine FcεRIα-based ELISA. The OD cutoff value was determined as the mean + 3 X SD of OD obtained from the healthy dogs' sera.

magnitude of response evident in the different samples varied, the reactivity evident in samples heated at 56°C for 1 hr was dramatically reduced to levels near or indistinguishable from negative sample responses. Important to this evaluation is the observation that heated negative serum samples were unaffected by the heating process; signals remained indistinguishable from background responses and no increase in non-specific reactions are evident.

Recombinant canine FcεRIα binding to D. farina-specific IgE in western blotting: The utility of recombinant canine FcεRIα in western blotting analysis was evaluated. Recombinant Der f 2 was electrophoresed by SDS-PAGE and then electrotransferred to PVDF membrane. The serum from a dog diagnosed with CAD and identified as Der f 2-sensitized by IDST was added to the membrane, and Der f 2-specific IgE was detected with biotinylated recombinant canine FcεRIα (Fig. 5, lane 1). To examine the IgE-specificity of this western blotting reagent, we adsorbed the biotinylated recombinant FcεRIα with purified canine IgE before adding to the membrane. The Der f 2-specific IgE signal evident with unadsorbed recombinant FcεRIα (Fig. 5, lane 1) was completely eliminated when biotinylated recombinant canine FcεRIα was adsorbed with purified canine IgE (Fig. 5, lane 2). In contrast, a signal of equal intensity to unadsorbed recombinant FcεRIα was evident when biotinylated recombinant canine FcεRIα was adsorbed with purified canine IgG (Fig. 5, lane 3). These results provide additional support for the IgE specificity of recombinant canine FcεRIα.

DISCUSSION

FcεRI is an oligomeric protein that is expressed on the surface of mast cells and basophils as a tetrameric complex consisting of one α, one β, and two γ subunits [1]. The FcεRIα binds to the Fc domain of IgE with high affinity; consequently, the FcεRI complex plays an important role in triggering allergic responses [1]. Expression and purification of the extracellular domain of human FcεRIα using a variety of systems has been reported. Chinese hamster ovary cell (CHO) transfectants [3], baculovirus-infected Sf-9 cells, yeast transformants [30], and *E. coli* transformants [28] have all been used to produce recombinant human FcεRIα. The utility of this molecule in detecting antigen-specific IgE in human sera as well as a variety of other animals has been well documented. In fact, one of the characterized commercial ELISA for allergen specific IgE in dogs [27] incorporates a human high affinity FcεRIα. However, Hakimi *et al.* reported that human FcεRIα exhibited lower affinity for rat IgE when compared to the affinity for human IgE [10] and it is likely that lowered cross species affinity exists for human FcεRIα in other animals as well. Therefore, successful expression, purification and characterization of a high affinity canine FcεRIα might represent a desirable alternative for assays intended for detecting antigen specific IgE in dogs.

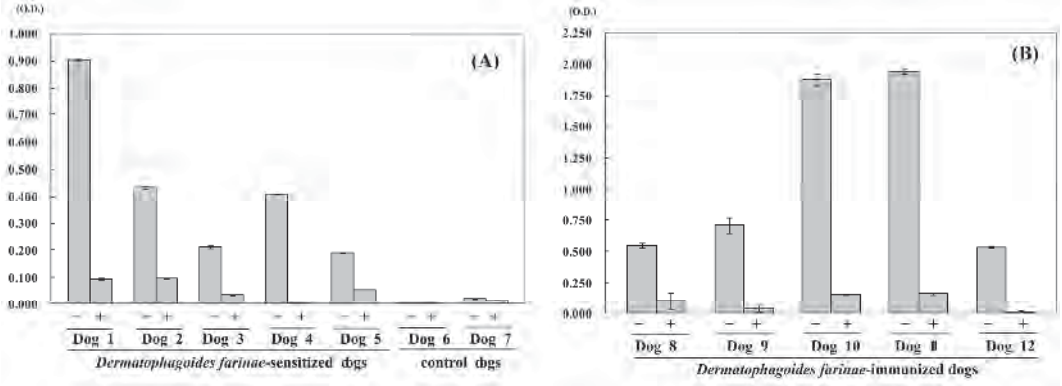

Fig. 4. Detection of *D. farinae* allergen-specific IgE and binding activity of recombinant canine FcεRIα in ELISA before and after heat inactivation. (A) Sera of *D. farinae*-sensitized dogs (Dog 1 to Dog 5) and healthy dogs used as controls (Dog 6 and Dog 7) and (B) Intact (−) and heat inactivated (+) sera of *D. farinae*-immunized dogs (Dog 8 to Dog 12) were assayed at 56°C for 1 hr by using recombinant canine FcεRIα.

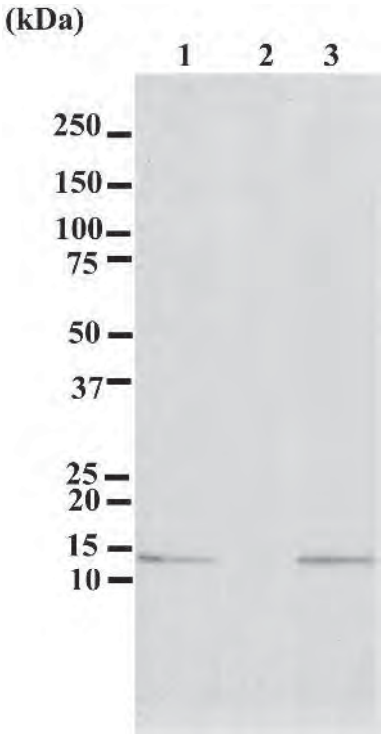

Fig. 5. Detection and inhibition of binding activity to Der f 2-specific IgE by western blotting: Der f 2 (15 kDa) was electrophoresed by SDS-PAGE and then electrotransferred to PVDF membrane. The serum of a naturally Der f 2-sensitized dog was assayed. Lane 1: detection with recombinant canine FcεRIα, Lane 2: detection with mixture of recombinant canine FcεRIα and canine IgE (1 μg/m*l*), Lane 3: detection with mixture of recombinant canine FcεRIα and canine IgG (10 μg/m*l*).

The recombinant canine FcεRIα used in the present study was expressed with GST. The commonly used GST gene fusion system [25] allowed us to successfully and more easily purify recombinant canine FcεRIα from *E. coli* lysate. Attempts to yield purified FcεRIα as a single protein containing only the extracellular domain of canine FcεRIα and free of GTS were unsuccessful. Nonetheless, the experiments conducted in this study demonstrate that the GST-FcεRIα fusion protein exhibits specific binding activity to canine IgE and confirms that GST has little influence on the application of FcεRIα for the detection of canine IgE. Whether or not the affinity of the canine GST-FcεRIα fusion protein is affected by the GST remains to be determined.

The specificity of recombinant canine FcεRIα binding to canine IgE was confirmed using three different approaches. Similar to the evaluation of human FcεRIα [27], we demonstrated IgE isotype specificity for the canine FcεRIα using ELISA for solid phase bound purified canine IgE and purified canine IgG. Our purified canine FcεRIα bound to canine IgE in an antigen dose dependent fashion that showed reactivity at concentrations as little as 3 *n*g, but reactivity of the purified canine FcεRIα to canine IgG was completely lacking even at a concentration of 100 *n*g. The utility of recombinant canine FcεRIα in western blotting analysis was confirmed using recombinant house dust mite allergen (Der f 2) and sera from mite reactive dogs. Further, Der f 2-specific IgE could not be detected using western blotting methods with biotinylated FcεRIα that was adsorbed (inhibition) with purified canine IgE. In contrast, adsorption with purified canine IgG did not interfere with immunoblot detection of Der f 2-specific IgE antibodies. Finally, mite reactivity evident in dog serum using an allergen-specific IgE ELISA that incorporates biotinylated canine FcεRIα was dramatically reduced (>80%) following heat treatment of the sera for 1 hr at 56°C. Such reduction in signal is consistent with the known heat lability of IgE [17, 24]. Equally important is the lack of reactivity in heated samples, which also contains very high levels of heat stable mite specific IgG (data not shown) thereby confirming the lack of canine FcεRIα reaction with IgG.

Although the performance characteristics of this detection reagent in an all encompassing allergen-specific IgE ELISA remains to be determined, it is logical to assume that its performance in detecting allergen-specific IgE in dog sera will parallel and exceed the performance characteristic of the human FcεRIα currently being used [27]. In essence, the FcεRIα behaves as a single epitope detecting tracer molecule. In this regard, its detection capability is akin to that of the Fab portion of monoclonal antibodies and as such might represent a good adjunct to currently available monoclonal cocktail based ELISA for allergen-specific IgE in dogs [17]. In fact, admixture of canine high affinity FcεRIα with high affinity canine IgE-specific monoclonal antibodies will likely yield an assay with increased sensitivity while maintaining specificity [7]. Continued development and characterization of such a detection system will undoubtedly result in the next generation of canine allergen-specific IgE detection ELISA and immunoblotting detection reagents.

ACKNOWLEDGMENTS. This work was partially supported by a Grant-in-Aid for scientific research from the Ministry of Health, Labor and Welfare of Japan and the Promotion and Mutual Aid Corporation for Private Schools of Japan, Grant-in-Aid for Matching Fund Subsidy for Private University.

REFERENCES

1. Abramson, J. and Pecht, I. 2007. Regulation of the mast cell response to the type I Fcε receptor. *Immunol. Rev.* **217**: 231–254. |Medline| |CrossRef|
2. Bensignor, E. and Carlotti, D. N. 2002. Sensitivity patterns to house dust mites and forage mites in atopic dogs: 150 cases. *Vet. Dermatol.* **13**: 37–42. |Medline| |CrossRef|
3. Blank, U., Ra, C. S. and Kinet, J. P. 1991. Characterization of truncated alpha chain products from human, rat, and mouse high affinity receptor for immunoglobulin E. *J. Biol. Chem.* **266**: 2639–2646. |Medline|
4. DeBoer, D. J. 1989. Survey of intradermal skin testing practices

in North America. *J. Am. Vet. Med. Assoc.* **195**: 1357–1363. [Medline]
5. DeBoer, D. J. and Hillier, A. 2001. The ACVD task force on canine atopic dermatitis (XV): fundamental concepts in clinical diagnosis. *Vet. Immunol. Immunopathol.* **81**: 271–276. [Medline] [CrossRef]
6. Foster, A. P., Littlewood, J. D., Webb, P., Wood, J. L., Rogers, K. and Shaw, S. E. 2003. Comparison of intradermal and serum testing for allergen-specific IgE using a Fcepsilon RIalpha-based assay in atopic dogs in the UK. *Vet. Immunol. Immunopathol.* **93**: 51–60. [Medline] [CrossRef]
7. Garcia-Gallo, M., Martin, L., Llorente, M., Kremer, L., Mas, A. and Alvarez, J. 2011. Production of an oligoclonal antibody to assay specific canine IgE. *Vet. Dermatol.* **22**: 468.
8. Goitsuka, R., Hayashi, N., Nagase, M., Sasaki, N., Ra, C., Tsujimoto, H. and Hasegawa, A. 1999. Molecular cloning of cDNAs encoding dog high-affinity IgE receptor alpha, beta, and gamma chains. *Immunogenetics* **49**: 580–582. [Medline] [CrossRef]
9. Griot-Wenk, M. E., Marti, E., DeBoer, D. J., de Weck, A. L. and Lazary, S. 1999. Domain mapping and comparative binding features of eight dog IgE-specific reagents in ELISA, immunoblots, and immunohistochemistry. *Vet. Immunol. Immunopathol.* **70**: 117–124. [Medline] [CrossRef]
10. Hakimi, J., Seals, C., Kondas, J. A., Pettine, L., Danho, W. and Kochan, J. 1990. The alpha subunit of the human IgE receptor (FcεRIα) is sufficient for high affinity IgE binding. *J. Biol. Chem.* **265**: 22079–22081. [Medline]
11. Halliwell, R. E. 1971. Atopic disease in the dog. *Vet. Rec.* **89**: 209–214. [Medline] [CrossRef]
12. Halliwell, R. E. and Longino, S. J. 1985. IgE and IgG antibodies to flea antigen in differing dog populations. *Vet. Immunol. Immunopathol.* **8**: 215–223. [Medline] [CrossRef]
13. Halliwell, R. E. and DeBoer, D. J. 2001. The ACVD task force on canine atopic dermatitis (III): the role of antibodies in canine atopic dermatitis. *Vet. Immunol. Immunopathol.* **81**: 159–167. [Medline] [CrossRef]
14. Hamilton, R. G. 2009. Laboratory tests for allergic and immunodeficiency diseases: principles and interpretations. pp.1247–1266. *In*: Allergy, 7th ed. (Adkinson, N.F., Holgate, S.T., Bochner, B., Lemanske, R.F., Busse, W.W. and Simons, F.E. eds.), Elsevier, Philadelphia.
15. Jeffers, J. G., Shanley, K. J. and Meyer, E. K. 1991. Diagnostic testing of dogs for food hypersensitivity. *J. Am. Vet. Med. Assoc.* **198**: 245–250. [Medline]
16. Kleinbeck, M. L., Hites, M. J., Loker, J. L., Halliwell, R. E. L. and Lee, K. W. 1989. Enzyme-linked immunosorbent assay for measurement of allergen-specific IgE antibodies in canine serum. *Am. J. Vet. Res.* **50**: 1831–1839. [Medline]
17. Lee, K. W., Blankenship, K. D., McCurry, Z. M., Esch, R. E., DeBoer, D. J. and Marsella, R. 2009. Performance characteristics of a monoclonal antibody cocktail based ELISA for detection of allergen specific IgE in dogs and comparison with a high affinity IgE receptor based ELISA. *Vet. Dermatol.* **20**: 157–164. [Medline] [CrossRef]
18. Masuda, K., Tsujimoto, H., Fujiwara, S., Kurata, K., Hasegawa, A., Yasueda, H., Yamashita, K., DeBoer, D. J., de Weck, A. L. and Sakaguchi, M. 1999. IgE sensitivity and cross-reactivity to crude and purified mite allergens (Der f 1, Der f 2, Der p 1, Der p 2) in atopic dogs sensitive to *Dermatophagoides* mite allergens. *Vet. Immunol. Immunopathol.* **72**: 303–313. [Medline] [CrossRef]
19. Masuda, K., Sakaguchi, M., Fujiwara, S., Kurata, K., Yamashita, K., Odagiri, T., Nakao, Y., Matsuki, N., Ono, K., Watari, T., Hasegawa, A. and Tsujimoto, H. 2000. Positive reactions to common allergens in 42 atopic dogs in Japan. *Vet. Immunol. Immunopathol.* **73**: 193–204. [Medline] [CrossRef]
20. Mueller, R. S., Burrows, A. and Tsohalis, J. 1999. Comparison of intradermal testing and serum testing for allergen-specific IgE using monoclonal IgE antibodies in 84 atopic dogs. *Aust. Vet. J.* **77**: 290–294. [Medline] [CrossRef]
21. Nerurkar, L. S., Namba, M., Brashears, G., Jacob, A. J., Lee, Y. J. and Sever, J. L. 1984. Rapid detection of herpes simplex virus in clinical specimens by use of a capture biotin-streptavidin enzyme-linked immunosorbent assay. *J. Clin. Microbiol.* **20**: 109–114. [Medline]
22. Olivry, T. 2010. New diagnostic criteria for canine atopic dermatitis. *Vet. Dermatol.* **21**: 124–127. [Medline] [CrossRef]
23. Peng, Z., Simons, F. E. and Becker, A. B. 1993. Measurement of ragweed-specific IgE in canine serum by use of enzyme-linked immunosorbent assays, containing polyclonal and monoclonal antibodies. *Am. J. Vet. Res.* **54**: 239–243. [Medline]
24. Prouvost-Danon, A., Abadie, A. and da Ponte, J. V. 1980. Heat inactivation of rat and mouse IgE. *Mol. Immunol.* **17**: 247–253. [Medline] [CrossRef]
25. Rojas, M., Donahue, J. P., Tan, Z. and Lin, Y. Z. 1998. Genetic engineering of proteins with cell membrane permeability. *Nat. Biotechnol.* **16**: 370–375. [Medline] [CrossRef]
26. Sakaguchi, M., Nakano, T., Tsujimoto, H., Sasaki, Y., DeBoerd, D. J. and Inouye, S. 1997. Specificity of an enzyme-linked immunosorbent assay for dog IgE antibody to Japanese cedar (*Cryptomeria japonica*) pollen. *Allergol. Int.* **46**: 207–212. [CrossRef]
27. Stedman, K., Lee, K., Hunter, S., Rivoire, B., McCall, C. and Wassom, D. 2001. Measurement of canine IgE using the alpha chain of the human high affinity IgE receptor. *Vet. Immunol. Immunopathol.* **78**: 349–355. [Medline] [CrossRef]
28. Takai, T., Okumura, K. and Ra, C. 2001. Direct expression of the extracellular portion of human FcεRIε chain as inclusion bodies in *Escherichia coli*. *Biosci. Biotechnol. Biochem.* **65**: 79–85. [Medline] [CrossRef]
29. Willemse, T. 1986. Atopic skin disease: a review and a reconsideration of diagnostic criteria. *J. Small Anim. Pract.* **27**: 771–778. [CrossRef]
30. Yagi, S., Yanagida, M., Tanida, I., Hasegawa, A., Okumura, K. and Ra, C. 1994. High-level expression of the truncated alpha chain of human high-affinity receptor for IgE as a soluble form by baculovirus-infected insect cells. Biochemical characterization of the recombinant product. *Eur. J. Biochem.* **220**: 593–598. [Medline] [CrossRef]

Comparative Immunology, Microbiology and Infectious Diseases 34 (2011) 157–161

Contents lists available at ScienceDirect

Comparative Immunology, Microbiology and Infectious Diseases

journal homepage: www.elsevier.com/locate/cimid

Induction of Th1 immune responses to Japanese cedar pollen allergen (Cry j 1) in mice immunized with Cry j 1 conjugated with CpG oligodeoxynucleotide

Y. Kaburaki[a], T. Fujimura[b], K. Kurata[c], K. Masuda[d], M. Toda[e], H. Yasueda[f], K. Chida[a], S. Kawarai[g], M. Sakaguchi[g,*]

[a] Department of Animal Resource Sciences, Graduate School of Agricultural and Life Sciences, The University of Tokyo, Yayoi 1-1-1, Bunkyo-ku, Tokyo 113-8657, Japan
[b] Department of Otolaryngology, Head and Neck Surgery, Graduate School of Medicine, Chiba University, 1-8-1 Inohana, Chuo-ku, Chiba 260-8670, Japan
[c] Institute of Tokyo Environmental Allergy, 2-2-4 Yushima, Bunkyo-ku, Tokyo 113-0034, Japan
[d] Animal Allergy Clinical Laboratories, 5-4-21 Nishihashimoto, Sagamihara, Kanagawa 229-1131, Japan
[e] Experimental Allergology, Paul-Ehrlich-Institut, Paul-Ehrlich-Street 59, Langen 63225, Germany
[f] Clinical Research Center for Allergy and Rheumatology, National Sagamihara Hospital, 18-1 Sakuradai, Sagamihara, Kanagawa 228-8522, Japan
[g] Department of Veterinary Microbiology, School of Veterinary Medicine, Azabu University, 1-17-71 Fuchinobe, Sagamihara, Kanagawa 229-8501, Japan

ARTICLE INFO

Article history:
Received 22 April 2010
Accepted 22 June 2010

Keywords:
Allergens
CpG
Pollen
IgE

ABSTRACT

We determined whether a major Japanese cedar pollen allergen (Cry j 1) conjugated with CpG oligodeoxynucleotide would enhance allergen-specific Th1 responses in mice. Cry j 1 conjugated with CpG (Cry j 1–CpG) induced IL-12 in the spleen cells of naïve mice. Cry j 1–CpG immunization of BALB/c mice suppressed anti-Cry j 1 IgE response and enhanced anti-Cry j 1 IgG_{2a} to subsequent Cry j 1 and alum adjuvant injection. $CD4^+$T cells isolated from the spleens in mice immunized with Cry j 1–CpG produced higher IFN-γ levels than did $CD4^+$T cells obtained from mice as negative controls. Our results suggested that Cry j 1–CpG immunization can induce Cry j 1-specific Th1 immune responses, thereby inhibiting IgE response to the pollen allergen.

1. Introduction

Japanese cedar (*Cryptomeria japonica*; CJ) pollinosis is a typical type I allergy induced by CJ pollen and one of the most common allergic diseases in Japan. In areas where there are CJ trees, approximately 10% of the population suffers from CJ pollinosis [1]. Two major allergens, Cry j 1 [2] and Cry j 2 [3] have been isolated from CJ pollen. More than 90% of 145 CJ pollinosis patients had specific IgE antibodies to both Cry j 1 and Cry j 2 allergens: the remainder had specific IgE to either one or the other [4]. The patients with CJ pollinosis had high levels of T-cell reactivity to Cry j 1 and Cry j 2 [5]. Recently, we isolated Cry j 3, which may play crucial roles in the cross-reactivity with oral allergy syndrome [6].

Bacterial DNA and synthetic oligodeoxynucleotides containing CpG are potent adjuvants of Th1 responses characterized by production of IFN-γ and IgG_{2a} [7–9]. Tokunaga and his colleagues had found that DNA extracted from *Mycobacterium bovis* activated NK cells to induce interferon and anti-tumor activities [10,11]. Several short DNA sequences containing CpG motif were determined by the sequencing of mycobacterium DNA.

The administration of allergen conjugated to CpG is an attractive approach to the prevention and treatment of allergic diseases [9]. In a clinical study, ragweed pollen allergen (Amb a 1) conjugated with CpG vaccine showed clinical efficacy in the treatment of ragweed allergic rhinitis

* Corresponding author. Tel.: +81 42 850 2481; fax: +81 42 850 2481.
E-mail address: sakagum@azabu-u.ac.jp (M. Sakaguchi).

0147-9571/$ – see front matter © 2010 Elsevier Ltd. All rights reserved.
doi:10.1016/j.cimid.2010.06.005

[12]. Moreover, allergens conjugated with CpG reduced the binding activity of specific IgE to native allergens and also reduced allergenesis of the allergens [9,13]. Recently, it was reported that Cry j 2 T-cell epitope peptides conjugated to CpG vaccine have no allergencity [14].

In this study, we investigated whether Cry j 1–CpG immunization suppressed the development of Cry j 1-specific IgE production in mice. Furthermore, we investigated the effect of Cry j 1–CpG on Th1 and Th2 cytokine production in Cry j 1-specific $CD4^+$T cells.

2. Materials and methods

2.1. Mice

Female BALB/c mice (7 weeks old) were obtained from Japan SLC Inc (Shizuoka, Japan). They were housed under specific pathogen-free conditions.

2.2. Antigens

Cry j 1 is a basic glycoprotein isolated from CJ pollen by affinity chromatography using monoclonal antibodies (mAb) specific to Cry j 1 [15,16].

2.3. Conjugation of CpG oligodeoxynucleotides to Cry j 1

The phosphorothioated CpG, consisting of 22 bases containing two CpG motifs 5′-TGACTGTGAACGTTCGAGATGA-3′ (immunostimulatory sequence: ISS 1018) [17,18] was produced by Invitrogen Corp. (Carlsbad, CA, USA). As a negative control, phosphorothioated oligodeoxynucleotide consisting of 22 bases containing the mutated 5′-TGACTGTGAAGGTTAGAGATGA-3′ (mCpG) was used in this study. Each of these CpGs had a molecular mass of approximately 7000. The 5′-phosphorothioate CpG was coupled to amino groups on Cry j 1. Cry j 1 was modified to incorporate thiol moieties by reacting to it with excess of succinimidyl-S-acetyl thiol acetate (Pierce Biotechnology, Rockford, IL, USA), as described previously [19]. Endotoxin levels were measured by Bio-Whittaker, QCL-1000 (Cambrex Bio Science Walkersville, Walkersville, MD, USA). The endotoxin levels of Cry j 1–CpG and Cry j 1–mCpG were <0.03 endotoxin unit/μg.

2.4. In vitro assay for IL-12 p40 assays in the naive spleen cells

Mice were sacrificed by means of anesthesia and their spleens were removed. Spleen cells (2×10^5) were added to wells in a total volume of 100 μL and stimulated with Cry j 1–CpG, CpG, and mCpG. Cultures were incubated for 0, 6, 11, 24, 35, and 48 h at 37 °C in 5% CO_2. Supernatants were harvested after each incubation period and frozen at −30 °C before being analyzed. The levels of IL-12 p40 in the culture supernatant were determined by sandwich ELISA (BD Biosciences, Franklin Lakes, NJ, USA).

2.5. Immunization

Ten BALB/c mice in each group were subcutaneously immunized with Cry j 1 (5 μg)–CpG, Cry j 1 (5 μg)–mCpG, or Cry j 1 (5 μg) in PBS three times weekly. All mice were intraperitoneally immunized with 5 μg of Cry j 1 and 2 mg of aluminum hydroxide (alum)(Pierce, Rockford, IL, USA) mixture at 3 and 6 weeks. Blood samples were collected by tail bleeding at weeks 1, 2, 4, 5, and 7 weeks, and serum samples were stored at −30 °C. Spleens for assays of IFN-γ, IL-4, and IL-5 were collected at 7 weeks.

2.6. Measurement of mouse anti-Cry j 1 IgG1, IgG_{2a}, IgE

IgG_1 and IgG_{2a} antibody responses to Cry j 1 were assayed by ELISA as described previously [20]. The IgE antibody response to Cry j 1 was analyzed by fluorometric ELISA as described previously [20].

2.7. ELISA inhibition with human anti-Cry j 1 IgE

The ability of Cry j 1–CpG to bind human Cry j 1-specific IgE was measured by using fluorometric ELISA inhibition as described previously [21].

2.8. Cytokine assays in $CD4^+$T cells from spleens of immunized mice

$CD4^+$T cells were purified from the spleens of mice by MACS [22]. Purified $CD4^+$T cells (2×10^5) were cultured with irradiated syngenic splenocytes (3×10^5) as antigen-presenting cells in 96-well plates for 3 days in the presence or absence of Cry j 1 (10 μg/ml). The culture supernatant was collected 3 days after cultivation and kept at −30 °C until use. IFN-γ, IL-4, and IL-5 levels were determined by ELISA using anti-IFN-γ mAb, anti-IL-4 mAb, and anti-IL-5 mAb (BD Biosciences) [20].

2.9. Statistics

The Kruskal–Wallis test was applied to compare data among the four groups. If the difference was significant, post hoc analysis using the Mann–Whitney *U*-test with Bonferroni correction in antibody levels and the Turkey–Kramer test in cytokine levels were performed to analyze the difference between the ODN-Cry j 1 group and the other group. Statistical significance was defined as $p < 0.05$.

3. Results

3.1. IL-12 p40 from naïve spleen cells

We investigated whether Cry j 1–CpG induced IL-12 p40 in the spleens of naïve mice. After spleen cells were cultivated for 36 h, significant IL-12 p40 production was observed in the cells stimulated with CpG-Cry j 1 and CpG as compared with mCpG as a negative control (Fig. 1).

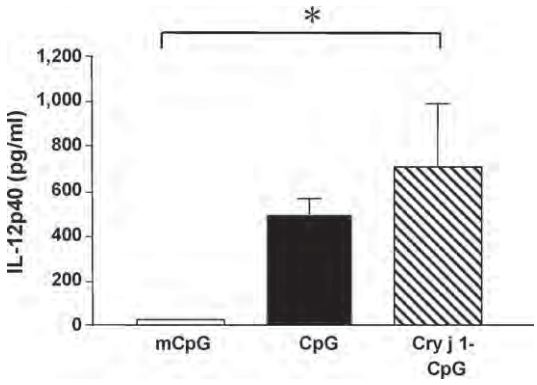

Fig. 1. IL-12 p40 production by Cry j 1–CpG or CpG stimulation in the spleens of naive mice. mCpG (1 μg/ml: 142 pmol), CpG (1 μg/ml: 142 pmol), Cry j 1–CpG (1 μg/ml: 142 pmol). *$p < 0.05$ for Cry j 1–CpG compared with mCpG.

3.2. Human anti-Cry j 1 IgE binding to Cry j 1–CpG

To determine whether the conjugation of CpG to Cry j 1 diminished the ability of Cry j 1 to react with anti-Cry j 1 IgE in pooled serum from patients with CJ pollinosis, the ability of Cry j 1–CpG to bind anti-Cry j 1 IgE was tested by the ELISA inhibition. Cry j 1–CpG reacted less well with anti-Cry j 1 IgE than did Cry j 1. An approximate 50-fold higher concentration of Cry j 1–CpG was necessary to achieve 50% inhibition compared with Cry j 1 (Fig. 2).

3.3. Anti-Cry j 1 IgE in mice immunized with Cry j 1–CpG

We investigated whether initial immunization of Cry j 1–CpG suppressed anti-Cry j 1 IgE development after immunization of Cry j 1 and alum. In groups immunized with Cry j 1 or Cry j 1–mCpG, anti-Cry j 1 IgE production was induced by boosting with Cry j 1 and alum at 4 and 6 weeks. Anti-Cry j 1 IgE production was significantly inhibited in mice immunized with Cry j 1–CpG up to 7 weeks (Fig. 3). Cry j 1–CpG immunization suppressed anti-Cry j 1 IgE production to a secondary immunization of Cry j 1 and alum.

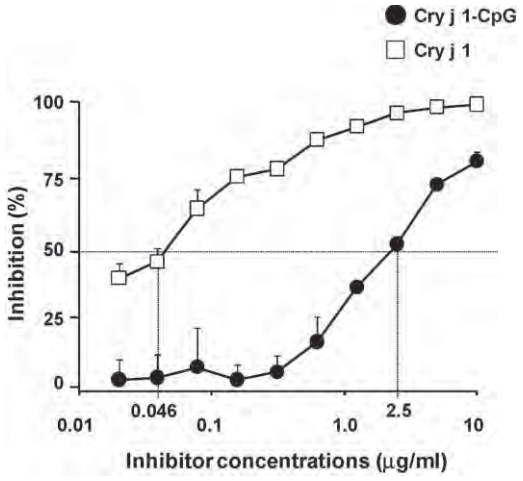

Fig. 2. Inhibition of human anti-Cry j 1 IgE from CJ allergic patients by Cry j 1 or Cry j 1–CpG.

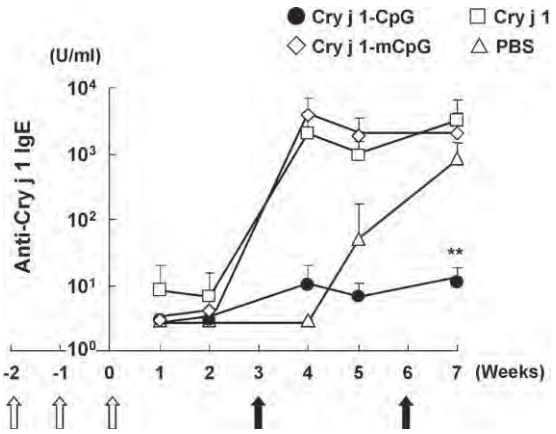

Fig. 3. Inhibition of anti-Cry j 1 IgE production by Cry j 1–CpG inoculation. BALB/c mice were immunized with 5 μg each of Cry j 1, Cry j 1–CpG, Cry j 1–mCpG, or PBS. **$p < 0.01$ for the group immunized with Cry j 1–CpG compared with other groups.

3.4. Anti-Cry j 1 IgG_1 and IgG_{2a} in mice immunized with Cry j 1–CpG

The effects of initial immunization of Cry j 1–CpG on the production of anti-Cry j 1 IgG_1 production were examined. After first immunization of Cry j 1 and alum at 3 weeks, anti-Cry j 1 IgG_1 production in groups immunized with Cry j 1 and Cry j 1–mCpG was enhanced (Fig. 4A). After secondary immunization of Cry j 1 and alum at 7 weeks, anti-Cry j 1 IgG_1 production showed no significant difference among any of the groups.

The effects of initial immunization of Cry j 1–CpG on the production of anti-Cry j 1 IgG_{2a} production were examined. At 1 and 2 weeks, anti-Cry j 1 IgG_{2a} levels showed no differences among any of the groups. After immunization of Cry j 1 and alum at 7 weeks, Cry j 1–CpG immunization developed significantly higher levels of anti-Cry j 1 IgG_{2a} compared with groups immunized with PBS, Cry j 1, or Cry j 1–mCpG ($p < 0.01$) (Fig. 4B).

3.5. Cytokine production in Cry j 1-specific $CD4^+$T cells cultures

The levels of IFN-γ, IL-4, and IL-5 in response to Cry j 1 were measured in $CD4^+$T cells obtained 2 weeks after the second boosting of Cry j 1 in alum. $CD4^+$T cells from mice immunized with Cry j 1–CpG secreted significantly higher levels of IFN-γ than did $CD4^+$T cells obtained from mice immunized with PBS, Cry j 1, or Cry j 1–mCpG ($p < 0.05$) (Fig. 5A).

Cry j 1-specific IL-5 levels in mice immunized with Cry j 1–CpG showed significantly lower than those in mice immunized with Cry j 1–mCpG, but showed no significant differences among other groups (Fig. 5B). Cry j 1-specific IL-4 levels in mice immunized with Cry j 1–CpG showed no significant differences among other groups (Fig. 5C).

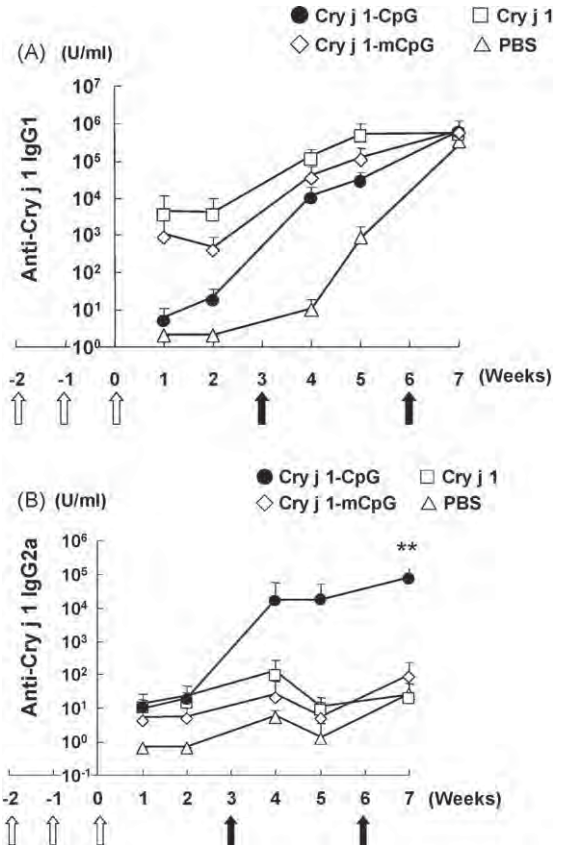

Fig. 4. Anti-Cry j 1 IgG_1 and IG_{2a} production by Cry j 1–CpG inoculation. BALB/c mice immunized with 5 μg each of either Cry j 1, Cry j 1–CpG, Cry j 1–mCpG, or PBS. (A) IgG_1 and (B) IgG_{2a}. $^{**}p < 0.01$ for the group immunized with Cry j 1–CpG compared with other groups.

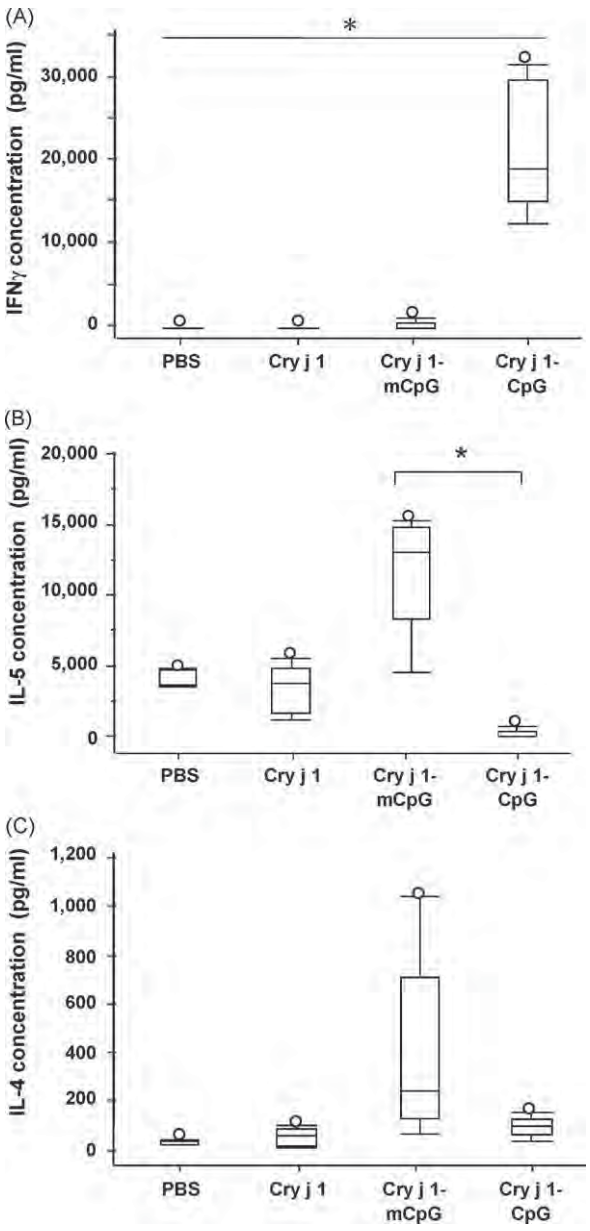

Fig. 5. The effect of Cry j 1–CpG on cytokine production in Cry j 1-specific $CD4^+$T-cell cultures. $CD4^+$T cells from mice immunized with Cry j 1, Cry j 1–CpG, Cry j 1–mCpG, or PBS were stimulated with 10 μg/ml of Cry j 1 for 3 days. (A) IFN-γ, (B) IL-5 and (C) IL-4. $^*p < 0.05$ for the group immunized with Cry j 1–CpG compared with other groups.

4. Discussion

It has been reported that IFN-γ induction is an IgM to IgG2a switch factor, which accounts for the association of IgG_{2a} with a Th1 response [23]. Cry j 1–CpG immunization significantly induced the production of IFN-γ from Cry j 1-specific $CD4^+$T cells. These observations are similar to those from the study of Iho et al. [24]. Those investigators showed that CpG oligodeoxynucleotide containing AACGTT induced the production of IFN-γ and the expansion of antigen-specific human peripheral blood mononuclear cells. In our study, we used CpG oligodeoxynucleotide containing AACGTT. This CpG might be a Th1 cell differentiation inducer and promote IFN-γ production.

In this study, inoculation with Cry j 1–CpG reduced anti-Cry j 1 IgE antibody and enhanced IgG_{2a} responses after immunization with alum-precipitated Cry j 1. Cry j 1–CpG induced the allergen-specific Th1-type immune response, resulting in the inhibition of the IgE response to the allergen. Tight et al. reported that in mice primed for Th2 response, injection with Amb a 1 (a major ragweed allergen)-conjugated CpG suppressed specific Amb a 1 IgE [9]. Also, Suzuki et al. reported that anti-Cry j 2 IgE levels were lower in mice immunized with Cry j 2 T-cell peptide conjugated with CpG [14]. These findings indicated the potential for a CpG-conjugated allergen or T-cell peptide vaccine to serve as a tool for the prevention and treatment of CJ pollinosis.

In the present study, IL-4 levels in mice immunized with Cry j 1–CpG were no different from those in any other immunized mice. IL-5 levels in mice immunized with Cry j 1–CpG showed significantly lower than those in mice immunized with Cry j 1–mCpG, but showed no significant differences among other groups. Similarly, our previous study showed that the inoculation of DNA vaccine encoding the $CD4^+$T-cell epitope in Cry j 2 (a major CJ allergen)

inhibited the allergen-specific IgE response to subsequent allergen and alum injection, but did not inhibit allergen-specific IL-4 and IL-5 production [22]. The alum can induce strong antigen-specific Th2 response and Th2-associated IL-4 production [25,26]. The subsequent allergen and alum injection in the present study might induce too strong Th2 responses to suppress Th2-cytokines in mice.

CpG oligodeoxynucleotide is a potent adjuvant of Th1 response, so it is hoped that it will be useful in the development of immunotherapies for allergic diseases and cancer. Marshall et al. demonstrated that ISS 1018-conjugated Amb a 1 allergen would induce IFN-γ production in peripheral blood mononuclear cells from human patients with ragweed allergy [18]. We used the same single strand synthetic ISS 1018-conjugated Cry j 1. Our data suggested that CpG played a role in switching on Th1 immunity to a protein antigen through the upregulation of IgG2a and IFN-γ. Furthermore, Cry j 1–CpG induced Th1 cell differentiation and suppressed anti-Cry j 1 IgE. This immunization may be useful as an immunotherapy for CJ pollinosis.

Acknowledgments

This work was supported by a Grant-in Aid for Scientific Research from the Ministry of Health, Labor, and Welfare of Japan, by the Promotion and Mutual Aid Corporation for Private Schools of Japan, by a Grant-in-Aid for Matching Fund Subsidy for Private University, and by a project grant awarded by the Azabu University Research Services Division.

References

[1] Okuda M. Epidemiology of Japanese cedar pollinosis throughout Japan. Ann Allergy Asth Immunol 2003;91:288–96.
[2] Yasueda H, Yui Y, Shimizu T, Shida T. Isolation and partial characterization of the major allergen from Japanese cedar (*Cryptomeria japonica*) pollen. J Allergy Clin Immunol 1983;71:77–86.
[3] Sakaguchi M, Inouye S, Taniai M, Ando S, Usui M, Matuhasi T. Identification of the second major allergen of Japanese cedar pollen. Allergy 1990;45:309–12.
[4] Hashimoto M, Nigi H, Sakaguchi M, Inouye S, Imaoka K, Miyazawa H, et al. Sensitivity to two major allergens (Cry j I and Cry j II) in patients with Japanese cedar (*Cryptomeria japonica*) pollinosis. Clin Exp Allergy 1995;25:848–52.
[5] Hirahara K, Tatuta T, Takatori T, Ohtsuki M, Kirinaka H, Kawaguchi J, et al. Preclinical evaluation of an immunotherapeutic peptide comprising 7 T-cell determinants of Cry j 1 and Cry j 2, the major Japanese cedar pollen allergens. J Allergy Clin Immunol 2001;108: 94–100.
[6] Fujimura T, Futamura N, Midoro-Horiuti T, Togawa A, Goldblum RM, Yasueda H, et al. Isolation and characterization of native Cry j 3 from Japanese cedar (*Cryptomeria japonica*) pollen. Allergy 2007;62:547–53.
[7] Sun S, Kishimoto H, Sprent J. DNA as an adjuvant: capacity of insect DNA and synthetic oligodeoxynucleotides to augment T cell responses to specific antigen. J Exp Med 1998;187:1145–50.
[8] Wagner H. Toll meets bacterial CpG-DNA. Immunity 2001;14:499–502.
[9] Tighe H, Takabayashi K, Schwartz D, Van Nest G, Tuck S, Eiden JJ, et al. Conjugation of immunostimulatory DNA to the short ragweed allergen amb a 1 enhances its immunogenicity and reduces its allergenicity. J Allergy Clin Immunol 2000;106:124–34.
[10] Tokunaga T, Yamamoto H, Shimada S, Abe H, Fukuda T, Fujisawa Y, et al. Antitumor activity of deoxyribonucleic acid fraction from *Mycobacterium bovis* BCG. I. Isolation, physicochemical characterization, and antitumor activity. J Natl Cancer Inst 1984;72:955–62.
[11] Yamamoto S, Kuramoto E, Shimada S, Tokunaga T. In vitro augmentation of natural killer cell activity and production of interferon-alpha/beta and -gamma with deoxyribonucleic acid fraction from *Mycobacterium bovis* BCG. Jpn J Cancer Res 1988;79:866–73.
[12] Creticos PS, Schroeder JT, Hamilton RG, Balcer-Whaley SL, Khattignavong AP, Lindblad R, et al. Immunotherapy with a ragweed-toll-like receptor 9 agonist vaccine for allergic rhinitis. New Eng J Med 2006;355:1445–55.
[13] Horner AA, Takabayashi K, Beck L, Sharma B, Zubeldia J, Baird S, et al. Optimized conjugation ratios lead to allergen immunostimulatory oligodeoxynucleotide conjugates with retained immunogenicity and minimal anaphylactogenicity. J Allergy Clin Immunol 2002;110:413–20.
[14] Suzuki M, Ohta N, Min WP, Matsumoto T, Min R, Zhang X, et al. Immunotherapy with CpG DNA conjugated with T-cell epitope peptide of an allergenic Cry j 2 protein is useful for control of allergic condition in mice. Ont Immunopharmacol 2007;7:46–54.
[15] Kawashima T, Taniai M, Taniguchi Y, Usui M, Ando S, Kurimoto M, et al. Antigenic analyses of Sugi basic protein by monoclonal antibodies: I. Distribution and characterization of B-cell-tropic epitopes of Cry j I molecules. Int Arch Allergy Immunol 1992;98:110–7.
[16] Kawashima T, Taniai M, Usui M, Ando S, Kurimoto M, Matuhasi T. Antigenic analyses of Sugi basic protein by monoclonal antibodies: II. Detection of immunoreactive fragments in enzyme-cleaved Cry j I. Int Arch Allergy Immunol 1992;98:118–26.
[17] Roman M, Martin-Orozco E, Goodman JS, Nguyen MD, Sato Y, Ronaghy A, et al. Immunostimulatory DNA sequences function as T helper-1-promoting adjuvants. Nat Med 1997;3:849–54.
[18] Marshall JD, Abtahi S, Eiden JJ, Tuck S, Milley R, Haycock F, et al. Immunostimulatory sequence DNA linked to the Amb a 1 allergen promotes T(H)1 cytokine expression while downregulating T(H)2 cytokine expression in PBMCs from human patients with ragweed allergy. J Allergy Clin Immunol 2001;108:191–7.
[19] Tighe H, Takabayashi K, Schwartz D, Van Nest G, Tuck S, Eiden JJ, et al. Conjugation of protein to immunostimulatory DNA results in a rapid, long-lasting and potent induction of cell-mediated and humoral immunity. Eur J Immunol 2000;30:1939–47.
[20] Toda M, Sato H, Takebe Y, Taniguchi Y, Saito S, Inouye S, et al. Inhibition of immunoglobulin E response to Japanese cedar pollen allergen (Cry j 1) in mice by DNA immunization: different outcomes dependent on the plasmid DNA inoculation method. Immunology 2000;99:179–86.
[21] Sakaguchi M, Toda M, Ebihara T, Irie S, Hori H, Imai A, et al. IgE antibody to fish gelatin (type I collagen) in patients with fish allergy. J Allergy Clin Immunol 2000;106:579–84.
[22] Toda M, Kasai M, Hosokawa H, Nakano N, Taniguchi Y, Inouye S, et al. DNA vaccine using invariant chain gene for delivery of $CD4^+$ T cell epitope peptide derived from Japanese cedar pollen allergen inhibits allergen-specific IgE response. Eur J Immunol 2002;32:1631–9.
[23] Finkelman FD, Katona IM, Mosmann TR, Coffman RL. IFN-γ regulates the isotypes of Ig secreted during in vivo humoral immune responses. J Immunol 1988;140:1022–7.
[24] Iho S, Yamamoto T, Takahashi T, Yamamoto S. Oligodeoxynucleotides containing palindrome sequences with internal 5′-CpG-3′ act directly on human NK and activated T cells to induce IFN-gamma production in vitro. J Immunol 1999;163:3642–52.
[25] Brewer JM, Conacher M, Satoskar A, Bluethmann H, Alexander J. In interleukin-4-deficient mice, alum not only generates T helper 1 responses equivalent to Freund's complete adjuvant, but continues to induce T helper 2 cytokine production. Eur J Immunol 1996;26:2062–6.
[26] Brewer JM, Conacher M, Hunter CA, Mohrs M, Brombacher F, Alexander J. Aluminium hydroxide adjuvant initiates strong antigen-specific Th2 responses in the absence of IL-4- or IL-13-mediated signaling. J Immunol 1999;163:6448–54.

Clinical Immunology (2011) 139, 65–74

available at www.sciencedirect.com

Clinical Immunology

www.elsevier.com/locate/yclim

Increase of regulatory T cells and the ratio of specific IgE to total IgE are candidates for response monitoring or prognostic biomarkers in 2-year sublingual immunotherapy (SLIT) for Japanese cedar pollinosis

Takashi Fujimura[a,1], Syuji Yonekura[a], Shigetoshi Horiguchi[a], Yuriko Taniguchi[b], Akemi Saito[c], Hiroshi Yasueda[c], Ayako Inamine[a], Toshinori Nakayama[b], Toshitada Takemori[d], Masaru Taniguchi[d], Masahiro Sakaguchi[e], Yoshitaka Okamoto[a,*]

[a] Department of Otolaryngology, Head and Neck Surgery, Graduate School of Medicine, Chiba University, Chiba, Japan
[b] Department of Immunology, Graduate School of Medicine, Chiba University, Chiba, Japan
[c] Clinical Research Center for Allergy and Rheumatology, Sagamihara National Hospital, Kanagawa, Japan
[d] Research Center for Allergy and Immunology, Yokohama Institute, RIKEN (The Institute of Physical and Chemical Research), Kanagawa, Japan
[e] Department of Veterinary Microbiology, School of Veterinary Medicine, Azabu University, Kanagawa, Japan

Received 24 September 2010; accepted with revision 31 December 2010

KEYWORDS
Allergic rhinitis;
Biomarker;
Immunotherapy;
Japanese cedar pollinosis;
Regulatory T cell;
Sublingual immunotherapy

Abstract The aims of this study were to examine the therapeutic effects of sublingual immunotherapy (SLIT) and to identify potential biomarkers that would predict the therapeutic response in a randomized, double-blind, placebo-controlled clinical trial. The trial was carried out over two pollinosis seasons in 2007 and 2008. Carry-over therapeutic effects were analyzed in 2009. SLIT significantly ameliorated the symptoms of pollinosis during the 2008 and 2009 pollen seasons. Cry j 1-specific cytokine production in a subgroup of patients with mild disease in the SLIT group was significantly attenuated. The ratio of specific IgE to total IgE before treatment correlated with the symptom-medication score in the SLIT group in 2008. Patients with increased

Abbreviations: DBPC, double-blind, placebo-controlled; ELISA, enzyme-linked immunosorbent assay; ELISPOT, enzyme-linked immunospot assay; iTreg, induced regulatory T cells; ITT analysis, intention-to-treat analysis; JAU, Japanese allergy unit; N.S., not significant; OT analysis, on-treatment analysis; PBMCs, peripheral blood mononuclear cells; RAST, radioallergosorbent test; SLIT, sublingual immunotherapy; SMS, symptom-medication score; Treg, regulatory T cells; QOL, quality-of-life.

* Corresponding author. Department of Otolaryngology, Head and Neck Surgery, Graduate School of Medicine, Chiba University, 1-8-1, Inohara, Chuo-ku, Chiba 260-8670, Japan. Fax: +81 43 227 3442.
E-mail address: yokamoto@faculty.chiba-u.jp (Y. Okamoto).
[1] Present address: Research Center for Allergy and Immunology, Yokohama Institute, RIKEN (The Institute of Physical and Chemical Research), Kanagawa, Japan.

1521-6616/$ - see front matter
doi:10.1016/j.clim.2010.12.022

Cry j 1-iTreg in the SLIT group had significantly improved QOL and QOL-symptom scores. In summary, the specific IgE to total IgE ratio and upregulation of Cry j 1-iTreg are candidates for biomarker of the clinical response to SLIT.

1. Introduction

Japanese cedar (*Cryptomeria japonica*) pollinosis is a common allergy in Japan, with a prevalence estimated to be 26.5% in a nationwide survey conducted in 2008 [1].

A 2000 Japanese allergy unit (JAU) sample of standardized extract from Japanese cedar pollen is the only available allergen for subcutaneous and sublingual immunotherapy (SLIT) against pollinosis in Japan. The 2000 JAU extract contains 1.5 to 4.2 μg of the major allergen, Cry j 1 [2]. The common monthly cumulative dose for SLIT is 8000 JAU, which contains approximately 10 μg of Cry j 1. This maintenance dose is 200-fold higher than that used in traditional subcutaneous immunotherapy using 0.2 ml of a 200 JAU/ml extract, which contains approximately 50 ng of Cry j 1. Despite using a low dose of the major allergen compared with that in European trials, positive effects on pollinosis have been shown in randomized double-blind, placebo-controlled (DBPC) studies, in which SLIT significantly ameliorated the symptom score, symptom-medication score (SMS), and quality-of-life (QOL) score [3,4].

SLIT induces Cry j 1-specific IgG4 production and attenuates the seasonal increase in the number of Th2 cells specific to epitopes from Cry j 1 and Cry j 2 [3]. Involvement of antigen-specific Tr1 cells or regulatory T cells (Treg) in the therapeutic mechanism has also been suggested [5,6]. We previously found that SLIT increased the levels of Cry j 1-specific induced Treg cells (Cry j 1-iTreg; $IL10^+Foxp3^+$ cells in $CD25^+CD4^+$ leukocytes) and that the increase in Cry j 1-iTreg after the pollen season may serve as a response monitoring biomarker that correlates with a positive therapeutic effect based on the QOL-symptom score and distinguishes responders from non-responders after SLIT [6].

In this report, we examined the reproducibility of the positive therapeutic effects and safety of SLIT and upregulation of iTregs as a response monitoring biomarker, with the goal of confirming our previous results in a larger randomized DBPC study. Therefore, the safety and clinical effect of SLIT for Japanese cedar pollinosis were used as the primary endpoint, and carry-over effects, immunological changes, and biomarkers for a positive clinical effect induced by SLIT were secondary endpoints.

2. Materials and methods

2.1. Study population

The study was conducted as a randomized, DBPC, parallel-group, single center trial in subjects with Japanese cedar pollinosis. This study was performed for two pollen seasons between September 2006 and May 2008, with follow-up in the pollen season in 2009. We recruited 130 participants in September 2006. Diagnosis of Japanese cedar pollinosis was based on clinical history and the presence of IgE specific to Japanese cedar pollen of at least class 2 (CAP-RAST method, Phadia, Tokyo, Japan). Participants with a history of immunotherapy or a diagnosis of asthma, or those who were pregnant, were excluded from the study. Patients who suffered seasonal or chronic rhinitis that required medical treatment were also excluded.

A total of 103 patients were eligible for the study, and all had moderate or severe symptoms in the previous pollen season [7]. We anticipated that some participants in the SLIT group would drop out from the study due to side effects and we planned to evaluate the risk of mild or severe side effects due to the vaccination. Therefore, we randomly divided the patients into treatment (SLIT) and placebo groups with a ratio of 6:4 according to the table of random numbers prepared by the Department of Pharmacy at Chiba University Hospital (Fig. 1). The sample size was determined based on a previous study [3]. Briefly, we planned to have 50 patients in each group with anticipation of dropout. We set 1.0 as a magnitude for the difference of average SMS between that from the SLIT and placebo groups and 1.5 as a standard deviation according to the result of previous study. Therefore, when the power was set to 0.8 and the α-error to 0.05, the number of required cases was 35 in each group. A person who was not directly involved in the study was responsible for group allocation. To prevent leakage of information, the allocation table was kept by this person and a member of the ethics committee who was also not directly involved in the study, until accessed with the key after completion of the study. The protocol was approved by the Ethics Committee of Chiba University, and written informed consent was obtained from each patient prior to participation in the study.

2.2. Clinical protocols

The SLIT group included 58 patients who received standardized Japanese cedar pollen extract (Torii Pharmaceutical Co. Ltd., Tokyo, Japan) [8], and the placebo group included 45 patients who received an inactive placebo. The protocol consisted of treatment with graded courses of the extract in 50% glycerol, followed by maintenance therapy [6]. Briefly, the extract was graded in three strengths: 20, 200, and 2000 JAU/ml. Patients received increasing doses with each vial, beginning with 0.2 ml from the 20 JAU/ml vial and increasing by 0.2 ml a day for 5 days per week. The vaccine was taken sublingually, kept in place for 2 min without a retention reagent, and then spit out. The procedure was repeated until the maximum dose (1.0 ml of 2000 JAU/ml) was reached. The maintenance dose was 1.0 ml of 2000 JAU/ml given once a week until the end of May 2008. The patients in the placebo group received inactive 50% glycerol in saline. All participants were allowed to take symptom-reducing drugs as needed.

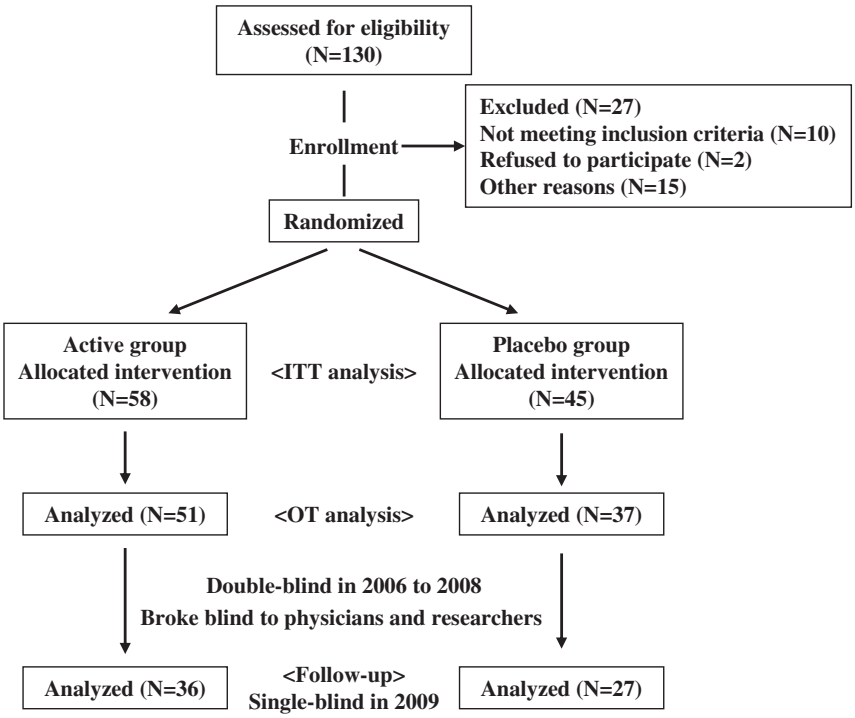

Figure 1 Flow diagram for groups and individuals in the phases of the randomized trial. Fifteen participants from the SLIT ($N=7$) and placebo ($N=8$) groups were lost to follow-up due to reasons such as moving house and transfer. The double-blind status was maintained until completion of analysis of all clinical and immunological parameters (December 2008). Follow-up analysis in 2009 was undertaken in a single-blind manner.

2.3. Clinical symptoms and safety measurements

The patients completed a pollinosis diary to record their nasal symptoms and use of symptom-reducing drugs in the 2007, 2008, and 2009 pollen seasons. The total amounts of pollen scattered from Japanese cedar and Japanese cypress (*Chamaecyparis obtusa*) in Chiba prefecture were 2777, 6596, and 5486 grains/cm^2 during the 2007, 2008, and 2009 pollen seasons, respectively, based on measurements with a Durham pollen sampler. The duration and amount of scattered Japanese cedar pollen differed greatly among these years, but the daily amount of scattered pollen typically followed a wide-based bell-shaped curve over the whole pollen season from the middle of January or early February to the middle or end of May. The duration of the peak pollen season was relatively constant in the 3 years, and therefore, we analyzed the SMS during the peak period. The peak pollen season was defined as the period from the first day that the pollen count was $\geq$20 grains/cm^2/day for 3 consecutive days until the last day that the pollen count was $\geq$20 grains/cm^2/day before a period in which the pollen count was $<$20 grains/cm^2/day for 7 consecutive days.

The daily SMS was calculated as described previously [3]. Briefly, daily episodes of sneezing and nose blowing were rated as 0–4: none, 0; 1–5 episodes, 1; 6–10 episodes, 2; 11–20 episodes, 3; $>$20 episodes, 4. Daily medication was recorded based on drug types and duration of usage using the following guidelines: antihistamines, mast cell stabilizers, and vasoconstrictors, 1; topical ocular or nasal steroids, 2. Patients with an average daily SMS in the peak pollen season of $\leq$4 were judged to have mild symptoms based on guidelines for allergic rhinitis [7].

In the middle of the 2007 and 2008 pollen seasons, the participants completed the Japanese Allergic Rhinitis QOL Standard Questionnaire No.1 (JRQLQ No.1) for assessment of QOL-symptom and total QOL scores [9]. These scores were calculated as previously described [4,6]. The total QOL-symptom score was calculated as the sum of each component score: none, 0; mild, 1; moderate, 2; severe, 3; and very severe, 4. Nasal and ocular symptoms covered by the questionnaire included runny nose, sneezing, nasal congestion, itchy nose, itchy eyes, and watery eyes. Adverse events were graded using Common Terminology Criteria for Adverse Events (CTCAE) v.3.0 [10]. Briefly, adverse events were graded as mild, grade 1; moderate, grade 2; severe, grade 3; life threatening, grade 4; death, grade 5 according to a category for allergy/immunology in the CTCAE v.3.0 scoring system.

2.4. Blood samples

Peripheral blood was obtained from each patient before treatment (September to October 2006) and before and after the pollen seasons in 2007 (December 2006 to January 2007, and May to June 2007, respectively) and 2008 (November to December 2007, and May 2008, respectively). Peripheral blood mononuclear cells (PBMCs) were isolated, frozen, and stored in liquid nitrogen [6]. However, the PBMCs isolated before treatment, and before and after the 2007 pollen season were damaged during storage and we were unable to

analyze their immunological responses. Therefore, immunological data were obtained only from PBMCs collected before and after the 2008 pollen season.

2.5. Total and antigen-specific immunoglobulin titer

The Cry j 1-specific IgE and IgG4 titers in plasma were measured by ELISA [3,11]. Total IgE and specific IgE titers for Japanese cedar, orchard grass, mugwort, and house dust mites were evaluated by the CAP-RAST method (Phadia).

2.6. Flow cytometric analysis

The levels of Cry j 1-iTreg were analyzed by flow cytometry [6]. Briefly, PBMCs were cultured with or without Cry j 1 for 3 days, followed by a culture with 10 ng/ml phorbol 12-myristate 13-acetate, 1 μM ionomycin, and 2 μM monensin for 6 h. The PBMCs were stained with PE-Cy7-anti-CD4 antibody, APC-anti-IL10 antibody (BD Biosciences, San Diego, CA, USA), PE-anti-CD25, and FITC-anti-Foxp3 (clone: PCH101) using a Foxp3 staining buffer set (eBioscience, San Diego, CA, USA).

2.7. Analysis of the number of IL4-producing cells and the concentration of cytokines

The number of IL4-producing cells stimulated with Cry j 1 was determined by enzyme-linked immunospot (ELISPOT) assay, and the concentrations of IL2, IL5, and IL13 in the culture supernatant were measured using a BD™ Cytometric bead assay (CBA) Flex system (BD Biosciences) [6]. Briefly, a 96-well sterile filter plate (Millipore, Billerica, MA, USA) was coated with monoclonal antibody to human IL4 (Mabtech AB, Nacka Strand, Sweden). The plate was pre-incubated with AIM-V medium at 37 °C for 1 h. The medium was discarded, and then PBMCs (3×10^5 cells/well) were cultured with fresh medium alone or with 10 μg/ml Cry j 1 for 17 h at 37 °C in AIM-V medium containing 5% human AB serum (Sigma-Aldrich, St. Louis, MO, USA). The plates were then incubated with a biotinylated monoclonal antibody to human IL4 for 2 h, and then with streptavidin-conjugated alkaline phosphatase for 1 h at room temperature. After washing with PBS, the plates were incubated with BCIP/NBT^{PLUS} (Mabtech) for 5 min at 37 °C. For the CBA, isolated PBMCs were cultured at 2.5×10^6 cells/ml with or without 5 μg/ml Cry j 1 for 3 days at 37 °C in AIM-V medium containing 5% human AB serum (Sigma-Aldrich). After centrifugation at 300×*g* for 10 min, the supernatant was divided into aliquots and stored at −20 °C until the cytokine assay was performed.

2.8. Data representation

The full analysis set ($N=103$) was used for the intention-to-treat (ITT) analysis and per protocol populations ($N=88$) were used for on-treatment (OT) analysis (Fig. 1). Cry j 1-specific cytokine production is shown as the difference between cells stimulated with Cry j 1 and controls stimulated with medium only. Changes after the 2008 pollen season are shown as differences between pre- and post-pollen season values.

2.9. Statistical analysis

Two-group comparisons were performed using a Wilcoxon *t*-test or Mann–Whitney *U*-test to determine the significance of differences, or using an unpaired *t*-test as indicated. *P*-values <0.05 were considered to be significant.

3. Results

3.1. Clinical effects and adverse events

A total of 103 patients were included in the overall analysis of efficacy for the 2007 and 2008 pollen seasons. These patients were randomly divided into the SLIT ($N=58$) and placebo ($N=45$) groups at a ratio of 6:4. Diaries and QOL questionnaires for 88 patients were available at the end of the DBPC study. The overall randomized population was considered to be the ITT population. The SMS in the SLIT group did not differ significantly from that in the placebo group in ITT analysis after 2-year SLIT (*P*=N.S.; Student *t*-test, data not shown).

The final sample size included 88 subjects for OT analysis (SLIT; $N=51$, placebo; $N=37$, ratio 4:3). The demographic characteristics of the OT population before treatment are shown in Table 1. The SMS in the SLIT group did not differ significantly from that in the placebo group in the 2007 peak pollen season (February 19 to March 31, *P*=N.S.; Student *t*-test). However, the average SMS in the 2008 peak pollen season (February 29 to April 1) was significantly ameliorated in the SLIT group compared with the placebo group (4.2 vs. 5.3, $P=0.02$; Student *t*-test). The percentages of subjects with mild symptoms (SMS ≤ 4) were 55% and 28% in the SLIT and placebo groups, respectively, in the peak pollen

Table 1 Clinical data of participants at the start of the study.

Group	SLIT	Placebo	*P*-value
Number	51	37	
Sex (M/F)	17/34	8/29	N.S.[a]
Mean age	44.4	42.3	N.S.[b]
Range	16–73	19–70	
Total IgE [IU/ml]	198	258	N.S.[b]
Range	6.8–1480	8.6–2090	
Specific IgE[c]	27	29	N.S.[b]
Range	0.8–100	1.5–100	
Class [mean]	3.5	3.8	N.S.[b]
Range	2–6	2–6	
Other allergies[d] (%)			
Orchard grass	16 (31%)	11 (30%)	N.S.[e]
Mugwort	5 (10%)	3 (8%)	<0.05[f]
House dust mite	24 (47%)	13 (35%)	N.S.[e]

[a] Yates2×2 Chi-squared test.
[b] Student *t*-test.
[c] Specific IgE to Japanese cedar pollen; CAP-RAST raw value [kAU/L], mean.
[d] Number of subjects with specific IgE of at least CAP-RAST class 2.
[e] 2×2 Chi-squared test.
[f] Fisher exact probability.

season (Fig. 2A). QOL-symptom and total QOL scores were also significantly ameliorated in the SLIT group compared to those in the placebo group in the middle of the 2008 pollen season (Fig. 2B).

There were no severe adverse events that required a patient to withdraw from the study; however, some subjects reported adverse events of mild discomfort: six of grade 2 (oral pruritus: 2; gingivostomatitis: 2; asthma: 1; rash in nasal cavity: 1) in the SLIT group (6/51; 11.8%); and one of grade 1 (bitter taste) in the placebo group (1/37; 2.7%).

3.2. Immunoglobulin production

There were no significant differences in Cry j 1-specific IgE and IgG4 production between patients in the SLIT and placebo groups before treatment, or before and after the pollen seasons. The SLIT group was divided into subgroups based on the SMS in the 2008 peak pollen season: a mild subgroup with SMS ≤ 4 (classified as responders; $N=28$) and a severe subgroup with SMS >4 (non-responders; $N=23$). IgE and IgG4 production in patients in the mild subgroup were both similar to those in patients in the severe subgroup and in the placebo group at various time points (data not shown).

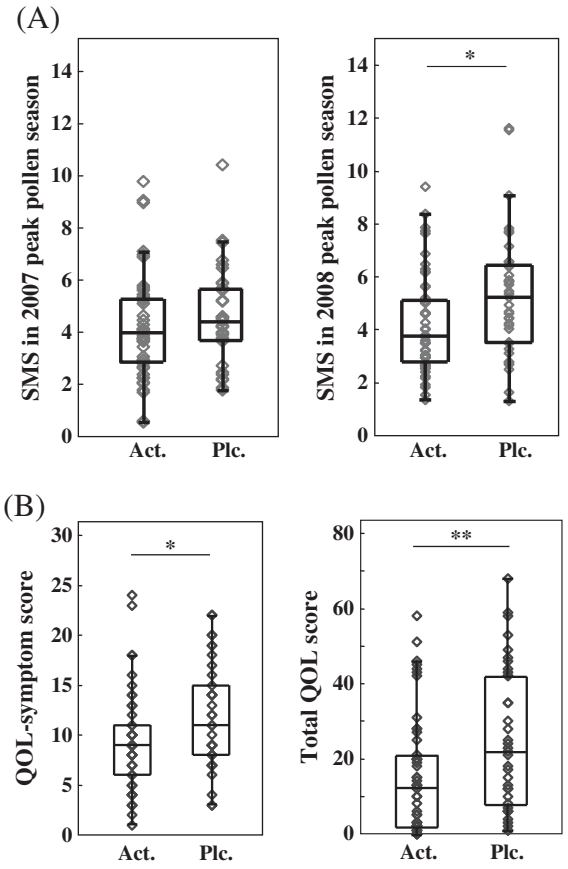

Figure 2 Clinical scores after 2-year SLIT. (A) Average daily symptom-medication scores (SMS) in the SLIT (Act.; $N=51$) and placebo (Plc.; $N=37$) groups in the 2007 and 2008 peak pollen seasons. (B) QOL-symptom and total QOL scores from the QOL questionnaire were plotted for the SLIT (Act.; $N=51$) and placebo (Plc.; $N=37$) groups in the middle of the 2008 pollen season. Each diamond shows a value for an individual. Two-group comparisons were performed using an unpaired Student t-test. *$P<0.05$, **$P<0.01$.

3.3. Cry j 1-specific cytokine production

IL2, IL5, and IL13 levels were analyzed in the culture supernatant. The number of IL4-producing cells was measured by ELISPOT because IL4 was undetectable in the supernatant. There were no significant differences between the SLIT and placebo groups in the production of each cytokine following stimulation with Cry j 1 (Fig. 3A). IL5 was significantly increased after the pollen season in all groups ($P<0.05$; Wilcoxon t-test), and the IL2 and IL13 levels and the number of IL4-producing cells were significantly increased after the pollen season in the SLIT and placebo groups and in the severe subgroup ($P<0.05$; Wilcoxon t-test). Patients in the mild subgroup (responder to SLIT) did not show significant increase of IL2 and IL13 or of IL4-producing cells after the pollen season (P=N.S.; Wilcoxon t-test). The increases in the number of IL4-producing cells and IL5 level after the pollen season in the mild subgroup were significantly less than those in the severe subgroup (non-responders) and the placebo group. The increase of IL13 in the mild subgroup was significantly less than that in the severe subgroup and showed a tendency to be attenuated compared with the placebo group (P=N.S.; Mann–Whitney U-test). The increase of IL2 in the mild subgroup was significantly less than that in the placebo group ($P<0.05$) and showed a tendency to be attenuated compared with the severe subgroup ($P=0.053$; Mann–Whitney U-test, Fig. 3B).

3.4. Prognostic biomarkers for clinical effects

The average ratio of Japanese cedar pollen-specific IgE to total IgE (sIgE/tIgE ratio) in all patients in the study was 0.193 before treatment. The SLIT group was divided into subgroups with a sIgE/tIgE ratio ≤ 0.19 (low, $N=28$) and >0.19 (high, $N=23$) before treatment. Similar subgroups were established in the placebo group. The SMS in the 2008 peak pollen season for the low subgroup was significantly improved compared to that in the high subgroup in the SLIT group ($P=0.02$; Mann–Whitney U-test); however, in the placebo group, the low and high subgroups had comparable SMSs (P=N.S.; Mann–Whitney U-test, Fig. 4A). Furthermore, the SMS was correlated with the sIgE/tIgE ratio in the SLIT group ($Rs=0.39$, $P<0.01$; Spearman correlation analysis), but not in the placebo group ($Rs=0.08$, P=N.S.; Spearman correlation analysis, Fig. 4B).

3.5. Upregulation of Cry j 1-iTreg levels as a response monitoring biomarker

A population of IL10$^+$Foxp3$^+$ cells in CD25$^+$CD4$^+$ leukocytes was evaluated as a potential marker for iTreg after stimulation with Cry j 1 or medium only before and after the pollen season in 2008. Neither the changes in Cry j 1-iTreg levels after stimulation with and without Cry j 1 nor the upregulation of Cry j 1-iTreg from pre- to post-pollen season differed significantly different between the groups (data not shown).

We previously reported that upregulation of Cry j 1-iTreg is a candidate biomarker that may distinguish SLIT responders from non-responders based on QOL-symptom scores [6]. Therefore, we divided the SLIT group into subgroups based on an increase ($N=24$) or decrease ($N=27$) in Cry j 1-iTreg levels from before to after the pollen season in 2008. QOL-symptom and total QOL scores in the increased iTreg subgroup significantly improved compared with those in the placebo group. In contrast, the scores in the decreased iTreg subgroup were similar to those in the placebo group (Fig. 4C).

3.6. Carry-over effects in the year after treatment

A total of 63 patients completed a pollinosis-symptom diary during the 2009 pollen season; 1 year after the 2-year SLIT treatment (Fig. 1). All participants remained blinded to their treatment with SLIT or a placebo. The SMS in the peak pollen season in 2009 (February 15 to March 6) in the SLIT group ($N=36$) was significantly attenuated compared to the placebo group ($N=27$, $P=0.03$). The average SMSs for the SLIT and placebo groups were 3.5 and 4.5, respectively, in the peak pollen season (Fig. 5).

4. Discussion

The primary endpoint of this randomized DBPC trial was the therapeutic effect evaluated in ITT analysis. No significant positive effect was observed between the SLIT and placebo groups after exchanging the perceived improvement of patients who dropped out with each median score from the counter group. In OT analysis, the SMS in the SLIT group was

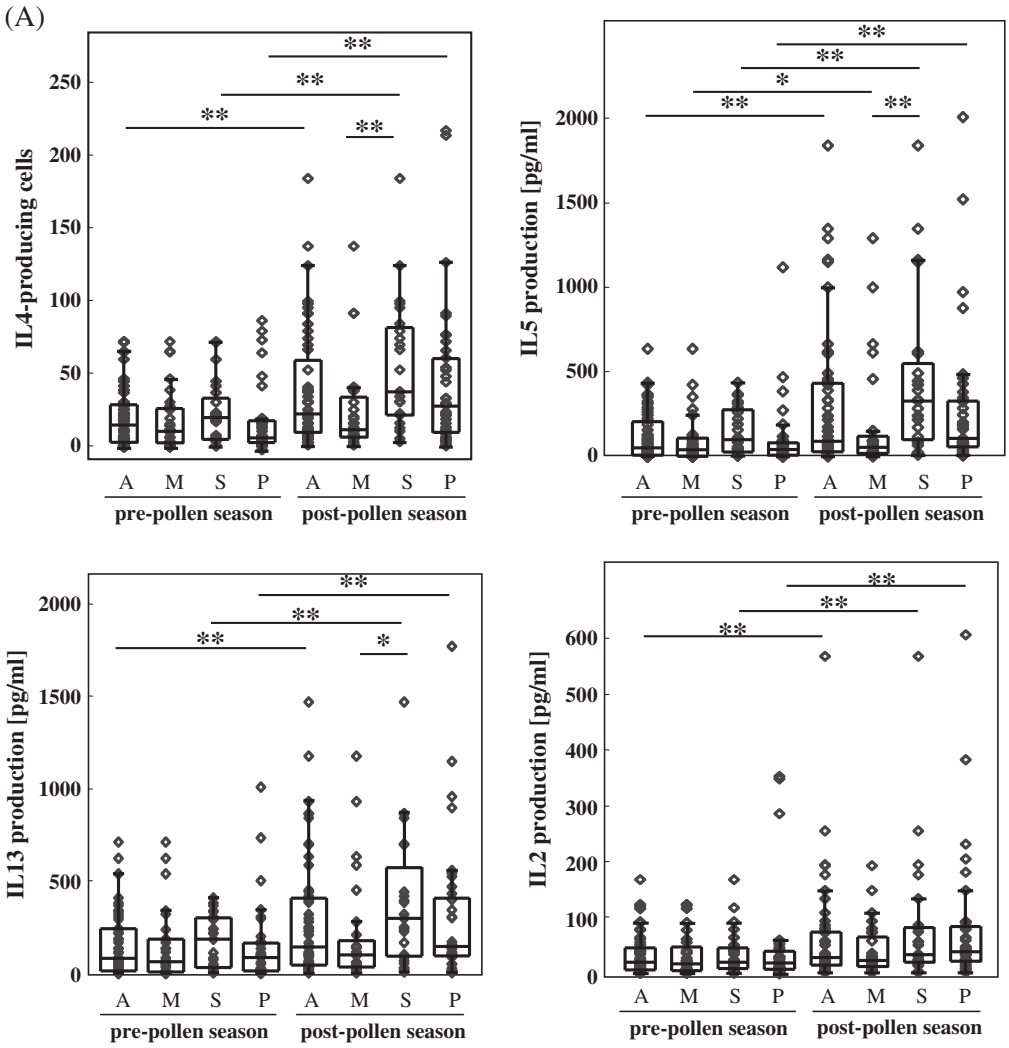

Figure 3 Cytokine production from PBMCs. (A) Number of Cry j 1-specific IL4-producing cells and Cry j 1-specific cytokine levels in the SLIT group (A; $N=51$), the mild subgroup of the SLIT group (M; $N=28$), the severe subgroup of the SLIT group (S; $N=23$), and the placebo group (P; $N=37$) at before and after the 2008 pollen season. Comparisons with a significant difference are indicated as * and **; otherwise, comparisons are not significantly different ($P=$N.S.). (B) Increases in the number of Cry j 1-specific IL4-producing cells and Cry j 1-specific cytokine levels occurred from before to after the 2008 pollen season in the SLIT group (Act.; $N=51$), the mild subgroup of the SLIT group (Mild; $N=28$), the severe subgroup of the SLIT group (Sev.; $N=23$), and the placebo group (Plc.; $N=37$). Each diamond shows the value for an individual. Two-group comparison was performed using a Mann–Whitney U-test. *$P<0.05$, **$P<0.01$.

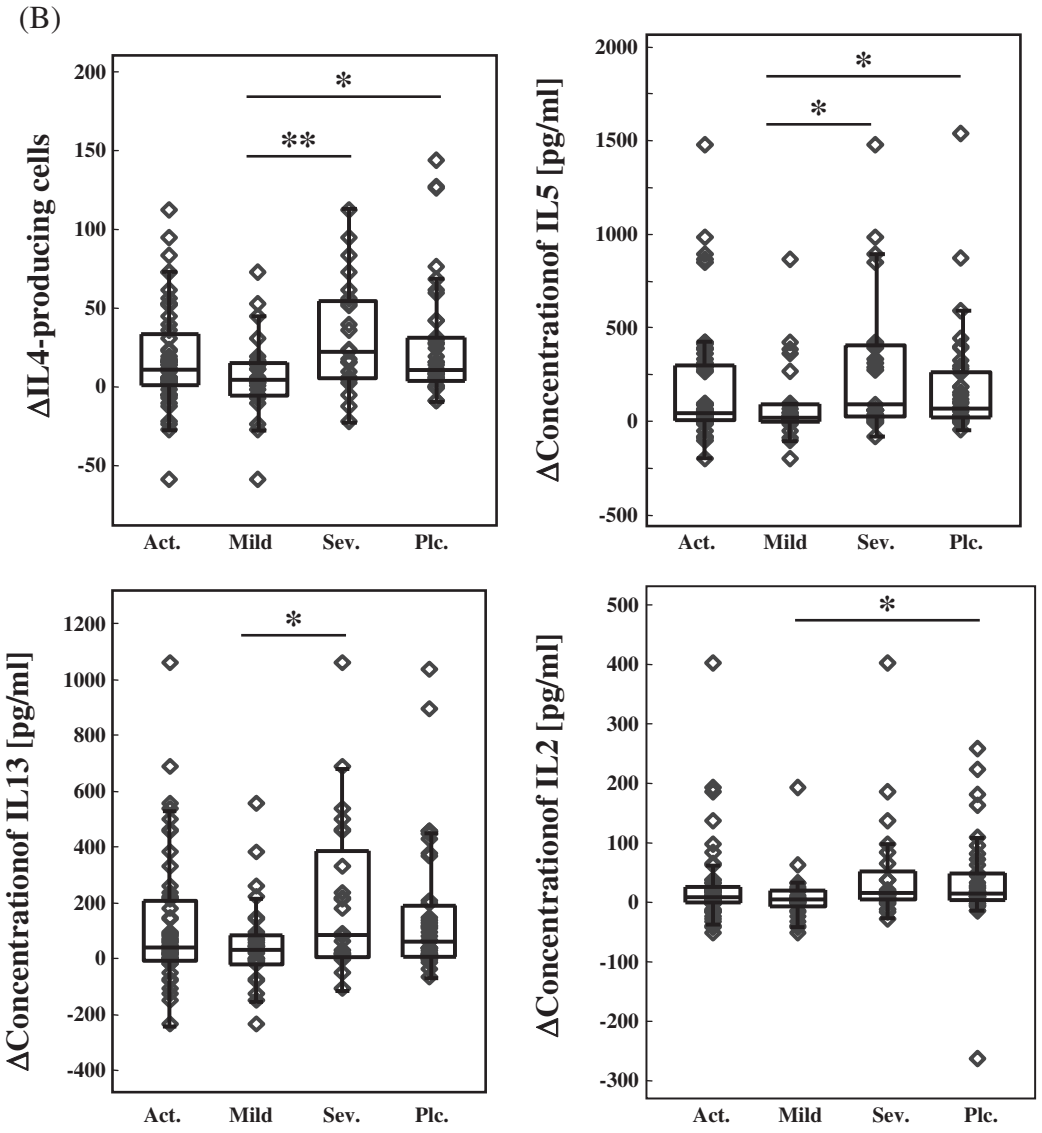

Figure 3 (*continued*).

significantly ameliorated compared to the placebo group in 2008. The percentage of mild subjects (SMS ≤ 4) in the SLIT group was 28% higher than that in the placebo group (SLIT, 55%; placebo, 27%), and the SMS was reduced by approximately 21% in the SLIT group compared with the placebo group (SLIT, 4.2; placebo, 5.3). This percentage of mild subjects differ significantly between the SLIT and placebo groups ($P=0.009$; 2×2 Chi-squared test). These effects following 2-year treatment were comparable to those in a trial of 1-year daily treatment using grass pollen tablets [12]. The low dose of the extract (about 1/40th of that used in Europe) may be one reason for the poor clinical outcome in the first year [13]. An extract of concentration >2000 JAU is not available for clinical use in Japan, and the clinical effects, safety, and optimum schedule for administration of an extract with a much higher allergen concentration remain unclear.

Positive clinical therapeutic effects were not obtained following 1-year treatment in our study, even in OT analysis (data not shown). In contrast, two previous reports demonstrated positive therapeutic effects after 1-year SLIT for Japanese cedar pollinosis [3,4]. However, in these studies, the annual pollen count (1154 grains/cm^2/season) [3] was less than in our study, and daily SMS was significantly attenuated on only 4 days in the pollen season [4]. The severity of SMS is affected by the amount of Japanese cedar pollen in the total and peak pollen season. Natural resolution and tolerance are not usually induced by natural exposure to Japanese cedar pollen, regardless of the amount of pollen [14].

Whether there are detectable alterations in peripheral T-cell responses after specific immunotherapy is still under debate [15–18]. The Cry j 1-specific cytokine profile from the SLIT group did not differ significantly from that in the placebo group. However, the increases in IL2, IL4, IL5, and IL13 production in the mild subgroup in the SLIT group were significantly attenuated (or showed a tendency to be attenuated) compared to the severe subgroup and the placebo

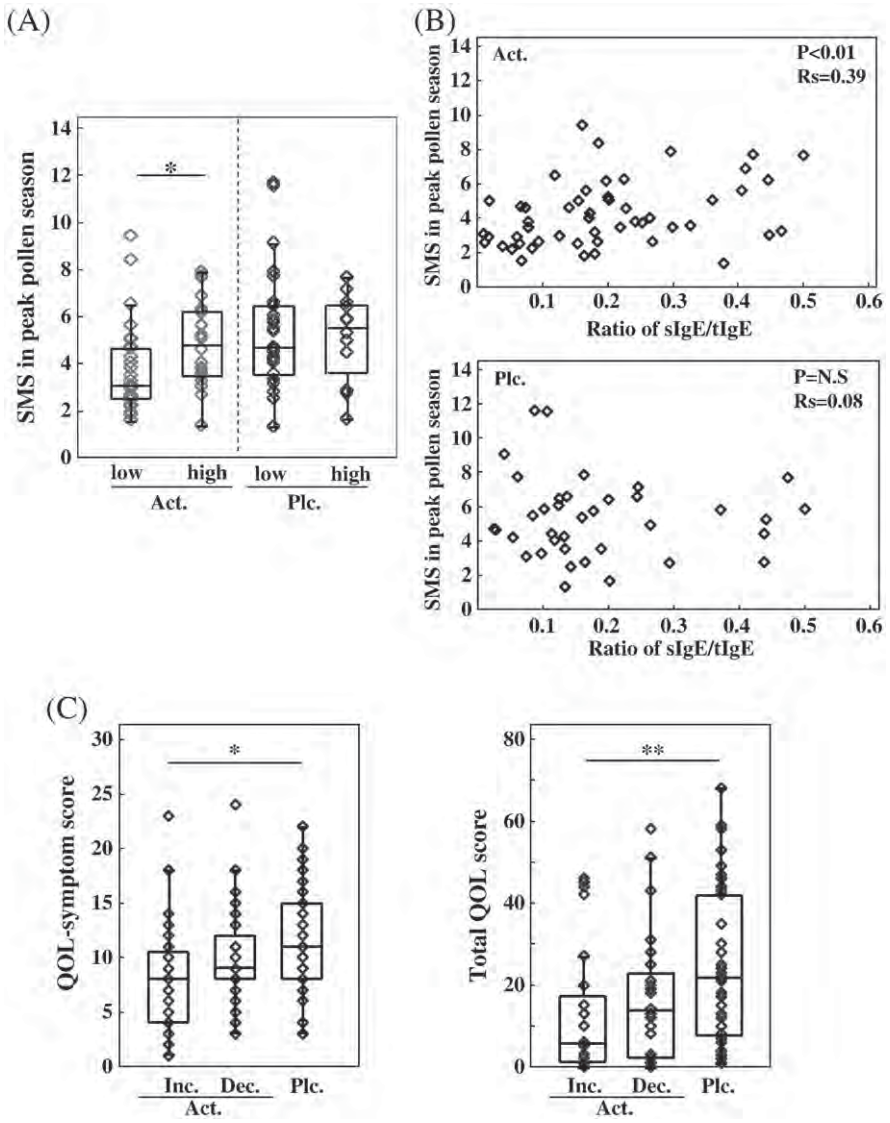

Figure 4 Biomarkers for positive therapeutic effects following SLIT. (A) SMSs in the 2008 peak pollen season for patients with low (low; $N=28$) and high (high; $N=23$) sIgE/tIgE ratios in the SLIT group (Act.), and for those with low ($N=25$) and high ($N=12$) sIgE/tIgE ratios in the placebo group (Plc.). *$P<0.05$. (B) Correlation between SMSs in the 2008 peak pollen season and sIgE/tIgE ratios before treatment in the SLIT (Act.; $N=51$) and placebo (Plc.; $N=37$) groups. Statistical data were obtained with Spearman correlation analysis. (C) QOL-symptom and total QOL scores from the QOL questionnaire plotted for a subgroup with increased Cry j 1-iTreg in the SLIT group (Inc.; $N=24$), a subgroup with decreased Cry j 1-iTreg in the SLIT group (Dec.; $N=27$), and the placebo group (Plc.; $N=37$) in the middle of the 2008 pollen season. Each diamond shows the value for an individual. *$P<0.05$, **$P<0.01$.

group (Fig. 3B). The SMS in all patients in the study correlated with the seasonal increases in IL4 ($R=0.35$, $P<0.01$), IL5 ($R=0.35$, $P<0.01$), and IL13 ($R=0.36$, $P<0.01$). The discrepancy in our current results and the results of previous studies with regard to downregulation of cytokine production from PBMCs may depend on the extent of the therapeutic effects achieved in each clinical trial.

Cry j 1-specific IgE production was not changed by treatment, even in the mild subgroup, as also found in our preliminary study [6]. We speculate that more time is required for changing antibody production following the changes of antigen-specific T cell profiles, because the alteration of T cell profiles strongly influences subsequent class switch recombination of B cells and antibody production. Another possibility is that the dose for SLIT used in this study was not high enough to alter the antibody profiles.

The sIgE/tIgE ratio has been found to be significantly higher in responders than in non-responders following 4-year immunotherapy [19]. In our trial, this ratio did not differ significantly between responders and non-responders (P=N.S.; Mann–Whitney U-test). However, subjects with a low sIgE/tIgE ratio before treatment were more likely to be responders to 2-year SLIT, and the ratio correlated with the SMS only in patients treated with SLIT (Fig. 4A, B). This suggests that SLIT was more effective in patients with a low sIgE/tIgE ratio than in those with a high sIgE/tIgE ratio. The range of total IgE levels for the participants were relatively wide (6.8–2090 IU/ml in all patients); however, the change of the total IgE for each

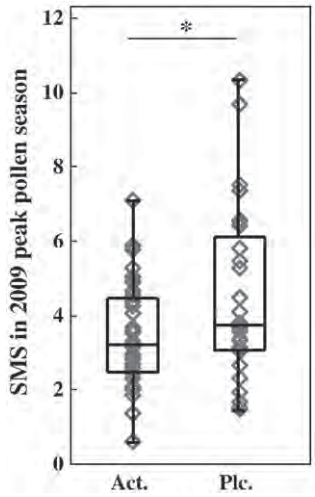

Figure 5 Carry-over effects following 2-year treatment with SLIT. SMSs in the 2009 peak pollen season were plotted for the SLIT (Act.; $N=36$) and placebo (Plc.; $N=27$) groups. Each diamond shows the value for an individual. Two-group comparisons were performed using an unpaired t-test.

individuals after 2-year treatment was not significantly different compared to before treatment (1.5±1.0 times higher, P=N.S.; paired t-test). Therefore, the wide range of total IgE levels was due to the variability on the allergic status for individuals, but not on method for measurement. The serum IgE level may affect the surface IgE level on effector cells such as mast cells and basophils, and Tregs can downregulate activation of mast cells and eosinophils [20,21]. We speculate that effector cells with a low specific IgE level are less likely to be activated by antigen crosslinking or are more susceptible to downregulation by Tregs than those with a high specific IgE level. It is also possible that the symptoms of patients with a low sIgE/tIgE ratio may be more readily attenuated by suboptimal potentiation of iTreg induced by SLIT.

We previously reported that an increased count of Cry j 1-iTregs was a candidate biomarker that could be used to distinguish between responders and non-responders to SLIT, as evaluated by the QOL-symptom score. In this report, the subgroup with increased Cry j 1-iTregs showed significant amelioration of the QOL-symptom and total QOL scores compared to the placebo group, while the subgroup with decreased Cry j 1-iTregs did not show this response (Fig. 4C). However, there was no significant difference in Cry j 1-specific cytokine production from PBMCs among patients with increased iTregs and decreased iTregs, and those in the placebo group (data not shown). Foxp3-expressing $CD25^+CD3^+$ cells and IL10-expressing $CD3^+$ cells, which are induced in the nasal mucosa after subcutaneous immunotherapy, have been linked to the clinical efficacy and suppression of seasonal inflammation [22]. Immunotherapy using an Amb a 1-immunostimulatory oligodeoxynucleotide conjugate also induced $CD4^+CD25^+$ T cells and IL10-producing cells in the nasal mucosa after the pollen season [23]. These data suggest that iTregs may downregulate effector cells at local sites of inflammation to suppress clinical symptoms. Induction of iTregs in the nasal mucosa and functional analysis of these cells may be necessary to determine the regulatory mechanisms affected by SLIT. Mucosal biopsy in the peak pollen season is useful for evaluation of local induction of iTregs and downregulation of effector cells. However, nasal biopsy in the pollen season significantly influences the daily SMS in the peak pollen season. Mucosal biopsy outside the pollen season after exposure using an artificial pollen chamber may be a powerful tool for evaluation of local regulatory mechanisms induced by SLIT [24]. Upregulation of iTregs in nasal mucosa may be difficult to determine since the evaluation may be painful for patients. However, upregulation of iTregs in peripheral blood is simple to analyze and may be a useful biomarker because an increase of peripheral Cry j 1-iTregs is correlated with QOL and QOL-symptom scores in the pollen season, as discussed here and elsewhere [6].

Cry j 1-specific IgG4 production was not induced by SLIT in this study to the same extent as that in our previous study [6]. A clinical trial showing that daily 2500 SQ-T (14 μg Phl p 5 per 4 weeks) tablets failed to induce IgG production supports our current results [13]. A change in the immunoglobulin profile may require a higher allergen dose or longer duration of exposure. However, our study suggests that detectable quantitative changes in IgG4 are not essential for the amelioration of clinical symptoms.

In summary, we suggest that the sIgE/tIgE ratio and upregulation of iTregs may be considered as prognostic and response monitoring biomarkers, respectively, for SLIT. However, further investigation of induction of iTregs at local inflammatory sites and downregulation of inflammatory cells is needed. Furthermore, validation studies with larger sample size would be required before either biomarkers should be applied widely in the clinical management of pollinosis patients. Development of a more effective vaccine and better protocols may reveal more significant differences in the Cry j 1-specific cytokine profiles and iTreg induction, and these results may increase our understanding of the roles of iTregs or Tr1 in the therapeutic mechanisms underlying the efficacy of SLIT.

Acknowledgments

We sincerely thank Drs. Takashi Saito, Yasuyuki Ishii, Masato Kubo, Tsuneyasu Kaisho, and Hisahiro Yoshida (RIKEN, Kanagawa, Japan) for their helpful comments and fruitful discussions. This work was partially supported by a grant from the Ministry of Health, Labour and Welfare in Japan, in part by the Global COE program (Global Center for Education and Research in Immune System Regulation and Treatment), MEXT, Japan, and in part by the Promotion and Mutual Aid Corporation for Private Schools of Japan, Grant-in-Aid for Matching Fund Subsidy for Private University, Japan.

References

[1] K. Baba, K. Nakae, Epidemiology of nasal allergy through Japan in 2008, Prog. Med. 28 (2008) 2001–2012, (In Japanese).
[2] H. Yasueda, K. Akiyama, Y. Maeda, T. Hayakawa, F. Kaneko, M. Hasegawa, et al., An enzyme-linked immunosorbent assay (ELISA) for the quantitation of sugi pollen and *Dermatophagoides* mite allergens and its application for standardization of allergen extracts, Arerugi 40 (1991) 1218–1225, (In Japanese).

[3] S. Horiguchi, Y. Okamoto, S. Yonekura, T. Okawa, H. Yamamoto, N. Kunii, et al., A randomized controlled trial of sublingual immunotherapy for Japanese cedar pollinosis, Int. Arch. Allergy Immunol. 146 (2008) 76–84.
[4] K. Okubo, M. Gotoh, S. Fujieda, M. Okano, H. Yoshida, H. Morikawa, et al., A randomized double-blind comparative study of sublingual immunotherapy for cedar pollinosis, Allergol. Int. 57 (2008) 265–275.
[5] K. Yamanaka, A. Yuta, M. Kakeda, R. Sasaki, H. Kitagawa, E. Gabazza, et al., Induction of IL-10-producing regulatory T cells with TCR diversity by epitope-specific immunotherapy in pollinosis, J. Allergy Clin. Immunol. 124 (2009) 842–845, e7.
[6] T. Fujimura, S. Yonekura, Y. Taniguchi, S. Horiguchi, A. Saito, H. Yasueda, et al., The induced regulatory T-cell level, defined as the proportion of $IL10^{+}Foxp3^{+}$ cells among $CD25^{+}CD4^{+}$ leukocytes, is an available response monitoring biomarker for sublingual immunotherapy: a preliminary report, Int. Arch. Allergy Immunol. 153 (2010) 378–387.
[7] Practical Guideline for the Management of Allergic Rhinitis in Japan—Perennial rhinitis and Pollinosis—2005 Edition (The fifth revision), Life Science Publishing Co. Ltd., Tokyo, 2005.
[8] K. Okubo, R. Takizawa, M. Gotoh, M. Okuda, Experience of specific immunotherapy with standardized Japanese cedar pollen extract, Arerugi 50 (2001) 520–527, (In Japanese).
[9] M. Okuda, K. Ohkubo, M. Goto, H. Okamoto, A. Konno, K. Baba, et al., Comparative study of two Japanese rhinoconjunctivitis quality-of-life questionnaires, Acta Otolaryngol. 125 (2005) 736–744.
[10] A. Trotti, A.D. Colevas, A. Setser, V. Rusch, D. Jaques, V. Budach, et al., CTCAE v3.0: development of a comprehensive grading system for the adverse effects of cancer treatment, Semin. Radiat. Oncol. 13 (2003) 176–181.
[11] H. Yasueda, A. Saito, M. Sakaguchi, T. Ide, S. Saito, Y. Taniguchi, et al., Identification and characterization of a group 2 conifer pollen allergen from *Chamaecyparis obtusa*, a homologue of Cry j 2 from *Cryptomeria japonica*, Clin. Exp. Allergy 30 (2000) 546–550.
[12] M. Calderon, T. Brandt, Treatment of grass pollen allergy: focus on a standardized grass allergen extract—Grazax, Ther. Clin. Risk Manage. 4 (2008) 1255–1260.
[13] S.R. Durham, W.H. Yang, M.R. Pedersen, N. Johansen, S. Rak, Sublingual immunotherapy with once-daily grass allergen tablets: a randomized controlled trial in seasonal allergic rhinoconjunctivitis, J. Allergy Clin. Immunol. 117 (2006) 802–809.
[14] Y. Okamoto, S. Horiguti, H. Yamamoto, S. Yonekura, T. Hanazawa, Present situation of cedar pollinosis in Japan and its immune responces, Allergol. Int. 58 (2009) 155–162.
[15] P.A. Wachholz, K.T. Nouri-Aria, D.R. Wilson, S.M. Walker, A. Verhoef, S.J. Till, et al., Grass pollen immunotherapy for hayfever is associated with increases in local nasal but not peripheral Th1:Th2 cytokine ratios, Immunology 105 (2002) 56–62.
[16] C. Rolinck-Werninghaus, M. Kopp, C. Liebke, J. Lange, U. Wahn, B. Niggemann, Lack of detectable alterations in immune responses during sublingual immunotherapy in children with seasonal allergic rhinoconjunctivitis to grass pollen, Int. Arch. Allergy Immunol. 136 (2005) 134–141.
[17] P. Moingeon, T. Batard, R. Fadel, F. Frati, J. Sieber, L. Van Overtvelt, Immune mechanisms of allergen-specific sublingual immunotherapy, Allergy 61 (2006) 151–165.
[18] G. Ciprandi, G.L. Marseglia, M.A. Tosca, Allergen-specific immunotherapy: an update on immunological mechanisms of action, Monaldi Arch. Chest Dis. 65 (2006) 34–37.
[19] G. Di Lorenzo, P. Mansueto, M.L. Pacor, M. Rizzo, F. Castello, N. Martinelli, et al., Evaluation of serum s-IgE/total IgE ratio in predicting clinical response to allergen-specific immunotherapy, J. Allergy Clin. Immunol. 123 (2009) 1103–1110, 1110 e1-4.
[20] G. Gri, S. Piconese, B. Frossi, V. Manfroi, S. Merluzzi, C. Tripodo, et al., $CD4^{+}CD25^{+}$ regulatory T cells suppress mast cell degranulation and allergic responses through OX40–OX40L interaction, Immunity 29 (2008) 771–781.
[21] Y. Ohkawara, K.G. Lim, Z. Xing, M. Glibetic, K. Nakano, J. Dolovich, et al., CD40 expression by human peripheral blood eosinophils, J. Clin. Invest. 97 (1996) 1761–1766.
[22] S. Radulovic, M.R. Jacobson, S.R. Durham, K.T. Nouri-Aria, Grass pollen immunotherapy induces Foxp3-expressing $CD4^{+}$ $CD25^{+}$ cells in the nasal mucosa, J. Allergy Clin. Immunol. 121 (2008) 1467–1472, e1.
[23] K. Asai, S.C. Foley, Y. Sumi, Y. Yamauchi, N. Takeda, M. Desrosiers, et al., Amb a 1-immunostimulatory oligodeoxynucleotide conjugate immunotherapy increases $CD4^{+}CD25^{+}$ T cells in the nasal mucosa of subjects with allergic rhinitis, Allergol. Int. 57 (2008) 377–381.
[24] P. Devillier, M. Le Gall, F. Horak, The allergen challenge chamber: a valuable tool for optimizing the clinical development of pollen immunotherapy, Allergy 66 (2011) 163–169.

Veterinary Immunology and Immunopathology 139 (2011) 99–106

Contents lists available at ScienceDirect

Veterinary Immunology and Immunopathology

journal homepage: www.elsevier.com/locate/vetimm

Research paper

Establishment of a quantitative ELISA for the measurement of allergen-specific IgE in dogs using anti-IgE antibody cross-reactive to mouse and dog IgE

Taro Okayama[a], Yukiko Matsuno[a], Nobutaka Yasuda[a], Toshihiro Tsukui[b], Yasuyuki Suzuta[b], Masanori Koyanagi[b], Masahiro Sakaguchi[c], Yasuyuki Ishii[d], Thierry Olivry[e], Kenichi Masuda[a,*]

[a] *Animal Allergy Clinical Laboratories Inc., SIC-2 #301 5-4-30 Nishihashimoto, Midori-ku, Sagamihara, Kanagawa 229-1131, Japan*
[b] *Zenoaq Nippon Zenyaku Kogyo Co., Ltd., Sasagawa Tairanoue 1-1, Asaka-machi, Koriyama, Fukushima 963-0196, Japan*
[c] *Department of Veterinary Microbiology, School of Veterinary Medicine, Azabu University, 1-17-71 Fuchinobe, Chuou-ku, Sagamihara, Kanagawa 229-8501, Japan*
[d] *Laboratory for Vaccine Design, RIKEN Research Center for Allergy and Immunology (RCAI), Suehiro-chou 1-7-22, Tsurumi-ku, Yokohama, Kanagawa 230-0045, Japan*
[e] *Department of Clinical Sciences and Center for Comparative Medicine and Translational Research, College of Veterinary Medicine, North Carolina State University, Raleigh, NC, USA*

ARTICLE INFO

Article history:
Received 3 March 2010
Received in revised form 2 August 2010
Accepted 5 September 2010

Keywords:
Dogs
IgE
Canine atopic dermatitis
ELISA
Allergy

ABSTRACT

As IgE plays a pivotal role in type I hypersensitivity-mediated allergic diseases, it is valuable to measure absolute quantity of serum antigen-specific IgE for clinical and research purposes. Here we describe a novel ELISA system that enables quantification of antigen-specific IgE in ng/ml in dogs. A newly developed monoclonal antibody (CRE-DM) was shown to recognize canine and mouse IgE equally in a dose dependent manner, but it did not recognize canine IgG. The reactivity of CRE-DM to canine IgE was also confirmed by an inhibition ELISA using canine IgE as an inhibitor and the maximum inhibition rate was 91.3%. In order to know whether canine IgE specific to an allergen could be quantitatively measured with an ELISA using CRE-DM, we established a quantitative ELISA that could measure canine IgE recognizing Cry j 1, one of the major allergens of Japanese cedar pollen. In this ELISA, a standard curve was created by using concentration-predetermined Cry j 1-specific monoclonal mouse IgE. According to the standard curve, the concentration of Cry j 1-specific IgE in dogs that were experimentally sensitized to Japanese cedar pollen could be calculated and determined in ng/ml. The specificity of the Cry j 1-specific IgE ELISA using CRE-DM was also confirmed by inhibition ELISA using canine IgE as an inhibitor and the inhibition rate was 97.0%. Reproducibility of the ELISA in three independent assays was determined using groups of pooled canine sera whose Cry j 1-IgE titers ranged from 155.9 to 888.2 ng/ml. Intra- and inter-assay reproducibility was determined with coefficient of variation ranging between 3.1–5.2% and 2.2–8.0%, respectively. These results demonstrated that the ELISA utilizing CRE-DM was a specific, reliable and robust new laboratory test that could quantify absolute amount of antigen-specific IgE in canine serum. The ELISA will serve as a useful tool in the clinics to evaluate the change of serum IgE titers during anti-allergic treatments as well as during seasonal fluctuation of allergen exposure.

1. Introduction

IgE plays a pivotal role in provoking IgE-mediated allergic reaction and inducing various allergic diseases such

* Corresponding author. Tel.: +81 042 770 9437; fax: +81 042 770 9438.
E-mail address: masuda@aacl.co.jp (K. Masuda).

0165-2427/$ – see front matter © 2010 Elsevier B.V. All rights reserved.
doi:10.1016/j.vetimm.2010.09.002

as canine atopic dermatitis (AD) and cutaneous adverse food reactions in dogs. The relationship between IgE and allergic diseases has been extensively investigated in dogs. Allergen-specific IgE has been known to initiate degranulation of the basophils in the skin of experimental flea allergy model dogs (Halliwell and Schemmer, 1987). It was also shown that the basophils of the peripheral blood of dogs with AD (Masuda et al., 2000) and food allergy (Ishida et al., 2003) are initiated to release histamines through antigen-IgE mediated stimulation. The serum titer of Japanese cedar pollen was reported to fluctuate in parallel to the manifestation of allergy-related clinical signs and the pollination season (Masuda et al., 2002). An oral exposure to food antigens in dogs with food allergy induced clinical signs, which were accompanied by the increase of allergen-specific IgE in the sera (Jackson et al., 2003). Because of the accumulating evidence suggesting the involvement of IgE in the pathogenesis of IgE-mediated allergic diseases in dogs, it is becoming quite important to detect allergen-specific IgE in clinical cases of canine AD and food allergy for diagnosis and therapeutic purposes (DeBoer and Hillier, 2001a).

Two major test methods have been used in dogs to detect allergen-specific IgE; intradermal test (IDT) and serum antigen-specific IgE test (serum IgE test). IDT is the *in vivo* test to see whether wheals are formed at the sites of intradermal injection of allergens. When a positive immediate reaction to an allergen solution is detected in IDT, it can be concluded that the patient has an IgE-mediated hypersensitivity to that allergen, thus supporting the diagnosis of IgE-mediated allergic disease. IDT has been popularly used in veterinary practice (Hillier and DeBoer, 2001), but however, there are some limitations for its clinical use. Because of the nature of this test as a qualitative method, the test results are only obtained as negative or positive. Therefore, it is difficult for clinicians to understand the magnitude of sensitization and to monitor the therapeutic efficacies using IDT results. It is also reported that IDT is prone to false negative results because the sufficient allergen concentrations that give the proper test results differ from allergen to allergen and from patient to patient (Hensel et al., 2004). Moreover, IDT is also reported to exhibit false positive reactions due to sub-clinical hypersensitivity (Pastorello, 1993; Codner and Tinker, 1995). In addition, because IDT requires particular procedures such as intradermal injections, antigen preparation and animals to be immobilized during the test, IDT is inconvenient for veterinary practitioners who are not specialized in allergic diseases to perform as a routine clinical test.

Serum IgE tests have been developed during the last three decades in expectation to overcome the limitations of IDT. Serum IgE tests are the methods to detect allergen-specific IgE in canine sera. Currently in most commercial tests available in the veterinary field, various forms of ELISAs are utilized as assay systems. For the detection of canine IgE, anti-IgE antibodies or recombinant extracellular segments of the human high affinity IgE receptor (rhFcεRIα) are used (DeBoer and Hillier, 2001b). The amount of the detecting reagent bound to IgE is measured by detecting the signals developed by enzyme-mediated methods. Thus the generated signals are deemed to reflect the amount of IgE in the tested serum. The intensity of signals is further converted into units, scores or grades that are defined by each laboratory and reported to the clinicians. Because the reference reagents and the data processing platforms used in the tests differ for each laboratory, it is difficult to compare results among the different laboratories. Also the results must be regarded as qualitative or semi-quantitative because the results are not given in an absolute quantification such as in ng/ml but in comparative scales. Moreover, there have been continuous debates until now on how to interpret and link the serum IgE test results with clinical findings (DeBoer and Hillier, 2001b; Zur et al., 2002). For these reasons, a truly quantitative serum IgE test has been sought.

In basic immunological research utilizing mice, there are a number of reports that utilize ELISAs which are able to quantify allergen-specific mouse IgE in μg/ml. In these ELISAs, anti-mouse IgE antibodies are used for the detection of IgE and pre-quantified allergen-specific monoclonal mouse IgEs are used to create standard curves. Then, the concentrations of allergen-specific IgE in mouse sera are calculated according to the standard curves. For instance, a quantitative ELISA system for ovalbumin (OVA)-specific mouse IgE was established with a monoclonal mouse IgE recognizing OVA and used to detect the serum titer of OVA-specific IgE at μg/ml in mice (Hamada et al., 2003). As in dogs, monoclonal canine IgE specific to filarial antigen has been developed and reported (Gebhard et al., 1995). However, the IgE described in the literature can only be used as a standard reference to measure the worm-specific IgE, which seems to have little use in allergy testing. In order to establish an ELISA for the measurement of allergen specific IgE in dogs by such systems, it is required to establish monoclonal canine IgE for each allergen to be tested, which seems to be difficult to achieve.

To overcome these issues, we attempted to establish a novel ELISA system that could measure the absolute quantity of antigen-specific serum IgE in dogs by using a newly developed anti-IgE antibody that cross reacts equally to IgEs of dog and mouse (CRE-DM). A monoclonal mouse IgE specific to Cry j 1, one of the major allergens of Japanese cedar pollen, was used as a reference standard to quantify Cry j 1-specific IgE in canine sera. This is the first report to demonstrate the method of an absolute quantification of allergen-specific IgE in ng/ml scale in canine sera.

2. Materials and methods

2.1. Preparation of anti-IgE mAb cross-reactive to canine and mouse IgE

Six female rats (Wistar/ST) were all immunized with 20 μg of mouse IgE (BD Biosciense, San Jose, CA, USA) and canine IgE (Bethyl Laboratories, Montgomery, TX, USA) two times with a 2-week interval. After 4 weeks, the spleen cells were obtained and fused with a mouse myeloma cell line, X63Ag8.653. A hybridoma cell clone that produced an antibody reacting with canine and mouse IgE in the culture supernatant was selected by direct ELISAs using mouse IgE or canine IgE as antigens. The cell clone was expanded and injected intraperitoneously into rats (Wistar/ST) and

ascites was obtained 6 months after the injection. From the ascites, rat IgG was purified with ammonium sulfate precipitation and biotinylated with a kit (EZ-Link, Pierce Biotechnology, Rockford, IL, USA). The IgG concentration was determined with a spectrophotometer at 280 nm. This anti-IgE antibody was supposed to be cross-reactive to IgEs of dog and mouse, thus the antibody was named CRE-DM. All aspects of this experiment were approved by Animal Care and Use Committee of Zenoaq Nippon Zenyaku Kogyo Co., Ltd. (Zenoaq, Fukushima, Japan).

2.2. Evaluation of the reactivity and the specificity of CRE-DM

Reactivity of the CRE-DM to canine IgE, canine IgG and mouse IgE were evaluated by ELISA using biotinylated CRE-DM as a detecting antibody. The microwells were coated with various concentrations ranging from 1 to 100 ng/ml of canine IgE (Bethyl Laboratories), canine IgG (Rockland Immunochemicals, Inc. Gilbertsville, PA, USA), or mouse IgE (BD Bioscienses). The wells were blocked with 1% gelatin in PBS for 2 h at room temperature. After washing three times with PBST, 100 μl of 0.5 μg/ml biotinylated CRE-DM diluted in dilution buffer (1% gelatin in PBST) was added to each well. After 2-h incubation at room temperature, the wells were washed three times with PBST and 100 μl of 0.05 U/ml Streptavidin-beta-Gal conjugate (Roche Diagnostics GmbH, Penzberg Germany) in dilution buffer was added to each well and incubated for 2 h at room temperature. The wells were then washed three times with PBST and 100 μl of 0.1 mM 4-methylumbelliferyl β-D-galactopyranoside (4MU, Sigma–Aldrich, Saint Louis, MS, USA) in reaction buffer (0.1% gelatin, 0.1 M NaCl and 1 mM $MgCl_2$ in phosphate buffer, pH 7.4) was added. Following 1-h incubation at room temperature, 100 μl of stop solution (0.25 M Na_2CO_3) was added and detected with microplate reader Gemini XPS (Molecular Devices, Sunnyvale, CA, USA). The data were analyzed using Softmax Pro (Molecular Devices). In the inhibition ELISA assay, which aims to qualify the specificity of the reaction, biotinylated CRE-DM was pre-incubated overnight at 4 °C with various amounts of canine IgE, and the assays were performed similarly as described above.

2.3. Serum samples from experimentally sensitized dogs

To obtain high titer serum used for the measurement and inhibition experiments in Cry j 1-specific IgE ELISA, a dog was experimentally sensitized to Japanese cedar pollen. The sensitization procedure was carried out as previously described (Yamashita et al., 2000). A dog was maintained and the experiment was carried out at Zenoaq. Briefly, a healthy beagle was subcutaneously injected twice at 2-week interval with 100 μg of Japanese cedar pollen antigen in 3 ml of saline-emulsified alum. Two weeks after the second injection, production of IgE to Japanese cedar pollen antigen was confirmed by IDT (data not shown), and serum sample was collected. All aspects of this experiment were approved by Animal Care and Use Committee of Zenoaq.

To obtain serum of various titers of IgE to Cry j 1, four Maltese-beagle atopic (MBA) dogs were sensitized with Cry j 1 with a combination of intraperitoneal and epicutaneous antigen stimulations. Dogs first received two intraperitoneal injections of 200 μg of a mixture of Cry j 1 and 2 (ratio: 5:2). Dogs were further sensitized with additional epicutaneous applications of 200 μg of crude Japanese cedar pollen in mineral oil, with or without tape stripping, on a weekly to monthly basis depending on their allergen-specific IgE serum levels. The serum samples were collected at several time points before and after the sensitization procedure. Successful sensitization was confirmed by the positive reactions to Cry j 1 in IDT, which showed wheal formation comparable to that of the histamine positive control. The sera were used for the quantification of serum Cry j 1-specific IgE pre- and post-sensitization and for determining the reproducibility of the Cry j 1-specific IgE ELISA utilizing CRE-DM. All aspects of the study were approved beforehand by North Carolina State University Institutional Animal Care and Use Committee (IACUC).

2.4. Determination of the optimal dilution rate for the dog serum sample

To address an issue that IgGs in the serum that share reactive antigens with IgEs could possibly influence the reactions between antigens and IgEs in the ELISA, it was considered essential to use the appropriate serum dilution rate to measure antigen-specific IgE in the serum. To determine the optimal dilution rate for serum samples, high Cry j 1-IgE titer serum described above was diluted to various dilution rates ranging from 10 to 100,000 and used in the ELISA. Because the dog was intensely immunized so as to produce large amounts of antibodies, the sample was considered to contain large amounts of IgGs specific for Cry j 1 as well, which should well exceed the amount of IgGs that could possibly be produced in the spontaneous sensitization to the allergen. From these reasons we used this serum as a representative sample. A serum of healthy beagle, obtained from Zenoaq, was diluted simultaneously and used in the assay to serve as a blank control for each dilution rates. Microwells were coated with 100 μl of 1 μg/ml Cry j 1 (Hayashibara Biochemical Labs., Inc., Okayama, Japan). Wells were blocked with 1% gelatin PBS for 2 h at room temperature and then washed three times with PBST. Then the diluted samples were applied to wells and incubated overnight at 4 °C. After washing three times with PBST, 100 μl of biotinylated CRE-DM in dilution buffer was added to each well. The rest of the procedure was carried out as described above.

2.5. Quantification of Cry j 1-specific IgE in canine serum

To determine whether canine IgE specific to an allergen could be quantitatively measured with an ELISA using CRE-DM and Cry j 1-specific monoclonal mouse IgE, we performed a quantitative ELISA specific for canine IgE to Cry j 1. Microwells were coated with 100 μl of 1 μg/ml Cry j 1 (Hayashibara Biochemical Labs., Inc.). Wells were

blocked with 1% gelatin PBS for 2 h at room temperature and then washed three times with PBST. Sera from clinical cases were diluted 1:1000 in dilution buffer and 100 μl were applied to microwells. To create a standard curve, anti-Cry j 1 monoclonal mouse IgE was obtained by a standard method to be used as a standard reference. Briefly, BALB/c mice were immunized twice in a week interval with 5 μg of Cry j 1 and 2 mg of alum per mouse. Three days after the last immunization, the mice were sacrificed and their splenic cells were fused with P3U1 myeloma cells at 3:1 ratio with polyethylene glycol 4000 (Wako Pure Chemical Industries, Osaka, Japan). The fused cells were seeded in 96 well flat bottom plate at the concentration of 6×10^4 cells per well (splenic cells) and cultured in HAT selection medium (complete RPMI with 10% FCS containing 0.1 mM hypoxanthine, 0.016 mM thymidine 0.4 nM aminopterin) for 10 days. The culture supernatants of growing cells were screened for the presence of mouse IgE with the Cry j 1-IgE ELISA using anti-mouse IgE monoclonal antibody (Yamasa Corporation, Chiba, Japan). Finally, a positive clone was established as a hybridoma secreting IgE specific to Cry j 1.

Obtained anti-Cry j 1 monoclonal mouse IgE was quantified with mouse IgE EIA kit (Yamasa Corporation) and diluted to concentrations ranging 0.156–10 ng/ml and 100 μl of each solution was applied to wells of ELISA plates. After incubating overnight at 4 °C, wells were washed and 100 μl of biotinylated CRE-DM diluted in dilution buffer at 0.5 μg/ml was added to each well. The rest of the procedure was carried out as described above. To further investigate whether CRE-DM could specifically detect IgE in canine serum, CRE-DM was incubated beforehand with canine IgE as an inhibitor for overnight at 4 °C (pre-treated CRE-DM). Inhibition ELISA was performed similarly as described above but replacing CRE-DM with the pre-treated CRE-DM.

2.6. Evaluation of the reproducibility of the ELISA utilizing CRE-DM

The reproducibility of the ELISA utilizing CRE-DM was evaluated by comparing results among the wells in three different plates within an assay (intra-assay) and among the wells of three independent assays which were performed on different days (inter-assay). Canine sera with various titers were prepared from the Cry j 1-sensitized MBA dogs as described above and the concentrations of Cry j 1-specific IgE in each serum were determined beforehand with the ELISA using CRE-DM. According to the concentrations, sera were divided into three groups, high, intermediate and low. Three serum samples were chosen from each group and pooled. On each plate the sera of high, intermediate and low groups were applied to wells. The first assay was carried out with three plates in parallel and the data were used for intra-assay evaluation. The second and third assays were carried out with one plate each. For inter-assay evaluation, data from three plates, each from three independent assays, were collected and analyzed. Coefficient of variation (CV) was calculated as (SD/mean) × 100 (%) for each sera group.

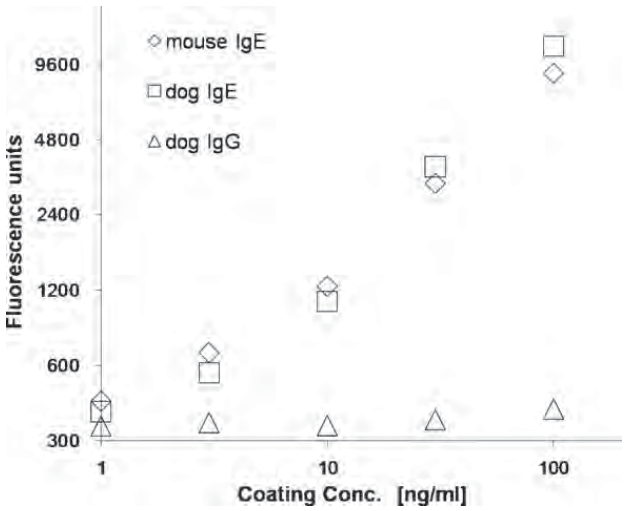

Fig. 1. Reactivity of CRE-DM against canine IgE, canine IgG and mouse IgE. Reactivity of the CRE-DM was evaluated in ELISA by applying the CRE-DM to the wells coated with canine IgE, canine IgG or mouse IgE. Resulting signals are plotted as fluorescence unit. Open diamonds, squares and triangles indicate signals from mouse IgE, canine IgE and canine IgG, respectively. The result is the representative of three independent experiments which gave similar results.

3. Results

3.1. Reactivity and specificity of CRE-DM

The reactivity of CRE-DM to IgE was first determined by the direct ELISA. It was shown that the CRE-DM reacted equally to canine IgE and mouse IgE in a dose dependent manner (Fig. 1). However, the CRE-DM did not react to canine IgG. The reactivity was further analyzed by an inhibition ELISA using canine IgE as an inhibitor. When CRE-DM was pre-incubated with various amounts of canine IgE, the reaction was obviously reduced. The inhibition rate ranged from 83.0% to 91.3% with the inhibitor/CRE-DM ratio varying from 0.5 to 10. The maximum reduction was obtained when the ratio was 10 (Fig. 2). Taken together, the CRE-DM was considered to react specifically to canine IgE and mouse IgE, but not to canine IgG.

3.2. Determination of the optimal dilution rate for the dog serum sample

To determine the serum dilution rate that is optimal for the quantification of Cry j 1-specific IgE in the dog serum, the serum with high IgE titer was diluted into indicated dilution rates and the ELISA was performed (Fig. 3). As the result, the fluorescence units and the dilution rates showed good correlation at the dilution rates between 100,000 and 1000 but plateaued at the dilution rates lower than 300. This was considered to indicate that the reactions between the Cry j 1-specific IgEs and the antigens were inhibited at the dilution rates <300 possibly due to the influence of the Cry j 1-specific IgGs in the serum that shared antigens with IgEs. From these results, we concluded that the dilution rate of 1000 was optimal in the measurement of allergen specific IgE in dog sera.

Inhibitor	Inhibition (%)					
IgE	0.0	83.0	84.7	88.8	89.9	91.3

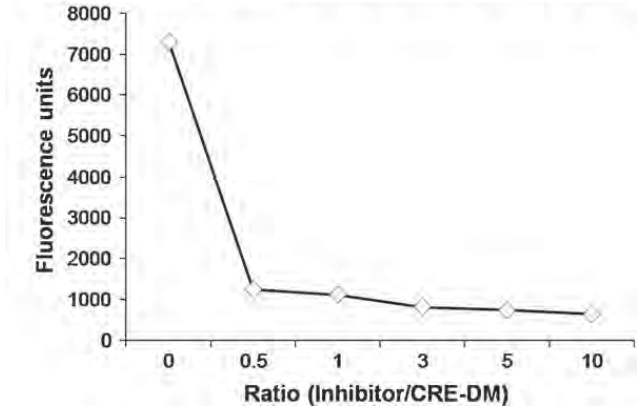

Fig. 2. Inhibition ELISA using canine IgE as an inhibitor. The CRE-DM was pre-incubated prior to ELISA with canine IgE to evaluate the specificity of the reaction. Resulting signals are plotted as fluorescence units with open diamonds. Percentages of the reductions are shown in the table. The result is the representative of three independent experiments that gave similar results.

3.3. Quantification of Cry j 1-specific IgE in canine serum samples

To test whether allergen-specific IgE in canine serum could be measured with an ELISA using CRE-DM, Cry j 1-specific IgE was measured in serum from the dog experimentally sensitized to Japanese cedar pollen. A standard curve in the ELISA was created by using the concentration-predetermined monoclonal mouse IgE specific to Cry j 1. As a result, Cry j 1-specific IgE in the serum could be measured and the concentration was determined as 11951.6 ng/ml. Furthermore, in order to confirm the specificity of this ELISA, an inhibition ELISA was performed with canine IgE as an inhibitor. When canine IgE was used as an inhibitor, the concentration of Cry j 1-specific IgE in the serum was reduced to 85.1 ng/ml, which indicated that the inhibition rate was 97.0% (Fig. 4). These data indicated that the reactivity of CRE-DM to canine IgE was maintained in the ELISA for canine serum as samples and allergen-specific IgE concentration in dog serum could be measured. To further confirm that serum antigen-specific IgE could be measured in other dog serum samples with different sensitization statuses, we measured the concentrations of Cry j 1-specific IgE in MBA dogs during pre- and post-sensitization with Cry j 1 (Table 1). The results clearly demonstrated that Cry j 1-specific IgE concentrations increased from nearly undetectable levels before the sensitization to high concentrations such as 544.8–1852.5 ng/ml after the sensitization. From these results, it was concluded that the ELISA utilizing CRE-DM could be used to measure allergen-specific IgE in the serum of dogs hypersensitive to Japanese cedar major allergens.

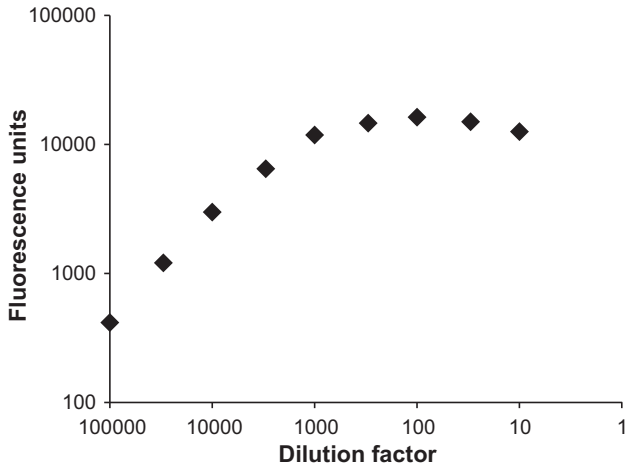

Fig. 3. Determination of the optimal dilution rate for the dog serum sample. The dog serum with high Cry j 1-specific IgE was diluted at various dilution rates as indicated. The resulting signals from each dilution rates are indicated as fluorescence units and plotted with solid diamonds. The result is the representative of two independent experiments that gave similar results.

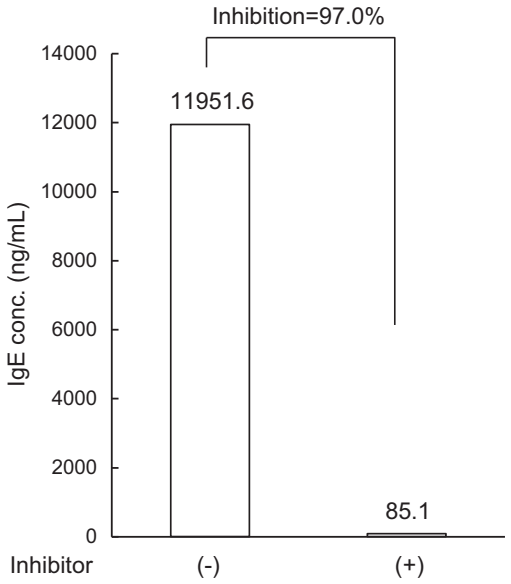

Fig. 4. Cry j 1-specific ELISA utilizing CRE-DM in canine serum samples. The absolute concentration of Cry j 1-specific IgE in canine sera was analyzed. Measurement of Cry j 1-specific IgE in a dog experimentally sensitized to Japanese cedar pollen. Also, the specificity of the ELISA was evaluated by pre incubating CRE-DM with canine IgE as an inhibitor. Inhibition rates are indicated in the figure. The result is the representative of two independent experiments that gave similar results.

3.4. Reproducibility of the Cry j 1-specific IgE ELISA utilizing CRE-DM

Using sera from MBA dogs experimentally sensitized to Cry j 1, the reliability of the Cry j 1-specific IgE ELISA was determined by evaluating the reproducibility of the values in pooled sera with the high, intermediate, and low

Table 1
Cry j 1-specific IgE concentration in MBA dogs sensitized with Cry j 1.

Dog no.	Pre-sensitization (ng/ml)	Post-sensitization (ng/ml)
1	15.6	1852.5
2	na[a]	1513.4
3	0	613.1
4	0	544.8

[a] Not applicable due to a failure in sample collection.

Table 2
Reproducibility of the Cry j 1-specific IgE ELISA utilizing CRE-DM.

Comparison	Groups	Data1 (ng/ml)	Data2 (ng/ml)	Data3 (ng/ml)	Mean (ng/ml)	CV (%)
Intra-assay	Low	155.9	172.2	168.7	165.6	5.2
	Intermediate	413.4	391.2	388.5	397.7	3.4
	High	841.3	888.2	841.9	857.1	3.1
Inter-assay	Low	172.2	156.0	180.0	169.4	7.2
	Intermediate	391.2	411.6	456.5	419.8	8.0
	High	888.2	887.4	854.2	876.6	2.2

concentrations of Cry j 1-specific IgE in three independent experiments. As the results, the intra-assay CV was found to be 5.3%, 3.4% and 3.1% in the pooled sera of low, intermediate and high IgE groups, respectively. Likewise, the inter-assay CV was 7.2%, 8.0% and 2.2% in the pooled sera of low, intermediate and high IgE groups, respectively (Table 2). These results indicated that the values obtained with the Cry j 1-specific IgE ELISA in this study were highly reproducible and reliable.

4. Discussion

In order to measure an absolute concentration of allergen-specific IgE in canine sera, it is necessary to use a monoclonal antibody that is highly specific to canine IgE. Since there are an excess amount of IgG which share reactive antigen with IgE in the serum (Hill et al., 1995), and that IgE and IgG have high similarities (Patel et al., 1995), IgE measurement will be influenced if the anti-IgE antibody used in the measurement can cross-react to IgG even at a low level. Therefore, an anti-IgE antibody used in the detection of IgE must be highly specific to IgE and required to be confirmed by proper assays so that the antibody does not react to IgG. We first examined the reactivity of the anti-IgE antibody, CRE-DM, especially focusing on the reactivity to canine IgE and IgG. In our study, it was shown that CRE-DM reacted specifically to purified canine IgE and mouse IgE in a dose dependent manner, but not to canine IgG, which was further confirmed by the inhibition ELISA. The specificity of CRE-DM was also confirmed in the ELISA for canine antigen-specific IgE using the serum of an experimentally sensitized dog. Unlike in the other previous studies that evaluated the reactivity of anti-IgE antibody or rhFcεRIα to canine IgE only by heating the serum at 56 °C (Stedman et al., 2001; Lee et al., 2009), we could obtain direct evidence that verified the reactivity of CRE-DM by the combination of ELISA and inhibition ELISA experiments. Also, in a currently ongoing study, we could determine the linear epitope sequence that is recognized by CRE-DM. CRE-DM was found to recognize an epitope located in the CH_3 regions of dog and mouse IgEs that showed high amino acid sequence similarity between both species (Tsukui T., et al., article in preparation). Furthermore, the identical sequence was not found in the amino acid sequence of dog IgG. According to these results, it was concluded that the ELISA using CRE-DM was highly specific for the measurement of canine IgE.

To measure an allergen-specific IgE by a quantitative ELISA, pre-quantified allergen-specific IgE is required as the reference standard for each allergen to be tested. However, the only purified canine allergen-specific IgE reported so far is against filarial antigen (Gebhard et al., 1995). Alternatively, the pooled serum of clinical cases sensitized to an allergen such as Japanese cedar pollen has been used as a reference in a comparative measurement ELISA whose test results were expressed at units/ml (Masuda et al., 2000). However, in a comparative measurement ELISA, the results must be considered as semi-quantitative and, as a drawback of this method, results cannot be compared among different allergens since the references must differ from assay to assay. In contrast, allergen-specific mouse IgE measurement has been implemented for different allergens by establishing pre-quantified allergen-specific monoclonal mouse IgE as reference standards for each allergen (Hamada et al., 2003). Therefore, the results could be expressed in, for example, μg/ml, which enables the comparison of the amount of allergen-specific IgE among different allergens. With this information, we conceived the objective that we could measure canine allergen-specific IgE by using allergen specific mouse IgE as a reference standard if we had an antibody that could cross-react to both canine and mouse IgE. Therefore, it was a great advantage to obtain an anti-IgE antibody, CRE-DM, which was proven to recognize both canine and mouse IgE in a dose dependent manner. In fact, we could quantify Cry j 1-specific IgE in canine sera at ng/ml by using Cry j 1-specific monoclonal mouse IgE as a reference standard in this study. The established method in this study can be applied to other allergen-specific IgE ELISAs by creating pre-quantified allergen-specific mouse IgE to various allergens. For this purpose, we are currently working on to expand the test system to measure allergen-specific canine IgE to various allergens by establishing reference standards using mouse sera sensitized with different allergens. With such a multi-allergen quantification system, it will become possible to compare the exact amount of allergen-specific IgEs among the different allergens in dogs. Since serum IgE levels have been shown to increase and decrease in parallel to allergen exposure (Masuda et al., 2002; Horiguchi et al., 2008), it will become possible to estimate the exposure levels of each allergen at the tested time point by comparing the serum IgE levels among allergens.

We conclude that the results obtained from the anti-Cry j 1 IgE ELISA were reliable since the dispersion of the results obtained by this assay had low CV (3.1–5.2% and 2.2–8.0% in intra- and inter-assay comparisons, respectively). These CV values are low compared to those in a previous report (Lee et al., 2009), which was considered to demonstrate the reliability of this assay. With such a low inter-assay variance among the results, this ELISA could be an appropriate test to monitor the possible seasonal fluctuation of serum allergen-specific IgE in dogs, since the amounts of

serum allergen-specific IgE in dogs were reported to fluctuate depending on seasonal allergen exposure (Masuda et al., 2002; Horiguchi et al., 2008). By monitoring the fluctuations of IgE to seasonal environmental allergens, it is possible to understand which environmental allergen might be associated with the manifestation of clinical signs in each patient at certain time points. This should aid clinicians to define more accurate therapeutic strategies by determining the specific target allergens at each time point. Another possible application of this ELISA is the evaluation of treatment effect of anti-allergic drugs, allergen avoidance and allergen immunotherapy. Efficacies of the therapies can be evaluated by comparing allergen-specific IgE concentrations before and after treatment (van Halteren et al., 1997; Takagi et al., 2005), which will serve as a valuable tool to evaluate the proof of concept of novel therapies under investigation. The other advantage of a quantitative system is the possible introduction of a standardization system by using pre-quantified reference standard as a universal calibrator. It will be beneficial for veterinarians and pet owners if the test results become able to be compared among different tests and the consistency of the test results are validated by a proper standardization program (DeBoer and Hillier, 2001b). Thus, the quantitative measurement of canine antigen-specific IgE utilizing this ELISA could be beneficial in many aspects of veterinary allergy.

A relationship between the concentration of serum antigen-specific IgE and the onset of *in vivo* allergic reaction has not yet been elucidated in dogs. In general, the test results in antigen-specific IgE ELISA have been compared with those from IDT, since IDT was long considered as a gold standard of the diagnosis of allergy (Mueller et al., 1999; Foster et al., 2003). However, in dogs, since IDT has been shown to exhibit false-positive reactions due to sub-clinical hypersensitivity (Pastorello, 1993; Codner and Tinker, 1995) and false negative results due to the insufficient antigen concentrations that are required to provoke *in vivo* reactions (Hensel et al., 2004), it is difficult to consider IDT as the definitive allergy test in dogs (DeBoer and Hillier, 2001b). Because it is advantageous to measure an absolute quantity of serum allergen-specific IgE by this ELISA, we are currently attempting to evaluate the threshold of IgE concentrations that are associated with *in vivo* allergic reactions instead of comparing the results between ELISA and IDT. In a currently on-going study, we have shown that a concentration of 100–200 ng/ml of antigen-specific IgE in dog serum is sufficient to provoke *in vivo* allergic reaction by Prausnitz–Kustner test using experimental dogs (unpublished data). Similar attempts have been made in human medicine to predict the outcome of food provocation test in human patients with food allergy by defining the threshold of serum allergen-specific IgE titers that elicit allergic reactions (Sampson and Ho, 1997; Sampson, 2001; Komata et al., 2009). However, because the levels of allergen-specific IgE are usually measured in specific units (kU_A/L) in human studies, it is not possible to extrapolate the results to dogs. By further accumulating data in dogs, we consider that this ELISA could be useful to determine a threshold concentration of serum IgE that elicit *in vivo* allergic reaction or clinical symptoms of allergy.

To summarize, we have established a novel ELISA system for the quantitative measurement of allergen-specific IgE in ng/ml in dogs. As we could demonstrate the reliability of the ELISA utilizing CRE-DM, we are aiming at the implementation of CRE-DM in multi-allergen IgE test, which might possibly become a standard allergy test. Since the concept of the quantitative measurement of serum allergen-specific IgE by ELISA utilizing CRE-DM can be further applied not only to dogs but also to other animal species including humans, the ELISA has a potential to be expanded to IgE testing in various species. In the future, comparison of the results on a same scale from medical, veterinary and experimental allergy model studies should enhance the understanding of the pathophysiological mechanism of IgE-mediated allergic diseases.

Conflict of interest statement

This study was funded by Animal Allergy Clinical Laboratories, Inc., Kanagawa, Japan. Dr. Masuda is CEO and stock-holder of this company.

Acknowledgement

We would thank Dr. Takashi Saito (Research Center of Allergy and Immunology, RIKEN) for providing monoclonal mouse IgE specific to Cry j 1.

References

Codner, E.C., Tinker, M.K., 1995. Reactivity to intradermal injections of extracts of house dust and housedust mite in healthy dogs and dogs suspected of being atopic. J. Am. Vet. Med. Assoc. 206, 812–816.

DeBoer, D.J., Hillier, A., 2001a. The ACVD task force on canine atopic dermatitis (XVI): laboratory evaluation of dogs with atopic dermatitis with serum-based "allergy" tests. Vet. Immunol. Immunopathol. 81, 277–287.

DeBoer, D.J., Hillier, A., 2001b. The ACVD task force on canine atopic dermatitis (XV): fundamental concepts in clinical diagnosis. Vet. Immunol. Immunopathol. 81, 271–276.

Foster, A.P., Littlewood, J.D., Webb, P., Wood, J.L.N., Rogers, K., Shaw, S.E., 2003. Comparison of intradermal and serum testing for allergen-specific IgE using a Fcepsilon RIalpha-based assay in atopic dogs in the UK. Vet. Immunol. Immunopathol. 93, 51–60.

Gebhard, D., Orton, S., Edmiston, D., Nakagaki, K., DeBoer, D., Hammerberg, B., 1995. Canine IgE monoclonal antibody specific for a filarial antigen: production by a canine × murine heterohybridoma using B cells from a clinically affected lymph node. Immunology 85, 429–434.

Halliwell, R.E., Schemmer, K.R., 1987. The role of basophils in the immunopathogenesis of hypersensitivity to fleas (*Ctenocephalides felis*) in dogs. Vet. Immunol. Immunopathol. 15, 203–213.

Hamada, K., Suzaki, Y., Goldman, A., Ning, Y.Y., Goldsmith, C., Palecanda, A., Coull, B., Hubeau, C., Kobzik, L., 2003. Allergen-independent maternal transmission of asthma susceptibility. J. Immunol. 170, 1683–1689.

Hensel, P., Austel, M., Medlau, L., Zhao, Y., Vidyashankar, A., 2004. Determination of threshold concentrations of allergens and evaluation of two different histamine concentrations in canine intradermal testing. Vet. Dermatol. 15, 304–308.

Hill, P.B., Moriello, K.A., DeBoer, D.J., 1995. Concentrations of total serum IgE, IgA, and IgG in atopic and parasitized dogs. Vet. Immunol. Immunopathol. 44, 105–113.

Hillier, A., DeBoer, D.J., 2001. The ACVD task force on canine atopic dermatitis (XVII): intradermal testing. Vet. Immunol. Immunopathol. 81, 289–304.

Horiguchi, S., Tanaka, Y., Uchida, T., Chazono, H., Ookawa, T., Sakurai, D., Okamoto, Y., 2008. Seasonal changes in antigen-specific T-helper clone sizes in patients with Japanese cedar pollinosis: a 2-year study. Clin. Exp. Allergy 38, 405–412.

Ishida, R., Masuda, K., Sakaguchi, M., Kurata, K., Ohno, K., Tsujimoto, H., 2003. Antigen-specific histamine release in dogs with food hypersensitivity. J. Vet. Med. Sci. 65, 435–438.

Jackson, H.A., Jackson, M.W., Coblentz, L., Hammerberg, B., 2003. Evaluation of the clinical and allergen specific serum immunoglobulin E responses to oral challenge with cornstarch, corn, soy and a soy hydrolysate diet in dogs with spontaneous food allergy. Vet. Dermatol. 14, 181–187.

Komata, T., Söderström, L., Borres, M.P., Tachimoto, H., Ebisawa, M., 2009. Usefulness of wheat and soybean specific IgE antibody titers for the diagnosis of food allergy. Allergol. Int. 58, 599–603.

Lee, K.W., Blankenship, K.D., McCurry, Z.M., Esch, R.E., DeBoer, D.J., Marsella, R., 2009. Performance characteristics of a monoclonal antibody cocktail-based ELISA for detection of allergen-specific IgE in dogs and comparison with a high affinity IgE receptor-based ELISA. Vet. Dermatol. 20, 157–164.

Masuda, K., Sakaguchi, M., Saito, S., Deboer, D.J., Fujiwara, S., Kurata, K., Yamashita, K., Hasegawa, A., Ohno, K., Tsujimoto, H., 2000. In vivo and in vitro tests showing sensitization to Japanese cedar (*Cryptomeria japonica*) pollen allergen in atopic dogs. J. Vet. Med. Sci. 62, 995–1000.

Masuda, K., Sakaguchi, M., Saito, S., Yamashita, K., Hasegawa, A., Ohno, K., Tsujimoto, H., 2002. Seasonal atopic dermatitis in dogs sensitive to a major allergen of Japanese cedar (*Cryptomeria japonica*) pollen. Vet. Dermatol. 13, 55–61.

Mueller, R.S., Burrows, A., Tsohalis, J., 1999. Comparison of intradermal testing and serum testing for allergen-specific IgE using monoclonal IgE antibodies in 84 atopic dogs. Aust. Vet. J. 77, 290–294.

Pastorello, E.A., 1993. 3. Skin tests for diagnosis of IgE-mediated allergy. Allergy 48, 57–62.

Patel, M., Selinger, D., Mark, G.E., Hickey, G.J., Hollis, G.F., 1995. Sequence of the dog immunoglobulin alpha and epsilon constant region genes. Immunogenetics 41, 282–286.

Sampson, H.A., 2001. Utility of food-specific IgE concentrations in predicting symptomatic food allergy. J. Allergy Clin. Immunol. 107, 891–896.

Sampson, H.A., Ho, D.G., 1997. Relationship between food-specific IgE concentrations and the risk of positive food challenges in children and adolescents. J. Allergy Clin. Immunol. 100, 444–451.

Stedman, K., Lee, K., Hunter, S., Rivoire, B., McCall, C., Wassom, D., 2001. Measurement of canine IgE using the alpha chain of the human high affinity IgE receptor. Vet. Immunol. Immunopathol. 78, 349–355.

Takagi, H., Hiroi, T., Yang, L., Tada, Y., Yuki, Y., Takamura, K., Ishimitsu, R., Kawauchi, H., Kiyono, H., Takaiwa, F., 2005. A rice-based edible vaccine expressing multiple T cell epitopes induces oral tolerance for inhibition of Th2-mediated IgE responses. Proc. Natl. Acad. Sci. U.S.A. 102, 17525–17530.

van Halteren, H.K., van der Linden, P.W., Burgers, J.A., Bartelink, A.K., 1997. Discontinuation of yellow jacket venom immunotherapy: follow-up of 75 patients by means of deliberate sting challenge. J. Allergy Clin. Immunol. 100, 767–770.

Yamashita, K., Masuda, K., Sakaguchi, M., Odagiri, T., Nakao, Y., Yamaki, M., Hasegawa, A., Matsuo, Y., Deboer, D.J., Ohno, K., Tsujimoto, H., 2000. Experimental sensitization with Japanese cedar pollen in dogs. J. Vet. Med. Sci. 62, 1223–1225.

Zur, G., Ihrke, P.J., White, S.D., Kass, P.H., 2002. Canine atopic dermatitis: a retrospective study of 266 cases examined at the University of California. Davis, 1992–1998. Part I. Clinical features and allergy testing results. Vet. Dermatol. 13, 89–102.

犬の緑内障および白内障の遺伝子解析

１．犬の緑内障の遺伝子解析

印牧信行、川原井晋平（麻布大学小動物臨床)、阪口雅弘（麻布大学微生物学第１）

研究要旨

緑内障は眼圧上昇を伴う視神経疾患である。原発性開放隅角緑内障がイヌ緑内障として最も典型的であり、シバイヌとシーズーが好発犬種である。これらの犬種では異常な虹彩角膜角と櫛状靭帯の発育不全が認められるが、遺伝学的背景は解明されていない。緑内障群と健常群のシバイヌ・シーズーの SRBD1、ELOVL5、ADAMTS10 遺伝子の SNP（一塩基多型）11 か所をダイレクトシーケンシング法で解析した。SRBD1 遺伝子について、シバイヌでは 3 か所の SNP（rs8655283, rs22018514, rs22018513）で、シーズーでは 1 か所の SNP（rs9172407）で、緑内障群と健常群の間に有意差を認めた。ELOVL5 遺伝子と ADAMTS10 遺伝子では有意差がなかった。このことより、SRBD1 遺伝子はシバイヌとシーズーさらにはヒトに共通した緑内障感受性遺伝子である可能性が示唆された。また、SRBD1 遺伝子の SNP 検査はイヌの緑内障発症リスクを予測できる検査法として有望と考えられた。

研究目的

緑内障は眼圧上昇を伴う視神経疾患であり、視野狭窄、神経節細胞の壊死、視神経変性などを伴う。緑内障は開放隅角緑内障（POAG)、閉鎖隅角緑内障（PCAG)、先天性緑内障（PCG）に分類され、POAG が最も一般的である。日本人では眼圧が上昇しない正常眼圧緑内障（NTG）の発症が多い。CYP1B1、MYOC、OPTN、OPTC 遺伝子はヒトとイヌの POAG、PCG との相関性について広く研究されている。日本緑内障学会の研究グループは日本人の NTG 感受性遺伝子として SRBD1、ELOVL5 遺伝子が候補となることを報告した。イヌ緑内障に関する研究は約 50 年前からあり、最近ではビーグル犬の緑内障候補遺伝子として ADAMTS10 の Gly661Arg が報告されている。加藤らは 29 犬種を比較し、POAG の好発犬種第 1 位がシバイヌ、第 2 位がシーズーであることを報告したが、遺伝学的背景は解明されていない。本研究ではシバイヌ、シーズーの緑内障候補遺伝子として SRBD1、ELOVL5、ADAMTS10 遺伝子に着目し解析を行うことを目的とした。

材料と方法

緑内障の診断：麻布大学附属動物病院を来院したシバイヌ 98 匹、シーズー67 匹を対象とした。両眼にベノキシールを点眼して局部麻酔を施し、眼圧をトノペンで測定した。眼圧 25mmHg 以上の個体を緑内障、25mmHg 未満の個体を健常と判定した。シバイヌ 42

匹とシーズー40匹が健常、シバイヌ56匹とシーズー27匹が緑内障と診断された。4歳以下のイヌは除外した。

DNAの精製：頚静脈より血液を採取し、DNA全血キット・スピン法（FUJI FILM社）でDNAを精製した。DNAの濃度と純度をGeneQuant Pro（GEヘルスサイエンス社）で測定した。

DNA塩基配列の決定：SRBD1遺伝子のSNP（rs22019922, rs8655283, rs22018514, rs22018513, rs9172407）、ELOVL5遺伝子のSNP（rs22226301, rs9194033, rs22202438, rs8643563, rs22194174）合わせて10か所を解析した。 ADMTS10遺伝子についてはGly661Arg（56097365 G>A)を解析した。PCRプライマーを表1に示す。PCR産物を1%アガロースゲルで電気泳動し、シングルバンドを切り出して-80℃で凍結した。サンプルを溶解し、Qiagen Dye Ex 2.0 スピンキット（QIAGEN社）でDNAを精製した。High Dye Mix（ライフテクノロジーズ社）を添加しサイクルシーケンシングを実施した。サンプルをシーケンシングチューブに移し、ABI 310 DNA Analyzer（ライフテクノロジーズ社）で塩基配列を解析した。

統計解析：緑内障群と健常群のSNPをHardy-Weinberg平衡で検定した。緑内障群と健常群のアレル頻度をχ自乗検定で評価した。メタ解析のための P 値とオッズ比をMantel-Haenszel法で検定した。 LD統計にはHaploview 4.1プログラムを使用した。ロジステック回帰分析にはPLINKを使用した。

結果および考察

緑内障群と健常群の平均年齢はシバイヌでは8.5±2.9歳と10.0±3.0歳、シーズーでは9.2±2.0歳と10.1±2.5歳であった。シバイヌ98匹とシーズー67匹のSRBD1、ELOVL5、ADAMTS10遺伝子の多型をダイレクトシーケンシング法で解析した（表１）。

表２はSRBD1遺伝子の5か所のSNPの解析結果を示す。シバイヌではrs22018513で最も強い相関（P=0.00039）を示し、Gアレルは緑内障リスクが3.03倍になることが判明した。rs8655283のTアレルが2.20倍（P=0.016）とrs22018514のGアレルが2.56倍（P=0.0037）リスクが高くなることが判明した。シーズーではrs9172407のGアレルが5.25倍（P=0.0014）リスクが高くなることが判明したが、シバイヌでは有意差とならなかった。シーズーではrs8655283のTアレル、rs22018514のGアレル、rs22019922のAアレルでオッズ比がそれぞれ2.43、2.43、2.49倍高くなったが有意差には至らなかった。

図１はSRBD1遺伝子の5か所のSNPのLDブロックを示す。シバイヌではrs8655283、rs22018514、rs22018513 の D'値が 0.78 以上と有意な相関を示した。シーズーではrs22019922とrs22018513のD'値は0.68以上と有意な相関を示した。

シバイヌ緑内障発症へのrs8655283、rs22018514、rs22018513の影響を解明するためロジスティック回帰分析を行った結果を表３に示す。rs22018513の関与が最も高いこと

が判明した。

表 4 は ELOVL5 と ADAMTS10 遺伝子の解析結果である。ELOVL5 遺伝子の rs9194033 と rs22202438 はシバイヌ、シーズーともに多型であったが緑内障との相関はなかった。ELOVL5 と ADAMTS10 遺伝子のその他の SNP では多型が存在しなかった。

この研究の目的は SRBD1、ELOVL5、ADAMTS10 遺伝子の全 11 か所の SNP のシバイヌ・シーズー緑内障発症への関与を解析することであった。その結果、シバイヌでは SRBD1 遺伝子のエクソン 4 に存在する rs22018513 が、シーズーではイントロン 1 に存在する rs9172407 が緑内障発症と有意な相関性を示し、緑内障感受性候補遺伝子と考えられた。BLAST 解析ではイヌ SRBD1 遺伝子はヒト SRBD1 遺伝子と 90%の相同性を示した。イヌ SRBD1 遺伝子の rs22018513 と rs9172407 に相当する配列はヒト SRBD1 遺伝子のエクソン 4 とイントロン 1 に存在するが SNP としては報告されていない。ヒト NTG 感受性候補遺伝子である SRBD1 遺伝子の rs32137871 はイントロン 17 に位置するが、エクソン 4 とイントロン 1 との連鎖が非常に強い。ヒト SRBD1 遺伝子のさらなる解析が必要である。

SRBD1 遺伝子は最初に大腸菌の S1 RNA 結合性ドメインとして発見され、ヒトでは DNA 結合性タンパク質の一部分と考えられている。ヒトとイヌの SRBD1 遺伝子の機能は不明である。イヌ SRBD1 は第 10 染色体に逆配列として存在する全長 186kb の遺伝子であり、3kb のエクソンを含む。マウスでは網膜神経節細胞への局在が知られているがイヌでの報告はない。

今回発見した rs22018513 と rs9172407 の変異はエクソン同義的置換とイントロン変異であり、遺伝子の発現に関連していると考えられた。ヒトでの研究のように mRNA レベルの解析が必要である。SRBD1 は間接的には細胞増殖、タンパク質合成、アポトーシス誘導、ホメオスタシスに関与することが知られており、SRBD1 の活性化は網膜神経節細胞の細胞死から緑内障を惹起すると考えられた。

ELOVL5 は長鎖不飽和脂肪酸の生合成に関与することが報告されている。日本緑内障学会研究グループはヒト ELOVL5 遺伝子が NTG 感受性遺伝子の候補であることを報告したが、この研究ではイヌ緑内障との相関性はなかった。これはヒト（NTG）とイヌ（POAG）の緑内障タイプの相違によると考えられる。一方、SRBD1 遺伝子はヒトとイヌの緑内障に共通していた。よってイヌ緑内障発症における SRBD1 遺伝子の機能を解明すればヒト緑内障の発症メカニズム解明につながる可能性があり、イヌが好適な動物モデルになると思われる。

加藤らの報告によるとビーグル犬はシバイヌ、シーズー、アメリカンコッカースパニエルに続く 4 番目の緑内障好発犬種である。Kuchtey らは最近、ビーグル犬 POAG 関連遺伝子として ADAMTS10 の Gly661Arg 変異を報告した。我々もこの SNP をシバイヌとシーズーで検査したが、変異を確認できず犬種に依存した SNP と考えられた。Kuchtey らは最近さらにこの SNP がビーグル犬特異的であり、他の犬種では存在しないことを報告した。イヌ遺伝子データベースでは ADAMTS10 遺伝子に 16 か所 SNP が存在する

ことがわかっており、これら SNP の緑内障との相関性を解析する必要がある。

イヌ緑内障発症を予想する有力な遺伝子検査方法はまだない。我々が今回シバイヌとシーズーで発見した SNP は緑内障遺伝子検査対象として有力と考えられた。しかし、どのような機構でイヌ緑内障が起きるかの研究は大きな課題である。ヒトとイヌでの SRBD1 遺伝子の機能のさらなる研究は緑内障の発症リスクの予測、予防医学、治療方法の樹立に大きく貢献すると期待される。また、SRBD1 遺伝子検査により、イヌの緑内障を早期に正確に診断することが可能となる。すでに緑内障を発症した個体では確定診断が可能となり、積極的な治療を早期に開始することで失明の危機を回避できる可能性も考えられる。

表 1　緑内障遺伝子解析に用いたプライマーの塩基配列

Gene	Allele	5′-3′ Forward	5′-3′ Reverse
SRBD1	rs22019922	TGTTGGTGTTGTCAGCAAGT	TCACACTCTTTCTCTCACTCTCTC
	rs8655283	TTAGGATGAAACCATGGAAC	TTGGCGATTTATTGAACTAAC
	rs22018513, rs22018514	GCTATTGCTGATGTTGATTTG	TGCAGTGCTGGCCCTGTTGGA
	rs9172407	GTGAACCTGAAATGGCAAA	TTAACTAGCTTCCTTGCTTCC
ELOVL5	rs22226301	AGTTGTGCTGCTTACATTAGG	AGCAAGGCAAGATGTGTTC
	rs9194033	AGTGATGCTGCTATGGGATG	GCTCAGGTCATGGGATCAAG
	rs22202438	CATGCTGAACATCTGGTGGT	GCTGGTCTGGATGATTGTCA
	rs8643563	AATTGTATGGCTGGGACCAA	ACCACCAGAGGACACGGATA
	rs22194174	AATGCTTATCCTACCCAATC	TCAGGCTCTATGCTCAGTG
ADAMTS10	Gly661Arg (56097365 G>A)	CACAGAGCAAGCAGGGAGT	GGGTGGAAGTGGGAGTG

doi:10.1371/journal.pone.0074372.t001

表 2　SRBD1 遺伝子解析結果

SNP ID	Chr.	Position (CanFam2.0)	Allele	SNP Type	Risk Allele	Breed	N		Risk Allele Frequency (%)		P	OR(95% CI)
							Cases	Controls	Cases	Controls		
rs22019922	10	50924623	A/C	Intron	A	Shiba-Inu	56	42	8.9	7.1	0.65	1.27 (0.44–3.66)
						Shih-Tzu	27	40	96.3	91.3	0.25	2.49(0.50–12.49)
						Overall	83	82			0.40	1.59 (0.66–3.80)
rs8655283	10	50989281	C/T	Intron	T	Shiba-Inu	56	42	37.5	21.4	0.016	2.20 (1.15–4.20)
						Shih-Tzu	27	40	92.6	83.8	0.13	2.43 (0.75–7.89)
						Overall	83	82			0.0068	2.25 (1.28–3.97)
rs22018514	10	51,049,600	C/G	Non-synonymous	G	Shiba-Inu	56	42	41.1	21.4	0.0037	2.56 (1.34–4.86)
						Shih-Tzu	27	40	92.6	83.8	0.13	2.43 (0.75–7.89)
						Overall	83	82			0.0018	2.52 (1.43–4.44)
rs22018513	10	51,049,604	A/G	Synonymous	G	Shiba-Inu	56	42	78.6	54.8	0.00039	3.03 (1.62–5.65)
						Shih-Tzu	27	40	94.4	93.8	0.87	1.13 (0.26–4.95)
						Overall	83	82			0.0015	2.59 (1.46–4.61)
rs9172407	10	51062753	A/G	Intron	G	Shiba-Inu	56	42	8.9	6.0	0.44	1.55 (0.51–4.71)
						Shih-Tzu	27	40	25.9	6.3	0.0014	5.25 (1.76–15.63)
						Overall	83	82			0.0074	2.90 (1.34–6.26)

OR, odds ratio; CI, confidence interval.
Overall P values and ORs for meta-analysis were calculated using the Mantel-Haenzel method.
doi:10.1371/journal.pone.0074372.t002

図１　SRBD1 遺伝子の LD ブロック（A はシバイヌ、B はシーズーの結果を示す）

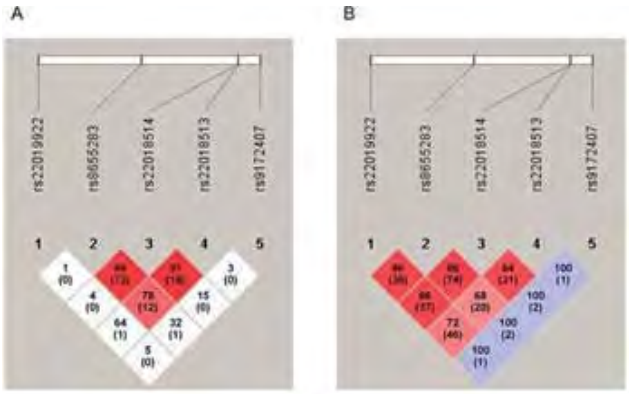

表３　シバイヌ SRBD1 遺伝子のロジスティック回帰分析

SNP ID	Risk Allele	Model	P*	P**		
				Covariates		
				rs8655283	rs22018514	rs22018513
rs8655283	T	Additive	0.021	–	0.92	0.15
rs22018514	G	Additive	0.0066	0.13	–	0.10
rs22018513	G	Additive	0.00025	0.0010	0.0021	–

*P values for each SNP under the recessive, additive, or dominant model that provided the best fit by logistic regression analysis. The lowest P value was selected as the best fit model. The indicated model showed the lowest P value for each SNP.
**P values adjusted for each SNP under the indicated model by conditional logistic regression analysis.
doi:10.1371/journal.pone.0074372.t003

表４　ELOVL5 遺伝子と ADAMTS10 遺伝子の解析結果

SNP ID	Chr.	Position (CanFam2.0)	Gene	Allele	SNP Type	Risk Allele*	Breed	N		Risk Allele Frequency (%)		P	OR (95% CI)
								Cases	Controls	Cases	Controls		
rs22226301	12	20733716	ELOVL5	C/T	3'UTR	T	Shiba-Inu	56	42	0.0	0.0	–	–
							Shih-Tzu	27	40	0.0	0.0	–	–
							Overall	83	82			–	–
rs9194033	12	20739417	ELOVL5	A/G	Intron	G	Shiba-Inu	56	42	33.9	26.2	0.25	1.45 (0.78–2.70)
							Shih-Tzu	27	40	55.6	68.8	0.12	0.57 (0.28–1.16)
							Overall	83	82			0.99	0.97 (0.61–1.54)
rs22202438	12	20743516	ELOVL5	A/G	Synonymous	G	Shiba-Inu	56	42	35.7	28.6	0.29	1.39 (0.75–2.56)
							Shih-Tzu	27	40	59.3	68.8	0.26	0.66 (0.32–1.36)
							Overall	83	82			0.98	1.02 (0.64–1.62)
rs8643563	12	20744701	ELOVL5	(–)/T	Frameshift coding	T	Shiba-Inu	56	42	0.0	0.0	–	–
							Shih-Tzu	27	40	0.0	0.0	–	–
							Overall	83	82			–	–
rs22194174	12	20749077	ELOVL5	A/C	Intron	A	Shiba-Inu	56	42	0.0	0.0	–	–
							Shih-Tzu	27	40	0.0	0.0	–	–
							Overall	83	82			–	–
Gly661Arg	20	56097365	ADAMTS10	A/G	Non-synonymous	A	Shiba-Inu	56	42	0.0	0.0	–	–
(56097365 G>A)							Shih-Tzu	27	40	0.0	0.0	–	–
							Overall	83	82			–	–

OR, odds ratio; CI, confidence interval.
Overall P values and ORs for meta-analysis were calculated using the Mantel-Haenzel method.
*Risk allele is for Shiba-Inu dogs.
doi:10.1371/journal.pone.0074372.t004

２．犬の白内障の遺伝子解析

印牧信行、川原井晋平（麻布大学附属動物病院）阪口雅弘、岡本憲明、高瀬有加里（麻布大学微生物学第１）

研究要旨

アメリカン・コッカー・スパニエルは若年性白内障における原因遺伝子の遺伝子解析を行った。以前からボストン・テリアなどで報告のあった遺伝子の変異は認められなかった。若年性白内障アメリカン・コッカー・スパニエルを DNA 採取順位に A と B の 2 つの集団に分けて解析をおこなった。A 集団においては網羅的な SNP アレーを行い、15 番染色体上の rs22428454(エンドセリン受容体タイプ A 遺伝子)と 31 番染色体上の遺伝子非コード領域 rs23685575（遺伝子非コード領域）が発症との関連を示唆する結果が得られた。しかし、B 集団においてはこの結果の再現性が得られなかった。

研究目的

アメリカン・コッカー・スパニエルは若年性白内障の好発犬種と知られている。若年性白内障は生後 3 歳くらいまでに水晶体の混濁を示し、視力が失われる疾患で常染色体性劣性遺伝と考えられているが原因遺伝子は不明である。本研究はアメリカン・コッカー・スパニエルにおける若年性白内障の原因遺伝子を検討するためにこの犬の若年性白内障の DNA を収集し、網羅的な SNP アレーを行い、その遺伝子解析を行った。

材料と方法

麻布大学附属動物病院に紹介されたアメリカン・コッカー・スパニエル犬で若年性白内障と診断された例を陽性例、若年性白内障を発症していない例を陰性例とした。最初に採取された陽性例 32 例、陰性例 8 例を A 集団とした。また、A 集団とは別に収集された陽性例 17 例、陰性例 16 例を B 集団とした。これらの犬から DNA を精製し、A 集団において網羅的な解析として SNP アレー（イルミナ社）を行った。その SNP 解析の結果から得られた所見から若年性白内障との関連が疑われる SNP を含むエンドセリン受容体タイプ A 遺伝子のエクソン部分の全遺伝子のシークエンスを A 集団の中から陽性例 21 例、陰性例 5 例を選んで調べた。また、SNP 解析の結果から得られた関連する遺伝子の SNP について別の集団である B 集団において遺伝子解析を行い、網羅的な SNP アレーの結果の確認を行った。

結果および考察

これまでに遺伝性白内障の原因遺伝子としては、ボストン・テリア、オーストラリアン・シェパード、スタッフォードシャー・ブル・テリアにおいて、Heat shock transcription

factor 4 遺伝子の変異が報告されている。これはこの遺伝子のエクソン９にある C が一塩基欠失して、その結果、フレームシフトがおこり、停止コドンが出現するというものであった。本研究において A 集団の若年性白内障の２５例について同じ変異が存在するか調べた。本研究において２５例すべて C 遺伝子の欠損は認められなかった。そのことからアメリカン・コッカー・スパニエル犬の若年性白内障はこれまでの報告とは異なる遺伝子変異で起こることが考えられた。

アメリカン・コッカー・スパニエル犬で若年性白内障と診断された例を陽性例、若年性白内障を発症していない例を陰性対照とした。最初に採取された陽性例 32 例、陰性例 8 例を網羅的な SNP アレーを行い、15 番染色体上の rs22428454(エンドセリン受容体タイプ A 遺伝子)と 31 番染色体上の遺伝子非コード領域 rs23685575（遺伝子非コード領域）が発症との関連を示唆する結果が得られた（図 1、表１）。

エンドセリン受容体タイプ A 遺伝子は７つのエクソンからなり、rs22428454 はエクソン１とエクソン２の間のイントロン領域に存在する（図２）。エンドセリン受容体にリガンドが結合すると、細胞内や細胞膜の Ca2＋チャネルが開放し、細胞内に Ca2＋が蓄積する。白内障水晶体内では Ca 濃度上昇がみられると、カルパイン（Ca によって活性するタンパク質分解酵素）によるクリスタリンの分解が亢進して水晶体の白濁化が起こると可能性がある。Ca 濃度に関わるエンドセリン受容体の異常は、白内障発症に関与する可能性が考えられた。これらのことからアメリカン・コッカー・スパニエルの白内障犬陽性例 21 例、陰性例 5 例のエンドセリン受容体タイプ A 遺伝子の全遺伝子配列の解析を行った。しかし、エクソン部分において他の変異は認められなかった。このエンドセリン受容体タイプ A 遺伝子のエクソン部分の遺伝子変異が白内障発症に関与する可能性は低いと考えられた。

図1　白内障犬のSNP解析（マンハッタンプロット）

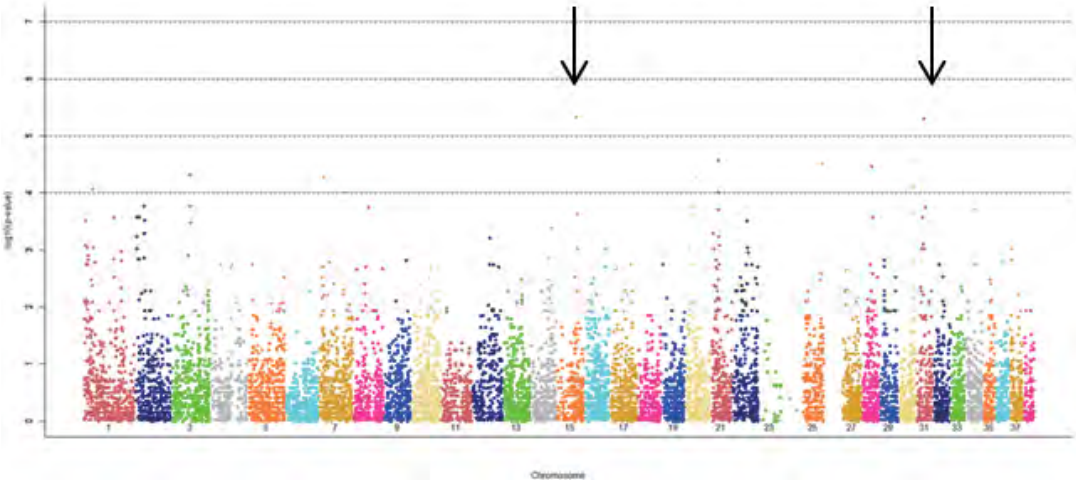

表１　白内障犬で高頻度に認められた SNP

CHR	BP	SNP	UNADJ	GC	BONF	HOLM
15	48. 862. 110	rs22428454	4. 75E-06	0. 00034	0. 06241	0. 06241
31	19. 139. 335	rs23685575	4. 99E-06	0. 00035	0. 06562	0. 0656
21	21. 080. 729	rs22920405	2. 69E-05	0. 00101	0. 3542	0. 3541
30	37. 955. 437	rs23659856	2. 69E-05	0. 00101	0. 3542	0. 3541
25	50. 884. 804	rs23231304	3. 13E-05	0. 00111	0. 4114	0. 4113
28	24. 817. 869	rs23394020	3. 46E-05	0. 00118	0. 4546	0. 4544

図2　エンドセリン受容体タイプA遺伝子の構造

研究発表

１．論文発表

1) 印牧信行、市川陽一朗、川原井晋平、落合秀治．麻布大学眼科に来院した緑内障症例の随伴症の分類、日本獣医師会雑誌、68、55-58、2015.

2) Kanemaki N, Tchedre K T, Imayasu M, Kawarai S, Sakaguchi M, Yoshino A, Itoh N, Meguro A, Mizuki N.: Dogs and humans share a common susceptibility gene SRBD1 for glaucoma risk. PLoS One, 8, 9, e74372, 2013.

2. 学会発表

1) Ota N, Kanemaki N, Tsujita H, Kobayashi Y, Abe M, Takimoto Y, Imayasu M, Meguro A, Mizuki N. Associations of single-nucleotide polymorphisms of SRBD1 gene 64 with glaucoma in Shiba-inu dog: A meta-analysis in six Japanese veterinary hospitals. ACVO Annual meeting, Coeur d’ Alene, ID, USA, Oct, 2015.

2) Imayasu M, Kanemaki N, Meguro A, Mizuki N. A novel single nucleotide polymerism asocial woth glaucoma in Shiba-inu and Shih-Tzu dogs, ARVO Annual Meeting, Orlando, FL, USA, May, 2014.

3) Kanemaki N, Tchedre KT, Imayasu M, Meguro A, Mizuki N. Identification of S1 RNA binding domain-1 SRBD1 as a major gene determing glaucoma in dogs. ARVO Annual Meeting, Seattle, WA, USA, May, 2013.

原　著

麻布大学眼科に来院した緑内障症例の随伴症の分類

印牧信行[1)]　市川陽一朗[2)]　川原井晋平[1)]　落合秀治[3)†]

1）麻布大学附属動物病院（〒252-5201　相模原市中央区淵野辺 1-17-71）
2）千葉県　開業（いちかわ動物病院：〒270-0011　松戸市根木内 168-1）
3）麻布大学生物科学総合研究所（〒252-5201　相模原市中央区淵野辺 1-17-71）

（2013 年 1 月 30 日受付・2014 年 9 月 22 日受理）

要　　約

麻布大学眼科に来院した犬の緑内障症例の発生状況と随伴症について調べた．1994 年 4 月から 2011 年 12 月までに麻布大学附属動物病院眼科に来院した犬2,981頭を対象とした．柴犬の緑内障罹患率は，来院数の上位21犬種のうちで，最も高かった（84 頭 /196 頭＝42.9%）．柴犬の緑内障眼 121 眼において，角膜混濁 57 眼（47.1%），眼球拡張 102 眼（84.3%），網膜視神経乳頭の萎縮及び陥凹 66 眼（54.5%），水晶体脱臼 50 眼（41.3%）が認められた．眼球拡張，視神経乳頭萎縮，水晶体脱臼を示す緑内障眼は高眼圧値を示した．水晶体脱臼を示す緑内障眼の 90%は水晶体亜脱臼であった．――キーワード：臨床徴候，緑内障，柴犬．

日獣会誌　68，55～58（2015）

緑内障は眼圧上昇に起因して視覚障害をもたらす疾患で，犬種依存性の高い眼科疾患の一つであることが知られる［1-3］．その罹患犬種には，アメリカンコッカースパニエル，ビーグル，バゼットハウンド，チャウチャウ，シャーペイ，ボストンテリア，ワイヤーフォックステリア，柴犬などがある［4, 5］．

緑内障の臨床徴候は病期によって変化し，急性期には赤目，角膜浮腫，突発的な視覚喪失がみられ，次いで慢性期には急性期の症候に加えて，網膜視神経乳頭の陥凹または萎縮，眼球拡張や水晶体脱臼がみられる［1］．

緑内障好発犬種では原発緑内障と続発緑内障が混在して発症することがある．また，原発緑内障は犬種間で，発症年齢，性差及び発症病態は異なる［2］．そのため，犬種間における緑内障の発生状況は，日常診療で遭遇する臨床所見を知る重要情報と考えられる．

そこで，今回，麻布大学附属動物病院眼科に来院した緑内障の発生状況と緑内障における随伴所見について調査した．

材 料 及 び 方 法

1994 年 4 月から 2011 年 12 月までに麻布大学附属動物病院眼科に来院した 2,981 頭を対象とした．眼疾患症例の集計は重複集計を避けるため，複数の診断名を有する症例では主原因あるいは症候が重度であった原因の疾患を診断名として集計した．緑内障症例は臨床症候と眼圧値 25mmHg 以上を示したものを緑内障と診断した．眼圧測定は眼圧計（TONO-PEN XL, Reichert, U.S.A.）を用いて，午前 9 時から午後 5 時までの外来診療時間帯で計測した．また，今回の調査では初診来院時に眼圧値が記録されていなかった症例で臨床症候，病歴から診断された緑内障を症候性緑内障とした．これらの症例はすべて，カルテの記載データ及び記録写真の所見から判断した．随伴所見は角膜混濁，眼球拡張，眼底像の視神経乳頭所見，水晶体脱臼について調べた．角膜混濁の程度は，肉眼では認めがたく細隙灯顕微鏡で識別可能な軽度の混濁を軽度，虹彩が透視できる中等度の混濁を中等度，また虹彩や瞳孔が見えない重度の混濁を重度とした．さらに，眼球拡張は肉眼的に明らかな症例とし，また水晶体脱臼は完全脱臼と亜脱臼のものに分類し，脱臼した位置について記録した．視神経乳頭所見は，乳頭の萎縮，陥凹と正常所見に分類とした．

統計処理：来院頻度及び症例の頻度はフィッシャーの直接確率検定または分割表分析で行った．また随伴所見における眼圧値の有意差検定は Welch の *t* 検定並びに Scheff 多重比較法で行った．

† 連絡責任者：落合秀治（麻布大学生物科学総合研究所）
〒252-5201　相模原市中央区淵野辺 1-17-71　☎ 042-754-7111　FAX 042-754-9930
E-mail : ochiaih@azabu-u.ac.jp

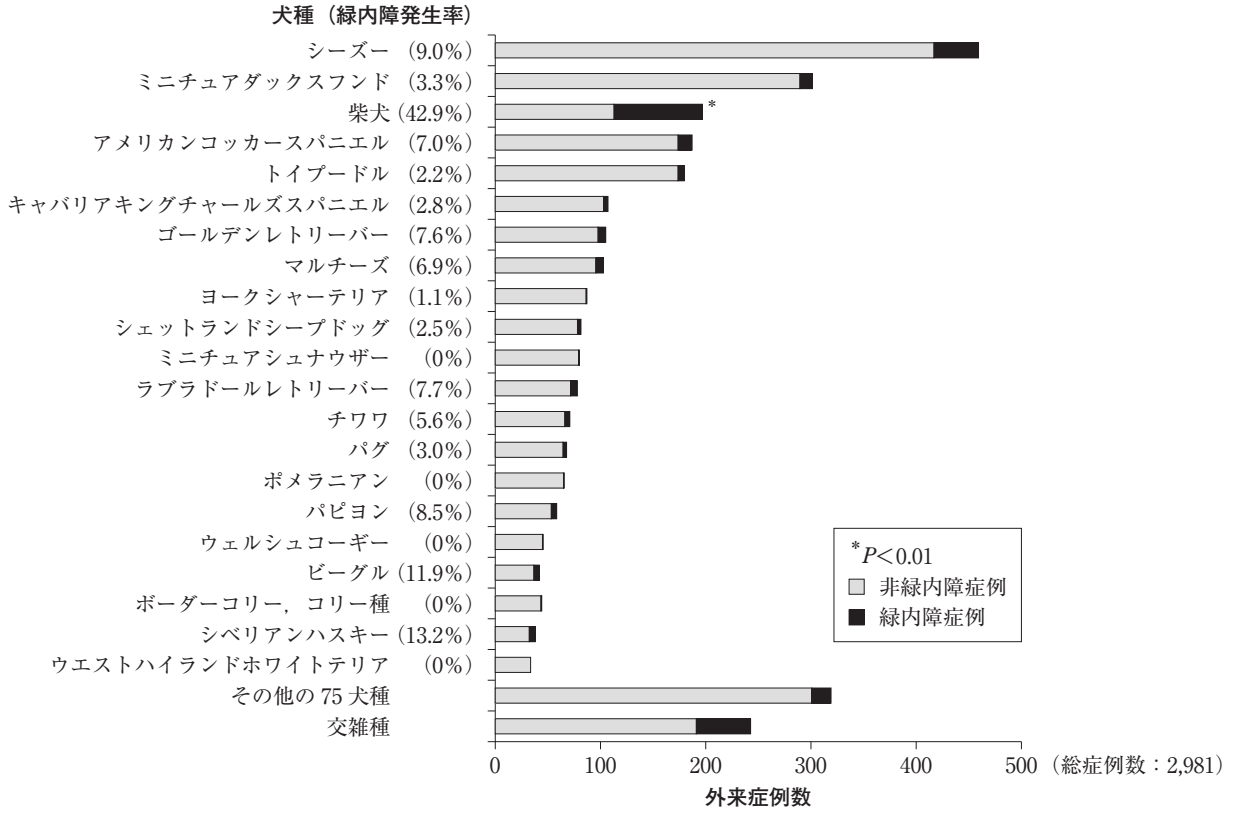

図1　犬種間における緑内障発生状況

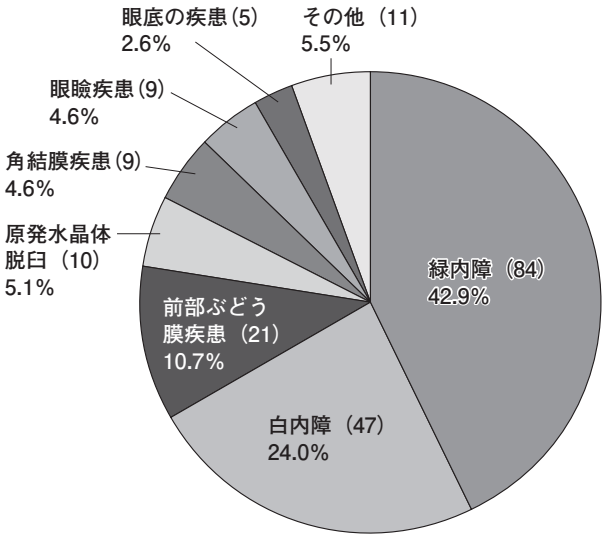

図2　柴犬の眼科疾患の発生頻度

表1　柴犬緑内障における患側眼，性及び年齢

分類	N	罹患眼数			性		初診来院年齢
	頭（眼）	片側性（右眼）	片側性（左眼）	両側性（両眼）	雄	雌	（平均±標準偏差）
緑内障症例	53（73）	20	13	40	21	32	7.4±2.38
症候性緑内障症例	20（26）	7	7	12	8	12	7.8±2.78
混合症例*	11（22）	—	—	22	5	6	7.5±1.75
計	84（121）	27	20	74	34	50	7.5±2.39

＊：1眼は緑内障で，他眼が症候性緑内障眼である症例

成　　績

犬種間における緑内障発生状況を調べた（図1）．その結果，緑内障の来院頻度は来院上位21犬種のうち，柴犬42.9%，シベリアンハスキー13.2%，ビーグル11.9%，シーズー9.0%，パピヨン8.5%の順にみられ，柴犬の緑内障罹患率は他の上位20犬種との間で有意に高かった（$P<0.01$）．また，柴犬196頭において緑内障と他の眼科疾患との来院状況（図2）をみると，緑内障が42.9%で第1位，次いで，白内障が24.0%，前房出血を含む前部ぶどう膜疾患10.7%，原発水晶体脱臼5.1%，角結膜疾患4.6%，眼瞼疾患4.6%，眼底の疾患2.6%，その他5.5%が認められた．

次いで柴犬緑内障における患眼の左右差，性差並びに初診来院年齢を調べた（表1）．調査対象とした緑内障は緑内障症例53頭73眼，症候性緑内障症例20頭26眼，その混合症例11頭22眼の計84頭121眼であった．緑内障症例と症候性緑内障症例において，性差，患眼の左右差はみられなかった．また，初診来院年齢は全体とし

表2　柴犬の緑内障眼及び症候性緑内障眼における随伴所見

所見		緑内障眼（N＝84）			緑内障眼及び症候性緑内障眼（N＝121）	
		N	（%）	眼圧値（mmHg）	N	（%）
角膜混濁の程度	重度	20	23.8	42.2±7.63	37	30.6
	中等度	13	15.5	40.9±10.14	18	14.9
	軽度	2	2.4	46.5±2.12	2	1.6
	なし	49	58.3	40.2±8.52	64	52.9
眼球拡張	ある	68	81.0	43.6±6.91[a]	102	84.3
	なし	16	19.0	29.5±3.80[a]	19	15.7
網膜視神乳頭所見	萎縮	38	45.2	44.7±6.92[a]	56	46.3
	陥凹	8	9.5	39.6±10.06[b]	10	8.2
	正常	13	15.5	30.2±3.85[a, b, c]	14	11.6
	判定*不能	25	29.8	41.1±7.25[c]	41	33.9
水晶体脱臼	完全脱臼	3	3.6	43.7±8.33	5	4.1
	亜脱臼	32	38.1	43.8±8.21[a]	45	37.2
	なし	49	58.3	38.8±8.24[a]	71	58.7

a–c：2群及び多重比較検定において，同一文字の間で有意差（$P<0.05$）を認める．

＊透光体の混濁により観察されなかった．

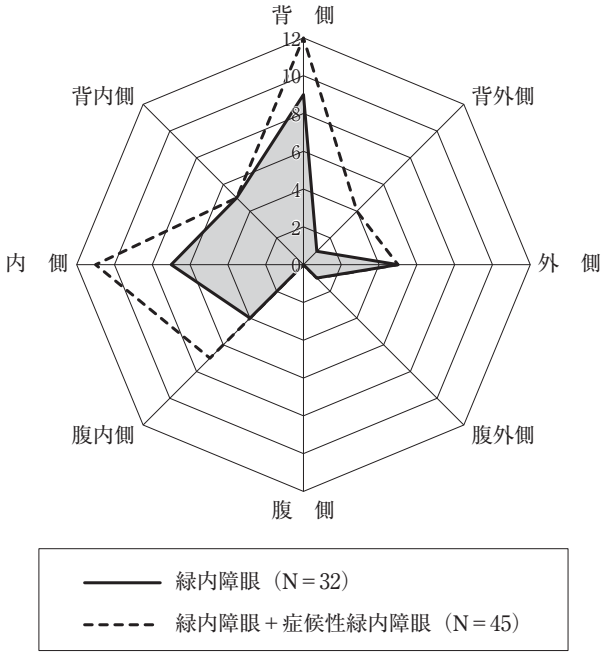

図3　柴犬緑内障における水晶体亜脱臼の脱臼変位方向

て7.5±2.39歳であった．

柴犬の緑内障眼及び症候性緑内障眼における随伴所見は表2に示した．全患眼121眼のうち，角膜混濁は患眼の45.5%が混濁明瞭な中等度及び重度を示したが，残りのうち52.9%は透明角膜を示した．眼球拡張は患眼の84.3%を示した．視神経乳頭の萎縮・陥凹所見は患眼の54.5%で認められたが，角膜・前房・水晶体・硝子体といった透光体の混濁によって乳頭観察が不能であった症例眼は33.9%を占めた．また随伴所見と眼圧値との関係では，眼球拡張，視神経乳頭陥凹・萎縮，水晶体亜脱臼を示す緑内障眼は高眼圧値を示した（表2）．

水晶体脱臼は患眼121眼のうち，水晶体脱臼を示さない眼球が71眼（58.7%）で，水晶体脱臼眼が50眼（41.3%）であった（表2）．また水晶体脱臼眼は完全脱臼5眼（4.1%），亜脱臼45眼（37.2%）が認められ，亜脱臼の発生頻度は水晶体脱臼眼の9割を占めた．その水晶体亜脱臼は腹内側から背側方向（腹内側，内側，背内側，背側）に変位したものが45眼中の35眼（77.8%）でみられた（図3）．

考　　察

日本国内において，緑内障の犬種発生率は，柴犬33%，シーズー16.5%，交雑種犬7.9%，アメリカンコッカースパニエル6.3%であるとKatoら［5］によって報告されている．今回の柴犬の罹患率42.9%はKatoらの報告よりも高く，眼科診療症例に限定されて集計したことに依ると考えられた．

種々の犬種で報告された原発緑内障の発症年齢は4～8歳の間で，およそ6歳である［4］．今回の柴犬の成績では初診来院年齢は平均7.5歳であった．これは本調査症例がすべて紹介症例であったことにより高齢であったと考えられた．また，性差では雌での発症が多いとの報告［4］もあるが犬種により異なり，柴犬では性差は認められなかった．

柴犬緑内障の随伴所見では，角膜混濁は調査緑内障眼の約4割が中等度及び重度の混濁で，隅角が可視できない程度の混濁を示した．また，眼球拡張並びに網膜視神経萎縮を示した緑内障眼は平均眼圧値が40mmHg以上を示し，Gelattら［2］の眼圧値分類による重度緑内障に相当した．緑内障は非可逆的病態を示す疾患であることから，眼球拡張並びに網膜視神経萎縮を示す疾患眼では眼圧測定は不可欠であることが認められた．

緑内障でみられる水晶体脱臼は，今回の調査眼の約6割で観察されなかったが，水晶体脱臼を示す患眼の9割（45/50眼）が水晶体亜脱臼を示し，またその脱臼方向は背・内側方向であることを示した．近年，水晶体脱臼の関連遺伝子が原発緑内障の素因に関わることが報告され，緑内障と水晶体脱臼の関連が指摘されるようになった［6, 7］．今回の緑内障眼における水晶体脱臼は眼球拡張に関連するものと推察されるが，水晶体小帯断裂の原因が眼圧上昇と眼球拡張だけに起因するかは，さらなる検討が必要であると考えられた．

成績の整理にご協力いただいた小松紘之氏に感謝の意を表する．

引 用 文 献

［1］ Brooks DE : Glaucoma in the dog and cat, Vet Clin North Am Small Anim Pract, 20, 775–797 (1990)

［2］ Gelatt KN, Brooks DE, Kallberg ME : The canine glaucomas, Veterinary Ophthalmology, Galatt KN, 4th ed, 767–786, Blackwell Publishing, Oxford (2007)

［3］ Bouhenni RA, Dunmire J, Sewell A, Edward DP : Animal models of glaucoma, J Biomed Biotechnol. doi: 10.1155/2012/692609 (2012)

［4］ Gelatt KN, MacKay EO : Prevalence of the breed-related glaucoma in pure-breed dogs in North America, Vet Ophthalmol, 7, 97–111 (2004)

［5］ Kato K, Sasaki N, Matsunaga S, Nishimura R, Ogawa H : Incidence of canine glaucoma with goniodysplasia in Japan: a retrospective study, J Vet Med Sci, 68, 853–858 (2006)

［6］ Kuchtey J, Olson LM, Rinkoski T, Mackay EO, Iverson TM, Gelatt KN, Haines JL, Kuchtey RW : Mapping of the disease locus and identification of ADAMTS10 as a candidate gene in a canine model of primary open angle glaucoma, PLoS Genet, 7, e1001306 (2011)

［7］ Morales J, Al-Sharif L, Khalil DS, Shinwari JM, Bavi P, Al-Mahrouqi RA, Al-Rajhi A, Alkuraya FS, Meyer BF, Al Tassan N : Homozygous mutations in ADAMTS10 and ADAMTS17 cause lenticular myopia, ectopia lentis, glaucoma, spherophakia, and short stature, Am J Hum Genet, 85, 558–568 (2009)

Classification of Clinical Findings of Glaucoma in Dogs Presenting at the Ophthalmic Department of Azabu Veterinary Teaching Hospital

Nobuyuki KANEMAKI[1)], Yoichiro ICHIKAWA[2)], Shinpei KAWARAI[1)] and Hideharu OCHIAI[3)†]

1) *Veterinary Teaching Hospital of Azabu University, 1–17–71 Fuchinobe, Chuo-ku, Sagamihara, 252–5201, Japan*
2) *Ichikawa Animal Hospital, 168–1 Negiuchi, Matusdo, 270–0011, Japan*
3) *Research Institute of Biosciences, Azabu University, 1–17–71 Fuchinobe, Chuo-ku, Sagamihara, 252–5201, Japan*

SUMMARY

We surveyed incidences and clinical findings of glaucoma according to breed in 2,981 dogs presented to the ophthalmic department at the Veterinary Teaching Hospital of Azabu University from April 1994 to December 2011. Among the 21 major breeds presented, Shiba Inu dogs displayed the highest rate of glaucoma, at 42.9% (84/196). Of 121 eyes of glaucomatous Shiba Inu dogs, there were 57 eyes with corneal opacity (47.1%), 102 eyes with enlargement of the eyeball (84.3%), 66 eyes with atrophy and cuppings of the retinal optic disc (54.5%) and 50 eyes with lens luxation (41.3%). High intraocular pressure was presented in glaucomatous Shiba Inu dogs with either enlargement of the eyeball, atrophy of the retinal optic disc or lens luxation. Subluxation of the lens accounted for 90% in the glaucomatous eyeballs with lens luxation.

—— Key words : Clinical signs, Glaucoma, Shiba Inu.

† *Correspondence to : Hideharu OCHIAI (Research Institute of Biosciences, Azabu University)*
1–17–71 Fuchinobe, Chuo-ku, Sagamihara, 252–5201, Japan
TEL 042–754–7111 FAX 042–754–9930 E-mail : ochiaih@azabu-u.ac.jp

J. Jpn. Vet. Med. Assoc., 68, 55～58 (2015)

OPEN ACCESS Freely available online

PLOS ONE

Dogs and Humans Share a Common Susceptibility Gene *SRBD1* for Glaucoma Risk

Nobuyuki Kanemaki[1], Kissaou T. Tchedre[2], Masaki Imayasu[2], Shinpei Kawarai[3], Masahiro Sakaguchi[3], Atsushi Yoshino[4], Norihiko Itoh[4], Akira Meguro[4], Nobuhisa Mizuki[4]*

1 Veterinary Teaching Hospital, Azabu University, Sagamihara, Kanagawa, Japan, **2** Central R&D Laboratory, Menicon Co., Ltd., Kasugai, Aichi, Japan, **3** Department of Veterinary Microbiology, School of Veterinary Medicine, Azabu University, Sagamihara, Kanagawa, Japan, **4** Department of Ophthalmology, Yokohama City University School of Medicine, Yokohama, Kanagawa, Japan

Abstract

Glaucoma is a degenerative optic neuropathy that is associated with elevated intraocular pressure. Primary open angle glaucoma is the most common type of glaucoma in canines, and its highest incidence among dog breeds has been reported in Shiba-Inus, followed by Shih-Tzus. These breeds are known to have an abnormal iridocorneal angle and dysplastic prectinate ligament. However, the hereditary and genetic backgrounds of these dogs have not yet been clarified. In this study, we investigated the association between polymorphisms of the glaucoma candidate genes, *SRBD1*, *ELOVL5*, and *ADAMTS10*, and glaucoma in Shiba-Inus and Shih-Tzus. We analyzed 11 polymorphisms in these three genes using direct DNA sequencing. Three *SRBD1* SNPs, rs8655283, rs22018514 and rs22018513 were significantly associated with glaucoma in Shiba-Inus, while rs22018513, a synonymous SNP in exon 4, showed the strongest association ($P = 0.00039$, OR = 3.03). Conditional analysis revealed that rs22018513 could account for most of the association of these SNPs with glaucoma in Shiba-Inus. In Shih-Tzus, only rs9172407 in the *SRBD1* intron 1 was significantly associated with glaucoma ($P = 0.0014$, OR = 5.25). There were no significant associations between the *ELOVL5* or *ADAMTS10* polymorphisms and glaucoma in Shiba-Inus and Shih-Tzus. The results showed that *SRBD1* polymorphisms play an important role in glaucoma pathology in both Shiba-Inus and Shih-Tzus. *SRBD1* polymorphisms have also been associated with normal- and high-tension glaucomas in humans. Therefore, *SRBD1* may be a common susceptibility gene for glaucoma in humans and dogs. We anticipate that the nucleotide sequencing data from this study can be used in genetic testing to determine for the first time, the genetic status and susceptibility of glaucoma in dogs, with high precision. Moreover, canine glaucoma resulting from *SRBD1* polymorphisms could be a useful animal model to study human glaucoma.

Citation: Kanemaki N, Tchedre KT, Imayasu M, Kawarai S, Sakaguchi M, et al. (2013) Dogs and Humans Share a Common Susceptibility Gene *SRBD1* for Glaucoma Risk. PLoS ONE 8(9): e74372. doi:10.1371/journal.pone.0074372

Editor: Reiner Albert Veitia, Institut Jacques Monod, France

Received December 17, 2012; **Accepted** August 6, 2013; **Published** September 9, 2013

Funding: This study was supported by the MEXT-Supported Program for the Strategic Research Foundation at Private Universities. The funders had no role in study design, data collection and analysis, decision to publish, or preparation of the manuscript.

Competing Interests: Two of the authors, KTT and MI are employed by the Menicon Co., Ltd. This does not alter the authors' adherence to all the PLOS ONE policies on sharing data and materials.

* E-mail: mizunobu@med.yokohama-cu.ac.jp

Introduction

Glaucoma is a degenerative optic neuropathy comprising a group of eye disorders, including visual field defects, progressive loss of retinal ganglion cells, and degeneration of optic nerve axons, and is frequently associated with elevated intraocular pressure (IOP) [1]. Glaucoma is classified into three types: primary open angle glaucoma (POAG), primary closed angle glaucoma (PCAG), and primary congenital glaucoma (PCG) [1]. POAG is the most common type of glaucoma, and is usually associated with high IOP. Japanese populations, however, have a substantially higher incidence of normal tension glaucoma (NTG), a form of glaucoma in which optic nerve damage occurs even though the IOP is not elevated [2,3].

It is well known that glaucoma is genetically heterogeneous and many genes, such as *CYP1B1*, *MYOC*, *OPTN*, and *OPTC*, are linked to POAG and PCG in humans and/or dogs [4–9]. Recently, the Normal Tension Glaucoma Genetic Study Group of the Japan Glaucoma Society performed a genome-wide association study with NTG patients and controls in a Japanese population [2]. The study identified two new susceptibility genes for NTG, *SRBD1* and *ELOVL5*, with strong statistical significance. Similarly, Mabuchi et al. also reported the association of an *SRBD1* polymorphism with Japanese POAG patients, including late-onset NTG and high tension glaucoma [10].

Canine primary glaucoma has been investigated since almost 50 years ago [11], and high incidences have been reported in Beagles [12–14], Welsh Springer Spaniels [15], and other breeds [16,17]. Recent study reported the Gly661Arg variant in *ADAMTS10* as the candidate disease-causing variant for POAG Beagles [12]. Kato et al. investigated the incidence of canine POAG, and reported that Shiba-Inus exhibited the highest incidence of glaucoma among 29 breeds, followed by Shih-Tzus [18]. They also reported that an abnormal iridocorneal angle and dysplastic prectinate ligament were associated with a high incidence of glaucoma in Shiba-Inus and Shih-Tzus. However, the hereditary and genetic backgrounds of glaucoma in these dogs have not yet been clarified.

In this study, to verify recent genetic findings, we investigated the association between glaucoma in Shiba-Inu and Shih-Tzu

dogs and polymorphisms of glaucoma candidate genes, *SRBD1*, *ELOVL5* and *ADAMTS10*, using direct sequencing.

Results

The average ages of glaucoma cases and controls were 8.5±2.9 and 10.0±3.0 years old, respectively, in Shiba-Inu dogs. Those in Shih-Tzu dogs were 9.2±2.0 and 10.1±2.5 years old, respectively. We genotyped 11 polymorphisms in *SRBD1*, *ELOVL5*, and *ADAMTS10* in 98 Shiba-Inu and 67 Shih-Tzu dogs using the direct DNA sequencing method (Table 1).

Table 2 shows the details of five single nucleotide polymorphisms (SNPs) in *SRBD1*, including their genomic locations and allele frequencies in Shiba-Inus and Shih-Tzus. In Shiba-Inus, the most statistically significant association was observed for rs22018513 ($P = 0.00039$); the G allele of rs22018513 had a 3.03-fold (95% CI = 1.62–5.65) increased risk of glaucoma, with a frequency of 78.6% in cases vs. 54.8% in controls. Significant associations were also observed for rs8655283 and rs22018514 in Shiba-Inus; the frequencies of the T allele of rs8655283 and the G allele of rs22018514 were significantly greater among glaucoma cases than among controls (rs8655283, 37.5% vs. 21.4%, $P = 0.016$, OR = 2.20, 95% CI = 1.15–4.20; rs22018514, 41.1% vs. 21.4%, $P = 0.0037$, OR = 2.56, 95% CI = 1.34–4.86). In Shih-Tzus, we observed a significant association for rs9172407 ($P = 0.0014$) and the G allele of rs9172407 had a 5.25-fold (95% CI = 1.76–15.63) increased risk of glaucoma (25.9% in cases vs. 6.3% in controls), whereas the frequency of this G allele was only moderately, but not significantly, increased in cases compared to controls in Shiba-Inus (8.9% vs. 6.0%, OR = 1.55, 95% CI = 0.51–4.71). rs22018513, which had the strongest association with glaucoma in Shiba-Inus, did not show a significant association in Shih-Tzus ($P = 0.868$, OR = 1.13, 95% CI = 0.26–4.95). Two other SNPs (rs8655283 and rs22018514), which were associated with glaucoma in Shiba-Inus, as well as rs22019922, also did not achieve statistically significant associations with glaucoma in Shih-Tzus. However, the odds-ratios of these variants in Shih-Tzus were suggestive of an association, with the T allele of rs8655283, the G allele of rs22018514, and the A allele of rs22019922, each having a 2.43 or 2.49-fold increased risk of glaucoma.

Figure 1 shows the strength of linkage disequilibrium (LD) for the five SNPs of *SRBD1* in Shiba-Inus and Shih-Tzus. Strong LD was observed between rs8655283, rs22018514 and rs22018513 in Shiba-Inus (D' ≥0.78) (Figure 1A). In Shih-Tzus, strong LD was observed throughout the region from rs22019922 to rs22018513 (D' ≥0.68) (Figure 1B). rs8655283 and rs22018514 were in almost complete LD in both Shiba-Inus and Shih-Tzus ($r^2 = 0.73$ and 0.74, respectively). rs9172407 was not linked with any of the other four SNPs in either breed.

To elucidate the effect of rs8655283, rs22018514 and rs22018513 on the disease susceptibility in Shiba-Inus, we performed conditional logistic regression analysis. Conditioning by rs22018513 eliminated the significant association of rs8655283 and rs22018514, while the association of rs22018513 remained significant after conditioning by rs8655283 or rs22018514 (Table 3). These results suggest that rs22018513 could account for most of the association of these SNPs with glaucoma in Shiba-Inus.

Table 4 shows the results of association analysis for the polymorphisms of *ELOVL5* and *ADAMTS10*. rs9194033 and rs22202438 of *ELOVL5* were polymorphic in Shiba-Inus and Shih-Tzus, while three *ELOVL5* polymorphisms (rs22226301, rs8643563 and rs22194174) and the *ADAMTS10* Gly661Arg variant were monomorphic. The G allele of rs9194033 and the G allele of rs22202438 had a 1.45- and a 1.39-fold increased risk of glaucoma in Shiba-Inus, respectively. Conversely, these alleles were decreased in cases compared to controls in Shih-Tzus (OR = 0.57 and 0.66, respectively). The differences in the allelic frequencies of rs9194033 or rs22202438 between cases and controls did not reach statistical significance for either breed.

Discussion

The aim of the present study was to assess the potential associations of polymorphisms in the candidate genes *SRBD1*, *ELOVL5*, and *ADAMTS10*, with the development of canine glaucoma. To this end, we genotyped 11 polymorphisms of these genes in two breeds of dogs with cases of glaucoma or without, as controls. Here we report that the *SRBD1* polymorphisms exhibited significant association with canine glaucoma, while the *ELOVL5* and *ADAMTS10* polymorphisms that were examined in this study were not associated with canine glaucoma. In Shiba-Inus, the strongest association with glaucoma in *SRBD1* was observed at rs22018513, which is a synonymous SNP in exon 4. Two other SNPs, rs8655283 and rs22018514, were also significantly associated with glaucoma; however, these significant associations were calculated only secondarily from a strong LD with rs22018513. In Shih-Tzus, however, rs22018513 was not associated with glaucoma. Only rs9172407 in intron 1 of *SRBD1* showed a statistically

Table 1. Primer pairs for PCR of glaucoma-related genes.

Gene	Allele	5′-3′ Forward	5′-3′ Reverse
SRBD1	rs22019922	TGTTGGTGTTGTCAGCAAGT	TCACACTCTTTCTCTCACTCTCTC
	rs8655283	TTAGGATGAAACCATGGAAC	TTGGCGATTTATTGAACTAAC
	rs22018513, rs22018514	GCTATTGCTGATGTTGATTTG	TGCAGTGCTGGCCCTGTTGGA
	rs9172407	GTGAACCTGAAATGGCAAA	TTAACTAGCTTCCTTGCTTCC
ELOVL5	rs22226301	AGTTGTGCTGCTTACATTAGG	AGCAAGGCAAGATGTGTTC
	rs9194033	AGTGATGCTGCTATGGGATG	GCTCAGGTCATGGGATCAAG
	rs22202438	CATGCTGAACATCTGGTGGT	GCTGGTCTGGATGATTGTCA
	rs8643563	AATTGTATGGCTGGGACCAA	ACCACCAGAGGACACGGATA
	rs22194174	AATGCTTATCCTACCCAATC	TCAGGCTCTATGCTCAGTG
ADAMTS10	Gly661Arg (56097365 G>A)	CACAGAGCAAGCAGGGAGT	GGGTGGAAGTGGGAGTG

doi:10.1371/journal.pone.0074372.t001

Table 2. Association analysis for five polymorphisms in the *SRBD1* gene region for Shiba-Inu and Shih-Tzu dog breeds.

SNP ID	Chr.	Position (CanFam2.0)	Allele	SNP Type	Risk Allele	Breed	N		Risk Allele Frequency (%)		P	OR(95% CI)
							Cases	Controls	Cases	Controls		
rs22019922	10	50924623	A/C	Intron	A	Shiba-Inu	56	42	8.9	7.1	0.65	1.27 (0.44–3.66)
						Shih-Tzu	27	40	96.3	91.3	0.25	2.49(0.50–12.49)
						Overall	83	82			0.40	1.59 (0.66–3.80)
rs8655283	10	50989281	C/T	Intron	T	Shiba-Inu	56	42	37.5	21.4	0.016	2.20 (1.15–4.20)
						Shih-Tzu	27	40	92.6	83.8	0.13	2.43 (0.75–7.89)
						Overall	83	82			0.0068	2.25 (1.28–3.97)
rs22018514	10	51,049,600	C/G	Non-synonymous	G	Shiba-Inu	56	42	41.1	21.4	0.0037	2.56 (1.34–4.86)
						Shih-Tzu	27	40	92.6	83.8	0.13	2.43 (0.75–7.89)
						Overall	83	82			0.0018	2.52 (1.43–4.44)
rs22018513	10	51,049,604	A/G	Synonymous	G	Shiba-Inu	56	42	78.6	54.8	0.00039	3.03 (1.62–5.65)
						Shih-Tzu	27	40	94.4	93.8	0.87	1.13 (0.26–4.95)
						Overall	83	82			0.0015	2.59 (1.46–4.61)
rs9172407	10	51062753	A/G	Intron	G	Shiba-Inu	56	42	8.9	6.0	0.44	1.55 (0.51–4.71)
						Shih-Tzu	27	40	25.9	6.3	0.0014	5.25 (1.76–15.63)
						Overall	83	82			0.0074	2.90 (1.34–6.26)

OR, odds ratio; CI, confidence interval.
Overall P values and ORs for meta-analysis were calculated using the Mantel-Haenzel method.
doi:10.1371/journal.pone.0074372.t002

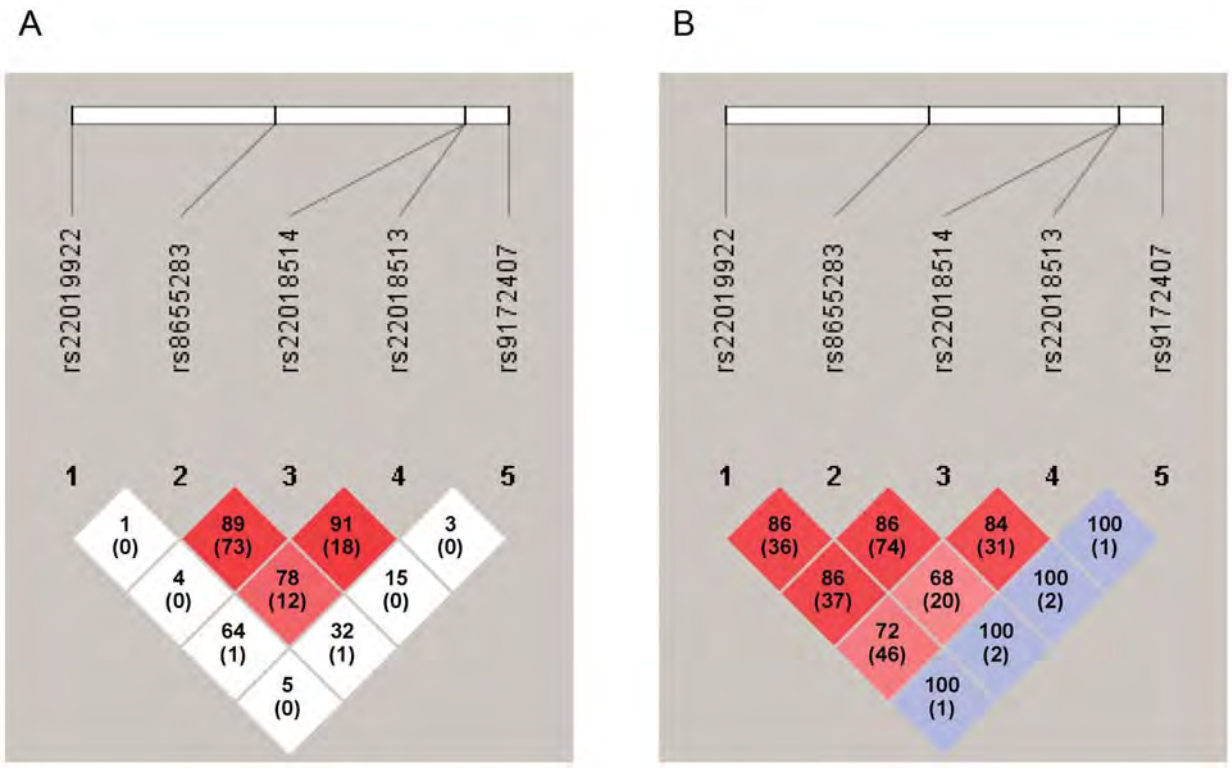

Figure 1. Linkage disequilibrium (LD) plot of five SNPs of the SRBD1 gene. A) LD structure in Shiba-Inus. B) LD structure in Shih-Tzus. The D′ value and r^2 value (in parentheses) corresponding to each SNP pair are expressed as a percentage and shown within the respective square. The color scheme is based on D′ and LOD score values: bright red (LOD ≥2 and D′ = 1); shades of pink/red (LOD ≥2 and D′ <1); blue (LOD <2 and D′ = 1); white (LOD <2 and D′ <1).
doi:10.1371/journal.pone.0074372.g001

Table 3. Conditional logistic regression analysis of rs8655283, rs22018514 and rs22018513 in the *SRBD1* gene for Shiba-Inus.

SNP ID	Risk Allele	Model	P*	P**		
				Covariates		
				rs8655283	rs22018514	rs22018513
rs8655283	T	Additive	0.021	–	0.92	0.15
rs22018514	G	Additive	0.0066	0.13	–	0.10
rs22018513	G	Additive	0.00025	0.0010	0.0021	–

*P values for each SNP under the recessive, additive, or dominant model that provided the best fit by logistic regression analysis. The lowest P value was selected as the best fit model. The indicated model showed the lowest P value for each SNP.
**P values adjusted for each SNP under the indicated model by conditional logistic regression analysis.
doi:10.1371/journal.pone.0074372.t003

significant association in Shih-Tzus, but not in Shiba-Inus. These results suggest that rs22018513 and rs9172407, or a respective neighboring polymorphism, may be a causative factor for glaucoma in Shiba-Inus and Shih-Tzus, respectively.

BLAST analysis (http://blast.ncbi.nlm.nih.gov/) reveals that the canine *SRBD1* amino acid sequence shares a high degree of similarity with its human homolog, with 90% identity. In humans, the nucleotide sequences corresponding to rs22018513 and rs9172407 are located within exon 4 and intron 1 of *SRBD1*, respectively. However, these sequences have never been reported as polymorphic in humans. While the human NTG-associated SNP, rs3213787, is located in intron 17 of *SRBD1* [2], the HapMap database shows strong LD across the entire human *SRBD1* region, suggesting that rs3213787 is strongly linked with polymorphisms in exon 4 and intron 1. Further investigation will be necessary to confirm the association of polymorphisms in the exon 4 and intron 1 regions of *SRBD1* in human glaucoma patients.

SRBD1 was initially identified as an S1 RNA-binding domain in *Escherichia coli* [19]. Many proteins contain S1 RNA-binding domains, such as the bacterial exonuclease polynucleotide phosphorylase, eukaryotic translation initiation factor 2 alpha, and even a human DNA-binding protein [20,21]. The function of *SRBD1* in humans and dogs remains unknown. Canine *SRBD1* is located on the reverse strand of chromosome 10, and is approximately 186 kb, including approximately 3 kb of the exon

Table 4. Association analysis for six polymorphisms in the ELOVL5 and ADAMTS10 gene regions for Shiba-Inu and Shih-Tzu dog breeds.

SNP ID	Chr.	Position (CanFam2.0)	Gene	Allele	SNP Type	Risk Allele*	Breed	N		Risk Allele Frequency (%)		P	OR (95% CI)
								Cases	Controls	Cases	Controls		
rs22226301	12	20733716	ELOVL5	C/T	3′UTR	T	Shiba-Inu	56	42	0.0	0.0	–	–
							Shih-Tzu	27	40	0.0	0.0	–	–
							Overall	83	82			–	–
rs9194033	12	20739417	ELOVL5	A/G	Intron	G	Shiba-Inu	56	42	33.9	26.2	0.25	1.45 (0.78–2.70)
							Shih-Tzu	27	40	55.6	68.8	0.12	0.57 (0.28–1.16)
							Overall	83	82			0.99	0.97 (0.61–1.54)
rs22202438	12	20743516	ELOVL5	A/G	Synonymous	G	Shiba-Inu	56	42	35.7	28.6	0.29	1.39 (0.75–2.56)
							Shih-Tzu	27	40	59.3	68.8	0.26	0.66 (0.32–1.36)
							Overall	83	82			0.98	1.02 (0.64–1.62)
rs8643563	12	20744701	ELOVL5	(–)/T	Frameshift coding	T	Shiba-Inu	56	42	0.0	0.0	–	–
							Shih-Tzu	27	40	0.0	0.0	–	–
							Overall	83	82			–	–
rs22194174	12	20749077	ELOVL5	A/C	Intron	A	Shiba-Inu	56	42	0.0	0.0	–	–
							Shih-Tzu	27	40	0.0	0.0	–	–
							Overall	83	82			–	–
Gly661Arg	20	56097365	ADAMTS10	A/G	Non-synonymous	A	Shiba-Inu	56	42	0.0	0.0	–	–
(56097365 G>A)							Shih-Tzu	27	40	0.0	0.0	–	–
							Overall	83	82			–	–

OR, odds ratio; CI, confidence interval.
Overall P values and ORs for meta-analysis were calculated using the Mantel-Haenzel method.
*Risk allele is for Shiba-Inu dogs.
doi:10.1371/journal.pone.0074372.t004

region (http://asia.ensembl.org/Canis_familiaris/Transcript/Exons?db=core;g=ENSCAFG00000002554;r=10:47923593-47924593;t=ENSCAFT00000049409). *SRBD1* transcript is reportedly expressed in the retinal ganglion cell and neuroblast layers in neonatal mouse tissue [2], but its localization in dogs remains unknown.

The present study found that a synonymous SNP (rs22018513) and intronic SNP (rs9172407) in *SRBD1* were associated with glaucoma in Shiba-Inus and Shih-Tzus, respectively. Synonymous and intronic polymorphisms can significantly affect gene expression by various mechanisms and lead to the development of disease [22–24]. We did not compare *SRBD1* mRNA levels in normal and affected dogs; however, a similar experiment has been conducted in humans [2]. Results from that study showed a significant correlation between increased *SRBD1* expression and the NTG-associated risk allele of intronic SNP. These results suggest that rs22018513 and rs9172407 in canine *SRBD1* could cause enhanced *SRBD1* expression. Reports show that *SRBD1* is indirectly involved in cell growth, general protein synthesis, induction of apoptosis, and maintaining homeostasis [2]. Therefore, we hypothesize that enhanced expression, leading to increased activity of SRBD1, which could induce apoptosis, could result in retinal ganglion cell death during the development of glaucoma.

ELOVL5 is a fatty acid condensing enzyme involved in the biosynthesis of long-chain polyunsaturated fatty acids [25], and is one of the candidate genes for retinitis pigmentosa [26]. The Normal Tension Glaucoma Genetics Study Group of the Japan Glaucoma Society reported *ELOVL5* as a new susceptibility gene for human NTG [2]. However, the present study did not show any significant association of *ELOVL5* polymorphisms with canine glaucoma. The difference between our results and those reported by the study group may be due to the different forms of glaucoma that were studied (human NTG without IOP elevation, and canine glaucoma with IOP elevation, respectively). In contrast, *SRBD1* polymorphisms were associated with canine glaucoma and human glaucoma independent of IOP, suggesting that *SRBD1* polymorphisms may affect a common disease condition in canine and human glaucoma. Therefore, detection of any common phenotypes in these glaucoma studies [2,10] is important because it will help to clarify how *SRBD1* affects the development of glaucoma. Moreover, canine glaucoma resulting from *SRBD1* polymorphisms could be used as an excellent genetic animal model for human glaucoma and contribute significantly to the development of novel diagnostic and therapeutic options for glaucoma.

Kato, et al., reported that the Beagle breed has the fourth-highest incidence of canine glaucoma, after Shiba-Inu, Shih-Tzu, and American Cocker Spaniel breeds [18]. Kuchtey et al. recently reported that the Gly661Arg variant (56097365 G>A) of *ADAMTS10* in Beagles with POAG is a candidate, predictive gene allele for canine POAG [12]. We did not observe an association between this 56097365 G>A variant and glaucoma in Shiba-Inus or Shih-Tzus, possibly because of breed-specific allelic differences between Beagles and Shiba-Inus or Shih-Tzus. More recently, Kuchtey, et al., reported that the Gly661Arg variant was not found in any of the other dog breeds analyzed, (Shiba-Inu, Shih-Tzu, American Cocker Spaniels, Chihuahua, Australian Cattle Dog, Jack Russell Terrier, Jindo, Siberian Husky, and Yorkshire Terrier), suggesting that this allele is Beagle-specific, and that other genes may be associated with glaucoma in other breeds [27]. However, *ADAMTS10* may be still a candidate gene for glaucoma in dogs, including Shiba-Inu and Shih-Tzu, because other *ADAMTS10* variants have yet to be investigated for their association with canine glaucoma. The Ensembl database (http://asia.ensembl.org/index.html) shows 16 genetic polymorphisms in the canine *ADAMTS10* gene region. Since the dog genome information is still incomplete, it is predicted that more even polymorphisms exist in the canine *ADAMTS10* gene region. Therefore, it is necessary to perform a comprehensive genetic analysis of the region and clarify whether *ADAMTS10* is a candidate gene for glaucoma not only in Beagles, but also in other breeds.

There are no genetic tests currently available to assist in glaucoma diagnosis, identification of people at risk, initiation of treatment, and timing of surgical intervention. We performed the present SNP analysis of candidate genes in Shiba-Inu and Shih-Tzu dog breeds for the possibility to help develop diagnostic, genetic analyses for glaucoma risk factors. However, the mechanism by which these genes contribute to the development of glaucoma remains to be determined. Future studies are expected to examine the roles of *SRBD1* in humans and dogs, in an effort to determine whether genetic testing might not only help predict whether someone will develop glaucoma, but may also, perhaps, be a valuable prognostic factor for the clinical course of the disease, and/or predictive factor for its treatment. Despite new and improving diagnostic and therapeutic options for glaucoma, blindness resulting from glaucoma remains a major public health problem. These future experiments will help to optimize glaucoma treatment.

Materials and Methods

Ethics Statement

This study was performed as part of research approved by the Ethical Committee of Azabu University (Permit Number: 110408-2). Informed written consent was obtained from each dog owner. All procedures in this study were conducted in accordance with the Guide for the Care and Use of Laboratory Animals of Azabu University.

Diagnosis of Glaucoma

98 Japanese Shiba-Inu dogs and 67 Shih-Tzu dogs were recruited from the Veterinary Teaching Hospital at Azabu University. All dogs received complete ophthalmologic examinations using a hand-held slit-lamp biomicroscope (SL-14; Kowa, Tokyo, Japan), indirect ophthalmoscopy, and tonometry. After the application of topical anesthesia (oxybuprocaine hydrochloride, Santen, Osaka, Japan), IOP was measured by tonometry using the Tono-Pen XL (Mentor O&O Inc., Norwell, MA). 42 Shiba-Inus and 40 Shih-Tzus were diagnosed as normal (<25 mmHg IOP). 56 Shiba-Inus and 27 Shih-Tzus had elevated IOP (>25 mmHg) in at least one eye, and were diagnosed with glaucoma. Since glaucoma is a late-onset disorder, we did not recruit dogs younger than four years in the control group, in an attempt to exclude potential glaucomatous dogs.

DNA Preparation

Genomic DNA from glaucomatous and normal dogs was collected from peripheral blood and purified using a DNA whole blood spin kit (Fuji Film, Tokyo, Japan). The purity and concentration of DNA were examined using GeneQuant Pro (GE Healthcare, Cambridge, UK).

Determination of DNA Sequences

In the *SRBD1* and *ELOVL5* gene regions, a total of ten polymorphisms were selected to cover the entire gene regions (rs22019922, rs8655283, rs22018514, rs22018513 and rs9172407 in *SRBD1*; rs22226301, rs9194033, rs22202438, rs8643563 and rs22194174 in *ELOVL5*) (Table 2,4). In the *ADAMTS10* gene

region, we selected the Gly661Arg variant (56097365 G>A) for analysis (Table 4). PCR primer pairs listed in Table 1 were used to amplify regions containing the SNPs mentioned above. The PCR products were electrophoretically separated on a 1% agarose gel, and the PCR product bands were cut and frozen at −80°C in Tris-EDTA buffer. The frozen samples were thawed, homogenized, and centrifuged at 15,000 *g* for 5 minutes. The supernatants were subjected to cycle sequencing using the Big Dye terminator sequencing kit (Life Technologies, Foster City, CA). The sequence cycling reaction products were purified using the Qiagen Dye Ex 2.0 Spin Kit (QIAGEN, Hilden, Germany) according to the manufacturer's instructions. After drying, the DNA samples were mixed with high Dye Mix (Life Technologies) and were directly sequenced using an ABI PRISM 310 genetic analyzer (Life Technologies). The sequence data were analyzed using Sequence Scanner v. 1.0 (Life Technologies) and GENETYX-WIN v. 4.0 (Genetyx, Tokyo, Japan). We did not find any novel DNA sequences deposited in GenBank in this study.

Statistical Analysis

Hardy-Weinberg equilibrium was tested for each SNP among glaucomatous and normal dogs. Differences in allele frequency between glaucomatous and normal dogs were assessed using the χ^2 test, and $P<0.05$ was considered statistically significant. Overall, *P* values and odds ratios (ORs) for meta-analysis were calculated by the Mantel-Haenszel method. The Haploview 4.1 program was used to compute pairwise LD statistics [28]. Conditional logistic regression analysis was performed to assess the effect of each SNP on the disease susceptibility using PLINK (http://pngu.mgh.harvard.edu/purcell/plink/) [29].

Acknowledgments

We sincerely thank all the dog owners who have provided samples for this study and all the veterinarians involved in sample collection and diagnosis.

Author Contributions

Conceived and designed the experiments: NK SK MS NI NM. Performed the experiments: NK KTT MI. Analyzed the data: MI AM AY. Contributed reagents/materials/analysis tools: NK KTT MI MS AM AY NM. Wrote the paper: KTT MI AM.

References

1. Quigley HA (1993) Open-angle glaucoma. N Engl J Med 328: 1097–1106.
2. Writing Committee for the Normal Tension Glaucoma Genetic Study Group of Japan Glaucoma Society, Meguro A, Inoko H, Ota M, Mizuki N, Bahram S (2010) Genome-wide association study of normal tension glaucoma: common variants in SRBD1 and ELOVL5 contribute to disease susceptibility. Ophthalmology 117: 1331–1338.
3. Nakano M, Ikeda Y, Taniguchi T (2009) Three susceptible loci associated with primary open-angle glaucoma identified by genome-wide association study in a Japanese polulation. Proc Natl Acad Sci 106: 12838–12842.
4. Kato K, Kamida A, Sasaki N, Shastry BS (2009) Evaluation of the CYP1B1 gene as a candidate gene in beagles with primary open-angle glaucoma (POAG). Mol Vis 15: 2470–2474.
5. Yang M, Guo X, Liu X, Shen H, Jia X, et al. (2009) Investigation of CYP1B1 mutations in Chinese patients with primary congenital glaucoma. Mol Vis 15: 432–437.
6. Kumar A, Basavaraj MG, Gupta SK, Qamar I, Ali AM, et al. (2007) Role of CYP1B1, MYOC, OPTN, and OPTC genes in adult-onset primary open-angle glaucoma: predominance of CYP1B1 mutations in Indian patients. Mol Vis 13: 667–676.
7. Sitorus R, Ardjo SM, Lorenz B, Preising M (2003) CYP1B1 gene analysis in primary congenital glaucoma in Indonesian and European patients. J Med Genet 40: e9.
8. Fan BJ, Wang DY, Fan DSP, Tam POS, Lam DSC, et al. (2005) SNPs and interaction analyses of myocilin, optineurin, and apolipoprotein E in primary open angle glaucoma patients. Mol Vis 11: 625–631.
9. Kato K, Sasaki N, Matsunaga S, Nishimura R, Ogawa H (2007) Cloning of canine myocilin cDNA and molecular analysis of the myocilin gene in Shiba Inu dogs. Vet Ophthalmol 10 suppl 1: 53–62.
10. Mabuchi F, Sakurada Y, Kashiwagi K, Yamagata Z, Iijima H, et al. (2011) Association between SRBD1 and ELOVL5 gene polymorphisms and primary open-angle glaucoma. Invest Ophthalmol Vis Sci 52: 4626–4629.
11. Lovekin LG (1964) Primary glaucoma in dogs. J Am Vet Med Assoc 145: 1081–1091.
12. Kuchtey J, Olson LM, Rinkoski T, MacKay EO, Iverson TM, et al. (2011) Mapping of the disease locus and identification of ADAMTS10 as a candidate gene in a canine model of primary open angle glaucoma. PLoS Genet 7: e1001306.
13. Gelatt KN, Gum GG (1981) Inheritance of glaucoma in the beagle. Am J Vet Res 42: 1691–1693.
14. Gelatt KN, Peiffer RL Jr, Gwin RM, Gum GG, Williams LW (1977) Clinical manifestations of inherited glaucoma in the beagle. Invest Ophthalmol Vis Sci 16: 1135–1148.
15. Cottrell BD, Barnett KC (1988) Primary glaucoma in the Welsh Springer Spaniel. J Small Anim Pract 29: 185–199.
16. Bedford PGC (1975) The aetiology of primary glaucoma in the dog. J Small Anim Pract 16: 217–239.
17. Martin CL, Wyman M (1978) Primary glaucoma in the dog. Vet Clin North Am 8: 257–286.
18. Kato K, Sasaki N, Matsunaga S, Nishimura R, Ogawa H, et al. (2006) Incidence of canine glaucoma with goniodysplasia in Japan: a retrospective study. J Vet Med Sci 68: 853–858.
19. Subramanian AR (1983) Structure and functions of ribosomal protein S1. Prog Nucleic Acid Res Mol Biol 28: 101–142.
20. Bycroft M, Hubbard TJ, Proctor M, Freund SM, Murzin AG (1997) The solution structure of the S1 RNA binding domain: a member of an ancient nucleic acid-binding fold. Cell 88: 235–242.
21. Eklund EA, Lee SW, Skalnik DG (1995) Cloning of a cDNA encoding a human DNA-binding protein similar to ribosomal protein S1. Gene 155: 231–235.
22. Sauna ZE, Kimchi-Sarfaty C (2011) Understanding the contribution of synonymous mutations to human disease. Nat Rev Genet 12: 683–691.
23. Nackley AG, Shabalina SA, Tchivileva IE, Satterfield K, Korchynskyi O, et al. (2006) Human catechol-O-methyltransferase haplotypes modulate protein expression by altering mRNA secondary structure. Science 314: 1930–1933.
24. Wang D, Guo Y, Wrighton SA, Cooke GE, Sadee W (2011) Intronic polymorphism in CYP3A4 affects hepatic expression and response to statin drugs. Pharmacogenomics J 11: 274–286.
25. Moon YA, Hammer RE, Horton JD (2009) Deletion of ELOVL5 leads to fatty liver through activation of SREBP-1c in mice. J Lipid Res 50: 412–423.
26. Barragan I, Marcos I, Borrego S, Antinolo G (2005) Mutation screening of three candidate genes, ELOVL5, SMAP1 and GLULD1 in autosomal recessive retinitis pigmentosa. Int J Mol Med 16: 1163–1167.
27. Kuchtey J, Kunkel J, Esson D, Sapienza JS, Ward DA, et al. (2013) Screening ADAMTS10 in dog populations supports Gly661Arg as the glaucoma-causing variant in beagles. Invest Ophthalmol Vis Sci 54: 1881–1886.
28. Barrett JC, Fry B, Maller J, Daly MJ (2005) Haploview: analysis and visualization of LD and haplotype maps. Bioinfomatics 21: 263–265.
29. Purcell S, Neale B, Todd-Brown K, Thomas L, Ferreira MA, et al. (2007) PLINK: a tool set for whole-genome association and population-based linkage analyses. Am J Hum Genet. 81: 559–575.

イヌにおけるヒトへの適合性に関する遺伝子解析

１．犬のヒト適応性に関する犬種差の検出
２．犬の家畜化過程における選択圧因子の推定
３．ヒトへの社会認知能力における犬種差の検出
４．犬の社会認知能力に関連する遺伝子の同定

菊水健史（麻布大学伴侶動物学研究室）、茂木一孝（麻布大学伴侶動物学研究室）、永澤美保（自治医科大学医学部生理学講座）

１．犬のヒト適応性に関する犬種差の検出

研究要旨

日本及び米国における一般の飼い主及びブリーダーを対象としたイヌの行動特性に関するアンケート調査を、インターネット媒体を用いて実施した。イヌの行動解析システムは、C-barq を用いた。質問は、米国 100 問、日本 78 問から成り、様々な場面における犬の行動を 5 段階で評価する内容である。犬種を既に報告されていた遺伝分岐図を元に 8 つのグループに分類し、犬の行動特性の犬種グループ比較に用いた。質問項目について因子分析及び平行分析を行い、各因子の平均値を因子得点として分析に使用した。

アンケート結果を因子分析したところ、11 の因子に分類された（訓練性、活発度、愛着、分離不安、侵入者に対する攻撃性、飼い主に対する攻撃性、見知らぬ人に対する攻撃性、見知らぬ犬に対する攻撃性、非社会的刺激に対する恐怖反応、見知らぬ人に対する恐怖反応、見知らぬ犬に対する恐怖反応）。そのうち、原始的な犬グループのイヌはどの犬種グループよりもヒトへの愛着が低いことが明らかとなった（$p<0.05$）。原始的な犬の愛着はその他のどの犬種グループよりも低く、先行研究で知られている遺伝分岐図と一致した結果である。その他の犬種グループでは、ワーキンググループは、見知らぬ人に対する恐怖反応、見知らぬ犬に対する恐怖反応、非社会的刺激に対する恐怖反応、飼い主に対する攻撃性、活発度が低いことが明らかとなった。また、ハーディンググループは訓練性が高く、トイグループは飼い主に対する攻撃性、見知らぬ人に対する攻撃性、侵入者に対する攻撃性が高かった。

研究目的

探索行動や逃避行動、遊び、訓練性能、不安傾向等の幾つかのイヌの行動特性には、犬種間で差が見られ、遺伝することが知られている。イヌの気質・行動や能力について犬種間で比較することにより、それらの犬種がどのように作成されていったのかその過程を知ることができる。特に、ゲノムワイド研究によって遺伝的に最もオオカミに近いことが知られている原始的な犬グループのイヌの行動特性は、祖先種に最も近いと考えられ、イヌの

家畜化（進化）を考える上で重要となる。そこで、原始的な犬グループのイヌの一般的な飼育下における行動特性について調査した。

材料と方法

犬の行動に関する調査は、犬の行動解析システムのひとつである Canine Behavioral Assessment and Research Questionare (C-barq)を用いて行った。C-barq はウェブサイト上（米国 http://www.cbarq.org、日本 http://cbarq.inutokurasu.jp/）で一般公開されており、データは一般の飼い主及びブリーダーを対象にして集められた。期間は、米国 2006 年 4 月、日本 2010 年 9 月より開始され、日本のウェブサイトは米国のものを日本用にアレンジしたものとなっている。質問は、米国 100 問、日本 78 問から成り、様々な場面における犬の行動を 5 段階で評価する内容である。また、犬の基本情報として、名前、生年月日、犬種、性別、体重、避妊去勢の実施状況や時期、疾患の有無、入手時期、入手元、飼い主の今までの飼育経験等を登録してもらった。

質問項目について因子分析を行い、各因子の平均値を因子得点として分析に使用した。犬種は既に報告されていた vonHoldt (2010)11 による遺伝分岐図を元に 8 つのグループに分類して犬の行動特性の犬種グループ比較に用いた。解析には一般化線型モデルを用い、解析は SPSS を用いて行った（SPSS v.19.0, SPSS Japan Inc., IBM company）。また、犬種グループの他にも、犬の行動特性に影響を及ぼすと思われる変数として、国、性別、年齢、避妊去勢の実施状況、体重、入手場所、入手時期、飼い主の今までの飼育経験を解析に含めた。クラスター解析は、SPSS を用いて、ウォード法で行った。

結果および考察

１．データ構造

日本及び米国に共通して見られた 59 犬種を選抜し、性別及び国の影響を除くためにそれぞれの国における犬種頭数と性別とを合わせた。その結果、各国 1252 頭となった。日本及び米国に共通していた 63 問の質問について因子分析を行った結果、12 の因子に分類された。因子負荷量が 0.4 より小さい項目を除き、再び因子分析を行った結果、再び 12 の因子に分類された。因子負荷量が 0.4 より小さい項目を再び除き、再び因子分析を行った結果、同じく因子得点における共通分散の 55.14%を占める 12 の因子に分類された。そのうち 11 の因子がクロンバックのアルファ値 0.7 以上を示した。11 の因子は、見知らぬ人に対する攻撃性、見知らぬ人に対する恐れ、訓練性、分離不安、興奮性、非社会的な刺激に対する恐れ、飼い主に対する攻撃性、見知らぬ犬に対する恐れ、見知らぬ犬に対する攻撃性、愛着、侵入者に対する攻撃性であり、11 の因子には総計 50 個の質問項目が含まれた。

２．C-barq 因子得点に対する犬種の影響

犬種を、既に報告されていた vonHoldt (2010)11 による遺伝分岐図（図 1-1）を基に、①原始的な犬（アンシエント）グループ、②トイグループ、③スパニエル、セントハウンド、

プードルから成るスパニエルグループ、④ワーキンググループ、⑤テリアグループ、⑥ハーディングとサイトハウンドから成るハーディンググループ、⑦レトリバーグループ、⑧マスチフグループの 8 つのグループに分類して解析を行った。柴犬は、vonHoldt (2010)による遺伝分岐図に含まれていないため、Parker (2004)による遺伝分岐図を基に原始的な犬のグループに分類した。その他の遺伝分岐図に含まれない犬種については、解析から除外した。一般化線型モデルを用いて解析を行った結果、11 の因子全てが犬種グループ及びその他 8 つの変数によって有意に説明された（$p<0.05$, 表 1-1, 図 1-2 参照）。

見知らぬ人に対する攻撃性：トイグループが最も高かった。トイグループは、ハーディンググループ、レトリバーグループ、マスチフグループよりも有意に攻撃的であった（$p<0.05$）。また、スパニエルグループは、レトリバーグループ及びマスチフグループ、原始的な犬グループはレトリバーグループ、ハーディンググループはレトリバーグループよりも有意に攻撃的であった（$p<0.05$）。

見知らぬ人に対する恐れ：ワーキンググループが最も低く、その他の全ての犬種グループよりも有意に低かった（$p<0.05$）。

訓練性：ハーディンググループが最も高かった。ハーディンググループの訓練性は、ワーキンググループ以外の全ての犬種グループよりも有意に高かった（$p<0.05$）。

分離不安：犬種グループによる違いは見られなかった。

興奮性：ワーキンググループが最も低かった。ワーキンググループの興奮性は、マスチフグループ以外の全ての犬種グループよりも有意に低かった（$p<0.05$）。ハーディンググループが最も高く、スパニエルグループ、ワーキンググループ、マスチフグループよりも有意に高かった（$p<0.05$）。

非社会的な刺激に対する恐れ：ワーキンググループが最も低く、ハーディンググループが最も高かった。ワーキンググループの非社会的な刺激に対する恐れは、マスチフグループ以外の全ての犬種グループよりも有意に低く、ハーディンググループの非社会的な刺激に対する恐れは、スパニエルグループ、ワーキンググループ、マスチフグループよりも有意に高かった（$p<0.05$）。

飼い主に対する攻撃性：ワーキンググループが最も低く、トイグループが最も高かった。ワーキンググループの飼い主に対する攻撃性は、その他の全ての犬種グループよりも低かった（$p<0.05$）。トイグループの飼い主に対する攻撃性は、ワーキンググループ、ハーディンググループ、レトリバーグループよりも有意に高かった（$p<0.05$）。また、スパニエルグループの飼い主に対する攻撃性は、ワーキンググループとハーディンググループよりも有意に高かった（$p<0.05$）。

見知らぬ犬に対する恐れ：ワーキンググループが最も低かった。ワーキンググループの見知らぬ犬に対する恐れは、その他の全ての犬種グループよりも有意に低かった（$p<0.05$）。

見知らぬ犬に対する攻撃性：レトリバーグループが最も低く、原始的な犬グループ、トイグループ、テリアグループ及びハーディンググループよりも有意に低かった（$p<0.05$）。

愛着：原始的な犬グループが最も低かった。原始的な犬グループの愛着スコアは、その他の全ての犬種グループよりも有意に低かった（$p<0.05$）。
侵入者に対する攻撃性：トイグループが最も高く、トイグループの侵入者に対する攻撃性は、マスチフグループよりも有意に高かった（$p<0.05$）。

３．C-barq 因子「愛着」の犬種クラスター解析

原始的な犬グループとその他の犬種グループとで違いが見られた愛着について、犬種クラスター解析を行った。その結果、犬種は大きく 2 つのクラスターに分類され、原始的な犬グループの 5 犬種全てがクラスター1 に分類された（図 1-3 参照）。原始的な犬グループの犬種以外には、ホワイトテリア、ウィペット、ケアンテリア、ボルゾイ、グレートデーンの 5 犬種がクラスター1 に分類され、その他の 36 犬種はクラスター2 に分類された。

表 1-1　一般化線型モデルを用いた因子得点の解析結果

	F1: Aggression to unfamiliar persons					F2: Fear of unfamiliar persons				
	χ^2	df	p	Pairwise comparison	B[5)]	χ^2	df	p	Pairwise comparison	B
Breed groups[1)]	50.570	7	0.000	1>7, 2>6, 2>7, 2>8, 3>7, 3>8, 5>7, 6>7		126.652	7	0.000	1>4, 2>4, 3>4, 5>4, 6>4, 7>4, 8>4	
Country	1.015	1	0.314			70.010	1	0.000	US>JPN	
Sex	1.683	1	0.195			69.123	1	0.000	F>M	
Neutered status[2)]	0.658	1	0.417			0.468	1	0.494		
Source where aquired[3)]	24.100	6	0.001	2>3, 5>3		1.940	6	0.925		
Dog-ownership experience[4)]	1.361	1	0.243			0.006	1	0.939		
Body weight	0.571	1	0.450			14.518	1	0.000		-0.029
Dog's age at evaluation	0.000	1	0.996			0.627	1	0.429		
Dog's age when acquired	14.696	1	0.000		-0.003	3.223	1	0.073		
Breed groups*Country	61.631	15	0.000			139.576	15	0.000		
Breed groups*Sex	63.198	15	0.000			127.814	15	0.000		
Country*Sex	12.030	3	0.007			85.804	3	0.000		
Breed groups*Country*Sex	79.827	31	0.000			141.411	31	0.000		
Omnibus	189.444	42	0.000			145.060	42	0.000		

	F3: Trainability					F4: Separation-related anxiety				
	χ^2	df	p	Pairwise comparison	B	χ^2	df	p	Pairwise comparison	B
Breed groups[1)]	51.531	7	0.000	6>1, 6>2, 6>3, 6>5, 6>7, 6>8		13.498	7	0.061		
Country	14.488	1	0.000	US>JPN		31.078	1	0.000	US>JPN	
Sex	0.749	1	0.387			0.000	1	0.996		
Neutered status[2)]	3.771	1	0.052			4.368	1	0.037	I>N	
Source where aquired[3)]	31.588	6	0.000	3>4, 7>4		12.795	6	0.046		
Dog-ownership experience[4)]	15.057	1	0.000	2>1		10.161	1	0.001	1>2	
Body weight	3.725	1	0.054			4.925	1	0.026		-0.012
Dog's age at evaluation	22.534	1	0.000		0.024	5.444	1	0.020		-0.039
Dog's age when acquired	5.055	1	0.025		0.000	1.083	1	0.298		
Breed groups*Country	89.920	15	0.000			96.176	15	0.000		
Breed groups*Sex	59.386	15	0.000			20.717	15	0.146		
Country*Sex	15.663	3	0.001			31.078	3	0.000		
Breed groups*Country*Sex	104.545	31	0.000			106.105	31	0.000		
Omnibus	248.373	42	0.000			237.075	42	0.000		

1, Ancient and spitz breeds: 1, Toy dogs: 2, Spaniels, scent hounds, and poodles: 3, Working dogs: 4, Small terriers: 5, Sight hounds and herding dogs: 6, Retrievers: 7, Mastiff-like dogs: 8

2, neutered: N, intact: I

3, bred by owner: 1, friend of relative: 2, breeder: 3, pet store: 4, shelter: 5, stray: 6, other: 7

4, first ownership: 1, second and more ownership: 2

5, partial regression coefficient

	F5: Energy and restless					F6: Fear of non-social stimuli				
	χ^2	df	p	Pairwise comparison	B	χ^2	df	p	Pairwise comparison	B
Breed groups[1)]	44.844	7	0.000	1>4, 2>4, 3>4, 5>4, 6>4, 7>4, 6>3, 6>8		44.844	7	0.000	1>4, 2>4, 3>4, 6>3, 5>4, 6>4, 7>4, 6>8	
Country	5.077	1	0.024	JPN>US		5.077	1	0.024	JPN>US	
Sex	0.161	1	0.688			0.161	1	0.688		
Neutered status[2)]	5.631	1	0.018	N>I		5.631	1	0.018	N>I	
Source where aquired[3)]	10.706	6	0.098			10.706	6	0.098		
Dog-ownership experience[4)]	2.130	1	0.144			2.130	1	0.144		
Body weight	7.906	1	0.005		-0.012	7.906	1	0.005		-0.012
Dog's age at evaluation	2.154	1	0.142			2.154	1	0.142		
Dog's age when acquired	4.155	1	0.042		0.001	4.155	1	0.042		0.001
Breed groups*Country	52.434	15	0.000			52.434	15	0.000		
Breed groups*Sex	47.984	15	0.000			47.984	15	0.000		
Country*Sex	5.752	3	0.124			5.752	3	0.124		
Breed groups*Country*Sex	65.671	31	0.000			65.671	31	0.000		
Omnibus	148.076	42	0.000			148.076	42	0.000		

	F7: Aggression to household members					F8: Fear of unfamiliar dogs				
	$\chi 2$	df	p	Pairwise comparison	B	χ^2	df	p	Pairwise comparison	B
Breed groups[1)]	84.719	7	0.000	1>4, 2>4, 2>6, 2>7, 3>4, 3>6, 5>4, 6>4, 7>4, 8>4		141.880	7	0.000	1>4, 2>4, 3>4, 5>4, 6>4, 7>4, 8>4	
Country	0.000	1	1.000			80.139	1	0.000	US>JPN	
Sex	0.000	1	1.000			78.662	1	0.000	F>M	
Neutered status[2)]	0.000	1	1.000			2.798	1	0.094		
Source where aquired[3)]	0.000	6	1.000			11.911	6	0.064		
Dog-ownership experience[4)]	0.000	1	1.000			1.017	1	0.313		
Body weight	0.023	1	0.881			5.361	1	0.021		-0.017
Dog's age at evaluation	0.000	1	0.986			1.257	1	0.262		
Dog's age when acquired	2.897	1	0.089			0.008	1	0.929		
Breed groups*Country	89.609	14	0.000			153.605	15	0.000		
Breed groups*Sex	85.619	14	0.000			142.858	15	0.000		
Country*Sex	20.113	3	0.000			98.852	3	0.000		
Breed groups*Country*Sex	91.284	29	0.000			155.422	31	0.000		
Omnibus	266.838	42	0.000			111.849	42	0.000		

	F9: Aggression to unfamiliar dogs					F11: Attachment and attention-seeking				
	χ^2	df	p	Pairwise comparison	B	χ^2	df	p	Pairwise comparison	B
Breed groups[1)]	26.211	7	0.000	1>7, 2>7, 5>7, 6>7		82.116	7	0.000	2>1, 3>1, 4>1, 5>1, 6>1, 7>1, 8>1	
Country	2.747	1	0.097			136.912	1	0.000	US>JPN	
Sex	5.105	1	0.024	M>F		3.030	1	0.082		
Neutered status[2)]	0.509	1	0.476			1.019	1	0.313		
Source where aquired[3)]	11.427	6	0.076			11.958	6	0.063		
Dog-ownership experience[4)]	0.780	1	0.377			0.042	1	0.837		
Body weight	1.718	1	0.190			7.023	1	0.008		-0.005
Dog's age at evaluation	16.415	1	0.000		0.069	11.145	1	0.001		-0.018
Dog's age when acquired	2.756	1	0.097			1.318	1	0.251		
Breed groups*Country	36.747	15	0.001			328.227	15	0.000		
Breed groups*Sex	38.165	15	0.001			86.349	15	0.000		
Country*Sex	9.449	3	0.024			145.751	3	0.000		
Breed groups*Country*Sex	52.726	31	0.009			344.926	31	0.000		
Omnibus	104.112	42	0.000			385.296	42	0.000		

	F12: Aggression to persons passing near the				
	χ^2	df	p	Pairwise comparison	B
Breed groups[1)]	19.286	7	0.007	2>8	
Country	3.724	1	0.054		
Sex	0.984	1	0.321		
Neutered status[2)]	0.543	1	0.461		
Source where aquired[3)]	8.539	6	0.201		
Dog-ownership experience[4)]	0.335	1	0.563		
Body weight	0.007	1	0.934		
Dog's age at evaluation	0.000	1	0.999		
Dog's age when acquired	8.065	1	0.005		-0.002
Breed groups*Country	29.034	15	0.016		
Breed groups*Sex	26.774	15	0.031		
Country*Sex	7.556	3	0.056		
Breed groups*Country*Sex	47.057	31	0.032		
Omnibus	72.384	42	0.002		

図 1-1　犬種の分類に用いた遺伝分岐図（vonHoldt 2010）

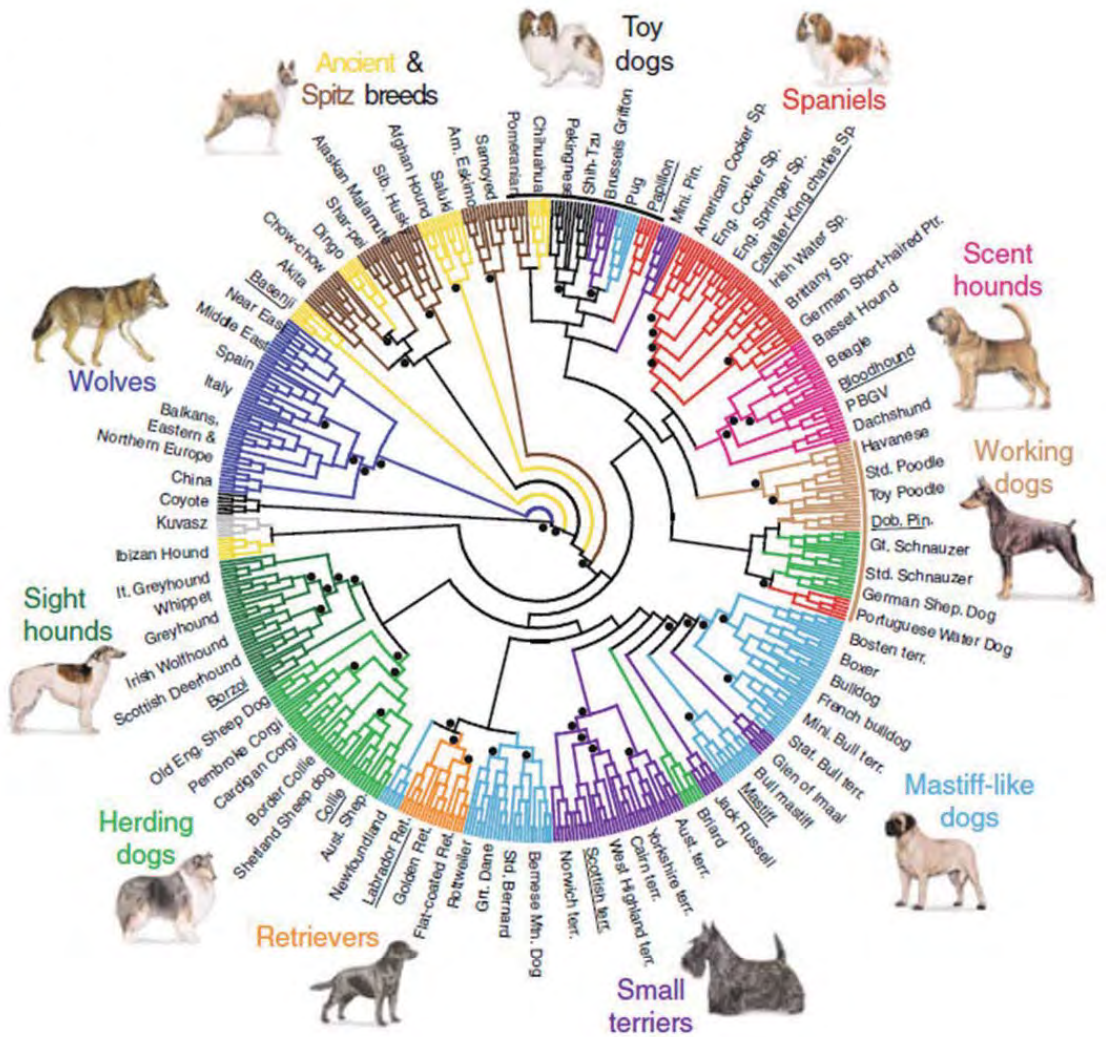

黒い点は、ブートストラップ値 95%以上を示す。

図 1-2　犬種グループにおける因子得点の平均スコア

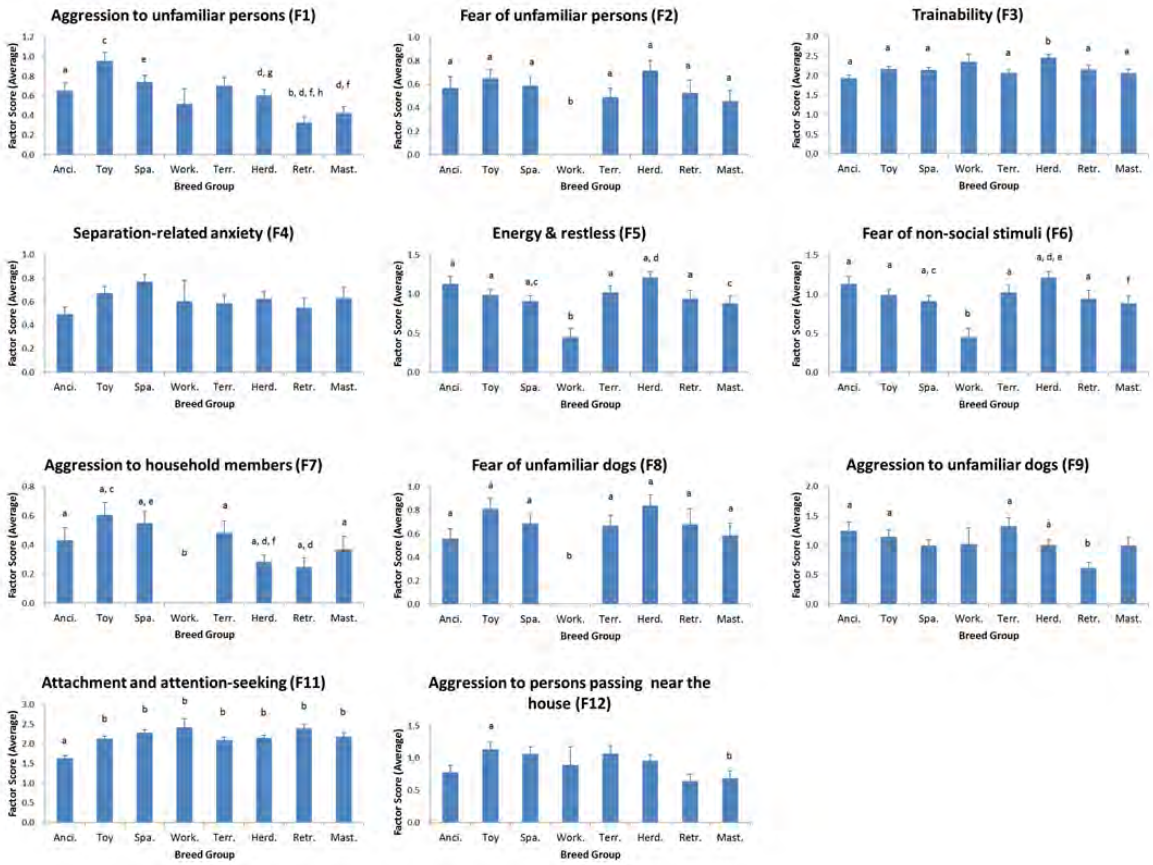

a vs b, p<0.05;　c vs d, p<0.05;　e vs f, p<0.05;　g vs h, p<0.05

Ancient and spitz breeds: Anci., Toy dogs: Toy, Spaniels, scent hounds, and poodles: Spa., Working dogs: Work., Small terriers: Terr., Sight hounds and herding dogs: Herd., Retrievers: Retr., Mastiff-like dogs: Mast.

図 1-3　愛着の犬種クラスター解析樹形図

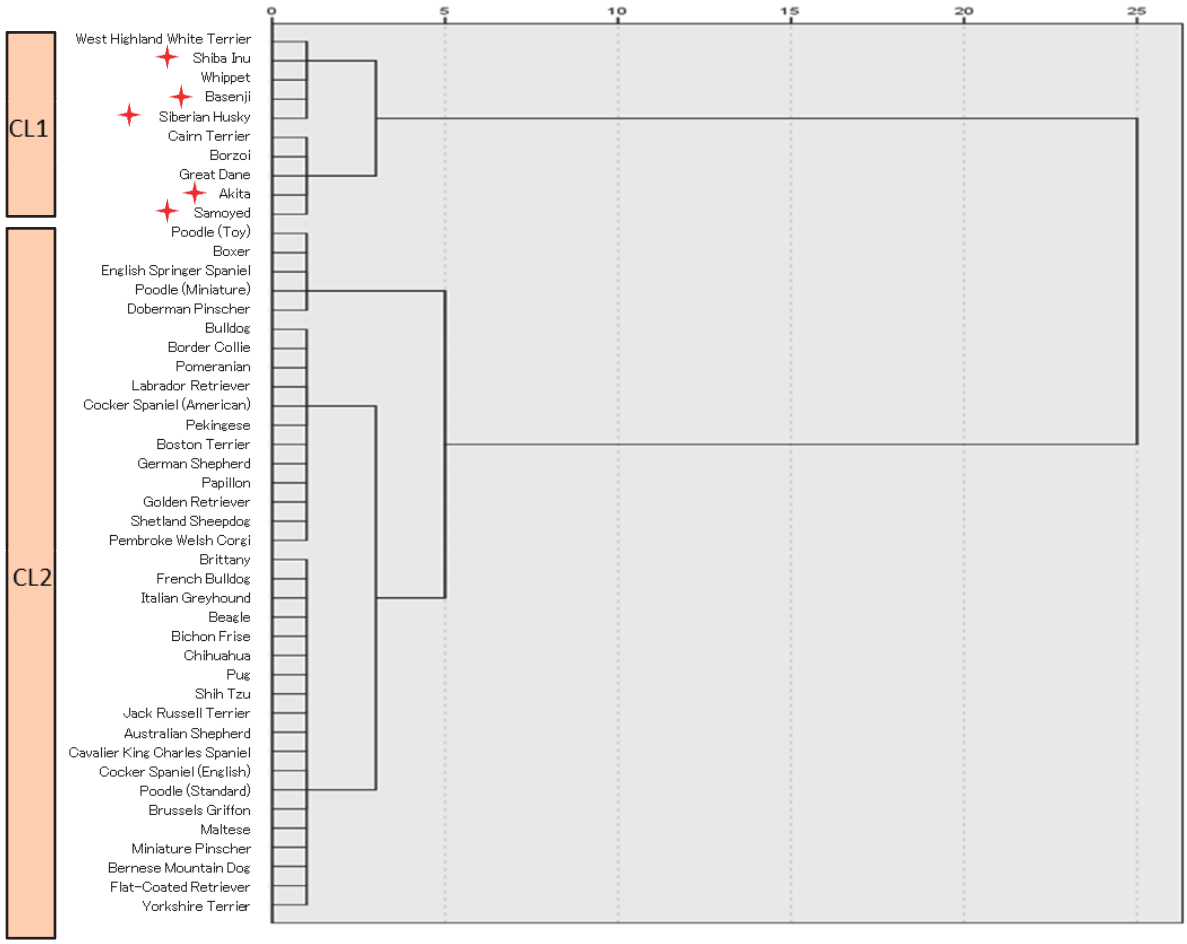

✦ 原始的な犬グループの犬種

２．犬の家畜化過程における選択圧因子の推定

研究要旨

オオカミ、秋田犬、柴犬、原始的な犬グループ以外のイヌ（ラブラドール、スタンダードプードル等の様々な犬種）のアミラーゼコピー数を調査した。柴犬は、一般的にペットとして飼われている柴犬と天然記念物柴犬保存会の厳しい管理の元で交配が行われている縄文柴を用いた。
オオカミのアミラーゼコピー数は先行研究で報告されているとおり、2 コピー程度であった。また、オオカミへの遺伝的近さから予想したとおり、秋田犬のコピー数はオオカミよりも多いが一般的な犬種より少なかった（$p<0.01$）。一方、秋田犬と同じく原始的な犬グループに含まれる柴犬のコピー数は、一般的な犬種と同程度であり、柴犬のオオカミへの遺伝的近さと反した結果となった。縄文柴のコピー数は、柴犬より少なく（$p<0.01$）、秋田犬より多かった（$p<0.05$）。

研究目的

2005 年のイヌの全ゲノム配列の解読以降、イヌの家畜化に関するゲノムワイドな研究が活発に行われた。それらの研究成果によりあげられたイヌの家畜化の過程で選択圧がかかったと思われる遺伝子の候補には、消化・代謝関連に関わるものが多く見られた 12-14。特に、でんぷん消化酵素である β-アミラーゼ遺伝子のコピー数が、オオカミに比べてイヌでは多くなっていることが明らかとなり、イヌの家畜化にはでんぷん消化能力の変化が大きく影響しているのではないかと推測された。
一方で、オオカミからイヌへと家畜化された「進化」（第 1 の段階）の選択圧としてでんぷん消化能力の変化が働いたのか、又は、ヒトが農耕を始めるとともにイヌの食糧源も変化しこれらの遺伝子に選択圧がかかったのかは明らかになっていない。本研究では第 1 章から第 3 章までの結果により、イヌの家畜化（進化）には気質が関連していたと推測しており、本章では、でんぷん消化能力がイヌの家畜化（進化）（第 1 の段階）の選択圧として働いたのかどうかを調査することとした。

材料と方法

オオカミ 12 頭、秋田犬 14 頭、柴犬 34 頭の血液又は肝臓の組織片より DNA を抽出した。血液の抗凝固剤は、エチレンジアミンテトラ酢酸（EDTA）を用いた。肝臓の組織片は、動物病院にて検体されたものを郵送いただいた。サンプルは全て-20℃にて冷凍保存した。柴犬は、一般的にペットとして飼われている柴犬 17 頭と天然記念物柴犬保存会の厳しい管理の元で交配が行われている縄文柴 17 頭を用いた。天然記念物柴犬保存会は古代のイヌの形態をめざして柴犬の交配を行っており、その結果、縄文柴は一般的な柴犬と比べて、浅い

額段、三角形の鋭い目、大きく鋭い歯等の縄文時代の遺跡から発掘されたイヌと近い形態を持つ。また原始的な犬グループ以外のイヌの代表として、ラブラドール、スタンダードプードル等の様々な犬種のイヌ 25 頭を用いた。

血液又は肝臓の組織片からの DNA 抽出は第 3 章と同様の手順で行った。

コピー数の測定には、TaqMan Genotyping Master Mix (Applied Biosystems)を用いた TaqMan Copy Number Assay 又は SYBR® Premix Ex Taq™ II (TaKaRa) を用いた qPCR を行った。プライマーやプローブの設計は Axelsson らの論文 10 に従い、方法はメーカーのプロトコルに従った。内部標準には、イヌゲノム上で 2 コピーで存在することが知られている C7orf28B を用い、サンプルは 1 個体 3 回ずつ測定した。TaqMan 法と qPCR 法との互換性を、同じサンプルを測ることにより確認した。

統計処理は SPSS statistic 17.0（SPSS Japan Inc.）を用い、有意水準は 5%とした。Kruskal-Wallis test 及び Mann Whitney U test（Bonferroni 補正）を行った。オオカミのうち 1 つのサンプルは、外れ値として除外した。

結果および考察

オオカミのアミラーゼコピー数は先行研究で報告されているとおり、2 コピー程度であった。また、オオカミへの遺伝的近さから予想したとおり、秋田犬のコピー数はオオカミよりも多いが一般的な犬種より少なかった。一方、秋田犬と同じく原始的な犬グループに含まれる柴犬のコピー数は、一般的な犬種と同程度であり、柴犬のオオカミへの遺伝的近さと反した結果となった。縄文柴のコピー数は、柴犬や一般的な犬種より少なく、秋田犬より多かった（図 2-1 参照）。

図 2-1　アミラーゼコピー数の犬種間ならびにオオカミとの比較

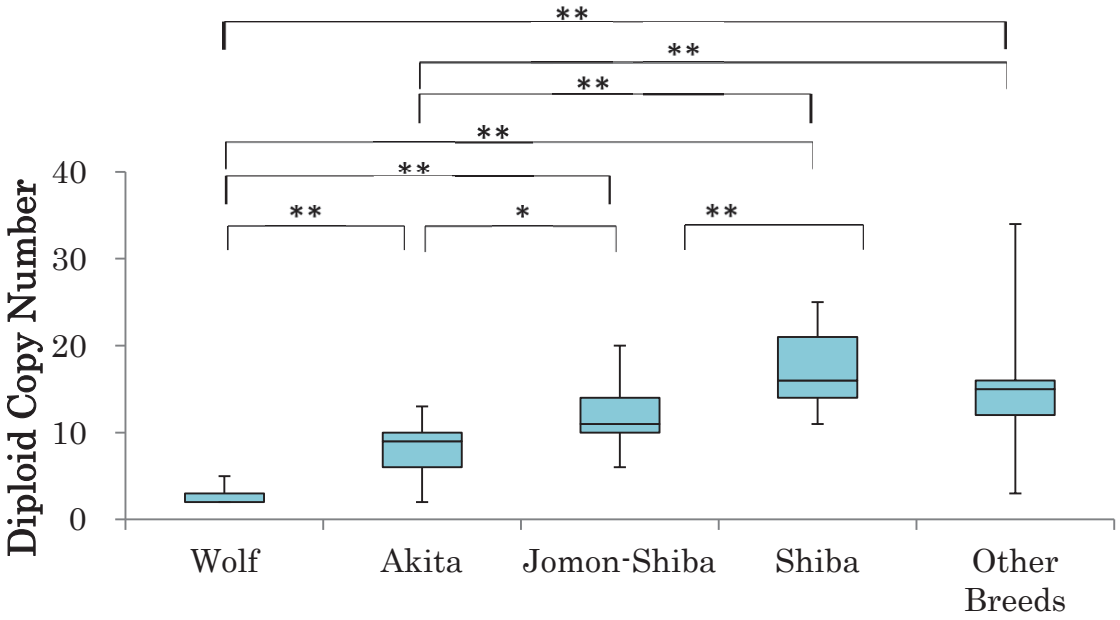

オオカミ（n=11），秋田犬（n=14），縄文柴（n=17），柴犬（n=17），一般的な犬種（n=25）.

Mann Whitney U-tests wih Bonferroni correction **, $p<0.01$ *, $p<0.05$

$\chi^2=48.3$, df=4, $p<0.01$

３．ヒトへの社会認知能力における犬種差の検出

研究要旨

様々な犬種のイヌを用い、イヌの認知能力の犬種差を解決不可能課題及び指差し二者選択課題により評価した。解決不可能課題では、餌を容器で覆い容器を固定した状態で、イヌがヒトを見るまでの時間、ヒトを見ている時間、ヒトを見る回数、交互凝視の回数を測定した。指差し二者選択課題では、２つのカップのどちらかに餌を隠した上で、ヒントを出すことによりイヌが餌の入っている方のカップを選ぶ回数を測定した。ヒントとしては容器をとんとんとたたく（タッピング）、容器へ視線を向ける（視線）、容器を指差す（指差し）の３種類を組み合わせて用いた。

解決不可能課題では、原始的な犬は、最初にヒトを見るまでの時間がトイグループ、スパニエルグループ、ハーディンググループよりも長く、ヒトを見ている時間がスパニエルグループ、ハーディンググループ、レトリバーグループよりも短く、ヒトを見る回数がスパニエルグループ、ハーディンググループよりも少なく、交互凝視の回数がトイグループ、スパニエルグループ、ハーディンググループ、レトリバーグループよりも少なかった。また、原始的な犬と一般的な犬種とで 2 群比較を行ったところ、最初にヒトを見るまでの時間、ヒトを見ている時間、ヒトを見る回数、交互凝視の回数の全てにおいて、原始的な犬は一般的な犬種よりも有意にヒトを見ない結果が得られた（$p<0.01$）。

指差し二者選択課題では、原始的な犬の成績は、視線＋指差し＋タッピング課題、視線＋指差し課題、指差し課題の全てにおいてその他の犬種グループと同等であり、犬種グループによる有意な差は見られなかった。原始的な犬と一般的な犬種とで２群比較を行ったところ、視線＋指差し＋タッピング課題において、原始的な犬は一般的な犬種よりも正答数が有意に高かった（$p<0.05$）。視線＋指差し課題、指差し課題では、有意な差は見られなかった。

研究目的

イヌの指差し理解力や解決不可能な場面でヒトを参照する能力は遺伝的基盤によると考えられ、これらの認知能力について犬種間で比較することにより、それらの犬種がどのように作成されていったのかその過程を知ることができる。特に、ゲノムワイド研究によって遺伝的に最もオオカミに近いことが知られている原始的な犬グループのイヌの行動特性は、祖先種に最も近いと考えられ、イヌの家畜化（進化）を考える上で重要となるが、犬種の遺伝分岐図におけるオオカミからの近縁度と指差し理解力や解決不可能課題における社会的認知能力との関連性の研究はこれまでに行われてきていない。第 2 章では、犬種をvonHoldt(2010)の遺伝分岐図を基に 8 つの犬種グループ（①原始的な犬グループ、②トイグループ、③スパニエル、セントハウンド、プードルから成るスパニエルグループ、④ワ

ーキンググループ、⑤テリアグループ、⑥ハーディングとサイトハウンドから成るハーディンググループ、⑦レトリバーグループ、⑧マスチフグループ）に分類し、社会的認知能力について、原始的な犬グループの特徴を調査することを目的とした。

材料と方法

一般家庭で飼育されているイヌ587頭を対象として行動テストを行った。イヌの募集は、公園、動物病院、しつけ教室、ドッグカフェなどでチラシを配布又は掲示して行い、飼い主様同意の上でテストに参加していただいた。

一般家庭で飼育されているイヌと犬舎で飼育されているイヌとの比較では、動物専門学校で飼育されているイヌ 75 頭を対象として行動テストを行った。トレーニング科のイヌは週に 2-3 回トレーニングを受けており、トリミング科のイヌは週に 1-2 回トリミングを受けている。犬舎で飼われており、数頭ずつ広い運動場に放されて適切な運動の機会を与えられている。入手先はほぼブリーダーであり、自家繁殖のイヌとペットショップからのイヌが数頭含まれている。

① 解決不可能課題

ウォーミングアップ試行：餌を板の上に置き、餌を容器で覆った状態で、板をイヌの前に置いた。イヌが自分で容器をどけて中の餌を食べるまで待った。これを 6 回繰り返し、容器をどけて中の餌を食べることをイヌに覚えさせた。

テスト試行：餌を板の上に置き、餌を容器で覆い、今度はイヌが容器を自分でどけられないように、容器を板に固定した。板をイヌの前に置き、イヌの行動を 2 分間観察した。イヌの行動をビデオカメラで撮影し、後でビデオ解析を行い、イヌが最初にヒトを見るまでの時間、ヒトを見ている時間、ヒトを見た回数、容器とヒトとの交互凝視の回数を計測した。

② 指差し二者選択課題

Hare ら(2002) 21 の手順を参考に行った。

ウォーミングアップ試行 : イヌを板の真ん中で、板から 1m の距離に実験者と対面するように座らせた。イヌが見ている前で餌を 2 つの容器のどちらか一方に入れた。イヌに開放の合図を出し、容器を選ばせた。イヌが餌の入っている方の容器に最初に触れた場合には、容器を持ち上げてイヌに餌を食べさせた。イヌが餌の入っていない方の容器に最初に触れた場合には、容器を持ち上げて、容器の中に何も入っていないこと確認させた。さらに、餌の入っている方の容器を持ち上げて、餌が入っていることをイヌに確認させた。ウォーミングアップ試行は、イヌが連続して 3 回、餌が入っている方のカップを選ぶまで続けられた。10 分間経ってもウォーミングアップ試行を通過できなかった場合には、テストは終了とし、そのイヌは除外された。

テスト試行:イヌを板の真ん中で、板から 1m の距離に実験者と対面するように座らせた。イヌの名前を呼び、餌を見せた後に、衝立の裏でイヌから見えないように餌を 2 つの容器

のどちらか一方に入れた。餌を隠す容器は、あらかじめ無作為に決められた。容器を板の両端にスライドさせた後に、衝立をどけた。イヌの名前を呼び注目させてから、指差し等のヒントを出した。ヒントは、容器をとんとんとたたく（タッピング）、容器を指差す（指差し）、容器へ視線を向ける（視線）、の三種類を組み合わせて用いた。ヒントの組み合わせは 4 パターン行い、視線＋指差し＋タッピング(GPT)課題、視線＋指差し(GP)課題、指差し(P)課題、コントロール(C、ヒントなし)の順番で行った。各パターンを 18 回ずつ行い、計 72 回の試行を行った（図 2-1 参照）。

統計解析は、まず犬種を既に報告されていた遺伝分岐図を元に 8 つのグループに分類し、イヌの社会的認知能力の犬種グループ間比較に用いた。なお、ワーキング、テリア、マスチフのグループについては、例数が少なかったため、分析からは除外し、5 つのグループで比較した。次に、原始的な犬グループ以外の 7 つのグループのイヌを一般的な犬種グループとしてまとめて、原始的な犬グループと一般的な犬種グループとの 2 群比較を行った。統計処理は SPSS statistic 17.0（SPSS Japan Inc.）を用い、有意水準は 5%とした。Kruskal-Wallis test 及び Mann Whitney U test（Bonferroni 補正）を行った。指差し二者選択課題と解決不可能課題の関連性の検討の統計処理は SPSS statistic 17.0（SPSS Japan Inc.）を用い、有意水準は 5%とし、相関解析を行った。

結果および考察

① 解決不可能課題

最初にヒトを見るまでの時間は、原始的な犬グループが、トイグループ、スパニエルグループ、ハーディンググループよりも有意に遅かった（$p<0.05$）。ヒトを見ている時間は、原始的な犬グループは、スパニエルグループ、ハーディンググループ、レトリバーグループよりも有意に少なかった（$p<0.05$）。ヒトを見る回数は、原始的な犬グループはスパニエルグループ、ハーディンググループよりも有意に少なく（$p<0.05$）、トイグループはスパニエルグループよりも有意に少なかった（$p<0.05$）。交互凝視の回数は、原始的な犬グループは、他の 4 つのグループ全てと比較して有意に少なく（$p<0.05$）、トイグループはハーディンググループのイヌよりも有意に少なかった（$p<0.05$）。（図 3-1 参照）

原始的な犬種グループとの比較では、最初にヒトを見るまでの時間、ヒトを見ている時間、ヒトを見る回数、交互凝視の回数、全てにおいて、原始的な犬グループのイヌは一般的な犬種よりも有意にヒトを見ない結果が得られた。（$p<0.01$, 図 3-2 参照）

② 指差し二者選択課題

犬種グループによる違いは見られなかった。（$p>0.05$, 図 3-3 参照）

原始的な犬種グループとの比較では、視線＋指差し＋タッピング課題において、原始的な犬グループのイヌは一般的な犬種よりも正答数が有意に高かった（$p<0.05$）。視線＋指差し課題、指差し課題では、有意な差は見られなかった。（$p>0.05$, 図 3-4 参照）

図 3-1　解決不可能課題でヒトを参照する能力について犬種グループ間比較

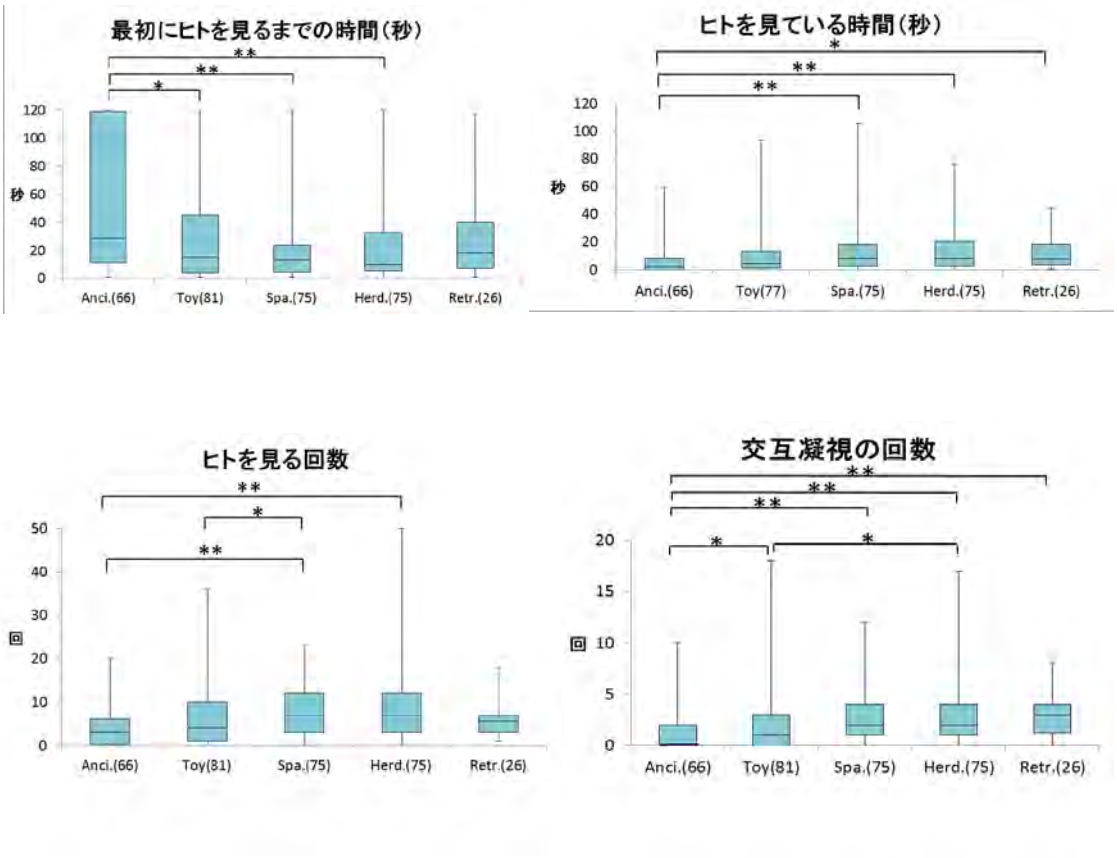

**, p<0.01　　*, p<0.05

Mann-Whitney U-test with Bonferroni correction

最初にヒトを見るまでの時間　χ^2＝19.732, df=4, p<0.01

ヒトを見ている時間　χ^2＝19.659, df=4, p<0.01

ヒトを見る回数　χ^2＝28.023, df=4, p<0.01

交互凝視の回数　χ^2＝36.956, df=4, p<0.01

図 3-2　解決不可能課題でヒトを参照する能力の原始的な犬と一般的な犬種の比較

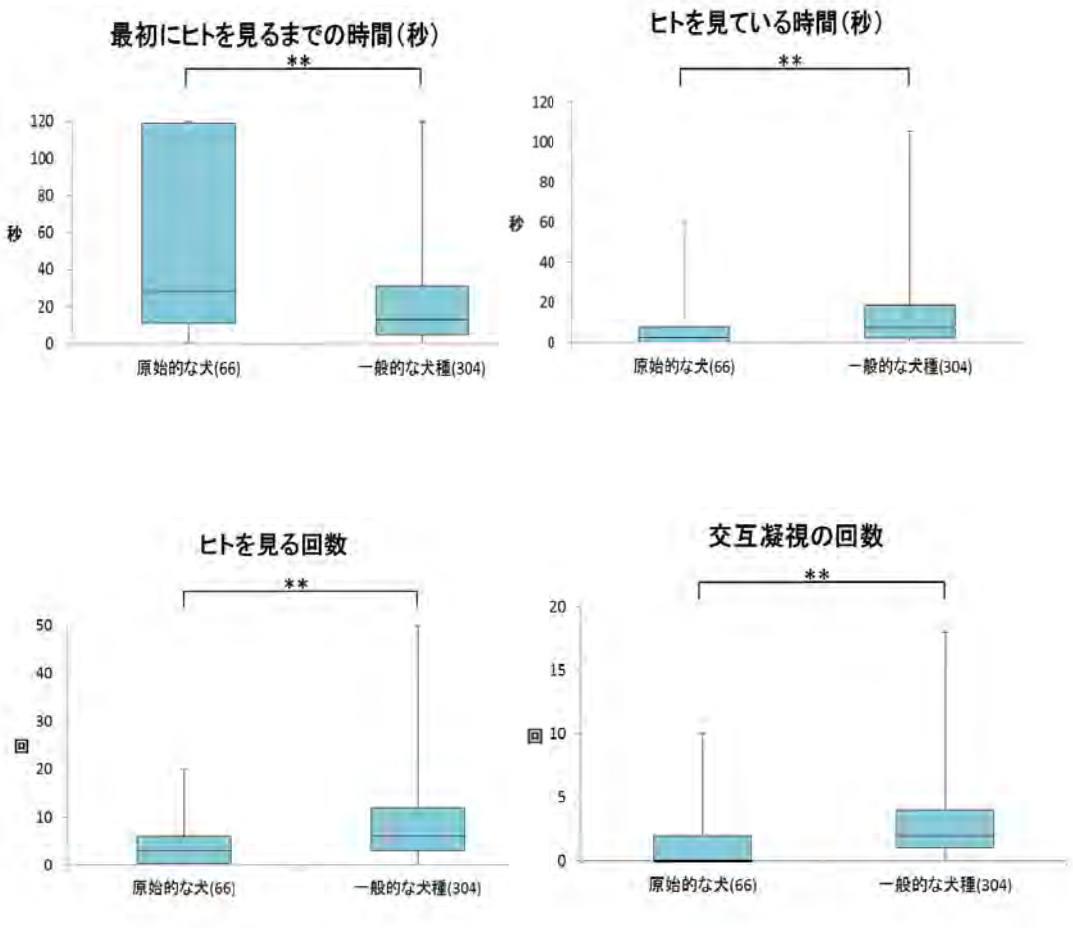

**, p<0.01

Mann-Whitney U-test

最初にヒトを見るまでの時間　χ^2＝17.691, df=1, p<0.01

ヒトを見ている時間　χ^2＝16.122, df=1, p<0.01

ヒトを見る回数　χ^2＝21.007, df=1, p<0.01

交互凝視の回数　χ^2＝26.659, df=1, p<0.01

図 3-3　指差し二者選択課題の正答数について犬種グループ間比較

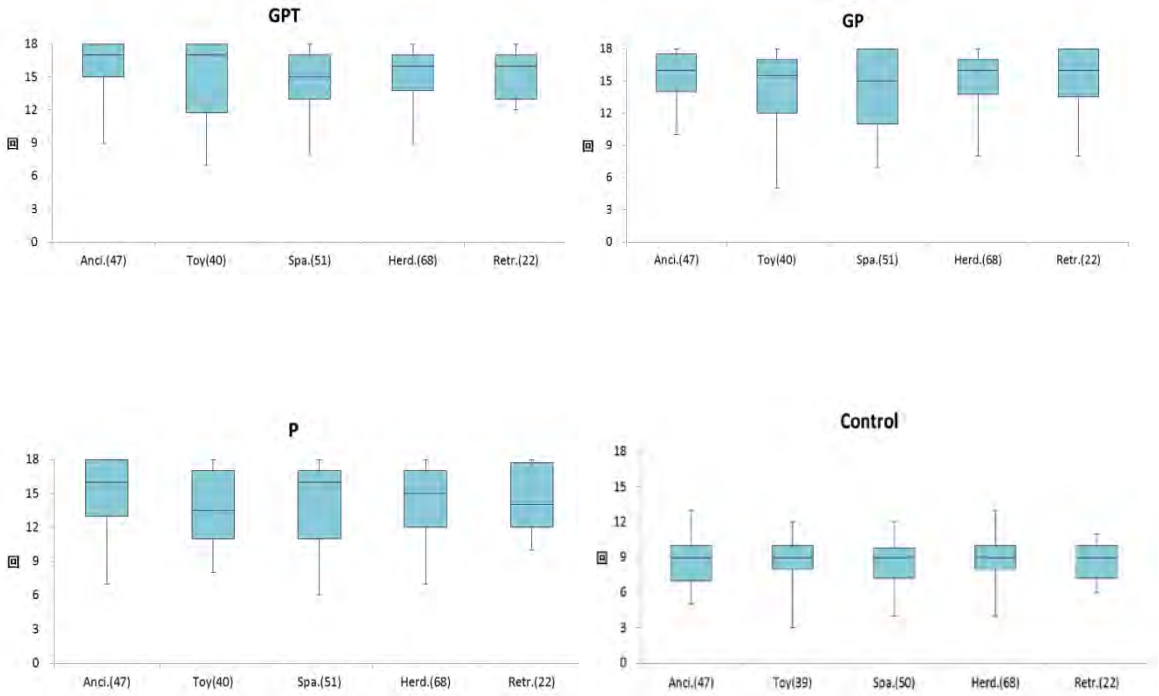

p>0.05

Mann-Whitney U-test with Bonferroni correction

視線＋指差し＋タッピング(GPT)**課題**　χ^2＝8.624, df=4, p>0.05

視線＋指差し(GP)**課題**　χ^2＝2.918, df=4, p>0.05

指差し(P)**課題**　χ^2＝4.771, df=4, p>0.05

コントロール(Control)**課題**　χ^2＝1.055, df=4, p>0.05

図 3-4　指差し二者選択課題の正答数の原始的な犬と一般的な犬種との比較

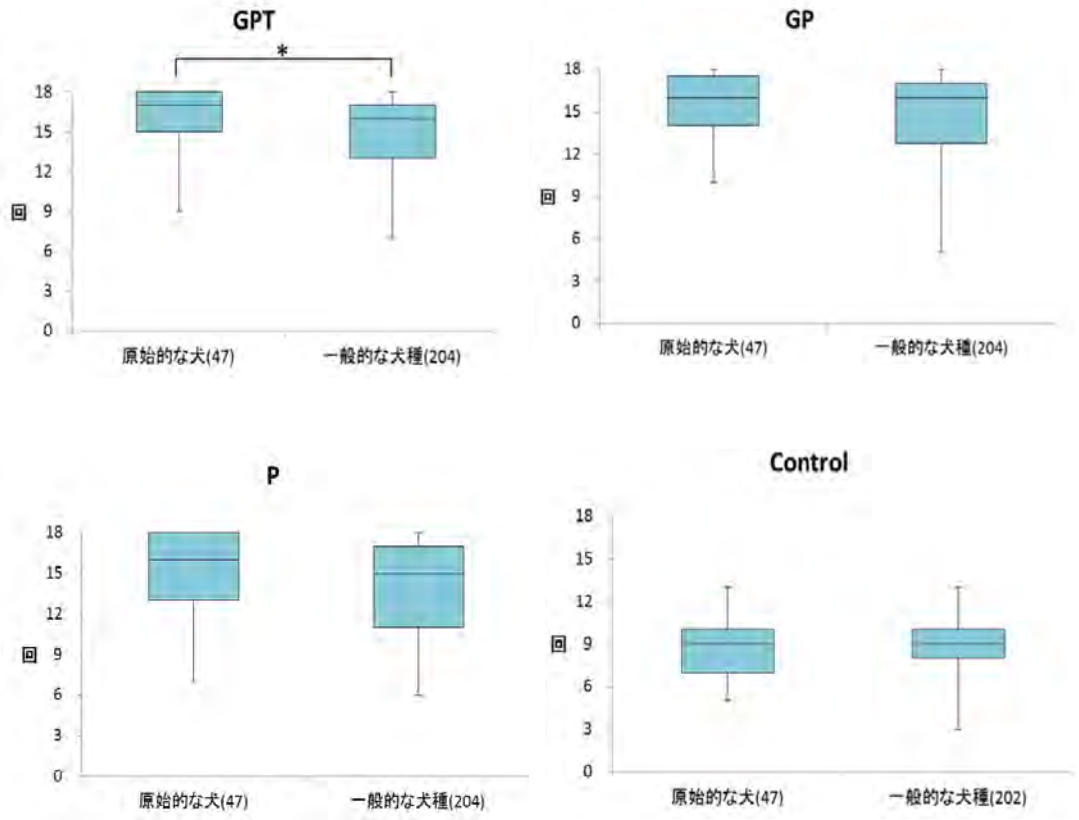

*, $p<0.05$

Mann-Whitney U-test

視線＋指差し＋タッピング(GPT)**課題**　$\chi^2=6.662$, df=1, $p<0.05$

視線＋指差し(GP)**課題**　$\chi^2=1.461$, df=1, $p>0.05$

指差し(P)**課題**　$\chi^2=3.299$, df=1, $p>0.05$

コントロール(Control)**課題**　$\chi^2=1.111$, df=1, $p>0.05$

４．犬の社会認知能力に関連する遺伝子の同定

研究要旨

コミュニケーション能力に関わるホルモンとして、オキシトシンとコルチゾールに着目し、メラノコルチン２受容体（MC2R）とオキシトシン、オキシトシン受容体の遺伝子を選択した。さらにゲノムワイド解析によってイヌの進化に関わると報告されている候補遺伝子から WBSCR17 を選抜し、これらに関連する遺伝子の多型を調べ、犬種差や行動実験の結果との関連性を調べた。

イヌの進化候補遺伝子である WBSCR17（ウィリアムズ症候群関連遺伝子）において、原始的な犬と一般的な犬種とで出現頻度の異なる一塩基多型(c.1179C>T)が検出され、原始的な犬では一般的な犬種に比べ T を持つ頻度が高かった。またこの T 型の遺伝子型を持つ個体では、指差し二者選択課題の視線＋指差し＋タッピングの課題の正答数が高い結果となった（$p<0.05$）。MC2R（メラノコルチン 2 受容体遺伝子）において、原始的な犬と一般的な犬種とで出現頻度の異なる一塩基多型（c.871G>A, Val291Ile）が検出され、原始的な犬では一般的な犬種に比べ A を持つ頻度が高かった。またこの A 型の遺伝子型を持つ個体を一般的な犬種内で比較した結果、指差し二者選択課題の視線＋指差し＋タッピング課題、視線＋指差し課題、指差し課題の正答数が低い結果となった（$p<0.05$）。OT（オキシトシン遺伝子）において、原始的な犬と一般的な犬種とで出現頻度の異なる一塩基多型（c322+50C>A）と反復数多型（c322+51_52repGGGGCC）が検出され、原始的な犬では一般的な犬種に比べ一塩基多型では A を持つ頻度が高く、反復数多型では 25 塩基及び 37 塩基の長さの配列を持つ頻度が低かった。原始的な犬に多い A/A 型の一塩基多型を持つ個体では、A/C 型の遺伝子型を持つ個体よりも、解決不可能課題のヒトを見ている時間、ヒトを見る回数、交互凝視の回数においてヒトを見ない結果となった（$p<0.05$）。反復数多型では 25 塩基又は 37 塩基の長さの配列をヘテロで持つ個体において、挿入を持たない個体よりも解決不可能課題でヒトを見る回数が多い傾向が見られた（$p=0.078$）。OTR（オキシトシン受容体遺伝子）においては、原始的な犬と一般的な犬種とで出現頻度の異なる一塩基多型が検出されたものの、行動実験の結果とは関連性が見られなかった。

研究目的

2005 年にイヌの全ゲノム配列が公表された 10。解読されたのはメスのボクサー「ターシャ」のゲノムである。その後、この「ターシャ」のゲノム解読結果（被覆度 7.5 倍）、2003 年に報告されていたスタンダードプードルのゲノム解読結果（被覆度 1.5 倍）29 及び、9 犬種（被覆度 0.02 倍）、オオカミやコヨーテから成る 5 種類のイヌ科動物（被覆度 0.04 倍）の塩基配列を決定した結果を比較することにより、250 万個以上の 1 塩基多型（SNPs）が同定

された 10。イヌの家畜化のプロセスには何らかの表現型による強い選択圧がかかっており、選択圧のシグナルがゲノム上に残されていると思われる。そのシグナルを探るために、2010 年にゲノムワイドな SNP ジェノタイピングアレイを用いた解析が報告された 14。その結果、ヒトにおいて肉体的・精神的に発達の遅れを示す発達障害であるウィリアムズ症候群に関連しているとされている遺伝子である WBSCR17 30 の近くに選択圧のシグナルが見られることが明らかとなった。ウィリアムズ症候群の人々は、反り返った鼻と小さな顎を持つ妖精のような顔つきをもち、肉体的にも精神的にも発達の遅れを示す。脳容積が小さく、知能低下が見られる。視覚空間認知の働きに著しい障害を持つ一方で、言語能力には問題がなく、多弁で、人を恐れず社交的な性格を持つ 31。脳容積が小さいことや、多弁であること、人を恐れず社交的な性格等は、イヌにも共通して見られる特徴であり、WBSCR17 遺伝子はイヌの家畜化（進化）と関連しているかもしれないと考え、本遺伝子を社会的認知能力に関連する遺伝子の第 1 候補とした。

さらに、同じくゲノムワイドな SNP ジェノタイピングアレイを用いた Chase らの研究成果では、家畜化関連遺伝子として MC2R（メラノコルチン 2 受容体）が挙げられている 32。Chase らの研究において、ハーディング関連遺伝子として挙げられている MC2R は、副腎にある ACTH 受容体でコルチゾールの産生に関与することが知られている。キツネの家畜化実験において人への攻撃性によって選択的に繁殖していくことにより、HPA 軸の活性が低下することや血漿中コルチゾール量が低下することが報告されている 33。また、in vitro の実験において、グルココルチコイドは細胞の分裂増殖の時間を調節し、細胞の分化を誘導することが報告されており 34、コルチゾールは発達速度・割合の調整に関与する可能性がある。イヌの家畜化（進化）において、人への攻撃性や恐怖心による選択圧が働き、その結果、発達速度や割合に変化が現れ現在の様々な犬種が作成されたとも考えられる。MC2R 遺伝子はイヌの家畜化（進化）と関連しているかもしれないと考え、本遺伝子を認知能力関連遺伝子の第 2 の候補とした。

材料と方法

イヌ 443 頭及びオオカミ 12 頭の血液、口内粘膜又は肝臓の組織片から DNA を抽出して遺伝子解析を行った。血液の抗凝固剤は、エチレンジアミンテトラ酢酸（EDTA）を用いた。口内粘膜の採取には、Endo Cervex ブラシ（アズワン）を用いた。肝臓の組織片は、動物病院にて検体されたものを郵送いただいた。サンプルは全て-20℃にて冷凍保存した。

血液及び口内粘膜からの DNA の抽出には QIAamp® DNA Mini Kit（QIAGEN）を用いた。抽出方法はメーカーのプロトコルに従った。肝臓の組織片からの DNA の抽出は、DNAzol(Invitrogen)を用いて行った。細胞の破砕には、ビーズ方式の高速細胞破砕システムである Precellys24 (Bertin Technologies) を用いた（5000rpm, 20sec×2）。DNA の抽出方法は、メーカーのプロトコルに従った。

Ensembl 及び National Center for Biotechnology Information (NCBI)のインターネッ

トデータベースを用いて 1 塩基多型（SNPs）を検索した。エクソン領域にある SNPs を対象とし、WBSCR17 では、イヌゲノム第 6 染色体の 2168245 番目塩基対にある同義突然変異(rs24319159)をターゲットとした。MC2R では、第 1 番染色体の 24388879 番目塩基対にある同義突然変異(rs21898857, SNP1)と第 1 番染色体の 24389137 番目塩基対にある同義突然変異(rs21898855, SNP2)をターゲットとした。OTR では、第 20 番染色体の 9359598 番目塩基対にあるミスセンス変異（rs22927823, SNP1）、9359610 番目塩基対にあるミスセンス変異（rs22927826, SNP2）、9360368 番目塩基対にある同義突然変異（rs22927829, SNP3）、9378164 番目塩基対にある同義突然変異（rs8679682, SNP4）及び 9378224 番目塩基対にある同義突然変異（rs22896457, SNP5）をターゲットとした。OT では、第 24 番染色体の 18193483 番目塩基対にある同義突然変異/スプライシング領域変異（rs23181992, SNP1）及び 18193484 番目塩基対にある同義突然変異/スプライシング領域変異（rs23181995, SNP2）をターゲットとした（図 4-1 参照）。これらのターゲットを増幅するようにプライマーを設計した。

上記の SNPs についてシークエンスした際に MC2R と OT にて新たに見つかったデータベースでは公開されていない多型もターゲットとして追加した。MC2R では、コーディング領域の 871 番目塩基対の非同義突然変異（c.871G>A, Val291Ile, SNP3)、及び OT ではイントロン領域の 1 塩基多型（c.322+50C>A, intron-SNP)と同じくイントロン領域の反復数多型（c.322+51_52ins, intron-repeat)である（図 4-1 参照）。なお、OT は 3 つのエクソン領域と 2 つのイントロン領域から成り、3 つのエクソン領域は、オキシトシンのポリペプチド及びオキシトシンの輸送タンパク質であるニューロフィジンをコードしている。

PCR は My Cycler ™ thermal Cycler（BIO RAD）又は PCR サーマルサイクラ―Dice Touch(Takara)を用いた。酵素は、KOD FX-Neo（TOYOBO）を用いて、反応液の組成はメーカーのプロトコルに従った。PCR 条件は、94℃2 分を 1 サイクル、98℃10 秒、65℃30 秒を 40 サイクル、72℃7 分を 1 サイクル、その後は 4℃で維持した。また、OT の PCR では一部のサンプルにおいて、LA-Taq（takara）を用いた。反応液の組成はメーカーのプロトコルに従い（GCI buffer 使用)、PCR 条件は、95℃2 分を 1 サイクル、95℃30 秒、65℃30 秒、74℃1min を 40 サイクル、74℃10 分を 1 サイクル、その後は 4℃で維持した。PCR 産物の精製には Nucleo Spin® Gel and PCR Clean-up（Takara）を用いて、方法はメーカーのプロトコルに従った。

プライマー混合済み鋳型からの迅速シーケンス受託サービスであるプレミックスシーケンス解析（takara）を利用した。PCR 産物及びプライマーの量は、メーカーのプロトコルに従った。PCR 産物の濃度は、電気泳動により確認したバンドの明るさを基に算出した。サンプルは-20℃にてあらかじめ冷凍し、ドライアイスを入れて、クール宅急便（冷凍タイプ、ヤマト運輸）にて郵送した。

OT-repeat 多型がヘテロの個体では、シークエンスをすると 2 つの波形が重なってしまいうまく判定することができなかった。そこで、Genetic Analyzer（AB Applied Biosystems）

による測定を行った。PCR を行った後に、サンプルをクール宅急便（冷蔵タイプ、ヤマト運輸）にて郵送し、測定は京都大学の野生動物研究センターに依頼した。PCR 酵素は、LA-Taq（takara）を用いて、反応液の組成はメーカーのプロトコルに従った（GCI buffer 使用）。PCR 条件は、95℃2 分を 1 サイクル、95℃30 秒、65℃30 秒、74℃1min を 35 サイクル、74℃10 分を 1 サイクル、その後は 4℃で維持した。

原始的な犬と一般的な犬種とで多型頻度を比較した。多型頻度の比較は、エクセル統計（Square Test）を用いて行った。また、遺伝子型と第 2 章の社会認知能力との関連解析を行った。関連解析には、SPSS statistic 17.0（SPSS Japan Inc.）を用いて、Mann Whitney U test を行った。有意水準は 5%とした。

結果および考察

① 多型頻度の比較

WBSCR17 の多型頻度は原始的な犬と一般的な犬種とで有意な差が見られ、原始的な犬において T/T 型のイヌが多い結果であった（$p<0.01$, 図 4-2 参照）。またオオカミ 6 頭でジェノタイピングを行ったところ、C/C 型が 4 頭、T/C 型が 2 頭であった。WBSCR17 については、エクソン領域全長について 11 頭のイヌでシークエンスを行い多型の検索を行ったが、イントロン領域には他にもいくつか多型が見られたものの（図 4-1 参照）、エクソン領域には他に多型は見られなかった。

MC2R の多型頻度は SNP1 及び SNP3 において原始的な犬と一般的な犬種とで有意な差が見られ、一般的な犬種において G/G 型のイヌが多い結果であった（$p<0.01$, 図 4-3 参照）。オオカミ 12 頭では、SNP1 では G/G 型が 1 頭、G/C 型が 4 頭、C/C 型が 7 頭で、SNP3 では G/G 型が 2 頭、A/G 型が 9 頭、A/A 型が 1 頭であった。SNP2 では、多型は見られるものの、原始的な犬と一般的な犬種とで有意な差は見られなかった（$p>0.05$）。また、イヌでは全ての個体が C/C 型であるのに対して、オオカミでは 12 頭中、C/C 型 9 頭、C/T 型 2 頭と T/T 型 1 頭である同義突然変異が SNP1 と SNP2 の間に 1 つ見られた（第 1 番染色体の 24389032 番目塩基対, SNP1.5）。

OTR の多型頻度は SNP4 において原始的な犬と一般的な犬種とで有意な差が見られ、原始的な犬において T/T 型のイヌが多い結果であった（$p<0.01$, 図 4-4 参照）。オオカミ 5 頭では、C/C 型が 4 頭、T/T 型が 1 頭であった。SNP1 と 2 では、全てのイヌが G/G 型であり、多型は見られなかった。SNP3 と SNP5 では、わずかに多型が見られるものの、95%以上のイヌが T/T 型であった。

OT の多型頻度は intron-SNP において原始的な犬と一般的な犬種とで有意な差が見られ、一般的な犬種において C/C 型のイヌが多い結果であった（$p<0.01$, 図 4-5 参照）。オオカミ 7 頭では、C/C 型が 2 頭、C/A 型が 2 頭、A/A 型が 3 頭であった。また、OT の intron-repeat 多型では、6 塩基欠失、挿入なし、6 塩基挿入、25 塩基挿入、37 塩基挿入型が見られた。6 塩基欠失型については、スタンダードプードルの一部の個体でのみ見られた。原始的な犬

と一般的な犬種とで比較したところ、原始的な犬において 25 塩基挿入と 37 塩基挿入型が少ないことが明らかとなった（図 4-5 参照）。また、オオカミではイヌとは異なる長さの挿入（12 塩基挿入と 18 塩基挿入）が見られた。さらに、オオカミでは 2 番目のエクソン領域の末尾 6 塩基からイントロン領域の最初 11 塩基までの領域で、イヌでは見られない多型が見られた。イヌではセリン、プロリンのところが、アスパラギン、アスパラギン酸になる非同義変異である。本変異はオオカミ 11 頭中 5 頭に見られた。SNP1 と 2 では、全てのイヌが A/A 型（SNP1）、C/C 型（SNP2）であり、多型は見られなかった（図 4-5 参照）。

② 認知能力と遺伝子型との関連解析

WBSCR17 において、遺伝子型と指差し二者選択課題の視線＋指差し＋タッピングの課題で関連性が有意に見られた（$p<0.05$, 図 4-6 参照）。原始的な犬に多い T/T 型のイヌの正答数が高い結果となった。視線＋指差しの課題と指差しの課題では、有意な差は見られなかった（$p>0.05$）。また、解決不可能課題の結果との関連性も見られ、ヒトを見ている時間、ヒトを見る回数において、一般的な犬種に多い C/C 型のイヌでヒトをよく見る結果が得られた（$p>0.05$, 図 4-7 参照）。

MC2R では、遺伝子型と認知能力テストとの間に有意な関連性は見られなかった（$p>0.05$, 図 4-8 参照）。SNP3 において、指差し二者選択課題の指差し課題で関連性の傾向($p=0.064$)が見られた。一般的な犬種に多い G/G 型で正答数の高い傾向であった。

OTR では、遺伝子型と認知能力テストとの間に有意な関連性は見られなかった（$p>0.05$）。

OT では、intron-SNP の遺伝子型と解決不可能課題で関連性が有意に見られた（$p<0.05$, 図 4-9 参照）。原始的な犬に多い intron-SNP A/A 型のイヌは、ヒトを見ている時間が短く、ヒトを見る回数と交互凝視の回数が少ない結果となった（$p<0.05$）。指差し二者選択課題では関連性が見られなかった（$p>0.05$）。intron-repeat 多型では、いずれの行動実験の結果とも有意な関連性が見られなかった（$p>0.05$）ものの、挿入なしと 25 塩基挿入、挿入なしと 37 塩基挿入のヘテロの個体において、解決不可能課題でヒトを見る回数が多いように思えた（$p>0.05$, 図 4-10 参照）。そこで、挿入なしのホモ、挿入なしと 25 塩基挿入又は挿入なしと 37 塩基挿入のヘテロ、25 塩基挿入又は 37 塩基挿入のホモの 3 群で比較したところ、挿入なしのホモの個体はヘテロの個体よりもヒトを見る回数が少ない傾向が得られた($p=0.078$)。

図 4-1　各遺伝子における多型箇所を示す概略図

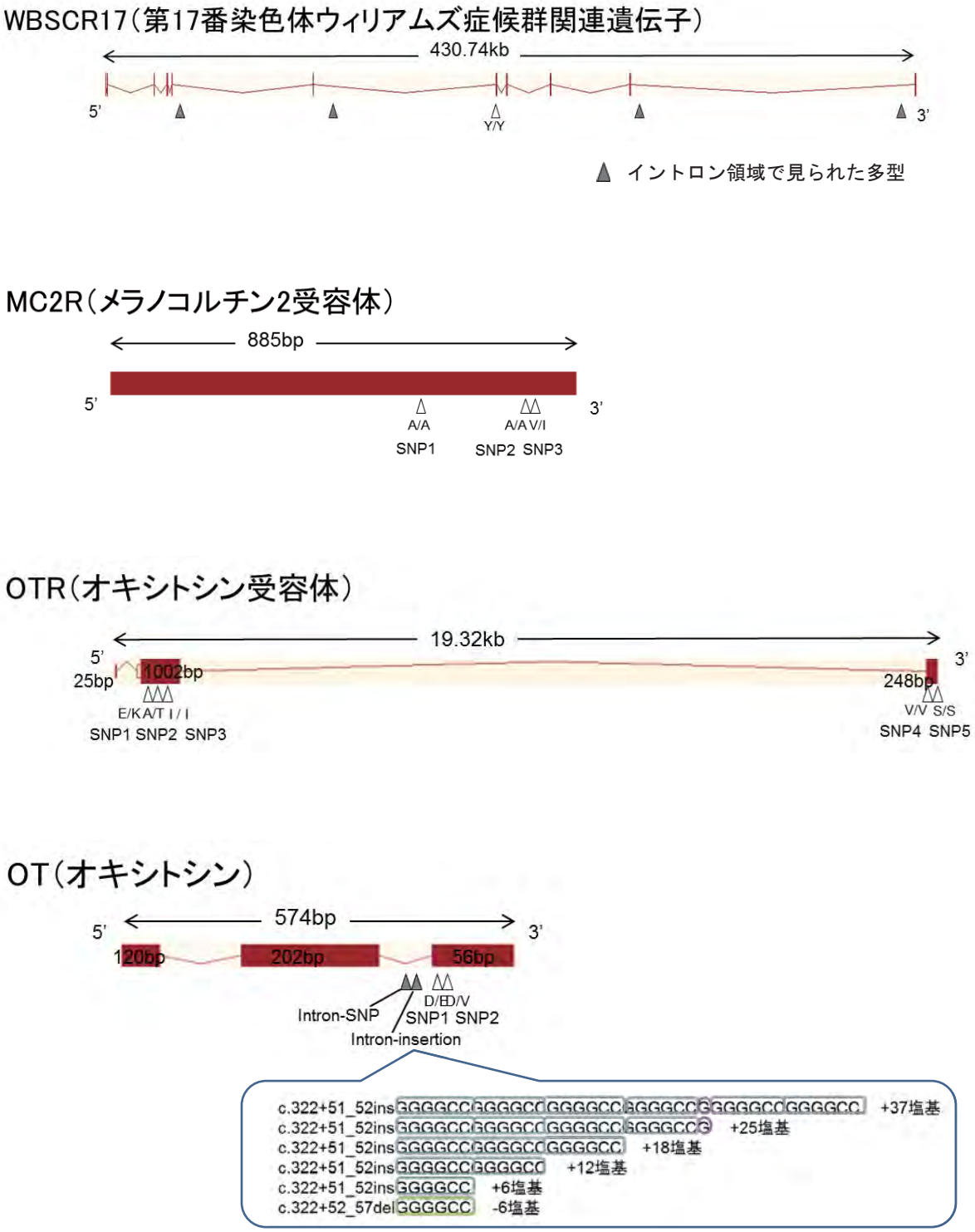

図 4-2　WBSCR17 多型頻度

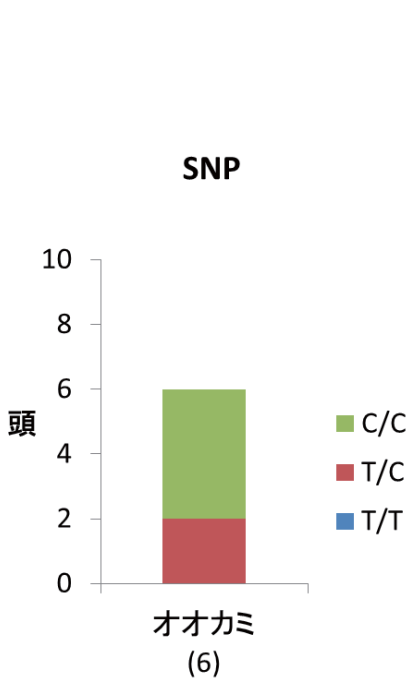

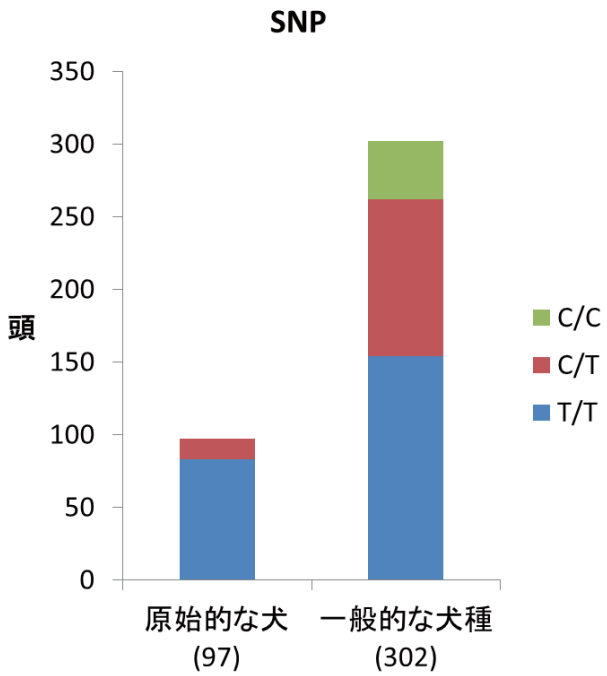

Square Test

$\chi^2 = 38.5$, df=2, $p<0.01$

図 4-3　MC2R 多型頻度

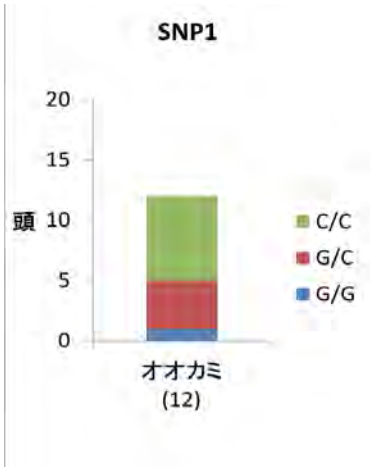

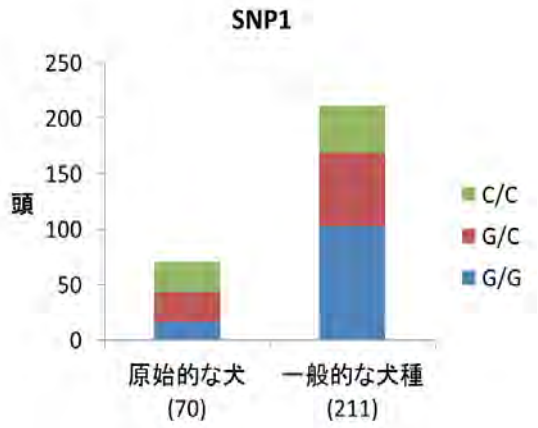

Square Test
χ^2=15.4, df=2, p<0.01

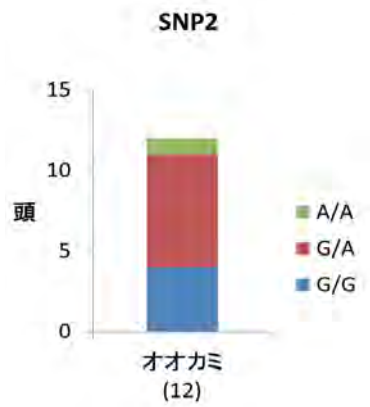

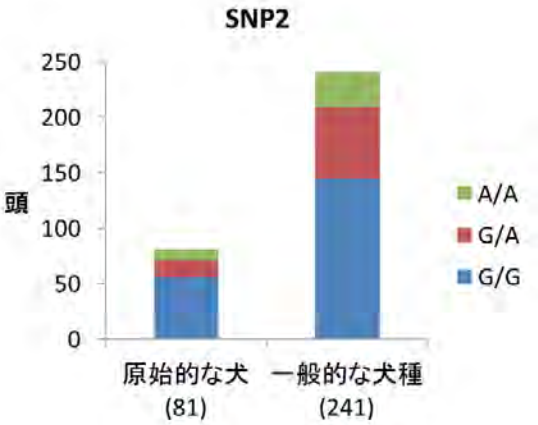

Square Test
χ^2=2.42, df=2, p>0.05

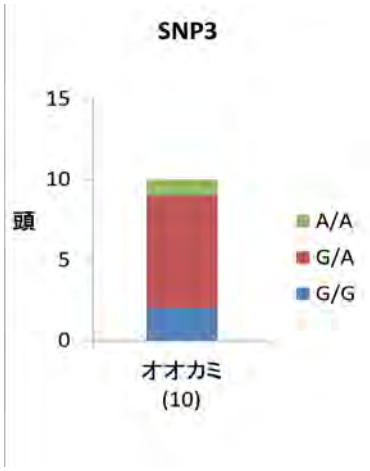

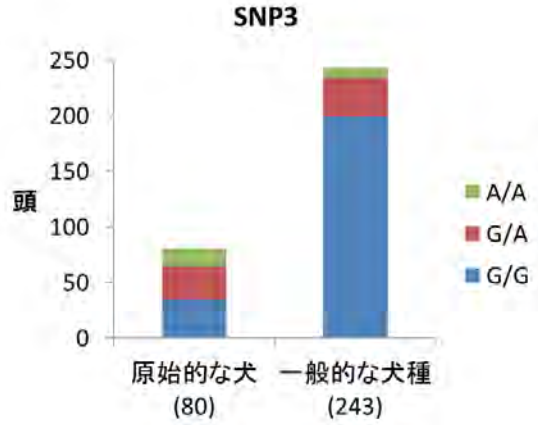

Square Test
χ^2=47.2, df=2, p<0.01

図 4-4　OTR 多型頻度

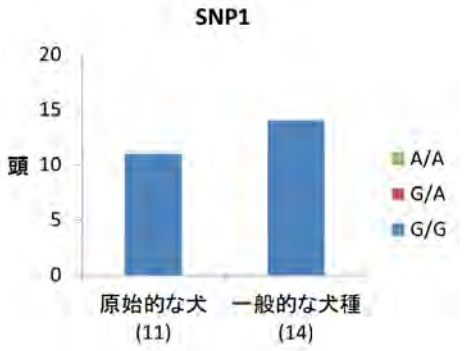

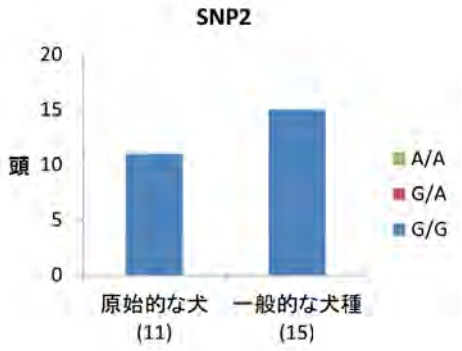

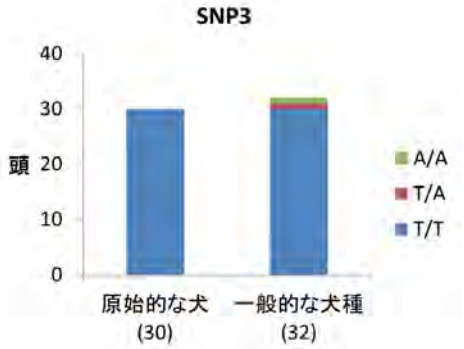

Square Test
χ^2＝1.94, df=2, p>0.05

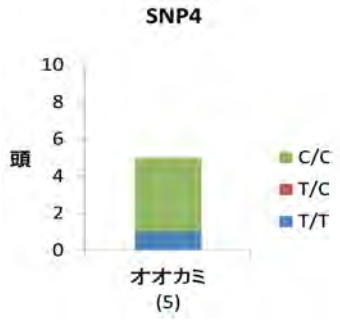

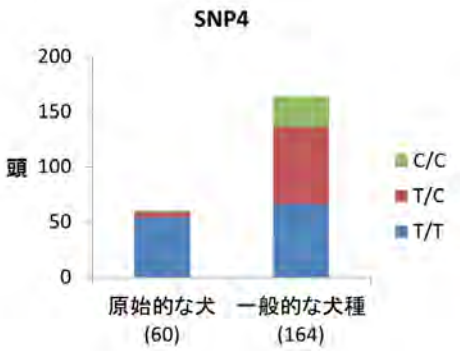

Square Test
χ^2＝43.8, df=2, p<0.01

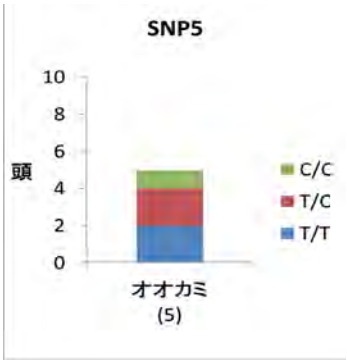

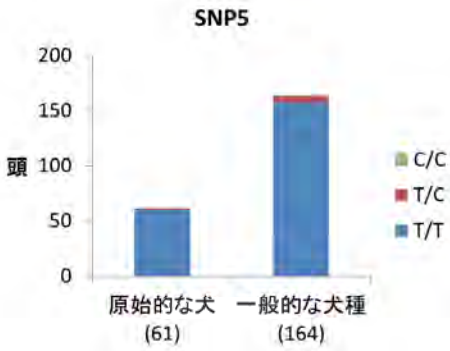

Square Test
χ^2＝0.986, df=2, p>0.05

図 4-5　OT 多型頻度

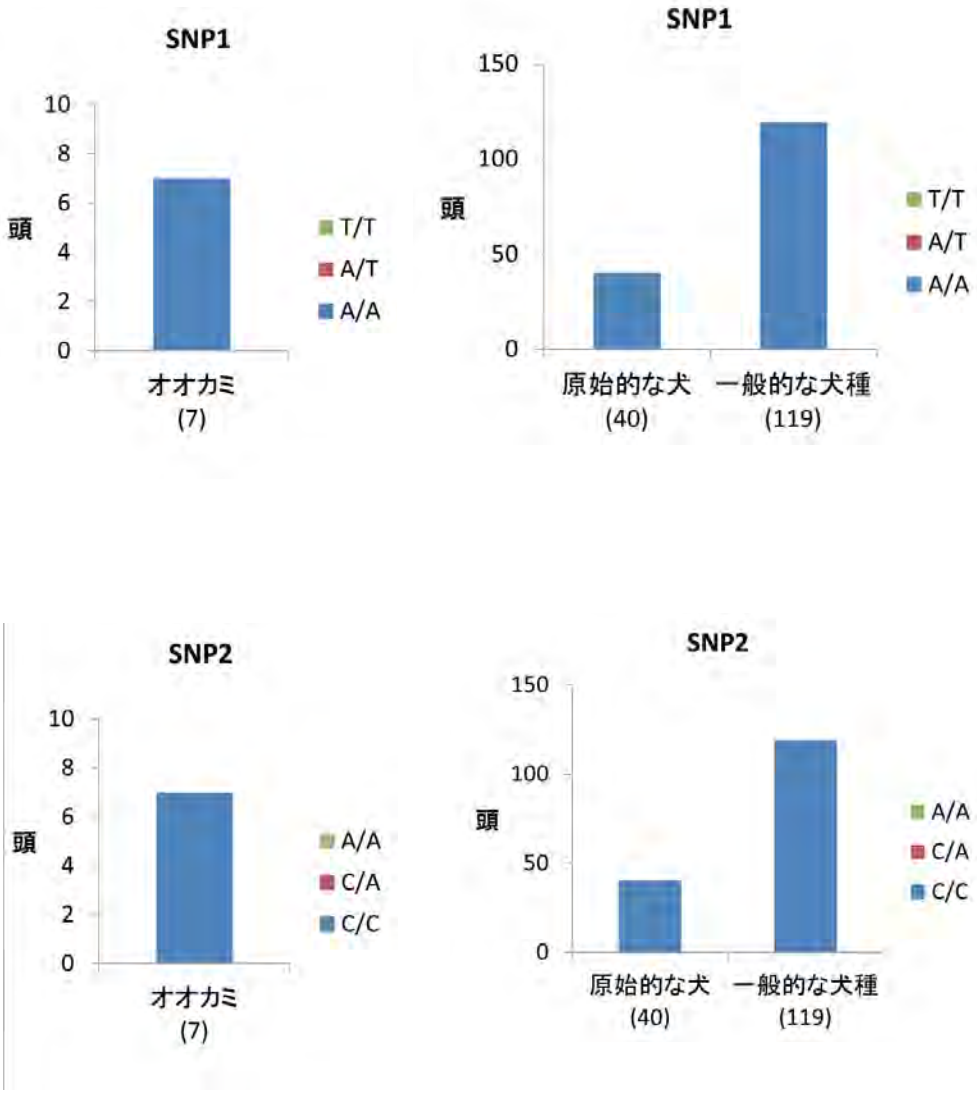
SNP1
頭
10
8
6
4
2
0
オオカミ
(7)
T/T
A/T
A/A
SNP1
頭
150
100
50
0
原始的な犬
(40)
一般的な犬種
(119)
T/T
A/T
A/A
SNP2
頭
10
8
6
4
2
0
オオカミ
(7)
A/A
C/A
C/C
SNP2
頭
150
100
50
0
原始的な犬
(40)
一般的な犬種
(119)
A/A
C/A
C/C

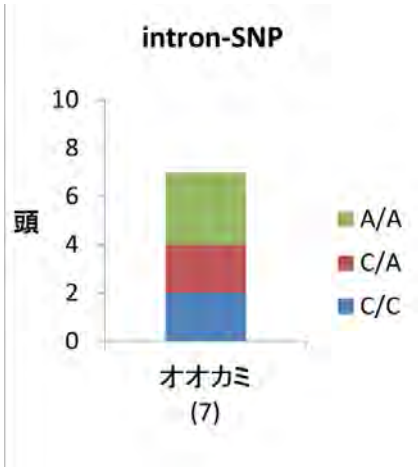

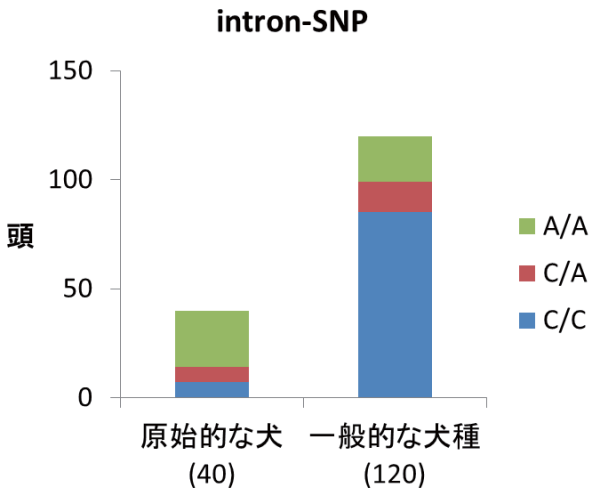

Square Test

$\chi^2 = 38.7$, df=2, $p<0.01$

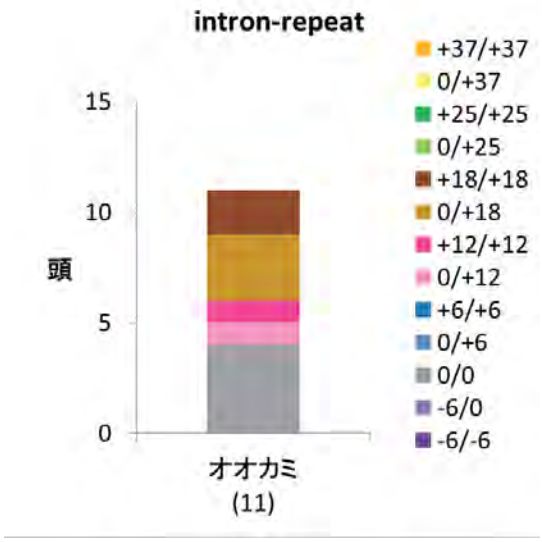

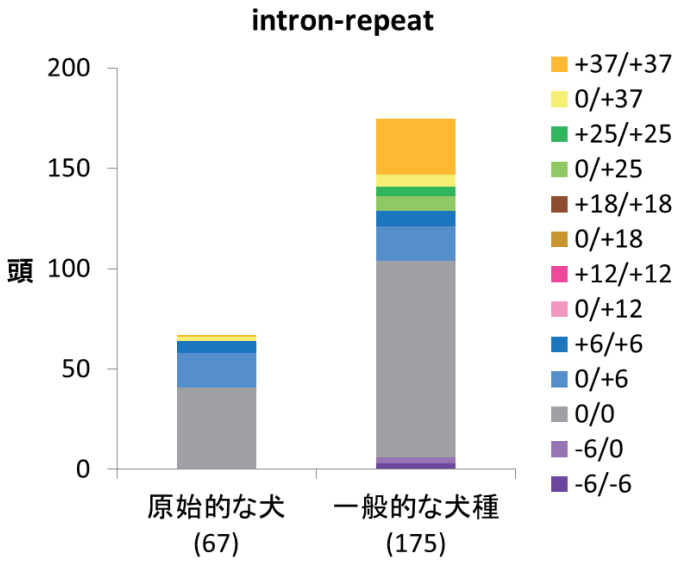

図 4-6　WBSCR17 遺伝子型と指差し二者選択課題

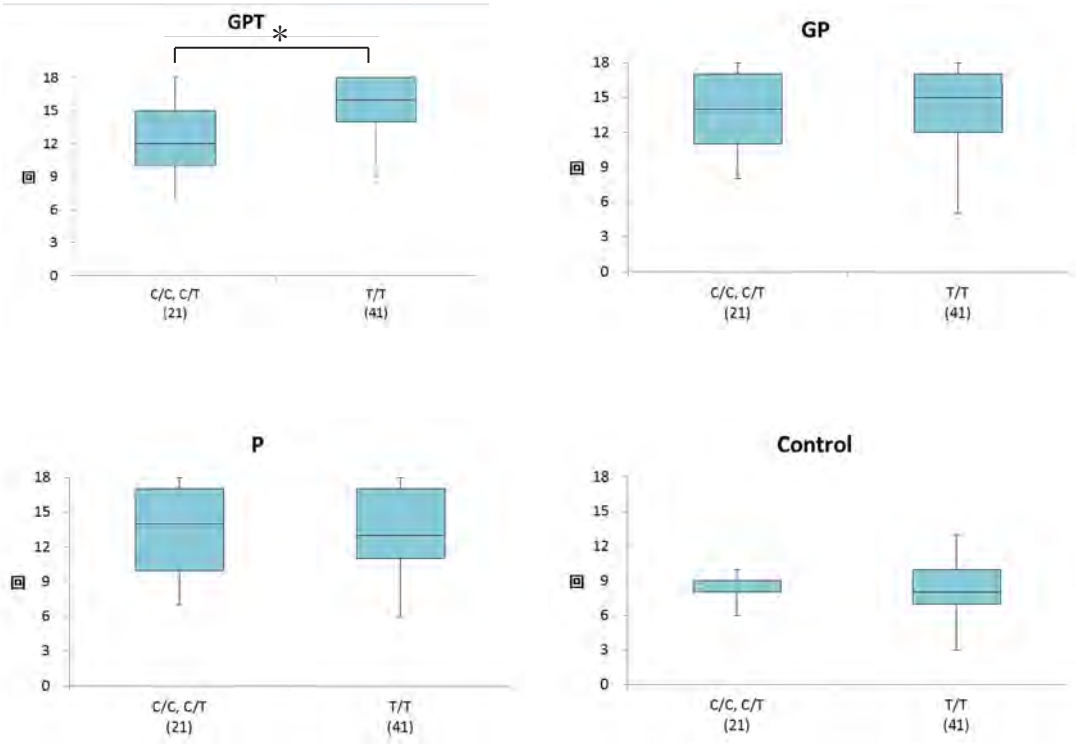

*, p<0.05

Mann-Whitney U-test

視線＋指差し＋タッピング(GPT)課題　χ^2＝9.682, df=1, p<0.01

視線＋指差し(GP)課題　χ^2＝1.101, df=1, p>0.05

指差し(P)課題　χ^2＝0.109, df=1, p>0.05

コントロール(Control)課題　χ^2＝0.138, df=1, p>0.05

図 4-7　WBSCR17 遺伝子型と解決不可能課題

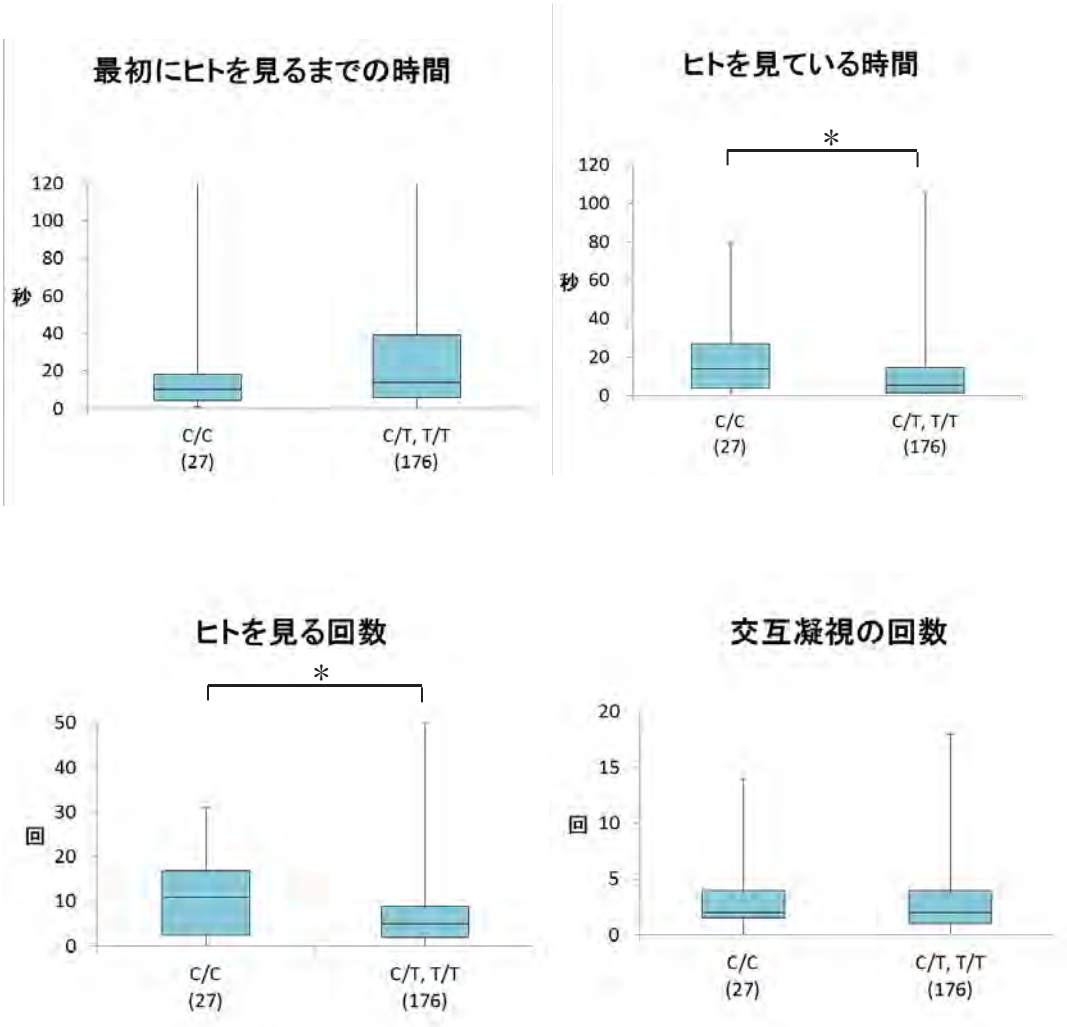

*, p<0.05

Mann-Whitney U-test

最初にヒトを見るまでの時間　$\chi^2=1.083$, df=1, p>0.05

ヒトを見ている時間　$\chi^2=4.647$, df=1, p<0.05

ヒトを見る回数　$\chi^2=5.297$, df=1, p<0.05

交互凝視の回数　$\chi^2=1.047$, df=1, p>0.05

図 4-8　MC2R SNP3 と指差し二者選択課題

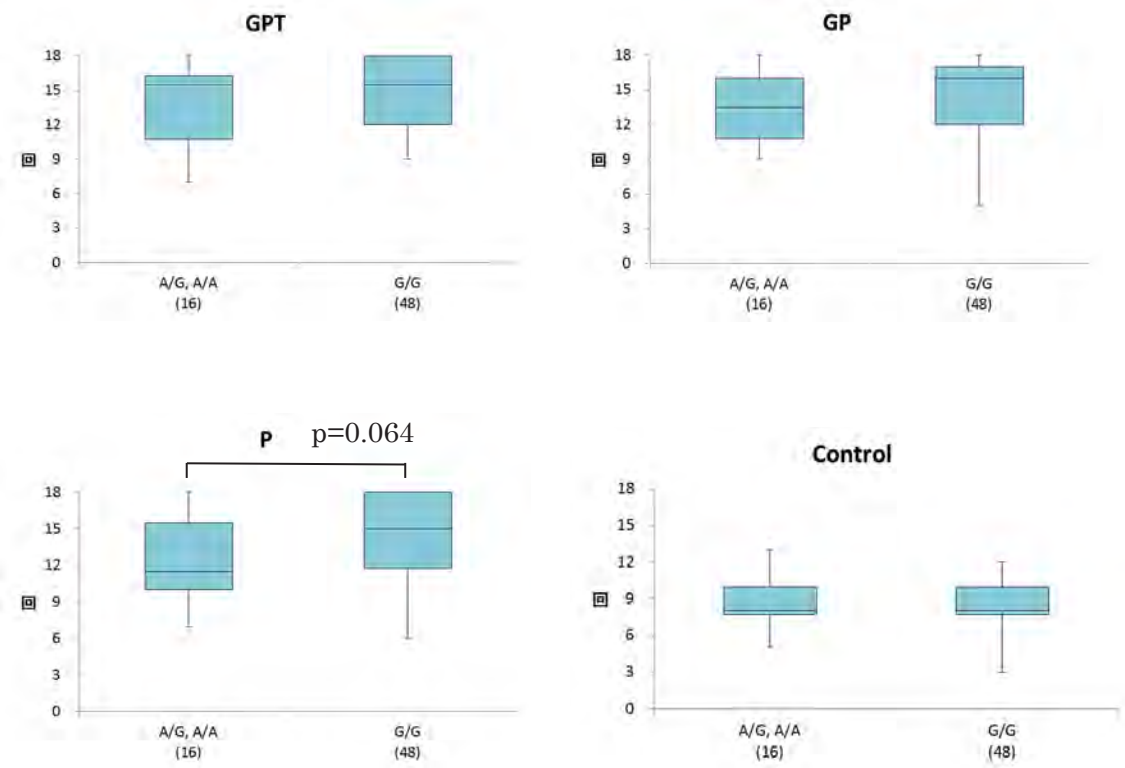

p>0.05

Mann-Whitney U-test

視線＋指差し＋タッピング(GPT)課題　χ^2＝0.630, df=1, p>0.05

視線＋指差し(GP)課題　χ^2＝1.469, df=1, p>0.05

指差し(P)課題　χ^2＝3.421, df=1, p=0.064

コントロール(Control)課題　χ^2＝0.020, df=1, p>0.05

図 4-9　OT intron-SNP と解決不可能課題

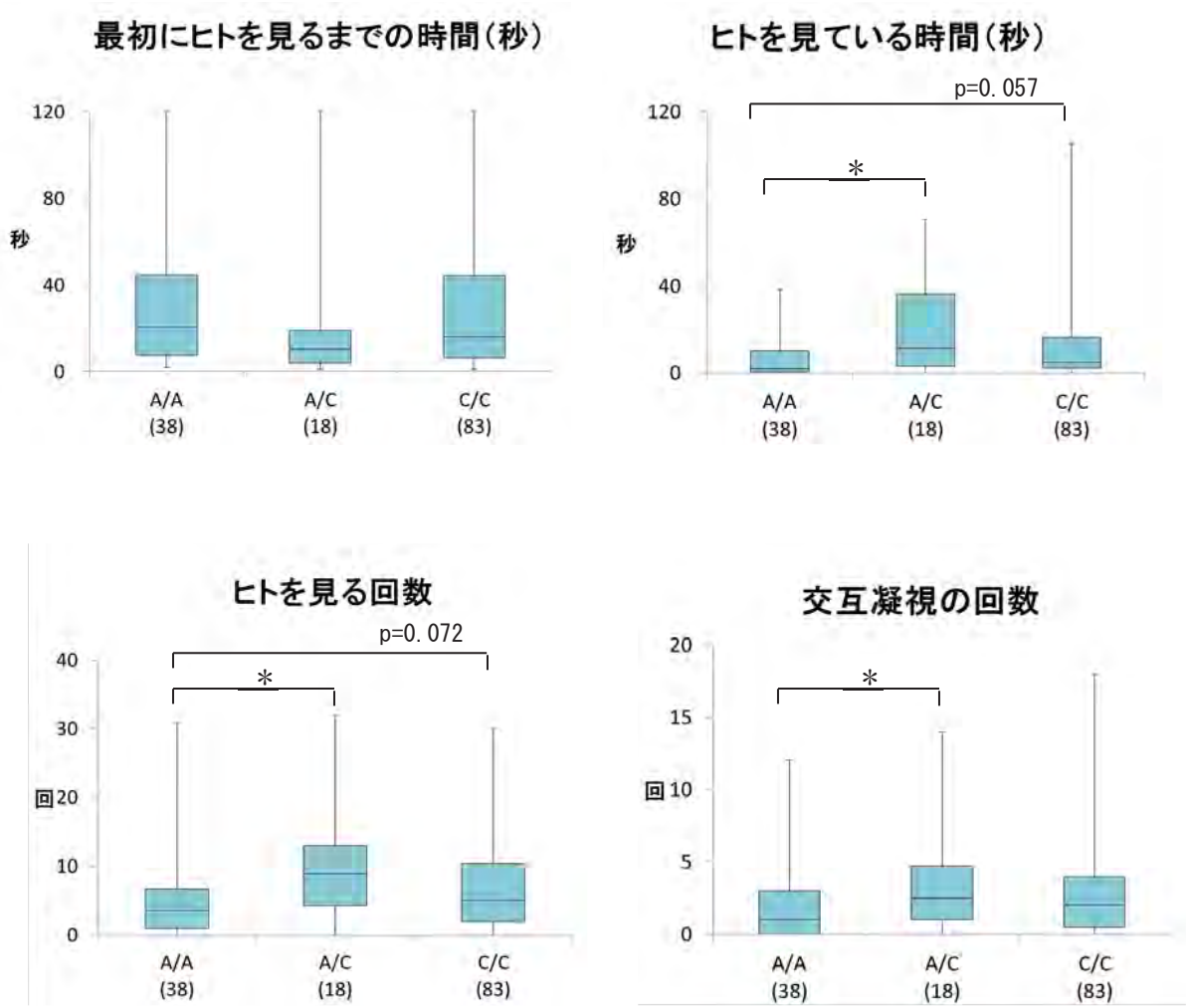

*,　p<0. 05

Mann-Whitney U-test with Bonferroni correction

最初にヒトを見るまでの時間　χ^2＝5.013, df=2, p>0.05

ヒトを見ている時間　χ^2＝9.345, df=2, p<0.05

ヒトを見る回数　χ^2＝9.508, df=2, p<0.05

交互凝視の回数　χ^2＝6.371, df=2, p<0.05

図 4-10　OT intron-repeat と解決不可能課題

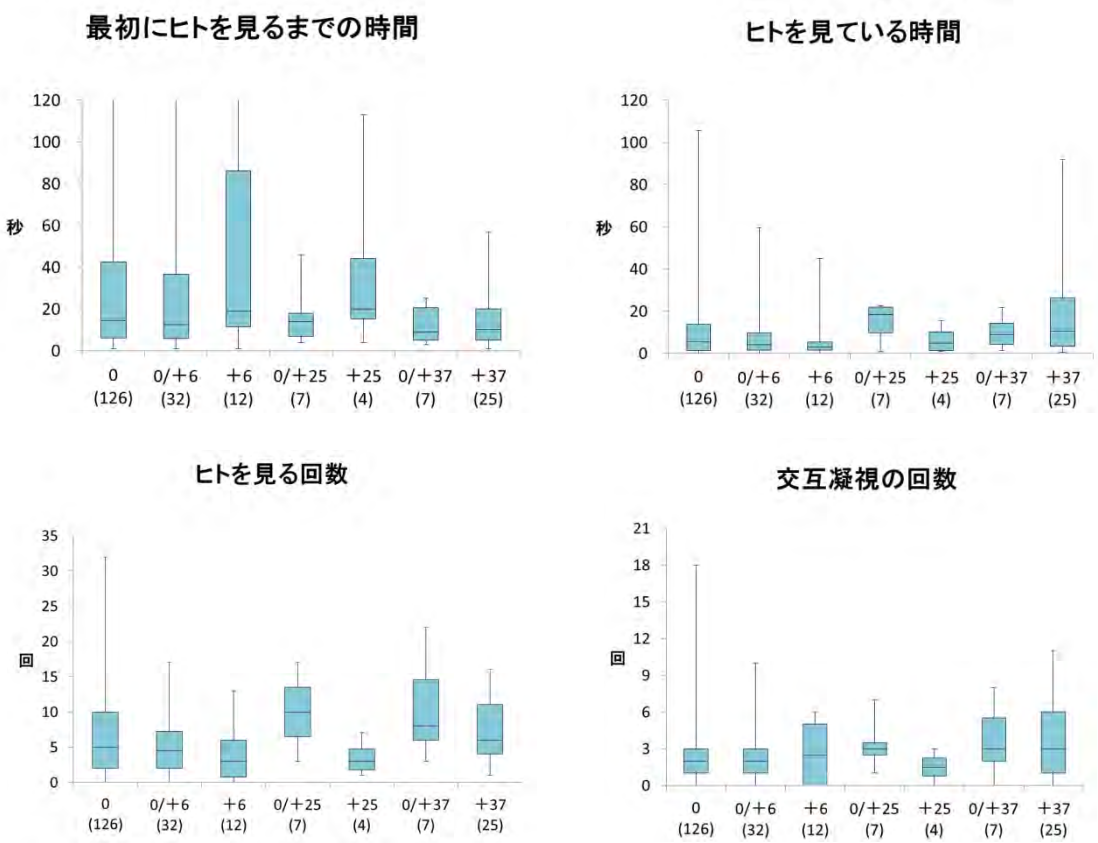

$p>0.05$

Mann-Whitney U-test with Bonferroni correction

最初にヒトを見るまでの時間　$\chi^2=4.215$, df=6, $p>0.05$

ヒトを見ている時間　$\chi^2=8.368$, df=6, $p>0.05$

ヒトを見る回数　$\chi^2=11.039$, df=6, $p=0.087$

交互凝視の回数　$\chi^2=7.258$, df=6, $p>0.05$

研究発表

１．論文発表

1) Ohkita M, Nagasawa M, Kazutaka M, Kikusui T: Owners' direct gazes increase dogs' attention-getting behaviors. Behav Processes. In press. 2016
2) Tonoike A, Nagasawa M, Mogi K, Serpell J, Ohtsuki H, Kikusui T: Comparison of owner-reported behavioral characteristics among genetically clustered breeds of dog (Canis familiaris). Sci Rep Dec 18;5:17710. 2016
3) Nagasawa M, Mogi K, Serpell J, Kikusui T: Comparison of behavioral characteristics of dogs in the United States and Japan. J Vet Med Sci, 78, 231-238,2016
4) Tonoike A, Terauchi G, Inoue-Murayama M, Nagasawa M, Mogi K, Kikusui T: The Frequency Variations of the Oxytocin Receptor Gene Polymorphisms among Dog Breeds. J Azabu Uni ,27,11-18, 2015
5) Tonoike A, Hori Y, Inoue-Murayama M, Konno A, Fujita K, Miyado M, Fukami M, Nagasawa M, Mogi K, Kikusui T: Copy number variations in the amylase gene in Japanese native dog breeds. Anim Genet 46:580-3, 2015
6) Nagasawa M, Mitsui S, En S, Ohtani N, Ohta M, Sakuma Y, Onaka T, Mogi K, Kikusui T: Oxytocin-gaze positive loop and the coevolution of human-dog bonds. Science 348, 333-6, 2015
7) Romero T, Nagasawa M, Mogi K, Hasegawa T, Kikusui T.: Intranasal administration of oxytocin promotes social play in domestic dogs. Commun Integra Biol 112, E311-320, 2015

2. 学会発表

1) 外池亜紀子、寺内豪、永澤美保、茂木一孝、菊水健史：イヌのヒトとのコミュニケーション能力の品種差, 関連遺伝子の探索. 日本動物心理学会第 73 回大会、筑波大学、9 月 2013 年
2) 片山真希、永澤美保、茂木一孝、菊水健史：体位や情動の変化がイヌの心拍変動に及ぼす影響. 日本動物心理学会第 73 回大会、筑波大学、9 月 2013 年
3) 寺内豪、永澤美保、外池亜紀子、坂田日香理、茂木一孝、菊水健史：イヌのヒトとの視線コミュニケーションの犬種差. 日本動物心理学会第 73 回大会、筑波大学、9 月 2013 年
4) 小川美里、圓史緒理、永澤美保、茂木一孝、菊水健史、：オキシトシン投与によるヒトへの視線増強の日本犬種と洋犬種の比較. 日本動物心理学会第 73 回大会、筑波大学、9 月 2013 年

3. 知的財産の出願・登録状況

該当なし

Behavioural Processes 125 (2016) 96–100

Contents lists available at ScienceDirect

Behavioural Processes

journal homepage: www.elsevier.com/locate/behavproc

Owners' direct gazes increase dogs' attention-getting behaviors

Midori Ohkita[a,c,*], Miho Nagasawa[b,c], Mogi Kazutaka[c], Takefumi Kikusui[c]

[a] Senshu University, Japan
[b] Jichi Medical University, Japan
[c] Azabu University, Japan

ARTICLE INFO

Article history:
Received 3 August 2015
Received in revised form 24 January 2016
Accepted 19 February 2016
Available online 23 February 2016

Keywords:
Gaze
Attention
Dogs

ABSTRACT

This study examined whether dogs gain information about human's attention via their gazes and whether they change their attention-getting behaviors (i.e., whining and whimpering, looking at their owners' faces, pawing, and approaching their owners) in response to their owners' direct gazes. The results showed that when the owners gazed at their dogs, the durations of whining and whimpering and looking at the owners' faces were longer than when the owners averted their gazes. In contrast, there were no differences in duration of pawing and likelihood of approaching the owners between the direct and averted gaze conditions. Therefore, owners' direct gazes increased the behaviors that acted as distant signals and did not necessarily involve touching the owners. We suggest that dogs are sensitive to human gazes, and this sensitivity may act as attachment signals to humans, and may contribute to close relationships between humans and dogs.

1. Introduction

Dogs, *Canis familiaris*, were domesticated at least 14,000 years ago (Druzhkova et al., 2013; Nobis, 1979; Vilá et al., 1997). Since then, humans and dogs have established close relationships. Communication by means of visual information is a crucial feature in these close relationships between humans and dogs. It is especially important for working dogs, such as hunting dogs, to understand human visual communicative information to aid them in making cooperative movements. Previous studies have revealed that dogs understand visual information given by humans very well (Hare et al., 2002; Miklósi et al., 1998).

In addition, dogs are able to understand the visual attention of humans as indicated by body orientation, the turning of the head, and gaze (Hare and Tomasello, 1999). In the current theory of human cognitive development, understanding the visual attention of others links to more complex social-cognitive skills, such as understanding intentions, or "theory of mind" (Baron-Cohen, 1995). Similarly, dogs' understanding of humans' visual attention may contribute to the communication between the two. This ability of dogs might be supported by the co-habitation between human and dogs.

Studies have examined whether dogs understand humans' attention based on their gazes (Call et al., 2003; Schwab and Huber, 2006). For example, Call et al. conducted a series of trials in which dogs were forbidden to take a piece of visible food (i.e., the experimenters spoke a "Don't take it" command). In some trials, the humans continued to look at the dogs throughout the trial (direct gaze condition), whereas in other trials, the humans closed their eyes (no-gaze condition). Call et al. reported that the dogs retrieved less food in the direct gaze condition than in the no-gaze condition, suggesting dogs respond to commands in different ways depending on whether humans gaze directly the dogs or not. Furthermore, the dogs understood the humans' attention as it was communicated by their gazes.

In Call et al.'s study, however, there are differences between the direct gaze and closed eyes condition in not only the directions of the gaze but also in the opening and closing of the eyes. Therefore, the true value of humans' gaze directions for the dogs was not clear. In humans, infants are sensitive to gaze direction, and they understand from the gaze direction whether others have directed attention to them (Farroni et al., 2002, 2000; Samuels, 1985). Therefore, in the current study, in order to examine whether dogs understand their owners' attention according to gaze direction, we

* Corresponding author at: School of Human Science, Senshu University, 2-1-1 Higashimita, Tama-ku, Kawasaki-shi, Kanagawa 214-8580, Japan.
E-mail address: m.ohkita.animalcognition@gmail.com (M. Ohkita).

http://dx.doi.org/10.1016/j.beproc.2016.02.013
0376-6357/

investigated whether they change their behaviors in different ways depending on owners' gazes.

In particular, we assessed dogs' attention-getting behaviors: whining and whimpering, looking at the owners' faces, pawing, and approaching. For the reason mentioned bellow, we focused on the attention-getting behaviors.

Studies of children with autism have revealed that their frequencies of affective expression and spontaneous social behaviors for others, such as looking at others or making physical contact with them, were lower than those observed among typically developing children in communicative situations (e.g., Baranek, 1999; Adrien et al., 1993). Studies have suggested that the lower frequencies found in communicative situations made it difficult for children with autism to establish closer relationships with others. Accordingly, spontaneous social behaviors, including the attention-getting behaviors, were important in subsequent reciprocal communication (Leavens et al., 2005).

In the present study, we examine whether dogs change their attention-getting behaviors according to humans' gazes in communicative situations. We compared the durations of the attention-getting behaviors in the Direct Gaze condition with those in the Avert Gaze condition. We predicted that if dogs are sensitive to humans' gazes and they understand humans' attention according to gaze, then the durations of the attention-getting behaviors would be longer in the Avert Gaze condition compared to the Direct Gaze condition.

2. Materials and methods

2.1. Subjects

The subjects were 20 pairs of owners and healthy household samples. The samples consisted of three Yorkshire Terriers, two Bolognese, two Chihuahuas, and two Pekingeses, as well as one of each of these breeds: Beagle, Bernese Mountain Dog, Italian Greyhound, Boston Terrier, Labrador Retriever, Shin-tzu, Papillon, and Welsh Corgi. In addition, three mixed breed dogs (two Miniature Dachshund and Toy Poodle, two Chihuahua and Toy Poodle). Ten dogs were male, and ten were female, with a mean age of 4.2 [SD: 3.1] years. One owner was male, and nineteen were female, with a mean age of 35.5 [SD: 12.8] years.

This study was approved by the Ethics Committee of Azabu University, Japan. Informed written consent was obtained from each participant.

2.2. Experimental procedures

The experiment was conducted in a room at Azabu University (Japan). The room was divided into partitions, yielding a space for the dog of 125 × 250 cm (Fig. 1a). The front of this space was a blank wall with an acrylic window. The owner sat outside the space in front of the window, and the dog was able to view the owner's face through the window (Fig. 1b).

The experiment consisted of two conditions. In the Direct Gaze condition, the owner faced the window and gazed directly at the dog on the other side. In the Avert Gaze condition, the owner faced the window but did not gaze at the dog (i.e., they gazed to either the left or the right). We asked the owners to have a neutral facial expression in both conditions. Each condition was conducted two times (i.e., 2 trials × 2 conditions), resulting in a total of 4 trials per dog. The order of the trials was an ABBA design and was counterbalanced within subjects. Each trial was lasted for 1 min. The interval between trials was 3 min. In the inter-trial interval, owners were able to interact freely with their dogs. The total experiment duration was 16 min. All trials were video-recorded (Sony video camera HDR-CX180 seated on a tripod) to analyze the dogs' behaviors.

2.3. Data analysis

Attention-getting behaviors, including standing in close proximity to the owner from the acrylic window (i.e., within an area of 70 × 70 cm from the windows; Fig. 1a), looking at the owner's face, whining and whimpering, and pawing, were recorded using an all-occurrence sampling. We analyzed the durations of these behaviors in the Direct Gaze and Avert Gaze conditions, using an Excel VBA-based event recorder. One of the authors (Midori Ohkita) analyzed all the videotaped data. In addition, a blind observer who did not know the purpose of the study analyzed randomly selected subjects (20%). Agreement reliability between the author and the naïve observer was excellent ($rs = .98$). We calculated sum durations for each behavior in each condition for each subject. Statistical analyses were performed using Wilcoxon signed-ranks test with an alpha level of .05.

3. Results

Fig. 2 shows the means of the sum durations (in seconds) for each attention-getting behaviors in each condition for each subject. The durations of whining and whimpering ($Z = 2.62$, $p = .01$, $r = .59$) and looking at the owners' faces ($Z = 4.43$, $p < .001$, $r = .99$) were longer in the Direct Gaze condition than in the Avert Gaze condition. There were no differences between the two conditions in durations of pawing ($Z = 1.47$, $p = .14$, $r = .33$) or standing close to the acrylic window ($Z = 0.71$, $p = .48$, $r = .16$).

4. Discussion

We investigated whether dogs change some of their attention-getting behaviors in different ways depending on owners' direct gazes by comparing their behavior under the avert gaze. Dogs usually perform attention-getting behaviors in order to get attention from humans. If dogs are sensitive to humans' gazes and they understand humans' attention according to gaze, then the durations of the attention-getting behaviors would be longer in the Avert Gaze condition compared to the Direct Gaze condition. An interesting finding, contrary to our expectations, was that the durations of whining and whimpering and looking at their owners' face were longer in the Direct Gaze condition than in the Avert Gaze condition. These results suggest that the dogs were sensitive to the direction of their owners' gazes. Subsequently, the dogs showed an increase of their own attention-getting behaviors. The question, then, arose; Why did the owners' attention behaviors—that is, the direct gaze—increase their dogs' attention-getting behaviors.

One possible explanation for this question is that attention-getting behaviors act as appetitive behavior whereas being touched by the owners or given a reward like food acts as a consummatory behavior. In general, owners' tend to touch their dogs after gazing at them directly (attending to them) in response to the dogs' attention-getting behaviors, dogs are more likely to act out attention-getting behaviors in response to their owners' gazes until these behaviors are reinforced by their owners' touches (Bentosela et al., 2008). In the present study, in the Direct Gaze condition, the dogs did perform attention-getting behaviors in response to their owners' gazes. In contrast, in the Avert Gaze condition, dogs did act out these behaviors a little, because their owners gazes were not present. In order to ensure these behaviors mainly occurred in the Direct Gaze condition, the durations of these behaviors were longer in that condition than in the Avert Gaze condition.

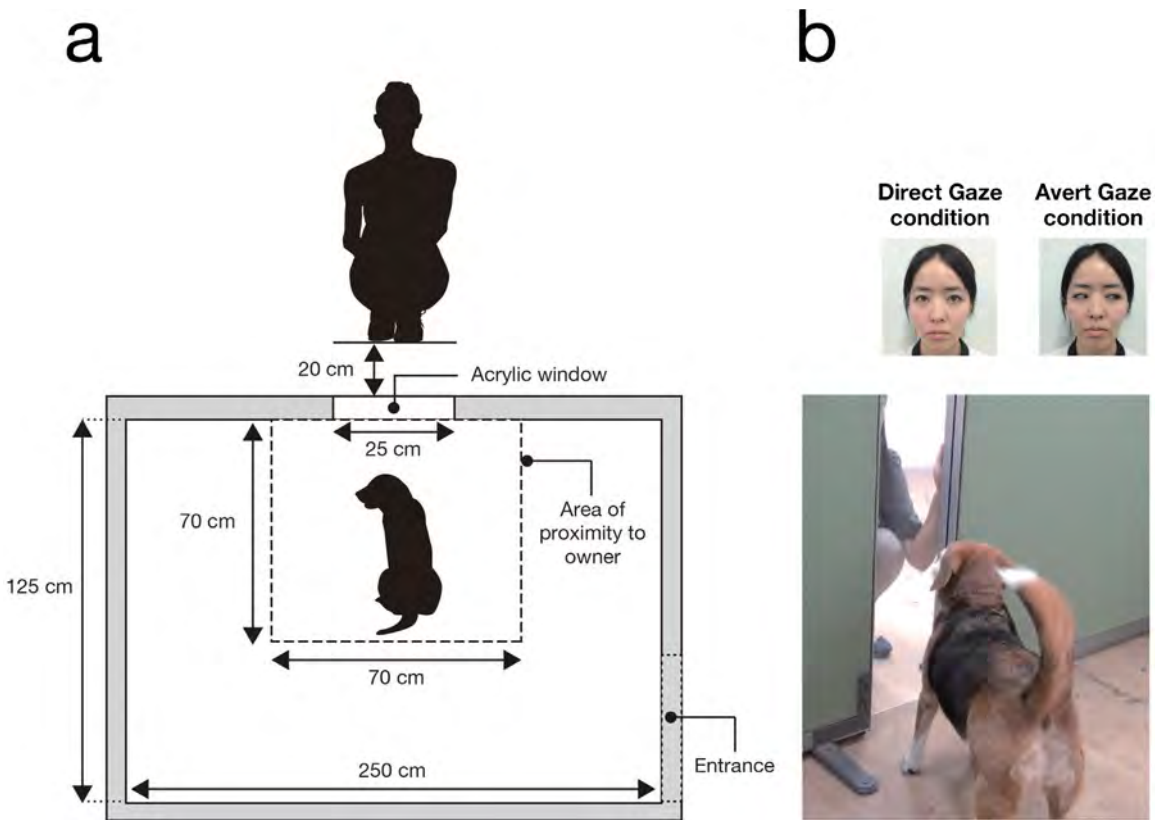

Fig. 1. Experimental setup.
(a) Schematic of the enclosed space for the dog and the position of the owner outside the enclosure. (b) Actual image of an owner behind the acrylic window with the dog.

Another possibility for the reasons why the owners' attention behaviors increased their dogs' attention-getting behaviors is that owners' gazes provide social rewards for dogs and increase dogs' behaviors toward the owners. Nagasawa et al. (2009, 2015) examined whether direct gaze contributes to the establishment of the relationships between humans and dogs. Dogs' behaviors of gazing at and touching their owners was longer when the owners interacted with their dogs (interaction experiment) than when the owners did not look at the dogs (control experiment). This suggested that the owners' gazes increased the dogs' attachment behaviors (dogs' gazes at their owners, dogs' approaching their owners, and dogs' touching their owners); therefore, there were positive loops of direct gaze and attachment behaviors between owners and their dogs. In this regards, it is feasible in the present study that owners' eye gaze enhance their dogs' whining and whimpering and looking at their owners' face as attachment behavior, as well as Nagasawa et al.'s studies.

Positive loops have been studied in mother-infant communication (Kendrick, 2004; see Nagasawa et al., 2013 for a review). These studies showed that mothers' parental behaviors (e.g., stroking) facilitated infants' attachment behaviors, which in turn increasingly facilitated the mothers' parental behaviors. Previous studies have also suggested that this positive loop stimulates the release of centrally acting oxytocin, and this oxytocin acts as a social reward within the nucleus accumbens. As a result, this positive loop might contribute to mother-infant bonding. In Nagasawa et al. (2009, 2015) studies, the positive loop of direct gaze between owners and dogs stimulated the release of oxytocin. That is, the positive loop of direct gaze functioned as a social reward for both owners and dogs (i.e., a primary reinforcer). This positive loop of direct gaze may establish a closer relationship between dogs and humans. Therefore, the findings of this present study are in line with those of Nagasawa et al., suggesting that owners' gazes provide social rewards for their dogs and increase the dogs' attachment behaviors, gazing at their owners. Further research is needed to examine whether dogs' increased behaviors according to humans' gazes are attention-getting behaviors or attachment behaviors.

In Nagasawa et al.'s studies, the durations of not only the dogs' gazes but also the dogs' touches, including pawing and approaching the owners, were longer when the owners interacted with the dogs in their usual way (eye gaze condition) than when the owners did not look at their dogs (non-eye gaze condition). The results of the present study are not consistent with these findings. In our study, the owner's direct gaze did not facilitate the dog's pawing or approaching the owner. Our experimental conditions were different from those used in Nagasawa et al. study (2009, 2015). In that study, the owners could touch their dogs. In the present study, a partition wall kept the owners from being able to touch their dogs. This difference in experimental conditions might lead to differences in the dogs' behaviors in response to their humans' gazes. This may be because floor and ceiling effects prevented differences between the conditions in terms of pawing and approaching their owners, respectively. It might be difficult for the dogs to paw the smooth acrylic window, so the dogs might not have wanted to paw in either condition. In addition, because each condition was shorter in the present study than in Nagasawa et al.'s studies, the duration might not have been long enough for the between-condition approaching differences to occur.

Even if a human's direct gaze signals rewards (i.e., being touched by humans) for dogs, they are nevertheless sensitive to human gazes. For many species, it is known that perceiving a direct gaze by a member of another species arouses an aversive response (Emery, 2000), probably because it is a salient signal of potential

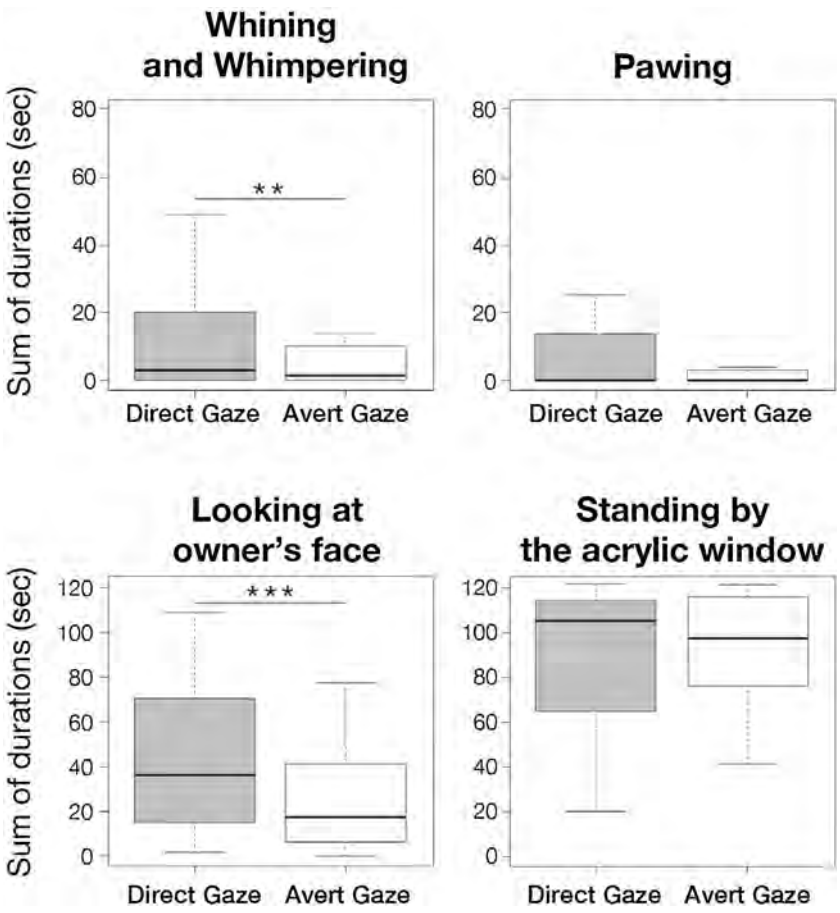

Fig. 2. Means of sum durations for attention-getting behaviors.
Box plots show means of sum durations (in seconds) for attention-getting behaviors in each condition for each subject. $^{*}p < .05$, $^{**}p < .01$, $^{***}p < .001$ (Wilcoxon signed-ranks test).

threat. In contrast, humans' direct gazes at dogs may contribute to close relationships between the two, although humans and dogs are phylogenetically very distant species. Therefore, these behavioral changes might be involved in convergent evolution of humans and dogs. By using adult dogs and their owners as subjects in the present study, however, we could not eliminate the possibility of prior learning. We intend to address these issues in future research.

Acknowledgments

This experiment was approved by the Animal Care and Use committee of Azabu University and was carried out according to Azabu University's Guidelines for Animal Research.

References

Adrien, J.L., Lenoir, P., Martineau, J., Perrot, A., Hameury, L., Larmande, C., Sauvage, D., 1993. Blind ratings of early symptoms of autism based upon family home movies. J. Am. Acad. Child Psychiatry 32, 617–626, http://dx.doi.org/10.1097/00004583-199305000-00019.

Baranek, T., 1999. Autism during infancy: a retrospective video analysis of sensory-motor and social behaviors at 9–12 months of age. J. Autism Dev. Disord. 29, 213–224.

Baron-Cohen, S., 1995. Mindblindness: An Essay on Autism and Theory of Mind. MIT Press, Cambridge, MA.

Bentosela, M., Barrera, G., Jakovcevic, A., Elgier, A.M., Mustaca, A.E., 2008. Effect of reinforcement: reinforcer omission and extinction on a communicative response in domestic dogs (*Canis familiaris*). Behav. Process. 78, 464–469.

Call, J., Bräuer, J., Kaminski, J., Tomasello, M., 2003. Domestic dogs (*Canis familiaris*) are sensitive to the attentional state of humans. J. Comp. Psychol. 117, 257–263, http://dx.doi.org/10.1037/0735-7036.117.3.257.

Druzhkova, A.S., Thalmann, O., Trifonov, V.A., Leonard, J.A., Vorobieva, N.V., 2013. Ancient DNA analysis affirms the canid from Altai as a primitive dog. PLoS One 8, e57754, http://dx.doi.org/10.1371/journal.pone.0057754.

Emery, N.J., 2000. The eyes have it: the neuroethology, function and evaluation of social gaze. Neurosci. Biobehav. Rev. 24, 581–604.

Farroni, T., Johnson, M.H., Brockband, M., Simon, F., 2000. Infants use of gaze direction to cue attention: the importance of perceived motion. Vis. Cogn. 7, 705–718, http://dx.doi.org/10.1080/135062800501443399.

Farroni, T., Csibra, G., Simon, F., Johnson, M.H., 2002. Eye contact detection in humans from birth. PNAS 99, 9602–9605, http://dx.doi.org/10.1073/pnas.152159999.

Hare, B., Tomasello, M., 1999. Domestic dogs (*Canis familiaris*) use human and conspecific social cues to locate hidden food. J. Comp. Psychol. 113, 173–177, http://dx.doi.org/10.1037/0735-7036.113.2.173.

Hare, B., Brown, M., Williamson, C., Tomasello, M., 2002. The domestication of social cognition in dogs. Science 298, 1634–1636, http://dx.doi.org/10.1126/science.1072702.

Kendrick, K.M., 2004. The neurobiology of social bonds. J. Neuroendocrinol. 16, 1007–1008, http://dx.doi.org/10.1111/j.1365-2826.2004.01262.x.

Leavens, D.A., Russell, J.L., Hopkins, W.D., 2005. Intentionality as measured in persistence and elaboration of communication by chimpanzees (*Pan troglodytes*). Child Dev. 76, 291–306, http://dx.doi.org/10.1111/j.1467-8624.2005.00845.x.

Miklósi, Á., Polgárdi, R., Topál, J., Csányi, V., 1998. Use of experimenter-given cues in dogs. Anim. Cogn. 1, 113–121, http://dx.doi.org/10.1007/s100710050016.

Nagasawa, M., Kikusui, T., Onaka, T., Ohta, M., 2009. Dog's gaze at its owner increases owner's urinary oxytocin during social interaction. Horm. Behav. 55, 434–441, http://dx.doi.org/10.1016/j.yhbeh.2008.12.002.

Nagasawa, M., Okabe, S., Mogi, K., Kikusui, T., 2013. The biological perspective on mother-infant bonding: the importance of oxytocin. Jpn. J. Anim. Psychol. 63, 47–63, http://dx.doi.org/10.2502/janip.63.1.4.

Nagasawa, M., Mitsui, S., En, S., Ohtani, N., Ohta, M., Sakuma, Y., Onaka, T., Mogi, K., Kikusui, T., 2015. Oxytocin-gaze positive loop and the coevolution of human-dog bonds. Science 348, 333–336, http://dx.doi.org/10.1126/science.1261022.

Nobis, G., 1979. Der älteste Haushund lebte vor 14,000 Jahren. Umschau 19, 610.

Samuels, C.A., 1985. Attention to eye contact opportunity and facial motion by three-month-old infants. J. Exp. Child. Psychol. 40, 105–114, http://dx.doi.org/10.1016/0022-0965(85)90067-0.
Schwab, C., Huber, L., 2006. Obey or not obey? Dogs (*Canis familiaris*) behave differently in response to attentional states of their owners. J. Comp. Psychol. 120, 169–175, http://dx.doi.org/10.1037/0735-7036.120.3.169.
Vilá, C., Savolainen, P., Maldonado, J.E., Amorim, I.R., Rice, J.E., Honeycutt, R.L., 1997. Multiple and ancient origins of the domestic dog. Science 276, 1687–1689, http://dx.doi.org/10.1126/science.276.5319.1687.

SCIENTIFIC REPORTS

OPEN

Comparison of owner-reported behavioral characteristics among genetically clustered breeds of dog (*Canis familiaris*).

Received: 06 May 2015
Accepted: 04 November 2015
Published: 18 December 2015

Akiko Tonoike[1], Miho Nagasawa[1,2], Kazutaka Mogi[1], James A. Serpell[3], Hisashi Ohtsuki[4] & Takefumi Kikusui[1]

During the domestication process, dogs were selected for their suitability for multiple purposes, resulting in a variety of behavioral characteristics. In particular, the ancient group of breeds that is genetically closer to wolves may show different behavioral characteristics when compared to other breed groups. Here, we used questionnaire evaluations of dog behavior to investigate whether behavioral characteristics of dogs were different among genetically clustered breed groups. A standardized questionnaire, the Canine Behavioral Assessment and Research Questionnaire (C-BARQ), was used, and breed group differences of privately-owned dogs from Japan (n = 2,951) and the United States (n = 10,389) were analyzed. Results indicated that dogs in the ancient and spitz breed group showed low attachment and attention-seeking behavior. This characteristic distinguished the ancient group from any other breed groups with presumed modern European origins, and may therefore, be an ancestral trait.

The dog *(Canis familiaris)* was the first animal to be domesticated[1] and today hundreds of different breeds are recognized. Breeds seem to be different in several aspects of their behavior due to the effects of artificial selection[2–5]. Although breeds are traditionally classified by the jobs they were originally selected to perform, parallel selection for other traits, such as suitability as pets, has also affected modern breed-typical behavior[6]. With the remarkable improvement of technologies available for genetic analysis, genetic relationships in dog breeds have recently been studied and genetic classifications of dog breeds have been constructed[7,8]. As a result, although dog breeds have traditionally been classified by their roles in human activities, historical records, and physical phenotypes, it is now possible to classify them based on patterns of genetic variation[9–11].

Cladogram analysis of dog genes showed the separation of several breeds with supposedly ancient origins from a large group of breeds with presumed modern European origins[7,8]. Modern European breeds are the products of controlled breeding practices since the Victorian era, and because they have originated recently and lack deep histories, the genetic groups have short internodes and low bootstrap support. On the other hand, ancient breeds are highly divergent and are distinct from modern European breeds. Since the dogs from these ancient breeds are genetically related most closely to wolves, they may exhibit remnants of wolves' behavioral, morphological and physiological characteristics.

The Canine Behavioral Assessment and Research Questionnaire (C-BARQ) is designed to provide dog owners and professionals with standardized evaluations of canine temperament and behavior[12]. The

[1]Department of Animal Science and Biotechnology, Azabu University, Sagamihara, Kanagawa, Japan. [2]Department of Physiology, Jichi Medical University, Shimotsuke, Tochigi, Japan. [3]School of Veterinary Medicine, University of Pennsylvania, Philadelphia, Pennsylvania, USA. [4]Department of Evolutionary Studies of Biosystems, School of Advanced Sciences, The Graduate University for Advanced Studies (SOKENDAI). Correspondence and requests for materials should be addressed to M.N. (email: nagasawa@carazabu.com)

C-BARQ has also been translated for use in Japan[13,14] after examination of the validity of questionnaire items[15]. In this study, we used C-BARQ evaluations of dogs to investigate whether the behavioral characteristics of dogs are different among genetically clustered breed groups. Although C-BARQ scores are obtained from dog owners and may therefore be influenced by subjective biases, the use of this instrument allows the standardized assessment of behavior in very large numbers of dogs, and has proven useful for studying breed differences in behavior[16–18]. Several studies comparing wolves, dogs, and other canids, suggest that behavioral changes were critical during the early stages of the domestication process[19–21]. We investigated the behavioral characteristics of breeds, especially those belonging to the ancient group, to understand the characteristics of this highly divergent group of ancient breeds.

Materials and Methods

Questionnaire. Behavioral data in the present study were collected from dog owners using the C-BARQ, which included 100 questions that asked owners to indicate how their dogs have responded in the recent past to a variety of common events and stimuli using a series of 0–4 rating scales. The C-BARQ is a standardized questionnaire that is widely used to assess the prevalence and severity of behavioral problems in dogs. The various C-BARQ item and subscale scores have also been shown to provide an accurate measure of canine behavioral phenotypes. Seven of the original 11 subscales were validated using a panel of 200 dogs previously diagnosed with specific behavior problems[12]. More recently, other studies have provided criterion validation of the C-BARQ by demonstrating associations between factor and item scores and training outcomes in working dogs[22], the performance of dogs in various standardized behavioral tests[23–26], and neurophysiological markers of canine anxiety and compulsive disorders[27,28]. The original C-BARQ was translated into Japanese by two behavioral professionals and reviewed by two professors[15]. Twenty-two out of 100 questions were eliminated due to the cultural and environmental differences between Japan and the USA, resulting in 78 questions for the Japanese version.

C-BARQ data were collected via the freely accessible websites http://www.cbarq.org (US, from April 2006) and http://cbarq.inutokurasu.jp/(JPN, from September 2010). Before answering the questionnaire, dog owners were asked to provide information about their dogs, such as its breed, age, sex, neuter status, body weight, age when acquired, where acquired, and the presence of any health problems. The online survey was advertised via articles in newspapers, magazines, online news, etc., in each country. The C-BARQ database was used for different purpose 29. The Ethical committee of Azabu University approved this study. We obtained the informed consent from all respondents and our methods were carried out in accordance with the approved guidelines.

Statistical analyses. Data from the completed questionnaires were subjected to factor analysis. Parallel analysis was used to determine the number of interpretable factors that could be extracted, and varimax rotation was used to identify empirical groupings of items that measured different behavioral traits. The Cronbach's α coefficient was calculated to assess internal consistency (reliability) of extracted factors; this coefficient describes how well a group of questionnaire items focuses on a single idea or construct. For comparison of the factors, we calculated the average of item scores composing each factor, which was analyzed as a factor score. The factor scores were then analyzed using generalized linear models These were analyzed by SPSS v.19.0 (SPSS Japan Inc., IBM company), except for the parallel analysis (R v. 3.0.0, 2013-04-03, The R Foundation for Statistical Computing).

Results

Subjects. A total of 5,377 C-BARQ questionnaires were completed in Japan. Dogs that were <1 or >7 years of age or had severe or chronic health problems were excluded, leaving a total of 3,098 completed questionnaires (57.76%) that were considered valid. The age cut-off was chosen to eliminate dogs whose behavior might have been affected by immaturity or senescence (in the case of some large or giant breeds). The response rates for each of the 78 questions in the questionnaire ranged from 39.22% to 99.86% (median, 98.39%, mode, 99.15%). The low response rates obtained for some questionnaire items were primarily due to the fact that the questionnaire's focus on events and stimuli occurring in recent past tended to exclude uncommon events and situations. Among the 14,481 questionnaires completed in the United States, 10,500 satisfied the requirements above (72.51%). The response rates for each of the 100 questions in the questionnaire ranged from 81.57% to 99.72% (median, 97.85%, mode, 98.04%). Fifteen questions with response rates $<85.0\%$ either in Japanese or US data were excluded for further analyses. Any questionnaires that had $<75.0\%$ response rates were also excluded, leaving 2,951 (54.88%) and 10,389 (71.74%) completed questionnaires that could be used in analyses in Japan and the United States, respectively.

Factor analysis. For the factor analysis we selected 59 breeds that were common to both countries and then matched the samples for sex and number of dog for each country in order to eliminate any sex or country biases ($n = 1,252$ each, Supplementary Table 1). Sixty-three of the questionnaire items common to both countries were analyzed by factor analysis and parallel analysis, and these items were sorted into 12 factors. After removing the items with factor loadings of <0.4, the remaining items were analyzed by factor analysis again, and yielded 12 factors. After removing the items with factor loadings of <0.4 again, the remaining items were analyzed by factor analysis, and again yielded 12 factors that accounted

Factors & questionnaire items	Factor loadings	SS loadings	Proportion Var	Cumulative Var	Cronbach's α
Aggression to unfamiliar persons		5.13	0.10	0.10	0.92
When approached directly by an unfamiliar adult while being walked or exercised on a leash	0.836				
When approached directly by an unfamiliar child while being walked or exercised on a leash	0.744				
When an unfamiliar person approaches the owner or a member of the owner's family at home	0.670				
When an unfamiliar person approaches the owner or a member of the owner's family away from home	0.792				
When mailmen or other delivery workers approach the home	0.604				
When an unfamiliar person tries to touch or pet the dog	0.806				
Toward unfamiliar persons visiting the home	0.717				
Fear of unfamiliar persons		2.79	0.05	0.15	0.90
When approached directly by an unfamiliar adult while away from the home	0.823				
When approached directly by an unfamiliar child while away from the home	0.747				
When unfamiliar persons visit the home	0.689				
When an unfamiliar person tries to touch or pet the dog	0.761				
Trainability		2.77	0.05	0.20	0.81
Returns immediately when called while off leash	0.667				
Obeys a sit command immediately	0.676				
Obeys a stay command immediately	0.717				
Seems to attend to or listen closely to everything the owner says or does	0.693				
Not slow to respond to correction or punishment	0.619				
Not easitly distracted by interesting sights, sounds, or smell	0.447				
Separation-related anxiety		2.73	0.05	0.25	0.76
Excessive salivation when left or about to be left on its owner	0.497				
Whining when left or about to be left on its owner	0.714				
Barking when left or about to be left on its owner	0.735				
Howling when left or about to be left on its owner	0.608				
Chewing/scratching at doors, floor, windows, curtains, etc.	0.462				
Loss of appetite when left or about to be left on its owner	0.403				
Energy and restless		2.65	0.05	0.30	0.72
Not shaking, shivering, or trembling when left or about to be left on its owner	0.441				
Restlessness, agitation, or pacing when left or about to be left on its owner	0.477				
When a member of the household returns home after a brief absence	0.690				
When visitors arrive at its home	0.480				
Playful, puppyish, boisterous	0.694				
Active, energetic, always on the go	0.493				
Continued					

Factors & questionnaire items	Factor loadings	SS loadings	Proportion Var	Cumulative Var	Cronbach's α
Fear of non-social stimuli		2.27	0.04	0.34	0.75
In response to sudden or loud noises	0.665				
In response to strange or unfamiliar objects on or near the sidewalk	0.671				
During thunderstorms	0.422				
When first exposed to unfamiliar situations	0.468				
In response to wind or wind-blown objects	0.699				
Aggression to household members		2.25	0.04	0.38	0.84
When toys, bones, or other objects are taken away by a member of the household	0.577				
When approached directly by a member of the household while it is eating	0.773				
When food is taken away by a member of the household	0.849				
When a member of the household retrieves food or objects stolen by the dog	0.626				
Fear of unfamiliar dogs		2.21	0.04	0.42	0.88
When approached directly by an unfamiliar dog of the same or larger size	0.769				
When approached directly by an unfamiliar dog of a smaller size	0.792				
When barked, growled, or lunged at by unfamiliar dog	0.756				
Aggression to unfamiliar dogs		2.10	0.04	0.46	0.89
When approached directly by an unfamiliar male dog while being walked or exercised on a leash	0.849				
When approached directly by an unfamiliar female dog while being walked or exercised on a leash	0.840				
When barked, growled, or lunged at by unfamiliar dog	0.642				
Attachment and attention-seeking		1.78	0.03	0.53	0.70
Tends to follow a member of household from room to room about the house	0.541				
Tends to sit close to or in contact with a member of the household when that individual is sitting down	0.672				
Tends to nudge, nuzzle, or paw a member of the household for attention when that individual is sitting down	0.701				
Becomes agitated when a member of the household shows affection for another person	0.466				
Aggression to persons passing near the house		1.15	0.02	0.55	0.89
When strangers walk past the home while the dog is in the yard	0.652				
When joggers, cyclists, roller skaters, or skateboarders pass the home while the dog is in the yard	0.607				

Table 1. Factor loading of questionnaire items constituting each factor.

for 54.96% of the common variance in item scores. Out of these twelve factors, eleven were found to have adequate Cronbach's α values ($\geq$0.7) (Table 1). The following eleven factors were extracted: aggression to unfamiliar persons (F1), fear of unfamiliar persons (F2), trainability (F3), separation-related behavior (F4), energy and restlessness(F5), fear of non-social stimuli (F6), aggression to household members (F7), fear of unfamiliar dogs (F8), aggression to unfamiliar dogs (F9), attachment and attention-seeking (F11), and aggression to persons passing near the house (F12). These results are shown in Table 1.

The influence of breeds on C-BARQ factor scores. Using the generalized linear model, the influence of breeds and various demographic variables on C-BARQ factor scores were examined. The dog

Breed groups	Breeds
Ancient and spitz breeds (152)	Basenji(JPN4, US4), Shiba Inu(64, 64), Akita(4, 4), Siberian Husky(2, 2), Samoyed(2, 2)
Toy dogs (612)	Shih Tzu(40, 40), Chihuahua(110, 110), Pug(46, 46), Papillon(24, 24), Pomeranian(50, 50), Miniature Pinscher(26, 26), Brussels Griffon(2, 2), Pekingese(8, 8)
Spaniels, scent hounds, and poodles (388)	American Cocker Spaniel(14, 14), English Cocker Spaniel(10, 10), English Springer Spaniel(4, 4), Cavalier King Charles Spaniel(36, 36), Brittany(2, 2), Beagle(42, 42), Bichon Frise(10, 10), Maltese(32, 32) , Toy Poodle(22, 22), Miniature Poodle(12, 12), Standard Poodle (10, 10)
Working dogs (32)	Doberman Pinscher(6, 6), German Shepherd(10, 10)
Small Terriers (236)	Cairn Terrier(4, 4), Jack Russell Terrier(58, 58), West Highland White Terrier(10, 10), Yorkshire Terrier(46, 46)
Sight hounds and herding dogs (408)	Italian Greyhound(18, 18), Whippet(6, 6), Borzoi(2, 2), Pembroke Welsh Corgi(48, 48), Australian Shepherd(6, 6), Border Collie(74, 74), Shetland Sheepdog(50, 50)
Retrievers (304)	Labrador Retriever(82, 82), Flat-Coated Retriever(8, 8), Golden Retriever(44, 44), Great Dane(2, 2), Bernese Mountain Dog(16, 16)
Mastiff-like dogs (112)	Boston Terrier(32, 32), Boxer(4, 4), Bulldog(2, 2), French Bulldog(18, 18)

Table 2. Genetically clustered breed groups used for statistical analysis. The numbers of selected dogs are shown in parentheses.

breeds were separated into eight breed groups according to the cladogram suggested by vonHoldt (2010). The eight groups consist of 1) ancient and spitz breeds, 2) toy dogs, 3) spaniels, scent hounds, and poodles, 4) working dogs, 5) small terriers, 6) sight hounds and herding dogs, 7) retrievers, and 8) mastiff-like dogs. As the Shiba Inu breed was not included in vonHoldt's cladogram, we classified them into the ancient and spitz breed group according to the cladogram suggested by Parker (2004). Other dog breeds not shown in vonHoldt's cladogram were eliminated from further analyses. The dog breeds in each breed group are shown in Table 2.

We analyzed the relationships between breed groups and C-BARQ factor scores while taking into account the possible intervening effects of the following 8 variables: country, sex, spay/neuter status, source from which dogs were acquired, owner's experience of dog-ownership, dog's age when acquired, dog's body weight, dog's age at the time of evaluation. These variables have previously been shown to influence the expression of behavior in dogs[16,30–32]. All of the factor scores were explained significantly by the variables, although most of the variance was explained by breed groups, country, sex, spay/neuter status, and source from which dogs were acquired. Significant interactions between breed group and other variables were also found. Results are shown in Table 3 and Fig. 1.

Toy dogs obtained the highest scores for Factor 1 (aggression to unfamiliar persons), and were significantly more aggressive in this context than sight hounds and herding dogs, retrievers, and mastiff-like dogs. Spaniels, scent hounds, and poodles were significantly more aggressive to unfamiliar persons than retrievers and mastiff-like dogs. The ancient and spitz breed group and sight hounds and herding dogs were significantly more aggressive to unfamiliar persons than retrievers. For F2 (fear of unfamiliar persons), working dogs obtained the lowest scores, and were significantly lower than all other breed groups. For F3 (trainability), sight hounds and herding dogs obtained the highest scores, and were significantly more trainable than all other breed groups except working dogs. For F4 (separation-related anxiety), there were no breed group differences. For F5 (energy and restlessness), working dogs obtained the lowest scores, and were significantly lower than all other breed groups except mastiff-like dogs. Sight hounds and herding dogs obtained the highest scores, and were significantly higher than the spaniels, scent hounds, and poodles breed group and mastiff-like dogs. For F6 (fear of non-social stimuli), sight hounds and herding dogs obtained the highest scores, and were significantly higher than the spaniels, scent hounds, and poodles breed group and mastiff-like dogs. Working dogs obtained the lowest scores, and were significantly lower than all other breed groups except mastiff-like dogs. For F7 (aggression to household members), working dogs obtained the lowest scores, and were significantly less aggressive in this context than all other breed groups. Toy dogs obtained the highest scores, and were significantly more aggressive to household members than the sight hounds and herding dogs breed group and retrievers. The spaniels, scent hounds, and poodles breed group was significantly more aggressive to household members than the sight hounds and herding dogs breed group. For F8 (fear of unfamiliar dogs), working dogs obtained the lowest score, and were significantly lower than all other breed groups. For F9 (aggression to unfamiliar dogs), retrievers obtained the lowest scores, and were significantly less aggressive in this context than ancient and spitz breeds, toy dogs, the small terriers, and the sight hounds and herding dogs breed group. For F11 (attachment and attention-seeking), the ancient and spitz breed group obtained the lowest scores, and were significantly lower than all other breed groups. For F12 (aggression to persons passing near the house), toy dogs obtained the highest scores, and were significantly more aggressive in this context than mastiff-like dogs.

	F1: Aggression to unfamiliar persons					F2: Fear of unfamiliar persons					F3: Trainability				
	χ^2	df	p	Pairwise comparison	B[5]	χ^2	df	p	Pairwise comparison	B	χ^2	df	p	Pairwise comparison	B
Breed groups[1]	50.570	7	0.000	1 > 7, 2 > 6, 2 > 7, 2 > 8, 3 > 7, 3 > 8, 5 > 7, 6 > 7		126.652	7	0.000	1 > 4, 2 > 4, 3 > 4, 5 > 4, 6 > 4, 7 > 4, 8 > 4		51.531	7	0.000	6 > 1, 6 > 2, 6 > 3, 6 > 5, 6 > 7, 6 > 8	
Country	1.015	1	0.314			70.010	1	0.000	US > JPN		14.488	1	0.000	US > JPN	
Sex	1.683	1	0.195			69.123	1	0.000	F > M		0.749	1	0.387		
Neutered status[2]	0.658	1	0.417			0.468	1	0.494			3.771	1	0.052		
Source where aquired[3]	24.100	6	0.001	2 > 3, 5 > 3		1.940	6	0.925			31.588	6	0.000	3 > 4, 7 > 4	
Dog-ownership experience[4]	1.361	1	0.243			0.006	1	0.939			15.057	1	0.000	2 > 1	
Body weight	0.571	1	0.450			14.518	1	0.000		−0.029	3.725	1	0.054		
Dog's age at evaluation	0.000	1	0.996			0.627	1	0.429			22.534	1	0.000		0.024
Dog's age when acquired	14.696	1	0.000		−0.003	3.223	1	0.073			5.055	1	0.025		0.000
Breed groups*Country	61.631	15	0.000			139.576	15	0.000			89.920	15	0.000		
Breed groups*Sex	63.198	15	0.000			127.814	15	0.000			59.386	15	0.000		
Country*Sex	12.030	3	0.007			85.804	3	0.000			15.663	3	0.001		
Breed groups*Country*Sex	31	0.000				141.411	31	0.000			104.545	31	0.000		
Omnibus	189.444	42	0.000			145.060	42	0.000			248.373	42	0.000		
	F4: Separation-related anxiety					F5: Energy and restless					F6: Fear of non-social stimuli				
	χ^2	df	p	Pairwise comparison	B	χ^2	df	p	Pairwise comparison	B	χ^2	df	p	Pairwise comparison	B
Breed groups[1]	13.498	7	0.061			44.844	7	0.000	1 > 4, 2 > 4, 3 > 4, 5 > 4, 6 > 4, 7 > 4, 6 > 3, 6 > 8		44.844	7	0.000	1 > 4, 2 > 4, 3 > 4, 6 > 3, 5 > 4, 6 > 4, 7 > 4, 6 > 8	
Country	31.078	1	0.000	US > JPN		5.077	1	0.024	JPN > US		5.077	1	0.024	JPN > US	
Sex	0.000	1	0.996			0.161	1	0.688			0.161	1	0.688		
Neutered status[2]	4.368	1	0.037	I > N		5.631	1	0.018	N > I		5.631	1	0.018	N > I	
Source where aquired[3]	12.795	6	0.046			10.706	6	0.098			10.706	6	0.098		
Dog-ownership experience[4]	10.161	1	0.001	1 > 2		2.130	1	0.144			2.130	1	0.144		
Body weight	4.925	1	0.026		−0.012	7.906	1	0.005		−0.012	7.906	1	0.005		−0.012
Dog's age at evaluation	5.444	1	0.020		−0.039	2.154	1	0.142			2.154	1	0.142		
Dog's age when acquired	1.083	1	0.298			4.155	1	0.042		0.001	4.155	1	0.042		0.001
Breed groups*Country	96.176	15	0.000			52.434	15	0.000			52.434	15	0.000		
Breed groups*Sex	20.717	15	0.146			47.984	15	0.000			47.984	15	0.000		
Country*Sex	31.078	3	0.000			5.752	3	0.124			5.752	3	0.124		
Breed groups*Country*Sex	106.105	31	0.000			65.671	31	0.000			65.671	31	0.000		
Omnibus	237.075	42	0.000			148.076	42	0.000			148.076	42	0.000		
	F7: Aggression to household members					F8: Fear of unfamiliar dogs					F9: Aggression to unfamiliar dogs				
	$\chi 2$	df	p	Pairwise comparison	B	χ^2	df	p	Pairwise comparison	B	χ^2	df	p	Pairwise comparison	B
Breed groups[1]	84.719	7	0.000	1 > 4, 2 > 4, 2 > 6, 2 > 7, 3 > 4, 3 > 6, 5 > 4, 6 > 4, 7 > 4, 8 > 4		141.880	7	0.000	1 > 4, 2 > 4, 3 > 4, 5 > 4, 6 > 4, 7 > 4, 8 > 4		26.211	7	0.000	1 > 7, 2 > 7, 5 > 7, 6 > 7	
Country	0.000	1	1.000			80.139	1	0.000	US > JPN		2.747	1	0.097		
Sex	0.000	1	1.000			78.662	1	0.000	F > M		5.105	1	0.024	M > F	
Neutered status[2]	0.000	1	1.000			2.798	1	0.094			0.509	1	0.476		
Source where aquired[3]	0.000	6	1.000			11.911	6	0.064			11.427	6	0.076		
Dog-ownership experience[4]	0.000	1	1.000			1.017	1	0.313			0.780	1	0.377		
Body weight	0.023	1	0.881			5.361	1	0.021		−0.017	1.718	1	0.190		

Continued

Dog's age at evaluation	0.000	1	0.986			1.257	1	0.262			16.415	1	0.000		0.069
Dog's age when acquired	2.897	1	0.089			0.008	1	0.929			2.756	1	0.097		
Breed groups*Country	89.609	14	0.000			153.605	15	0.000			36.747	15	0.001		
Breed groups*Sex	85.619	14	0.000			142.858	15	0.000			38.165	15	0.001		
Country*Sex	20.113	3	0.000			98.852	3	0.000			9.449	3	0.024		
Breed groups*Country*Sex	91.284	29	0.000			155.422	31	0.000			52.726	31	0.009		
Omnibus	266.838	42	0.000			111.849	42	0.000			104.112	42	0.000		
	F11: Attachment and attention-seeking					F12: Aggression to persons passing near the house									
	χ^2	df	p	Pairwise comparison	B	χ^2	df	p	Pairwise comparison	B					
Breed groups[1)]	82.116	7	0.000	2 > 1, 3 > 1, 4 > 1, 5 > 1, 6 > 1, 7 > 1, 8 > 1		19.286	7	0.007	2 > 8						
Country	136.912	1	0.000	US > JPN		3.724	1	0.054							
Sex	3.030	1	0.082			0.984	1	0.321							
Neutered status[2)]	1.019	1	0.313			0.543	1	0.461							
Source where aquired[3)]	11.958	6	0.063			8.539	6	0.201							
Dog-ownership experience[4)]	0.042	1	0.837			0.335	1	0.563							
Body weight	7.023	1	0.008		−0.005	0.007	1	0.934							
Dog's age at evaluation	11.145	1	0.001		−0.018	0.000	1	0.999							
Dog's age when acquired	1.318	1	0.251			8.065	1	0.005		−0.002					
Breed groups*Country	328.227	15	0.000			29.034	15	0.016							
Breed groups*Sex	86.349	15	0.000			26.774	15	0.031							
Country*Sex	145.751	3	0.000			7.556	3	0.056							
Breed groups*Country*Sex	344.926	31	0.000			47.057	31	0.032							
Omnibus	385.296	42	0.000			72.384	42	0.002							

Table 3. Results for the analysis of factor scores using generalized linear models. 1) Ancient and spitz breeds: 1, Toy dogs: 2, Spaniels, scent hounds, and poodles: 3, Working dogs: 4, Small terriers: 5, Sight hounds and herding dogs: 6, Retrievers: 7, Mastiff-like dogs: 8. 2) neutered: N, intact: I. 3) bred by owner: 1, friend of relative: 2, breeder: 3, pet store: 4, shelter: 5, stray: 6, other: 7. 4) first ownership: 1, second and more ownership: 2. 5) partial regression coefficient".

Some factors were different between US and Japan (US > JPN; F2, F3, F4, F8, F11 JPN > US; F5, F6), and between male and female (male > female; F9 female > male; F2, F8). Some factors were affected by spay/neuter status (intact > neutered; F4 neutered > intact; F5, F6), source from which dogs were acquired (F1; friend or relative > breeder, shelter > breeder F3; breeder > pet store, other > pet store) and owner's experience of dog-ownership (first ownership > second and more ownership; F4 second and more ownership > first ownership; F3). Body weight, dog's age at the time of evaluation and dog's age when acquired also influenced some factors (body weight; F2, F4, F5, F6, F8, F11 dog's age at evaluation; F3, F4, F9, F11 dog's age when acquired; F1, F3, F5, F6, F12). The environment for dogs and their owners are different in Japan and US. For example, pet stores are a popular source of dog acquisition in Japan compared with the US where most purebred dogs are acquired directly from breeders. In order to investigate the effect of country on breed group differences, we separated the questionnaire data into two groups -dogs living in Japan and the USA- and analyzed for the breed group differences separately in each group. There were some differences between countries, the primary breed group differences remained the same in both countries, especially with respect to F11 (attachment and attention-seeking), even though there were large differences in the environment surrounding the dogs in two countries. The results are shown in Supplemental Table 2.

Additionally, we conducted cluster analyses of the factors using breed medians and Ward's method. All of the breeds of the ancient and spitz breed group are clustered in one group in the dendrogram branches associated with F2 (fear of unfamiliar persons), F4 (separation-related anxiety) and F11 (attachment and attention-seeking). Four out of five breeds of the ancient and spitz breed group are also clustered in one group in the branch associated with F8 (fear of unfamiliar dogs). In F11 (attachment and attention-seeking), two clusters were identified and all of five breeds of ancient and spitz breed group were classified into the same cluster. Five other breeds also clustered as showing low levels of attachment and attention-seeking, including two terriers (West Highland White Terrier, Cairn Terrier), two sight hounds (Whippet, Borzoi), and the Great Dane. In F4 (separation-related anxiety), two clusters

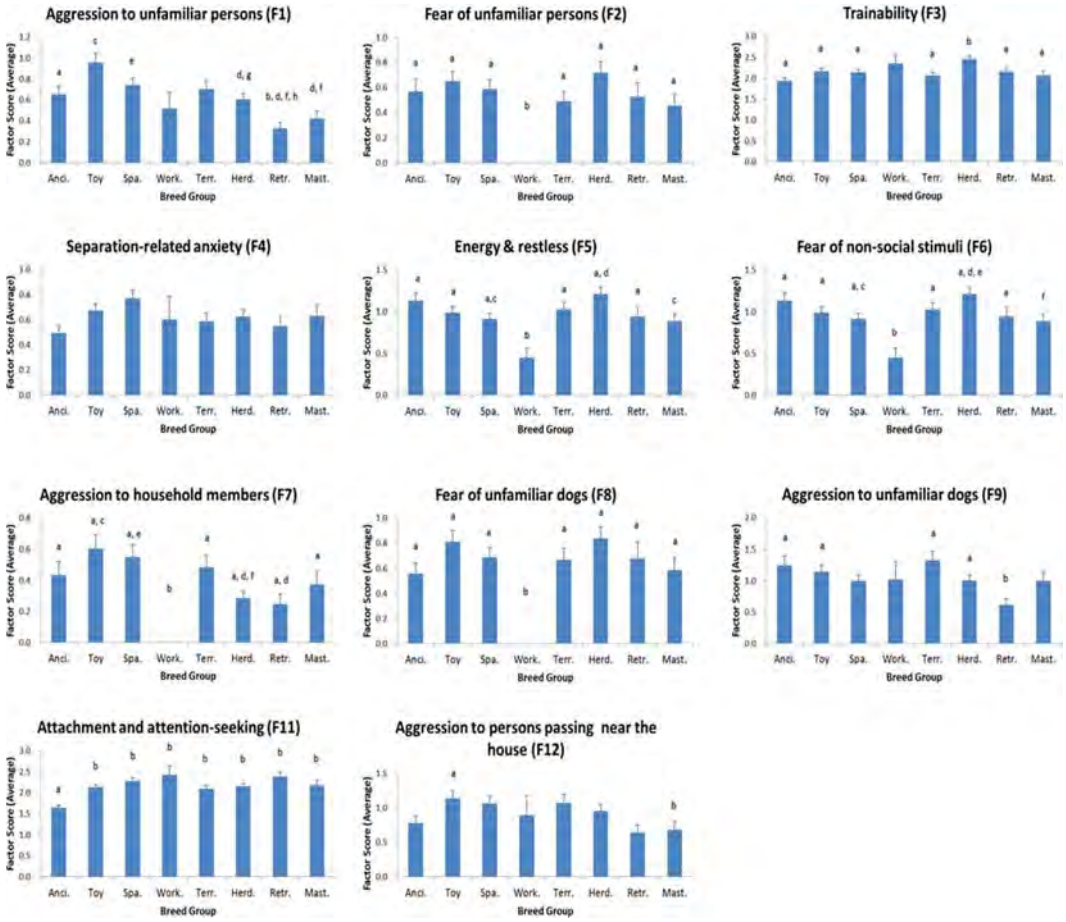

Figure 1. Average factor scores for breed groups. The dog breeds were separated into eight breed groups according to the cladogram, Ancient and spitz breeds: 1, Toy dogs: 2, Spaniels, scent hounds, and poodles: 3, Working dogs: 4, Small terriers: 5, Sight hounds and herding dogs: 6, Retrievers: 7, Mastiff-like dogs: 8. a vs b, $p < 0.05$; c vs d, $p < 0.05$; e vs f, $p < 0.05$; g vs h, $p < 0.05$.

were identified and all of five breeds of ancient and spitz breed group were classified into the same cluster. Fifteen other breeds are also clustered as showing low levels of separation anxiety. In F2 (fear of unfamiliar persons), two clusters were identified and eleven breeds (Chihuahua, Poodle (Toy), Boxer, Yorkshire Terrier, Shetland Sheepdog, Whippet, Maltese, Miniature Pinscher, Great Dane, Cocker Spaniel (American), and Italian Greyhound) were in one cluster and all other breeds were in the other. The trees for F2, F4 and F11 are shown in Supplementary Figure 1, 2 and 3.

Discussion

Using a validated online behavioral evaluation system (C-BARQ), we collected data on the behavioral characteristics of dogs in Japan and the United States, and investigated differences among genetically classified breed groups. Overall, most of the variance in C-BARQ factor scores was explained by the variables; breed group, country, sex, spay/neuter status, and source from which dogs were acquired. Significant interactions between breed group and other variables were also found, indicating that the behaviors evaluated by C-BARQ were influenced by genetic origins, hormonal status and environmental factors, such as country. Some factors were clearly explained by breed group differences. These differences may be related to the effects of direct selection for behavioral characteristics or due to differences in the conditions of life that different breeds experience during development. Since it is hard to believe that all ancient breeds grew up in similar environments that were distinct from those of all modern breeds, it appears unlikely that the observed breed group differences are due solely to environmental factors. Furthermore, when we separated the questionnaire data into two groups—dogs living in Japan and the United States—and analyzed for breed group differences separately in each group (Supplementary Table 2), we identified similar breed group differences in behavior in both countries. This finding supports the view that these differences are primarily due to genetic factors. The most unique among the eight breed groups is the working dog group, which shows the lowest levels of fear of unfamiliar persons, non-social stimuli, and unfamiliar dogs, and the lowest scores for energy, hyperactivity, and aggression to household members. Working dogs are used as police dogs, military dogs, watch dogs, and may be under strong

selection for these characteristics. Even those that live as family pets, may still retain the the effects of past selection for working roles. Since the data for working dogs are from only two breeds, Doberman Pinscher and German Shepherd, there is a possibility that the uniqueness of the working dog group is related to the small size of this group. Similarly, the trainability of sight hounds and herding dogs may be high because of direct selection for this characteristic. Most interestingly, the scores for attachment and attention-seeking of the ancient and spitz breeds group is different from the scores of any other breed group with presumed modern European origins. Some studies suggested that even hand-reared wolves did not show attachment-like behavior like dogs[21,33]; therefore, the unique characteristic of this breed group may be one of the remnants of wolves' behavioral characteristics and may be very informative of understanding the dog domestication processes. "Attachment" in C-BARQ is defined by owners' responses to questions concerning the dog's tendency "to follow members of the household from room to room about the house," "to sit close to or in contact with a member of the household when that individual is sitting down," "to nudge, nuzzle, or paw a member of the household for attention when that individual is sitting down," and "to become agitated when a member of the household shows affection for another person or animal." Considering the history of these breeds, it seems unlikely that dogs in the ancient and spitz breed group were selected for low degrees of attachment and attention seeking. Rather, it is more likely that the capacity to form attachments for humans was an important component of the evolution of modern dogs. Furthermore, we believe that the cluster analysis of the attachment and attention-seeking traits, in which all five breeds in the ancient and spitz breeds groups clustered in a small tightly clustered group of 10 breeds, clearly separated from the 36 other breeds, supports our interpretation that low levels of attachment and attention-seeking are a distinctive behavioral characteristic of the ancient and spitz breed groups. The five other breeds that clustered with the ancient and spitz breeds for attachment and attention-seeking may have developed lower levels of attachment secondarily as adaptations for hunting independently of human guidance. We also investigated the influence of the two different grouping methods, of vonHoldt *et al.*[8] and Parker *et al.*[11] on the low attachment tendency in the ancient and spitz breed group. The low attachment tendency in the ancient and spitz breed group was stable for both grouping methods.

Although some of the breeds in the ancient and spitz group have practical functions such as pulling sleds (e.g. Siberian husky), their C-BARQ scores for attachment and attention-seeking are not different from the other breeds in the ancient and spitz group. This may be because they are primarily motivated to run in groups without formal training or the need to attend to or follow instructions from a human handler[1]. We also need to be careful about interpreting the close relationship of these breeds to wolves in the cladogram because there may be an influence of recent crossing with wolves.

Previous discussions of the behavioral changes associated with the domestication of the dog have tended to emphasize the role of selection for the trait of "tameness" (i.e. loss of fearful or aggressive responses toward humans)[34,35]. However, a previous study of species differences in behavior towards humans between hand-reared dogs and wolf pups also revealed that even wolves that have been intensively socialized do not show the same levels of attachment behavior towards humans that dogs do[33]. This suggests that in addition to tameness, dogs may acquired high levels of attachment and attention-seeking behavior toward humans during the domestication process. In a famous series of experiments involving farmed foxes (*Vulpes vulpes*), individuals with low aggressive-fearful reactions to humans were selectively bred for over forty generations. This led to a unique population of foxes that also gradually showed high attachment behaviors, such as actively seeking contact with humans, tail-wagging in anticipation of social contact, licking experimenters' faces and hands, and following them like dogs[36]. Considering the results of our study, together with the results of such experiments, we believe that one of the earliest stages of dog domestication may have involved selection for not only low aggressive-fearful tendencies in ancestral wolves toward humans, but also the early development of human-directed attachment behavior.

Despite their low attachment and attention-seeking tendencies, the aggressive and fearful reactions towards humans were relatively low in the ancient and spitz breed group. It is possible that domestication may have involved a two-stage process, with selection for low aggressive and fearful tendencies occurring in the first stage, and selection for prosociality (attachment and attention-seeking) occurring later, perhaps in association with the development of more specialized working roles. As a result, the ancient and spitz breeds may retain the low aggressive and fearful tendencies associated with stage 1, but lack the strong prosocial traits associated with stage 2 and more modern breeds of dog. Viewed in this light, the aggressiveness toward humans characteristic of toy dogs may be a secondary development concomitant with their small body size which renders them less of a threat to humans. Or it may be that toy breeds are less adequately socialized by their owners. This association between small body size and aggression in dogs confirms the findings of previous studies[17].

The findings of the present study, namely that the ancient and spitz breed group shows the lowest attachment levels and is significantly different from other breed groups, confirms the idea that selective processes may have taken place during domestication on genetic changes affecting the attachment system, and that the consistently low attachment levels found in this group of breeds may be a remnant of an earlier stage of dog evolution. Since we could not fully describe the contribution of environmental factors to these observed breed differences in behavior, future investigations will need to take into account the possible effects of breed-specific environmental influences.

References

1. Serpell, J. *The Domestic Dog: Its Evolution, Behaviour, and Interactions with People*. (Cambridge University Press, 1995).
2. Bradshaw, J. W., Goodwin, D., Lea, A. M. & Whitehead, S. L. A survey of the behavioural characteristics of pure-bred dogs in the United Kingdom. *Vet. Rec.* **138,** 465–468 (1996).
3. Mahut, H. Breed differences in the dog's emotional behaviour. *Can. J. Exp. Psychol.* **12,** 35 (1958).
4. Seksel, K., Mazurski, E. J. & Taylor, A. Puppy socialisation programs: short and long term behavioural effects. *Appl. Anim. Behav. Sci.* **62,** 335–349 (1999).
5. Scott, J. P. & Fuller, J. F. *Genetics and the social behavior of the dog*. (University of Chicago Press, 1965).
6. Svartberg, K. Breed-typical behaviour in dogs—Historical remnants or recent constructs? *Appl. Anim. Behav. Sci.* **96,** 293–313 (2006).
7. Parker, H. G. *et al.* Genetic structure of the purebred domestic dog. *Science* **304,** 1160–1164 (2004).
8. vonHoldt, B. M. *et al.* Genome-wide SNP and haplotype analyses reveal a rich history underlying dog domestication. *Nature* **464,** 898–902 (2010).
9. Wayne, R. K. & Ostrander, E. A. Lessons learned from the dog genome. *Trends Genet.* **23,** 557–567 (2007).
10. Turcsán, B., Kubinyi, E. & Miklósi, Á. Trainability and boldness traits differ between dog breed clusters based on conventional breed categories and genetic relatedness. *Appl. Anim. Behav. Sci.* **132,** 61–70 (2011).
11. Parker, H. G. *et al.* Breed relationships facilitate fine-mapping studies: A 7.8-kb deletion cosegregates with collie eye anomaly across multiple dog breeds. *Genome Res.* **17,** 1562–1571 (2007).
12. Hsu, Y. & Serpell, J. A. Development and validation of a questionnaire for measuring behavior and temperament traits in pet dogs. *J. Am. Vet. Med. Assoc.* **223,** 1293–1300 (2003).
13. Kutsumi, A., Nagasawa, M., Ohta, M. & Ohtani, N. Importance of puppy training for future behavior of the dog. *J. Vet. Med. Sci.* **75,** 141–149 (2013).
14. Nagasawa, M., Mogi, K. & Kikusui, T. Continued distress among abandoned dogs in Fukushima. *Sci. Rep*. **2,** 724 (2012).
15. Nagasawa, M. *et al.* Assessment of the Factorial Structures of the C-BARQ in Japan. *J. Vet. Med. Sci.* **73,** 869 (2011).
16. Serpell, J. A. & Hsu, Y. Effects of breed, sex, and neuter status on trainability in dogs. *Anthrozoös*. **18,** 196–207 (2005).
17. Duffy, D. L., Hsu, Y. & Serpell, J. A. Breed differences in canine aggression. *Appl. Anim. Behav. Sci*. **114,** 441–460 (2008).
18. Mehrkam, L. R. & Wynne C. D. L. Behavioral differences among breeds of domestic dogs (Canis lupus familiaris): Current status of the science. *Appl. Anim. Behav. Sci*. **155,** 12–27 (2014).
19. Goodwin, D., Bradshaw, J. W. S. & Wickens, S. M. Paedomorphosis affects agonistic visual signals of domestic dogs. *Anim. Behav.* **53,** 297–304 (1997).
20. Kubinyi, E., Virányi, Z. & Miklósi, Á. Comparative social cognition: from wolf and dog to humans. *Comp. Cogn. Behav. Rev*. **2,** 26–46 (2007).
21. Miklósi, Á. *et al.* A simple reason for a big difference: wolves do not look back at humans, but dogs do. *Curr. Biol.* **13,** 763–766 (2003).
22. Duffy, D. L. & Serpell, J. A. Predictive validity of a method for evaluating temperament in young guide and service dogs. *Appl. Anim. Behav. Sci.* **138,** 99–109 (2012).
23. Barnard, S., Siracusa, C., Reisner, I., Valsecchi, P. & Serpell, J. A. Validity of model devices used to assess canine temperament in behavioral tests. *Appl. Anim. Behav. Sci.* **138,** 79–87 (2012).
24. De Meester, R. H. *et al.* A preliminary study on the use of the socially acceptable behavior test as a test for shyness/confidence in the temperament of dogs. *J. Vet. Behav*. **3,** 161–170 (2008).
25. Foyer, P., Bjällerhag, N., Wilsson, E. & Jensen, P. Behaviour and experiences of dogs during the first year of life predict the outcome in a later temperament test. *Appl. Anim. Behav. Sci.* **155,** 93–100 (2014).
26. Svartberg, K. A comparison of behaviour in test and in everyday life: Evidence of three consistent boldness-related personality traits in dogs. *Appl. Anim. Behav. Sci.* **91,** 103–128 (2005).
27. Vermeire, S. *et al.* Neuro-imaging the serotonin 2A receptor as a valid biomarker for canine behavioural disorders. *Res. Vet. Sci.* **91,** 465–472 (2011).
28. Vermeire, S. *et al.* Serotonin 2A receptor, serotonin transporter and dopamine transporter alterations in dogs with compulsive behaviour as a promising model for human obsessive-compulsive disorder. *Psychiatry Res.* **201,** 78–87 (2012).
29. Nagasawa, M., Kanbayashi, S., Mogi, K., Serpell, J. A. & Kikusui, T. Comparison of behavioral characteristics of dogs in the United States and Japan. *J. Vet. Med. Sci*. in press.
30. Houpt, K. A. *et al.* Proceedings of a workshop to identify dog welfare issues in the US, Japan, Czech Republic, Spain and the UK. *Appl. Anim. Behav. Sci.* **106,** 221–233 (2007).
31. McGreevy, P. D. *et al.* Dog behavior co-varies with height, bodyweight and skull shape. *PloS one* **8,** e80529 (2013).
32. McMillan, F. D., Serpell, J. A., Duffy, D. L., Masaoud, E. & Dohoo, I. R. Differences in behavioral characteristics between dogs obtained as puppies from pet stores and those obtained from noncommercial breeders. *J. Am. Vet. Med. Assoc.* **242,** 1359–1363 (2013).
33. Topál, J. *et al.* Attachment to humans: a comparative study on hand-reared wolves and differently socialized dog puppies. *Anim. Behav.* **70,** 1367–1375 (2005).
34. Coppinger, R. & Coppinger, L. *Dogs: A startling new understanding of canine origin, behavior & evolution*. (Simon and Schuster 2001).
35. Driscoll, C. A., Macdonald, D. W. & O'Brien, S. J. From wild animals to domestic pets, an evolutionary view of domestication. *Proc. Natl. Acad. Sci. USA* **106** Suppl 1, 9971–9978 (2009).
36. Trut, L., Plyusnina, I. & Oskina, I. An experiment on fox domestication and debatable issues of evolution of the dog. *Russ. J. Genet.* **40,** 644–655 (2004).

Acknowledgements

This work was financially supported by MEXT*-Supported Program for the Strategic Research Foundation at Private universities, 2011–2015, and Grant-in-Aid for Scientific Research on Innovative Areas No. 25118007 "The Evolutionary Origin and Neural Basis of the Empathetic Systems".

Author Contributions

A.T., M.N. and T.K. wrote the main manuscript text and A.T. prepared Fig. 1 and supplementary Figures 1–3. T.K., M.N. and H.O. conducted statistical analysis and prepared all tables. T.K., K.M. and J.A.S. collected data and prepared experimental design. All authors reviewed the manuscript.

Additional Information

Supplementary information accompanies this paper at http://www.nature.com/srep

Competing financial interests: The authors declare no competing financial interests.

How to cite this article: Tonoike, A. *et al.* Comparison of owner-reported behavioral characteristics among genetically clustered breeds of dog (*Canis familiaris*). *Sci. Rep.* **5**, 17710; doi: 10.1038/srep17710 (2015).

FULL PAPER *Ethology*

Comparison of behavioral characteristics of dogs in the United States and Japan

Miho NAGASAWA[1,2], Shunichi KANBAYASHI[2], Kazutaka MOGI[2], James A. SERPELL[3] and Takefumi KIKUSUI[2]*

[1]*The Department of Physiology, Jichi Medical University, 3311–1 Yakushiji, Shimotsuke, Tochigi 329–0498, Japan*
[2]*The Department of Animal Science and Biotechnology, Azabu University, 1–17–71 Fuchinobe, Chuo-ku, Sagamihara, Kanagawa 252–5201, Japan*
[3]*School of Veterinary Medicine, University of Pennsylvania, 3900 Delancey Street, Philadelphia, PA 19104–6010, U.S.A.*

(Received 28 April 2015/Accepted 14 September 2015/Published online in J-STAGE 27 September 2015)

ABSTRACT. This study examined the difference in dog owning between Japan and the United States, and the effect of these differences on dogs' behavioral characteristics. Behavioral evaluations of privately-owned dogs were obtained by using online questionnaire. We compared background and demographic information from the two countries and analyzed the effects of these differences on behavioral characteristics in dogs. The results indicated that there was a bias in the dog breeds kept in Japan compared to the United States and that Japanese dogs' body weight was lower than the US dogs. The main source of dog acquisition was pet stores in Japan and breeders and/or shelters in the United States. Multiple linear regression analysis found that Japanese dogs showed more aggression to household members and higher energy, restlessness and fear of non-social stimuli than US dogs, while US dogs showed more fear of unfamiliar persons, separation-related behavior and excitability. US dogs also showed higher levels of trainability and attachment to owners. The lower dog's body weight was, the higher the behavioral scores except for trainability were. When dogs that were obtained under 3 months of age were analyzed, the younger the dogs were when their owners obtained them, the higher the scores on some behavioral problem factors w ere. The higher rates of problem behaviors among Japanese dogs compared with US dogs suggest that the preference for small breed dogs an d poor early development environment influenced the behavioral characteristics of dogs.
KEY WORDS: behavioral characteristics, canine, C-BARQ, questionnaire

doi: 10.1292/jvms.15-0253; *J. Vet. Med. Sci.* 78(2): 231–238, 2016

It is estimated that there are 10,346,000 pet dogs in Japan [7]. Japanese dogs are treated as "family members" and provided with the kind of socialization and training more typical of western countries, such as the United States. On the other hand, as dogs have become increasingly integrated into human habitats, behavioral problems have also become more apparent, and these behaviors can sometimes lower the dog owners' quality of life.

In order to solve and prevent these behavior problems, evaluation methods have been developed to help understand dogs' behavioral characteristics [4, 8, 18, 21, 23]. The Canine Behavioral Assessment and Research Questionnaire (C-BARQ) is designed to provide dog owners and professionals with standardized evaluations of canine temperament and behavior [6]. The C-BARQ is also used in Japan [11, 17] after examination of the validity of questionnaire items [16].

The goal of the present study was to use C-BARQ evaluations of dogs from Japan and the United States to investigate whether cultural differences in dog ownership between the two countries influence the behavioral characteristics of their dogs. A number of general differences between the two countries may be important for understanding variation in dog behavior. First, there are differences in the typical household living environment. Japanese homes are generally smaller than in the United States, making some particular small breed dogs more desirable in Japan. Second, the practice of dog acquisition from breeders is not yet typical among Japanese dog owners, and it is still common to acquire dogs from pet stores. A recent study in the United States has confirmed that puppies acquired from pet stores tend to display higher rates of behavioral problems as adults than those acquired from non-commercial breeders [14]. The Japanese tendency to acquire puppies from pet stores may therefore result in higher rates of undesirable behavior than in the US. In light of these differences, we hypothesized that Japanese and American dogs would display consistent differences in the prevalence of particular behavior problems.

The second goal of this study was to examine factors that influenced the behavioral characteristics in each country. It is well-established that experiences when young influence the behavioral characteristics of adults in human and nonhuman animals, including dogs [1, 2, 5, 12, 19, 25]. Therefore, we focused primarily on those factors related to experiences in youth.

MATERIALS AND METHODS

Questionnaire: Behavioral data in the present study were collected from dog owners using the C-BARQ, which includes 100 items that ask owners to indicate how their dogs have responded "in the recent past" to a variety of common

*CORRESPONDENCE TO: KIKUSUI, T., Department of Animal Science and Biotechnology, Azabu University, 1–17–71 Fuchinobe, Chuo-ku, Sagamihara, Kanagawa 252–5201, Japan.
e-mail: kikusui@azabu-u.ac.jp

events and stimuli using a series of 0–4 rating scales (see supplemental data). The C-BARQ is a standardized questionnaire designed to assess the prevalence and severity of behavioral problems in dogs. The validation and reliability of C-BARQ have been described elsewhere [3, 6, 20]. The original C-BARQ was translated into Japanese by 2 behavioral professionals and corrected by 2 professors.

Subjects: C-BARQ data were collected via the freely accessible websites http://www.cbarq.org (US, from April 2006 to November 2012) and http://cbarq.inutokurasu.jp/ (JPN, from September 2010 to November 2012). Before answering the questionnaire, dog owners were asked to provide information about their dogs, such as its breed, age, sex, neuter status, body weight, age when acquired, where acquired and the presence of any health problems. The online survey was advertised via articles in newspapers, magazines, online news and so on, in each country. The C-barq database was used for different purpose [24].

Statistical analyses: Demographic data on the dogs were analyzed by Mann-Whitney *U*-tests, χ^2 tests and Kruskal-Wallis tests (all tests were 2-tailed). If a significant difference was found in a Kruskal-Wallis test, we conducted Mann-Whitney U-tests for multiple comparisons, applying the Bonferroni correction.

Data from the completed questionnaires were subjected to factor analysis. Kaiser's eigenvalue rule was used to determine the number of interpretable factors that could be extracted, and varimax rotation was used to identify empirical groupings of items that measured different behavioral traits. The Cronbach's α coefficient was calculated to assess internal consistency (reliability) of extracted factors; this coefficient describes how well a group of questionnaire items focuses on a single idea or construct. For comparison of the factors, we calculated the average of item scores composing each factor, which was analyzed as a factor score. The factor scores were analyzed by multiple linear regression analysis and Mann-Whitney U-tests to investigate the association with the demographic characteristics of the dogs. Results are expressed as medians ± interquartile ranges (SPSS v.19.0, SPSS Japan Inc., IBM company, Tokyo, Japan), and the results of post-hoc tests were described by the corrected *P*-values.

RESULTS

There were 5,107 C-BARQ questionnaires completed in Japan. Dogs that were <1 or >7 years of age or had severe or chronic health problems were excluded, leaving a total of 2,933 completed questionnaires (57.43%) that were considered valid. The response rates for each of the 78 items in the questionnaire ranged from 39.22 to 99.86% (median, 97.48%, mode, 98.84%). Among the 14,481 questionnaires completed in the United States, 10,500 satisfied the requirements above (72.51%). The response rates for each of the 100 items in the questionnaire ranged from 81.57% to 99.72% (median, 97.85%, mode, 98.04%). Fifteen items with response rates <85.0% either in Japanese or US data were excluded for further analyses. In each dog case, the data of response rates <75.0% were also excluded, leaving 2,789 (54.61%) and 10,389 (71.74%) completed questionnaires that could be used in analyses in Japan and the United States, respectively.

Demographic data: There were 113 and 194 pure breeds represented, respectively, in the Japanese and US data, and there were mixed or unknown breeds in the both countries. In Japan, approximately half of all dogs belonged to the most popular 9 breeds, of which the only large breed was the Labrador Retriever. In the United States, the most popular 27 breeds accounted for 50% of all dogs (Supplementary Table 1). The median age of the dogs was 3.23 ± 1.46 years in Japan and 3.00 ± 1.50 years in the United States. There was no significant difference in the sex ratios of dogs between the 2 countries. However, the proportions of dogs that were neutered/spayed were significantly different (χ^2 (1)=226.85, P<0.001) with a greater proportion of dogs in the United States being neutered/spayed (JPN: 63.8%, US: 77.8%; U=12467505, P<0.001). The body weights of dogs in Japan were significantly lower than in the United States (JPN: 7.00 ± 3.75 kg, US: 24.00 ± 9.50 kg; U=4911742, P<0.001). The median age of dogs when acquired was also significantly lower in Japan than in the United States (JPN: 8.00 ± 8.00 weeks; US: 12.00 ± 22.00 weeks; U=13310688, P<0.001). The proportion of sources from which dogs were acquired showed significant biases in both countries. In Japan, the most common answer was "pet stores" (40.7%), and the second was "breeders" (25.3%), while "breeders" (42.4%) was first and "shelters" (33.6%) was second in the United States. This information is shown in Table 1a.

For the Factor Analysis, we selected 59 breeds that were common to both countries and then matched the samples for sex and number of dog of each breed in order to eliminate any breed or sex biases (n=1,234 each, Supplementary Table 1). The median ages of the dogs were not significantly different in the 2 countries, but the dogs' body weights in Japan were lower than in the United States even after standardization of the numbers and sex ratios of each breed (JPN: 8.0 ± 4.5, US: 9.0 ± 5.5; U=691119.5, P<0.001). Dog's age when acquired in Japan was younger than in the United States (JPN: 10 ± 3.5 weeks, US: 12 ± 21.5 weeks; U=591855.5, P<0.001). The proportion of sources from which dogs were acquired showed the same tendencies as the analysis above in both countries (Table 1b). The median body weights of dogs were significantly different across sources of acquisition in both countries (except for "Bred by owners", "other" and "N/A"). In Japan, dogs from pet stores had significantly lower body weight than dogs from friends or relatives, breeders and shelters. In the United States, dogs acquired from breeders were significantly heavier than dogs from pet stores and shelters. The median ages of dogs when acquired were also significantly different across sources in both countries. In both countries, dogs from shelters and adopted as strays were significantly older than dogs from friends or relatives, breeders and pet stores. However, in the United States, dogs from friends or relatives were significantly older than dogs from breeders. This information is summarized in Table 2.

Factor analysis: Sixty-three of the questionnaire items

Table 1. The source from which dogs were acquired

a. All dogs

		Bred by owner	Friend or relative	Breeder	Pet store	Shelter	Stray	Other	N/A	Total
Japan	(n)	22	237	707	1,136	194	32	70	391	2,789
	(%)	0.8	8.5	25.3	40.7	7.0	1.1	2.5	14.0	100.0
The United States	(n)	519	716	4,407	308	3,488	463	488	0	10,389
	(%)	5.0	6.9	42.4	3.0	33.6	4.5	4.7	0.0	100.0
Total	(n)	541	953	5,114	1,444	3,682	495	558	391	13,178
	(%)	4.1	7.2	38.8	11.0	27.9	3.8	4.2	3.0	100.0

χ^2 (7)=4,086.466, P<0.001.

b. Dogs after breed- and sex-matched selection for factor analysis

		Bred by owner	Friend or relative	Breeder	Pet store	Shelter	Stray	Other	N/A	Total
Japan	(n)	6	98	389	575	32	10	30	94	1,234
	(%)	0.5	7.9	31.5	46.6	2.6	0.8	2.4	7.6	100.0
The United States	(n)	52	110	596	73	304	34	65	0	1,234
	(%)	4.2	8.9	48.3	5.9	24.6	2.8	5.3	0.0	100.0
Total	(n)	58	208	985	648	336	44	95	94	2,468
	(%)	2.4	8.4	39.9	26.3	13.6	1.8	3.8	3.8	100.0

χ^2 (7)=713.144, P<0.001.

Table 2. The comparison of dog's current body weight and age when acquired among the source in acquisition

	Friends or relatives	Breeders	Pet stores	Shelters	Stray	χ^2 (4)	P-value
Japan							
Body weight	8.00 ± 8.25 [a)]	9.00 ± 8.88 [a)]	6.00 ± 2.50 [b)]	9.00 ± 7.25 [a)]	10.50 ± 6.50	60.712	<0.01
Dog's age when acquired	10.00 ± 7.50 [a)]	9.00 ± 5.88 [a)]	11.00 ± 3.50 [a)]	89.00 ± 68.75 [b)]	116.00 ± 82.38 [b)]	91.008	<0.01
The United States							
Body weight	8.00 ± 7.00	10.00 ± 9.38 [a)]	7.00 ± 2.50 [b)]	8.00 ± 4.50 [b)]	9.00 ± 5.88	20.161	<0.01
Dog's age when acquired	12.00 ± 25.50 [a)]	9.00 ± 5.88 [b)]	10.00 ± 4.00 [a,b)]	78.00 ± 67.50 [c)]	77.00 ± 48.00 [c)]	392.48	<0.01

The significance probabilities are 1% except for the following comparison; Body weight: Pet sotres vs. Shelters in Japan, Breeders vs. Shelters in the United States, Age when acquired: Friends or relatives vs. Stray in Japan, P<0.05.

common to the 2 countries were analyzed by factor analysis in each country to compare the behavioral characteristics of the 2 countries, and these items were sorted into 16 factors. After removing the items with factor loadings of <0.4, the remaining items were analyzed by factor analysis again and yielded 12 factors that accounted for 55.47% of the common variance in item scores. Eleven factors were found to have adequate Cronbach's α values (≥0.7) (Table 3). The following factors were extracted: Aggression to unfamiliar persons (F1), Fear of unfamiliar persons (F2), Separation-related behavior (F3), Aggression to household members (especially resource guarding) (F4), Energy and restlessness (F5), Fear of non-social stimuli (F6), Fear of unfamiliar dogs (F7), Trainability (F8), Aggression to unfamiliar dogs (F9), Excitability (F10), Attachment and attention-seeking (F11), and Aggression to persons passing near the house (F12). These results are shown in Table 3. We compared these results with the previous study (11 factors) [16] and found that 8 factors (F2, F3, F4, F6, F7, F8, F9 and F11) were almost the same as the previous analysis. Other 2 factors in the previous study split respectively into 2 factors (F1 and F12, and F5 and F10). The other factor in the previous study was chasing, however, the questionnaire items about chasing did not meet the criterion of response rate and were excluded in this analysis.

Multiple linear analyses of factor scores: We examined the influence of country and the various demographic variables on C-BARQ factor scores using multiple linear regression analysis. We analyzed each factor score using the following 7 explanatory variables: country, sex, spay/neuter status, owner's experience of dog-ownership, the source in acquisition of dogs, dog's age and body weight at the time of evaluation, and dog's age when acquired. Regarding the source in acquisition of dogs, the cases acquired from breeders were set as the baseline, and the standardized partial regression coefficient of each of the explanatory variable indicated the influence on the factor score compared to this baseline. In addition, we limited dog's age when acquired under 3 months of age and reanalyzed the same explanatory variables in order to investigate the influence of early experi-

Table 3. Factor loading of questionnaire items constituting each factor

Factors & questionnaire items	Factor loading	Eigenvalue	Contribution ratio	Cronbach's α
Aggression to unfamiliar persons		9.367	9.798	0.918
When approached directly by an unfamiliar adult while being walked or exercised on a leash	0.837			
When an unfamiliar person tries to touch or pet the dog	0.803			
When an unfamiliar person approaches the owner or a member of the owner's family away from home	0.788			
When approached directly by an unfamiliar child while being walked or exercised on a leash	0.752			
Toward unfamiliar persons visiting the home	0.713			
When an unfamiliar person approaches the owner or a member of the owner's family at home	0.664			
When mailmen or other delivery workers approach the home	0.599			
Fear of unfamiliar persons		4.218	5.375	0.900
When approached directly by an unfamiliar male adult while away from the home	0.823			
When an unfamiliar person tries to touch or pet the dog	0.770			
When approached directly by an unfamiliar child while away from the home	0.752			
When unfamiliar persons visit the home	0.693			
Separation-related behavior		3.838	5.055	0.804
Barking when left or about to be left on its owner	0.736			
Whining when left or about to be left on its owner	0.711			
Howling when left or about to be left on its owner	0.616			
Excessive salivation when left or about to be left on its owner	0.490			
Chewing/scratching at doors, floor, windows, curtains, etc.	0.476			
Loss of appetite when left or about to be left on its owner	0.405			
Aggression to members of the household (especially related to possession)		3.314	5.009	0.723
When food is taken away by a member of the household	0.831			
When approached directly by a member of the household while it is eating	0.772			
When a member of the household retrieves food or objects stolen by the dog	0.689			
When toys, bones or other objects are taken away by a member of the household	0.642			
When verbally corrected or punished by a member of the household	0.401			
Energy and restless		2.275	4.861	0.841
Playful, puppyish, boisterous	0.709			
When a member of the household returns home after a brief absence	0.685			
Active, energetic, always on the go	0.526			
When visitors arrive at its home	0.489			
Restlessness, agitation or pacing when left or about to be left on its owner	0.462			
Fear of non-social stimuli		2.142	4.432	0.758
In response to wind or wind-blown objects	0.699			
In response to strange or unfamiliar objects on or near the sidewalk	0.677			
In response to sudden or loud noises	0.664			
When first exposed to unfamiliar situations	0.478			
During thunderstorms	0.427			
Fear of unfamiliar dogs		1.887	4.114	0.883
When approached directly by an unfamiliar dog of the same or larger size	0.810			
When barked, growled or lunged at by unfamiliar dog	0.759			
When approached directly by an unfamiliar dog of a smaller size	0.755			
Trainability		1.734	4.028	0.800
Obeys a stay command immediately	0.769			
Obeys a sit command immediately	0.731			
Seems to attend to or listen closely to everything the owner says or does	0.622			
Returns immediately when called while off leash	0.609			
Aggression to unfamiliar dogs		1.537	4.026	0.897
When approached directly by an unfamiliar male dog while being walked or exercised on a leash	0.853			
When approached directly by an unfamiliar female dog while being walked or exercised on a leash	0.841			
When barked, growled or lunged at by unfamiliar dog	0.641			
Excitability		1.370	3.443	0.678
Just before being taken on a car trip	0.680			
Just before being taken on a walk	0.640			
When playing with you or other familiy member of your house	0.433			
Displays a strong attachment for one particular member of the household	0.422			
Attachment and attention-seeking		1.255	3.368	0.705
Tends to nudge, nuzzle or paw a member of the household for attention when that individual is sitting down	0.710			
Tends to sit close to or in contact with a member of the household when that individual is sitting down	0.656			
Tends to follow a member of household from room to room about the house	0.532			
Becomes agitated when a member of the household shows affection for another person	0.473			
Aggression to persons passing near the house		1.016	2.239	0.877
When strangers walk past the home while the dog is in the yard	0.662			
When joggers, cyclists, roller skaters or skateboarders pass the home while the dog is in the yard	0.599			

Table 4. The standardized partial regression coefficient of demographic variables in multiple linear regression analysis of factor scores

	F1 Aggression to unfamiliar persons		F2 Fear for unfamiliar persons		F3 Separation- related anxiety		F4 Aggression to house member	
	All	Acquired under 3 months of age	All	Acquired under 3 months of age	All	Acquired under 3 months of age	All	Acquired under 3 months of age
Country [a)]	–0.031	–0.043	0.127 **	0.089 **	0.249 **	0.267 **	–0.633 **	–0.655 **
Sex [b)]	–0.058 **	–0.072 **	0.065 **	0.039	–0.030	–0.027	–0.019	–0.020
Neutered status [c)]	0.031	0.014	–0.016	–0.022	0.033	0.009	0.015	0.009
Dog–ownership experience [d)]	–0.012	–0.020	–0.002	–0.024	–0.093 **	–0.105 **	–0.025	–0.020
The source in acquisition [e)]								
Bred by owner	–0.013	–0.060 *	0.003	–0.010	–0.011	–0.060 *	–0.004	–0.039
Friend or relative	0.108 **	0.135 **	–0.001	0.006	0.039	0.043	0.048 **	0.057 **
Pet store	0.058 *	0.086 **	0.023	0.052	0.040	0.053	0.057 **	0.040
Shelter	0.094 **	0.053 *	0.051 *	0.037	0.096 **	0.091 **	0.043 *	0.023
Stray	0.053 *	0.020	0.003	–0.012	0.078 **	0.047	0.038 *	0.007
Body weight	–0.160 **	–0.181 **	–0.178 **	–0.182 **	–0.148 **	–0.179 **	–0.023	–0.033
Dog's age at evaluation	0.014	0.035	–0.038	–0.028	–0.057 **	–0.040	–0.145 **	–0.137 **
Dog's age when acquired	–0.079 **	–0.104 **	0.054 *	–0.067 *	–0.032	–0.092 **	–0.056 **	–0.061 **
Adj R^2	0.046 **	0.071 **	0.063 **	0.043 **	0.112 **	0.130 **	0.461 **	0.465 **

	F5 Energy & restless		F6 Fear for non-social objects		F7 Fear for unfamiliar dogs		F8 Trainability	
	All	Acquired under 3 months of age	All	Acquired under 3 months of age	All	Acquired under 3 months of age	All	Acquired under 3 months of age
Country [a)]	–0.165 **	–0.187 **	–0.103 **	–0.132 **	0.007	–0.007	0.153 **	0.148 **
Sex [b)]	–0.082 **	–0.078 **	0.027	0.038	0.089 **	0.096 **	0.036	0.057 *
Neutered status [c)]	0.041 *	0.025	–0.048 *	–0.033	–0.044 *	–0.015	–0.063 **	–0.039
Dog–ownership experience [d)]	–0.039	–0.046	–0.045 *	–0.057 *	–0.019	–0.019	0.083 **	0.091 **
The source in acquisition [e)]								
Bred by owner	–0.027	–0.111 **	–0.028	–0.050	–0.014	–0.051	–0.023	–0.005
Friend or relative	0.047 *	0.021	–0.027	–0.035	–0.011	–0.011	–0.037	–0.041
Pet store	0.158 **	0.149 **	0.048	0.060 *	0.086 **	0.110 **	–0.153 **	–0.145 **
Shelter	0.059 *	0.024	–0.016	0.024	0.020	0.011	–0.063 *	–0.013
Stray	0.034	–0.004	0.017	0.002	–0.015	–0.030	–0.029	0.010
Body weight	–0.106 **	–0.144 **	–0.139 **	–0.149 **	–0.136 **	–0.154 **	0.156 **	0.164 **
Dog's age at evaluation	–0.022	–0.034	0.048 *	0.064 *	0.005	0.007	0.105 **	0.095 **
Dog's age when acquired	–0.032	–0.147 **	0.044	–0.027	–0.005	–0.057	–0.091 **	0.045
Adj R^2	0.099 **	0.127 **	0.048 **	0.063 **	0.038 **	0.052 **	0.113 **	0.107 **

	F9 Aggression to unfamiliar dogs		F10 Excitability		F11 Attachment and attention-seeking		F12 Aggression to passers around house	
	All	Acquired under 3 months of age	All	Acquired under 3 months of age	All	Acquired under 3 months of age	All	Acquired under 3 months of age
Country [a)]	0.035	0.039	0.255 **	0.270 **	0.395 **	0.395 **	0.077 **	0.070 *
Sex [b)]	–0.078 **	–0.077 **	–0.049 *	–0.037	–0.016	–0.024	–0.022	–0.022
Neutered status [c)]	–0.014	–0.029	0.077 **	0.080 **	0.021	0.017	0.029	0.019
Dog–ownership experience [d)]	–0.024	–0.020	–0.044 *	–0.029	0.017	0.021	–0.002	–0.001
The source in acquisition [e)]								
Bred by owner	0.007	–0.018	–0.009	–0.046	–0.041 *	–0.094 **	0.005	–0.016
Friend or relative	0.076 **	0.113 **	0.047 *	0.041	0.023	0.018	0.083 **	0.109 **
Pet store	0.029	0.072 *	0.048 *	0.046	0.036	0.016	0.045	0.053
Shelter	0.105 **	0.036	0.058 *	0.045	0.058 *	0.016	0.066 *	0.026
Stray	0.053 *	0.016	0.037	0.001	0.036	0.023	0.029	–0.010
Body weight	–0.078 **	–0.079 **	–0.053 **	–0.063 *	–0.068 **	–0.094 **	–0.133 **	–0.161 **
Dog's age at evaluation	0.115 **	0.135 **	0.012	0.027	–0.079 **	–0.061 *	0.014	0.035
Dog's age when acquired	–0.055 *	–0.072 *	–0.093 **	–0.070 *	–0.018	–0.075 **	–0.096 **	–0.048
Adj R^2	0.034 **	0.043 **	0.066 **	0.075 **	0.156 **	0.149 **	0.027 **	0.035 **

a) Japan: 0, US: 1, b) male: 0, female: 1, C) intact: 0, neuterd: 1, d) first ownership: 0, second and more ownership: 1, e) Acquired from there: 1/ Not acquired from there: 0. The cases acquired from breeders are set as the baseline, and the standardized partial regression coefficient of each of the explanatory variable indicated the influence on the factor score compared to this baseline. *P<0.05, **P<0.01.

ence more properly. The results are shown in Table 4. In the case that all data were included, all of the factor scores except F1, F7 and F9 were explained significantly by the variable 'country', and the standardized partial regression coefficient in F4, F5 and F6 indicated that dogs in Japan tended to display higher factor scores than dogs in the US. Sex differences explained F1, F2, F5, F7, F9 and F10, and male dogs tended to obtain higher factor scores than female dogs on F1, F5, F9 and F10. Neuter/Spay status explained F5, F6, F7, F8 and F10, and intact dogs showed higher scores on F6, F7 and F8. Previous experience of dog-owning explained F3, F6, F8 and F10, and the score of F8 was higher when owners had previous dog-owning experience. In the source in acquisition of dogs, acquisition from a shelter explained 10 factors (except for F6 and F7). The case of friend or relative and pet store explained 6 factors respectively (Friend or relative: F1, F4, F5, F9, F10 and F12, pet store: F1, F4, F5, F7, F8 and F10). These factor scores except for F8 were higher in comparison to the acquisition from breeders. Body weight explained all factors except F4, and the lower dog's body weights were, the higher their factor scores were except for F8. Age at evaluation explained F3, F4, F6, F8, F9 and F11, and older dogs obtained higher factor scores for F6, F8 and F9. Age when dogs were acquired explained F1, F2, F4, F8, F9, F10 and F12, and the younger the dogs were when their owners obtained them, the higher their scores on these factors except for F2 were. In the case of only dogs that were obtained under 3 months of age (n=1,516), the source in acquisition of dogs which explained the factors mostly is from pet stores (F1, F5, F6, F7, F8 and F9), of which factor scores except for F8 were higher in comparison to the acquisition from breeders. Dogs from friend or relative showed highest scores in the factors related with aggression (F1, F4, F9 and F12). Age when dogs were acquired explained the factor scores except for F6, F7, F8 and F12, and the younger the dogs were when their owners obtained them, the higher their scores on these factors were.

DISCUSSION

Using an online behavioral evaluation system, we collected data on the behavioral characteristics of dogs in Japan and the United States, and investigated differences between the 2 countries. First, we compared background and demographic information for the dogs using all valid data. The results showed that there was a bias in the dog breeds that are chosen by the owners in Japan compared to the United States, which has a wide variety in the breeds that are common; and Japanese dogs' body weights were significantly lower than those of US dogs even after standardization for the number and sexes of each breed, indicating both a Japanese preference for small-sized dogs and a tendency for US dogs to be heavier irrespective of breed and sex. From a historical perspective, most breeds were produced in Europe and the United States, while there were few breeds native to Japan; lack of diversity of breeds in Japan might bring a bias towards owning particular breeds. Japanese owners commonly acquire their dogs from pet stores, while the main sources from which dogs were acquired in the United States were breeders and shelters. This might be due to the easy access to animal shelters as a source for acquiring dogs in the United States. The ratio of neutered dogs was higher in the United States than in Japan, suggesting a cultural difference in attitudes to surgical sterilization between the two countries. Dog's age when acquired was significantly greater in the United States than in Japan. This result may be due to the larger proportion of dogs acquired from shelters in the US sample.

After breed- and sex-matched selection for Factor Analysis, we compared the demographic information again. We found a significant difference in three parameters. First, body weight differences remained despite breed-matched selection between two countries. Second, with respect to dog's age when acquired, there was no significant difference between dogs from breeders and those from pet stores in each country. Considering the time-lag from weaning to acquisition from pet stores [15], dogs from pet stores may be taken from their litters earlier than dogs from breeders. Third, the body weight of dogs from pet stores was significantly lower than that from breeders in each country, suggesting that small breeds were acquired mainly from pet stores.

In order to investigate which demographic variables affected the dog's behavioral characteristics, we analyzed C-BARQ factor scores using multiple linear regression analysis. We found that the variable 'country' affected 9 out of 12 factors. Dogs in Japan showed the more aggression toward household members, more energy and restlessness, and more fear of non-social stimuli than dogs in the United States. On the other hand, dogs in the United States showed more fear of unfamiliar persons, more separation-related behavior and greater excitability, while showing also higher scores for trainability and attachment and attention-seeking. Further research will be needed to identify the reasons for these differences in behavior between the two countries. In all sources in acquisition of dogs except for "bred by owner", most factor scores were higher than those of breeder (except for trainability). The source in acquisition of dogs that explained the factors mostly was from pet stores when dog's age when acquired was limited under 3 months of age, although that was from shelter in the case of all data. The factor scores except for trainability of dogs from pet stores were higher than from breeders, suggesting the possibility that the early developmental experience was not appropriate in pet stores. In addition, it is notable that acquisition from friend or relative was strongly related to aggression. We found also that dog's body weight correlated with most behavioral characteristics, indicating that small breed dogs tended to display a greater potential for problem behaviors as well as reduced trainability. This finding replicates those from a previous study that found that dogs' skull shape, height and bodyweight co-vary with their behavior [13]. The standardized partial regression coefficients of other demographic variables were also significant, but very low.

We hypothesized that dog's age at time of acquisition was related to their behavioral characteristics. Multiple linear regression analysis in this study did not show a large effect

of age of acquisition on factor scores, because these data included dogs that were acquired in adulthood. Analysis which limited dogs that were acquired under 3 months of age revealed that the effect of age of acquisition on factor scores became higher than the analysis which included all dogs in most factors. This suggests that the earlier the dogs were acquired in their developmental period (that is, dogs were separated from their mother too early), the worse the dog's behavioral characteristics may be influenced. In rodent models, it has been demonstrated that the maltreatment of pups in early developmental periods, such as early weaning, influences adult temperament. We previously demonstrated that early weaning caused exposure to high levels of glucocorticoids in the central nervous system of mouse pups [9]. These can increase the stress response of pups and decrease nutritional factors in the central nervous system, leading to excessive anxiety and aggression and decreased learning capacity, among other effects [10]. From these previous studies, the current data suggested that the high fear, high aggression, high excitability and low trainability found in dogs from pet stores were related to early weaning. In addition, Slabbert and Rasa [22] found that dogs that had been separated from their mothers and nest sites (but not their littermates) at 6 weeks of age were prone to exhibit loss of appetite and weight and increased distress, mortality and susceptibility to disease compared to dogs that had remained at the nest sites with their mothers until 12 weeks of age. It can be inferred that while it is important for dogs to be exposed to human society during the early developmental period for socialization, very early mother-infant separation could cause adverse effects in dogs during adulthood.

In conclusion, the comparison of demographic data and behavioral characteristics of dogs between Japan and the United States, using an online questionnaire, showed that Japanese owners were more likely to have acquired their dogs from pet stores and had preferences for a few particular small breeds. We also found a greater potential for the development of problem behaviors in dogs in Japan compared with the United States. The Japanese preference for acquiring small breed dogs from pet stores may have been responsible for these negative behavioral effects, but further research is needed to clarify the precise causal mechanism (s) involved.

ACKNOWLEDGMENT. This work was financially supported by MEXT*-Supported Program for the Strategic Research Foundation at Private universities.

REFERENCES

1. Agid, O., Shapira, B., Zislin, J., Ritsner, M., Hanin, B., Murad, H., Troudart, T., Bloch, M., Heresco-Levy, U. and Lerer, B. 1999. Environment and vulnerability to major psychiatric illness: a case control study of early parental loss in major depression, bipolar disorder and schizophrenia. *Mol. Psychiatry* **4**: 163–172. [Medline] [CrossRef]
2. Caldji, C., Tannenbaum, B., Sharma, S., Francis, D., Plotsky, P. M. and Meaney, M. J. 1998. Maternal care during infancy regulates the development of neural systems mediating the expression of fearfulness in the rat. *Proc. Natl. Acad. Sci. U.S.A.* **95**: 5335–5340. [Medline] [CrossRef]
3. Duffy, D. L. and Serpell, J. A. 2012. Predictive validity of a method for evaluating temperament in young guide and service dogs. *Appl. Anim. Behav. Sci.* **138**: 99–109. [CrossRef]
4. Goddard, M. E. and Beilharz, R. G. 1985. Individual variation in agonistic behaviour in dogs. *Anim. Behav.* **33**: 1338–1342. [CrossRef]
5. Heim, C. and Nemeroff, C. B. 2001. The role of childhood trauma in the neurobiology of mood and anxiety disorders: preclinical and clinical studies. *Biol. Psychiatry* **49**: 1023–1039. [Medline] [CrossRef]
6. Hsu, Y. and Serpell, J. A. 2003. Development and validation of a questionnaire for measuring behavior and temperament traits in pet dogs. *J. Am. Vet. Med. Assoc.* **223**: 1293–1300. [Medline] [CrossRef]
7. Japan Pet Food Association Available at: http://www.petfood.or.jp/data/chart2014/01.html (in Japanese). Accessed April 26, 2015.
8. Jones, A. C. and Gosling, S. D. 2005. Temperament and personality in dogs (Canis familiaris): A review and evaluation of past research. *Appl. Anim. Behav. Sci.* **95**: 1–53. [CrossRef]
9. Kikusui, T., Ichikawa, S. and Mori, Y. 2009. Maternal deprivation by early weaning increases corticosterone and decreases hippocampal BDNF and neurogenesis in mice. *Psychoneuroendocrinology* **34**: 762–772. [Medline] [CrossRef]
10. Kikusui, T. and Mori, Y. 2009. Behavioural and neurochemical consequences of early weaning in rodents. *J. Neuroendocrinol.* **21**: 427–431. [Medline] [CrossRef]
11. Kutsumi, A., Nagasawa, M., Ohta, M. and Ohtani, N. 2013. Importance of puppy training for future behavior of the dog. *J. Vet. Med. Sci.* **75**: 141–149. [Medline] [CrossRef]
12. Liu, D., Diorio, J., Tannenbaum, B., Caldji, C., Francis, D., Freedman, A., Sharma, S., Pearson, D., Plotsky, P. M. and Meaney, M. J. 1997. Maternal care, hippocampal glucocorticoid receptors, and hypothalamic-pituitary-adrenal responses to stress. *Science* **277**: 1659–1662. [Medline] [CrossRef]
13. McGreevy, P. D., Georgevsky, D., Carrasco, J., Valenzuela, M., Duffy, D. L. and Serpell, J. A. 2013. Dog behavior co-varies with height, bodyweight and skull shape. *PLoS ONE* **8**: e80529. [Medline] [CrossRef]
14. McMillan, F. D., Serpell, J. A., Duffy, D. L., Masaoud, E. and Dohoo, I. R. 2013. Differences in behavioral characteristics between dogs obtained as puppies from pet stores and those obtained from noncommercial breeders. *J. Am. Vet. Med. Assoc.* **242**: 1359–1363. [Medline] [CrossRef]
15. Ministry of the Environment Government of Japan Available at: http://www.env.go.jp/council/14animal/y140-21/ref01_1.pdf (in Japanese). Accessed April 26, 2015. According to the Ministry of the Environment survey in 2008, the average of age when puppies were offered for sale in the pet stores was 60.1 day-old; however, the average age when pet stores purchased puppies from distributors and auctions were 43.3 and 41.6 day-old, respectively. The Act on Welfare and Management of Animals which was revised in 2013 prohibits the sale of dogs which are under 45 day-old. This act aims to increase the age limit for sale up to 56 day-old with a phased approach; however, there are no regulatory about separation from the mother and littermates yet.
16. Nagasawa, M., Tsujimura, A., Tateishi, K., Mogi, K., Ohta, M., Serpell, J. A. and Kikusui, T. 2011. Assessment of the factorial structures of the C-BARQ in Japan. *J. Vet. Med. Sci.* **73**: 869–875. [Medline] [CrossRef]
17. Nagasawa, M., Mogi, K. and Kikusui, T. 2012. Continued dis-

tress among abandoned dogs in Fukushima. *Sci. Rep.* **2**: 724. [Medline] [CrossRef]
18. Netto, W. J. and Planta, D. J. U. 1997. Behavioural testing for aggression in the domestic dog. *Appl. Anim. Behav. Sci.* **52**: 243–263. [CrossRef]
19. Serpell, J. A. and Jagoe, J. A. 1995. Early experience and the development of behavior. pp. 79–102. *In*: The Domestic Dog: Its Evolution, Behaviour and Interactions with People. (Serpell, J.A. ed.), Cambridge University Press, Cambridge.
20. Serpell, J. A. and Hsu, Y. 2005. Effects of breed, sex, and neuter status on trainability in dogs. *Anthrozoos* **18**: 196–207. [CrossRef]
21. Sforzini, E., Michelazzi, M., Spada, E., Ricci, C., Carenzi, C., Milani, S., Luzie, F. and Verga, M. 2009. Evaluation of young and adult dogs' reactivity. *J. Vet. Behav.* **4**: 3–10. [CrossRef]
22. Slabbert, J. M. and Rasa, O. A. 1993. The effect of early separation from the mother on pups in bonding to humans and pup health. *J. S. Afr. Vet. Assoc.* **64**: 4–8. [Medline]
23. Svartberg, K. and Forkman, B. 2002. Personality traits in the domestic dog (Canis familiaris). *Appl. Anim. Behav. Sci.* **79**: 133–155. [CrossRef]
24. Tonoike, A., Nagasawa, M., Mogi, K., Serpell, J. A., Ohtsuki, H. and Kikusui, T. 2015. Comparison of owner-reported behavioral characteristics among genetically clustered breeds of dog (Canis familiaris). *Sci. Rep.* **5**: 17710.
25. Winslow, J. T., Noble, P. L., Lyons, C. K., Sterk, S. M. and Insel, T. R. 2003. Rearing effects on cerebrospinal fluid oxytocin concentration and social buffering in rhesus monkeys. *Neuropsychopharmacology* **28**: 910–918. [Medline]

原　著　麻布大学雑誌　第 27 巻　11－18

The Frequency Variations of the Oxytocin Receptor Gene Polymorphisms among Dog Breeds

Akiko TONOIKE[1], Go TERAUCHI[1], Miho INOUE-MURAYAMA[2], Miho NAGASAWA[1], Kazutaka MOGI[1], Takefumi KIKUSUI[1]

[1]Graduate School of Veterinary Sciences, Azabu University,
1-17-71 Chuo-ku, Fuchinobe, Sagamihara, Kanagawa 252-5201, Japan
[2]Wildlife Research Center, Kyoto University, 2-24 Tanaka-Sekiden-cho, Sakyo, Kyoto 606-8203, Japan
[1] 麻布大学大学院　獣医学研究科
〒 252-5201　神奈川県相模原市中央区淵野辺 1-17-71
[2] 京都大学野生動物研究センター
〒 606-8203　京都市左京区田中関田町 2-24　関田南研究棟

Abstract: The domestic dog (*Canis familiaris*) has been diverged from wolves 15,000–100,000 years ago and certain genetic changes may have enabled them to adapt to the human social niche. In this study, we investigated the polymorphisms of the oxytocin receptor gene in dogs and wolves in order to investigate the possibility of the genetic change in the oxytocin system during dog domestication processes. Genotypes of the oxytocin receptor gene polymorphisms were determined in dogs and wolves. The single nucleotide polymorphisms (SNP; rs22927829, rs8679682, rs22896457) were observed in the sampled dogs. On the other hand, for the SNPs rs22927823 and rs22927826, only homozygous GG genotypes were observed (n=25). The frequencies of the SNPs (rs8679682 and rs22896457) were significantly different among wolves and dogs, and also among dog breed groups ($p<0.05$, chi-square test). The frequency profile of these SNPs among dog breed groups supports the hypothesis that there were selections on the oxytocin receptor gene during the dog domestication processes.
Key words: dogs, wolves, domestication, oxytocin receptor gene, single nucleotide polymorphisms.

Introduction

The domestic dog (*Canis familiaris*) belongs to the Canidae family which contains 34 closely related species which diverged within the last 10 million years[1]. Recent phylogenetic analysis of 30 out of 34 living wild canids had revealed that the grey wolf is the most closely related living relative of the domestic dog[2]. At present, there are more than 700 breeds in the world, 194 of which are recognized by the Japan Kennel Club (JKC) (http://www.jkc.or.jp/modules/worlddogs/). Recent studies on dog genes have successively created genetic cladograms of dog breeds[3, 4]. Especially, in the cladogram suggested by vonHoldt (2010), there was a surprising correspondence between genetic and phenotypic/functional breed groupings[4]. The grey wolf and the domestic dog are estimated to be diverged 14.9 thousand years ago[5], however the process of dog domestication is still poorly understood.

The process of domestication involves selection of specific phenotypes. Some researchers believe that domestication started when a population of ancient wolves started to exploit human-related food sources[6]. Certain genetic changes may have enabled them to adapt to the human social niche during an early phase of the domestication process. Recent genome-wide research have revealed some signals of selection in the dog genome,

including the signals near genes which relate to memory formation, behavioral sensitization, and/or the Williams –Beuren syndrome in humans characterized by social traits such as exceptional gregariousness[7]. Later research also has revealed some signals of selection in the genes related to the reproduction, digestion and metabolism, and neurological process[8]. The genes related to the neurological process may be especially strong candidates for one of the genes selected for in the early stages of dog domestication, since the domestication process often involves behavioral and neurological traits, such as the reduction of aggression, which allows for complex interactions with humans[9]. Indeed, recent research had revealed the association of dopamine and serotonin related genes with aggression in domestic dogs[10].

The neuropeptide oxytocin is known to be involved in social behavior, including social bonding and social cognition[11-14]. Oxytocin increases trust and more frequently directs the gaze to the eye region of faces in humans[11, 12]. Oxytocin knockout (OTKO) mice are also more aggressive than wild-type mice[13]. Remarkably, OTKO mice are deficit of recognizing familiar conspecifics after repeated social encounters, although olfactory and non-social memory functions are intact[13]. Oxytocin is further suggested to be critical for the formation of a partner preference in the female prairie vole[14]. Some studies have also shown that some oxytocin receptor polymorphisms are related to stress response and attachment behaviors[15, 16]. A study in humans has shown that genetic variation of the oxytocin receptor modulates the effectiveness of social buffering[15]. Another study in infants has shown that an oxytocin receptor polymorphism is associated with attachment security[16]. Since oxytocin system has been shown to be widely related to the formation and function of social groups, we have investigated the polymorphisms of the oxytocin receptor in dogs and wolves, which is located on chromosome 20 in dogs, in order to understand the contribution of the changes in the oxytocin system to the processes of dog domestication.

Materials and Methods

Animals and DNA isolation

Blood samples of 228 dogs were collected from voluntary recruited dogs in Japan. Blood samples of three wolves (2 *Canis lupus lupus* and 1 *Canis lupus arctos*) were collected from privately owned wolves in Japan. Each of them was owned by different owners and none of the wolf samples were related by blood. Two DNA samples of wolves (*Canis lupus subsp.*) were also kindly shared from the Wildlife Research Center of Kyoto University. Genomic DNA was isolated using the QIAamp® DNA Mini Kit (QIAGEN, Hilden, Germany). The number of dogs in each breed is shown in Table 1.

Data Base Search for the Polymorphism

The polymorphisms were searched by using the Ensembl and National Center for Biotechnology Information (NCBI) data base. Two missense variants and three synonymous variants in the exon were selected for further analyses (rs22927823, rs22927826, rs22927829, rs8679682, rs22896457).

PCR amplification

Three fragments including the five selected polymorphisms of the oxytocin receptor gene were amplified by PCR using primer pairs shown in Table 2. The PCR reactions were performed in a total volume of 50 μl containing 20-50 ng genomic DNA, 0.2 μM of each primer, 0.4 mM of dNTP, 1 U KOD-FX Neo DNA polymerase (TOYOBO, Osaka, Japan) and 25 μl 2×PCR buffer in a PCR Thermal Cycler Dice Touch (Takara, Shiga, Japan). Samples were initially denatured at 94°C for 2 min, followed by 40 cycles of 98°C for 10 s, 65°C for 30 s, and a final extension at 72°C for 7 min.

Genotyping and sequencing

The PCR products were purified using Nucleo Spin® Gel and PCR Clean-up Kit (Takara) after confirmed by 1.5% agarose gel electrophoresis. The concentration of the purified-PCR products were calculated using 1.5% agarose gel electrophoresis. The 30 ng purified-PCR products are

Table 1. The number of dogs in each breeds and the genetically clustered breed groups used for the analysis.

Ancient and Spitz					Toy				
	n					n			
Breeds	rs22927823 rs22927826	rs22927829	rs8679682	rs22896457	Breeds	rs22927823 rs22927826	rs22927829	rs8679682	rs22896457
Akita	0	0	1	1	Pomeranian	1	1	2	2
Shiba	11	29	53	54	Chihuahua	0	0	6	6
Samoyed	0	0	1	1	Shih Tzu	1	3	23	23
Spaniels, Scent hounds, and Poodles					Working				
	n					n			
Breeds	rs22927823 rs22927826	rs22927829	rs8679682	rs22896457	Breeds	rs22927823 rs22927826	rs22927829	rs8679682	rs22896457
American Cocker Spaniel	0	1	7	7	German shepherd	0	0	3	3
English Cocker Spaniel	0	0	3	3					
Cavalier King Charles Spaniel	0	0	2	2					
Beagle	1	2	4	4					
Basset Hound	0	0	3	3					
Toy Poodle	0	0	18	18					
Standard Poodle	1	3	11	11					
Sight hounds and Herding					Retrievers				
	n					n			
Breeds	rs22927823 rs22927826	rs22927829	rs8679682	rs22896457	Breeds	rs22927823 rs22927826	rs22927829	rs8679682	rs22896457
Borzoi	0	2	2	2	Golden Retriever	2	2	8	8
Welsh Corgi Pembroke	0	0	2	2	Labrador Retriever	5	6	13	13
Collie	0	1	2	2	Barnese Mountain Dog	0	0	1	1
Austrlian Shepherd	0	0	1	1					
Shetland Sheepdog	0	2	4	4					
Border Collie	1	2	8	8					
Small terriers					Mastiff-like				
	n					n			
Breeds	rs22927823 rs22927826	rs22927829	rs8679682	rs22896457	Breeds	rs22927823 rs22927826	rs22927829	rs8679682	rs22896457
Yorkshire Terrier	0	0	5	5	Jack Russel Terrier	0	0	4	4
Cairn Terrier	0	0	1	1	Boxer	1	1	1	1
					Other Breeds and Mix				
	n					n			
Breeds	rs22927823 rs22927826	rs22927829	rs8679682	rs22896457	Breeds	rs22927823 rs22927826	rs22927829	rs8679682	rs22896457
Kai	0	1	2	2	Maltese	0	1	1	1
Shikoku	0	0	2	2	Great Pyrenees	0	0	1	1
Kishu	0	0	1	1	Welsh Terrier	0	0	1	1
Spitz	0	0	1	1	Bedlington Terrier	0	0	1	1
Miniature Schnauzer	1	5	6	6	Norfolk Terrier	0	0	1	1
Miniature Dachshund	0	0	8	8	Wire-haired Fox Terrier	0	0	4	4
Boronese	0	0	1	1	Mix	0	1	8	8

Blood samples were collected and the oxytocin receptor gene polymorphisms were investigated in dogs. The dog breeds were separated into eight breed groups: 1) ancient and spitz breeds, 2) toy dogs, 3) spaniels, scent hounds, and poodles, 4) working dogs, 5) small terriers, 6) sight hounds and herding dogs, 7) retrievers, and 8) mastiff-like dogs following cladograms of vonHoldt and Parker for analysis.

mixed with 7.5 pmoles primer in a total volume of 15 μl. The samples were shipped to the Takara CDM Center (Mie, Japan) and subjected to the Premix Sequence Analysis (Takara).

Statistical analysis

The dog breeds were separated into eight breed groups: 1) ancient and spitz breeds, 2) toy dogs, 3) spaniels, scent hounds, and poodles, 4) working dogs, 5) small terriers, 6) sight hounds and herding dogs, 7) retrievers, and 8) mastiff-like dogs following vonHoldt's (2010) cladogram[4] (Table 1). Since the Shiba Inu breed was not included in vonHoldt's cladogram, we classified them into the ancient and spitz breed group according to the cladogram suggested by

Table 2. Primers used for PCR amplification to genotype the dog oxytocin receptor gene polymorphisms.

	Primer	Sequence (5'-3')
rs22927823 and rs22927826	Forward	CCTCCTCCGAAGGGCTTG
	Reverse	CGCAGCGAGAAGATGTGC
rs22927829	Forward	ACCTACCTGCTGCTGCTCAT
	Reverse	GCTCCCTCCTCCGAGGTC
rs8679682 and rs22896457	Forward	ACCCCTACCCTCCCTTCAG
	Reverse	AAGCCCTTGGAGGCAGTC

Parker (2004)[3]. Other dog breeds not shown in vonHoldt' s cladogram were eliminated from further analyses. The working dogs breed group was eliminated from further analyses since there were only three individuals. The dog breeds in each breed group are shown in Table 1.

The frequencies of each single nucleotide polymorphisms (SNP) were assessed for deviation from Hardy–Weinberg equilibrium and were compared between dogs and wolves and between dog breed groups using chi-square test. $P<0.05$ was considered significant.

Results

For the SNPs, rs22927823 and rs22927826, only homozygous GG genotypes were observed (n=25). For the SNP, rs22927829, 97% (n=61) of the sampled dogs (n=63) owned homozygous TT genotypes. Heterozygous AT genotype was observed in one Boxer and homozygous AA genotype was observed in one Miniature Schnauzer. For the SNP, rs8679682, 53% (n=120) owned homozygous TT genotypes, 34% (n=78) owned heterozygous CT genotypes and 13% (n=29) owned homozygous CC genotypes. For the SNP, rs22896457, 96% (n=220) owned homozygous TT genotypes, 3% (n=7) owned heterozygous CT genotypes and homozygous CC genotype was observed in only one Boxer. The SNPs, rs8679682 and rs22896457, were genotyped in five wolf samples. For the SNP, rs8679682, homozygous TT genotype was observed in only one out of five wolves, and homozygous CC genotypes were observed in four of five wolves. For the SNP, rs22896457, two out of five wolves owned homozygous TT genotypes, other two out of five wolves owned heterozygous CT genotypes and one out of five wolves owned homozygous CC genotype.

As shown in Table 3 and Fig. 1, there were significant differences of oxytocin receptor variant (rs8679682 and rs22896457) frequencies among wolves and dogs ($p<0.05$, chi-square test). For the SNP, rs8679682, C variant allele was more common in wolves (80%) than in dogs (30%), whilst the T variant allele was less common in wolves (20%) than in dogs (70%). For the SNP, rs22896457, C variant allele was more common in wolves (40%) than in dogs (2%), whilst the T variant allele was less common in wolves (60%) than in dogs (98%). The frequencies of each SNPs were not in Hardy–Weinberg Equilibrium ($p<0.05$) except for the rs22896457 SNP in wolf population.

As shown in Table 3 and Fig. 1, there were significant differences of oxytocin receptor variant (rs8679682 and rs22896457) frequencies among dog breed groups ($p<0.05$, chi-square test). The frequencies of each SNPs were in Hardy–Weinberg Equilibrium ($p>0.05$) except for the rs8679682 SNP in the ancient and spitz breed group and for the rs22896457 SNP in the mastiff-like dog group. The frequency of C variant allele of the rs8679682 SNP was more common in the mastiff-like dog group (80%), which is very close to the frequency in wolves (80%), compared to the toy dogs, the spaniels, scent hounds, and poodles breed group, small terriers, the sight hounds and herding dogs bred group, and the retrievers (32-42%). The frequency of C variant allele of the rs8679682 SNP was less common in the ancient and spitz breed group (5%) than in the toy dogs, the spaniels, scent hounds, and poodles breed group, small terriers, the sight hounds and herding dogs bred group, and the retrievers (32-42%). The frequency of C variant allele of the rs22896457 SNP

Table 3. Frequency of oxytocin receptor single nucleotide polymorphisms (SNPs) and combined genotypes in wolves and dogs.

SNPs	Wolf or Dog or Dog Breed Group	Genotype Frequency			HWE	Allele Frequency				
rs8679682		CC	CT	TT		C	T			
	Wolf (n=5)	0.80	0.00	0.20	p=0.025	0.80	0.20			
	Dog (n=227)	0.13	0.34	0.53	p=0.006	0.30	0.70			
	Ancient and Spitz (n=55)	0.02	0.05	0.93	p=0.006	0.05	0.95			
	Toy (n=31)	0.06	0.52	0.42	p=0.314	0.32	0.68			
	Spaniels, Scent hounds, and Poodles (n=48)	0.19	0.40	0.42	p=0.255	0.39	0.61			
	Sight hounds and Herding (n=19)	0.11	0.47	0.42	p=0.820	0.34	0.66			
	Retrievers (n=22)	0.09	0.55	0.36	p=0.402	0.36	0.64			
	Small terriers (n=6)	0.33	0.17	0.50	p=0.108	0.42	0.58			
	Mastiff-like (n=5)	0.60	0.40	0.00	p=0.576	0.80	0.20			
rs22896457		CC	CT	TT		C	T			
	Wolf (n=5)	0.20	0.40	0.40	p=0.709	0.40	0.60			
	Dog (n=228)	0.00	0.03	0.96	p=0.002	0.02	0.98			
	Ancient and Spitz (n=56)	0.00	0.02	0.98	p=0.946	0.01	0.99			
	Toy (n=31)	0.00	0.00	1.00	p=0.946	0.00	1.00			
	Spaniels, Scent hounds, and Poodles (n=48)	0.00	0.02	0.98	p=0.942	0.01	0.99			
	Sight hounds and Herding (n=19)	0.00	0.00	1.00	p=0.942	0.00	1.00			
	Retrievers (n=22)	0.00	0.05	0.95	p=0.913	0.02	0.98			
	Small terriers (n=6)	0.00	0.33	0.67	p=0.624	0.17	0.83			
	Mastiff-like (n=5)	0.20	0.00	0.80	p=0.025	0.20	0.80			
Combined genotype rs8679682-rs22896457		CC-CC	CC-CT	CC-TT	CT-CC	CT-CT	CT-TT	TT-CC	TT-CT	TT-TT
	Wolf (n=5)	0.20	0.40	0.20	0.00	0.00	0.00	0.00	0.00	0.20
	Dog (n=227)	0.00	0.01	0.11	0.00	0.01	0.33	0.00	0.00	0.52
	Ancient and Spitz (n=55)	0.00	0.02	0.00	0.00	0.00	0.05	0.00	0.00	0.93
	Toy (n=31)	0.00	0.00	0.06	0.00	0.00	0.52	0.00	0.00	0.42
	Spaniels, Scent hounds, and Poodles (n=48)	0.00	0.00	0.19	0.00	0.02	0.38	0.00	0.00	0.42
	Sight hounds and Herding (n=19)	0.00	0.00	0.11	0.00	0.00	0.47	0.00	0.00	0.42
	Retrievers (n=22)	0.00	0.00	0.09	0.00	0.00	0.55	0.00	0.05	0.32
	Small terriers (n=6)	0.00	0.17	0.17	0.00	0.17	0.00	0.00	0.00	0.50
	Mastiff-like (n=5)	0.20	0.00	0.40	0.00	0.00	0.40	0.00	0.00	0.00

The proportion of each genotype, allele and combined genotype are provided for wolves, dogs and seven dog breed groups.
Statistical tests for Hardy-Weinberg Equilibrium (HWE) are also provided.

was more common in the mastiff-like dog group (20%) and in the small terriers (17%), which is about the half of the frequency in wolves (40%), than in the toy dogs, the spaniels, scent hounds, and poodles breed group, the sight hounds and herding dogs bred group, and the retrievers (0-2%).

Discussion

The oxytocin system is widely related to the behaviors and cognition in many mammals as shown in mice[13], prairie voles[14] and humans[11, 12, 15, 16]. In order to investigate the possibility of the genetic change in the oxytocin system during dog domestication processes, we investigated the polymorphisms of the oxytocin receptor gene in dogs and wolves. Genome-wide studies on dog genes had revealed that there are at least two domestication bottlenecks[2, 5]. The first would have been related to the divergence of the domestic dog from wolves 15,000–100,000 years ago[2]. The recent one would be related to the breed creation and the artificial selection conducted within the past few hundred years[5]. Breeds seem to be different in several aspects of their behavior due to the effects of these artificial selections[17-19], and we hypothesized that there would be variations in the oxytocin receptor genes among dog breeds.

As predicted, there were frequency variations in the oxytocin receptor genes among dog breeds. For the rs8679682 SNP, the ancient and spitz breed group had the least frequency of C allele among seven breed groups. This is surprising since even though the ancient and spitz breed group is genetically related most closely to wolves,

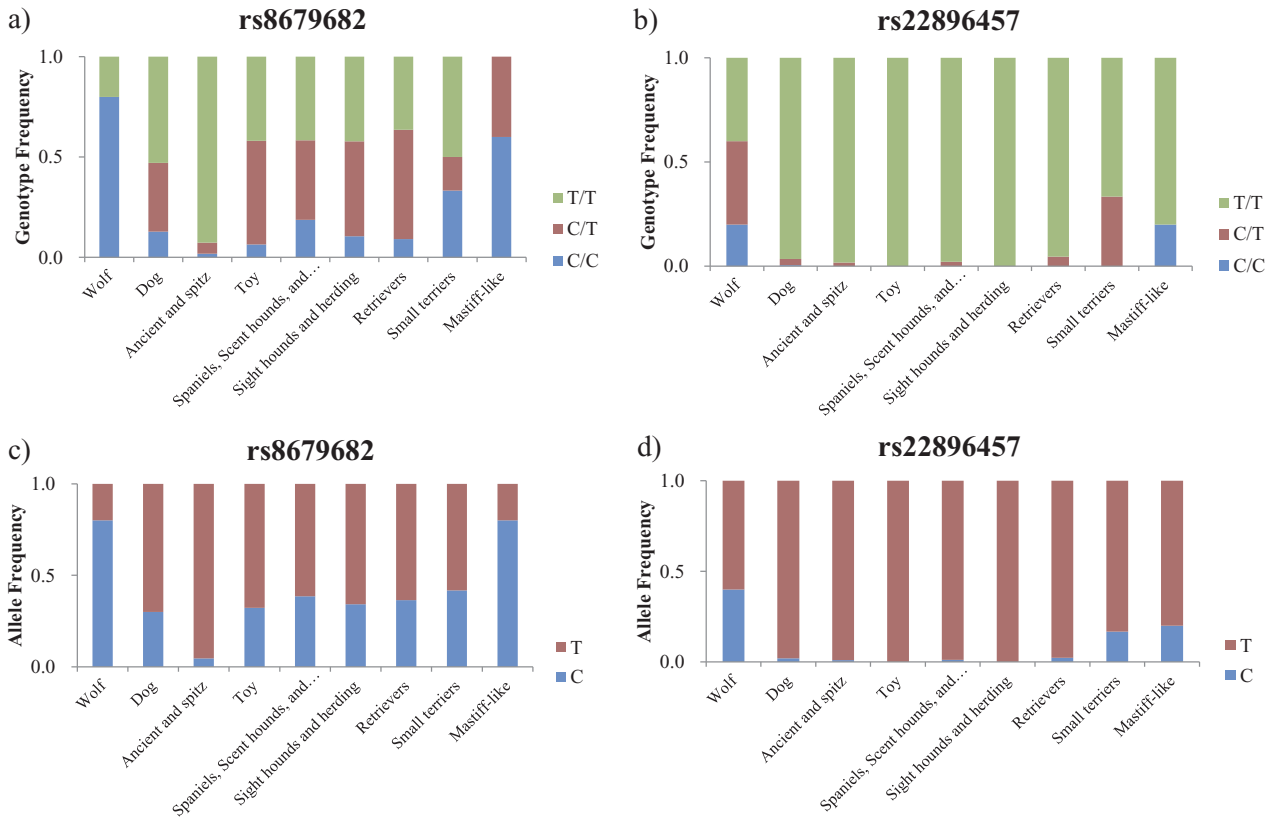

Fig. 1 Genotype frequency and Allele frequency for the SNPs, rs8679682 and rs22896457, in wolves and dogs.
Genotype frequency and allele frequency for the SNPs rs8679682 and rs22896457, in wolves and dogs and in dog breed groups (Ancient and spitz, Toy, Spaniels, Scent hounds, and Poodles, Sight hounds and herding, Retrievers, Small terriers and Mastiff-like) were compared. The frequencies were significantly different for both SNPs between wolves and dogs and also among dog breed groups ($p<0.05$, chi-square test). (a) Genotype frequency of rs8679682 (b) Genotype frequency of rs22896457 (c) Allele frequency of rs8679682 (d) Allele frequency of rs22896457

rs8679682 SNP profile was most different from the profile in wolves. On the other hand, the mastiff-like dog group, which is genetically furthest from wolves, had the most frequency of C allele, which is at almost the same level as in wolves. This can be interpreted as during the early domestication processes, there was a selection or genetic drift related to this SNP and the frequency of the C allele dropped dramatically in the domestic dogs. As the artificial selection began and humans started to control the breeding, C allele gradually increased. Considering the artificial selection creating the mastiff-like dogs, the C allele frequency increased to reach almost the same level in the mastiff-like dogs as the wolves. The rs22896457 SNP also shows the same tendency as the rs8679682 SNP. The C allele frequency, which was almost 40% in wolves is almost 0% in the ancient and spitz breed group, stays at almost 0% for the toy dogs, spaniels, scent hounds, and poodles, working dogs, sight hounds and herding dogs, retrievers, is about 17% for the small terriers, and in the mastiff-like dogs which is believed to be the furthest away genetically show almost 20%.

Recently, three oxytocin receptor gene polymorphisms associated with human directed social behavior in dogs have been reported[20]. This study suggested that oxytocin receptor gene polymorphisms have an impact on proximity seeking tendency towards an unfamiliar person and their owner, as well as friendliness of the dogs toward strangers, although the mediating molecular regulatory mechanisms are yet unknown[20]. Although the direct influence on the behaviors would be hard to interpret since the SNPs in the present study, rs22896457 and rs8679682, are synonymous variants, the frequency profile of these SNPs among dog breed groups supports the hypothesis that there were selections on oxytocin receptor gene during the

dog domestication processes. Further studies on oxytocin receptor gene polymorphisms and their associations with dog behaviors are required.

Acknowledgements

This work was supported by JSPS KAKENHI (grant numbers 25118007, 25290082, and 25118005), a research project grant from the MEXT* Program for the Strategic Research Foundation at Private Universities, a research project grant awarded by Azabu University, and the Cooperation Research Program of Wildlife Research Center, Kyoto University.

Notes

1) Wayne, R. K., Geffen E., Girman D.J., Koepfli K.P., Lau L.M. and Marshall C.R. Molecular systematics of the Canidae. *Syst. Biol*. **46**, 622-653 (1997).
2) Lindblad-Toh, K., Wade, C.M., Mikkelsen, T.S., Karlsson, E.K., Jaffe D.B., Kamal, M., Clamp, M., Chang, J.L., Kulbokas III E.J., Zody, M.C., Mauceli, E., Xie, X., Breen, M., Wayne, R.K., Ostrander, E.A., Ponting, C.P., Galibert, F., Smith, D.R., deJong, P.J., Kirkness, E., Alvarez, P., Biagi, T., Brockman, W., Butler, J., Chin, C.W., Cook, A., Cuff, J., Daly, M.J., DeCaprio, D., Gnerre, S., Grabherr, M., Kellis, M., Kleber, M., Bardeleben, C., Goodstadt, L., Heger, A., Hitte, C., Kim, L., Koepfli, K.P., Parker, H.G., Pollinger, J.P., Searle, S.M.J., Sutter, N.B., Thomas, R., Webber, C., Broad Institute Genome Sequencing Platform and Lander, E.S. Genome sequence, comparative analysis and haplotype structure of the domestic dog. *Nature* **438**, 803-819 (2005).
3) Parker, H.G., Kim, L.V., Sutter,N.B., Carlson, S., Lorentzen, T.D., Malek, T.B., Johnson,G.S., DeFrance, H.B., Ostrander, E.A. and Kruglyak, N. Genetic structure of the purebred domestic dog. *Science* **304**, 1160-1164 (2004).
4) vonHoldt, B.M., Pollinger, J.P., Lohmueller, K.E., Han, E., Parker, H.G., Quignon, P., Degenhardt, J.D., Boyko, A.R., Earl, D.A., Auton, A., Reynolds, A., Bryc, K., Brisbin, A., Knowles, J.C., Mosher, D.S., Spady, T.C., Elkahloun, A., Geffen, E., Pilot, M., Jedrzejewski, W., Greco, C., Randi, E., Bannasch, D., Wilton, A., Shearman, J., Musiani, M., Cargill, M., Jones, P.G., Qian, Z., Huang, W., Ding, Z.L., Zhang, Y., Bustamante, C.D., Ostrander, E.A., Novembre, J. and Wayne, R.K. Genome-wide SNP and haplotype analyses reveal a rich history underlying dog domestication. *Nature* **464**, 898-902 (2010).
5) Freedman, A.H., Gronau, I., Schweizer, R.M., Vecchyo, D.O.D., Han, E., Silva, P.M., Galaverni, M., Fan, Z., Marx, P., Lorente-Galdos, B., Beale, H., Ramirez, O., Hormozdiari, F., Alkan, C., Vila`, C., Squire, K., Geffen, E., Kusak, J., Boyko, A.R., Parker, H.G., Lee, C., Tadigotla, V., Siepel, A., Bustamante, C.D., Harkins, T.T., Nelson, S.F., Ostrander, E.A., Marques-Bonet, T., Wayne, R.K., and Novembre, J. Genome sequencing highlights the dynamic early history of dogs. *PLOS Genetics* **10**, 1-12 (2014).
6) Coppinger, R. P. and Coppinger, L. Dogs: A New Understanding of Canine Origin, Behavior, and Evolution. Chicago: University of Chicago Press, p.39-68 (2001).
7) vonHoldt B.M., Pollinger, J.P., Lohmueller, K.E., Han, E., Parker, H.G., Quignon, P., Degenhardt, J.D., Boyko, A.R., Earl, D.A., Auton, A., Reynolds, A., Bryc, K., Brisbin, A., Knowles, J.C., Mosher, D.S., Spady, T.C., Elkahloun, A., Geffen, E., Pilot, M., Jedrzejewski, W., Greco, C., Randi, E., Bannasch, D., Wilton, A., Shearman, J., Musiani, M., Cargill1, M., Jones, P.G., Qian, Z., Huang, W., Ding, Z.L., Zhang, Y., Bustamante, C.D., Ostrander, E.A., Novembre, J., and Wayne, R.K. Genome-wide SNP and haplotype analyses reveal a rich history underlying dog domestication. *Nature* **464**, 898-903 (2010).
8) Wang,G., Zhai, W., Yang, H., Fan, R., Cao, X., Zhong, L., Wang, L., Liu, F., Wu, H., Cheng, L., Poyarkov, A.D., Poyarkov JR, N.A., Tang, S., Zhao, W., Gao, Y., Lv, X., Irwin, D.M., Savolainen, P., Wu, C.I., and Zhang, Y. The genomics of selection in dogs and the parallel evolution between dogs and humans. *Nature Commun*. **4**, 1860. DOI: 10.1038/ncomms2814.
9) Belyaev, D.K. The Wilhelmine E. Key 1978 invitational lecture. Destabilizing selection as a factor in domestication. *J. Hered*. **70**, 301–308 (1979).
10) Vage, J., Wade, C., Biagi, T., Fatjo, J., Amat, M., Lindblad-Toh, K., and Lingaas, F. Association of dopamine- and serotonin-related genes with canine aggression. *Genes, Brain and Behavior* **9**, 372-378 (2010).
11) Kosfeld, M., Heinrichs, M., Zak, P.J., Fischbacher, U. and Fehr, E. Oxytocin increases trust in humans. *Nature* **435**, 673-676 (2005).

12) Guastella, A.J., Mitchell, P.B. and Dadds, M.R. Oxytocin increases gaze to the eye region of human faces. *Biol. Psychiatry* **63**, 3-5 (2008).
13) Winslow, J.T. and Insel, T.R. The social deficits of the oxytocin knockout mouse. *Neuropeptides* **36**, 221-229 (2002).
14) Insel, T.R. and Hulihan, T.J. A gender-specific mechanism for pair bonding: Oxytocin and partner preference formation in monogamous voles. *Behav. Neurosci*. **109**, 782-789 (1995)
15) Chen, F.S., Kumsta, R., Dawans, B., Monakhov, M., Ebstein, R.P., and Heinrichsa, M. Common oxytocin receptor gene (OXTR) polymorphism and social support interact to reduce stress in humans. *PNAS* **108**, 19937–19942 (2011).
16) Chen, F.S., Barth, M.E., Johnson, S.L., Gotlib, I.H. and Johnson, S.C. Oxytocin receptor (*OXTR*) polymorphisms and attachment in human infants. *Front. Psychol*. **2**, 1-6 (2011).
17) Bradshaw, J.W., Goodwin, D., Lea, A.M., and Whitehead, S.L. A survey of the behavioural characteristics of pure-bred dogs in the United Kingdom. *Vet. Rec*. **138**, 465-468 (1996).
18) Mahut, H. Breed differences in the dog's emotional behaviour. *Can. J. Psychol*. **12**, 35-44 (1958).
19) Scott, J.P. and Fuller, J.F. Genetics and the Social Behavior of the Dog. Chicago: University of Chicago Press, p.185-260 (1965).
20) Kis, A., Bence, M., Lakatos, G., Pergel, E., Turcsan, B., Pluijmakers, J., Vas, J., Elek, Z., Bruder, I., Foldi, L., Sasvari-Szekely, M., Miklosi, A., Ronai, Z., and Kubinyi, E. Oxytocin receptor gene polymorphisms are associated with human directed social behavior in dogs (*Canis familiaris*). *PLOS One* **9**, DOI: 10.1371/journal.pone.0083993.

ANIMAL GENETICS Immunogenetics, Molecular Genetics and Functional Genomics

SHORT COMMUNICATION

doi: 10.1111/age.12344

Copy number variations in the amylase gene (*AMY2B*) in Japanese native dog breeds

A. Tonoike*, Y. Hori†, M. Inoue-Murayama†, A. Konno†, K. Fujita†, M. Miyado‡, M. Fukami‡, M. Nagasawa*§, K. Mogi* and T. Kikusui*

*Companion Animal Research, School of Veterinary Medicine, Azabu University, Sagamihara, Kanagawa 252-5201, Japan. †Department of Psychology, Kyoto University, Sakyo, Kyoto 606-8501, Japan. ‡Department of Molecular Endocrinology, National Research Institute for Child Health and Development, Tokyo 157-8535, Japan. §Department of Physiology, Jichi Medical University, Shimotsuke, Tochigi 329-0498, Japan.

Summary

A recent study suggested that increased copy numbers of the *AMY2B* gene might be a crucial genetic change that occurred during the domestication of dogs. To investigate *AMY2B* expansion in ancient breeds, which are highly divergent from modern breeds of presumed European origins, we analysed copy numbers in native Japanese dog breeds. Copy numbers in the Akita and Shiba, two ancient breeds in Japan, were higher than those in wolves. However, compared to a group of various modern breeds, Akitas had fewer copy numbers, whereas Shibas exhibited the same level of expansion as modern breeds. Interestingly, average *AMY2B* copy numbers in the Jomon-Shiba, a unique line of the Shiba that has been bred to maintain their appearance resembling ancestors of native Japanese dogs and that originated in the same region as the Akita, were lower than those in the Shiba. These differences may have arisen from the earlier introduction of rice farming to the region in which the Shiba originated compared to the region in which the Akita and the Jomon-Shiba originated. Thus, our data provide insights into the relationship between the introduction of agriculture and *AMY2B* expansion in dogs.

Keywords agriculture, *AMY2B* expansion, ancient breeds, domestication, Shiba, wolf

Recently, whole-genome resequencing in dogs and wolves has identified genomic regions that were under selection during dog domestication. From these analyses, researchers found that copy numbers of the *AMY2B* locus increased by several fold in dogs compared to wolves (Axelsson *et al.* 2013). The *AMY2B* gene encodes a protein with amylase activity that is crucial to the digestion of starch-rich diets, and studies have suggested that increased *AMY2B* copy numbers allowed ancestors of dogs to thrive on starch-rich diets. This finding also suggested that the development of agriculture might have catalysed dog domestication. Previous phylogenetic studies in dogs and wolves revealed that breeds of dogs are genetically distinct and that some breeds with Asian and African origins are highly divergent from modern breeds of presumed European origins (Parker *et al.* 2004; vonHoldt *et al.* 2010). Despite these previous studies, it is still not known whether ancient breeds have only a few *AMY2B* copy numbers, as is the case in wolves. Moreover, the influence of regional agricultural histories on *AMY2B* expansion is unclear.

Japan is an island country located in the Pacific Ocean; the western end of Japan is close to the Korean peninsula. It is believed that rice farming was brought to Japan from the Korean peninsula along with human migration in the fourth to third century BC, with expansion then occurring to the north-east regions (Hudson 1999). Japanese native dog breeds, the Shiba and the Akita, have been classified as ancient breeds (Parker *et al.* 2004; vonHoldt *et al.* 2010). The Shiba is believed to have originated in the western part of Japan (from Shimane to Nagano prefectures), whereas the Akita is believed to have originated in the north-east region (Akita prefecture) (Tanabe 1991). Here, we compared variations in *AMY2B* copies among Shibas, Akitas, a group of various modern breeds and wolves. We also analysed a unique line of Shibas, known as the Jomon-Shiba, which originated in the eastern part of Japan. Compared to the Shiba, Jomon-Shibas have skulls with more acute orbital angles and larger teeth, resembling dog skulls excavated from archaeological sites belonging to the

Address for correspondence

K. Mogi, Companion Animal Research, School of Veterinary Medicine, Azabu University, Sagamihara, Kanagawa 252-5201, Japan.
E-mail: mogik@azabu-u.ac.jp

Accepted for publication 02 July 2015

Jomon period (14 500–300 BC) in Japan (Tanabe 1991). The breeding of Jomon-Shibas has been strictly controlled by the Japan Society for Preservation of the Natural-Monument Shiba-Dog, founded in 1959, through the use of morphological characteristics, such as a shallower stop and larger teeth when compared to the Shiba, as indexes (Fig. 1a,b).

Blood samples were collected, and DNA was extracted from wolves ($n = 12$; Table 1), Akitas ($n = 14$), Jomon-Shibas ($n = 17$), Shibas ($n = 17$) and dogs of various modern breeds ($n = 25$). Variations in *AMY2B* copy numbers were analysed by Multiplex TaqMan assays, as described by Axelsson *et al.* (2013), or standard qPCR assays using SYBR Premix Ex Taq II (TaKaRa). For the Multiplex TaqMan assays, reference assays were designed to amplify *C7orf28B*, which is present in two copies in the canine genome. The standard qPCR assays were performed on a Thermal Cycler Dice Real Time System II (TaKaRa), according to the manufacturer's protocol. Relative copy numbers were calculated according to the ΔΔCt method using *C7orf28B* as a reference gene. The results for several samples analysed using both the methods were comparable. For each sample, three replications were performed. Statistical analysis was carried out using Kruskal–Wallis tests with *post hoc* Mann–Whitney *U*-tests with Bonferroni correction (SPSS v. 19.0; SPSS Japan Inc.). One of the wolf samples was excluded as result of outlier statistics.

The average *AMY2B* copy number in wolves was low (mean ± standard deviation: 2.7 ± 0.9; Fig. 1c), consistent with previous studies (Axelsson *et al.* 2013; Freedman *et al.* 2014). However, the copy number in Akitas was significantly higher (8.1 ± 3.2) than that in wolves but lower than those of modern breeds (15.0 ± 6.7). When considered together with a recent report showing that the average *AMY2B* copy number in the Samoyed, another ancient breed, was similar to that of the Akita (Arendt *et al.* 2014), these data suggest that expansion of *AMY2B* copy numbers occurring in ancient breeds was less than that in modern breeds. We also found that the average copy number in the Shiba was similar (17.1 ± 4.2) to that of modern breeds (Fig. 1c), despite the observation that Shibas are highly divergent from modern breeds of presumed European origins (Parker *et al.* 2004). This observation may be related to the agricultural history of Japan, in which rice farming was introduced earlier to the region where the Shiba originated than to the region where the Akita originated. This is supported by another analysis focusing on other breeds (Freedman *et al.* 2014), which suggested that breeds historically bred in areas of intensive agriculture seem to have more *AMY2B* copy numbers than do breeds historically associated with nomadic hunter gatherers. This also raises the possibility that agriculture accelerated *AMY2B* expansion even after the domestication of dogs as well as during the process of domestication. Interestingly, the *AMY2B* copy number in the Jomon-Shiba was significantly lower (11.9 ± 3.6) than that in the Shiba (Fig. 1c). Because the Jomon-Shiba originated in the eastern part of Japan, these dogs may have been influenced less by agriculture than the Shiba was, as was observed with the Akita. Alternatively, selective breeding to maintain the

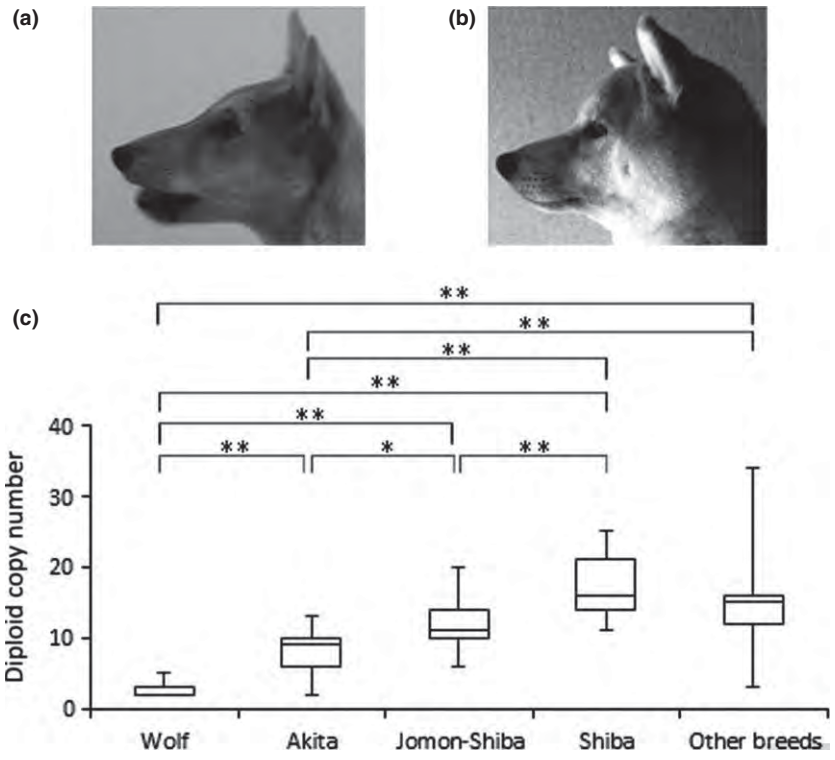

Figure 1 Facial views of Jomon-Shiba (a) and Shiba (b) from the left angle. *AMY2B* diploid copy number analysis (c). Box plot showing the diploid amylase copy number in wolves ($n = 11$), Akitas ($n = 14$), Jomon-Shibas ($n = 17$), Shibas ($n = 17$) and other breeds ($n = 25$). Significance was determined using Mann–Whitney *U*-tests with Bonferroni correction: $^{**}P < 0.01$; $^{*}P < 0.05$.

Table 1 Diploid copy numbers in individual dogs and wolves.

Wolf/dog	Diploid copy number
Wolf 1	3
Wolf 2	3
Wolf 3	5
Wolf 4	3
Wolf 5	3
Wolf 6	2
Wolf 7	2
Wolf 8	3
Wolf 9	2
Wolf 10	2
Wolf 11	2
Wolf 12	10
Akita 1	13
Akita 2	8
Akita 3	10
Akita 4	9
Akita 5	9
Akita 6	6
Akita 7	4
Akita 8	10
Akita 9	12
Akita 10	11
Akita 11	9
Akita 12	6
Akita 13	5
Akita 14	2
Jomon-Shiba 1	18
Jomon-Shiba 2	15
Jomon-Shiba 3	11
Jomon-Shiba 4	11
Jomon-Shiba 5	9
Jomon-Shiba 6	14
Jomon-Shiba 7	12
Jomon-Shiba 8	20
Jomon-Shiba 9	11
Jomon-Shiba 10	10
Jomon-Shiba 11	15
Jomon-Shiba 12	9
Jomon-Shiba 13	6
Jomon-Shiba 14	13
Jomon-Shiba 15	8
Jomon-Shiba 16	10
Jomon-Shiba 17	11
Shiba 1	21
Shiba 2	21
Shiba 3	15
Shiba 4	22
Shiba 5	12
Shiba 6	13
Shiba 7	15
Shiba 8	19
Shiba 9	17
Shiba 10	25
Shiba 11	19
Shiba 12	15
Shiba 13	23
Shiba 14	11
Shiba 15	13
Shiba 16	14
Shiba 17	16
Labrador 1	16
Labrador 2	34
Labrador 3	29
Labrador 4	10
Labrador 5	12
Labrador 6	7
Labrador 7	12
Labrador 8	15
Labrador 9	15
Labrador 10	10
Labrador 11	17
Labrador 12	8
Labrador 13	15
Labrador 14	15
Labrador 15	9
Standard Poodle 1	14
Standard Poodle 2	12
Miniature Dachshund 1	20
Shih Tzu 1	15
Bolognese 1	24
Beagle 1	3
Miniature Dachshund × Toy Poodle 1	14
Miniature Dachshund × Toy Poodle 2	20
Mongrel 1	14
Mongrel 2	16

appearance of the Jomon-Shiba may have prevented the expansion of *AMY2B* copy numbers. Further studies are required to examine these possibilities.

In conclusion, this analysis revealed that *AMY2B* expansion occurred in ancient dogs in Japan. The level of *AMY2B* expansion in Japanese native breeds was equal to or lower than that of modern breeds. Such differences may be attributed to the timing of the introduction of agriculture in the regions of origin.

Acknowledgements

This work was supported by JSPS KAKENHI (grant numbers 25118007, 25290082, and 25118005), a research project grant MEXT*-Supported Program for the Strategic Research Foundation at Private Universities, a research project grant awarded by Azabu University and the Cooperation Research Program of Wildlife Research Center, Kyoto University. We thank Mrs. Maki Kuroi and Dr. Eri Iwata for kindly providing us dog photos.

References

Arendt M., Fall T., Lindblad-Toh K. & Axelsson E. (2014) Amylase activity is associated with *AMY2B* copy numbers in dog: implications for dog domestication, diet and diabetes. *Animal Genetics* **45**, 716–22.

Axelsson E., Ratnakumar A., Arendt M., Maqbool K., Webster M.T., Perloski M., Liberg O., Arnemo J.M., Hedhammar Å. & Lindblad-Toh K. (2013) The genomic signature of dog domestication reveals adaptation to a starch-rich diet. *Nature* **495**, 360–4.

Freedman A.H., Gronau I., Schweizer R.M., Ortega-Del Vecchyo D., Han E., Silva P.M., Galaverni M., Fan Z., Marx P. & Lorente-Galdos B. (2014) Genome sequencing highlights the dynamic early history of dogs. *PLoS Genetics* **10**, e1004016.

vonHoldt B.M., Pollinger J.P., Lohmueller K.E. *et al.* (2010) Genome-wide SNP and haplotype analyses reveal a rich history underlying dog domestication. *Nature* **464**, 898–902.

Hudson M. (1999) *Ruins of Identity: Ethnogenesis in the Japanese Islands*. University of Hawaii Press, Honolulu, HI.

Parker H.G., Kim L.V., Sutter N.B., Carlson S., Lorentzen T.D., Malek T.B., Johnson G.S., DeFrance H.B., Ostrander E.A. & Kruglyak L. (2004) Genetic structure of the purebred domestic dog. *Science* **304**, 1160–4.

Tanabe Y. (1991) The origin of Japanese dogs and their association with Japanese people. *Zoological Science* **8**, 639–51.

The dilution hypothesis provides an alternative framework with which to explain observations of the apparent recalcitrance of DOC and lends a physiological meaning to the operationally defined "semi-labile" and "semi-refractory" fractions (*16*, *17*). We hypothesize that under the dilution hypothesis, very heterogeneous mixtures of labile compounds appear semirefractory, whereas increasingly less diverse DOM assemblages containing larger concentrations of some substrates will present higher microbial growth and DOC turnover rates, resulting in increasing degrees of apparent lability. The microbial generation of apparently recalcitrant material (*18*) from labile substrates in a process recently dubbed the "microbial carbon pump" (*19*) can also be explained with the dilution hypothesis. Microbial utilization of abundant, labile compounds results in hundreds of different metabolites (*20*), which are subsequently consumed down to the lowest utilizable concentration. This mechanism explains observations of relatively concentrated, labile materials being transformed into apparently recalcitrant matter through microbial consumption (*18*) but does not necessarily imply the formation of structurally recalcitrant molecules. Indeed, "recalcitrant" DOC is not defined structurally, but operationally, as the DOC pool remaining after long experimental incubations or as the fraction transported in an apparently conservative manner with the ocean circulation (*1*). Thus, the dilution hypothesis severely limits the feasibility of geoengineering efforts to enhance carbon storage in the deep ocean (*21*) by using the microbial carbon pump.

FT-ICR-MS characterization of DOC from different oceans (*13*, *14*, *22*, *23*) and also from this study (fig. S5) shows no indication of prevalent, intrinsically recalcitrant compounds accumulating in substantial amounts. Conversely, FT-ICR-MS data show that oceanic DOC is a complex mixture of minute quantities of thousands of organic molecules, which is in good agreement with the dilution hypothesis. Mean radiocarbon ages of deep oceanic DOC in the range of 4000 to 6000 years have been considered as evidence for its recalcitrant nature (*24*, *25*). However, these are average ages of a pool containing a mixture of very old molecules >12,000 years old but also featuring a large proportion of contemporary materials (*26*). Moreover, elevated radiocarbon ages only demonstrate that these old molecules are not being newly produced at any appreciable rate—because that would lower their isotopic age—but does not necessarily imply that they are structurally recalcitrant. Furthermore, it is unlikely that natural organic molecules can accumulate in the ocean in substantial concentrations and remain recalcitrant or be preserved for millennia when degradation pathways for novel synthetic pollutants evolve soon after these compounds are released in nature (*27*).

Although there might be a truly recalcitrant component in deep oceanic DOC, our results clearly show that the concentration of individual labile molecules is a major factor limiting the utilization of a substantial fraction of deep oceanic DOC. These results provide, therefore, a robust and parsimonious explanation for the long-term preservation of labile DOC into one of the largest reservoirs of organic carbon on Earth, opening a new avenue in our understanding of the global carbon cycle.

REFERENCES AND NOTES

1. D. A. Hansell, *Annu. Rev. Mar. Sci.* **5**, 421–445 (2013).
2. E. B. Kujawinski, *Annu. Rev. Mar. Sci.* **3**, 567–599 (2011).
3. H. W. Jannasch, *Limnol. Oceanogr.* **12**, 264–271 (1967).
4. H. W. Jannasch, *Global Planet. Change* **9**, 289–295 (1994).
5. R. T. Barber, *Nature* **220**, 274–275 (1968).
6. Materials and methods are available as supplementary materials on *Science* Online.
7. T. Dittmar, B. Koch, N. Hertkorn, G. Kattner, *Limnol. Oceanogr. Methods* **6**, 230–235 (2008).
8. D. L. Kirchman, X. A. G. Morán, H. Ducklow, *Nat. Rev. Microbiol.* **7**, 451–459 (2009).
9. T. Reinthaler *et al.*, *Limnol. Oceanogr.* **51**, 1262–1273 (2006).
10. A. Nebbioso, A. Piccolo, *Anal. Bioanal. Chem.* **405**, 109–124 (2013).
11. D. A. Hansell, C. A. Carlson, D. J. Repeta, R. Schlitzer, *Oceanography (Wash. D.C.)* **22**, 202–211 (2009).
12. A. Konopka, *Curr. Opin. Microbiol.* **3**, 244–247 (2000).
13. G. Kattner, M. Simon, B. Koch, in *Microbial Carbon Pump in the Ocean*, N. Jiao, F. Azam, S Sanders, Eds. (Science/AAAS, Washington, DC, 2011), pp. 60–61.
14. T. Dittmar, J. Paeng, *Nat. Geosci.* **2**, 175–179 (2009).
15. M. V. Zubkov, P. H. Burkill, J. N. Topping, *J. Plankton Res.* **29**, 79–86 (2007).
16. C. A. Carlson, H. W. Ducklow, A. F. Michaels, *Nature* **371**, 405–408 (1994).
17. J. H. Sharp *et al.*, *Estuaries Coasts* **32**, 1023–1043 (2009).
18. H. Ogawa, Y. Amagai, I. Koike, K. Kaiser, R. Benner, *Science* **292**, 917–920 (2001).
19. N. Jiao *et al.*, *Nat. Rev. Microbiol.* **8**, 593–599 (2010).
20. R. P. Maharjan, S. Seeto, T. Ferenci, *J. Bacteriol.* **189**, 2350–2358 (2007).
21. R. Stone, *Science* **328**, 1476–1477 (2010).
22. R. Flerus *et al.*, *Biogeosciences* **9**, 1935–1955 (2012).
23. O. J. Lechtenfeld *et al.*, *Geochim. Cosmochim. Acta* **126**, 321–337 (2014).
24. P. M. Williams, E. R. M. Druffel, *Nature* **330**, 246–248 (1987).
25. J. E. Bauer, in *Biogeochemistry of Marine Dissolved Organic Matter*, D. A. Hansell, C. A. Carlson, Eds. (Academic Press, San Diego, CA, 2002), pp. 405–453.
26. C. L. Follett, D. J. Repeta, D. H. Rothman, L. Xu, C. Santinelli, *Proc. Natl. Acad. Sci. U.S.A.* **111**, 16706–16711 (2014).
27. S. D. Copley, *Trends Biochem. Sci.* **25**, 261–265 (2000).

ACKNOWLEDGMENTS

This is a contribution to the Malaspina 2010 Expedition project, funded by the CONSOLIDER-Ingenio 2010 program of the from the Spanish Ministry of Economy and Competitiveness (Ref. CSD2008-00077). J.M.A. was supported by a "Ramón y Cajal" research fellowship from the Spanish Ministry of Economy and Competitiveness. E.M. was supported by a fellowship from the Junta para la Ampliación de Estudios program of CSIC. G.J.H. and R.L.H. were supported by the Austrian Science Fund (FWF) projects I486-B09 and P23234-B11 and by the European Research Council (ERC) under the European Community's Seventh Framework Programme (FP7/2007-2013)/ERC grant agreement 268595 (MEDEA project). We thank A. Dorsett for assistance with DOC analyses, participants in the Malaspina Expedition and the crews of the BIO Hespérides, and RV Pelagia and the personnel of the Marine Technology Unit of CSIC for their invaluable support. Original data sets are available online at http://digital.csic.es/handle/10261/111563. J.M.A. designed the experimental setup, carried out part of the experiments, measured prokaryotic abundance, analyzed the data, and wrote the manuscript. E.M. carried out part of the experiments and data analysis. C.M.D. designed the Malaspina 2010 Expedition, was responsible for DOC analyses, and together with G.J.H. contributed to the design of the experiments and discussion of results. R.L.H. and T.D. analyzed the FT-ICR-MS samples. All authors discussed the results and contributed to the manuscript.

SUPPLEMENTARY MATERIALS

www.sciencemag.org/content/348/6232/331/suppl/DC1
Materials and Methods
Figs. S1 to S9
Tables S1 and S2
References (*28*–*35*)

18 July 2014; accepted 4 March 2015
Published online 19 March 2015;
10.1126/science.1258955

SOCIAL EVOLUTION

Oxytocin-gaze positive loop and the coevolution of human-dog bonds

Miho Nagasawa,[1,2] Shouhei Mitsui,[1] Shiori En,[1] Nobuyo Ohtani,[1] Mitsuaki Ohta,[1] Yasuo Sakuma,[3] Tatsushi Onaka,[2] Kazutaka Mogi,[1] Takefumi Kikusui[1]*

Human-like modes of communication, including mutual gaze, in dogs may have been acquired during domestication with humans. We show that gazing behavior from dogs, but not wolves, increased urinary oxytocin concentrations in owners, which consequently facilitated owners' affiliation and increased oxytocin concentration in dogs. Further, nasally administered oxytocin increased gazing behavior in dogs, which in turn increased urinary oxytocin concentrations in owners. These findings support the existence of an interspecies oxytocin-mediated positive loop facilitated and modulated by gazing, which may have supported the coevolution of human-dog bonding by engaging common modes of communicating social attachment.

Dogs are more skillful than wolves and chimpanzees, the closest respective relatives of dogs and humans, at using human social communicative behaviors (*1*). More specifically, dogs are able to use mutual gaze as a communication tool in the context of needs of affiliative help from others (*2*). Convergent evolution between humans and dogs may have led to the acquisition of human-like communication modes in dogs, possibly as a by-product of temperament changes, such as reduced fear and aggression (*1*). This idea yields interesting implications that dogs were domesticated by coopting social cognitive systems in humans that

Corrected 12 June 2015; see full text.

are involved in social attachment. The development of human-unique social cognitive modes may depend on specific temperament and social affiliation changes and may have consequently evolved differently from those of chimpanzees and bonobos (*3*). Thus, although humans and dogs exist on different branches of the evolutionary tree, both may have independently acquired tolerance of one another because of alterations in neural systems that mediate affiliation (*1*). These alterations may be related to paedomorphic characteristics in dogs, which enabled them to retain a degree of social flexibility and tolerance similar to that of humans (*4*, *5*); therefore, it is plausible that a specific affiliative relationship developed between humans and dogs despite interspecies differences. This common social relationship change may have enabled cohabitation between humans and dogs and the eventual development of human-like modes of social communication in dogs.

Gaze plays an important role in human communication. Gaze not only facilitates the understanding of another's intention but also the establishment of affiliative relationships with others. In humans, "mutual gaze" is the most fundamental manifestation of social attachment between a mother and infant (*6*), and maternal oxytocin is positively associated with the duration of mother-to-infant gaze (*7*). Oxytocin plays a primary role in regulating social bonding between mother and infants and between sexual partners in monogamous species (*8*, *9*). Moreover, activation of the oxytocin system enhances social reward (*10*) and inhibits stress-induced activity of the hypothalamic-pituitary-adrenal axis (*11*). It has therefore been suggested that these functions may facilitate dyadic interaction, such as an oxytocin-mediated positive loop of attachment and maternal behaviors between mother and infant (*12*, *13*): Maternal nurturing activates the oxytocinergic system in the infant, thus enhancing attachment; this attachment then stimulates oxytocinergic activity in the mother, which facilitates further maternal behavior (*9*). Because the establishment of such an oxytocin-mediated positive loop requires the sharing of social cues and recognition of a particular partner, the study of oxytocin-mediated bonding has been restricted to intraspecies relationships.

The human-dog relationship is exceptional because it is an interspecies form of attachment. Dogs can discriminate individual humans (*14*, *15*). Furthermore, dogs show distinctly different behavior toward caregivers as compared with hand-raised wolves (*14*), and interaction with dogs confers a social buffering effect to humans. Likewise, dogs also receive more social buffering effects from interacting with humans than from conspecifics (*16*). Tactile interaction between humans and dogs increases peripheral oxytocin concentrations in both humans and dogs (*17*, *18*). Further, social interaction initiated by a dog's gaze increases urinary oxytocin in the owner, whereas obstruction of the dog's gaze inhibits this increase (*19*). These results demonstrate that the acquisition of human-like social communication improves the quality of human-dog affiliative interactions, leading to the establishment of a human-dog bond that is similar to a mother-infant relationship. We hypothesized that an oxytocin-mediated positive loop, which originated in the intraspecies exchange of social affiliation cues, acts on both humans and dogs, is coevolved in humans and dogs, and facilitates human-dog bonding. However, it is not known whether an oxytocin-mediated positive loop exists between humans and dogs as has been postulated between mother and infants, and whether this positive loop emerged during domestication.

We tested the hypothesis that an oxytocin-mediated positive loop exists between humans and dogs that is mediated by gaze. First, we examined whether a dog's gazing behavior affected urinary oxytocin concentrations in dogs and owners during a 30-min interaction. We also conducted the same experiment using hand-raised wolves, in order to determine whether this positive loop has been acquired by coevolution with humans. Second, we determined whether manipulating oxytocin in dogs through intranasal administration would enhance their gazing behavior toward their owners and whether this gazing behavior affected oxytocin concentrations in owners.

In experiment 1, urine was collected from the dogs and owners right before and 30 min after the interaction, and the duration of the following behaviors was measured during the interaction: "dog's gaze at owner (dog-to-owner gaze)," "owner's talking to dog (dog-talking)," and "owner's touching of dog (dog-touching)." Dog owners were assigned to one of two groups: long gaze or short gaze (fig. S1). Wolves were tested with the same procedure and were compared with the two dog groups. Dogs in the long-gaze group gazed most at their owners among the three groups. In contrast, wolves rarely showed mutual gazing to their owners (Fig. 1A and fig. S2). After a 30-min interaction, only owners in the long-gaze group showed a significant increase in urinary oxytocin concentrations and the highest change ratio of oxytocin (Fig. 1, B and C). The oxytocin change ratio in owners correlated significantly with that of dogs, the duration of dog-to-owner gaze, and dog-touching. Moreover, the duration of the dog-to-owner gaze correlated with dog-talking and dog-touching (table S2A); however, through multiple linear regression analysis, we found that only the duration of dog-to-owner gaze significantly explained the oxytocin change ratio in owners. The duration of dog-touching showed a trend toward explaining oxytocin concentrations in owners (Table 1A). Similarly, a significantly higher oxytocin change ratio was observed in the dogs of the long-gaze group than in those of the short-gaze group (Fig. 1, D and E). The duration of dog-to-owner gaze also significantly explained the oxytocin change ratio in dogs, and the duration of dog-touching showed a trend toward explaining oxytocin concentrations in dogs by multiple linear regression analysis (Table 1A). In wolves, in contrast, the duration of wolf-to-owner gaze did

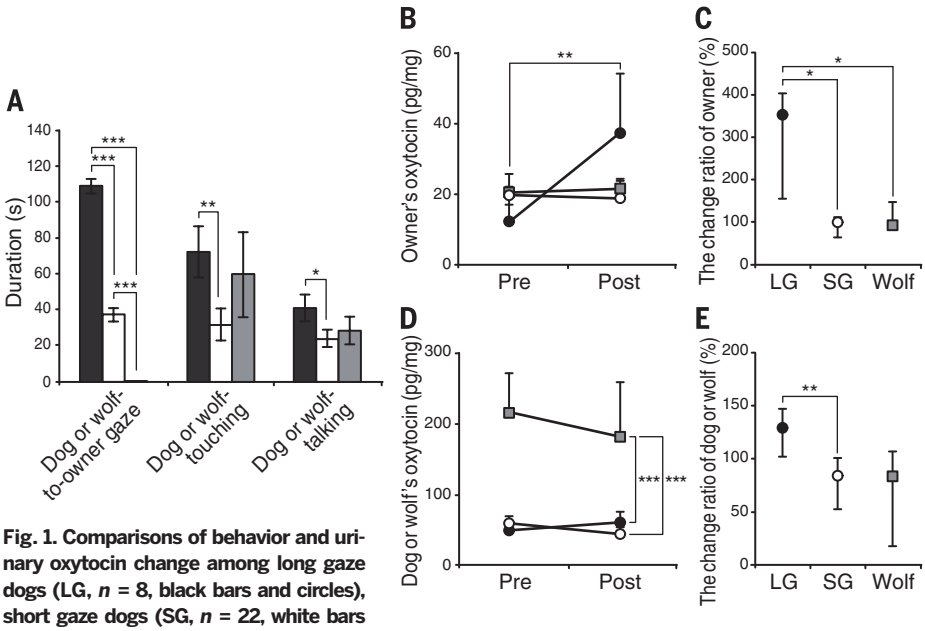

Fig. 1. Comparisons of behavior and urinary oxytocin change among long gaze dogs (LG, *n* = 8, black bars and circles), short gaze dogs (SG, *n* = 22, white bars and circles), and wolves (wolf, *n* = 11, gray bars and square). (**A**) Behavior during the first 5-min interaction. (**B**) and (**D**) Changes of urinary oxytocin concentrations after a 30-min interaction. Urinary oxytocin concentrations in owners (B) and dogs or wolves (D) collected before and after a 30-min interaction are shown. (**C**) and (**E**) Comparisons of the change ratio of urinary oxytocin among LG, SG, and wolf for owners (C) and dogs or wolves (E). The results of (A), (B), and (D) are expressed as mean ± SE. (C) and (E) reflect median ± quartile. ***$P < 0.001$, **$P < 0.01$, *$P < 0.05$.

[1]Department of Animal Science and Biotechnology, Azabu University, Sagamihara, Kanagawa, Japan. [2]Department of Physiology, Jichi Medical University, Shimotsuke, Tochigi, Japan. [3]University of Tokyo Health Sciences, Tama, Tokyo, Japan.
***Corresponding author. E-mail: kikusui@azabu-u.ac.jp**

not correlate with the oxytocin change ratio in either owners or wolves, and wolf-to-owner gaze did not explain the oxytocin change ratio in owners and wolves (tables S2B and S3). These results suggest that wolves do not use mutual gaze as a form of social communication with humans, which might be expected because wolves tend to use eye contact as a threat among conspecifics (*20*) and avoid human eye contact (*21*). Thus, dog-to-owner gaze as a form of social communications probably evolved during domestication and triggers oxytocin release in the owner, facilitating mutual interaction and affiliative communication and consequently activation of oxytocin systems in both humans and dogs in a positive loop.

In experiment 2, we evaluated the direct evidence of whether oxytocin administration enhanced dog gazing behavior and the subsequent increase in urinary oxytocin concentration in owners. This experiment involved 27 volunteers and their dogs, and participants unfamiliar to the dogs. A solution containing oxytocin or saline was administered to the dog and the dog then entered the experimental room, where the owner and two unfamiliar people were seated (fig. S4). Human behavior toward dogs was restricted to prevent the influence of extraneous stimuli on dog behavior and/or urinary oxytocin concentration. They were forbidden to talk to each other or to touch the dog voluntarily. Urine samples from the owner and the dog were collected before and after the interaction and were later compared. The total amount of time that the dog gazed at, touched, and was close to the owner and the unfamiliar participants was also measured.

Oxytocin administration to dogs significantly increased the duration that the dog gazed at the owner in female dogs but not male dogs (Fig. 2A). Further, urinary oxytocin concentration significantly increased in the owners of female dogs that received oxytocin versus saline, even though oxytocin was not administered to the owners (Fig. 2D). No significant effect of oxytocin administration was observed in the other measured dog behaviors (Fig. 2, B and C). Furthermore, multiple linear regression analysis revealed that the duration of gazing behavior significantly explained the oxytocin change ratio in owners (Table 1B). Thus, oxytocin administration enhances the gazing behavior of female dogs, which stimulates oxytocin secretion in their owners. Conversely, when interaction from humans was limited, no significant difference in urinary oxytocin concentrations in dogs was observed after the interaction in either the oxytocin or the saline conditions, and no significant oxytocin change ratio was found in dogs (Fig. 2, F and G). These results thus suggest that, although oxytocin administration may enhance dog gazing behavior and lead to an oxytocin increase in owners, limited owner-to-dog interaction may prevent the increased oxytocin secretion in dogs by breaking the oxytocin-mediated positive loop.

Table 1. Results of multiple linear regression analysis of oxytocin change ratio and behavioral variables in owners and dogs. *$P < 0.05$, †$P < 0.1$; R, multiple correlation coefficient; **, $P < 0.01$.

(A) Experiment 1

	Oxytocin change ratio	
	Owners	**Dogs**
Owner talking to dog	−0.107	−0.264
Owner touching dog	0.321†	0.335†
Dog-to-owner gaze	0.458*	0.388*
R	0.619	0.575
Adjusted R^2	0.306	0.247
P	0.008	0.020

(B) Experiment 2

	Oxytocin change ratio	
	Owners	**Dogs**
Dog's sex	0.090	0.138
Oxytocin administration	0.202	0.234
Dog-to-owner gaze	0.458**	0.030
Dog touching owner	−0.040	−0.054
Proximity to owner	0.048	−0.023
R	0.574	0.275
Adjusted R^2	0.248	−0.046
P	0.005	0.686

Sex: Female = 1, male = 0; oxytocin administration: oxytocin = 1, saline = 0.

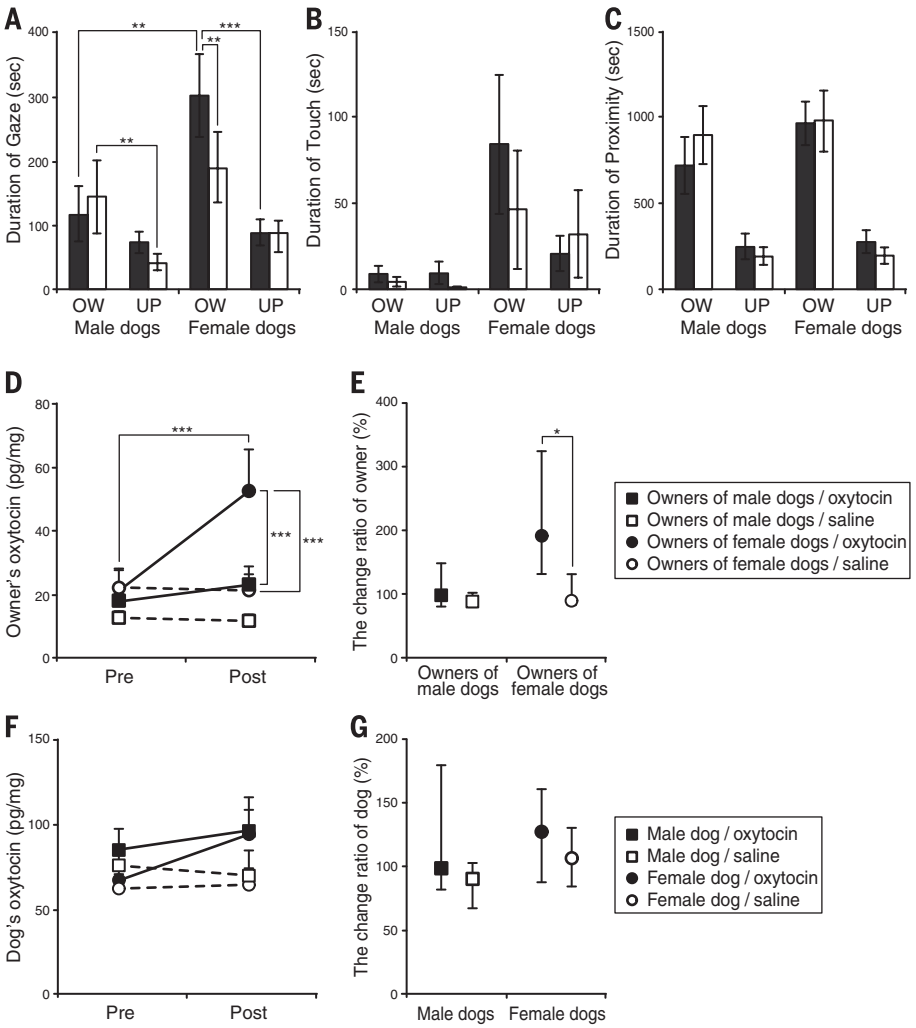

Fig. 2. Comparisons of behavior and urinary oxytocin between oxytocin and saline treatment conditions. (A) to (C) The effects of oxytocin administration on dog behaviors. Panels show the mean duration of dogs' gaze at participants (**A**), touching participants (**B**), and time spent in the proximity of less than 1 m from each participant (**C**). Black and white bars indicate, respectively, oxytocin- and saline treatment conditions. OW, owner; UP, unfamiliar person. (D) to (G) Change in urinary oxytocin concentrations after a 30-min interaction after oxytocin or saline administration. Urinary oxytocin concentrations of owners (**D**) and dogs (**F**) before and after a 30-min interaction are shown for oxytocin and saline groups. The change ratio of urinary oxytocin in owners (**E**) and dogs (**G**) is compared between male and female dogs. ***$P < 0.001$, **$P < 0.01$, *$P < 0.05$. The results of (A) to (D) and (F) are expressed as mean ± SE. (E) and (G) reflect median ± quartile.

Corrected 12 June 2015; see full text.

Interestingly, oxytocin administration only increased mutual gaze duration in female dogs, whereas sex differences were not observed in experiment 1, which did not include unfamiliar individuals. Sex differences in the effects of intranasal oxytocin have been reported in humans as well (*22*), and it is possible that females are more sensitive to the affiliative effects of oxytocin or that exogenous oxytocin may also be activating the vasopressin receptor system preferentially in males. Oxytocin and the structurally related vasopressin affect social bonding and aggression in sexually dimorphic manners in monogamous voles (*8*, *9*), and oxytocin possibly increases aggression (*23*, *24*). Therefore, the results of experiment 2 may indicate that male dogs were attending to both their owners and to unfamiliar people as a form of vigilance. The current study, despite its small sample size, implies a complicated role for oxytocin in social roles and contexts in dogs.

In human infants, mutual gaze represents healthy attachment behavior (*25*). Human functional magnetic resonance imaging studies show that the presentation of human and canine family members' faces activated the anterior cingulate cortex, a region strongly acted upon by oxytocin systems (*26*). Urinary oxytocin variation in dog owners is highly correlated with the frequency of behavioral exchanges initiated by the dogs' gaze (*19*). These results suggest that humans may feel affection for their companion dogs similar to that felt toward human family members and that dog-associated visual stimuli, such as eye-gaze contact, from their dogs activate oxytocin systems. Thus, during dog domestication, neural systems implementing gaze communications evolved that activate the humans' oxytocin attachment system, as did gaze-mediated oxytocin release, resulting in an interspecies oxytocin-mediated positive loop to facilitate human-dog bonding. This system is not present in the closest living relative of the domesticated dog.

In the present study, urinary oxytocin concentrations in owners and dogs were affected by the dog's gaze and the duration of dog-touching. In contrast, mutual gaze between hand-raised wolves and their owners was not detected, nor was there an increase of urinary oxytocin in either wolves or their owners after a 30-min experimental interaction (experiment 1). Moreover, the nasal administration of oxytocin increased the total amount of time that female dogs gazed at their owners and, in turn, urinary oxytocin concentrations in owners (experiment 2). We examined the association between our results and early-life experience with humans in dogs and wolves in order to test the possibility that our results were due to differences in early-life experience with humans. The results did not indicate a significant association between the animals' early-life experiences with humans and the findings of the current study (see the supplementary methods). Moreover, there were no significant differences between dogs in the long-gaze group and wolves in either the duration of dog/wolf-touching and dog/wolf-talking, suggesting that the shorter gaze of the wolves was not due to an unstable relationship. These results support the existence of a self-perpetuating oxytocin-mediated positive loop in human-dog relationships that is similar to that of human mother-infant relations. Human-dog interaction by dogs' human-like gazing behavior brought on social rewarding effects due to oxytocin release in both humans and dogs and followed the deepening of mutual relationships, which led to interspecies bonding.

REFERENCES AND NOTES

1. B. Hare, M. Tomasello, *Trends Cogn. Sci.* **9**, 439–444 (2005).
2. A. Miklósi *et al.*, *Curr. Biol.* **13**, 763–766 (2003).
3. A. P. Melis, B. Hare, M. Tomasello, *Science* **311**, 1297–1300 (2006).
4. R. Coppinger *et al.*, *Ethology* **75**, 89–108 (1987).
5. M. Somel *et al.*, *Proc. Natl. Acad. Sci. U.S.A.* **106**, 5743–5748 (2009).
6. S. Dickstein, R. A. Thompson, D. Estes, C. Malkin, M. E. Lamb, *Infant Behav. Dev.* **7**, 507–516 (1984).
7. S. Kim, P. Fonagy, O. Koos, K. Dorsett, L. Strathearn, *Brain Res.* **1580**, 133–142 (2014).
8. L. J. Young, Z. Wang, *Nat. Neurosci.* **7**, 1048–1054 (2004).
9. H. E. Ross, L. J. Young, *Front. Neuroendocrinol.* **30**, 534–547 (2009).
10. G. Dölen, A. Darvishzadeh, K. W. Huang, R. C. Malenka, *Nature* **501**, 179–184 (2013).
11. I. D. Neumann, *Prog. Brain Res.* **139**, 147–162 (2002).
12. M. Nagasawa, S. Okabe, K. Mogi, T. Kikusui, *Front. Hum. Neurosci.* **6**, 31 (2012).
13. J. K. Rilling, L. J. Young, *Science* **345**, 771–776 (2014).
14. J. Topál *et al.*, *Anim. Behav.* **70**, 1367–1375 (2005).
15. M. Nagasawa, K. Mogi, T. Kikusui, *Jpn. Psychol. Res.* **51**, 209–221 (2009).
16. D. S. Tuber, S. Sanders, M. B. Hennessy, J. A. Miller, *J. Comp. Psychol.* **110**, 103–108 (1996).
17. J. S. Odendaal, R. A. Meintjes, *Vet. J.* **165**, 296–301 (2003).
18. S. Mitsui *et al.*, *Horm. Behav.* **60**, 239–243 (2011).
19. M. Nagasawa, T. Kikusui, T. Onaka, M. Ohta, *Horm. Behav.* **55**, 434–441 (2009).
20. M. W. Fox, *The Soul of the Wolf* (Burford Books, New York, 1997).
21. M. Gácsi, J. Vas, J. Topál, Á. Miklósi, *Appl. Anim. Behav. Sci.* **145**, 109–122 (2013).
22. J. K. Rilling *et al.*, *Psychoneuroendocrinology* **39**, 237–248 (2014).
23. I. D. Neumann, *J. Neuroendocrinol.* **20**, 858–865 (2008).
24. C. K. De Dreu *et al.*, *Science* **328**, 1408–1411 (2010).
25. E. Meins, *Security of Attachment and the Social Development of Cognition* (Psychology Press, Philadelphia, 1997).
26. J. Shinozaki, T. Hanakawa, H. Fukuyama, *Neuroreport* **18**, 993–997 (2007).

ACKNOWLEDGMENTS

This study was supported in part by the Grant-in-Aid for Scientific Research on Innovative Areas (No. 4501) from the Japan Society for the Promotion of Science, in Japan. We thank all human and canine participants, Howlin' Ks Nature School, U.S. Kennel, R. Ooyama and N. Yoshida-Tsuchihashi from Azabu University, and Drs. Kato and Takeda from University of Tokyo Health Sciences. We are also grateful to Cody and Charley for their significant contributions. The analyzed data are included in the supplementary materials.

SUPPLEMENTARY MATERIALS

www.sciencemag.org/content/348/6232/333/suppl/DC1
Materials and Methods
Figs. S1 to S5
Tables S1 to S4
References (*27* –*30*)
Movies S1 to S3
Data Tables 1 and 2

9 September 2014; accepted 3 March 2015
10.1126/science.1261022

PLANT ECOLOGY

Anthropogenic environmental changes affect ecosystem stability via biodiversity

Yann Hautier,[1,2,3]* David Tilman,[2,4] Forest Isbell,[2] Eric W. Seabloom,[2] Elizabeth T. Borer,[2] Peter B. Reich[5,6]

Human-driven environmental changes may simultaneously affect the biodiversity, productivity, and stability of Earth's ecosystems, but there is no consensus on the causal relationships linking these variables. Data from 12 multiyear experiments that manipulate important anthropogenic drivers, including plant diversity, nitrogen, carbon dioxide, fire, herbivory, and water, show that each driver influences ecosystem productivity. However, the stability of ecosystem productivity is only changed by those drivers that alter biodiversity, with a given decrease in plant species numbers leading to a quantitatively similar decrease in ecosystem stability regardless of which driver caused the biodiversity loss. These results suggest that changes in biodiversity caused by drivers of environmental change may be a major factor determining how global environmental changes affect ecosystem stability.

Human domination of Earth's ecosystems, especially conversion of about half of the Earth's ice-free terrestrial ecosystems into cropland and pasture, is simplifying ecosystems via the local loss of biodiversity (*1*, *2*). Other major global anthropogenic changes include nutrient eutrophication, fire suppression and elevated fire frequencies, predator decimation, climate warming, and drought, which likely affect many aspects of ecosystem functioning, especially ecosystem productivity, stability, and biodiversity (*1*, *3*–*7*). However, to date there has been little evidence showing whether or how these three ecosystem responses may be mechanistically

SHORT COMMUNICATION

Communicative & Integrative Biology 8:3, e1017157; May/June 2015; Published with license by Taylor & Francis Group, LLC

Intranasal administration of oxytocin promotes social play in domestic dogs

Teresa Romero[1,2,*], Miho Nagasawa[3], Kazutaka Mogi[3], Toshikazu Hasegawa[1], and Takefumi Kikusui[3]

[1]Department of Cognitive and Behavioral Sciences; Graduate School of Arts and Science; The University of Tokyo; Tokyo, Japan; [2]Japanese Society for the Promotion of Sciences; Tokyo, Japan; [3]Department of Animal Science and Biotechnology; Azabu University; Kanagawa, Japan

Keywords: companion animals, domestic dogs, oxytocin, social play, social bonds

In a recent paper,[1] we examined whether oxytocin in the domestic dog modulates the maintenance of close social bonds in non-reproductive contexts. We found that exogenous oxytocin promotes positive social behaviors not only toward conspecifics, but also toward human partners. Here we examined in further detail the effect that oxytocin manipulation has on social play. When sprayed with oxytocin, subjects initiated play sessions more often and played for longer periods of time than when sprayed with saline. Furthermore, after oxytocin nasal intake dogs displayed play signals more often than after saline administration, suggesting that oxytocin enhances dogs' play motivation. To our knowledge, this study provides the first evidence that oxytocin promotes social play in the domestic dog. We use these results to hypothesize on the potential therapeutic use of oxytocin for promoting social behaviors and treating social deficits in the domestic dog.

Over the past several decades, extensive animal research has shown that the hypothalamic neuropeptide oxytocin plays an important role in the regulation of several behaviors associated with sociality, such as sexual behavior, pair-bonding, parental care, peer recognition, and social memory (for reviews see refs.[2,3]). More recent studies in humans have revealed that oxytocin is also involved in aspects of social cognition including social perception, emotion recognition, sensibility to the experiences of others, and pro-social behaviors (for reviews see refs.[4,5]).

Building on these findings, researchers have suggested that the manipulation of the oxytocin system may be used as a tool for improving socio-cognitive abilities in individuals with social deficit disorders (e.g. autism spectrum disorder, social anxiety disorder, and borderline personality disorder; for reviews see refs.[6,7]). In fact, in the last decade the effect of administered oxytocin has been tested in clinical populations, with several of these studies reporting beneficial effects of oxytocin on social attention and emotion recognition in autistic individuals, and a reduction of social anxiety in patients with social phobia and borderline personality disorder (e.g., refs.[8-11]). While at this point much remains unknown about the lasting effects of these benefits and the extent to which personality and personal history mitigate these beneficial effects, such findings are clearly grounds for optimism about the therapeutic potential of oxytocin.

A similar therapeutic use of oxytocin could be relevant to animal health. This clinical approach could be particularly interesting for companion animals showing behavioral problems related to social deficits. Each year, millions of dogs and cats arrive in animal shelters after abandonment, abuse, or relinquishment by their previous caregivers. The most widely reported reasons for relinquishment of dogs in USA are behavioral problems due to lack of proper socialization and habituation (i.e. fear and aggression directed to strangers or other dogs).[12,13] Although in many countries there are approved drugs for the treatment of anxiety related disorders in domestic animals,[14] to date there is no drug for the treatment of social deficits. Thus, the development of pharmacotherapies that promote social integration in companion animals may be helpful in the treatment of selected behavior problems.

In a recent paper,[1] we showed that nasal intake of oxytocin promotes social bonding in domestic dogs. A total of 16 adult dogs from different breeds participated as subjects in a randomized placebo-controlled experiment (females = 8; male = 8; mean age 6.1 y (SEM = 0.7)). Each dog received a nasal spray of 100μl of oxytocin (40 IU, Peptide institute, Japan) or 100μl of saline solution, depending on the testing condition. All subjects received both conditions and each condition was carried out on different days. After spray intake, dogs stay in the experimental room (11.5 × 6.5m) with their owners and a familiar dog partner, and their behaviors were video recorded for 60 minutes. Owners were instructed to sit quietly in the experimental room and not to actively interact with their dogs; while dogs could move freely in the room (for further details, see[1]). We found that

*Correspondence to: Teresa Romero; Email: tromero@darwin.c.u-tokyo.ac.jp
Submitted: 11/13/2014; Revised: 01/06/2015; Accepted: 01/09/2015
http://dx.doi.org/10.1080/19420889.2015.1017157

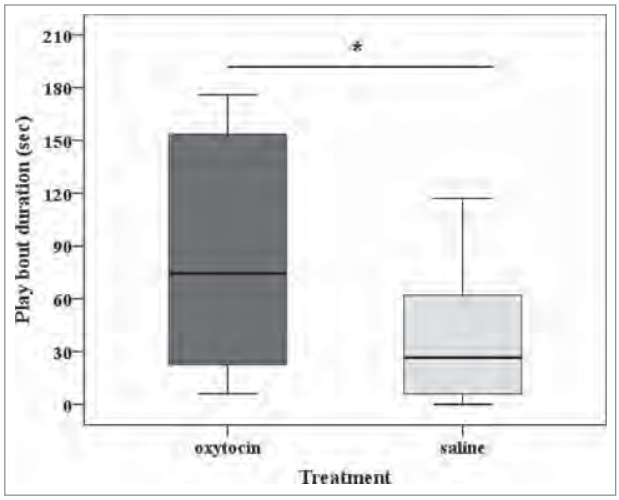

Figure 1. Duration of play bouts during the oxytocin and the saline conditions. The box plots represent the median and upper and lower quartiles; and the whiskers indicate the values within 1.5 times the interquartile range. *$P < 0.05$

oxytocin caused dogs to engage in higher levels of affiliation and approach with their dog partners, suggesting that the experimental intranasal administration of oxytocin in dogs promotes affiliative motivation and facilitates bond formation and maintenance.

Here, we analyze in more detail the episodes of social play that took play during the experimental sessions in order to address the question of whether intranasal administration of oxytocin enhances social play in dogs. Play is a highly plastic and versatile behavior that generally occurs when animals are free from environmental and social stressors.[15] Although play is characteristic of early life stages, in many species social play continues into adulthood (e.g. rodents,[16] canids,[17,18] primates[19,20]). Social play is thought to help animals to develop social and emotional flexibility, conflict resolution skills and appropriate reactions to unexpected situations.[15,21-24] It could also serve to assess social relationships and/or increase social affinity between individuals.[19,25,26] Social play is also associated with immediate benefits for the animals. Recent evidence shows that through play animals reduce tension around stressful situations,[27] or turn a stranger into a familiar individual.[28] Furthermore, play is frequently used as part of therapies to correct behavioral problems in dogs.[29] Thus, the combination of behavioral interventions with pharmacotherapies that promote affiliation in general and play in particular might be a potential fruitful strategy for the treatment of behavior problems in companion animals.

In the present study, all dogs that participated as partners had a friendly relationship with the subjects. Thus, we did not observe any agonistic behavior during the experimental sessions and none of the play sessions resembled or escalated into aggression. A play session started when an individual directed a play signal (including play bow, face paw, and exaggerated approaches and retreats[18,21,30]) or any playful behavior (including nipping, inhibited bite, play-chasing, mounting, play-fighting, and play-tackling[18,21,30]) toward the partner, and ended when their activity ceased or one of the subjects moved away (>1 m). A new play session was recorded if at least 5 seconds elapsed between the end of the first bout and the start of the new bout. Only play sessions that lasted more than 5 seconds were included in the analysis (N = 74). All subjects but one were involved in at least one social play session (mean duration in seconds = 161.3 ± 52.6 SE), and only one subject engaged in solitary play. Thus, solitary play sessions were excluded from the analyses. The type of treatment dogs were administered with did not affect how often subjects were involved in social play (Wilcoxon signed rank test: $z = -1.749$, $N = 15$, $p = 0.08$), nor how often they engaged in play after receiving a play invitation ($z = 0.479$, $N = 15$, $p = 0.6384$). However, after oxytocin nasal spray intake, dogs initiated play sessions significantly more often than after saline treatment ($z = -1.997$, $N = 15$, $p = 0.046$). We then examined the total amount of time dogs spent playing with their partners. We found that oxytocin treatment was associated with longer play sessions ($z = -2.040$, $N = 15$, $p = 0.041$, **Fig. 1**).

Given that social play is an interaction that requires the active involvement of both partners, the total time that 2 individuals play together depends on both individuals' motivation. Thus, we evaluated the subject's relative role in maintaining the play session by examining the production of play signals that are known to promote and/or facilitate play interactions.[18,31] We did not find any effect of treatment type on the frequency of play signals received ($z = -0.255$, $N = 15$, $p = 0.799$, **Fig. 2A**). However, after oxytocin nasal intake dogs directed play signals to their play-mates significantly more often than after saline treatment ($z = -2.090$, $N = 15$, $p = 0.037$, **Fig. 2B**). These findings suggest that the experimental administration of oxytocin had positive effects on dogs' motivation to interact in a playful way with conspecifics. Play has long been identified as a potential welfare indicator,[15] a facilitator of social-emotional learning,[22] and an implicitly rewarding behavior.[32] Thus, increasing

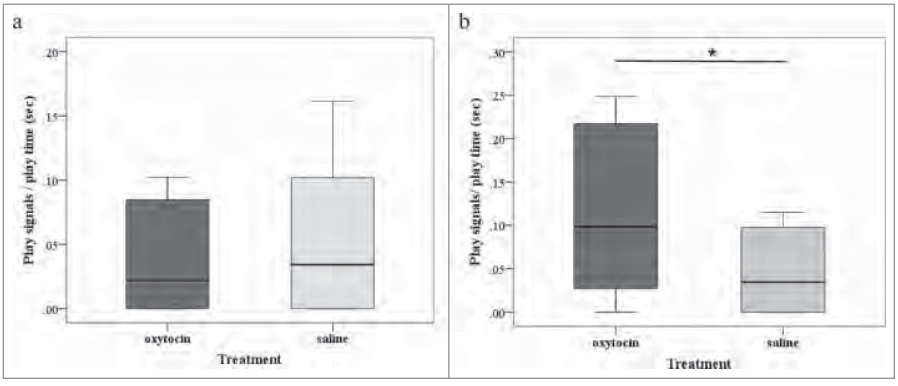

Figure 2. Frequency of play signals received (**A**) and given (**B**) during the oxytocin and the saline experimental conditions. The box plots represent the median and the upper and lower quartiles; and the whiskers indicate the values within 1.5 times the interquartile range. *$P < 0.05$.

play interactions could be beneficial for dogs. Previous results[1] have provided behavioral evidence that exogenous oxytocin promotes positive social behaviors in the domestic dog. The present study extends this data showing that oxytocin manipulation also enhances play motivation, suggesting that this pharmacological intervention may be used to help manage a range of animal behavioral problems. The reader should note, however, that the positive effects of oxytocin on social approach, general affiliation[1] and play (this study) were observed in healthy dog participants. Hence, a key question is whether administration of oxytocin can influence social behaviors in animals with behavioral disorders. Caution is therefore warranted in the interpretation of our results, and further studies on whether and how oxytocin influences social interactions in clinic populations are clearly necessary.

In summary, this study provides the first evidence that administration of oxytocin increases dogs' motivation to play with conspecifics and refines our knowledge about the behavioral effects of exogenous oxytocin in dogs. A more thorough understanding of this peptide and its behavioral consequences in healthy individuals may help to design pharmacological interventions aimed at promoting social behavior in companion animals whose social skills have been compromised, such as dogs with poor socialization at earlier life stages. Further investigation is clearly necessary to further test oxytocin's behavioral effects on clinical populations.

Disclosure of Potential Conflicts of Interest

No potential conflicts of interest were disclosed.

Acknowledgments

We thank the dogs and their owners for their participation in the study. We are also grateful to Darby Proctor for useful comments on a previous version of the manuscript.

Funding

The present study was approved by the Ethics Committee of Azabu University (Japan) (No. 130304–2). This research was supported by the JSPS Research Fellowships for Foreign Researchers (No. P10311) and the MEXT Grant-in-aid for Scientific Research (No. 26380981) to T. R., the MEXT Grant-in-aid for Challenging Exploratory Research (No. 23650132) to T. H., and the Grant-in-Aid for Scientific Research on Innovative Areas (No. 4501) to T.K. and T. H.

References

1. Romero T, Nagasawa M, Mogi K, Hasegawa T, Kikusui T. Oxytocin promotes social bonding in dogs. Proc Natl Acad Sci USA 2014; 111:9085-90; PMID:24927552; http://dx.doi.org/10.1073/pnas.1322868111
2. Ross HE, Young LJ. Oxytocin and the neural mechanisms regulating social cognition and affiliative behavior. Front Neuroendocrinol 2009; 30:534-47; PMID:19481567; http://dx.doi.org/10.1016/j.yfrne.2009.05.004
3. Insel TR. The challenge of translation in social neuroscience: a review of oxytocin, vasopressin, and affiliative behavior. Neuron 2010; 65:768-79; PMID:20346754; http://dx.doi.org/10.1016/j.neuron.2010.03.005
4. Bartz JA, Zaki J, Bolger N, Ochsner KN. Social effects of oxytocin in humans: context and person matter. Trends Cogn Sci 2010; 15:301-9.
5. Heinrichs M, von Dawans B, Domes G. Oxytocin, vasopressin, and human social behavior. Front Neuroendocrinol 2009; 30:548-57; PMID:19505497; http://dx.doi.org/10.1016/j.yfrne.2009.05.005
6. Modi ME, Young LJ. The oxytocin system in drug discovery for autism: Animal models and novel therapeutic strategies. Horm Behav 2012; 61:340-50; PMID:22206823; http://dx.doi.org/10.1016/j.yhbeh.2011.12.010
7. Bakermans-Kranenburg MJ, van Ijzendoorn MH. Sniffing around oxytocin: review and meta-analyses of trials in healthy and clinical groups with implications for pharmacotherapy. Transl Psych 2013; 3:e258; http://dx.doi.org/10.1038/tp.2013.34
8. Andari E, Duhamel J-R, Zalla T, Herbrecht E, Leboyer M, Sirigu A. Promoting social behavior with oxytocin in high-functioning autism spectrum disorders. Proc Natl Acad Sci USA 2010; 107:4389-94; PMID:20160081; http://dx.doi.org/10.1073/pnas.0910249107
9. Guastella AJ, Einfeld SL, Gray KM, Rinehart NJ, Tonge BJ, Lambert TJ, Hickie IB. Intranasal oxytocin improves emotion recognition for youth with autism spectrum disorders. Biol Psych 2010; 67:692-4; http://dx.doi.org/10.1016/j.biopsych.2009.09.020
10. Tachibana M, Kagitani-Shimono K, Mohri I, Yamamoto T, Sanefuji W, Nakamura A, Oishi M, Kimura T, Onaka T, Ozono K, Taniike M. Long-term administration of intranasal oxytocin is a safe and promising therapy for early adolescent boys with autism spectrum disorders. J Child Adolesc Psychopharmacol 2013; 23:123-7; PMID:23480321; http://dx.doi.org/10.1089/cap.2012.0048
11. Stavropoulos KK, J CL. Research review: Social motivation and oxytocin in autism—implications for join attention development and intervention. J Child Psychol Psych 2013; 54:603-18; http://dx.doi.org/10.1111/jcpp.12061
12. Salman MD, Hutchison J, Ruch-Gallie R, Kogan L, New JCJ, Kass PH, Scarlett JM. Behavioral reasons for relinquishment of dogs and cats to 12 shelters. J Appl Anim Welf Sci 2010; 3:93-106; http://dx.doi.org/10.1207/S15327604JAWS0302_2
13. Duffy DL, Kruger KA, Serpell JA. Evaluation of a behavioral assessment tool for dogs relinquished to shelters. Prev Vet Med 2014; PMID:25457136
14. Simpson BS, Papich MG. Pharmacologic management in veterinary behavioral medicine. Veterinary Clinics of North America: Small Animal Practice 2003; 33:365-404; http://dx.doi.org/10.1016/S0195-5616(02)00130-4
15. Held SDE, Spinka M. Animal play and animal welfare. Anim Behav 2011; 81:891-9; http://dx.doi.org/10.1016/j.anbehav.2011.01.007
16. Pellis SM. Sex-differences in play fighting revisited: traditional and nontraditional mechanisms for sexual differentiation in rats. Arch Sex Behav 2002; 31:11-20; http://dx.doi.org/10.1023/A:1014070916047
17. Bauer EB, Smuts BB. Cooperation and competition during dyadic play in domestic dogs, *Canis familiaris*. Anim Behav 2007; 73:489-99; http://dx.doi.org/10.1016/j.anbehav.2006.09.006
18. Horowitz L. Attention to attention in domestic dog (*Canis familiaris*) dyadic play. Anim Cogn 2009; 12:107-18; PMID:18679727; http://dx.doi.org/10.1007/s10071-008-0175-y
19. Pellis SM, Iwaniuk AN. Adult-adult play in primates: comparative analyses of its origin, distribution and evolution. Ethology 2000; 106:1083-104; http://dx.doi.org/10.1046/j.1439-0310.2000.00627.x
20. Palagi E, Paoli T. Play in adult bonobos (*Pan paniscus*): modality and potential meaning. Am J Phys Anthropol 2007; 134:219-25; PMID:17596855; http://dx.doi.org/10.1002/ajpa.20657
21. Bekoff M. Social play behavior. Bioscience 1984; 34:228-33; http://dx.doi.org/10.2307/1309460
22. Spinka M, Newberry RC, Bekoff M. Mammalian play: training for the unexpected. Q Rev Biol 2011; 76:141-68; http://dx.doi.org/10.1086/393866
23. Smith EFS. Does play matter: functional and evolutionary aspects of animal and human play. Behav Brain Sci 1982; 5:139-55; http://dx.doi.org/10.1017/S0140525X0001092X
24. Palagi E, Cordoni G, Borgognini Tarli TS. Immediate and delayed benefits of play behaviour: new evidence from chimpanzees (*Pan troglodytes*). Ethology 2004; 110:949-62; http://dx.doi.org/10.1111/j.1439-0310.2004.01035.x
25. Palagi E. Social play in bonobos (*Pan paniscus*) and chimpanzees (*Pan troglodytes*): Implications for natural social systems and interindividual relationships. Am J Phys Anthropol 2006; 129:418-26; PMID:16323189; http://dx.doi.org/10.1002/ajpa.20289
26. Ciani F, Dall'Olio S, Stanyon R, Palagi E. Social tolerance and adult play in macaque societies: a comparison with different human cultures. Anim Behav 2012; 84:1313-22; http://dx.doi.org/10.1016/j.anbehav.2012.09.002
27. Palagi E, Paoli T, Tarli SB. Short-term benefits of play behavior and conflict prevention in *Pan paniscus*. Int J Primatol 2006; 27:1257-70; http://dx.doi.org/10.1007/s10764-006-9071-y
28. Antonacci D, Norscia I, Palagi E. Stranger to familiar: wild strepsirhines manage xenophobia by playing. PLoS ONE 2010; 5:e13218; PMID:20949052; http://dx.doi.org/10.1371/journal.pone.0013218
29. Landsberg GM, Hunthausen WL, Ackerman LJ. Behavior problems of the dog and cat. Elsevier Health Sciences, 2012.
30. Abrantes R. Dog language. Napierville, Illinois: Wakan Tanka Publishers, 1997.
31. Bekoff M. The development of social interaction, play, and meta-communication in mammals: an ethological perspective. Q Rev Biol 1972; 47:412-34; http://dx.doi.org/10.1086/407400
32. Vanderschuren LJMJ, Niesink RJM, Van Ree JM. The neurobiology of social play-behavior in rats. Neurosci Biobehav Rev 1997; 21:309-26; PMID:9168267; http://dx.doi.org/10.1016/S0149-7634(96)00020-6

犬の腫瘍壊死因子(TNF-α)遺伝子に関する研究

１．正常犬における TNF-αの遺伝子の解析

２．免疫介在性疾患および腫瘍疾患における TNFN の遺伝子の解析

久末正晴（麻布大学内科学第二）　田中和明（麻布大学動物工学）
渡辺　征（麻布大学内科学第二）

１．正常犬における TNF-αの遺伝子の解析

研究要旨

ヒトの医学領域では TNF-αは様々な免疫介在性疾患で、その異常が認められている。本研究では犬の TNF-αの遺伝子である TNFA 遺伝子においてマイクロサテライト変異の解析を試みた。犬の遺伝的リスク因子を特定する目的で、まず正常犬の TNF-αの遺伝子である TNFA 遺伝子の塩基配列を解析することとした。ビーグル、チワワ、ミニチュアダックス、トイプードル、コーギーおよび柴犬、各 20 頭以上からなる合計 139 頭の DNA 試料を用い、PCR 産物は 3130 Genetic analyzer を用いた遺伝子型判定に供した。その結果、第１イントロン内に 4 塩基を単位とするマイクロサテライト(tetra-nucleotide repeats;以後 TNR)変異を見出した。さらに第１イントロン内の TNR 多型を判定するために、約 120 塩基対の産物が得られるプライマーを設計した。犬 TNFA 遺伝子の第１イントロンに GAAT を反復単位とする TNR が存在し、繰り返し数多型が存在することが明らかになった。調査した 139 個体から 5 回, 6 回, 7 回, 8 回型の 4 対立遺伝子が検出された。ビーグル種からは 5 回型から 8 回型まで全ての対立遺伝子が検出されたが、他の 5 品種からは 8 回型は検出されなかた。ヘテロ接合度の期待値 (He) および多型情報量(PIC)は、品種によって、それぞれ 0.389－0.749 と 0.333－0.682 の間で差異が認められた。このマイクロサテライトマーカーは、多型性に富み同時に型判定が容易であるため、犬 TNFA 遺伝子のランドマークとして、伝達不平衡テストなどの疾患相関解析に利用可能であると予想された。

研究目的

近年、小動物臨床において犬では免疫介在性溶血性貧血、免疫介在性血小板減少症、全身性紅斑性狼瘡、多発性関節炎、膜性腎症などの様々な免疫介在性疾患の発生が認められている。ヒトの医学領域では TNF-αは特発性血小板減少性紫斑病(イヌの免疫介在性血小板減少症)、リウマチ性関節炎、全身性紅斑性狼瘡といった膠原病などの様々な免疫介在性疾患で、その異常が認められている。そこで、本研究ではイヌの炎症性疾患に対する遺伝的リスク因子を発見する目的で TNFA 遺伝子の多型を検索した。

材料と方法

当初は、ビーグル犬の第一エクソンおよびイントロンを含む広い領域をコードする TNFA 遺伝子解析を PCR 法にて実施した。その結果、同一犬種ににもかかわらず塩基長の異なるバンドが検出されハプロタイプが存在するものと予想された(図 1, 2)。この予備研究の解析結

果を以て、他犬種においても同様の塩基長の変化があることを予想し TNFA 遺伝子解析を実施した。

研究対象として、ビーグル、チワワ、ミニチュアダックス、トイプードル、コーギーおよび 柴犬、各 20 頭以上からなる合計 139 頭の DNA 試料を用いた。第１イントロン内の TNR 多型を判定するために、約 120 塩基対の産物が得られる TNFA-STR1-F (5’-GGAAGATGCTCATGGATTGCT-3’) と TNFA-STR1-R (5’-TACCCACACCCCACATCTCT-3’) プライマーを設計した(図 3)。PCR 産物は 3%アガロースゲルで電気泳動および蛍光物質 FAM で標識し 3130 Genetic analyzer を用いた遺伝子型判定に供した。

結果および考察

調査した 139 個体からすべての犬種において 5 回, 6 回, 7 回, 8 回型の 4 対立遺伝子が検出された。これらの結果から、イヌ TNFA 遺伝子の第１イントロンに GAAT を反復単位とする(tetra-nucleotide repeats;以後 TNR)が存在し、繰り返し数多型が存在することが明らかになった(図 4)。この特徴的な配列は、マイクロサテライトと呼ばれ真核生物のゲノム上には、いたる所に様々な数の反復 DNA 配列が存在する。同一個体のゲノム内部であっても反復回数は場所ごとに異なり、個体間でも異なる。この種の反復配列のうち 2~5 塩基対を反復単位とするものをマイクロサテライト反復配列といい（短塩基縦列配列:STR ともいう)、イントロンに存在している。

興味深いことに、ビーグル種からは 5 回型から 8 回型まで全ての対立遺伝子が検出されたが、他の 5 品種からは 8 回型は検出されなかた。ヘテロ接合度の期待値 (He) および多型情報量(PIC)は、品種によって、それぞれ 0.389 - 0.749 と 0.333 - 0.682 の間で差異が認められた。このマイクロサテライトマーカーは、多型性に富むばかりでなく同時に型判定が容易であるため、イヌ TNFA 遺伝子のランドマークとして、伝達不平衡テストなどの疾患相関解析に利用可能である。

本研究の結果から犬の TNFA 遺伝子にマイクロサテライトが見出され、これらが免疫介在性疾患や腫瘍疾患の病態発生や診断法の確立に寄与するものと考えられた。

図 1

正常犬(ビーグル)のシークエンス内に見られたハプロタイプ

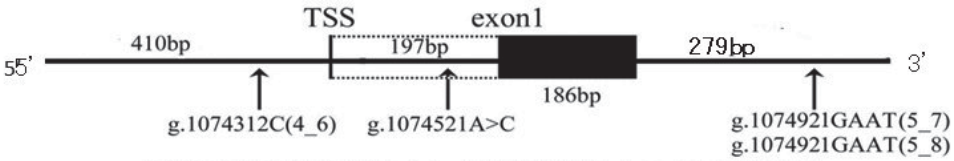

黒塗りBOXはCDSを示す。TSSは推定上の転写開始点

多型
1. 5' 側転写開始点(TSS)より上流のCの繰り返し数4から6への多型
2. エクソン1の非翻訳領域のA>CのSNP
3. 第1イントロン内のGAATを単位とする4塩基反復多型(マイクロサテライト)

以上3か所の多型は組み合わせることにより、3つの新規なハプロタイプとして分類し、AB819627からAB819629の登録番号でデータベースに登録した.

CanFam3.1	g.[1041312C[4]; 1074521A ; 1074921GAAT[5]]
AB819627	g.[1041312C[4]; 1074521C ; 1074921GAAT[5]]
AB819628	g.[1041312C[6]; 1074521C ; 1074921GAAT[7]]
AB819629	g.[1041312C[6]; 1074521C ; 1074921GAAT[8]]

図 2

アガロース･ゲル電気泳動によるマイクロサテライトの遺伝子型判定

(犬種:ビーグル; 3% アガロースゲル, EtBr染色)

第1イントロン内の$(GAAT)_{5-8}GAT(GAAT)_2$をモチーフとするGAAT反復配列多型のヘテロ接合が存在することが明らかとなった

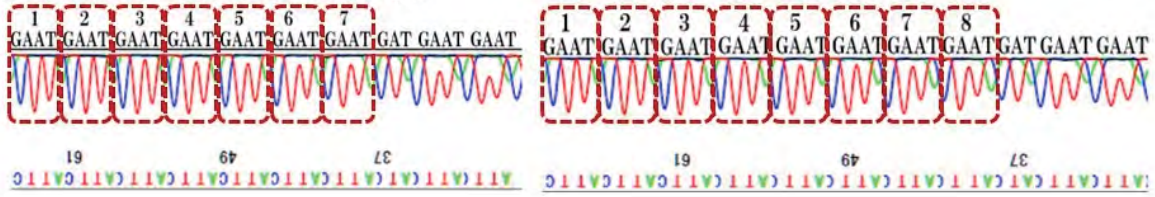

図 3

CanFam3.1に基ずいて作成した犬 *TNF-α*遺伝子の構造図

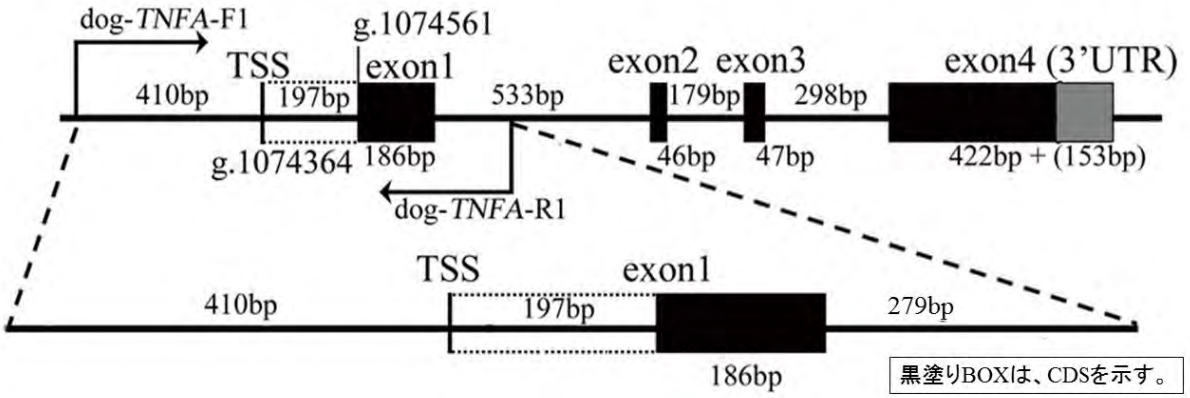

(CanFam3.1, dog genome assembly NW_003726081)

図 4

犬 *TNF-α*遺伝子の4塩基反復マイクロサテライトの対立遺伝子頻度

犬種(頭数)	対立遺伝子頻度 5	6	7	8	*He*[a)]	*PIC*[b)]	HWE[c)]
ビーグル (22)	0.295	0.136	0.295	0.273	0.749	0.682	P<0.05
ミニチュア・ダックスフンド (20)	0.625	0.075	0.300	0.000	0.527	0.438	NS
チワワ (26)	0.692	0.250	0.058	0.000	0.464	0.391	NS
ミニチュア・プードル (24)	0.604	0.167	0.229	0.000	0.566	0.493	P<0.05
ウエルシュ・コーギー (22)	0.558	0.250	0.182	0.000	0.595	0.516	NS
柴犬 (25)	0.760	0.040	0.200	0.000	0.389	0.333	NS

[a)]ヘテロ接合度の期待値, [b)]多型情報含有値, [c)]ハーディ・ワインベルグ平衡からの逸脱

2. 免疫介在性疾患および腫瘍疾患における TNFN の遺伝子の解析

久末正晴（麻布大学内科学第二）

研究要旨

マイクロサテライトは、犬の免疫介在性血液疾患および腫瘍性疾患の診断応用に有力と考え探索を行った。免疫介在性疾患では、最終的に 36 例の犬の免疫介在性血小板減少で解析を実施したが、特異的な SNP の解析には至らなかった。さらに、リンパ腫および悪性黒色腫の計 10 例において TNFA 遺伝子のマイクロサテライト解析を実施していたが、変異は見出だすことは困難で特異的な SNP の解析には至らなかった。本研究では、犬の他の免疫介在性血液疾患および腫瘍性疾患について解析中で達成度は 20%であった。この原因として、免疫介在性血液疾患はそもそも母集団が少なく、かつ確定診断要件を満たすものが少なったことが挙げられる。また腫瘍性疾患においては、二次診療施設に来院するリンパ腫および悪性黒色腫の検体数が減少傾向であることも挙げられる。このように解析数がごく少数であるため、変異の有無を確認できないこととプライマーの設計自体に問題があった可能性があり、今後検討する必要があるものと考えられた。

研究目的

前述したように犬では免疫介在性疾患および腫瘍疾患の臨床例が多く存在する。免疫介在性血小板減少症(IMT)は、犬で比較的多発する血液疾患であり中には難治性の症例も存在する。治療はプレドニゾロンの投与が一般的ではあるが、最近治療抵抗性の IMT の発生例も多く見受けられ、免疫抑制剤や脾臓摘出などの治療も行われている。例えば、炎症性腸疾患(IBD)、特にリンパ球性形質細胞性腸炎(LPE)では，IL-1，IL-2，IL-5，IL-6，IL-12 の他に TNF-αの血中レベルの上昇が報告されている.

さらに、リンパ腫などの血液腫瘍による疾患は犬猫において発生率が高く、臨床上重要な疾患である。現在の血液腫瘍の検査は血液検査や細胞診が主である。しかし、これらの検査方法にはもちろん検出限界があり、病理検査は侵襲性が高いこともあり経過観察に頼らなくてはならない。そこで注目されているのがマイクロサテライトを用いた遺伝子診断法である。マイクロサテライト解析による腫瘍診断は、針生検材料などのごく少量の検体での検査が可能であり、また客観的に血液腫瘍の悪性を評価できるなどの利点が挙げられる。この診断方法を確立するには不安定性を示すマイクロサテライトマーカーの絞り込みが課題となっている。

通常、細胞は分化・代謝の過程で異常が生じるとアポトーシスによって異常な細胞は消滅する。しかし、悪性度の高い癌細胞ではアポトーシスが生じずに癌細胞は増殖していく。一方、白血病においてはこのマイクロサテライト領域において遺伝子欠損 (LOH) や長さの変化が生じてだんだん蓄積され、マイクロサテライトの不安定性が見受けられるようになる。すなわち、マイクロサテライトマーカーを調べてゲノムの不安定性が見られれば、その組織が腫瘍性であることの証拠になる。

これらのマイクロサテライトは、犬の免疫介在性血液疾患および腫瘍性疾患の診断応用に有力と考え探索を行った。

材料と方法

免疫介在性疾患では、最終的に 36 例の犬の免疫介在性血小板減少で解析を実施した。IMT の症例は、麻布大学付属動物病院もしくは東京大学 動物医療センターに来院した犬 36 頭であった。全症例で、血小板数減少の原因となる基礎疾患は認められず、さらに凝固系検査を実施したが、PT、APTT、フィブリノーゲン及び FDP のいずれにおいても明らかな異常値を示した個体はなく DIC の発生は疑われなかった。

リンパ腫は 6 例の多中心型であり、腫脹したリンパ節より細胞を針生検にて採取した。患部の細胞より DNA を抽出した。悪性黒色腫の犬は 4 例で、口腔の腫瘤より腫瘍細胞を針生検にて採取した。

結果および考察

IMT の解析においては、一犬種につき最低 10 例以上の罹患犬と同数の犬を確保する必要があった。しかしながら、最も多いウェリッシュ・コーギーでも最大 7 例であり統計学的解析に必要な症例数の確保は困難であり、特異的な SNP の解析には至らなかった（図 5)。図 6 に示すように、犬の TFNA 遺伝子の第一イントロンおよびエクソン部分には、多様な変異が見られたもののその統一性は見いだせずかなり大規模な解析が必要であると考えられた。

さらに、リンパ腫 10 例および悪性黒色腫において TNFA 遺伝子のマイクロサテライト解析を実施していたが、プライマー増幅は困難で変異は見出だすことは困難で特異的な SNP の解析には至らなかった。この原因として、免疫介在性血液疾患はそもそも母集団が少なく、かつ確定診断要件を満たすものが少なったことが挙げられる。また腫瘍性疾患においては、二次診療施設に来院するリンパ腫および悪性黒色腫の検体数が減少傾向であることも挙げられる。このように解析数がごく少数であるため、変異の有無を確認できないこととプライマーの設計自体に問題があった可能性があり、今後検討する必要があるものと考えられた。

図 5

IMT　解析対象の品種の内訳

2016年　3月末	36例
ウェリッリュコーギー	7例
ミニチュア・ダックス	6例
ヨーキシャ・テリア	2例
トイ・プードル	6例
コッカースパニエル	4例
秋田犬	1例
甲斐犬	1例
バーニーズマウンテン	1例
ペキニーズ	1例
ラブラドール	1例
ラサ・アプソ	2例
雑種	4例

麻布大学
　患者 28例
東京大学附属動物医療センター
　患者 8例

本研究の期間内に解析に必要なn数を確保できなかった

図 6　IMT 症例に見られた遺伝子変異

	Promoter (F1/R1)				Exon 1(F1/R1)			Intron 1(F1/R1)					
	C(-385)	A(-375)	A(-364)	A(+137)	G(+323)	G(+326)	ins A(+380)	C(+488)	T(+581)	T(+584)	T(+486)	TGAAMS	
1.	del C		del A	del A	C (G)							8	
2.	del C (del G)		del A (del T)	del A (del T)	C (G)					C	A	7	
3.	del C		del A	del A								8	
4.			del A		C		ins A					9	
5.			del A		C	C						8	
6.			del A									9	
7.			del A									8	
8.			del A		C							8	
9.			del A		C (G)		del G					8	
10.			del A (del T)	del A				del C		A	C	7	
11.			del A	del A								9	
12.			del A	del A								8	
13.			del A	del A	C							8	
14.			del A	del A								8	
15.	del C		del A									8	
16.	del C		del A		C							8	
17.	del C		del A	del A								9	
18.			del A	del A	C(G)							8	

1. 論文発表

1) Horimoto T, Gen F, Murakami S, Iwatsuki-Horimoto K, Kato K, Hisasue M, Sakaguchi M, Nidom CA, Kawaoka Y. : Cats as a potential source of emerging influenza virus infections. Virol Sin. 30, 221-3, 2015.
2) Kawarai S, Hisasue M, Matsuura S, Ito T, Inoue Y, Neo S, Fujii Y, Madarame H, Shirota K, Tsuchiya R. : Canine pemphigus foliaceus with concurrent immune-mediated thrombocytopenia. Am Anim Hosp Assoc. 51, 56-63, 2015.
3) Watanabe M, Tanaka K, Takizawa T, Segawa K, Neo S, Tsuchiya R, Murata M, Murakami M, Hisasue M.: Characterization of a canine tetranucleotide microsatellite marker located in the first intron of the tumor necrosis factor alpha gene. J Vet Med Sci. 76, 119-22, 2014.
4) Kamiie J, Shimoyama N, Aihara N, Hisasue M, Naya Y, Ogihara K, Shirota K. : Quantitative analysis of CD3ε in a cloned canine lymphoma cell line by selected reaction monitoring assay. Biosci Biotechnol Biochem. 78, 271-5, 2014.
5) Horimoto T, Gen F, Murakami S, Iwatsuki-Horimoto K, Kato K, Akashi H, Hisasue M, Sakaguchi M, Kawaoka Y, Maeda K. : Serological evidence of infection of dogs with human influenza viruses in Japan. Vet Rec. 174:96, (Epub 2013 Dec 11) 2014.
6) Watanabe S, Ito J, Baba T, Hiratsuka T, Kuse K, Ochi H, Anai Y, Hisasue M, Tsujimoto H, Nishigaki K.J : Notch2 transduction by feline leukemia virus in a naturally infected cat. Vet Med Sci. 76, 553-7. 2014.
7) Kurihara Y, Suzuki T, Sakaue M, Murayama O, Miyazaki Y, Onuki A, Aoki T, Saito M, Fujii Y, Hisasue M, Tanaka K, Takizawa T. : Valproic acid, a histone deacetylase inhibitor, decreases proliferation of and induces specific neurogenic differentiation of canine adipose tissue-derived stem cells. J Vet Med Sci. 76:15-23. 2014.
8) Fujimoto A, Neo S, Ishizuka C, Kato T, Segawa K, Kawarai S, Ogihara K, Hisasue M, Tsuchiya R. : Identification of cell surface antigen expression in canine hepatocellular carcinoma cell lines. Vet Med Sci. 75:831-5. 2013.
9) Kato T, Hisasue M, Segawa K, Fujimoto A, Makiishi E, Neo S, Yasuno K, Kobayashi R, Tsuchiya R. : Accumulation of xenotransplanted canine bone marrow cells in NOD/SCID/γc(null) mice with acute hepatitis induced by CCl4. Vet Med Sci. 75:847-55. 2013.
10) Segawa K, Kondo T, Kimura S, Fujimoto A, Kato T, Ishikawa T, Neo S, Hisasue M, Yamada T, Tsuchiya R. : Effects of prostaglandin E1 on the preparation of platelet concentrates in dogs. J Vet Intern Med. 26:370-6. 2012.

2. 学会発表

1) 渡辺征，田中和明，滝沢達也，瀬川和仁，根尾櫻子，土屋亮，村田倫子, 村上賢，久末正晴：イヌ腫瘍壊死因子(TNFA)遺伝子の第 1 イントロンに存在する 4 塩基反復マイクロサテライトの特徴. 第 156 回日本獣医学会、岐阜、2013 年 9 月

NOTE *Biochemistry*

Characterization of a Canine Tetranucleotide Microsatellite Marker Located in the First Intron of the Tumor Necrosis Factor Alpha Gene

Masashi WATANABE[1)]**, Kazuaki TANAKA[2)]**, Tatsuya TAKIZAWA[2)], Kazuhito SEGAWA[1)], Sakurako NEO[1)], Ryo TSUCHIYA[1)], Michiko MURATA[3)], Masaru MURAKAMI[3)] and Masaharu HISASUE[1)]*

[1)]*Laboratory of Veterinary Internal Medicine II, Faculty of Veterinary Medicine, Azabu University, Chuo-ku, Sagamihara, Kanagawa 252–5201, Japan*
[2)]*Laboratory of Animal Biotechnology, Faculty of Veterinary Medicine, Azabu University, Chuo-ku, Sagamihara, Kanagawa 252–5201, Japan*
[3)]*Laboratory of Molecular Biology, Faculty of Veterinary Medicine, Azabu University, Chuo-ku, Sagamihara, Kanagawa 252–5201, Japan*

(Received 18 June 2013/Accepted 21 August 2013/Published online in J-STAGE 13 September 2013)

ABSTRACT. A polymorphic tetranucleotide $(GAAT)_n$ microsatellite in the first intron of the canine tumor necrosis factor alpha (*TNFA*) gene was characterized in this study; 139 dogs were analyzed: 22 Beagles, 26 Chihuahuas, 20 Miniature Dachshunds, 24 Miniature Poodles, 22 Pembroke Welsh Corgis and 25 Shiba Inus. We detected the presence of the 4 alleles $(GAAT)_5$, $(GAAT)_6$, $(GAAT)_7$ and $(GAAT)_8$, including 9 of the 10 expected genotypes. The expected heterozygosity (*He*) and the polymorphic information content (*PIC*) value of this microsatellite locus varied from 0.389 to 0.749 and from 0.333 to 0.682, respectively, among the 6 breeds. The allelic frequency differed greatly among breeds, but this microsatellite marker was highly polymorphic and could be a useful marker for the canine *TNFA* gene.
KEY WORDS: canine *TNFA* gene, tetranucleotide microsatellite.

doi: 10.1292/jvms.13-0316; *J. Vet. Med. Sci.* 76(1): 119–122, 2014

Tumor necrosis factor alpha (TNFA) is a multifunctional pro-inflammatory cytokine, which is secreted mainly by monocytes and macrophages (Online Mendelian Inheritance in Man (*OMIM, 191160*),. In humans, genetic variations in the *TNFA* gene are associated with various disorders, e.g., septic shock [14], rheumatoid arthritis [15], cystic fibrosis [3], inflammatory bowel diseases [11] and insulin resistance syndrome [8].

In the veterinary field, TNFA is also considered to be one of the most important cytokines involved with many inflammatory diseases, including bacterial and protozoan infections and sepsis [6, 13, 17]. For example, increased expression of *TNFA* mRNA in colonic mucosa has been reported on dogs with idiopathic lymphocytic-plasmacytic colitis [16].

The canine *TNFA* gene is located on dog chromosome 12 (CanFam3.1, dog genome assembly *NW_003726081*), and it comprises 4 exons and 3 introns. However, the genetic polymorphisms in the canine *TNFA* gene have not been clarified.

Microsatellites are tandem repeated sequences, usually di-, tri- and tetranucleotide motifs, which display high levels of polymorphism, making them ideal genetic markers [7, 18]. Microsatellites were thought to be evolutionarily neutral and to have no generalized function [18]. In recent years, however, many reports have indicated that microsatellites in the promoter regions and introns of functional genes exert genetic effects in many cases [1, 5, 9, 10, 12, 19]. Thus, microsatellites in known functional genes are good targets for analyzing genetic polymorphisms.

In this study, we focused on a $(GAAT)_n$ repeat motif located in the first intron of the canine *TNFA* gene and demonstrated that this microsatellite locus was highly polymorphic, so it could be a useful marker for genetic analysis.

Whole blood, swabs of the oral mucosa or nail samples were collected from dogs at veterinary hospitals and dog grooming shops in Japan. The 139 samples obtained were from 22 Beagles, 26 Chihuahuas, 20 Miniature Dachshunds, 24 Miniature Poodles, 22 Pembroke Welsh Corgis and 25 Shiba Inus. This study was approved by the Institutional Animal Care and Use Committee (Permission number: 1306094) and carried out according to the Azabu University Animal Experimentation Regulations. DNA was extracted from these samples using a Quick Gene DNA tissue kit (Fuji Film, Tokyo, Japan) or a NucleoSpin Blood Quick Pure kit (Macherey-Nagel, Duren, Germany), according to the manufacturer's protocols.

The primers used for polymerase chain reaction (PCR) analysis were designed using CanFam3.1. A 1.1-kb DNA fragment containing about 400 bp upper stream from the putative transcription start site, a 5′- untranslated region (5′- UTR), the first exon and about 240 bp of the first intron of the canine *TNFA* gene was amplified by PCR using the forward primer dog-*TNFA*-F1 (5′-AAGCCCCACCCCTTG-

*CORRESPONDENCE TO: HISASUE, M., Laboratory of Veterinary Internal Medicine II, Faculty of Veterinary Medicine, Azabu University, 1–17–71, Fuchinobe, Chuo-ku, Sagamihara, Kagagawa 252–5201, Japan.
e-mail: hisasue@azabu-u.ac.jp
**The first two authors contributed equally to this work.

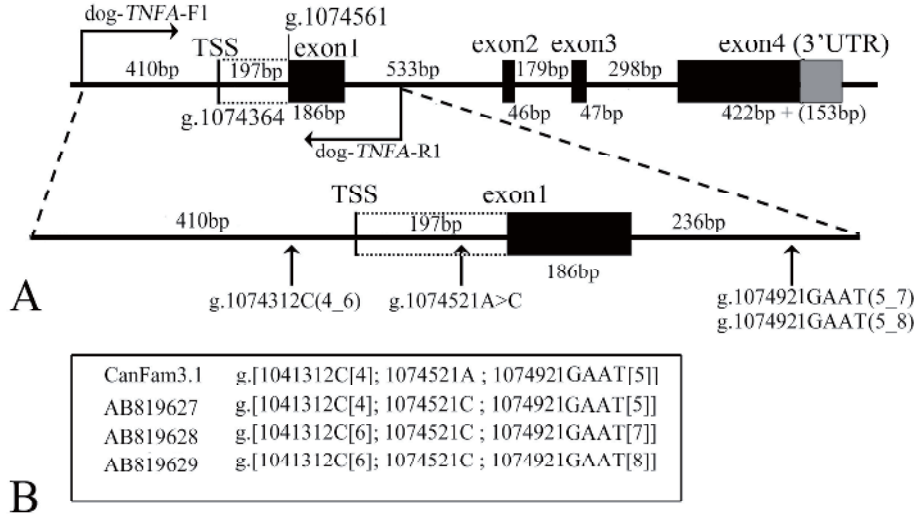

Fig. 1. Scheme of the canine *TNFA* gene showing the region sequenced and the polymorphisms detected. (A) Structure of the canine *TNFA* gene (above) and its sequenced region (below). The protein-coding sequences are indicated by dark boxes. The numbering of base positions was based on the reference sequence, NW_003726081 (CanFam3.1; chromosome 12). In the reference sequence, g.1074364 and g.1074561 were the putative transcription start site (TSS) and the head of the translation initiation codon of the *TNFA* gene, respectively. (B) The variations detected in the partial *TNFA* gene in 7 Beagles.

CACCTT-3′) and the reverse primer dog-*TNFA*-R1 (5′-CCACACCCCACATCTCTCCACACA-3′) (Fig. 1A). PCR was performed using 30 μl reaction volumes, according to the manufacturer's instructions for GoTaq Green Master Mix (Promega, Fitchburg, WI, U.S.A.). The program comprised initial denaturation at 94°C for 3 min, followed by 30 cycles of denaturation at 94°C for 20 sec, annealing at 59°C for 25 sec and extension at 72°C for 60 sec with a final extension at 72°C for 7 min. The amplified products were purified using a QIAquick PCR Purification kit (Qiagen, Hilden, Germany). The purified DNA was sequenced directly using a Big Dye Terminator version 3.1 Cycle Sequencing kit (Applied Biosystems, Foster City, CA, U.S.A.) with dog-*TNFA*-F1 and dog-*TNFA*-R1 primers. First, we analyzed the DNA sequences of 22 Beagles. However, 15 of the 22 individuals produced poor results, because of widespread double peak from the dog_*TNFA*_R1 primer side. As a result, we determined the target sequences successfully in 7 individuals only.

After multiple alignments of the partial *TNFA* sequences of the 7 Beagles with the canine reference sequence, we found 3 polymorphic sites: a cytosine direct repeat variation in the 5′ gene flanking region (g.1074312C (4_6)), an adenine to cytosine substitution in the 5′ UTR (g.1074521A>C) and GAAT microsatellite variations in the first intron (g.1074922GAAT (5_7) and g.1074922GAAT (5_8)) (Fig. 1A). Next, we identified 3 *TNFA* variations: TNFA-Beagle1 (1 dog), TNFA-Beagle2 (2 dogs) and TNFA-Beagle3 (4 dogs) in the 7 individuals (Fig. 1B).These nucleotide sequences were deposited in the DDBJ, EMBL and GenBank nucleotide databases under accession numbers AB819627–AB819629.

Based on their electropherograms, we also found that the suboptimal sequencing results for the 15 Beagles resulted from the heterozygosity (*He*) in different numbers of (GAAT) repeats in the [$(GAAT)_{5–8}$ (GAT) $(GAAT)_2$] microsatellite motif in the first intron (Fig. 1). To genotype this microsatellite locus, we designed the following primer set: CFA12-*TNFA*-STR1-F (5′-GGAAGATGCTCATGGATTGCT-3′) and CFA12-*TNFA*-STR1-R (5′-TACCCACACCCCACATCTCT-3′). PCR was performed using 25 μl reaction volumes, according to the manufacturer's instructions for GoTaq Master Mix (Promega). The program comprised initial denaturation at 94°C for 3 min, followed by either 30 or 40 cycles of denaturation at 94°C for 20 sec, annealing at 55°C for 15 sec and extension at 72°C for 30 sec with a final extension at 72°C for 7 min. The PCR products were electrophoresed on a 3.0% agarose gel and visualized by ethidium bromide staining (Fig. 2). Four alleles, i.e., $(GAAT)_5$, $(GAAT)_6$, $(GAAT)_7$ and $(GAAT)_8$, were detected in the CFA12-*TNFA*-STR1 tetranucleotide microsatellite locus, and the lengths of their PCR products were 114, 118, 122 and 126 bp, respectively. Subsequently, we surveyed the allele distribution of this microsatellite marker in 6 dog breeds. We used the FAM-labeled CFA12-*TNFA*-STR1-F primer, and the fragment lengths of the PCR products were determined automatically using an ABI 3130 genetic analyzer with GeneMapper Ver. 4.0 (Applied Biosystems). Table 1 shows the genotypic and allele distribution in 6 dog breeds. Four alleles were present in 22 Beagles, whereas only 3 alleles were detected in 117 dogs from the other 5 breeds. This is because the $(GAAT)_8$ allele was absent from Chihuahuas, Miniature Dachshunds, Miniature Poodles,

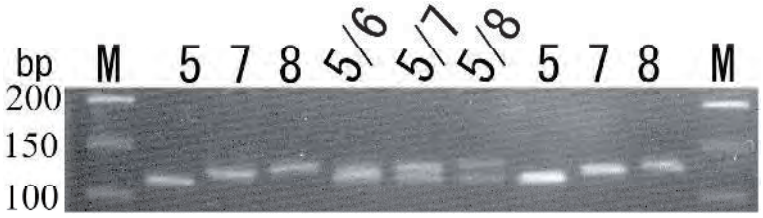

Fig. 2. Genotyped patterns of the tetranucleotide microsatellite polymorphism in the first intron of the canine *TNFA* gene on a 3.0% agarose gel. The genotypes relate to the upper lanes of the gel. M is a 50-bp DNA ladder molecular size marker (Toyobo, Osaka, Japan).

Table 1. Genotypic and allelic frequency of $(GAAT)_n$ tetranucleotide microsatellite in canine *TNFA* gene among dog breeds

Breeds (number of animals)	Genotype										Allelic frequency				*He*[a]	*PIC*[b]	Deviations of HWE[c]
	5	6	7	8	5/6	5/7	5/8	6/7	6/8	7/8	5	6	7	8			
Beagle (22)	1	0	2	4	5	5	1	1	0	3	0.295	0.136	0.295	0.273	0.749	0.682	$P<0.05$
Miniature Dachshund[d] (20)	8	0	2	0	2	7	0	1	0	0	0.625	0.075	0.300	0.000	0.527	0.438	NS[e]
Chihuahua[d] (26)	12	2	0	0	9	3	0	0	0	0	0.692	0.250	0.058	0.000	0.464	0.391	NS
Miniature Poodle (24)	6	1	0	0	6	11	0	0	0	0	0.604	0.167	0.229	0.000	0.566	0.493	$P<0.05$
Pembroke Welsh Corgi (22)	8	1	0	0	5	4	0	4	0	0	0.568	0.250	0.182	0.000	0.595	0.516	NS
Shiba Inu (25)	13	0	0	0	2	10	0	0	0	0	0.760	0.040	0.200	0.000	0.389	0.333	NS

a) Expected heterozygosity, b) Polymorphic information content, c) Deviations of Hardy-Weinberg Equilibrium, d) All the indivduals had long-coate. e) Not significant.

Pembroke Welsh Corgis and Shiba Inus. $(GAAT)_5$ was the most common allele in the 6 dog breeds. An exact test of the Hardy–Weinberg equilibrium using a Markov chain and calculation of the expected *He* were performed using Arlequin ver. 3.1 [4]. The polymorphic information content (*PIC*) value for this microsatellite locus was estimated using a formula described previously [2]. The deviations from the Hardy–Weinberg equilibrium were statistically significant ($P<0.05$) for Beagles and Miniature Poodles. *He* was deficient in Beagles, whereas an excess of *He* was observed in Miniature Poodles. The expected *He* and *PIC* value for this microsatellite locus varied from 0.389 (Shiba Inu) to 0.749 (Beagle) and from 0.333 (Shiba Inu) to 0.682 (Beagles), respectively, in the 6 breeds (Table 1). The allelic frequency differed greatly among breeds, but this microsatellite marker was highly polymorphic and could be a useful marker for the canine *TNFA* gene. Given the important roles of TNFA in many inflammatory reactions, the tetranucleotide microsatellite alleles could be associated with susceptibility to inflammatory disorders during the lifetime of the domestic dog due to a direct gene effect or linkage disequilibrium with adjacent nucleotide variations. Further studies are needed to test for possible correlations between this microsatellite variation and canine diseases.

ACKNOWLEDGMENTS. We thank Dr. Hidekatsu Shimakura from the First Department of Microbiology, Faculty of Veterinary Medicine, Azabu University for collecting canine DNA samples. This work was supported by the MEXT Program for the Strategic Research Foundation at Private Universities, 2011–2015. The authors would like to thank Enago (www.enago.jp) for the English language review.

REFERENCES

1. Aoki, T., Koch, K. S. and Leffert, H. L. 1997. Attenuation of gene expression by a trinucleotide repeat-rich tract from the terminal exon of the rat hepatic polymeric immunoglobulin receptor gene. *J. Mol. Biol.* **267**: 229–236. [Medline] [CrossRef]
2. Botstein, D., White, R. L., Skolnick, M. and Davis, R. W. 1980. Construction of a genetic linkage map in man using restriction fragment length polymorphisms. *Am. J. Hum. Genet.* **32**: 314–331. [Medline]
3. Buranawuti, K., Boyle, M. P., Cheng, S., Steiner, L. L., McDougal, K., Fallin, M. D., Merlo, C., Zeitlin, P. L., Rosenstein, B. J., Mogayzel, P. J. Jr., Wang, X. and Cutting, G. R. 2007. Variants in mannose-binding lectin and tumour necrosis factor alpha affect survival in cystic fibrosis. *J. Med. Genet.* **44**: 209–214. [Medline] [CrossRef]
4. Excoffier, L., Laval, G. and Schneider, S. 2005. Arlequin ver. 3.0: An integrated software package for population genetics data analysis. *Evol. Bioinform. Online* **1**: 47–50.
5. Gardezi, A. Z., Ziaei, Y. Z. and Marashi, S. M. 2008. Microsatellite polymorphism of the human leptin gene and risk of obesity. *J. Crit. Care* **23**: 440–444. [Medline] [CrossRef]
6. Guedes, P. M., Veloso, V. M., Afonso, L. C., Caliari, M. V., Carneiro, C. M., Diniz, L. F., Marques-da-Silva, E. A., Caldas, I. S., Do Valle Matta, M. A., Souza, S. M., Lana, M., Chiari, E., Galvão, L. M. and Bahia, M. T. 2009. Development of chronic cardiomyopathy in canine Chagas disease correlates with high IFN-gamma, TNF-alpha, and low IL-10 production during the acute infection phase. *Vet. Immunol. Immunopathol.* **130**: 43–52. [Medline] [CrossRef]
7. Hearne, C. M., Ghosh, S. and Todd, J. A. 1992. Microsatellites for linkage analysis of genetic traits. *Trends Genet.* **8**: 288–294. [Medline]

8. Ishii, T., Hirose, H., Saito, I., Nishikai, K., Maruyama, H. and Saruta, T. 2000. Tumor necrosis factor alpha gene G-308A polymorphism, insulin resistance, and fasting plasma glucose in young, older, and diabetic Japanese men. *Metabolism* **49**: 1616–1618. [Medline] [CrossRef]
9. Kashi, Y., King, D. and Soller, M. 1997. Simple sequence repeats as a source of quantitative genetic variation. *Trends Genet.* **13**: 74–78. [Medline] [CrossRef]
10. Klesert, T. R., Otten, A. D., Bird, T. D. and Tapscott, S. J. 1997. Trinucleotide repeat expansion at the myotonic dystrophy locus reduces expression of *DMAHP*. *Nature Genet.* **16**: 402–406. [Medline] [CrossRef]
11. Koss, K., Satsangi, J., Fanning, G. C., Welsh, K. I. and Jewell, D. P. 2000. Cytokine (TNF-alpha, LT-alpha, and IL-10) polymorphisms in inflammatory bowel diseases and normal controls: differential effects on production and allele frequencies. *Genes Immun.* **1**: 185–190. [Medline] [CrossRef]
12. Meloni, R., Albanèse, V., Ravassard, P., Treilhou, F. and Mallet, J. 1998. A tetranucleotide polymorphic microsatellite, located in the first intron of the tyrosine hydroxylase gene, acts as a transcription regulatory element *in vitro*. *Hum. Mol. Genet.* **7**: 423–428. [Medline] [CrossRef]
13. Menezes-Souza, D., Corrêa-Oliveira, R., Guerra-Sá, R., Giunchetti, R. C., Teixeira-Carvalho, A., Martins-Filho, O. A., Oliveira, G. C. and Reis, A. B. 2011. Cytokine and transcription factor profiles in the skin of dogs naturally infected by *Leishmania (Leishmania) chagasi* presenting distinct cutaneous parasite density and clinical status. *Vet. Parasitol.* **177**: 39–49. [Medline] [CrossRef]
14. Mira, J.P., Cariou, A., Grall, F., Delclaux, C., Losser, M.R., Heshmati, F., Cheval, C., Monchi, M., Teboul, J.L., Riche, F., Leleu, G., Arbibe, L., Mignon, A., Delpech, M. and Dhainaut, J.F. 1999. Association of *TNF2*, a TNF-alpha promoter polymorphism, with septic shock susceptibility and mortality: a multicenter study. *JAMA* **282**: 561–568. [Medline] [CrossRef]
15. Mulcahy, B., Waldron-Lynch, F., McDermott, M. F., Adams, C., Amos, C. I., Zhu, D. K., Ward, R. H., Clegg, D. O., Shanahan, F., Molloy, M. G. and O'Gara, F. 1996. Genetic variability in the tumor necrosis factor-lymphotoxin region influences susceptibility to rheumatoid arthritis. *Am. J. Hum. Genet.* **59**: 676–683. [Medline]
16. Ridyard, A. E., Nuttall, T. J., Else, R. W., Simpson, J. W. and Miller, H. R. P. 2002. Evaluation of Th1, Th2 and immunosuppressive cytokine mRNA expression within the colonic mucosa of dogs with idiopathic lymphocytic-plasmacytic colitis. *Vet. Immunol. Immunopathol.* **86**: 205–214. [Medline] [CrossRef]
17. Song, R., Kim, J., Yu, D., Park, C. and Park, J. 2012. Kinetics of IL-6 and TNF-α changes in a canine model of sepsis induced by endotoxin. *Vet. Immunol. Immunopathol.* **146**: 143–149. [Medline] [CrossRef]
18. Weber, J. L. and May, P. E. 1989. Abundant class of human DNA polymorphisms which can be typed using the polymerase chain reaction. *Am. J. Hum. Genet.* **44**: 388–396. [Medline]
19. Wei, J., Ramchand, C. N. and Hemmings, G. P. 1995. Association of polymorphic VNTR region in the first intron of the human *TH* gene with disturbances of the catecholamine pathway in schizophrenia. *Psychiatr. Genet.* **5**: 83–88. [Medline] [CrossRef]

Bioscience, Biotechnology, and Biochemistry, 2014
Vol. 78, No. 2, 271–275

Note

Quantitative analysis of CD3ε in a cloned canine lymphoma cell line by selected reaction monitoring assay

Junichi Kamiie[1], Naoto Shimoyama[1], Naoyuki Aihara[1], Masaharu Hisasue[2], Yuko Naya[3], Kikumi Ogihara[3,*] and Kinji Shirota[1,4]

[1]*Laboratory of Veterinary Pathology, School of Veterinary Medicine, Azabu University, Sagamihara, Japan;* [2]*Laboratory of Veterinary Internal Medicine II, School of Veterinary Medicine, Azabu University, Sagamihara, Japan;* [3]*Laboratory of Pathology, School of Life and Environmental Science, Azabu University, Sagamihara, Japan;* [4]*Research Institute of Biosciences, Azabu University, Sagamihara, Japan*

Received August 7, 2013; accepted October 28, 2013
http://dx.doi.org/10.1080/09168451.2014.878216

We established a mass spectrometry-based quantitative method of assaying CD3ε, a component of the T-cell receptor complex. It revealed a CD3ε level of 1 mol per cell in a newly derived canine T-cell lymphoma cell line. Our results suggest that this method has sufficient sensitivity to quantify CD3ε levels in canine lymphoma cells reliably.

Key words: CD3; lymphoma; quantitative proteomics; selected reaction monitoring; mass spectrometry

CD3ε, a component of the CD3 complex, is one of the most abundantly expressed cell-surface proteins of the T-cell lineage. The CD3 complex is composed of four polypeptide chains (δ, ε, γ, and ζ) and is associated with the T-cell receptor (TCR). These chains form δε and γε heterodimers and ζζ homodimers. The δε and γε heterodimers are associated with TCR-α and –β, respectively, and generate intermediate complexes.[1,2] The ζζ homodimers bind to TCR complexes and are transported to the cell surface.[3,4]

In T-cell lineage differentiation, TCR complexes are expressed on thymocytes beginning at the early stages of maturation, and expression of them increases during the maturation process. In addition, each component of the TCR complex changes its expression level during the development of the T-cell lineage.[5,6] Stoichiometric analyses based on absolute quantification of the levels of TCR components are important in understanding their roles in development, but no such quantitative measurements of TCR components yet been reported. Although TCR components are integral membrane proteins, it is difficult to develop quantitative immunological assays, such as the enzyme-linked immunosorbent assay (ELISA), due to the insolubility of these membrane proteins.

Several quantitative proteomics techniques that employ mass spectrometry have been reported recently.[7–9] In particular, absolute quantitative proteomics in the selected reaction monitoring (SRM) mass spectrometry mode is suitable for the highly sensitive and accurate quantification of such proteins.[9] A quantitative approach by SRM has been applied to the study of integral membrane proteins, including drug transporters[10] and G protein-coupled receptors.[11]

In this study, we aimed to develop a quantitative method of determining the levels of canine CD3ε in cells. To verify the usefulness of the method with biological samples, we applied it to establish a novel canine T-cell lymphoma cell line, and we determined the expression level of CD3ε in these cells.

To establish a novel CD3ε-expressing canine T-cell lymphoma cell line, we analyzed cells from the intestinal mass of a 5-year-old male beagle. Cytological examination of the aspirates revealed that the mass was composed of large heteromorphic lymphoid cells with numerous mitoses. Based on these findings, we diagnosed the intestinal mass as a lymphoma. One month after cytological examination, the beagle died at the owner's home and a necropsy was performed with the owner's approval. The intestinal mass was fixed in 10% phosphate-buffered formalin pH 7.4, processed routinely, embedded in paraffin, and cut into sections by 3 μm thick. The paraffin-embedded sections were stained with hematoxylin and eosin or subjected to immunohistochemistry. The de-waxed sections were pretreated by microwaving them in citrate buffer and then incubating them with mouse anti-human-CD3ε antibody (clone F7.2.38, DAKO Japan, Tokyo) for 1 h at room temperature. The signals were visualized with horseradish peroxidase-conjugated rabbit anti-mouse IgG (Nichirei Biosciences, Tokyo) and 3,3′-diaminobenzidine.

The surface of the intestinal tumor mass was sterilized with 70% ethyl alcohol and pipetted into a single-cell

*Corresponding author. Email: ogiwarak@azabu-u.ac.jp
Abbreviations: TCR, T-cell receptor; ELISA, enzyme-linked immunosorbent assay; SRM, selected reaction monitoring; PBS, phosphate-buffered saline; CV, coefficient of variation.

suspension in culture medium. The cell suspension was centrifuged and resuspended in fresh culture medium. This procedure was repeated several times. Primary culture of the cells obtained was carried out in an RPMI-1640 growth medium containing 18% heat-inactivated fetal bovine serum (Gibco BRL, Cergy-Pontoise, France), 0.1% glutamine, 1 mM sodium pyruvate, 0.1% spectinomycin, and 0.035% $NaHCO_3$ in 60-mm Petri dishes at 37 °C in a CO_2 incubator. The medium was replaced approximately twice per week, and confluent cultures were subcultured. The cell line was subjected to cloning by limiting dilution in 96-well plates in an RPMI-1640 medium containing 10% fetal bovine serum. At 4 to 7 days after cultivation, the clones that had grown were trypsinized and subjected to a further limiting dilution step. The cloned cell line was eventually established after three limiting dilution steps.

Flow cytometry analysis of the CD antigens expressed by the cloned cell line was done with antibodies for mouse anti-canine CD3 (clone CA17.2A12, Serotec, Oxford, UK), mouse anti-canine CD4 (clone CA13.1E4, Serotec), or mouse anti-canine CD8α (clone CA9.JD3, Serotec) diluted to 1:200, 1:20, and 1:20, respectively, in Dulbecco's phosphate-buffered saline (PBS) with 1% bovine albumin. We incubated 1×10^6 cells/100 μL for 1 h at 4 °C with 10 μL of each primary antibody. After they were washed twice in PBS, the cells were fixed with 0.5% paraformaldehyde in PBS for 1 h at 4 °C. After further washing in PBS, FITC-conjugated goat anti-mouse IgG (Cappel, Durham, NC) was added, and the mixture was incubated for 1 h at 4 °C. The cells were then washed and fixed with 0.5% paraformaldehyde in PBS. After washing in PBS, the cells were resuspended in PBS and analyzed with a flow cytometer (Epics XL/XL–MCL, Beckman Coulter, San Jose, CA).

For western blotting, 2×10^8 cells were washed three times with PBS and then centrifuged at $250 \times g$ for 10 min. The cell pellets were homogenized with 10 times the initial volume of 0.1% SDS and 10 mM Tris–HCl (pH 8.0). Protein concentrations were measured with a DC Protein Assay Kit (Bio-Rad Laboratories, Hercules, CA) with bovine serum albumin (Bio-Rad) as standard. A total of 10 μg of protein from the cells was resolved by 5–20% SDS-polyacrylamide gel electrophoresis and electro-transferred to PVDF membranes (Bio-Rad). After treatment with a blocking buffer (4% skim milk in 25 mM Tris–HCl pH 8.0, 125 mM NaCl, and 0.1% Tween 20), the membranes were incubated with anti-human CD3ε antibody at 4 °C for 16 h. They were then washed with the blocking buffer three times and incubated with horseradish peroxidase-conjugated polyclonal rabbit anti-mouse immunoglobulin (Dako Japan, Tokyo). Signals were visualized with a chemiluminescence kit (ECL-plus; GE Healthcare UK, Buckinghamshire).

According to a histopathological analysis, the intestinal mass of the beagle was comprised of a monoclonal cluster of large round proliferating tumor cells. The tumor cells were 5–20 μm in diameter with a sharp, irregularly indented nucli (Fig. 1(A)). Mitosis was observed to have occurred frequently. Immunohistochemistry revealed strong expression of CD3ε in the cytoplasm of the tumor cells (Fig. 1(B)). Flow cytometry revealed that the cells expressed CD3ε (Fig. 1(C)), but not CD4, CD8α, or CD79α (data not shown). By Western blotting, expression of CD3ε in the cells was also detected (Fig. 1(D)), whereas CD79α, a B-cell marker, was not detectable in them (data not shown).

We established a quantitative method of detecting CD3ε-derived peptide by mass spectrometry in SRM mode. First, a target peptide sequence was selected from among 27 tryptic peptides derived from the canine CD3ε sequence (SWISS-PROT: P27597) according to previously described peptide selection criteria.[10] Briefly, the target peptide was selected by the following criteria: (i) the target peptide sequence is unique for canine CD3ε, (ii) it does not contain chemically reactive residues (cysteine or methionine), and (iii) it does not contain post-translational modifications or continuous sequences of K or R. The sequence NDNLVEGASNR, a canine-specific sequence, was selected as quantitative target. An isotope-labeled peptide of the target sequence that contained a labeled alanine residue ($^{13}C_3$, ^{15}N) was synthesized by Thermoelectron Corporation (Sedanstrabe, Germany), as reference for the quantitative assay.

SRM transitions were determined with high sensitivity. Seven transitions derived from the y3 to y9 product ions were identified for the endogenous and isotope-labeled forms of NDNLVEGASNR. To verify that, we commanded sufficient sensitivity to detect each of the transitions, SRM analysis of the cultured cell sample was done for the 14 transitions. Tryptic digestion of the cultured cells was done as described previously.[12] We solubilized the cultured cells in 7 M guanidine HCl, 0.5 M Tris–HCl (pH 8.5), and 50 mM EDTA. The protein concentration of the lysate was measured with a protein assay kit (DC Protein Assay, Bio-Rad) with bovine serum albumin as standard. One μg of proteins was reduced with equal amounts of dithiothreitol and *S*-carbamoylmethylated and with 2.5 times the amount of iodoacetamide. The proteins were precipitated with methanol and chloroform (4:1/v:v). The precipitated proteins were dissolved in 1.2 M urea and 500 mM Tris–HCl (pH 8.0), and then digested with trypsin (Promega, Fichburg, WI) at an enzyme to substrate ratio of 1:100 at 37 °C over 16 h. The efficiency of tryptic digestion was checked by SDS-PAGE followed by Western blotting for CD3ε. The specific band of CD3ε disappeared in the digested sample (Fig. 1(D)). We spiked the tryptic digest with 200 fmol of isotope-labeled peptide. The tryptic digests were acidified with formic acid to a pH of < 2.0. The acidified samples were centrifuged at $21{,}500 \times g$ for 15 min, and then the supernatants were injected into a nano-LC system (Paradigm MS4, AMR, Tokyo) connected to an ESI-triple-quadrupole mass spectrometer (TSQ vantage, Thermo Fisher Scientific, Yokohama, Japan). The nano-LC system was run with a reversed phase column (L-column ODS; 0.1 mm inner diameter × 50 mm, 3 μm particles) with a gradient starting at 5% B to 45% B in 45 min, at a flow rate of 500 nL/min. The gradient was generated by mixing water containing 0.1% formic acid (A) and acetonitrile containing 0.1% formic acid (B). The spectrometer was operated in SRM mode with a 1 s cycle time. Collision energies for each transition were

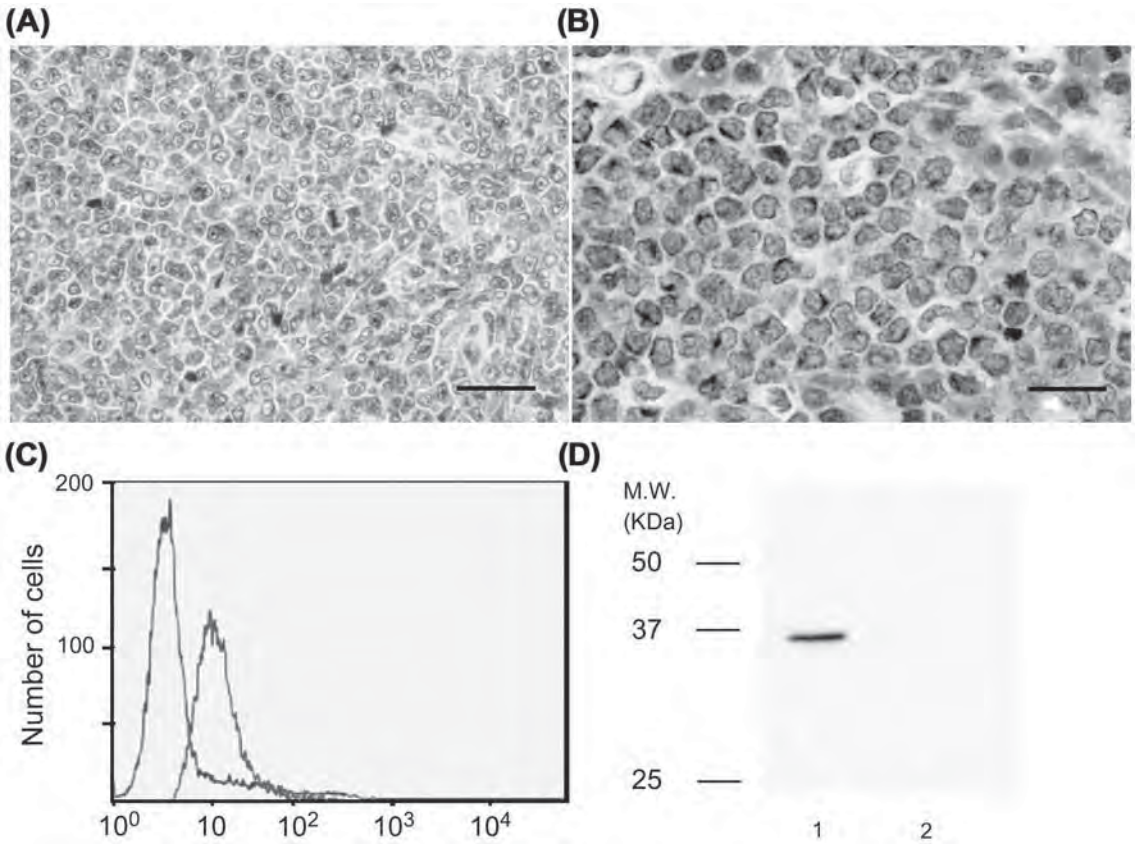

Fig. 1. Morphological findings and CD3ε expression in intestinal tumor cells and cultured cells.

Note: (A) Hematoxylin and eosin staining of the intestinal tumor. Tumor cells were 5–20 μm in diameter with sharp, irregularly indented nuclei. Mitosis was observed to have occurred frequently. Scale bar represents 50 μm. (B) Immunohistochemical detection of CD3ε in the intestinal tumor. Tumor cells showed strong CD3ε expression. Scale bar represents 25 μm. (C) Detection of CD3ε in the cultured cells by flow cytometry. (D) Detection of CD3ε in cultured canine T-cell lymphoma cells. A total of 10 μg of protein from cells (lane 1) and a tryptic digest of cells (lane 2) were analyzed by Western blotting to detect CD3ε.

determined by Pinpoint software, version 1.0 (Thermo Fisher Scientific).

We generated SRM chromatograms of the endogenous and isotope-labeled peptides in 1 μg of protein from the cultured cells spiked with 200 fmol of the isotope-labeled peptides. All transitions showed signal peaks at the same retention time of 10.95 min (Fig. 2(A)). Identity confirmation of the targeted peptide relied on the composite MS/MS spectra displayed. The consistency of the SRM fragmentation patterns is illustrated in Fig. 2(B). The transitions, 594.8$[M+H]^{2+}$/504.3$[M+H]^{+}$, 594.8$[M+H]^{2+}$/633.3$[M+H]^{+}$, and 594.8$[M+H]^{2+}$/732.4$[M+H]^{+}$, derived from the y5, y6, and y7 endogenous peptides respectively, exhibited more than 2 to 5-fold higher signal intensities than the other four transitions (Fig. 2(B)). The order of the peak areas derived from the y-series ions in the SRM analysis was reflected the MS/MS spectrum signal intensity results (y6 > y7 > y5 > y3 > y8 > y9 > y4) (Fig. 2(B)).

Quantitative values were calculated based on the peak area ratio (endogenous/isotope-labeled peptide). We calculated the quantitative values for each product ion in 0.1 μg of protein from cultured cells spiked with 200 fmol of isotope-labeled peptide. The transitions for y5, y6, and y7 showed excellent accuracy, with a coefficient of variation (CV) < 5%, although the other four transitions had CVs of 8.5–13.9% (Table 1). These results suggest that the transitions for y5, y6, and y7 are suitable for sensitive and accurate quantification of CD3ε levels. We used a total of six transitions that contained three transitions derived from y5, y6, and y7 of the endogenous and isotope-labeled peptides to quantify the CD3ε levels.

To assess the linearity of this method, dilution series of the cells were analyzed. The cell suspension was diluted with 1% BSA containing PBS to dilutions of 1:100, 1:1,000, and 1:10,000 in low-binding tubes. The cell concentration in each tube was measured with a Neubauer counting chamber under light microscopy. Aliquots of 1×10^3, 1×10^5, and 1×10^6 cells were transferred to new tubes from the dilutions of 1:100, 1:1000, and 1:10,000, respectively. For each sample, the quantitative value of CD3ε per cell was calculated as the average of nine quantitative values for the y5, y6, and y7 transitions from three different experiments. Quantitative values were correlated with cell numbers ranging from 5000 to 50,000, and the regression line was represented by the equation $y = 0.0005\,x^{1.1}$ ($R^2 = 1.0$; Fig. 2(C)). Our results indicate that the established method has a 100-fold dynamic range with excellent linearity.

The established method measured 0.82 ± 0.06 fmol of CD3ε in 5×10^3 cells in linearity (Fig. 2(C)). This result suggest that the limit of quantification of the established method is femto mol per assay, and that method nearly equaled that of ELISA in sensitivity, the sensitivity of which is approximately 0.1 to 1 fmol.[13)]

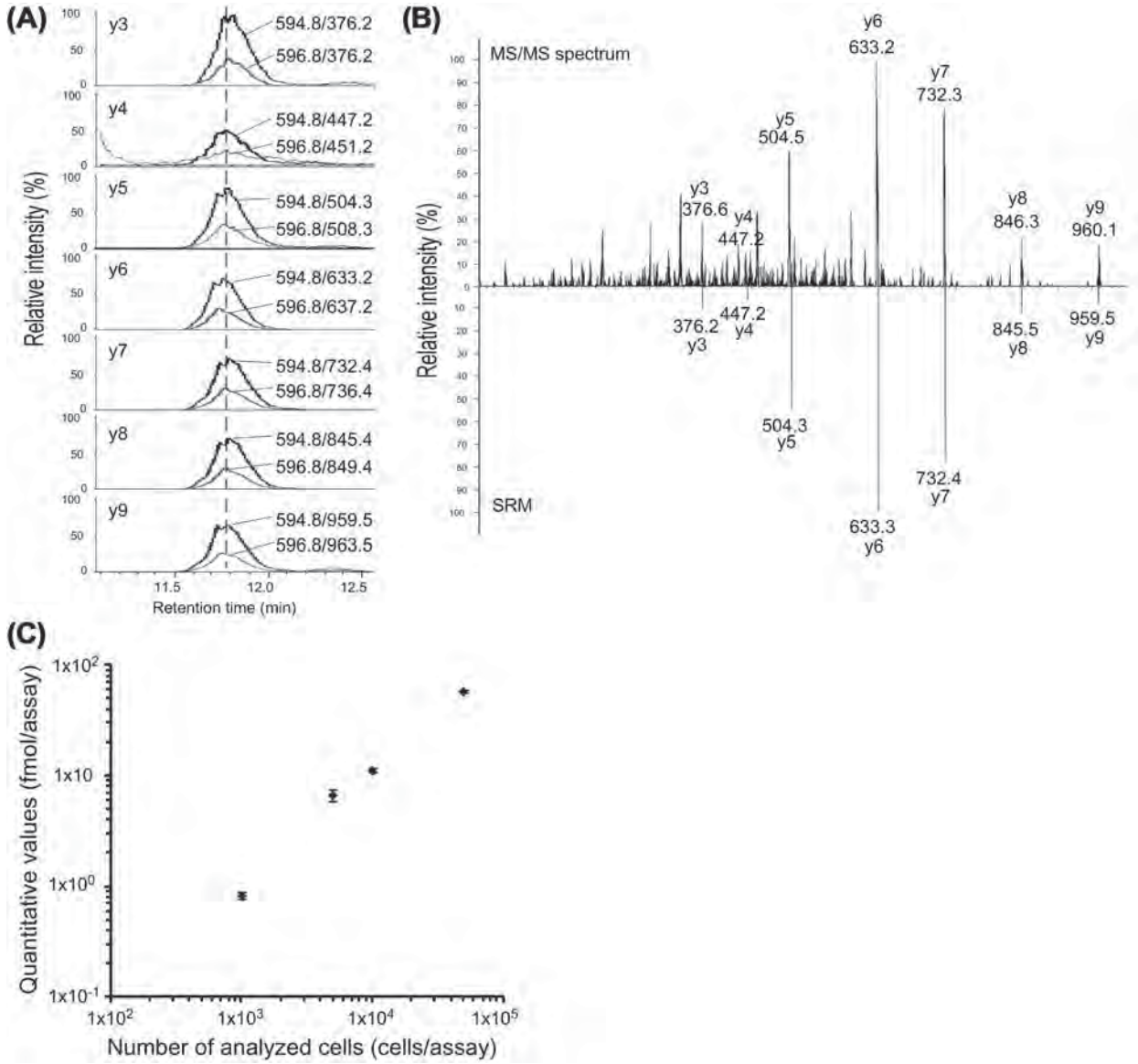

Fig. 2. Relative signal intensities of transitions representing endogenous and stable isotope-labeled CD3ε peptides in cultured cells and linearity of the quantitatively measured CD3ε levels.

Note: Stable isotope-labeled peptide (200 fmol) was spiked into 1 μg of protein from cultured canine cells (A and B) or, a dilution series of the cultured cells (C). LC/MS/MS with SRM transitions was done to quantify endogenous and stable isotope-labeled CD3ε peptides. (A) Chromatograms of transitions for y-series ions derived from endogenous and isotope-labeled peptides. *Y*-axes represent relative signal intensity, and the highest signal intensity in each chromatogram was defined as 100%. (B) Signal intensities of SRM transitions for the NDNLVEGASNR peptide as a spectrum imitation (lower layer) as compared to the corresponding MS/MS spectrum of the doubly charged precursor mass of NDNLVEGASNR peptide (upper layer). *Y*-axes represent relative signal intensity, and the highest signal intensity in each chromatogram was defined as 100%. (C) The amount of CD3ε was determined by the ratio of the peak area of the unlabeled and stable isotope-labeled peptides (unlabeled/labeled) in a dilution series of a cell line. Each point represents the mean value ± SD ($n = 3$).

Table 1. Quantitative values for transitions in 0.1 μg of Protein from cultured canine T-Cell lymphoma.

	Quantitative values (fmol/assay)				
Productions	Assay 1	Assay 2	Assay 3	Mean ± SD	C.V. (%)
y3	11.1	12.0	10.1	11.1 ± 0.94	8.46
y4	7.25	9.49	9.10	8.62 ± 1.20	13.9
y5	8.62	9.30	9.25	9.06 ± 0.38	4.20
y6	8.19	8.62	8.86	8.56 ± 0.34	3.94
y7	8.18	8.63	8.87	8.56 ± 0.35	4.08
y8	7.42	8.58	9.15	8.38 ± 0.88	10.5
y9	7.54	9.75	8.09	8.46 ± 1.15	13.6

We calculated the CD3ε levels per cell that we determined based on three transitions that we replicated in three experiments with a digest of 5000 cells. There was no significant difference (ANOVA, $p > 0.05$) in mean values based on the Q1/Q3 transitions 594.8/504.3, 594.8/633.3, and 594.8/732.4. The calculated values were 1.08, 1.12, and 1.15 amol/cell, respectively. Finally, the amount of protein in each sample was determined to be 1.12 amol/cell with a CV of 1.35% as average of the calculated values for the three transitions. These quantitative results indicate the high sensitivity and reproducibility of the method.

In conclusion, we established a quantitative assay for measuring CD3ε levels by SRM-based mass spectrometry. This assay measured the absolute expression level of CD3ε in a canine T-cell lymphoma cell line. It should be possible to develop quantitative assays for other components of the TCR by the approach described here. In addition, 300 SRM transitions were run in a single analysis by means of one of several modern mass spectrometers. Therefore, it should be possible to develop simultaneous quantitative assays for TCR components by mass spectrometry in the SRM mode. Analysis of the quantitative profiles of components of the TCR should contribute to a better understanding of lymphocyte biology.

Acknowledgments

We would like to thank Ms Ai Uchida and Mr Hirotaka Kawakami for technical assistance. This study was partially supported by a Grant-in-Aid for the development of intellectual property by Azabu University.

References

[1] Alarcon B, Berkhout B, Breitmeyer J, Terhorst C. Assembly of the human T cell receptor-CD3 complex takes place in the endoplasmic reticulum and involves intermediary complexes between the CD3-gamma.delta.epsilon core and single T cell receptor alpha or beta chains. J. Biol. Chem. 1988;263:2953–2961.

[2] San José E, Sahuquillo AG, Bragado R, Alarcón B. Assembly of the TCR/CD3 complex: CD3 epsilon/delta and CD3 epsilon/gamma dimers associate indistinctly with both TCR alpha and TCR beta chains. Evidence for a double TCR heterodimer model. Eur. J. Immunol. 1998;28:12–21.

[3] Minami Y, Weissman AM, Samelson LE, Klausner RD. Building a multichain receptor: synthesis, degradation, and assembly of the T-cell antigen receptor. Proc. Natl. Acad. Sci. USA. 1987;84:2688–2692.

[4] Sancho J, Chatila T, Wong RC, Hall C, Blumberg R, Alarcon B, Geha RS, Terhorst C. T-cell antigen receptor (TCR)-alpha/beta heterodimer formation is a prerequisite for association of CD3-zeta 2 into functionally competent TCR.CD3 complexes. J. Biol. Chem. 1989;264:20760–20769.

[5] Lanier LL, Allison JP, Phillips JH. Correlation of cell surface antigen expression on human thymocytes by multi-color flow cytometric analysis: implications for differentiation. J. Immunol. 1986;137:2501–2507.

[6] Wilson A, MacDonald HR. Expression of genes encoding the pre-TCR and CD3 complex during thymus development. Int. Immunol. 1995;7:1659–1664.

[7] Gygi SP, Rist B, Gerber SA, Turecek F, Gelb MH, Aebersold R. Quantitative analysis of complex protein mixtures using isotope-coded affinity tags. Nat. Biotechnol. 1999;17:994–999.

[8] Ong SE, Foster LJ, Mann M. Mass spectrometric-based approaches in quantitative proteomics. Methods. 2003;29:124–130.

[9] Picotti P, Rinner O, Stallmach R, Dautel F, Farrah T, Domon B, Wenschuh H, Aebersold R. High-throughput generation of selected reaction-monitoring assays for proteins and proteomes. Nat. Methods. 2009;7:43–46.

[10] Kamiie J, Ohtsuki S, Iwase R, Ohmine K, Katsukura Y, Yanai K, Sekine Y, Uchida Y, Ito S, Terasaki T. Quantitative atlas of membrane transporter proteins: development and application of a highly sensitive simultaneous LC/MS/MS method combined with novel in-silico peptide selection criteria. Pharm. Res. 2008;25:1469–1483.

[11] Barnidge DR, Dratz EA, Martin T, Bonilla LE, Moran LB, Lindall A. Absolute quantification of the G protein-coupled receptor rhodopsin by LC/MS/MS using proteolysis product peptides and synthetic peptide standards. Anal. Chem. 2003;75:445–451.

[12] Mawuenyega KG, Kaji H, Yamauchi Y, Shinkawa T, Saito H, Taoka M, Takahashi N, Isobe T. Large-scale identification of Caenorhabditis elegans proteins by multidimensional liquid chromatography-tandem mass spectrometry. J. Proteome Res. 2003;2:23–35.

[13] Harlow ED, Lane D. Antibodies a laboratory manual. New York, NY: Cold Spring Harbor Laboratory Press; 1988. p. 578–583.

NOTE *Virology*

Notch2 Transduction by Feline Leukemia Virus in a Naturally Infected Cat

Shinya WATANABE[1)], Jumpei ITO[2)], Takuya BABA[2)], Takahiro HIRATSUKA[2)], Kyohei KUSE[2)], Haruyo OCHI[2)], Yukari ANAI[2)], Masaharu HISASUE[3)], Hajime TSUJIMOTO[4)] and Kazuo NISHIGAKI[1,2)]*

[1)]*Laboratory of Molecular Immunology and Infectious Disease, United Graduate School of Veterinary Science, Yamaguchi University, 1677–1 Yoshida, Yamaguchi 753–8515, Japan*
[2)]*Laboratory of Molecular Immunology and Infectious Disease, Joint Faculty of Veterinary Medicine, Yamaguchi University, 1677–1 Yoshida, Yamaguchi 753–8515, Japan*
[3)]*Laboratory of Veterinary Internal Medicine II, School of Veterinary Medicine, Azabu University, 1–17–71 Fuchinobe, Chuo-ku, Sagamihara-shi, Kanagawa 252–5201, Japan*
[4)]*Department of Veterinary Internal Medicine, Graduate School of Agricultural and Life Sciences, The University of Tokyo, 1–1–1 Yayoi, Bunkyo-ku, Tokyo 113–8657, Japan*

(Received 3 July 2013/Accepted 25 November 2013/Published online in J-STAGE 9 December 2013)

ABSTRACT. Feline leukemia virus (FeLV) induces neoplastic and nonneoplastic diseases in cats. The transduction of cellular genes by FeLV is sometimes observed and associated with neoplastic diseases including lymphoma and sarcoma. Here, we report the first natural case of feline *Notch2* transduction by FeLV in an infected cat with multicentric lymphoma and hypercalcemia. We cloned recombinant FeLVs harboring *Notch2* in the *env* gene. *Notch2* was able to activate expression of a reporter gene, similar to what was previously reported in cats with experimental FeLV-induced thymic lymphoma. Our findings suggest that the transduction of *Notch2* strongly correlates with FeLV-induced lymphoma.

KEY WORDS: feline leukemia virus, hypercalcemia, lymphoma, *Notch2*, transduction.

doi: 10.1292/jvms.13-0344; *J. Vet. Med. Sci.* 76(4): 553–557, 2014

Feline leukemia virus (FeLV), a gammaretrovirus that can cause a variety of both proliferative and degenerative diseases, is a major pathogen of feline lymphoma [4, 6]. The transduction and activation of cellular proto-oncogenes by FeLV are mechanisms associated with the occurrence of lymphomas and sarcomas. Some recombinant FeLVs harboring cellular sequences, such as the transcription factor *myc* [3, 5, 10, 16, 18–20, 26] and T-cell receptor β chain gene *tcr* [10], have been cloned from cats with naturally occurring lymphoma. FeLV, which transduces the intracellular region of *Notch2*, has been cloned from cats with experimental FeLV-induced thymic lymphoma [24].

Notch2 is a single-spanning transmembrane receptor that belongs to the Notch family of proteins, which play a role in cell differentiation and generation of tumors. The physical contact between cells expressing Notch ligands (e.g., delta-like ligands DLL1, 3 and 4 and Jagged1 and 2) and cells expressing the Notch protein induces proteolytic cleavage of Notch. This leads to release of the intracellular region of Notch into the nucleus, resulting in activation of responsive gene expression [reviewed in 11]. The active forms of Notch receptors have been reported in human patients with lymphoma and leukemia [8, 15, 27, 30]. Here, we report, for the first time, transduction of feline *Notch2* sequence by FeLV (*Notch2*-FeLV) in a naturally infected cat with multicentric lymphoma and hypercalcemia.

A 2-year-old, 2.0-kg, spayed female Japanese domestic cat was referred to the Veterinary Medical Center, The University of Tokyo, in 1995 with consecutive debilitation, dehydration and leanness. The cat was tested positive for FeLV p27-Gag antigen and diagnosed with multicentric lymphoma. Although the tumor had temporally gone into remission after chemotherapy, relapse occurred, and severe hypercalcemia was observed in its blood biochemistry profile (Table 1). Radiography showed extensive calcification in the pulmonary field and concurrent decalcification in the scapula and humerus. Despite treatment with furosemide, infusion of sodium chloride saline, porcine calcitonin (4 IU/kg) and salmon calcitonin (4 IU/kg) for hypercalcemia, little effective palliation was observed, and the cat died with neural manifestations on day 21. Marked invasion of the tumor cells was seen in the multiple tissues at necropsy.

We extracted DNA from the tumor tissue and amplified the entire *env* gene of the FeLV provirus using two PCRs as described previously and employing specific primer pairs (5′-CAT CGA GAT GGA AGG TCC AAC G-3′ (Fe-8S) and 5′-CAT GGT YGG TCY GGA TCG TAT TG-3′(Fe-3R) and 5′-GAG ACC TCT AGC GGC GGC CTA C-3′ (Fe-9S) and 5′-GTC AAC TGG GGA GCC TGG AGA C-3′ (Fe-7R)) [28]. Amplicons were cloned using Zero Blunt PCR Cloning Kit (Invitrogen, Carlsbad, CA, U.S.A.). Two FeLV clones (KeyN2-1 and KeyN2-2) contained feline *Notch2*-like sequences; the nucleotide sequences of the clones were deposited in GenBank under accession numbers AB818695 and AB818696, respectively (Fig. 1). Both sequences contained

*CORRESPONDENCE TO: NISHIGAKI, K., Laboratory of Molecular Immunology and Infectious Disease, Joint Faculty of Veterinary Medicine, Yamaguchi University, 1677–1 Yoshida, Yamaguchi 753–8515, Japan. e-mail: kaz@yamaguchi-u.ac.jp

Table 1. Blood tests for the cat with lymphoma

Complete blood count			Blood biochemistry profile		
	Patient	Reference range		Patient	Reference range
RBC ($\times 10^6/\mu l$)	6.59	5.00–10.00	BUN (mg/d*l*)	45.0	17.6–32.8
Ht (%)	28	24–45	Cre (mg/d*l*)	1.8	0.8–2.4
Hb (g/d*l*)	9.5	8.0–15.0	ALT (U/*l*)	199	12–130
TP (g/d*l*)	6.8	5.7–7.8	ALP (U/*l*)	1	14–111
PLT ($\times 10^3/\mu l$)	95	300–800	LDH (U/*l*)	711	0–798
WBC ($\times 10^3/\mu l$)	15.8	4.9–20.0	Ca (mg/d*l*)	17.3	8.8–11.9
Eos (%)	1	2–10	P (mmol/*l*)	8.0	2.6–6.0
Band (%)	0	0–2	Na (mmol/*l*)	148	147–156
Seg (%)	72	35–75	K (mmol/*l*)	4.2	3.4–4.6
Lym (%)	26	20–55	Cl (mmol/*l*)	115	107–120
Mono (%)	1	1–4			

ALP, alkaline phosphatase; ALT, alanine aminotransferase; Band, banded neutrophil; BUN, blood urea nitrogen; Ca, calcium concentration; Cl, chloride; Cre, creatinine; Eos, eosinophil; RBC, red blood cells; Ht, hematocrit; Hb, hemoglobin; K, potassium; LDH, lactate dehydrogenase; Lym, lymphocyte; Mono, monocyte; Na, sodium; P, phosphate; PLT, platelet; Seg, segmented neutrophil; TP, total protein; WBC, white blood cells.

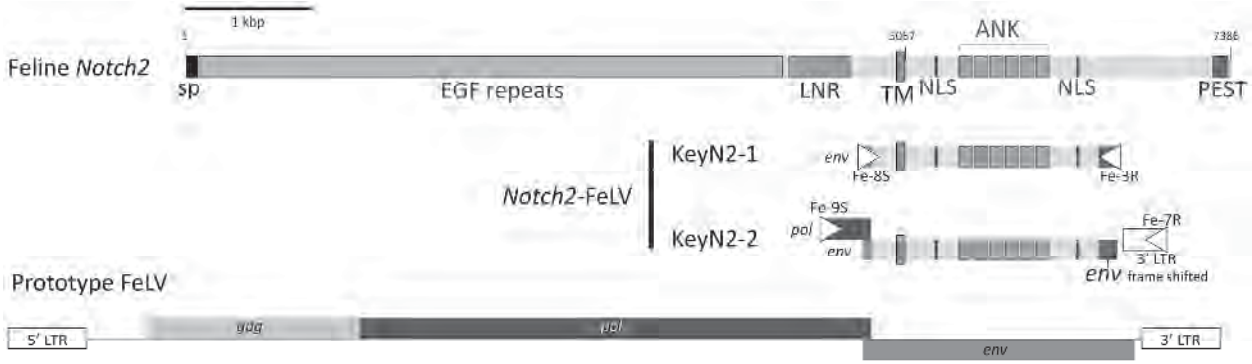

Fig. 1. Genetic structures of *Notch2*-FeLV. Schematic structures of the two clones of *Notch2*-FeLV (KeyN2-1 and KeyN2-2), feline *Notch2* and prototype FeLV provirus. Notch2 contains EGF (blue) and Lin-12-Notch repeats (LNR; pink) in its extracellular region and ANK repeats (orange), two NLSs (green) and proline/glutamic acid/serine/threonine-rich motifs (PEST; purple) in its intracellular region. TM; Notch2 transmembrane. Triangle indicates the primers used for cloning the two *Notch2*-FeLVs. sp, signal peptide.

the same recombinant junctions, along with 5′ and 3′ terminal sequences derived from FeLV *env* gene, and an intracellular region harboring transmembrane (TM) and ankyrin (ANK)-repeats of the feline *Notch2* gene. Both clones had short 23-amino-acid open reading frame (ORF), possibly derived from the FeLV *env* gene (Fig. 2A). A second ORF contained a sequence with a frame-shifted *env* sequence at its C-terminal, and this ORF possibly expresses viral Notch2 (v-Notch2) fusion protein (Fig. 2B). Other researchers have reported similar *Notch2* transduction during experimental infection of cats with FeLV 61E, a cloned virus, and have isolated four clones of *Notch2*-FeLV from two cats [24]. Three recombinants had the same 5′ junctions as those seen in our clones; however, the 3′ junctions were dissimilar. The second ORF of the recombinant v-Notch2 protein is translated by using the internal ribosome entry site (IRES) activity within the TM region of *Notch2* [14]. All variants isolated to date include the intracellular region of *Notch2* with functional ANK repeats and two nuclear location signals (NLSs). Such truncated expression of Notch receptors can lead to the constitutive activation of Notch signaling [reviewed in 12]. Direct repeat sequences of the enhancer or the upstream of the enhancer (URE) [21] were not seen in the LTR of KeyN2-2.

We further analyzed activation of Notch signaling pathway by the v-Notch2 protein using transient luciferase reporter assays. The predicted second ORF of clone KeyN2-2 was amplified by PCR using specific primers (5′-GAG GAT CCA TGG CGA AAC GAA AGC GTA A-3′ (Fe-250S) and 5′-TTG AAT TCT TAC AGG TCT TCT TCA GAG ATC AGT TTC TGT TCG CTG GAA GTC ATG GTT GG-3′ (Fe-223R), tagged with Myc at the C-terminus and then cloned into the pFUΔss expression vector [1]. The v-Notch2 protein was transiently expressed in HEK293T cells using Screen-Fect A (Wako, Osaka, Japan) as manufacturer's instructions (Fig. 3A). Co-transfection of our plasmid with pGa981-6

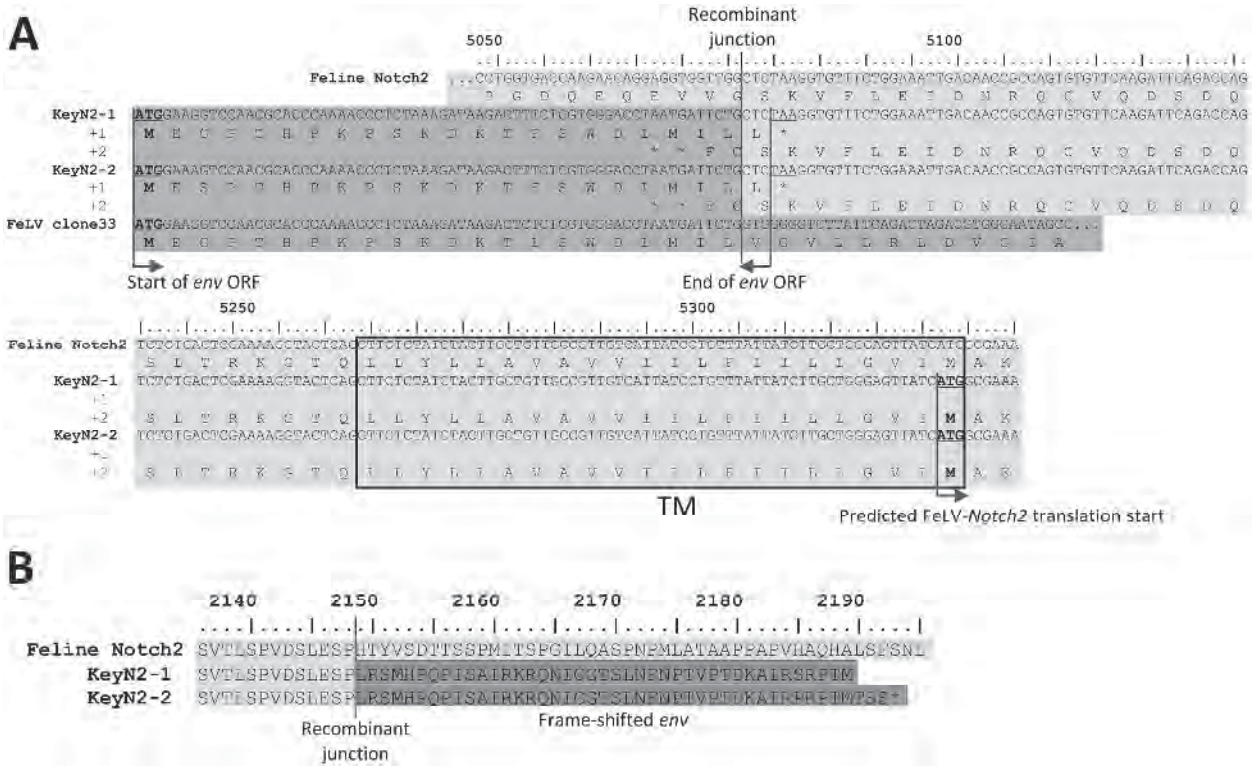

Fig. 2. The sequence alignment of *Notch2*-FeLV recombinant junctions flanking the 5′ (A) and 3′ (B) regions. Predicted start codons of the *env* gene and the recombinant *Notch2* are underlined and in bold. FeLV clone 33 (GenBank accession no. AB060732) [22] was used as a prototype FeLV reference sequence. The reading frame of the 3′ terminus of the *env* gene was frame-shifted (red). *Stop codon. TM; *Notch2* transmembrane.

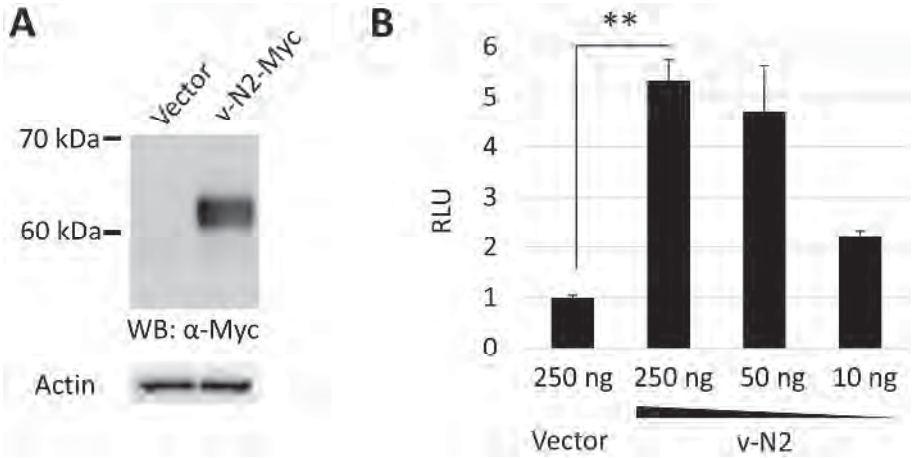

Fig. 3. Expression and activation of v-Notch2 protein. (A) Expression of Myc-tagged v-Notch2 proteins in transiently transfected HEK293T cells. HEK293T cells were transfected with pFUΔss expression vector (vector) [1] or pFUΔss-KeyN2-Myc (v-N2-Myc). Cells were collected after 48 hr, and total cell lysates were subjected to Western blotting analysis using mouse anti-Myc (Wako, Osaka, Japan) or mouse anti-β-Actin antibody (Santa Cruz Biotechnology, Santa Cruz, CA, U.S.A.). (B) HEK293T cells in 24-well plate were co-transfected with pGa981-6 (50 *n*g), phRL-CMV (5 *n*g) and v-Notch2 expressing plasmids (v-N2). Luciferase assay was performed in triplicate, and the relative luciferase activity was measured using Dual-Luciferase Reporter Assay System (Promega) at 48 hr post transfection. The relative luciferase unit (RLU) is shown relative to the negative control (vector). Error bars denote the standard deviation (SD). $^{**}P<0.01$ using unpaired *t*-test.

[13], a firefly luciferase reporter containing the RBP-Jκ binding promoter and phRL-CMV reference plasmid (Promega, Madison, WI, U.S.A.) that constitutively expresses renilla luciferase showed dose-dependent activation of the v-Notch2 protein (Fig. 3B).

Lymphoma and refractory hypercalcemia was observed in our cat. Hypercalcemia is commonly linked to malignancy in dogs and humans, especially in lymphoma [7, 23]. In most cases of feline lymphoma, elevation of the serum calcium concentration or parathyroid hormone-related peptide (PTHrP) is uncommon [2, 25]. Recently, an association between bone metabolism and Notch signaling has been revealed; RANKL-induced association of Notch2 and Jagged1 in pre-osteoclasts can lead to the differentiation into osteoclasts and activates osteoclastgenesis in them through the NF-κB pathway [9, 29]. Our v-Notch2 protein lacked extracellular region of Notch2. Therefore, v-Notch2 likely possesses the potential to activate osteoclastgenesis independent of RANKL stimulation when overexpressed in osteoclast/monocyte lineage cells.

Because of the recombination-prone property of gammaretroviruses, we observed numerous recombination events and various recombinant forms of FeLVs transducing cellular genes, including endogenous FeLV (enFeLV) [28] and ERV-DC [1]. The emergence of such recombinant viruses could alter the disease specificity, potential and outcome in FeLV-infected cats. Additionally, various numbers of proto-oncogenes, which function as a key regulator of proliferation and differentiation, have been historically identified in such recombinant gammaretroviruses. Although Notch2 has been recognized as tumor suppressor in some human tumors [17], transduction of *Notch2* gene seems to be a feasible mechanisms for FeLV-induced lymphomagenesis. Finally, our report may provide a new insight into the relationship between the Notch signaling pathway and humoral hypercalcemia.

ACKNOWLEDGMENTS. The pGa981-6 reporter construct was provided by RIKEN BRC, which participates in the National Bio-Resources Project of the Ministry of Education, Culture, Sports, Science and Technology (MEXT), Japan. This study was supported by a grant from the MEXT, Japan (Grant# 22380168).

REFERENCES

1. Anai, Y., Ochi, H., Watanabe, S., Nakagawa, S., Kawamura, M., Gojobori, T. and Nishigaki, K. 2012. Infectious endogenous retroviruses in cats and emergence of recombinant viruses. *J. Virol.* **86**: 8634–8644. [Medline] [CrossRef]
2. Bolliger, A. P., Graham, P. A., Richard, V., Rosol, T. J., Nachreiner, R. F. and Refsal, K. R. 2002. Detection of parathyroid hormone − related protein in cats with humoral hypercalcemia of malignancy. *Vet. Clin. Pathol.* **31**: 3–8. [Medline] [CrossRef]
3. Braun, M. J., Deininger, P. L. and Casey, J. W. 1985. Nucleotide sequence of a transduced *myc* gene from a defective feline leukemia provirus. *J. Virol.* **55**: 177–183. [Medline]
4. Cotter, S. M. 1992. Feline leukemia virus: Pathophysiology, prevention, and treatment. *Cancer Invest.* **10**: 173–181. [Medline] [CrossRef]
5. Doggett, D. L., Drake, A. L., Hirsch, V., Rowe, M. E., Stallard, V. and Mullins, J. I. 1989. Structure, origin, and transforming activity of feline leukemia virus-*myc* recombinant provirus FTT. *J. Virol.* **63**: 2108–2117. [Medline]
6. Dorn, C. R., Taylor, D. O. and Hibbard, H. H. 1967. Epizootiologic characteristics of canine and feline leukemia and lymphoma. *Am. J. Vet. Res.* **28**: 993–1001. [Medline]
7. Elliott, J., Dobson, J. M., Dunn, J. K., Herrtage, M. E. and Jackson, K. F. 1991. Hypercalcaemia in the dog: A study of 40 cases. *J. Small Anim. Pract.* **32**: 564–571. [CrossRef]
8. Ellisen, L. W., Bird, J., West, D. C., Soreng, A. L., Reynolds, T. C., Smith, S. D. and Sklar, J. 1991. TAN-l, the human homolog of the Drosophila Notch gene, is broken by chromosomal translocations in T lymphoblastic neoplasms. *Cell* **66**: 649–661. [Medline] [CrossRef]
9. Fukushima, H., Nakao, A., Okamoto, F., Shin, M., Kajiya, H., Sakano, S., Bigas, A., Jimi, E. and Okabe, K. 2008. The association of Notch2 and NF-kappaB accelerates RANKL-induced osteoclastogenesis. *Mol. Cell. Biol.* **28**: 6402–6412. [Medline] [CrossRef]
10. Fulton, R., Forrest, D., McFarlane, R., Onions, D. and Neil, J. C. 1987. Retroviral transduction of T-cell antigen receptor beta-chain and *myc* genes. *Nature* **326**: 190–194. [Medline] [CrossRef]
11. Greenwald, I. 1994. Structure/function studies of lin-12/Notch proteins. *Curr. Opin. Genet. Dev.* **4**: 556–562. [Medline] [CrossRef]
12. Kopan, R. and Ilagan, M. X. G. 2009. The canonical Notch signaling pathway: unfolding the activation mechanism. *Cell* **137**: 216–233. [Medline] [CrossRef]
13. Kurooka, H., Kuroda, K. and Honjo, T. 1998. Roles of the ankyrin repeats and C-terminal region of the mouse notch1 intracellular region. *Nucl. Acids Res.* **26**: 5448–5455. [Medline] [CrossRef]
14. Lauring, A. S. and Overbaugh, J. 2000. Evidence that an IRES within the Notch2 Coding Region Can Direct Expression of a Nuclear Form of the Protein. *Mol. Cell Biol.* **6**: 939–945. [Medline] [CrossRef]
15. Lee, S., Kumano, K., Nakazaki, K., Sanada, M., Matsumoto, A., Yamamoto, G., Nannya, Y., Suzuki, R., Ota, S., Ota, Y., Izutsu, K., Sakata-Yanagimoto, M., Hangaishi, A., Yagita, H., Fukayama, M., Seto, M., Kurokawa, M., Ogawa, S. and Chiba, S. 2009. Gain-of-function mutations and copy number increases of Notch2 in diffuse large B-cell lymphoma. *Cancer Sci.* **100**: 920–926. [Medline] [CrossRef]
16. Levy, L. S., Gardner, M. B. and Casey, J. W. 1984. Isolation of a feline leukaemia provirus containing the oncogene *myc* from a feline lymphosarcoma. *Nature* **308**: 853–856. [Medline] [CrossRef]
17. Lobry, C., Oh, P. and Aifantis, I. 2011. Oncogenic and tumor suppressor functions of Notch in cancer: it's NOTCH what you think. *J. Exp. Med.* **208**: 1931–1935. [Medline] [CrossRef]
18. Mullins, J. I., Brody, D. S., Binari, R. C. Jr. and Cotter, S. M. 1984. Viral transduction of c-*myc* gene in naturally occurring feline leukaemias. *Nature* **308**: 856–858. [Medline] [CrossRef]
19. Neil, J. C., Forrest, D., Doggett, D. L. and Mullins, J. I. 1987. The role of feline leukaemia virus in naturally occurring leukaemias. *Cancer Surv.* **6**: 117–137. [Medline]
20. Neil, J. C., Hughes, D., McFarlane, R., Wilkie, N. M., Onions, D. E., Lees, G. and Jarrett, O. 1984. Transduction and rearrangement of the *myc* gene by feline leukaemia virus in naturally occurring T-cell leukaemias. *Nature* **308**: 814–820. [Medline]

[CrossRef]
21. Nishigaki, K., Okuda, M., Endo, Y., Watari, T., Tsujimoto, H. and Hasegawa, A. 1997. Structure and function of the long terminal repeats of feline leukemia viruses derived from naturally occurring acute myeloid leukemias in cats. *J. Virol.* **71**: 9823–9827. [Medline]
22. Nishigaki, K., Hanson, C., Thompson, D., Yugawa, T., Hisasue, M., Tsujimoto, H. and Ruscetti, S. K. 2002. Analysis of the disease potential of a recombinant retrovirus containing Friend murine leukemia virus sequences and a unique long terminal repeat from feline leukemia virus. *J. Virol.* **76**: 1527–1532. [Medline] [CrossRef]
23. Potts, J. T. 1996. Hyperparathyroidism and other hypercalcemic disorders. *Adv. Intern. Med.* **41**: 165–212. [Medline]
24. Rohn, J. L., Lauring, A. S., Linenberger, M. L. and Overbaugh, J. 1996. Transduction of Notch2 in feline leukemia virus-induced thymic lymphoma. *J. Virol.* **70**: 8071–8080. [Medline]
25. Savary, K. C., Price, G. S. and Vaden, S. L. 2000. Hypercalcemia in cats: a retrospective study of 71 cases (1991–1997). *J. Vet. Intern. Med.* **14**: 184–189. [Medline]
26. Stewart, M. A., Forrest, D., McFarlane, R., Onions, D., Wilkie, N. and Neil, J. C. 1986. Conservation of the c-*myc* coding sequence in transduced feline v-*myc* genes. *Virology* **154**: 121–134. [Medline] [CrossRef]
27. Trøen, G., Wlodarska, I., Warsame, A., Hernández Llodrà, S., De Wolf-Peeters, C. and Delabie, J. 2008. NOTCH2 mutations in marginal zone lymphoma. *Haematologica* **93**: 1107–1109. [Medline] [CrossRef]
28. Watanabe, S., Kawamura, M., Odahara, Y., Anai, Y., Ochi, H., Nakagawa, S., Endo, Y., Tsujimoto, H. and Nishigaki, K. 2013. Evolutionary dynamics of the feline leukemia virus: phylogenetic and structural diversity in the *env* gene. *PLoS one* **8**: e61009. [Medline] [CrossRef]
29. Weber, J. M., Forsythe, S. R., Christianson, C. A., Frisch, B. J., Gigliotti, B. J., Jordan, C. T., Milner, L. A., Guzman, M. L. and Calvi, L. M. 2006. Parathyroid hormone stimulates expression of the Notch ligand Jagged1 in osteoblastic cells. *Bone* **39**: 485–493. [Medline] [CrossRef]
30. Weng, A. P., Ferrando, A. A., Lee, W., Morris, J. P., Silverman, L. B., Sanchez-Irizarry, C., Blacklow, S. C., Look, A. T. and Aster, J. C. 2004. Activating mutations of NOTCH1 in human T cell acute lymphoblastic leukemia. *Science* **306**: 269–271. [Medline] [CrossRef]

NOTE *Clinical Pathology*

Identification of Cell Surface Antigen Expression in Canine Hepatocellular Carcinoma Cell Lines

Ayumi FUJIMOTO[1)], Sakurako NEO[1)], Chinatsu ISHIZUKA[1)], Takashi KATO[1)], Kazuhito SEGAWA[1)], Shinpei KAWARAI[2)], Kikumi OGIHARA[3)], Masaharu HISASUE[1)]* and Ryo TSUCHIYA[1)]

[1)]*Laboratory of Veterinary Internal Medicine II, School of Veterinary Medicine, Azabu University, 1–17–71 Fuchinobe, Chuoku, Sagamihara, Kanagawa 252–5201, Japan*
[2)]*Department of Veterinary Teaching Hospital, School of Life and Environmental Science, Azabu University, 1–17–71 Fuchinobe, Chuoku, Sagamihara, Kanagawa 252–5201, Japan*
[3)]*Laboratory of Pathology, School of Life and Environmental Science, Azabu University, 1–17–71 Fuchinobe, Chuoku, Sagamihara, Kanagawa 252–5201, Japan*

(Received 17 December 2012/Accepted 30 January 2013/Published online in J-STAGE 13 February 2013)

ABSTRACT. The characteristics of surface antigens in canine hepatocellular carcinoma (cHCC) have not been clarified. The objective of this study was to investigate surface antigens, which are considered as stem/progenitor or cancer cell markers, in cHCC cell lines. Expression of various antigens including CD29, CD34, CD44, CD90, CD133 and Dlk-1 was assessed in four cHCC cell lines by flow cytometry. CD44, CD133 and Dlk-1 expression was detectable in all cell lines, and three cell lines expressed CD29. These results indicate that CD29, CD44, CD133 and Dlk-1 have potential as suitable markers in cHCC identification, suggesting that these findings will contribute to the establishment of an early diagnostic tool for the identification of hepatocellular maturation processes.

KEY WORDS: canine, hepatocellular carcinoma, liver, stem cell, tumor marker.

doi: 10.1292/jvms.12-0549; *J. Vet. Med. Sci.* 75(6): 831–835, 2013

Canine hepatocellular carcinoma (cHCC) is an uncommon condition, accounting for <1% of all canine tumors. However, cHCC is the most common primary liver tumor, accounting for 50% of cases [13]. To date, no breed and sex predisposition has been confirmed for cHCC, but male dogs and dogs in general aged >10 years are over-represented in some studies [6, 9, 12]. Clinical signs of hepatic tumors are non-specific, mostly indiscernible from those of other liver diseases. Hepatic tumors are usually recognized only in the advanced stages or when metastasis has already been established. Characterization of hepatic progenitor cells (HPCs) is one of the key parameters in understanding the cellular mechanisms involved in tumorigenesis, along with the establishment of early diagnostic tools and the development of a therapeutic method. In human medicine, it is widely accepted that cancer cells arise from stem/progenitor cells, as these are the only single cells persisting in tissues for sufficient time to acquire the requisite number of genetic changes for neoplastic development [1]. Although it has been reported that various antigens expressed in liver stem/progenitor cells match with hepatocellular carcinoma (HCC) cell surface markers, including cancer stem cells, controversy continues in regard to the biological significance and specificity of various antigens in liver tissue [8]. Furthermore, identification of hepatic stem/progenitor cells is required to perform analysis of hepatocyte differentiation and maturation. Hepatic stem and/or progenitor cells not only play a pivotal role in liver regeneration but are also able to accumulate mutations in the target genes, resulting in malignant transformation [3].

In human medicine, HPCs can be more easily identified on the basis of their expression of immunohistochemical markers including CD13, CD44, CD90, CD133, epithelial cell adhesion molecule and OV6 [10]. However, research on the identification of stem/progenitor cell markers in cHCC is limited [4]. Cogliati *et al.* reported that CD44 and keratin 19 were expressed in most cHCC cases, while CD133 was expressed in some cases [4]. The usefulness of these markers has not been investigated, and analytical research into other HCC-specific antigens, including cancer stem cells and hepatocellular stem/progenitor cell markers, has not been conducted. Alison maintained that the rodent counterparts to HPCs described in human models are often referred to as oval cells, which express certain antigens traditionally associated with hematopoietic cells (CD34, c-kit, flt-3 and Thy-1) [1]. The informtaion of expressing antigens in cHCC cell line may be helpful to select specific antigens in cHCC tissue, and it will contribute to the diagnosis of cHCC using immunohistochemistry of biopsy samples obtained from clinical case. In the present study, we investigated the expression level of some surface antigens recognized as tumor makers in four cHCC cell lines (930-599A, 95-0112, 95-1044 and CHKS-rL) by flow cytometry.

All tumors were removed from dogs with cHCC and diagnosed histologically. 95-0112 was established after transplantation to Rowett nude rats and cultured through >30 passages, whereas 930-599A and 95-1044 were cul-

*CORRESPONDENCE TO: HISASUE, M., Laboratory of Veterinary Internal Medicine II, School of Veterinary Medicine, Azabu University, 1–17–71 Fuchinobe, Chuoku, Sagamihara, Kanagawa 252–5201, Japan.
e-mail: hisasue@azabu-u.ac.jp

tured through >200 passages. A CHKS-rL cell line secreting α-fetoprotein has been established and reported previously [7]. All cell lines were grown in Isocove's modified Dulbecco's medium (Gibco Brl, Tokyo, Japan) supplemented with 10% fetal bovine serum, 5,000 units/*l* penicillin, 50 mg/*l* streptomycin (Gibco Brl) and 2 mmol/*l* L-glutamine (Sigma, St. Louis, MO, U.S.A.) in 100-mm non-coated plastic dishes at 37°C in a 5% CO_2 humidified incubator. Morphological characters were as follows: 930-599A cells had spindle-shaped cytoplasm; 95-0112 cells had flattened, polygonal cytoplasm and some projections, and cell–cell adherence was not recognized; 95-1044 cells had spindle-shaped cytoplasm with tight cell–cell junctions and cell–matrix adherence; and CHKS-rL cells were of polygonal shape with strong cell–cell adherence and rounded nuclei (Fig. 1). The medium was changed every 3 days, and cells were used for flow cytometry analysis after 3–5 passages from the start of culture.

Liver tissue from 3 adult dogs was used for analysis of the mature hepatocyte population. The left lateral lobe (approximately 30 g) was surgically removed from clinically healthy 1-year-old beagles under anesthesia with atropine (0.05 mg/kg SC), propofol (8 mg/kg IV) and isoflurane. All experiments were conducted with humane care and in compliance with the guidelines of Azabu University for the treatment of experimental animals (100323-1). The portal branch was cannulated and perfused with 300 m*l* of Ca^{2+}- and Mg^{2+}-free Hanks' buffered salt solution supplemented with HEPES (2.38 g/*l*) and EGTA (0.19 g/*l*). Tissues were then incubated at 37°C for 20 min with a perfusate of 300 m*l* collagenase solution [(Hanks' buffered salt solution supplemented with HEPES (2.38g/*l*) and $CaCl_2$ (0.56 g/*l*)]. The digested tissue was perfused again with the addition of 300 m*l* serum-free Dulbecco's modified Eagle's medium (Gibco Brl), and the cell suspension was collected. The cells were centrifuged at 50 ×*g* for 3 min, and the separated hepatocytes were used for flow cytometry analysis.

The samples were adjusted to a density of 1×10^7/m*l* and incubated at 4°C for 30 min with monoclonal antibodies, which were diluted ×50 in phosphate-buffered saline. Antibodies used were as follows: CD29 (PE-conjugated mouse anti-human CD29, $IgG_{1,\kappa}$, 303004; BioLegend, San Diego, CA, U.S.A.); CD34 (PE-conjugated mouse anti-canine CD34, $IgG_{1,\kappa}$, 559369; BD Biosciences, San Diego, CA, U.S.A.); CD44 (PE-conjugated rat anti-mouse/human CD44, $IgG_{2b,\kappa}$, 103008; BioLegend); CD90 (Thy-1) (PE-conjugated rat anti-canine CD90, $IgG_{2b,\kappa}$, 12-5900; eBioscience, San Diego, CA, U.S.A.); CD133 (PE-conjugated rat anti-mouse CD133, $IgG_{1,\kappa}$, 12-1331; eBioscience) and Dlk-1 (FITC-conjugated rat anti-mouse Dlk-1, IgG_1, D187-4; MBL, Nagoya, Japan). Isotype-matched immunoglobulins serving as negative controls were as follows: PE-labeled mouse $IgG_{1,\kappa}$ (550617; BD Biosciences) for CD29 and CD34; PE-labeled rat $IgG_{2b,\kappa}$ (556925; BD Biosciences) for CD44 and CD90; PE-labeled rat $IgG_{1,\kappa}$ (12-4301; eBioscience) for CD133 and FITC-labeled rat IgG_1 (M080-4; MBL) for Dlk. Samples were analyzed using an EC800 cell analyzer (SONY, Tokyo, Japan) and Flowjo 7.6.3 software (TreeStar, Ashland, OR, U.S.A.). A positive result was defined as fluorescence values >10%, and high, moderate and low levels were defined as those >70, 40 and 10%, respectively. All experiments were conducted independently and in triplicate. Statistical analysis was performed using EXCEL (Microsoft) and add-in software EXCEL Toukei (Social Survey Research Information). Data regarding expression of surface antigens on mature hepatocytes are expressed as mean ± standard deviation.

All four cHCC cell lines expressed CD44, CD133 and Dlk-1 (Fig. 2 and Table 1). Marked CD29 expression was detected in 930-599A, 95-1044 and CHKS-rL (99.30, 84.43 and 94.30%, respectively), but 95-0112 did not express this antigen (1.88%). All cell lines did not express CD34, with the range of the expression level being between 0.13 and 5.04%. Markedly high CD44 expression was detected in 930-599A, 95-0112 and CHKS-rL (98.87, 78.90 and 86.63%, respectively), while a low expression level was observed in 95-1044 (29.07%). CD90 expression was detectable in 930-599A alone, but at a high level (98.57%). CD133 was moderately expressed in 930-599A (57.53%), but was expressed at low levels in 95-0112, 95-1044 and CHKS-rL (20.97, 34.67 and 19.70%, respectively). Dlk-1 was highly expressed in 930-599A (86.50%), but at low levels in 95-0112, 95-1044 and CHKS-rL (20.90, 26.43 and 21.17%, respectively). Expression of all surface antigens on mature hepatocytes of liver tissue derived from normal healthy dogs was recorded at very low levels (n=3; range, 2.16 ± 0.02 to 7.75 ± 0.09%).

In this study, CD44, CD133 and Dlk-1 were expressed in all cHCC cell lines, but not in normal hepatocytes. All cell lines showed high expression of CD44, a member of the family of transmembrane glycoproteins. This finding is relatively consistent with that of cHCC studies, indicating that $CD44^+$ cell populations are involved as stem/progenitor cells [4, 10, 22]. One recent study indicated that CD44 is a specific marker for small or immature hepatocytes, with 61.6% of cHCC cases showing immature $CD44^+$ hepatocytes [4]. Interestingly, expression of CD133, a surface antigen of hematopoietic stem cells, was observed in cHCC. In addition, another recent study demonstrated that hepatocellular cancer stem cells expressed CD133, and the $CD133^+$ population had both *in vitro* and *in vivo* tumourigenic potential [11, 15]. Indeed, when Cogliati *et al.* investigated CD133 expression among cHCC cases, only two (15.8%) showed a high expression level [4]. We suspect that the low CD133 expression level in the present study was caused by the method of immunohistochemical analysis used, because antigen-specific reactivity decreased by less than that measured by flow cytometry. Dlk-1, a transmembrane-secreted protein with epidermal growth factor-like repeats, was identified as a hepatic stem/progenitor cell marker, and in the present study, it was expressed among all cell lines analyzed. This surface antigen was found to be associated with early liver tissue development, because it was strongly expressed in mouse fetal liver between E10.5 and E16.5 and decreased in adult liver tissue [17]. Furthermore, Yanai *et al.* reported that Dlk-1 was expressed in 79 of 386 cases (20.5%) of HCC according to immunohistochemical analysis [21].

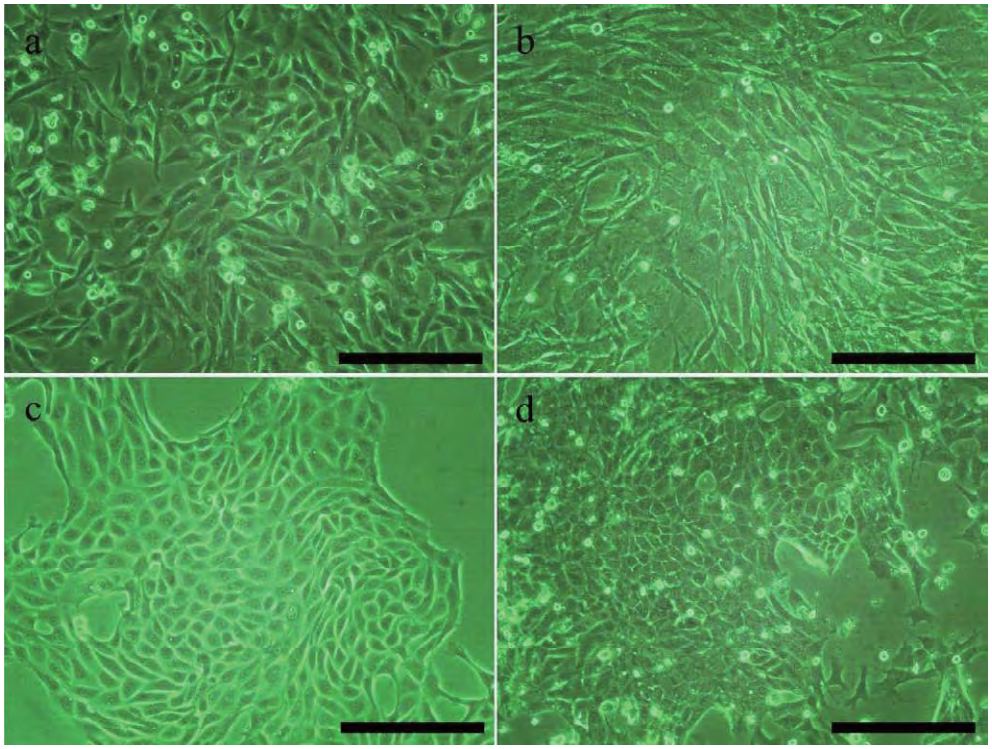

Fig. 1. Morphology of cHCC cell lines. 930-599A (a), 95-0112 (b), 95-1044 (c) and CHKS-rL (d) were used for flow cytometry analysis in cell cultures that reached 70–80% confluency after 3–5 passages. Bar=50 μm.

In the present study, 3 of 4 cell lines showed high CD29 expression, suggesting that this might be a progenitor surface marker for canine liver tissue. CD29 (β-integrin) is a cell surface adhesion receptor; integrin is composed of α and β subunits, which mediate the cell–extracellular matrix and cell–cell interactions. In particular, β-integrin transduces biochemical signals from the extracellular environment, mainly with respect to growth, differentiation, invasiveness and metastatic aspects of malignant cells. Suzuki *et al*. demonstrated that fetal mouse liver cell populations expressing CD29 and CD49f differentiated to form colonies containing mature hepatocytes and cholangiocytes, indicating that these markers have potential as hepatic stem cell markers [16]. Furthermore, we noted that CD29 was expressed in regenerative liver tissue after hepatectomy, and this marker has shown potential as a stem/progenitor cell marker (data not shown).

The presence of $CD90^+$ cells was found to be associated with a high incidence of distant organ metastasis, suggesting that CD90 is a cancer stem cell surface antigen [20]. In this study, only cell line 930-599A strongly expressed CD90, while expression was absent in the other cell lines investigated. However, because the proportion of cancer stem cells involved in HCC is relatively low, further analysis will be required to elucidate whether CD90 is suitable for the purpose of determining cHCC stem cells. In addition, Arends *et al.* reported that progenitor cells derived from healthy mature canine liver expressed CD90, suggesting its potential as a progenitor cell marker [2]. Therefore, further investigation will be needed to measure CD90 expression in hepatic cancer stem cells.

CD34, a hematopoietic stem cell antigen that is also considered a stem cell marker, was not expressed among all cell lines studied, suggesting that it would not be a suitable marker in cHCC identification. Some studies reported that CD34 was found to be valuable in distinguishing HCC from metastatic neoplasms [14, 18]. However, Saad *et al.* reported $CD34^+$ sinusoidal endothelial cells in 27/30 (90%) cases of human HCC, but this antigen was either not or poorly expressed in human normal liver tissue [14]. Conigliaro *et al.* demonstrated that murine liver stem cells are Sca^+, $CD34^-$, $CD45^-$, α-fetoprotein$^+$ and albumin$^-$, suggesting that hepatic stem/progenitor cells have a non-hematopoietic origin [5]. The present study findings indicate that CD34 may not be specific to cHCC.

There is a possibility that CD29, CD44, CD133 and Dlk-1 are expressed only in situations where liver regeneration is enhanced, as α-fetoprotein [19], when it might be difficult to distinguish between tumor and normal tissue using only these antigens. In the present study, these surface antigens were not assessed in liver tissue after hepatectomy or hepatitis, and further research is required to determine appropriate cancer cell markers. The biological significance and pathogenic role of these antigens were not investigated in this study. Furthermore, the expression of surface antigens in cHCC cell lines may be transformed by abundant repeated

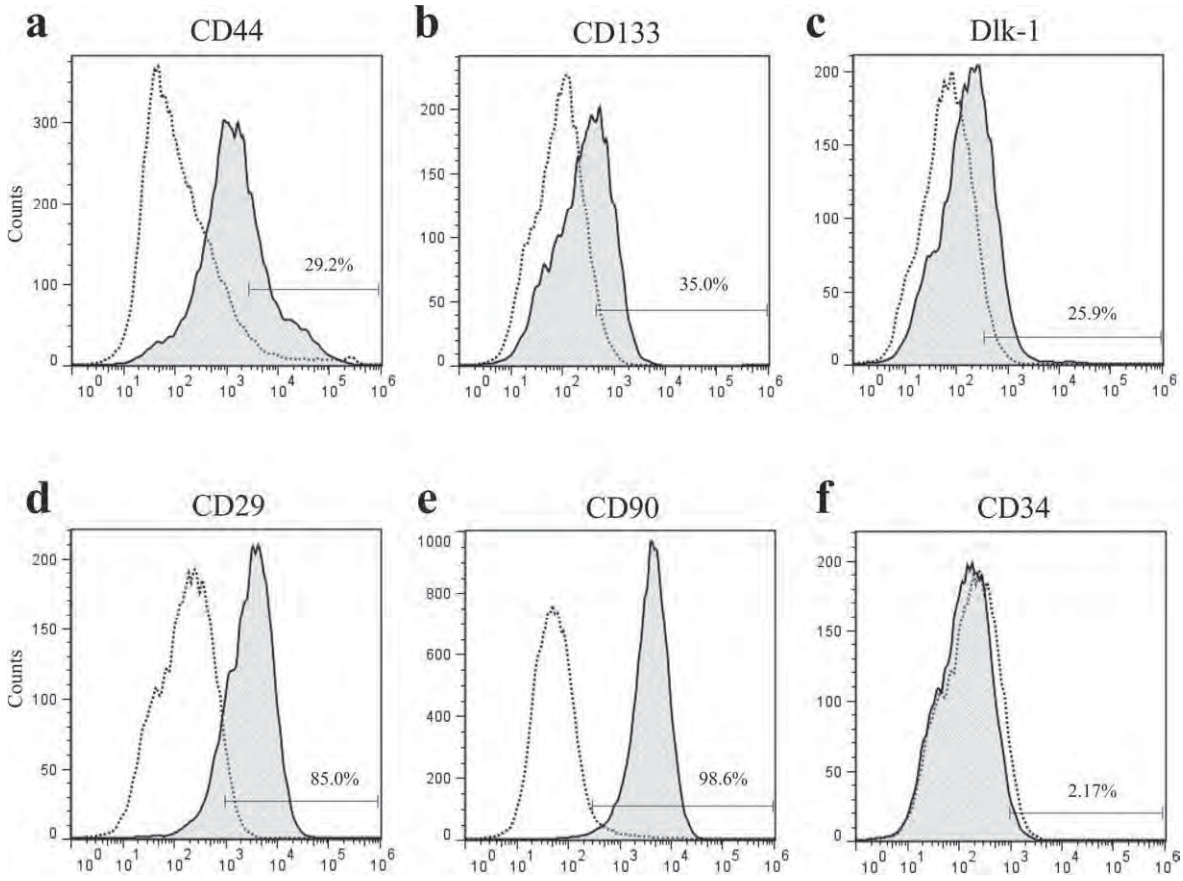

Fig. 2. Flow cytometry was performed to analyze the expression of CD29, CD34, CD44, CD90, CD133 and Dlk-1 in four cHCC cell lines: 930-599A, 95-0112, 95-1044 and CHKS-rL. The expression of PE-labelled CD44 (a), PE-labelled CD133 (b), FITC-labelled Dlk-1 (c), PE-labelled CD29 (d) and PE-labelled CD34 (f) in 95-1044. PE-labelled CD90 was expressed only in 930-599A (e). Broken line, isotype control; solid line, cHCC cell lines.

Table 1. Expression status of surface antigens in cHCC cell lines and hepatocyte

	930-599A	95-0112	95-1044	CHKS-rL	Hepatocyte
CD44	98.87%	78.90%	29.07%	86.63%	7.75 ± 0.09%
CD133	57.53%	20.97%	34.67%	19.70%	4.00 ± 0.04%
Dlk-1	86.50%	20.90%	26.43%	21.17%	3.01 ± 0.02%
CD29	99.30%	1.88%	84.43%	94.30%	2.46 ± 0.02%
CD90	98.57%	1.62%	0.67%	1.79%	2.16 ± 0.02%
CD34	0.13%	1.36%	2.81%	5.04%	2.66 ± 0.02%

passage *in vitro*. In particular, transplantation experiment and characterization of cell populations established using these antigens are expected to clarify the biological significance, and investigation of gene m-RNA/protein expression of other oncogenes, transcription factors and factors associated with hepatocyte differentiation/maturation will be required.

In conclusion, CD29, CD44, CD133 and Dlk-1 were expressed in cHCC cell lines, suggesting that these surface markers have potential as diagnostic tools and will be helpful in cHCC characterization. In addition, they have the potential to detect hepatocellular stem/progenitor cells in canine, similar to those in humans. We expect that evaluation of expression of these markers in biopsy samples may be helpful in establishing cHCC diagnosis. However, to determine the usefulness of this diagnostic tool in veterinary clinical pathology, the sensitivity and specificity of these antigens should be investigated among cHCC, hepatitis and hyperplastic tissues from clinical cases.

ACKNOWLEDGMENTS. This study was supported by the Science Research Promotion Fund of the Promotion and Mutual Aid Corporation for Private Schools of Japan and a Grant-in-Aid for Matching Fund Subsidy for Private Universities.

REFERENCES

1. Alison, M. R. 2005. Liver stem cells: implications for hepatocarcinogenesis. *Stem Cell Rev.* **1**: 253–260. [Medline] [CrossRef]
2. Arends, B., Spee, B., Schotanus, B. A., Roskams, T., Van den Ingh, T. S., Penning, L. C. and Rothuizen, J. 2009. *In vitro* differentiation of liver progenitor cells derived from healthy dog livers. *Stem Cells Dev.* **18**: 351–358. [Medline] [CrossRef]
3. Chiba, T., Zheng, Y. W., Kita, K., Yokosuka, O., Saisho, H., Onodera, M., Miyoshi, H., Nakano, M., Zen, Y., Nakanuma, Y., Nakauchi, H., Iwama, A. and Taniguchi, H. 2007. Enhanced self-renewal capability in hepatic stem/progenitor cells drives cancer initiation. *Gastroenterology* **133**: 937–950. [Medline] [CrossRef]
4. Cogliati, B., Aloia, T. P., Bosch, R. V., Alves, V. A., Hernandez-Blazquez, F. J. and Dagli, M. L. 2010. Identification of hepatic stem/progenitor cells in canine hepatocellular and cholangiocellular carcinoma. *Vet. Comp. Oncol.* **8**: 112–121. [Medline] [CrossRef]
5. Conigliaro, A., Colletti, M., Cicchini, C., Guerra, M. T., Manfredini, R., Zini, R., Bordoni, V., Siepi, F., Leopizzi, M., Tripodi, M. and Amicone, L. 2008. Isolation and characterization of a murine resident liver stem cell. *Cell Death Differ.* **15**: 123–133. [Medline] [CrossRef]
6. Evans, S. M. 1987. The radiographic appearance of primary liver neoplasia in dogs. *Vet. Radiol.* **28**: 192–196. [CrossRef]
7. Kawarai, S., Hashizaki, K., Kitao, S., Nagano, S., Madarame, H., Neo, S., Ishikawa, T., Furuichi, M., Hisasue, M., Tsuchiya, R., Tsujimoto, H. and Yamada, T. 2006. Establishment and characterization of primary canine hepatocellular carcinoma cell lines producing alpha-fetoprotein. *Vet. Immunol. Immunopathol.* **113**: 30–36. [Medline] [CrossRef]
8. Knight, B., Tirnitz-Parker, J. E. and Olynyk, J. K. 2008. C-kit inhibition by imatinib mesylate attenuates progenitor cell expansion and inhibits liver tumor formation in mice. *Gastroenterology* **135**: 969–979. [Medline] [CrossRef]
9. Liptak, J. M., Dernell, W. S., Monnet, E., Powers, B. E., Bachand, A. M., Kenney, J. G. and Withrow, S. J. 2004. Massive hepatocellular carcinoma in dogs: 48 cases (1992–2002). *J. Am. Vet. Med. Assoc.* **225**: 1225–1230. [Medline] [CrossRef]
10. Liu, L. L., Fu, D., Ma, Y. and Shen, X. Z. 2011. The power and the promise of liver cancer stem cell makers. *Stem Cells Dev.* **20**: 2023–2030. [Medline] [CrossRef]
11. Ma, S., Chan, K. W., Hu, L., Lee, T. K., Wo, J. Y., Ng, I. O., Zheng, B. J. and Guan, X. Y. 2007. Identification and characterization of tumorigenic liver cancer stem/progenitor cells. *Gastroenterology* **132**: 2542–2556. [Medline] [CrossRef]
12. Patnaik, A. K., Hurvitz, A. I. and Lieberman, P. H. 1980. Canine hepatic neoplasms: a clinicopathologic study. *Vet. Pathol.* **17**: 553–564. [Medline] [CrossRef]
13. Patnaik, A. K., Hurvitz, A. I., Lieberman, P. H. and Johnson, G. F. 1981. Canine hepatocellular carcinoma. *Vet. Pathol.* **18**: 427–438. [Medline]
14. Saad, R. S., Luckasevic, T. M., Noga, C. M., Johnson, D. R., Silverman, J. F. and Liu, Y. L. 2004. Diagnostic value of HepPar1, pCEA, CD10, and CD34 expression in separating hepatocellular carcinoma from metastatic carcinoma in fine-needle aspiration cytology. *Diagn. Cytopathol.* **30**: 1–6. [Medline] [CrossRef]
15. Suetsugu, A., Osawa, Y., Nagaki, M., Moriwaki, H., Saji, S., Bouvet, M. and Hoffman, R. M. 2010. Simultaneous color-coded imaging to distinguish cancer "stem-like" and non-stem cells in the same tumor. *J. Cell. Biochem.* **111**: 1035–1041. [Medline] [CrossRef]
16. Suzuki, A., Zheng, Y., Kondo, R., Kusakabe, M., Takada, Y., Fukao, K., Nakauchi, H. and Taniguchi, H. 2000. Flow-cytometric separation and enrichment of hepatic progenitor cells in the developing mouse liver. *Hepatology* **32**: 1230–1239. [Medline] [CrossRef]
17. Tanimizu, N., Nishikawa, M., Saito, H., Tsujimura, T. and Miyajima, A. 2003. Isolation of hepatoblasts based on the expression of Dlk/Pref-1. *J. Cell Sci.* **116**: 1775–1786. [Medline] [CrossRef]
18. Varma, V. and Cohen, C. 2004. Immunohistochemical and molecular markers in the diagnosis of hepatocellular carcinoma. *Adv. Anat. Pathol.* **11**: 239–249. [Medline] [CrossRef]
19. Yamada, T., Fujita, M., Kitao, S., Ashida, Y., Nishizono, K., Tsuchiya, R., Shida, T. and Kobayashi, K. 1999. Serum alpha-fetoprotein values in dogs with various hepatic diseases. *J. Vet. Med. Sci.* **61**: 657–659. [Medline] [CrossRef]
20. Yamashita, T., Honda, M., Nakamoto, Y., Baba, M., Nio, K., Hara, Y., Zeng, S. S., Kondo, T. H., Takatori, H., Yamashita, T., Mizukoshi, E., Ikeda, H., Zen, Y., Takamura, H., Wang, X. W. and Kaneko, S. 2013. Discrete nature of EpCAM(+) and CD90(+) cancer stem cells in human hepatocellular carcinoma. *Hepatology* **57**: 1484–1497. [Medline]
21. Yanai, H., Nakamura, K., Hijioka, S., Kamei, A., Ikari, T., Ishikawa, Y., Shinozaki, E., Mizunuma, N., Hatake, K. and Miyajima, A. 2010. Dlk-1, a cell surface antigen on foetal hepatic stem/progenitor cells, is expressed in hepatocellular, colon, pancreas and breast carcinomas at a high frequency. *J. Biochem.* **148**: 85–92. [Medline] [CrossRef]
22. Zhu, Z., Hao, X., Yan, M., Yao, M., Ge, C., Gu, J. and Li, J. 2010. Cancer stem/progenitor cells are highly enriched in $CD133^{+}CD44^{+}$ population in hepatocellular carcinoma. *Int. J. Cancer* **126**: 2067–2078. [Medline]

FULL PAPER *Surgery*

Accumulation of Xenotransplanted Canine Bone Marrow Cells in NOD/SCID/γ_c^{null} Mice with Acute Hepatitis Induced by CCl_4

Takashi KATO[1)], Masaharu HISASUE[1)]*, Kazuhito SEGAWA[1)], Ayumi FUJIMOTO[1)], Eri MAKIISHI[1)], Sakurako NEO[1)], Kyohei YASUNO[2)], Ryosuke KOBAYASHI[2)] and Ryo TSUCHIYA[1)]

[1)]*Laboratory of Internal Medicine II, School of Veterinary Medicine, Azabu University, 1–17–71 Fuchinobe, Chuoku, Sagamihara, Kanagawa 252–5201, Japan*
[2)]*Research Institute of Biosciences, School of Veterinary Medicine, Azabu University, 1–17–71 Fuchinobe, Chuoku, Sagamihara, Kanagawa 252–5201, Japan*

(Received 7 December 2012/Accepted 2 February 2013/Published online in J-STAGE 15 February 2013)

ABSTRACT. Bone marrow cell infusion (BMI) has recently been suggested as an effective therapy for refractory liver disease; however, the efficiency of BMI using canine bone marrow cells (cBMCs) has not been reported. We evaluated the accumulation potential of cBMCs in a mouse model of acute liver failure. Acute hepatitis was induced by carbon tetrachloride (CCl_4) treatment in NOD/SCID/γ_c^{null}(NOG) mice and wild-type (WT) C57BL mice, and the characteristics of liver dysfunction and the degree of hepatic injury and regeneration were compared between the two mouse models. Next, female CCl_4-treated NOG mice were xenotransplanted with male PKH26-labeled cBMCs, and the potential of cBMCs to accumulate in injured liver tissue compartments was examined. Fluorescence microscopy was perform ed to histologically detect the infused cBMCs, and DNA polymerase chain reaction was performed for detection of the male Y chromosome (SRY gene) in the recipient female NOG mice. The number of PKH26-positive cBMCs transplanted in the liver tissue gradually increased in the NOG mice. The infused cBMCs were located in the necrotic area of the liver at an early stage after transplantation, and most had accumu - lated a week after transplantation. However, the therapeutic efficacy of the xenotransplantation remained unclear, because no significant differences were observed concerning the extent liver injury and regeneration between the cBMC-transplanted and saline control mice. These results suggest that cBMCs will specifically accumulate in injured liver tissue and that BMC transplantation may have the potential to repair liver deficiency.

KEY WORDS: canine bone marrow cell, carbon tetrachloride (CCl_4), cell therapy, liver regeneration, NOD/SCID/γ_c^{null}(NOG) mouse.

doi: 10.1292/jvms.12-0530; *J. Vet. Med. Sci.* 75(7): 847–855, 2013

Chronic hepatitis (CH) and cirrhosis have long been recognized in many dog breeds by both primary and referral veterinary practices [18, 21]. These disorders are often perceived as extremely difficult to treat, and there are no cures. Therefore, more effective therapies are needed. In human medicine, liver transplantation is the only effective cure for CH and cirrhosis, but the limitations of transplantation, such as a lack of donors, surgical complications, rejection and high cost, have led to proposals for less invasive regenerative therapy procedures.

Recent reports demonstrated that murine bone marrow cells (BMCs) transplanted via peripheral vein populated and differentiated into albumin-producing hepatocytes via hepatoblast intermediates [1, 26, 29]. Interestingly, BMC infusion improves hepatic function, including elevation of serum albumin levels, and in mice or rats, it reduces liver fibrosis, corrects liver dysfunction and improves survival rate in human cirrhosis patient [10, 12]. On the basis of these results, a clinical trial of autologous BMC infusion was conducted, wherein it was shown that BMCs administered through a peripheral vein improved liver function in patients with liver cirrhosis [13, 22]. Therefore, BMC infusion may prove to be a curative therapy for liver cirrhosis in the future [27].

Recent studies have shown that the effects of BMC therapy on liver failure depend on many factors such as specific accumulation ability, immunomodulation, trophic support, differentiation (plasticity), revascularization and tissue regeneration [16, 17]. In particular, specific accumulation ability is one of the most important factors in cell transplant therapy [4, 28]. In murine models, accumulation ability has been established for specific disorders of the liver and pancreas [24]. In another study of liver cirrhosis patients with splenomegaly, splenectomy enhanced the repopulation of BMCs into the cirrhotic liver microenvironment and tended to result in greater improvement of liver function [12]. These studies suggest that the specific accumulation of BMCs in the disordered liver is important for effective results.

We previously demonstrated the capacity of canine BMCs (cBMCs) for differentiation into albumin-producing hepatocyte-like cells [15]. It has also been shown that bone marrow stromal cells (BMSCs), which are one of the components of BMCs, have various therapeutic potentials such as matrix metalloproteinase activity [7]. Furthermore, xenotransplantation using canine BMSCs may be effective in resolving inflammatory fibrotic liver in CCl_4-treated immunodeficient mice [8]. Although some reports described

*CORRESPONDENCE TO: HISASUE, M., Laboratory of Veterinary Internal Medicine II, School of Veterinary Medicine, Azabu University, 1–17–71 Fuchinobe, Chuoku, Sagamihara, Kanagawa 252–5201, Japan.
e-mail: hisasue@azabu-u.ac.jp

autologous transplantation of BMCs in liver injured models, studies demonstrating the ability of cBMCs to accumulate in the disordered liver have been limited. In addition, the systemic effects of infused BMC populations are not well known in both dogs and rodents. Haraguchi *et al*. reported that the donor genomic DNAs of xenotransplanted canine BMSCs were detectable in recipient nude mice administered cyclosporin A (CSA) [8]. Cho *et al*. described that infused mice BMCs have a specific homing capacity to the liver in CCl_4-injected recipient mice [4]. However, these studies have not elucidated the localization of transplanted cells in injured liver tissue. To analyze the accumulation of BMCs in the liver, we used NOD/SCID/γ_c^{null}(NOG) mice in this study because this model accepts heterologous cells much more readily compared with any other immunodeficient model [11].

Therefore, the present study used an NOG mouse model with acute hepatitis induced by CCl_4 treatment to investigate the ability of xenotransplanted cBMCs to accumulate in injured murine liver tissue and estimate the specificity of this accumulation in the liver.

MATERIALS AND METHODS

Animals: Six-week-old NOG mice were purchased from the Central Institute for Experimental Animals (Kawasaki, Japan). Same age C57BL6J Jcl mice were purchased from CLEA Japan, Inc. (Kawasaki, Japan) to serve as the wild-type (WT) murine control. All mice were shipped to the Research Institute of Biosciences of Azabu University and handled with humane care under pathogen-free conditions. The mice were housed in a room under controlled temperature (25°C), humidity and lighting (12-hr light/dark cycle). Access to food and tap water was *ad libitum* throughout the study period. All of male NOG and C57BL mice were used in research for an experimental model of liver injury, and female NOG mice were used for cBMC transplant experimentation. A 2-year-old male beagle dog that was clinically healthy was used as a donor of cBMCs for transplantation into NOG mice. All experiments in this study were performed in accordance with the Animal Protection Guidelines of Azabu University (authorization no. 10–79).

Experimental model of liver injury: Forty male NOG mice and 20 male WT mice were divided into three groups: NOG + CCl_4 (n=20), NOG + oil (n=20) and WT + CCl_4 (n=20). CCl_4 (Wako Pure Chemical Industries, Osaka, Japan) dissolved in olive oil (1 m*l*/kg) was administered via intraperitoneal injection in the NOG + CCl_4 and WT + CCl_4 groups, and the extent of liver injury and regeneration was investigated in these mice. The mice were sacrificed at 0 hr, 24 hr, 48 hr, 72 hr and 1 week after CCl_4 injection, and the livers were sectioned and fixed in phosphate-buffered 10% formaldehyde for histological examination.

Preparation of donor BMCs: cBMCs were harvested from the humerus and femur of the dog under general anesthesia with intravenous injection of medetomidine (20 μg/kg) and pentobarbital (10 mg/kg). The cells were collected in a heparin-containing syringe. After fat removal, cBMCs were extracted, and single-cell suspensions were prepared by passing the cells through a 100-μm mesh filter (BD Falcon) into new tubes. Mononuclear cells (MNCs) were isolated with Ficoll solution (Lymphoprep; Axis-Shield, Oslo, Norway) and washed and concentrated three times. The isolated MNCs were labeled with red fluorescent dye using a PKH26 Red Fluorescent Cell Linker Kit (Sigma–Aldrich, St Lous, MO, U.S.A.) according to the manufacturer's protocol. Incubation was performed for 5 min at room temperature with 1×10^7 MNCs/m*l*, followed by washing in phosphate-buffered saline (PBS) to remove proteins from the culture medium for optimal staining. The staining reaction was stopped with addition of 1% bovine serum albumin, followed by washing with PBS. Labeling and viability were verified by cultivation in hepatocyte growth medium as previously described [15].

Transplantation: Fifteen female NOG mice were grouped as follows: CCl_4 + cBMC (n=5), oil + cBMC (n=5) and CCl_4 + saline (n=5). At 1.5–2 hr after BMC harvesting, prepared MNCs (1×10^6) or saline was administered to the tail veins of CCl_4- or oil-treated NOG mice. The mice were sacrificed after 1 week, and the livers, lungs and spleens were removed to evaluate the systemic distribution of the administered cBMCs (Fig. 1A). To investigate the time course of BMC accumulation in the injured liver, 32 female NOG mice were grouped into CCl_4 + cBMC (n=16) and CCl_4 + saline (n=16) groups and injected as above. These mice were sacrificed, and the livers were removed at 0 hr, 24 hr, 48 hr and 1 week after BMC transplantation (Fig. 1B).

Laboratory analysis: The mice were anesthetized with pentobarbital (Somnopentyl; Kyoritu Seiyaku Corporation, Tokyo, Japan), and their blood was collected from the heart and centrifuged at 15,00G for 15 min at 4°C. Albumin, alanine aminotransferase (ALT) and aspartate amino transferase (AST) levels were analyzed with a Hitachi 9,000 series automatic analyzer.

Histological examination: Liver samples were fixed in a 10% neutral-buffered formaldehyde solution, embedded in paraffin and sectioned. The 3-μm-thick sections were stained with hematoxylin and eosin (HE). The relative necrotic area, expressed as a percentage of the total liver area, was determined in the HE-stained liver sections. Each field was acquired as 5 nonoverlapping random fields (×200 magnification) and analyzed using ImageJ software version 1.41 (http://rsb.info.nih.gov/ij).

Immunohistochemistry: Tissue sections were subjected to immunohistochemistry using rat monoclonal antibody to the Ki-67 antigen (1:200; Dako, Tokyo, Japan), which detects proliferating cells. Microwave antigen retrieval was performed in citrate buffer (pH 6.0) for 10–20 min. The sections were treated with 0.3% H_2O_2 in methanol for 20 min. For the primary antibody reaction, slides were incubated in a wet chamber overnight at 4°C. The immunoreactive materials were visualized using a peroxidase staining kit (Histofine Simple Stain MAX PO; Nichirei, Tokyo, Japan) and diaminobenzidine (Histofine Simple Stain DAB; Nichirei). The sections were counterstained with hematoxylin. The number of cells and the number of Ki-67-positive cells per field in each mouse liver were measured at ×400 magnification, and

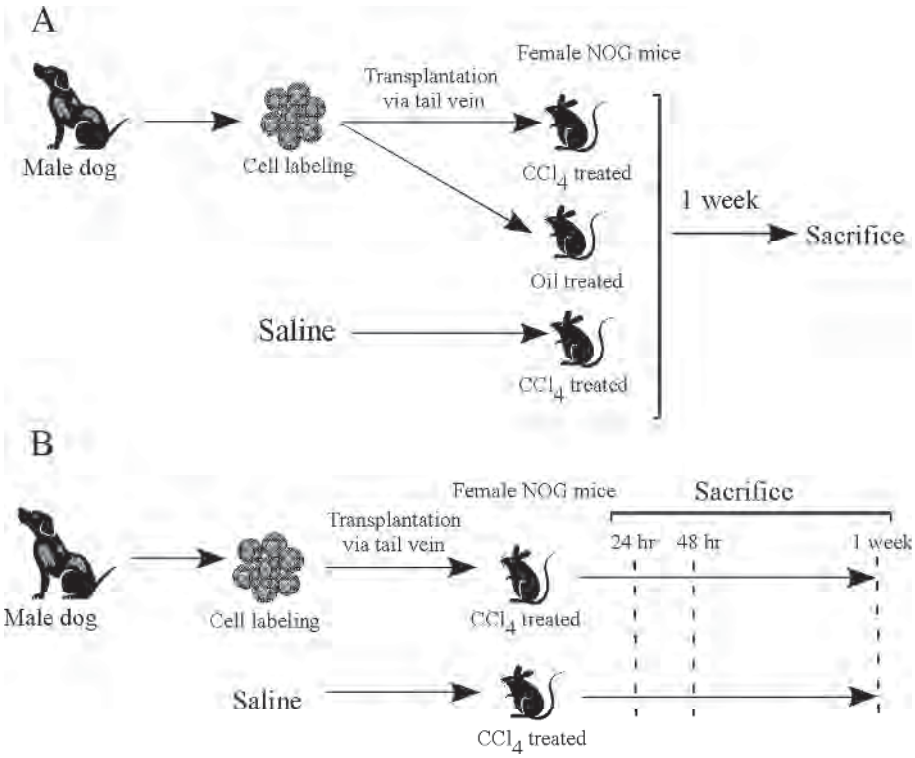

Fig. 1. Experimental design of cBMC transplantation into NOG mice. (A) The cBMCs were collected from a male dog, red fluorescence-labeled with PKH26, and transplanted into female NOG mice with liver injury induced by CCl_4 treatment. The mice were grouped as CCl_4 + cBMC, oil + cBMC and CCl_4 + saline groups (n=5, respectively). The systemic distribution of the transplanted male cBMCs was evaluated 1 week after transplantation. (B) Sampling times after cBMC transplantation. The CCl_4 + cBMC (n=12) and CCl_4 + saline (n=12) groups were sacrificed, and their livers were removed at 0 hr, 24 hr, 48 hr and 1 week after BMC transplantation (n=4, respectively).

the ratio of Ki-67-positive cells was calculated.

Double fluorescence analysis: For fluorescence analysis, freshly isolated lungs, spleens and livers were embedded in optimal cutting temperature medium and frozen. Frozen sections (5 μm) were obtained using a cryostat (model HM505; Microm) equipped with a tungsten carbide knife. After fixation with 3.7% paraformaldehyde, polymerized actin was stained with phalloidin (Alexa Fluor 488 phalloidin, Invitrogen, Carlsbad, CA, U.S.A.). Vectashield mounting medium with DAPI (Vector Laboratories Inc., Burlingame, CA, U.S.A.) was used for nuclear staining. The lung and spleen sections were nuclear stained with DAPI alone. Images were observed and captured by fluorescence microscopy (FSX100; Olympus, Tokyo, Japan). Computer-assisted image analysis was performed using ImageJ software version 1.41.

Canine Y chromosome (SRY)-specific PCR: Genomic DNA was isolated from NOG mouse liver tissue homogenates using a QIAamp DNA Mini Kit (Qiagen, Hilden, Germany). The presence or absence of the sex-determination region of the male Y chromosome (SRY gene) in the recipient female NOG mice was assessed by PCR as previously described [25]. Primer sequences for the SRY gene were obtained from published sequences (forward primer, 5′-CAAGATGGCTCTAGAGAATCCC-3′; reverse primer, 5′-AGCTGTCCGTGTAGGTGA-3′), which amplified a 284-bp product. The PCR conditions were as follows: incubation at 94°C for 2 min; 40 cycles of incubation at 94°C for 30 sec, 57°C for 30 sec and 72°C for 30 sec. PCR products were separated using 2% agarose gel electrophoresis and stained with ethidium bromide. Positive (male canine genomic DNA) and negative (female canine genomic DNA) controls were included in each assay.

Statistical analysis: Data are expressed as means ± standard error of the mean (SEM). The Mann–Whitney U test was used to compare the different groups as appropriate. P values of <0.05 were considered statistically significant. Analyses were performed using GraphPad Prism 5.

RESULTS

Characterization of CCl_4-induced acute liver dysfunction in NOG mice: The degree of liver injury was assessed by measuring serum liver enzymes (Fig. 2A). Serum albumin levels were significantly decreased at 48 hr after CCl_4 injection, after which the levels improved to within the normal range in both NOG and WT mice. Both serum ALT and AST

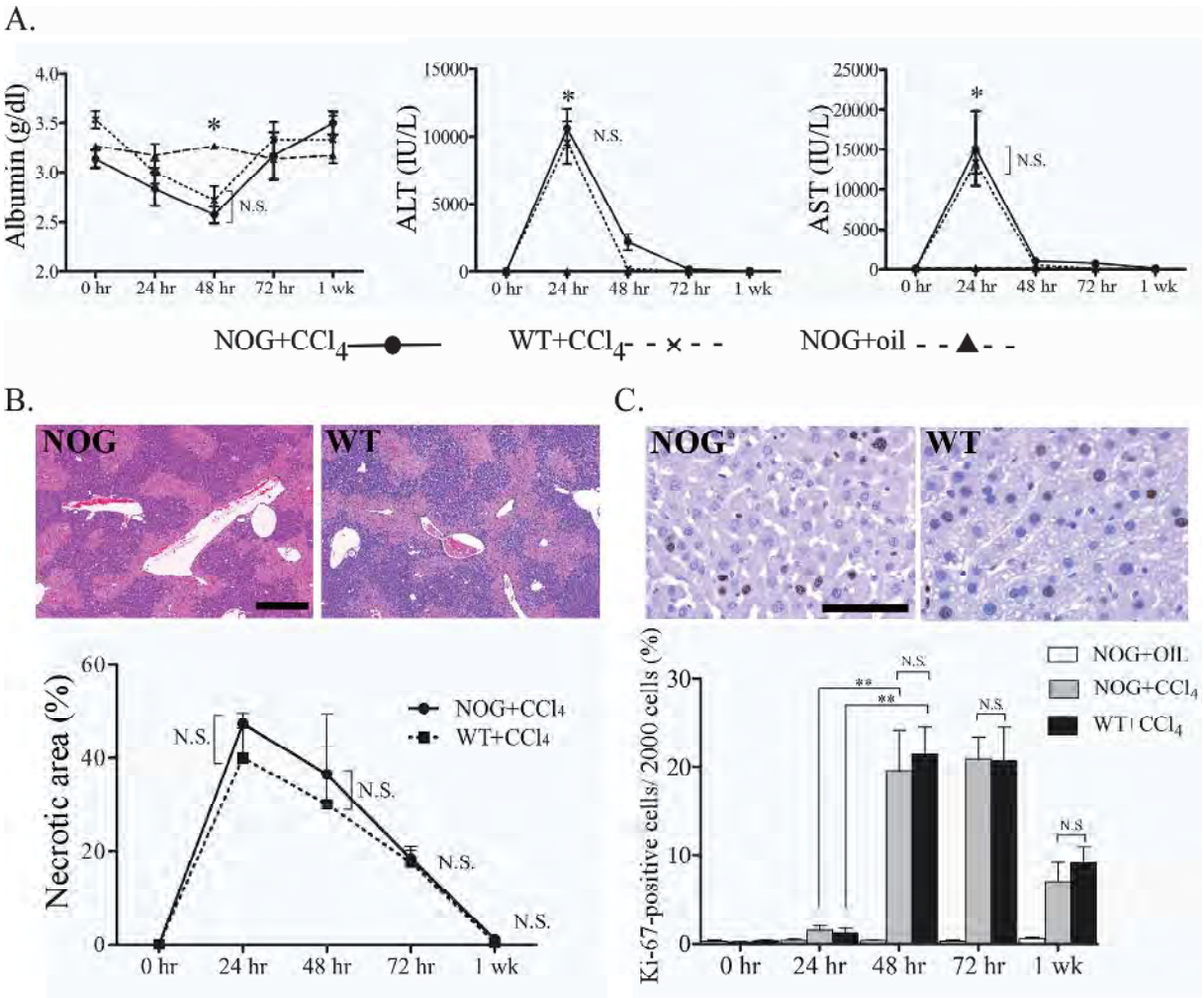

Fig. 2. CCl_4-induced acute liver injury and regeneration in NOG and WT mice. (A) Serum albumin, ALT and AST levels before and 7 days after CCl_4 injection. (B) Histological findings of necroses in the centrilobular and midzonal liver areas. The necrotic area of the liver was increased by more than 50% 24 hr after CCl_4 injection in both WT and NOG mice. Scale bar=200 μm. (C) Regeneration of liver tissue was estimated by detection of Ki-67-positive cells. The ratios of Ki-67-positive cells were calculated in 2,000 hepatocytes. Scale bar=100 μm. Bars indicate means ± SEM. N.S., not significant. *Significant difference compared with the NOG + oil group (n=4 per group; $P<0.05$). **Significant difference compared with that 24 hr after CCl_4 treatment of NOG and WT mice (n=4 per group; $P<0.05$).

increased markedly 24 hr after CCl_4 injection; however, they decreased to within the normal range 48 hr after CCl_4 injection, with no differences between the NOG and WT mice. To evaluate liver damage and regeneration, the necrotic areas of the liver were measured in NOG and WT mice injected with CCl_4. There were no significant differences in the extent of liver necrosis between the NOG and WT mice (Fig 2B). Immunohistochemistry using Ki-67, a marker for cell proliferation, was performed to assess hepatocyte regeneration (Fig. 2C). Ki-67-positive hepatocytes were limited 24 hr after CCl_4 injection; however, there were many positive cells 48 hr after CCl_4 injection, with no differences between the NOG and WT mice.

Migration of PKH26-positive cBMCs into injured liver lobules: PKH26-positive cBMCs (1×10^6) were injected into liver-damaged and control (undamaged) female NOG mice. Infused cBMCs could be visualized by fluorescence microscopy a week after transplantation (Fig. 3). A few PKH26-positive cells were detected in sections of the liver from undamaged controls (Fig. 3A), and there were no PKH26-positive cells in CCl_4-damaged mice without cBMC transplantation. In contrast, in the transplanted CCl_4-treated mice, the number of PKH26-positive cells gradually increased, spreading into the liver lobules (Fig. 3A, 3B). Some PKH26-positive cells were observed in the lung tissue of both liver-damaged and control mice (Fig. 3A, 3B), while no PKH26-positive cells were detected in spleen tissue from any of the groups (Fig. 3A).

Detection of the SRY gene in transplanted NOG mice: PCR amplification of the canine SRY gene, located on the Y

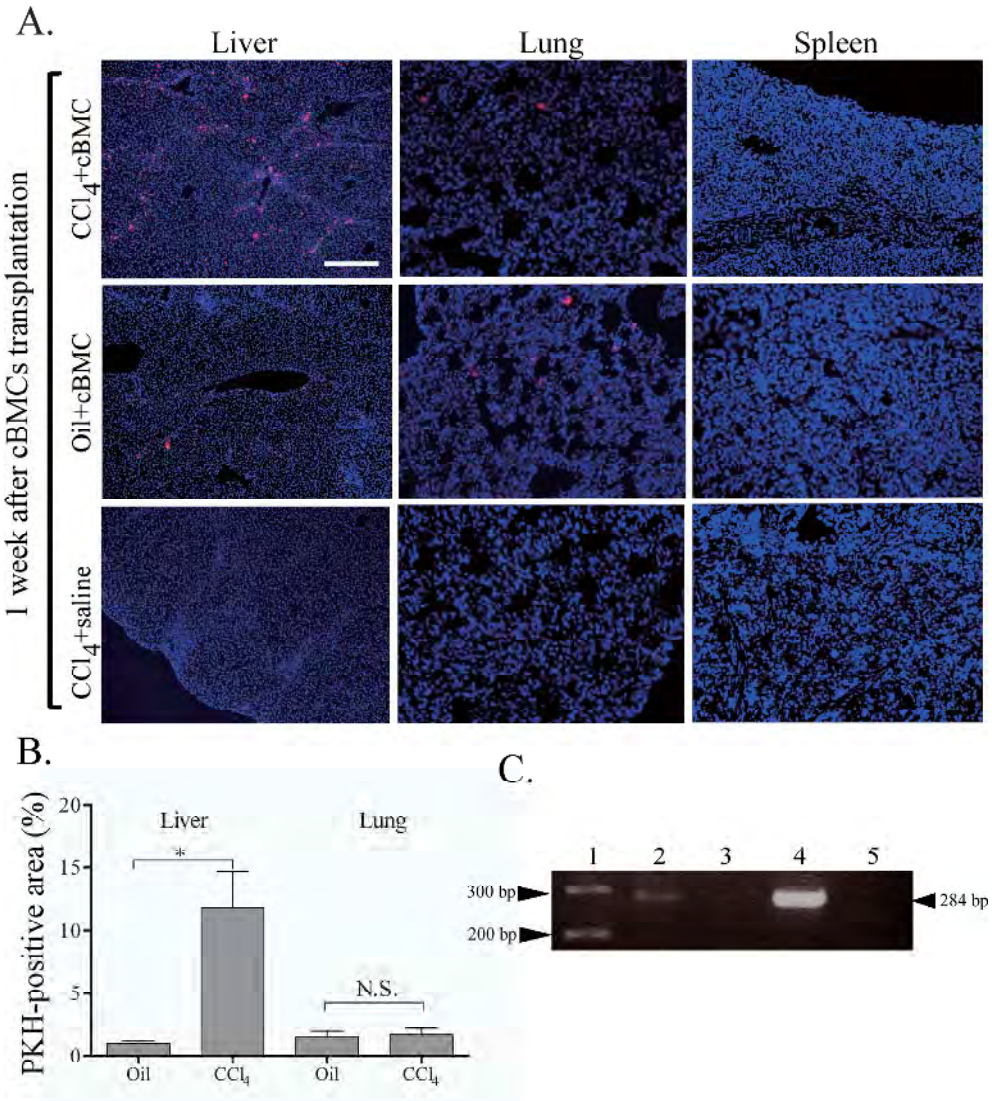

Fig. 3. Engraftment of donor cBMCs in liver, lung, and spleen tissues was examined 1 week after transplantation. (A) Detection of PKH26-labeled infused cells in liver tissues by fluorescence microscopy. A number of PKH26-positive cBMCs were detected in livers of the CCl_4 + cBMC group, but only a few cBMCs were detected in livers of the oil + cBMC group. In both the CCl_4 + cBMC and oil + cBMC groups, some PKH26-positive cells were detected in the lung tissue, but not in the spleen tissue. Scale bar=200 μm (B) Quantitative comparison of PKH26-positive cBMCs in liver and lung tissues. PKH26-positive cells were significantly increased in the CCl_4 + cBMC group compared with the oil + cBMC group, but the number of PKH26-positive cells in the lung tissue did not differ between the groups. *Significant difference compared with the Oil+cBMCs group (n=4 per group; $P<0.05$). (C) The canine male-specific SRY gene (284 bp) was amplified exclusively in the livers of the female xenotransplanted mice. Lane 1, molecular weight standard; lane 2, cBMC-infused liver tissue; lane 3, saline-treated liver tissue; lane 4, male dog liver tissue (positive control); lane 5, female dog liver tissue (negative control).

chromosome, demonstrated that transplanted cBMCs were present in the livers of the transplanted female mice, indicating that male cBMCs accumulated in the liver tissue of the female mice (Fig. 3C).

Localization of infused cBMCs in the injured Liver: Phalloidin staining of frozen liver sections was performed to further elucidate the localization of cBMCs in the mouse liver. The actin cytoskeleton was disordered in necrotic tissue, and PKH26-positive cells were slightly accumulated in the necrotic areas 24 and 48 hr after transplantation (Fig. 4A). One week after transplantation, the number of accumulated cBMCs (PKH26-positive cells) gradually increased and spread into the liver lobules (Fig. 4A, 4B).

Effects of cBMC transplantation on CCl_4-induced acute

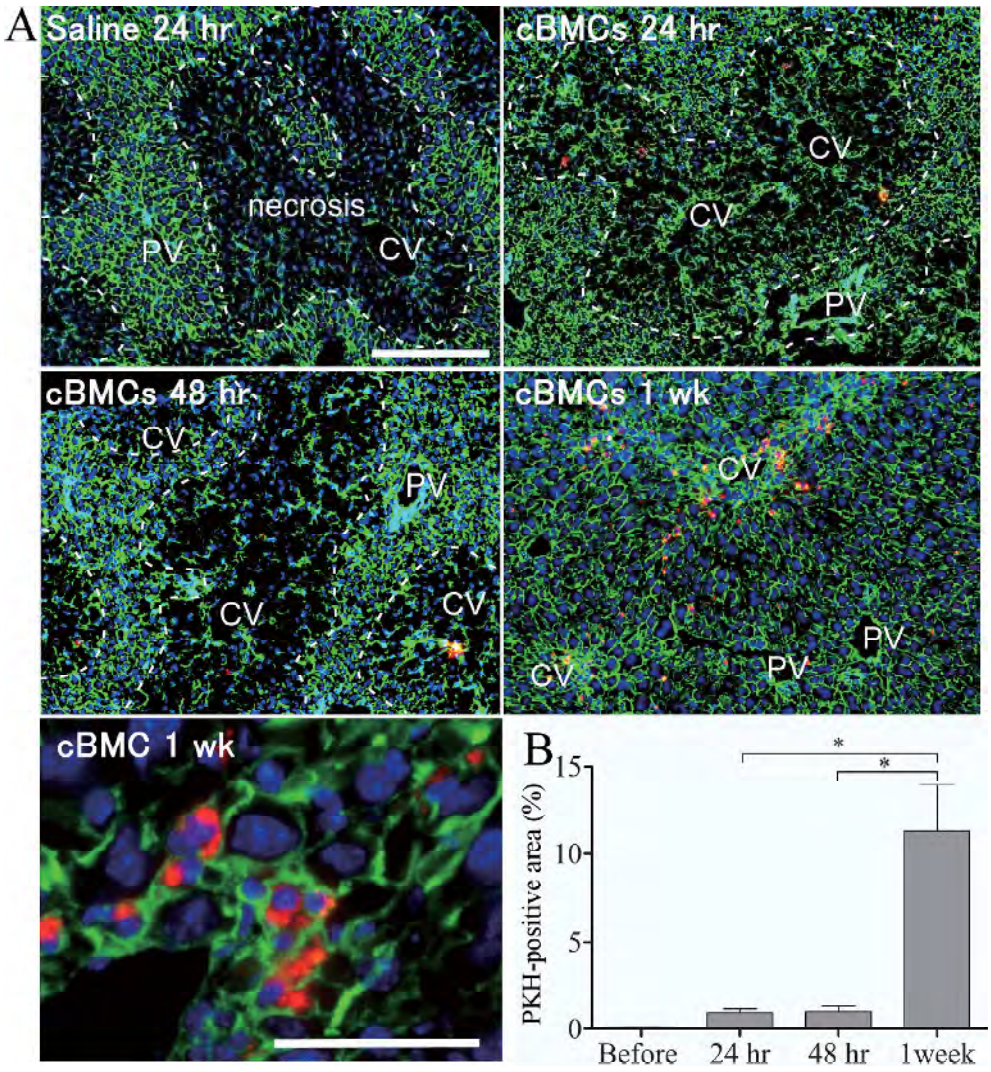

Fig. 4. Combined analysis of actin phalloidin (green), PKH26 (red) and DAPI (blue). (A) The left liver lobes of NOG mice were analyzed 24 hr, 48 hr and 1 week after cBMC transplantation. The dotted lines indicated the necrotic area of the liver tissue. Red fluorescence indicates the position of the PKH26-labeled cBMCs. At 24 and 48 hr after transplantation, cBMCs were sparsely distributed, corresponding to the necrotic areas. These cells had accumulated 1 week after transplantation. (B) Quantitative comparison of PKH26-positive cBMCs in liver tissues. Bars indicate means ± SEM. CV, central vein; PV, portal vein. *Significant difference compared with that in the oil + cBMC group (n=4 per group; $P<0.05$). Scale bar=Small bar=200 μm, Large Bar=50 μm (Fig. A).

liver dysfunction in the NOG mice: To clarify the therapeutic efficacy of cBMC transplantation in an acute liver hepatitis model, the degrees of hepatic injury and regeneration were compared between the cBMC-transplantation and saline (control) groups (Fig. 5). As parameters of hepatic injury, serum albumin and hepatic enzyme levels (Fig. 5A) and necrotic areas (Fig. 5B) were measured. As a measure of hepatocyte regeneration, the Ki-67-positive ratios were measured in each group (Fig. 5C). However, none of these parameters were significantly different between the control and transplantation groups ($P=0.872$).

DISCUSSION

In the present study, the infused cBMCs not only accumulated in the injured mouse liver at an early stage after transplantation but also accumulated specifically in injured tissue. Although several investigators have reported the ability of BMCs to engraft in experimental models, including rodent models [3, 6, 14], to our knowledge, this is the first study to investigate whether canine BMCs can accumulate in the injured liver tissue of an immunodeficient mouse model. Transplantation of cBMCs into recipient mice was success-

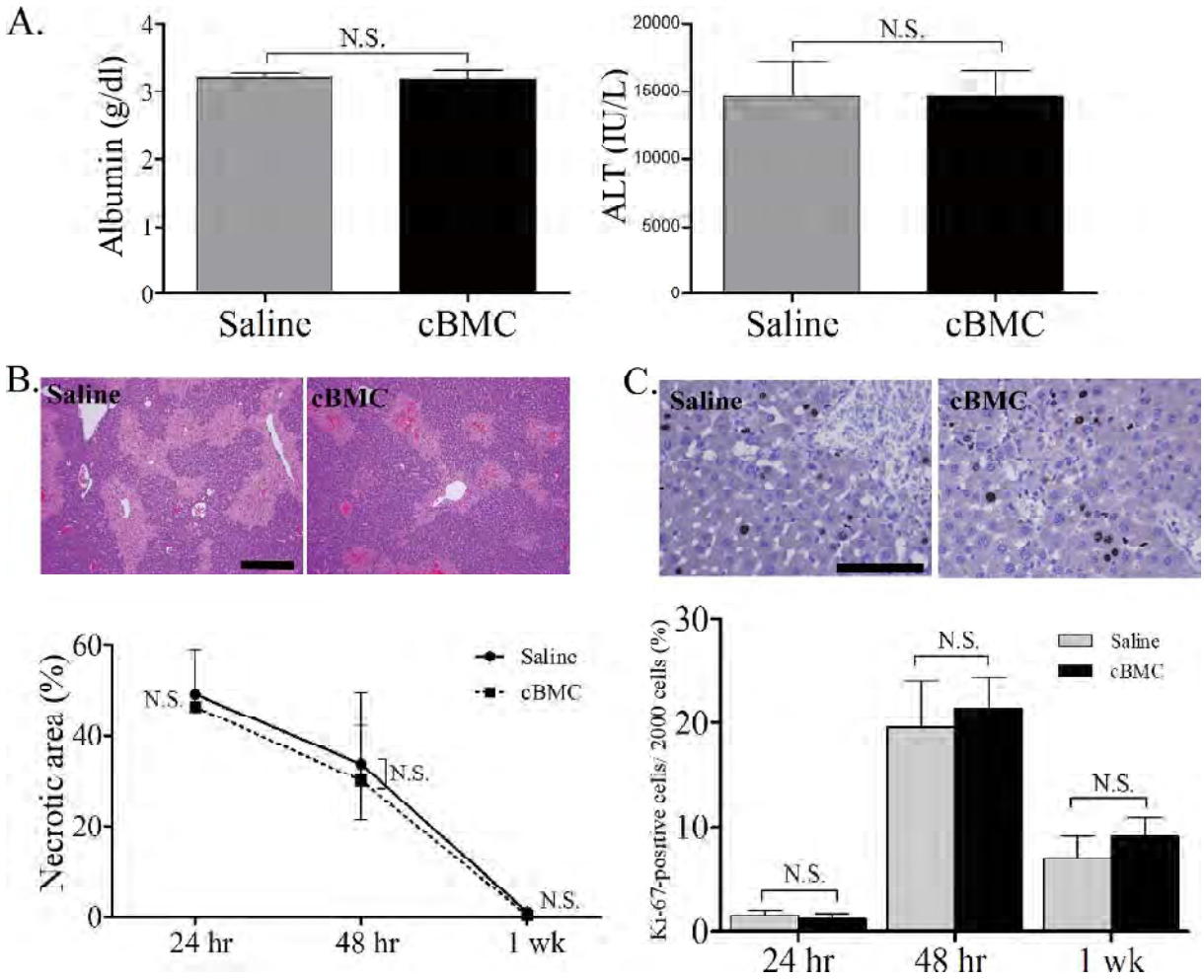

Fig. 5. Influence of cBMC transplantation on acute liver injury and regeneration. (A) Serum albumin and ALT levels at 24 hr after transplantation were not significantly different between the saline and cBMC groups. (B) Histology of the liver confirmed necrotic hepatocytes as eosinophilic cytoplasm in the centrilobular and midzonal areas. There were no significant differences at any time point between the saline and cBMC groups. Scale bar=200 μm. (C) Hepatocyte regeneration was measured by immunohistochemistry of Ki-67 48 hr after CCl_4 injection. Regeneration was unchanged at each time point in both the saline and cBMC groups. Scale bar=100 μm. Bars indicate means ± SEM. N.S., not significant.

ful, as indicated by the detection of both PKH26-labeled cBMCs and the canine SRY gene in the liver tissue of female NOG mice. In particular, infused cBMCs were located in the necrotic area of the liver an early stage after transplantation, with the largest accumulation at 1 week after transplantation. CCl_4-induced acute liver injury in NOG mice peaked at 24 hr, and most liver regeneration occurred at 48 hr after CCl_4 injection. However, the time course of cBMC migration to the injured liver tissue did not correspond to the time course of liver injury or regeneration, because most cBMC accumulation occurred more than 48 hr after transplantation. Previously, Thomas *et al*. demonstrated that macrophage therapy was effective for improving liver fibrosis in a murine hepatic fibrosis model. Their migration of infused macrophages was detected in liver tissue from 1 to 7 days after transplantation, but the number of cells was not increased [28]. Chronic hepatitis and developed hepatic fibrosis models were used for their study, which they were established by a long-term protocol of CCl_4 injection on two consecutive days per week for at least 6 weeks. In the present study, NOG mice were injected with CCl_4 a single time and used as an acute hepatitis model, so its pathogenesis might be the cause of the different time course of cell accumulation in chronic hepatic injury. Therefore, we suggested that transplanted cell accumulation in the injured liver might be affected by the difference in acute or chronic hepatic deficiency, or transplanted cell fraction.

Several immunodeficiency models, such as NOG mice, have been developed for heterograft experimentation [2]. NOG mice can accept heterologous cells much more readily than any other immunodeficient rodent model [9, 12]. Although the immune system plays an important role in liver

regeneration [5, 19], it is not known whether NOG mice are an appropriate model for spontaneous acute hepatitis. In the present study, we further confirmed these findings by comparing CCl_4-induced hepatitis and liver regeneration between NOG and WT mouse models of acute hepatitis, which suggested that NOG mice can be used as an acute liver injury model similar to WT mice. Both serum hepatic enzyme levels and necrotic areas showed maximum increases 24 hr after CCl_4 injection, and Ki-67-positive hepatocytes appeared 48 hr after CCl_4 injection (Fig. 2). These findings were consistent with those of a previous study [20]. It is well known that the hepatocyte growth factor (HGF) is the most important factor for hepatic regeneration [23]. We expect that liver regeneration is not influenced by the immunodeficiency of NOG mice, because HGF may be secreted normally in these mice.

Infused cBMCs also accumulated in the liver and lung but not in the spleen. Thomas *et al*. [28] and Cho *et al*. [4] have demonstrated the efficient trafficking of rodent BMSCs to various target organs following transplantation, with a major portion of the input cells retained in the lung. In the green fluorescent protein (GFP)/CCl_4 mouse model, Iwamoto *et al*. [12] demonstrated that splenectomy enhanced the migration of GFP-positive BMCs to the damaged liver. With the exception of migration to the lung, our findings agree with these data, although it is difficult to precisely evaluate the accumulation in the spleen in NOG mice because they have natural splenic atrophy.

In this study, cBMC transplantation did not improve hepatic function and regeneration. Serum ALT increased extremely (approximately 15,000 IU/*l*) 24 hr after CCl_4 injection in both the saline and cBMC groups. In this study, the hepatic necrotic area 24 hr after CCl_4 injection was 50% of the liver, indicating that change was the greatest value in this acute hepatitis model. We suggested that CCl_4-induced acute liver injury may have been so severe that it became impossible to evaluate the therapeutic effects of cBMC transplantation. In the hepatic fibrosis model, some studies indicated that bone marrow-derived cells could decrease collagen fibers and reduce hepatic fibrosis through expression of matrix metalloproteinases (MMPs) [4, 7, 8]. Haraguchi *et al*. reported that transplanted cBMSCs migrated into liver regions exhibiting severe inflammation and fibrosis, and fibrosis was significantly reduced in CCl_4/CSA mice transplanted with canine bone marrow stromal cells (cBMSCs) [8]. Therefore, the therapeutic effects of cBMC transplantation should be evaluated in clinical canine cases or in a hepatic fibrosis model.

In conclusion, we demonstrated that cBMCs accumulate after xenotransplantation in NOG mice with induced liver injury. These results suggest that cBMCs may have potential in relation to liver regeneration, although the precise mechanisms for regulating cBMC stimulation in the damaged liver remain uncertain. A further study of these mechanisms is required to develop cell therapies that utilize cBMCs for repair of the damaged liver.

ACKNOWLEDGMENTS. This study was supported by the Science Research Promotion Fund of the Promotion and Mutual Aid Corporation for Private Schools of Japan, by a Matching Fund Subsidy for Private Universities and by a grant from the Ministry of Education, Culture, Sports, Science and Technology (No 80333144).

REFERENCES

1. Almeida-Porada, G., Zanjani, E. D. and Porada, C. D. 2010. Bone marrow stem cells and liver regeneration. *Exp. Hematol.* **38**: 574–580. [Medline] [CrossRef]
2. Bosma, G. C., Custer, R. P. and Bosma, M. J. 1983. A severe combined immunodeficiency mutation in the mouse. *Nature* **301**: 527–530. [Medline] [CrossRef]
3. Brulport, M., Schormann, W., Bauer, A., Hermes, M., Elsner, C., Hammersen, F. J., Beerheide, W., Spitkovsky, D., Härtig, W., Nussler, A., Horn, L. C., Edelmann, J., Pelz-Ackermann, O., Petersen, J., Kamprad, M., von Mach, M., Lupp, A., Zulewski, H. and Hengstler, G. 2007. Fate of extrahepatic human stem and precursor cells after transplantation into mouse livers. *Hepatology* **46**: 861–870. [Medline] [CrossRef]
4. Cho, K. A., Lim, G. W., Joo, S. Y., Woo, S. Y., Seoh, J. Y., Cho, S. J., Han, H. S. and Ryu, K. H. 2011. Transplantation of bone marrow cells reduces CCl_4 -induced liver fibrosis in mice. *Liver Int.* **31**: 932–939. [Medline] [CrossRef]
5. Diehl, A. M. 2000. Cytokine regulation of liver injury and repair. *Immunol. Rev.* **174**: 160–171. [Medline] [CrossRef]
6. Doshi, M., Koyanagi, M., Nakahara, M., Saeki, K., Saeki, K. and You, A. 2006. Identification of human neutrophils during experimentally induced inflammation in mice with transplanted CD34+ cells from human umbilical cord blood. *Int. J. Hematol.* **84**: 231–237. [Medline] [CrossRef]
7. Haraguchi, T., Tani, K., Koga, M., Oda, Y., Itamoto, K., Yamamoto, N., Terai, S., Sakaida, I., Nakazawa, H. and Taura, Y. 2012. Matrix metalloproteinases (MMPs) activity in cultured canine bone marrow stromal cells (BMSCs). *J. Vet. Med. Sci.* **74**: 633–636. [Medline] [CrossRef]
8. Haraguchi, T., Tani, K., Takagishi, R., Oda, Y., Itamoto, K., Yamamoto, N., Terai, S., Sakaida, I., Nakazawa, H. and Taura, Y. 2012. Therapeutic potential of canine bone marrow stromal cells (BMSCs) in the carbon tetrachloride (CCl_4) induced chronic liver dysfunction mouse model. *J. Vet. Med. Sci.* **74**: 607–611. [Medline] [CrossRef]
9. Hasegawa, M., Kawai, K., Mitsui, T., Taniguchi, T., Monnai, M., Wakui, M., Ito, M., Suematsu, M., Peltz, G., Nakamura, G. and Suemizu, H. 2011. The reconstituted 'humanized liver' in TK-NOG mice is mature and functional. *Biochem. Biophys. Res. Commun.* **405**: 405–410. [Medline] [CrossRef]
10. Ishikawa, T., Terai, S., Urata, Y., Marumoto, Y., Aoyama, K., Sakaida, I., Murata, T., Nishina, H., Shinoda, K., Uchimura, S., Hamamoto, Y. and Okita, K. 2006. Fibroblast growth factor 2 facilitates the differentiation of transplanted bone marrow cells into hepatocytes. *Cell Tissue Res.* **323**: 221–231. [Medline] [CrossRef]
11. Ito, M., Hiramatsu, H., Kobayashi, K., Suzue, K., Kawahata, M., Hioki, K., Ueyama, Y., Koyanagi, Y., Sugamura, K., Tsuji, K., Heike, T. and Nakahata, T. 2002. NOD/SCID/γc^{null} mouse: an excellent recipient mouse model for engraftment of human cells. *Blood* **100**: 3175–3182. [Medline] [CrossRef]
12. Iwamoto, T., Terai, S., Mizunaga, Y., Yamamoto, N., Omori, K., Uchida, K., Yamasaki, T., Fujii, Y., Nishina, H. and Sakaida, I. 2012. Splenectomy enhances the anti-fibrotic effect of bone marrow cell infusion and improves liver function in cirrhotic

mice and patients. *J. Gastroenterol.* **47**: 300–312. [Medline] [CrossRef]
13. Kim, J. K., Park, Y. K., Kim, J. S., Park, M. S., Paik, Y. H., Seok, J. Y., Chung, Y. E., Kim, H. O., Kim, K. S., Ahn, S. H., Kim, Y., Kim, M. J., Lee, K. S., Chon, C. Y., Kim, S. J., Terai, S., Sakaida, I. and Han, K. H. 2010. Autologous bone marrow infusion activates the progenitor cell compartment in patients with advanced liver cirrhosis. *Cell Transplant.* **19**: 1237–1246. [Medline] [CrossRef]
14. Meyerrose, T. E., De Ugarte, D. A., Hofling, A. A., Herrbrich, P. E., Cordonnier, T. D., Shultz, L. D., Eagon, J. C., Wirthlin, L., Sands, M. S., Hedrick, M. A. and Nolta, J. A. 2007. *In vivo* distribution of human adipose-derived mesenchymal stem cells in novel xenotransplantation models. *Stem Cells* **25**: 220–227. [Medline] [CrossRef]
15. Neo, S., Ishikawa, T., Ogiwara, K., Kansaku, N., Nakamura, M., Watanabe, M., Hisasue, M., Tsuchiya, R. and Yamada, T. 2009. Canine bone marrow cells differentiate into hepatocyte-like cells and placental hydrolysate is a potential inducer. *Res. Vet. Sci.* **87**: 1–6. [Medline] [CrossRef]
16. Parekkadan, B., van Poll, D., Megeed, Z., Kobayashi, N., Tilles, A. W., Berthiaume, F. and Yarmush, M. L. 2007. Immunomodulation of activated hepatic stellate cells by mesenchymal stem cells. *Biochem. Biophys. Res. Commun.* **363**: 247–252. [Medline] [CrossRef]
17. Parekkadan, B., van Poll, D., Suganuma, K., Carter, E. A., Berthiaume, F., Tilles, A. W. and Yarmush, M. L. 2007. Mesenchymal stem cell-derived molecules reverse fulminant hepatic failure. *PLoS One* **2**: e941. [CrossRef]
18. Poldervaart, J. H., Favier, J. P., Penning, L. C., van den Ingh, T. S. G. A. M. and Rothuizen, J. 2009. Primary Hepatitis in Dogs: A Retrospective Review (2002–2006). *J. Vet. Intern. Med.* **23**: 72–80. [Medline] [CrossRef]
19. Racanelli, V. and Rehermann, B. 2006. The liver as an immunological organ. *Hepatology* **43**: S54–62. [Medline] [CrossRef]
20. Recknagel, R. O. 1967. Carbon tetrachloride hepatotoxicity. *Pharmacol. Rev.* **19**: 145–208. [Medline]
21. Rutgers, H. C. and Haywood, S. 1988. Chronic hepatitis in the dog. *J. Small. Anim. Pract.* **29**: 679–690. [CrossRef]
22. Saito, T., Okumoto, K., Haga, H., Nishise, Y., Ishii, R., Sato, C., Watanabe, H., Okada, A., Ikeda, M., Togashi, H., Ishikawa, T., Terai, S., Sakaida, I. and Kawata, S. 2011. Improved liver function in patients with liver cirrhosis after autologous bone marrow cell infusion therapy. *Stem Cells Dev.* **20**: 1503–1510. [Medline] [CrossRef]
23. Strain, A. J., Ismail, T., Tsubouchi, H., Arakaki, N., Hishida, T., Kitamura, N., Daikuhara, Y. and McMaster, P. 1991. Native and recombinant human hepatocyte growth factors are highly potent promoters of DNA synthesis in both human and rat hepatocytes. *J. Clin. Invest.* **87**: 1853–1857. [Medline] [CrossRef]
24. Takeshita, F., Kodama, M., Yamamoto, H., Ikarashi, Y., Ueda, S., Teratani, T., Yamamoto, Y., Tamatani, T., Kanegasaki, S., Ochiya, T. and Quinn, G. 2006. Streptozotocin-induced partial beta cell depletion in nude mice without hyperglycaemia induces pancreatic morphogenesis in transplanted embryonic stem cells. *Diabetologia* **49**: 2948–2958. [Medline] [CrossRef]
25. Tateishi-Yuyama, E., Matsubara, H., Murohara, T., Ikeda, U., Shintani, S., Masaki, H., Amano, K., Kishimoto, Y., Yoshimoto, K., Akashi, H., Shimada, K., Iwasaka, T. and Imaizumi, T. 2002. Therapeutic angiogenesis for patients with limb ischemia by autologous transplantation of bone-marrow cells: A pilot study and a randomised controlled trial. *Lancet* **360**: 427–435. [Medline] [CrossRef]
26. Terai, S., Sakaida, I., Yamamoto, N., Omori, K., Watanabe, T., Shinya, O., Katada, T., Miyamoto, K., Shinoda, K., Nishina, H. and Okita, K. 2003. An *in vivo* model for monitoring transdifferentiation of bone marrow cells into functional hepatocytes. *J. Biochem.* **134**: 551–558. [Medline] [CrossRef]
27. Terai, S., Tanimoto, H., Maeda, M., Zaitsu, J., Hisanaga, T., Iwamoto, T., Fujisawa, K., Mizunaga, Y., Matsumoto, T., Urata, Y., Marumoto, Y., Hidaka, I., Ishikawa, T., Yokoyama, Y., Aoyama, K., Tsuchiya, M., Takami, T., Omori, K., Yamamoto, N., Segawa, M., Uchida, K., Yamasaki, T., Okita, K. and Sakaida, I. 2012. Timeline for development of autologous bone marrow infusion (ABMi) therapy and perspective for future stem cell therapy. *J. Gastroenterol.* **47**: 491–497. [Medline] [CrossRef]
28. Thomas, J. A., Pope, C., Wojtacha, D., Robson, A. J., Gordon-Walker, T. T., Hartland, S., Ramachandran, P., Van Deemter, M., Hume, D. A., Iredale, J. P. and Forbes, S. J. 2011. Macrophage therapy for murine liver fibrosis recruits host effector cells improving fibrosis, regeneration, and function. *Hepatology* **53**: 2003–2015. [Medline] [CrossRef]
29. Yamamoto, N., Terai, S., Ohata, S., Watanabe, T., Omori, K., Shinoda, K., Miyamoto, K., Katada, T., Sakaida, I., Nishina, H. and Okita, K. 2004. A subpopulation of bone marrow cells depleted by a novel antibody, anti-Liv8, is useful for cell therapy to repair damaged liver. *Biochem. Biophys. Res. Commun.* **313**: 1110–1118. [Medline] [CrossRef]

J Vet Intern Med 2012;26:370–376

Effects of Prostaglandin E_1 on the Preparation of Platelet Concentrates in Dogs

K. Segawa, T. Kondo, S. Kimura, A. Fujimoto, T. Kato, T. Ishikawa, S. Neo, M. Hisasue, T. Yamada, and R. Tsuchiya

Background: Platelet concentrates (PC) are prepared by centrifugation of platelet-rich plasma (PRP) that is prepared by centrifugation of whole blood. The resuspension of the platelet pellet during PC preparation from dogs is difficult because of platelet activation induced by centrifugation.

Objectives: To investigate the efficacy of adding prostaglandin E_1 (PGE_1) to prevent platelet activation during PC preparation from dogs.

Animals: Fifteen healthy Beagle dogs.

Methods: Prospective, experimental trial: PGE_1 was added to PRP before the high-speed centrifugation during PC preparation. To estimate the effect of this addition, we assessed the platelet aggregability before transfusion, the survival of the platelets after transfusion, and the platelet reactivity after transfusion, which is estimated by the P-selectin expression of the platelets when stimulated by thrombin.

Results: The difficulty associated with platelet resuspension was resolved by PGE_1. PGE_1 strongly inhibited platelet aggregation induced by collagen and ADP; however, it recovered after the platelets were resuspended in plasma without PGE_1 (mean aggregation ratio; collagen: 10.00–80.80%, ADP: 8.20–53.60%). Survival of the platelets after transfusion was not affected by PGE_1 (mean 8.04 and 7.56 days, without and with PGE_1), and thrombin-induced P-selectin expression after transfusion in PGE_1-treated PC was also well maintained (mean positive ratio 53.7 and 47.9%, before and 24 hours after transfusion).

Conclusions and Clinical Importance: The addition of PGE_1 in PRP before the centrifugation of PRP can improve the preparation efficiency of PC from dogs, while maintaining the therapeutic efficacy of the platelets.

Key words: Aggregability; P-selectin; Survival; Transfusion.

Platelet transfusions are indicated when animals have bleeding tendencies associated with thrombocytopenia, thrombocytopathy, or both. This is especially important before surgery or until immunosuppressive drugs become effective in the face of life-threatening bleeding in immune-mediated thrombocytopenia.[1–3] In the context of platelet transfusion, platelet concentrates (PC) have advantages over whole blood transfusion because of the decreased risk of hemolytic transfusion reactions, volume overload, and the development of polycythemia.

Platelet concentrates from dogs are prepared by serial differential centrifugation of fresh whole blood[4,5] or apheresis.[6,7] Apheresis results in high quality PC, but it requires special equipment and general anesthesia in veterinary practices. Consequently, PC preparation by the serial differential centrifugation of fresh whole blood is more practical in most veterinary clinics.

Abbreviations:

PGE_1	prostaglandin E_1
PRP	platelet-rich plasma
PC	platelet concentrates
PPP	platelet-poor plasma
ADP	adenosine diphosphate
PE	phycoerythrin
PBS	phosphate buffered physiological saline
ANOVA	analysis of variance
SD	standard deviation

A protocol for the preparation of PC from dogs by using serial differential centrifugation was first reported in 1993.[4] In the serial differential centrifugation method, PC are harvested by a high-speed centrifugation of platelet-rich plasma (PRP) after a low-speed centrifugation of fresh whole blood. However, it is difficult to resuspend platelet pellets following the high-speed centrifugation caused by platelet activation. Platelet activation during PC preparation contributes to the development of platelet storage lesions and decreased platelet viability.[8–10] It is therefore important to develop a method to minimize platelet activation during the preparation of PC.

Prostaglandin E_1 (PGE_1) is a reversible inhibitor of platelet activation because of its ability to increase cyclic AMP levels within the platelets.[9,11] Although early studies showed that the addition of PGE_1 to human PRP facilitated the separation, concentration, and resuspension of platelets,[9,12–14] there have been no studies of the effects of PGE_1 on the preparation of PC in dogs. The aim of this study was to investigate

From The Laboratory of Internal Medicine II, School of Veterinary Medicine, Azabu University, Kanagawa, Japan. This work was done in The Laboratory of Internal Medicine II, School of Veterinary Medicine, Azabu University. Previously presented at the 150th Meeting of the Japanese Society of Veterinary Science, 2010.

Corresponding author: Ryo Tsuchiya, DVM, PhD, The Laboratory of Internal Medicine II, School of Veterinary Medicine, Azabu University, 1-17-71 Fuchinobe, Chuou-ku, Sagamihara-shi, Kanagawa 252-5201, Japan; e-mail: tsutiyar@azabu-u.ac.jp.

Submitted May 30, 2011; Revised November 20, 2011; Accepted December 16, 2011.

10.1111/j.1939-1676.2011.00881.x

the efficacy of adding PGE_1 during PC preparation. We estimated the ease of platelet resuspension after high-speed centrifugation of PGE_1-treated PC and then confirmed platelet function before and after transfusion, and also evaluated survival of the PGE_1-treated platelets after transfusion.

Materials and Methods

Study Design

The platelet aggregability in PC before transfusion, the survival of the platelets after transfusion, and the platelet reactivity after transfusion were assessed to evaluate the benefits of modifying the PC preparation by adding PGE_1. The platelet viability in PC prepared with PGE_1 was confirmed by the comparing platelet aggregability before and after PGE_1 treatment (n = 5). The survival of the platelets after transfusion was assessed by flow cytometry using a biotin label. The platelets in PC prepared with PGE_1 and that in PRP without PGE_1 (both n = 5) were labeled with biotin and then were reinfused into the same individuals. Blood samples were collected 1 hour after transfusion (Day 0) and at the same time on Days 1 through 7. The survival time of the transfused platelets were calculated by the changes in the biotin-positive ratio of the platelets. Subsequently, the biotinylated PC prepared with PGE_1 (n = 5) were reinfused and blood samples were collected 1 and 24 hours after reinfusion. The P-selectin expression following thrombin stimulation in the biotin-labeled platelets was analyzed by flow cytometry using FITC-labeled anti-P-selectin antibody to estimate the reactivity after transfusion.

Experimental Animals

Research protocols were approved by the Animal Experiment Committee of Azabu University. Fifteen healthy Beagle dogs, 11 intact males and 4 intact females, 1–12 years of age and weighing 9–15 kg, were used for the experiments. Some dogs were rotated and used for more than 1 experiment (the number of dogs used in each experiment is described below).They were maintained in the Institute of Life Sciences or in the Veterinary Clinical Center, Azabu University, according to the Animal Experiment Guidelines of the university. They had no history of venipuncture or treatment with any drug, including nonsteroidal anti-inflammatory agents, for at least 2 weeks before the study. They were allowed free access to water but were fasted for at least 12 hours before blood collection and were fed after the last sampling was complete on each experimental day.

PC Preparation

A quantity of 200 mL of whole blood was drawn into 200 mL blood transfusion bags[a] containing citrate-phosphate dextrose adenine 1 (CPDA-1) at the standard mixing ratio (1 part CPDA-1 to 6.5 parts blood) from the jugular vein through 17-gauge needles. The bag was weighed during blood collection, and the collection tubing was clamped off when it reached the intended collection volume.

Platelet concentrates were prepared by serial differential centrifugation of fresh whole blood.[4,5] All blood components containing platelets were handled gently at 20–24°C (room temperature) to minimize platelet activation. After resting for 30 minutes, the whole blood was centrifuged (soft spin) for 3.5 minutes at 1,000 × *g* to prepare PRP. The PRP were then transferred into a satellite bag[b] using a plasma extractor. Extraction was stopped when the red blood cell interface was 1 cm from the top of the collecting bag, and the PRP was left undisturbed for 15 minutes. For PC that were to be treated with PGE_1, PGE_1[c] (1 mmol/L in ethanol) was injected into the PRP (final concentration, 1 μmol/L) through an outlet port, and then mixed manually by rocking the bags back and forth. The PRP was centrifuged (hard spin) for 10 minutes at 2,000 × *g* to produce a platelet pellet. The platelet-poor plasma (PPP) was transferred to another satellite bag, leaving behind 20 mL of plasma with the platelet pellet. The platelet pellet was left undisturbed for 1 hour to promote platelet disaggregation, and then the platelets were resuspended by gentle manual back and forth rocking and massaging of the bag.

Aggregability of Platelets in PC Prepared with PGE_1

The aggregability of the platelets in PC treated with and without PGE_1 was assessed. Four samples for platelet aggregometry were collected from the transfusion bags at each step of PC preparation. First, a sample of the PRP was collected from the satellite bag when the PRP was produced, and the remainder was divided in 2 satellite bags. Second, the PGE_1 was added to one of the separated PRP bags, and then a sample (PGE_1^+ PRP) was collected immediately. Third, the PGE_1^+ PRP was centrifuged (hard spin), and then the supernatant was replaced with PGE_1-free autologous plasma. The platelet pellet was resuspended after a 1 hour incubation, and a sample of the PGE_1-removed PC was collected. Fourth, a control PC sample was also collected from the paired untreated PRP bag after high-speed centrifugation, after a 1-hour incubation, and resuspension according to the reported method.[4,5]

Aggregometry was performed as follows. First, the platelet counts were measured using an automated cell counter[d] and adjusted to approximately 250,000/μL by adding autologous PPP. After a 30 minute rest for the resuspended platelets, optical platelet aggregometry was performed by using an aggregometer.[e] Collagen[f] and adenosine diphosphate (ADP)[g] were used as agonists. Because CPDA-1 is not an ideal anticoagulant for aggregometry,[15,16] the stimulating conditions were modified with the addition of $CaCl_2$ to a final concentration of 15 mmol/L to accelerate the platelet reaction, and the addition of low molecular weight heparin[h] at a final concentration 0.6 IU anti-Xa/mL to prevent the plasma coagulation induced by adding the $CaCl_2$. The final concentrations of collagen and ADP were 100 μg/mL and 20 μmol/L, respectively.

Survival of Platelets after Transfusion

The survival of the platelets after transfusion in PC prepared with PGE_1 and that in PRP without PGE_1 were investigated according to Heilmann's technique of biotinylation.[7,16,17] The PC and PRP were produced as described above. Next, the platelet survival was assessed as follows: N-hydroxysuccinimido biotin (0.2 mg/mL PC or PRP)[i] dissolved at 20 mg/mL in dimethylsulphoxide was added into PC prepared with PGE_1 or PRP, and then mixed well. After a 10-minute incubation at room temperature, the biotin-treated platelets were infused to the same individuals through a cephalic vein over 30 minutes. Quantities of 2.5 mL of blood samples were collected 1 hour after reinfusion (Day 0) and at the same time on Days 1 to 7 to assess the survival of the reinfused platelets. The samples were anticoagulated with ethylenediaminetetraacetic acid disodium salt and centrifuged for 1 minute at 2,000 × *g* to separate the PRP. Then the PRP were stored at 4°C until the final sample was collected.

After collecting all the samples for the platelet survival study, the platelet counts of each PRP sample were adjusted to approximately 10,000/μL using a phosphate buffered physiological saline

containing 3% bovine serum albumin at pH 7.2 (PBS). A quantity of 10 μL of phycoerythrin-streptavidin (PE-SA)[j] was added to 100 μL of the platelet suspensions. The percentages of biotinylated platelets were measured by PE positive events using flow cytometry.

The samples were analyzed using an Epics XL flow cytometer[k] or a Cyflow SL instrument.[l] The light scatter and fluorescence channels were set on a logarithmic scale. DNA-check beads[m] were used to calibrate the fluorescence. The forward scatter threshold was set to exclude debris and machine noise. Platelets were identified by their forward and side light scatter. A minimum of 2,000 platelets were analyzed. The background fluorescence was evaluated by use of nonbiotinylated platelets, and gates were established so that approximately 95% of the events had no fluorescence.

The survival of the platelets after transfusion was calculated using a linear regression model.[18,19]

Platelet Reactivity after Transfusion

To investigate the platelet reactivity after transfusion, thrombin-induced P-selectin expression was analyzed. The Heilmann platelet biotinylation technique described above was also used to discriminate the transfused platelets from the other platelets.[7,16,17] Biotinylated PC prepared with PGE_1 were reinfused as described above. A quantity of 2.5 mL of blood was collected into sodium citrate at 1 and 24 hours after reinfusion to assess platelet P-selectin expression with thrombin stimulation.[7,20,21]

Because the P-selectin expression changed over time, the analyses of P-selectin expression were performed at 1 and 24 hours after reinfusion. The PRP was separated from these samples as described above. After a 15-minute incubation of the PRP, PGE_1 at final concentration of 1 μmol/L was added to the PRP to stop the activation of the platelets. Next, the PRP was centrifuged for 3 minutes at 2,000 × *g*, and platelets were resuspended in PBS at approximately 10,000/μL. A total of 100 μL of the platelet suspension was incubated with 20 μL of FITC-labeled anti-human P-selectin mouse monoclonal antibody[7,21,n] and 10 μL of PE-SA.

While they were incubated with the antibody, the platelets were activated with thrombin[o] at a final concentration 0.25 U/mL in the stimulus group. This was done to determine if the transfused platelets maintained their reactivity to thrombin stimulation. After a 20-minute incubation at room temperature and 2 washes, the platelets were resuspended in 150 μL of PBS and analyzed immediately using flow cytometry.

The positive and negative control data were also acquired from preliminary studies where platelets were not transfused, but where they were thrombin stimulated or were left unstimulated.

The FITC-labeled mouse IgG_1[p] was used as an isotypic control for the anti-P-selectin monoclonal antibody, and no nonspecific binding was observed (data not shown). Although the same flow cytometer settings as described above were used, the background fluorescence was evaluated by use of nonstimulated platelets. Compensation was performed for all dual-labeled samples to ensure adequate separation of events with and without fluorescence.

Statistical Analysis

All data were analyzed using the same statistical software program.[q] Normality was confirmed by the Kolmogorov-Smirnov test. The maximal aggregation values were compared between the PRP and other fractions using Dunnett's posthoc test. The unpaired t-test was used for the analysis of the platelet survival after transfusion. Unpaired t-tests were performed to analyze the differences in the platelet reactivity between the positive control and the values after transfusion. In addition, the paired t-test was used to compare the platelet reactivity between samples collected at 1 and 24 hours after transfusion. Data were expressed as the means ± standard deviation (SD). Box plots were also used as descriptive parameters within figures. Values of $P < .05$ were considered to be significant.

Results

Platelet Resuspension after High-Speed Centrifugation

Platelets were packed tightly to the bottom, irrespective of the presence of PGE_1 (Fig 1A). The platelet pellets prepared with PGE_1 achieved uniform resuspension after the 20-minute agitation (Fig 1B). Because the untreated platelet pellet was difficult to disaggregate, there were more platelet aggregates in the bag without PGE_1 (Fig 1C). The platelet pellets without PGE_1 took 30 minutes or more to achieve uniform resuspension.

Aggregability of Platelets in PC Prepared with PGE_1

Although there were significant differences in the aggregability between PRP and PGE_1[+] PRP (collagen: $P < .001$; n = 5, ADP: $P < .001$; n = 5, Fig 2A and 2B), there was no significant difference in the aggregability between PRP and PGE_1-removed PC using either agonist. As a result of the replacement of PGE_1-containing plasma with intact PPP, the collagen or ADP-induced platelet aggregation recovered similar to the PRP.

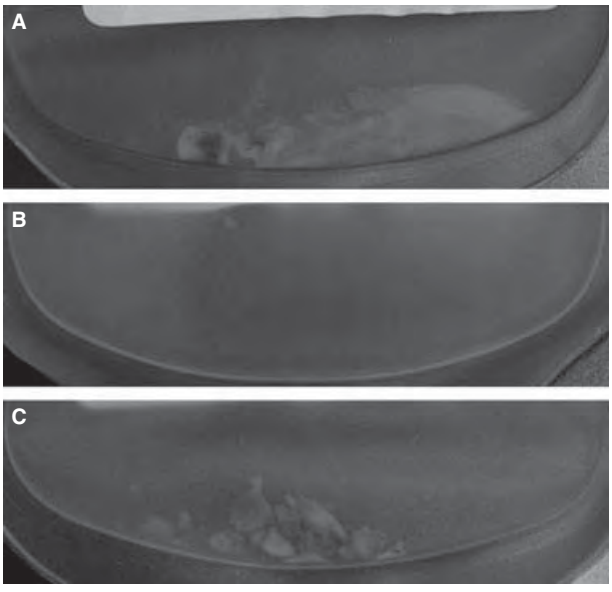

Fig 1. The platelet resuspension after high-speed centrifugation and a 1-hour resting period with (**B**) and without (**C**) PGE_1 in dogs. Platelet pellets (**A**) were manipulated gently by hand for 20 minutes to achieve uniform resuspension. A lot of platelet aggregates were still found in bag C.

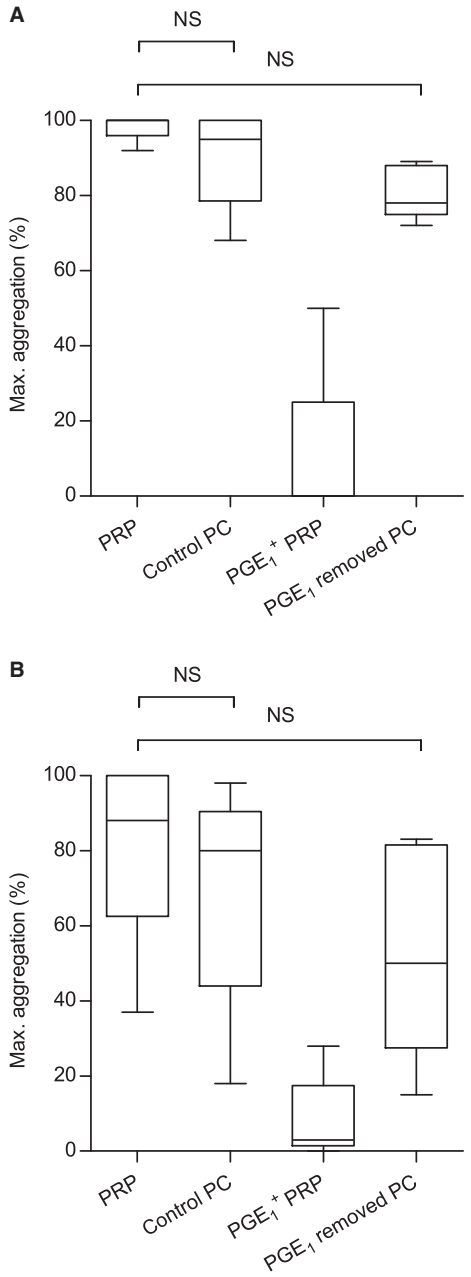

Fig 2. The aggregability of platelets in platelet concentrates (PC) prepared with prostaglandin E_1 (PGE_1) as analyzed by turbidimetric aggregometry in dogs. The samples of platelet-rich plasma (PRP), control PC (without PGE_1), PGE_1^+ PRP, and PGE_1 removed PC were collected from transfusion bags at each step of PC preparation. The final concentrations of collagen (**A**; n = 5) and ADP (**B**; n = 5) were 100 μg/mL and 20 μmol/L, respectively. Dunnett's posthoc test was used to compare the PRP and other fractions. For box graphs, the line within the box represents the median value, the limits of the box represent the 25th and 75th percentile values, and the whiskers represent the range. NS, not significant (same in Figs 4 and 6).

Survival of Platelets after Transfusion

Transfused platelets were discriminated as biotin/PE-SA positive events (Fig 3). The platelet survival

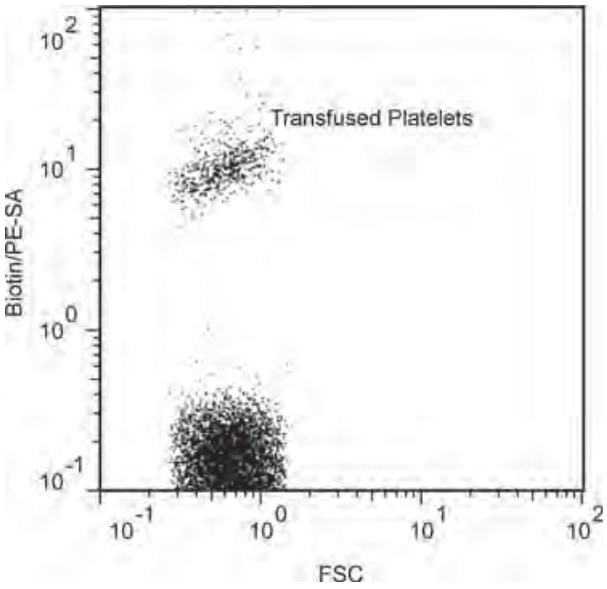

Fig 3. A dot plot of the transfused platelets evaluated by flow cytometry in dogs. Biotin/phycoerythrin-streptavidin (SA) labeled platelets were discriminated as PE positive events (upper scatters).

was 8.04 ± 0.49 days (n = 5) in the group that was transfused with PRP without PGE_1 and was 7.56 ± 0.81 days (n = 5) in the group that was transfused with PC prepared with PGE_1 (Fig 4). No significant difference was found between the groups in the platelet survival (P = .3).

Platelet Reactivity after Transfusion

Transfused platelets were completely discriminated from other platelets as PE-positive events (Fig 5). There were no significant differences between PE-positive and PE-negative platelets with regard to the P-selectin expression that was evaluated as FITC positive events. Thrombin-induced P-selectin expression events were compared between transfused PC and control data (Fig 6). There were no significant differences between the positive control (P-selectin positive ratio: 53.7 ± 5.1%; n = 5) and transfused PC prepared with PGE_1 (1 hour after transfusion: 42.0 ± 13.0%; n = 5, 24 hour after transfusion: 47.9 ± 13.3%; n = 5) by unpaired t-tests. No significant difference was found between the values at 1 and 24 hours after transfusion by the paired t-test.

Discussion

This study suggests that the addition of PGE_1 during preparation of PC by serial differential centrifugation is an effective tool for decreasing platelet activation.

It is often difficult to resuspend platelet pellets following high-speed centrifugation of PRP according to the reported protocol,[4,5] and treatment with PGE_1 made platelet resuspension easier and faster. Therefore,

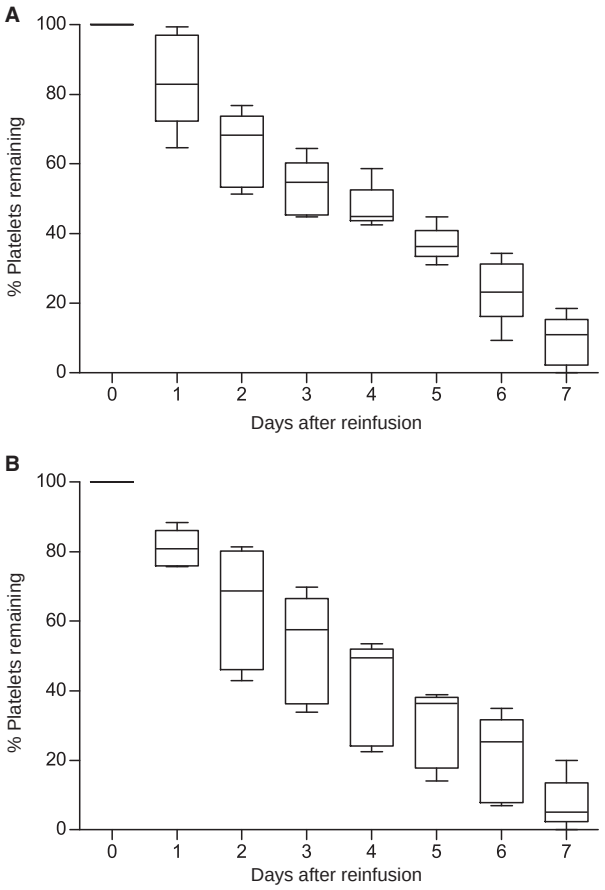

Fig 4. The survival of biotin-labeled autologous platelets in dogs, reinfused as platelet-rich plasma (**A**; n = 5) or PC prepared with prostaglandin E_1 (**B**; n = 5). The percentage of biotinylated platelets at various times was quantitated by flow cytometry as indicated in Figure 3. The percentage of biotin-positive platelets on Day 0 in each dog was estimated as 100% remaining. According to the consensus opinion of the Biomedical Excellence for Safer Transfusion Collaborative, only time points beyond 20 hours after infusion were used to analyze the survival of platelets after transfusion. No significant difference in the platelet survival was found between the groups according to the unpaired t-test. For box graphs, the line within the box represents the median value, the limits of the box represent the 25th and 75th percentile values, and the whiskers represent the range.

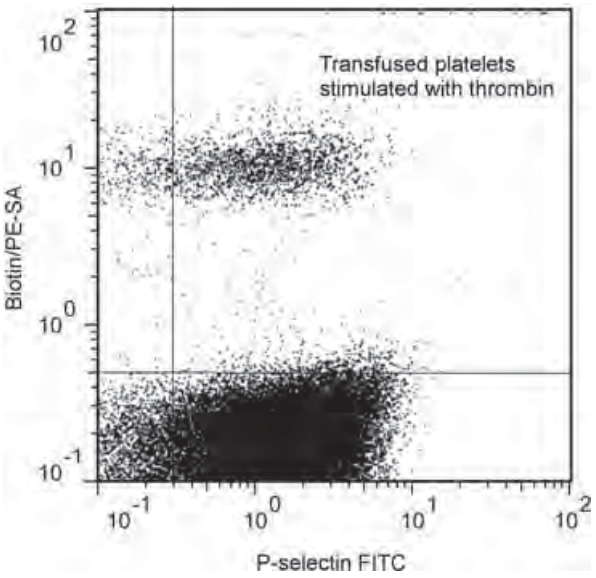

Fig 5. A dot plot of the transfused platelet responses to thrombin as quantitated by the P-selectin expression in dogs. To detect platelet surface P-selectin, an FITC-labeled anti-human P-selectin monoclonal antibody was used. Transfused platelets were discriminated as indicated in Figure 3.

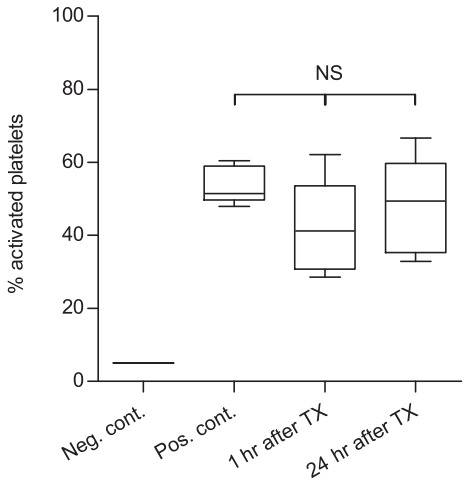

Fig 6. The reactivity of the transfused platelets in dogs. The platelet responses at 1 and 24 hours after transfusion were quantitated by thrombin-induced P-selectin expression as indicated in Figure 5. The positive and negative controls were derived from platelets before transfusion with and without thrombin stimulation (n = 5). There were no significant differences between the positive control and transfused Platelet concentrates as determined by unpaired *t*-tests. There was also no significant difference found between the values at 1 and 24 hours after transfusion by the paired t-test. Neg. cont., negative control; Pos. cont., positive control; after TX, after transfusion. For box graphs, the line within the box represents the median value, the limits of the box represent the 25th and 75th percentile values, and the whiskers represent the range. NS, not significant.

addition of PGE_1 resolved the difficulties associated with platelet pellet resuspension in dogs.

To treat hemostatic abnormalities caused by thrombocytopenia, thrombocytopathy, or both, platelets in PGE_1-treated PC should act normally after transfusion. The inhibitory effect of PGE_1 on platelets is considered to be reversible,[9,11] but it was necessary to confirm the reversibility in vitro before a PGE_1-treated PC transfusion is performed. In this study, the collagen- or ADP-induced platelet aggregation was clearly inhibited by PGE_1 treatment. After replacement of the supernatant plasma containing PGE_1 with autologous intact PPP, the inhibitory effects of PGE_1 were lost. This reversibility of the effect of PGE_1 suggested that platelets in PGE_1-treated PC act normally during hemostasis when they are diluted with a larger amount of circulating plasma after transfusion.

Whenever new platelet-rich products are produced, an assessment of the in vivo platelet survival is essential to predict the platelet viability after transfusion. We found that the platelet survival after transfusion of PGE_1-treated PC was equal to that of intact PRP.

The reversible effect of PGE_1 on platelets was confirmed in vitro using platelet aggregometry as described above. However, the viability of platelets after transfusion in PGE_1-treated PC is not necessarily guaranteed by evidence of their aggregation. Therefore, we investigated the platelet reactivity after transfusion. Although there are many kinds of laboratory examinations that can be used to assess the quality of PC, there are no in vivo methods to predict the clinical efficacy.[22] For this study, we combined the thrombin-induced P-selectin expression analysis with Heilmann's biotinylation technique[7,16,17] which distinguishes transfused platelets from other intact platelets using flow cytometry. This original technique was considered to be quite powerful to estimate the viability of the platelets after transfusion. Our results showed that the strong inhibitory effect of PGE_1 on platelet function had disappeared after PC transfusion, and that platelets in PGE_1-treated PC maintain their reactivity for at least 24 hours after transfusion.

Because the PGE_1 solution is available commercially and is licensed for clinical use, the addition of PGE_1 during preparation of PC is easily implemented and practical. In human medicine, the addition of PGE_1 to the preparation of PC and 5 days of storage reduced the survival of platelets after transfusion to 5.8 ± 1.6 days compared with 6.9 ± 1.4 days in control PC prepared without PGE_1.[9] Although the addition of PGE_1 did not shorten the survival of platelets after transfusion in this study, we did not assess the in vivo survival of stored platelets treated with PGE_1. Therefore, the addition of PGE_1 should only be considered when fresh PC is transfused immediately in dogs. Furthermore studies are needed to investigate the storage stability of PC prepared with PGE_1.

Footnotes

[a] Teruflex, BB-SCD207J01, Terumo Company, Tokyo, Japan
[b] Transfer Bags, BB-T015CJ, Terumo Company
[c] Prostaglandin E_1, Sigma Chemical Company, Saint Louis, MO
[d] Sysmex F-820, Sysmex Corporation, Kobe, Japan
[e] Chrono-log C550 dual-channel aggregometer, Chrono-log Corp, Havertown, PA
[f] Chrono-collagen, Chrono-log Corp
[g] Chrono-ADP, Chrono-log Corp
[h] FRAGMINiv5,000, Pfizer Japan Inc, Tokyo, Japan
[i] N-hydroxysuccinimido biotin, Sigma Chemical Company
[j] Phycoerythrin-streptavidin, Sigma Chemical Company
[k] EPICS XL, Beckman Coulter, Fullerton, CA
[l] CyFlow SL, Partec Gmbh, Munster, Germany
[m] DNA-check Beads, Beckman Coulter, Fullerton, CA
[n] Anti-human CD62P-FITC, clone AC1.2, Becton Dickinson, San Jose, CA
[o] Thrombin, Sigma Chemical Company
[p] Mouse IgG_1 isotype control-FITC, clone MOPC-21, Becton Dickinson, San Jose, CA
[q] Prism, Version 5.0, Graphpad Software, San Diego, CA

Acknowledgments

This study was partially supported by The Promotion and Mutual Aid Corporation for Private Schools of Japan, and a Grant-in-Aid for Matching Fund Subsidy for Private Universities.

References

1. Abrams-Ogg AC. Triggers for prophylactic use of platelet transfusions and optimal platelet dosing in thrombocytopenic dogs and cats. Vet Clin North Am Small Anim Pract 2003;33:1401–1418.

2. Stroncek DF, Rebulla P. Platelet transfusions. Lancet 2007;370:427–438.

3. Callan MB, Appleman EH, Sachais BS. Canine platelet transfusions. J Vet Emerg Crit Care (San Antonio) 2009;19:401–415.

4. Abrams-Ogg AC, Kruth SA, Carter RF, et al. Preparation and transfusion of canine platelet concentrates. Am J Vet Res 1993;54:635–642.

5. Allyson K, Abrams-Ogg AC, Johnstone IB. Room temperature storage and cryopreservation of canine platelet concentrates. Am J Vet Res 1997;58:1338–1347.

6. Callan MB, Appleman EH, Shofer FS, et al. Clinical and clinicopathologic effects of plateletpheresis on healthy donor dogs. Transfusion 2008;48:2214–2221.

7. Appleman EH, Sachais BS, Patel R, et al. Cryopreservation of canine platelets. J Vet Intern Med 2009;23:138–145.

8. Rinder HM, Snyder EL. Activation of platelet concentrate during preparation and storage. Blood Cells 1992;18:445–456; discussion 457-460.

9. Hawker RJ, Turner VS, Mitchell SG. Use of prostaglandin E_1 during preparation of platelet concentrates. Transfus Med 1996;6:249–254.

10. Shrivastava M. The platelet storage lesion. Transfus Apher Sci 2009;41:105–113.

11. Feinstein MB, Fraser C. Human platelet secretion and aggregation induced by calcium ionophores. Inhibition by PGE1 and dibutyryl cyclic AMP. J Gen Physiol 1975;66:561–581.

12. Becker GA, Chalos MK, Tuccelli M, et al. Prostaglandin E_1 in preparation and storage of platelet concentrates. Science 1972;175:538–539.

13. Shio H, Ramwell PW. Prostaglandin E_1 in platelet harvesting: An *in vitro* study. Science 1972;175:536–538.

14. Valeri CR, Zaroulis CG, Rogers JC, et al. Prostaglandins in the preparation of blood components. Science 1972;175:539–542.

15. Moroff G, Morse EE, Kakaiya RM, et al. Platelet viability following storage for 5 days. Influence of holding whole blood for 8 hours at 20 to 24 degrees C before concentrate preparation. Transfusion 1984;24:382–385.

16. Tsuchiya R, Yagura H, Hachiya Y, et al. Aggregability and post-transfusion survival of canine platelets in stored whole blood. J Vet Med Sci 2003;65:825–829.

17. Heilmann E, Friese P, Anderson S, et al. Biotinylated platelets: A new approach to the measurement of platelet life span. Br J Haematol 1993;85:729–735.

18. Dumont LJ. Analysis and reporting of platelet kinetic studies. Transfusion 2006;46:67S–73S.

19. Valeri CR, Ragno G. Platelet radiolabeling procedure. Transfusion 2007;47:946–947; author reply 947.

20. Yeo EL, Gemmell CH, Sutherland DR, et al. Characterization of canine platelet P-selectin (CD 62) and its utility in flow cytometry platelet studies. Comp Biochem Physiol B 1993;105: 625–636.

21. Wills TB, Wardrop KJ, Meyers KM. Detection of activated platelets in canine blood by use of flow cytometry. Am J Vet Res 2006;67:56–63.

22. Maurer-Spurej E, Chipperfield K. Past and future approaches to assess the quality of platelets for transfusion. Transfus Med Rev 2007;21:295–306.

犬のアロペシアX（ポメラニアン脱毛症）の遺伝子解析

村上　賢（麻布大学分子生物学）

研究要旨

本研究では、DNA マイクロアレイ法や real-time RT-PCR 法による定量的遺伝子発現比較解析を用いて、犬のアロペシア X 症の原因候補遺伝子として、Dlx3 及び Lef1 の 2 つを選定した。続いて、これらの遺伝子の発現を転写段階で評価するレポーターアッセイ系を構築した。イヌ Lef1 転写因子はイヌ Dlx3 遺伝子発現を促進した。Lef1 転写因子の新たな結合部位が推測された。発毛・育毛効果がある R&U には、Dlx3 プロモーター及びLef1-プロモーター -ルシフェラーゼレポーター評価系においてこれら遺伝子の発現促進作用があることを示した。今後は、本評価系をイヌの発毛・育毛に関わる物質のスクリーニングアッセイとして利用するとともに、イヌ毛乳頭初代培養細胞の確立を試み、それを利用した、より精度の高いアッセイ系の構築を目指す。イヌのアロペシア X は、成年発症型、非炎症性、非掻痒性の脱毛という点で、人の脱毛と似た現象であり、当該スクリーニングアッセイ系の確立は、イヌだけでなく人の発毛・育毛関連因子のスクリーニングや作用機序解明への貢献が期待できる。

研究目的

犬のアロペシア X は、成年発症型非炎症性非掻痒性の先天性脱毛疾患である。1〜4 歳で発症し、痛みや痒みを伴わない脱毛が頭部と四肢端以外に起こる皮膚疾患である。脱毛を示す外観異常以外には特に病気は認められない。犬種特異性があり、特にポメラニアンに好発する。原因は不明であり、治療法は確立されていない。本研究では、疾患の発症原因を遺伝子からアプローチし、アロペシア X の疾患関連原因遺伝子を同定することを第一の目的とし、その成果を遺伝子発現レベルでの治療候補薬の開発、スクリーニングアッセイ系へ応用することを第二の目的とする。

材料と方法

健常犬の皮膚とアロペシア X 症ポメラニアン犬の脱毛部の皮膚から RNA を抽出し、DNA マイクロアレイによる網羅的遺伝子発現比較解析を実施し、発現変動のある遺伝子群を疾患関連原因候補遺伝子とした。次に、アロペシア X 疾患犬と健常犬及びカラーダイリューションアロペシア(CDA)疾患犬の数多くの個体の皮膚から RNA を抽出し、これら疾患関連原因候補遺伝子について新規に設定したプライマーを用いて、real-time RT-PCR 法による定量的遺伝子発現を解析した。最有力の疾患関連遺伝子（アロペシア X のみで減少している遺伝子）の候補として注目した Dlx3（Distal-less homeobox 3）及び Lef1（Lymphoid Enhancer-Binding Factor 1）について、以下のプラスミドコンストラクト

を作製した。即ち、DNA 国際データバンクに登録されているイヌゲノム配列を参考に、イヌ Dlx3 遺伝子の推定プロモーター領域（-2125～+15：+1 は転写開始点）を PCR 増幅し、ルシフェラーゼレポータープラスミドを構築した。-1675～-125 の間で様々な長さのプロモーター領域をもつデリーションミュータントのレポーターベクターも作製し、C2C12 細胞を用いたレポーターアッセイ系を構築した。また、イヌ Lef1 遺伝子のタンパク質コード領域の cDNA をもつ発現系ベクターを作製した。さらに、Lef1 遺伝子のプロモーター領域をもつルシフェラーゼレポーターベクターも作製した。

結果と考察

DNA マイクロアレイによる網羅的遺伝子発現比較解析の結果、アロペシア X 症の皮膚組織で健常皮膚に比べて有意に発現量の減少が見られた複数の遺伝子について疾患原因候補遺伝子として注目した。次に、これらの候補遺伝子について、アロペシア X 疾患犬と健常犬及び CDA 疾患犬の数多くの個体の皮膚における厳密な定量的発現解析を real-time RT-PCR 法を用いて実施した。その結果、最有力候補遺伝子（アロペシア X のみで減少している遺伝子）として、Dlx3 及び Lef1 が得られた（図 1)。Dlx3 遺伝子産物は毛包の分化や毛の周期に関与するタンパク質の 1 つであり、Lef1 遺伝子産物は Dlx3 遺伝子発現を促進する転写因子であることがマウスで知られている。

イヌ Dlx3 遺伝子の推定プロモーター領域（-2125～+15）にルシフェラーゼ遺伝子を組み込んだ新規のレポータープラスミド、及びそのデリーションミュータントのレポーターベクターを用いて、C2C12 細胞内で発現系ベクターを用いてイヌ Lef1 遺伝子のタンパク質を一過性に過剰発現させ、ルシフェラーゼ活性を測定した。この評価系で、Lef1 転写因子の発現は、期待通りに Dlx3 遺伝子の発現を増加させた（図 2)。興味深いことに、マウスで報告されている Lef1 転写因子が応答する結合部位（-158～-150）以外にも、Dlx3 遺伝子の発現を制御する応答エレメントが Dlx3 遺伝子のプロモーター領域に存在することが示唆された（図 2)。さらに、イヌアロペシア X に対して劇的な発毛効果があることが報告されている市販の動物用健康補助食品 R&U（生理活性物質を含むリゾープス菌 *rhizopus oryzae* 由来抽出物）を本評価系でアッセイしたところ、R&U は用量依存的に Dlx3 遺伝子発現を促進した（図 3)。R&U の発毛・育毛効果をサポートする一つの機序であるかもしれない。また、構築した Lef1 遺伝子のプロモーター領域をもつルシフェラーゼレポータープラスミドによるレポーターアッセイ系を用いて R&U を評価したところ、R&U は転写段階での Lef1 遺伝子の発現も促進することがわかった（図 4)。これらのレポーター評価系を用いて、Dlx3 遺伝子発現の制御機構に関する分子生物学的解析をするとともに、当該遺伝子発現を促進する物質の探索を行っている。本研究でのレポーター評価系では、いくつかの培養細胞株を検討した上で、C2C12 細胞株を用いたが、より信頼性の高い発毛・育毛効果を評価するためにイヌ毛乳頭初代培養細胞株を確立し用いるのが望ましいと思われる。

また、アロペシア X 疾患犬と健常犬におけるプロモーター領域を含む Dlx3 遺伝子の塩基配列を決定し比較したが、調べた領域における両者の塩基配列に相違は認められなかった。

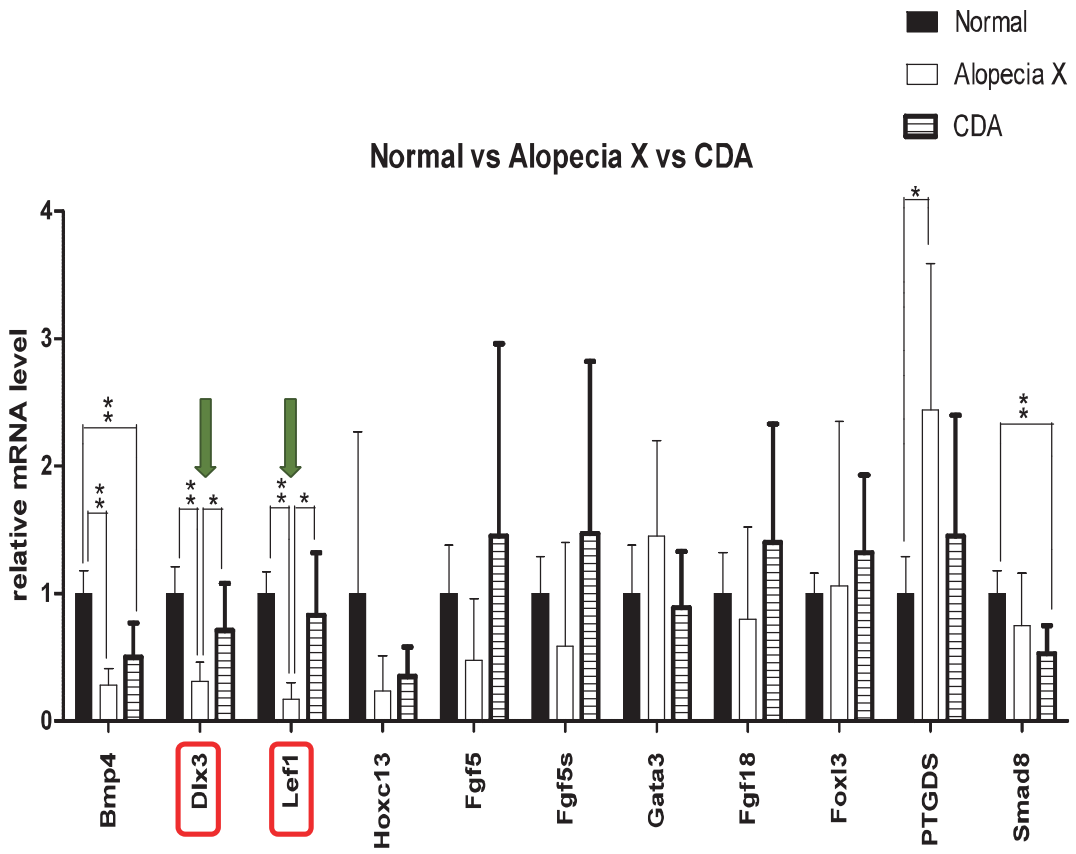

図1　real-time RT-PCRによる各種遺伝子の定量的発現解析

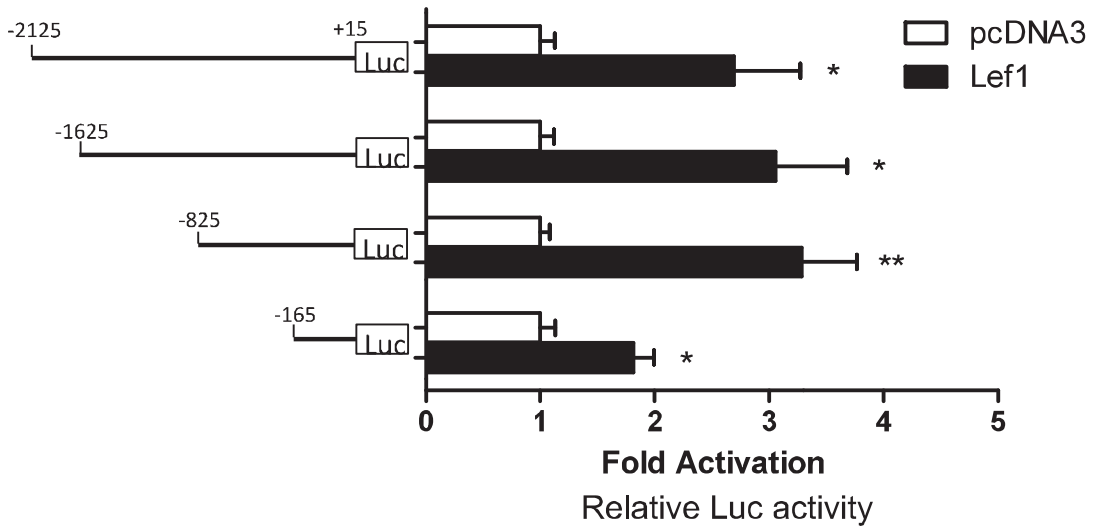

図2　レポーターアッセイによるDlx3プロモーター領域におけるLef1タンパク質の反応性

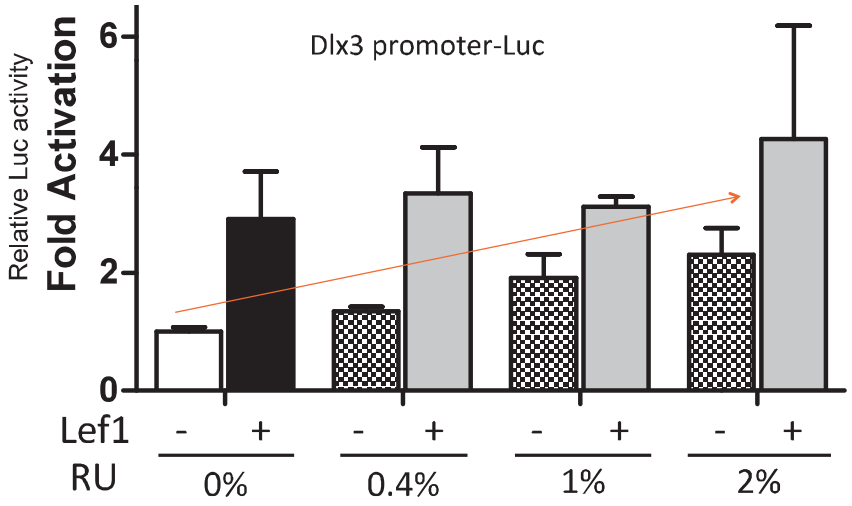

図3　R&Uによる濃度依存的Dlx3遺伝子発現の促進

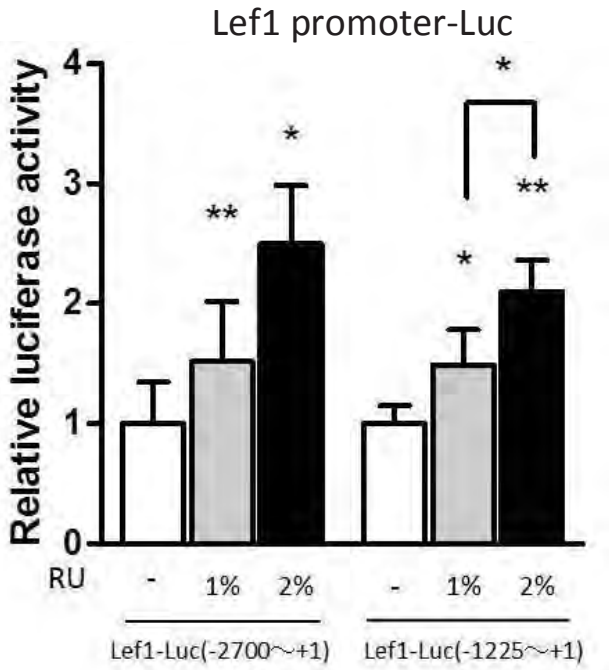

図4　R&Uによる濃度依存的Lef1遺伝子発現の促進

1.論文発表

1) Katakawa Y, Funaba M, Murakami M.: Smad8/9 is regulated through the BMP pathway. J. Cell. Biochem. [Epub ahead of print] 2016.
2) Nishino Y, Murakami M, Funaba M.: Expression and role of the TGF-β family in glial cells infected with Borna disease virus. Microbes and Infection., 18, 128-36, 2016.
3) Kida R, Yoshida H, Murakami M, Shirai M, Hashimoto O, Kawada T, Matsui T, Funaba M.: Direct action of capsaicin in brown adipogenesis and activation of brown adipocytes. Cell Biochem. Funct., 34, 34-41, 2016.
4) Kasai T, Kato Y, Saegusa S, Murakami M.: Distribution of major staphylococcalca cassette chromosome mec types and exfoliative toxin genes in Staphylococcus pseudintermedius strains from dogs with superficial pyoderma. J Azabu Uni., 27, 27-31, 2015.
5) Yamada A, Kodo Y, Murakami M, Kuroda M, Aoki T, Fujimoto T, Arai K.: Hybrid origin of gynogenetic clones and the introgression of their mitochondrial genome into sexual diploids through meiotic hybridogenesis in the loach, Misgurnus anguillicuadatus. J Exp Zool A Ecol Genet Physiol 323, 593-606, 2015.
6) Shirai M, Nomura R, Kato Y, Murakami M, Kondo C, Takahashi S, Yamasaki Y, Matsumoto-Nakano M, Arai N, Yasuda H, Nakano K, Asai F.: Short communication: Distribution of Porphyromonas gulae fimA genotypes in oral specimens from dogs with mitral regurgitation. Res Vet Sci 102, 49-52, 2015.

7) Kanamori Y, Murakami M, Matsui T, Funaba M.: Role of TPA-responsive element in hepcidin transcription induced by the bone morphogenetic protein pathway. Biochem Biophys Res Commun 466, 162-6, 2015.
8) Murakami M, Ohi M, Ishikawa S, Shirai M, Horiguchi H, Nishino Y, Funaba M.: Adaptive expression of uncoupling protein 1 in the carp liver and kidney in response to changes in ambient temperature. Comp Biochem Physiol Part A, 185, 142-9, 2015. 査読有
9) Kanamori Y, Murakami M, Matsui T. and Funaba M.: The regulation of hepcidin expression by serum treatment: requirements of the BMP response element and STAT- and AP-1-binding sites. Gene 551, 119-126, 2014.
10) Kanamori Y, Murakami M, Matsui T, Funaba M.:Hepcidin expression in liver cells: evaluation of mRNA levels and transcriptional regulation.Gene 546, 50-5, 2014. 査読有
11) Yamaguchi S, Sano A, Hiruma M, Murata M, Kaneshima T, Murata Y, Takahashi H, Takahashi S, Takahashi Y, Chibana H, Touyama H, Nguyen Thi Thanh Ha, Nakazato Y, Uehara Y, Hirakawa M, Imura Y, Terashima Y, Kawamoto Y,Takahashi K,Sugiyama K, Hiruma M, Murakami M, Hosokawa A, Uezato H.: Isolation of Dermatophytes and Related Species from Domestic Fowl (Gallus gallus domesticus). Mycopathologia., 178, 135-43, 2014.
12) Nishita T, Yatsu J, Murakami M, Kamoshida S, Orito K, Ichihara N, Arishima K, Ochiai H.: Isolation and sequencing of swine carbonic anhydrase VI, an enzyme expressed in the swine kidney. BMC Res Notes 7, 116, 2014.
13) Asai K, Funaba M, Murakami M.: Enhancement of RANKL-induced MITF-E expression and osteoclastogenesis by TGF-β. Cell Biochem Funct 32, 401-9, 2014.
14) Murata M, Murakami M.: Two distinct mtDNA lineages among captive African penguins in Japan. J Vet Med Sci 76, 559-63, 2014.
15) Watanabe M, Tanaka K, Takizawa T, Segawa K, Neo S, Tsuchiya R, Murata M, Murakami M, Hisasue M.: Characterization of a canine tetranucleotide microsatellite marker located in the first intron of the tumor necrosis factor alpha gene. J Vet Med Sci 76, 119-22. 2014.
16) Shibuya E, Murakami M, Kondo M, Kamei Y, Tomonaga S, Matsui T, Funaba M.: Downregulation of Pgc-1α expression by tea leaves and their by-products. Cell Biochem Funct 32, 236-40, 2013.
17) Suenaga M, Kurosawa N, Asano H, Kanamori Y, Umemoto T, Yoshida H, Murakami M, Kawachi H, Matsui T, Funaba M.: Bmp4 expressed in preadipocytes is required for the onset of adipocyte differentiation. Cytokine 64, 138-45, 2013.
18) Dong J, Murakami M, Fujimoto T, Yamaha E, Arai K.: Genetic characterization of the progeny of a pair of the tetraploid silver crucian carp Carassius auratus langsdorfii. Fish Sci 79, 935-41, 2013.

19) Iida N, Fukushima H, Hiroi M, Yagi M, Kanda T, Murakami M, Sugiyama K.: Development of duplex SYBR green real-time PCR for rapid and simultaneous detection of 16 specific genes of 16 major foodborne bacteria. Jpn J Food Microbiol (日本食品微生物学会雑誌), 30, 160-4, 2013.
20) Yoshida H, Kanamori Y, Asano H, Hashimoto O, Murakami M, Kawada T, Matsui T, Funaba M.: Regulation of brown adipogenesis by the Tgf-β family: Involvement of Srebp1c in Tgf-β- and Activin-induced inhibition of adipogenesis. Biochim Biophys Acta 1830, 5027–35, 2013.
21) Ohnishi M, Okatani AT, Harada K, Sawada T, Marumo K, Murakami M, Sato R, Esaki H, Shimura K, Kato H, Uchida N, Takahashi T.: Genetic characteristics of CTX-M-Type extended-spectrum-β-lactamase (ESBL)-producing enterobacteriaceae involved in mastitis cases on Japanese dairy farms, 2007 to 2011. J Clin Microbiol 51, 3117-22, 2013.
22) Ohnishi M, Okatani AT, Esaki H, Harada K, Sawada T, Murakami M, Marumo K, Kato Y, Sato R, Shimura K, Hatanaka N, Takahashi T.: Herd prevalence of Enterobacteriaceae producing CTX-M-type and CMY-2 β-lactamases among Japanese dairy farms. J Appl Microbiol 115, 282-9, 2013.
23) Hirai N, Shirai M, Kato Y, Murakami M, Nomura R, Yamasaki Y, Takahashi S, Matsumoto-Nakano M, Nakano K, Asai F.: Correlation of age with distribution of periodontitis-related bacteria in Japanese dogs. J Vet Med Sci 75, 999-1001, 2013.
24) Murakami M, Shirai M, Ooishi R, Tsuburaya A, Asai K, Hashimoto O, Ogawa K, Nishino Y, Funaba M.: Expression of activin receptor-like kinase 7 in adipose tissues. Biochem Genet 51, 202-10, 2013.
25) Murata M, Takahashi H, Takahashi S, Takahashi Y, Chibana H, Murata Y, Sugiyama K, Kaneshima T, Yamaguchi S, Miyasato H, Murakami M, Kano R, Hasegawa A, Uezato H, Hosokawa A, Sano A.: Isolation of Microsporum gallinae from a fighting cock (*Gallus gallus domesticus*) in Japan. Med. Mycol., 51, 144-9, 2013.
26) Yamasaki Y, Nomura R, Nakanoa K, Inaba H, Kuboniwa M, Hirai N, Shirai M, Kato Y, Murakami M, Naka S, Iwai S, Matsumoto-Nakano M, Ooshima T, Amano A, Asai F.: Distribution and molecular characterization of *Porphyromonas gulae* carrying a new fimA genotype. Vet Microbiol 161, 196-205, 2012.
27) Haishima A, Murakami M, Ikeda T, Inoue K, Kamiie J, Shirota K.: Detection of Bcl-2 mRNA and its product in the glomerular podocytes of the normal rat kidney. Exp. Toxicol. Pathol., 64, 633-7, 2012.
28) Nomura R, Shirai M, Kato Y, Murakami M, Nakano K, Hirai N, Mizusawa T, Naka S, Yamasaki Y, Matsumoto-Nakano M, Ooshima T, Asai F.: Diversity of fimbrillin among *Porphyromonas gulae* clinical isolates from Japanese dogs. J Vet Med Sci 74, 885-91,

2012.
29) Tanaka M, Izawa T, Kuwamura M, Nakao T, Maezono Y, Ito S, Murata M, Murakami M.,, Sano A,Yamate J.: Deep granulomatous dermatitis of the fin caused by fusarium solani in a false killer whale (*Pseudorca crassidens*). J. Vet. Med. Sci., 74, 779-82, 2012.
30) Nishikawa O, Arishima K, Kobayashi T, Shirai M, Murakami M, Sakaue M,Yamamoto M.: Maternal exposure to low doses of DES altered mRNA expression of hepatic microsomal enzymes in male rat offspring. J. Vet. Med. Sci., 74, 247-53, 2012.
31) Ishii Y, Takizawa T, Iwasaki H, Fujita Y, Murakami M, Groppe JC, Tanaka K.: Nucleotide polymorphisms in the canine Noggin gene and their distribution among dog (*Canis lupus familiaris*) breeds. Biochem Genet 50, 12-8, 2012.
32) Ooishi R, Shirai M, Funaba M, Murakami M.: Microphthalmia-associated transcription factor is required for mature myotube formation. Biochim Biophys Acta 1820, 76–83, 2012.
33) Umemoto T, Furutani Y, Murakami M, Matsui T, Funaba M.: Endogenous Bmp4 in myoblasts is required for myotube formation in C2C12 cells. Biochim. Biophys. Acta., 1810, 1127-35, 2011.
34) Morita H, Nakano A, Onoda H, Toh H, Oshima K, Takami H, Murakami M, Fukuda S, Takizawa T, Kuwahara T, Ohno H, Tanabe S,Hattori M.: *Bifidobacterium kashiwanohense* sp. nov., isolated from healthy infant faeces. Int. J. Syst. Evol. Microbiol., 61(Pt 11), 2610-5, 2011.
35) Kato Y, Shirai M, Murakami M, Mizusawa T, Hagimoto A, Wada K, Nomura R, Nakano K, Ooshima T, Asai F.: Molecular detection of human periodontal pathogens in oral swab specimens from dogs in Japan. J Vet Dent 28, 84-89, 2011.

2. 学会発表

1) 片川優子、舟場正幸、村上賢：BMP 経路による Smad8/9 遺伝子発現制御. 第 38 回日本分子生物学会年会、神戸、2015 年 12 月
2) 大久保倫子、赤池かんな、村上賢：国内ケープペンギンの個体識別および父子鑑定におけるマイクロサテライト DNA マーカーの有用性. 第 158 回日本獣医学会学術集会、十和田、2015 年 9 月
3) 黒田真道、村上賢、藤本貴史、荒井克俊：反復配列をプローブとした FISH による染色体識別とクローンドジョウの雑種起源解明. 平成 26 年度日本水産学会秋季大会、福岡、2014 年 9 月
4) 村田倫子、亀井早紀、村上賢：フンボルトペンギン属 3 種のペンギンの核型分析による特徴付け. 第 157 回日本獣医学会学術集会、札幌、2014 年 9 月
5) 片川優子、舟場正幸、村上賢：BMP による Smad8 発現調節メカニズムの解析. 第 157

回日本獣医学会学術集会、札幌、2014 年 9 月

6) 浅井久美子、舟場正幸、村上賢：TGF-βによる RANKL 誘導性 Mitf-E の発現と破骨細胞分化への影響. 第 36 回日本分子生物学会年会、神戸、2013 年 12 月

7) 片川優子、堀口昌秀、舟場正幸、村上賢：BMP による Smad8 発現調節. 第 36 回日本分子生物学会年会、神戸、2013 年 12 月

8) Murata K, Murakami S.: Characterization of DNA markers isolated from the African penguin (Spheniscus demersus) by using RDA and MASA techniques. 6th Asian Meeting on Zoo and Wildlife Medicine/Conservation, Singapore, Oct, 2013.

9) 金森耀平、村上賢、松井徹、舟場正幸：肝細胞培養系とヘプシジン遺伝子発現. 第 30 回日本微量栄養素学会学術集会、京都、2013 年 6 月

10) 杉山和寿、小久保聖子、内田貴大、村上賢：*Chaetomium globosum* 及び *Microsporum canis* の PCR による鑑別診断の検討. 第 87 回麻布獣医学会、相模原、2012 年 11 月

Microbes and Infection 18 (2016) 128–136
www.elsevier.com/locate/micinf

Original article

Expression and role of the TGF-β family in glial cells infected with Borna disease virus

Yoshii Nishino [a,*], Masaru Murakami [b], Masayuki Funaba [c,*]

[a] Department of Animal Medical Sciences, Faculty of Life Sciences, Kyoto Sangyo University, Kyoto 603-8555, Japan
[b] Laboratory of Molecular Biology, Azabu University School of Veterinary Medicine, Sagamihara 252-5201, Japan
[c] Division of Applied Biosciences, Kyoto University Graduate School of Agriculture, Kyoto 606-8502, Japan

Received 24 June 2015; accepted 9 October 2015
Available online 19 October 2015

Abstract

A previous study revealed that the expression of the Borna disease virus (BDV)-encoding phosphoprotein in glial cells was sufficient to induce neurobehavioral abnormalities resembling Borna disease. To evaluate the involvement of the TGF-β family in BDV-induced changes in cell responses by C6 glial cells, we examined the expression levels of the TGF-β family and effects of inhibiting the TGF-β family pathway in BDV-infected C6 (C6BV) cells. The expression of activin βA and BMP7 was markedly increased in BDV-infected cells. Expression of Smad7, a TGF-β family-inducible gene, was increased by BDV infection, and the expression was decreased by treatment with A-83-01 or LDN-193189, inhibitors of the TGF-β/activin or BMP pathway, respectively. These results suggest autocrine effects of activin A and BMP7 in C6BV cells. IGFBP-3 expression was also induced by BDV infection; it was below the detection limit in C6 cells. The expression level of IGFBP-3 was decreased by LDN-193189 in C6BV cells, suggesting that endogenous BMP activity is responsible for IGFBP-3 gene induction. Our results reveal the regulatory expression of genes related to the TGF-β family, and the role of the enhanced BMP pathway in modulating cell responses in BDV-infected glial cells.

Keywords: Borna disease virus; TGF-β family; Glial cells; BMP; IGFBP-3

1. Introduction

Borna disease virus (BDV) is a non-segmented negative-strand RNA virus belonging to the family *Bornaviridae* [1]. The genome of BDV encodes at least 6 proteins: a nucleoprotein (N), nonstructural protein (X), phosphoprotein (P), matrix protein (M), envelope protein (G), and RNA polymerase (L) [2]. BDV naturally infects a wide range of warm-blooded hosts [3]; BDV infection induces severe signs of neurological disease, including behavioral abnormalities [3]. Responses to BDV infection vary according to differences in the species, animal strain, age of the host at the time of infection, or viral strain, indicating that host-dependent factors as well as virus-specific factors determine the onset of Borna disease [4–6]. However, the precise mechanism underlying the BDV-induced onset of behavioral disorders currently remains unclear.

Previous studies have attempted to identify the BDV-derived molecule(s) responsible for the onset of Borna disease in BDV-infected animals [7,8], and found that the forced expression of P in glial cells [7] but not N in neurons and glial cells [8] induced behavioral abnormalities such as enhanced intermale aggressiveness, hyperactivity, and spatial reference memory deficits resembling the neurobehavioral abnormalities exhibited in BDV-infected animals. Furthermore, the ectopic expression of BDV P did not affect neurodegenerative reactions [7]. Thus, functional modulations in glial cells have been implicated in these behavioral abnormalities [7].

* Corresponding authors.
E-mail addresses: nishino@cc.kyoto-su.ac.jp (Y. Nishino), mfunaba@kais.kyoto-u.ac.jp (M. Funaba).

http://dx.doi.org/10.1016/j.micinf.2015.10.001

We previously demonstrated that the expression of transforming growth factor (TGF)-β family members and their signal components was altered in the brains of 3-week-old rats infected with BDV [6]; the expression of TGF-β1, activin βE, and GDF15 was increased in the brain in response to BDV infection, whereas that of TGF-β2, inhibin α, and BMP2 was decreased [6]. Furthermore, the expression of TβRII and ALK5, receptors for TGF-β [9,10], was shown to be increased in BDV-infected brains, while that of Smads, signal mediators and regulators of the TGF-β family [9,10], was generally increased by BDV infection [6]. Cell growth and differentiation are potently regulated by the TGF-β family in many types of cell, and alteration of TGF-β family signal is implicated in the pathogenesis of diseases through disturbances of cell response [9,10]. In view of the (patho-)physiological role of the TGF-β family, we hypothesized the involvement of the TGF-β family in the BDV-induced functional modulation of the central nervous system; previous findings on the Borna disease-like phenotype resulting from the glial expression of BDV P [7] and modulated expression of TGF-β family signaling components [6] prompted us to hypothesize that BDV infection in glial cells induces behavioral disturbances through the modulation of TGF-β family signaling. In order to validate our hypothesis, the present study examined 1) the regulatory expression of the signal components of the TGF-β family in glial cells infected with BDV, and 2) the effects of inhibiting the TGF-β family pathway on cell responses in BDV-infected glial cells.

2. Materials and methods

2.1. Materials

The following reagents were purchased: TGF-β1 and BMP7 were from R & D Systems (Minneapolis, MN, USA); LDN-193189, an inhibitor of BMP type I receptors [11,12], was from Stemgent (San Diego, CA, USA); A-83-01, an inhibitor of TGF-β/activin type I receptors [13], was from Calbiochem (La Jolla, CA, USA); rabbit polyclonal antibodies against phospho-Smad1 (Ser463/Ser465)/Smad5 (Ser463/Ser465)/Smad8 (Ser465/Ser467) (#9511), phospho-Smad2 (Ser465/Ser467) (#3101), or phospho-ERK (Thr202/Tyr204) (#9101) were from Cell Signaling Technology (Danvers, MA, USA); and a mouse monoclonal antibody against α-tubulin (B-5-1-2) was from Abcam (Cambridge, MA, USA).

2.2. Cell culture

C6 glioma cells [14] and C6 glioma cells infected with the BDV He/80 strain (C6BV, [15]) were cultured in Dulbecco's modified Eagle's medium (DMEM) supplemented with 10% heat-inactivated fetal bovine serum (FBS), 100 U/mL penicillin, and 100 μg/mL streptomycin. In order to examine the effects of inhibitors of the TGF-β family on gene expression, C6 and C6BV cells were plated at the density of 1×10^4/mL. Sixteen hours after plating, cells were treated with A-83-01 (5 μM) or LDN-193189 (100 pM) or both for 72 h.

2.3. Western blot

C6 and C6BV cells were plated at the density of 2.5×10^5/mL to examine the phosphorylation of Smad and ERK. Twenty hours after plating, cells were cultured in DMEM medium with 0.2% FBS for 4 h to eliminate the effects of serum on phosphorylation. Cells were pretreated with A-83-01 (5 μM) or LDN-193189 (100 pM) for 15 min, followed by a treatment with TGF-β1 (100 pM) or BMP7 (2 nM) for 1 h. Western blot analyses were performed as described previously [16]. Immunoreactive proteins were visualized using the ECL Select Western blotting detection system (GE Healthcare, Buckinghamshire, UK), according to the manufacturer's protocol.

2.4. RNA isolation, cDNA synthesis, and real-time quantitative PCR

Total RNA was isolated from C6 and C6BV cells using the RNeasy Mini Kit (Qiagen, Venlo, the Netherlands). The concentration of RNA was calculated from absorbance at 260 nm. The ratio of absorbance at 260 nm to that at 280 nm was comparable among samples. The cDNA was synthesized from 1 μg of total RNA by the ReverTra Ace qPCR Master Mix (Toyobo, Osaka, Japan), according to the manufacturers' protocols. The cDNA corresponding to 5 ng of total RNA, i.e., 0.5% of the cDNA, was used as a template to evaluate expression levels, except for IGFBP-3, for RT-quantitative PCR (RT-qPCR); the cDNA corresponding to 20 ng of total RNA (2% of the cDNA) was used to examine the expression of IGFBP-3. qPCR was performed using Thunderbird qPCR Mix (Toyobo) in Applide Biosystems StepOnePlus Real Time PCR Systems (Life Technologies, Carlsbad, CA, USA), according to the manufacturers' protocol. The qPCR profile was as follows: after denaturing for 20 s at 95 °C, 40 cycles consisted of 15 s at 95 °C and 60 s at 60 °C. The oligonucleotide primers for RT-qPCR and PCR efficiency [17] are shown in Table 1. All the primer sets were designed to span an exon–exon junction to exclude the possibility of amplification of genomic DNA. After 40 cycles of RT-qPCR, the dissociation (melting) curve of the products was examined by changes in the ramp temperature from 60 °C to 95 °C. Each sample showed a single peak, suggesting the expected PCR products. The abundance of gene transcripts was calculated by the standard curve method, and the value was normalized against HPRT1, GAPDH or TBP. The expression level of genes in C6 cells treated without the inhibitor was set to 1, except for IGFBP-3. Since the expression of IGFBP-3 in C6 cells was below the detection limit, its level in C6BV cells treated without the inhibitor was set at 1. The cell culture experiments, i.e., comparison of gene expression between C6 cells and C6BV cells as well as effect of inhibitors for the TGF-β family pathway on gene expression, were performed at least two times, and showed similar results.

Table 1
Nucleotide sequences of primers used in RT-qPCR analyses, sizes of PCR products, and mean PCR efficiency.

Gene	Primer	Sequence	GenBank accession number	Size (bp)	Efficiency (%)[a]
TGF-β family:					
TGF-β1	5′	5′-cctggaaagggctcaacac-3′	X52498	100	97.5
	3′	5′-ctgccgtacacagcagttct-3′			
TGF-β2	5′	5′-agtgggcagcttttgctc-3′	NM_031131	73	120.9
	3′	5′-gtagaaagtgggcgggatg-3′			
TGF-β3	5′	5′-agtggctgttgcggagag-3′	NM_013174	72	102.9
	3′	5′-gctgaaaggtatgacatggaca-3′			
Inhibin α	5′	5′-gcacaggacctctgaaccag-3′	NM_012590	88	94.5
	3′	5′-agctgcctgatcctcacag-3′			
Activin βA	5′	5′-atcatcacctttgccgagtc-3′	NM_017128	71	94.2
	3′	5′-tcactgccttccttggaaat-3′			
Activin βB	5′	5′-gatcatcagctttgcagagaca-3′	XM_001053684	137	92.9
	3′	5′-cataggggagcagtttcaggta-3′			
Activin βC	5′	5′-ggaaaccctgttggagca-3′	BC089799	90	104.4
	3′	5′-agacgggtttggttgatgtt-3′			
Activin βE	5′	5′-ccccaggcagcactgaccaga-3′	AF140032	120	97.0
	3′	5′-gcggtaggttgaagtggatt-3′			
BMP2	5′	5′-cggactgcggtctcctaa-3′	NM_017178	70	99.6
	3′	5′-ggggaagcagcaacactaga-3′			
BMP4	5′	5′-cgggcttgagtaccctgag-3′	NM_012827	85	109.0
	3′	5′-tgggatgttctccagatgttc-3′			
BMP7	5′	5′-cctgggcttacagctctcc-3′	XM_001053727	82	101.1
	3′	5′-tccatgccgtccaatcag-3′			
GDF15	5′	5′-cggatactcagtccagaggtg-3′	NM_019216	99	86.6
	3′	5′-gcggtaggcttcggggaga-3′			
Type I receptors:					
ALK1	5′	5′-ctaaccgactggcagcagat-3′	L36088	66	117.0
	3′	5′-ggtaccagcactctcgcatca-3′			
ALK2	5′	5′-tgggcctttggcctcgttctg-3′	BC167754	77	84.3
	3′	5′-ggtggcttgtaatcttccactatac-3′			
ALK3	5′	5′-ctgtattgtcgccatgatcg-3′	D38082	86	93.3
	3′	5′-ggttgtaacgacctctgcttg-3′			
ALK4	5′	5′-tccttcttccccttgttgtcct-3′	S76466	84	96.1
	3′	5′-gcatgcacacagcagagcct-3′			
ALK5	5′	5′-ggccaaatattcccaacagat-3′	BC087035	65	94.8
	3′	5′-tctcataattttggccatcactc-3′			
ALK6	5′	5′-tccccaatcgatggagcagt-3′	BC092609	68	100.2
	3′	5′-cgcccagcactctgtcata-3′			
Type II receptors:					
TβRII	5′	5′-ctactctgtctgtggatgac-3′	S67770	93	86.1
	3′	5′-ccaaattcatcctggattct-3′			
ActRIIA	5′	5′-cctaccctcctgtacttgttcc-3′	S48190	78	99.1
	3′	5′-gcaatggcttcaaccctagtaa-3′			
ActRIIB	5′	5′-ggctcagctcatgaacgact-3′	BC097358	69	108.8
	3′	5′-ctctgccacgactgcttgt-3′			
BMPRII	5′	5′-gagccctccctggacttg-3′	NM_080407	60	97.0
	3′	5′-atatcgaccccgtccaatca-3′			
Smad:					
Smad1	5′	5′-gcagccctttcagatgccag-3′	BC061757	85	95.2
	3′	5′-ggctgagagccatcctgggc-3′			
Smad2	5′	5′-caggacgattagatgagcttg-3′	BC127497	113	96.0
	3′	5′-cgtatttgctgtactcagtcccc-3′			
Smad3	5′	5′-cctgccactgtctgcaagata-3′	U66479	65	99.5
	3′	5′-gcaaattcctggttgttgaagat-3′			
Smad4	5′	5′-gaacactggatggacgactg-3′	AF056002	69	103.0
	3′	5′-acagacgggcatagatcaca-3′			
Smad5	5′	5′-cagcctatggacacaagcaa-3′	AB010955	78	98.6
	3′	5′-ggcaacaggctgaacatctc-3′			
Smad6	5′	5′-gttgcaacccctaccacttc-3′	NM_001109002	76	93.3
	3′	5′-ggaggagacagccgagaata-3′			
Smad7	5′	5′-acccccatcaccttagtcg-3′	AF159626	73	94.2
	3′	5′-aaatccatcgggtatctgga-3′			

(*continued on next page*)

Table 1 (*continued*)

Gene	Primer	Sequence	GenBank accession number	Size (bp)	Efficiency (%)[a]
Smad8	5′	5′-accattaccgcagagtggaga-3′	AF012347	73	91.2
	3′	5′-tgagggttgtactcgctgtg-3′			
Target genes:					
p21WAF	5′	5′-gcagtgcccgagttaagg-3′	U24174	91	92.8
	3′	5′-ccaggatcggacatggtg-3′			
IGFBP-3	5′	5′-ggaaagacgacgtgcattg-3′	NM_012588	78	101.5
	3′	5′-gcgtatttgagctccacgtt-3′			
Corrected gene:					
Hprt1	5′	5′-gaccggttctgtcatgtcg-3′	NM_012583	61	82.2
	3′	5′-acctggttcatcatcactaatcac-3′			
GAPDH	5′	5′-acaactttggcatcgtgga-3′	NM_017008	62	92.9
	3′	5′-cttctgagtggcagtgatgg-3′			
TBP	5′	5′-cccaccagcagttcagtagc-3′	NM_001004198	75	97.6
	3′	5′-caattctgggtttgatcattctg-3′			

[a] Mean value.

2.5. Statistical analyses

Data are expressed as the mean ± SE. Gene expression levels were log-transformed to provide an approximation of a normal distribution before being analyzed. Regarding the expression of genes related to the TGF-β family, differences between C6 cells and C6BV cells were examined using an unpaired *t*-test. Data for the expression of Smad7, p21WAF, and IGFBP-3 were analyzed by ANOVA using the GLM procedures of SAS [18]. Considered factors were cell type, A-83-01, LDN-193189, interaction of cell type and A-83-01 (cell × A-83-01), the interaction of cell type and LDN-193189 (cell × LDN-193189), interaction of A-83-01 and LDN-193189 (A-83-01 × LDN-193189), and interaction of cell type, A-83-01, and LDN-193189 (cell × A-83-01 × LDN-193189). The expression of IGFBP-3 was below the detection limit in C6 cells irrespective of the treatment; therefore, the factors were A-83-01, LDN-193189, and the interaction of A-83-01 and LDN-193189 (A-83-01 × LDN-193189). The effects of the inhibitor treatment in each cell type, and the effects of the cell type treated with the respective inhibitor (for the expression of Smad7 and p21WAF) were examined by Dunnett's test. Differences of $P < 0.05$ were considered significant.

3. Results

3.1. Expression of the TGF-β family was modulated in BDV-infected C6 glioma cells

TGF-β family consists of three major subfamilies, i.e., TGF-βs, activins and BMPs. TGF-β family transmits signals through specific heteromeric complexes with type I receptors, called activin-like kinases (ALKs), and type II receptors. Both type I and type II receptors have intracellular serine/threonine kinase domains. In canonical signal transduction, TGF-βs signal via the TβRII type II receptor and uses the ALK5 type I receptor. Activins associates with ActRIIA and ActRIIB type II receptors, and the ALK4 type I receptor. BMP signaling is mediated by BMPRII, ActRIIA, and ActRIIB type II receptors, and ALK2/3/6 type I receptors. According to current models, constitutively active type II receptor kinases trans-phosphorylate and activate type I receptors, which subsequently transmit signals downstream by phosphorylating serines at the carboxyl terminus of receptor-regulated (R)-Smads. There are two R-Smad subclasses: activin/TGF-β pathway-specific R-Smads (Smad2 and Smad3) and BMP pathway-specific R-Smads (Smad1, Smad5, and Smad8). Once activated by phosphorylation, R-Smads form complexes with Smad4, and accumulate in the nucleus where they interact with transcriptional regulators for target genes [9,10].

We first explored the regulatory expression of 12 members of the TGF-β family in C6 glioma cells in response to BDV infection (Fig. 1). C6BV cells did not exhibit cytopathic

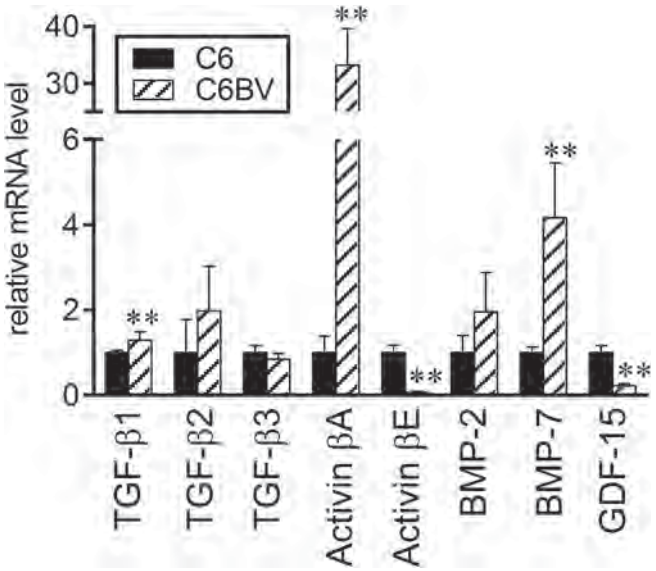

Fig. 1. Expression of TGF-β family members in C6 glioma cells infected with BDV. Total RNA was isolated from C6 and C6BV cells, and expression of the TGF-β family was evaluated by RT-qPCR. Expression was normalized to that of HPRT1, and expression in C6 cells was set to 1. Data are shown as the mean ± SE ($n = 5$). **: $P < 0.01$.

effects (data not shown), and the growth rate of C6BV cells was similar to that of C6 cells (data not shown). The expression of TGF-β1, activin βA, and BMP7 was significantly increased in BDV-infected cells. The expression of activin βA was clearly up-regulated; its expression level in C6BV cells was 33-fold higher than that in C6 cells. In contrast, the expression of activin βE and GDF15 was significantly lower in C6BV cells than in C6 cells; the expression of activin βE was down-regulated in C6BV cells (17-fold). The altered expression of the TGF-β family in BDV-infected cells did not result from changes in the expression level of HPRT1, the reference gene; the expression pattern was essentially unchanged by the correction by GAPDH or TBP (data not shown). Furthermore, expression pattern of the other genes shown as below was also comparable, irrespective of the reference gene (data not shown). Expression levels of inhibin α, activin βB, activin βC, and BMP4 were below the detection limit (data not shown).

We next examined the expression levels of receptors for the TGF-β family (Fig. 2). The expression levels of ALK3 and ALK4 were significantly decreased in C6BV cells (Fig. 2), and the BDV infection also decreased the expression of ActRIIA (Fig. 2). In contrast, the expression levels of ActRIIB and BMPRII were significantly higher in C6BV cells than in C6 cells (Fig. 2). The expression of ALK1 and ALK6 was below the detection limit (data not shown). We further evaluated the expression levels of Smad (Fig. 3). The expression of Smad1 and Smad7 was significantly lower and higher in C6BV cells than in C6 cells, respectively.

3.2. BDV infection affected endogenous activities of TGF-β family members in C6 glioma cells

In order to explore the role of the aberrant expression of TGF-β family components, we used A-83-01 and LDN-193189, inhibitors of the TGF-β/activin type I receptors [13] and BMP type I receptors [11,12], respectively. Inhibition of the type I receptor serine/threonine kinase leads to block Smad phosphorylation and subsequent signaling [11–13]. As expected, the TGF-β1 treatment induced the phosphorylation of Smad2 in C6 and C6BV cells; this phosphorylation was blocked by the pretreatment with A-83-01, but not by that with LDN-193189 (Fig. 4A, *second line*). In C6 cells, BMP7 potentiated the phosphorylation of Smad1/5/8, which was blocked by the pretreatment with LDN-193189 (Fig. 4A, *top*). The treatment with TGF-β only slightly induced the phosphorylation of Smad1/5/8, and this phosphorylation was blocked by A-83-01, but not by LDN-193189. The phosphorylation of Smad1/5/8 was stronger in C6BV cells than in C6 cells. Furthermore, BMP7 did not induce the phosphorylation of Smad1/5/8 in C6BV cells; this may have resulted from the full activation of Smad1/5/8 in C6BV cells under basal conditions.

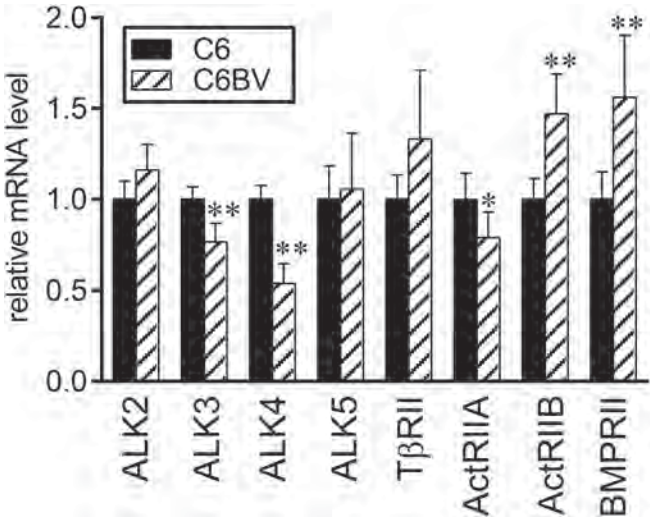

Fig. 2. Expression of receptors for the TGF-β family in C6 glioma cells infected with BDV. Total RNA was isolated from C6 and C6BV cells, and the expression of type I and type II receptors for the TGF-β family was evaluated by RT-qPCR. Expression was normalized to that of HPRT1, and expression in C6 cells was set to 1. Data are shown as the mean ± SE ($n = 5$). * and **: $P < 0.05$ and $P < 0.01$, respectively.

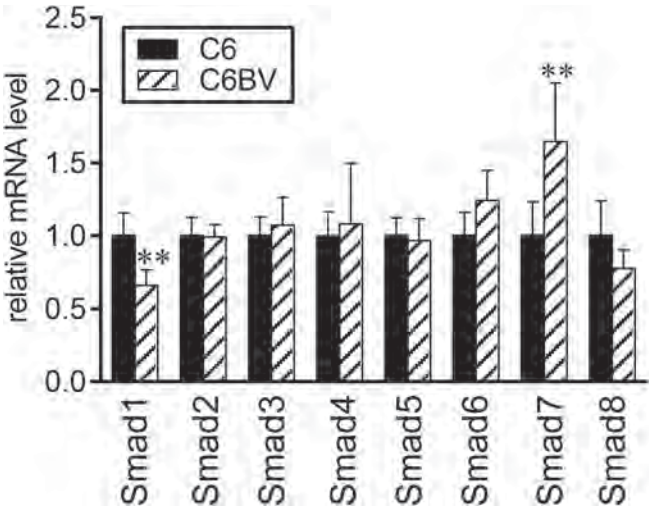

Fig. 3. Expression of Smads in C6 glioma cells infected with BDV. Total RNA was isolated from C6 and C6BV cells, and the expression of Smad was evaluated by RT-qPCR. Expression was normalized to that of HPRT1, and expression in C6 cells was set to 1. Data are shown as the mean ± SE ($n = 5$). **: $P < 0.01$.

Previous studies showed the modulation of the ERK MAP kinase pathway in BDV-infected PC12 neuronal cells [19], primary cultured neurons [20], and oligodendroglial cells [21]. In addition, the functional interaction between the TGF-β family pathway and the ERK pathway has been reported in many biological systems [9,10]. Thus, we measured phosphorylated ERK levels (Fig. 4A, *third line*), because ERK is known to be phosphorylated and activated [22]. The phosphorylation level of ERK was lower in C6BV cells than in C6 cells. In C6 cells, TGF-β1 and BMP7 decreased the phosphorylation of ERK, as did the treatment with A-83-01 or LDN-193189, suggesting that the phosphorylation of ERK is regulated by the TGF-β family with dual effects, i.e., efficient ERK phosphorylation by the optimal activity of the TGF-β family. In contrast, BMP7 increased phosphorylated ERK levels in C6BV cells. Furthermore, A-83-01 increased the phosphorylation of ERK, irrespective of the treatment with

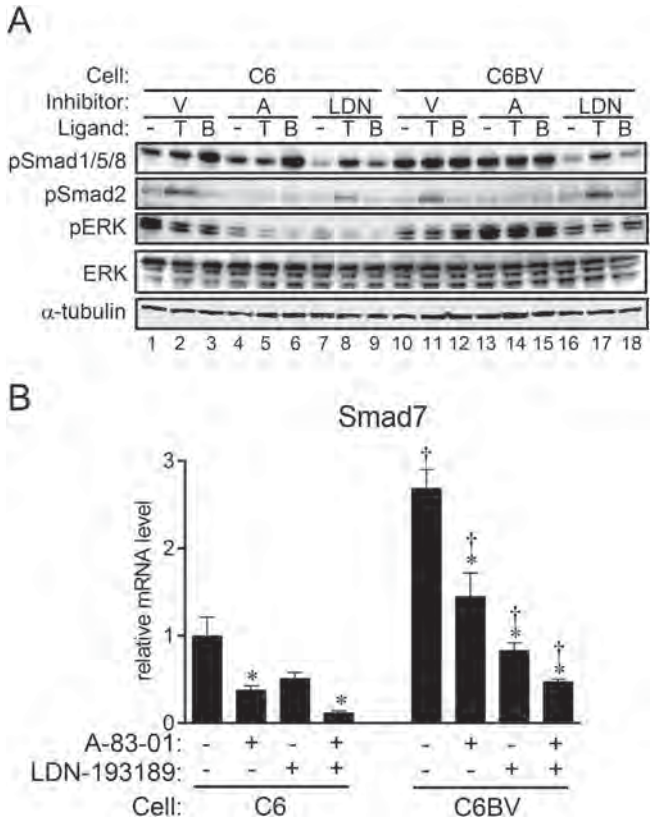

Fig. 4. Smad7 expression and phosphorylation of Smad and ERK regulated by BDV infection and the TGF-β family. A: The phosphorylation of Smad and ERK in C6 and C6BV cells. After being cultured in DMEM medium with 0.2% FBS for 4 h, C6 and C6BV cells were pretreated with vehicle (V), A-83-01 (A: 5 μM) or LDN-193189 (LDN: 100 pM) for 15 min, followed by a treatment with TGF-β1 (T: 100 pM) or BMP7 (B: 2 nM) for 1 h. The phosphorylation of Smad and ERK was examined by Western blot analyses. B: Smad7 expression in C6 and C6BV cells treated with inhibitors of the TGF-β family. C6 and C6BV cells were treated with A-83-01 (5 μM) or LDN-193189 (100 pM) or both for 72 h. Smad7 mRNA levels were normalized to those of HPRT1 mRNA. Expression in wild-type C6 cells without the inhibitor treatment was set to 1. Data are shown as the mean ± SE ($n = 6$). *: $P < 0.05$, significantly different from that in respective cells without the inhibitor treatment, and †: $P < 0.05$, significantly different from that in C6 cells treated with the respective inhibitor.

TGF-β1 or BMP7. These results suggested that the phosphorylation status of ERK was distinct between C6 cells and C6BV cells, and that the involvement of TGF-β1 and BMP7 in ERK phosphorylation was also dependent on the cell context.

The expression of Smad7, which inhibits Smad-mediated signaling [9,10], is regulated by the TGF-β family; TGF-β, activin A, and BMP were previously shown to increase Smad7 mRNA levels in various cell types [23–25]. Not only A-83-01, but also LDN-193189 effectively decreased the expression of Smad7 in C6 cells and C6BV cells, except for the treatment with LDN-193189 alone in C6 cells (Table 2, Fig. 4B). These results suggested that the endogenous activities of TGF-β/activin and BMP regulated Smad7 expression in C6 cells and C6BV cells. Consistent with the results in Fig. 3, the expression of Smad7 was significantly higher in C6BV cells than in C6 cells (Fig. 4B). In view of the marked up-regulation in the expression of activin βA and lack of expression of inhibin α in C6BV cells, activin A (a homodimer of activin βA), but not inhibin A (a heterodimer of inhibin α and activin βA) was produced in C6BV cells, which may stimulate Smad7 expression in an autocrine manner. In contrast, BMP7 may be the principle molecule responsible for enhanced BMP activity in C6BV cells, as suggested by the higher level of Smad7 (Fig. 4B) and phosphorylated Smad1/5/8 (Fig. 4A) in C6BV cells.

3.3. Expression levels of p21WAF and IGFBP-3 were modulated in C6 glioma cells infected with BDV

A previous study showed that BDV P inhibited the p53-induced expression of p21WAF, a cyclin-dependent kinase inhibitor [26]. Furthermore, IGFBP-3 was identified by cDNA microarray analyses as a gene that was more strongly expressed in BDV P-expressing C6 cells than in C6 cells [27]. Therefore, we determined whether the expression of p21WAF and IGFBP-3 was modulated in C6BV cells, and also if the TGF-β/activin pathway or BMP pathway was involved in their expression. Consistent with previous findings [26,27], the expression of p21WAF was decreased in BDV-infected cells (Fig. 5A). In addition, although the expression level of IGFBP-3 was below the detection limit in C6 cells, its reproducible expression was detected in C6BV cells, indicating that its expression was up-regulated. An analysis of variance on the expression of p21WAF indicated a significant effect of cell type and the interaction of cell type, A-83-01, and LDN-193189 (Table 2); however, the effects of the inhibitors were small (Fig. 5A). In contrast, LDN-193189 markedly decreased the expression of IGFBP-3 in C6BV cells (Table 2, Fig. 5B).

Table 2
Effects of cell type, A-83-01, and LDN-193189 on gene expression.

	Effects of						
	Cell[a]	A[b]	LDN[c]	Cell × A	Cell × LDN	A × LDN	Cell × A × LDN
Smad7	0.001	0.001	0.001	0.009	NS[d]	NS	NS
p21WAF	0.001	NS	NS	NS	NS	NS	0.04
IGFBP-3	–[e]	NS	0.001	–	–	NS	–

[a] Cell type.
[b] A-83-01.
[c] LDN-193189.
[d] Non-significant.
[e] Not examined.

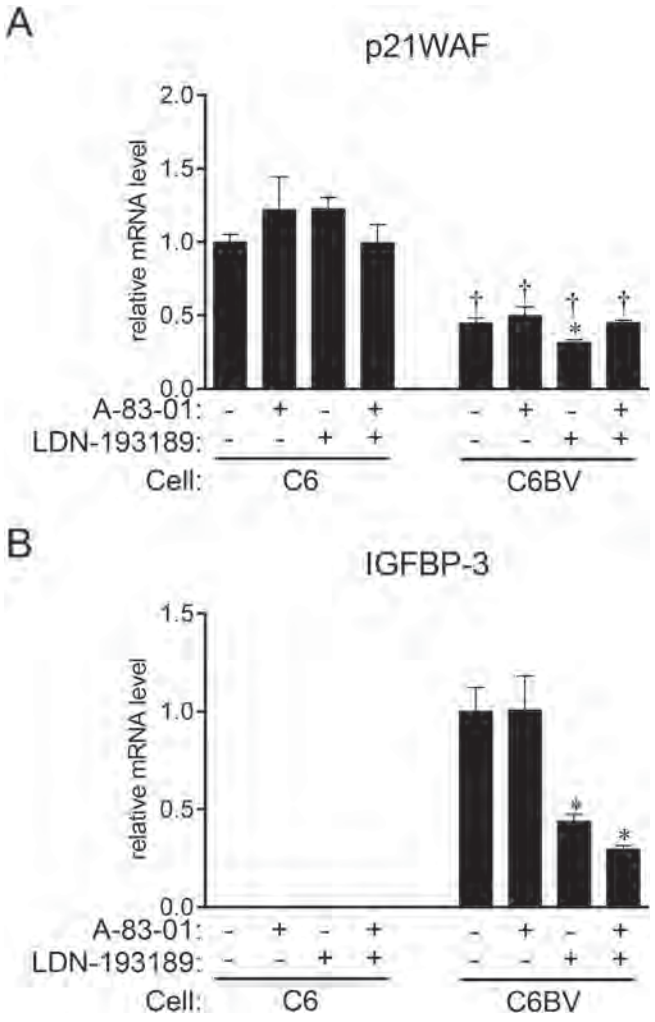

Fig. 5. Expression of p21WAF and IGFBP-3 in C6 glioma cells infected with BDV. C6 and C6BV cells were treated with A-83-01 (5 μM) or LDN-193189 (100 pM) or both for 72 h. The expression of p21WAF (A) and IGFBP-3 (B) was evaluated by RT-qPCR. Expression was normalized to that of HPRT1. The expression of p21WAF in C6 cells without the inhibitor treatment was set to 1, and the expression of IGFBP-3 in C6BV cells without the inhibitor treatment was set to 1. Data are shown as the mean ± SE ($n = 6$). *: $P < 0.05$, significantly different from that in respective cells without the inhibitor treatment, and †: $P < 0.05$, significantly different from that in C6 cells treated with the respective inhibitor.

4. Discussion

Previous studies reported that the forced expression of BDV P, but not N in glial cells induced neurobehavioral abnormalities resembling those in BDV-infected animals [7,8]. These findings suggested that the expression of BDV P in glial cells was sufficient for the onset of Borna disease. We previously revealed changes in the expression of genes related to TGF-β family signaling in the brains of BDV-infected rats [6]. The TGF-β family has been shown to regulate diverse physiological processes including cell differentiation, cell-cycle progression, reproductive function, development, bone morphogenesis, immune surveillance, motility, adhesion, neuronal growth, and wound healing [28–30]. Thus, malfunctions in TGF-β family members have been implicated in the pathogenesis of severe diseases [9,10]. We hypothesize that alteration of the TGF-β family signaling is related to the onset of neurological disturbances induced by BDV infection. As the first step to elucidate the molecular mechanisms underlying behavioral disturbances induced by BDV infection, the present study initially explored the regulatory expression of the signal components of the TGF-β family in BDV-infected glial cells as well as the possible role of the TGF-β family. We demonstrated that 1) the expression of the TGF-β family, especially activin βA, activing βE, BMP7, and GDF15, was markedly altered in C6 glioma cells infected with BDV, 2) the endogenous activity of activin and BMP was stimulated by BDV infection, possibly through the autocrine action of activin A and BMP7, respectively, and 3) the BMP pathway was involved in the BDV-induced expression of IGFBP-3. Honda et al. [27] suggested the involvement of IGFBP-3 produced in BDV-infected glial cells in onset of neurological disturbances. Also, considering that IGFBP-3 has growth inhibitory and proapoptotic effects [31], the present results provide novel information on the role of the BMP-mediated regulation of cell responses in glial cells infected with BDV.

In addition to inhibiting the interaction between IGFs and their receptors, IGFBP-3 has been shown to function through the IGF/IGF receptor-independent pathway; this is now widely recognized [32]. IGFBP-3 binds to the low-density lipoprotein receptor-related protein-1/α2M receptor, which has also been recognized as a type V TGF-β receptor [33]. IGFBP-3-mediated signaling has been reciprocally related to TGF-β/activin signaling [34–36]; however, the precise relationship between these two signaling pathways remains unclear. Future studies are warranted to identify the target cells and determine the role of IGFBP-3 produced by BDV-infected glial cells. Furthermore, the regulation of IGFBP-3 by the BMP pathway needs to be clarified.

The expression of activin βA was markedly increased in C6BV cells, suggesting the up-regulated expression of activin A. Previous studies revealed that the expression of activin A was increased in T cells, B cells, macrophages, mast cells, and microglial cells in response to activation [37,38]. Furthermore, serum concentrations of activin A were increased in patients infected with influenza [39]. Therefore, the increased expression of activin A may be a general phenotype of activated cells.

Previous studies demonstrated that activin A potentiated the up-regulated expression of p21WAF [40–42]. Since the expression of activin A was markedly increased in C6BV cells (Fig. 1), we expected that of p21WAF to also be up-regulated in C6BV cells. However, similar to previous findings [26], the expression of p21WAF was significantly lower in C6BV cells than in C6 cells (Fig. 5A). The activin A-induced expression of p21WAF is known to be dependent on the cell context [43]; therefore, the enhanced expression of activin A in C6BV cells regulates the expression of genes other than p21WAF. Alternatively, activin A produced in C6BV cells may act on neurons. Activin A has been identified as a neuron survival factor [44]. In addition, an activin A infusion into the dentate gyrus,

but not the CA1 pyramidal cell layer of the hippocampus produced an antidepressant-like effect in a behavioral model of depression [45].

We previously reported that the expression of TGF-β1 and activin βE was up-regulated in the brains of rats infected with BDV, whereas that of activin βA and BMP7 was unaffected by the infection [6]. These results are inconsistent with the present results: the expression of activin βA and BMP7 was markedly higher in C6BV cells than in C6 cells, whereas that of activin βE and GDF15 was decreased. These controversial results may be related to differences in the materials examined; in our previous study, 3-week-old rats were infected with BDV and inflammatory cells infiltrated the brain [6]. The expression of TGF-β1 was generally up-regulated in activated immune cells [46,47]. Thus, the induction of brain TGF-β1 may be a result of the infiltration of immune cells; however, its expression was increased in BDV-infected brains without the infiltration of immune cells [48]. The expression of the TGF-β family may also be affected in BDV-infected neurons. The modulation of gene expression in glial cells and neurons and changes in the cell population of brains infected with BDV may result in an inconsistent expression pattern of the TGF-β family.

The present results suggest aberrant signaling of the ubiquitous pathway in glial cells infected with BDV. Endogenous BMP activity was enhanced in C6BV cells, which may have been due to the enhanced expression of BMP7. Smad1/5/8 could not be further phosphorylated in response to BMP7 (Fig. 4A), suggesting the full activation of the BMP pathway in C6BV cells. The phosphorylation of ERK was also modulated by BDV infection; phosphorylation levels of ERK were lower in C6BV cells than in C6 cells (Fig. 4A). There are inconsistent results regarding ERK phosphorylation in BDV-infected cells; ERK phosphorylation was decreased in primary cultured neurons infected with BDV [20]. In contrast, BDV infection induced the constitutive phosphorylation of ERK in PC12 neuronal cells and oligodendroglial cells, whereas the nuclear translocation of ERK was inhibited by the infection [19,21]. The present study also showed that ERK phosphorylation was modulated by the TGF-β/activin and BMP pathways; it was stimulated by the inhibition of the TGF-β/activin pathway in C6BV cells, whereas endogenous TGF-β/activin activity was required for ERK phosphorylation in C6 cells. Modulation of the ubiquitous signaling pathways in glial cells infected with BDV may lead to dysregulation of the central nervous system.

The present study extends basic information on BDV-induced cell responses; our results clearly indicate the involvement of the BMP pathway in IGFBP-3 gene induction in C6BV cells. Previous studies revealed that BDV P negatively regulates p53-mediated signaling pathway as well as transcription of interferon-β gene through association with Traf family member-associated NF-κB activator-binding kinase-1 [26,49]. Future studies are needed to evaluate the regulatory role of TGF-β family in these pathways, which may be helpful in understanding the onset of Borna disease in detail.

Conflict of interest

The authors have no conflicting financial or commercial interests.

Acknowledgments

We thank Dr. K. Matsumoto for guidance of real-time quantitative PCR analyses. The present study was supported by JSPS KAKENHI Grant Number 25450433 and Program to supporting research activities of female researchers from the Japan Society for the Promotion of Science.

References

[1] Kishi M, Tomonaga K, Lai P, de la Torre JC. In: Carbone KM, editor. Borna disease virus and its role in neurobehavioral disease. Washington, DC: ASM Press; 2002. p. 23–43.
[2] Schneider U. Novel insights into the regulation of the viral polymerase complex of neurotropic Borna disease virus. Virus Res 2005;111:148–60.
[3] Rott R, Becht H. Natural and experimental Borna disease in animals. Curr Top Microbiol Immunol 1995;190:17–30.
[4] Pletnikov MV, Gonzalez-Dunia D, Stitz L. In: Carbone KM, editor. Borna disease virus and its role in neurobehavioral disease. Washington, DC: ASM Press; 2002. p. 125–78.
[5] Nishino Y, Kobasa D, Rubin SA, Pletnikov MV, Carbone KM. Enhanced neurovirulence of Borna disease virus variants associated with nucleotide changes in the glycoprotein and L polymerase genes. J Virol 2002;76:8650–8.
[6] Nishino Y, Ooishi R, Kurokawa S, Fujino K, Murakami M, Madarame H, et al. Gene expression of the TGF-β family in rat brain infected with Borna disease virus. Microbes Infect 2009;11:737–43.
[7] Kamitani W, Ono E, Yoshino S, Kobayashi T, Taharaguchi S, Lee BJ, et al. Glial expression of Borna disease virus phosphoprotein induces behavioral and neurological abnormalities in transgenic mice. Proc Natl Acad Sci U S A 2003;100:8969–74.
[8] Rauer M, Götz J, Schuppli D, Staeheli P, Hausmann J. Transgenic mice expressing the nucleoprotein of Borna disease virus in either neurons or astrocytes: decreased susceptibility to homotypic infection and disease. J Virol 2004;78:3621–32.
[9] Massagué J. TGFβ signalling in context. Nat Rev Mol Cell Biol 2012;13:616–30.
[10] Sakaki-Yumoto M, Katsuno Y, Derynck R. TGF-β family signaling in stem cells. Biochim Biophys Acta 2013;1830:2280–96.
[11] Cuny GD, Yu PB, Laha JK, Xing X, Liu JF, Lai CS, et al. Structure-activity relationship study of bone morphogenetic protein (BMP) signaling inhibitors. Bioorg Med Chem Lett 2008;18:4388–92.
[12] Yu PB, Deng DY, Lai CS, Hong CC, Cuny GD, Bouxsein ML, et al. BMP type I receptor inhibition reduces heterotopic ossification. Nat Med 2008;14:1363–9.
[13] Tojo M, Hamashima Y, Hanyu A, Kajimoto T, Saitoh M, Miyazono K, et al. The ALK-5 inhibitor A-83-01 inhibits Smad signaling and epithelial-to-mesenchymal transition by transforming growth factor-β. Cancer Sci 2005;96:791–800.
[14] Van Dinter S, Flintoff WF. Rat glial C6 cells are defective in murine coronavirus internalization. J Gen Virol 1987;68:1677–85.
[15] Carbone KM, Rubin SA, Sierra-Honigmann AM, Lederman HM. Characterization of a glial cell line persistently infected with Borna disease virus (BDV): influence of neurotrophic factors on BDV protein and RNA expression. J Virol 1993;67:1453–60.
[16] Funaba M, Murakami M. A sensitive detection of phospho-Smad1/5/8 and Smad2 in Western blot analyses. J Biochem Biophys Methods 2008;70:816–9.

[17] Jacob F, Guertler R, Naim S, Nixdorf S, Fedier A, Hacker NF, et al. Careful selection of reference genes is required for reliable performance of RT-qPCR in human normal and cancer cell lines. PLoS One 2013;8:e59180.
[18] SAS Institute. SAS user's guide: statistics, ver. 9.2. Cary: SAS Institute; 2001.
[19] Hans A, Syan S, Crosio C, Sassone-Corsi P, Brahic M, Gonzalez-Dunia D. Borna disease virus persistent infection activates mitogen-activated protein kinase and blocks neuronal differentiation of PC12 cells. J Biol Chem 2001;276:7258–65.
[20] Hans A, Bajramovic JJ, Syan S, Perret E, Dunia I, Brahic M, et al. Persistent, noncytolytic infection of neurons by Borna disease virus interferes with ERK 1/2 signaling and abrogates BDNF-induced synaptogenesis. FASEB J 2004;18:863–5.
[21] Liu X, Yang Y, Zhao M, Bode L, Zhang L, Pan J, et al. Proteomics reveal energy metabolism and mitogen-activated protein kinase signal transduction perturbation in human Borna disease virus Hu-H1-infected oligodendroglial cells. Neuroscience 2014;268:284–96.
[22] Torii S, Nakayama K, Yamamoto T, Nishida E. Regulatory mechanisms and function of ERK MAP kinases. J Biochem 2004;136:557–61.
[23] Nakao A, Afrakhte M, Morén A, Nakayama T, Christian JL, Heuchel R, et al. Identification of Smad7, a TGFβ-inducible antagonist of TGF-β signalling. Nature 1997;389:631–5.
[24] Ishisaki A, Yamato K, Nakao A, Nonaka K, Ohguchi M, ten Dijke P, et al. Smad7 is an activin-inducible inhibitor of activin-induced growth arrest and apoptosis in mouse B cells. J Biol Chem 1998;273:24293–6.
[25] Karaulanov E, Knöchel W, Niehrs C. Transcriptional regulation of BMP4 synexpression in transgenic Xenopus. EMBO J 2004;23:844–56.
[26] Zhang G, Kobayashi T, Kamitani W, Komoto S, Yamashita M, Baba S, et al. Borna disease virus phosphoprotein represses p53-mediated transcriptional activity by interference with HMGB1. J Virol 2003;77:12243–51.
[27] Honda T, Fujino K, Okuzaki D, Ohtaki N, Matsumoto Y, Horie M, et al. Upregulation of insulin-like growth factor binding protein 3 in astrocytes of transgenic mice that express Borna disease virus phosphoprotein. J Virol 2011;85:4567–71.
[28] Schilling SH, Hjelmeland AB, Rich JN, Wang XF. In: Derynck R, Miyazono K, editors. The TGF-β family. Cold Spring Harbor, NY: Cold Spring Harbor Laboratory Press; 2008. p. 45–77.
[29] Wiater E, Vale W. In: Derynck R, Miyazono K, editors. The TGF-β family. Cold Spring Harbor, NY: Cold Spring Harbor Laboratory Press; 2008. p. 79–120.
[30] Katagiri T, Suda T, Miyazono K. In: Derynck R, Miyazono K, editors. The TGF-β family. Cold Spring Harbor, NY: Cold Spring Harbor Laboratory Press; 2008. p. 121–49.
[31] Butt AJ, Fraley KA, Firth SM, Baxter RC. IGF-binding protein-3-induced growth inhibition and apoptosis do not require cell surface binding and nuclear translocation in human breast cancer cells. Endocrinology 2002;143:2693–9.
[32] Jogie-Brahim S, Feldman D, Oh Y. Unraveling insulin-like growth factor binding protein-3 actions in human disease. Endocr Rev 2009;30:417–37.
[33] Huang SS, Ling TY, Tseng WF, Huang YH, Tang FM, Leal SM, et al. Cellular growth inhibition by IGFBP-3 and TGF-β1 requires LRP-1. FASEB J 2003;17:2068–81.
[34] Leal SM, Liu Q, Huang SS, Huang JS. The type V transforming growth factor β receptor is the putative insulin-like growth factor-binding protein 3 receptor. J Biol Chem 1997;272:20572–6.
[35] Leal SM, Huang SS, Huang JS. Interactions of high affinity insulin-like growth factor-binding proteins with the type V transforming growth factor-β receptor in mink lung epithelial cells. J Biol Chem 1999;274:6711–7.
[36] Fanayan S, Firth SM, Butt AJ, Baxter RC. Growth inhibition by insulin-like growth factor-binding protein-3 in T47D breast cancer cells requires transforming growth factor-β (TGF-β) and the type II TGF-β receptor. J Biol Chem 2000;275:39146–51.
[37] Ogawa K, Funaba M. Activin in humoral immune responses. Vitam Horm 2011;85:235–53.
[38] Sugama S, Takenouchi T, Kitani H, Fujita M, Hashimoto M. Activin as an anti-inflammatory cytokine produced by microglia. J Neuroimmunol 2007;192:31–9.
[39] Linko R, Hedger MP, Pettilä V, Ruokonen E, Ala-Kokko T, Ludlow H, et al. Serum activin A and B, and follistatin in critically ill patients with influenza A(H1N1) infection. BMC Infect Dis 2014;14:253.
[40] Yamato K, Koseki T, Ohguchi M, Kizaki M, Ikeda Y, Nishihara T. Activin A induction of cell-cycle arrest involves modulation of cyclin D2 and p21CIP1/WAF1 in plasmacytic cells. Mol Endocrinol 1997;11:1044–52.
[41] Chen JL, Walton KL, Winbanks CE, Murphy KT, Thomson RE, Makanji Y, et al. Elevated expression of activins promotes muscle wasting and cachexia. FASEB J 2014;28:1711–23.
[42] Chen L, Zhang W, Liang HF, Zhou QF, Ding ZY, Yang HQ, et al. Activin A induces growth arrest through a SMAD-dependent pathway in hepatic progenitor cells. Cell Commun Signal 2014;12:18.
[43] Bauer J, Sporn JC, Cabral J, Gomez J, Jung B. Effects of activin and TGFβ on p21 in colon cancer. PLoS One 2012;7:e39381.
[44] Schubert D, Kimura H, LaCorbiere M, Vaughan J, Karr D, Fischer WH. Activin is a nerve cell survival molecule. Nature 1990;344:868–70.
[45] Dow AL, Russell DS, Duman RS. Regulation of activin mRNA and Smad2 phosphorylation by antidepressant treatment in the rat brain: effects in behavioral models. J Neurosci 2005;25:4908–16.
[46] Letterio JJ, Roberts AB. Regulation of immune responses by TGF-β. Annu Rev Immunol 1998;16:137–61.
[47] Rubtsov YP, Rudensky AY. TGFβ signaling in control of T-cell-mediated self-reactivity. Nat Rev Immunol 2007;7:443–53.
[48] Plata-Salamán CR, Ilyin SE, Gayle D, Romanovitch A, Carbone KM. Persistent Borna disease virus infection of neonatal rats causes brain regional changes of mRNAs for cytokines, cytokine receptor components and neuropeptides. Brain Res Bull 1999;49:441–51.
[49] Unterstab G, Ludwig S, Anton A, Planz O, Dauber B, Krappmann D, et al. Viral targeting of the interferon-β-inducing Traf family member-associated NF-κB activator (TANK)-binding kinase-1. Proc Natl Acad Sci U S A 2005;102:13640–5.

CELL BIOCHEMISTRY & FUNCTION

CELL BIOCHEMISTRY AND FUNCTION
Cell Biochem Funct 2016; **34**: 34–41.
Published online in Wiley Online Library
(wileyonlinelibrary.com) **DOI**: 10.1002/cbf.3162

Direct action of capsaicin in brown adipogenesis and activation of brown adipocytes

Ryosuke Kida[1], Hirofumi Yoshida[1], Masaru Murakami[2], Mitsuyuki Shirai[3], Osamu Hashimoto[4], Teruo Kawada[5], Tohru Matsui[1] and Masayuki Funaba[1]*

[1]*Division of Applied Biosciences, Kyoto University Graduate School of Agriculture, Kyoto, Japan*
[2]*Laboratory of Molecular Biology, Azabu University School of Veterinary Medicine, Sagamihara, Japan*
[3]*Laboratory of Veterinary Pharmacology, Azabu University School of Veterinary Medicine, Sagamihara, Japan*
[4]*Laboratory of Experimental Animal Science, Kitasato University School of Veterinary Medicine, Towada, Japan*
[5]*Division of Food Science and Biotechnology, Kyoto University Graduate School of Agriculture, Kyoto, Japan*

The ingestion of capsaicin, the principle pungent component of red and chili peppers, induces thermogenesis, in part, through the activation of brown adipocytes expressing genes related to mitochondrial biogenesis and uncoupling such as peroxisome proliferator-activated receptor (Ppar) γ coactivator-1α (Pgc-1α) and uncoupling protein 1 (Ucp1). Capsaicin has been suggested to induce the activation of brown adipocytes, which is mediated by the stimulation of sympathetic nerves. However, capsaicin may directly affect the differentiation of brown preadipocytes, brown adipocyte function, or both, through its significant absorption. We herein demonstrated that *Trpv1*, a capsaicin receptor, is expressed in brown adipose tissue, and that its expression level is increased during the differentiation of HB2 brown preadipocytes. Furthermore, capsaicin induced calcium influx in brown preadipocytes. A treatment with capsaicin in the early stage of brown adipogenesis did not affect lipid accumulation or the expression levels of *Fabp4* (a gene expressed in mature adipocytes), *Pparγ2* (a master regulator of adipogenesis) or brown adipocyte-selective genes. In contrast, a treatment with capsaicin in the late stage of brown adipogenesis slightly increased the expression levels of *Fabp4*, *Pparγ2* and *Pgc-1α*. Although capsaicin did not affect the basal expression level of *Ucp1*, *Ucp1* induction by forskolin was partially inhibited by capsaicin, irrespective of the dose of capsaicin. The results of the present study suggest the direct effects of capsaicin on brown adipocytes or in the late stage of brown adipogenesis. Copyright © 2015 John Wiley & Sons, Ltd.

KEY WORDS—capsaicin; Trpv1; brown adipocytes; brown adipogenesis; Ucp1

INTRODUCTION

There are two kinds of thermogenesis, shivering and non-shivering. The latter mainly occurs in brown adipocytes; non-shivering thermogenesis in brown adipocytes has been attributed to the expression of a series of genes related to mitochondrial biogenesis and enhancements in cellular respiration that is uncoupled from ATP synthesis.[1] This uncoupling occurs through the expression of uncoupling protein 1 (Ucp1), a proton channel located at the inner mitochondrial membrane.[1] Non-shivering thermogenesis in brown adipocytes is induced by the dissipation of chemical energy in the form of heat against cold exposure.[1] The stimulatory effects of cold exposure on brown adipocyte activation are known to be mediated through the activation of the sympathetic nervous system, initiated by the peripheral stimulation of transient receptor potential (Trp) channels in sensory neurons.[2,3]

The ingestion of capsaicin, the principle pungent component of red pepper,[4] and non-pungent capsaicin analogs (capsinoids) has been shown to increase energy expenditure and brown adipocyte-mediated thermogenesis.[3,5–7] Because capsaicin stimulates Trpv1,[8] the capsaicin-induced stimulation of brown adipocytes may be mediated through the activation of sympathetic nervous activity.[3] Previous studies reported that capsaicin and capsinoids stimulated sympathetic nerve activity,[9,10] and capsinoid-induced energy expenditure was attenuated by denervation of the spinal and vagus nerves or in mice lacking the *Trpv1* gene.[11]

However, the activation of brown adipocytes may also be directly induced by capsaicin. Capsaicin is effectively absorbed from the gastrointestinal tract.[12] Trpv1 is predominantly expressed in sensory nerves, but is also expressed in other tissues including the brain, lung, liver, testis and white adipocytes.[13,14] These findings suggest that absorbed capsaicin directly acts on the other tissues expressing Trpv1. During an investigation of *Trpv1* expression in the whole body, we detected its expression in brown adipose tissue

*Correspondence to: Masayuki Funaba, Division of Applied Biosciences, Kyoto University Graduate School of Agriculture, Kitashirakawa Oiwakecho, Kyoto, Japan.
E-mail: mfunaba@kais.kyoto-u.ac.jp

Received 3 November 2015
Revised 16 December 2015
Accepted 16 December 2015

(BAT). Capsaicin has been shown to induce calcium influx via Trpv1,[8] and increases in the concentration of intracellular calcium inhibit the differentiation of white preadipocytes.[15,16] These findings prompted us to pursue the possibility of the direct activation of brown adipocytes as well as brown adipogenesis by capsaicin without the mediation of sympathetic nerve activation. In the present study, we employed a cell culture system that avoids the effects of sympathetic nerve activation in order to evaluate the direct role of capsaicin.

MATERIALS AND METHODS

Materials

The following reagents were purchased: capsaicin and forskolin, an activator of adenylate cyclase,[17] were from Wako (Osaka, Japan); iRTX (5′-iodoresiniferatoxin), an antagonist of Trpv1,[18] was from Alomone Labs (Jerusalem, Israel); A23187, a calcium ionophore,[19] was from Cayman (Ann Arbor, MI, USA) and Fluo-8-AM, a fluorescence-based calcium indicator,[20] was from AAT Bioquest (Sunnyvale, CA, USA).

Cell culture

HB2 brown preadipocytes,[21] which were isolated from mouse interscapular BAT and were kindly provided by Dr. M. Saito, Emeritus Professor of Hokkaido University, were cultured in Dulbecco's modified eagle medium with 10% FBS and antibiotics as described previously;[22] HB2 cells were stimulated to differentiate into brown adipocytes by insulin (20 nM) 2 days after confluence (day 0). In order to examine the effects of capsaicin on brown adipogenesis, capsaicin with or without iRTX at the indicated concentration (0–10 μM) was added to the culture medium from day 0 to day 8. We also evaluated the ability of capsaicin to activate brown adipocytes by treating cells with capsaicin from day 8 to day 12, followed by a stimulation with forskolin (10 μM) for 4 h. Lipid accumulation was examined by Oil Red O staining on day 8 or 12. Images were obtained by scanning stained wells (GT-9400UF, EPSON, Tokyo, Japan).

Calcium imaging

The calcium imaging reagent was freshly prepared as follows: 5-μM Fluo-8 AM (Invitrogen, Paisley, UK) and 0.04% Pluronic F-127 (AnaSpec Inc., Fremont, CA, USA) were suspended in phosphate buffered saline with 1.27 mM Ca^{2+} (PBS(Ca^{2+})), and treated with ultrasonication for 10 s. HB2 cells plated in 96-well plates were washed with PBS(Ca^{2+}) twice, and loaded with 100 μl of the calcium imaging reagent for 20 min at 37 °C under a 5% CO_2/95% air. Cells were subsequently washed with PBS(Ca^{2+}) twice, and 50 μl of PBS(Ca^{2+}) was added, followed by a stimulation with or without capsaicin or A23187. Fluo-8 fluorescence was captured using a fluorescence microscope (FSX100, Olympus, Tokyo, Japan). At least three independent experiments were performed, and representative results are shown.

RNA isolation, RT-PCR and RT-quantitative PCR

Interscapular BAT was obtained from adult female C57BL/6 mice (Japan SLC, Hamamatsu, Japan); mice were cared for under a protocol approved by the Azabu University Animal Experiment Committee. Total RNA isolation and RT-PCR were performed to examine *Trpv* expression as previously described.[23] The cDNA synthesized from 20 ng of total RNA was used as the template for RT-PCR. Thermal cycling parameters consisted of 40 cycles for *Trpv* or 35 cycles for *Tbp* (TATA-binding protein) of denaturation at 95 °C for 20 s, annealing at 58 °C for 20 s and extension at 72 °C for 20 s. The PCR products were electrophoresed in agarose gels, and subsequently stained with ethidium bromide.

The expression levels of *Trpv* and genes related to brown adipogenesis in HB2 brown (pre)adipocytes were examined by RT-real-time quantitative PCR (RT-qPCR) as described previously.[24] The oligonucleotide primers used are shown in Table 1. The Ct value was determined, and the abundance of gene transcripts was analysed using the $^{\Delta\Delta}$Ct method with *Tbp* as the reference gene.[25]

Statistical analyses

Data are expressed as the mean ± standard error (SE). Data on gene expression were log-transformed to provide an approximation of a normal distribution before analyses. Differences between gene expression levels in cells were examined using unpaired *t*-tests. Differences of $p < 0.05$ were considered significant.

RESULTS

Regulatory expression of Trpv1 during brown adipogenesis

We examined the expression of *Trpv* family members in mouse BAT (Figure 1A). The significant expression of *Trpv1*, *Trpv2*, *Trpv3* and *Trpv4* was detected. Based on these results, we next evaluated changes in the expression of *Trpv* family members during brown adipogenesis using HB2 brown preadipocytes (Figure 1B–E). The expression of *Trpv1* increased with time after day 4 of the induction of differentiation, whereas that of *Trpv2* and *Trpv4* decreased after the induction of differentiation. The expression of *Trpv3* increased on day 6 after the induction of differentiation; however, this increase was not significant because of large variations. The expression levels of *TrpV5* and *Trpv6* were lower than the detection limit throughout brown adipogenesis (data not shown).

Capsaicin induces calcium influx in brown preadipocytes

Capsaicin induces calcium influx via the activation of Trpv1; the overexpression of Trpv1, but not that of Trpv2 or Trpv4, was previously reported to induce calcium influx

Table 1. Nucleotide sequences of primers used in RT-qPCR analyses

Gene	Primer	Sequence	GenBank accession number	Size (bp)
Trpv family:				
Trpv1	5′	5′-caacaagaaggggcttacacc-3′	NM_001001445	77
	3′	5′-tctggagaatgtaggccaagac-3′		
Trpv2	5′	5′-caccatagttgcctaccacca-3′	NM_011706	63
	3′	5′-gtcgcttttgatgagggaat-3′		
Trpv3	5′	5′-tcgtctacaacaccaacattga-3′	NM_145099	77
	3′	5′-tttcgtgtgtagcagcgtatg-3′		
Trpv4	5′	5′-tcagaagatcctcttcaaagacct-3′	NM_022017	98
	3′	5′-acggattcaggagggtgac-3′		
Trpv5	5′	5′-atggaggagaccacctgaag-3′	NM_001007572	124
	3′	5′-cgcttccgtttctgcattag-3′		
Trpv6	5′	5′-gctcagagccgagacgag-3′	NM_022413	61
	3′	5′-gaagaggtgattcccagatcc-3′		
Adipocyte-related genes:				
Fabp4	5′	5′-aaggtgaagagcatcataaccct-3′	NM_024406	133
	3′	5′-tcacgcctttcataacacattcc-3′		
Pgc-1α	5′	5′-tgtggaactctctggaactgc-3′	NM_008904	81
	3′	5′-gccttgaaagggttatcttgg-3′		
Pparγ2	5′	5′-tgctgttatgggtgaaactctg-3′	NM_011146	110
	3′	5′-ctgtgtcaaccatggtaatttctt-3′		
Ucp1	5′	5′-ctttgcctcactcaggattgg-3′	NM_009463	123
	3′	5′-actgccacacctccagtcatt-3′		
Reference gene:				
Tbp	5′	5′-ccaatgactcctatgaccccta-3′	NM_013684	104
	3′	5′-cagccaagattcacggtagat-3′		

in response to capsaicin.[8,26,27] Furthermore, capsaicin modulated membrane currents in cells expressing Trpv1,[8] but not in those expressing Trpv2[26] or Trpv3.[28] Thus, Trpv1, but not Trpv2, Trpv3 or Trpv4, mediates capsaicin-induced cell responses. In order to evaluate the activation of Trpv1 by capsaicin, calcium influx was examined using fluorescent analyses (Figure 2). The treatment of cells with capsaicin at 10 μM, but not 0.1 or 1 μM, increased fluorescent intensity, suggesting the induction of calcium influx by a high dose of capsaicin. Capsaicin-induced calcium influx was detected within 10 s, and continued for at least 120 s. A23187, a calcium ionophore, expectedly induced rapid and robust calcium influx within 10 s, which thereafter decreased. These results are consistent with previous findings obtained in white preadipocytes; capsaicin induced the prolonged influx of calcium in 3T3-L1 preadipocytes,[29] although the effective concentration of capsaicin to induce calcium influx was lower (~0.01 μM). In addition, A23187-induced calcium influx was found to be transient in human white preadipocytes.[16] We also attempted to examine calcium influx in mature brown adipocytes, but were unsuccessful because of autofluorescence (data not shown).

Effects of capsaicin on brown adipogenesis

The result that *Trpv1* is expressed in brown preadipocytes and its expression is increased with differentiation suggests the direct action of capsaicin in the early stage of brown adipogenesis. Thus, we treated cells with capsaicin or iRTX for 8 days after the induction of differentiation in order to examine their effects on the early stage of brown adipogenesis. Neither Trpv1 activation by capsaicin nor Trpv1 inhibition by iRTX affected lipid accumulation, as evaluated by Oil Red O staining (Figure 3A). In addition, the expression level of *Fabp4*, a marker of maturation in white and brown adipocytes,[30,31] was unaffected by capsaicin (Figure 3B). Because peroxisome proliferator-activated receptor (Ppar) γ2 is a master regulator of white and brown adipogenesis,[32] we also measured the expression level of *Pparγ2* and showed that it was not affected by capsaicin (Figure 3C). Pparγ coactivator-1α (Pgc-1α) and Ucp1 are genes that are more strongly expressed in brown fat than in white fat[33] and are the principle genes for thermogenesis in brown adipocytes.[1] The treatment of cells with capsaicin during brown adipogenesis did not affect the expression levels of *Pgc-1α* (Figure 3D) or *Ucp1* (Figure 3E). Because the expression levels of these genes reflect the activity of brown adipocytes,[1,34,35] these results suggest that capsaicin does not significantly affect the early stage of brown adipogenesis.

Effects of capsaicin on activation of brown adipocytes

We next examined the role of capsaicin in the function of brown adipocytes and late stage of brown adipogenesis; HB2 brown adipocytes were treated for 4 days with capsaicin, i.e. the treatment was performed during the period between day 8 and 12. The treatment of these cells with capsaicin did not affect lipid accumulation, irrespective of the dose of capsaicin (Figure 4A). However, the expression of *Fabp4* was up-regulated by increases in the concentration of capsaicin used; the expression level of *Fabp4* in cells treated with 10 μM of capsaicin was significantly higher than that in control cells (Figure 4B). The expression levels

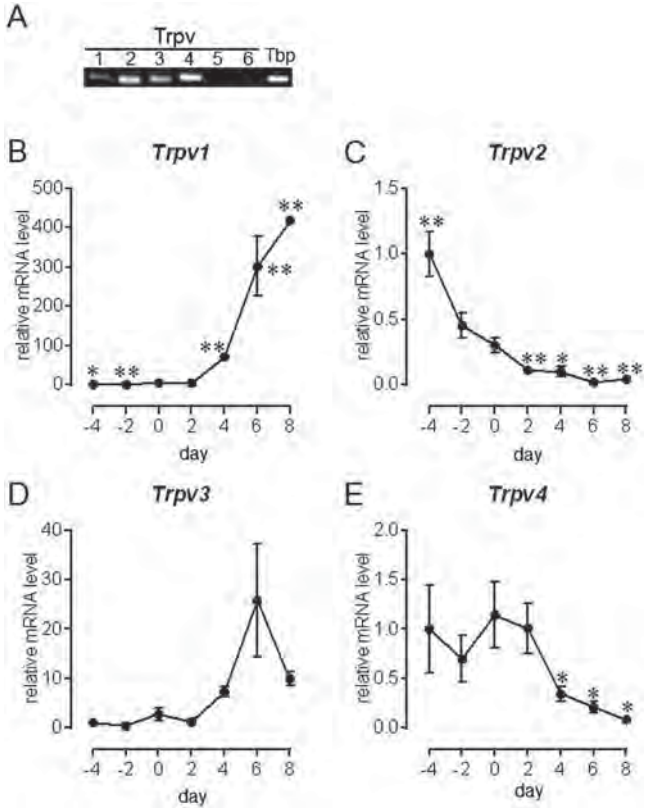

Figure 1. Expression of *Trpv* in mouse brown adipose tissues and HB2 cells. (A) Total RNA was isolated from the brown adipose tissue of adult C57BL/6 mice, and RT-PCR was performed in order to examine the expression of *Trpv*. PCR products were electrophoresed on agarose gels, followed by staining with ethidium bromide. A representative result is shown. (B–E) Two days after confluence (day 0), HB2 brown preadipocytes were differentiated into brown adipocytes by a treatment with insulin. The expression of *Trpv1* (B), *Trpv2* (C), *Trpv3* (D) and *Trpv4* (E) was examined using RT-qPCR and expressed as ratios to *Tbp*, with the level being set to 1 in cells on day −4. Data shown are the mean ± SE ($n = 4$). * and **: $p < 0.05$ and $p < 0.01$ significantly different from expression levels on day 0, respectively

of *Pparγ2* and *Pgc-1α* were significantly increased in brown adipocytes treated with 0.1 μM or 10 μM of capsaicin (Figure 4C and D). Although capsaicin did not affect *Ucp1* expression under the unstimulated state, it partially inhibited *Ucp1* expression induced by forskolin, irrespective of the dose used (Figure 4E). These results suggest that brown adipocytes are target cells of capsaicin or that capsaicin affects the late stage of brown adipogenesis.

DISCUSSION

The present study showed that the capsaicin receptor *Trpv1* is expressed in mouse BAT, and also that its expression level is increased with brown adipogenesis. By taking these results together with the efficient absorption of capsaicin from the gastrointestinal tract,[12] we expected capsaicin to directly modulate brown adipogenesis, the activation of brown adipocytes or both. We revealed that capsaicin modulates brown adipogenesis in the late stage rather than brown adipogenesis in the early stage. Furthermore, capsaicin modulates the activation of brown adipocytes; a treatment with capsaicin during the late stage of brown adipogenesis increased the expression levels of *Pparγ2* and *Pgc-1α*, and blunted forskolin-induced *Ucp1* expression. Our results indicate the direct action of capsaicin in brown (pre)adipocytes.

Previous studies reported the expression of *Trpv1* in white adipose tissue (WAT),[36] and that the expression levels of *Trpv1* decreased with time during white adipogenesis.[29,37] This is in contrast to the changes observed in the expression levels of *Trpv1* during brown adipogenesis, which suggests the differential regulation of *Trpv1* expression between brown and white (pre)adipocytes. *Trpv1* transcription is known to be stimulated by the transcription factors Sp1, Sp4, Runx1 and C/ebpβ in neuronal cells.[38,39] Gene transcription is regulated in a cell context-dependent manner,[40] and the transcriptional regulation in adipogenic cells currently remains unclear. Nevertheless, in view of the regulation of adipogenesis by Sp1 and C/ebpβ,[31] the above described transcription factors may be involved in changes in *Trpv1* during brown adipogenesis.

Capsaicin at 0.1 μM or 10 μM increased the expression of *Pparγ2* and *Pgc-1α* when cells were treated during the late stage of brown adipogenesis. Pparγ2 promotes a transcriptional cascade involved in the function of adipocytes,[31,32] while Pgc-1α stimulates mitochondrial biogenesis as well as brown adipocyte function including the transcriptional activation of *Ucp1*.[1] Therefore, the present results suggest that capsaicin stimulates the differentiation of brown preadipocytes present in the late stage of brown adipogenesis, increases expression levels in brown adipocytes or both.

In contrast to the treatment with capsaicin during the late stage of brown adipogenesis, the up-regulated expression of *Pparγ2* and *Pgc-1α* was not detected when cells were treated with capsaicin during the early stage of brown adipogenesis. This differential response to capsaicin may be related to increases in the expression level of *Trpv1* during brown adipogenesis. Capsaicin-induced calcium influx may be greater in brown adipocytes than in brown preadipocytes. Previous studies demonstrated that increases in the concentration of intracellular calcium induced the up-regulated expression of *Pparγ2* in human white adipocytes,[16] and the calcium signalling pathway activated the transcription of the *Pgc-1α* gene.[41] Alternatively, the cell response itself is likely to change during brown adipogenesis. Norepinephrine-induced increases in intracellular calcium concentrations were found to be slower in brown preadipocytes than in brown adipocytes.[42] Shi *et al.*[16] also revealed differential white adipogenesis in response to calcium signalling in a stage-dependent manner; increases in intracellular calcium inhibited adipogenesis in the early stages of differentiation, whereas they promoted adipogenesis in the late stage.

The cell stage-dependent effects of capsaicin might be related to changes in expression level of *Trpv1* during brown adipogenesis. We explored calcium flux in response

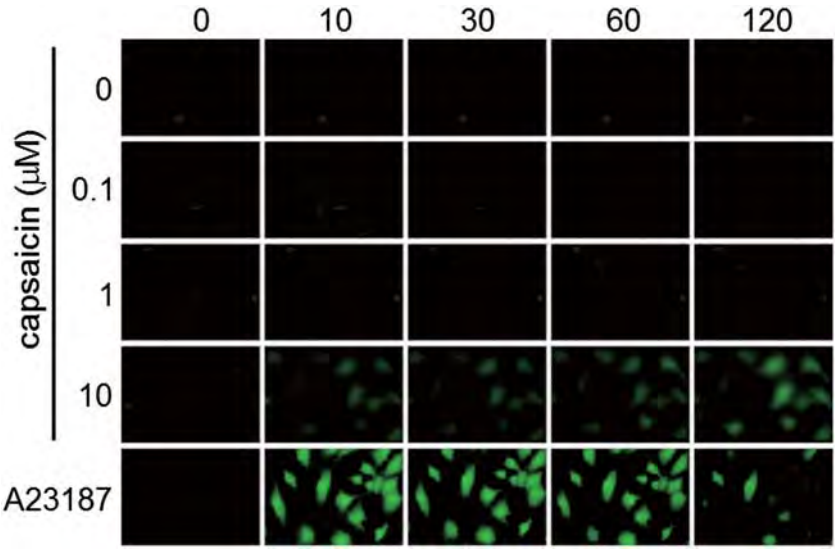

Figure 2. Calcium influx by capsaicin or A23187 in HB2 brown preadipocytes. HB2 brown preadipocytes loaded Fluo-8 AM were treated with the indicated concentration of capsaicin or A23187 (1 μM) for the indicated time. A representative fluorescent image is shown

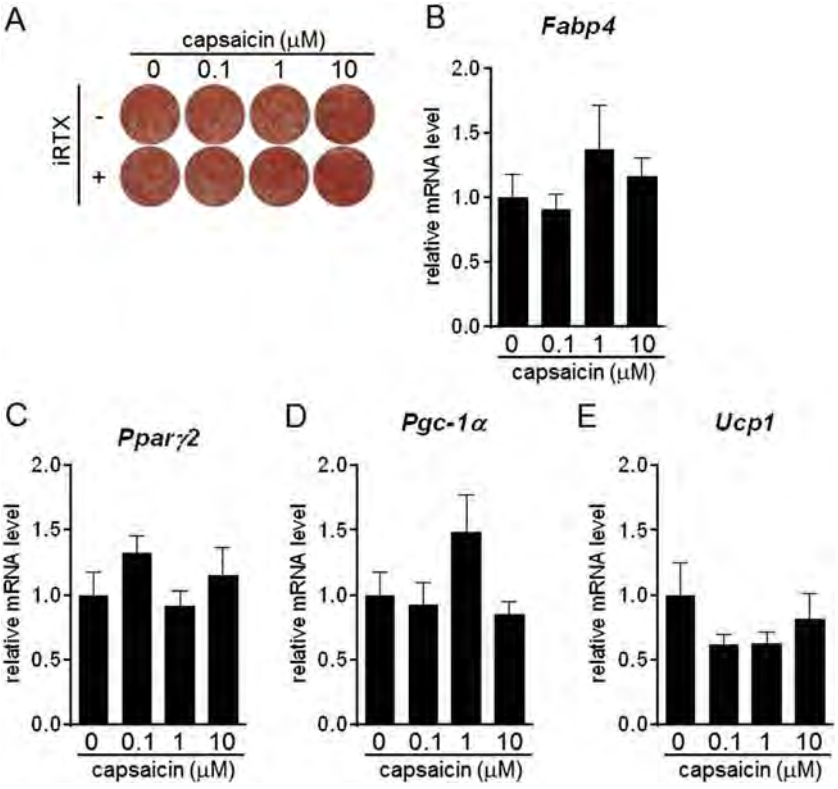

Figure 3. Effects of capsaicin and the Trpv1 antagonist on brown adipogenesis. Two days after confluence (day 0), HB2 brown preadipocytes were differentiated into brown adipocytes by a treatment with insulin in the presence or absence of the indicated concentration of capsaicin or iRTX, a Trpv1 antagonist (200 nM). (A) Cells on day 8 were examined by Oil Red O staining. The expression of *Fabp4* (B), *Pparγ2* (C), *Pgc-1α* (D) and *Ucp1* (E) was examined using RT-qPCR and expressed as ratios to *Tbp*, with the level being set to 1 in cells treated without capsaicin and iRTX. Data shown are the mean ± SE ($n = 4$)

to capsaicin in brown preadipocytes but not in mature brown adipocytes because of autofluorescence as described above. In view of higher concentration of capsaicin to induce calcium influx effectively in brown preadipocytes than in 3T3-L1 preadipocytes,[29] capsaicin-induced calcium influx in brown preadipocytes may not be mediated by Trpv1.

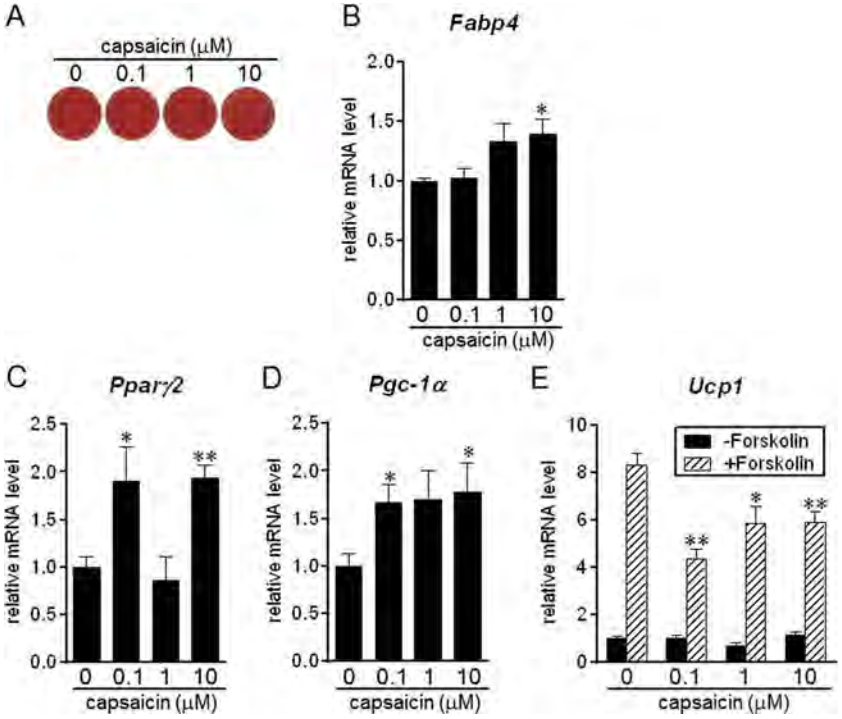

Figure 4. Effects of capsaicin on brown adipocyte function. HB2 brown preadipocytes were differentiated into brown adipocytes by a treatment with insulin. Brown adipocytes were treated with or without the indicated concentration of capsaicin in the presence of insulin on days 8–12. (A) Cells on day 12 were examined by Oil Red O staining. The expression of *Fabp4* (B), *Pparγ2* (C) and *Pgc-1α* (D) was examined. In addition, on day 12, cells were treated with or without forskolin (10 μM) for 4 h, and the expression of *Ucp1* (E) was examined using RT-qPCR and expressed as ratios to *Tbp*, with the level being set to 1 in cells treated without capsaicin and forskolin. Data shown are the mean ± SE ($n = 4$). * and **: $p < 0.05$ and $p < 0.01$ significantly different from expression levels in cells treated without capsaicin (and with forskolin (E)), respectively

Molecules responsible for capsaicin-induced calcium influx at the higher concentration should be explored in future.

There are two kinds of thermogenic adipocytes, i.e. brown and beige. In mice, BAT consists of brown adipocytes, whereas beige adipocytes relatively exhibit sparse distribution in WAT.[43] Both adipocyte types express genes involved in thermogenesis such as *Ucp1* and *Pgc-1α* at similar levels,[44] and forskolin has been shown to up-regulate Ucp1 expression in both types of adipocytes.[45] However, molecular signatures differ between brown and beige adipocytes,[44–47] as do the cell lineages; brown adipocytes are derived from skeletal muscle cells,[48] whereas beige adipocytes are from smooth muscle-derived cells.[44] Baboota *et al.*[37] recently revealed that the treatment of cells with capsaicin during the early stage of 3T3-L1 white adipogenesis induced the up-regulation of *Pparγ2*, *Pgc-1α* and *Ucp1* expression, suggesting the promotion of differentiation to beige adipocytes. Capsaicin has the potential to increase the activity of brown/beige adipocytes. However, the action point of capsaicin may differ between brown and beige (pre)adipocytes; the target of capsaicin is brown adipocytes or brown preadipocytes present in the late stage of brown adipogenesis, whereas capsaicin induces beige adipocytes through the promotion of adipogenesis in the early stage.

Forskolin-induced *Ucp1* expression was partially inhibited by capsaicin, which suggests the inhibitory effect of capsaicin on the activation of brown adipocytes. This effect of capsaicin is in contrast to the *in vivo* effects of capsaicin and capsinoids on brown adipocytes.[7,49,50] In adult humans, the chronic ingestion of capsinoids for 6 weeks did not affect basal energy expenditure, but increased cold-induced thermogenesis;[7] capsaicin or capsinoid-induced thermogenesis in animals has been attributed to sympathetic nerve-mediated events,[3] whereas capsaicin intrinsically inhibits the activation of brown adipocytes.

The precise reason why capsaicin partially inhibited forskolin-induced *Ucp1* expression currently remains unclear. Forskolin activates adenylate cyclase,[17] which increases cAMP concentrations and the subsequent stimulation of the protein kinase A pathway, leading to the transcription of the *Ucp1* gene.[1] Capsaicin-induced calcium influx may stimulate the activity of calmodulin-dependent phosphodiesterase, which degrades cAMP.[51] This enhancement in phosphodiesterase activity with increases in intracellular calcium concentrations has also been suggested in brown adipocytes.[52]

Chaiyasit *et al.*[53] reported that peak concentration of plasma concentration was 2.47 ng/ml (8.1 nM) in humans ingested capsicum containing 26.6 mg of capsaicin. The concentration is lower than that examined effect on brown adipogenesis and brown adipocyte function in this study. Therefore, it is not clear whether capsaicin at the concentration detected in plasma affects brown adipogenesis and brown adipocyte function. Future studies are needed to clarify the effect of physiological concentration of capsaicin.

CONFLICT OF INTEREST

The authors declare no conflict of interest.

ACKNOWLEDGEMENTS

The authors thank Prof. Dr. Masayuki Saito for providing HB2 brown preadipocytes.

REFERENCES

1. Cannon B, Nedergaard J. Brown adipose tissue: function and physiological significance. *Physiol Rev* 2004; **84**: 277–359.
2. Nakamura K. Central circuitries for body temperature regulation and fever. *Am J Physiol Regul Integr Comp Physiol* 2011; **301**: R1207–R1228.
3. Saito M, Yoneshiro T. Capsinoids and related food ingredients activating brown fat thermogenesis and reducing body fat in humans. *Curr Opin Lipidol* 2013; **24**: 71–77.
4. Bode AM, Dong Z. The two faces of capsaicin. *Cancer Res* 2011; **71**: 2809–2814.
5. Snitker S, Fujishima Y, Shen H, *et al.*. Effects of novel capsinoid treatment on fatness and energy metabolism in humans: possible pharmacogenetic implications. *Am J Clin Nutr* 2009; **89**: 45–50.
6. Yoneshiro T, Aita S, Kawai Y, Iwanaga T, Saito M. Nonpungent capsaicin analogs (capsinoids) increase energy expenditure through the activation of brown adipose tissue in humans. *Am J Clin Nutr* 2012; **95**: 845–850.
7. Yoneshiro T, Aita S, Matsushita M, *et al.*. Recruited brown adipose tissue as an antiobesity agent in humans. *J Clin Invest* 2013; **123**: 3404–3408.
8. Caterina MJ, Schumacher MA, Tominaga M, Rosen TA, Levine JD, Julius D. The capsaicin receptor: a heat-activated ion channel in the pain pathway. *Nature* 1997; **389**: 816–824.
9. Hachiya S, Kawabata F, Ohnuki K, *et al.*. Effects of CH-19 Sweet, a non-pungent cultivar of red pepper, on sympathetic nervous activity, body temperature, heart rate, and blood pressure in humans. *Biosci Biotechnol Biochem* 2007; **71**: 671–676.
10. Watanabe T, Kawada T, Kurosawa M, Sato A, Iwai K. Adrenal sympathetic efferent nerve and catecholamine secretion excitation caused by capsaicin in rats. *Am J Physiol* 1988; **255**: E23–E27.
11. Kawabata F, Inoue N, Masamoto Y, Matsumura S, Kimura W, Kadowaki M, Higashi T, Tominaga M, Inoue K, Fushiki T. Non-pungent capsaicin analogs (capsinoids) increase metabolic rate and enhance thermogenesis via gastrointestinal TRPV1 in mice. *Biosci Biotechnol Biochem* 2009; **73**: 2690–2677.
12. Kawada T, Suzuki T, Takahashi M, Iwai K. Gastrointestinal absorption and metabolism of capsaicin and dihydrocapsaicin in rats. *Toxicol Appl Pharmacol* 1984; **72**: 449–456.
13. Jang Y, Lee Y, Kim SM, Yang YD, Jung J, Oh U. Quantitative analysis of TRP channel genes in mouse organs. *Arch Pharm Res* 2012; **35**: 1823–1830.
14. Ye L, Kleiner S, Wu J, *et al.*. TRPV4 is a regulator of adipose oxidative metabolism, inflammation, and energy homeostasis. *Cell* 2012; **151**: 96–110.
15. Ntambi JM, Takova T. Role of Ca^{2+} in the early stages of murine adipocyte differentiation as evidenced by calcium mobilizing agents. *Differentiation* 1996; **60**: 151–158.
16. Shi H, Halvorsen YD, Ellis PN, Wilkison WO, Zemel MB. Role of intracellular calcium in human adipocyte differentiation. *Physiol Genomics* 2000; **3**: 75–82.
17. Seamon KB, Daly JW. Forskolin: a unique diterpene activator of cyclic AMP-generating systems. *J Cyclic Nucleotide Res* 1981; **7**: 201–224.
18. Wahl P, Foged C, Tullin S, Thomsen C. Iodo-resiniferatoxin, a new potent vanilloid receptor antagonist. *Mol Pharmacol* 2001; **59**: 9–15.
19. Reed PW, Lardy HA. A23187: a divalent cation ionophore. *J Biol Chem* 1972; **247**: 6970–6977.
20. Martin VV, Beierlein M, Morgan JL, Rothe A, Gee KR. Novel fluo-4 analogs for fluorescent calcium measurements. *Cell Calcium* 2004; **36**: 509–514.
21. Irie Y, Asano A, Cañas X, Nikami H, Aizawa S, Saito M. Immortal brown adipocytes from p53-knockout mice: differentiation and expression of uncoupling proteins. *Biochem Biophys Res Commun* 1999; **255**: 221–225.
22. Yoshida H, Kanamori Y, Asano H, *et al.*. Regulation of brown adipogenesis by the Tgf-β family: involvement of Srebp1c in Tgf-β- and Activin-induced inhibition of adipogenesis. *Biochim Biophys Acta* 1830; **2013**: 5027–5035.
23. Murakami M, Ohi M, Ishikawa S, Shirai M, Horiguchi H, Nishino Y, Funaba M. Adaptive expression of uncoupling protein 1 in the carp liver and kidney in response to changes in ambient temperature. *Comp Biochem Physiol A Mol Integr Physiol* 2015; **185**: 142–149.
24. Kanamori Y, Murakami M, Matsui T, Funaba M. Hepcidin expression in liver cells: evaluation of mRNA levels and transcriptional regulation. *Gene* 2014; **546**: 50–55.
25. Duran EM, Shapshak P, Worley J, *et al.*. Presenilin-1 detection in brain neurons and FOXP3 in peripheral blood mononuclear cells: normalizer genes selection for real time reverse transcriptase PCR using the deltadeltaCt method. *Front Biosci* 2005; **10**: 2955–2965.
26. Kanzaki M, Zhang YQ, Mashima H, Li L, Shibata H, Kojima I. Translocation of a calcium-permeable cation channel induced by insulin-like growth factor-I. *Nat Cell Biol* 1999; **1**: 165–170.
27. Strotmann R, Harteneck C, Nunnenmacher K, Schultz G, Plant TD. OTRPC4, a nonselective cation channel that confers sensitivity to extracellular osmolarity. *Nat Cell Biol* 2000; **2**: 695–702.
28. Xu H, Ramsey IS, Kotecha SA, *et al.*. TRPV3 is a calcium-permeable temperature-sensitive cation channel. *Nature* 2002; **418**: 181–186.
29. Zhang LL, Yan Liu D, Ma LQ, *et al.*. Activation of transient receptor potential vanilloid type-1 channel prevents adipogenesis and obesity. *Circ Res* 2007; **100**: 1063–1070.
30. Kang S, Bajnok L, Longo KA, Petersen RK, Hansen JB, Kristiansen K, MacDougald OA. Effects of Wnt signaling on brown adipocyte differentiation and metabolism mediated by PGC-1α. *Mol Cell Biol* 2005; **25**: 1272–1282.
31. Tang QQ, Lane MD. Adipogenesis: from stem cell to adipocyte. *Annu Rev Biochem* 2012; **81**: 715–736.
32. Kajimura S, Seale P, Spiegelman BM. Transcriptional control of brown fat development. *Cell Metab* 2010; **11**: 257–262.
33. Seale P, Kajimura S, Yang W, *et al.*. Transcriptional control of brown fat determination by PRDM16. *Cell Metab* 2007; **6**: 38–54.
34. Kajimura S, Saito M. A new era in brown adipose tissue biology: molecular control of brown fat development and energy homeostasis. *Annu Rev Physiol* 2014; **76**: 225–249.
35. Tseng YH, Kokkotou E, Schulz TJ, *et al.*. New role of bone morphogenetic protein 7 in brown adipogenesis and energy expenditure. *Nature* 2008; **454**: 1000–1004.
36. Chen J, Li L, Li Y, *et al.*. Activation of TRPV1 channel by dietary capsaicin improves visceral fat remodeling through connexin43-mediated Ca^{2+} influx. *Cardiovasc Diabetol* 2015; **14**: 22.
37. Baboota RK, Singh DP, Sarma SM, *et al.*. Capsaicin induces "brite" phenotype in differentiating 3T3-L1 preadipocytes. *PLoS One* 2014; **9**: e103093.
38. Chu C, Zavala K, Fahimi A, *et al.*. Transcription factors Sp1 and Sp4 regulate TRPV1 gene expression in rat sensory neurons. *Mol Pain* 2011; **7**: 44.
39. Ugarte GD, Diaz E, Biscaia M, Stehberg J, Montecino M, van Zundert B. Transcription of the pain-related TRPV1 gene requires Runx1 and C/EBPβ factors. *J Cell Physiol* 2013; **228**: 860–870.
40. Erhard F, Haas J, Lieber D, *et al.*. Widespread context dependency of microRNA-mediated regulation. *Genome Res* 2014; **24**: 906–919.
41. Handschin C, Rhee J, Lin J, Tarr PT, Spiegelman BM. An autoregulatory loop controls peroxisome proliferator-activated receptor gamma coactivator 1α expression in muscle. *Proc Natl Acad Sci U S A* 2003; **100**: 7111–7116.
42. Dolgacheva LP, Abzhalelov BB, Zhang SJ, Zinchenko VP, Bronnikov GE. Norepinephrine induces slow calcium signalling in murine brown preadipocytes through the β-adrenoceptor/cAMP/protein kinase A pathway. *Cell Signal* 2003; **15**: 209–216.

43. Ishibashi J, Seale P. Beige can be slimming. *Science* 2010; **328**: 1113–1114.
44. Long JZ, Svensson KJ, Tsai L, *et al.*. A smooth muscle-like origin for beige adipocytes. *Cell Metab* 2014; **19**: 810–820.
45. Wu J, Boström P, Sparks LM, *et al.*. Beige adipocytes are a distinct type of thermogenic fat cell in mouse and human. *Cell* 2012; **150**: 366–376.
46. Sharp LZ, Shinoda K, Ohno H, *et al.*. Human BAT possesses molecular signatures that resemble beige/brite cells. *PLoS One* 2012; **7**: e49452.
47. Shinoda K, Luijten IH, Hasegawa Y, *et al.*. Genetic and functional characterization of clonally derived adult human brown adipocytes. *Nat Med* 2015; **21**: 389–394.
48. Seale P, Bjork B, Yang W, *et al.*. PRDM16 controls a brown fat/skeletal muscle switch. *Nature* 2008; **454**: 961–967.
49. Ono K, Tsukamoto-Yasui M, Hara-Kimura Y, Inoue N, Nogusa Y, Okabe Y, Nagashima K, Kato F. Intragastric administration of capsiate, a transient receptor potential channel agonist, triggers thermogenic sympathetic responses. *J Appl Physiol* 2011; **110**: 789–798.
50. Yoshida T, Yoshioka K, Wakabayashi Y, Nishioka H, Kondo M. Effects of capsaicin and isothiocyanate on thermogenesis of interscapular brown adipose tissue in rats. *J. Nutr. Sci. Vitaminol. (Tokyo)* 1988; **34**: 587–594.
51. Goraya TA, Cooper DM. Ca^{2+}-calmodulin-dependent phosphodiesterase (PDE1): current perspectives. *Cell Signal* 2005; **17**: 789–797.
52. Bronnikov GE, Zhang SJ, Cannon B, Nedergaard J. A dual component analysis explains the distinctive kinetics of cAMP accumulation in brown adipocytes. *J Biol Chem* 1999; **274**: 37770–37780.
53. Chaiyasit K, Khovidhunkit W, Wittayalertpanya S. Pharmacokinetic and the effect of capsaicin in *Capsicum frutescens* on decreasing plasma glucose level. *J Med Assoc Thai* 2009; **92**: 108–113.

ARTICLE
Journal of Cellular Biochemistry 9999:1–9 (2016)

Journal of Cellular Biochemistry

Smad8/9 Is Regulated Through the BMP Pathway

Yuko Katakawa,[1] Masayuki Funaba,[2*] and Masaru Murakami[1**]

[1]*Laboratory of Molecular Biology, Azabu University School of Veterinary Medicine, Sagamihara 252-5201, Japan*

[2]*Division of Applied Biosciences, Graduate School of Agriculture, Kyoto University, Kyoto 606-8502, Japan*

ABSTRACT

Members of the transforming growth factor-β (TGF-β) family function through Smad-dependent and Smad-independent pathways. The Smad-dependent pathway is stimulated through the phosphorylation of receptor-regulated Smad (R-Smad) and inhibited through the dephosphorylation of R-Smad or the gene induction of inhibitory Smad (I-Smad). Little information is available on the regulation of R-Smad gene expression. BMP4 potentiated the up-regulation of Smad8/9 expression in C2C12, H9c2, 3T3-L1, HepG2, B16, and primary fibroblasts. BMP4-induced Smad8/9 expression was cycloheximide-insensitive and LDN-193189-sensitive, suggesting a direct event mediated through BMP type I receptors. BMP4 transcriptionally stimulated the Smad8/9 gene, and BMP-responsive elements (BREs) spanning nt −121 to nt −44 are involved in the up-regulation of Smad8/9 expression in response to BMP4. Phosphorylated Smad1/5/8/9 specifically bound to the BREs of Smad8/9 gene. The present study reveals that Smad8/9 is a unique R-Smad regulated through the BMP pathway at the mRNA level. J. Cell. Biochem. 9999: 1–9, 2016.

KEY WORDS: BMP; SMAD8/9; TRANSCRIPTION

The transforming growth factor-β (TGF-β) family, comprising three subfamilies, TGF-β, activin, and BMP groups [Miyazono et al., 2010; Massagué, 2012; Sakaki-Yumoto et al., 2013], plays diverse physiological roles, including the control of cell division, early embryonic patterning, cell differentiation, and cell determination [Derynck et al., 2008]. Compared with these diverse functions, the signal transduction pathways of these transcription factors, collectively referred to as the Smad pathway, are relatively simple. Members of the TGF-β family transmit signals through specific heteromeric complexes through type I and type II receptors, followed by the phosphorylation of the type I receptor via the type II receptor serine/threonine kinase. The phosphorylation of the type I receptor activates the serine/threonine kinase activity of this receptor, resulting in the phosphorylation of C-terminal serines of receptor-regulated (R)-Smads (Smad1, 2, 3, 5, and 8 [or 9]: Smad1/5/8/9 are regulated through BMP receptor complexes, and Smad2/3 are regulated via activin or TGF-β receptor complexes), complex formation with common Smads (Smad4) and the transactivation of target genes [Miyazono et al., 2010; Massagué, 2012; Sakaki-Yumoto et al., 2013].

The negative regulation of TGF-β family signaling is also partly mediated through the Smad proteins. The expression of inhibitory (I)-Smads (Smad6 and Smad7) is up-regulated through TGF-β1, activin A, BMP2, and BMP7 [Nakao et al., 1997; Ishisaki et al., 1998; Takase et al., 1998], and I-Smads directly associate with activated type I receptors to compete with R-Smads [Hayashi et al., 1997]. Alternatively, I-Smads interact with a Smad-interacting ubiquitin ligase known as Smurf, leading to the ubiquitination and proteasomal degradation of these receptors [Ebisawa et al., 2001; Murakami et al., 2003]. The signaling of the TGF-β family is further negatively regulated through the de-phosphorylation of R-Smads [Duan et al., 2006; Knockaert et al., 2006; Lin et al., 2006].

In contrast to I-Smads, the activity of R-Smads is not generally regulated at the expression level; the TGF-β family does not affect the expression of R-Smad [Nakao et al., 1997; Poncelet et al., 1999; Herrera et al., 2009; Murakami et al., 2009], although a few studies have reported the modulation of Smad3 expression through TGF-β [Yanagisawa et al., 1998; Poncelet et al., 1999; Winbanks et al., 2011]. We previously showed that the expression of Smad8/9, but not Smad1 and Smad5, is decreased in response to the differentiation stimulation of myoblasts into myotubes [Furutani et al., 2011]; the dynamic changes in Smad8/9 expression paralleled changes in endogenous BMP activity. The results suggested that unlike the other R-Smads, Smad8/9 is a target gene for the BMP pathway. Here we

Conflicts of interest: The authors declare that there are no conflicts of interest.

Grant sponsor: Azabu University; Grant number: 2013K08.

*Correspondence to: Dr. Masayuki Funaba, Ph.D., Division of Applied Biosciences, Graduate School of Agriculture, Kyoto University, Kyoto 606-8502, Japan. E-mail: mfunaba@kais.kyoto-u.ac.jp **Correspondence to: Dr. Masaru Murakami, Laboratory of Molecular Biology, Azabu University School of Veterinary Medicine, Sagamihara 252-5201, Japan. E-mail: murakami@azabu-u.ac.jp

Manuscript Received: 21 May 2015; Manuscript Accepted: 4 January 2016

Accepted manuscript online in Wiley Online Library (wileyonlinelibrary.com): 00 Month 2015

DOI 10.1002/jcb.25478 • © 2016 Wiley Periodicals, Inc.

showed that the BMP pathway up-regulates Smad8/9 expression in multiple cell types, indicating the unique regulation of the BMP-induced Smad-dependent signaling pathway.

MATERIALS AND METHODS

MATERIALS

The following reagents were purchased: BMP2, BMP4, TGF-β1, and activin A were from R & D Systems (Minneapolis, MN); LDN-193189, an inhibitor for BMP type I receptor [Yu et al., 2008], was from Stemgent (San Diego, CA); a rabbit monoclonal antibody against Smad5 (D4G2, #12534), and rabbit polyclonal antibodies against phospho-Smad1 (Ser463/Ser465)/Smad5 (Ser463/Ser465)/Smad8 (Ser465/Ser467) (#13820 for Western blot and #11971 for chromatin immunoprecipitation [ChIP]) were from Cell Signaling Technology (Danvers, MA); a rabbit monoclonal antibody against Smad1 (EP565Y, ab33902), a goat polyclonal antibody against Smad8/9 (ab48011), and a mouse monoclonal antibody against α-tubulin (B-5-1-2, ab11304) were from Abcam (Cambridge, MA).

CELL CULTURE

C2C12, H9c2, 3T3-L1, HepG2, and B16 cells were cultured in Dulbecco's modified Eagle's medium (DMEM) supplemented with 10% heat-inactivated fetal bovine serum (FBS), 100 U/ml penicillin and 100 μg/ml streptomycin. C2C12, 3T3-L1, and B16 are mouse-originated cell lines. H9c2 and HepG2 are rat- and human-originated cell lines, respectively. Rat primary fibroblasts were prepared from skin of Wistar rats [Messenger, 1984] and cultured in DMEM supplemented with 10% FBS and antibiotics.

RNA ISOLATION AND QUANTITATIVE RT-PCR (QRT-PCR)

Total RNA isolation and qRT-PCR analyses were performed as previously described [Murakami et al., 2015]; total RNA was isolated using the RealTime ready Cell Lysis Kit (Roche, Mannheim, Germany), and cDNA was synthesized using Transcriptor Universal cDNA Master (Roche). The oligonucleotide primers for qRT-PCR are shown in Table I. As described above, because we used cell lines and primary cells originated from several species, that is, C2C12 (mouse), H9c2 (rat), 3T3-L1 (mouse), HepG2 (human), B16 (mouse), and primary fibroblasts (rat), we designed PCR primers to detect human, rat, and mouse genes. The mRNA levels were expressed relative to β-actin or GAPDH mRNA levels.

KARYOTYPE ANALYSES

To prepare the metaphase chromosomes, 3T3-L1 cells were grown to 80% confluency in 100-mm dishes. Colchicine (Calbiochem, La Jolla, CA) was added at a final concentration of 0.1 μg/ml for 1 h to stop the cell cycle. The cells were collected and subsequently treated with 0.075 M potassium chloride for 30 min at 37°C. The cells were fixed in Carnoy's solution (methanol: acetic acid, 3:1) and spread onto glass slides using the air-drying method. After staining with a 5% Giemsa solution, the number of chromosomes with 23 metaphases was counted.

WESTERN BLOT

The cells were lysed using the EzRIPA Lysis Kit (Atto, Tokyo, Japan), according to the manufacturer's instructions. The protein concentration was determined using the Pierce BCA Protein Assay Kit (Thermo Fisher Scientific, Waltham, MA). After heating for 5 min at 95°C, 10 μg of the protein samples was subjected to 10% SDS–polyacrylamide gel electrophoresis, followed by blotting onto iBlot Gel Transfer Stacks PVDF, Mini membranes (Life Technologies, Grand Island, NY) using an iBlot Gel Transfer Device (Life Technologies). The membranes were blocked with EzBlock (Atto) for 2 h and reacted with primary antibody diluted 1:1,000–5,000 in Can Get Signal solution (Toyobo, Tokyo, Japan) overnight at 4°C. Subsequently, the membranes were reacted with the appropriate secondary antibody conjugated with HRP for 1 h at room temperature. The immunoreactive proteins were visualized using the ECL Select Western blotting detection system (GE Healthcare, Buckinghamshire, UK) according to the manufacturer's instructions.

PLASMIDS

The DNA sequence spanning nt −1000 to nt +113 of the mouse Smad8/9 promoter was amplified and cloned into a pGL4 basic vector containing the firefly luciferase reporter (Smad8/9(−1000)-luc); nt +1 was defined as the transcriptional initiation site. Reporter plasmids with deleted promoters or point mutations were prepared using a PCR-based method. The plasmids were verified through DNA sequencing.

REPORTER ASSAYS

C2C12 and 3T3-L1 cells were transiently transfected with the Smad8/9 reporter construct and a plasmid expressing Renilla luciferase under the control of thymidine kinase promoter (pRL-tk) using Polyethylenimine Max reagent (Polysciences, Warrington, PA). At 24 h post-transfection, the cells were cultured with members of the TGF-β family in the presence of 0.2% FBS in DMEM for 16 h. The firefly luciferase activity in the cell lysate was normalized to the Renilla luciferase activity.

ChIP

C2C12 cells were treated with or without BMP4 (4 nM) for 2 h, and ChIP assays were performed by use of a commercial kit (Simple ChIP Plus Enzymatic Chromatin IP (#9005), Cell Signaling Technology). Binding of Smad1/5/8/9 to the region including BMP-responsive elements (BREs) of Smad8/9 gene (nt −164 to nt +21) was evaluated by PCR. Nucleotide sequence of the used PCR primers is shown in Table I. Because the GC-content of the region is extremely high (~77%), we amplified the region by use of PrimeSTAR GXL DNA polymerase (TaKaRa, Otsu, Japan), which is suitable for amplification of the GC-rich template. According to the manufacturer's protocol, the PCR profile was as follows: after denaturing for 2 min at 98°C, 30 cycles consisted of 10 sec at 98°C and 20 sec at 68°C, followed by extension for 3 min at 68°C. We also amplified outside region of the BREs of Smad8/9 (nt −2861 to nt −2702), the unrelated region to BMP signaling of hepcidin (nt −150 to nt −35), and the region including BREs of Id2 gene (nt −2872 to nt −2673, Nakahiro et al., 2010); hepcidin is a BMP-responsive gene, but the region spanning nt −150 to nt −35 is not involved in

TABLE I. Oligonucleotide Sequences For qRT-PCR and ChIP Assay

Gene	5′-primer	3′-primer	GenBank accession number
Human			
Smad1	5′-caacagccacccgtttcct-3′	5′-gtttgggtaactgctattggga-3′	U59423
Smad2	5′-tcatagcttggatttacagccag-3′	5′-acaccaaaatgcaggttctgag-3′	BC014840
Smad3	5′-tggacgcaggttctccaaac-3′	5′-gtgctggggacatcggattc-3′	BC0550743
Smad4	5′-gccaactttcccaacattcctg-3′	5′-tgctgctgtcctggctgag-3′	BC002379
Smad5	5′-ctttccaccagcccaacaacac-3′	5′-taggcaggaggaggcgtatcag-3′	AF009678
Smad6	5′-tctcctcgcgacgagtacaa-3′	5′-ccggagcagtgatgagggagt-3′	NM_005585
Smad7	5′-acccgatggattttctcaaac-3′	5′-gccagataattcgttcccccc-3′	AF015261
Smad9	5′-atgtgatttactgctgcgtgt-3′	5′-cggtagtggtaagggttaatgc-3′	BC011559
β-*actin*	5′-ccaaccgcgagaagatga-3′	5′′-ccagaggcgtacagggatag -3′	NM_001101
Mouse			
Smad1	5′-tgaaaacaccaggcgacata-3′	5′-tgaggcattccgcatacac-3′	NM_008539
Smad2	5′-tgtgcagagccccaactgt-3′	5′-gcctggtgggatcttacacact-3′	U60530
Smad3	5′-ggaatgcagccgtggaact-3′	5′-aagacctcccctccgatgtag-3′	AB008192
Smad4	5′-aagctgccctgttgtgactgt-3′	5′′-ggagagttgacccaagcaaaag-3′	NM_008540
Smad5	5′-gcagtaacatgattcctcagacc-3′	5′-gcgacaggctgaacatctc-3′	AF063006
Smad6	5′-gttgcaacccctaccacttc-3′	5′-ggaggagacagccgagaata-3′	AF010133
Smad7	5′-acccccatcaccttagtcg-3′	5′-gaaaatccattgggtatctgga-3′	AF015260
Smad8/9	5′-cggatgagctttgtgaagg-3′	5′-gggtgctcgtgacatcct-3′	AY145520
β-*actin*	5′-ctaaggccaaccgtgaaaag-3′	5′-accagaggcatacagggaca-3′	NM_007393
GAPDH	5′-cgtgttcctacccccaatgt-3′	5′-tgtcatcatacttggcaggtttct-3′	NM_008084
Rat			
Smad1	5′-gcagccctttcagatgccag-3′	5′-ggctgagagccatcctgggc-3′	NM_013130
Smad2	5′-caggacgattagatgagcttg-3′	5′-cgtatttgctgtactcagtcccc-3′	NM_019191
Smad3	5′-cctgccactgtctgcaagata-3′	5′-gcaaattcctggttgttgaagat-3′	NM_013095
Smad4	5′-gaacactggatggacgactg-3′	5′-acagacgggcatagatcaca-3′	NM_019275
Smad5	5′-cagcctatggacacaagcaa-3′	5′-ggcaacaggctgaacatctc-3′	NM_021692
Smad6	5′-gttgcaacccctaccacttc-3′	5′-ggaggagacagccgagaata-3′	NM_001109002
Smad7	5′-acccccatcaccttagtcg-3′	5′′-aaatccatcgggtatctgga-3′	NM_030858
Smad9	5′-accattaccgcagagtggaga-3′	5′-tgagggttgtactcgctgtg-3′	AF012347
β-*actin*	5′-ctaaggccaaccgtgaaaag-3′	5′-accagaggcatacagggaca-3′	NM_031144
ChIP			
BRE of Smad8	5′-aaggctctctgcaggcatgatgtg-3′	5′-tccagaggcgtcagtcaggctgga-3′	NC_000069.6
Outside BRE of Smad8	5′-gggtggtgccagtcaggtttgctt-3′	5′-cacatcaatcataaactaagaaaa-3′	NC_000069.6
Unrelated to responsiveness to BMP in hepcidin	5′-cactattttcttggaaatgagtcagagc-3′	5′-tgtgtggtggctgtctaggagcc-3′	NC_000073.6
BRE of Id2	5′-gctgagtgacggcgcggttgctat-3′	5′-gtgatccctgacaggtgatgaatt-3′	NC_000078.6

BMP-mediated transcriptional activation [Truksa et al., 2009]. Because the GC-content of the former two sequences was 43% and 53%, respectively, we amplified the region by use of *Ex-Taq* DNA polymerase (TaKaRa) with the PCR profile of initial denaturation for 3 min at 95°C, 30 cycles consisted of 20 sec at 95°C, 20 sec at 60°C and 20 sec at 72°C, followed by extension for 3 min at 72°C. The region including BREs of Id2 gene is GC-rich (∼75%). Thus, we used PrimeSTAR GXL DNA polymerase; the two-step PCR profile to detect the BREs of Smad8/9 gene; however, did not properly amplify the Id2 promoter. Therefore, we performed three-step PCR with the PCR profile of initial denaturation for 2 min at 98°C, 30 cycles consisted of 10 sec at 98°C, 15 sec at 55°C and 20 sec at 68°C, followed by extension for 3 min at 68°C, according to the manufacturer's protocol. The PCR products were electrophoresed in agarose gels, followed by ethidium bromide staining and visualization under ultraviolet light. We also examined several antibodies against Smad for ChIP assays in preliminary experiments; reproducible results were obtained, when antibody against phosphorylated Smad1/5/8/9 was used. Thus, chromatin samples were reacted with control IgG as a negative control or anti-phosphorylated Smad1/5/8/9 antibody.

STATISTICAL ANALYSES

The data are expressed as the means ± standard error (SE). Differences in the gene expression between cells were examined using unpaired *t*-tests. Differences of $P < 0.05$ were considered significant.

RESULTS

SMAD8/9 EXPRESSION IS UP-REGULATED THROUGH BMP4 IN MULTIPLE CELL TYPES

In a previous study, we revealed that changes in Smad8/9 expression, but not Smad1/5, paralleled endogenous BMP activity during myogenesis [Furutani et al., 2011]. We explored whether Smad8/9 expression is up-regulated through exogenous BMP and determined whether this regulation is detected in multiple cell types. Treatment with BMP4 for 2 h increased Smad8/9 expression in all examined cells (Fig. 1); expectedly, the expression of I-Smads, Smad6 and Smad7 were increased as previously shown [Nakao et al., 1997; Takase et al., 1998]. In addition, the expression levels of R-Smads other than Smad8/9 were unaffected after BMP4 treatment. The up-regulation of Smad8/9 expression was also detected in cells treated with BMP2, a closely related molecule to BMP4 (Fig. 2, data not shown).

Smad8 is closely related to Smad9; the nucleotide sequence of mouse Smad9 (GenBank accession number: NM_019483) indicates that six nucleotides (5′-cgagtc-3′) are inserted at nt +961 of mouse Smad8 (AF175408, Fig. 3A), leading to differences of two amino acids between Smad8 and Smad9. To characterize Smad8/9 in the cells examined in Figure 1, the nucleotide sequence of the region spanning the six nucleotides was determined (Fig. 3B). The insertion of the six nucleotides was detected in all cells examined (Fig. 3B upper, data not shown), except for C2C12 cells (Fig. 3B middle), indicating that C2C12 cells express Smad8, whereas the other cells express Smad9. Treatment with BMP4 did

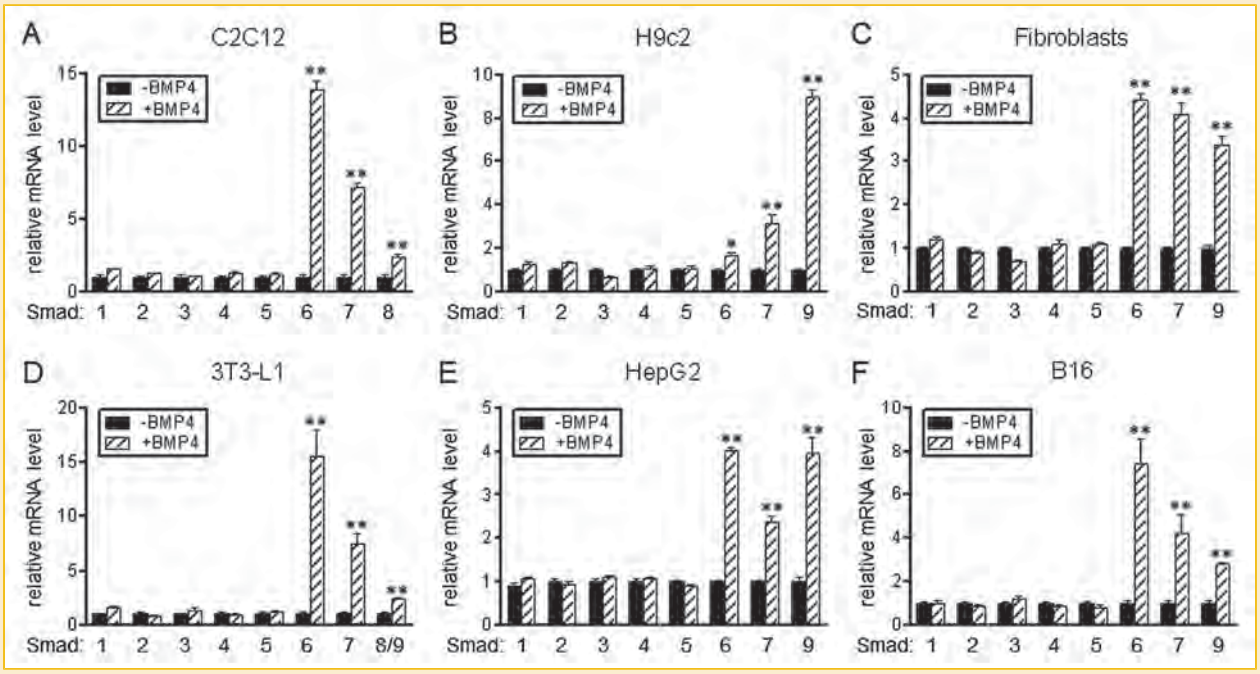

Fig. 1. Smad expression in response to BMP4 in multiple cell types. Smad expression in response to treatment with BMP4 was examined in C2C12 cells (A), H9c2 cells (B), primary fibroblasts (C), 3T3-L1 cells (D), HepG2 cells (E), and B16 cells (F). The cells were cultured in the presence or absence of BMP4 (4 nM) for 2 h. Expression of Smad was examined using qRT-PCR and expressed as ratios to β-actin, with the level set to 1 in cells cultured in the absence of BMP4. The data are presented as the means ± SE (n = 4). *, **: $P < 0.05$ and $P < 0.01$, respectively, compared with expression in cells treated without BMP4.

not induce expression of Smad9 in C2C12 cells, which was verified by direct sequencing of the RT-PCR products (data not shown). Notably, the nucleotide sequencing in 3T3-L1 cells reproducibly indicated the expression of both Smad8 and Smad9 (Fig. 3B bottom). We cloned Smad8/9 mRNA expressed in 3T3-L1 cells and determined the nucleotide in a total of 58 clones: 24 clones (41%) of Smad8 and 34 clones (59%) of Smad9 (data not shown). The karyotype analyses of a total of 23 cells showed 63 ± 15

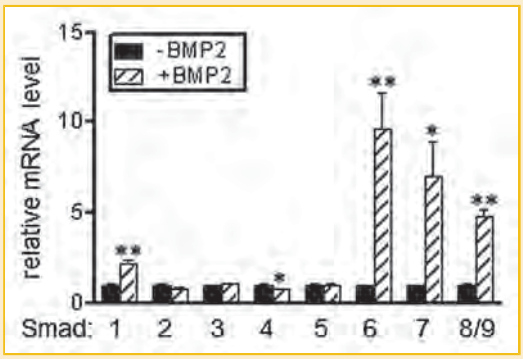

Fig. 2. Smad expression in response to BMP2 in 3T3-L1 cells. Smad expression in response to treatment with BMP2 was examined in 3T3-L1 cells. The cells were cultured in the presence or absence of BMP2 (4 nM) for 2 h. The expression of Smad was examined using qRT-PCR and expressed as ratios to GAPDH, with the level set to 1 in cells cultured in the absence of BMP2. The data are presented as the means ± SE (n = 4). *, **: $P < 0.05$ and $P < 0.01$, respectively, compared with expression in cells treated without BMP2.

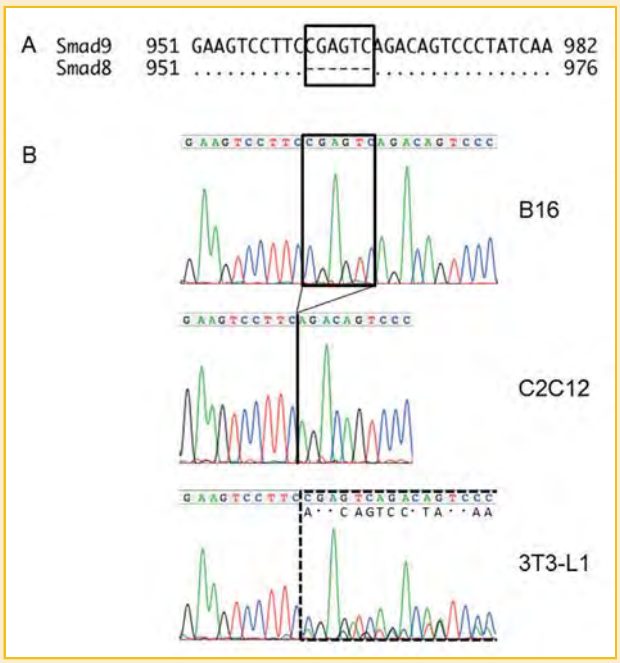

Fig. 3. Nucleotide sequence of Smad8/9 in multiple cell types. A: Nucleotide sequence surrounding nt +961 of mouse Smad9 compared with that of mouse Smad8. B: Waveform of the nucleotide sequence of Smad8/9 in B16 (upper), C2C12 (middle), and 3T3-L1 cells (bottom).

chromosomes in 3T3-L1 cells. Considering the 40 chromosomes observed in normal mice, the mixed and uneven ratio of Smad8 and Smad9 might reflect abnormal chromosomes.

We next evaluated the effects of the other members of the TGF-β family, TGF-β1, and activin A, on Smad8/9 expression (Fig. 4). As expected, TGF-β1 increased the expression of I-Smad in C2C12 cells (Fig. 4A) and 3T3-L1 cells (Fig. 4B). Activin A potentiated the up-regulation of I-Smad expression in 3T3-L1 cells. In contrast, activin A did not up-regulate I-Smad expression in C2C12 cells, although the effects of activin A were statistically significant. Both TGF-β1 and activin A did not substantially increase Smad8/9 expression. These results indicate that Smad8/9 is a unique R-Smad gene regulated at the mRNA level through BMPs.

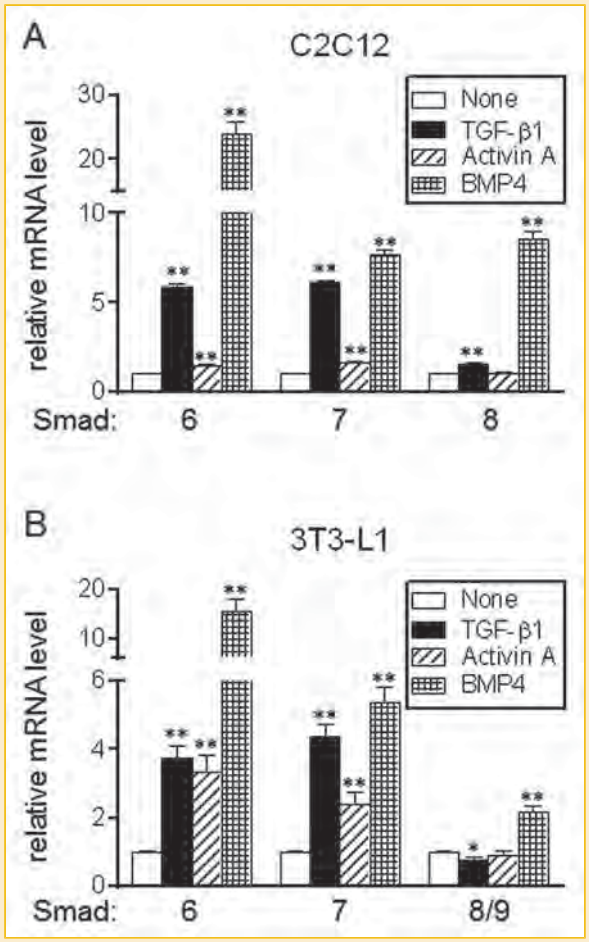

Fig. 4. Smad expression in response to the TGF-β family in C2C12 and 3T3-L1 cells. Smad expression in response to treatment with TGF-β1, activin A, or BMP4 was examined in C2C12 cells (A) and 3T3-L1 cells (B). The cells were cultured in the presence or absence of TGF-β1 (100 pM), activin A (4 nM), or BMP4 (4 nM) for 2 h. The expression of Smad was examined using qRT-PCR and expressed as ratios to β-actin, with the level set to 1 in cells cultured in the absence of ligand. The data are presented as the means ± SE ($n = 4$). *, **: $P < 0.05$ and $P < 0.01$, respectively, compared with expression in cells treated without ligand.

BMP4-INDUCED SMAD8/9 EXPRESSION IS TRANSCRIPTIONALLY REGULATED

To examine the molecular mechanism underlying the regulation of Smad8/9 expression, the effects of cycloheximide, an inhibitor of protein synthesis, on BMP-induced Smad8/9 expression were examined (Fig. 5). Smad8/9 expression in response to BMP4 treatment was up-regulated, irrespective of treatment with cycloheximide, suggesting that the Smad8/9 induction is a direct event. Thus, we speculated that BMP-induced Smad8/9 expression is transcriptionally regulated. To this end, luciferase-based reporter assays using the Smad8/9 promoter were performed.

Initially, we examined the BMP4-induced transcription of Smad8/9 using a reporter containing 1,000 bp of the Smad8/9 gene promoter (Fig. 6A and B). BMP4 increased the expression of luciferase, and pretreatment with LDN-193189, an inhibitor of BMP type I receptors [Yu et al., 2008], suppressed the responsiveness to BMP4 in C2C12 and 3T3-L1 cells, indicating that BMP4-induced Smad8/9 expression is transcriptionally regulated through the activation of BMP type I receptors. Considering that, BMP type I receptors phosphorylate and activate Smad1/5/8/9 [Miyazono et al., 2010; Massagué, 2012; Sakaki-Yumoto et al., 2013], the stimulated Smad8/9 transcription is likely achieved through a Smad-dependent pathway. Indeed, LDN-193189 inhibited the BMP4-induced phosphorylation of Smad1/5/8/9 (Fig. 6C).

MULTIPLE BMP-RESPONSIVE ELEMENTS ARE REQUIRED FOR BMP4-INDUCED SMAD8/9 TRANSCRIPTION

We next explored the potential region within the Smad8/9 promoter responsible for transcriptional activation in response to BMP4 treatment using deleted mutants of the Smad8/9 reporter (Fig. 7). The deletion of 330 bp within 1,000 bp upstream of the Smad8/9 gene decreased responsiveness to BMP4 in C2C12 cells (Fig. 7A); nevertheless, significant transcriptional activation through BMP4 was detected. Compared with Smad8/9(−338)-luc, further deletions of the Smad8/9 promoter resulted in gradual decrease of BMP4-induced transcription. The responsiveness to BMP4 nearly disappeared when Smad8/9(−43)-luc was used as a reporter. Similar effects of BMP4 were detected in 3T3-L1 cells, although the responsiveness to BMP4 in Smad8/9(−1000)-luc was not different from that in Smad8/9(−670)-luc (Fig. 7B). Similar to the response in C2C12 cells, BMP4 did not induce transcriptional activation, when Smad8/9(−43)-luc was used in 3T3-L1 cells. These results suggest that BREs are located at the distal region of nt −43 of the Smad8/9 promoter.

The BMP-induced phosphorylation of Smad1/5/8/9 stimulates transcription through binding to a GCCG or GC-rich sequence located in the promoter region of the target gene [Kusanagi et al., 2000; López-Rovira et al., 2002]. Examination of the nucleotide sequence indicated five potential regions of GCCG (BRE-1, 2, 4, and 5) or GC-rich sequence (BRE-3) within nt −121 of the Smad8/9 promoter (Fig. 8A). To examine the involvement of these BREs in BMP4-induced transcription, reporter plasmids with individual or combinational mutations of the BREs were prepared.

All five mutations of the BREs completely inhibited responsiveness to BMP4 (Fig. 8B). The mutations of individual BREs partially decreased the BMP response; specifically, BRE-3 mutations markedly reduced luciferase activity in response to BMP4. BRE-1 and BRE-2 mutations did not have the additive effects of BRE-3

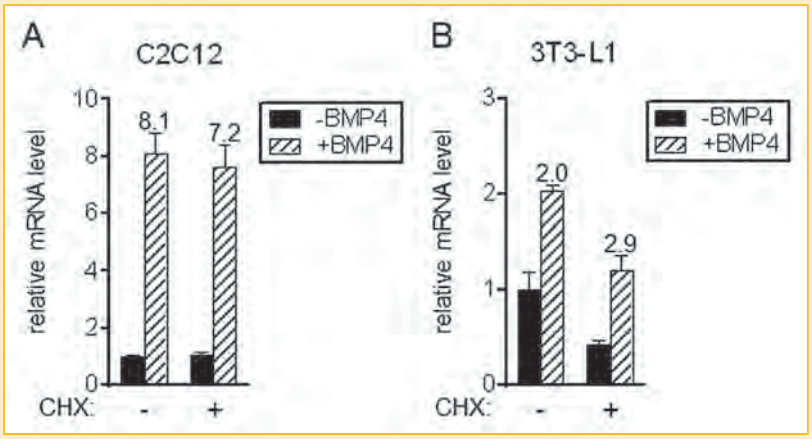

Fig. 5. Modulation of BMP4-induced Smad8/9 expression through cycloheximide. The necessity of new protein synthesis was examined for BMP4-induced mRNA expression of Smad8 in C2C12 cells (A) and 3T3-L1 cells (B). The cells were treated with or without BMP4 (4 nM) for 12 h after pre-treatment with or without cycloheximide (0.5 μg/ml) for 15 min. Smad8/9 expression was examined using qRT-PCR and expressed as ratios to β-actin, with the level set to 1 in cells cultured in the absence of BMP4 and cycloheximide. The data are presented as the means ± SE (n = 4). The numbers on the bar indicate fold-induction.

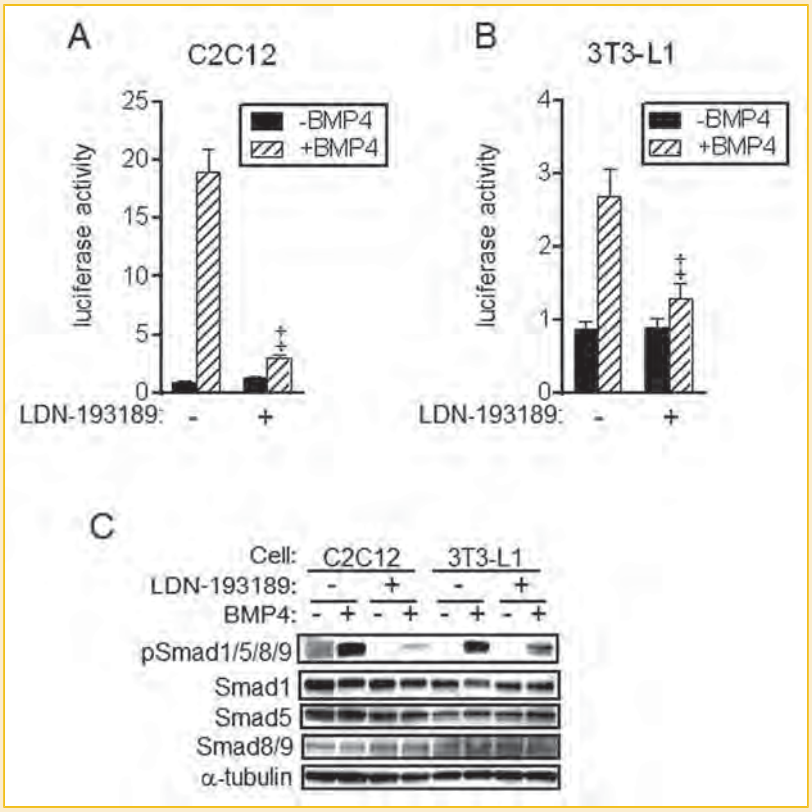

Fig. 6. Modulation of BMP4-induced Smad8/9 transcription through LDN-193189. BMP type I receptor kinase activity was examined for the BMP4-induced transcription and phosphorylation of Smad8/9 in C2C12 cells (A and C) and 3T3-L1 cells (B and C). The cells were treated with or without BMP4 (4 nM) for 1 h (C) or 16 h (A and B) after pre-treatment with or without LDN-193189 (100 nM) for 15 min. A, B: Smad8/9 transcription was evaluated as Smad8/9(−1000)-luc expression. Firefly, luciferase activity was expressed as a ratio to Renilla luciferase activity, with the level set to 1 in cells cultured in the absence of BMP4 and LDN193189. The data are presented as the means ± SE (n = 6). ‡ $P < 0.01$, compared with the respective treatment with BMP4, but not with LDN-193189. C: The effects of LDN-193189 on the phosphorylation of Smad1/5/8/9 in C2C12 and 3T3-L1 cells were examined through western blot analyses. Expression level of total Smad1, Smad5, Smad8/9, and α-tubulin was also examined.

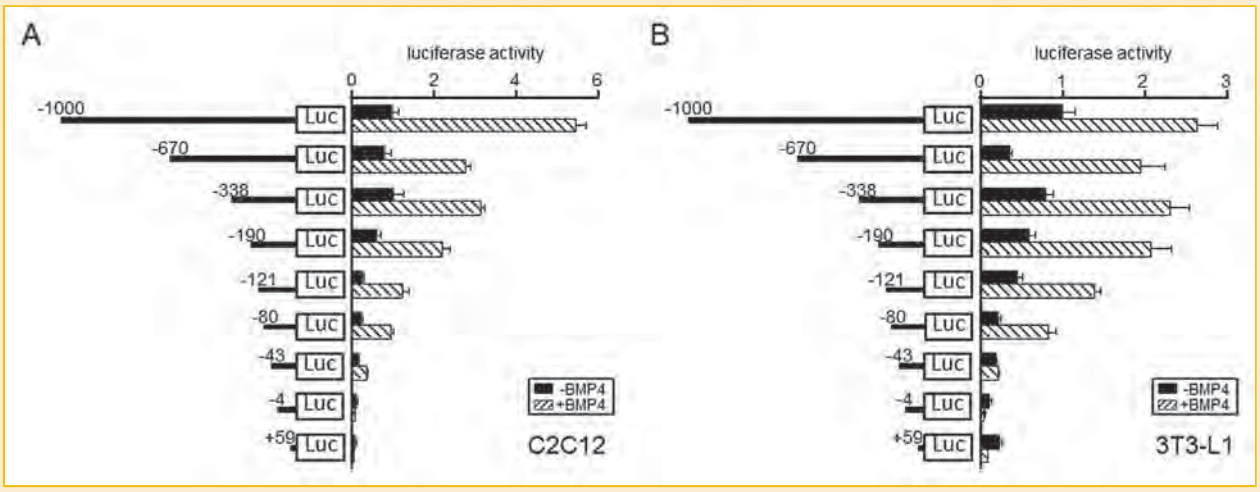

Fig. 7. Transcriptional regulation of Smad8/9 through BMP4. The BRE in Smad8/9 promoter was examined using a series of Smad8/9 reporters with deleted promoters in C2C12 cells (A) and 3T3-L1 cells (B). The cells were transiently transfected with the indicated reporter plasmid with Renilla-luc and treated with or without BMP4 (4 nM) for 16 h. Firefly luciferase activity was expressed as a ratio to Renilla luciferase activity, with the level set to 1 in cells transfected with Smad8/9(−1000)-luc and cultured in the absence of BMP4. The data are presented as the means ± SE (n = 4).

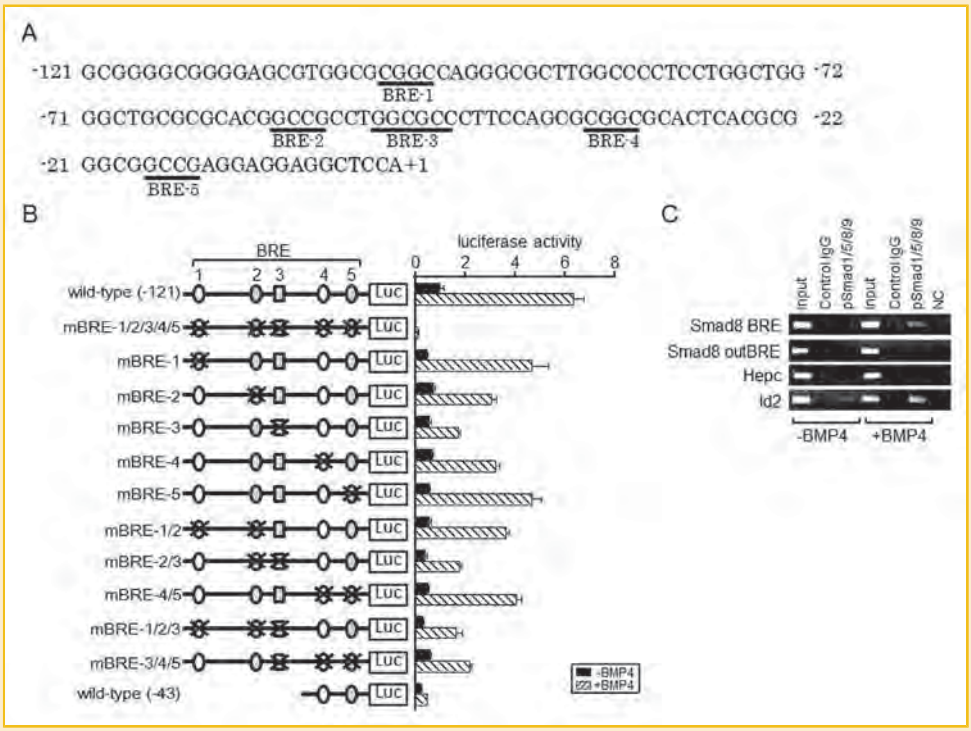

Fig. 8. Identification of BRE in Smad8/9. A: Nucleotide sequence of BRE-1 to BRE-5 of Smad8/9. B: BRE in Smad8/9 promoter was explored through reporter assays using Smad8/9 promoter with point mutations in C2C12 cells. The cells were transiently transfected with the indicated reporter plasmid with Renilla-luc and treated with or without BMP4 (4 nM) for 16 h. Firefly luciferase activity was expressed as a ratio to Renilla luciferase activity, with the level set to 1 in cells cultured in the absence of BMP4. The data are presented as the means ± SE (n = 4). C: C2C12 cells were treated with (+BMP4) or without BMP4 (-BMP4, 4 nM) for 2 h. Chromatin extracts were immunoprecipitated with antibody against phosphorylated Smad1/5/8/9 or control IgG, followed by amplification of the region spanning BREs of Smad8 gene (Smad8 BRE), outside BREs of Smad8 gene (Smad8 outBRE), unrelated to responsiveness to BMP in hepcidin gene (Hepc), and BREs of Id2 gene (Id2). PCR was also performed using distilled water as the negative control (NC). The PCR products were electrophoresed in agarose gels and stained by ethidium bromide. A representative result is shown.

mutations. Similar results were obtained with BRE-4 and BRE-5 mutations; mutations of both BRE-4 and BRE-5 did not inhibit the responsiveness to BMP4 induced through BRE-3 mutations. These results suggest that all five BREs are necessary for BMP-induced Smad8/9 transcription, although BRE-3 is the most critical region.

We further explored whether Smad1/5/8 binds to the region including BREs of Smad8 gene, that is, nt −164 to nt +21, in C2C12 cells by ChIP assay (Fig. 8C). When anti-phosphorylated Smad1/5/8 antibody but not control IgG was used for ChIP assay, the region including the BREs of Smad8 was amplified; the band intensity tended to increase in response to BMP4 treatment. Phosphorylated Smad1/5/8 also bound to the region including the BREs of Id2 in a BMP4-dependent manner. On the contrary, significant band was not detected, when the primer sets to detect the outside BREs of Smad8 gene or the unrelated region to BMP responsiveness in hepcidin gene were used. These results suggest that phosphorylated Smad1/5/8 binds to the BREs of Smad8 gene, and that the binding is dependent on BMP signaling in C2C12 cells.

DISCUSSION

BMPs elicit physiological effects through the transcriptional activation of target genes; BMPs induce phosphorylation of R-Smads and complex formation with Smad4, leading to transcriptional activation of the target genes. The signaling model of BMP indicates that the dephosphorylation of R-Smads and gene induction of I-Smads terminate the stimulated BMP signaling [Miyazono et al., 2010; Massagué, 2012; Sakaki-Yumoto et al., 2013]; the activity of R-Smads is not regulated through expression, but rather through the phosphorylation status [Miyazono et al., 2010]. The present study revealed that Smad8/9 is an exceptional R-Smad positively regulated via the BMP pathway at the mRNA level, and that gene induction occurs in multiple cell types; recently, Tsukamoto et al. [2014] reported similar results that BMP regulates expression of Smad9. The present study extends their results [Tsukamoto et al., 2014]: expression of Smad8 and Smad9 is cell-type dependent, Smad8/9 gene expression is transcriptionally regulated by BMP, and several BREs are involved in the transcriptional activation of Smad8/9.

Functional role of Smad8/9 is still controversial. As described above, Smad8/9 is categorized as R-Smad that is phosphorylated in response to treatment with BMP [Miyazono et al., 2010; Massagué, 2012; Sakaki-Yumoto et al., 2013]. Similar to Smad1 and Smad5, Smad8/9 mediates the transcription of a reporter with BREs derived from the Id1 gene [Kawai et al., 2000; Tsukamoto et al., 2014], suggesting that functions of Smad8/9 are compatible with those of Smad1 and Smad5. Indeed, Smad8/9 is required for brain development [Hester et al., 2005] and dorso-ventral patterning during embryogenesis [Wei et al., 2014]; these effects were similar to those of Smad1. In contrast, Tsukamoto et al. [2014] recently demonstrated the inhibition of the BMP pathway by Smad8/9; BMP induced phosphorylation of Smad1 and Smad8/9, and phosphorylated Smad8/9 formed complex with Smad1 to inhibit Smad1-mediated transcription. These results suggest a dominant-negative role of Smad8/9 in transcriptional activation by Smad1. In the case of similar role of Smad8/9 to Smad1 and Smad5, the present results on BMP-induced up-regulation of Smad8/9 expression is interpreted to accelerate the BMP signaling. Taken the role with well-characterized gene induction of I-Smad, that is, Smad6 and Smad7, by the BMP pathway [Miyazono et al., 2010] together, net BMP signaling may be finely tuned by simultaneous stimulation and inhibition of BMP activity. In contrast, in the case of inhibitory role of Smad8/9 in BMP pathway, the present results reflect a negative feedback of BMP signaling. The dominant-negative role of Smad8/9 suggested by Tsukamoto et al. [2014] has not been shown in biological process yet. Further studies to explore the biological role of Smad8/9 clarify the significance of Smad8/9 gene induction.

There is an alternative splicing variant of Smad8/9 gene, designated Smad8B in humans, which lacks C-terminal serines phosphorylated through receptor complexes [Nishita et al., 1999]. We examined Smad8B expression in HepG2 cells, a human-derived cell line, using previously reported PCR primers [Nishita et al., 1999], but could not detect significant Smad8B expression, irrespective of the BMP treatment (data not shown). We also explored the corresponding sequence of murine Smad8/9, but did not detect Smad8B. Thus, we concluded that the induction of Smad8/9 gene expression through BMP4 in multiple cell types does not reflect the expression of Smad8/9 variant lacking region with C-terminal serines.

A search of the nucleotide database indicated mouse Smad8/9 variants with inserted sequences between exons 1 and 2 (variant 1: GenBank accession number XM_006501728) and the deletion of a part of exon 2 (variant 2: XM_00651729). Furthermore, other human Smad8/9 variants lacking lack exons 2 and 3, or exon 3 alone have been identified [Cheng et al., 2004]. The expression of these Smad8/9 variants and effects of BMP4 treatment were further examined using RT-PCR analyses with primers to discriminate these variants in C2C12 cells. We detected Smad8/9 variants 1 and 2, but not Smad8/9 variants lacking exons 2 and 3, or exon 3 alone as previously reported [Cheng et al., 2004] (data not shown). BMP4 increased the gene transcript levels of all 3 Smad8/9, that is, wild-type Smad8/9, Smad8/9 variants 1 and 2 (data not shown). The amino acid sequence of Smad8/9 variant 1 is identical to that of wild-type Smad8/9. In addition, differences in the amino acid sequences between wild-type Smad8/9 and Smad8/9 variant 2 only involves 13 amino acids; the first nine amino acids of wild-type Smad8/9 are deleted in Smad8/9 variant 2, and four amino acids within the next five amino acids are different between wild-type Smad8/9 and Smad8/9 variant 2. Thus, the present results suggest that the stimulated BMP pathway substantially increases activity of wild-type Smad8/9.

The R-Smads, except for Smad2, and Smad4 can bind to preferred DNA sequences. However, the affinity of Smads to the DNA sequence is not sufficient to support the association of Smads with regulatory promoter sequences [Miyazono et al., 2010; Massagué, 2012; Sakaki-Yumoto et al., 2013]. Therefore, Smad complexes interact and cooperate with the other transcription factors, leading to transcriptional regulation of target genes with the help of transcriptional coactivators and corepressors [Miyazono et al., 2010; Massagué, 2012; Sakaki-Yumoto et al., 2013]. Future studies are needed to characterize Smad complexes bound to the BREs of Smad8/9.

ACKNOWLEDGMENT

This work was supported by a research project grant awarded by the Azabu University (2013K08).

REFERENCES

Cheng KH, Ponte JF, Thiagalingam S. 2004. Elucidation of epigenetic inactivation of SMAD8 in cancer using targeted expressed gene display. Cancer Res 64:1639–1646.

Derynck R, Piek E, Schneider RA, Choy L, Alliston T. 2008. TGF-b family signaling in mesenchymal differentiation. In: Derynck R, Miyazono K, editors. The TGF-b family. New York: Cold Spring Harbor Laboratory Press. pp 613–665.

Duan X, Liang YY, Feng XH, Lin X. 2006. Protein serine/threonine phosphatase PPM1A dephosphorylates Smad1 in the bone morphogenetic protein signaling pathway. J Biol Chem 281:36526–36532.

Ebisawa T, Fukuchi M, Murakami G, Chiba T, Tanaka K, Imamura T, Miyazono K. 2001. Smurf1 interacts with transforming growth factor-b type I receptor through Smad7 and induces receptor degradation. J Biol Chem 276:12477–12480.

Furutani Y, Umemoto T, Murakami M, Matsui T, Funaba M. 2011. Role of endogenous TGF-β family in myogenic differentiation of C2C12 cells. J Cell Biochem 112:614–624.

Hayashi H, Abdollah S, Qiu Y, Cai J, Xu YY, Grinnell BW, Richardson MA, Topper JN, Gimbrone MA, Jr., Wrana JL, Falb D. 1997. The MAD-related protein Smad7 associates with the TGFb receptor and functions as an antagonist of TGFb signaling. Cell 89:1165–1173.

Herrera B, van Dinther M, Ten Dijke P. 2009. Autocrine bone morphogenetic protein-9 signals through activin receptor-like kinase-2/Smad1/Smad4 to promote ovarian cancer cell proliferation. Cancer Res 69:9254–2962.

Hester M, Thompson JC, Mills J, Liu Y, El-Hodiri HM, Weinstein M. 2005. Smad1 and Smad8 function similarly in mammalian central nervous system development. Mol Cell Biol 25:4683–4692.

Ishisaki A, Yamato K, Nakao A, Nonaka K, Ohguchi M, Ten Dijke P. 1998. Smad7 is an activin-inducible inhibitor of activin-induced growth arrest and apoptosis in mouse B cells. J Biol Chem 273:24293–24296.

Kawai S, Faucheu C, Gallea S, Spinella-Jaegle S, Atfi A, Baron R, Roman SR. 2000. Mouse smad8 phosphorylation downstream of BMP receptors ALK-2, ALK-3, and ALK-6 induces its association with Smad4 and transcriptional activity. Biochem Biophys Res Commun 271:682–687.

Knockaert M, Sapkota G, Alarcón C, Massagué J, Brivanlou AH. 2006. Unique players in the BMP pathway: Small C-terminal domain phosphatases dephosphorylate Smad1 to attenuate BMP signaling. Proc Natl Acad Sci USA 103:11940–11945.

Kusanagi K, Inoue H, Ishidou Y, Mishima HK, Kawabata M, Miyazono K. 2000. Characterization of a bone morphogenetic protein-responsive Smad-binding element. Mol Biol Cell 11:555–565.

Lin X, Duan X, Liang YY, Su Y, Wrighton KH, Long J, Hu M, Davis CM, Wang J, Brunicardi FC, Shi Y, Chen YG, Meng A, Feng XH. 2006. PPM1A functions as a Smad phosphatase to terminate TGFb signaling. Cell 125:915–928.

López-Rovira T, Chalaux E, Massagué J, Rosa JL, Ventura F. 2002. Direct binding of Smad1 and Smad4 to two distinct motifs mediates bone morphogenetic protein- specifictranscriptional activation of Id1 gene. J Biol Chem 277:3176–3185.

Massagué J. 2012. TGFβ signalling in context. Nat Rev Mol Cell Biol 13:616–630.

Messenger AG. 1984. The culture of dermal papilla cells from human hair follicles. Br J Dermatol 110:685–689.

Miyazono K, Kamiya Y, Morikawa M. 2010. Bone morphogenetic protein receptors and signal transduction. J Biochem 147:35–51.

Murakami M, Kawachi H, Ogawa K, Nishino Y, Funaba M. 2009. Receptor expression modulates the specificity of transforming growth factor-β signaling pathways. Genes Cells 14:469–482.

Murakami M, Ohi M, Ishikawa S, Shirai M, Horiguchi H, Nishino Y, Funaba M. 2015. Adaptive expression of uncoupling protein 1 in the carp liver and kidney in response to changes in ambient temperature. Comp Biochem Physiol A Mol Integr Physiol 185:142–149.

Murakami G, Watabe T, Takaoka K, Miyazono K, Imamura T. 2003. Cooperative inhibition of bone morphogenetic protein signaling by Smurf1 and inhibitory Smads. Mol Biol Cell 14:2809–2817.

Nakahiro T, Kurooka H, Mori K, Sano K, Yokota Y. 2010. Identification of BMP-responsive elements in the mouse Id2 gene. Biochem Biophys Res Commun 399:416–421.

Nakao A, Afrakhte M, Morén A, Nakayama T, Christian JL, Heuchel R, Itoh S, Kawabata M, Heldin NE, Heldin CH, Ten Dijke P. 1997. Identification of Smad7, a TGFb-inducible antagonist of TGF-b signalling. Nature 389:631–635.

Nishita M, Ueno N, Shibuya H. 1999. Smad8B, a Smad8 splice variant lacking the SSXS site that inhibits Smad8-mediated signaling. Genes Cells 4:583–591.

Poncelet AC, de Caestecker MP, Schnaper HW. 1999. The transforming growth factor-b /SMAD signaling pathway is present and functional in human mesangial cells. Kidney Int 56:1354–1365.

Sakaki-Yumoto M, Katsuno Y, Derynck R. 2013. TGF-β family signaling in stem cells. Biochim Biophys Acta 1830:2280–2296.

Takase M, Imamura T, Sampath TK, Takeda K, Ichijo H, Miyazono K, Kawabata M. 1998. Induction of Smad6 mRNA by bone morphogenetic proteins. Biochem Biophys Res Commun 244:26–29.

Truksa J, Lee P, Beutler E. 2009. Two BMP responsive elements, STAT, and bZIP/HNF4/COUP motifs of the hepcidin promoter are critical for BMP, SMAD1, and HJV responsiveness. Blood 113:688–695.

Tsukamoto S, Mizuta T, Fujimoto M, Ohte S, Osawa K, Miyamoto A, Yoneyama K, Murata E, Machiya A, Jimi E, Kokabu S, Katagiri T. 2014. Smad9 is a new type of transcriptional regulator in bone morphogenetic protein signaling. Sci Rep 4:7596.

Wei CY, Wang HP, Zhu ZY, Sun YH. 2014. Transcriptional factors smad1 and smad9 act redundantly to mediate zebrafish ventral specification downstream of smad5. J Biol Chem 289:6604–6618.

Winbanks CE, Wang B, Beyer C, Koh P, White L, Kantharidis P, Gregorevic P. 2011. TGF-b regulates miR-206 and miR-29 to control myogenic differentiation through regulation of HDAC4. J Biol Chem 286:13805–13814.

Yanagisawa K, Osada H, Masuda A, Kondo M, Saito T, Yatabe Y, Takagi K, Takahashi T, Takahashi T. 1998. Induction of apoptosis by Smad3 and down-regulation of Smad3 expression in response to TGF-b in human normal lung epithelial cells. Oncogene 17:1743–1747.

Yu PB, Deng DY, Lai CS, Hong CC, Cuny GD, Bouxsein ML, Hong DW, McManus PM, Katagiri T, Sachidanandan C, Kamiya N, Fukuda T, Mishina Y, Peterson RT, Bloch KD. 2008. BMP type I receptor inhibition reduces heterotopic ossification. Nat Med 14:1363–1369.

原　著　麻布大学雑誌　第 27 巻　27－31

Distribution of Major Staphylococcal Cassette Chromosome *mec* Types and Exfoliative Toxin Genes in *Staphylococcus pseudintermedius* Strains from Dogs with Superficial Pyoderma in Japan

Tomoko KASAI[1,3], Yukio KATO[2], Sanae SAEGUSA[3], Masaru MURAKAMI[1]

[1]Laboratory of Molecular Biology, [2]Laboratory of Public Health 2, School of Veterinary Medicine, Azabu University, 1-17-71 Fuchinobe, Chuou-ku, Sagamihara, Kanagawa 252-5201 Japan
[3]Kitagawa Veterinary Hospital, 1-39-1 Minamitokiwadai, Itabashi-ku, Tokyo, 174-0072 Japan

Abstract: *Staphylococcus pseudintermedius* is a major pathogen of canine pyoderma, known to produce exfoliative toxins that could be involved in formation of cutaneous lesions. To understand the genotypic distribution of *S. pseudintermedius*, we surveyed 74 dogs with pyoderma in three veterinary hospitals in Japan. Seventy-four *S. pseudintermedius* strains were isolated, 52 of which (70.3%) were *mecA*-positive methicillin-resistant *S. pseudintermedius* (MRSP). Staphylococcal cassette chromosome *mec* (SCC*mec*) typing of the identified MRSP strains revealed that the most prevalent genotype was type III-like (63.4%) followed by type V (34.6%). These data suggest high prevalence of MRSP strains consisting of two major SCC*mec* types among canine pyoderma in Japan. We found low prevalence of exfoliative toxin genes (*exp*) in the MRSP strains: *expA* and *expB* were present in 1.9% and 0%, respectively. These findings suggest no association in carriage between *mecA* and *exp* genes in *S. pseudintermedius* from canine pyoderma.

Key words: *Staphylococcus pseudintermedius*; superficial pyoderma; methicillin resistance; SCC*mec*; exfoliative toxin

Introduction

Staphylococcus pseudintermedius is a normal inhabitant of the skin and mucosae of dogs[1, 2]. This species is also known to be the major pathogen of superficial pyoderma, one of the most common infectious diseases of canine cutaneous disorder[3]. Previous studies have revealed that *S. pseudintermedius* possess virulence factors such as exfoliative toxins (ETs) ExpA and B, which cause skin exfoliation[4-6]. However, few studies have described the distribution of ETs in *S. pseudintermedius* from canine superficial pyoderma[4, 5], and the presence of ETs in methicillin-resistant *S. pseudintermedius* (MRSP) has not been reported.

Since the first report of a *mecA*-positive MRSP strain in 1999[7], MRSP infections have been increasing in small animal medicine[8-12]. According to previous studies, MRSP strains are mainly classified into two genotypes based on the type of staphylococcal cassette chromosome *mec* (SCC*mec*): SCC*mec* type III-like clones (informally designated type II-III by Descloux *et al.*[13]), which are found in Europe and many other areas across the world[14-18], and type V clones, which are prevalent in North America, Korea and Thailand[14, 15, 19-22]. Genotyping is important and helpful in understanding the geographic distribution and estimating the epidemic nature and spread of MRSP clones. However, only a few studies have performed genotype-based analysis of canine

superficial pyoderma caused by MRSP in Japan[18]. We therefore conducted molecular analysis of MRSP strains isolated from canine superficial pyoderma and determined SCC*mec* types in Japan. We also analyzed two exfoliative toxin genes, *expA* and *expB*, to investigate the association between methicillin resistance and the carriage of toxin genes. Here, we describe the prevalence of methicillin resistance and exfoliative toxin genes in the genome of *S. pseudintermedius* among 74 dogs with superficial pyoderma from three veterinary hospitals in Japan.

Materials and Methods

Sample collecting

We examined 74 dogs with superficial pyoderma in three private veterinary hospitals in three prefectures of Japan between April 2010 and December 2012. The 74 dogs (37 males, 37 females; mean age, 7.9 years [range, 10 months to 15 years]) were 10 Shih Tzu dogs, 9 French Bulldogs, 9 Poodles, 7 Miniature Dachshunds, 5 Shiba Inu dogs, 5 Pugs, 4 Chihuahuas, 4 Cocker Spaniels, 2 West Highland white terriers, 2 Retrievers, 2 Malteses, 2 Yorkshire terriers, 2 Cavalier King Charles Spaniels, 2 Jack Russells, 1 Basset, 1 Chin, 1 German shepherd, 1 Pekingese, 1 Schnauzer, 1 Weimaraner and 3 Mixed breeds. A total of 74 specimens were collected by swabbing skin lesions. Bacterial strains from the specimens were cultivated on tryptic soy agar containing 5% sheep blood (BD Japan, Co., Ltd., Tokyo, Japan) at 37°C for 18 h. All strains were identified as staphylococci based on colony morphology, Gram stain appearance and the catalase test.

Species identification, determination of methicillin resistance and SCC*mec* typing

Crude DNA extraction from a single colony and staphylococcal species identification using multiplex PCR (M-PCR) were performed as previously described by Sasaki *et al.*[23].

To identify methicillin resistance, a PCR method[24] for detection of the *mecA* gene was used. Subsequently, SCC*mec* typing of the MRSP strains identified was performed. To discriminate SCC*mec* types I to V, including type III-like, classified based on the *ccr* and *mec* gene complexes, two M-PCRs[25] and one duplex PCR[15] were carried out.

Detection of exfoliative toxin genes

Fragments from two exfoliative toxin genes, *expA* and *expB*, were amplified by conventional PCR. The oligonucleotide primers were as previously reported (Yamamoto *et al.*, 2012, 15th Annual meeting of The Japanese Society of Veterinary Dermatology): 5´-ATTTGTTCACATGGATTTATT-3´ (forward) and 5´-AGGGGCATTAACAATAAGATC-3´ (reverse) for *expA*, and 5´-TTTATGACAGCTATGCTCATT-3´ (forward) and 5´-TCCTAAATTAGCGTCAAAAAT-3´ (reverse) for *expB*. The thermal cycling parameters consisted of an initial denaturation at 95°C for 3 min followed by 30 cycles of denaturation at 95°C for 30 s, annealing at 55°C for 30 s, and extension at 72°C for 30 s, with an additional final extension step of 72°C for 2 min. PCR products were separated on 1.0% agarose gel with TAE buffer and visualized with ethidium bromide.

Results and Discussion

A total of 74 staphylococci from 74 dogs with superficial pyoderma were obtained. All strains were identified as *S. pseudintermedius* as previously described[23]. Molecular characteristics of the isolated *S. pseudintermedius* were investigated using several conventional PCR methods as previously described[15, 25]. As shown in Table 1, MRSP with *mecA* accounted for 70.3% (52/74) of the strains. This frequency was very high compared to previous surveillance data from other countries: 5.1% in the UK[26], 29.3% in Korea[20] and 47.8% in North China[17], and was similar to the previously reported 66.5% in Japan[27]. This indicates a high prevalence of MRSP in canine superficial pyoderma in Japan. Sixty-five (87.8%) out of 74 dogs had been treated with antimicrobials previously: 50 (96.2%) of 52 dogs infected with MRSP and 15 (68.2%) of 22 dogs infected with MSSP. Dogs infected with MRSP tended to have greater exposure to antibiotics than MSSP-infected dogs.

Table 1 Distribution of methicillin-resistant *S. pseudintermedius* strains from canine pyoderma

	No. of strains (%)
S. pseudintermedius	74 (100)
Methicillin-susceptible	22 (29.7)
Methicillin-resistant	52 (70.3)
SCC*mec*-type III-like	33
SCC*mec*-type V	18
Nontypeable	1

Table 2 Distribution of two exfoliative toxin genes among *S. pseudintermedius* strains

S. pseudintermedius	n	No. of positive strains (%)	
		expA	*expB*
Methicillin-susceptible	22	5 (22.7)	1 (4.5)
Methicillin-resistant	52	1 (1.9)	0 (0)

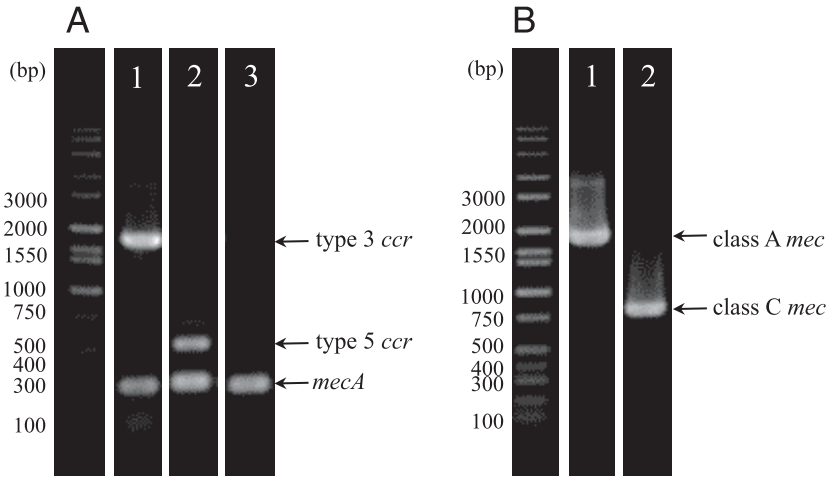

Fig. 1 Multiplex PCR analysis of *ccr* gene complex (A) and *mec* gene complex (B).
Lane 1, SCC*mec* type III-like MRSP; lane 2, SCC*mec* type V MRSP; lane 3, SCC*mec* nontypeable MRSP. (A) Upper bands in lanes 1 and 2 represent types 3 and 5 *ccr* genes, respectively. Lane 3 is a nontypeable strain that possesses *mecA* gene only. (B) Lanes 1 and 2 show single bands specific to class A and C *mec* gene complexes.

Previous use of antimicrobials may be associated with MRSP infection in dogs.

Furthermore, multiplex and duplex PCR assays for SCC*mec* typing revealed that 33 (63.4%) of 52 MRSP strains were type III-like, 18 (34.6%) belonged to type V, and only one was determined as nontypeable. The representative electrophoretic patterns of SCC*mec* type III-like (with fragments of both type 3 *ccr* and class A *mec*) and V (with fragments of both type 5 *ccr* and class C *mec*) are shown in Fig. 1.

To examine the presence of ET genes, amplification of the *expA* and *B* genes was conducted as shown in Fig. 2 (representative data). Table 2 shows the frequency of *expA* and *B* in the isolated *S. pseudintermedius* strains. The *expA*

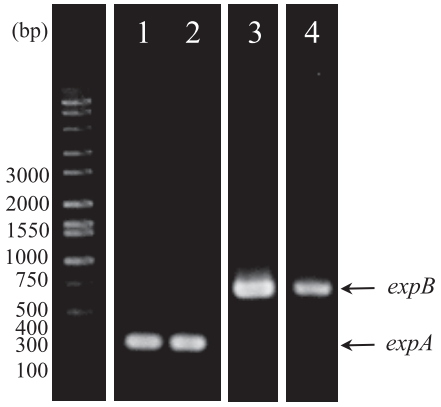

Fig. 2 PCR analysis of exfoliative genes.
Lane 1, a MSSP isolate carrying the *expA* gene; lane 2, positive control strain for *expA*; lane 3, a MSSP carrying the *expB* gene; lane 4, positive control strain for *expB*.

gene was detected at a rate of 22.7% (5/22) in methicillin-susceptible *S. pseudintermedius* (MSSP) strains in contrast to 1.9% (1/52) in MRSP strains; the latter MRSP strain was SCC*mec* type V. One MSSP isolate possessed the *expB* gene; however, the gene was not detected in any MRSP strain. There was no significant possession of ETs in *S. pseudintermedius* carrying the *mecA* gene, although they may be important virulence factors in canine pyoderma.

This study demonstrated that as many as 70.3% of 74 dogs diagnosed with superficial pyoderma had MRSP, implying the prevalence of MRSP in veterinary clinical practice in Japan. It is therefore important to rapidly, easily and feasibly determine *S. pseudintermedius* strains carrying the *mecA* gene and identify their genotypes not only to understand the epidemiological pattern but also for implementation of infection-control measures in veterinary clinical practice. To detect MRSP strains and their SCC*mec* types, we used several traditional PCR techniques that were complicated, cumbersome and time-consuming. We are currently designing improved multiplex PCR strategies.

Acknowledgements

We are grateful to Dr. Koji Nishifuji (Tokyo University of Agriculture and Technology, Japan) for providing control strains for detection of exfoliative toxin genes. We also thank Ms. Akemi Suto and Dr. Reiko Usui for their help in collecting specimens.

References

1) Allaker, R. P., Lloyd, D. H., and Simpson, A. I., Occurrence of *Staphylococcus intermedius* on the hair and skin of normal dogs. *Res. Vet. Sci*. **52**, 174-176 (1992).
2) Allaker, R. P., Lloyd, D.H., and Bailey, R.M., Population sizes and frequency of staphylococci at mucocutaneous sites on healthy dogs. *Vet. Rec*. **130**, 303-304 (1992).
3) Bannoehr, J. and Guardabassi, L., *Staphylococcus pseudintermedius* in the dog: taxonomy, diagnostics, ecology, epidemiology and pathogenicity. *Vet. Dermatol*. **23**, 253-266, e251-252 (2012).
4) Futagawa-Saito, K., Makino, S., Sunaga, F., Kato, Y., Sakurai-Komada, N., Ba-Thein, W., and Fukuyasu, T., Identification of first exfoliative toxin in *Staphylococcus pseudintermedius*. *FEMS Microbiol. Lett*. **301**, 176-180 (2009).
5) Iyori, K., Hisatsune, J., Kawakami, T., Shibata, S., Murayama, N., Ide, K., Nagata, M., Fukata, T., Iwasaki, T., Oshima, K., Hattori, M., Sugai, M., and Nishifuji, K., Identification of a novel *Staphylococcus pseudintermedius* exfoliative toxin gene and its prevalence in isolates from canines with pyoderma and healthy dogs. *FEMS Microbiol. Lett*. **312**, 169-175(2010).
6) Iyori, K., Futagawa-Saito, K., Hisatsune, J., Yamamoto, M., Sekiguchi, M., Ide, K., Son, W. G., Olivry, T., Sugai, M., Fukuyasu, T., Iwasaki, T., and Nishifuji, K., *Staphylococcus pseudintermedius* exfoliative toxin EXI selectively digests canine desmoglein 1 and causes subcorneal clefts in canine epidermis. *Vet. Dermatol*. **22**, 319-326 (2011).
7) Gortel, K., Campbell, K. L., Kakoma, I., Whittem, T., Schaeffer, D. J., and Weisiger, R. M., Methicillin resistance among staphylococci isolated from dogs. *Am. J. Vet. Res*. **60**, 1526-1530 (1999).
8) Bemis, D. A., Jones, R. D., Frank, L. A., and Kania, S. A., Evaluation of susceptibility test breakpoints used to predict *mecA*-mediated resistance in *Staphylococcus pseudintermedius* isolated from dogs. *J. Vet. Diagn. Invest*. **21**, 53-58 (2009).
9) Jones, R. D., Kania, S. A., Rohrbach, B. W., Frank, L. A., and Bemis, D. A., Prevalence of oxacillin- and multidrug-resistant staphylococci in clinical samples from dogs: 1,772 samples (2001-2005). *J. Am. Vet. Med. Assoc*. **230**, 221-227 (2007).
10) Kania, S. A., Williamson, N. L., Frank, L. A., Wilkes, R. P., Jones, R. D., and Bemis, D. A., Methicillin resistance of staphylococci isolated from the skin of dogs with pyoderma. *Am. J. Vet. Res*. **65**, 1265-1268 (2004).
11) Loeffler, A., Linek, M., Moodley, A., Guardabassi, L., Sung, J. M., Winkler, M., Weiss, R., and Lloyd, D. H., First report of multiresistant, *mecA*-positive *Staphylococcus intermedius* in Europe: 12 cases from a veterinary dermatology referral clinic in Germany. *Vet. Dermatol*. **18**, 412-421 (2007).
12) Zubeir, I. E., Kanbar, T., Alber, J., Lammler, C., Akineden, O., Weiss, R., and Zschock, M., Phenotypic and genotypic characteristics of methicillin/oxacillin-resistant *Staphylococcus intermedius* isolated from clinical specimens during routine veterinary microbiological examinations. *Vet. Microbiol*. **121**, 170-176 (2007).

13) Descloux, S., Rossano, A., and Perreten, V., Characterization of new staphylococcal cassette chromosome *mec* (SCC*mec*) and topoisomerase genes in fluoroquinolone- and methicillin-resistant *Staphylococcus pseudintermedius*. *J. Clin. Microbiol*. **46**, 1818-1823 (2008).
14) Moodley, A., Stegger, M., Ben Zakour, N. L., Fitzgerald, J. R., and Guardabassi, L., Tandem repeat sequence analysis of staphylococcal protein A (*spa*) gene in methicillin-resistant *Staphylococcus pseudintermedius*. *Vet. Microbiol*. **135**, 320-326 (2009).
15) Perreten, V., Kadlec, K., Schwarz, S., Gronlund Andersson, U., Finn, M., Greko, C., Moodley, A., Kania, S. A., Frank, L. A., Bemis, D. A., Franco, A., Iurescia, M., Battisti, A., Duim, B., Wagenaar, J. A., van Duijkeren, E., Weese, J. S., Fitzgerald, J. R., Rossano, A., and Guardabassi, L., Clonal spread of methicillin-resistant *Staphylococcus pseudintermedius* in Europe and North America: an international multicentre study. *J. Antimicrob. Chemother*. **65**, 1145-1154 (2010).
16) Ruscher, C., Lubke-Becker, A., Semmler, T., Wleklinski, C. G., Paasch, A., Soba, A., Stamm, I., Kopp, P., Wieler, L. H., and Walther, B., Widespread rapid emergence of a distinct methicillin- and multidrug-resistant *Staphylococcus pseudintermedius* (MRSP) genetic lineage in Europe. *Vet. Microbiol*. **144**, 340-346 (2010).
17) Wang, Y., Yang, J., Logue, C. M., Liu, K., Cao, X., Zhang, W., Shen, J., and Wu, C., Methicillin-resistant *Staphylococcus pseudintermedius* isolated from canine pyoderma in North China. *J. Appl. Microbiol*. **112**, 623-630 (2012).
18) Onuma, K., Tanabe, T., and Sato, H., Antimicrobial resistance of *Staphylococcus pseudintermedius* isolates from healthy dogs and dogs affected with pyoderma in Japan. *Vet. Dermatol*. **23**, 17-22, e15 (2012).
19) Black, C. C., Solyman, S. M., Eberlein, L. C., Bemis, D. A., Woron, A. M., and Kania, S. A., Identification of a predominant multilocus sequence type, pulsed-field gel electrophoresis cluster, and novel staphylococcal chromosomal cassette in clinical isolates of *mecA*-containing, methicillin-resistant *Staphylococcus pseudintermedius*. *Vet. Microbiol*. **139**, 333-338 (2009).
20) Youn, J-H., Koo, H. C., Ahn, K. J., Lim, S-K., and Park, Y. H., Determination of staphylococcal exotoxins, SCC*mec* types, and genetic relatedness of *Staphylococcus intermedius* group isolates from veterinary staff, companion animals, and hospital environments in Korea. *J. Vet. Sci*. **12**, 221 (2011).
21) Feng, Y., Tian, W., Lin, D., Luo, Q., Zhou, Y., Yang, T., Deng, Y., Liu, Y. H., and Liu, J. H., Prevalence and characterization of methicillin-resistant *Staphylococcus pseudintermedius* in pets from South China. *Vet. Microbiol*. **160**, 517-524 (2012).
22) Chanchaithong, P., Perreten, V., Schwendener, S., Tribuddharat, C., Chongthaleong, A., Niyomtham, W., and Prapasarakul, N., Strain typing and antimicrobial susceptibility of methicillin-resistant coagulase-positive staphylococcal species in dogs and people associated with dogs in Thailand. *J. Appl. Microbiol*. **117**, 572-586 (2014).
23) Sasaki, T., Tsubakishita, S., Tanaka, Y., Sakusabe, A., Ohtsuka, M., Hirotaki, S., Kawakami, T., Fukata, T., and Hiramatsu, K., Multiplex-PCR method for species identification of coagulase-positive staphylococci. *J. Clin. Microbiol*. **48**, 765-769 (2010).
24) Zhang, K., McClure, J. A., Elsayed, S., Louie, T., and Conly, J. M., Novel multiplex PCR assay for characterization and concomitant subtyping of staphylococcal cassette chromosome *mec* types I to V in methicillin-resistant *Staphylococcus aureus*. *J. Clin. Microbiol*. **43**, 5026-5033 (2005).
25) Kondo, Y., Ito, T., Ma, X. X., Watanabe, S., Kreiswirth, B. N., Etienne, J., and Hiramatsu, K., Combination of multiplex PCRs for staphylococcal cassette chromosome *mec* type assignment: rapid identification system for *mec*, *ccr*, and major differences in junkyard regions. *Antimicrob. Agents Chemother*. **51**, 264-274 (2007).
26) Maluping, R. P., Paul, N. C., and Moodley, A., Antimicrobial susceptibility of methicillin-resistant *Staphylococcus pseudintermedius* isolated from veterinary clinical cases in the UK. *Br. J. Biomed. Sci*. **71**, 55-57 (2014).
27) Kawakami, T., Shibata, S., Murayama, N., Nagata, M., Nishifuji, K., Iwasaki, T., and Fukata, T., Antimicrobial susceptibility and methicillin resistance in *Staphylococcus pseudintermedius* and *Staphylococcus schleiferi* subsp. *coagulans* isolated from dogs with pyoderma in Japan. *J. Vet. Med. Sci*. **72**, 1615-1619 (2010).

RESEARCH ARTICLE

Hybrid Origin of Gynogenetic Clones and the Introgression of Their Mitochondrial Genome Into Sexual Diploids Through Meiotic Hybridogenesis in the Loach, *Misgurnus anguillicuadatus*

JOURNAL OF EXPERIMENTAL ZOOLOGY
PART A
ECOLOGICAL GENETICS AND PHYSIOLOGY
A Journal of Integrative Biology

AYA YAMADA[1], YUKIHIRO KODO[2], MASARU MURAKAMI[2], MASAMICHI KURODA[1], TAKAO AOKI[1], TAKAFUMI FUJIMOTO[1], AND KATSUTOSHI ARAI[1]*

[1]Faculty and Graduate School of Fisheries Sciences, Hokkaido University, Hakodate, Hokkaido, Japan
[2]Faculty of Veterinary Medicine, Azabu University, Sagamihara, Kanagawa, Japan

ABSTRACT

In a few Japanese populations of the loach *Misgurnus anguillicaudatus* (Teleostei: Cobitidae), clonal diploid lineages produce unreduced diploid eggs that normally undergo gynogenetic reproduction; however the origin of these clones remains elusive. Here, we show the presence of two diverse clades, A and B, within this loach species from sequence analyses of two nuclear genes *RAG1* (recombination activating gene 1) and *IRBP2* (interphotoreceptor retinoid-binding protein, 2) and then demonstrate heterozygous genotypes fixed at the two loci as the evidence of the hybrid nature of clonal lineages. All the clonal individuals were identified by clone-specific mitochondrial DNA haplotypes, microsatellite genotypes, and random amplified polymorphic DNA fingerprints; they commonly showed two alleles, one from clade A and another from clade B, whereas other wild-type diploids possessed alleles from either clade A or B. However, we also found wild-type diploids with clone-specific mitochondrial DNA and nuclear genes from clade B. One possible explanation is an introgression of a clone-specific mitochondrial genome from clonal to these wild-type loaches. These individuals likely arose by a cross between haploid sperm from bisexual B clade males and haploid eggs with clone-specific mtDNA and clade B nuclear genome, produced by meiotic hybridogenesis (elimination of unmatched A genome followed by meiosis after preferential pairing between two matched B genomes) in clone-origin triploid individual (ABB). *J. Exp. Zool. 323A:593–606, 2015.* © 2015 Wiley Periodicals, Inc.

How to cite this article: Yamada A, Kodo Y, Murakami M, Kuroda M, Aoki T, Fujimoto T, Arai K. 2015. Hybrid origin of gynogenetic clones and the introgression of their mitochondrial genome into sexual diploids through meiotic hybridogenesis in the loach, *Misgurnus anguillicuadatus*. J. Exp. Zool. 323A:593–606.

J. Exp. Zool. 323A:593–606, 2015

The loach *Misgurnus anguillicaudatus* (Teleostei: Cobitidae) is a gonochoristic diploid with $2n = 50$ chromosomes and it reproduces sexually, but clonal diploid lineages have been found in the northern area of Hokkaido Prefecture and the Notojima Island of Ishikawa Prefecture, Japan (Morishima et al., 2002, 2008a). These clonal diploid loaches are essentially all-female and generate unreduced diploid eggs by premeiotic endomitosis, that is, chromosome doubling without cytokinesis (Itono et al., 2006). Most clonal diploid eggs initiate gynogenetic development after fertilization by sperm of sympatric sexually reproducing wild-type males, whereas some incorporate the sperm nucleus into the egg to develop as triploid animal (Itono et al., 2007). Genetics and atypical reproduction of clonal diploid and other polyploid *Misgurnus* loaches have been reviewed by Arai and Fujimoto (2013).

Interspecific hybridization is considered to be involved in the origin of unisexual vertebrates, which atypically reproduce by parthenogenesis, gynogenesis (sperm-dependent parthenogenesis), or hybridogenesis, and this is often accompanied by polyploidy (reviewed in Dawley, '89; Vrijenhoek et al., '89; Vrijenhoek, '94), although nonhybrid origins were recently reported in parthenogenetically reproducing lizard *Lepidophyma* genus (Sinclair et al., 2010). Hybridization often causes a disruption of regular meiosis because of unsuccessful pairing between non-homologous chromosomes derived from different species, and it often results in sterility, but it seldom induces atypical gametogenesis and unusual modes of reproduction in fish species (Dawley et al., '85; Fujimoto et al., 2008). Examples of unisexual fish with an apparent hybrid origin are included in the genera *Poecilia*, *Poeciliopsis*, *Menidia*, *Phoxinus*, *Squalius*, *Carassius*, and *Cobitis* (reviewed in Dawley, '89; Vrijenhoek et al., '89; Gui and Zhou, 2010; Collares-Pereira et al., 2013). Recent large-scale multi-locus analyses revealed the hybrid origin of asexuality, establishment of clones in different ploidy levels, and effect of asexual complexes to the initiation of clonality and polyploidy in *Cobitis* loach, different members of the family Cobitidae (Janko et al., 2012). In the *Misgurnus* loach, however, a relationship between clonal reproduction in certain diploids and hybridization is ambiguous, because *M. anguillicaudatus* has been identified as a single species entity (Saitoh, '89).

Grant sponsor: JSPS-KAKENHI; grant number: 21380114.
*Correspondence to: Katsutoshi Arai, Faculty and Graduate School of Fisheries Sciences, Hokkaido University, 3-1-1, Minato, Hakodate, Hokkaido 041-8611, Japan.
E-mail: araikt@fish.hokudai.ac.jp
Received 2 February 2015; Revised 9 May 2015; Accepted 29 May 2015
DOI: 10.1002/jez.1950
Published online 14 July 2015 in Wiley Online Library (wileyonlinelibrary.com).

There are two major groups of Japanese *M. anguillicaudatus*, namely, A and B, which are further clustered into two sub-groups, B-1 and B-2, based on highly differentiated sequences (average sequence divergence, 13%) of the mitochondrial DNA control region (mtDNA-CR) (Morishima et al., 2008a). Similar intergeneric equivalent diversity has also been observed in *M. anguillicaudatus* (Koizumi et al., 2009), in which different mtDNA regions, particularly cytochrome b sequences, were analyzed, and a large genetic divergence was observed (average sequence divergence, 15–18%). However, recent molecular phylogenetic studies strongly suggest that the entire mitochondrial genome of group B *Misgurnus* must have originated from the ancestral loach genus *Cobitis* through introgression; thus, the presence of two different lineages diverging early in the speciation process within *M. anguillicaudatus* is highly spurious (Šlechtová et al., 2008; Kitagawa et al., 2011). The hypotheses about the mitochondrial introgression are supported by the recent analyses of the complete mitochondrial genomes of different polyploid *M. anguillicaudatus* (Zhou et al., 2014). Although these results raise the question of genealogy based on previous mtDNA analyses (Morishima et al., 2008a; Koizumi et al., 2009), the presence of two different groups in the Japanese wild populations have also been demonstrated by using allozymes (Khan and Arai, 2000) and microsatellite analyses (Arias-Rodriguez et al., 2006). Recent molecular phylogenetic studies on *Misgurnus* from the Far Eastern region of Russia also suggested the presence of different species within *M. anguillicaudatus* (Perdices et al., 2012). Disruption of normal meiosis and subsequent gametogenesis was also reported in inter-populational *M. anguillicaudatus* hybrids between group A females and group B males as in atypical reproduction occurred in inter-specific hybrids: most hybrids generated unreduced diploid and other types of unusual gametes (Arias-Rodriguez et al., 2009, 2010). All these studies support the hybrid-origin theory for the occurrence of gynogenetically reproducing clones in nature.

In natural triploid loaches arising from the spontaneous incorporation of a haploid sperm nucleus from a wild-type diploid into an unreduced diploid egg of clonal lineage, haploid eggs are formed by meiotic hybridogenesis: one of the two different chromosome-sets (haploid genome) of the clone preferentially pairs with the genetically similar haploid set from a sperm donor to form bivalents and then they produce haploid gametes by regular meiosis, but another haploid set of the clone is eliminated before meiosis because of the low pairing affinity between the two haploid genomes of the clone (Morishima et al., 2008b). This unusual pattern of meiotic hybridogenesis also suggests that the genomic constitution of the clonal loach might be heterozygous because of its presumptive hybrid origin.

All the above-mentioned results support the involvement of hybridization in the origin of clonal diploid loaches in nature, but direct genetic evidence has not been obtained so far. In the

present study, we analyzed sequences of the nuclear genes, *RAG1* (recombination activating gene 1) and *IRBP2* (interphotoreceptor retinoid-binding protein 2), which have been utilized for molecular phylogenetic studies in Cypriniformes fishes, including loach species (Šlechtová et al., 2008; Saitoh et al., 2010; Perdices et al., 2012), in putative clonal diploid loaches and wild-type diploid loaches from different localities. Here, we demonstrate that the sequences of the *RAG1* and *IRBP2* genes can be classified into two different clades, which closely correspond to two groups that were previously observed in mtDNA-CR sequences. We then show that clonal diploid specimens with clone-specific mtDNA-CR sequences and microsatellite genotypes are heterozygotes possessing two different alleles from diverse clades at both *RAG1* and *IRBP2* loci, indicating the hybrid origin of clonal lineage.

MATERIALS AND METHODS

Ethics

All experiments procedures were performed in accordance with Institutional guidelines on animal experimentation and care, and were approved by the Animal Research Committee of Hokkaido University.

Fish Specimens

From 2000 to 2010, *M. anguillicaudatus* ($n = 54$) were collected from 12 Japanese localities (Table 1). The ploidy status of each individual was examined by flow cytometry according to Morishima et al. (2002) and one triploid individual was detected among the specimens collected from site number 1. Clonal individuals (#3 and #6) were previously identified by reproduction experiments including artificial fertilization with normal sperm, hybridization with goldfish sperm, and induced gynogenesis with UV-irradiated sperm as well as genetically identical genotypes in several microsatellite loci and multi-locus DNA fingerprinting (Morishima et al., 2002). Clone 1 strain was established by reproduction of the identified female (#3: Morishima et al., 2002) and then maintained in the Aquarium room of the Environment Control Experiment Building of the Faculty of Fisheries Sciences, Hokkaido University, Hakodate. Clone 1 strain was used as reference for clone 1. The other clonal strains (2 to 4) were later identified by the presence of mtDNA-CR haplotype III as well as absolutely identical profiles in random amplified polymorphic DNA (RAPD)-PCR analyses using several random primers and multi-locus DNA fingerprinting using a tetranucleotide probe (Morishima et al., 2008a). Preserved specimens of clones 2 to 4 were also used as reference control samples to identify clonal strains. The mud loach *M. mizolepis* specimen ($n = 1$), obtained from a commercial aquarium shop, was also used in the analysis.

Mitochondrial DNA Analysis

DNA was extracted from fin clips or muscle tissue by using the standard phenol/chloroform protocol (Asahida et al., '96). The mtDNA-CR was amplified and subjected to restriction fragment length polymorphism (RFLP) analysis, followed by determination of the partial sequences of the mtDNA-CR region (444–448 bp)

Table 1. Sampling sites, sample size, and year of sampling of specimens used in the present.

		Locality		
Site no.	Prefecture	City/town/village (former name) (Site no. in Morishima et al. [2008a])	N	Year of sampling
1	Hokkaido	Ozora (Memanbetsu) [5]	12 (1)[1]	1998/2009
2	Hokkaido	Iwamizawa [8]	8	1996
3	Aomori	Yomogita	2	2009
4	Iwate	Hanamaki [18]	2	2004
5	Yamagata	Tsuruoka [20]	2	2004
6	Miyagi	Osaki (Naruko) [22]	1	1998
7	Niigata	Niigata (Maki) [30]	9	1996
8	Saitama	Hanyu [27]	4	1998
9	Aichi	Inazawa [40]	2	2003
10	Mie	Yokkaichi [42]	2	2004
11	Ishikawa	Nanao[2] [33]	9	2009
12	Shimane	Izumo [49]	1	1997
Total			54	

[1]Number of triploid individual is indicated in parentheses.
[2]Hannoura region, Notojima island.

according to the procedures described in Morishima et al. (2008a). Precise group identification of each specimen was performed by 100 to 99.3% matching in the corresponding site between the deposited 942–954 bp mtDNA-CR sequences (AB306717-AB306793) clustered into different genetic groups (A, B-1, and B-2; Morishima et al., 2008a) and present partial 444–448 bp sequences by using Bioedit (http://www.mbio.ncsu.edu/BioEdit/bioedit.html).

Identification of Clonal Diploid Individuals by DNA Marker Analyses

Since all the previously identified clonal individuals and clone-origin triploid individuals had mtDNA-CR RFLP haplotype III, that is, sequences III-1 or III-2 (Morishima et al., 2008a), candidates of clones were predicted to have such a clone-specific haplotype. Thus, samples taken from localities (site no, 1, 7, and 11), where previously known clones were found, were firstly screened to separate candidates of clones among diploid loaches by presence or absence of the clone-specific mtDNA-CR haplotype.

Next, selected candidates of clones were analyzed by independent microsatellite loci (*Mac* 3, *Mac37, Mac* 404, *Mac458* and *Mac477*; Morishima et al., 2008b, c, 2012) in order to find out clonal individuals with genotypes identical to those of the reference control samples of clones 1, 2, 3, and 4. These five loci were used to genotype progeny of clone 1 in Morishima et al. (2008b, 2012).

Candidates of clones were further examined by RAPD (random amplified polymorphic DNA) fingerprinting using three different random primers, Wako-01 (Arbitorary Primer set A-01, Wako, Osaka, Japan), OPA-11 (Kit A-11, Operon Technologies, Alameda, CA, USA) and OPA-12 (Kit A-12) according to the procedures described by Itono et al. (2006, 2007) and Morishima et al. (2008a). The other specimens without clone-specific mtDNA-CR haplotype, clonal microsatellite genotypes and clonal RAPD fingerprints were conveniently categorized to wild-type diploids, although the bisexual reproductive mode was not individually confirmed by reproduction experiments.

For microsatellite genotyping, PCR was performed with a 10 μL mixture containing 1.0 μL of the DNA sample, 6.45 μL of DDW, 0.8 μL of dNTP mixture (TaKaRa, Otsu, Shiga, Japan), 1.0 μL of 10×PCR buffer (TaKaRa), 0.05 μL of *r Taq* DNA Polymerase (TaKaRa), 0.37 μL of the primer mix (Forward:Reverse = 1:10), and 0.33 μL of the M13-tailed forward primer (with fluorescence-labeled 5′ ends). The PCR conditions were as follows: initial denaturation at 94° for 1 min, 35 cycles of 94° for 15 sec, 56° for 15 sec, and 72° for 1 min 30 sec. The reaction was completed by a final extension at 72° for 60 min. Electrophoresis was carried out using ABI PRISM 3130xl (Applied Biosystems, Foster City, CA, USA). The alleles were distinguished by differences in the molecular size using the Gene Scan 500LIZ (Applied Biosystems). Genotyping was performed using the Gene Mapper Software v.3.7 (Applied Biosystems).

The amplification reactions were conducted for RAPD fingerprinting in a mixture comprising DNA template (100 ng/μL), DDW 16.0 μL, dNTP mixture (TaKaRa) 1.6 μL, 10× PCR buffer (TaKaRa) 2.0 μL, *rTaq* polymerase (TaKaRa) 0.2 μL and random primer 0.2 μL in 0.2 mL microtube. Amplification profiles were follows: initial step of 3 min at 95°, subsequent 30 cycles of 30 sec at 95°, 1 min at 36°, and 1 min at 72°, followed by final primer extension for 7 min at 72°. About 5 μL of PCR products were electrophoresed on 1.5% agalose gel and stained with ethidium bromide and photographed on a UV transilluminator using a gel documentation system (UVP BioDoc-It™ Imagining System, Cambridge, UK).

Sequencing of the *RAG1* Gene

RAG1 was amplified using the primer RAG-1F (5′-AGCTGTAGTCAGTAYCACAARATG-3′: Quenouille et al., 2004) and RAG-RV1 (5′-TCCTGRAAGATYTTGTAGAA-3′: Šlechtová et al., 2007). PCR was performed with a 20 μL mixture containing 1.0 μL of the DNA sample, 13.3 μL of DDW, 1.6 μL of a dNTP mixture (TaKaRa), 2.0 μL of 10x*Ex Taq* Buffer (TaKaRa), 0.1 μL of *Ex Taq* DNA Polymerase (TaKaRa), 1.0 μL of 10 μM RAG-1F primer, and 1.0 μL of 10 μM RAG-RV1 primer. The PCR conditions were as follows: initial denaturation at 95° for 5 min, touch-down profile of 1 min at 94°, 1 min 30 sec at 60–55° (1° /cycle), and 2 min at 72° followed by 30 cycles with annealing temperature held at 54°. The reaction was completed by a final extension at 72° for 7 min. The PCR products were purified using AMPure Kits (Beckman Coulter, Brea, CA, USA) and the purified products were sequenced with PCR primers using BigDye Terminator v3.1 Cycle Sequencing Kit (Applied Biosystems). The sequence products were purified using Clean SEQ (Beckman Coulter) and resolved on an ABI PRISM 3130xl (Applied Biosystems). The sequences were aligned using ClustalW in the program BioEdit (http://www.mbio.- ncsu.edu/BioEdit/bioedit.html), and the alleles were identified when no or only one double-peaked site was observed. When two or more double-peaked sites were detected, the PCR product was cloned again using the TA Cloning Kit (Invitrogen, Paisley, UK), and each allele per clone was identified.

Sequencing of the *IRBP-2* Gene

IRBP-2 was amplified using the primer IRBP 76F (5′-CTTRTTGTGGATATGGCAAAAAT-3′) and IRBP 1162R (5′-TGGTGGWCTTYAGGCACTTGT-3′) (Chen et al., 2008). PCR was performed with a 20 μL mixture containing 1.0 μL of the DNA sample, 13.3 μL of DDW, 1.6 μL of dNTP mixture (TaKaRa), 2.0 μL of 10× *Ex* Taq Buffer (TaKaRa), 0.1 μL of *Ex* Taq DNA polymerase (TaKaRa), 1.0 μL of 10 μM IRBP 76F primer, and 1.0 μL of 10 μM IRBP 1162R primer. The PCR conditions were as follows: initial denaturation at 95° for 4 min, 30 cycles of 95° for 40 sec, 58° for 40 sec, and 72° for 1 min 30 sec. The reaction was completed by a final extension at 72° for 7 min. The PCR products were purified using AMPure Kits (Beckman Coulter), and the

purified products were sequenced using PCR primers and the BigDye Terminator v3.1 Cycle Sequencing Kit (Applied Biosystems). The sequence products were purified using Clean SEQ (Beckman Coulter) and resolved on ABI PRISM 3130xl (Applied Biosystems). The sequences were aligned using ClustalW in the program BioEdit (http://www.mbio.ncsu.edu/BioEdit/bioedit.html), and alleles were identified when no or only one double-peaked site was observed. When two or more double-peaked sites were detected, the PCR product was cloned using a TA Cloning Kit (Invitrogen), and alleles were identified in the clone.

Data Analysis

We conducted maximum likelihood (ML) phylogenetic analysis by using MEGA 5 (Tamura et al., 2011). The best-fit substitution models indicated that the Kimura 2-parameter+ discrete gamma model (Kimura, '80; Yang, '94) was the best fit implemented in MEGA 5. Bootstrap analysis was performed on 1,000 replications in the phylogenetic tree. We obtained *Cobitis biwae* (RAG-1: AB531299, IRBP-2: AB531238), *Cobitis striata* (RAG-1: AB531286, IRBP-2: AB531223), and *Acantopsis choirorhynchos* (RAG-1: AB531313, IRBP-2: 531254) as the outgroup from DDBJ/GenBank/EMBL. The genetic distance between the groups was also calculated using MEGA5 against the *p*-distance.

RESULTS

Table 2 shows the genetic groups inferred from mtDNA-CR RFLP haplotypes and the partial sequences of all the loach specimens examined. Clone-specific mtDNA-CR haplotypes (III-1 or III-2) were detected in six out of 12 samples from site number 1, one out of 9 samples from site number 7, and six out of nine samples from site number 11. No clone-specific mtDNA-CR haplotypes were detected in specimens from other sampling sites.

When microsatellite genotyping was performed at five different loci in above-mentioned samples, five candidates from site number 1 were identified as clone 1, because they exhibited microsatellite genotypes identical to the reference control of clone 1 and other samples gave polymorphic variations (Table 3). On the other hand, clone 2 was found in site number 7, and clones 3 and 4 were detected in site no. 11 (Table 3). Clonal individual was not detected by microsatellite genotyping in other candidates from site number 11, although they had clone-specific mtDNA-CR III-1 or III-2 haplotype (Tables 2 and 3). A naturally triploid individual (fish no. 7 from site no. 1) harbored two microsatellite alleles specific to clone 2, which may presumably be a spontaneous triploid progeny of clone 2 (Table 3).

RAPD-fingerprinting with three different random primers (Wako-01, OPA-11, and OPA-12) verified genetically identical characteristics of five candidates from site number 1 (clone 1), one candidate from site number 7 (clone 2) and two candidates from site number 11 (clone 3 and 4), because they gave fingerprints identical to that of reference control samples of clone 1–4 (Fig. 1). Triploid sample (no. 7 from site no. 1; lane 12 in left gels) gave DNA fingerprints comprising all fragments of clone 2 and additional fragments (Fig. 1). Genetic variation was found by RAPD fingerprinting in other diploids from site number 1, 7, and 11 (Fig. 1). Several samples that had clone-specific mtDNA-CR III-1 or III-2 haplotype also gave polymorphic fingerprints (Fig. 1).

The 527-bp *RAG1* gene sequence was determined in 52 individuals of *M. anguillicaudatus* and one individual of *M. mizolepis*. Consequently, 16 different sequences were distinguished among *M. anguillicaudatus* specimens examined and all these sequences were deposited in DDBJ/GenBank/EMBL as accession numbers AB698049 to AB698064, with allele names serially designated as *RAG1-01* to *RAG1-16* in the present study. Two sequences (AB704298, 704299) from a *M.mizolepis* specimen were also deposited in DDBJ/GenBank/EMBL and designated as *RAG1-a* and *RAG1-b*, respectively. ML phylogenetic analysis resulted in the construction of a tree (Fig. 2), which clustered in two major clades, A and B, with clade B further divided in two sub-clades, B-1 and B-2. *RAG1* sequences of *M. anguillicaudatus* were clearly distinguished from those of *M. mizolepis* and this difference indicated the presence of genetically diversified groups within the species. The genetic distance of *RAG1* by mean uncorrected *p*-distance was $4.3 \pm 0.8\%$ between *Cobitis* and *Misgurnus*, $3.1 \pm 0.6\%$ between *M. anguillicaudatus* and *M. mizolepis*, $2.6 \pm 0.6\%$ between clade A and B, and $2.4 \pm 0.6\%$ between sub-clades B-1 and B-2.

Among *M. anguillicaudatus* and *M. mizolepis* specimens examined, 20 genotypes were detected in the *RAG1* gene locus (Table 2). In wild-type diploids of *M. anguillicaudatus* from site numbers 2 to 5, 7, 9, 10, and 12, the individuals were either homozygous (*Rag1-01/Rag1-01*, *Rag1-02/Rag1-02*) or heterozygous (*Rag1-01/Rag1-02*, *Rag1-01/Rag1-11*, *Rag1-01/Rag1-12*) for the *RAG1* alleles of the sub-clade B-1. All these genotypes had mtDNA-CR sequences classified in the B-1 group. Loaches from site number 8 were either homozygous (*Rag1-13/Rag1-13*) or heterozygous (*Rag1-13/Rag1-14*, *Rag1-13/Rag1-16*, *Rag1-14/Rag1-15*) for the *RAG1* alleles of the sub-clade B-2. All these genotypes contained an mtDNA-CR classified as B-2. In 13 loaches from site number 1, five wild-type diploids were either homozygous (*Rag1-05/Rag1-05*) or heterozygous (*Rag1-03/Rag1-04*, *Rag1-04/Rag1-05*, *Rag1-05/Rag1-06*) for the *RAG1* alleles of clade A. The wild-type diploids with *RAG1* alleles of the clades A, B-1, and B-2 were categorized into genetic groups A, B-1, and B-2, as inferred from mtDNA-CR, respectively (Table 2).

On the other hand, clonal diploid loaches from site numbers 1, 7, and 11 showed the characteristic *RAG1* genotype: all clonal individuals were heterozygous for clade A and clade B-1 (*Rag1-01/Rag1-07*, *Rag1-07/Rag1-10*), that is, hybrids between genetically different clades. In site number 11, however, wild-type diploid loaches with homozygous (*Rag1-10/Rag1-10*) or heterozygous genotypes (*Rag1-01/Rag1-09*, *Rag1-01/Rag1-10*, *Rag1-01/Rag1-11*) within the same B-1 clade showed clone-specific mtDNA-CR.

Table 2. Clones and wild-type diploids inferred from mtDNA-CR haplotypes, microsatellite genotypes and RAPD fingerprinting and clade A and B alleles of *RAG1* and *IRBP2* loci.

		mtDNA-CR					*RAG1* Genotype[5]		*IRBP2* Genotype[5]	
Site no.	Fish no.	RFLP	Haplotype (444–448 bp)	Group[1]	Clone-specific Haplotype[2]	Identification of Clone[3]	Clade A allele	Clade B allele	Clade A allele	Clade B allele
1	1	III	III-1, III-2	A	+	Clone 1	7	1	9	6
	2	I	I-3, I-4, I-5	A	–	–	4 5	–	11 12	–
	3	III	III-1, III-2	A	+	Clone 1	7	1	9	6
	4	III	III-1, III-2	A	+	Clone 1	7	1	9	6
	5	III	III-1, III-2	A	+	Clone 1	7	1	9	6
	6	IV	IV-1	A	–	–	5 5	–	11 12	–
	7	III	III-1, III-2	A	+	Triploid [4]	7	1	.n.d.[6]	
	8	III	III-1, III-2	A	+	Clone 1	7	1	9	6
	9	I	I-3, I-4, I-5	A	–	–	3 4	–	n.d.	
	10	I	I-7	A	–	–	5 5	–	12 13	–
	11	I	I-7	A	–	–	5 6	–	10 12	–
	12	I	I-7	A	–	–	.n.d.		10 12	–
2	1	V	V-1, V-4	B-1	–	–	–	1 1	–	1 1
	2	V	V-3	B-1	–	–	–	1 2	–	1 2
	3	V	V-1, V-4	B-1	–	–	–	2 2	–	2 2
	4	V	V-1, V-4	B-1	–	–	–	1 2	–	1 2
	5	V	V-1, V-4	B-1	–	–	–	2 2	n.d.	
	6	V	V-1, V-4	B-1	–	–	–	1 1	–	1 2
	7	V	V-1, V-4	B-1	–	–	–	2 2	n.d.	
	8	V	V-1, V-4	B-1	–	–	–	2 2	–	2 3
3	1	V	V-5, V-6, V-24	B-1	–	–	–	1 1	–	1 2
	2	V	V-5, V-6, V-24	B-1	–	–	–	1 12	–	1 2
4	1	V	V-2, V-21	B-1	–	–	–	1 12	–	2 4
	2	V	V-27	B-1	–	–	–	1 1	–	2 4
5	1	V	V-5, V-6, V-24	B-1	–	–	–	1 1	n.d.	
	2	V	V-5, V-6, V-24	B-1	–	–	–	1 1	–	2 2
6	1	X	n.d.	A	–	–	8 8		7 7	
7	1	V	V-23	B-1	–	–	–	1 1	–	6 6
	2	VII	VII-8, VII-15	B-1	–	–	–	1 1	n.d.	
	3	V	V-23	B-1	–	–	–	1 1	n.d.	
	4	VII	VII-8, VII-15	B-1	–	–	–	1 1	n.d.	
	5	V	V-5, V-6, V-24	B-1	–	–	–	1 1	n.d	
	6	V	V-23	B-1	–	–	–	1 1	n.d.	
	7	IX	IX-1	B-1	–	–	–	1 1	n.d.	–
	8	V	V-23	B-1	–	–	n.d.		–	6 6

Table 2. (*Continued*)

Site no.	Fish no.	mtDNA-CR RFLP	mtDNA-CR Haplotype (444–448 bp)	mtDNA-CR Group[1]	mtDNA-CR Clone-specific Haplotype[2]	Identification of Clone[3]	*RAG1* Genotype[5] Clade A allele	*RAG1* Genotype[5] Clade B allele	*IRBP2* Genotype[5] Clade A allele	*IRBP2* Genotype[5] Clade B allele
	9	III	III-1, III-2	A	+	Clone 2	7	1	9	6
8	1	VII	VII-1, VII-12	B-2	–	–	–	14 15	n.d.	
	2	VII	VII-4, VII-9	B-2	–	–	–	13 13	n.d.	
	3	VII	VII-14	B-2	–	–	–	13 14	n.d.	
	4	VII	VII-1, VII-12	B-2	–	–	–	13 16	–	14 15
9	1	V	V-19, V-26	B-1	–	–	–	1 1	n.d.	
	2	V	V-23	B-1	–	–	–	1 1	n.d.	–
10	1	V	V-20	B-1	–	–	–	1 11	d.d.	–
	2	V	V-20	B-1	–	–	–	1 11	n.d	–
11	1	III	III-1, III-2	A	+	Clone 4	7	10	8	5
	2	III	III-1, III-2	A	+	–	–	1 9	–	6 6
	3	III	III-1, III-2	A	+	–	–	10 10	–	6 6
	4	III	III-1, III-2	A	+	–	–	1 9	–	5 6
	5	V	V-7	B-1	–	–	–	1 10	–	5 6
	6	III	III-1, III-2	A	+	–	–	1 10	–	6 6
	7	VII	VII-7	B-1	–	–	–	1 9	–	5 6
	8	V	V-7	B-1	–	–	–	1 10	–	6 6
	9	III	III-1, III-2	A	+	Clone 3	7	1	8	5
12	1	VII	VII-11	B-1	–	–	–	1 1	n.d.	

[1]Group inferred from mtDNA-CR haplotypes (RFLP, sequences) by Morishima et al. (2008a).
[2]Presence (+) or absence (–) of clone-specific mtDNA haplotypes based on Morishima et al. (2008a).
[3]Clone-candidates were first screened for presence of clone-specific mtDNA haplotypes and then identified as clone 1 to 4 based on identical microsatellite genotypes as shown in Table 3 and identical RAPD fingerprints as shown Figure 1. Symbol "–" means non-clonal wild-type.
[4]Triploid probably derived from clone 1 diploid by accidental sperm nucleus incorporation into diploid egg.
[5]Symbol "–" means absence of allele categorized to clade A or B.
[6]Not determined.

Table 3. Identification of clonal individuals by matching of genotypes of five independent microsatellite loci with those of reference control samples identified as clones 1–4 by Morishima et al. (2002, 2008a, b, 2012).

		Microsatellite locus (Linkage group)					
Site No.	Fish No.	Mac 3(12)	Mac37 (10)	Mac404 (4)	Mac458 (16)	Mac477 (11)	Identification of clone
Reference control	clone 1	103/145	101/107	207/211	224/232	124/192	clone 1
	clone 2	103/145	101/105	213/223	232/232	124/202	clone 2
	clone 3	103/161	101/107	203/211	228/234	124/196	clone 3
	clone 4	103/161	101/107	203/211	216/238	124/196	clone 4
1	1*	103/145	101/107	207/211	224/232	124/192	clone 1
	2	113/113	99/105	195/199	228/244	126/126	
	3*	103/145	101/107	207/211	224/232	124/192	clone 1
	4*	103/145	101/107	207/211	224/232	124/192	clone 1
	5*	103/145	101/107	207/211	224/232	124/192	clone 1
	6	117/117	79/85	181/189	250/264	126/126	
	7*	103/113/145	93/101/105	201/213/223	232/260	124/126/202	clone 2 origin 3n
	8*	103/145	101/107	207/211	224/232	124/192	clone 1
7	7	123/151	105/109	193/243	234/264	136/140	
	8	109/163	107/107	193/201	212/260	138/202	
	9*	103/145	101/105	213/223	232/232	124/202	clone 2
11	1*	103/161	101/107	203/211	216/238	124/196	clone 4
	2*	137/143	105/131	203/219	200/200	178/194	
	3*	135/135	105/107	219/219	218/236	196/216	
	4*	135/151	105/107	203/219	202/216	178/214	
	5	103/145	105/107	203/229	218/234	178/178	
	6*	105/135	105/131	203/205	200/200	178/196	
	7	137/151	115/117	203/219	202/228	194/212	
	8	103/143	105/107	203/219	202/230	178/216	
	9*	103/161	101/107	203/211	228/234	124/196	clone 3

*Samples with clone-specific mtDNA haplotypes.

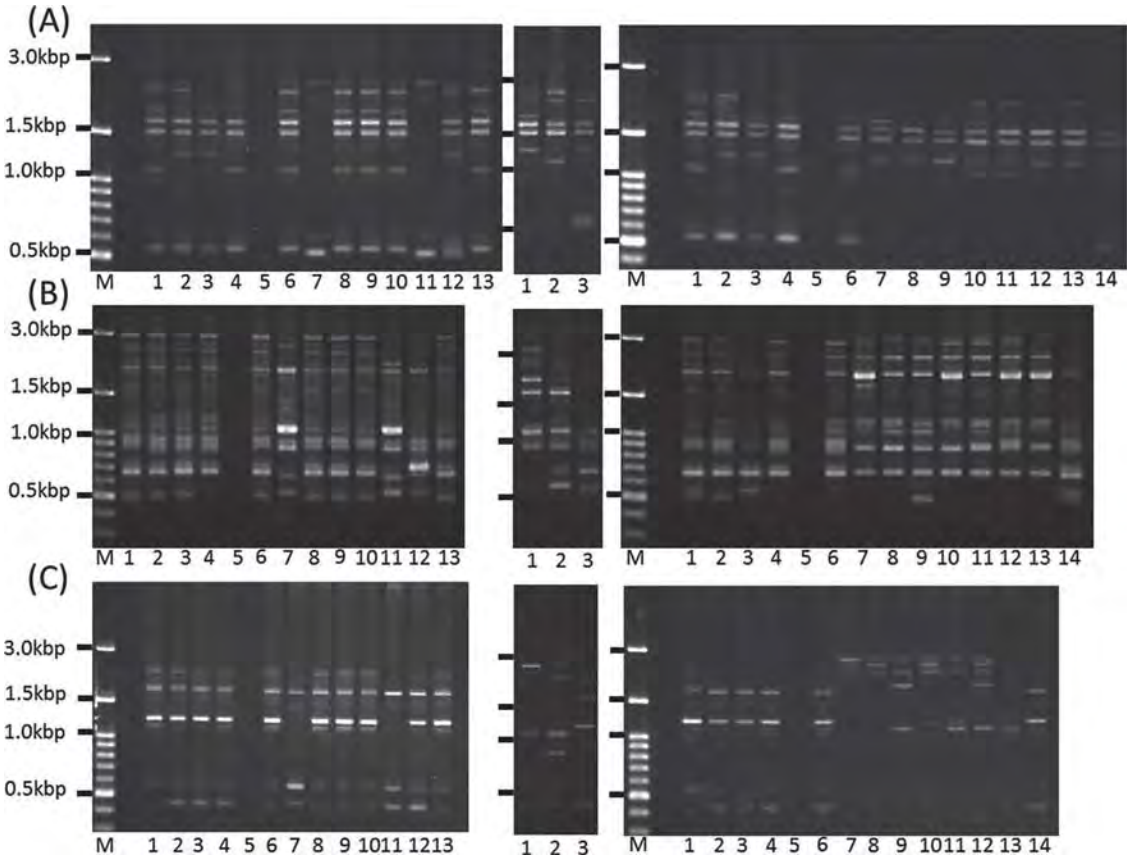

Figure 1. RAPD-PCR fingerprints using random primers WAKO-01(A), OPA-11(B), and OPA-12(C). Left gels: Lanes 1–4 denote reference control samples of clone 1, 2, 3, and 4, respectively. Lane 5, blank. Lanes 6–13 denote fish no. 1–8 from site number 1 (see Table 1 and 2). Central gels: Lanes 1–3 denote fish no. 7, 8, and 9 from site number 7 (see Table 1 and 2). Right gels: Lanes 1–4 denote reference control samples of clone 1, 2, 3, and 4, respectively. Lane 5, blank. Lanes 6–13 denote fish number 1–9 from site number 11 (see Table 1 and 2). M in a gel indicates size marker. Left bars also indicate molecular size marker of 3.0, 1.5, 1.0, and 0.5 kbp.

The 575-bp *IRBP2* gene sequence was determined in 35 individuals of *M. anguillicaudatus* and one individual of *M. mizolepis*. Consequently, 15 different alleles were detected in *M. anguillicaudatus* specimens and all these sequences were deposited in DDBJ/GenBank/EMBL under accession numbers AB702651 to AB702665, with allele names serially designated as*IRBP2-01* to *IRBP2-15*. Two sequences (AB704300 and 704301) from a *M. mizolepis* specimen were also deposited in DDBJ/GenBank/EMBL and designated as *IRBP2-a* and *IRBP2-b*, respectively. ML phylogenetic analysis resulted in the construction of a tree (Fig. 3), which clustered at two major clades, A and B. The *IRBP2* sequences of *M. anguillicaudatus* were clearly distingusished from those of *M. mizolepis* and indicated the presence of two genetically differentiated groups in *M. anguillicaudatus*. Further sub-clade analysis was not possible using the phylogenetic tree. The genetic distance of *IRBP2* by mean uncorrected *p*-distance was $5.3 \pm 0.7\%$ between *Cobitis* and *Misgurnus*, $3.8 \pm 0.6\%$ between *M. anguillicaudatus* and *M. mizolepis*, and $2.9 \pm 0.6\%$ between clades A and B.

A total 15 genotypes were detected in the *IRBP2* gene locus (Table 2). Wild-type diploid samples from site numbers 2 to 5, 7, and 8 were either homozygous (*IRBP2-01/ IRBP2-01*, *IRBP2-02/ IRBP2-02*, *IRBP2-06/ IRBP2-06*) or heterozygous (*IRBP2-01/ IRBP2-02*, *IRBP2-02/ IRBP2-04*, *IRBP2-05/ IRBP2-06*, *IRBP2-14/ IRBP2-15*) for *IRBP2* sequences of the clade B. All these genotypes harbored an mtDNA-CR that was classified as belonging to either the B-1 or B-2 subgroup. In loaches from site number 1, five diploid included only the *IRBP2* alleles of clade A (*IRBP2-11/ IRBP2-12*, *IRBP2-12/ IRBP2-13*, *IRBP2-10/ IRBP2-12*). The wild-type loach individuals with *IRBP2* alleles of the clades A and B were categorized into genetic groups A and B, as inferred from mtDNA-CR, respectively.

On the other hand, all the clonal diploid individuals from site numbers 1, 7, and 11 exhibited heterozygosity between alleles

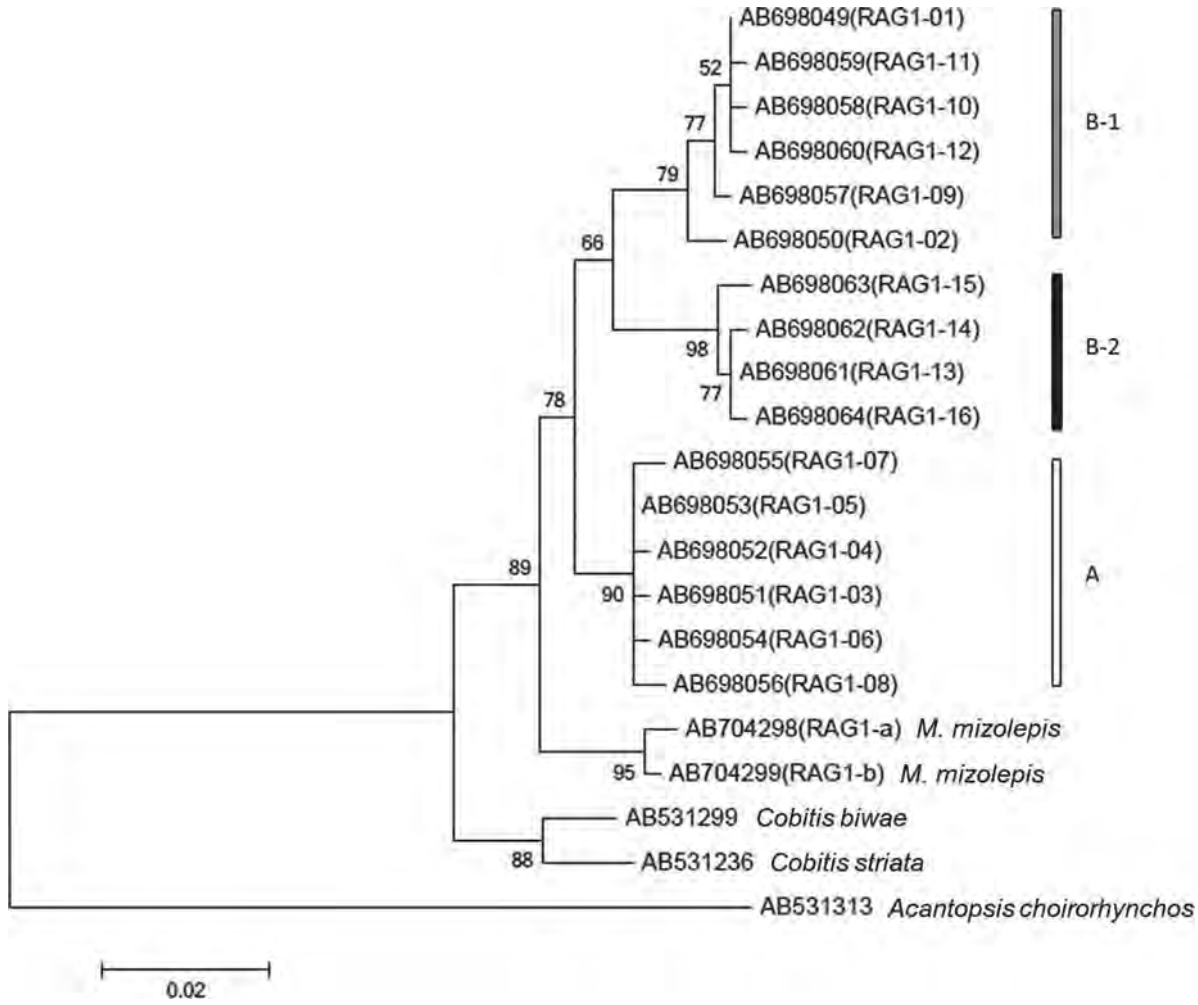

Figure 2. ML phylogenetic tree using *RAG1* sequences. The numbers on the branches are bootstrap values.

from clades A and B of the *IRBP2* gene (*IRBP2-05/ IRBP2-08*, *IRBP2-06/ IRBP2-09*). However, in wild-type diploid loaches from site number 11, four individuals showed *IRBP2* gene sequences exclusively from clade B (*IRBP2-06/ IRBP2-06*), although these showed an mtDNA-CR belonging to group A (Table 2).

DISCUSSION

Although recent molecular phylogenetic studies using both nuclear genes and mitochondrial DNA markers suggest that the entire mitochondrial genome of one of the two major groups in Japanese *M. anguillicaudatus* should have been replaced by that of the genus *Cobitis* due to introgression after a hybridization event that occurred approximately 7 to 10 million years ago (Slechtova et al., 2008; Kitagawa et al., 2011; Pardices et al., 2012), both *RAG1* and *IRBP2* sequences examined in this study were clustered into two clades of the same species. Among wild-type diploid *M. anguillicaudatus* specimens within clade A of both *RAG1* and *IRBP2* gene sequences were categorized as group A, as inferred from its mtDNA-CR, whereas those within clade B of both gene sequences as that of group B. Specimens within the subclade B-1 of *RAG1* and those within the subclade B-2 also correspond to the B-1 and B-2 groups, as inferred from the mtDNA-CR, respectively. Thus, genetic results from mtDNA and nuclear gene sequence analyses strongly suggest the presence of different groups within *M. anguillicaudatus*.

The inter-clade genetic distance for *RAG1* ($2.6 \pm 0.6\%$) estimated in the present study was slightly higher than the inter-specific genetic distance reported for several *Misgurnus* species ($2.1 \pm 0.8\%$; Perdices et al., 2012) and similar to that for the *Cobitis* species ($2.5 \pm 0.5\%$; Perdices et al., 2012). A similar inter-clade distance was also estimated in the present study for

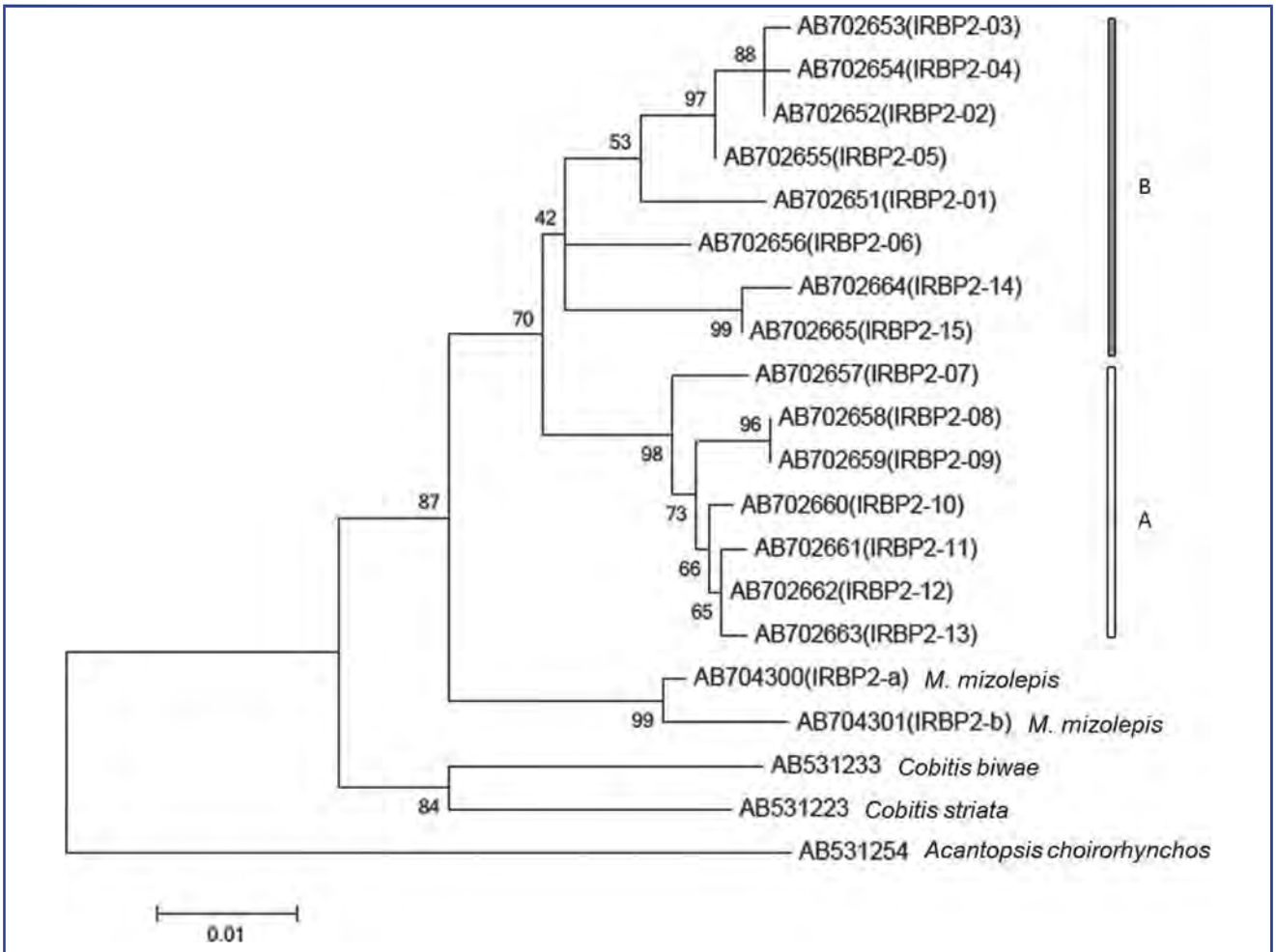

Figure 3. ML phylogenetic tree using *IRBP2* sequences. The numbers on the branches are bootstrap values.

IRBP2 (2.9 ± 0.6%). Molecular systematics of Asian and Far Eastern *Misgurnus* are poorly understood (Perdices et al., 2012), but present *RAG1* and *IRBP2* genetic distances between clades of the Japanese *M. anguillicaudatus* suggest the presence of genetically diverse groups or cryptic species in loaches.

Wild-type loaches were homozygous or heterozygous for *RAG1* and *IRBP2* gene alleles within the same clade. In contrast, all the clonal diploid individuals that were identified by mtDNA-CR haplotype, microsatellite genotype analyses and RAPD fingerpinting showed heterozygous genotypes between clades A and B alleles in both *RAG1* and *IRBP2* genes. These results show that natural clonal diploid loaches may have occurred from an earlier hybridization event between the loaches from different genetic groups (Fig. 4). Hybridization presumably caused a disruption of normal meiosis and subsequent irregular gametogenesis because of the failure of pairing between chromosomes, with each set originating from a different species or genetic group. However, in the inter-populational (or inter-clade) *Misgurnus* hybrids, females might have generated genetically identical unreduced eggs to recover fertility, and very few such eggs might have acquired the developing mode of gynogenesis through mutation for clonal reproduction. The unreduced diploid egg formation was reported in inter-populational *M. anguillicaudatus* hybrids between group A and B-1, as inferred from mtDNA-CR sequences (Arias-Rodriguez et al., 2009). Recently in the genus *Cobitis* spinous loaches, clonality and polyploidy were artificially synthesized by hybridization: F_1 hybrids between two bisexual species produced unreduced eggs, a few of which initiated gynogenesis in nature (Choleva et al., 2012). The formation of unreduced diploid eggs has also been reported in inter-specific hybridizations in *Salmo* (Johnson and Wright, '86), *Oryzias* (Shimizu et al., 2000), *Lepomis* (Dawley et al., '85) and in the inter-generic hybridization between *Carassius* and *Cyprinus* (Liu et al., 2001). As a cytological mechanism responsible for

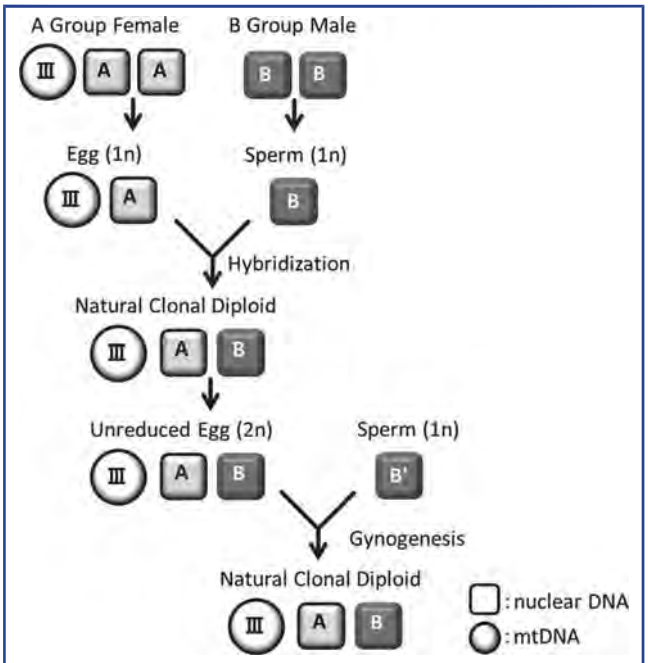

Figure 4. A scenario for the formation of natural clonal diploids through the hybridization of a group A female and a group B male in *Misgurnus* loaches. III in figure means clone-specific mitochondrial DNA control region haplotype transmitted from A group female.

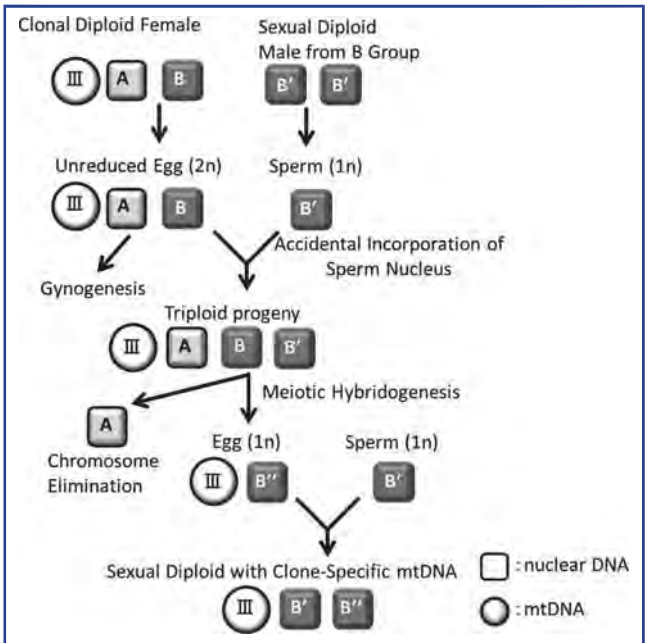

Figure 5. A scenario of introgression of clone-specific mtDNA from clonal diploid loaches to sexual diploid loaches through meiotic hybridogenesis of triploid progeny with one group A genome and two group B genomes, accidentally formed by incorporation of a group B sperm nucleus into a diploid unreduced egg from a clonal diploid loach. III in figure means clone-specific mitochondrial DNA control region haplotype transmitted from A group female.

unreduced oogenesis, premeiotic endomitosis has been proposed because natural clonal diploid loaches were shown to form unreduced diploid eggs through this mechanism (Itono et al., 2006), probably occurring at an early germ cell stage (Yoshikawa et al., 2009; Morishima et al., 2012).

In specimens from site number 11 (Hannoura, Notojima, Nanao City, Ishikawa Prefecture, site no. 33 in Morishima et al., 2008a), wild-type diploid loaches with clone-specific mtDNA-CR haplotypes occurred sympatrically with clonal diploid individuals, although these harbored *RAG1* and *IRBP2* gene sequences exclusively from clade B. The mitochondrial genome of clade B loaches may have thus been replaced by that from the natural clonal lineage. One possible explanation to this occurrence is an introgression of clone-specific mitochondrial genomes from clones to sympatric wild-type diploid loaches. However, introgression of mitochondrial genome by backcrossing of paternal species (group) to hybrids is not realistic, because most hybrids from intergeneric crosses are often sterile or sometimes nonviable (reviewed in Chevassus, '83). Intergeneric hybrids between *M. anguillicaudatus* and *Cobitis* species have been reported to produce viable progeny (Minamori, '53; Kusunoki et al., '94), although sterility in most hybrids has also been reported by Minamori ('57). It is also been shown that inter-populational *Misgurnus* hybrids derived from genetically different groups are generally sterile or undergo unusual reproduction. Experimental *Misgurnus* hybrids from groups A and B-1 produce a small number of haploid eggs, a large number of unreduced diploid eggs, and other genetically abnormal eggs, including aneuploids and mosaicisms (Arias-Rodriguez et al., 2009). The inter-populational male hybrids generated a very small number of fertile haploid or/and diploid spermatozoa (Arias-Rodriguez et al., 2010). Similar results were also obtained in hybrids within the genus *Cobitis* (Choleva et al., 2012). Production of functional gametes by hybrids is a prerequisite for the introgression theory by subsequent backcrossing of fertile hybrids with its original species or population.

Wild-type diploid genotypes with clone-specific mtDNA-CR are likely to occur through meiotic hybridogenesis (Morishima et al., 2008b). Unreduced diploid eggs with a heterozygous genotype (AB) are formed by a clone from a crossing between a clade A female with clone-specific mtDNA and a clade B male (Fig. 4) and these diploid eggs infrequently develop into triploid fish with genotype ABB: a haploid sperm from a wild-type male

from clade B was thus accidentally incorporated into an unreduced diploid egg (genotype AB) of the clonal diploid (Fig. 5). These clone-derived triploid loaches (genotype ABB) are known to produce haploid eggs by meiotic hybridogenesis (Morishima et al., 2008b), that is, elimination of an unmatched chromosome set from clade A and pairing between two chromosome sets from clade B, followed by quasinormal meiosis (Fig. 5). Thus, the occurrence of wild-type diploid loaches with chromosome sets of clade B and a mtDNA-CR of group A in site number 11 is well explained by this meiotic hybridogenetic mechanism. Consequently, the formation of triploids from clonal lineages and the subsequent reproduction through meiotic hybridogenesis presumably produce bisexually reproducing diploid loaches with clone-specific mtDNA. Therefore, introgression of clonal mtDNA through meiotic hybridogenesis of clone-origin triploids produces bisexually reproducing loaches with clone-derived group A mitochondrial genomes.

The present study concluded that the *RAG1* and *IRBP2* genotypes in natural clonal loaches, that generate unreduced diploid eggs with identical genotypes and develop through gynogenesis, arose through the hybridization of two genetically different groups of *M. anguillicaudatus*.

ACKNOWLEDGMENTS

We thank the staff of the Ishikawa Prefecture Fisheries Research Center for sampling loaches in the Ishikawa Prefecture.

LITERATURE CITED

Arai K, Fujimoto T. 2013. Genome constitution and atypical reproduction in polyploid and unisexual lineages of the *Misgurnus* loach, a teleost fish. Cytogenet Genome Res 140:226–240.

Arias-Rodriguez L, Morishima K, Arai K. 2006. Genetically diversified populations in the loach *Misgurnus anguillicaudatus* inferred from newly developed microsatellite markers. Mol Ecol Notes 7:82–85.

Arias-Rodriguez L, Yasui GS, Arai K. 2009. Disruption of normal meiosis in artificial inter-populational hybrid female *Misgurnus* loach. Genetica 136:49–56.

Arias-Rodriguez L, Yasui GS, Kusuda S, Arai K. 2010. Reproductive and genetic capacity of spermatozoa of inter-populational hybrid males in the loach, *Misgurnus anguillicaudatus*. J Appl Ichthyol 26: 653–658.

Asahida T, Kobayashi T, Saitoh K, Nakayama I. 1996. Tissue preservation and total DNA extraction from fish stored at ambient temperature using buffer containing high concentration of urea. Fish Sci 62:727–730.

Chen WJ, Miya M, Saitoh K, Mayden RL. 2008. Phylogenetic utility of two existing and four novel nuclear gene loci in reconstructing tree of life of ray-finned fishes: the order Cypriniformes (Ostariophysi) as a case study. Gene 425:125–134.

Chevassus B. 1983. Hybridization in fish. Aquaculture 33:245–262.

Choleva L, Janko K, De Gelas K, et al. 2012. Synthesis of clonality and polyploidy in vertebrate animals by hybridization between two sexual species. Evolution 66–7:2191–2203.

Collares-Pereira MJ, Matos I, Morgado-Santos M, Coelho MM. 2013. Natural pathways towards polyploidy in animals: the *Squalius alburnoides* fish complex as a model system to study genome size and genome reorganization in polyploids. Cytogenet Genome Res 140:97–116.

Dawley RM. 1989. An introduction to unisexual vertebrates. In: Dawley RM, Bogart JP, editors. Evolution and ecology of unisexual vertebrates. Albany: New York State Museum. Bulletin 466, p 1–18.

Dawley RM, Graham JH, Schultz RJ. 1985. Triploid progeny of pumpkinseed x green sunfish hybrids. J Hered 76:251–257.

Fujimoto T, Yasui GS, Yoshikawa H, Yamaha E, Arai K. 2008. Genetic and reproductive potential of spermatozoa of diploid and triploid males obtained from interspecific hybridization of *Misgurnus anguillicaudatus* female with *M. mizolepis* male. J Appl Ichthyol 24:430–437.

Gui JF, Zhou L. 2010. Genetic basis and breeding application of clonal diversity and dual reproduction modes in polyploidy *Carassius auratus gibelio*. Sci China Life Sci 53:409–415.

Itono M, Morishima K, Fujimoto T, et al. 2006. Premeiotic endomitosis produces diploid eggs in the natural clone loach, *Misgurnus anguillicaudatus* (Teleostei: Cobitidae). J Exp Zool 305A:513–523.

Itono M, Okabayashi N, Morishima K, et al. 2007. Cytological mechanisms of gynogenesis and sperm incorporation in unreduced diploid eggs of the clonal loach, *Misgurnus anguillicaudatus* (Teleostei: Cobitidae). J Exp Zool 307A:35–50.

Janko K, Kotusz J, De Gelas K, et al. 2012. Dynamic formation of asexual diploid and polyploidy lineages: multilocus analysis of *Cobitis* reveals the mechanisms maintaining the diversity of clones. PLoS ONE 7:e45384.

Johnson KR, Wright JE. 1986. Female brown trout x Atlantic salmon hybrids produce gynogens and triploids when backcrossed to male Atlantic salmon. Aquaculture 57:345–358.

Khan MMR, Arai K. 2000. Allozyme variation and genetic differentiation in the loach, *Misgurnus anguillicaudatus*. Fish Sci 66:211–222.

Kimura M. 1980. A simple method for estimating evolutionary rates of base substitutions through comparative studies of nucleotide sequences. J Mol Evol 16:111–120.

Kitagawa T, Fujii Y, Koizumi N. 2011. Origin of the two major distinct mtDNA clades of the Japanese population of the oriental weather loach *Misgurnus anguillicaudatus* (Teleostei: Cobitidae). Folia Zool 60:340–346.

Koizumi N, Takemura T, Watabe K, Mori A. 2009. Genetic variation and diversity of Japanese loach inferred from mitochondrial DNA—phylogenetic analysis using the cytochrome b gene sequence. Trans Jap Soc Irrig Drain Rural Engin 77:7–16.

Kusunoki T, Arai K, Suzuki R. 1994. Viability and karyotypes of interracial and intergeneric hybrids in loach species. Fish Sci 60:415–422.

Liu S, Liu Y, Zhou G, et al. 2001. The formation of tetraploid stocks of red crucian carp x common carp hybrids as an effect of interspecific hybridization. Aquaculture 192:171–186.

Minamori S. 1953. Physiological i-solation in cobitidae II. Inviability of hybrids between the mud loach and some local races of spinous loaches. J Sci Hiroshima Univ Series B Div 1 14:125–149.

Minamori S. 1957. Physiological isolation in cobitidae V. Sterility of the hybrids between the mud loach and six races of spinous loaches. J Sci Hiroshima Univ Series B Div 1 17:55–65.

Morishima K, Horie S, Yamaha E, Arai K. 2002. A cryptic clonal line of the loach *Misgurnus anguillicaudatus* (Teleostei: Cobitidae) evidenced by induced gynogenesis, interspecific hybridization, microsatellite genotyping and multilocus DNA fingerprinting. Zool Sci 19:565–575.

Morishima K, Nakamura-Shiokawa Y, Bando E, et al. 2008a. Cryptic clonal lineages and genetic diversity in the loach *Misgurnus anguillicaudatus* (Teleostei: Cobitidae) inferred from nuclear and mitochondrial DNA analyses. Genetica 132:159–171.

Morishima K, Yoshikawa H, Arai K. 2008b. Meiotic hybridogenesis in triploid *Misgurnus* loach derived from a clonal lineage. Heredity 100:581–586.

Morishima K, Nakayama I, Arai K. 2008c. Genetic linkage map of the loach *Misgurnus anguillicaudatus* (Teleostei: Cobitidae). Genetica 132:227–241.

Morishima K, Yoshikawa H, Arai K. 2012. Diploid clone produces unreduced diploid gametes but tetraploid clone generates reduced diploid gametes in the *Misgurnus* loach. Biol Reprod 86 33:1–7.

Perdices A, Vasil'ev V, Vasil'eva E. 2012. Molecular phylogeny and intraspecific structure of loaches (genera Cobitis and Misgurnus) from the Far East region of Russia and some conclusion on their systematic. Ichthyol Res 59:113–123.

Quenouille B, Bermingham E, Planes S. 2004. Molecular systematic of the damselfishes (Teleostei: Pomacentridae): Bayesian phylogenetic analyses of mitochondrial and nuclear DNA sequences. Mol Phylogenet Evol 31:66–68.

Saitoh K. 1989. Asian Pond loach. In: Kawanabe H, Mizuno N, editors. Freshwater fishes of Japan. Tokyo: Yamakei Pub. p 382–385.

Saitoh K, Chen WJ, Mayden RL. 2010. Extensive hybridization and tetraploidy in spined loach fish. Mol Phylogenet Evol 56:1001–1010.

Shimizu Y, Shibata N, Sakaizumi M, Yamashita M. 2000. Production of diploid eggs through premeiotic endomitosis in the hybrid medaka between *Oryzias latipes* and *O. curvinotus*. Zool Sci 17:951–958.

Sinclair EA, Pramuk JB, Bezy RL, Crandall KA, Sites JW, Jr. 2010. DNA evidence for nonhybrid origins of parthenogenesis in natural populations of vertebrates. Evolution 64:1346–1357.

Šlechtová V, Bohlen J, Perdices A. 2008. Molecular phylogeny of the freshwater fish family Cobitidae (Cypriniformes: Teleostei): delimination of genera, mitochondrial introgression and evolution of sexual dimorphism. Mol Phylogenet Evol 47:812–831.

Tamura K, Peterson D, Peterson N, et al. 2011. MEG A5: molecular evolutionary genetics analysis using maximum likelihood, evolutionary distance, and maximum parsimony method. Mol Biol Evol 28:2731–2739.

Vrijenhoek RC. 1994. Unisexual fish: model systems for studying ecology and evolution. Annu Rev Ecol Syst 25:71–96.

Vrijenhoek RC, Dawley RM, Cole CJ, Bogart JP. 1989. A list of the known unisexual vertebrates. In: Dawley RM, Bogart JP, editors. Evolution and ecology of unisexual vertebrates. Albany: New York State Museum. Bulletin 466, p 19–23.

Yang Z. 1994. Maximum likelihood phylogenetic estimation from DNA sequences with variable rates over: approximate methods. J Mol Evol 39:306–314.

Yoshikawa H, Morishima K, Fujimoto T, et al. 2009. Chromosome doubling in early spermatogonia produces diploid spermatozoa in a natural clone fish. Biol Reprod 80:973–979.

Zhou X, Yu Y, Li Y, et al. 2014. Comparative analysis of mitochondrial genomes in distinct nuclear ploidy loach *Misgurnus anguillicaudatus* and its implications for polyploidy evolution. PLoS ONE 9: e92033.

Research in Veterinary Science 102 (2015) 49–52

Contents lists available at ScienceDirect

Research in Veterinary Science

journal homepage: www.elsevier.com/locate/yrvsc

Short communication: Distribution of *Porphyromonas gulae fimA* genotypes in oral specimens from dogs with mitral regurgitation

Mitsuyuki Shirai [a,1], Ryota Nomura [b,*,1], Yukio Kato [c], Masaru Murakami [d], Chihiro Kondo [a], Soraaki Takahashi [a], Yoshie Yamasaki [e], Michiyo Matsumoto-Nakano [e], Nobuaki Arai [f], Hidemi Yasuda [f], Kazuhiko Nakano [b], Fumitoshi Asai [a]

[a] *Department of Pharmacology, School of Veterinary Medicine, Azabu University, Sagamihara, Kanagawa 252–5201, Japan*
[b] *Department of Pediatric Dentistry, Osaka University Graduate School of Dentistry, Suita, Osaka 565–0871, Japan*
[c] *Department of Veterinary Public Health II, School of Veterinary Medicine, Azabu University, Sagamihara, Kanagawa 252–5201, Japan*
[d] *Department of Molecular Biology, School of Veterinary Medicine, Azabu University, Sagamihara, Kanagawa 252–5201, Japan*
[e] *Department of Pediatric Dentistry, Okayama University Graduate School of Medicine, Dentistry and Pharmaceutical Sciences, Okayama 700–8556, Japan*
[f] *Yasuda Veterinary Clinic, Meguro, Tokyo 152–0034, Japan*

ARTICLE INFO

Article history:
Received 18 November 2014
Received in revised form 8 July 2015
Accepted 13 July 2015

Keywords:
fimbriae
mitral regurgitation
periodontal disease
Porphyromonas gulae

ABSTRACT

Porphyromonas gulae, a suspected pathogen for periodontal disease in dogs, possesses approximately 41-kDa fimbriae (FimA) that are encoded by the *fimA* gene. In the present study, the association of *fimA* genotypes with mitral regurgitation (MR) was investigated. Twenty-five dogs diagnosed with MR (age range 6–13 years old, average 10.8 years) and 32 healthy dogs (8–15 years old, average 10.8 years) were selected at the participating clinics in a consecutive manner during the same time period. Oral swab specimens were collected from the dogs and bacterial DNA was extracted, then polymerase chain reaction analysis was performed using primers specific for each *fimA* genotype, with the dominant genotype determined. The rate for genotype C dominant specimens was 48.0% in the MR group, which was significantly higher than that in the control group (18.8%) ($P < 0.05$). These results suggest that *P. gulae fimA* genotype C is associated with MR.

Periodontal disease, including gingivitis and periodontitis, is commonly found in dogs, with prevalence rates ranging from 50-70% (Harvey and Emily, 1993). Gingivitis involves inflammation of the gingiva, whereas periodontitis is a more progressive form of periodontal disease that involves the loss of tooth supporting tissues (i.e., periodontal ligament, cementum, alveolar bone). Proper periodontal therapy can reduce gingival bleeding, tooth mobility, and, in some cases, sophisticated methods can be utilized to regenerate lost tissues. The distribution of bacterial species related to periodontal disease has been investigated using oral swab specimens taken from dogs, with *Porphyromonas gulae*, a Gram-negative black-pigmented anaerobe, one of the species frequently detected (Kato et al., 2011). The cell surface component Fimbrillin (FimA), a 41-kDa fimbriae subunit, of *P. gulae* has also been characterized and shown to be a possible factor related to periodontal disease in dogs (Hamada et al., 2008). In our recent study, FimA of *P. gulae* was classified into 3 major genotypes; A, B, and C, with type C shown to have a high virulence for periodontal disease, followed by B and A (Nomura et al., 2012; Yamasaki et al., 2012).

The association of periodontal disease with systemic diseases has recently been gaining attention (Pavlica et al., 2008; Rawlinson et al., 2011). Mitral regurgitation (MR) caused by myxomatous mitral valve disease is one of the most common types of cardiovascular diseases occurring in dogs (Serfass et al., 2006; Atkins et al., 2009) and characterized by chronic progression, with the condition worsening from mild to severe over time (Borgarelli et al., 2008). A few reports have shown an association of periodontal disease with MR in dogs (Glickman et al., 2009). In the present study, oral specimens from dogs diagnosed with MR were analyzed to investigate the association of the disease with the presence of *P. gulae* and genotypes of *fimA* encoding FimA.

Twenty-five dogs diagnosed with MR and treated at veterinary clinics in Tokyo in 2012 and 2013 were consecutively enrolled (MR group). In addition, 36 dogs older than 6 years old and without periodontitis, MR, diabetes mellitus, or other relevant clinical history, were selected as Control group. Among them, we removed the 4 larger breed dogs that weighed more than 20 kilograms and used the remaining 32 as controls. The study protocol was approved by the Animal Research Committee of Azabu University (No. 130307–3). Prior to

* Corresponding author at: Department of Pediatric Dentistry, Osaka University Graduate School of Dentistry, 1–8 Yamada-oka, Suita, Osaka 565–0871, Japan.
E-mail addresses: shirai@azabu-u.ac.jp (M. Shirai), rnomura@dent.osaka-u.ac.jp (R. Nomura), katohy@azabu-u.ac.jp (Y. Kato), murakami@azabu-u.ac.jp (M. Murakami), v09058@azabu-u.ac.jp (C. Kondo), v09083@azabu-u.ac.jp (S. Takahashi), yoca777@live.jp (Y. Yamasaki), mnakano@cc.okayama-u.ac.jp (M. Matsumoto-Nakano), narai@slj.co.jp (N. Arai), hidemi@yasuda-vet.org (H. Yasuda), nakano@dent.osaka-u.ac.jp (K. Nakano), asai@azabu-u.ac.jp (F. Asai).
[1] These authors contributed equally to this work.

http://dx.doi.org/10.1016/j.rvsc.2015.07.009
0034-5288/

sample collection, the owners were informed of the purpose of the study and gave approval for their participation. None of the dogs or their owners received antibiotic treatment within the previous 3 months prior to collection. Oral specimens were obtained from supra- and sub-gingival areas of the left and/or right upper fourth premolar and/or lower first molar using Seed-Swab^{R} g-1 or −2 swabs (Eiken Chemical, Tokyo, Japan), then bacterial DNA was extracted using a method previously described (Kato et al., 2011).

According to the ACVIM (American College of Veterinary Internal Medicine) functional classification (Atkins et al., 2009), the 25 dogs in the MR group (18 males, 7 females; 10.8 ± 0.3 year old) were diagnosed based on physical examination, thoracic radiography, electrocardiography, and echocardiography findings, as follows; Stage A ($n = 0$), Stage B1 ($n = 4$), Stage B2 ($n = 10$), Stage C ($n = 7$), and Stage D ($n = 4$). In addition, the severity of MR has been reported to be associated with murmur intensity and audibility (Ljungvall et al., 2009). Thus, these dogs were also evaluated using the Levine classification, which is a scoring system used to classify the intensity or loudness of a heart murmur (Freeman and Levine, 1933), as follows; I/VI ($n = 0$), II/VI ($n = 8$), II-III/VI ($n = 2$), III/VI ($n = 7$), IV/VI ($n = 7$), V/VI ($n = 0$), and VI/VI ($n = 1$). Breeds represented in the MR group are listed in Supplementary Table 1. The 32 healthy dogs in the control group (17 males, 15 females, 10.8 ± 0.4 years old) had no abnormal cardiac conditions shown in physical examination, thoracic radiography, electrocardiography, and echocardiography findings. Breeds represented in the control group are listed in Supplementary Table 2.

Statistical analyses were performed using the computational software packages StatView 5.0[e] and Prism 4[f]. Fisher's protected least-significant difference test was utilized to compare the detection frequencies of each *fimA* genotype for each gingival condition. Odds ratio (OR) and 95% confidence interval (CI_{95}) values were calculated to determine the significance of the association of each *fimA* genotype in the dogs with each periodontal condition. A P value of <0.05 was considered to be statistically significant.

We evaluated calculus coverage, and gingival and periodontal scores based on methods previously described, with some modifications (Warrick and Gorrel, 1997; Harvey and Emily, 1993; Löe, 1967; Wolf et al., 2005). For each dog, 22 teeth were scored according to a previously described technique (Kate and Cecilia, 1999). Dental calculus accumulation was scored visually, as follows; (3) more than half of the area of the portion of the tooth from the gingival margin to the tip of the crown, (2) less than half of that area, (1) slight, only at gingival margin, and (0) none. Gingival scores were evaluated visually as follows; (3) prominent inflammation (intensive redness with gingival swelling) identified throughout entire area, (2) prominent inflammation (intensive redness with gingival swelling) identified in limited area, (1) slight inflammation (slight redness without gingival swelling) identified only in gingival margin, and (0) no significant findings. Periodontal scores were evaluated based on visual examination and palpation, as follows; (3) tooth mobility with severe attachment loss, (2) attachment loss identified in more than one quarter of the portion of the tooth but no tooth mobility, (1) attachment loss identified in less than one quarter of that portion, and (0) no significant findings. Table 1 summarizes the oral conditions in the MR and Control groups. There were no significant differences in regard to dental calculus and gingival scores. As for periodontal scoring, the MR group had higher scores than the control group, though there were no significant differences between the groups.

Detection of *P. gulae* and *fimA* genotypes in addition to *Tannerella forsythia* and *Campylobacter rectus* were performed by PCR using species-specific sets of primers (Kato et al., 2011; Nomura et al., 2012; Yamasaki et al., 2012). PCR amplification was performed in a total volume of 20 μl with 1 μl of bacterial DNA using Ex Taq polymerase (Takara Bio, Shiga, Japan) with the following cycling parameters: initial denaturation at 95 °C for 4 minutes and then 30 cycles consisting of 95 °C for 30 seconds, 60 °C for 30 seconds, and 72 °C for 30 seconds, with a final extension at 72 °C for 7 minutes. Specificity with this method was shown in our previous study, with the minimum detection level reported to be 10–100 cells (Nomura et al., 2012; Yamasaki et al., 2012). The dominant genotypes were determined using samples with multiple *fimA* genotypes detected. PCR was performed with titrated DNA samples (1/10, 1/100, 1/1000) from each specimen. The dominant genotype was determined as that with the lowest detection limit. When the detection limits were similar for at least two genotypes, the results were described as no dominancy. Fig. 1A shows the results of detection using the PCR system with genomic DNA extracted from titrated cultures of representative strains of each type. The lowest numbers of tested strains for identification were the same for all 3 *fimA* genotypes. Fig. 1B, C, and D show

Table 1
Oral conditions and distribution frequency of *P. gulae* and its *fimA* genotypes in oral specimens in MR and Control groups.

	MR ($n = 25$)	Control ($n = 32$)	Statistical analysis
Age in years Mean ± SE [a] (range)	10.8 ± 0.3 (6–13)	10.8 ± 0.4 (8–15)	NS [b]
Body weight in kg Mean ± SE [a] (range)	5.7 ± 0.8 (1.6-14.6)	5.7 ± 0.7 (1.6-18.8)	NS [b]
Oral condition			
Dental calculus score (mean ± SE [a])	1.7 ± 0.1	1.8 ± 0.2	NS [b]
Gingival score (mean ± SE [a])	0.8 ± 0.2	0.8 ± 0.1	NS [b]
Periodontal score(mean ± SE [a])	0.6 ± 0.2	0.3 ± 0.1	NS [b]
PCR detection			
P. gulae-positive	24 (96.0%)	30 (93.8%)	NS [b]
A-dominant	5 (20.0%)	17 (53.1%)	$P = 0.0143$ OR: 0.22 (CI_{95}: 0.07-0.73)
B-dominant	3 (12.0%)	4 (12.5%)	NS [b]
C-dominant	12 (48.0%)	6 (18.8%)	$P = 0.0240$ OR [c]: 4.00 (CI_{95} [d]: 1.22-13.08)
A = C	2 (8.0%)	1 (3.1%)	NS [b]
A = B = C	0 (0%)	1 (3.1%)	NS [b]
Untypeable	2 (8.0%)	1 (3.1%)	NS [b]

[a] SE, standard error.
[b] NS, not significant.
[c] OR, odds ratio.
[d] CI_{95}, 95% confidence interval.

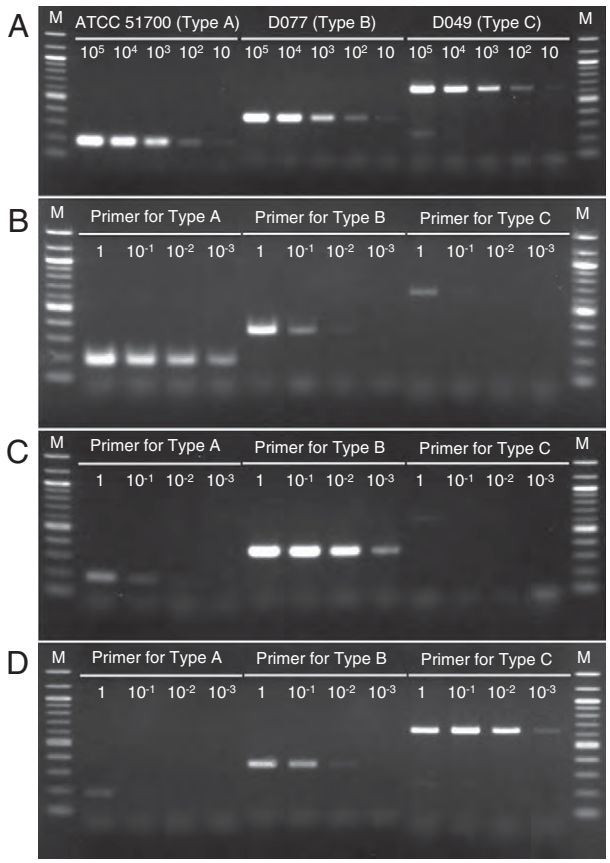

Fig. 1. Methodology designed to identify the dominant genotype *fimA* of *P. gulae*, using polymerase chain reaction (PCR). A. Comparisons of PCR products using diluted genomic DNA extracted from *P. gulae* strains with each *fimA* genotype. M; molecular size marker (100-bp DNA ladder). B, C, D. Representative results obtained with clinical specimens using PCR system constructed for the present study.

representative results obtained using titrated bacterial DNA samples from the original concentration to 10^{-3} in the PCR system constructed for the present study. Fig. 1B presents a representative specimen, in which positive bands were observed in the original and 10^{-1} dilution samples for type B and the original dilution for type C, while positive bands were observed when applying the original, 10^{-1}, 10^{-2}, and even 10^{-3} dilution samples for type A detection. Thus, this specimen was classified as "type A-dominant." Fig. 1C and D present representative results of other "type B-dominant" and "type C-dominant" specimens, respectively. The detection rates for both *T. forsythia* and *C. rectus* were not significantly between the Control and MR groups (Supplementary Tables 1 and 2).

Table 1 summarizes the distribution frequencies of *P. gulae* and its *fimA* genotypes in oral specimens obtained from the MR and Control groups. *P. gulae* was detected in nearly all specimens from both groups. On the other hand, there was a significantly larger number of type A-dominant specimens in the Control group ($P<0.05$) and a significantly larger number of type C-dominant specimens in the MR group ($P<0.05$). The odds ratios for type-A and type-C detection in the MR group were 0.22 and 4.00, respectively.

This is the first known study to analyze oral specimens obtained from dogs with MR in comparison to those from healthy dogs, though the number of subjects, variety of breeds, and clinical assessment parameters were limited. We previously reported that genomic DNA specific for *P. gingivalis* was detected in approximately 10% of heart valves and 20-30% of atheromatous plaque specimens, indicating a possible association between periodontal disease and cardiovascular diseases (Nakano et al., 2009). That notion is also supported by previous evidence showing that frequent detection of *fimA* genotype organisms, such as type II and IV, indicated that they are highly virulent for periodontitis (Nakano et al., 2008). In addition, it is interesting that analysis of the evolutionary relationship revealed that type C *fimA* of *P. gulae* is close to type IV *fimA* of *P. gingivalis* (Yamasaki et al., 2012). Taken together, these results indicate the possibility of an association of periodontal disease with MR.

In summary, the present results indicate a possible association between the presence of a specific genotype of *fimA* of *P. gulae* with MR. In addition, our novel method used to specify the dominant genotype of *P. gulae* in the specimens obtained may enable identification of subjects at risk and in need of preventive approaches.

Supplementary data to this article can be found online at http://dx.doi.org/10.1016/j.rvsc.2015.07.009.

Conflicts of interest

The authors declare that they have no competing interests.

Acknowledgements

This study was supported by Grants-in-Aid for Scientific Research for Challenging Exploratory Research (No. 23658256 and 25670873) from the Japan Society for Promotion of Science, the Promotion and Mutual Aid Corporation of Private Schools of Japan, and a Grant-in-Aid for Matching Fund Subsidy for Private Universities. We also thank Prof. Howard K. Kuramitsu (State University of New York at Buffalo) for editing the manuscript.

References

Atkins, C., Bonagura, J., Ettinger, S., Fox, P., Gordon, S., Haggstrom, J., Hamlin, R., Keene, B., Luis-Fuentes, V., Stepien, R., 2009. Guidelines for the diagnosis and treatment of canine chronic valvular heart disease. J. Vet. Intern. Med. 23, 1142–1150.

Borgarelli, M., Savarino, P., Crosara, S., Santilli, R.A., Chiavegato, D., Poggi, M., Bellino, C., La Rosa, G., Zanatta, R., Haggstrom, J., Tarducci, A., 2008. Survival characteristics and prognostic variables of dogs with mitral regurgitation attributable to myxomatous valve disease. J. Vet. Intern. Med. 22, 120–128.

Freeman, A.R., Levine, S.A., 1933. Clinical significance of systolic murmurs: Study of 1000 consecutive "noncardiac" cases. Ann. Intern. Med. 6, 1371–1379.

Glickman, L.T., Glickman, N.W., Moore, G.E., Goldstein, G.S., Lewis, H.B., 2009. Evaluation of the risk of endocarditis and other cardiovascular events on the basis of the severity of periodontal disease in dogs. J. Am. Vet. Med. Assoc. 234, 486–494.

Hamada, N., Takahashi, Y., Watanabe, K., Kumada, H., Oishi, Y., Umemoto, T., 2008. Molecular and antigenic similarities of the fimbrial major components between *Porphyromonas gulae* and *P. gingivalis*. Vet. Microbiol. 128, 108–117.

Harvey, C.E., Emily, P.P., 1993. Small Animal Dentistry. 1st ed. Mosby – Year Book Inc, St. Loius, p. 413.

Kate, E.I., Cecilia, Gorrel, 1999. Assessing oral health and hygiene in dogs. Waltham Focus 9, 32–33.

Kato, Y., Shirai, M., Murakami, M., Mizusawa, T., Hagimoto, A., Wada, K., Nomura, R., Nakano, K., Ooshima, T., Asai, F., 2011. Molecular detection of human periodontal pathogens in oral swab specimens from dogs in Japan. J. Vet. Dent. 28, 84–89.

Ljungvall, I., Ahlstrom, C., Höglund, K., Hult, P., Kvart, C., Borgarelli, M., Ask, P., Häggström, J., 2009. Use of signal analysis of heart sounds and murmurs to assess severity of mitral valve regurgitation attribute to myxomatous mitral valve disease in dogs. Am. J. Vet. Res. 70, 604–613.

Löe, H., 1967. The gingival index, the plaque index and the retention index systems. J. Periodontol. 38, 610–616.

Nakano, K., Inaba, H., Nomura, R., Nemoto, H., Takeuchi, H., Yoshioka, H., Toda, K., Taniguchi, K., Amano, A., Ooshima, T., 2008. Distribution of *Porphyromonas gingivalis fimA* genotypes in cardiovascular specimens from Japanese patients. Oral Microbiol. Immunol. 23, 170–172.

Nakano, K., Nemoto, H., Nomura, R., Inaba, H., Yoshioka, H., Taniguchi, K., Amano, A., Ooshima, T., 2009. Detection of oral bacteria in cardiovascular specimens. Oral Microbiol. Immunol. 24, 64–68.

Nomura, R., Shirai, M., Kato, Y., Murakami, M., Nakano, K., Hirai, N., Mizusawa, T., Naka, S., Yamasaki, Y., Matsumoto-Nakano, M., Ooshima, T., Asai, F., 2012. Diversity of Fimbrillin among *Porphyromonas gulae* clinical isolates from Japanese dogs. J. Vet. Med. Sci. 74, 885–891.

Pavlica, Z., Petelin, M., Juntes, P., Erzen, D., Crossley, D.A., Skaleric, U., 2008. Periodontal disease burden and pathological changes in organs of dogs. J. Vet. Dent. 25, 97–105.

Rawlinson, J.E., Goldstein, R.E., Reiter, A.M., Attwater, D.Z., Harvey, C.E., 2011. Association of periodontal disease with systemic health indices in dogs and the systemic response to treatment of periodontal disease. J. Am. Vet. Med. Assoc. 238, 601–609.

Serfass, P., Chetboul, V., Sampedrano, C.C., Nicolle, A., Benalloul, T., Laforge, H., Gau, C., Hébert, C., Pouchelon, J.L., Tissier, R., 2006. Retrospective study of 942 small-sized

dogs: Prevalence of left apical systolic heart murmur and left-sided heart failure, critical effects of breed and sex. J. Vet. Cardiol. 8, 11–18.
Warrick, J., Gorrel, C.A., 1997. More sensitive method of scoring calculus. Proceedings of the 11th Annual Veterinary Dental Forum, Denver, USA, 30 Oct-2 Nov, pp. 134–136.
Wolf, H.F., Rateitschak, E.M., Rateitschak, K.H., Hassel, T.M., 2005. Color atlas of dental medicine: periodontology. 3rd ed. Georg Thieme Verlag, Stuttgart.
Yamasaki, Y., Nomura, R., Nakano, K., Inaba, H., Kuboniwa, M., Hirai, N., Shirai, M., Kato, Y., Murakami, M., Naka, S., Iwai, S., Matsumoto-Nakano, M., Ooshima, T., Amano, A., Asai, F., 2012. Distribution and molecular characterization of *Porphyromonas gulae* carrying a new *fimA* genotype. Vet. Microbiol. 28, 196–205.

Biochemical and Biophysical Research Communications 466 (2015) 162–166

Contents lists available at ScienceDirect

Biochemical and Biophysical Research Communications

journal homepage: www.elsevier.com/locate/ybbrc

Role of a TPA-responsive element in hepcidin transcription induced by the bone morphogenetic protein pathway

Yohei Kanamori [a], Masaru Murakami [b], Tohru Matsui [a], Masayuki Funaba [a, *]

[a] Division of Applied Biosciences, Graduate School of Agriculture, Kyoto University, Kyoto 606-8502, Japan
[b] Laboratory of Molecular Biology, Azabu University School of Veterinary Medicine, Sagamihara 252-5201, Japan

ARTICLE INFO

Article history:
Received 21 August 2015
Accepted 28 August 2015
Available online 3 September 2015

Keywords:
Hepcidin
TPA-Responsive element
BMP
AP-1

ABSTRACT

Systemic iron balance is governed by the liver-derived peptide hormone hepcidin. The transcription of hepcidin is primarily regulated by the bone morphogenetic protein (BMP) and inflammatory cytokine pathways through the BMP-response element (BMP-RE) and STAT-binding site, respectively. In addition to these elements, we previously identified a TPA-responsive element (TRE) in the hepcidin promoter and showed that it mediated the transcriptional activation of hepcidin through activator protein (AP)-1 induced by serum. In the present study, we examined the role of TRE in the BMP-induced transcription of hepcidin in HepG2 liver cells. The serum treatment increased the basal transcription of hepcidin; however, responsiveness to the expression of ALK3(QD), a constitutively active BMP type I receptor, was unaffected. Consistent with these results, mutations in TRE in the hepcidin promoter decreased basal transcription, whereas responsiveness to the expression of ALK3(QD) remained unchanged. HepG2 cells significantly expressed AP-1 components in the basal state, whereas BMP did not up-regulate the expression of these components. The expression of c-fos enhanced the basal transcription of hepcidin as well as ALK3(QD)-mediated hepcidin transcription, whereas that of dominant-negative c-fos decreased hepcidin transcription. The results of the present study suggested that the *cis*-elements of the hepcidin promoter, BMP-RE and TRE, individually transmitted BMP-mediated and AP-1-mediated signals, respectively, whereas transcription was synergistically increased by the stimulation of BMP-RE and TRE.

1. Introduction

Hepcidin is a peptide hormone that regulates systemic iron balance. Under iron overload conditions, hepcidin is mainly produced in the liver, and inhibits intestinal iron absorption and iron release from macrophages, thereby decreasing iron concentrations in the blood [1,2]. The expression of hepcidin was also previously shown to be induced by inflammation caused by infection; this has been suggested as a host defense mechanism to reduce the availability of iron for pathogens [3,4]. The ability of hepcidin to decrease systemic iron levels is primarily regulated at its expression level; hepcidin mRNA levels are primarily controlled by transcription [1,2].

Accumulating evidence has indicated that the transcription of hepcidin is mainly regulated by the BMP-Smad and inflammatory cytokine-STAT pathways [1,2]. Under iron overload conditions, BMP6 produced in the liver binds to its receptors, consisting of type I receptor and type II receptors, which phosphorylate and activate Smad1/5/8 and subsequently stimulate the transcription of hepcidin via promoter elements, i.e., BMP-response element (BMP-RE) 1 located at nt −155 to nt −150 (nt + 1 is defined as the translational initiation site of hepcidin) and BMP-RE2 (nt −1678 to nt −1673) [5–8]. In contrast, inflammatory cytokines such as interleukin (IL)-6 and oncostatin M have been shown to induce the phosphorylation and activation of STAT3, which result in the transcriptional activation of hepcidin through binding to the STAT-binding site (STAT-BS, nt −143 to nt −134) [9,10].

We recently revealed that serum exhibited potency to stimulate the transcription of hepcidin [11]. A TPA-responsive element (TRE, *nt −133 to nt −127*), which has not yet been characterized, was found to play a role in the serum-induced transcription of hepcidin; mutations in TRE resulted in decreases in hepcidin promoter activity induced by serum. The inhibition of basal BMP activity or

Abbreviations: AP, activator protein; BMP, bone morphogenetic protein; BMP-RE, BMP-response element; IL, interleukin; STAT-BS, STAT-binding site; TRE, TPA-responsive element.

* Corresponding author. Division of Applied Biosciences, Graduate School of Agriculture, Kyoto University, Kitashirakawa Oiwakecho, Kyoto 606-8502, Japan.
E-mail address: mfunaba@kais.kyoto-u.ac.jp (M. Funaba).

http://dx.doi.org/10.1016/j.bbrc.2015.08.123
0006-291X/

mutations in BMP-REs also inhibited the serum-induced transcription of hepcidin, suggesting a functional interaction between BMP-REs and TRE. However, the involvement of TRE in hepcidin transcription mediated by the BMP pathway currently remains obscure. The aim of the present study was to determine the role of TRE in the transcriptional activation of hepcidin by the BMP pathway in luciferase-based reporter assays using the hepcidin promoter.

2. Materials and methods

2.1. Plasmids, cell culture, and reporter assays

The hepcidin reporter construct, i.e., the hepcidin promoter spanning nt −2018 to nt −35 inserted into the luciferase reporter vector pGL4 (hepcidin(-2018)-luc), and the mutated plasmids were previously described [11]. The expression plasmid for ALK3(QD) [12], a constitutively active BMP type I receptor, was kindly provided by Dr. K. Miyazono. HepG2 human hepatoma cells were cultured in DMEM supplemented with 10% heat-inactivated fetal bovine serum (FBS) and antibiotics. HepG2 cells (6×10^4 cells per well) seeded onto 24-well plates were transfected with hepcidin(-2018)-luc or the indicated reporter plasmid (0.5 μg), indicated expression plasmid, or empty plasmid (0.5 μg) and β-galactosidase expression plasmid under the control of a cytomegalovirus-derived promoter (pCMV-βGal, 0.1 μg) using polyethylenimine Max reagent (Polysciences, Warrington, PA, USA). Cells were harvested 30 h after transfection. In the ligand stimulation, transfected cells were cultured in DMEM with 0.2% FBS for 4 h, followed by a culture with or without 4 nM of BMP2 (R & D Systems, Minneapolis, MN, USA) or 2.5 nM of IL-6 (R & D Systems) for 24 h. In order to examine the effects of inhibiting the BMP pathway, transfected cells were treated with or without LDN-193189 (100 nM, Stemgent, San Diego, CA, USA), an inhibitor of the BMP type I receptor [13] for 24 h. Luciferase activity was normalized to β-galactosidase activity as previously described [14].

2.2. RNA isolation, RT-PCR, and RT-quantitative PCR

Total RNA isolation, cDNA synthesis, PCR, and real-time quantitative PCR (qPCR) were performed as described previously [15]. The following primers were used: 5′-ACTACCACTCACCCGCAGAC-3′ and 5′-CCAGGTCCGTGCAGAAGT-3′ for *c-fos*, 5′-AGGATAGTGCGATGTTTCAGG-3′ and 5′-GACTTCTCAGTGGGCTGTCC-3′ for *c-jun*, 5′-ATACACAGCTACGGGATACGG-3′ and 5′-GCTCGGTTTCAGGAGTTTGT-3′ for *junB*, 5′-CAGTTCCTCTACCCCAAGGTG-3′ and 5′-TTCTGCTTGTGTAAATCCTCCA-3′ for *junD*, 5′-CAGAGACAAAATATTTCCCATTTGT-3′ and 5′-CAGAGACAAAATATTTCCCATTTGT-3′ for *Fra1*, 5′-TTCTCCGGCTCCTTTTCTAA-3′ and 5′-ATTTCAGACAGGGCCAAAAA-3′ for *Fra2*, and 5′-AGCCACATCGCTCAGACAC-3′ and 5′-GCCCAATACGACCAAATCC-3′for *GAPDH*. The ΔΔCt method was used to normalize the levels of target transcripts to *GAPDH* levels [16].

3. Results and discussion

In order to evaluate the role of TRE in hepcidin transcription induced by the BMP pathway, the effects of serum and the expression of ALK3(QD) were examined in luciferase-based reporter assays using the hepcidin promoter (Fig. 1A). Consistent with previous findings [11,15], the treatment with serum or expression of ALK3(QD) increased luciferase expression, indicating the stimulation of hepcidin transcription. The ALK3(QD)-induced transcription of hepcidin was enhanced in the presence of serum, whereas the fold-induction of luciferase activity by the expression

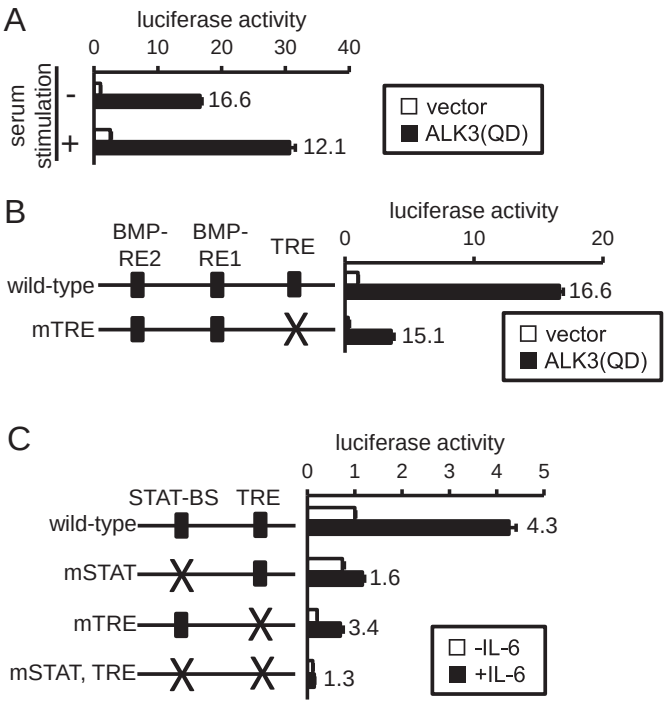

Fig. 1. TRE was required for the full activation of hepcidin transcription induced by the BMP pathway and IL-6 pathway. (A) HepG2 cells were transfected with hepcidin(-2018)-luc and pCMV-βGal with or without ALK3(QD). Cells were stimulated with or without 10% FBS for 24 h (B and C) HepG2 cells were transfected with the indicated reporter and pCMV-βGal. Cells were also co-transfected with or without ALK3(QD) (B) or treated with or without IL-6 (2.5 nM) for 24 h (C). Luciferase activity was normalized to β-galactosidase activity, and luciferase activity in cells in the absence of ALK3(QD) and FBS (A) or in cells transfected with the wild-type reporter, but not ALK3(QD) (B) or IL-6 (C) was set to 1. Results are shown as the mean ± SE (n = 3). The number at the side of the bar indicates fold-induction.

of ALK3(QD) was similar between cells treated with (12.1-fold) and without serum (16.6-fold). Mutations in TRE decreased the basal transcription of hepcidin, whereas responsiveness to ALK3(QD) expression was unchanged, i.e., the fold-induction in response to the stimulation of the BMP pathway was 16.6 for the wild-type reporter and 15.1 for the reporter with TRE mutations (Fig. 1B).

These results indicated the synergistic effects of TRE on the BMP-mediated transcription of hepcidin; although TRE was required for the basal transcription of hepcidin, TRE-mediated transcription did not modulate the efficiency of transcriptional activation by the BMP pathway.

We subsequently investigated the role of TRE in IL-6-mediated hepcidin transcription (Fig. 1C). A previous study revealed that IL-6 induced STAT3 phosphorylation and hepcidin transcription via STAT-BS [9], whereas another study showing that mutations in STAT-BS did not change responsiveness to IL-6 did not support these findings [17]. Since STAT-BS was located adjacent to TRE, we examined the role of TRE as well as STAT-BS in IL-6-induced hepcidin transcription (Fig. 1C). Mutations in STAT-BS blocked the transcriptional activation of hepcidin by IL-6, whereas TRE mutations did not affect fold-induction in response to the IL-6 treatment on hepcidin transcription. These results suggested that, similar to the regulation of BMP-induced hepcidin transcription, TRE did not affect the efficiency of IL-6-induced hepcidin transcription, but was required for the maximal transcription of hepcidin.

Activator protein (AP)-1 has been shown to bind to TRE and stimulate the transcription of its target genes [18,19]. We examined the expression of AP-1 components in cells treated with or without BMP2 (Fig. 2). All AP-1 components examined were significantly

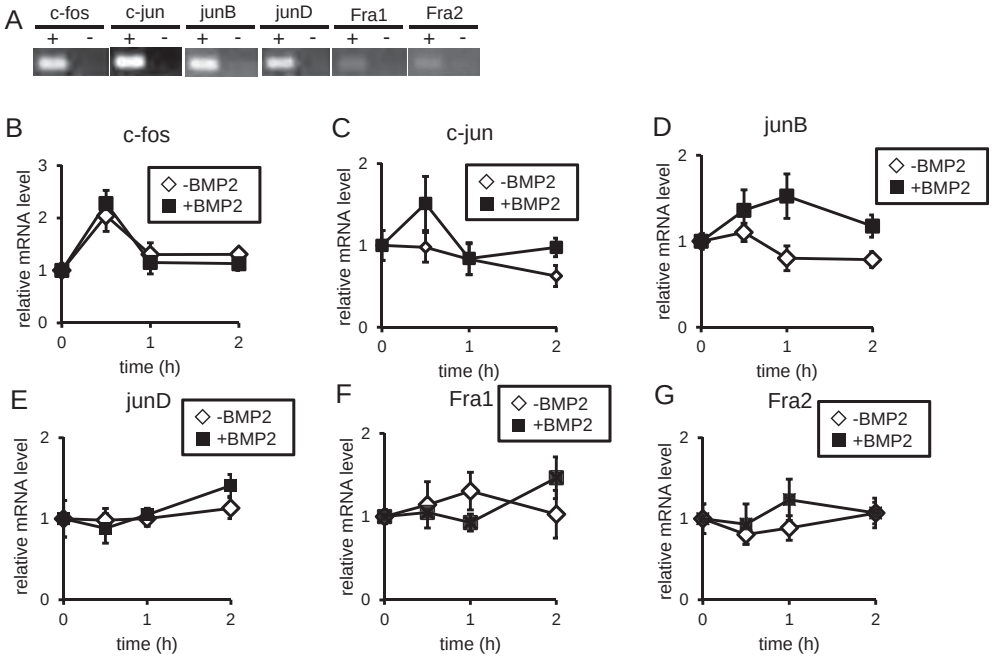

Fig. 2. BMP did not induce the expression of AP-1 components. (A) The basal expression of AP-1 components in HepG2 cells. Total RNA was isolated from basal HepG2 cells, and the expression of the indicated gene was evaluated by RT-PCR. cDNA was synthesized by a treatment with reverse transcriptase, and was used as the template of PCR (RT(+)). As the negative control, an equal amount of RNA was treated without reverse transcriptase, followed by PCR (RT(−)). (B–G) Time-course changes in the expression of AP-1 components in response to the BMP2 treatment. The expression of c-fos (B), c-jun (C), junB (D), junD (E), Fra1 (F), and Fra2 (G) was quantified and expression levels in cells before the treatment with BMP2 were set to 1. Results are shown as the mean ± SE (n = 4).

expressed under the basal condition (Fig. 2A), and BMP2 did not affect the expression of these components (Fig. 2B–G). Provided that TRE plays a role in the basal transcription of hepcidin, as shown in Fig. 1B and C, we suspected that at least one of the AP-1 components expressed in unstimulated cells was important for the basal transcription of hepcidin. Thus, the effects of the forced expression of c-fos, a representative AP-1 component, were examined (Fig. 3A). The expression of c-fos increased the basal transcription of hepcidin, which was blocked by the TRE mutations. ALK3(QD)-induced hepcidin transcription was further increased by the expression of c-fos, for which TRE in the promoter was required; enhancements in ALK3(QD)-induced hepcidin transcription by the expression of c-fos were not detected with mutations in TRE. The fold-induction of the transcription of the reporter with TRE mutations in response to ALK3(QD) expression was unaffected by c-fos expression, whereas that of the wild-type reporter was decreased by the overexpression of c-fos; the precise reason for the decrease observed in the fold-induction in the presence of overexpressed c-fos currently remains unknown, but may reflect the saturation of transcriptional activation induced by ALK3(QD) and c-fos. The involvement of c-fos in the basal transcription of hepcidin was also examined by the expression of dominant-negative c-fos; although dominant-negative c-fos inhibited the basal transcription of hepcidin, responsiveness to BMP2 remained unchanged (Fig. 3B).

In contrast to the effects of c-fos, the forced expression of c-jun did not affect the basal transcription of hepcidin, but decreased responsiveness to the stimulation of the BMP pathway, irrespective of TRE mutations (Fig. 3C). These results suggested that c-jun negatively regulated the BMP-mediated transcription of hepcidin through regions other than TRE in the hepcidin promoter. AP-1 components may regulate the BMP-mediated transcription of hepcidin differently.

The role of endogenous BMP activity in the TRE-mediated basal transcription of hepcidin was further evaluated using LDN-193189, an inhibitor of the BMP pathway [13] (Fig. 4A). In this case, we used reporter plasmids with the hepcidin promoter spanning nt −270 to nt −35, which included both BMP-RE1 and TRE; BMP-RE1 rather than BMP-RE2, which was previously shown to be involved in serum-induced hepcidin transcription [11]. The treatment with LDN-193189 decreased the expression of the wild-type reporter gene to one-fifth; transcriptional activity in cells treated with LDN-193189 was similar to that of the reporter gene with BMP-RE1 mutations in cells treated without LDN-193189. In addition, the transcriptional activity of the BMP-RE1-mutated reporter was insensitive to LDN-193189. Consistent with the results shown in Fig. 1B and C, the expression of the reporter with TRE mutations was lower than that of the wild-type reporter, and the treatment with LDN-193189 further decreased the transcription of the TRE-mutated reporter. The extent of this decrease was less than that induced by LDN-193189 on the transcription of the wild-type reporter; LDN-193189 decreased transcription by as much as one-half. Luciferase expression of the reporter with mutations in BMP-RE1 and TRE was similar to that of the TRE-mutated reporter in cells treated with LDN-193189, and the expression of the double mutated reporter was LDN-193189-insensitive. These results suggested that not only AP-1 expression in the steady state, but also endogenous BMP activity was required for the basal transcription of hepcidin. Our previous findings also suggested the necessity of endogenous BMP activity for the basal transcription of hepcidin [11]. The differential fold-inhibition in response to LDN-193189 between the wild-type reporter (0.21) and TRE-mutated reporter (0.47) may be explained by the regulation of molecules related to BMP signaling by AP-1 (Fig. 4B). For example, Smurf1 has been identified as a negative regulator of the BMP pathway through the degradation of BMP receptors [20], and the transcriptional activation of Smurf1 is known to be stimulated by AP-1 [21]. Liberated AP-1 resulting from TRE mutations may stimulate Smurf1 transcription, thereby decreasing endogenous BMP activity. As a result, the expression of the TRE-mutated reporter gene may be decreased more than luciferase expression resulting from the loss of TRE-

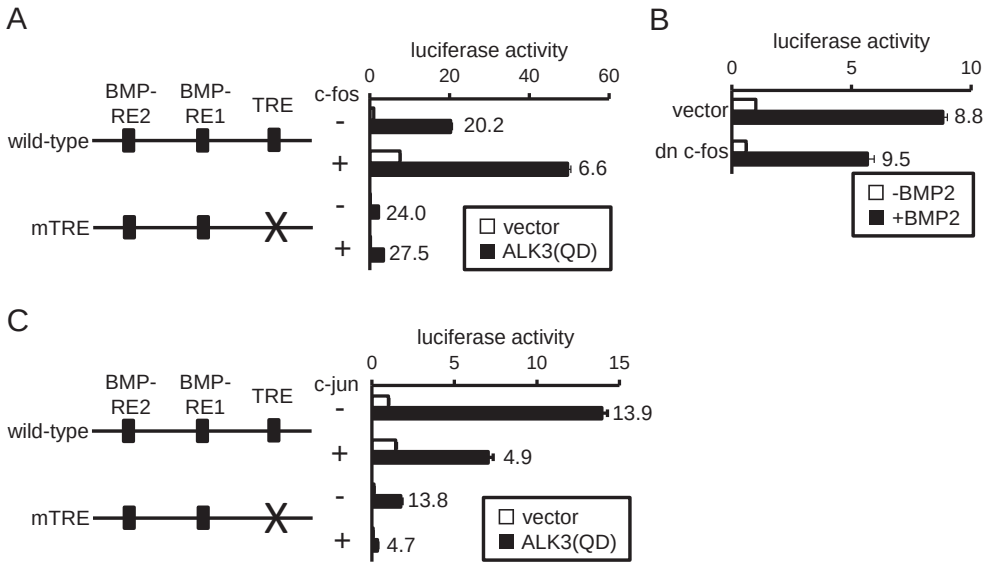

Fig. 3. AP-1 components regulated BMP-induced hepcidin transcription differently. (A and C) HepG2 cells were transfected with the indicated reporter and pCMV-βGal with or without c-fos (A) or c-jun (C). (B) HepG2 cells were transfected with hepcidin(-2018)-luc and pCMV-βGal with or without dominant-negative c-fos. Cells were stimulated with or without BMP2 (4 nM) for 24 h. Luciferase activity was normalized to β-galactosidase activity, and luciferase activity in cells transfected with the wild-type reporter, but not the AP-1 component (A and C) or in cells transfected without dominant-negative c-fos and BMP2 (B) was set to 1. Results are shown as the mean ± SE (n = 3). The number at the side of the bar indicates fold-induction.

mediated transcription itself, ultimately reducing responsiveness to LDN-193189. In any case, the results of the present study suggest that the *cis*-elements of the hepcidin promoter, BMP-RE and TRE, individually transmitted BMP-mediated and AP-1-mediated signals, respectively; however, transcription was synergistically increased by the stimulation of BMP-RE and TRE, indicating that BMP-RE and TRE are both required for the maximal transcription of hepcidin.

Two relationships are likely to exist between TRE- and BMP-RE-mediated hepcidin transcription; they individually or interactively regulate its transcription. When the transcription of hepcidin is individually regulated through TRE or BMP-RE, TRE- and BMP-RE-mediated transcription may be additively or synergistically increased. The first case is that TRE-mediated transcription is independent of and additive to BMP-induced transcription; the extent of decreases in BMP-induced hepcidin transcription by TRE mutations corresponds to those in basal transcription. The second case is that TRE-mediated transcription is independent of BMP-induced transcription, similar to the first case, whereas transcription is synergistically increased. In this case, responsiveness to the stimulation of the BMP pathway, which is evaluated by the fold-induction of hepcidin transcription, is not changed by TRE mutations, whereas basal transcription is decreased. Furthermore, when hepcidin transcription is interactively regulated through TRE and BMP-RE, BMP-induced hepcidin transcription may be blocked by TRE mutations; not only basal transcription but also responsiveness to the stimulation of the BMP pathway is reduced (the third case). The present study revealed that TRE is required for basal transcription of hepcidin, but does not affect efficiency of BMP-mediated transcription. We conclude that hepcidin transcription via TRE and BMP-RE is regulated by the mode indicated by the second case.

Various relationships are known to exist between AP-1 and the BMP pathway. BMP2 was previously found to block AP-1-dependent gene transcription in monocytes, suggesting the negative regulation of AP-1 activity by the BMP pathway [22]. A previous study demonstrated that BMP6 and AP-1 had reciprocal effects on miRNA-21 expression; AP-1 stimulated the transcription of miRNA-

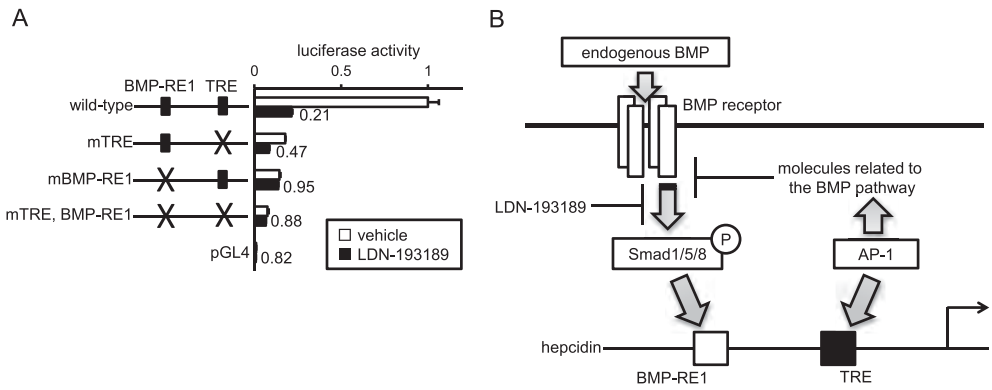

Fig. 4. Functional interaction between the BMP-responsive element and TRE in BMP-mediated hepcidin transcription. (A) HepG2 cells were transfected with the indicated reporter and pCMV-βGal. Cells were treated with or without LDN-193189 (100 nM) for 24 h. Luciferase activity was normalized to β-galactosidase activity, and luciferase activity in cells transfected with the wild-type reporter and treated with vehicle was set to 1. Results are shown as the mean ± SE (n = 3). The number at the side of the bar indicates fold-induction. (B) A proposed model for the role of TRE in hepcidin transcription mediated by endogenous BMP activity.

21, whereas BMP6 inhibited it by blocking the binding of AP-1 to the promoter of the miRNA-21 gene [23]. In contrast, a cooperative relationship has been reported between AP-1 and the BMP pathway; BMP4 promoted hematopoiesis in concert with AP-1, which was partly achieved through the up-regulation of junD expression [24]. Furthermore, BMP2 has been shown to stimulate GlcAT-1 gene transcription, which is mediated by AP-1 binding to the AP-1 binding site of the GlcAT-1 gene promoter; mutations in the AP-1 binding site completely blocked the BMP2-induced transcription of GlcAT-1 [25]. Similar to previous findings reported by Lee et al. [24] and Hiyama et al. [25], the results of the present study suggest a cooperative relationship between AP-1 and the BMP pathway for transcriptional activation. However, BMP2 did not induce AP-1 gene expression in the present study, and the basal expression of c-fos was important for the transcription of hepcidin. Furthermore, AP-1 did not affect the efficiency of transcriptional activation by the BMP pathway. The interactive mode between AP-1 and the BMP pathway depends on the regulated gene, which leads to the diverse effects of BMP and AP-1 in various physiological processes.

Conflict of interest

All authors have no conflict of interest.

Acknowledgments

We thank Dr. K. Miyazono for providing the plasmid for ALK3(QD). This work was partly supported by JSPS KAKENHI (15J02394 to Y.K.), research project grants from the Azabu University (2014-K-6 to M.M.) and from Tokyo Institute of Technology (to Y.K.).

References

[1] M.W. Hentze, M.U. Muckenthaler, B. Galy, C. Camaschella, Two to tango: regulation of mammalian iron metabolism, Cell 142 (2010) 24–38.
[2] D. Meynard, J.L. Babitt, H.Y. Lin, The liver: conductor of systemic iron balance, Blood 123 (2014) 168–176.
[3] M. Nairz, D. Haschka, E. Demetz, G. Weiss, Iron at the interface of immunity and infection, Front. Pharmacol. 5 (2014) 152.
[4] J. Arezes, G. Jung, V. Gabayan, E. Valore, P. Ruchala, P.A. Gulig, T. Ganz, E. Nemeth, Y. Bulut, Hepcidin-induced hypoferremia is a critical host defense mechanism against the siderophilic bacterium *Vibrio vulnificus*, Cell Host Microbe 17 (2015) 47–57.
[5] L. Kautz, D. Meynard, A. Monnier, V. Darnaud, R. Bouvet, R.H. Wang, C. Deng, S. Vaulont, J. Mosser, H. Coppin, M.P. Roth, Iron regulates phosphorylation of Smad1/5/8 and gene expression of Bmp6, Smad7, Id1, and Atoh8 in the mouse liver, Blood 112 (2008) 1503–1509.
[6] P.B. Yu, C.C. Hong, C. Sachidanandan, J.L. Babitt, D.Y. Deng, S.A. Hoyng, H.Y. Lin, K.D. Bloch, R.T. Peterson, Dorsomorphin inhibits BMP signals required for embryogenesis and iron metabolism, Nat. Chem. Biol. 4 (2008) 33–41.
[7] B. Andriopoulos Jr., E. Corradini, Y. Xia, S.A. Faasse, S. Chen, L. Grgurevic, M.D. Knutson, A. Pietrangelo, S. Vukicevic, H.Y. Lin, J.L. Babitt, BMP6 is a key endogenous regulator of hepcidin expression and iron metabolism, Nat. Genet. 41 (2009) 482–487.
[8] J. Truksa, P. Lee, E. Beutler, Two BMP responsive elements, STAT, and bZIP/HNF4/COUP motifs of the hepcidin promoter are critical for BMP, SMAD1, and HJV responsiveness, Blood 113 (2009) 688–695.
[9] D.M. Wrighting, N.C. Andrews, Interleukin-6 induces hepcidin expression through STAT3, Blood 108 (2006) 3204–3209.
[10] J. Kanda, T. Uchiyama, N. Tomosugi, M. Higuchi, T. Uchiyama, H. Kawabata, Oncostatin M and leukemia inhibitory factor increase hepcidin expression in hepatoma cell lines, Int. J. Hematol. 90 (2009) 545–552.
[11] Y. Kanamori, M. Murakami, T. Matsui, M. Funaba, The regulation of hepcidin expression by serum treatment: requirements of the BMP response element and STAT- and AP-1-binding sites, Gene 551 (2014) 119–126.
[12] T. Imamura, M. Takase, A. Nishihara, E. Oeda, J. Hanai, M. Kawabata, K. Miyazono, Smad6 inhibits signalling by the TGF-β superfamily, Nature 389 (1997) 622–626.
[13] P.B. Yu, D.Y. Deng, C.S. Lai, C.C. Hong, G.D. Cuny, M.L. Bouxsein, D.W. Hong, P.M. McManus, T. Katagiri, C. Sachidanandan, N. Kamiya, T. Fukuda, Y. Mishina, R.T. Peterson, K.D. Bloch, BMP type I receptor inhibition reduces heterotopic ossification, Nat. Med. 14 (2008) 1363–1369.
[14] M. Murakami, H. Kawachi, K. Ogawa, Y. Nishino, M. Funaba, Receptor expression modulates the specificity of transforming growth factor-β signaling pathways, Genes Cells 14 (2009) 469–482.
[15] Y. Kanamori, M. Murakami, T. Matsui, M. Funaba, Hepcidin expression in liver cells: evaluation of mRNA levels and transcriptional regulation, Gene 546 (2014) 50–55.
[16] E.M. Duran, P. Shapshak, J. Worley, A. Minagar, F. Ziegler, S. Haliko, I. Moleon-Borodowsky, P.A. Haslett, Presenilin-1 detection in brain neurons and FOXP3 in peripheral blood mononuclear cells: normalizer gene selection for real time reverse transcriptase pcr using the deltadeltaCt method, Front. Biosci. 10 (2005) 2955–2965.
[17] J. Truksa, P. Lee, E. Beutler, The role of STAT, AP-1, E-box and TIEG motifs in the regulation of hepcidin by IL-6 and BMP-9: lessons from human HAMP and murine Hamp1 and Hamp2 gene promoters, Blood Cells Mol. Dis. 39 (2007) 255–262.
[18] E. Shaulian, M. Karin, AP-1 as a regulator of cell life and death, Nat. Cell Biol. 4 (2002) E131–E136.
[19] J. Hess, P. Angel, M. Schorpp-Kistner, AP-1 subunits: quarrel and harmony among siblings, J. Cell Sci. 117 (2004) 5965–5973.
[20] G. Murakami, T. Watabe, K. Takaoka, K. Miyazono, T. Imamura, Cooperative inhibition of bone morphogenetic protein signaling by Smurf1 and inhibitory Smads, Mol. Biol. Cell 14 (2003) 2809–2817.
[21] H.L. Lee, T. Yi, K. Baek, A. Kwon, H.R. Hwang, A.S. Qadir, H.J. Park, K.M. Woo, H.M. Ryoo, G.S. Kim, J.H. Baek, Tumor necrosis factor-α enhances the transcription of Smad ubiquitination regulatory factor 1 in an activating protein-1- and Runx2-dependent manner, J. Cell. Physiol. 228 (2013) 1076–1086.
[22] E.M. Egorina, T.A. Sovershaev, J.B. Hansen, M.A. Sovershaev, BMP-2 inhibits TF expression in human monocytes by shutting down MAPK signaling and AP-1 transcriptional activity, Thromb. Res. 129 (2012) e106–e111.
[23] J. Du, S. Yang, D. An, F. Hu, W. Yuan, C. Zhai, T. Zhu, BMP-6 inhibits microRNA-21 expression in breast cancer through repressing deltaEF1 and AP-1, Cell Res. 19 (2009) 487–496.
[24] S.Y. Lee, J. Yoon, M.H. Lee, S.K. Jung, D.J. Kim, A.M. Bode, J. Kim, Z. Dong, The role of heterodimeric AP-1 protein comprised of JunD and c-Fos proteins in hematopoiesis, J. Biol. Chem. 287 (2012) 31342–31348.
[25] A. Hiyama, S.S. Gogate, S. Gajghate, J. Mochida, I.M. Shapiro, M.V. Risbud, BMP-2 and TGF-β stimulate expression of β1,3-glucuronosyl transferase 1 (GlcAT-1) in nucleus pulposus cells through AP1, TonEBP, and Sp1: role of MAPKs, J. Bone Min. Res. 25 (2010) 1179–1190.

Comparative Biochemistry and Physiology, Part A 185 (2015) 142–149

Contents lists available at ScienceDirect

Comparative Biochemistry and Physiology, Part A

journal homepage: www.elsevier.com/locate/cbpa

Adaptive expression of uncoupling protein 1 in the carp liver and kidney in response to changes in ambient temperature

Masaru Murakami [a,*], Masahiro Ohi [a], Shoko Ishikawa [a], Mitsuyuki Shirai [b], Hiroki Horiguchi [a], Yoshii Nishino [c], Masayuki Funaba [d,*]

[a] Laboratory of Molecular Biology, Azabu University School of Veterinary Medicine, Sagamihara 252-5201, Japan
[b] Laboratory of Veterinary Pharmacology, Azabu University School of Veterinary Medicine, Sagamihara 252-5201, Japan
[c] Department of Animal Medical Sciences, Faculty of Life Sciences, Kyoto Sangyo University, Kyoto 603-8555, Japan
[d] Division of Applied Biosciences, Graduate School of Agriculture, Kyoto University, Kyoto 606-8502, Japan

ARTICLE INFO

Article history:
Received 17 May 2014
Received in revised form 16 October 2014
Accepted 2 April 2015
Available online 10 April 2015

Keywords:
UCP1
PPAR
PGC-1
RXR
Ambient temperature
Carps

ABSTRACT

The expression of uncoupling protein (UCP1) is up-regulated in mammalian brown adipocytes during cold exposure. However, a previous study revealed that UCP1 was highly expressed in the liver of common carps, and that the hepatic expression of UCP1 was down-regulated during cold exposure. The present study examined the effects of temperature on the recovery of UCP1 expression levels and the expression of genes involved in UCP1 transcription in the livers and kidneys of common carps. The hepatic and renal expressions of UCP1 were decreased by acclimation from 22 °C to 8 °C, and a subsequent increase in the water temperature from 8 °C to 28 °C recovered the renal, but not hepatic expression of UCP1. Changes in the expression of peroxisome proliferator-activator receptor (PPAR) γ, retinoid X receptor (RXR) α and PPARγ co-activator (PGC)-1α, genes that are involved in the expression of UCP1 in mammals, with ambient temperature indicated that the expressions of PPARγ and RXRα, but not expression of PGC-1α was decreased in response to cold exposure; the hepatic and renal expressions of PPARγ and RXRα recovered to basal levels with the cessation of cold exposure, although this was not complete for hepatic expression of PPARγ. The results of the present study indicate that a unique regulatory mechanism is responsible for the hepatic and renal expressions of carp UCP1 during cold exposure and subsequent reacclimation, and is distinct from that in murine brown adipocytes.

1. Introduction

Uncoupling protein (UCP) 1 increases proton leakage from the mitochondrial inner membrane, resulting in a decreased proton motive force, which leads to increased oxygen consumption and heat generation without the concomitant generation of ATP. The restricted expression of UCP1 in mammalian brown adipocytes located in brown and white fat renders these cells responsible for non-shivering heat production (Cannon and Nedergaard, 2004).

The expression of UCP1 and its orthologs has been detected not only in placental mammals, but also in ectothermic vertebrates (Gesta et al., 2007). UCP1 was identified in the common carp (*Cyprinus carpio*), an ectothermic vertebrate, based on the conserved synteny within the mammalian lineage (Jastroch et al., 2005). It was found to be highly expressed in the liver and to a lesser extent in the kidney. The expression of UCP1 could not be detected in carp adipose tissues, which suggested that the role of UCP1 in energy expenditure in fish differed from that in placental mammals (Jastroch et al., 2005).

The expression of UCP1 in murine brown fat was previously shown to be up-regulated in response to cold exposure (Puigserver et al., 1998; Barbatelli et al., 2010), whereas hepatic UCP1 transcript levels were lower in the common carp acclimated at 8 °C for 4 weeks than in those kept at 20 °C (Jastroch et al., 2005). Similar responses were observed in gilthead sea bream (*Sparus aurata*); expression levels of hepatic UCP1 were lower in winter than in summer and fall (Bermejo-Nogales et al., 2010). The mechanism underlying the regulation of fish UCP1 expression currently remains unknown. In addition, changes in UCP1 expression upon recovery from cold exposure have not experimentally been examined. Furthermore, studies are needed to elucidate the relationship between the expression of UCP1 and non-shivering heat production in ectothermic vertebrates.

In murine brown fat, the transcription of UCP1 is regulated by several key molecules including the tissue-restricted transcription factors peroxisome proliferator-activator receptor (PPAR) α, β/δ and γ, thyroid hormone receptor (TR) α, and the transcriptional co-activator PPARγ co-activator (PGC)-1α (Puigserver et al., 1998; Barbera et al., 2001;

* Corresponding authors.
E-mail addresses: murakami@azabu-u.ac.jp (M. Murakami), mfunaba@kais.kyoto-u.ac.jp (M. Funaba).

http://dx.doi.org/10.1016/j.cbpa.2015.04.003
1095-6433/

Cannon and Nedergaard, 2004; Cao et al., 2004; Komatsu et al., 2010; Seebacher and Glanville, 2010). In addition, PGC-1β, a molecule structurally related to PGC-1α, is known to be highly expressed in murine brown fat (Lin et al., 2002; Seale et al., 2007). PPAR and TR heterodimerize with retinoid X receptor (RXR), and the formed complex regulates transcription of target genes including UCP1 and PGC-1 (Cannon and Nedergaard, 2004; Evans and Mangelsdorf, 2014). Furthermore, a transcription factor, cAMP responsive element binding protein (CREB) is phosphorylated and activated by protein kinase A, which leads to stimulation of UCP1 transcription (Cannon and Nedergaard, 2004). The expression levels of nuclear respiratory factor 1 (NRF1), which stimulates mitochondrial biogenesis by interacting with PGC-1α (Scarpulla, 2008), have been closely related to those of UCP1, PPARδ, and PGC-1α during cold exposure in murine brown fat (Seebacher and Glanville, 2010).

We hypothesized that regulation of carp UCP1 expression is similar to that established in murine UCP1 expression, although response to cold exposure is different between common carps and mice. As the first step to clarify regulation of fish UCP1 expression, we isolated not only 5′ flanking region of carp UCP1 gene but also coding region of carp mRNA for several molecules involved in regulation of murine UCP1 expression partially, because the information has not yet been available yet. By use of the information, we examined the effects of ambient temperature on expression levels of UCP1 and the candidates to regulate UCP1 expression in common carps.

2. Materials and methods

2.1. Animals

A total of 30 common carps aged 7 months were used. These carps were fed with commercial pellets *ad libitum* with a 12-h light/12-h dark cycle. They were kept in a temperature-controlled recirculating water system maintained at 22 °C for at least 2 weeks (day 0). The water temperature was gradually lowered to 8 °C over 3 days. After 14 days at 8 °C (days 3–17), the water temperature was gradually returned to 28 °C over 3–5 days and kept at 28 °C for 14 days (days 21–35). Carps were sacrificed on days 0, 17, and 35, and the livers and kidneys were removed.

2.2. RNA isolation and RT-quantitative real-time PCR

RNA isolation and reverse transcription (RT)-quantitative real-time PCR (qPCR) analyses were performed as described previously (Murakami et al., 2008; Asai et al., 2014). Total RNA was isolated from the livers and kidneys of carps using QuickGene RNA tissue kit S (Wako, Osaka, Japan) in QuickGene-810 (Wako, Osaka, Japan), an automatic nucleic acid extraction system, according to the manufacturer's protocol. The concentration of RNA was determined from absorbance at 260 nm. In RT-qPCR analyses, cDNA was synthesized using the high capacity cDNA reverse transcription kit with an RNase inhibitor (Life Technologies, Carlsbad, CA, USA), according to the manufacturer's protocol. The cDNA corresponding to 5 ng of total RNA was used as a template of qPCR; the qPCR was performed using KAPA SYBR FAST Universal qPCR Master Mix (Kapa Biosystems, Boston, MA, USA) in Thermal Cycler Dice Real Time System TP800 (Takara, Otsu, Japan), according to the manufacturer's protocol. The qPCR profile was as follows: after denaturing for 30 s at 95 °C, 40 cycles consisted of 5 s at 95 °C and 30 s at 60 °C. The oligonucleotide primers for qPCR are shown in Table 1. After 40 cycles of RT-qPCR, the dissociation (melting) curve of the products was examined by changes in the ramp temperature from 60 °C to 95 °C. Each sample showed a single peak, suggesting the expected PCR products. The mRNA levels were expressed relative to EF1α mRNA levels, and the expression level in the liver of control carps was set at 100.

2.3. Isolation of 5′ flanking region of UCP1 gene from carps

The 5′ flanking region of carp UCP1 gene was isolated by two rounds of PCR; we designed 4 PCR primers. Because of lack of information on 5′ flanking region of carp UCP1 gene, forward primers were designed on the basis of information of zebrafish UCP1 gene; 5′-gttgtagttttgg tttattacacaagg-3′ named as primer A that corresponds to nt −4500 to nt −4474 of zebrafish UCP1 gene (GenBank accession number NC_007112) and 5′-taaagtcctgctgcagtggaaacag-3′ as primer B that is nt −3000 to nt −2976 of zebrafish UCP1 gene. The reverse primers were designed based on the carp UCP1 gene (AY461434), *i.e.*, 5′-gatggagtgacaggatgatgcctcgtg-3′ (nt +45 to nt +19) and 5′-ctgacagctgtgattgagttcctctg-3′ (nt +74 to nt +49) as primer C and primer D, respectively. The first round PCR was performed using genomic DNA, which was isolated from carp muscle cells, as a template DNA as well as primers A and D; PCR was conducted in a total volume of 50 μL by use of PrimeSTAR GXL DNA Polymerase that is a high fidelity polymerase (TaKaRa). The PCR profile consisted of 35 cycles of denature for 10 s at 98 °C, annealing for 15 s at 55 °C and extension for 4 min at 68 °C. The second round of PCR re-amplified using one-fiftieth of the PCR products as the template, and primers B and C with the same PCR profile. The products of the nested-PCR were electrophoresed in agarose gels, followed by ethidium bromide staining and visualization under ultraviolet light. A significant band was detected at ~2800 bp, which was within the range of expected size. The band was excised from the gels, and the nucleotide sequence was determined by direct sequencing and deposited in GenBank (LC003596). To examine the validity of sequence, PCR was performed by use of genomic DNA as a template DNA and PCR primers spanning nt −434 to nt −412 (5′-tttctgagctc ctttaatgcatc-3′) and nt +930 to nt +908 (5′-gcggtgtccagaggg aaggtgac-3′), and the nucleotide sequence of PCR product was confirmed by direct sequencing. The 5′ flanking region of carp, human, mouse, rat and zebrafish UCP gene was compared by use of Pairwise Sequence Alignment of EMBOSS (http://emboss.open-bio.org/).

Table 1
Nucleotide sequence of primers used in RT-qPCR analyses.

Gene	Forward primer	Reverse primer	GenBank accession number
CREB	5′-ctcagcagattgccaccttgg-3′	5′-gggcagctgaactaaggtcac-3′	LC000680[1]
EF1α	5′-atgcggtggaatcgacaa-3′	5′-cagagagcaatgtcaatggtg-3′	AF485331
NRF1	5′-aagccctgaggactattgtt-3′	5′-gctcctgtgccaacctgtat-3′	AB924641[1]
PGC-1α	5′-tgcctgagcttgacctctct-3′	5′-cgtcttcatccactgggatac-3′	AB767302[1]
PGC-1β	5′-tggggaagaggaggtctgc-3′	5′-ccgtccaggctgtctgtg-3′	AB767303[1]
PPARα	5′-gggaaagagcagcacgagtcc-3′	5′-ggtaggcttcatgcatctgtc-3′	FJ849065
PPARβ/δ	5′-tggctttgtggatctcttcc-3′	5′-gatctcgccgaaaggtttgc-3′	LC000683[1]
PPARγ	5′-aggcaactctacgagtcctatct-3′	5′-agttgatcatctgctcgccttcc-3′	FJ849064
RXRα	5′-cacccaatgatccagtcacaaaca-3′	5′-agctcattccatcctgctcgtaga-3′	LC000682[1]
TRα	5′-aatcacccgcaaccagtgccag-3′	5′-tcgatcagacgcctcttggcc-3′	LC000681[1]
UCP1	5′-cgccttctacaaaggtttcg-3′	5′-cgaatgacacgaacatcacc-3′	AY461434

[1] Nucleotide sequence was determined in this study.

2.4. Isolation of PGC-1α, PGC-1β, PPARβ/δ, TRα, RXRα, CREB, and NRF1 mRNA from carp livers

To isolate PGC-1α, PGC-1β, PPARβ/δ, TRα, RXRα, CREB, and NRF1 cDNA from carp livers, 1 μg of the recovered RNA was treated with RNase-free DNase I (Invitrogen) to remove residual DNA. RNA was subsequently reverse-transcribed in a 21 μl volume reaction using the oligo(dT) primer and Superscript III First-Strand Synthesis System for RT-PCR (Invitrogen) to generate first-strand cDNA (Murakami et al., 2008).

Based on the nucleotide sequence of the PGC-1α mRNAs of goldfish (*Carassius auratus*, FJ710611 and EU426842), zebrafish (*Danio rerio*, FJ710604), grass carp (*Ctenopharyngodon idella*, JN195739), and golden shiner (*Notemigonus crysoleucas*, FJ710606), the following PCR primers were designed to isolate PGC-1α cDNA: 5′-atggcgtgggacaggtgtaatc-3′ and 5′-tcaaaggaagtggcaagatggt-3′. To isolate PGC-1β mRNA, the following PCR primers were designed based on the nucleotide sequence of zebrafish PGC-1β (XM_009291061): 5′-atggcggactgcgcttcactgttagatg-3′ and 5′-agacccccgactccgtcctcaacaat-3′. To isolate PPARβ/δ mRNA, the PCR primers, 5′-cagtgcaccacagtggaaactg-3′ and 5′-gaatgccatcctgaatctgctc-3′, were designed based on the nucleotide sequence of zebrafish PPARδb (NM_131468 and XM_683192). The mRNA of TRα was isolated on the bases of nucleotide sequences of goldfish TRα1 (AY973629) and TRα2 (DQ172902) and zebrafish TRαa (NM_131396) by use of 5′-gcatcacatgtgagggctgcaa-3′ and 5′-tctccatacagcagcctttcag-3′ as PCR primers. The mRNA of RXRα was isolated on the bases of nucleotide sequences of goldfish RXRα (AY197562) and zebrafish RXRαa (NM_001161551 and XM_001923838) by use of 5′-cagaagtgtttggccatgggc-3′ and 5′-gcaaaccttccaggttgttcag-3′ as PCR primers. The mRNA of CREB was isolated on the bases of nucleotide sequences of goldfish CREB1 (AM886438) and zebrafish CREB1 (NM_001161551 and XM_001923838) by use of 5′-caggagcagatgtccagcagg-3′ and 5′-gcatactgcaggatggtggtg-3′ as PCR primers. As for NRF1 mRNA, the following PCR primers were designed based on the nucleotide sequence of zebrafish NRF1 (XM_005164709) and Japanese pufferfish (*Takifugu rubripes*) NRF1-like isoform 1 (XM_003972802): 5′-caggcccagctccgagcgttcat-3′ and 5′-ggccacagcctgcgtggcctct-3′. Using these primers, cDNA was isolated from common carp livers, and agarose gel electrophoresis of the PCR products indicated bands with an expected size of ~920 bp for PGC-1α, ~350 bp for PGC-1β, ~270 bp for PPARβ/δ, ~440 bp for TRα, ~450 bp for RXRα, ~440 bp for CREB, and ~560 bp for NRF1. The nucleotide sequence of the PCR product was determined by direct sequencing.

2.5. Statistical analyses

Data are expressed as the mean ± SE. Data were log-transformed to provide an approximation of a normal distribution before analysis. Differences between groups in each tissue were analyzed by Tukey's multiple comparison test. $P < 0.05$ was considered significant.

3. Results

The expression of UCP1 was evaluated in the livers and kidneys of common carps acclimatized at various temperatures (Fig. 1). A decrease in the water temperature from 22 °C to 8 °C significantly reduced the expression of UCP1 in the liver and kidney within 14 days. Although increasing the water temperature from 8 °C to 28 °C did not change the hepatic expression of UCP1, the renal expression of UCP1 returned to basal levels. Consistent with previous findings (Jastroch et al., 2005), the expression level of UCP1 was higher in the liver than in the kidney.

Expression of mammalian UCP1 gene is transcriptionally regulated (Cannon and Nedergaard, 2004). We determined nucleotide sequence of 5′ flanking region of carp UCP1 gene, because it has not yet been available. Whole genome sequence of common carps is not known, and, therefore, we isolated 2634 bases upstream sequence of the

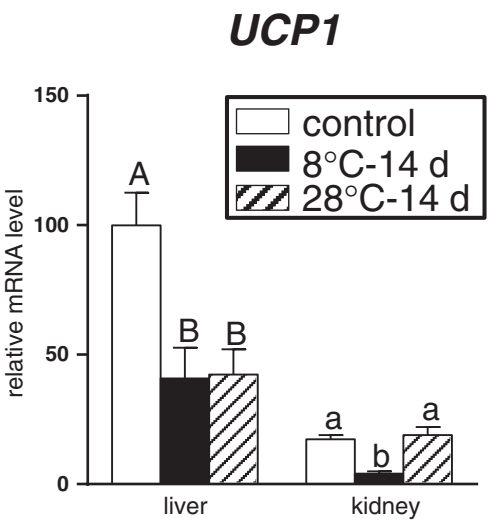

Fig. 1. UCP1 expression in the livers and kidneys of common carps acclimated to various temperatures. Common carps acclimated at 22 °C were subjected to cold exposure for 14 days at 8 °C. They were then acclimated at 28 °C for 14 days. The gene transcript levels of UCP1 were determined by RT-qPCR and are expressed relative to the expression of EF1α, with the hepatic level determined on day 0 (control) set to 100. Data shown are the mean ± SE (n = 10). A, B and a, b: $P < 0.05$.

putative transcriptional initiation site of carp UCP1 through the nested-PCR strategy in reference to the nucleotide sequence of 5′ flanking region of zebrafish UCP1 gene (Fig. 2A). When genomic DNA from three carps was individually used as the template DNA, comparable results were obtained (data not shown). The validity of the isolated nucleotide sequence was also determined by the expected amplification of genomic DNA using PCR primers designed within the region of determined nucleotide (data not shown).

The nucleotide sequence indicated the lack of the first 18 bases (5′-tggatccaaagaattcgg-3′) within 5′ untranslated region of carp UCP1 mRNA in GenBank accession number AY461434, and three nucleotide substitutions, T, C, and T instead of A, G, and G of the 20th, 22nd, and 25th nucleotides, respectively. We performed RT-PCR using liver cDNA as the template DNA and the first 22 bases of AY461434 (primer E: 5′-tggatccaaagaattcggcacg-3′) as the forward primer and primer for the RT-qPCR as the reverse primer, and found no band (Fig. 2B, lanes 1–3). In contrast, when the first 22 bases overlapping to AY461434 determined in this study (primer F: 5′-ctccagtcatcatcctgtcact-3′), *i.e.*, corresponding region spanning the 19th nucleotide to the 40th nucleotide of AY461434, were used as the forward primer, we detected the PCR product with the expected size (Fig. 2B, lanes 5–7). Therefore, we conclude that the 19th nucleotide of DNA sequence recorded in AY461434 is the putative transcriptional initiation site of UCP1 gene in common carps used in this study; the 19th nucleotide is designated as nt + 1. The nucleotide sequence near 5′′ untranslated region of carp UCP mRNA may be different between the strains. The nucleotide sequence has limited homology with that of 5′ flanking region of human, mouse, and rat UCP1 genes (Fig. 2C). The less homology of the nucleotide sequence was also detected between carps and zebrafish.

Previous studies identified and characterized the brown adipose tissue (BAT)-specific enhancer region (~220 bp) around nt −2500 upstream of murine UCP1 transcriptional initiation site (Kozak et al., 1994; Rim and Kozak, 2002). The region plays a critical role in the regulation of UCP1 that includes responsive element to PPAR, TR, and CREB (Cannon and Nedergaard, 2004). Homology search indicated no similarity between the murine BAT-specific enhancer and the carp UCP1 promoter (data not shown). In addition, there was no consensus responsive element to PPAR, TR, and CREB within the carp UCP1 promoter, *i.e.*, direct repeats (DR) 1 and 2 (core sequence 5′-agg(a/t)ca-3′ separated by one and two base-pairs, respectively) for PPAR (Evans and Mangelsdorf,

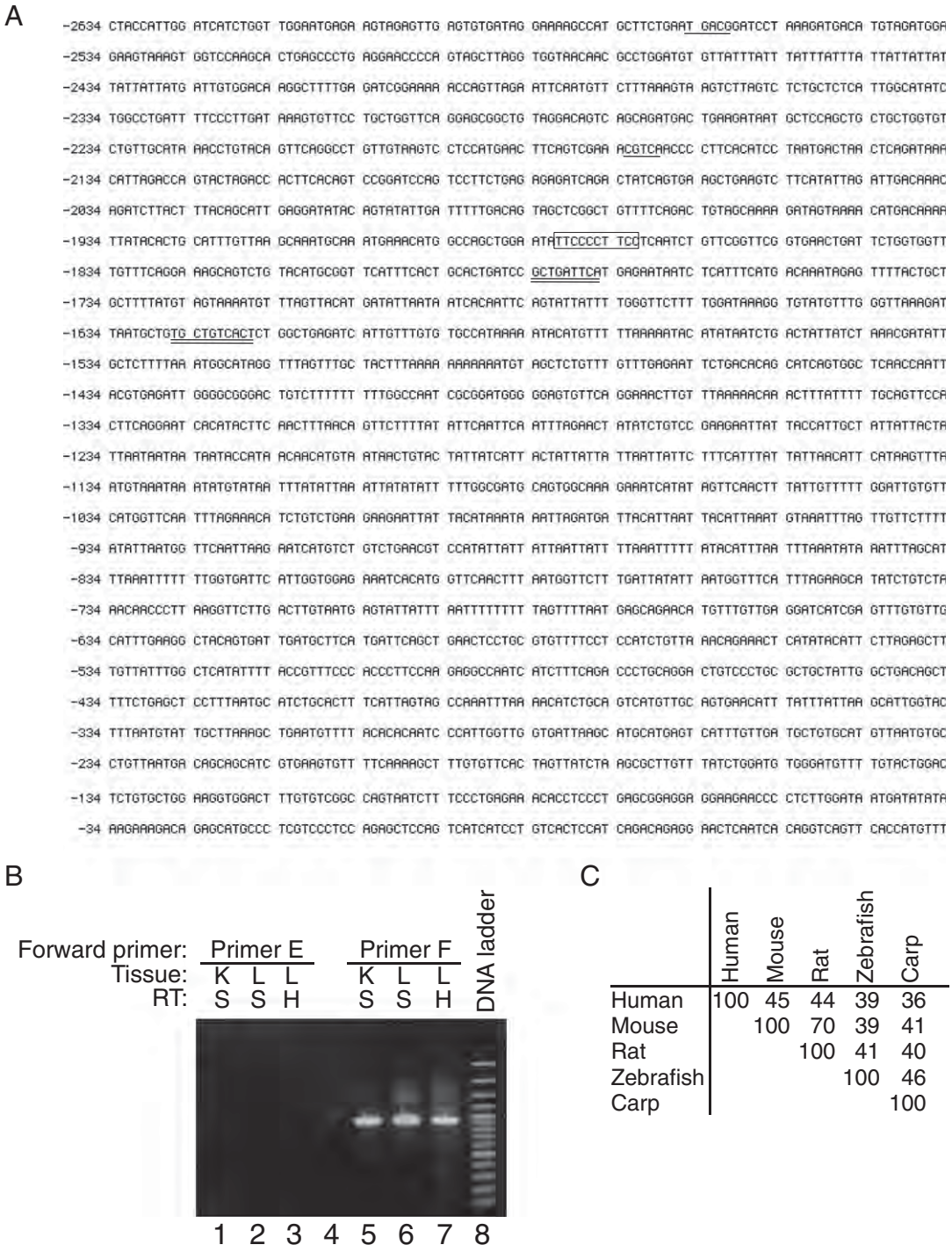

	Human	Mouse	Rat	Zebrafish	Carp
Human	100	45	44	39	36
Mouse		100	70	39	41
Rat			100	41	40
Zebrafish				100	46
Carp					100

Fig. 2. Nucleotide sequence of the 5′ flanking region of the carp UCP1 gene. (A) Nucleotide sequence of the 5′ flanking region of the carp UCP1 gene. The nt +1 is defined as putative transcriptional-initiation site. Possible CRE, BRE-1, and NF-E2 recognition sequences are shown with underline, box, and double underline, respectively. (B) RT-PCR analyses were performed using cDNA prepared from kidney (K: lanes 1 and 5) and liver (L: lanes 2, 3, 6 and 7) as the template. The cDNA was prepared by Superscript III First-Strand Synthesis System (S) to isolate full-length of carp UCP1 mRNA (lanes 1, 2, 5 and 6) or by high capacity cDNA reverse transcription kit (H: lanes 3 and 7). Lanes 1–3 and 5–7 indicate PCR products using primer E and the reverse primer for RT-qPCR, and primer F and the reverse primer for RT-qPCR, respectively. Lanes 4 and 8: negative control and 100-bp DNA ladder, respectively. (C) Homology between nucleotide sequences spanning nt −2634 to nt −1 of UCP1 gene of various animal species.

2014), DR-4 for TR (Evans and Mangelsdorf, 2014), and cAMP response element (5′-tgacgtca-3′) for CREB (Montminy, 1997). We also searched specific sequence motifs present in the murine BAT-specific enhancer region, and found two half-site consensus sequence of CRE (5′-cgtca-3′ and its complementary sequence 5′-tgacg-3′, Fig. 2A, underline), two contiguous TTCC motifs within brown adipocyte-regulatory element 1 (BRE-1, Fig. 2A, box), and two possible NF-E2 sites (Fig. 2A, double underline).

The expression of genes involved in the expression of UCP1 in mammals (Puigserver et al., 1998; Barbera et al., 2001; Cannon and Nedergaard, 2004; Cao et al., 2004; Komatsu et al., 2010; Seebacher and Glanville, 2010) was examined next. Sequence information for

common carp PGC-1α, PGC-1β, PPARβ/δ, TRα, RXRα, CREB, and NRF1 cDNAs was unavailable; thus, we isolated gene transcripts from the liver of the common carp. The partial amino acid sequences deduced from the nucleotide sequences exhibited sequence similarity to fish PGC-1α, PGC-1β, PPARβ/δ, TRα, RXRα, CREB, and NRF1, respectively (Fig. 3), which suggested that these are orthologs of respective genes

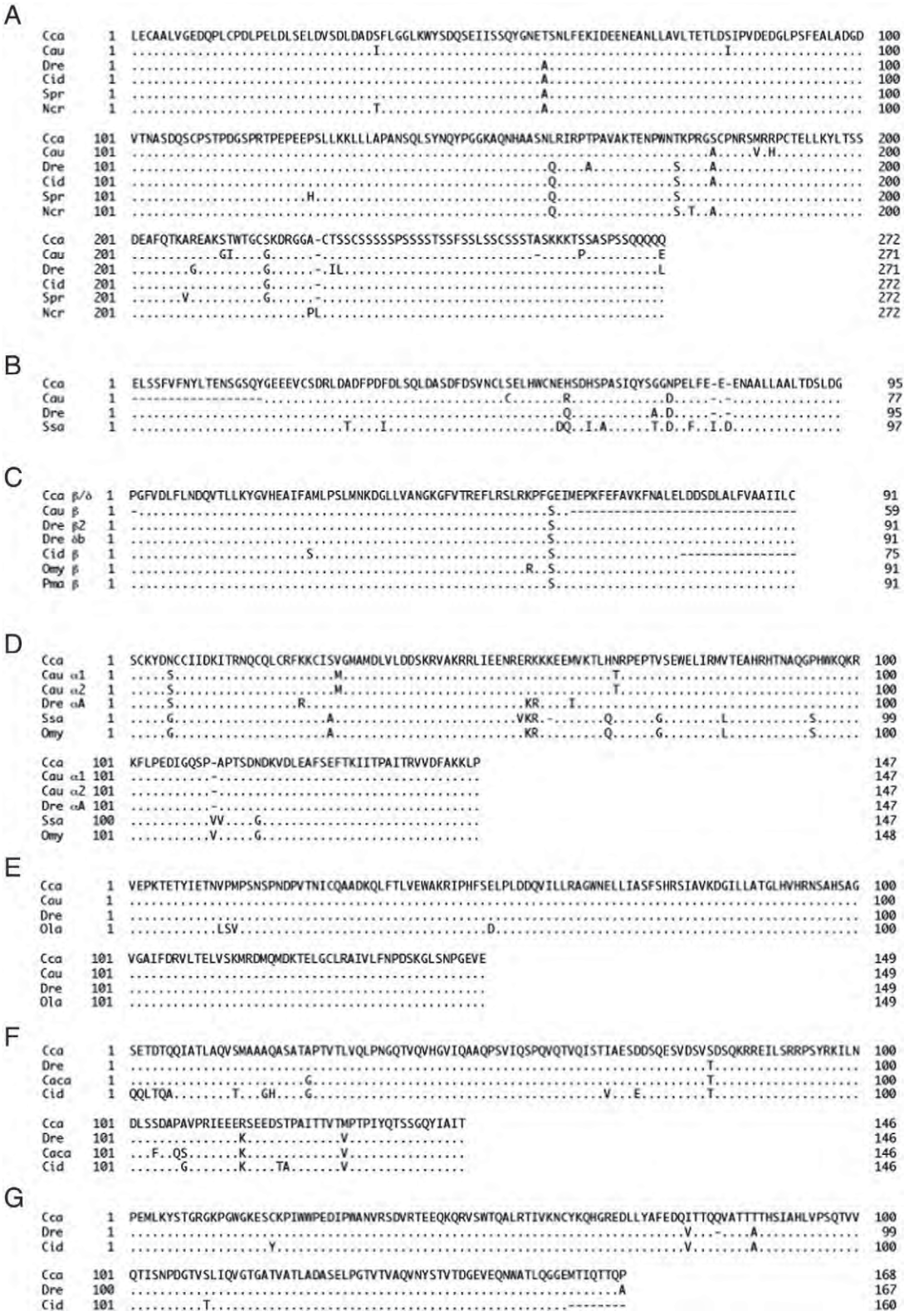

Fig. 3. Comparison of the amino acid sequence deduced from the nucleotide sequence of PGC-1, PPARβ/δ, TRα, RXRα, CREB, and NRF1. The partial gene transcripts of PGC-1α, PGC-1β, PPARβ/δ, TRα, RXRα, CREB, and NRF1 were isolated and sequenced. The deduced amino acid sequences of PGC-1α (A), PGC-1β (B), PPARβ/δ (C), TRα (D), RXRα (E), CREB (F), and NRF1 (G) were compared to that of fish PGC-1α, PGC-1β, PPARβ/δ, TRα, RXRα, CREB, and NRF1, respectively. The dot stands for the same amino acid as that in Cca. Cca: *Cyprinus carpio*, Cau: *Carassius auratus*, Dre: *Danio rerio*, Cid: *Ctenopharyngodon idella*, Spr: *Schizothorax prenanti*, Ncr: *Notemigus crysoleucas*, Ssa: *Salmo salar*, Caca: *Carassius carassius*, Omy: *Oncorhynchus mykiss*, Pma: *Pagrus major*, Ola: *Oryzias latipes*. β/δ, β, and β2 and δb: PPARβ/δ, PPARβ, PPARβ2, and PPARδb, respectively. α1, α2, and αA: TRα1, TRα2, and TRαA, respectively.

in common carps. Since fish PGC-1α, PGC-1β, PPARβ/δ, TRα, RXRα, CREB, and NRF1 consist of ~878, ~495, ~517, ~421, ~343, ~318, and ~514 amino acids, respectively, the gene transcripts clarified in the present study are expected to correspond to approximately one-fifth of PGC-1β and PPARβ/δ, one-third of PGC-1α, TRα, and NRF1, and half of RXRα and CREB of the coding regions.

Unlike the hepatic and renal expressions of UCP1, the expression level of PGC-1α did not decrease with a reduction in the water temperature from 22 °C to 8 °C; the renal expression of PGC-1α was increased by cold exposure (Fig. 4A). The hepatic expression of PGC-1α remained unchanged by increases in the water temperature from 8 °C to 28 °C, whereas the cold-induced expression of renal PGC-1α returned to basal levels with increases in the water temperature from 8 °C to 28 °C. Decreasing the water temperature from 22 °C to 8 °C decreased the expression of PGC-1β in the kidney, but not significantly in the liver (Fig. 4B). The renal expression of PGC-1β tended to return to basal levels with increases in the water temperature from 8 °C to 28 °C.

The hepatic expression of PPARα was unaffected by cold exposure, but decreased with increases in the water temperature from 8 °C to 28 °C (Fig. 5A). In contrast, changes in the water temperature did not affect the renal expression of PPARα. Expression of hepatic and renal PPARβ/δ was increased by cold exposure, and the increase in water temperature from 8 °C to 28 °C decreased the expressions; hepatic expression levels at 28 °C were lower than those at 22 °C (Fig. 5B). Both the hepatic and renal expressions of PPARγ were markedly reduced with decreasing water temperature from 22 °C to 8 °C, and the cessation of cold exposure returned to these expression levels back to basal levels; however, hepatic expression was not completely recovered (Fig. 5C). Expression of renal TRα was decreased during the cold exposure, and the cessation of cold exposure further decreased the expression; hepatic expression of TRα was also decreased by the increase in water temperature from 8 °C to 28 °C (Fig. 5D). Similar to the regulatory expression of PPARγ, RXRα expressions in the liver and kidney were significantly decreased during cold exposure, and the re-warming resulted in return to the basal expression levels (Fig. 5E).

Cold exposure did not affect expression levels of hepatic and renal expressions of CREB, but the increase in water temperature from 8 °C to 28 °C significantly decreased renal CREB expression (Fig. 6A). The cold exposure increased the hepatic and renal expression levels of NRF1, and an increase in the water temperature from 8 °C to 28 °C decreased expression levels; expression levels at 28 °C were lower than those at 22 °C (Fig. 6B).

4. Discussion

This study revealed six aspects of the regulation of the hepatic and renal expressions of UCP1 in carps in response to changes in ambient temperature 1) both the hepatic and renal expressions of UCP1 were down-regulated by cold exposure, 2) expression levels in the kidney, but not in the liver recovered with the cessation of cold exposure, 3) water temperature-related changes in the renal expression of UCP1 paralleled those in the renal expression of PPARγ and RXRα, 4) the cold-induced down-regulation of hepatic PPARγ partially recovered with the cessation of cold exposure, 5) contrary to hepatic PPARγ and RXRα expressions, expressions of hepatic and renal PPARβ/δ and NRF1 were up-regulated during cold exposure, and the cessation of cold exposure returned the expression, and 6) the expression of hepatic and renal PGC-1α was not decreased by cold exposure. Of these, the down-regulation observed in the hepatic expression of UCP1 during cold exposure was consistent with previous findings (Jastroch et al., 2005); considering that the common carp is an ectothermic animal, down-regulation of UCP1, a drive engine of non-shivering thermogenesis, during cold exposure is reasonable. The other 5 points were not evaluated in the study by Jastroch et al. (2005). Our results confirm that regulatory expression of carp UCP1 during cold exposure and subsequent recovery from cold exposure is distinct from that of mammalian UCP1 expression, but suggests that expression level of carp UCP1 is partly but not completely related to that of molecules involved in regulation of mammalian UCP1 expression. The present study has provided a novel insight into the regulatory expression of carp UCP1.

Although expression levels of UCP1 were closely related to those of molecules regulating UCP1 expression in murine brown adipocytes during the changes in ambient temperature in common carps, the detailed regulation was distinct between murine brown adipocytes and carp tissues such as liver and kidney. In murine brown adipocytes, the cold-induced stimulation of the sympathetic nervous system and accompanying β3 adrenergic receptor activation induce the transcription of PGC-1α, which in turn stimulates UCP1 transcription through complex formation with PPARγ (Oberkofler et al., 2002; Cao et al., 2004). The expression level of PGC-1α, but not PPARγ was shown to increase during cold exposure in murine brown fat (Seale et al., 2007; Karamitri et al., 2009; Komatsu et al., 2010). The present study indicates that renal expression of UCP1 is closely related to that of PPARγ rather than PGC-1α; water temperature-related changes in the renal expression of UCP1 paralleled those in the expression of PPARγ, but not in PGC-1α. Cold exposure also decreased hepatic expressions of UCP1 and PPARγ, but the expression level of hepatic PGC-1α was unaffected.

Consistent with previous findings on the effects of cold on the expression of PPARα in murine brown fat (Komatsu et al., 2010), the hepatic and renal expression levels of PPARα in common carps were unaffected by cold exposure. In addition, hepatic and renal expressions of PPARβ/δ were rather increased during cold exposure. Taking the expression level of PPARs and PGC-1α together, the down-regulation of PPARγ expression during cold exposure may be responsible for the down-regulation of UCP1 expression in common carps. Changes in expression levels of RXRα, a PPARγ partner (Evans and Mangelsdorf,

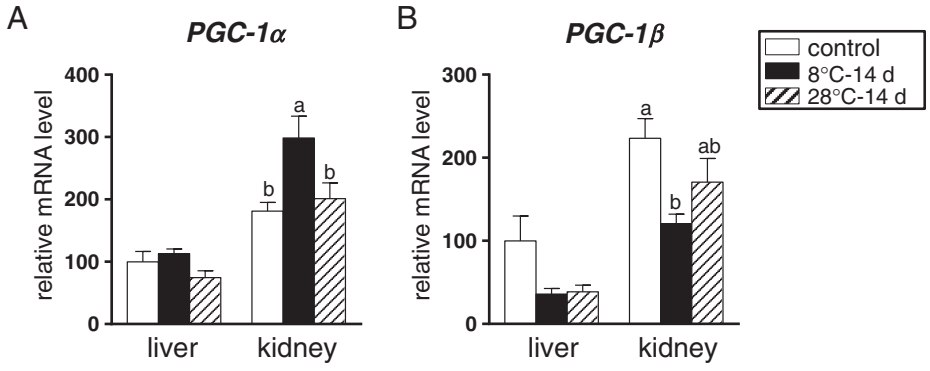

Fig. 4. PGC-1 expression in the livers and kidneys of common carps acclimated to various temperatures. Common carps acclimated at 22 °C were subjected to cold exposure for 14 days at 8 °C. They were then acclimated at 28 °C for 14 days. Transcript levels of PGC-1α (A) and PGC-1β (B) were determined by RT-qPCR and are expressed relative to the expression of EF1α, with the hepatic level determined on day 0 (control) set to 100. Data shown are the mean ± SE (n = 10). a, b: $P < 0.05$.

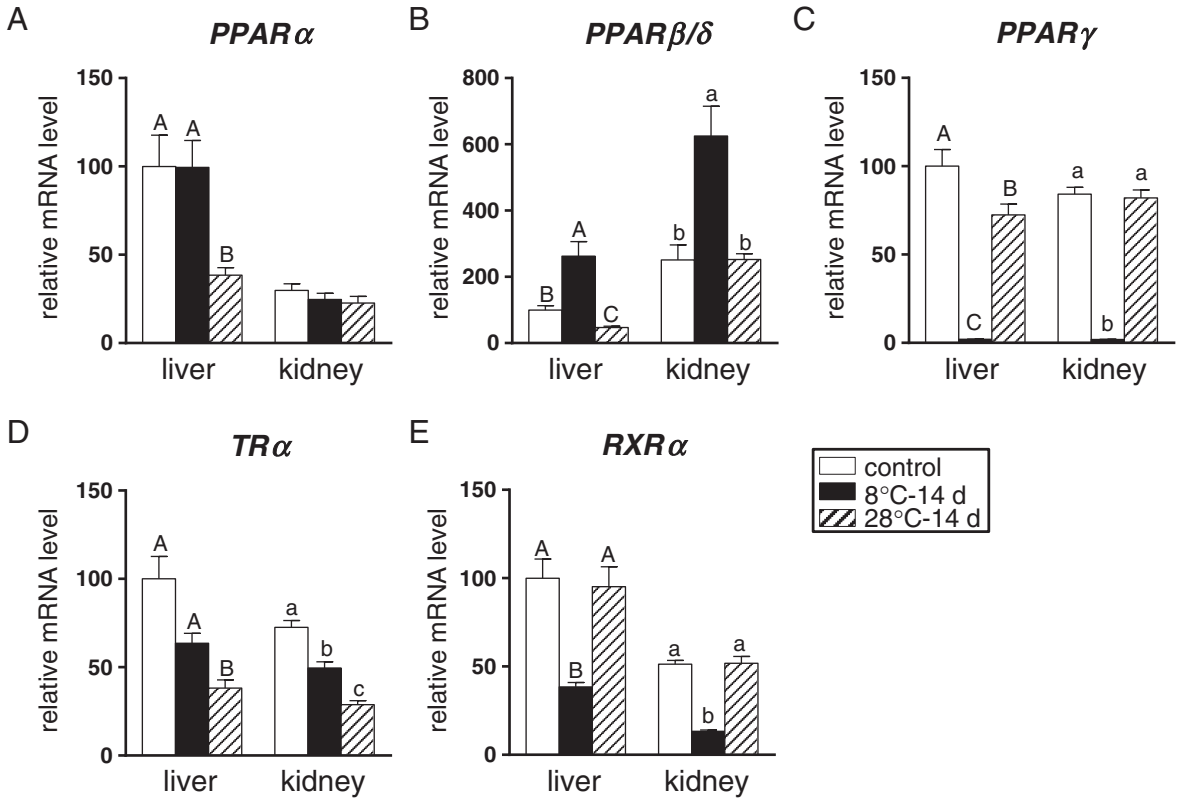

Fig. 5. Expression of PPAR, TRα, and RXRα in the livers and kidneys of common carps acclimated to various temperatures. Common carps acclimated at 22 °C were subjected to cold exposure for 14 days at 8 °C. They were then acclimated at 28 °C for 14 days. Transcript levels of PPARα (A), PPARβ/δ (B), PPARγ (C), TRα (D), and RXRα (E) were determined by RT-qPCR and are expressed relative to the expression of EF1α, with the hepatic level determined on day 0 (control) set to 100. Data shown are the mean ± SE (n = 10). A, B, C and a, b, c: $P < 0.05$.

2014), basically paralleled to those of PPARγ. Therefore, expression levels of RXRα may be also involved in regulation of UCP1 expression by PPARγ during cold exposure.

However, the regulatory expressions of PPARγ/RXRα do not explain UCP1 expression in liver of common carps during the water temperature from 8 °C to 28 °C; the cessation of cold exposure increased hepatic expressions of PPARγ and RXRα but not UCP1. It is possible that inhibitory factor(s) on UCP1 expression is induced in carp livers during the recovery period from cold exposure.

We isolated 2634 bases upstream to putative transcription initiation site of UCP1 gene. The nucleotide sequence has low homology to corresponding region of humans, mice, rats, and even zebrafish, although some sequence motifs in the murine BAT-specific enhancer are present scattered widely. The enhancer region of human UCP1 gene, which includes responsive elements to PPAR, TR, and CREB, is located around nt −3800 (Rim and Kozak, 2002; Shore et al., 2013). It is possible that the transcriptional enhancer is located in a more distal region of UCP1 promoter. In addition, the sequence motifs in fish may not match to those suggested in mammals. These should be evaluated in future studies.

We also evaluated the expression of NRF1, because NRF1 has been shown to regulate energy metabolism in concert with PGC-1α in mammals (Scarpulla, 2008). A previous study revealed that changes in NRF1 expression paralleled those in UCP1, PGC-1α, and PPARδ expressions during cold exposure and physical activity in murine brown fat (Seebacher and Glanville, 2010). Cold exposure increased the renal expression of PGC-1α, PPARβ/δ, and NRF1, and the cessation of cold exposure decreased the expression of these genes; similar changes

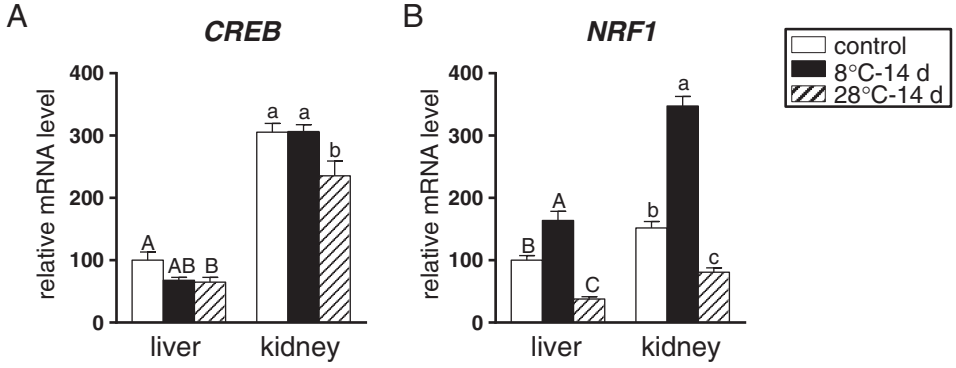

Fig. 6. Expression of CREB and NRF1 in the livers and kidneys of common carps acclimated to various temperatures. Common carps acclimated at 22 °C were subjected to cold exposure for 14 days at 8 °C. They were then acclimated at 28 °C for 14 days. Transcript levels of CREB (A) and NRF1 (B) were determined by RT-qPCR and are expressed relative to the expression of EF1α, with the hepatic level determined on day 0 (control) set to 100. Data shown are the mean ± SE (n = 10). A, B, C and a, b, c: $P < 0.05$.

were also detected in hepatic expressions of PPARβ/δ and NRF1. However, water temperature-related changes in the expression pattern of PGC-1α, PPARβ/δ, and NRF1 differed from those in UCP1 expression. PGC-1α, PPARβ/δ, and NRF1 may cooperatively function through their up-regulation during cold exposure, and this is distinct from the regulation of energy metabolism through the modulation of UCP1 expression.

A previous study showed that the hepatic expressions of PGC-1α, PGC-1β, and PPARβ and NRF1 were higher in goldfish acclimated at 4 °C for 3 weeks than in those acclimated at 20 °C, and PPARα expression was lower during cold exposure (LeMoine et al., 2008). Bremer et al. (2012) observed that cold exposure significantly increased expression of PGC-1β and NRF1, decreased expression of PGC-1α, PPARα, and TRα, and did not affect expression of PPARβ/δ and RXRα in white muscle of goldfish. The temperature-related changes in gene expression were partly but not completely consistent with the previous results. At present, it is difficult to understand relationships among expression levels of these genes comprehensively; effects of cold exposure are also different among tissues in gold fish (LeMoine et al., 2008), and there may be species differences on cold-related changes in gene expression.

Although carp UCP1 may be a functional uncoupling protein, similar to its mammalian counterpart (Jastroch et al., 2007), a correlation between the expression of UCP1 and non-shivering heat production has yet to be established in fish. Future studies are needed to determine the role of UCP1 expression, the physiological significance of regulatory changes in the hepatic and renal expressions of UCP1, and the molecular mechanisms underlying altered expression levels of genes during cold exposure and subsequent recovery from cold exposure in common carps. Also, aging, diet, feed restriction, and hypoxia are known to affect expression levels of UCP2 and UCP3, structurally related molecules to UCP1, in gilthead sea bream (Bermejo-Nogales et al., 2010, 2014). To understand uncoupling-related regulation of energy metabolism in ectothermic animals fully, it is needed to explore regulatory expressions of UCP2 and UCP3 in addition to UCP1.

Acknowledgments

We thank Dr. Masaaki Hasegawa for providing the common carps. Also, we are grateful to anonymous reviewer's constructive comments. This work was supported by a research project grant awarded by the Azabu University (2013K08).

References

Asai, K., Funaba, M., Murakami, M., 2014. Enhancement of RANKL-induced MITF-E expression and osteoclastogenesis by TGF-β. Cell Biochem. Funct. 32, 401–409.
Barbatelli, G., Murano, I., Madsen, L., Hao, Q., Jimenez, M., Kristiansen, K., Giacobino, J.P., De Matteis, R., Cinti, S., 2010. The emergence of cold-induced brown adipocytes in mouse white fat depots is determined predominantly by white to brown adipocyte transdifferentiation. Am. J. Physiol. Endocrinol. Metab. 298, E1244–E1253.
Barbera, M.J., Schluter, A., Pedraza, N., Iglesias, R., Villarroya, F., Giralt, M., 2001. Peroxisome proliferator-activated receptor α activates transcription of the brown fat uncoupling protein-1 gene. A link between regulation of the thermogenic and lipid oxidation pathways in the brown fat cell. J. Biol. Chem. 276, 1486–1493.
Bermejo-Nogales, A., Calduch-Giner, J.A., Pérez-Sánchez, J., 2010. Gene expression survey of mitochondrial uncoupling proteins (UCP1/UCP3) in gilthead sea bream (*Sparus aurata L.*). J. Comp. Physiol. B. 180, 685–694.
Bermejo-Nogales, A., Calduch-Giner, J.A., Pérez-Sánchez, J., 2014. Tissue-specific gene expression and functional regulation of uncoupling protein 2 (UCP2) by hypoxia and nutrient availability in gilthead sea bream (*Sparus aurata*): implications on the physiological significance of UCP1-3 variants. Fish Physiol. Biochem. 40, 751–762.
Bremer, K., Monk, C.T., Gurd, B.J., Moyes, C.D., 2012. Transcriptional regulation of temperature-induced remodeling of muscle bioenergetics in goldfish. Am. J. Physiol. Regul. Integr. Comp. Physiol. 303, R150–R158.
Cannon, B., Nedergaard, J., 2004. Brown adipose tissue: function and physiological significance. Physiol. Rev. 84, 277–359.
Cao, W., Daniel, K.W., Robidoux, J., Puigserver, P., Medvedev, A.V., Bai, X., Floering, L.M., Spiegelman, B.M., Collins, S., 2004. p38 mitogen-activated protein kinase is the central regulator of cyclic AMP-dependent transcription of the brown fat uncoupling protein 1 gene. Mol. Cell. Biol. 24, 3057–3067.
Evans, R.M., Mangelsdorf, D.J., 2014. Nuclear receptors, RXR, and the big bang. Cell 157, 255–266.
Gesta, S., Tseng, Y.H., Kahn, C.R., 2007. Developmental origin of fat: tracking obesity to its source. Cell 131, 242–256.
Jastroch, M., Wuertz, S., Kloas, W., Klingenspor, M., 2005. Uncoupling protein 1 in fish uncovers an ancient evolutionary history of mammalian nonshivering thermogenesis. Physiol. Genomics 22, 150–156.
Jastroch, M., Buckingham, J.A., Helwig, M., Klingenspor, M., Brand, M.D., 2007. Functional characterisation of UCP1 in the common carp: uncoupling activity in liver mitochondria and cold-induced expression in the brain. J. Comp. Physiol. B. 177, 743–752.
Karamitri, A., Shore, A.M., Docherty, K., Speakman, J.R., Lomax, M.A., 2009. Combinatorial transcription factor regulation of the cyclic AMP-response element on the Pgc-1α promoter in white 3 T3-L1 and brown HIB-1B preadipocytes. J. Biol. Chem. 284, 20738–20752.
Komatsu, M., Tong, Y., Li, Y., Nakajima, T., Li, G., Hu, R., Sugiyama, E., Kamijo, Y., Tanaka, N., Hara, A., Aoyama, T., 2010. Multiple roles of PPARα in brown adipose tissue under constitutive and cold conditions. Genes. Cells 15, 91–100.
Kozak, U.C., Kopecky, J., Teisinger, J., Enerbäck, S., Boyer, B., Kozak, L.P., 1994. An upstream enhancer regulating brown-fat-specific expression of the mitochondrial uncoupling protein gene. Mol. Cell. Biol. 14, 59–67.
LeMoine, C.M., Genge, C.E., Moyes, C.D., 2008. Role of the PGC-1 family in the metabolic adaptation of goldfish to diet and temperature. J. Exp. Biol. 211, 1448–1455.
Lin, J., Puigserver, P., Donovan, J., Tarr, P., Spiegelman, B.M., 2002. Peroxisome proliferator-activated receptor gamma coactivator 1β (PGC-1β), a novel PGC-1-related transcription coactivator associated with host cell factor. J. Biol. Chem. 277, 1645–1648.
Montminy, M., 1997. Transcriptional regulation by cyclic AMP. Annu. Rev. Biochem. 66, 807–822.
Murakami, M., Kondo, S., Funaba, M., 2008. Expression and function of alternative splice variants of the mouse TGF-β type I receptor. Cell Biol. Int. 32, 848–854.
Oberkofler, H., Esterbauer, H., Linnemayr, V., Strosberg, A.D., Krempler, F., Patsch, W., 2002. Peroxisome proliferator-activated receptor (PPAR) γ coactivator-1 recruitment regulates PPAR subtype specificity. J. Biol. Chem. 277, 16750–16757.
Puigserver, P., Wu, Z., Park, C.W., Graves, R., Wright, M., Spiegelman, B.M., 1998. A cold-inducible coactivator of nuclear receptors linked to adaptive thermogenesis. Cell 92, 829–839.
Rim, J.S., Kozak, L.P., 2002. Regulatory motifs for CREB-binding protein and Nfe2l2 transcription factors in the upstream enhancer of the mitochondrial uncoupling protein 1 gene. J. Biol. Chem. 277, 34589–34600.
Scarpulla, R.C., 2008. Transcriptional paradigms in mammalian mitochondrial biogenesis and function. Physiol. Rev. 88, 611–638.
Seale, P., Kajimura, S., Yang, W., Chin, S., Rohas, L.M., Uldry, M., Tavernier, G., Langin, D., Spiegelman, B.M., 2007. Transcriptional control of brown fat determination by PRDM16. Cell Metab. 6, 38–54.
Seebacher, F., Glanville, E.J., 2010. Low levels of physical activity increase metabolic responsiveness to cold in a rat (*Rattus fuscipes*). PLoS One 5, e13022.
Shore, A., Emes, R.D., Wessely, F., Kemp, P., Cillo, C., D'Armiento, M., Hoggard, N., Lomax, M.A., 2013. A comparative approach to understanding tissue-specific expression of uncoupling protein 1 expression in adipose tissue. Front. Genet. 3, 304.

Gene 551 (2014) 119–126

Contents lists available at ScienceDirect

Gene

journal homepage: www.elsevier.com/locate/gene

The regulation of hepcidin expression by serum treatment: Requirements of the BMP response element and STAT- and AP-1-binding sites

Yohei Kanamori [a], Masaru Murakami [b], Tohru Matsui [a], Masayuki Funaba [a,*]

[a] Division of Applied Biosciences, Graduate School of Agriculture, Kyoto University, Kyoto 606-8502, Japan
[b] Laboratory of Molecular Biology, Azabu University School of Veterinary Medicine, Sagamihara 252-5201, Japan

ARTICLE INFO

Article history:
Received 9 April 2014
Received in revised form 26 June 2014
Accepted 20 August 2014
Available online 21 August 2014

Keywords:
Hepcidin
Serum
AP-1
BMP
Liver

ABSTRACT

Expression of hepcidin, a central regulator of systemic iron metabolism, is transcriptionally regulated by the bone morphogenetic protein (BMP) pathway. However, the factors other than the BMP pathway also participate in the regulation of hepcidin expression. In the present study, we show that serum treatment increased hepcidin expression and transcription without inducing the phosphorylation of Smad1/5/8 in primary hepatocytes, HepG2 cells or Hepa1-6 cells. Co-treatment with LDN-193189, an inhibitor of the BMP type I receptor, abrogated this hepcidin induction. Reporter assays using mutated reporters revealed the involvement of the BMP response element-1 (BMP-RE1) and signal transducers and activator of transcription (STAT)- and activator protein (AP)-1-binding sites in serum-induced hepcidin transcription in HepG2 cells. Serum treatment induced the expression of the AP-1 components c-fos and junB in primary hepatocytes and HepG2 cells. Forced expression of c-fos or junB enhanced the response of hepcidin transcription to serum treatment. By contrast, the expression of dominant negative (dn)-c-fos and dn-junB decreased hepcidin transcription. The present study reveals that serum contains factors stimulating hepcidin transcription. Basal BMP activity is essential for the serum-induced hepcidin transcription, although serum treatment does not stimulate the BMP pathway. The induction of c-fos and junB by serum treatment stimulates hepcidin transcription, through possibly cooperation with BMP-mediated signaling. Considering that AP-1 is induced by various stimuli, the present results suggest that hepcidin expression is regulated by more diverse factors than had been previously considered.

1. Introduction

Iron is essential for fundamental metabolic processes in cells and organisms. Iron homeostasis is strictly maintained through cellular and systemic systems. Cellular iron metabolism is regulated through iron-regulatory proteins that bind iron-responsive elements in regulated mRNAs. By contrast, systemic iron metabolism is mainly governed by the synthesis and secretion of the iron-regulating hormone hepcidin. Hepcidin is produced by liver parenchymal cells and orchestrates systemic iron fluxes and decreases plasma iron levels by binding to and degrading the iron exporter ferroportin on the surface of iron-releasing cells, especially on the basolateral membrane of enterocytes (Anderson et al., 2012; Hentze et al., 2010; Lee and Beutler, 2009).

Hepcidin expression is transcriptionally regulated; bone morphogenetic protein (BMP), a member of the transforming growth factor-β (TGF-β) family, potently stimulates the process (Finberg, 2013; Hentze et al., 2010; Lee and Beutler, 2009; Muckenthaler, 2008). Members of the TGF-β family, including BMP, TGF-β, and activin, elicit their activities through similar but distinct signal transduction pathways. Upon ligand binding, the receptor complexes phosphorylate carboxyl-terminal serines of receptor-regulated (R-) Smad; BMP induces the phosphorylation of Smad1/5/8, whereas TGF-β/activin does Smad2/3 phosphorylation. Phosphorylated R-Smad forms complexes with the common Smad, Smad4, and these translocate into the nucleus where they participate in the regulation of gene transcription (Massagué, 2012; Miyazono et al., 2010; Sakaki-Yumoto et al., 2013).

In addition to the BMP pathway, several other molecules, such as interleukin (IL)-6, IL-22, oncostatin M and testosterone, also regulate hepcidin transcription (Chung et al., 2010; Guo et al., 2013; Kanda

Abbreviations: BMP, bone morphogenetic proteins; TGF-β, transforming growth factor-β; IL, interleukin; AP, activator protein; STAT, signal transducers and activator of transcription; BMP-RE, BMP response element; CMF, calcium and magnesium-free; HBSS, Hank's buffered salt solution; DMEM, Dulbecco's modified Eagle's medium; FBS, fetal bovine serum; RT-qPCR, reverse transcription-quantitative polymerase chain reaction; Gapdh, glyceraldehyde-3-phosphate dehydrogenase; pCMV-βGal, plasmid expressing β-galactosidase under the control cytomegalovirus promoter; SE, standard error; TRE, TPA-responsive element.

* Corresponding author at: Division of Applied Biosciences, Graduate School of Agriculture, Kyoto University, Kitashirakawa Oiwakecho, Kyoto 606-8502, Japan.
E-mail address: mfunaba@kais.kyoto-u.ac.jp (M. Funaba).

http://dx.doi.org/10.1016/j.gene.2014.08.037
0378-1119/

et al., 2009; Nemeth et al., 2003; Smith et al., 2013); other factors and mechanisms that regulate hepcidin expression have not yet been fully elucidated.

During the exploration of BMP-induced hepcidin expression, we noticed that serum starvation down-regulates hepcidin expression in hepatocytes. This observation prompted us to pursue the role of serum as a positive regulator in hepcidin expression. Here we show that serum stimulates hepcidin transcription via the following: an activator protein (AP)-1 binding site within the hepcidin promoter, which spans nt −133 to nt −127 and was identified previously but was not characterized (Truksa et al., 2007); the signal transducers and activator of transcription (STAT)-binding site (STAT-BS), which spans nt −143 to nt −134; and the BMP response element 1 (BMP-RE1), which spans nt −155 to nt −150. Although serum treatment does not stimulate the BMP pathway, the basal BMP activity is indispensable for serum-induced hepcidin transcription. In addition, the AP-1 components c-fos and junB induced by serum treatment would be involved in the transcriptional activation. The present study extends our understanding of hepcidin expression. AP-1 is induced by various stimuli, such as stress, infections and inflammations, and certain stimuli that are mediated by cytokines and growth factors (Hess et al., 2004). Thus, the present results suggest that hepcidin is regulated by more factors than were previously considered.

2. Materials & methods

2.1. Materials

The following reagents were purchased and used: BMP2 was from R&D Systems (Minneapolis, MN, USA); BMP6 was from GeneTex (Irvine, CA, USA); LDN-193189, an inhibitor for BMP type I receptor (Yu et al., 2008a) was from Stemgent (San Diego, CA, USA); rabbit polyclonal antibodies against phospho-Smad1 (Ser463/Ser465)/Smad5 (Ser463/Ser465)/Smad8 (Ser426/Ser428) (#9511) and p38 (#9212) were from Cell Signaling Technology (Danvers, MA, USA); a mouse monoclonal antibody against Smad1 (A-4, sc-7965) was from Santa Cruz Biotechnology (Santa Cruz, CA, USA); and a rabbit monoclonal antibody against Smad1 (EP565Y, ab33902) and a mouse monoclonal antibody against β-actin (AC-15, ab6276) were from Abcam (Cambridge, MA, USA).

2.2. Cell culture

Animal experiments were approved by the Kyoto University Animal Experiment Committee. Primary rat hepatocytes were isolated by collagenase digestion of livers from male Sprague–Dawley rats aged 4 weeks. The livers were perfused from the portal vein to the incised inferior vena cava with calcium and magnesium-free (CMF) buffer (40 mM Hepes, pH 7.4, 120 mM NaCl, 5.4 mM KCl, 5.0 mM $NaHCO_3$ and 5.6 mM glucose supplemented with 100 U/mL penicillin, 100 μg/mL streptomycin and 250 ng/mL amphotericin B) for 10 min at a rate of ~12 mL/min followed by perfusion with CMF buffer containing 0.05% collagenase (Wako, Osaka, Japan) for 10 min. Subsequently, hepatocytes were liberated into Hank's buffered salt solution (HBSS), i.e., 140 mM NaCl, 5.4 mM KCl, 0.34 mM Na_2HPO_4, 0.44 mM KH_2PO_4, 0.81 mM $MgSO_4 \cdot 7H_2O$, 1.3 mM $CaCl_2$, 4.2 mM $NaHCO_3$ and 5.6 mM glucose supplemented with 100 U/mL penicillin, 100 μg/mL streptomycin and 250 ng/mL amphotericin B. After cell recovery by centrifugation at 50 ×g for 2 min, the cells were washed with HBSS three times and were then resuspended in Dulbecco's modified Eagle's medium (DMEM) with 10% heat-inactivated fetal bovine serum (FBS) and antibiotics. Cells (>90% hepatocytes by microscopy) were seeded on collagen-coated plates at 1.5×10^5 cells per well in 12-well plates. Attached cells were subsequently used. HepG2 hepatoma cells and Hepa1-6 hepatoma cells were cultured in DMEM with 10% heat-inactivated FBS and antibiotics.

2.3. RNA isolation and RT-quantitative PCR

Total RNA was isolated from rat primary hepatocytes by using TRIZOL (Invitrogen, Grand Island, NY, USA) and cDNA was synthesized by the ABI high capacity cDNA reverse transcription kit (Applied Biosystems, Foster City, CA, USA), according to the manufacturers' protocols. The cDNA that was reverse-transcribed from 5 ng of total RNA was used as a template for RT-quantitative PCR (RT-qPCR) as previously described (Asano et al., 2013). The oligonucleotide primers for RT-qPCR are as follows: 5′-gatggcactcagcactgga-3′ and 5′-gctgcagctctgtagtctgtct-3′ for hepcidin, 5′-gaacactggatggacgactg-3′ and 5′-acagacgggcatagatcaca-3′ for Smad4, and 5′-cgtgttcctacccccaatgt-3′ and 5′-tgtcatcatacttggcaggtttc-3′ for glyceraldehyde-3-phosphate dehydrogenase (Gapdh). The Ct value was determined, and the abundance of gene transcripts was analyzed using the $^{\Delta\Delta}$Ct method and by normalizing against the Gapdh gene (Duran et al., 2005).

2.4. Western blot

Western blot analyses were performed as previously described (Funaba and Murakami, 2008). The immunoreactive proteins were visualized using the ECL Select Western blotting detection system (GE Healthcare, Buckinghamshire, UK) according to the manufacturer's protocol.

2.5. Plasmids

The DNA sequence that spans nt −2018 to nt −35 of the mouse hepcidin (Hamp1) promoter was amplified and cloned into a pGL4 basic vector that contained the firefly luciferase reporter (Hepcidin (−2018)-luc); nt +1 was defined as the translation initiation site. Reporter plasmids with deleted promoters or point mutations were prepared by a PCR-based method. The dominant negative (dn)-c-fos, which lacks region encoding amino acid 133 to amino acid 159 (Ransone et al., 1990), was also prepared by a PCR-based method. The plasmids were verified by DNA sequencing. Expression vectors for c-fos, junB and dn-jun B were kindly provided by Dr. M. Hibi.

2.6. Reporter assays

HepG2 and Hepa1-6 hepatoma cells were transiently transfected with the described expression vectors, reporter construct and a plasmid expressing β-galactosidase (pCMV-βGal) with the use of the polyethylenimine Max reagent (Polysciences, Warrington, PA, USA) according to the manufacturer's protocol. DNA transfection was performed in the absence of heat-inactivated FBS. Equal amounts of DNA, adjusted with empty vector, were transfected in each experiment. At 4 h post-transfection, cells were cultured with medium with or without heat-inactivated FBS for 24 h. Luciferase activity in the cell lysate was normalized to β-galactosidase activity.

2.7. Statistical analyses

Data are expressed as the mean ± standard error (SE). Data on gene expression were log-transformed to provide an approximation of a normal distribution before analysis. Differences between gene expressions in the cells were examined using unpaired *t*-tests. Differences of $P < 0.05$ were considered significant.

3. Results and discussion

3.1. Serum stimulates hepcidin transcription in liver cells

When effects of exogenous ligand are examined, cells are typically cultured with a reduced concentration of heat-inactivated FBS before and during ligand stimulation. During the analysis of BMP-induced

hepcidin expression in rat primary hepatocytes, we reproducibly observed that serum starvation itself down-regulates hepcidin expression significantly ($P < 0.05$, Fig. 1A). The decreased expression levels of hepcidin were not caused by a non-specific down-regulation of gene expression, because serum starvation did not affect Smad4 expression. These results suggest that serum has a stimulatory effect on hepcidin expression. Thus, we aimed to verify the up-regulation of hepcidin expression levels in response to serum treatment. Attached rat primary hepatocytes were cultured in the absence of heat-inactivated FBS followed by treatment with or without 10% FBS. Consistent with the results on the effects of serum starvation (Fig. 1A), the serum treatment clearly increased the expression of hepcidin but not Smad4 in primary hepatocytes ($P < 0.01$, Fig. 1B).

Previous studies revealed that hepcidin expression is primarily increased by the activation of the BMP pathway (Finberg, 2013; Hentze et al., 2010; Lee and Beutler, 2009). Especially, BMP6 principally regulates hepcidin transcription in livers; mice lacking BMP6 exhibited inappropriately low level of hepcidin and massive iron overload (Andriopoulos et al., 2009; Meynard et al., 2009). BMP2 is relatively heat-stable, and heat-inactivation of FBS for 30 min at 56 °C did not decrease the bioactivity of BMP2 (Ohta et al., 2005), although the stability of BMP6 in response to the heat treatment is unknown. Thus, it is possible that BMP or the related molecule(s) in heat-inactivated FBS is responsible for serum-induced hepcidin expression. To this end, we evaluated phosphorylated Smad1/5/8 in response to serum stimulation in primary hepatocytes because BMPs elicit their activities through the phosphorylation of carboxyl-terminal serines of Smad1/5/8 (Massagué, 2012; Miyazono et al., 2010; Sakaki-Yumoto et al., 2013).

Serum treatment did not increase the phosphorylation levels of Smad1/5/8 in primary hepatocytes; rather, phosphorylated Smad1/5/8 levels tended to decrease with serum treatment, implying the presence of inhibitor(s) for the BMP pathway in serum (Fig. 1C, lanes 2–9). As expected, Smad1/5/8 was clearly phosphorylated within 1 h after BMP2 treatment in primary hepatocytes (Fig. 1C, lanes 10 and 11). Pretreatment with LDN-193189 decreased phosphorylation levels of Smad1/5/8 (Fig. 1D) and abrogated serum-induced hepcidin expression (Fig. 1E).

To explore serum-induced hepcidin expression in detail, experiments were next performed in HepG2 cells and Hepa1-6 cells. Consistent with the results from primary hepatocytes, serum treatment did not induce the phosphorylation of Smad1/5/8 in either HepG2 cells or Hepa1-6 cells (Fig. 2A). We next examined hepcidin transcription by luciferase-based reporter assays in HepG2 cells and Hepa1-6 cells; these cell lines are suitable to examine hepcidin transcription but not hepcidin expression at the mRNA level (Kanamori et al., 2014). Serum treatment increased the expression levels of hepcidin (−2018)-luc in

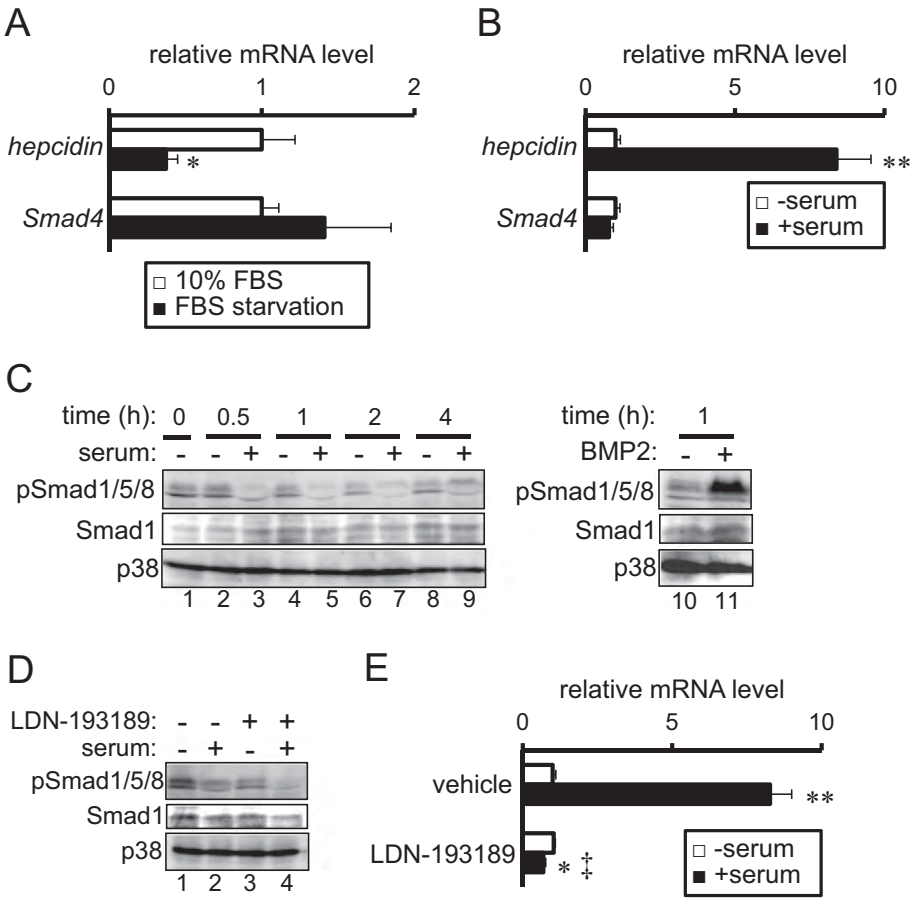

Fig. 1. Modulation of hepcidin expression levels by serum concentrations in rat primary hepatocytes. (A) Attached rat primary hepatocytes were cultured in the presence or absence of heat-inactivated FBS for 12 h. Hepcidin expression was examined by RT-qPCR and expressed as ratios to Gapdh, with the level set to 1 in cells cultured in the presence of heat-inactivated FBS. Data shown are the mean ± SE (n = 3). *: $P < 0.05$, vs. cells treated with 10% FBS. (B) Attached rat primary hepatocytes were cultured in the absence of heat-inactivated FBS for 4 h, followed by culturing with or without 10% heat-inactivated FBS for 12 h. Hepcidin expression was examined by RT-qPCR and is expressed as ratios to Gapdh, with the level set to 1 in cells treated without FBS. Data shown are the mean ± SE (n = 4). **: $P < 0.01$, vs. cells treated without serum. (C) Attached rat primary hepatocytes were cultured in the presence or absence of heat-inactivated FBS for the indicated time. Phosphorylated Smad1/5/8, Smad1 and p38 were examined by Western blot analysis. As a positive control, rat primary hepatocytes were also treated with BMP2 (4 nM) for 1 h. (D and E). Attached rat primary hepatocytes were treated with or without LDN-193189 for 20 min followed by treatment with or without 10% heat-inactivated FBS for 1 h (D) or 12 h (E). (D) Phosphorylated Smad1/5/8, Smad1 and p38 were examined by Western blot analysis. (E) Hepcidin expression was examined by RT-qPCR and is expressed as ratios to Gapdh, with the level set to 1 in cells treated without LDN-193189 and FBS. Data shown are the mean ± SE (n = 4). **: $P < 0.01$, vs. cells treated with the respective reagent (vehicle or LDN-193189) but without serum. ‡: $P < 0.01$, vs. cells treated with vehicle and serum.

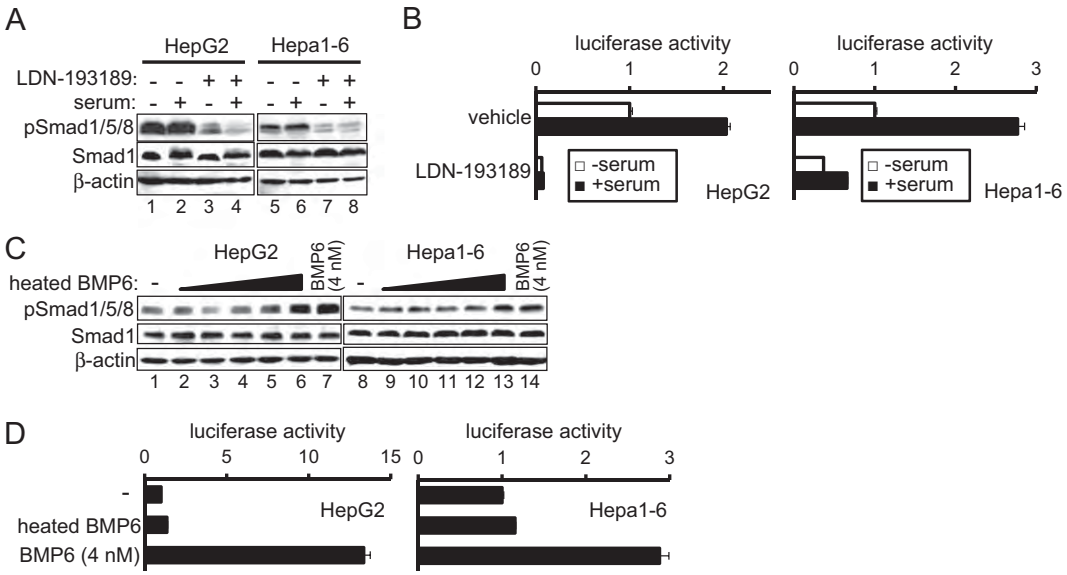

Fig. 2. Role of endogenous BMP activity in serum-induced hepcidin expression. (A and C) HepG2 cells and Hepa1-6 cells were cultured in the absence of heat-inactivated FBS for 4 h. (A) After pre-treatment with or without LDN-193189 for 20 min, cells were cultured with or without 10% heat-inactivated FBS for 1 h. (C) Cells were treated with or without various concentrations of BMP6, which was heated for 30 min at 56 °C, for 1 h. Concentration of the treated BMP6 is as follows; lanes 2 and 9: 0.24 pM, lanes 3 and 10: 1.2 pM, lanes 4 and 11: 6 pM, lanes 5 and 12: 30 pM, and lanes 6 and 13: 150 pM. As a positive control, cells were treated with 4 nM BMP6 (lanes 7 and 14). (A and C) Phosphorylated Smad1/5/8, Smad1 and β-actin were examined by Western blot analysis. (B and D) After transfection with hepcidin(−2018)-luc and CMV-βGal, HepG2 cells and Hepa1–6 cells were cultured in the absence of heat-inactivated FBS for 4 h. (B) After pre-treatment with or without LDN-193189 for 20 min, cells were cultured with or without 10% heat-inactivated FBS for 24 h. (D) Cells were treated with or without 30 pM BMP6, which was heated for 30 min at 56 °C, for 24 h. As a positive control, cells were treated with 4 nM BMP6. (B and D) Luciferase activity was normalized to β-galactosidase activity, and the luciferase activity in cells cultured in the absence of LDN-193189 and FBS was set to 1. Data were expressed as the mean ± SE from a representative experiment (n = 3).

HepG2 cells and Hepa1-6 cells (Fig. 2B), which indicated that serum-induced hepcidin expression is regulated at the level of transcription. In addition, pre-treatment with LDN-193189 decreased the luciferase activity and blocked serum-induced hepcidin transcription (Fig. 2B). These results indicate that the BMP activity is not further enhanced by serum treatment but that the endogenous BMP activity is required for serum-induced hepcidin expression and transcription in liver cells.

We also evaluated the effects of BMP6 in heat-inactivated FBS on Smad1/5/8 phosphorylation and hepcidin transcription in HepG2 cells and Hepa1-6 cells. Herrera and Inman (2009) reported that FBS contains ~300 pM of BMP6, which was determined by the transcriptional activity of BMP-responsive reporter. Thus, it is estimated that the culture medium, i.e., DMEM with 10% FBS, contains ~30 pM of BMP6 that was heated for 30 min for 56 °C. Significant induction of Smad1/5/8 phosphorylation and hepcidin transcription could not be detected in HepG2 cells and Hepa1-6 cells treated with below 30 pM of the heat-treated BMP6 (Fig. 2C and D). Taken failure of Smad1/5/8 phosphorylation in response to serum treatment in primary hepatocytes (Fig. 1C and D) with the inability to phosphorylate Smad1/5/8 and transactivate hepcidin by 30 pM of the heat-treated BMP6 in live cell lines together, BMP in the FBS is not likely to explain the serum-induced up-regulation of hepcidin expression. Previous studies also revealed that a BMP concentration greater than 100 pM is required to induce hepcidin expression (Maes et al., 2010; Truksa et al., 2006; Wu et al., 2012).

3.2. Serum-induced hepcidin transcription is mediated via BMP-RE1, TRE and STAT-BS

Previous studies revealed that the hepcidin promoter has two BMP responsive elements: BMP-RE1 (spanning nt −155 to nt −150) and BMP-RE2 (spanning nt −1678 to nt −1673) (Casanovas et al., 2009; Truksa et al., 2009). We performed reporter assays using a series of deleted reporters of mouse hepcidin promoter. The responsiveness to serum treatment was still detected by a deletion of BMP-RE2, although basal transcription was reduced and the extent of the increase in luciferase expression in response to serum treatment was decreased (Fig. 3A). The deletion of BMP-RE1 further decreased the basal transcription and inhibited the responsiveness to serum treatment (Fig. 3A), which suggests an essential role of BMP-RE1 in serum-induced hepcidin transcription. Consistent with these results, reporter assays that used reporters with point mutations in BMP-RE1, BMP-RE2 or both revealed that serum-induced hepcidin transcription was inhibited in reporters containing mutations in BMP-RE1 but not BMP-RE2 (Fig. 3B).

Serum treatment is known to induce the expression of AP-1 components, which stimulate transcription by binding to the TPA-responsive element (TRE) located in the transcriptional regulatory region of the gene (Hess et al., 2004; Shaulian and Karin, 2002). The TRE consensus sequence is $TGA^{G}/_{C}TCA$ (Hess et al., 2004; Shaulian and Karin, 2002), but the closely related sequence TGAGACA also binds to AP-1 and confers AP-1-mediated transcription (Kim et al., 1990). A search for the hepcidin gene identified a possible TRE sequence from nt −133 to nt −127 (Fig. 4A).

Truksa et al. (2007) reported the existence of the TRE sequence in the hepcidin gene and explored its function in IL-6 and BMP9-induced hepcidin transcription by using a reporter plasmid containing the hepcidin promoter with TRE mutations. However, to create the "TRE mutated reporter" they mutated sequence outside of the core TRE sequence ($TGA^{G}/_{C}TCA$) (Truksa et al., 2007), and therefore the role of TRE was not strictly evaluated in their study. Additionally, adjacent to the TRE sequence, a STAT-BS sequence spans nt −143 to nt −134 (Fig. 4A). Although the STAT-BS sequence has been reported to function in IL-6-induced transcription (Wrighting and Andrews, 2006), mutations in the STAT-BS in mouse hepcidin (Hamp1) did not affect the responsiveness to IL-6 (Truksa et al., 2007). In the present study, we prepared reporter plasmids with mutated core TRE sequence (mTRE), STAT-BS sequence (mSTAT) or both (mSTAT, TRE) by introducing point mutations at distal sites from the mutual elements (Fig. 4B). In this case, we used a reporter plasmid with a shorter hepcidin promoter, hepcidin(−270)-luc, as a wild-type plasmid to evaluate serum responsiveness (Fig. 3A).

Serum-induced hepcidin transcriptional activation was decreased when the TRE or STAT-BS was mutated (Fig. 4C), and the double

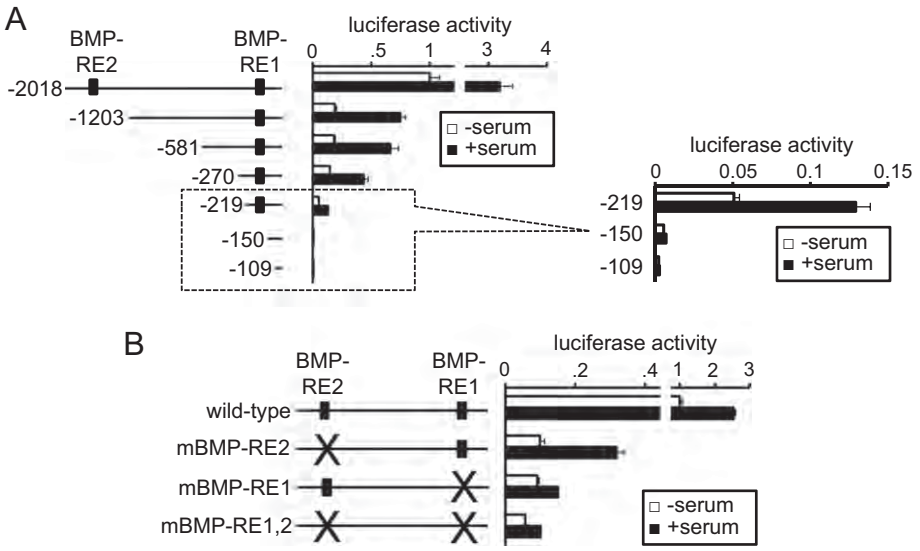

Fig. 3. Role of BMP-RE in serum-induced hepcidin expression. After transfection with the indicated reporter plasmid and CMV-βGal, HepG2 cells were cultured in the absence of heat-inactivated FBS for 4 h. After pre-treatment with or without LDN-193189 for 20 min, cells were cultured with or without 10% heat-inactivated FBS for 24 h. Luciferase activity was normalized to β-galactosidase activity, and the luciferase activity in cells that were cultured in the absence of FBS and were transfected with hepcidin(−2018)-luc was set to 1. Data were expressed as the mean ± SE from a representative experiment (n = 3). Hepcidin transcription was examined by the use of reporter genes with series of deletions (A) or a reporter gene with point mutations in BMP-RE1 and -RE2 (B). BMP-RE1 (GGCGCC) was mutated to aGaaCC, and BMP-RE2 (GGCGCC) was mutated to tcaGCC; the mutated nucleotides are shown in small characters.

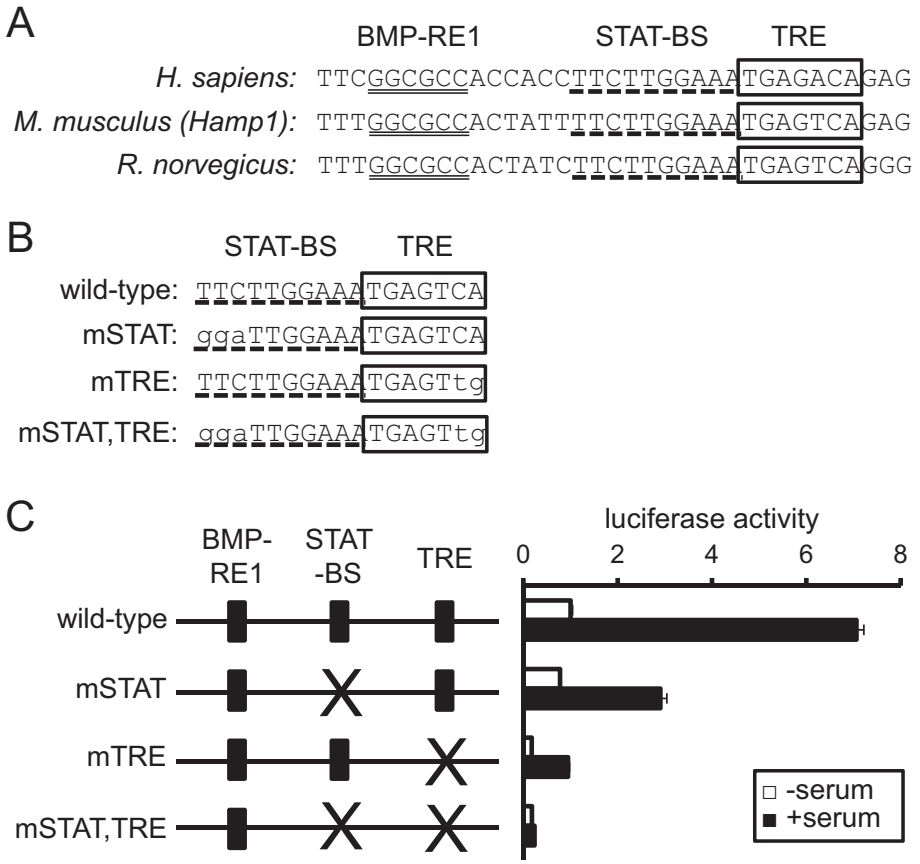

Fig. 4. TRE in the hepcidin promoter. (A) Nucleotide sequence of the hepcidin promoter around TRE. Possible TRE sequence is indicated by a box, and BMP-RE1 and STAT-BS are indicated by a double underline and a dotted underline, respectively. (B) Mutations in STAT-BS and TRE. TRE and STAT-BS are indicated by a box and a dotted underline, respectively. The mutated nucleotides are shown in small characters. (C) The role of TRE and STAT-BS in serum-induced hepcidin transcription. After transfection with the indicated reporter plasmid and CMV-βGal, HepG2 cells were cultured in the absence of heat-inactivated FBS for 4 h followed by culture with or without 10% heat-inactivated FBS for 24 h. Luciferase activity was normalized to β-galactosidase activity, and the luciferase activity in cells that were cultured in the absence of FBS and were transfected with hepcidin(−270)-luc was set to 1. Data were expressed as the mean ± SE from a representative experiment (n = 3).

mutations completely abrogated serum-induced hepcidin transcription. In addition, mutations in the TRE decreased basal transcription levels of hepcidin. These results suggest that both the TRE and STAT-BS are required for full activation of hepcidin transcription induced by serum; especially, TRE is essential for the basal transcription of hepcidin.

Verga Falzacappa et al. (2007) identified a possible AP-1 binding site but not the TRE in the human hepcidin gene, which extends from nt −313 to nt −304, by the use of the nucleotide database on putative transcription factor binding sites. The nucleotide database did not indicate the corresponding region of mouse hepcidin gene (Hamp1), nt −292 to nt −283, as a putative AP-1 binding site (Fig. 5A). Nevertheless, we examined the role of the region spanning from nt −292 to nt −283 by the use of hepcidin(−581)-luc as a wild-type plasmid. The responsiveness to serum was not changed by the mutations of the region (Fig. 5B). The results are consistent with those that deletion of nt −581 to nt 271 did not affect hepcidin transcription in response to serum (Fig. 3A). Thus, we conclude that the putative AP-1 site suggested by Verga Falzacappa et al. (2007) is not functional for serum-induced transcription of mouse hepcidin.

3.3. Serum induces c-fos and junB expressions in liver cells, which are responsible for hepcidin transcription via TRE and STAT-BS

We examined the induction of AP-1 in response to serum treatment in primary hepatocytes (Fig. 6A) and HepG2 cells (Fig. 6B). The time-course changes that occurred during serum stimulation were similar between the two cell types but were different among the genes analyzed; c-fos expression was transiently induced within 30 min after serum treatment, and c-fos expression levels returned to basal levels at 1.5 h after serum treatment in primary hepatocytes and at 2 h in HepG2 cells. Expression levels of junB were significantly higher in cells treated with serum at 1 h of serum treatment in primary hepatocytes and from 0.5 h to 4 h in HepG2 cells. In contrast, serum treatment did not significantly affect c-jun expression in primary hepatocytes, although it slightly but significantly increased from 0.5 to 4 h in HepG2 cells.

Considering that serum treatment stimulated hepcidin expression and transcription in primary hepatocytes and HepG2 cells, the expression of c-fos and junB but not c-jun may be involved in serum-induced hepcidin transcription. Thus, we explored that the effects of the forced expression

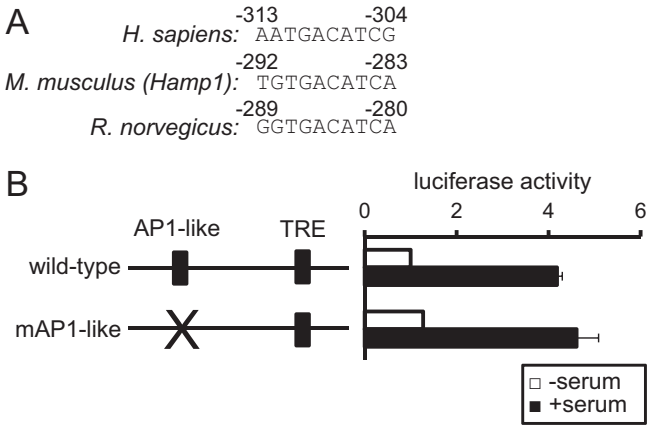

Fig. 5. Role of a putative AP-1 binding site in serum-induced hepcidin expression. (A) Nucleotide sequence of human putative AP-1 binding site and the corresponding region in mouse and rat hepcidin promoter. (B) The role of the putative AP-1 binding site in serum-induced hepcidin transcription. After transfection with the indicated reporter plasmid and CMV-βGal, HepG2 cells were cultured in the absence of heat-inactivated FBS for 4 h followed by culture with or without 10% heat-inactivated FBS for 24 h. Luciferase activity was normalized to β-galactosidase activity, and the luciferase activity in cells that were cultured in the absence of FBS and were transfected with hepcidin(−581)-luc was set to 1. Data were expressed as the mean ± SE from a representative experiment (n = 3). The corresponding region to human putative AP-1 binding site (TGTGACATCA) was mutated to TGTGttATCA; the mutated nucleotides are shown in small characters.

of c-fos and junB were examined (Fig. 7). The expression of c-fos alone increased the transcription of hepcidin, and it also increased serum-induced hepcidin transcription. The responsiveness to serum also increased with junB expression, although junB expression alone did not stimulate hepcidin transcription. Mutations of either the STAT-BS or TRE sequences decreased hepcidin transcription, irrespective of serum stimulation. The effects of the TRE mutations were more remarkable, but the reporters still responded to serum treatment. Double mutations in both the STAT-BS and TRE sequences completely inhibited hepcidin transcription.

We further examined the effects of the expression of dn-c-fos or dn-junB on hepcidin transcription (Fig. 8). Basal transcription of hepcidin was decreased by the expression of dn-c-fos or dn-junB. In addition, the extent of the increase in luciferase activity in response to serum treatment was smaller in cells expressing dn-c-fos or dn-junB than in those expressing empty vector.

Here, we showed that the withdrawal of heat-inactivated FBS decreased the expression of hepcidin in primary hepatocytes and that serum treatment increased hepcidin expression and transcription (and vice versa) in primary hepatocytes, HepG2 cells and Hepa1-6 cells. We also demonstrated that serum treatment does not stimulate the BMP pathway but the basal BMP activity is required for hepcidin induction through the BMP-RE1 region of its promoter. The serum induced expression of c-fos and junB and both the TRE and STAT-BS sequences within the hepcidin promoter are essential for serum-induced transcription. AP-1 enhances the transcription of the α2-macroglobulin gene through complex formation with STAT3 (Ginsberg et al., 2007). The requirement of adjacent STAT-BS and TRE sequences suggests the cooperative role of AP-1 and STAT3 in AP-1-mediated hepcidin transcription, similar to that for the α2-macroglobulin gene.

Hepcidin transcription, via both STAT-BS and TRE regulation, may be elicited by some cytokines. For example, oncostatin M, a stimulator of hepcidin expression (Chung et al., 2010; Kanda et al., 2009), can induce the expression of AP-1 components (Botelho et al., 1998). Not only JAK inhibition but also MEK1/2 inhibition blocked oncostatin M-mediated hepcidin expression (Chung et al., 2010; Kanda et al., 2009); JAK phosphorylates and activates STAT (Ihle, 2001), and MEK1/2 is a MAPK kinase and an upstream molecule that induces AP-1 components (Shaulian and Karin, 2002).

The present study reveals the requirements of BMP-RE1, TRE and STAT-BS for the full induction of hepcidin transcription by serum treatment; BMP-RE1 is essential for the responsiveness to serum, although the BMP activity is not enhanced by serum. In view of a central role of the BMP pathway in hepcidin transcription, AP-1 possibly accelerates hepcidin transcription through enhancement of the basal BMP activity. Previous studies revealed that AP-1 cooperatively enhanced TGF-β-mediated transcription through activated Smad3 and Smad4 (Busnadiego et al., 2013; Funaba et al., 2006; Wong et al., 1999; Zhang et al., 1998), but at present, no direct evidence is available on the role of AP-1 in BMP-mediated signaling. Members of the Jun family physically interact with Smad4 (Liberati et al., 1999), a common Smad that transmits both TGF-β and BMP signals (Massagué, 2012; Miyazono et al., 2010; Sakaki-Yumoto et al., 2013). In addition, a liver-specific disruption of Smad4 decreased the expression of hepcidin in mice, and the overexpression of Smad4 increased the transcription of hepcidin in Hepa1-6 cells (Wang et al., 2005), which indicates the involvement of Smad4 in hepcidin expression. To clarify the role of AP-1 in BMP signaling, the effects of exogenous BMP should be examined in future studies.

During the preparation of this manuscript, the effect of serum treatment on hepcidin transcription was reported (Shanmugam and Cherayil, 2013). These researchers showed that heat-inactivated FBS treatment increased the phosphorylation levels of Smad1/5/8 and hepcidin mRNA levels in HepG2 cells, which were blocked by co-treatment with dorsomorphin, an inhibitor of the BMP type I receptor, as well as AMPK (Yu et al., 2008b; Zhou et al., 2001). These authors concluded that BMP or BMP-related proteins in heat-inactivated FBS are responsible for the serum-induced hepcidin mRNA changes, and these

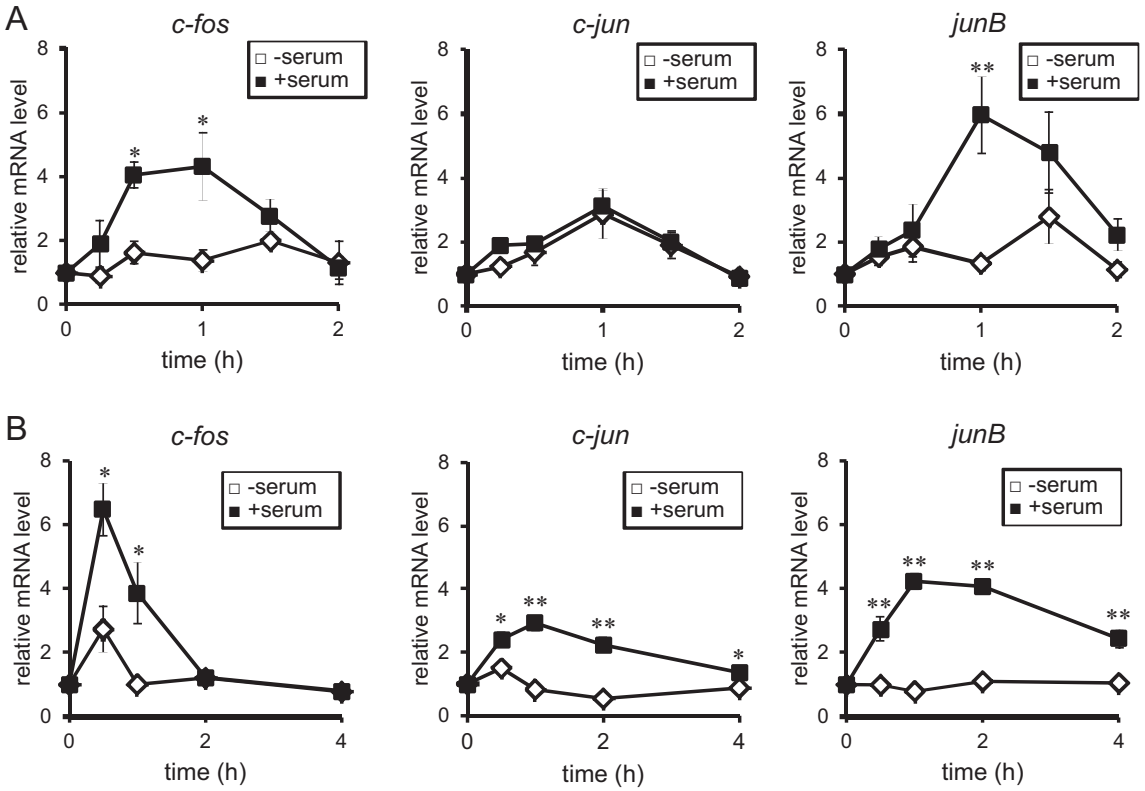

Fig. 6. The induction of AP-1 components in response to serum stimulation. Primary hepatocytes (A) and HepG2 cells (B) were cultured in the absence of heat-inactivated FBS for 4 h followed by culturing with or without 10% heat-inactivated FBS for the indicated time. The expression of AP-1 components such as c-fos, c-jun and junB was examined by RT-qPCR and expressed as ratios to Gapdh, with the level in cells at time = 0 set to 1. Data shown are the mean ± SE (n = 4). * and **: $P < 0.05$ and $P < 0.01$, respectively, vs. cells treated without serum at the same time point.

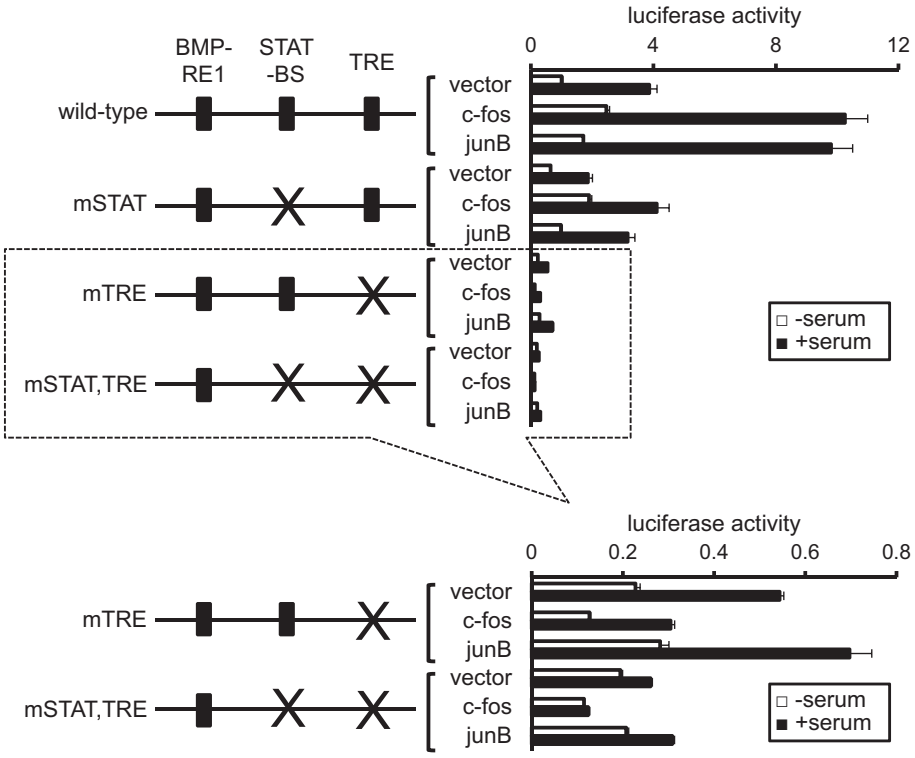

Fig. 7. Enhancement of hepcidin transcription by AP-1 via TRE. The role of AP-1 components in serum-induced hepcidin transcription. After transfection with the indicated AP-1 component expression vector and reporter plasmid, and CMV-βGal, HepG2 cells were cultured in the absence of heat-inactivated FBS for 4 h followed by culturing with or without 10% heat-inactivated FBS for 24 h. Luciferase activity was normalized to β-galactosidase activity, and the luciferase activity was set to 1 in cells that were cultured in the absence of exogenous AP-1 components and FBS and were transfected with hepcidin(−270)-luc. Data were expressed as the mean ± SE from a representative experiment (n = 3).

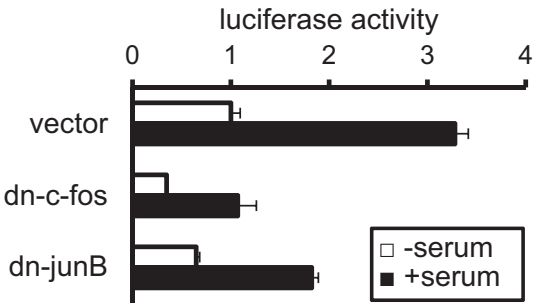

Fig. 8. Inhibition of hepcidin transcription by dn-c-fos and dn-junB. After transfection with the indicated dominant negative form of the AP-1 component expression vector and reporter plasmid, and CMV-βGal, HepG2 cells were cultured in the absence of heat-inactivated FBS for 4 h followed by culturing with or without 10% heat-inactivated FBS for 24 h. Luciferase activity was normalized to β-galactosidase activity, and the luciferase activity was set to 1 in cells that were cultured in the absence of exogenous AP-1 components and FBS and were transfected with hepcidin(−270)-luc. Data were expressed as the mean ± SE from a representative experiment (n = 3).

researchers' results on serum-induced hepcidin expression are consistent with those of the present study. However, the underlying mechanism clearly contrasts with our results; the reason for this inconsistency is currently unknown.

Acknowledgments

We thank Dr. M. Hibi for providing plasmids. This work was partly supported by a research project grant that was awarded by the Azabu University (2013K08) and a grant awarded by the Tokyo Institute of Technology.

References

Anderson, C.P., Shen, M., Eisenstein, R.S., Leibold, E.A., 2012. Mammalian iron metabolism and its control by iron regulatory proteins. Biochim. Biophys. Acta 1823, 1468–1483.
Andriopoulos Jr., B., Corradini, E., Xia, Y., Faasse, S.A., Chen, S., Grgurevic, L., Knutson, M.D., Pietrangelo, A., Vukicevic, S., Lin, H.Y., Babitt, J.L., 2009. BMP6 is a key endogenous regulator of hepcidin expression and iron metabolism. Nat. Genet. 41, 482–487.
Asano, H., Yamada, T., Hashimoto, O., Umemoto, T., Sato, R., Ohwatari, S., Kanamori, Y., Terachi, T., Funaba, M., Matsui, T., 2013. Diet-induced changes in Ucp1 expression in bovine adipose tissues. Gen. Comp. Endocrinol. 184, 87–92.
Botelho, F.M., Edwards, D.R., Richards, C.D., 1998. Oncostatin M stimulates c-Fos to bind a transcriptionally responsive AP-1 element within the tissue inhibitor of metalloproteinase-1 promoter. J. Biol. Chem. 273, 5211–5218.
Busnadiego, O., González-Santamaría, J., Lagares, D., Guinea-Viniegra, J., Pichol-Thievend, C., Muller, L., Rodríguez-Pascual, F., 2013. LOXL4 is induced by transforming growth factor β1 through Smad and JunB/Fra2 and contributes to vascular matrix remodeling. Mol. Cell. Biol. 33, 2388–2401.
Casanovas, G., Mleczko-Sanecka, K., Altamura, S., Hentze, M.W., Muckenthaler, M.U., 2009. Bone morphogenetic protein (BMP)-responsive elements located in the proximal and distal hepcidin promoter are critical for its response to HJV/BMP/SMAD. J. Mol. Med. (Berl.) 87, 471–480.
Chung, B., Verdier, F., Matak, P., Deschemin, J.C., Mayeux, P., Vaulont, S., 2010. Oncostatin M is a potent inducer of hepcidin, the iron regulatory hormone. FASEB J. 24, 2093–2103.
Duran, E.M., Shapshak, P., Worley, J., Minagar, A., Ziegler, F., Haliko, S., Moleon-Borodowsky, I., Haslett, P.A., 2005. Presenilin-1 detection in brain neurons and FOXP3 in peripheral blood mononuclear cells: normalizer gene selection for real time reverse transcriptase PCR using the deltadeltaCt method. Front. Biosci. 10, 2955–2965.
Finberg, K.E., 2013. Regulation of systemic iron homeostasis. Curr. Opin. Hematol. 20, 208–214.
Funaba, M., Murakami, M., 2008. A sensitive detection of phospho-Smad1/5/8 and Smad2 in Western blot analyses. J. Biochem. Biophys. Methods 70, 816–819.
Funaba, M., Ikeda, T., Murakami, M., Ogawa, K., Nishino, Y., Tsuchida, K., Sugino, H., Abe, M., 2006. Transcriptional regulation of mouse mast cell protease-7 by TGF-β. Biochim. Biophys. Acta 1759, 166–170.
Ginsberg, M., Czeko, E., Müller, P., Ren, Z., Chen, X., Darnell Jr., J.E., 2007. Amino acid residues required for physical and cooperative transcriptional interaction of STAT3 and AP-1 proteins c-Jun and c-Fos. Mol. Cell. Biol. 27, 6300–6308.
Guo, W., Bachman, E., Li, M., Roy, C.N., Blusztajn, J., Wong, S., Chan, S.Y., Serra, C., Jasuja, R., Travison, T.G., Muckenthaler, M.U., Nemeth, E., Bhasin, S., 2013. Testosterone administration inhibits hepcidin transcription and is associated with increased iron incorporation into red blood cells. Aging Cell 12, 280–291.
Hentze, M.W., Muckenthaler, M.U., Galy, B., Camaschella, C., 2010. Two to tango: regulation of mammalian iron metabolism. Cell 142, 24–38.
Herrera, B., Inman, G.J., 2009. A rapid and sensitive bioassay for the simultaneous measurement of multiple bone morphogenetic proteins. Identification and quantification of BMP4, BMP6 and BMP9 in bovine and human serum. BMC Cell Biol. 10, 20.
Hess, J., Angel, P., Schorpp-Kistner, M., 2004. AP-1 subunits: quarrel and harmony among siblings. J. Cell Sci. 117, 5965–5973.
Ihle, J.N., 2001. The Stat family in cytokine signaling. Curr. Opin. Cell Biol. 13, 211–217.
Kanamori, Y., Murakami, M., Matsui, T., Funaba, M., 2014. Hepcidin expression in liver cells: evaluation of mRNA levels and transcriptional regulation. Gene 546, 50–55.
Kanda, J., Uchiyama, T., Tomosugi, N., Higuchi, M., Uchiyama, T., Kawabata, H., 2009. Oncostatin M and leukemia inhibitory factor increase hepcidin expression in hepatoma cell lines. Int. J. Hematol. 90, 545–552.
Kim, S.J., Angel, P., Lafyatis, R., Hattori, K., Kim, K.Y., Sporn, M.B., Karin, M., Roberts, A.B., 1990. Autoinduction of transforming growth factor β1 is mediated by the AP-1 complex. Mol. Cell. Biol. 10, 1492–1497.
Lee, P.L., Beutler, E., 2009. Regulation of hepcidin and iron-overload disease. Annu. Rev. Pathol. 4, 489–515.
Liberati, N.T., Datto, M.B., Frederick, J.P., Shen, X., Wong, C., Rougier-Chapman, E.M., Wang, X.F., 1999. Smads bind directly to the Jun family of AP-1 transcription factors. Proc. Natl. Acad. Sci. U. S. A. 96, 4844–4849.
Maes, K., Nemeth, E., Roodman, G.D., Huston, A., Esteve, F., Freytes, C., Callander, N., Katodritou, E., Tussing-Humphreys, L., Rivera, S., Vanderkerken, K., Lichtenstein, A., Ganz, T., 2010. In anemia of multiple myeloma, hepcidin is induced by increased bone morphogenetic protein 2. Blood 116, 3635–3644.
Massagué, J., 2012. TGFβ signalling in context. Nat. Rev. Mol. Cell Biol. 13, 616–630.
Meynard, D., Kautz, L., Darnaud, V., Canonne-Hergaux, F., Coppin, H., Roth, M.P., 2009. Lack of the bone morphogenetic protein BMP6 induces massive iron overload. Nat. Genet. 41, 478–481.
Miyazono, K., Kamiya, Y., Morikawa, M., 2010. Bone morphogenetic protein receptors and signal transduction. J. Biochem. 147, 35–51.
Muckenthaler, M.U., 2008. Fine tuning of hepcidin expression by positive and negative regulators. Cell Metab. 8, 1–3.
Nemeth, E., Valore, E.V., Territo, M., Schiller, G., Lichtenstein, A., Ganz, T., 2003. Hepcidin, a putative mediator of anemia of inflammation, is a type II acute-phase protein. Blood 101, 2461–2463.
Ohta, H., Wakitani, S., Tensho, K., Horiuchi, H., Wakabayashi, S., Saito, N., Nakamura, Y., Nozaki, K., Imai, Y., Takaoka, K., 2005. The effects of heat on the biological activity of recombinant human bone morphogenetic protein-2. J. Bone Miner. Metab. 23, 420–425.
Ransone, L.J., Visvader, J., Wamsley, P., Verma, I.M., 1990. Trans-dominant negative mutants of Fos and Jun. Proc. Natl. Acad. Sci. U. S. A. 87, 3806–3810.
Sakaki-Yumoto, M., Katsuno, Y., Derynck, R., 2013. TGF-β family signaling in stem cells. Biochim. Biophys. Acta 1830, 2280–2296.
Shanmugam, N.K., Cherayil, B.J., 2013. Serum-induced up-regulation of hepcidin expression involves the bone morphogenetic protein signaling pathway. Biochem. Biophys. Res. Commun. 441, 383–386.
Shaulian, E., Karin, M., 2002. AP-1 as a regulator of cell life and death. Nat. Cell Biol. 4, E131–E136.
Smith, C.L., Arvedson, T.L., Cooke, K.S., Dickmann, L.J., Forte, C., Li, H., Merriam, K.L., Perry, V.K., Tran, L., Rottman, J.B., Maxwell, J.R., 2013. IL-22 regulates iron availability in vivo through the induction of hepcidin. J. Immunol. 191, 1845–1855.
Truksa, J., Peng, H., Lee, P., Beutler, E., 2006. Bone morphogenetic proteins 2, 4, and 9 stimulate murine hepcidin 1 expression independently of Hfe, transferrin receptor 2 (Tfr2), and IL-6. Proc. Natl. Acad. Sci. U. S. A. 103, 10289–10293.
Truksa, J., Lee, P., Beutler, E., 2007. The role of STAT, AP-1, E-box and TIEG motifs in the regulation of hepcidin by IL-6 and BMP-9: lessons from human HAMP and murine Hamp1 and Hamp2 gene promoters. Blood Cells Mol. Dis. 39, 255–262.
Truksa, J., Lee, P., Beutler, E., 2009. Two BMP responsive elements, STAT, and bZIP/HNF4/COUP motifs of the hepcidin promoter are critical for BMP, SMAD1, and HJV responsiveness. Blood 113, 688–695.
Verga Falzacappa, M.V., Vujic Spasic, M., Kessler, R., Stolte, J., Hentze, M.W., Muckenthaler, M.U., 2007. STAT3 mediates hepatic hepcidin expression and its inflammatory stimulation. Blood 109, 353–358.
Wang, R.H., Li, C., Xu, X., Zheng, Y., Xiao, C., Zerfas, P., Cooperman, S., Eckhaus, M., Rouault, T., Mishra, L., Deng, C.X., 2005. A role of SMAD4 in iron metabolism through the positive regulation of hepcidin expression. Cell Metab. 2, 399–409.
Wong, C., Rougier-Chapman, E.M., Frederick, J.P., Datto, M.B., Liberati, N.T., Li, J.M., Wang, X.F., 1999. Smad3-Smad4 and AP-1 complexes synergize in transcriptional activation of the c-Jun promoter by transforming growth factor β. Mol. Cell. Biol. 19, 1821–1830.
Wrighting, D.M., Andrews, N.C., 2006. Interleukin-6 induces hepcidin expression through STAT3. Blood 108, 3204–3209.
Wu, X., Yung, L.M., Cheng, W.H., Yu, P.B., Babitt, J.L., Lin, H.Y., Xia, Y., 2012. Hepcidin regulation by BMP signaling in macrophages is lipopolysaccharide dependent. PLoS One 7, e44622.
Yu, P.B., Deng, D.Y., Lai, C.S., Hong, C.C., Cuny, G.D., Bouxsein, M.L., Hong, D.W., McManus, P.M., Katagiri, T., Sachidanandan, C., Kamiya, N., Fukuda, T., Mishina, Y., Peterson, R.T., Bloch, K.D., 2008a. BMP type I receptor inhibition reduces heterotopic ossification. Nat. Med. 14, 1363–1369.
Yu, P.B., Hong, C.C., Sachidanandan, C., Babitt, J.L., Deng, D.Y., Hoyng, S.A., Lin, H.Y., Bloch, K.D., Peterson, R.T., 2008b. Dorsomorphin inhibits BMP signals required for embryogenesis and iron metabolism. Nat. Chem. Biol. 4, 33–41.
Zhang, Y., Feng, X.H., Derynck, R., 1998. Smad3 and Smad4 cooperate with c-Jun/c-Fos to mediate TGF-β-induced transcription. Nature 394, 909–913.
Zhou, G., Myers, R., Li, Y., Chen, Y., Shen, X., Fenyk-Melody, J., Wu, M., Ventre, J., Doebber, T., Fujii, N., Musi, N., Hirshman, M.F., Goodyear, L.J., Moller, D.E., 2001. Role of AMP-activated protein kinase in mechanism of metformin action. J. Clin. Invest. 108, 1167–1174.

Gene 546 (2014) 50–55

Contents lists available at ScienceDirect

Gene

journal homepage: www.elsevier.com/locate/gene

Hepcidin expression in liver cells: evaluation of mRNA levels and transcriptional regulation

Yohei Kanamori [a], Masaru Murakami [b], Tohru Matsui [a], Masayuki Funaba [a,*]

[a] Division of Applied Biosciences, Kyoto University Graduate School of Agriculture, Kyoto 606-8502, Japan
[b] Laboratory of Molecular Biology, Azabu University School of Veterinary Medicine, Sagamihara 252-5201, Japan

ARTICLE INFO

Article history:
Received 3 February 2014
Received in revised form 7 May 2014
Accepted 19 May 2014
Available online 20 May 2014

Keywords:
Hepcidin
mRNA
Transcription
BMP
Liver cells

ABSTRACT

Hepcidin produced in the liver negatively regulates intestinal iron absorption, and the bone morphogenetic protein (BMP) pathway is well-known to stimulate hepcidin expression. However, the regulation of hepcidin expression has not been fully elucidated. In this study, we evaluate different systems that can be used to determine how hepcidin expression is regulated. The basal expression of hepcidin in liver cell lines, such as HepG2 cells and Hepa1-6 cells, was lower than that in the liver and primary hepatocytes; the expression levels of hepcidin in the cell lines were near the limit of detection for RT-PCR and RT-qPCR analyses. Treatment with trichostatin A, RNAlater, or MG-132 enhanced the expression of hepcidin in HepG2 cells, suggesting that histone deacetylation, instability of mRNA, or proteosomal degradation of the protein(s) that positively regulate hepcidin expression may be responsible for the decreased expression of hepcidin in HepG2 cells. In luciferase-based reporter assays, BMP induced the transcription of a reporter, hepcidin(−2018)-luc, that contains nt −2018 through nt −35 of the hepcidin promoter in HepG2 cells and Hepa1-6 cells. However, BRE-luc, a representative reporter used to evaluate BMP signaling, was unresponsive to BMP in HepG2 cells. These results suggest that hepcidin transcription can be best evaluated in liver cell lines and that the hepcidin promoter senses BMP signaling with high sensitivity. The present study demonstrates that studies regarding the regulation of hepcidin expression at the mRNA level should be evaluated in primary hepatocytes, and liver cell lines are well-suited for studies examining the transcriptional regulation of hepcidin.

1. Introduction

The iron uptake of the body is tightly regulated through the modulation of its absorption from the intestine (Lee and Beutler, 2009). Ferric iron is reduced at the luminal site by intestinal cytochrome b, and ferrous iron is transferred into the enterocyte via the transmembrane protein divalent metal transporter-1. On the basolateral side, ferrous iron is exported from enterocytes to the circulatory system via ferroportin, and after being oxidized by the membrane bound ferroxidase hephaestin, iron is incorporated into transferrin (Ganz and Nemeth, 2012).

Hepcidin is a 25-amino acid antimicrobial peptide that serves as the central regulator of intestinal iron absorption (Lee and Beutler, 2009). Hepcidin binds to the iron exporter ferroportin and induces its endocytosis and proteolysis, thus preventing intestinal absorption of iron (De Domenico et al., 2007; Nemeth et al., 2004). Previous studies suggested that hepcidin activity is mainly regulated at the gene transcript level (Ganz and Nemeth, 2012). The ratio of intestinal iron absorption to iron intake decreases as dietary iron levels increase (Laftah et al., 2004), and this is achieved by the up-regulation of hepatic hepcidin expression (Corradini et al., 2009; Kautz et al., 2008). The current model suggests that hepcidin expression is transcriptionally regulated by the pathway induced by bone morphogenetic proteins (BMPs) such as BMP2, BMP4, BMP6 and BMP9 (Babitt et al., 2006, 2007; Lee and Beutler, 2009; Muckenthaler, 2008; Truksa et al., 2006). Increased levels of iron have been shown to increase the hepatic expression of BMP6 (Kautz et al., 2008), and the disruption of BMP6 resulted in decreased hepatic hepcidin expression and the accumulation of iron in the liver (Andriopoulos et al., 2009; Meynard et al., 2009). However, factors other than the BMPs are also involved in modulating hepcidin expression (Goodnough et al., 2012; Lee and Beutler, 2009; Muckenthaler, 2008), indicating that the mechanisms governing hepcidin expression have not yet been fully elucidated.

Abbreviations: BMP, bone morphogenetic protein; CMF, calcium and magnesium-free; HBSS, Hank's buffered salt solution; DMEM, Dulbecco's modified Eagle's medium; FBS, fetal bovine serum; ALK, activin receptor-like kinase; RT-PCR, reverse transcription-polymerase chain reaction; RT-qPCR, reverse transcription-quantitative polymerase chain reaction; Gapdh, glyceraldehyde-3-phosphate dehydrogenase; pCMV-βGal, plasmid expressing β-galactosidase under the control cytomegalovirus promoter; SEM, standard error of the mean; Id1, inhibitor of differentiation 1; Hprt1, hypoxanthine phosphoribosyltransferase 1.

* Corresponding author at: Division of Applied Biosciences, Kyoto University Graduate School of Agriculture, Kitashirakawa Oiwakecho, Kyoto 606-8502, Japan.
E-mail address: mfunaba@kais.kyoto-u.ac.jp (M. Funaba).

http://dx.doi.org/10.1016/j.gene.2014.05.040
0378-1119/

While exploring the factors that affect hepcidin expression, we noticed that hepcidin expression in liver cell lines is extremely low compared to that in the liver and primary hepatocytes, and this low level of expression makes it difficult to evaluate the regulation of hepcidin at the mRNA level. The main objective of this study is to clarify the differences of the hepcidin expression level among the livers, primary hepatocytes and liver cell lines. The present study provides information on cultured cell systems suitable for evaluating hepcidin expression.

2. Materials & methods

2.1. Animals and cell culture

Animal experiments were approved by the Kyoto University Animal Experiment Committee or the Azabu University Animal Experiment Committee. Mouse and rat livers were obtained from normal adult C57BL/6 mice and Sprague–Dawley rats, respectively. Primary rat hepatocytes were isolated by collagenase digestion of livers from male Wistar rats weighing 200 to 300 g. Livers were perfused from the portal vein to the incised inferior vena cava with calcium and magnesium-free (CMF) buffer consisting of 40 mM Hepes, pH 7.4, 120 mM NaCl, 5.4 mM KCl, 5.0 mM $NaHCO_3$ and 5.6 mM glucose supplemented with 100 U/mL penicillin, 100 μg/mL streptomycin and 250 ng/mL amphotericin B for 10 min at a rate of ~12 mL/min followed by perfusion with CMF buffer containing 0.05% collagenase (Wako, Tokyo, Japan) for 10 min. Subsequently, hepatocytes were liberated into Hank's buffered salt solution (HBSS), i.e., 140 mM NaCl, 5.4 mM KCl, 0.34 mM Na_2HPO_4, 0.44 mM KH_2PO_4, 0.81 mM $MgSO_4 \cdot 7H_2O$, 1.3 mM $CaCl_2$, 4.2 mM $NaHCO_3$ and 5.6 mM glucose supplemented with 100 U/mL penicillin, 100 μg/mL streptomycin and 250 ng/mL amphotericin B. After cell recovery by centrifugation at 50 ×*g* for 2 min, the cells were washed with HBSS three times and resuspended in Dulbecco's modified Eagle's medium (DMEM) with 10% fetal bovine serum (FBS) and antibiotics. Cells (>90% hepatocytes by microscopy) were seeded on collagen-coated plates at 1.5×10^5 cells per well in 12-well plates. After attachment, the medium was replaced with the same medium, and the cells were incubated for 24 h. Then, the cells were treated with or without BMP2 (4 nM; R&D Systems, Minneapolis, MN, USA) in the presence or absence of cycloheximide (0.5 μg/mL) for 12 h.

HepG2 hepatoma cells, Hepa1-6 hepatoma cells and 3T3-L1 preadipocytes were cultured in DMEM with 10% FBS and antibiotics. For the luciferase-based reporter assays, these cells were transiently transfected using PolyFect transfection reagent (Qiagen, Valencia, CA, USA) or polyethylenimine Max reagent (Polysciences, Warrington, PA, USA), according to the manufacturers' protocols. At 24 h post-transfection, the cells were pre-treated with or without LDN-193189 (100 nM), an inhibitor of the BMP type I receptor (Cuny et al., 2008), for 15 min before BMP2 (4 nM) treatment for 16 h. To evaluate the expression of constitutively active activin receptor-like kinase (ALK) 3 (ALK3(QD)), cells were harvested at 36 h post-transfection. To evaluate the levels of hepcidin mRNA, HepG2 cells and Hepa1-6 cells were treated for 24 h with or without trichostatin A (TSA: 0.1 μg/mL; Wako, Tokyo, Japan), an inhibitor of class I and II histone deacetylases (Gräff and Tsai, 2013), RNAlater (0.1 or 1%; Life Technologies, Carlsbad, CA, USA) to denature RNase at a controlled pH (Zaitoun et al., 2010) or MG-132 (20 μM; EMD Millipore, Billerica, MA, USA), a proteasome inhibitor (Tsubuki et al., 1993). In Hepa1-6 cells, treatment with MG-132 at 20 μM caused detachment of the cells from culture dish, and, therefore, we also treated with MG-132 at 10 μM.

2.2. RNA isolation, RT-PCR and RT-quantitative PCR

Total RNA was isolated from the livers and cells, and cDNA was synthesized using TRIZOL (Invitrogen, Grand Island, NY, USA) and ReverTra Ace qPCR RT kit (Toyobo, Osaka, Japan), respectively, according to the manufacturers' protocols. The cDNA reverse-transcribed from 5 or 20 ng of total RNA was used as a template for conventional reverse transcription-polymerase chain reaction (RT-PCR) or RT-quantitative PCR (RT-qPCR) using SYBR Green I (Thunderbird SYBR qPCR mix, Toyobo, Osaka, Japan) as described previously (Asano et al., 2013). The oligonucleotide primers for the conventional RT-PCR and RT-qPCR are presented in Table 1. The Ct value was determined, and the abundance of gene transcripts was analyzed using the $^{\Delta\Delta}$Ct method using glyceraldehyde-3-phosphate dehydrogenase (Gapdh) as the normalization gene (Duran et al., 2005).

2.3. Plasmids and reporter assays

Plasmids were obtained as follows: BRE-luc reporter plasmids (Korchynskyi and ten Dijke, 2002) was from Dr. P. ten Dijke, and ALK3(QD) (Imamura et al., 1997) was obtained from Dr. K. Miyazono. The DNA fragment spanning from −2018 bp to −35 bp of the mouse hepcidin (Hamp1) promoter was amplified and cloned into the basic vector pGL4 containing the firefly luciferase reporter (Hepcidin (−2018)-luc) with nt +1 as the translation initiation site. The product was verified through nucleotide sequencing. Luciferase-based reporter

Table 1
Oligonucleotide PCR primers for RT-PCR and RT-qPCR.

	Oligonucleotide		GenBank accession number
	5′-primer	3′-primer	
RT-PCR and qPCR:			
Gapdh	5′-TTCATTGACCTCAACTACATGGT-3′	5′-GCTAAGCAGTTGGTGGTGCAGGA-3′	NM_002046 (human) NM_008084 (mouse) NM_017008 (rat)
Hprt1	5′-ATGGGAGGCCATCACATTG-3′	5′-CTTTCCAGTTAAAGTTGAGAGATCA-3′	NM_000194 (human) NM_013556 (mouse) NM_012583 (rat)
mhHepcidin[a]	5′-TGCCTCCTGCTCCTCCTCCT-3′	5′-GCAGAAAATGCAGATGGGGAAGT-3′	NM_021175 (human) NM_032541 (mouse)
mrHepcidin[b]	5′-GCTGCCTGTCTCCTGCTT-3′	5′-TTACAGCATTTACAGCAGAAGAGG-3′	NM_053469 (rat) NM_032541 (mouse)
RT-PCR:			
Tmprss6	5′-CACTGTGACTGTGGCCTCCAGG-3′	5′-CGTCGTAGTCATGGCTGTCCTC-3′	NM_153609 (human) NM_027902 (mouse) NM_001130556 (rat)
RT-qPCR:			
rGapdh	5′-ACAACTTTGGCATCGTGGA-3′	5′-CTTCTGAGTGGCAGTGATGG-3′	NM_017008 (rat)
rHepcidin	5′-GCTGCCTGTCTCCTGCTT-3′	5′-AGCCGTAGTCTGTCTCGTCT-3′	NM_053469 (rat)

[a] PCR primers common to mouse and human hepcidin.
[b] PCR primers common to mouse and rat hepcidin.

assays were conducted as described previously (Murakami et al., 2009). Cells were transiently transfected with the indicated expression vectors, reporter construct and a plasmid expressing β-galactosidase under the control cytomegalovirus promoter (pCMV-βGal). Equal amounts of DNA were transfected in each experiment and adjusted with empty vector. Luciferase activity was normalized to the β-galactosidase activity, and the luciferase activity in the cell lysate transfected without BMP treatment or with the empty vector was set at 1.

2.4. Statistical analyses

Data are expressed as the mean ± standard error of the mean (SEM). Data on gene expression were log-transformed to provide an approximation of a normal distribution before analysis. Differences between control cells and BMP2-treated cells, between cycloheximide-treated and untreated cells, and between LDN-193189-treated and untreated cells were examined using unpaired *t*-tests. Differences of $P < 0.05$ were considered significant.

3. Results and discussion

3.1. Hepcidin expression is lower in cell lines than in liver and primary hepatocytes

Hepcidin expression was examined in mouse and rat livers, rat primary hepatocytes and the human HepG2 and mouse Hepa1-6 liver cell lines. To compare the hepcidin expression levels, we designed PCR primers to amplify both mouse hepcidin (Hamp1) and rat hepcidin (Fig. 1A), and both human hepcidin and mouse hepcidin (Fig. 1B). Significant hepcidin expression was detected in livers and primary hepatocytes, but the levels of hepcidin expression in HepG2 cells and Hepa1-6 cells was lower or below the limit of detection. Gapdh and hypoxanthine phosphoribosyltransferase 1 (Hprt1), house-keeping genes, were individually amplified by use of common PCR primers applicable to human, mouse and rat Gapdh and Hprt1. The Gapdh levels tended to be higher in HepG2 cells and Hepa1-6 cells than in the livers and primary hepatocytes, and the Hprt1 levels were higher in primary hepatocytes and liver cell lines (Fig. 1C).

We also examined hepcidin expression by RT-qPCR analyses (Fig. 2). Consistent with the RT-PCR analyses (Fig. 1), hepcidin expression level in primary hepatocytes was as high as that in the livers (Fig. 2A), whereas hepcidin expression level was below detection limit in the liver cell lines, including HepG2 cells and Hepa1-6 cells (Fig. 2B). In some samples, we could detect significant fluorescence in qPCR more than 35 cycles in HepG2 cells, but it was not reproducible (data not shown). Hepcidin mRNA level has been clearly detected in liver cell lines including HepG2 cells (Ravasi et al., 2012); the discrepancy could be due to the differences of the sensitivity of RT-qPCR analyses. The RT-qPCR analyses for Gapdh and Hprt1 indicated clear expression in all samples (Fig. 2C and D); similar to the RT-PCR analyses (Fig. 1), expression level in the liver samples tended to be lower than that in the primary hepatocytes and liver cell lines. All these results suggest that hepcidin expression levels in liver cell lines are lower than those in the livers and primary hepatocytes, and that the lower expression of hepcidin in the liver cell lines is not due to a non-specific decrease in gene transcript levels.

There are several possible explanations for the lower hepcidin mRNA levels in the liver cell lines. Hepcidin mRNA is negatively regulated by Tmprss6, a transmembrane matriptase-2 (Du et al., 2008); the increase in Tmprss6 mRNA levels in response to BMP treatment is delayed compared to the up-regulation of hepcidin expression, indicating a negative feedback loop to avoid excess hepcidin expression (Meynard et al., 2011). Because the lower expression of hepcidin in the liver cell lines likely results from higher expression of Tmprss6, we examined the Tmprss6 expression level in liver cell lines. However, Tmprss6 expression was undetectable in the liver cell lines (Fig. 1D). Thus, the low level of hepcidin expression in the liver cell lines is not due to high levels of Tmprss6.

We also examined the potential roles of histone deacetylase activation and mRNA instability in the low expression of hepcidin in liver

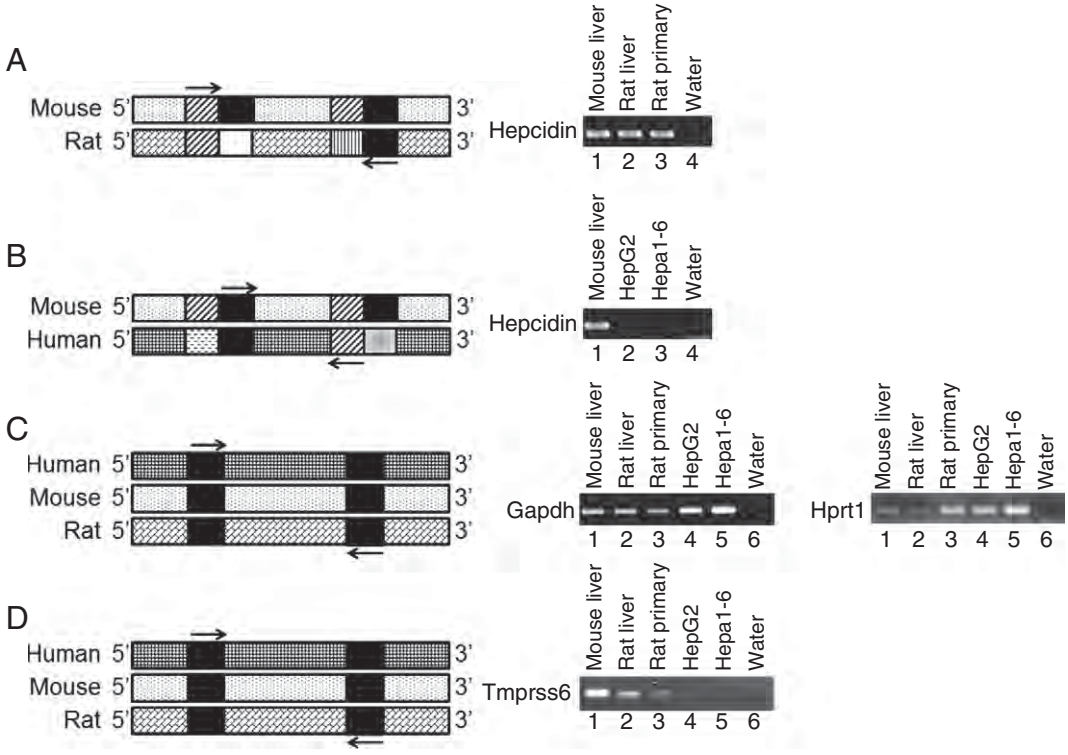

Fig. 1. Hepcidin expression in the liver, primary hepatocytes and liver cell lines. The cDNA was prepared from total RNA from mouse and rat livers, rat primary hepatocytes and the liver cell lines HepG2 and Hepa1-6. RT-PCR was performed using primers to detect (A) mouse and rat hepcidin using mrHepcidin primer set, (B) human and mouse hepcidin using mhHepcidin primer set, (C) human, mouse and rat Gapdh and Hprt1 and (D) human, mouse and rat Tmprss6. The PCR products were electrophoresed on 2% agarose gels and stained with ethidium bromide. A representative result is shown.

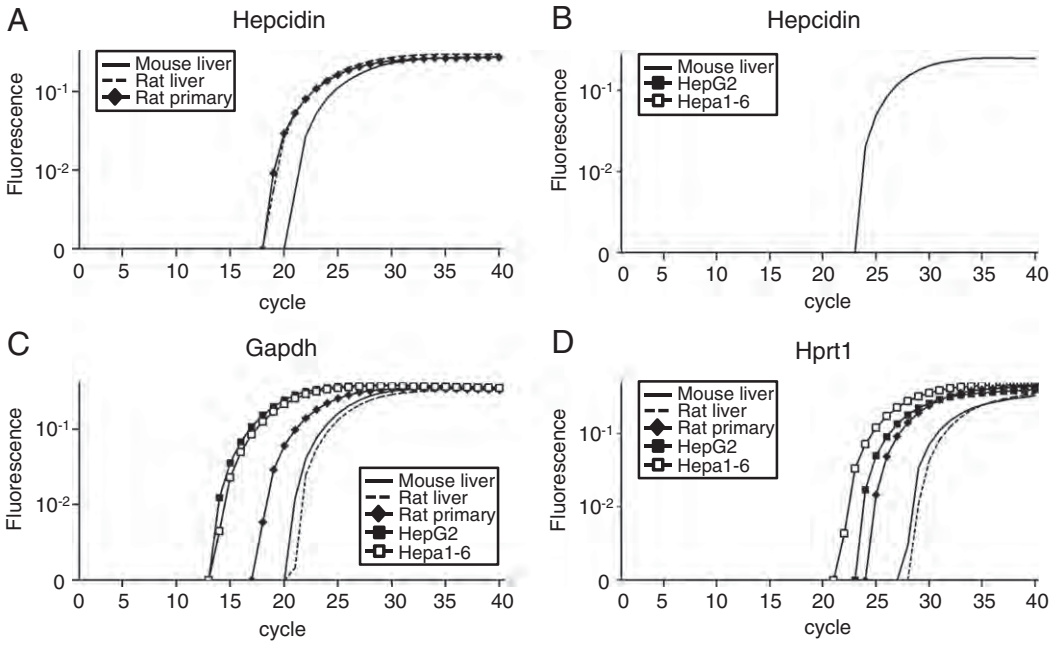

Fig. 2. Lower hepcidin expression in liver cell lines than in the liver and primary hepatocytes. The cDNA was prepared from total RNA from mouse and rat livers, rat primary hepatocytes and the liver cell lines HepG2 and Hepa1-6. RT-qPCR was performed using primers to detect (A) mouse and rat hepcidin using mrHepcidin primer set, (B) human and mouse hepcidin using mhHepcidin primer set, (C) human, mouse and rat Gapdh and (D) human, mouse and rat Hprt1. The amplification plots are shown. Note that cDNA from HepG2 cells and Hepa1-6 cells was not amplified (B).

cell lines. Treatment with TSA robustly increased the expression of hepcidin in HepG2 cells but not in Hepa1-6 cells, although the expression level in cells without TSA treatment was near the limit of detection (Fig. 3A). Hepcidin expression was also induced by treatment with an RNase inhibitor in HepG2 cells but not in Hepa1-6 cells (Fig. 3B). Unlike Hepa1-6 cells, transcriptional repression due to histone deacetylation, mRNA instability or both may be responsible for the low levels of hepcidin in HepG2 cells. We further examined the effect of MG-132 on hepcidin expression. Treatment with MG-132 increased hepcidin transcription in HepG2 cells but not in Hepa1-6 cells (Fig. 3C). These results suggest the different reasons underlying the lower expression level of hepcidin between HepG2 cells and Hepa1-6 cells. Future studies are needed to clarify the reason of the lower expression of hepcidin in Hepa1-6 cells. Additionally, histone acetylation within the hepcidin promoter and hepcidin mRNA instability should be also evaluated to clarify the relation to the silencing of hepcidin in HepG2 cells. Furthermore, the

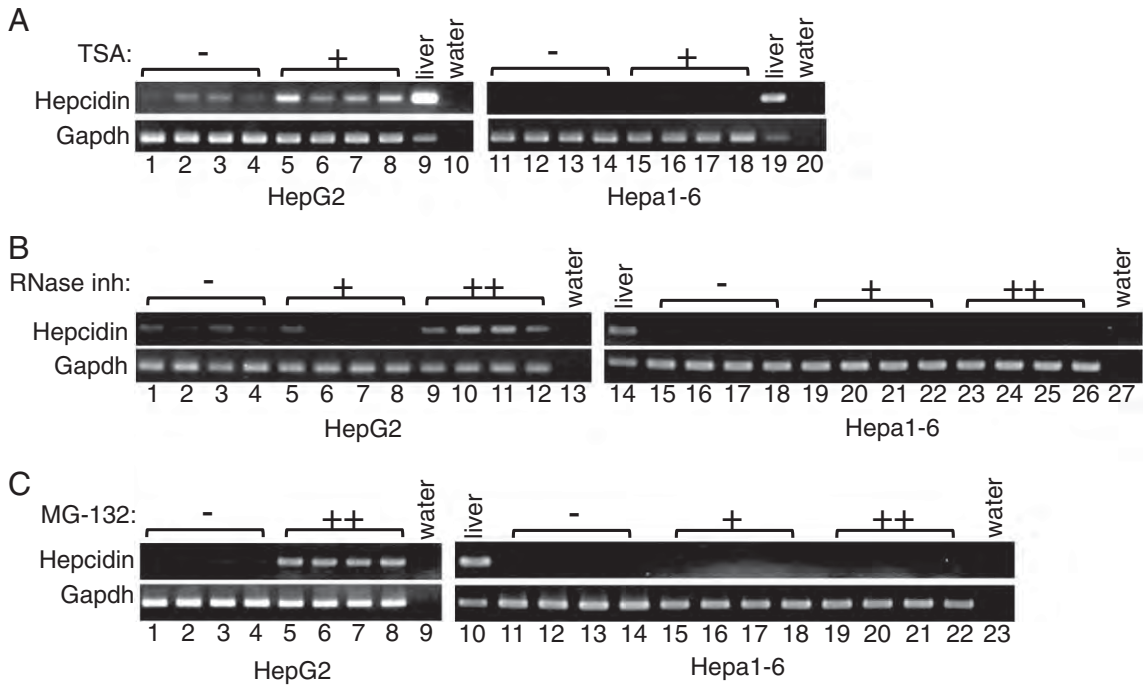

Fig. 3. Altered expression of hepcidin by histone deacetylases, RNase and the proteasome in HepG2 cells but not in Hepa1-6 cells. HepG2 cells were treated with TSA (A), RNase inhibitor (B) or MG-132 (C) as described in the Materials and methods section. The treatments were performed in quadruplicate. The hepcidin (upper) and Gapdh (lower) expression levels were examined by RT-PCR. The PCR products were electrophoresed on 2% agarose gels and stained with ethidium bromide. A representative result is shown.

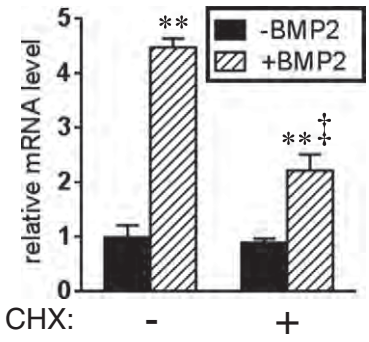

Fig. 4. Hepcidin expression and transcription in response to BMP2 in liver cells. Rat primary hepatocytes were treated with or without BMP2 in the presence (+) or absence (−) of cycloheximide (CHX). Hepcidin expression examined by RT-qPCR using rHepcidin primer set was normalized to Gapdh expression, which was quantified by use of rGapdh primer set. The expression level in cells treated without BMP2 or cycloheximide was set at 1. **: $P < 0.01$ vs. cells treated without BMP2. ‡: $P < 0.01$ vs. cells treated with BMP2 and without cycloheximide.

molecule(s) that positively regulate hepcidin, which is degraded by proteasome, should be identified in HepG2 cells.

As described above, the activation of hepcidin expression by the BMP pathway is well-known (Babitt et al., 2006, 2007; Lee and Beutler, 2009; Muckenthaler, 2008). We also evaluated hepcidin expression in response to BMP treatment and the effect of cycloheximine, a protein synthesis inhibitor, in rat primary hepatocytes. BMP increased hepcidin expression 4.5-fold, and cycloheximide partially blocked the up-regulation of hepcidin expression (Fig. 4). The results indicate that BMP-induced hepcidin expression is partially a direct event, and that it is also enhanced through de novo protein synthesis; the results clearly disagree with a previous study using HepG2 cells in which cycloheximide did not affect BMP-induced hepcidin expression (Babitt et al., 2006). The contradicting conclusions are possibly due to the different cell types used in the studies.

The BMP-regulated expression of hepcidin has been studied in various systems, including the liver cell lines such as HepG2, Hep3B and Huh7 cells (Babitt et al., 2006, 2007; Mleczko-Sanecka et al., 2010; Truksa et al., 2007, 2009). The Lin group has examined hepcidin mRNA by RT-qPCR analyses, and their studies revealed that treatment with BMP increased the expression of hepcidin by 50 to 1100-fold and 12 to 25-fold in Hep3B cells and HepG2 cells, respectively. An approximately 8-fold induction was detected in mouse and rat primary hepatocytes, and intraperitoneal injection of BMP resulted in only a 1.3 to 2-fold increase in hepatic hepcidin expression (Andriopoulos et al., 2009; Babitt et al., 2006, 2007; Corradini et al., 2009, 2010; Theurl et al., 2011). One explanation for the larger effect BMP treatment on hepcidin expression in the liver cell lines may be related to a lower basal expression level; the magnitude of the increase in the hepcidin mRNA copy number in response to BMP treatment relative to the total hepcidin mRNA is larger when the basal expression is lower. Examining hepcidin mRNA in liver cell lines can allow one to overlook factor(s) that positively and negatively affect hepcidin expression.

3.2. Hepcidin transcription can be examined in cell lines

Primary hepatocytes are suitable for examining hepcidin mRNA levels, but they are inappropriate for studying the transcriptional regulation of hepcidin using a reporter gene; it is generally difficult to transfect primary cells with plasmid DNA, although plasmid DNA can be highly transfected in primary cells by use of a special apparatus (Gresch and Altrogge, 2012). In contrast, cell lines can be easily transfected with plasmid DNA, and the transcriptional regulation of hepcidin has been examined by luciferase-based reporter assays in many studies (Goodnough et al., 2012; Mleczko-Sanecka et al., 2010; Pandur et al., 2013; Truksa et al., 2009). Consistent with the results of previous studies, the expression of hepcidin(−2018)-luc was significantly increased by BMP treatment in HepG2 cells ($P < 0.01$) and was inhibited by pretreatment with LDN-193189; both basal expression of the luciferase

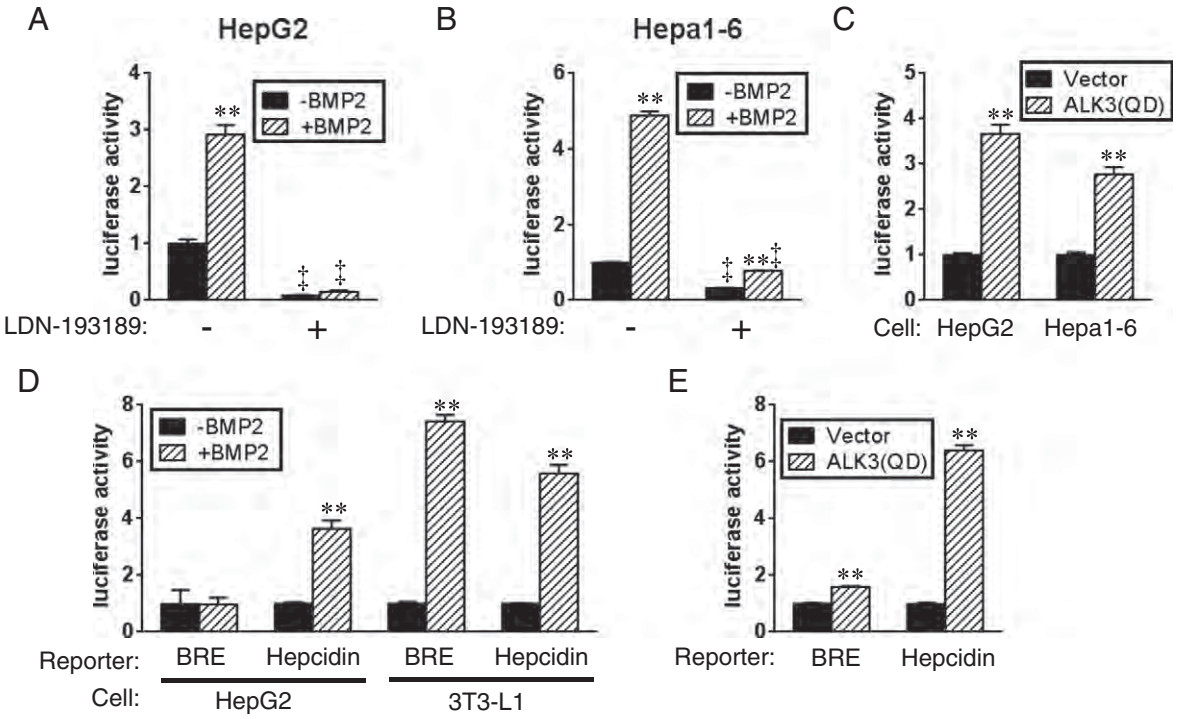

Fig. 5. Hepcidin expression and transcription in response to BMP2 in liver cells. HepG2 cells (A) and Hepa1-6 cells (B) were transiently transfected with Hepcidin(−2018)-luc and pCMV-βGal and treated with or without BMP2 in the presence (+) or absence (−) of LDN-193189. (C) Hepcidin(−2018)-luc, ALK3(QD) and pCMV-βGal were transfected into the indicated cells. (D) The indicated reporter gene and pCMV-βGal were transfected in HepG2 and 3T3-L1 cells, and the cells were treated with or without BMP2. (E) HepG2 cells were transfected with the indicated reporter, ALK3(QD) and pCMV-βGal. Luciferase activity was normalized to β-galactosidase activity, and luciferase activity in the cell lysates in the absence of BMP2, ALK3(QD) and LDN-193189 was set at 1. Data are expressed as the mean ± S.E. (n = 3). **: $P < 0.01$ vs. cells treated without BMP2. ‡: $P < 0.01$ vs. cells treated without LDN-193189.

and the induced expression in response to BMP treatment were significantly decreased ($P < 0.01$, Fig. 5A). Similar results were obtained in Hepa1-6 cells (Fig. 5B). Furthermore, the enhanced transcription of hepcidin(−2018)-luc was significantly elicited by the forced expression of ALK3(QD), a constitutively active BMP type I receptor (Imamura et al., 1997) ($P < 0.01$, Fig. 5C). These results confirm previous results that showed that BMP-induced hepcidin transcription is evaluated in liver cell lines.

BRE-luc, which is derived from the promoter region of inhibitor of differentiation 1 (Id1), a BMP target gene, is a representative reporter that transmits canonical BMP signaling (Korchynskyi and ten Dijke, 2002). Provided that hepcidin transcription is stimulated by the BMP pathway in liver cells (Fig. 5A–C), we expected that not only hepcidin(−2018)-luc but also BRE-luc is transcriptionally stimulated by the BMP pathway. However, the BMP-induced transcriptional activation of BRE-luc was not detected in HepG2 cells. 3T3-L1 cells and C2C12 cells are non-liver cells that can transmit canonical BMP signaling (Korchynskyi and ten Dijke, 2002; Rebbapragada et al., 2003); in these cells, BMP treatment increased expression of BRE-luc and hepcidin(−2018)-luc ($P < 0.01$, Fig. 5D, data not shown). The higher response of hepcidin(−2018)-luc than BRE-luc was also detected when the BMP signal was transmitted by ALK3(QD) expression, although ALK3(QD) expression significantly increased expression of hepcidin(−2018)-luc ($P < 0.01$, Fig. 5E). The results suggest that it is difficult to evaluate BMP signaling by BRE-luc and that the hepcidin promoter senses exogenous BMP with high sensitivity in liver cell lines, thus extending the current understanding of how hepcidin expression is regulated by the BMP pathway.

4. Conclusions

The present study revealed that 1) compared with expression in the livers and primary hepatocytes, hepcidin expression levels are lower in liver cell lines, 2) the activation of histone deacetylase and the accelerated degradation of mRNA or protein(s) may be involved in the lower expression levels of hepcidin in HepG2 cells, and 3) the transcriptional regulation of hepcidin, which is highly responsive to BMP, can be evaluated in liver cell lines. We conclude that primary hepatocytes should be used to examine the regulation of hepcidin expression at the mRNA level. In addition, liver cell lines such as HepG2 cells and Hepa1-6 cells should be limited to studies that aim to evaluate the transcriptional regulation of hepcidin.

Conflict of interest

The authors have declared that there is no conflict of interest.

Acknowledgments

We thank Drs. K. Miyazono and P. ten Dijke for providing plasmids. This work was partly supported by a research project grant awarded by the Azabu University (2013K08).

References

Andriopoulos Jr., B., Corradini, E., Xia, Y., Faasse, S.A., Chen, S., Grgurevic, L., Knutson, M.D., Pietrangelo, A., Vukicevic, S., Lin, H.Y., Babitt, J.L., 2009. BMP6 is a key endogenous regulator of hepcidin expression and iron metabolism. Nat. Genet. 41, 482–487.

Asano, H., Yamada, T., Hashimoto, O., Umemoto, T., Sato, R., Ohwatari, S., Kanamori, Y., Terachi, T., Funaba, M., Matsui, T., 2013. Diet-induced changes in Ucp1 expression in bovine adipose tissues. Gen. Comp. Endocrinol. 184, 87–92.

Babitt, J.L., Huang, F.W., Wrighting, D.M., Xia, Y., Sidis, Y., Samad, T.A., Campagna, J.A., Chung, R.T., Schneyer, A.L., Woolf, C.J., Andrews, N.C., Lin, H.Y., 2006. Bone morphogenetic protein signaling by hemojuvelin regulates hepcidin expression. Nat. Genet. 38, 531–539.

Babitt, J.L., Huang, F.W., Xia, Y., Sidis, Y., Andrews, N.C., Lin, H.Y., 2007. Modulation of bone morphogenetic protein signaling in vivo regulates systemic iron balance. J. Clin. Invest. 117, 1933–1939.

Corradini, E., Garuti, C., Montosi, G., Ventura, P., Andriopoulos Jr., B., Lin, H.Y., Pietrangelo, A., Babitt, J.L., 2009. Bone morphogenetic protein signaling is impaired in an HFE knockout mouse model of hemochromatosis. Gastroenterology 137, 1489–1497.

Corradini, E., Schmidt, P.J., Meynard, D., Garuti, C., Montosi, G., Chen, S., Vukicevic, S., Pietrangelo, A., Lin, H.Y., Babitt, J.L., 2010. BMP6 treatment compensates for the molecular defect and ameliorates hemochromatosis in Hfe knockout mice. Gastroenterology 139, 1721–1729.

Cuny, G.D., Yu, P.B., Laha, J.K., Xing, X., Liu, J.F., Lai, C.S., Deng, D.Y., Sachidanandan, C., Bloch, K.D., Peterson, R.T., 2008. Structure–activity relationship study of bone morphogenetic protein (BMP) signaling inhibitors. Bioorg. Med. Chem. Lett. 18, 4388–4392.

De Domenico, I., Ward, D.M., Langelier, C., Vaughn, M.B., Nemeth, E., Sundquist, W.I., Ganz, T., Musci, G., Kaplan, J., 2007. The molecular mechanism of hepcidin-mediated ferroportin down-regulation. Mol. Biol. Cell 18, 2569–2578.

Du, X., She, E., Gelbart, T., Truksa, J., Lee, P., Xia, Y., Khovananth, K., Mudd, S., Mann, N., Moresco, E.M., Beutler, E., Beutler, B., 2008. The serine protease TMPRSS6 is required to sense iron deficiency. Science 320, 1088–1092.

Duran, E.M., Shapshak, P., Worley, J., Minagar, A., Ziegler, F., Haliko, S., Moleon-Borodowsky, I., Haslett, P.A., 2005. Presenilin-1 detection in brain neurons and FOXP3 in peripheral blood mononuclear cells: normalizer gene selection for real time reverse transcriptase pcr using the deltadeltaCt method. Front. Biosci. 10, 2955–2965.

Ganz, T., Nemeth, E., 2012. Hepcidin and iron homeostasis. Biochim. Biophys. Acta 1823, 1434–1443.

Goodnough, J.B., Ramos, E., Nemeth, E., Ganz, T., 2012. Inhibition of hepcidin transcription by growth factors. Hepatology 56, 291–299.

Gräff, J., Tsai, L.H., 2013. Histone acetylation: molecular mnemonics on the chromatin. Nat. Rev. Neurosci. 14, 97–111.

Gresch, O., Altrogge, L., 2012. Transfection of difficult-to-transfect primary mammalian cells. Methods Mol. Biol. 801, 65–74.

Imamura, T., Takase, M., Nishihara, A., Oeda, E., Hanai, J., Kawabata, M., Miyazono, K., 1997. Smad6 inhibits signalling by the TGF-β superfamily. Nature 389, 622–626.

Kautz, L., Meynard, D., Monnier, A., Darnaud, V., Bouvet, R., Wang, R.H., Deng, C., Vaulont, S., Mosser, J., Coppin, H., Roth, M.P., 2008. Iron regulates phosphorylation of Smad1/5/8 and gene expression of Bmp6, Smad7, Id1, and Atoh8 in the mouse liver. Blood 112, 1503–1509.

Korchynskyi, O., ten Dijke, P., 2002. Identification and functional characterization of distinct critically important bone morphogenetic protein-specific response elements in the Id1 promoter. J. Biol. Chem. 277, 4883–4891.

Laftah, A.H., Ramesh, B., Simpson, R.J., Solanky, N., Bahram, S., Schümann, K., Debnam, E.S., Srai, S.K., 2004. Effect of hepcidin on intestinal iron absorption in mice. Blood 103, 3940–3944.

Lee, P.L., Beutler, E., 2009. Regulation of hepcidin and iron-overload disease. Annu. Rev. Pathol. 4, 489–515.

Meynard, D., Kautz, L., Darnaud, V., Canonne-Hergaux, F., Coppin, H., Roth, M.P., 2009. Lack of the bone morphogenetic protein BMP6 induces massive iron overload. Nat. Genet. 41, 478–481.

Meynard, D., Vaja, V., Sun, C.C., Corradini, E., Chen, S., López-Otín, C., Grgurevic, L., Hong, C.C., Stirnberg, M., Gütschow, M., Vukicevic, S., Babitt, J.L., Lin, H.Y., 2011. Regulation of TMPRSS6 by BMP6 and iron in human cells and mice. Blood 118, 747–756.

Mleczko-Sanecka, K., Casanovas, G., Ragab, A., Breitkopf, K., Müller, A., Boutros, M., Dooley, S., Hentze, M.W., Muckenthaler, M.U., 2010. SMAD7 controls iron metabolism as a potent inhibitor of hepcidin expression. Blood 115, 2657–2665.

Muckenthaler, M.U., 2008. Fine tuning of hepcidin expression by positive and negative regulators. Cell Metab. 8, 1–3.

Murakami, M., Kawachi, H., Ogawa, K., Nishino, Y., Funaba, M., 2009. Receptor expression modulates the specificity of transforming growth factor-β signaling pathways. Genes Cells 14, 469–482.

Nemeth, E., Tuttle, M.S., Powelson, J., Vaughn, M.B., Donovan, A., Ward, D.M., Ganz, T., Kaplan, J., 2004. Hepcidin regulates cellular iron efflux by binding to ferroportin and inducing its internalization. Science 306, 2090–2093.

Pandur, E., Sipos, K., Grama, L., Nagy, J., Poór, V.S., Sétáló, G., Miseta, A., Fekete, Z., 2013. Prohepcidin binds to the HAMP promoter and autoregulates its own expression. Biochem. J. 451, 301–311.

Ravasi, G., Pelucchi, S., Trombini, P., Mariani, R., Tomosugi, N., Modignani, G.L., Pozzi, M., Nemeth, E., Ganz, T., Hayashi, H., Barisani, D., Piperno, A., 2012. Hepcidin expression in iron overload diseases is variably modulated by circulating factors. PLoS One 7, e36425.

Rebbapragada, A., Benchabane, H., Wrana, J.L., Celeste, A.J., Attisano, L., 2003. Myostatin signals through a transforming growth factor β-like signaling pathway to block adipogenesis. Mol. Cell. Biol. 23, 7230–7242.

Theurl, I., Schroll, A., Sonnweber, T., Nairz, M., Theurl, M., Willenbacher, W., Eller, K., Wolf, D., Seifert, M., Sun, C.C., Babitt, J.L., Hong, C.C., Menhall, T., Gearing, P., Lin, H.Y., Weiss, G., 2011. Pharmacologic inhibition of hepcidin expression reverses anemia of chronic inflammation in rats. Blood 118, 4977–4984.

Truksa, J., Peng, H., Lee, P., Beutler, E., 2007. Different regulatory elements are required for response of hepcidin to interleukin-6 and bone morphogenetic proteins 4 and 9. Br. J. Haematol. 139, 138–147.

Truksa, J., Peng, H., Lee, P., Beutler, E., 2006. Bone morphogenetic proteins 2, 4, and 9 stimulate murine hepcidin 1 expression independently of Hfe, transferrin receptor 2 (Tfr2), and IL-6. Proc. Natl. Acad. Sci. U.S.A. 103, 10289–10293.

Truksa, J., Lee, P., Beutler, E., 2009. Two BMP responsive elements, STAT, and bZIP/HNF4/COUP motifs of the hepcidin promoter are critical for BMP, SMAD1, and HJV responsiveness. Blood 113, 688–695.

Tsubuki, S., Kawasaki, H., Saito, Y., Miyashita, N., Inomata, M., Kawashima, S., 1993. Purification and characterization of a Z-Leu-Leu-Leu-MCA degrading protease expected to regulate neurite formation: a novel catalytic activity in proteasome. Biochem. Biophys. Res. Commun. 196, 1195–1201.

Zaitoun, I., Erickson, C.S., Schell, K., Epstein, M.L., 2010. Use of RNAlater in fluorescence-activated cell sorting (FACS) reduces the fluorescence from GFP but not from DsRed. BMC Res. Notes 3, 328.

Mycopathologia (2014) 178:135–143
DOI 10.1007/s11046-014-9758-0

Isolation of Dermatophytes and Related Species from Domestic Fowl (*Gallus gallus domesticus*)

Sayaka Yamaguchi · Ayako Sano · Midori Hiruma · Michiko Murata · Takashi Kaneshima · Yoshiteru Murata · Hideo Takahashi · Sana Takahashi · Yoko Takahashi · Hiroji Chibana · Hidemi Touyama · Nguyen Thi Thanh Ha · Yasutomo Nakazato · You Uehara · Morihiko Hirakawa · Yoshimi Imura · Yoshie Terashima · Yasuhiro Kawamoto · Keji Takahashi · Kazutoshi Sugiyama · Masataro Hiruma · Masaru Murakami · Atsushi Hosokawa · Hiroshi Uezato

Received: 25 January 2014 / Accepted: 9 May 2014 / Published online: 22 June 2014

Abstract We investigated 793 bird combs [645 chickens and 148 fighting cocks (Shamo)] to determine the prevalence of dermatophytes and their related fungal species. The targeted fungal species were recovered from 195 of the 793 examined birds (24.6 %). Prevalence ratios were compared in temperate (the mainland) and subtropical (Nansei Islands) areas, genders, strains, breeding scale (individual and farm), and housing system (in cage and free ranging). The frequency of the fungal species in the mainland, males, fighting cocks, breeding scale by individual nursing, and free-range housing system exhibited significantly higher positive ratios than that in the other groups. A total of 224 dermatophytes and related species were isolated, including 101 *Arthroderma* (*Ar.*) *multifidum*, 83 *Aphanoascus* (*Ap.*) *terreus*, five *Uncinocarpus queenslandicus*, two *U. reesii*, two *Ap. pinarensis*, one *Amauroascus kuehnii*, one *Ar. simii*, one *Gymnoascus petalosporus*, one *Microsporum gallinae*, and 28 *Chrysosporium*-like (*Chrysosporium* spp.) isolates, which were identified using internal transcribed spacer regions of ribosomal RNA gene

S. Yamaguchi · H. Uezato
Department of Dermatology, Faculty of Medicine, University of the Ryukyus, Okinawa, Japan

A. Sano (✉) · H. Touyama · N. T. T. Ha · Y. Nakazato · Y. Uehara · M. Hirakawa · Y. Imura · Y. Kawamoto
Faculty of Agriculture, University of the Ryukyus, 1 Sembaru, Nishihara-cho, Nakagusuku, Okinawa 903-0213, Japan
e-mail: aya_grimalkin@yahoo.co.jp

M. Hiruma · M. Hiruma
Department of Dermatology, Faculty of Medicine, Juntendo University, Tokyo, Japan

M. Murata · S. Takahashi · M. Murakami
Faculty of Veterinary Medicine, Azabu University, Kanagawa, Japan

T. Kaneshima
Ryukyu Animal Clinic Center, Okinawa, Japan

Y. Murata
Murata Animal Hospital, Chiba, Japan

Y. Murata · H. Takahashi
Committee of Infectious Diseases, Chiba Veterinary Medical Association, Chiba, Japan

H. Takahashi
A-Land Oyumino Animal Hospital, Chiba, Japan

Y. Takahashi · H. Chibana
Medical Mycology Research Center, Chiba University, Chiba, Japan

Y. Terashima
Tropical Bioresources Research Center, University of the Ryukyus, Okinawa, Japan

K. Takahashi
Chiba Prefectural Government, Chiba, Japan

sequences. The predominant fungal species in the mainland was *Ap. terreus* and that in the Nansei Islands was *Ar. multifidum*. Pathogenic fungal species to humans and animals were limited to *M. gallinae* and *Ar. simii*, which corresponded to 0.025 % of the isolates in this study.

Keywords Dermatophyte · Ketanophilic · *Gallus gallus domesticus* · Internal transcribed spacer (ITS) rDNA

Introduction

Chickens (*Gallus gallus domesticus*) and their nursing environments contain dermatophytes and related species. The predominant dermatophyte species related to chickens are *Microsporum gallinae* and *Arthroderma* (*Ar.*) *simii*; these are known causative agents of mycotic zoonoses [1, 2]. The former fungal species was isolated from a human [3] and from a fighting cock [4] in Japan. The latter fungal species caused ringworm in an imported chimpanzee [5].

According to Chermette et al., human *Ar. simii* infections are rare [2]; however, the fungal species is spread worldwide [6]. Furthermore, dermatophyte-related species, mainly keratinophilic fungi represented by *Chrysosporium*-like species, have also been isolated from chickens and their raising habitats in Egypt [7, 8], India [9, 11], Nigeria [12], Iran [13], Germany [14], Bahrain [15], and Saint Kitts and Nevis [16].

We previously reported the isolation of chicken dermatophytes; one human case of *M. gallinae* infection was found in a subtropical area of Japan [3], and one case from a fighting cock was reported in a temperate area [4]. However, no other dermatophytes or species related to chicken have been investigated in Japan. The present study, as a representative study in the Far East, aims to investigate the prevalence ratio of dermatophytes and their related fungal species in chickens and fighting cocks (Shamo) with comparisons between temperate and subtropical areas of Japan.

K. Sugiyama
Sugiyama Veterinary Clinic, Shizuoka, Japan

A. Hosokawa
AM Dermatological Clinic, Okinawa, Japan

Materials and Methods

Animals

Seven hundred ninety-three chickens nursing in Japan, including 293 from the mainland and 500 from the Nansei Island areas, were investigated. Prefectures are not mentioned to comply with the privacy policy. The survey was carried out from December 2008 to March 2013. The details of the chickens are given in Table 1. Approval was obtained from the ethics committee for animal welfare of the University of the Ryukyus (No. 2011-5271 and 2012-5437).

Isolation

Transparent plastic tape 18 mm in width (Scotch® Sumitomo 3A, Tokyo, Japan) was cut into strips approximately 10 cm in length. Both 1-cm ends were folded for handling. The adhesive surface (approximately 6 cm in length) was placed on the comb and gently rubbed with both the thumb and index finger to collect scales. The tape was incubated at 42 °C for 4 h to remove the mites. Afterward, the tape was stamped on BBL™ Mycosel™ Agar (Becton, Dickinson and Company (BD), Sparks, MD, USA) plates in duplicate and cultured at 35 °C for up to 28 days.

White to slightly beige colored, cottony or powdery colonies, which are characteristics of dermatophytes and/or related species, were picked and transferred onto potato dextrose agar (Difco™ Potato Dextrose Agar; PDA, BD) slants and incubated at 25 °C for further molecular biological analysis. In addition, we placed the transparent tape on the first colonies to appear and observed them by light microscopy after staining with lactophenol cotton blue to detect round or pyriform conidia attached to the right angle of the hyaline septate hyphae.

Following molecular biological identification, plural fungal sprouts from one comb sample with different genotypes of identical species were treated as individual isolates.

Molecular Biological Identification

Sequences of the internal transcribed spacer (ITS) 1-5.8S-ITS 2 region of the rRNA gene (ITS rDNA) were obtained by routine methods [17]. Briefly, DNA was extracted with a DEXPAT® kit (TaKaRa, Ohtsu,

Table 1 Number of positive samples from a total number of samples classified based on areas, sex, strains, breeding scale, and form

Area	Sex		Strain				Breeding scale		Housing system		Total
	Female	Male	Chicken		Shamo		Individual	Farm	Cage	Free range	
			Female	Male	Female	Male					
Mainland	42/136	47/147	28/115	28/113	14/21	19/44	28/78	61/215	8/19	81/274	89/293
293	(30.9)	(40.0)	(24.3)	(24.8)	(66.6)	(43.2)	(37.8)	(28.4)	(42.1)	(29.6)	(30.4)
Nansei Islands	50/337	56/163	46/321	40/96	4/16	16/67	54/185	52/315	47/348	59/152	106/500
500	(14.8)	(34.4)	(14.3)	(41.7)	(25.0)	(23.9)	(29.2)	(16.5)	(21.2)	(49.2)	(21.2)
Total	92/473	103/320	74/436	68/209	18/37	35/111	82/263	113/530	55/367	140/426	195/793
793	(19.5)	(32.2)	(17.0)	(32.5)	(48.6)	(31.5)	(31.7)	(21.3)	(24.6)	(32.9)	(24.6)

The data are shown as the number of dermatophyte-positive/total number of chickens with the percentage in parentheses

Japan) using a modified procedure. Approximately 100 μL fungal cells from the cultures that were incubated at 25 °C for 1 month on PDA slants was placed in a sterile microtube (1.5 mL); subsequently, 0.5 mL DEXPAT® solution was added, and the mixture was homogenized with a plastic pestle. The tube was incubated at 100 °C for 10 min and then centrifuged at 13,200×*g* for 10 min, and the supernatants were used as DNA samples. Although this type of kit is designed to extract DNA from paraffin-embedded tissue samples, we routinely use it to isolate genes from DNA from fungal cultures because of its convenience [17].

We mixed 2.5 μL DNA extract with Ready-To-Go polymerase chain reaction (PCR) beads (Amersham Pharmacia Tokyo, Japan), 2.5 μL 10 pM primers ITS-5 (5′-GGAAGTAAAAGTCGTAACAAGG-3′) and ITS-4 (5′-TCCTCCGCTTATTGATATGC-3′) [18], and 17.5 μL distilled water. The reaction mixture was subjected to one denaturation cycle at 95 °C for 4 min; 30 amplification cycles at 94 °C for 1 min, 50 °C for 1 min, and 72 °C for 2 min; and a final extension cycle at 72 °C for 10 min in a PCR Thermal Cycler MP (TaKaRa).

The PCR products were visualized by electrophoresis on 1.0 % agarose gels in 1× TBE buffer [0.04 M Tris-boric acid, and 0.001 M ethylenediaminetetraacetic acid (EDTA, pH 8.0)] followed by ethidium bromide staining. The PCR samples were purified using a PCR purification kit (QIAquick, Qiagen Co. Ltd., Tokyo, Japan) and labeled with BigDye Terminator ver. 1.1 (Applied Biosystems, Foster City, CA, USA) following the manufacturer's protocol. The labeled samples were directly sequenced on an ABI PRISM 3100 sequencer (Applied Biosystems) using the primers ITS-5, ITS-4, ITS-2 (5′-GCTGCGTTC TTCATCGATGC-3′), and ITS3 (5′-GCATCGATG AAGAACGCAGC-3′) [18]. The DNA sequences were aligned using GENETEX-MAC genetic information processing software (Software Development Co., Ltd., Tokyo, Japan). Sequences were analyzed by a basic local alignment search tool (BLAST) (http://www.ncbi.nlm.nih.gov/BLAST/Blast.cgi), and closely related sequences were obtained. The confirmation of fungal species was based on >99 % identity to the known fungal species, and those of fungal genera was <98 %.

Statistical Analysis

The comparison of the prevalence ratios of the chickens between the mainland and Nansei Islands, the females and males, the chickens and fighting cocks (Shamo strain), breeding scale (e.g., individual habits and commercial or institutional farms), and housing system (in cage including battery and individual cage and free range) were evaluated using Pearson's chi-square method with odds ratios and two-tailed Fischer's exact probability test via the website http://vassarstats.net/odds2x2.html and the text http://vassarstats.net/textbook/index.html. *P* values <0.05 were considered statistically significant. The area-dependent appearance of the fungal species of *Ar. multifidum* and *Aphanoascus* (*Ap.*) *terreus* was also compared by the same method mentioned above.

Table 2 Statistic comparisons of the prevalence ratio of dermatophyte and their related species in the poultries

Comparisons	Data Number of dermatophyte-positive/ total number of birds (%)	Significance	Odds ratio (range)
Area			
Mainlands versus Nansei Islands	**89/293 (30.4)** versus 106/500 (21.2)	$P < 0.001$	1.6216 (1.1674–2.2525)
Gender			
Males versus females in total birds	**217/320 (67.8)** versus 92/473 (19.5)	$P < 0.0001$	1.9657 (1.4176–2.7256)
Males versus females in mainland	50/158 (31.6) versus 39/135 (28.9)	Not significant	–
Males versus females in Nansei Islands	**50/163 (30.7)** versus 56/337 (16.6)	$P < 0.001$	2.2203 (1.3463–3.4455)
Strain			
Chickens versus fighting cocks in total birds	142/503 (28.2) versus **53/148 (35.8)**	$P < 0.001$	1.9762 (1.3458–2.9019)
Chickens versus fighting cocks in males	68/209 (32.5) versus 35/111 (31.5)	Not significant	–
Chickens versus fighting cocks in Females	74/436 (17.0) versus **18/37 (48.6)**	$P < 0.001$	4.6344 (2.3211–9.2534)
Chickens versus fighting cocks in Mainland	56/228 (24.6) versus **33/65 (50.8)**	$P < 0.001$	3.1674 (1.7873–5.6131)
Chickens versus fighting cocks in Nansei Islands	86/417 (20.6) versus 20/96 (20.8)	Not significant	–
Breeding scale			
Individual versus Farm in total birds	**82/263 (31.2)** versus 113/530 (21.3)	$P < 0.01$	1.6718 (1.1976–2.3338)
Individual versus farm in males[a]	58/166 (34.9) versus 48/155 (31.0)	Not significant	–
Individual versus farm in females[a]	24/97 (24.7) versus 65/375 (17.3)	Not significant	–
Individual versus farm in mainland	28/78 (35.9) versus 61/215 (28.4)	Not significant	–
Individual versus farm in Nansei Islands	**54/185 (29.2)** versus 52/315 (16.5)	$P < 0.001$	2.0849 (1.3499–3.2200)
Housing system			
Cage versus free range in total birds	55/367 (24.6) versus **140/426 (32.9)**	$P < 0.001$	2.7769 (2.0429–5.6727)
Cage versus free range in males[a]	29/115 (25.2) versus 32/205 (15.6)	Not significant	–
Cage versus free range in females[a]	26/252 (10.4) versus **66/221 (29.9)**	$P < 0.001$	3.7012 (2.3485–8.6923)
Cage versus free range in mainland[a]	8/19 (42.1) versus 81/274 (29.6)	Not significant	–
Cage versus free range in Nansei Islands[a]	47/348 (13.5) versus **59/152 (38.8)**	$P < 0.001$	4.0629 (1.6152–6.3607)

[a] Data were not shown in Table 1

Significantly higher data were indicated in bold letters

Results

Of the 793 birds that were examined, dermatophytes or related species were recovered from the combs of 195 (24.6 %). The prevalence ratios based on the gender, strain, breeding scale, and housing system are shown in Table 1. In addition, a marked clinical change was detected in a fighting cock that was positive for *M. gallinae* [4].

The results of the comparisons of area, gender, strain, breeding scale, and housing system are shown in Table 2. The prevalence ratio of the birds from the mainland was significantly higher than that of the Nansei Islands ($P < 0.001$; odds ratio 1.6216).

The prevalence ratio of the males was higher than that of the females ($P < 0.001$; odds ratio 1.9657). No significant difference was noted between the ratios of males and females from the mainland. However, the prevalence ratio of males from the Nansei Islands was significantly higher than that of the females ($P < 0.001$; odds ratio 2.2203).

The prevalence of dermatophyte-related fungi in the Shamo strain was higher than that in chickens of both sexes ($P < 0.001$; odds ratio 1.9762). The comparison between female chickens and female Shamo strain birds showed a significant difference ($P < 0.001$; odds ratio 4.6344). The significance was also detected in the comparison of females from the mainland and those from the Nansei Islands ($P < 0.001$; odds ratio 3.1674). The comparisons in males were not significantly different.

The breeding scale by individual habit exhibited a significantly higher positive ratio than that of commercial or institutional nursing farms ($P < 0.01$; odds ratio 1.6718). There was no significant difference in the prevalence of dermatophyte-related fungi according to the breeding scale of birds in the mainland and birds grouped by gender, while a significant difference was detected in the individual breeding scale in the Nansei Islands ($P < 0.001$; odds ratio 2.0849).

The free-range housing system had a significantly higher positive ratio than that of birds in cages ($P < 0.001$; odds ratio 2.7769). No significant difference was noted in the housing system of the male sex, but a significant difference was observed in the prevalence of dermatophyte-related fungi according to the housing system of females ($P < 0.001$; odds ratio 3.7012). No significant difference was observed in the prevalence of dermatophyte-related fungi according to the housing system of the mainland samples, while a significantly higher prevalence was observed in the free-range housing system in the Nansei Islands ($P < 0.001$; odds ratio 4.0629).

Two hundred twenty-four dermatophytes and related species were isolated in this survey. The number of positive birds and the number of isolates did not match because of duplicate or more isolates and/or genotypes from ten females and 13 males. Isolated species were identified based on ITS rDNA gene sequences with more than 99 % identity to the known isolates in the GenBank database and included 101 *Ar. multifidum*, 83 *Ap. terreus*, five *Uncinocarpus queenslandicus*, two *U. reesii*, one *Ap. pinarensis*, one *Amauroascus* (*Am.*) *kuehnii*, one *Ar. simii*, one *Gymnoascus petalosporus*, and one *M. gallinae* isolates [4]. In addition, 28 *Chrysosporium* spp. isolates were identified based on the gene sequences with <99 % homology to the known species (Table 3). The ITS rDNA gene sequences of the isolates were deposited in the GenBank database under the accession numbers AB861650–AB861872 and AB667976 for *M. gallinae* [4].

Ar. multifidum, *Ap. terreus*, and *Chrysosporium* spp. were isolated from all areas, genders, strains, breeding scales, and housing systems. The background of the *M. gallinae* isolate from a male Shamo has been described in a previous report [4]. *U. queenslandicus* isolates were recorded from the mainland in both sexes of chicken strains with individual breeding and housing in cages. The remaining species were limited to the Nansei Islands. *U. reesii* was isolated from males and females, breeding scales, and housing systems in the Shamo strain. *Ap. pinarensis* was isolated from a female chicken, *Am. kuehnii* was isolated from a male chicken, and *Ar. simii* was isolated from a male Shamo with individual breeding scale and housing in cages, whereas *G. petalosporus* was isolated from a female chicken in farm housing in a battery cage (Table 3).

Ar. multifidum had a significantly higher dermatophyte prevalence ratio in the Nansei Islands than in the mainland ($P < 0.001$; odds ratio 7.4622). The prevalence ratio of *Ar. multifidum* in chickens was higher than that in Shamo ($P < 0.05$; odds ratio 1.9518). The prevalence ratio of dermatophytes and related fungi in *Ap. terreus* was significantly higher in the mainland than in the Nansei Islands ($P < 0.001$; odds ratio 4.7866). Both *Ar. multifidum* and *Ap. terreus* exhibited

Table 3 Details of 224 isolates

Species or genus (number of isolates)	Area		Sex		Strain of bird		Breeding scale	Housing system		
	ML	NI	F	M	C	S	I	FA	CA	FR
Arthroderma multifidum (101)	17 (18.7)	84 (63.2)	44 (42.3)	57 (47.5)	81 (49.4)	20 (33.3)	61 (59.2)	40 (33.1)	40 (60.6)	61 (38.6)
Aphanoascus terreus (83)	53 (58.2)	30 (22.6)	43 (41.3)	40 (33.3)	55 (33.5)	28 (46.7)	21 (20.4)	62 (51.2)	13 (19.7)	70 (44.3)
Chrysosporium sp. (28)	17 (18.7)	11 (8.3)	10 (9.6)	18 (15.0)	20 (12.2)	8 (13.3)	11 (10.7)	17 (14.0)	2 (3.0)	26 (16.5)
Uncinocarpus queenslandicum (5)	5 (5.5)	0 (0)	4 (3.8)	1 (0.8)	5 (3.0)	0 (0)	5 (4.9)	0 (0)	5 (7.6)	0 (0)
Uncinocarpus reesii (2)	0 (0)	2 (1.5)	1 (1.0)	1 (0.8)	0 (0)	2 (3.3)	1 (1.0)	1 (0.8)	1 (1.5)	1 (0.6)
Aphanoascus pinarensis (1)	0 (0)	1 (0.8)	1 (1.0)	0 (0)	1 (0.6)	0 (0)	1 (1.0)	0 (0)	1 (1.5)	0 (0)
Amauroascus kuehnii (1)	0 (0)	1 (0.8)	0 (0)	1 (0.8)	1 (0.6)	0 (0)	1 (1.0)	0 (0)	1 (1.5)	0 (0)
Arthroderma simii (1)	0 (0)	1 (0.8)	0 (0)	1 (0.8)	0 (0)	1 (1.7)	1 (1.0)	0 (0)	1 (1.5)	0 (0)
Gymnoascus petalosporus (1)	0 (0)	1 (0.8)	1 (1.0)	0 (0)	1 (0.6)	0 (0)	0 (0)	1 (0.8)	1 (1.5)	0 (0)
Microsporum gallinae (1)	1 (1.1)	0 (0)	0 (0)	1 (0.8)	0 (0)	1 (1.7)	1 (1.0)	0 (0)	1 (1.5)	0 (0)
Total numbers of isolates (224)	93	131	104	120	164	60	103	121	66	158

The percentage was calculated from the number of isolate(s) divided by the total number of isolates times 100

ML mainland, *NI* Nansei Islands, *F* female, *M* male, *C* chicken, *S* fighting cock (Shamo); *I* individual, *FA* farm, *CA* battery and individual cage, *FR* indoor and outdoor free-range housing

significantly higher prevalence ratios in individual breeding scales than in farms ($P < 0.001$; odds ratios 1.9861 and 4.1033, respectively). On the other hand, *Ar. multifidum* showed a significantly higher ratio in birds housed in cages ($P < 0.001$; odds ratio 2.4464), while *Ap. terreus* exhibited a significantly higher ratio in free-range housing birds ($P < 0.001$; odds ratio 3.2430) (Table 4).

Discussion

The average temperature in Tokyo, as a representative area of the mainland, is 16.8 °C and that of Naha of the Nansei Islands is 23.1 °C based on the data by the Japan Meteorological Agency. Chickens in the temperate regions (mainland) showed significantly higher prevalence ratio of dermatophyte and related species than chickens in the subtropical area (Nansei Islands), indicating that the prevalence of dermatophyte and related species was not correlated with the mean annual temperature.

The prevalence ratio was higher in males than in females and in Shamo strain than in chickens, which seems to reflect the vigorous action of males and Shamo strain. Breeding scales also influenced the prevalence ratio. Sloppy management of the individual housing of the birds could increase the number of target fungal species, because the housing management was out of political control until October 1, 2011. Direct contact with soil by the free-range housing system of the birds may increase the prevalence ratio of the fungal species. We supposed that the prevalence ratio might reflect soil and environmental fungal flora.

There were only two pathogenic dermatophyte isolates: one *Ar. simii* isolate and one *M. gallinae* isolate. The ratio of pathogenic species was extremely low: two of 793 chickens, corresponding to 0.025 %. Furthermore, these fungal species rarely caused zoonotic infection. Human records of *Ar. simii* infections worldwide were reviewed by Beguin et al. [6]. However, both the rare zoonotic dermatophyte species derived from the Shamo strain seemed to be endemic to Japan. To our knowledge, the isolation of *Ar. simii* from autochthonous animals is the first record in Japan, although a previous study showed the isolation of the fungal species from an imported chimpanzee [5].

Interestingly, there were regional differences in the prevalence ratio of the major two fungal species, *Ar. multifidum* and *Ap. terreus*. The former specie was the predominant species in the Nansei Islands and the latter one in the mainlands. These results suggest that the differences are climate and environmental based.

The above two major species may not become pathogenic. According to Chanasee et al. [19],

Table 4 Statistical comparisons of the prevalence ratio of *Ar. multifidum* and *Ap. terreus* in poultry

Comparisons	Data Number of dermatophyte-positive/ total number of isolates (%)	Significance	Odds ratio (range)
Arthroderma multifidum			
Mainland versus Nansei Islands	17/91 (18.7) versus **84/133 (63.2)**	$P < 0.001$	7.4622 (3.9582–14.068)
Males versus females	44/104 (42.3) versus 57/120 (47.5)	Not significant	–
Chickens versus fighting cocks	**81/164 (49.4)** versus 20/60(33.3)	$P< 0.05$	1.9518 (1.0521–3.6207)
Individual versus farm	**51/103 (49.5)** versus 40/121 (33.1)	$P< 0.05$	1.9861 (1.1562–3.4115)
Cage versus free range	**40/66 (60.6)** versus 61/158 (38.6)	$P< 0.001$	2.4464 (1.3581–4.4068)
Aphanoascus terreus			
Mainland versus Nansei Islands	**53/91 (58.2)** versus 30/133 (22.6)	$P< 0.001$	4.7866 (2.6753–8.5712)
Males versus females	43/104 (41.3) versus 40/120 (33.3)	Not significant	–
Chickens versus fighting cocks	55/164 (33.5) versus 28/60 (46.7)	Not significant	–
Individual versus farm	21/103 (20.4) versus **62/121 (51.2)**	$P< 0.001$	4.1033 (2.2579–7.4571)
Cage versus free range	13/66 (19.7) versus **70/158 (44.3)**	$P< 0.001$	3.2430 (1.6380–6.4207)

Significantly higher data were indicated in bold letters

pathogenicity of *Ar. multifidum* to guinea pig skin and the peritoneal cavity of mice were negative. Therefore, we suspect that there is currently no need for concern regarding to *Ar. multifidum* infection. *Ap. terreus* is a keratinophilic fungus and has been isolated from soil and birds [20–23], however, this fungal species has no record of pathogenicity.

Uncinocarpus queenslandicus (*Chrysosporium queenslandicus* anamorph) has been isolated from indoor samples from India [24], soil from Egypt [25] and Kuwait [26]. This species also caused infections in snakes [27]. The present isolates are correspondent to the first isolates of this species in Japan.

U. reesii is related to highly pathogenic fungi, for example, *Coccidioides* spp. and *Paracoccidioides* spp. [28]. Isolation of this fungal species has been recorded in India [29] and Egypt [25]. The present isolates are also the first report in Japan.

The identification of the present *Ap. pinarensis* isolate was based on ITS rDNA gene sequences (AB861811) exhibiting 99 % identity to AJ439433 derived from *Ap. pinarensis* isolated in Cuba. However, we did not detect ascospores with an irregularly reticulate wall and two prominent and delicate equatorial rims under microscopy described by Cano et al. [30].

Am. kuehnii was isolated from crater soil in India [31]. However, identification based on ITS rDNA gene sequences was insufficient because of more than 10 % of diversities among the species tree *via* BLAST search. The identity of the present *Am. kuehnii* to the ex-type strain: CBS 539.72 was 98 %; however, the homologies to the other *Am. kuehnii* sequences were more than 99 % located at the same subcluster at the "Distance tree of results" via BLAST search. Then, we confirm the isolate as *Am. kuehnii*.

G. petalosporus was isolated from a bird sanctuary [32], suggesting the isolate is related to a chicken-breeding environment.

Identification of *Chrysosporium*-like isolates at the species level requires further investigation. *Chrysosporium* spp. are known causative agents for mycotic disease in poultry [9, 10] and are often isolated from feathers [15, 16, 22] and animal-related environments [7–15, 19, 23, 26]. Human cases of onychomycosis [33] and systemic infection in a patient with acute lymphocytic leukemia caused by *Chrysosporium* sp. [34] have been reported. However, the present isolates were not matched to pathogenic *Chrysosporium* spp. based on the ITS rDNA sequences.

In conclusion, the predominant fungal species in the Main Lands was *Ap. terreus* and that in the Nansei

Islands was *Ar. multifidum*. In addition, pathogenic fungal species for humans and animals were limited to *M. gallinae* [4] and *Ar. simii* corresponding to 0.025 % in the present study.

Acknowledgments This study was supported in part by the Special Research Fund for Emerging and Re-emerging Infections of the Ministry of Health, Welfare and Labour (Grant No. H-21-Shinkou-004) and by a Grant-in-Aid for Scientific Research (c) by the Japan Society for the Promotion of Science (JSPS, No. 23580419). We express our gratitude to Drs. Takako Murano (Chiba Prefecture), Tadao Ikeda (Association Pasteur Japan), Eichiro Matayoshi and Taketoshi Kawamitsu (Okinawa Veterinary Medical Association), Takako Okubo and Masami Sudo (Ibaraki Prefecture), Tomo Inomata (Azabu University), and Shigeyuki Matsui and Moriji Iketani (Shizuoka Prefecture). We also thank Ms. Kyoko Yarita, Akiko Takayama, and Yuki Hanami (Medical Mycology Research Center, Chiba University) for technical support.

Conflict of interest The authors report no conflict of interest. The authors alone are responsible for the content and writing of the paper.

References

1. Cabañes FJ. Dermatophytes in domestic animals. In: Kushwaha RKS, Guarro J, editors. Biology of dermatophytes and other keratinophilic fungi, Revista Iberoamericana de Micología, Bilbao; 2000. p. 104–8. http://dermatophytes.reviberoammicol.com/contents.php?104108.
2. Chermette R, Ferreiro L, Guillot J. Dermatophytoses in animals. Mycopathologia. 2008;166:385–405.
3. Miyasato H, Yamaguchi S, Taira K, Hosokawa A, Kayo S, Sano A, Uezato H, Takahashi K. Tinea corporis caused by *Microsporum gallinae*. The first clinical case in Japan. J Dermatol. 2011;38:473–8.
4. Murata M, Takahashi H, Takahashi S, Takahashi Y, Chibana H, Murata Y, Sugiyama K, Kaneshima T, Yamaguchi S, Miyasato H, Murakami M, Kano R, Hasegawa A, Uezato H, Hosokawa A, Sano A. Isolation of *Microsporum gallinae* from a fighting cock (*Gallus gallus domesticus*) in Japan. Med Mycol. 2013;51:144–9.
5. Okoshi S, Takashio M, Hasegawa A. Ringworm caused by *Trichophyton simii* in a captive chimpanzee. Jpn J Med Mycol. 1966;7:204–8.
6. Beguin H, Goens K, Hendrikx M, Planard C, Stubbe D, Detandt M. Is *Trichophyton simii* endemic to the Indian subcontinent? Med Mycol. 2013;51:444–8.
7. Abdel-Gawad KM, Moharram AM. Keratinophilic fungi from the duck nails in Egypt. J Basic Microbiol. 1989;29:259–63.
8. el-Naghy MA, el-Ktatny MS, Fadl-Allah EM, Nazeer WW. Degradation of chicken feathers by *Chrysosporium georgiae*. Mycopathologia. 1998;143:77–84.
9. Dixit AK, Kushwaha RK. Occurrence of keratinophilic fungi on Indian Birds. Folia Microbiol (Praha). 1991;36:383–6.
10. Saidi SA, Bhatt S, Richard JL, Sikdar A, Ghosh GR. *Chrysosporium tropicum* as a probable cause of mycosis of poultry in India. Mycopathologia. 1994;125:143–7.
11. Saxena P, Kumar A, Shrivastava JN. Diversity of keratinophilic mycoflora in the soil of Agra (India). Folia Microbiol (Praha). 2004;49:430–4.
12. Efuntoye MO, Fashanu SO. Occurrence of keratinophilic fungi and dermatophytes on domestic birds in Nigeria. Mycopathologia. 2001;153:87–9.
13. Khosravi AR, Mahmoudi M. Dermatophytes isolated from domestic animals in Iran. Mycoses. 2003;46:222–5.
14. Gründer S, Mayser P, Redmann T, Kaleta EF. Mycological examinations on the fungal flora of the chicken comb. Mycoses. 2005;48:114–9.
15. Mandeel Q, Nardoni S, Mancianti F. Keratinophilic fungi on feathers of common clinically healthy birds in Bahrain. Mycoses. 2011;54:71–7.
16. Gungnani HC, Sharma S, Gupta B. Keratinophilic fungi recovered from feathers of different species of birds in St Kitts and Nevis. West Indian Med J. 2012;61(9):912–5.
17. Murata Y, Sano A, Ueda Y, Inomata T, Takayama A, Poonwan N, Nanthawan M, Mikami Y, Miyaji M, Nishimura K, Kamei K. Molecular epidemiology of canine histoplasmosis in Japan. Med Mycol. 2007;45:233–47.
18. White TJ, Bruns T, Lee S, Taylor JW. Amplification and direct sequencing of fungal ribosomal RNA genes for phylogenetics. In: Innis MH, Gelfand DH, Sninsky JJ, White TJ, editors. PCR protocols: a guide to methods and applications. San Diego, CA: Academic Press; 1990. p. 315–22.
19. Chabasse D, De Gentile L, Bouchara JP. Pathogenicity of some *Chrysosporium* species isolated in France. Mycopathologia. 1989;106:171–7.
20. Hubalek Z. Interspecific affinity among keratinolytic fungi associated with birds. Folia Parasitol (Praha). 1976;23:267–72.
21. Sur B, Ghosh GR. Keratinophilic fungi from Orissa, India, I: isolation from soils. Sabouraudia. 1980;18:269–74.
22. Sur B, Ghosh GR. Keratinophilic fungi from Orissa, India, II: isolations from feathers of wild birds and domestic fowls. Sabouraudia. 1980;18:275–80.
23. Hubalek Z. Keratinophilic fungi associated with free-living mammals and birds. In: Kushwaha RKS, Guarro J, editors. Biology of dermatophytes and other keratinophilic fungi, Revista Iberoamericana de Micología, Bilbao; 2000. p. 93–102. http://dermatophytes.reviberoammicol.com/contents.php?093103.
24. Mitra SK, Sikdar A, Das P. Dermatophytes isolated from selected ruminants in India. Mycopathologia. 1998;142:13–6.
25. Zaki SM, Mikami Y, El-Din AA, Youssef YA. Keratinophilic fungi recovered from muddy soil in Cairo vicinities, Egypt. Mycopathologia. 2005;160:245–51.
26. Al-Musallam AA. Distribution of keratinophilic fungi in animal folds in Kuwait. Mycopathologia. 1990;112:65–70.
27. Vissiennon T, Schüppel KF, Ullrich E, Kuijpers AF. Case report. A disseminated infection due to *Chrysosporium queenslandicum* in a garter snake (*Thamnophis*). Mycoses. 1999;42:107–10.
28. Desjardins CA, Champion MD, Holder JW, Muszewska A, Goldberg J, Bailðo AM, Brigido MM, Ferreira ME, Garcia AM, Grynberg M, Gujja S, Heiman DI, Henn MR, Kodira CD, Leðn-Narvðez H, Longo LV, MaL J, Malavazi I,

Matsuo AL, Morais FV, Pereira M, Rodrðguez-Brito S, Sakthikumar S, Salem-Izacc SM, Sykes SM, Teixeira MM, Vallejo MC, Walter ME, Yandava C, Young S, Zeng Q, Zucker J, Felipe MS, Goldman GH, Haas BJ, McEwen JG, Nino-Vega G, Puccia R, San-Blas G, Soares CM, Birren BW, Cuomo CA. Comparative genomic analysis of human fungal pathogens causing paracoccidioidomycosis. PLoS Genet. 2011;7:e1002345. doi:10.1371/journal.pgen.1002345.

29. Deshmukh SK. Isolation of dermatophytes and other keratinophilic fungi from the vicinity of salt pan soils of Mumbai, India. Mycopathologia. 2004;157:265–7.
30. Cano J, Sagués M, Barrio E, Vidal P, Castañeda RF, Gené J, Guarri J. Molecular taxonomy of *Aphanoascus* and description of two species from soil. Stud Mycol. 2002;47:153–64.
31. Deshmukh SK, Verekar SA. Keratinophilic fungi from the vicinity of meteorite crater soils of Lonar (India). Mycopathologia. 2006;162:303–6.
32. Dhib I, Fathallah A, Yaacoub A, Zemni R, Gaha R, Said MB. Clinical and mycological features of onychomycosis in central Tunisia: a 22 years retrospective study (1986–2007). Mycoses. 2013;56:273–80.
33. Apinis AE, Rees RG. An undescribed keratinophilic fungus from southern Queensland. Trans Brit Mycol Soc. 1977;67:522–24.
34. Levy FE, Larson JT, George E, Maisel RH. Invasive *Chrysosporium* infection of the nose and paranasal sinuses in an immunocompromised host. Otolaryngol Head Neck Surg. 1991;104:384–8.

Nishita et al. BMC Research Notes 2014, 7:116
http://www.biomedcentral.com/1756-0500/7/116

BMC Research Notes

RESEARCH ARTICLE Open Access

Isolation and sequencing of swine carbonic anhydrase VI, an enzyme expressed in the swine kidney

Toshiho Nishita[1*], Juro Yatsu[2], Masaru Murakami[3], Shino Kamoshida[3], Kensuke Orito[4], Nobutune Ichihara[5], Kazuyoshi Arishima[6] and Hideharu Ochiai[7*]

Abstract

Background: Carbonic anhydrase VI (CA-VI) is produced by the salivary gland and is secreted into the saliva. Although CA-VI is found in the epithelial cells of distal straight tubule of swine kidneys, the exact function of CA-VI in the kidneys remains unclear.

Results: CA-VI was located in the epithelial cells of distal straight tubule of swine kidneys.
A full-length cDNA clone of CA-VI was generated from the swine parotid gland by reverse transcription polymerase chain reaction, using degenerate primers designed based on conserved regions of the same locus in human and bovine tissues.
The cDNA sequence was 1348 base pairs long and was predicted to encode a 317 amino acid polypeptide with a putative signal peptide of 17 amino acids. The deduced amino acid sequence of mature CA-VI was most similar (77.4%) to that of human CA-VI. CA-VI expression was confirmed in both normal and nephritic kidneys, as well as parotid. As the primers used in this study spanned two exons, the influence of genomic DNA was not detected. The expression of CA-VI was demonstrated in both normal and nephritic kidneys, and mRNA of CA-VI in the normal kidneys which was the normalised to an endogenous β–actin was 0.098 ± 0.047, while it was significantly lower in the diseased kidneys (0.012 ± 0.007). The level of CA-VI mRNA in normal kidneys was 19-fold lower than that of the parotid gland (1.887).

Conclusions: The localisation of CA-VI indicates that it may play a specialised role in the kidney.

Keywords: Carbonic anhydrase VI, cDNA, Swine kidney, mRNA, RT-PCR, Kidney disease

Background

Carbonic anhydrase (CA; EC 4.2.1.1) is a well-characterised enzyme that catalyses the reversible hydration of CO_2 to form HCO_3^- and protons according to the following reaction: $CO_2 + H_2O \leftrightarrow H_2CO_3 \leftrightarrow HCO_3^- + H^+$. The first reaction is catalysed by CA and the second reaction occurs instantaneously. The mammalian α-CA gene family includes at least 15 enzymatically active isoforms with different structural and catalytic properties. Six of the active CA isozymes are cytosolic (CA-I, –II, –III, –VII, –VIII, and -XIII), 4 are membrane-associated (CA-IV, –IX, –XII, and -XIV), 2 are mitochondrial (CA-VA and CA-VB), and 1 is secretory form (CA-VI), while 2 CA-related proteins (CA-X and XI) are inactive variants [1-3]. The physiological function of carbonic anhydrase is to maintain the acid–base balance in various tissues and biological fluids [4].

CA-VI has been previously purified from the saliva and parotid glands of sheep [5] humans [6], cattle [7], pigs [8], and dogs [9]. The enzyme is localised in the serous acinar and demilune cells of the parotid and submandibular glands [7,10], from which it is secreted into saliva. CA-VI may participate in the regulation of salivary pH and buffer capacity, and protect the mouth and upper alimentary canal against excess acidity [11]. On

* Correspondence: nishida@azabu-u.ac.jp; ochiaih@azabu-u.ac.jp
[1]Laboratory of Physiology I, School of Veterinary Medicine, Azabu University, 1-17-71 Fuchinobe, Sagamihara, Kanagawa 252-5201, Japan
[7]Research Institute of Biosciences, School of Veterinary Medicine, Azabu University, 1-17-71 Fuchinobe, Sagamihara, Kanagawa 252-5201, Japan
Full list of author information is available at the end of the article

the other hand, Hooper et al. [12] suggested that the unique oligosaccharide structures on bovine CA-VI might have an antibacterial function. Karhumaa et al. [13] also suggested that the glycoproteins on CA-VI confer multifunctionality on the enzyme.

To date, human, bovine, mouse, canine, and equine CA-VI cDNAs have been cloned successfully [14-18]. CA-VI was previously reported to be present in the parotid gland, saliva, bile, and serum of pigs [19]. However, the exact physiological and clinical significance of swine CA-VI has not been established. Here, we demonstrated immunohistochemical localization of CA-VI in the swine kidney and deduced the nucleotide sequence of swine CA-VI. Furthermore, we demonstrate expression of CA-VI in both normal and diseased kidneys of pigs. These data provide an initial step toward exploring the physiological and pathological roles of CA-VI.

Methods

Tissue samples

Samples from normal kidneys (n = 9), parotid gland (n = 1), and diseased kidneys (n = 19) of domestic pigs were taken from a slaughterhouse in Miyagi prefecture (Japan).

Macroscopically, diseased swine kidneys showed signs of necrosis (n = 7), nephritis (n = 7), pyelectasis (n = 3), and cystic kidney (n = 2).

All samples were obtained in accordance with the guidelines of the Laboratory Animal Care Committee of Azabu University, Japan, and programs accredited by the Office of Laboratory Animal Welfare (OLAW) USA (#A5393-01) were used.

The samples were immediately fixed in neutralised 10% formalin and Bouin's solution, dehydrated with a graded series of alcohols, cleared with xylene, and then embedded in paraffin wax blocks that were cut into 4-μm-thick histological sections. To observe the morphologic changes, renal tissue samples were stained with hematoxylin and eosin. Microscopic inspection of diseased kidney revealed predominantly renal tubule necrosis and stromal cell permeation.

Immunohistochemical staining of CA-VI in kidney

Biopsies of pig kidneys were performed. The samples were immediately fixed in neutralized 10% formalin and Bouin's solution, dehydrated with a graded series of alcohols, cleared with xylene and then embedded in paraffin wax blocks that were cut into 4 μm-thick histological sections.

Endogenous peroxidase activity was blocked in deparaffinized and rehydrated sections using 0.3% H_2O_2 in methanol, and immersion in normal goat serum (2% in PBS) for 20 min blocked fragment crystallizable receptors. Monospecific primary antisera (diluted 1:2000) against swine CA-VI produced in our laboratory [8] was used to detect the respective isozymes during a 1-h incubation. Antibody binding was visualized using the Vectastain Elite avidin-biotin-peroxidase complex kit (ABC-POD reagent kit; Vector) and diaminobenzidine (DAB) according to the manufacturer's protocol.

The kidney sections were stained with hematoxylin, dehydrated through a graded alcohol series, and mounted on coverslips.

Samples were observed and photographed under a light microscope.

cDNA sequence of pig CA-VI

Total RNA was isolated from the parotid gland of a healthy pig by using RNA extraction solution (Isogen; Nippon Gene, Japan). Degenerate primers used for the amplification of a central region of swine CA-VI cDNA were designed based on the conserved sequences in human [14] and bovine [15] cDNAs. Reverse transcription-polymerase chain reaction (RT-PCR) amplification was then performed using the SuperScript One-Step RT-PCR system (Life Technologies, MS, USA), according to the manufacturer's instructions. The RT-PCR products were verified to be single bands on agarose gel electrophoresis and were then purified using Ultrafree-DA (Millipore, MA, USA) and Microcon YM-100 (Millipore). The purified DNA was cloned into a pGEM-T Easy cloning vector (Promega, WI, USA) and sequenced using a Thermo Sequenase Fluorescent Labeled Primer Cycle sequencing kit (Amersham Biosciences, NJ, USA) and a DSQ2000L DNA sequencer (Shimadzu, Japan). In order to minimise PCR errors, sequences from several clones were analysed. The consensus nucleotide sequence showed a high similarity of approximately 80% to bovine CA-VI cDNA sequences. In order to amplify the 3′ and 5′ regions of pig CA-VI cDNA, 3′- and 5′ -rapid amplification of cDNA ends (3′- and 5′-RACE) methods were employed. 3′-RACE was performed as previously described [20] and 5′-RACE was carried out using a SMART RACE cDNA amplification kit (Clontech, CA, USA), according to the manufacturer's protocol.

Each RACE product was cloned into the pGEM-T Easy vector and sequenced by employing an AmpliTaq Dye Terminator Cycle Sequencing FS Ready Reaction kit (Applied Biosystems, CA, USA) on a 373A DNA sequencer (Applied Biosystems).

RNA extraction from FFPE tissue

A total of 19 diseased and 9 healthy kidney samples in formalin-fixed, paraffin-embedded (FFPE) were used in this study. The 4 pieces of 10-μm-thick FFPE sections were cut from each paraffin block and collected in a 1.5-mL tube. A NucleoSpin FFPE RNA isolation kit for FFPE Tissues (Takara, Kyoto, Japan) was then used according to the manufacturer's protocol. Briefly, 1 mL of xylene

was added into the 4 pieces of 20-μm-thick FFPE sections to remove traces of paraffin. The tissues were digested with proteinase K at 60°C for 3 h and treated with DNase I. After washing, total RNA, including a small miRNA fraction, was eluted with distilled water and stored at −80°C until use.

cDNA synthesis and PCR evaluation of pig CA-VI

Reverse transcription was performed using a SuperScript III First-Strand Synthesis System (Invitrogen, Carlsbad, CA) according to the manufacturer protocol, and the resulting cDNA was used as a template for RT-PCR. Primer set used was purchased from Takara (Kyoto, Japan). Primer sequences for the CA-VI genes were following; forward: 5′-AGAATGTCCACTGGTTTGTGCTTG-3′; reverse: 5′-GGATGGTCTTGTTCTGGTCATTCA-3′. The expected product size of the PCR using this primer set is 102 bp. PCR reaction was performed using Takara *Ex Taq*™ Hot Start version (Takara, Kyoto, Japan). Amplification was conducted using the following protocol: initial denaturation phase at 95°C for 30 s, and then 40 cycles at 95°C for 15 s for denaturation, then at 60°C for 30 s for annealing and extension step. PCR products were loaded in 3% agarose gel.

Real-time PCR evaluation of pig CA-VI

Real-time quantitative PCR was performed using a Thermal Cycler Dice® Real Time System II (Takara). Samples (final volume of 25 μL) were run in duplicate and contained the following: X1 SYBR® *Premix Ex Taq*™ II (Takara) 1 μL 10 mM of each primer and 2 μL cDNA template. Amplification conditions were carried out as manufacturer's protocol. The primer set used in CA-VI amplification was the same as described above. The housekeeping gene β-actin was used as a reference gene (forward: 5′-TCTGGCACCACACCTTCT-3′, reverse; 5′-TGATCTGGGTCATCTTCTCAC-3′; DDBJ accession number AY550069). The Real-Time RT-PCR results are presented as the gene expression of the target gene (CA-VI) relative to that of the housekeeping gene (β-actin), and CA-VI gene expression levels are achieved using the $2^{-\Delta\Delta CT}$ method of quantification [21].

Statistical analysis

To compare differences in the relative levels of CA-VI mRNA between normal and nephritic kidneys, statistical analysis was carried out using an unpaired *t*-test. Values of $P < 0.01$ were considered to be statistically significant.

Results

Immunohistochemical study

The results of immunohistochemical localization of CA-VI in the kidneys of clinically normal pigs were shown in Figure 1. CA-VI was located in the epithelial cells of distal straight tubule of swine kidneys.

Nucleotide sequence of swine CA-VI cDNA

A 1348-bp nucleotide sequence corresponding to full-length swine CA-VI cDNA was obtained (accession number AB333806), consisting of a 951-bp open reading frame encoding swine CA-VI of 317 amino acids (Figure 2A). A typical polyadenylation signal was found in the 3′ untranslated region. The deduced 317 amino acids included a signal peptide (17 amino acids) typical of most secreted proteins where the region was enriched with hydrophobic residues [22]; thus, the predicted mature protein consisted of 300 amino acids. To determine the genomic structure, the UCSC genome browser site (http://genome.ucsc.edu/) was used to align canine genomic sequences and the cDNA sequence of CA-VI (Figure 2B).

The amino acid sequence of the deduced swine mature CA-VI was 3 residues shorter than that of canine CA-VI, and 9 residues (in the carboxy-terminal region) longer than that of mouse and human CA-VI, respectively. The sequence of swine CA-VI showed approximately 77.4% identity to human CA-VI (Figure 3). Two cysteine residues (amino acid positions 25 and 207), which are known to form intra-molecular disulphide bonds in sheep CA-VI [23], are conserved, and 3 histidine residues (amino acid positions 94, 96, and 121) responsible for zinc binding were also found. In addition, 2 potential N-glycosylation sites (Asn-X-Thr/Ser) were detected; 1 of these (amino acid positions 239–241, Asn-Lys-Thr) is known to be glycosylated in sheep CA-VI [23].

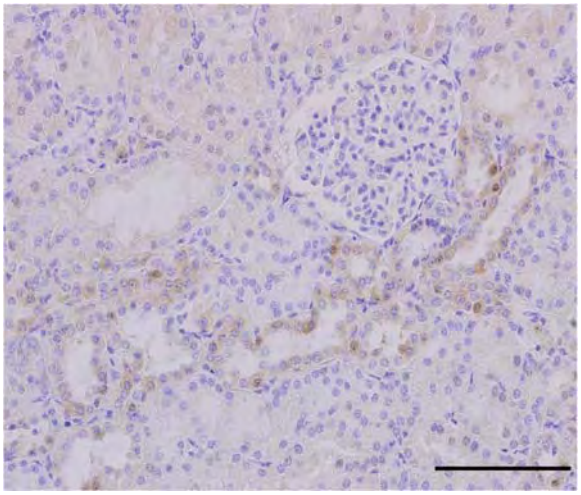

Figure 1 Immunohistochemical localization of CA-VI in the swine kidney. CA-VI was found in the epithelial cells of the distal straight tubule of swine kidneys. Scale bar: 50 μm.

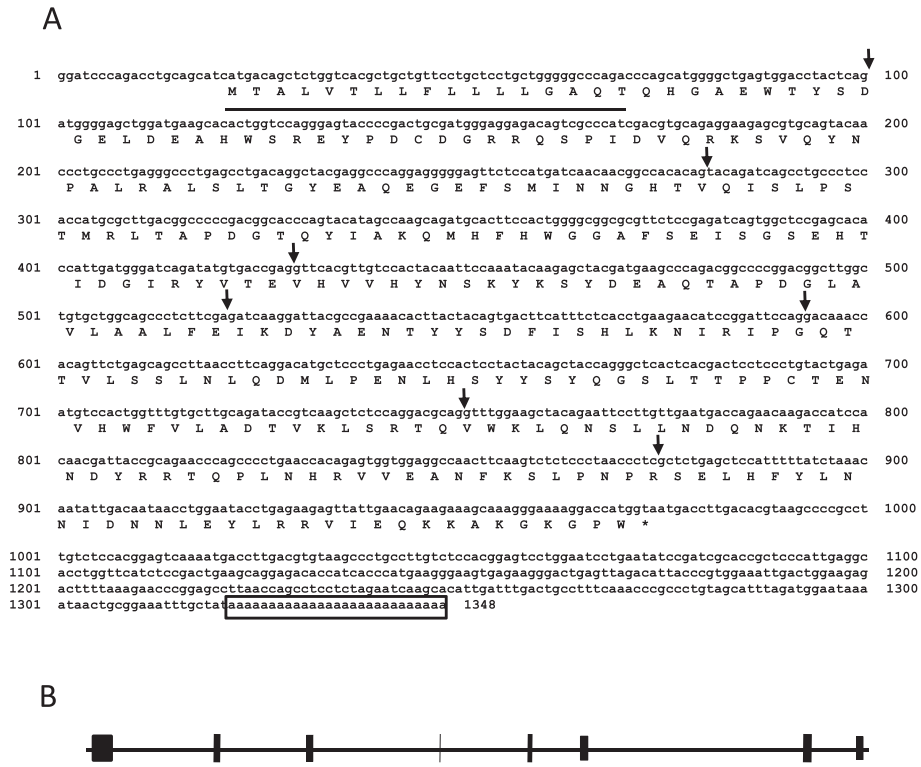

Figure 2 Nucleotide and deduced amino acid sequences of swine *CA-VI* cDNA. The DDBJ accession number is AB333806. The termination codon is asterisked and the polyadenylation signal is boxed. The putative signal peptides consisting of 17 amino acid is underlined. Arrows indicate the positions of introns **(A)**. Alignment of the cDNA sequence with swine genome chromosome 1 predicts 8 exons of 70–447 base pairs. Exon ■: intron **—(B)**.

Figure 3 Comparison of the amino acid sequences of mature CA-VI in pigs, dogs, humans, sheep, and cattle. Multiple sequence alignments were performed using the Genetyx program (version 12). Asterisks and dots indicate identical residues and conservative substitution, respectively. Cys residues are indicated by diamonds, and His residues, by triangles. These are likely to form an intra-molecular disulphide bond and to bind to zinc, respectively. The potential glycosylation sites are indicated by circles.

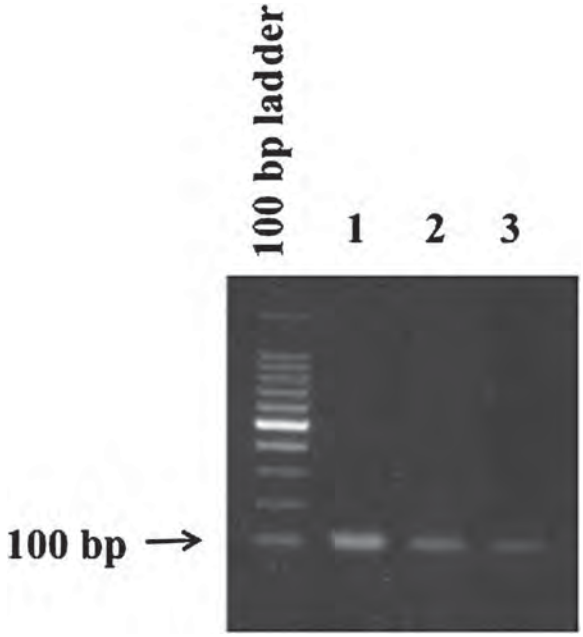

Figure 4 RT-PCR analysis of CA-VI expression from FFPE samples. m; 100-bp ladder, 1; parotid, 2; normal kidney, 3; nephritic kidney.

Expression of swine CA-VI mRNA in kidney

Figure 4 shows the RT-PCR analysis of CA-VI expression from FFPE samples. CA-VI expression was confirmed in both normal and nephritic kidneys, as well as parotid. As the primers used in this study spanned two exons, the influence of genomic DNA was not detected.

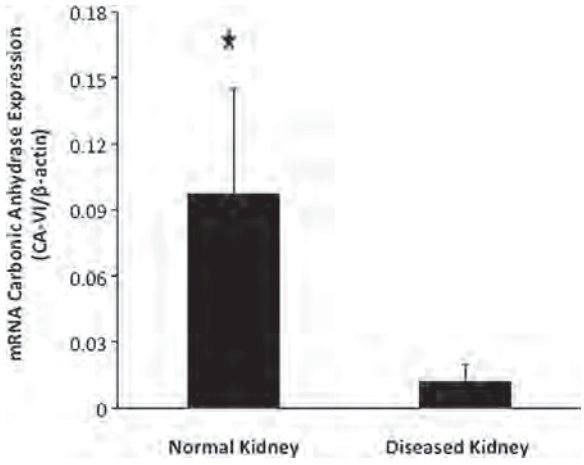

Figure 5 Comparison of CA-VI expression in normal or diseased kidneys from FFPE samples as shown by quantitative RT-PCR. CA-VI levels were normalised to an endogenous β-actin mRNA. The values represent the mean ± SD. Asterisks indicate a significant difference between the normal and diseased kidneys ($P < 0.05$, unpaired *t*-test).

The levels of CA-VI mRNA in the kidney

Expression levels of CA-VI mRNA were measured by qRT-PCR in FFPE samples of normal and diseased kidneys (Figure 4). The relative level of CA-VI mRNA in the normal kidneys was 0.098 ± 0.047, while it was significantly lower in the diseased kidneys (0.012 ± 0.007; $p = 2.71 \times 10^{-8}$, Figure 5). The level of CA-VI mRNA in normal kidneys was 19-fold lower than that of the parotid gland (1.887).

Discussion

Fernley et al., [24] reported that CA-VI was absent from the sublingual salivary gland, kidney, lung, adrenal, brain, skeletal muscle, liver, heart, pancreas, small intestine, and cerebrospinal fluid of sheep. However, CA-VI was found in the lung, skeletal muscle, liver, heart, and pancreas of pigs by using ELISA [19]. In the present study, we show for the first time that CA-VI is expressed in the epithelial cells of distal straight tubule of swine kidneys.

The expression of bovine CA-VI mRNA has previously been detected in the parotid gland, liver, and mammary gland of cow [25,26]. Canine CA-VI mRNA signals were strong in the major salivary glands and weaker in the minor salivary glands and esophagus, and were absent in the pancreas, liver, and almost all parts of the digestive tract, except the esophagus [17]. In the horse, CA-VI mRNA was detected in the digestive tract, salivary glands, testis, thyroid gland, and liver, but not in nerve tissue, skeletal muscle, spleen, or lymph node [18].

To our knowledge, there have been no previous studies on CA-VI mRNA expression in normal and diseased kidneys. Although the levels of CA-VI mRNA were lower in diseased kidneys, further studies are necessary to determine whether CA-VI is a suitable biomarker for kidney disorders.

In the kidney, cytosolic CA-II accounts for >95% of all CA activity. In humans, rabbits, and bovine species, most of the remaining ~ 5% of renal CA is membrane associated and consists of CA-IV and CA-XII [27] CA-II is expressed in the renal proximal tubule; thin descending limb; thick ascending limb; and intercalated cells of the cortical collecting duct, outer medullary collecting duct, and inner medullary collecting duct. Schwartz [28] described that the function of CA-II in renal H^+/HCO_3^- transport is perhaps best understood by examining CA-II interactions with specific transporters.

Räisänen et al., [29] suggested that CA-III is an oxyradical scavenger that protects cells from oxidative damage. Using HK-2 cells, which represent an established model for normal human proximal tubule cells, Gailly et al. [30] reported that exposure to 1 mM H_2O_2 induced a significant increase in CA-III mRNA expression. This suggests that CA-III may be a multifunctional

enzyme, and that 1 of the functions is to protect cells from oxidative damage.

Recently, Pertovaara et al. [31] reported that the levels of anti-CA-VI antibody were significantly higher in patients with primary Sjogren's syndrome (pSS). The amount of antibody correlated significantly with urinary pH, and inversely with serum sodium concentrations. Anti-CA-VI antibody seems to be associated with renal acidification capacity in patients with pSS. However, the role of CA-VI autoantibodies in modulating urinary pH in the kidney remained perplexing, since the presence of CA-VI has never been demonstrated in the human kidneys. Pertovaara et al. [31] speculated that anti-CA-VI antibodies might exhibit cross-reactivity with CA-XIII expressed in the kidneys. However, the molecular weight of CA-XIII is 30 kDa [2] and the subunit molecular weight of swine CA-VI is 37 kDa [8]. Furthermore, the amino acid sequence homology between human CA-VI and CA-XIII is only 35%, which is also the degree of homology between CA-VI and CA-II [2]. We feel it is unlikely that cross-reactivity explains the results above. In support of this, despite a 62% amino acid sequence homology between equine CA-I and CA-II, sera raised against each of these isoforms do not exhibit cross-reactivity with the other [32]. These results indicate that anti human CA-VI serum does not cross-react with both human CA-XIII and CA-II.

The exact function of CA-VI in the kidneys remains unclear at this stage. However, based on our preliminary data, additional studies should be conducted to determine whether measuring the CA-VI concentration in the urine of pigs with kidney disorders is of clinical utility.

Conclusions

CA-VI was located in the epithelial cells of distal straight tubule of swine kidneys.

The cDNA sequence was 1348 base pairs long and was predicted to encode a 317 amino acid polypeptide with a putative signal peptide of 17 amino acids. The deduced amino acid sequence of mature CA-VI was most similar (77.4%) to that of human CA-VI. The expression of CA-VI was demonstrated in both normal and nephritic kidneys, and the relative levels of CA-VI mRNA in the nephritic kidneys were significantly lower than in normal kidneys. The level of CA-VI mRNA in normal kidneys was 19-fold lower than that of the parotid gland.

Abbreviations

CA-VI: Carbonic anhydrase VI; RT-PCR: Reverse transcription- polymerase chain reaction.

Competing interests

The authors declare that they have no competing interests.

Authors' contributions

TN, JY and HO were responsible for the study conception and design, development of the questionnaire, carried out the data collection, performed descriptive statistical analyses and drafted and revised the manuscript. KO helped in the descriptive statistical analyses. MM and KA helped in the design of the study and coordination. SK and NI performed the drafting of the manuscript. All authors read and approved the final manuscript.

Acknowledgement

The authors declare that no funding support was obtained for this study.

Author details

[1]Laboratory of Physiology I, School of Veterinary Medicine, Azabu University, 1-17-71 Fuchinobe, Sagamihara, Kanagawa 252-5201, Japan. [2]Miyagi Prefectural Meat Sanitation Inspection Station, 314 Imaizumi, Sakuraoka, Yoneyamacho, Tome-city, Miyagi 987-0031, Japan. [3]Laboratory of Molecular Biology, School of Veterinary Medicine, Azabu University, 1-17-71 Fuchinobe, Sagamihara, Kanagawa 252-5201, Japan. [4]Laboratory of Physiology II, School of Veterinary Medicine, Azabu University, 1-17-71 Fuchinobe, Sagamihara, Kanagawa 252-5201, Japan. [5]Laboratory of Anatomy I, School of Veterinary Medicine, Azabu University, 1-17-71 Fuchinobe, Sagamihara, Kanagawa 252-5201, Japan. [6]Laboratory of Anatomy II, School of Veterinary Medicine, Azabu University, 1-17-71 Fuchinobe, Sagamihara, Kanagawa 252-5201, Japan. [7]Research Institute of Biosciences, School of Veterinary Medicine, Azabu University, 1-17-71 Fuchinobe, Sagamihara, Kanagawa 252-5201, Japan.

Received: 17 October 2013 Accepted: 24 February 2014
Published: 28 February 2014

References

1. Hewett-Emmett D, Tashian RE: **Functional diversity, conservation, and convergence in the evolution of the alpha-, beta-, and gamma-carbonic anhydrase gene families.** *Mol Phylogenet Evol* 1996, **1:**550–577.
2. Fujikawa-Adachi K, Nishimori I, Taguchi T, Onishi S: **Human carbonic anhydrase XIV (CA14): cDNA cloning, mRNA expression, and mapping to chromosome 1.** *Genomics* 1999, **61:**74–81.
3. Lehtonen J, Shen B, Vihinen M, Casini A, Scozzafava A, Supuran CT, Parkkila AK, Saarnio J, Kivelä AJ, Waheed A, Sly WS, Parkkila S: **Characterization of CA XIII, a novel member of the carbonic anhydrase isozyme family.** *J Biol Chem* 2004, **279:**2719–2727.
4. Carter MJ: **Carbonic anhydrase: isoenzymes, properties, distribution, and functional significance.** *Biol Rev Camb Philos Soc* 1972, **47:**465–513.
5. Fernley RT, Coghlan JP, Wright RD: **Purification and characterization of a high-Mr carbonic anhydrase from sheep parotid gland.** *Biochem J* 1988, **249:**201–207.
6. Murakami H, Sly WS: **Purification and characterization of human salivary carbonic anhydrase.** *J Biol Chem* 1987, **262:**1382–1388.
7. Asari M, Miura K, Ichihara N, Nishita T, Amasaki H: **Distribution of carbonic anhydrase isozyme VI in the developing bovine parotid gland.** *Cells Tissues Organs* 2000, **167:**18–24.
8. Nishita T, Sakomoto M, Ikeda T, Amasaki H, Shino M: **Purification of carbonic anhydrase isozyme VI (CA-VI) from swine saliva.** *J Vet Med Sci* 2001, **63:**1147–1149.
9. Kasuya T, Shibata S, Kaseda M, Ichihara N, Nishita T, Murakami M, Asari M: **Immunohistolocalization and gene expression of the secretory carbonic anhydrase isozymes (CA-VI) in canine oral mucosa, salivary glands and oesophagus.** *Anat Histol Embryol* 2007, **36:**53–57.
10. Parkkila S, Kaunisto K, Rajaniemi L, Kumpulainen T, Jokinen K, Rajaniemi H: **Immunohistochemical localization of carbonic anhydrase isoenzymes VI, II, and I in human parotid and submandibular glands.** *J Histochem Cytochem* 1990, **38:**941–947.
11. Parkkila S, Parkkila AK, Lehtola J, Reinilä A, Södervik HJ, Rannisto M, Rajaniemi H: **Salivary carbonic anhydrase protects gastroesophageal mucosa from acid injury.** *Dig Dis Sci* 1997, **42:**1013–1019.
12. Hooper LV, Beranek MC, Manzella SM, Baenziger JU: **Differential expression of GalNAc-4-sulfotransferase and GalNAc-transferase results in distinct glycoforms of carbonic anhydrase VI in parotid and submaxillary glands.** *J Biol Chem* 1995, **270:**5985–5993.
13. Karhumaa P, Leinonen J, Parkkila S, Kaunisto K, Tapanainen J, Rajaniemi H: **The identification of secreted carbonic anhydrase VI as a constitutive**

glycoprotein of human and rat milk. *Proc Natl Acad Sci U S A* 2001, **98:**11604–11608.
14. Aldred P, Fu P, Barrett G, Penschow JD, Wright RD, Coghlan JP, Fernley RT: **Human secreted carbonic anhydrase: cDNA cloning, nucleotide sequence, and hybridization histochemistry.** *Biochemistry* 1991, **30:**569–575.
15. Jiang W, Woitach JT, Gupta D: **Sequence of bovine carbonic anhydrase VI: potential recognition sites for N-acetylgalactosaminyltransferase.** *Biochem J* 1996, **318:**291–296.
16. Sok J, Wang XZ, Batchvarova N, Kuroda M, Harding H, Ron D: **CHOP-Dependent stress-inducible expression of a novel form of carbonic anhydrase VI.** *Mol Cell Biol* 1999, **19:**495–504.
17. Murakami M, Kasuya T, Matsuba C, Ichihara N, Nishita T, Fujitani H, Asari M: **Nucleotide sequence and expression of a cDNA encoding canine carbonic anhydrase VI (CA-VI).** *DNA Seq* 2003, **14:**195–198.
18. Ochiai H, Kanemaki N, Kamoshida S, Murakami M, Ichihara N, Asari M, Nishita T: **Determination of full-length cDNA nucleotide sequence of equine carbonic anhydrase VI and its expression in various tissues.** *J Vet Med Sci* 2009, **71:**1233–1237.
19. Nishita T, Itoh S, Arai S, Ichihara N, Arishima K: **Measurement of carbonic anhydrase isozyme VI (CA-VI) in swine sera, colostrums, saliva, bile, seminal plasma and tissues.** *Anim Sci J* 2011, **82:**673–678.
20. Frohman MA, Dush MK, Martin GR: **Rapid production of full-length cDNAs from rare transcripts: amplification using a single gene-specific oligonucleotide primer.** *Proc Natl Acad Sci U S A* 1988, **85:**8998–9002.
21. Takara K, Yamamoto K, Matsubara M, Minegaki T, Takahashi M, Yokoyama T, Okumura K: **Effects of α-adrenoceptor antagonists on ABCG2/BCRP-mediated resistance and transport.** *PLoS One* 2012, **7**(2):e30697.
22. von Heijne G: **A new method for predicting signal sequence cleavage sites.** *Nucleic Acids Res* 1986, **14:**4683–4690.
23. Fernley RT, Wright RD, Coghlan JP: **Complete amino acid sequence of ovine salivary carbonic anhydrase.** *Biochemistry* 1988, **27:**2815–2820.
24. Fernley RT, Wright RD, Coghlan JP: **Radioimmunoassay of carbonic anhydrase VI in saliva and sheep tissues.** *Biochem J* 1991, **274:**313–316.
25. Nishita T, Tanaka Y, Wada Y, Murakami M, Kasuya T, Ichihara N, Matsui K, Asari M: **Measurement of carbonic anhydrase isozyme VI (CA-VI) in bovine sera, saliva, milk and tissues.** *Vet Res Commun* 2007, **31:**83–92.
26. Kitade K, Nishita T, Yamato M, Sakamoto K, Hagino A, Katoh K, Obara Y: **Expression and localization of carbonic anhydrase in bovine mammary gland and secretion in milk.** *Comp Biochem Physiol Part A* 2003, **134:**349–354.
27. Purkerson JM, Schwartzm GJ: **The role of carbonic anhydrases in renal physiology.** *Kidney Int* 2007, **71:**103–115.
28. Schwartz GJ: **Physiology and molecular biology of renal carbonic anhydrase.** *J Nephrol* 2002, **15:**S61–S74.
29. Räisänen SR, Lehenkari P, Tasanen M, Rahkila P, Härkönen PL, Väänänen HK: **Carbonic anhydrase III protects cells from hydrogen peroxide-induced apoptosis.** *FASEB J* 1999, **13:**513–522.
30. Gailly P, Jouret F, Martin D, Debaix H, Parreira KS, Nishita T, Blanchard A, Antignac C, Willnow TE, Courtoy PJ, Scheinman SJ, Christensen EI, Devuyst O: **A novel renal carbonic anhydrase type III plays a role in proximal tubule dysfunction.** *Kidney Int* 2008, **1999**(74):52–61.
31. Pertovaara M, Bootorabi F, Kuuslahti M, Pasternack A, Parkkila S: **Novel carbonic anhydrase autoantibodies and renal manifestations in patients with primary Sjogren's syndrome.** *Rheumatology* 2011, **50:**1453–1457.
32. Nishita T, Matsushita H: **Comparative immunochemical studies of carbonic anhydrase III in horses and other mammalian species.** *Comp Biochem Physiol* 1988, **91:**91–96.

doi:10.1186/1756-0500-7-116
Cite this article as: Nishita *et al.*: Isolation and sequencing of swine carbonic anhydrase VI, an enzyme expressed in the swine kidney. *BMC Research Notes* 2014 **7**:116.

CELL BIOCHEMISTRY & FUNCTION

CELL BIOCHEMISTRY AND FUNCTION
Cell Biochem Funct (2014)
Published online in Wiley Online Library
(wileyonlinelibrary.com) **DOI**: 10.1002/cbf.3028

Enhancement of RANKL-induced MITF-E expression and osteoclastogenesis by TGF-β

Kumiko Asai[1], Masayuki Funaba[2]* and Masaru Murakami[1]*

[1]*Laboratory of Molecular Biology, Azabu University School of Veterinary Medicine, Sagamihara, Japan*
[2]*Division of Applied Biosciences, Graduate School of Agriculture, Kyoto University, Kyoto, Japan*

Microphthalmia-associated transcription factor (MITF) is a transcription factor that is expressed in limited types of cells, including osteoclasts, but the expression and role of MITF during osteoclastogenesis have not been fully elucidated. The expression of the MITF-E isoform but not that of the MITF-A isoform was induced in response to differentiation stimulation towards osteoclasts by receptor activator of NF-κB ligand (RANKL) in both RAW264.7 cells and primary bone marrow cells. The RANKL-induced formation of tartrate-resistant acid phosphatase (TRAP)-positive multinucleated cells was inhibited in RAW264.7 cells expressing siRNA for MITF-E. Transforming growth factor-β (TGF-β) enhanced RANKL-induced MITF-E expression and -TRAP positive multinucleated cell formation. In particular, TGF-β potentiated the formation of larger osteoclasts. The expression levels of NFATc1, TRAP and CtsK, genes related to osteoclast development and activity, were concurrently enhanced by TGF-β in the presence of RANKL. Furthermore, the expression of dendritic cell-specific transmembrane protein (DC-STAMP), Itgav, Itga2, Itga5, Itgb1, Itgb3 and Itgb5, genes related to cell adhesion and fusion, were up-regulated by co-treatment with TGF-β. In particular, the regulatory expression of Itgav and Itgb5 in response to RANKL with or without TGF-β resembled that of MITF-E. Because MITF is involved in cell fusion in some cell systems, these results imply a role for MITF-E as an enhancer of osteoclastogenesis and that RANKL-induced levels of both MITF-E mRNA and of MITF-dependent gene expression are enhanced by treatment with TGF-β. Copyright © 2014 John Wiley & Sons, Ltd.

KEY WORDS—osteoclastogenesis; MITF; TGF-β; cell fusion; integrins

INTRODUCTION

Osteoclasts, which degrade bone matrix through the secretion of acid and various enzymes,[1–3] are tartrate-resistant acid phosphatase (TRAP)-positive multinucleated cells formed by the fusion of precursor cells of monocyte–macrophage lineage.[4,5] Osteoclast differentiation is supported by osteoblasts and stromal cells, which produce factors affecting the number and activity of osteoclasts. Macrophage-colony-stimulating factor (M-CSF) and receptor activator of NF-κB ligand (RANKL) principally regulate osteoclastogenesis. M-CSF is required for the survival and proliferation of osteoclast precursor cells.[4,5] In contrast, RANKLstimulates osteoclast differentiation through regulatory expression of osteoclastogenesis-related transcription factors including nuclear factor of activated T-cells c1 (NFATc1).[4,5]

In addition to these molecules, various cytokines, including transforming growth factor-β (TGF-β), are involved in osteoclastogenesis.[3,6,7] TGF-β is a pluripotent growth factor that modulates cell differentiation and maturation in diverse types of cells.[7,8] Although the effects of TGF-β on osteoclast differentiation depend on the cell culture system and the stage of osteoclast differentiation,[7,8] TGF-β consistently stimulates RANKL-induced osteoclastogenesis in differentiation models using RAW264.7 cells.[9–11] The detailed mechanism underlying the enhanced osteoclastogenesis by TGF-β in RAW264.7 cells is not, as of yet, fully characterized.

The regulation of osteoclast differentiation and maturation is not determined only by secreted proteins from osteoblasts and stromal cells. Microphthalmia-associated transcription factor (MITF) is a transcription factor expressed in a tissue-specific manner.[12,13] MITF is also expressed in monocyte–macrophage lineage cells and osteoclasts.[14] The *Mitf*^{mi} allele produces an impaired bone phenotype. The bones of *Mitf*^{mi}/*Mitf*^{mi} mice present signs of osteopetrosis due to a lack of functional osteoclasts.[14,15] MITF regulates osteoclastogenesis in at least two steps. First, MITF up-regulates the expression of genes related to osteoclast activity such as TRAP,[16] chloride channel 7,[17] cathepsin K (CtsK)[18] and v-ATPase d2.[19] Second, MITF governs osteoclast development through the regulation of cell fusion. Dendritic cell-specific transmembrane protein (DC-STAMP) is required for efficient cell–cell fusion of osteoclasts,[20] and transcription of DC-STAMP is positively regulated by MITF.[21] The activity of MITF in stimulating cell fusion has also been shown in different cell types. MITF expression in myoblasts and nascent myotubes is essential for

*Correspondence to: Masayuki Funaba, Division of Applied Biosciences, Graduate School of Agriculture, Kyoto University.E-mail: mfunaba@kais.kyoto-u.ac.jp; Masaru Murakami, Laboratory of Molecular Biology, Azabu University School of Veterinary Medicine. E-mail: murakami@azabu-u.ac.jp

Received 11 November 2013
Revised 14 January 2014
Accepted 15 January 2014

Table 1. Oligonucleotide PCR primers for RT-qPCR

	Oligonucleotide		GenBank accession number
	5′-primer	3′-primer	
MITF			
MITF-A	5′-GAGGAGTTTCACGAAGAACC-3′	5′-GCTGGCGTAGCAAGATGCGTGA-3′	AB_009397
MITF-E	5′-CCAGATACACAGACAGTCACAG-3′	5′-GCTGGCGTAGCAAGATGCGTGA-3′	AF_465624
Osteoclast-related genes			
NFATc1	5′-TCCAAAGTCATTTTCGTGGA-3′	5′-CTTTGCTTCCATCTCCCAGA-3′	NM_016791
TRAP	5′-GCCAAAGAGATCGCCAGAAC-3′	5′-GAAGTAGAAATTGTCCCCCAGAGA-3′	NM_007388
CtsK	5′-TGGACTGTGTGACTGAGAATTATGG-3′	5′-CCGTTCTGCTGCACGTATTG-3′	NM_007802
Cell fusion-related genes			
DC-STAMP	5′-CGAAGCTCCTTGAGAAACGA-3′	5′-GGACTGGAAACCAGAAATGAA-3′	AB_109560
Itgav	5′-GGTGTGGATCGAGCTGTCTT-3′	5′-CAAGGCCAGCATTTACAGTG-3′	NM_008402
Itga2	5′-ACTTCCGGCATACGAAAGAAT-3′	5′-TCAGCCAGCAGGTGATGTTA-3′	NM_008396
Itga5	5′-CACCATTCAATTTGACAGCAA-3′	5′-TCCTCTCCCTTGGCACTGTA-3′	NM_010577
Itgb1	5′-ATGCAGGTTGCGGTTTGT-3′	5′-CATCCGTGGAAAACACCAG-3′	NM_010578
Itgb3	5′-GTGGGAGGGCAGTCCTCTA-3′	5′-CAGGATATCAGGACCCTTGG-3′	NM_016780
Itgb5	5′-TGCCACCTGCCAAGATGGCATA-3′	5′-CACGGACACTTCAAAGGATG-3′	NM_010580
ADAM8	5′-AAAGGCTCCGAGACAAATCC-3′	5′-TTGGAGAGCCCCGAGATAG-3′	NM_007403
ADAM12	5′-CAGAGCATCCCAGCCAAG-3′	5′-CAGGCTGAGGATCAGGTCTC-3′	NM_007400
Housekeeping gene			
G3PDH	5′-CGTGTTCCTACCCCCAATGT-3′	5′-TGTCATCATACTTGGCAGGTTTCT-3′	NM_008084

RT-qPCR, reverse transcription quantitative polymerase chain reaction; MITF, microphthalmia-associated transcription factor; NFATc1, Nuclear factor of activated T-cells c1; TRAP, tartrate-resistant acid phosphatase; CtsK, cathepsin K; DC-STAMP, dendritic cell-specific transmembrane protein; Itg, integrin; ADAM, a disintegrin and metalloirotease domein; G3PDH, glyceraldehyde-3-phosphate dehydrogenase.

the maturation of myotubes via the up-regulation of integrin α_9 (Itga9) expression.[13]

Microphthalmia-associated transcription factor is expressed as a series of isoforms differing in their first exons and promoters.[22–24] For most isoforms, the initial exon, which is isoform-specific exon, is spliced onto the later part of exon 1B and then to the common exons 2–9[22–24]; at present, nine MITF isoforms have been identified in mice, i.e. MITF-A, -B, -C, -D, -E, -H, -J, -M and -mc. MITF isoforms are expressed in a cell type-specific manner.[25–28] Transcriptional activities of MITF are overlapped but distinct among MITF isoforms depending on the target gene.[29–33]

Here, we explored the role of MITF during osteoclastogenesis and the relationship between MITF-E isoform and the TGF-β pathway. Our results indicate that the MITF-E isoform is induced in differentiating osteoclasts, and the expression is required for efficient osteoclast formation. In addition, TGF-β enhances the expression level of MITF-E induced by RANKL and potentiates the formation of larger osteoclasts, possibly through the up-regulation of integrins.

MATERIALS AND METHODS

Materials

The following reagents were purchased, recombinant murine M-CSF and recombinant murine soluble RANKL from Peprotech (Rocky Hill, NJ, USA) and recombinant human TGF-β1 from R&D Systems (Minneapolis, MN, USA).

Cell culture

RAW264.7 cells were cultured in alpha minimal essential medium (α-MEM) with 6% heat-inactivated fetal bovine serum (FBS), 100 U/ml penicillin and 100 μg/ml streptomycin at 37 °C under a humidified 5% CO_2 atmosphere. Primary osteoclasts were basically differentiated as described by Sankar *et al.*[34] Bone marrow cells were obtained from the femurs of adult C57BL/6 mice and cultured for 3 days in basal medium, i.e. Dulbecco's modified Eagle's medium (DMEM) with 10% heat-inactivated FBS, 100 U/ml penicillin and 100 μg/ml streptomycin, supplemented with M-CSF (50 ng/ml). Subsequently, the cells were cultured in the basal medium supplemented with M-CSF (25 ng/ml) in the presence or absence of recombinant soluble RANKL (50 ng/ml). The animal experiments were approved by the Animal Care and Use Committees of Azabu University.

Histochemical detection of TRAP

Tartrate-resistant acid phosphatase was detected by staining of fixed cells by the use of an acid phosphatase, leukocyte kit (Sigma, St. Louis, MO, USA) according to the manufacturer's protocol. The cells were counter-stained with hematoxylin, and the number of cells with more than three nuclei was counted. In addition, the area of TRAP-positive cells was measured by the use of Image J software, and the number of TRAP-positive cells was counted for every cell size.

Osteoclast function assay

Osteoclast functionality was examined via a pit formation assay using 96-well Corning Osteo Assay plates (Corning

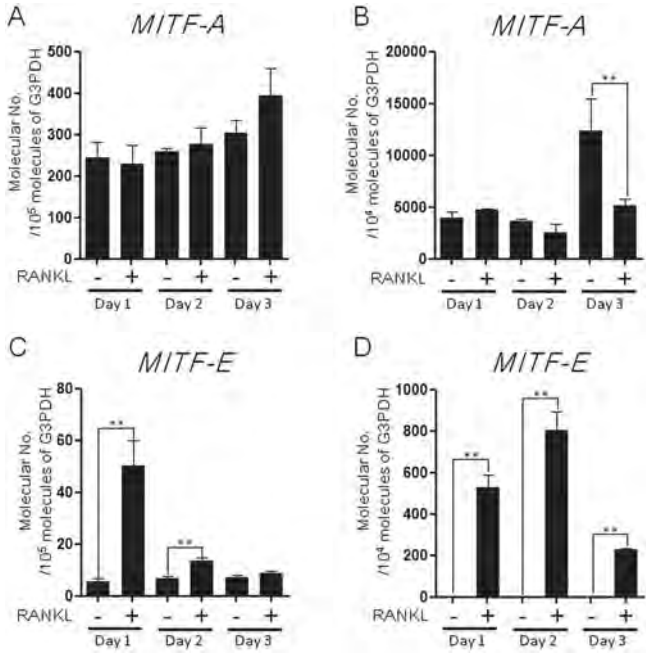

Figure 1. MITF-E is induced during osteoclastogenesis. Gene transcript levels of the MITF-A isoform (A and B) and MITF-E isoform (C and D) were quantified by RT-qPCR during osteoclastogenesis in RAW264.7 macrophage cells (A and C) and primary cultures of bone marrow cells (B and D). (A and C) RAW264.7 cells were treated with or without RANKL (100 ng/ml) for 3 days. (B and D) Bone marrow cells were treated with M-CSF (50 ng/ml) for 3 days. Non-adherent cells were subsequently treated with M-CSF (50 ng/ml) with or without RANKL (100 ng/ml) for an additional 3 days. The expression of the MITF isoforms was normalized to G3PDH expression ($n = 3$). $^{**}p < 0.01$

Inc., Corning, NY, USA) according to the manufacturer's protocol. The pits were observed via light microscopy. The pit area was measured using Image J software, and the total pit area per well was calculated.

siRNA transfection

The siRNA for MITF-E were prepared (Bonac Inc., Kurume, Japan). The nucleotide sequences used were 5′-GGUUACG UAUCUUGUCCACAG-3′ and 5′- GUGGACAAGAUACG UAACCUC-3'. As a control, siRNA for green fluorescent protein (GFP) was used.[35] For reverse transcription-quantitative polymerase chain reaction (RT-qPCR) analyses, 20 pmol of siRNA was transfected into RAW264.7 cells seeded at a density of 2.5×10^4 cells in 24-well plates at 24 h before transfection. For morphological evaluation, 4 pmol of siRNA was transfected in cells seeded at a density of 4×10^3 cells in 96-well plates. The transfection of siRNA was conducted by the use of Lipofectamine RNAiMAX (Life Technologies, Carlsbad, CA, USA) according to the manufacturer's protocol. At 8 h after transfection, the cells were treated with RANKL (50 ng/ml) for 24 h.

RNA isolation and RT-quantitative PCR

Total RNA was isolated by the use of QuickGene RNA cultured cell kit S (Wako, Osaka, Japan) in QuickGene-810 (Wako, Osaka, Japan), an automatic nucleic acid extraction system, according to the manufacturer's protocol. The concentration of RNA was determined from the absorbance at 260 nm. The cDNA was synthesized by the use of high capacity cDNA reverse transcription kit with rnase inhibitor (Life Technologies, Carlsbad, CA, USA), according to the manufacturer's protocol. The cDNA corresponding to 5 ng of total RNA was used as a template of real-time qPCR; qPCR was performed by the use of SYBR Premix Ex-taq II (Takara, Otsu, Japan) in Thermal Cycler Dice Real Time System TP800 (Takara, Otsu, Japan), according to the manufacturer's protocol. The profile of qPCR is as follows: after denature for 30 s at 95 °C, 40 cycles consisting of 5 s at 95 °C and 30 s at 60 °C. Subsequently, melting curve analyses were performed by increasing temperature from 60 °C to 95 °C to verify that the PCR products are not primer dimers but single products. Gene transcript level in each sample was determined by standard curve method; the standard DNA was prepared as described in the succeeding texts. The PCR primers used are presented in Table 1. The 5′-primers for MITF-A and -E were selected from the respective isoform-specific region; the specificity of the PCR primers was also verified by agarose gel electrophoresis of the PCR product and subsequent staining with ethidium bromide. The relative mRNA level was expressed as a ratio with the G3PDH mRNA level. When the gene expression level was below detection limit, it was assumed to express at the detection limit.

Preparation of standard DNA

To examine time-course changes in the expression of MITF isoforms, the number of cDNA molecules was precisely quantified as described previously.[35] Briefly, the cDNA for MITF-A, MITF-E and G3PDH was individually amplified by PCR. The PCR product by the use of Wizard SV Gel and PCR Clean-Up System (Promega, Madison, WI, USA). The amount of the PCR product was precisely quantified by the use of a DNA 1000 Lab Chip Kit (Agilent Technologies, Santa Clara, CA, USA) in an Agilent2100 bioanalyzer (Agilent Technologies, Santa Clara, CA, USA). The molecular number of the PCR product was calculated from the DNA mass and the molecular weight. Several levels of the PCR product were prepared by serial dilution and used as standard solutions of qPCR.

Statistical analysis

All the experiments were basically performed two or more times; each experiment was performed in triplicate. The data of a representative experiment are presented as the mean ± SE ($n = 3$). Comparisons between the cells treated with RANKL alone and the other cells and comparisons between cells transfected with siRNA for green fluorescent protein and those with MITF-E siRNA were conducted using student's *t*-test. The results were considered statistically significant at $p < 0.05$.

RESULTS AND DISCUSSION

The changes in gene expression of MITF isoforms during osteoclastogenesis were examined (Figure 1). Because RAW264.7 cells synthesize sufficient M-CSF,[36] only exogenous RANKL is required for the formation of TRAP-positive multinucleated cells. In contrast, both M-CSF and RANKL must be exogenously supplied in primary bone marrow cell culture. The MITF-A isoform was expressed in both RAW264.7 cells (Figure 1A) and bone marrow cells (Figure 1B). The expression level was relatively constant during osteoclastogenesis in both RAW264.7 cells and bone marrow cells, except for the higher expression of MITF-A in bone marrow cells on day 3 without RANKL (Figure 1B). In contrast, the gene transcript levels of MITF-E were increased within 1 day in response to treatment with RANKL in RAW264.7 cells (ninefold, Figure 1C) and in bone marrow cells (1000-fold, Figure 1D). RANKL-induced MITF-E expression was gradually decreased with incubation days in RAW264.7 cells, and the effect of RANKL treatment was not significant on day 3. In contrast, the up-regulation of MITF-E with treatment with M-CSF and RANKL was maintained for at least 3 days in bone marrow cells. Treatment with M-CSF alone had no effects on MITF-E expression in bone marrow cells (data not shown). Significant expression of the other MITF isoforms was not detected (data not shown). Lu *et al*. showed the up-regulation of MITF-E expression in response to RANKL treatment by semi-quantitative RT-PCR analyses.[37] In the present study, we quantitatively reveal the specific induction of MITF-E mRNA during osteoclastogenesis.

The role of induced MITF-E in the formation of osteoclastic cells was evaluated next. RAW264.7 cells were transfected with MITF-E siRNA prior to RANKL treatment. MITF-E siRNA potentiated a decrease in the number of TRAP-positive multinucleated cells (Figure 2A and 2B), suggesting a positive role for the induced MITF-E in osteoclastogenesis. The MITF-E gene transcript level was reproducibly decreased by transfection with the siRNA (Figure 2C, data not shown). MITF-E isoform-specific region is only 139 bp. We designed possible 2 siRNAs for MITF-E; the knockdown efficiency and reproducibility of the knockdown is better for the siRNA used in this study (data not shown), although nevertheless the inhibition of MITF-E expression is limited. The knockdown of MITF-E gene did not affect the expression level of MITF-A (Figure 2D). Transfection of siRNA for MITF-E inhibited RANKL-induced expression of TRAP and CtsK, genes related to osteoclast activity,[16,18] on day 3 (Figure 2E and 2F). Lu *et al*. also showed the blockage of MITF-E gene

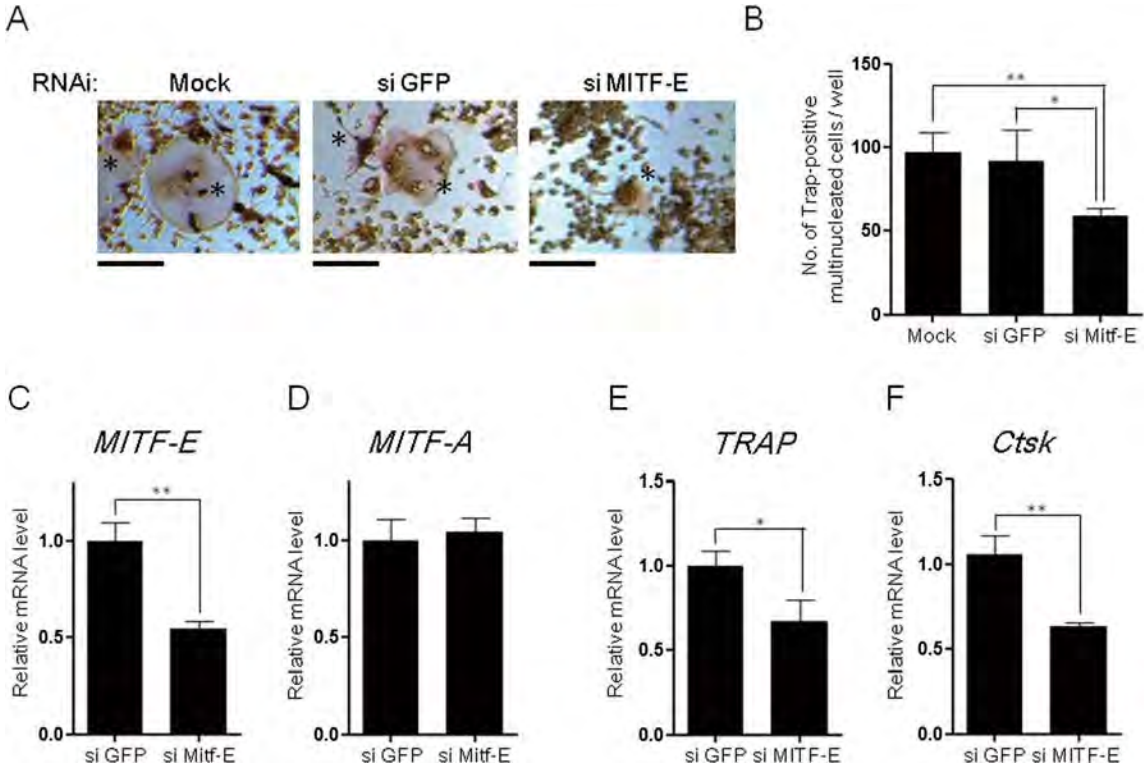

Figure 2. MITF-E expression is required for osteoclastogenesis. RAW264.7 cells were transfected with MITF-E siRNA or GFP or treated with RNA transfection reagent only (mock). At 8 h after transfection, the cells were treated with or without RANKL (100 ng/ml) for 3 days. (A) The cells were stained for TRAP and counter-stained with hematoxylin. A representative result is shown. *, TRAP-positive multinucleated cell. The bar in each photograph indicates 100 μm. (B) The number of TRAP-positive multinucleated cells in a well of 96-well plate was counted ($n = 3$). (C–F) The gene transcript level of MITF-E (C) and MITF-A (D) on day 1 and that of TRAP (E) and CtsK (F) on day 3 were quantified by RT-qPCR, and the expression was normalized to G3PDH expression. The expression in cells treated with siRNA for GFP was set to 1 ($n = 3$). * and **, $p < 0.05$ and $p < 0.01$, respectively

induction results in the impaired formation of osteoclasts[37]; we also observed the similar results. All these results suggest that transient induction of MITF-E by RANKL is essential for efficient osteoclastogenesis.[37]

Next, the effects of TGF-β on osteoclastogenesis were examined in RAW264.7 cells. Treatment with TGF-β alone did not induce formation of TRAP-positive multinucleated cells, but TGF-β increased the number of TRAP-positive multinucleated cells induced by RANKL (Figure 3A and 3B), which was consistent with previous results.[9–11] We also noticed that larger TRAP-positive multinucleated cells were formed by co-treatment with TGF-β compared with the treatment with RANKL alone. Chin *et al.*[11] described the TGF-β-induced formation of giant osteoclasts but did not quantitatively analyze them. To characterize the cell size in detail, the number of TRAP-positive multinucleated cells was counted for every cell size (Figure 3C). The proportion of cells with areas $>1\times10^4$ and $<2\times10^4\,\mu m^2$ was significantly increased by TGF-β treatment, whereas the proportion of cells with areas $<5\times10^3\,\mu m^2$ tended to be decreased, indicating that TGF-β accelerates the formation of larger TRAP-positive multinucleated cells. TGF-β also increased bone resorption activity, and RANKL-induced pit formation was enhanced by the co-treatment with TGF-β (Figure 3D and 3E). The present results suggest that TGF-β acts not only as an enhancer of osteoclast formation induced by RANKL but also as an accelerator of mature osteoclast formation through cell fusion of nascent osteoclasts.

The molecular basis of enhanced osteoclastogenesis by TGF-β was then explored. The expression of NFATc1, which is involved in the onset of osteoclastogenesis,[38,39] was increased within 1 day after treatment with RANKL, and TGF-β enhanced RANKL-induced NFATc1 expression (Figure 4A). Similarly, RANKL-induced MITF-E

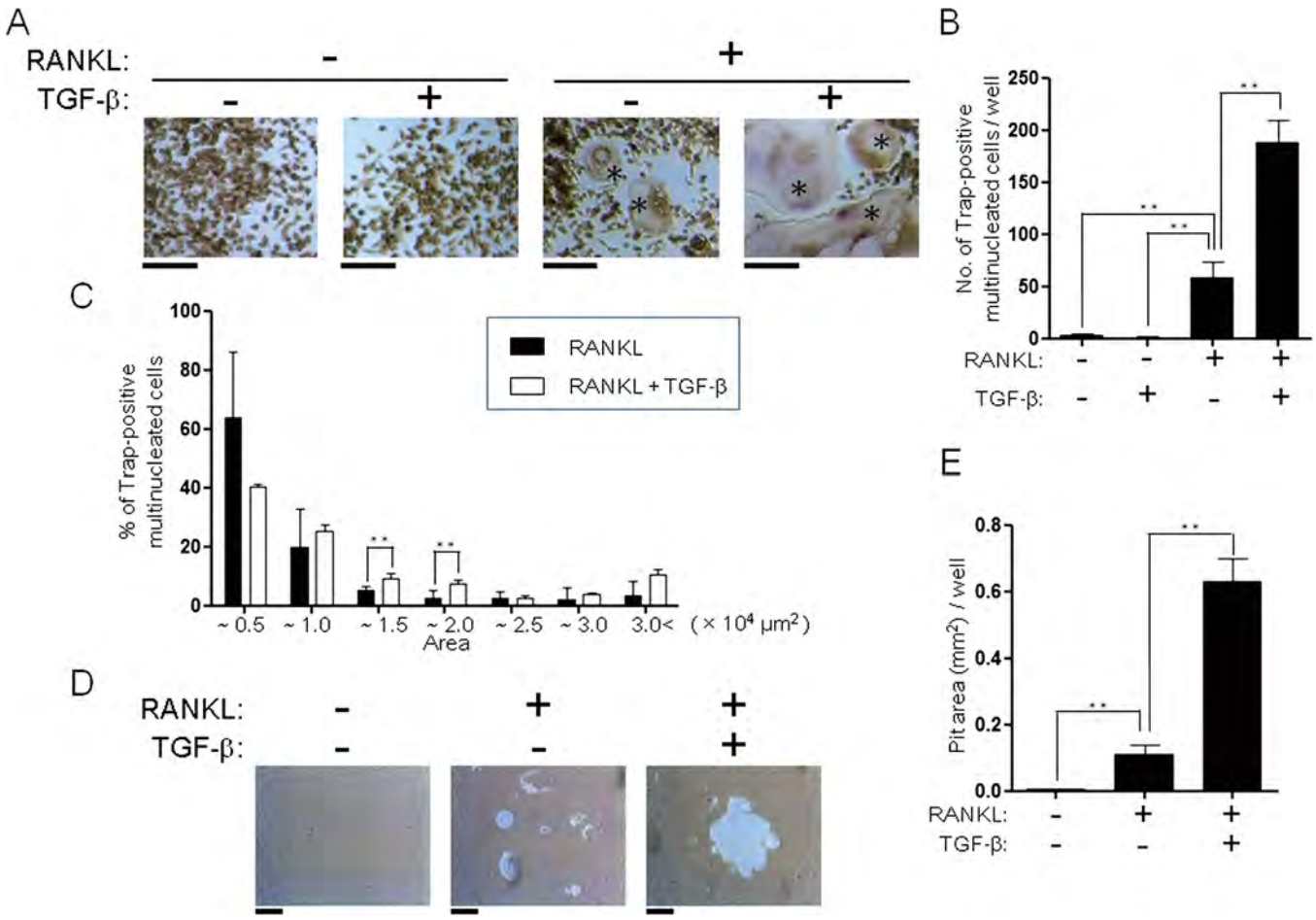

Figure 3. TGF-β enhances RANKL-induced osteoclastogenesis. RAW264.7 cells were pre-treated with or without TGF-β1 (100 pM) for 12 h, followed by the co-treatment with or without RANKL (100 ng/ml) for 3 days. (A) Cells were stained for TRAP and counter-stained with hematoxylin. A representative result is shown. *, TRAP-positive multinucleated cell. The bar in each photograph indicates 100 μm. (B) The total number of TRAP-positive multinucleated cells in a well of 96-well plate was counted ($n=3$). (C) The number of TRAP-positive multinucleated cells induced by RANKL alone or RANKL plus TGF-β was counted for every cell size. The percentage of the respective TRAP-positive multinucleated cell number to the total TRAP-positive multinucleated cell number was calculated ($n=3$). (D) Osteoclast functionality was evaluated by pit formation assays ($n=3$). A representative result is shown. The bar in each photograph indicates 100 μm. (E) The total area of pit in a well of 96-well plate was measured ($n=3$). **, $p<0.01$

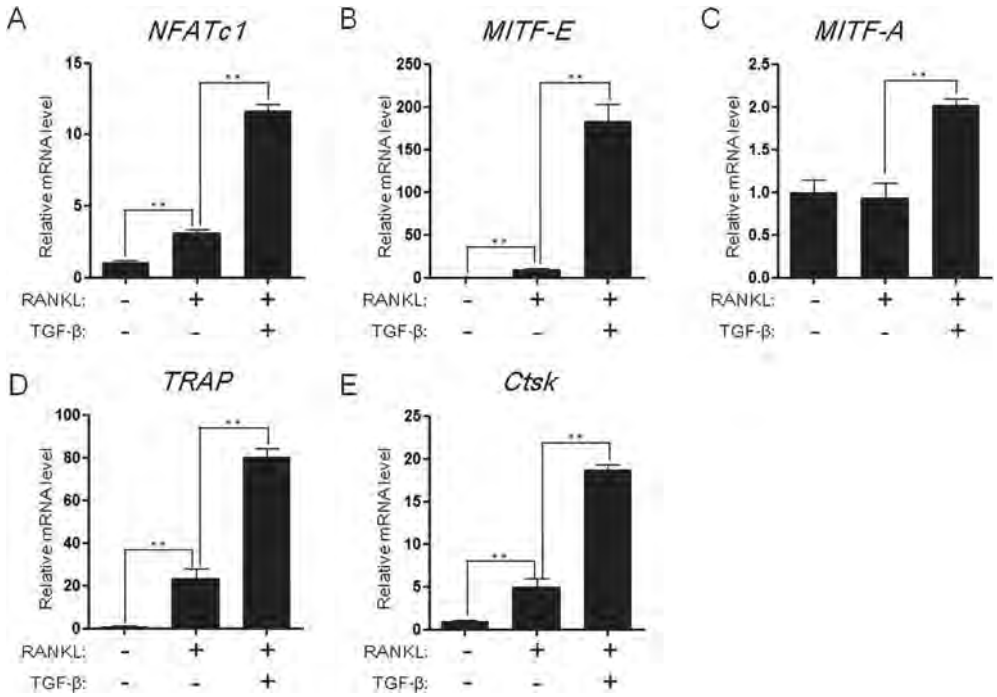

Figure 4. TGF-β enhances the expression of MITF-E and genes related to osteoclastogenesis. RAW264.7 cells were pre-treated with or without TGF-β1 (100 pM) for 12 h, followed by the co-treatment with RANKL (100 ng/ml) for 3 days. The gene transcript levels of NFATc1 (A), MITF-E (B) and MITF-A (C) on day 1 and TRAP (D) and CtsK (E) on day 3 were quantified by RT-qPCR. The expression was normalized to G3PDH expression, and the expression in cells treated without RANKL and TGF-β1 was set to 1 ($n = 3$). **, $p < 0.01$

expression was further up-regulated by TGF-β (Figure 4B). The TGF-β treatment also significantly increased gene transcript level of MITF-A, but the extent of increase in the expression was relatively small (~twofold, Figure 4C). In accordance with the enhancement of expression related to the triggering of osteoclastogenesis, TGF-β further increased the expression of TRAP and CtsK on day 3 (Figure 4D and 4E).

The expression of the genes involved in cell fusion was further examined. DC-STAMP is a master regulator of cell fusion in osteoclast formation.[40,41] The expression of DC-STAMP was induced by RANKL treatment, and TGF-β slightly but significantly enhanced the RANKL-induced expression (Figure 5A).

We evaluated the gene transcript levels of integrins and a disintegrin and metalloprotease (ADAM). Integrins and ADAMs are also involved in the adhesion and fusion of monocyte/macrophage-lineage cells.[41,42] Several integrin proteins, such as integrin α_V (Itgav), α_2(Itga2), α_5(Itga5), β_1(Itgb1) and β_5 (Itgb5), are expressed in human osteoclasts.[43] The forced expression of Itgav stimulated the formation of TRAP-negative multinucleated cells in RAW264.7 cells, and RANKL changed these cells to TRAP-positive cells.[11] Anti-Itga9 antibody partly inhibited M-CSF and RANKL-induced osteoclast formation.[44] Bone marrow cells prepared from integrin β_3 (Itgb3)-null mice are less differentiated into osteoclasts *in vitro*.[45] Furthermore, the down-regulation of ADAM8 and ADAM12 expression inhibits osteoclast formation as well as cell fusion of macrophages.[46,47] The expression levels of Itgav, Itga2, Itga5, Itgb1, Itgb3 and Itgb5 were significantly higher in cells treated with RANKL and TGF-β than in cells treated with RANKL alone (Figure 5B–5G). In contrast, the expression of ADAM8 and ADAM12 was not increased by TGF-β treatment (Figure 5H and 5I). RANKL treatment significantly increased the expression of Itgav, Itgb5 and ADAM12 (Figure 5B, 5G and 5I). The changes in the expression level of Itgav and Itgb5 in response to treatment with RANKL with or without TGF-β resembled those of MITF-E expression; RANKL increased the expression (Figure 4B), but the extent of the increased gene expression was much smaller than that of the increase following co-treatment with TGF-β.

In the present study, DC-STAMP expression was increased by RANKL treatment, which coincides with the induction of MITF-E but not MITF-A. Previous studies showed that the transcriptional activation of DC-STAMP, a master regulator of cell fusion during osteoclastogenesis, is regulated by MITF,[21,48] although isoform of MITF responsible for the cell fusion has not been identified. It is possible that one of the roles of MITF-E induces transcriptional activation of DC-STAMP. However, the role of MITF-E expression in response to treatment with RANKL and TGF-β is likely to be distinct from that with RANKL alone; the extent of further increase in DC-STAMP expression in response to TGF-β was relatively smaller than that in MITF-E expression. Considering that TGF-β formed larger osteoclasts with more nuclei, the further increased MITF-E by TGF-β might regulate the

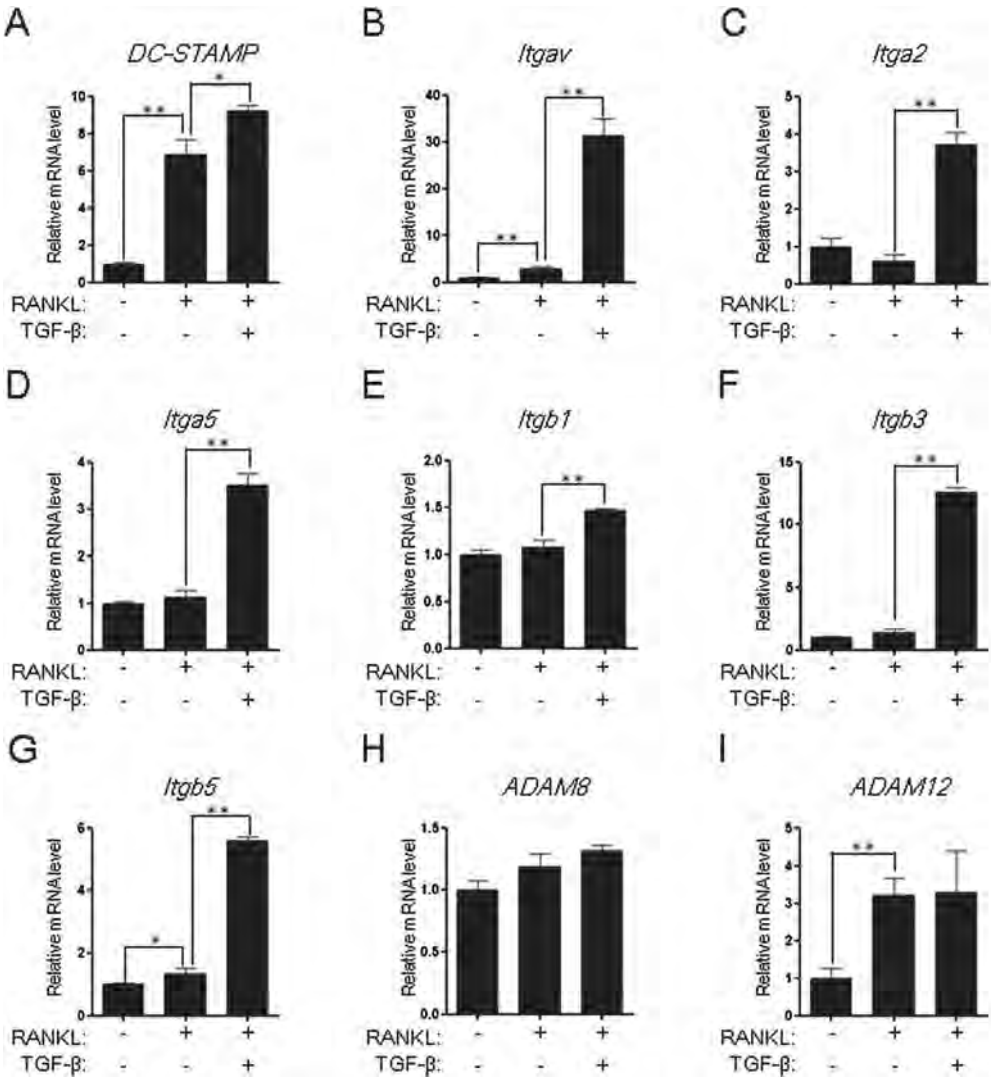

Figure 5. TGF-β increases the expression of genes related to cell adhesion and fusion. RAW264.7 cells were pre-treated with or without TGF-β1 (100 pM) for 12 h, followed by the co-treatment with RANKL (100 ng/ml) for 3 days. The gene transcript levels of DC-STAMP (A), ItgaV (B), Itga2 (C), Itga5 (D), Itgb1 (E), Itgb3 (F), Itgb5 (G), ADAM8 (H) and ADAM12 (I) on day 3 were quantified by RT-qPCR. The expression was normalized to G3PDH expression, and the expression in cells treated without RANKL and TGF-β1 was set to 1 ($n = 3$). * and **, $p < 0.05$ and $p < 0.01$, respectively

transcription of gene(s) other than DC-STAMP, leading to the acceleration of cell fusion.

Integrins are involved in cell fusion as described earlier.[11,13] In addition, integrin α4 (Itga4) expression is induced by MITF in hematopoietic stem/progenitor cells,[49] and the regulatory expression of Itga4 depends on the isoform of MITF.[53] Thus, we speculate that TGF-β-mediated up-regulation of MITF-E expression is responsible for the formation of larger osteoclasts through increased expression of integrins; especially, the regulatory expression of Itgav and Itgb5 may be important, because changes in expression of MITF-E paralleled to those of Itgav and Itgb5 in response to treatment with RANKL with or without TGF-β. The present results suggest the critical role of DC-STAMP and integrins in osteoclastogenesis induced by RANKL and in osteoclast maturation by TGF-β, respectively; MITF-E may regulate both processes.

The present study extends the knowledge of the expression and role of MITF-E expression in developing osteoclasts. We previously demonstrated the functional interaction between MITF and the TGF-β pathway. TGF-β enhances MITF-E-mediated transcription,[30,31] whereas the MITF-M isoform negatively regulates TGF-β-mediated signalling.[50] In the present study, additional regulation of MITF activity by the TGF-β pathway, i.e. enhancement of MITF expression by TGF-β, was clarified. Recently, it was shown that TGF-β represses the transcription of MITF-M in melanoma cells.[51] Taken the present results with the results of a previous study[51] together, MITF expression may be regulated by TGF-β in an isoform-dependent or cell type-dependent manner or both.

Balancing bone resorption and bone formation is important for bone and mineral homeostasis. Differentiation into multinucleated TRAP-positive cells resulting from the

fusion of monocyte/macrophage lineage cells is a critical step in determining osteoclast activity. Therefore, fine-tuning of osteoclastogenesis through the regulation of TGF-β activity is likely to maintain preferable bone mass. Further studies are needed to clarify the molecular mechanisms underlying the regulation of MITF-E expression by TGF-β, osteoclast formation and maturation by MITF-E and the regulatory expression of integrins by MITF-E and TGF-β.

CONFLICT OF INTEREST

The authors have declared that there is no conflict of interest.

ACKNOWLEDGEMENTS

This work was supported by a Grant-in-Aid for Scientific Research (24580437) from The Japan Society for the Promotion of Science and a research project grant awarded by Azabu University.

REFERENCES

1. Blair HC. How the osteoclast degrades bone. *Bioessays* 1998; **20**: 837–846.
2. Bar-Shavit Z. The osteoclast: a multinucleated, hematopoietic-origin, bone-resorbing osteoimmune cell. *J Cell Biochem* 2007; **102**: 1130–1139.
3. Nakamura I, Takahashi N, Jimi E, Udagawa N, Suda T. Regulation of osteoclast function. *Mod Rheumatol* 2012; **22**: 167–177.
4. Boyle WJ, Simonet WS, Lacey DL. Osteoclast differentiation and activation. *Nature* 2003; **423**: 337–342.
5. Negishi-Koga T, Takayanagi H. Ca^{2+}-NFATc1 signaling is an essential axis of osteoclast differentiation. *Immunol Rev* 2009; **231**: 241–256.
6. Fox SW, Lovibond AC. Current insights into the role of transforming growth factor-β in bone resorption. *Mol Cell Endocrinol* 2005; **243**: 19–26.
7. Janssens K, ten Dijke P, Janssens S, Van Hul W. Transforming growth factor-b1 to the bone. *Endocr Rev* 2005; **26**: 743–774.
8. Alliston T, Piek E, Derynck R. TGF-β family signaling in skeletal development, maintenance, and disease. In *The TGF-β Family*, Derynck R, Miyazono K (eds.). Cold Spring Harbor Laboratory Press: Cold Spring Harbor, 2008; 667–723.
9. Koseki T, Gao Y, Okahashi N, *et al*. Role of TGF-b family in osteoclastogenesis induced by RANKL. *Cell Signal* 2002; **14**: 31–36.
10. Shui C, Riggs BL, Khosla S. The immunosuppressant rapamycin, alone or with transforming growth factor-β, enhances osteoclast differentiation of RAW264.7 monocyte-macrophage cells in the presence of RANK-ligand. *Calcif Tissue Int* 2002; **71**: 437–446.
11. Chin SL, Johnson SA, Quinn J, *et al*. A role for αV integrin subunit in TGF-β-stimulated osteoclastogenesis. *Biochem Biophys Res Commun* 2003; **307**: 1051–1058.
12. Hodgkinson CA, Moore KJ, Nakayama A, *et al*. Mutations at the mouse microphthalmia locus are associated with defects in a gene encoding a novel basic-helix-loop-helix-zipper protein. *Cell* 1993; **74**: 395–404.
13. Ooishi R, Shirai M, Funaba M, Murakami M. Microphthalmia-associated transcription factor is required for mature myotube formation. *Biochim Biophys Acta* 1820; **2012**: 76–83.
14. Weilbaecher KN, Motyckova G, Huber WE, *et al*. Linkage of M-CSF signaling to Mitf, TFE3, and the osteoclast defect in Mitf(mi/mi) mice. *Mol Cell* 2001; **8**: 749–758.
15. Hershey CL, Fisher DE. Mitf and Tfe3: members of a b-HLH-ZIP transcription factor family essential for osteoclast development and function. *Bone* 2004; **34**: 689–696.
16. Luchin A, Purdom G, Murphy K, *et al*. The microphthalmia transcription factor regulates expression of the tartrate-resistant acid phosphatase gene during terminal differentiation of osteoclasts. *J Bone Miner Res* 2000; **15**: 451–460.
17. Meadows NA, Sharma SM, Faulkner GJ, Ostrowski MC, Hume DA, Cassady AI. The expression of Clcn7 and Ostm1 in osteoclasts is coregulated by microphthalmia transcription factor. *J Biol Chem* 2007; **282**: 1891–1904.
18. Motyckova G, Weilbaecher KN, Horstmann M, Rieman DJ, Fisher DZ, Fisher DE. Linking osteopetrosis and pycnodysostosis: regulation of cathepsin K expression by the microphthalmia transcription factor family. *Proc Natl Acad Sci U S A* 2001; **98**: 5798–5803.
19. Feng H, Cheng T, Steer JH, *et al*. Myocyte enhancer factor 2 and microphthalmia-associated transcription factor cooperate with NFATc1 to transactivate the V-ATPase d2 promoter during RANKL-induced osteoclastogenesis. *J Biol Chem* 2009; **284**: 14667–14676.
20. Yagi M, Miyamoto T, Sawatani Y, *et al*. DC-STAMP is essential for cell-cell fusion in osteoclasts and foreign body giant cells. *J Exp Med* 2005; **202**: 345–351.
21. Courtial N, Smink JJ, Kuvardina ON, Leutz A, Göthert JR, Lausen J. Tal1 regulates osteoclast differentiation through suppression of the master regulator of cell fusion DC-STAMP. *FASEB J* 2012; **26**: 523–532.
22. Steingrímsson E, Copeland NG, Jenkins NA. Melanocytes and the microphthalmia transcription factor network. *Annu Rev Genet* 2004; **38**: 365–411.
23. Hou L, Pavan WJ. Transcriptional and signaling regulation in neural crest stem cell-derived melanocyte development: do all roads lead to Mitf? *Cell Res* 2008; **18**: 1163–1176.
24. Vachtenheim J, Borovanský J. "Transcription physiology" of pigment formation in melanocytes: central role of MITF. *Exp Dermatol* 2010; **19**: 617–627.
25. Amae S, Fuse N, Yasumoto K, *et al*. Identification of a novel isoform of microphthalmia-associated transcription factor that is enriched in retinal pigment epithelium. *Biochem Biophys Res Commun* 1998; **247**: 710–715.
26. Takemoto CM, Yoon YJ, Fisher DE. The identification and functional characterization of a novel mast cell isoform of the microphthalmia-associated transcription factor. *J Biol Chem* 2002; **277**: 30244–30252.
27. Murakami M, Iwata Y, Funaba M. Expression and transcriptional activity of alternative splice variants of Mitf exon 6. *Mol Cell Biochem* 2007; **303**: 251–257.
28. Bharti K, Liu W, Csermely T, Bertuzzi S, Arnheiter H. Alternative promoter use in eye development: the complex role and regulation of the transcription factor MITF. *Development* 2008; **135**: 1169–1178.
29. Murakami M, Ikeda T, Ogawa K, Funaba M. Transcriptional activation of mouse mast cell protease-9 by microphthalmia-associated transcription factor. *Biochem Biophys Res Commun* 2003; **311**: 4–10.
30. Funaba M, Ikeda T, Murakami M, Ogawa K, Abe M. Up-regulation of mouse mast cell protease-6 gene by transforming growth factor-b and activin in mast cell progenitors. *Cell Signal* 2005; **17**: 121–128.
31. Murakami M, Ikeda T, Saito T, Ogawa K, Nishino Y, Nakaya K. Transcriptional regulation of plasminogen activator inhibitor-1 by transforming growth factor-b, activin A and microphthalmia-associated transcription factor. *Cell Signal* 2006; **18**: 256–265.
32. Park HY, Wu C, Yonemoto L, *et al*. MITF mediates cAMP-induced protein kinase C-beta expression in human melanocytes. *Biochem J* 2006; **395**: 571–578.
33. Shahlaee AH, Brandal S, Lee YN, Jie C, Takemoto CM. Distinct and shared transcriptomes are regulated by micophtalmia-associated transcription factor isoforms in mast cells. *J Immunol* 2007; **178**: 378–388.
34. Sankar U, Patel K, Rosol TJ, Ostrowski MC. RANKL coordinates cell cycle withdrawal and differentiation in osteoclasts through the cyclin-dependent kinase inhibitors p27KIP1 and p21CIP1. *J Bone Miner Res* 2004; **19**: 1339–1348.
35. Murakami M, Kawachi H, Ogawa K, Nishino Y, Funaba M. Receptor expression modulates the specificity of transforming growth factor-b signaling pathways. *Genes Cells* 2009; **14**: 469–482.
36. Islam S, Hassan F, Tumurkhuu G, *et al*. Receptor activator of nuclear factor-kB ligand induces osteoclast formation in RAW 264.7 macrophage

cells via augmented production of macrophage-colony-stimulating factor. *Microbiol Immunol* 2008; **52**: 585–590.
37. Lu SY, Li M, Lin YL. Mitf induction by RANKL is critical for osteoclastogenesis. *Mol Biol Cell* 2010; **21**: 1763–1771.
38. Ishida N, Hayashi K, Hoshijima M, *et al*. Large scale gene expression analysis of osteoclastogenesis in vitro and elucidation of NFAT2 as a key regulator. *J Biol Chem* 2002; **277**: 41147–41156.
39. Takayanagi H, Kim S, Koga T, *et al*. Induction and activation of the transcription factor NFATc1 (NFAT2) integrate RANKL signaling in terminal differentiation of osteoclasts. *Dev Cell* 2002; **3**: 889–901.
40. Yagi M, Miyamoto T, Toyama Y, Suda T. Role of DC-STAMP in cellular fusion of osteoclasts and macrophage giant cells. *J Bone Miner Metab* 2006; **24**: 355–358.
41. Oursler MJ. Recent advances in understanding the mechanisms of osteoclast precursor fusion. *J Cell Biochem* 2010; **110**: 1058–1062.
42. Brodbeck WG, Anderson JM. Giant cell formation and function. *Curr Opin Hematol* 2009; **16**: 53–57.
43. Hughes DE, Salter DM, Dedhar S, Simpson R. Integrin expression in human bone. *J Bone Miner Res* 1993; **8**: 527–533.
44. Rao H, Lu G, Kajiya H, *et al*. a9b1: a novel osteoclast integrin that regulates osteoclast formation and function. *J Bone Miner Res* 2006; **21**: 1657–1665.
45. Faccio R, Takeshita S, Zallone A, Ross FP, Teitelbaum SL. c-Fms and the avb3 integrin collaborate during osteoclast differentiation. *J Clin Invest* 2003; **111**: 749–758.
46. Abe E, Mocharla H, Yamate T, Taguchi Y, Manolagas SC. Meltrin-a, a fusion protein involved in multinucleated giant cell and osteoclast formation. *Calcif Tissue Int* 1999; **64**: 508–515.
47. Choi SJ, Han JH, Roodman GD. ADAM8: a novel osteoclast stimulating factor. *J Bone Miner Res* 2001; **16**: 814–822.
48. Maruyama K, Uematsu S, Kondo T, *et al*. Strawberry notch homologue 2 regulates osteoclast fusion by enhancing the expression of DC-STAMP. *J Exp Med* 2013; **210**: 1947–1960.
49. Khurana S, Buckley S, Schouteden S, *et al*. A novel role of BMP4 in adult hematopoietic stem and progenitor cell homing via Smad independent regulation of integrin-α4 expression. *Blood* 2013; **121**: 781–790.
50. Funaba M, Ikeda T, Murakami M, *et al*. Transcriptional activation of mouse mast cell protease-7 by activin and transforming growth factor-b is inhibited by microphthalmia-associated transcription factor. *J Biol Chem* 2003; **278**: 52032–52041.
51. Pierrat MJ, Marsaud V, Mauviel A, Javelaud D. Expression of microphthalmia-associated transcription factor (MITF), which is critical for melanoma progression, is inhibited by both transcription factor GLI2 and transforming growth factor-β. *J Biol Chem* 2012; **287**: 17996–18004.

NOTE *Wildlife Science*

Two Distinct mtDNA Lineages among Captive African Penguins in Japan

Michiko MURATA[1)] and Masaru MURAKAMI[1)]*

[1)]*Laboratory of Molecular Biology, School of Veterinary Medicine, Azabu University, 1–17–71 Fuchinobe, Chuo-ku, Sagamihara, Kanagawa 252–5201, Japan*

(Received 25 July 2013/Accepted 25 November 2013/Published online in J-STAGE 9 December 2013)

ABSTRACT. The African penguin (*Spheniscus demersus*) is one of the world's most endangered seabirds. In Japan, although the number of African penguins in captivity continues to increase, genetic data have not been collected for either wild or captive populations. To reveal genetic diversity and characterization in captive African penguins, we analyzed the nucleotide sequences of mitochondrial DNA (mtDNA) from a sample of 236 African penguins. Analysis of 433 bp of the control region and 1,140 bp of cytochrome b sequences revealed the existence of two mtDNA clades. Control region haplotypes were much more divergent (d=3.39%) between the two clades than within each clade. The divergence of these clades may reflect differences at the subspecies or geographical population level in African penguins. These findings suggest that at least two distinct maternal lineages exist in the wild populations of the African penguin.

KEY WORDS: African penguin, control region, genetic diversity, mitochondrial DNA.

doi: 10.1292/jvms.13-0377; *J. Vet. Med. Sci.* 76(4): 559–563, 2014

The African penguin (*Spheniscus demersus*), which is endemic to southern Africa, inhabits 31 islands and four mainland sites in Namibia and South Africa, ranging from southern Angola in the north to Nelson Mandela Bay in the east [4]. Wild African penguin populations markedly decreased in the 20th century. Approximately 56,000 pairs estimated in 2001 have declined to 21,000 pairs in 2009 [5]. This population decline is thought to be primarily due to food scarcity, resulting from overfishing, overexploitation and environmental fluctuations, such as increased sea surface temperature linked to climate change. In addition, oil pollution has become a major factor in African penguin mortality. Consequently, the African penguin is listed in Appendix II of the Convention on International Trade in Endangered Species and classified as Endangered by the 2010 International Union for Conservation of Nature.

While wild African penguin populations continue to decrease, properly maintained captive populations are increasing year on year. According to the 2011 Japanese regional studbook for the African penguin, their original introduction to Japan was in 1935, and from 1973 to 2011, 156 additional founders were introduced: 92 from South Africa, 30 from overseas zoos and aquariums and the remaining 34 from unknown locations. The time and number of introductions varied. The captive African penguin populations in Japan contain 485 individuals, comprising an estimated 87 different founder lineages. In order to avoid close inbreeding and to maintain genetic diversity, the Japanese Association of Zoos and Aquariums (JAZA) keeps studbooks which it uses to promote longer-term breeding plans. However, no genetic data on the foundering population of African penguins introduced to Japan are described in the studbook, and the genetic relationship of captive African penguins in Japan is unclear.

Genetic data have not been collected on either wild or captive African penguins in Japan so far. In this study, we examined the genetic diversity of the captive Japanese populations of African penguins by analyzing the control region and cytochrome b sequences of mitochondrial DNA (mtDNA), since mtDNA sequences have higher rates of nucleotide substitution than nuclear DNA sequences [2]. Analysis of mtDNA sequences can reveal genetic relationships among closely related species. This molecular information may prove useful to JAZA for future management and implementation of breeding programs.

Blood or feather samples from African penguins (n=236) were collected from 20 Japanese zoos and aquariums. Blood samples were also collected from captive populations of Humboldt penguins (*Spheniscus humboldti*) (n=20) and Magellanic penguins (*Spheniscus magellanicus*) (n=2). Genomic DNA was extracted using Dr. GenTLE^{TM} (TaKaRa Bio, Otsu, Japan) or Get pureDNA Kit-Cell, Tissue (Dojindo Molecular Technologies, Kumamoto, Japan). Two mtDNA fragments of 653 bp (control region) and 1,140 bp (cytochrome b) were amplified by polymerase chain reaction (PCR). The control region fragments and the entire cytochrome b gene were amplified using the primer pair L-tRNA^{Glu}(5′-CCTGCTTGGCTTTTYTCCAAGACC) and H-Dbox (5′-CTGACCGAGGAACCAGAGGCGC) [13] and the primer pair BCL1 (5′-AGGCCTACCTAGGATCCTTCGCCCT) and BCH1 (GTCTTTGGTTAATTACAAGACCAATGTTT) [8], respectively. The H-Dbox, BCL1 and BCH1 primers were also used as sequencing primers. Amplification reactions were carried out in a 50 μl solution containing 10–100 ng genomic DNA, 1 × buffer (20 mM Tris-HCl, pH8.0, 100 mM KCL and 2 mM $MgCl_2$), 200

*CORRESPONDENCE TO: MURAKAMI, M., Laboratory of Molecular Biology, School of Veterinary Medicine, Azabu University, 1–17–71 Fuchinobe, Chuo-ku, Sagamihara, Kanagawa 252–5201, Japan.
e-mail: murakami@azabu-u.ac.jp

μM each of deoxyribonucleotides, 1.25 units of *Ex Taq*® HS DNA polymerase (TaKaRa Bio) and 0.2 μM of each primer. Reaction mixtures were incubated in a PCR thermal cycler (TaKaRa PCR Thermal Cycler Dice™; TaKaRa Bio) with initial denaturation of 3 min at 95°C with a typical profile of 32 cycles, each consisting of 30 sec at 95°C, 30 sec at 60°C (for the control region) or 55°C (for cytochrome b) and 30 sec (control region) or 1 min (cytochrome b) at 72°C with final extension of 5 min at 72°C. PCR products were checked by electrophoresis on 1.5% agarose gel with TAE buffer, and the gel was stained with ethidium bromide. PCR products were purified by exonuclease I (Wako, Osaka, Japan) and shrimp alkaline phosphatase (TaKaRa Bio) and were sequenced directly using an ABI PRISM 3130 Genetic Analyzer and BigDye® Terminator v3.1 Cycle Sequencing Kit (Applied Biosystems, Foster, CA, U.S.A.). The sequences of 433 nucleotides of the control region and 1,140 nucleotides of cytochrome b were determined. Phylogenetic analyses were conducted using MEGA version 5 [16]. Multiple sequence alignment was performed by using Clustal W [17]. Genetic distances between haplotypes were obtained using the Tamura-Nei model [15]. Phylogenetic trees were constructed by the neighbor-joining (NJ), maximum parsimony (MP) and maximum likelihood (ML) methods. The reliability of tree topology was assessed by 1,000 bootstrap replications [7]. Lastly, Neighbor-Net analysis [3] was performed to construct a phylogenetic network using SplitsTree4 software [9] (http://www.splitstree.org/).

DNA sequences of the mitochondrial control region of 236 African penguin individuals were determined. Multiple sequence alignments of the 433 bp constituting the partial control region showed 39 polymorphic sites, generating a total of 30 different haplotypes (Table 1). All substitutions were transitions. Our nucleotide sequencing data are available under the accession numbers AB775475-775504 from the DDBJ/EMBL/GenBank databases. The available 45 of the total 64 South African founder populations were also examined, resulting in 27 haplotypes. This indicated that the founder populations were derived from 27 maternal ancestors. These maternal genetic results are consistent with traceable records of captive breeding detailed in the studbook. We also investigated the Humboldt penguin and Magellanic penguin, which belong to *Spheniscus*, the same genus as the African penguin. Eight different haplotypes were obtained from these species (accession numbers AB775505-775512).

NJ phylogenetic tree analysis using mitochondrial DNA control region sequences revealed that the captive African penguin populations kept in a total of 20 Japanese zoos and aquariums clustered into two clades (A and B) as supported by high bootstrap values (Fig. 1). Clades A and B contained 26 and 4 haplotypes, respectively. The 27 haplotypes from South Africa described above belonged to both clades A and B, suggesting 2 maternal lineages derived from South Africa. Five substitutions at nucleotide numbers 110, 166, 217, 225 and 285 in the control region were characteristic of clade B (Table 1). The mean genetic distance of the control region sequences between the 2 clades was 3.39%, and the genetic distances within clades A and B were 0.93% and 1.18%, respectively. Both MP and ML analyses also showed a similar topology with the captive African penguins arranged in 2 different clades (data not shown). A network analysis further supported the division of the maternal lineages of the captive African penguins into these 2 different clades (Fig. 2).

The complete 1,140 bp sequences (accession numbers AB776002-776009) in the cytochrome b gene were obtained from 54 captive African penguins in Japan. There were 8 haplotypes defined by 11 variable sites. Nine nucleotide substitutions were synonymous, and the remaining 2 substitutions were non-synonymous. The same two clades as those of the control region were separated by 1 non-synonymous substitution (data not shown).

The mtDNA diversities of rockhopper penguin (*Eudyptes* spp.) and blue penguin (*Eudyptula minor*) samples from wild populations have been previously reported. The rockhopper penguin, which had been considered a single species with two subspecies [6], was suggested to be two distinct species based on the average genetic distance (6.1%) of the control region sequences between its northern and southern clades [10]. The blue penguin, a single species comprising 6 morphologically determined subspecies [11], can be divided into an Australian-Otago clade and a New Zealand clade from analyses of 3 mtDNA sequences [1]. The control region sequences between these two clades have been found to differ by 11.8%. Moreover, examination of the control region sequences of individuals collected from 7 southern Australian *E. m. novaehollandiae* colonies [11] showed no geographic clustering of closely related genetic variations among colonies [12]. The average genetic distance among colonies of this subspecies was 1.0%, based on our calculations made from sequence data for EU043384-043403. Considering these molecular data found in studies of the rockhopper penguin and blue penguin, the divergence of African penguin clades A and B (d=3.39%) seen in the present study may reflect either a difference in geographical populations or the existence of undefined subspecies of African penguins, although it must be noted that our data focused on captive-bred individuals.

This is the first report of molecular data obtained by mtDNA analyses of captive African penguins. Here, we demonstrated the existence of two divergent clades of captive African penguins with moderate genetic distance (d=3.39%). Although we currently have no descriptive information on the founders of the captive African penguin population and genetic data from wild African penguin populations must also be examined, our data imply that captive African penguins in Japan are derived from two distinct maternal lines. We are presently analyzing nuclear DNA markers, including microsatellite diversity and repetitive DNA sequences, to elucidate further the genetic characterization of African penguin populations.

In other endangered species, such as the Oriental white stork (*Ciconia boyciana*), mtDNA control region analysis has been utilized to develop an effective breeding plan in Japan [18, 19]. Likewise, careful genetic management is needed to maintain genetic variability in the African penguin and to use captive breeding projects to save this endangered species from extinction.

Table 1. Haplotypes and variable sites of the mitochondrial control region found in Japanese captive populations of African penguins (*Spheniscus demersus*)

Haplotype		Nucleotide position																																					Number of individuals
		13	11	30	31	107	108	110	117	121	122	134	135	139	141	161	165	166	170	177	184	198	217	220	225	237	239	243	275	285	286	288	292	293	294	295	305	306	309	326	
CladeA	type1	A	G	T	T	T	T	A	A	A	G	A	T	C	T	G	A	A	G	G	C	G	G	G	G	A	T	A	G	A	T	G	G	G	T	T	A	A	T	T	22
	type2	G	.	.	.	.	.	.	G	.	.	.	.	.	.	.	.	.	A	.	.	.	.	.	.	.	.	.	.	.	.	.	.	.	.	.	.	.	.	.	C	3
	type3	G	.	.	.	C	.	.	G	.	.	.	.	.	.	.	.	.	A	.	.	.	.	.	.	.	.	.	.	.	.	.	.	.	.	.	.	.	.	.	.	9
	type4	.	.	.	.	.	.	.	G	.	.	.	.	.	.	.	.	.	.	.	.	.	.	.	.	.	.	.	.	.	.	.	.	.	.	.	.	.	.	.	C	20
	type5	G	.	.	.	.	.	.	G	.	.	.	.	.	.	.	.	.	.	.	.	.	.	.	.	.	.	.	.	.	.	.	.	.	.	.	G	.	.	C	28
	type6	.	.	.	.	C	.	.	G	.	.	.	.	.	.	.	.	.	.	.	.	.	.	.	.	.	.	.	.	.	.	.	.	.	.	.	.	.	.	.	C	7
	type8	G	.	.	.	.	.	.	G	.	.	.	.	.	.	.	.	.	A	.	.	.	.	.	.	.	.	.	.	.	.	.	.	.	.	C	.	.	.	C	25
	type9	G	.	.	.	.	.	.	G	.	.	.	.	.	.	.	.	.	.	.	.	.	.	A	.	.	.	.	.	.	.	.	.	.	.	.	.	.	.	.	C	27
	type10	G	.	.	.	.	.	.	G	.	.	.	.	.	.	.	.	.	.	.	.	.	.	.	.	.	.	.	.	.	.	.	A	.	.	.	.	.	.	.	C	9
	type11	.	.	.	.	.	.	.	G	G	.	.	.	.	.	.	.	.	.	.	.	.	.	.	.	.	.	.	.	.	.	.	.	.	.	.	.	.	.	.	C	3
	type12	G	.	.	.	.	.	.	G	.	.	.	.	.	.	.	.	.	.	.	.	A	.	.	.	.	.	.	.	.	.	.	.	.	.	.	.	.	.	.	C	3
	type13	G	.	.	.	.	.	.	G	G	.	.	.	.	.	.	.	.	A	.	.	.	.	.	.	.	.	.	.	.	.	.	.	.	.	.	.	.	.	.	C	8
	type14	G	.	.	.	.	.	.	G	.	.	.	.	.	.	.	.	.	.	.	.	.	.	.	.	.	.	.	.	.	.	.	.	.	.	.	.	.	.	.	C	18
	type15	G	.	.	.	.	.	.	G	.	.	G	C	.	C	.	.	.	.	.	.	.	.	.	.	.	C	.	.	.	.	A	.	.	.	.	.	.	.	.	C	8
	type17	G	.	.	.	.	.	.	G	.	.	.	.	.	.	.	.	.	.	.	T	.	.	.	.	.	C	.	.	.	.	.	.	.	.	.	.	.	.	.	C	3
	type18	G	.	.	.	.	C	.	G	.	.	.	.	.	.	.	.	.	.	.	.	A	.	.	.	.	.	.	.	.	A	.	.	.	.	.	.	.	.	.	1
	type19	G	.	.	.	C	.	.	G	.	A	.	.	.	.	.	.	.	A	.	.	.	.	.	.	.	.	.	.	.	.	.	.	.	.	.	.	.	.	.	.	1
	type20	G	.	.	.	.	.	.	G	.	.	.	.	.	.	.	.	.	.	.	T	.	.	.	.	.	.	.	.	.	A	.	A	.	.	.	.	.	.	C	4
	type21	G	.	.	.	.	.	.	G	.	.	.	.	.	.	.	.	.	.	.	.	.	.	.	.	.	.	.	.	.	.	A	C	.	.	.	.	.	.	C	2
	type22	G	.	.	.	.	C	.	G	.	.	.	.	.	.	.	.	.	.	.	.	A	.	.	.	.	.	.	.	.	A	.	.	.	.	.	.	C	.	.	1
	type23	G	.	.	.	.	.	.	G	.	.	.	.	.	.	.	.	.	.	.	.	A	.	.	.	.	.	.	.	.	.	A	.	.	.	.	.	.	.	C	1
	type25	G	.	.	.	.	.	.	G	.	.	.	.	.	.	.	.	.	.	.	.	.	.	.	.	.	.	.	.	.	.	.	A	.	.	.	.	.	.	C	1
	type26	G	.	.	.	.	.	.	G	.	.	.	.	.	.	A	.	.	.	.	.	.	.	.	.	.	C	.	.	.	.	A	.	.	.	.	.	.	.	C	3
	type27	G	.	.	.	.	.	.	G	G	.	.	.	T	.	.	.	A	.	.	.	.	.	.	.	.	.	.	.	.	.	.	.	.	.	.	.	.	.	.	C	11
	type29	G	.	.	.	.	.	.	G	G	.	.	.	.	.	.	.	.	.	.	.	.	.	.	.	.	.	.	.	.	.	A	.	.	.	.	.	.	.	.	C	2
	type30	.	.	.	.	.	.	.	G	.	.	.	.	.	.	.	G	.	.	.	.	.	.	.	.	.	.	.	.	.	.	.	.	.	.	.	.	.	.	.	.	C	3
CladeB	type7	.	A	C	.	C	.	G	G	.	.	.	.	.	.	A	.	G	.	R	.	.	A	.	A	.	.	.	A	G	.	A	.	.	.	.	.	G	.	C	7
	type16	.	.	.	C	C	.	G	G	.	.	.	.	.	.	A	.	G	.	.	.	.	A	.	A	G	.	G	A	G	C	A	.	.	.	.	.	.	.	C	1
	type24	.	.	.	C	C	.	G	G	.	.	.	.	.	.	A	.	G	.	.	.	.	A	.	A	G	.	G	.	G	.	A	.	.	.	.	.	.	.	C	1
	type28	.	A	C	.	C	.	G	G	.	.	.	.	.	.	A	.	G	.	.	.	.	A	.	A	.	.	.	A	G	.	A	.	.	.	.	.	G	.	C	4
																																								total	236

ACKNOWLEDGMENTS. We thank Sunshine International Aquarium, Ueno Zoological Gardens, Awashima Marine Park, Nagasaki Penguin Aquarium, Yokohama Hakkeijima Sea Paradise Aqua Museum, Kakegawa Kachoen, Matsue Vogel Park, EPSON Shinagawa Aqua Stadium, Futami Sea Paradise, Kobe Kachoen, Marine World Uminonakamichi, Tohoku Safari Park, Nasu Safari Park, Kurume City Bird Center, Yodel Forest, Izu Mito Sea Paradise, Noboribetsu Marine Park, Marinepia Matsushima Aquarium, Miyazaki City Phoenix Zoo and Kyoto Aquarium for their contribution of samples used in this study. We particularly thank Mr. M. Tomiyama for his assistance with field collections.

REFERENCES

1. Banks, J. C., Mitchell, A. D., Waas, J. R. and Paterson, A. M. 2002. An unexpected pattern of molecular divergence within the blue penguin (*Eudyptula minor*) complex. *Notornis* **49**: 29–38.
2. Brown, W. M., George, M. Jr. and Wilson, A. C. 1979. Rapid evolution of animal mitochondrial DNA. *Proc. Natl. Acad. Sci. U. S. A.* **76**: 1967–1971. [Medline] [CrossRef]
3. Bryant, D. and Moulton, V. 2004. Neighbor-net: an agglomerative method for the construction of phylogenetic networks. *Mol. Biol. Evol.* **21**: 255–265. [Medline] [CrossRef]
4. Crawford, R. J. M., Underhill, L. G., Upfold, L. and Dyer, B. M. 2007. An altered carrying capacity of the Benguela upwelling ecosystem for African penguins (*Spheniscus demersus*). *ICES J. Mar. Sci.* **64**: 570–576. [CrossRef]
5. Crawford, R. J. M., Altwegg, R., Barham, B. J., Barham, P. J., Durant, J. M., Dyer, B. M., Geldenhuys, D., Makhado, A. B., Pichegru, L., Ryan, P. G., Underhill, L. G., Upfold, L., Visagie, J., Waller, L. J. and Whittington, P. A. 2011. Collapse of South Africa's penguins in the early 21st century. *Afr. J. Mar. Sci.* **33**: 139–156. [CrossRef]
6. del Hoyo, J., Elliott, A. and Sargatal, J., editors. 1992. Spheniscidae (Penguin) pp. 140–160 *In*: Handbook of the bird of the world, vol.1, Lynx Edicions, Barcelona.
7. Felsenstein, J. 1985. Confidence limits on phylogenies: an approach using the bootstrap. *Evolution* **39**: 783–791. [CrossRef]
8. Hitosugi, S., Tsuda, K., Okabayashi, H. and Tanabe, Y. 2007.

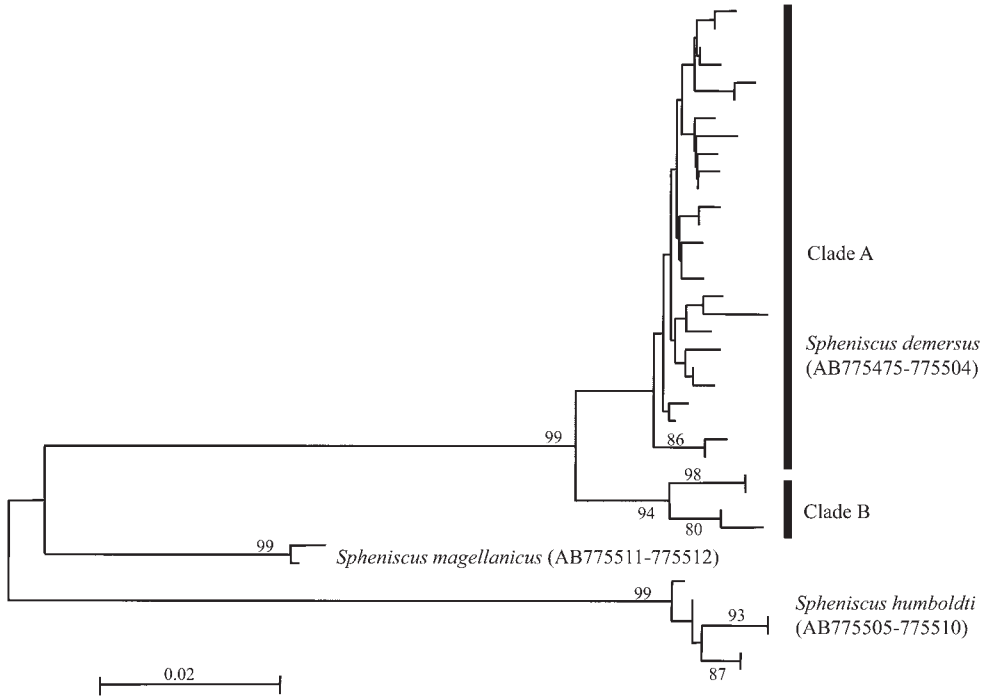

Fig. 1. Neighbor-joining tree of mitochondrial DNA control region haplotypes of African penguins. The tree was constructed as described by Saitou and Nei [14] and was rooted using Humboldt penguins (*Spheniscus humboldti*) as an outgroup. Phylogenetic analyses were conducted with MEGA5. Only bootstrap values greater than 70% are shown.

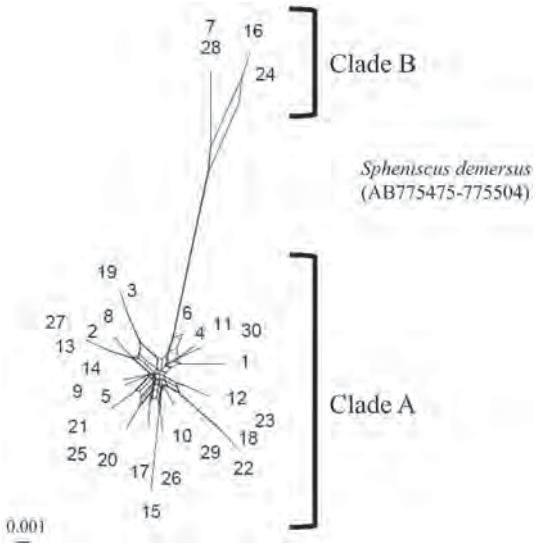

Fig. 2. Neighbor-Net diagram of captive African penguin populations. A network of relationships among the 30 haplotypes detected in 236 individuals of the captive African penguin was generated by Neighbor-Net analysis of polymorphisms of the control region. Digits represent the haplotype number.

Phylogenetic Relationships of mitochondrial DNA cytochrome b gene in East Asian ducks. *J. Poult. Sci.* **44**: 141–145. [CrossRef]

9. Huson, D. H. and Bryant, D. 2006. Application of phylogenetic networks in evolutionary studies. *Mol. Biol. Evol.* **23**: 254–267. [Medline] [CrossRef]
10. Jouventin, P., Cuthbert, R. J. and Ottvall, R. 2006. Genetic isolation and divergence in sexual traits: Evidence for the northern rockhopper penguin *Eudyptes moseleyi* being a sibling species. *Mol. Ecol.* **15**: 3413–3423. [Medline] [CrossRef]
11. Kinsky, F. C. and Falla, R. A. 1976. A subspecific revision of the Australasian Blue Penguin (Eudyptula minor) in the New Zealand region. *National Museum of New Zealand Records* **1:** 105–126.
12. Overeem, R. L., Peucker, A. J., Austin, C. M., Dann, P. and Burridge, C. P. 2008. Contrasting genetic structuring between colonies of the world's smallest penguin, *Eudyptula minor* (aves: Spheniscidae). *Conserv. Genet.* **9**: 893–905. [CrossRef]
13. Roeder, A. D., Ritchie, P. A. and Lambert, D. M. 2002. New DNA markers for penguins. *Conserv. Genet.* **3**: 341–344. [CrossRef]
14. Saitou, N. and Nei, M. 1987. The neighbor-joining method: a new method for reconstructing phylogenetic trees. *Mol. Biol. Evol.* **4**: 406–425. [Medline]
15. Tamura, K. and Nei, M. 1993. Estimation of the number of nucleotide substitutions in the control region of mitochondrial DNA in humans and chimpanzees. *Mol. Biol. Evol.* **10**: 512–526. [Medline]
16. Tamura, K., Peterson, D., Peterson, N., Stecher, G., Nei, M. and Kumar, S. 2011. MEGA5: Molecular evolutionary genetics analysis using maximum likelihood, evolutionary distance, and

maximum parsimony methods. *Mol. Biol. Evol.* **28**: 2731–2739. [Medline] [CrossRef]

17. Thompson, J. D., Higgins, D. G. and Gibson, T. J. 1994. CLUSTAL W: improving the sensitivity of progressive multiple sequence alignment through sequence weighting, position-specific gap penalties and weight matrix choice. *Nucleic Acids Res.* **22**: 4673–4680. [Medline] [CrossRef]
18. Yamamoto, Y. 2011. New haplotypes in the mitochondrial control region of Oriental White Storks, *Ciconia boyciana*. *Reintroduction* **1**: 77–80.
19. Yamamoto, Y., Murata, K., Matsuda, H., Hosoda, T., Tamura, K. and Furuyama, J. 2000. Determination of the complete nucleotide sequence and haplotypes in the D-loop region of the mitochondrial genome in the oriental white stork, *Ciconia boyciana*. *Genes Genet. Syst.* **75**: 25–32. [Medline] [CrossRef]

NOTE *Biochemistry*

Characterization of a Canine Tetranucleotide Microsatellite Marker Located in the First Intron of the Tumor Necrosis Factor Alpha Gene

Masashi WATANABE[1)]**, Kazuaki TANAKA[2)]**, Tatsuya TAKIZAWA[2)], Kazuhito SEGAWA[1)], Sakurako NEO[1)], Ryo TSUCHIYA[1)], Michiko MURATA[3)], Masaru MURAKAMI[3)] and Masaharu HISASUE[1)]*

[1)]*Laboratory of Veterinary Internal Medicine II, Faculty of Veterinary Medicine, Azabu University, Chuo-ku, Sagamihara, Kanagawa 252–5201, Japan*
[2)]*Laboratory of Animal Biotechnology, Faculty of Veterinary Medicine, Azabu University, Chuo-ku, Sagamihara, Kanagawa 252–5201, Japan*
[3)]*Laboratory of Molecular Biology, Faculty of Veterinary Medicine, Azabu University, Chuo-ku, Sagamihara, Kanagawa 252–5201, Japan*

(Received 18 June 2013/Accepted 21 August 2013/Published online in J-STAGE 13 September 2013)

ABSTRACT. A polymorphic tetranucleotide $(GAAT)_n$ microsatellite in the first intron of the canine tumor necrosis factor alpha (*TNFA*) gene was characterized in this study; 139 dogs were analyzed: 22 Beagles, 26 Chihuahuas, 20 Miniature Dachshunds, 24 Miniature Poodles, 22 Pembroke Welsh Corgis and 25 Shiba Inus. We detected the presence of the 4 alleles $(GAAT)_5$, $(GAAT)_6$, $(GAAT)_7$ and $(GAAT)_8$, including 9 of the 10 expected genotypes. The expected heterozygosity (*He*) and the polymorphic information content (*PIC*) value of this microsatellite locus varied from 0.389 to 0.749 and from 0.333 to 0.682, respectively, among the 6 breeds. The allelic frequency differed greatly among breeds, but this microsatellite marker was highly polymorphic and could be a useful marker for the canine *TNFA* gene.
KEY WORDS: canine *TNFA* gene, tetranucleotide microsatellite.

doi: 10.1292/jvms.13-0316; *J. Vet. Med. Sci.* 76(1): 119–122, 2014

Tumor necrosis factor alpha (TNFA) is a multifunctional pro-inflammatory cytokine, which is secreted mainly by monocytes and macrophages (Online Mendelian Inheritance in Man (*OMIM, 191160*),. In humans, genetic variations in the *TNFA* gene are associated with various disorders, e.g., septic shock [14], rheumatoid arthritis [15], cystic fibrosis [3], inflammatory bowel diseases [11] and insulin resistance syndrome [8].

In the veterinary field, TNFA is also considered to be one of the most important cytokines involved with many inflammatory diseases, including bacterial and protozoan infections and sepsis [6, 13, 17]. For example, increased expression of *TNFA* mRNA in colonic mucosa has been reported on dogs with idiopathic lymphocytic-plasmacytic colitis [16].

The canine *TNFA* gene is located on dog chromosome 12 (CanFam3.1, dog genome assembly *NW_003726081*), and it comprises 4 exons and 3 introns. However, the genetic polymorphisms in the canine *TNFA* gene have not been clarified.

Microsatellites are tandem repeated sequences, usually di-, tri- and tetranucleotide motifs, which display high levels of polymorphism, making them ideal genetic markers [7, 18]. Microsatellites were thought to be evolutionarily neutral and to have no generalized function [18]. In recent years, however, many reports have indicated that microsatellites in the promoter regions and introns of functional genes exert genetic effects in many cases [1, 5, 9, 10, 12, 19]. Thus, microsatellites in known functional genes are good targets for analyzing genetic polymorphisms.

In this study, we focused on a $(GAAT)_n$ repeat motif located in the first intron of the canine *TNFA* gene and demonstrated that this microsatellite locus was highly polymorphic, so it could be a useful marker for genetic analysis.

Whole blood, swabs of the oral mucosa or nail samples were collected from dogs at veterinary hospitals and dog grooming shops in Japan. The 139 samples obtained were from 22 Beagles, 26 Chihuahuas, 20 Miniature Dachshunds, 24 Miniature Poodles, 22 Pembroke Welsh Corgis and 25 Shiba Inus. This study was approved by the Institutional Animal Care and Use Committee (Permission number: 1306094) and carried out according to the Azabu University Animal Experimentation Regulations. DNA was extracted from these samples using a Quick Gene DNA tissue kit (Fuji Film, Tokyo, Japan) or a NucleoSpin Blood Quick Pure kit (Macherey-Nagel, Duren, Germany), according to the manufacturer's protocols.

The primers used for polymerase chain reaction (PCR) analysis were designed using CanFam3.1. A 1.1-kb DNA fragment containing about 400 bp upper stream from the putative transcription start site, a 5′- untranslated region (5′- UTR), the first exon and about 240 bp of the first intron of the canine *TNFA* gene was amplified by PCR using the forward primer dog-*TNFA*-F1 (5′-AAGCCCCACCCCTTG-

*CORRESPONDENCE TO: HISASUE, M., Laboratory of Veterinary Internal Medicine II, Faculty of Veterinary Medicine, Azabu University, 1–17–71, Fuchinobe, Chuo-ku, Sagamihara, Kagagawa 252–5201, Japan.
e-mail: hisasue@azabu-u.ac.jp
**The first two authors contributed equally to this work

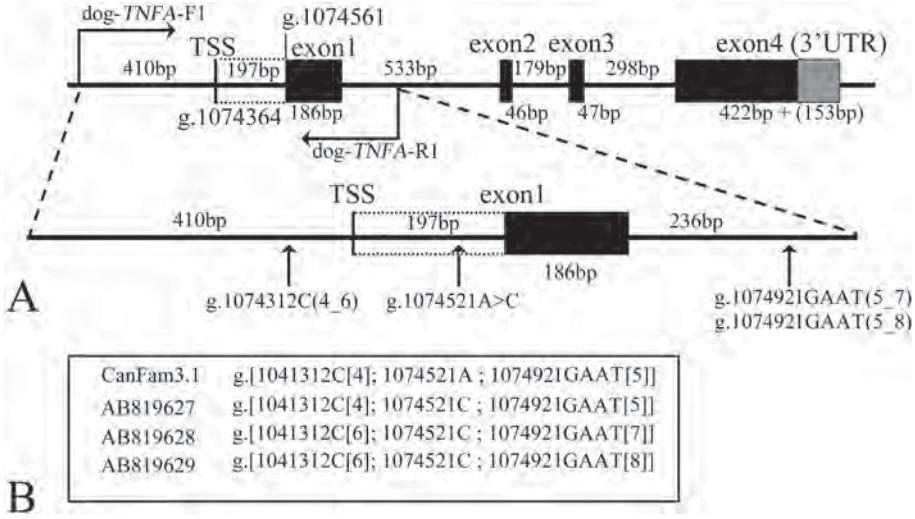

Fig. 1. Scheme of the canine *TNFA* gene showing the region sequenced and the polymorphisms detected. (A) Structure of the canine *TNFA* gene (above) and its sequenced region (below). The protein-coding sequences are indicated by dark boxes. The numbering of base positions was based on the reference sequence, NW_003726081 (CanFam3.1; chromosome 12). In the reference sequence, g.1074364 and g.1074561 were the putative transcription start site (TSS) and the head of the translation initiation codon of the *TNFA* gene, respectively. (B) The variations detected in the partial *TNFA* gene in 7 Beagles.

CACCTT-3′) and the reverse primer dog-*TNFA*-R1 (5′-CCACACCCCACATCTCTCCACACA-3′) (Fig. 1A). PCR was performed using 30 μl reaction volumes, according to the manufacturer's instructions for GoTaq Green Master Mix (Promega, Fitchburg, WI, U.S.A.). The program comprised initial denaturation at 94°C for 3 min, followed by 30 cycles of denaturation at 94°C for 20 sec, annealing at 59°C for 25 sec and extension at 72°C for 60 sec with a final extension at 72°C for 7 min. The amplified products were purified using a QIAquick PCR Purification kit (Qiagen, Hilden, Germany). The purified DNA was sequenced directly using a Big Dye Terminator version 3.1 Cycle Sequencing kit (Applied Biosystems, Foster City, CA, U.S.A.) with dog-*TNFA*-F1 and dog-*TNFA*-R1 primers. First, we analyzed the DNA sequences of 22 Beagles. However, 15 of the 22 individuals produced poor results, because of widespread double peak from the dog_*TNFA*_R1 primer side. As a result, we determined the target sequences successfully in 7 individuals only.

After multiple alignments of the partial *TNFA* sequences of the 7 Beagles with the canine reference sequence, we found 3 polymorphic sites: a cytosine direct repeat variation in the 5′ gene flanking region (g.1074312C (4_6)), an adenine to cytosine substitution in the 5′ UTR (g.1074521A>C) and GAAT microsatellite variations in the first intron (g.1074922GAAT (5_7) and g.1074922GAAT (5_8)) (Fig. 1A). Next, we identified 3 *TNFA* variations: TNFA-Beagle1 (1 dog), TNFA-Beagle2 (2 dogs) and TNFA-Beagle3 (4 dogs) in the 7 individuals (Fig. 1B).These nucleotide sequences were deposited in the DDBJ, EMBL and GenBank nucleotide databases under accession numbers AB819627–AB819629.

Based on their electropherograms, we also found that the suboptimal sequencing results for the 15 Beagles resulted from the heterozygosity (*He*) in different numbers of (GAAT) repeats in the [$(GAAT)_{5–8}$ (GAT) $(GAAT)_2$] microsatellite motif in the first intron (Fig. 1). To genotype this microsatellite locus, we designed the following primer set: CFA12-*TNFA*-STR1-F (5′-GGAAGATGCTCATGGATTGCT-3′) and CFA12-*TNFA*-STR1-R (5′-TACCCACACCCCACATCTCT-3′). PCR was performed using 25 μl reaction volumes, according to the manufacturer's instructions for GoTaq Master Mix (Promega). The program comprised initial denaturation at 94°C for 3 min, followed by either 30 or 40 cycles of denaturation at 94°C for 20 sec, annealing at 55°C for 15 sec and extension at 72°C for 30 sec with a final extension at 72°C for 7 min. The PCR products were electrophoresed on a 3.0% agarose gel and visualized by ethidium bromide staining (Fig. 2). Four alleles, i.e., $(GAAT)_5$, $(GAAT)_6$, $(GAAT)_7$ and $(GAAT)_8$, were detected in the CFA12-*TNFA*-STR1 tetranucleotide microsatellite locus, and the lengths of their PCR products were 114, 118, 122 and 126 bp, respectively. Subsequently, we surveyed the allele distribution of this microsatellite marker in 6 dog breeds. We used the FAM-labeled CFA12-*TNFA*-STR1-F primer, and the fragment lengths of the PCR products were determined automatically using an ABI 3130 genetic analyzer with GeneMapper Ver. 4.0 (Applied Biosystems). Table 1 shows the genotypic and allele distribution in 6 dog breeds. Four alleles were present in 22 Beagles, whereas only 3 alleles were detected in 117 dogs from the other 5 breeds. This is because the $(GAAT)_8$ allele was absent from Chihuahuas, Miniature Dachshunds, Miniature Poodles,

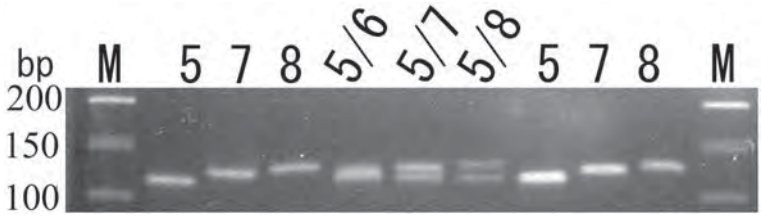

Fig. 2. Genotyped patterns of the tetranucleotide microsatellite polymorphism in the first intron of the canine *TNFA* gene on a 3.0% agarose gel. The genotypes relate to the upper lanes of the gel. M is a 50-bp DNA ladder molecular size marker (Toyobo, Osaka, Japan).

Table 1. Genotypic and allelic frequency of $(GAAT)_n$ tetranucleotide microsatellite in canine *TNFA* gene among dog breeds

Breeds (number of animals)	Genotype										Allelic frequency				*He*[a)]	*PIC*[b)]	Deviations of HWE[c)]
	5	6	7	8	5/6	5/7	5/8	6/7	6/8	7/8	5	6	7	8			
Beagle (22)	1	0	2	4	5	5	1	1	0	3	0.295	0.136	0.295	0.273	0.749	0.682	$P<0.05$
Miniature Dachshund[d)] (20)	8	0	2	0	2	7	0	1	0	0	0.625	0.075	0.300	0.000	0.527	0.438	NS[e)]
Chihuahua[d)] (26)	12	2	0	0	9	3	0	0	0	0	0.692	0.250	0.058	0.000	0.464	0.391	NS
Miniature Poodle (24)	6	1	0	0	6	11	0	0	0	0	0.604	0.167	0.229	0.000	0.566	0.493	$P<0.05$
Pembroke Welsh Corgi (22)	8	1	0	0	5	4	0	4	0	0	0.568	0.250	0.182	0.000	0.595	0.516	NS
Shiba Inu (25)	13	0	0	0	2	10	0	0	0	0	0.760	0.040	0.200	0.000	0.389	0.333	NS

a) Expected heterozygosity, b) Polymorphic information content, c) Deviations of Hardy-Weinberg Equilibrium, d) All the indivduals had long-coate. e) Not significant.

Pembroke Welsh Corgis and Shiba Inus. $(GAAT)_5$ was the most common allele in the 6 dog breeds. An exact test of the Hardy–Weinberg equilibrium using a Markov chain and calculation of the expected *He* were performed using Arlequin ver. 3.1 [4]. The polymorphic information content (*PIC*) value for this microsatellite locus was estimated using a formula described previously [2]. The deviations from the Hardy–Weinberg equilibrium were statistically significant ($P<0.05$) for Beagles and Miniature Poodles. *He* was deficient in Beagles, whereas an excess of *He* was observed in Miniature Poodles. The expected *He* and *PIC* value for this microsatellite locus varied from 0.389 (Shiba Inu) to 0.749 (Beagle) and from 0.333 (Shiba Inu) to 0.682 (Beagles), respectively, in the 6 breeds (Table 1). The allelic frequency differed greatly among breeds, but this microsatellite marker was highly polymorphic and could be a useful marker for the canine *TNFA* gene. Given the important roles of TNFA in many inflammatory reactions, the tetranucleotide microsatellite alleles could be associated with susceptibility to inflammatory disorders during the lifetime of the domestic dog due to a direct gene effect or linkage disequilibrium with adjacent nucleotide variations. Further studies are needed to test for possible correlations between this microsatellite variation and canine diseases.

ACKNOWLEDGMENTS. We thank Dr. Hidekatsu Shimakura from the First Department of Microbiology, Faculty of Veterinary Medicine, Azabu University for collecting canine DNA samples. This work was supported by the MEXT Program for the Strategic Research Foundation at Private Universities, 2011–2015. The authors would like to thank Enago (www.enago.jp) for the English language review.

REFERENCES

1. Aoki, T., Koch, K. S. and Leffert, H. L. 1997. Attenuation of gene expression by a trinucleotide repeat-rich tract from the terminal exon of the rat hepatic polymeric immunoglobulin receptor gene. *J. Mol. Biol.* **267**: 229–236. [Medline] [CrossRef]
2. Botstein, D., White, R. L., Skolnick, M. and Davis, R. W. 1980. Construction of a genetic linkage map in man using restriction fragment length polymorphisms. *Am. J. Hum. Genet.* **32**: 314–331. [Medline]
3. Buranawuti, K., Boyle, M. P., Cheng, S., Steiner, L. L., McDougal, K., Fallin, M. D., Merlo, C., Zeitlin, P. L., Rosenstein, B. J., Mogayzel, P. J. Jr., Wang, X. and Cutting, G. R. 2007. Variants in mannose-binding lectin and tumour necrosis factor alpha affect survival in cystic fibrosis. *J. Med. Genet.* **44**: 209–214. [Medline] [CrossRef]
4. Excoffier, L., Laval, G. and Schneider, S. 2005. Arlequin ver. 3.0: An integrated software package for population genetics data analysis. *Evol. Bioinform. Online* **1**: 47–50.
5. Gardezi, A. Z., Ziaei, Y. Z. and Marashi, S. M. 2008. Microsatellite polymorphism of the human leptin gene and risk of obesity. *J. Crit. Care* **23**: 440–444. [Medline] [CrossRef]
6. Guedes, P. M., Veloso, V. M., Afonso, L. C., Caliari, M. V., Carneiro, C. M., Diniz, L. F., Marques-da-Silva, E. A., Caldas, I. S., Do Valle Matta, M. A., Souza, S. M., Lana, M., Chiari, E., Galvão, L. M. and Bahia, M. T. 2009. Development of chronic cardiomyopathy in canine Chagas disease correlates with high IFN-gamma, TNF-alpha, and low IL-10 production during the acute infection phase. *Vet. Immunol. Immunopathol.* **130**: 43–52. [Medline] [CrossRef]
7. Hearne, C. M., Ghosh, S. and Todd, J. A. 1992. Microsatellites for linkage analysis of genetic traits. *Trends Genet.* **8**: 288–294. [Medline]

8. Ishii, T., Hirose, H., Saito, I., Nishikai, K., Maruyama, H. and Saruta, T. 2000. Tumor necrosis factor alpha gene G-308A polymorphism, insulin resistance, and fasting plasma glucose in young, older, and diabetic Japanese men. *Metabolism* **49**: 1616–1618. [Medline] [CrossRef]
9. Kashi, Y., King, D. and Soller, M. 1997. Simple sequence repeats as a source of quantitative genetic variation. *Trends Genet.* **13**: 74–78. [Medline] [CrossRef]
10. Klesert, T. R., Otten, A. D., Bird, T. D. and Tapscott, S. J. 1997. Trinucleotide repeat expansion at the myotonic dystrophy locus reduces expression of *DMAHP*. *Nature Genet.* **16**: 402–406. [Medline] [CrossRef]
11. Koss, K., Satsangi, J., Fanning, G. C., Welsh, K. I. and Jewell, D. P. 2000. Cytokine (TNF-alpha, LT-alpha, and IL-10) polymorphisms in inflammatory bowel diseases and normal controls: differential effects on production and allele frequencies. *Genes Immun.* **1**: 185–190. [Medline] [CrossRef]
12. Meloni, R., Albanèse, V., Ravassard, P., Treilhou, F. and Mallet, J. 1998. A tetranucleotide polymorphic microsatellite, located in the first intron of the tyrosine hydroxylase gene, acts as a transcription regulatory element *in vitro*. *Hum. Mol. Genet.* **7**: 423–428. [Medline] [CrossRef]
13. Menezes-Souza, D., Corrêa-Oliveira, R., Guerra-Sá, R., Giunchetti, R. C., Teixeira-Carvalho, A., Martins-Filho, O. A., Oliveira, G. C. and Reis, A. B. 2011. Cytokine and transcription factor profiles in the skin of dogs naturally infected by *Leishmania (Leishmania) chagasi* presenting distinct cutaneous parasite density and clinical status. *Vet. Parasitol.* **177**: 39–49. [Medline] [CrossRef]
14. Mira, J.P., Cariou, A., Grall, F., Delclaux, C., Losser, M.R., Heshmati, F., Cheval, C., Monchi, M., Teboul, J.L., Riche, F., Leleu, G., Arbibe, L., Mignon, A., Delpech, M. and Dhainaut, J.F. 1999. Association of *TNF2*, a TNF-alpha promoter polymorphism, with septic shock susceptibility and mortality: a multicenter study. *JAMA* **282**: 561–568. [Medline] [CrossRef]
15. Mulcahy, B., Waldron-Lynch, F., McDermott, M. F., Adams, C., Amos, C. I., Zhu, D. K., Ward, R. H., Clegg, D. O., Shanahan, F., Molloy, M. G. and O'Gara, F. 1996. Genetic variability in the tumor necrosis factor-lymphotoxin region influences susceptibility to rheumatoid arthritis. *Am. J. Hum. Genet.* **59**: 676–683. [Medline]
16. Ridyard, A. E., Nuttall, T. J., Else, R. W., Simpson, J. W. and Miller, H. R. P. 2002. Evaluation of Th1, Th2 and immunosuppressive cytokine mRNA expression within the colonic mucosa of dogs with idiopathic lymphocytic-plasmacytic colitis. *Vet. Immunol. Immunopathol.* **86**: 205–214. [Medline] [CrossRef]
17. Song, R., Kim, J., Yu, D., Park, C. and Park, J. 2012. Kinetics of IL-6 and TNF-α changes in a canine model of sepsis induced by endotoxin. *Vet. Immunol. Immunopathol.* **146**: 143–149. [Medline] [CrossRef]
18. Weber, J. L. and May, P. E. 1989. Abundant class of human DNA polymorphisms which can be typed using the polymerase chain reaction. *Am. J. Hum. Genet.* **44**: 388–396. [Medline]
19. Wei, J., Ramchand, C. N. and Hemmings, G. P. 1995. Association of polymorphic VNTR region in the first intron of the human *TH* gene with disturbances of the catecholamine pathway in schizophrenia. *Psychiatr. Genet.* **5**: 83–88. [Medline] [CrossRef]

CELL BIOCHEMISTRY & FUNCTION

CELL BIOCHEMISTRY AND FUNCTION
Cell Biochem Funct 2014; **32**: 236–240.
Published online 20 September 2013 in Wiley Online Library
(wileyonlinelibrary.com) **DOI**: 10.1002/cbf.3006

Downregulation of Pgc-1α expression by tea leaves and their by-products

Erika Shibuya[1], Masaru Murakami[2], Makoto Kondo[3], Yasutomi Kamei[4], Shozo Tomonaga[1], Tohru Matsui[1] and Masayuki Funaba[1]*

[1]*Division of Applied Biosciences, Graduate School of Agriculture, Kyoto University, Kyoto, Japan*
[2]*Laboratory of Molecular Biology, Azabu University School of Veterinary Medicine, Sagamihara, Japan*
[3]*Graduate School of Bioresources, Mie University, Tsu, Japan*
[4]*Graduate School of Life and Environmental Sciences, Kyoto Prefectural University, Kyoto, Japan*

Previous studies indicate that muscle Pgc-1α expression governs the proportion of muscle fibre types. As a first step in using diet to manipulate the proportion of muscle fibre types by using Pgc-1α expression, the present study investigates the modulation of Pgc-1α expression by feedstuffs. A luciferase-based Pgc-1α reporter construct (Pgc-1α(-2553)-luc) that contains the mouse Pgc-1α promoter (−2553 to +78 bp) was prepared. A screen of ethanol extracts from 33 feedstuffs indicated that oolong tea and roasted green tea extracts decreased Pgc-1α(-2553)-luc expression in C2C12 myoblasts. The transcriptional repression of Pgc-1α by tea leaf extracts was reproduced in hepatic HepG2 cells. We further examined the effects of the alcohol extracts of tea waste and its silage on Pgc-1α transcription; the tea waste silage extract inhibited Pgc-1α transcription. Treatment with the extracts of raw tea leaves, tea waste and tea waste silage effectively decreased Pgc-1α mRNA levels during myogenesis of myosatellite cells. The present results suggest that tea leaves and their by-products could be used to modulate proportions of muscle fibre types.

KEY WORDS—Pgc-1α; skeletal muscle; tea leaf; muscle fibre type; feedstuffs

INTRODUCTION

Pparγ co-activator-1α (Pgc-1α) was originally identified as a co-activator of Pparγ; Pgc-1α enhances the expression of the Ucp1 gene, which encodes an uncoupling protein found in the mitochondria of brown adipocytes and is essential to generating heat by nonshivering thermogenesis.[1] Subsequent analyses in cultured cells and transgenic mice have established that the biological function of Pgc-1α is to regulate mitochondrial oxidative metabolism as well as mitochondrial biogenesis in diverse cell types.[2–4] In skeletal muscle, Pgc-1α expression is enhanced by exercise in humans and rodents[5–7] and is involved in the maintenance of muscle function; transgenic mice with enhanced Pgc-1α expression in skeletal muscles preserve muscle integrity and function during ageing. This phenotype is related to the maintenance of the activity of enzymes involved in oxidative phosphorylation, the reduction of apoptosis, autophagy and proteasomal degradation.[8] In addition, the transgenic mice exhibited resistance to age-related obesity and increased insulin sensitivity.[8] In contrast, reduced muscle function and exercise capacity were detected in skeletal muscle-specific Pgc-1α knock-out mice.[9]

Metabolic changes related to muscle Pgc-1α expression can be partly explained by the modulation of muscle fibre types. Muscle fibres are divided into two types, slow twitch and fast twitch. Reddish slow-twitch myofibres contain a high number of mitochondria and use oxidative metabolism as their primary energy source, whereas whitish fast-twitch myofibres contain more glycogens and predominantly use glycolytic metabolism.[10] Mouse muscles forced to express Pgc-1α state contained more slow-twitch muscle fibres,[11] whereas gene targeting of skeletal muscle Pgc-1α increased expression of fast-twitch muscle fibre-specific myosin heavy chain (Myhc) 2b and decreased the expression of Myhc 1, which is slow-twitch muscle fibre-specific.[9]

Pgc-1α activity is closely linked to its expression level, because it is primarily regulated at the transcriptional level. MEF2 activates Pgc-1α gene transcription, and MEF2 repression decreases Pgc-1α mRNA levels, leading to the downregulation of genes involved in fatty acid oxidation in the heart.[12] In addition, selective expression of constitutively active CAMK IV in skeletal muscle increases Pgc-1α transcription, mRNA levels and mitochondrial DNA copy number.[13] Therefore, Pgc-1α activity can be potentially monitored by evaluation of its mRNA levels. The objective of this study is to identify feedstuffs that affect Pgc-1α expression. We screened for Pgc-1α expression using luciferase under the control of the Pgc-1α promoter as a reporter.

*Correspondence to: Masayuki Funaba, Division of Applied Biosciences, Graduate School of Agriculture, Kyoto University, Kitashirakawa Oiwakecho, Kyoto 606-8502, Japan. E-mail: mfunaba@kais.kyoto-u.ac.jp

Received 12 June 2013
Revised 21 August 2013
Accepted 28 August 2013

Here, we show that tea leaves and their by-products contain factors that downregulate Pgc-1α expression through transcriptional inhibition.

MATERIALS AND METHODS

Cell culture

Animal experiments were approved by the Kyoto University Animal Experiment Committee. Myosatellite cells were isolated from rat plantaris muscles; male Wistar rats weighing 200–300 g were sacrificed by exsanguination under isoflurane anaesthesia, and the plantaris muscle was collected. Muscles were washed with phosphate-buffered saline and minced with scissors in digestion buffer containing 0.1% (w/v) collagenase I (Wako Pure Chemical Industries, Ltd., Osaka, Japan) and 1,000 U/ml dispase (Invitrogen, Grand Island, NY, USA) in 140 NaCl, 5.4 KCl, 0.34 Na_2HPO_4, 0.44 KH_2PO_4, 0.81 $MgSO_4{\cdot}7H_2O$, 1.3 $CaCl_2$, 4.2 $NaHCO_3$ and 5.6 mM glucose supplemented with 10 U/mL penicillin, 100 μg/mL streptomycin and 2.5 μg/mL amphotericin B, followed by enzyme digestion shaking at 100 rpm for 60 min at 37 °C. After filtering through 50 μm nylon mesh, cells were washed with Dulbecco's modified Eagle's medium (DMEM) with 10% fetal bovine serum and antibiotics twice and seeded on cell culture dishes. On day one post confluence, cells were differentiated into myotubes by using differentiation medium, i.e. DMEM with 2% horse serum and antibiotics. Ethanol extracts of feedstuffs (20 μg/mL) or forskolin (10 μM) were simultaneously added to the differentiation medium. Cells were harvested 12 days post-differentiation to analyse Pgc-1α expression.

C2C12 cells, COS7 cells and HepG2 cells were cultured in DMEM with 10% fetal bovine serum and antibiotics. The DMEM used for C2C12 cells contained 1 g/L of glucose, whereas the medium used for COS7 and HepG2 cells contained 4.5 g/L of glucose. For luciferase-based reporter assays, plasmid vectors were transiently transfected using Lipofectamine LTX reagent (Invitrogen) for C2C12 cells or PolyFect transfection reagent (Qiagen, Valencia, CA, USA) for COS7 and HepG2 cells according to the manufacturers' protocol. At 24 h post-transfection, cells were treated with or without the extracts from feedstuffs (20 μg/mL) or forskolin (10 μM) for 24 h.

Preparation of ethanol extract

A total of 41 feedstuffs were used. Wet tea wastes were obtained from a local beverage company that produces canned and bottled tea drinks. Tea waste was ensiled in laboratory silos by using the method described by Nishino *et al.*[14] Two grammes of food was mixed with 40 mL of ethanol and vigorously shaken for 60 min at room temperature followed by filtration through filter paper. For tea waste and its silage, the ethanol extraction was performed after freeze drying the samples. The ethanol extracts were concentrated to ~20 mg/mL ethanol extract by using a centrifugal evaporator (RD-400, Yamato Scientific Co., Ltd, Tokyo, Japan). The samples were stored under N_2 gas at −20 °C until analysis.

RNA isolation and RT-qPCR

Total RNA isolation from myosatellite cells and cDNA synthesis were performed using TRIZOL (Invitrogen) and the ReverTra Ace qPCR RT kit (Toyobo, Osaka, Japan) respectively according to the manufacturers' protocols. The cDNA was reverse transcribed from 5 ng of total RNA and was used as a template for reverse transcription-quantitative polymerase chain reaction (RT-qPCR) as described previously.[15] The oligonucleotide primers were 5'-TGTGGAACTCTCTGGAACTGC-3' and 5'-GCCTTGAAAGGGTTATCTTGG-3' for Pgc-1α and 5'-CTAAGGCCAACCGTGAAAAG-3' and 5'-ACCAGAGGCATACAGGGACA-3' for β-actin. The Ct values were determined, and the abundance of gene transcripts was analysed using the $^{\Delta\Delta}$Ct method by using β-actin as the normalization gene.

Plasmids and reporter assays

The DNA fragment encompassing −2554 and +79 bp of the mouse Pgc-1α promoter was amplified and cloned into the pGL4 basic vector containing the firefly luciferase reporter gene (Pgc-1α(-2553)-luc); nt +1 is the transcription initiation site. The reporter construct contains the promoter region used in study by Amat *et al.*,[16] who showed transcriptional regulation of Pgc-1α by MyoD. The coding region of mouse MyoD was cloned into pcDNA3. The product was verified by nucleotide sequencing. Cells were transiently transfected with the indicated expression vectors: Pgc-1α(-2553)-luc and a plasmid expressing Renilla luciferase under the control of thymidine kinase (pRenilla-luc). Luciferase activity was normalized to Renilla luciferase activity, and the firefly luciferase activity in the cell lysate treated with vehicle was set at 1.

Statistical analyses

The data are expressed as the mean ± SEM. Data from the reporter assays and gene expression data were log transformed to provide an approximation of a normal distribution before analysis. Differences between control cells and cells treated with the feedstuff extracts were examined using an unpaired *t*-test. Differences of $P < 0.05$ were considered significant.

RESULTS AND DISCUSSION

To evaluate the transcriptional activity of Pgc-1α, a luciferase-based reporter assay using the Pgc-1α promoter were performed in C2C12 myoblasts; ethanol extracts from 33 feedstuffs were evaluated. The extracts were evaluated at a concentration of 20 μg/mL, except for the red bell pepper extract. Because the red bell pepper extract had a cytotoxic effect in C2C12 cells, the transcriptional activity was examined at a concentration of 2 μg/mL. The reporter assay screen

was replicated in at least three independent experiments. Representative results are shown in Figure 1. Luciferase expression was significantly lower in cells treated with oolong tea or roasted green tea extracts of than in control cells. None of the extracts reproducibly increased luciferase expression more than twofold (data not shown).

Next, we examined whether the inhibitory effects of tea leaf extract can be detected in the other cells. Pgc-1α transcription is stimulated by forskolin, an activator of adenylate cyclase[17] and by MyoD, a muscle-specific transcription factor.[16] However, Pgc-1α transcription was unaffected by forskolin in COS7 cells, even when MyoD was co-expressed (Figure 2A). In contrast, HepG2 hepatoma cells were responsive to forskolin irrespective of MyoD expression (Figure 2A), indicating that Pgc-1α transcription can be evaluated in HepG2 cells. The inhibitory effects of tea leaf extracts on Pgc-1α transcription were weaker in HepG2 cells (Figure 2B) relative to C2C12 cells (Figure 1) but were detected in green tea, black tea, roasted green tea and oolong tea extracts. These results suggest that tea leaves contain factor(s) that inhibit Pgc-1α transcription; the activity of the tea leaves is not limited to C2C12 myogenic cells but is also detected in liver cells. Pgc-1α orchestrates a complex program of metabolic changes that occur during the transition from a fed liver to a fasted liver, including gluconeogenesis; these effects on fasting adaptation are achieved through co-activation of hepatic transcription factors such as hepatic nuclear factor 4α, Pparα, glucocorticoid receptor, Foxo1 and the liver X receptor.[18] Therefore, the tea leaves may also be able to modulate hepatic glucose metabolism.

Effects of tea waste and its silage on Pgc-1α transcription were further evaluated in C2C12 cells (Figure 3). The tea

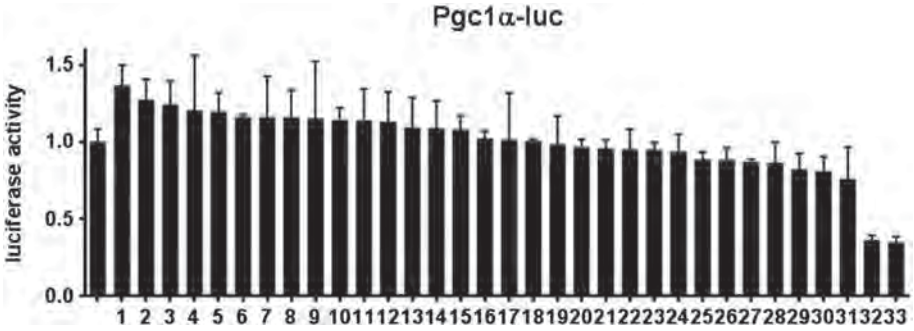

Figure 1. Inhibition of Pgc-1α transcription by tea leaf extracts in C2C12 cells. C2C12 cells were transiently transfected with Pgc-1α(-2553)-luc and pRenilla-luc, and treated with vehicle or feedstuff extracts for 24 h. The firefly luciferase activity was normalized to the Renilla luciferase activity, and the firefly luciferase activity in cell lysates treated with vehicle was set to 1. Data are expressed as the mean ± SE ($n = 3$). **: $P < 0.01$ vs. vehicle. (1) fish meal, (2) glycated rice meal, (3) chicken meal, (4) wine residues, (5) yellow grease, (6:) red bell pepper extract, (7) dried distiller's grains with solubles, (8) black soybean branch, (9) cassava starch pulp, (10) skim milk, (11) rapeseed meal, (12) corn gluten meal, (13) black soybean leaf, (14) corn germ meal, (15) wheat flour, (16) shochu distillery by-product, (17) tall fescue, (18) soybean meal, (19) corn gluten feed, (20) yogurt, (21) rice alcohol cake, (22) meat and bone meal, (23) dehulled soybean meal, (24) sake kasu, (25) butter oil, (26) soybean flour, (27) feather meal, (28) wine lees, (29) defatted rice bran, (30) soy protein concentrate, (31) wheat bran, (32) oolong tea and (33) roasted green tea

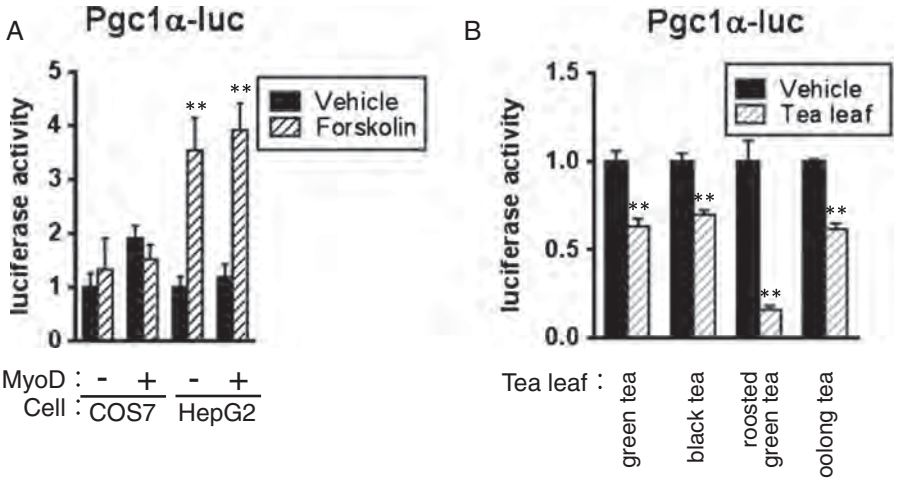

Figure 2. Transcriptional repression of Pgc-1α(-2553)-luc by tea leaf extracts in HepG2 cells. (A) COS7 cells or HepG2 cells were transiently transfected with Pgc-1α(-2553)-luc and pRenilla-luc with or without the MyoD expression plasmid and treated with vehicle or forskolin (10 μM) for 24 h. (B) C2C12 cells were transiently transfected with Pgc-1α(-2553)-luc and pRenilla-luc and treated with vehicle or the indicated extract for 24 h. Firefly luciferase activity was normalized to Renilla luciferase activity, and the firefly luciferase activity in the cell lysates treated with vehicle was set to 1. Data are expressed as the mean ± SE ($n = 3$). **: $P < 0.01$ vs. vehicle

waste extracts from green tea, black tea and oolong tea did not significantly decrease expression of the Pgc-1α(-2553)-luc construct, but the silage extract effectively repressed Pgc-1α transcription; the effects of oolong tea waste silage were not statistically significant but had a tendency to repress expression ($P = 0.08$).

Screening feedstuffs using Pgc-1α(-2553)-luc indicates that the extracts from tea leaves and their by-products cause inhibitory effects on Pgc-1α transcription. We further verified whether these feedstuffs actually downregulate Pgc-1α expression in myogenic cells; cells were treated during myogenesis with or without the extracts of tea leaves or their by-products, and Pgc-1α mRNA levels were examined by RT-qPCR. Because C2C12 myoblasts and myotubes did not express Pgc-1α mRNA significantly (data not shown), we used primary myosatellite cells from rat plantaris muscle. Consistent with the reporter assay results (Figure 1), the oolong tea leaf extract decreased Pgc-1α mRNA expression, whereas cassava starch pulp or dehulled soybean meal extracts did not affect Pgc-1α expression (Figure 4A). Forskolin treatment increased Pgc-1α expression as expected (Figure 4A). The extracts from tea waste silage also had the ability to down-regulate Pgc-1α expression (Figure 4B). Unlike Pgc-1α transcription, Pgc-1α mRNA level was decreased also by the tea waste extract (Figure 4B); the inconsistent result between the reporter assay and expression at the mRNA level may be due to (1) transcriptional repression via a region not contained in the Pgc-1α reporter gene or (2) post-transcriptional regulation such as mRNA stability.

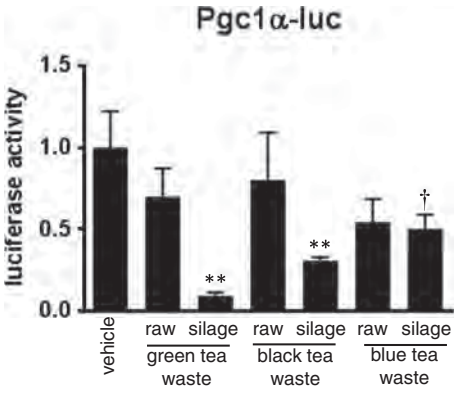

Figure 3. Transcriptional repression of Pgc-1α(-2553)-luc by extracts of tea waste and its silage in C2C12 cells. C2C12 cells were transiently transfected with Pgc-1α(-2553)-luc and pRenilla-luc and were treated with vehicle or the indicated extract for 24 h. Firefly luciferase activity was normalized to Renilla luciferase activity, and the firefly luciferase activity in the cell lysates treated with vehicle was set to 1. Data are expressed as the mean ± SE ($n = 3$). † and **: $P < 0.10$ and $P < 0.01$, respectively, vs. vehicle

The present study identifies tea leaves and their by-products as negative regulators of Pgc-1α expression. As described previously, muscle fibre type is modulated by the expression level of Pgc-1α; higher expression of Pgc-1α increases the proportion of slow-twitch oxidative muscle fibre type,[11] whereas the suppression of Pgc-1α expression increases fast-twitch glycolytic muscle fibre type.[9] Therefore, tea leaves and their by-products may act as a switch of muscle fibre types, although future studies should be carried out to clarify whether they affect muscle fibre types through modulation of Pgc-1α expression *in vivo*.

Pgc-1α transcription is accelerated through calcium signaling pathway in skeletal muscle; activation of calcineurin stimulates Pgc-1α transcription mediated by activated CREB and MEF2.[18] In addition, Pgc-1α expression is enhanced by glucagon and glucocorticoid signaling in liver.[18] Although mechanisms underlying why tea leaves and their by-products inhibit Pgc-1α transcription are unclear, the inhibition may be elicited by negative regulation of the transcriptional activation.

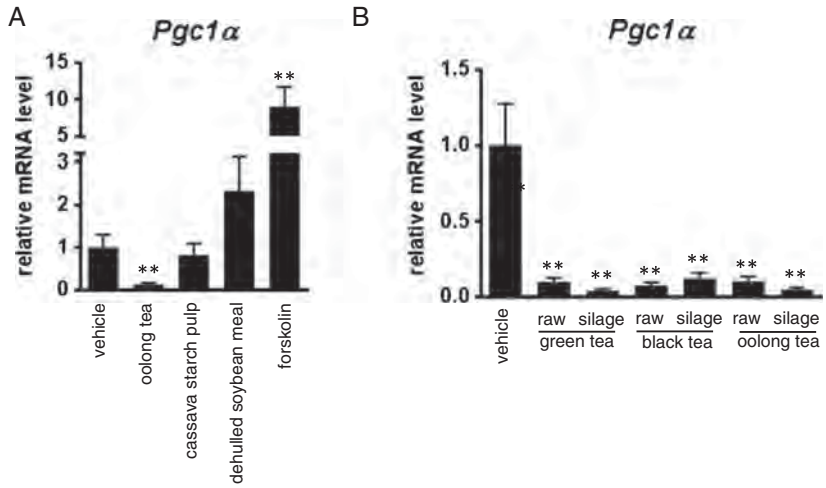

Figure 4. Downregulation of Pgc-1α expression by extracts of tea waste and its silage in primary myosatellite cells. Myosatellite cells from rat plantaris muscle were differentiated into myotubes by reducing the serum concentration of the culture medium. After simulating differentiation, the cells were treated with the indicated extract or forskolin 12 days. Pgc-1α mRNA levels were examined by reverse transcription-quantitative polymerase chain reaction and normalized to β-actin mRNA levels. The expression level in cells treated with vehicle was set to 1. Data are expressed as the mean ± SE ($n = 6$). **: $P < 0.01$ vs. vehicle

Considering that Pgc-1α expression levels in skeletal muscle are positively correlated with the health benefits described previously,[8,9] tea leaves and their by-products may have a negative effect on skeletal muscle Pgc-1α-mediated improvement of whole-body health in humans. However, the downregulation of Pgc-1α expression may be beneficial to beef production. Beef colour is one important factor in determining the wholesale price of beef in Japan. The dark red colour of beef decreases the commodity value of beef in Japan; Japanese consumers prefer lightly coloured beef. Muscle fibre type affects beef colour; longissimus muscle and psoas major muscle are a mixture of fast-twitch and slow-twitch muscle fibres; slow-twitch muscle fibres are reddish, and fast-twitch muscle fibres are whitish. Thus, the tea leaves and their by-products could potentially enable the production of the preferred colour of beef through increased proportion of fast-twitch muscle fibres mediated by the downregulation of Pgc-1α expression. Furthermore, considering the correlation between slow-twitch muscle fibre content and cooking loss, a beef quality trait,[19] tea leaves and their by-products may be effective at improving beef quality by decreasing cooking loss. Effects of muscle fibre type in beef on human nutrition are unknown. Comparison of amino acid composition between fast-twitch myosin and slow-twitch myosin indicates no substantial difference (data not shown).

Canned and bottled tea drinks have become a favourite beverage in Japan. Over 100 000 t of tea waste per year are emitted from beverage companies; however, much of these wastes are burned or composted.[14] Tea waste can be preserved by ensiling because of its high moisture content, thus tea waste silage would be a practical feedstuff to improve beef production.

Downregulation of Pgc-1α expression by tea leaf by-products may also lead to an improvement of fattening efficacy, i.e. weight gain per feed intake. Transgenic mice with elevated muscle Pgc-1α expression are resistant to age-related obesity;[8] one of the underlying the events in this process is increased energy expenditure resulting from Irisin production and secretion from the skeletal muscle in response to the upregulation of skeletal muscle Pgc-1α expression.[20] Future studies should identify the specific molecule(s) in the extract of tea leaves and their by-products that represses Pgc-1α expression, and how these molecule(s) induce transcriptional repression. Considering the abundance of various phenols, polyphenols and tannins in tea leaves,[21,22] these compounds could be candidates.

CONFLICT OF INTEREST

The authors have declared that there is no conflict of interest.

ACKNOWLEDGEMENTS

This work was supported by a Grant-in-Aid for Scientific Research (23380158) from the Japan Society for the Promotion of Science and a research project grant awarded by the Azabu University.

REFERENCES

1. Puigserver P, Wu Z, Park CW, Graves R, Wright M, Spiegelman BM. A cold-inducible coactivator of nuclear receptors linked to adaptive thermogenesis. *Cell* 1998; **92**: 829–839.
2. Handschin C, Spiegelman BM. Peroxisome proliferator-activated receptor g coactivator 1 coactivators, energy homeostasis, and metabolism. *Endocr Rev* 2006; **27**: 728–735.
3. Feige JN, Auwerx J. Transcriptional coregulators in the control of energy homeostasis. *Trends Cell Biol* 2007; **17**: 292–301.
4. Lin JD. The PGC-1 coactivator networks: chromatin-remodeling and mitochondrial energy metabolism. *Mol Endocrinol* 2009; **23**: 2–10.
5. Goto M, Terada S, Kato M, *et al*. cDNA Cloning and mRNA analysis of PGC-1 in epitrochlearis muscle in swimming-exercised rats. *Biochem Biophys Res Commun* 2000; **274**: 350–354.
6. Baar K, Wende AR, Jones TE, *et al*. Adaptations of skeletal muscle to exercise: rapid increase in the transcriptional coactivator PGC-1. *FASEB J* 2002; **16**: 1879–1886.
7. Norrbom J, Sundberg CJ, Ameln H, Kraus WE, Jansson E, Gustafsson T. PGC-1a mRNA expression is influenced by metabolic perturbation in exercising human skeletal muscle. *J Appl Physiol* 2004; **96**: 189–194.
8. Wenz T, Rossi SG, Rotundo RL, Spiegelman BM, Moraes CT. Increased muscle PGC-1α expression protects from sarcopenia and metabolic disease during aging. *Proc Natl Acad Sci U S A* 2009; **106**: 20405–20410.
9. Handschin C, Chin S, Li P, *et al*. Skeletal muscle fiber-type switching, exercise intolerance, and myopathy in PGC-1α muscle-specific knockout animals. *J Biol Chem* 2007; **282**: 30014–30021.
10. Schiaffino S, Reggiani C. Fiber types in mammalian skeletal muscles. *Physiol Rev* 2011; **91**: 1447–1531.
11. Lin J, Wu H, Tarr PT, *et al*. Transcriptional co-activator PGC-1α drives the formation of slow-twitch muscle fibres. *Nature* 2002; **418**: 797–801.
12. Czubryt MP, McAnally J, Fishman GI, Olson EN. Regulation of peroxisome proliferator-activated receptor gamma coactivator 1a (PGC-1a) and mitochondrial function by MEF2 and HDAC5. *Proc Natl Acad Sci U S A* 2003; **100**: 1711–1716.
13. Wu H, Kanatous SB, Thurmond FA, *et al*. Regulation of mitochondrial biogenesis in skeletal muscle by CaMK. *Science* 2002; **296**: 349–352.
14. Nishino N, Kawai T, Kondo M. Changes during ensilage in fermentation products, tea catechins, antioxidative activity and in vitro gas production of green tea waste stored with or without dried beet pulp. *J Sci Food Agric* 2007; **87**: 1639–1644.
15. Asano H, Yamada T, Hashimoto O, *et al*. Diet-induced changes in Ucp1 expression in bovine adipose tissues. *Gen Comp Endocrinol* 2013; **184**: 87–92.
16. Amat R, Planavila A, Chen SL, Iglesias R, Giralt M, Villarroya F. SIRT1 controls the transcription of the peroxisome proliferator-activated receptor-g co-activator-1a (PGC-1a) gene in skeletal muscle through the PGC-1a autoregulatory loop and interaction with MyoD. *J Biol Chem* 2009; **284**: 21872–21880.
17. Karamitri A, Shore AM, Docherty K, Speakman JR, Lomax MA. Combinatorial transcription factor regulation of the cyclic AMP-response element on the Pgc-1α promoter in white 3T3-L1 and brown HIB-1B preadipocytes. *J Biol Chem* 2009; **284**: 20738–20752.
18. Liu C, Lin JD. PGC-1 coactivators in the control of energy metabolism. *Acta Biochim Biophys Sin (Shanghai)* 2011; **43**: 248–257.
19. Ozawa S, Mitsuhashi T, Mitsumoto M, *et al*. The characteristics of muscle fiber types of longissimus thoracis muscle and their influences on the quantity and quality of meat from Japanese Black steers. *Meat Sci* 2000; **54**: 65–70.
20. Boström P, Wu J, Jedrychowski MP, *et al*. A PGC1-α-dependent myokine that drives brown-fat-like development of white fat and thermogenesis. *Nature* 2012; **481**: 463–468.
21. Higdon JV, Frei B. Tea catechins and polyphenols: health effects, metabolism, and antioxidant functions. *Crit Rev Food Sci Nutr* 2003; **43**: 89–143.
22. Clifford MN. Diet-derived phenols in plasma and tissues and their implications for health. *Planta Med* 2004; **70**: 1103–1114.

Cytokine 64 (2013) 138–145

Contents lists available at SciVerse ScienceDirect

Cytokine

journal homepage: www.journals.elsevier.com/cytokine

Bmp4 expressed in preadipocytes is required for the onset of adipocyte differentiation

Masashi Suenaga [a], Norio Kurosawa [a], Hiroki Asano [a], Yohei Kanamori [a], Takenao Umemoto [a], Hirofumi Yoshida [a], Masaru Murakami [b], Hiroyuki Kawachi [a,1], Tohru Matsui [a], Masayuki Funaba [a,*]

[a] Division of Applied Biosciences, Kyoto University Graduate School of Agriculture, Kyoto 606-8502, Japan
[b] Laboratory of Molecular Biology, Azabu University School of Veterinary Medicine, Sagamihara 229-5201, Japan

ARTICLE INFO

Article history:
Received 23 February 2013
Received in revised form 3 July 2013
Accepted 8 July 2013
Available online 2 August 2013

Keywords:
Bmp4
Adipocyte differentiation
Preadipocytes
Interleukin-11

ABSTRACT

We previously revealed that endogenous bone morphogenetic protein (Bmp) activity is required for lipid accumulation in 3T3-L1 adipocytes. The present study characterized the role of endogenous Bmp activity in preadipocytes. Endogenous Bmp activity was monitored by analyzing the level of phosphorylation of Smad1/5/8, downstream molecules in the Bmp pathway. Higher levels of phosphorylated Smad1/5/8 were detected in adipogenic cells but not in non-adipogenic cells prior to differentiation induction. The inhibition of the Bmp pathway during this period decreased the expression of *Pparγ2* and *C/ebpα*, which are transcription factors responsible for adipocyte differentiation. The expression of these transcription factors were also down-regulated by *Bmp4* knockdown. In addition, endogenous Bmp4 was required for the repression of *Intrleukin-11* expression. Endogenous Bmp4 in preadipocytes is indispensable for the onset of the adipogenic program, and may help to maintain the preadipocytic state during adipocyte differentiation.

1. Introduction

In addition to its role as the major energy-storage tissue, adipose tissue integrates a wide array of homeostatic processes by secreting various cytokines. Because excess and deficient levels body fat are related to various (patho-)physiological conditions, optimal body fat mass is essential for the maintenance of health [1]. The amount of adipose tissue is determined by the size and number of adipocytes. Adipocyte size largely reflects the amount of stored triglycerides, whereas adipocyte number is regulated by the commitment of mesenchymal stem cells in the adipocyte lineage and by the proliferation and differentiation of preadipocytes. Peroxisome proliferator-activated receptor γ (Pparγ, a nuclear hormone receptor, is the dominant regulator for adipocyte differentiation, and various molecules including growth factors and hormones affect adipogenesis through the modulation of Pparγ expression and activity [2].

Bone morphogenetic proteins (Bmps), members of the transforming growth factor-β (Tgf-β) family, regulate diverse physiological processes including adipose tissue formation [3]. The role of Bmps in the commitment of pluripotent stem cells to the adipocyte lineage (adipocyte progenitors) has been well established [4]. The addition of Bmp4 to the culture medium stimulated the adipocyte differentiation of multipotential C3H10T1/2 cells [5,6] and mouse embryonic fibroblasts [7]. A33 cells, a subline of C3H10T1/2 cells treated with the DNA methylation inhibitor 5-azacytidine, were committed to the adipocyte lineage and highly expressed and secreted Bmp4 [8]. In contrast, the roles of Bmps in the differentiation of preadipocytes into adipocytes are controversial; treatment with Bmp2 decreased insulin-induced lipid accumulation in 3T3-F442A preadipocytes [9], whereas Bmp7 stimulated the adipocyte differentiation of 3T3-L1 preadipocytes [10].

3T3-L1 preadipocytes are frequently used as a cell model for adipocyte differentiation. In a standard differentiation program, growth-arrested confluent 3T3-L1 preadipocytes are treated with the appropriate hormonal agents, which induce synchronous reentrance into the cell cycle and undergo at least 2 rounds of mitosis, referred to as mitotic clonal expansion. Subsequently, the preadipocytes exit the cell cycle and begin to differentiate into adipocytes [11]. We previously analyzed endogenous Bmp activity during the adipocyte differentiation of 3T3-L1 activity was higher before differentiation induction, and the inhibition of this activity decreased lipid accumulation [12]. These results suggest a novel activity of Bmp in preadipocytes, but the following points remained to be clarified: (1) the levels of endogenous Bmp activity in the other adipogenic and non-adipogenic cells, (2) the effects of exogenous Bmp after differentiation induction in 3T3-L1 cells, (3) the

* Corresponding author. Tel.: +81 75 753 6055; fax: +81 75 753 6344.
E-mail address: mfunaba@kais.kyoto-u.ac.jp (M. Funaba).
[1] Present address: Department of Animal Bioscience, Faculty of Bioscience, Nagahama Institute of Bio-Science and Technology, Nagahama 526-0829, Japan.

1043-4666/$ - see front matter © 2013 Elsevier Ltd. All rights reserved.
http://dx.doi.org/10.1016/j.cyto.2013.07.011

Table 1
Oligonucleotide PCR primers for RT-qPCR.

	Oligonucleotide		GenBank accession number
	5′-primer	3′-primer	
Actr2a	5′-CCCTCCTGTACTTGTTCCTACTCA-3′	5′-GCAATGGCTTCAACCCTAGT-3′	M65287
Actr2b	5′-GCTCAGCTCATGAACGACT-3′	5′-CTCTGCCACGACTGCTTGT-3′	M84120
Alk2	5′-AGGGCTCATCACCACCAAT-3′	5′-GCCACTTCCTGATGTACACG-3′	L15436
Alk3	5′-TGACCTGGGCCTAGCTGTTA-3′	5′-TTCAGGCTTTCATCCAGCA-3′	Z23154
Bmp4	5′-GAGGAGTTTCCATCACGAAGA-3′	5′-GCTCTGCCGAGGAGATCA-3′	NM_007554
Bmpr2	5′-TGGGAGGTGTTTATGAGGTGT-3′	5′-GAAAAGCCATCTGGTAATCTGG-3′	U78048
C/ebpα	5′-CAAGAACAGCAACGAGTACCG-3′	5′-GTCACTGGTCAACTCCAGCAC-3′	NM_007678
Fabp4	5′-AAGGTGAAGAGCATCATAACCCT-3′	5′-TCACGCCTTTCATAACACATTCC-3′	NM_024406
Hprt1	5′-TCCTCCTCAGACCGCTTTT-3′	5′-CCTGGTTCATCATCGCTAATC-3′	NM_013556
Interleukin-11	5′-CGCCGTTTACAGCTCTTGA-3′	5′-CAGGGGGATCACAGGTTG-3′	NM_008350
Lox	5′-CAGGCTGCACAATTTCACC-3′	5′-CAAACACCAGGTACGGCTTT-3′	NM_010728
Pparγ2	5′-TGCTGTTATGGGTGAAACTCTG-3′	5′-CTGTGTCAACCATGGTAATTTCTT-3′	NM_011146
Pref-1	5′-CGGGAAATTCTGCGAAATAG-3′	5′-TGTGCAGGAGCATTCGTACT-3′	NM_010052
Zfp423	5′-CGTGAAGTTCGAGAGTGCTG-3′	5′-GGCACTTGATACACTGGTACGTC-3′	NM_033327

identities of the molecule(s) responsible for the higher Bmp activity prior to differentiation induction in 3T3-L1 cells, and (4) the possible target process(es) involved in the progression of the adipogenic program. In this study, we explored these unknowns to understand the precise role of Bmp during adipogenesis.

2. Materials and methods

2.1. Materials

The following reagents were purchased: dorsomorphin (compound C: 6-[4-(2-piperidin-1-yl-ethoxy)phenyl]-3-pyridin-4-yl-pyrazolo[1,5-a] pyrimidine) was from Calbiochem (La Jolla, CA, USA);LDN-193189 was from Stemgent (San Diego, CA, USA);purified Tgf-β1 was from Becton Dickinson (Franklin Lakes, NJ, USA);recombinant Activin A, Bmp2 and Bmp4 were from R & D Systems (Minneapolis, MN, USA);rabbit polyclonal antibody against phospho-Smad1 (Ser463/Ser465)/Smad5 (Ser463/Ser465)/Smad8 (Ser426/Ser428) (#9511) and rabbit polyclonal antibody against phospho-Smad2 (Ser465/Ser467) were from Cell Signaling Technology (Danvers, MA, USA);and rabbit monoclonal antibody against Smad1 (ab33902), rabbit polyclonal antibody against Smad2 (ab63576), and mouse monoclonal antibody against and β-actin (AC-15) were from Abcam (Cambridge, MA, USA).

2.2. Cell culture

3T3-L1 preadipocytes were cultured and differentiated as described previously [12]. Bovine stromal–vascular (SV) cells were isolated from perirenal adipose tissues as follows. The tissues from 28- to 32-month-old Japanese Black steers were digested by with type I collagenase (1 mg/ml) in Hank's balanced salt solution containing penicillin (100 U/ml), streptomycin (100 μg/ml) and amphotericin B (250 ng/ml) and subsequently filtered through a 250 μm nylon mesh filter to remove undigested tissue fragments and debris. After centrifugation, the cell pellet consisting of SV cells containing preadipocytes was washed with growth medium, i.e., Dulbecco's modified Eagle's medium (DMEM) containing 10% FBS, ascorbic acid phosphate magnesium salt (100 μM) and antibiotics, followed by resuspension in the growth medium containing 10% DMSO and storage in liquid nitrogen. The adipocyte differentiation of the SV cells was induced as described previously [13]. Two days after reaching confluence (day 0), cells were cultured in the growth medium in the presence of differentiation inducers (3-isobutyl-1-methylxanthine (0.5 mM), dexamethasone (0.25 μM) and insulin (10 μg/ml)) for 2 days, followed by culture with insulin (5 μg/ml) in the growth medium. To investigate the effects of dorsomorphin and LDN-193189 on adipocyte differentiation, dorsomorphin (10 μM) or LDN-193189 (100 nM) dissolved in DMSO was added to the culture medium for the indicated period; treatments with the concentration of the inhibitors effectively blocked Bmp-induced phosphorylation of Smad1 and transcriptional activation of a Bmp-responsive gene Id1 [14,15]. An equal concentration of DMSO (0.1%) was used as a control. Lipid accumulation was examined by Oil Red O staining on day 8. The images were obtained by scanning stained wells (GT-9400UF;EPSON, Tokyo, Japan). Subsequently, dye was extracted with 2-propanol. The absorbance of the solution was measured at 510 nm for quantification [12].

2.3. Western blotting

To examine changes in phosphorylated Smad1/5/8 expression over time, cells were recovered in 200 mM phosphate buffer, pH 7.4, 2 M NaCl, 2 mM Na3VO4, 1 mM PMSF and 1% aprotinin and then lysed by ultrasonication. DNA content was measured by the method of Labarca and Paigen [16]. Samples containing equal amounts of DNA were subjected to SDS–PAGE, followed by immunoblotting as described previously [17]. The reacted proteins were visualized using the ECL Plus Western Blotting Detection System (GE Healthcare) according to the manufacturer's protocol. After stripping the antibodies and the detection reagents, the membranes were reprobed with anti-Smad1 antibody or anti-β-actin antibody.

To examine effects of protein kinase inhibitors on ligand-induced Smad phosphorylation, cells were cultured in medium with 0.2% FBS for 4 h, treated with vehicle (DMSO), dorsomorphin (5 μM) or LDN-193189 (100 nM) with 0.2% FBS for 20 min, and subsequently stimulated with Tgf-β1 (200 pM), Activin A (4 nM) or Bmp2 (4 nM) in the presence of the kinase inhibitor for 1 h.

2.4. RT-qPCR

RNA isolation and RT-qPCR were performed as described previously [12]. The oligonucleotide primers for RT-qPCR are presented in Table 1. The C_t value was determined, and the abundances of gene transcripts were calculated from the C_t value using *Hprt1* as the normalization gene.

2.5. Double-stranded RNA transfection

Double-stranded RNAs (dsRNAs) targeting the expression of *Bmp4* and *green fluorescent protein* (*GFP*) were synthesized by BONAC corporation (Kurume, Japan). The coding sequence of the

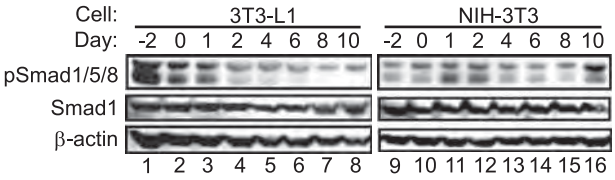

Fig. 1. Endogenous Bmp activity is higher prior to differentiation induction in 3T3-L1 cells. Phosphorylation status of Smad1/5/8 during adipocyte differentiation in 3T3-L1 and NIH-3T3 cells. 3T3-L1 and NIH-3T3 cells were stimulated with differentiation inducers for 2 days starting on day 0. Samples containing 1 μg of DNA were subjected to Western blotting to detect phosphorylated Smad1/5/8 at C-terminal serines (*upper panel*). The membranes were re-blotted with an antibody against Smad1 (*middle panel*) or β-actin (*lower panel*).

dsRNA for *GFP* is as described previously [16]. Four oligonucleotides were designed to target *Bmp4*, 5'-GUUGAAAAAUUAUCAGGAGAU-3' (set 1), 5'-CUCCUGAUAAUUUUUCAACAC-3' (set 1), and 5'-CAGACUAGUCCAUCACAAUGU-3' (set 2), and 5'-AUUGUGAUGGACUAGUCUGGU-3' (set 2). To make dsRNA, the two oligonucleotides of each set were mixed, and 1:1 mixtures of the dsRNA were prepared. dsRNA transfection was performed using the Lipofectamine RNAiMAX regent (Invitrogen: Carlsbad, CA, USA) according to the manufacturer's protocol.

2.6. Plasmids and reporter assay

BRE-luc was kindly provided by Dr. P. ten Dijke. The other reporter genes were constructed by a PCR-based method, and all constructs were verified by DNA sequencing. Luciferase-based reporter assays were conducted as described previously [18]. 3T3-L1 cells were transiently transfected with the indicated firefly luciferase-based reporter construct using Lipofectamine LTX reagent (Invitrogen). A *Renilla reniformis* luciferase vector driven by the thymidine kinase promoter (Renilla-luc; Promega, Madison, WI, USA) was co-transfected to serve as an internal control for transfection efficiency. At 24 h after transfection, the cells were treated with Bmp4 (4 nM) for 16 h. Firefly luciferase activity was normalized to Renilla luciferase activity, and the luciferase activity in the cell lysate in the absence of ligand was set to 1.

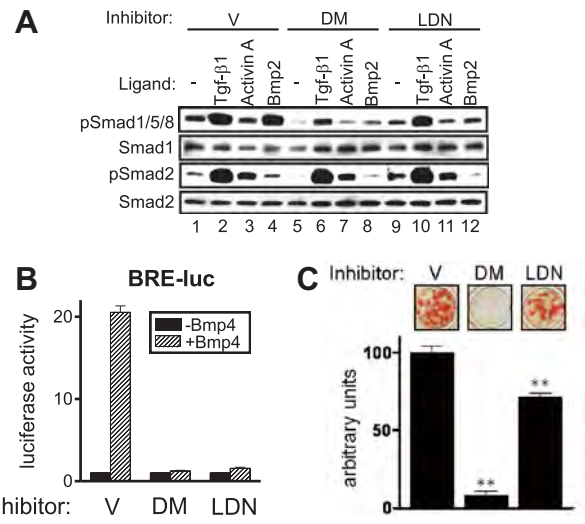

Fig. 3. Endogenous Bmp activity prior to differentiation induction is required for efficient lipid accumulation in 3T3-L1 cells. (A) Smad phosphorylation in response to the Tgf-β family in 3T3-L1 cells treated with dorsomorphin or LDN-193189. 3T3-L1 cells at 70% confluence were pre-treated with dorsomorphin (DM: 5 μM), LDN-193189 (LDN: 100 nM) or DMSO as a vehicle control (V) for 20 min, followed by treatment with Tgf-β1 (200 pM), Activin A (4 nM) or Bmp2 (4 nM) for 1 h. Phosphorylated Smad1/5/8 (*upper panel*) and Smad2 (*third panel*) were examined by Western blotting, and the membranes were then re-blotted for total Smad1 (*second panel*) and Smad2 (*fourth panel*). (B) Effects of dorsomorphin and LDN-193189 on Bmp-mediated transcription. 3T3-L1 cells were transiently transfected with BRE-luc and Renilla-luc and treated with dorsomorphin (DM: 5 μM), LDN-193189 (LDN: 100 nM) or DMSO as a vehicle control (V) for 20 min, followed by treatment with or without Bmp4 (4 nM) for 16 h. Firefly luciferase activity was normalized to Renilla luciferase activity, and the luciferase activity in cell lysates in the absence of Bmp4 and inhibitors was set to 1. Data were expressed as the mean ± SE of triplicates from a representative experiment. (C) Suppression of lipid accumulation by the inhibition of Bmp activity in 3T3-L1 cells. Dorsomorphin (DM: 5 μM), LDN-193189 (LDN: 100 nM) or DMSO as a vehicle control (V) was added to the culture medium from day −2 to day 0, and lipid accumulation on day 8 was examined by Oil Red O staining (*upper panel*). After staining, the dye was extracted with 2-propanol, and the amount was quantified by measuring the absorbance at 510 nm. The absorbance of the extracted dye from cells treated with vehicle was set to 100. Data are expressed as the mean ± SE of quadruplicates. $^{**}P < 0.01$ vs. vehicle. (For interpretation of the references to colour in this figure legend, the reader is referred to the web version of this article.)

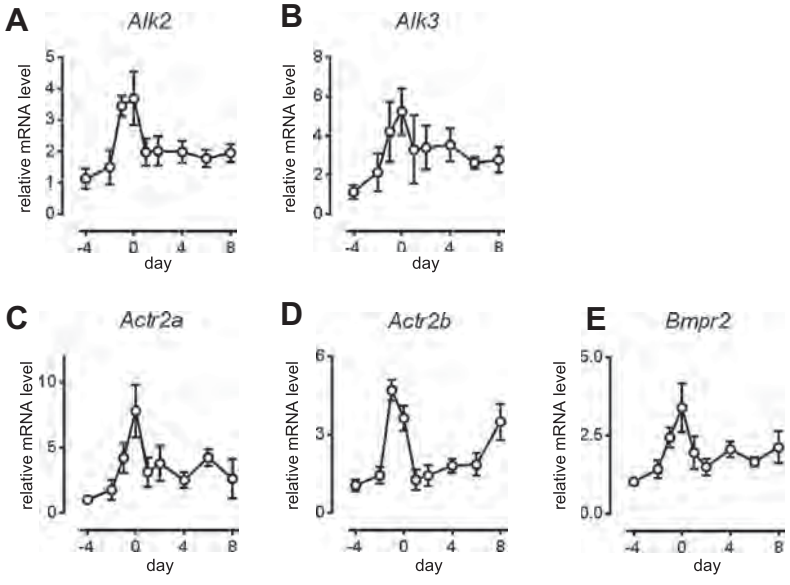

Fig. 2. Expression of Bmp receptors dynamically changes during adipogenesis in 3T3-L1 cells. Time-course changes in the gene expression of *Alk2* (A), *Alk3* (B), *Actr2a* (C), *Actr2b* (D) and *Bmpr2* (E) during adipogenesis were examined by RT-qPCR analyses in 3T3-L1 cells. The gene transcript levels were examined on day −4, −2, −1, 0, 1, 2, 4, 6 and 8, and are expressed as ratios relative to *Hprt1* expression, with the level in 3T3-L1 cells on day −4 set to 1. Data are expressed as the mean ± SE of quadruplicates.

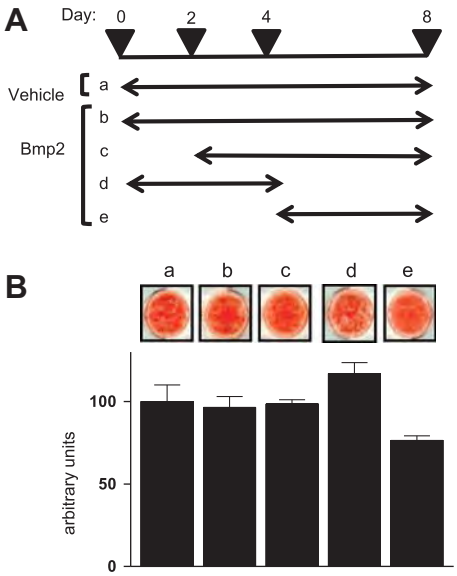

Fig. 4. Exogenous Bmp does not affect lipid accumulation in 3T3-L1 cells (A and B) Limited effect of exogenous Bmp on lipid accumulation in 3T3-L1 cells. Bmp2 (4 nM) was added to the culture medium for the indicated period (A), and lipid accumulation on day 8 was examined by Oil Red O staining (B, *upper panel*). After staining, the dye was extracted with 2-propanol, and the amount was quantified by measuring the absorbance at 510 nm. The absorbance of the extracted dye from cells treated with vehicle was set to 100 (B, *lower panel*). Data are expressed as the mean ± SE of quadruplicates.

2.7. Statistical analyses

Data are expressed as the mean ± SEM. Differences between treatments were examined by Student's *t*-test. Differences of $P < 0.05$ were considered significant.

3. Results and discussion

Bmp transmits signals through the phosphorylation of Smad1/5/8 at the C-terminus after complex formation with ligand, type I receptors and type II receptors [19,20]. Phosphorylated Smad1/5/8 levels were monitored to evaluate endogenous Bmp activity during adipocyte differentiation (Fig. 1). Consistent with a previous study [12], the intensity of the bands was higher for 3T3-L1 preadipocytes on day −2 (lane 1) and gradually decreased with the progression of differentiation (lanes 2–8). NIH-3T3 cells did not significantly differentiate into cells with lipid droplets, even if cells were treated using the differentiation protocol for 3T3-L1 cells (data not shown). Unlike 3T3-L1 cells, NIH-3T3 cells did not exhibit higher levels of phosphorylated Smad1/5/8 expression prior to treatment with differentiation inducers (Fig. 1, lane 9), although the expression levels on days 1, 2 and 10 were relatively higher (lanes 11, 12 and 16).

We next evaluated time-course changes in expression of Bmp receptors during adipogenesis in 3T3-L1 cells (Fig. 2). Alk2, Alk3 and Alk6 are type I receptors for Bmp, whereas Actr2a, Actr2b and Bmpr2 function as type II receptors for Bmp [19,20]. No significant expression of *Alk6* was detected throughout the adipogenesis of 3T3-L1 cells (data not shown). Expression level of all the Bmp receptors, except for *Actr2b*, tended to increase from day −4 to day 0, and decrease in response to the differentiation stimulation. Thereafter, the decreased level continued at least to day 8. *Actr2b* expression tended to increase day −4 to day −1, and increase again from day 6 to day 8. Changes in Bmp receptor expression during adipogenesis suggest that responsiveness to Bmp changes before and after the differentiation stimulation, i.e., higher responsiveness to Bmp just before the differentiation stimulation and lower after the stimulation.

Dorsomorphin was identified as an inhibitor of the Bmp pathway by screening for compounds that disrupt dorsoventral axis formation, which is governed by Bmp, in zebrafish [14]. Subsequently, LDN-193189 was synthesized as a structurally related compound capable of efficiently inhibiting Bmp4-induced Smad1/5/8 phosphorylation in murine pulmonary artery smooth muscle cells [21]. To examine the ability of the compounds to inhibit Bmp signaling in 3T3-L1 cells, ligand-induced Smad phosphorylation (Fig. 3A) and Bmp-mediated transcriptional activation (Fig. 3B) were evaluated. Pretreatment with dorsomorphin or LDN-193189 effectively inhibited the Bmp2-induced phosphorylation of Smad1/5/8 (Fig. 3A, upper panel, lanes 4, 8 and 12). As in the other cell types [18,22–25], treatment of 3T3-L1 cells with Tgf-β1 induced the phosphorylation of Smad1/5/8 (Fig. 3A, upper panel, lanes 1 and 2), which was also partially inhibited by pretreatment with dorsomorphin but not with LDN-193189 (Fig. 3A, upper panel, lanes 6 and 10). The phosphorylation and activation of Smad2 is a canonical Tgf-β1 and Activin A pathway [19]. Dorsomorphin and LDN-193189 did not affect the Tgf-β1- or Activin A-induced phosphorylation of Smad2 (Fig. 3A, third panel, lanes 2, 3, 6, 7, 10 and 11). Luciferase-based reporter assays also showed that both dorsomorphin and LDN-193189 effectively blocked Bmp4-induced expression of BRE-luc, a sensitive Bmp-responsive reporter gene [26] (Fig. 3B). These results indicate that dorsomorphin and

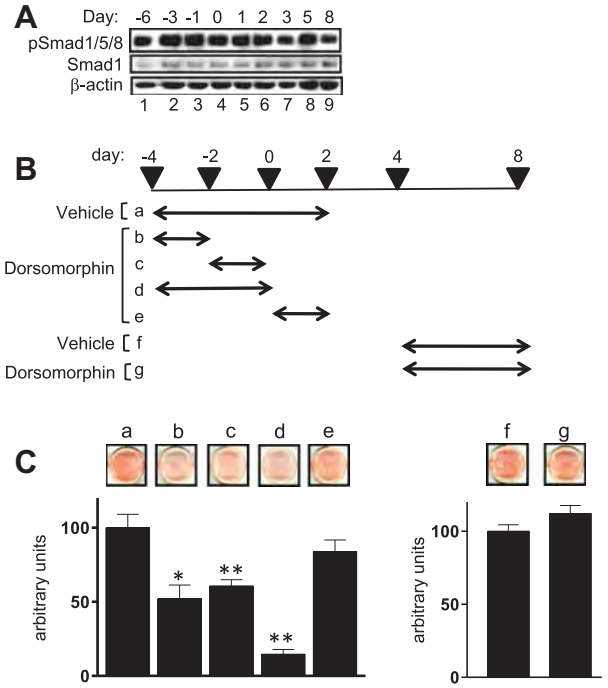

Fig. 5. Endogenous Bmp activity prior to differentiation induction is also required for lipid accumulation in bovine SV cells (A) Phosphorylation status of Smad1/5/8 during adipocyte differentiation in bovine SV cells. Bovine SV cells were stimulated with differentiation inducers for 2 days starting on day 0. Samples containing 1 μg of DNA were subjected to Western blotting to detect Smad1/5/8 phosphorylated at C-terminal serines (*upper panel*). The membranes were re-blotted with an antibody against Smad1 (*middle panel*) or β-actin (*lower panel*). (B and C) Suppression of lipid accumulation by the inhibition of Bmp activity in bovine SV cells. Dorsomorphin (5 μM) or DMSO as a vehicle control was added to the culture medium for the indicated period (B), and lipid accumulation on day 8 was examined by Oil Red O staining (C, *upper panel*). After staining, the dye was extracted with 2-propanol, and the amount was quantified by measuring the absorbance at 510 nm. The absorbance of the extracted dye from cells treated with vehicle was set to 100 (C, *lower panel*). Data are expressed as the mean ± SE of quadruplicates. * and $^{**}P < 0.05$ and 0.01, respectively, vs. vehicle. (For interpretation of the references to colour in this figure legend, the reader is referred to the web version of this article.)

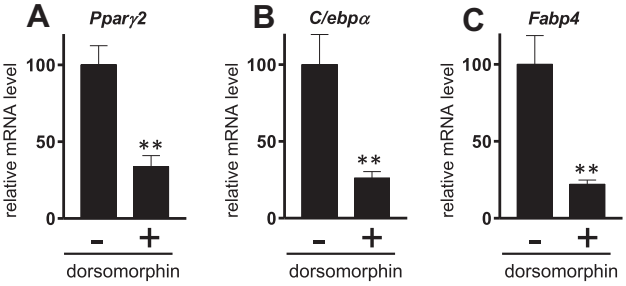

Fig. 6. Inhibition of Bmp activity prior to differentiation induction inhibits adipocyte differentiation in 3T3-L1 cells Effects of inhibition of Bmp activity prior to differentiation induction on adipocyte differentiation. Dorsomorphin (5 μM) or DMSO as a vehicle control was added to the culture medium from day -2 to day 0. The gene transcript levels of *Pparγ2* (A), *C/ebpα* (B) and *Fabp4* (C) on day 8 were measured by RT-qPCR and are expressed as ratios relative to *Hprt1* expression, with the level in 3T3-L1 cells treated with vehicle set to 100. Data shown are the mean ± SE ($n = 4$). $^{**}P < 0.01$ vs. control.

LDN-193189 selectively inhibit Bmp-induced phosphorylation of Smad1/5/8 in 3T3-L1 cells.

To examine the role of the high Bmp activity in preadipocytes, 3T3-L1 cells were treated with dorsomorphin or LDN-193189 before differentiation induction, i.e., from day −2 to day 0, and lipid accumulation was evaluated on day 8. Although LDN-193189 was less effective, both inhibitors inhibited lipid accumulation, as demonstrated by lower lipid levels on day 8 (Fig. 3C). The reason of the less potency of LDN-193189 on lipid accumulation, irrespective of compatible inhibition of Bmp4-mediated transcriptional activation between dorsomorphin and LDN-193189, is currently unknown. Dorsomorphin inhibits not only the Bmp pathway but also the AMPK pathway; dorsomorphin, also known as compound C, is originally identified as the AMPK inhibitor [27]. It is possible that the AMPK activity is involved in lipid accumulation of 3T3-L1 cells; endogenous AMPK activity was detected in 3T3-L1 preadipocytes [12]. Whatever the reason may be, these results definitely suggest that the high Bmp activity in preadipocytes is necessary for lipid accumulation. Alternatively, decreasing Bmp activity in response to differentiation induction may be required for efficient lipid accumulation. Thus, the effects of additional Bmp on lipid accumulation were examined in 3T3-L1 cells (Fig. 4). Bmp2 was added to the culture medium for various periods of time (Fig. 4A), and lipid accumulation was evaluated by Oil Red O staining on day 8. The presence of additional Bmp2 after differentiation induction did not affect lipid accumulation in 3T3-L1 cells (Fig. 4B). As described above, the inconsistent results have been reported on the role of exogenous Bmps in adipogenesis [9,10]. The precise reason of the results is unknown; the discrepancy may relate to subtle differences in cell systems or culture conditions.

The role of endogenous Bmp activity in adipogenic cells other than 3T3-L1 cells was next evaluated. Bovine SV cells can be differentiated into adipocytes in response to treatment with the differentiation inducers used on 3T3-L1 cells [13]. Endogenous Bmp activity was relatively constant during the adipocyte differentiation of SV cells (Fig. 5A). As in 3T3-L1 cells, treatment with dorso-

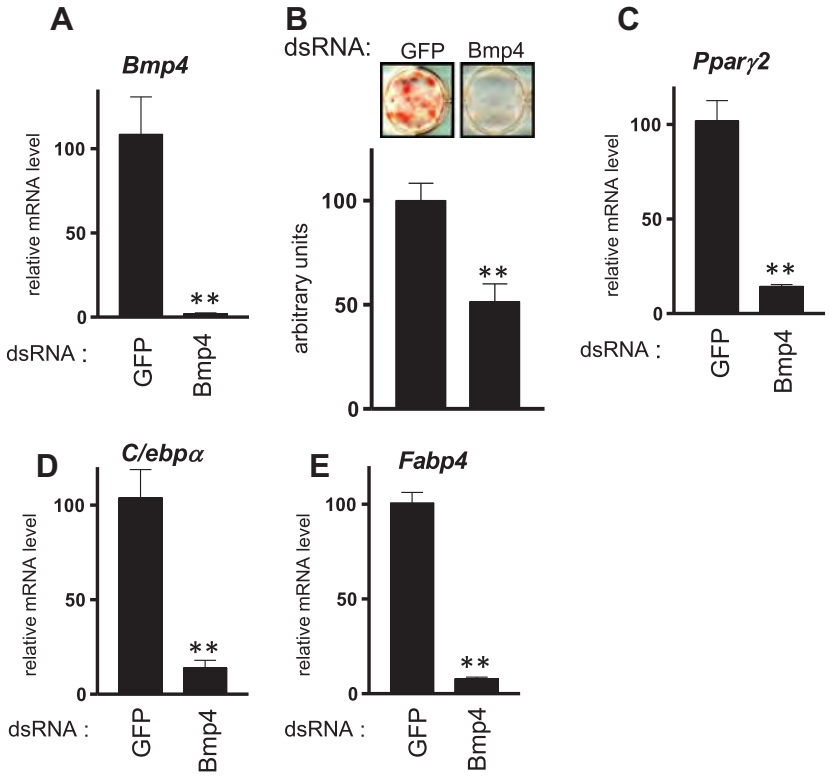

Fig. 7. Down-regulation of Bmp4 prior to differentiation is sufficient to inhibit adipocyte differentiation in 3T3-L1 cells (A) The down-regulation of Bmp4 expression in 3T3-L1 cells. 3T3-L1 cells were transfected with dsRNA for *Bmp4* or *GFP* on day −3. The gene transcript level of *Bmp4* on day 0 was measured by RT-qPCR and expressed as a ratio relative to *Hprt1* expression, with the level in 3T3-L1 cells treated with dsRNA for *GFP* set to 100. Data shown are the mean ± SE ($n = 4$). $^{**}P < 0.01$ vs. GFP. (B) Suppression of lipid accumulation in 3T3-L1 cells transfected with dsRNA for Bmp4. 3T3-L1 cells were transfected with dsRNA for *Bmp4* or *GFP* as a negative control on day -3, and lipid accumulation on day 8 was examined by Oil Red O staining (*upper panel*). After staining, the dye was extracted with 2-propanol, and the amount was quantified by the measuring absorbance at 510 nm. The absorbance of the extracted dye from cells treated with dsRNA for *GFP* was set to 100. Data are expressed as the mean ± SE of quadruplicates. $^{**}P < 0.01$ vs. GFP. (C-E) Inhibition of adipocyte differentiation by knockdown of *Bmp4*. 3T3-L1 cells were transfected with dsRNA for *Bmp4* or *GFP* on day −3. The gene transcript levels of *Pparγ2* (C), *C/ebpα* (D) and *Fabp4* (E) on day 8 were measured by RT-qPCR and expressed as ratios relative to *Hprt1* expression, with the level in 3T3-L1 cells treated with dsRNA for *GFP* set to 100. Data shown are the mean ± SE ($n = 4$). $^{**}P < 0.01$ vs. GFP.

morphin prior to differentiation induction but not after differentiation induction decreased lipid accumulation in SV cells (Fig. 5B and C). All of these results suggest that endogenous Bmp activity before differentiation induction is necessary for lipid accumulation during the adipogenic program.

To identify the process that endogenous Bmp activity regulates, we next examined the expression of genes regulating adipocyte differentiation. Pparγ, a dominant and essential regulator of adipocyte differentiation [28–30], controls the transcriptional pathway of adipogenesis in concert with CCAAT/enhancer-binding proteinα (C/ebpα [31]. The inhibition of endogenous Bmp activity down-regulated the expression of *Pparγ2* and *C/ebpα* (Fig. 6A and B). Consistent with these results, the expression of *Fabp4*, a late differentiation marker of adipogenesis and a representative target gene of C/ebpα and Pparγ [32], was decreased in 3T3-L1 cells pretreated with dorsomorphin (Fig. 6C). These results suggest that endogenous Bmp activity prior to differentiation induction is responsible for adipocyte differentiation.

Our previous study indicated that the expression of *Bmp4* was higher in preadipocytes and decreased after day 1 [12]. In view of the parallel changes in *Bmp4* expression and the phosphorylation of Smad1/5/8, Bmp4 may be responsible for the higher Bmp activity before differentiation induction. The down-regulation of *Bmp4* expression by transfection of cells with dsRNA for *Bmp4* on day −3 to day 0 decreased lipid accumulation on day 8 (Fig. 7A and B). The treatment also decreased the expression of *Pparγ2*, *C/ebpα* and *Fabp4* (Fig. 7C–E), suggesting that higher Bmp4 activity in preadipocytes is indispensable for adipocyte differentiation.

We further explored the molecular process regulated by Bmp4 in 3T3-L1 cells. The gene expression of molecules involved in adipocyte differentiation, including *Zfp423*, *Interleukin-11*, *Pref-1* and *lysyl oxidase* (*Lox*), was examined. Zfp423 was identified as a gene highly expressed in fibroblasts committed to the adipocyte lineage and was found to be responsible for adipocyte differentiation [32,33]. Analysis of the nucleotide sequence from −3 kb to the transcriptional initiation site of the *Zfp423* gene revealed 6 possible Bmp-responsive elements (BRE: GCCGnCGC) in Drosophila cells [34] and mammalian cells [35] in the region from nt −883 to nt −800;5 of these BREs partially overlapped (Fig. 8A). *Zfp423* transcription was not decreased by treatment with Bmp inhibitors, and Bmp4 addition did not increase the expression of Zfp423-luc, even when the possible BREs were isolated (Fig. 8A and B). Furthermore, treatment with dorsomorphin or dsRNA for *Bmp4* did not significantly decrease *Zfp423* expression (Fig. 8C). Thus, we concluded that Zfp423 is not a target gene for endogenous Bmp activity in preadipocytes.

Interleukin-11 was cloned based on its inhibitory activity on the differentiation of 3T3-L1 preadipocytes [36]. The knockdown of Bmp4 significantly increased the expression of *Interleukin-11* on day 0 and day 2 in 3T3-L1 cells (Fig. 9A). Pref-1 is highly expressed in preadipocytes, and down-regulation of the expression of Pref-1 triggers the progression of the adipogenic program [37–41]. Transfection with dsRNA for *Bmp4* significantly decreased the expression of *Pref-1* on day 0 and day 2 (Fig. 9B). Lox was identified as a gene that mediates Bmp-induced commitment to the adipocyte lineage [6]. Transfection with dsRNA for *Bmp4* did not decrease *Lox* expression (data not shown).

Our previous study revealed that endogenous Bmp activity in preadipocytes is required for lipid accumulation in adipocytes [12]. Here, we extend this information: higher expression of Bmp4 in preadipocytes is indispensable for adipocyte differentiation. Previous studies revealed that a number of molecules are involved in the regulation of adipocyte differentiation, and most of these studies evaluated effects of the factors by treating with dif-

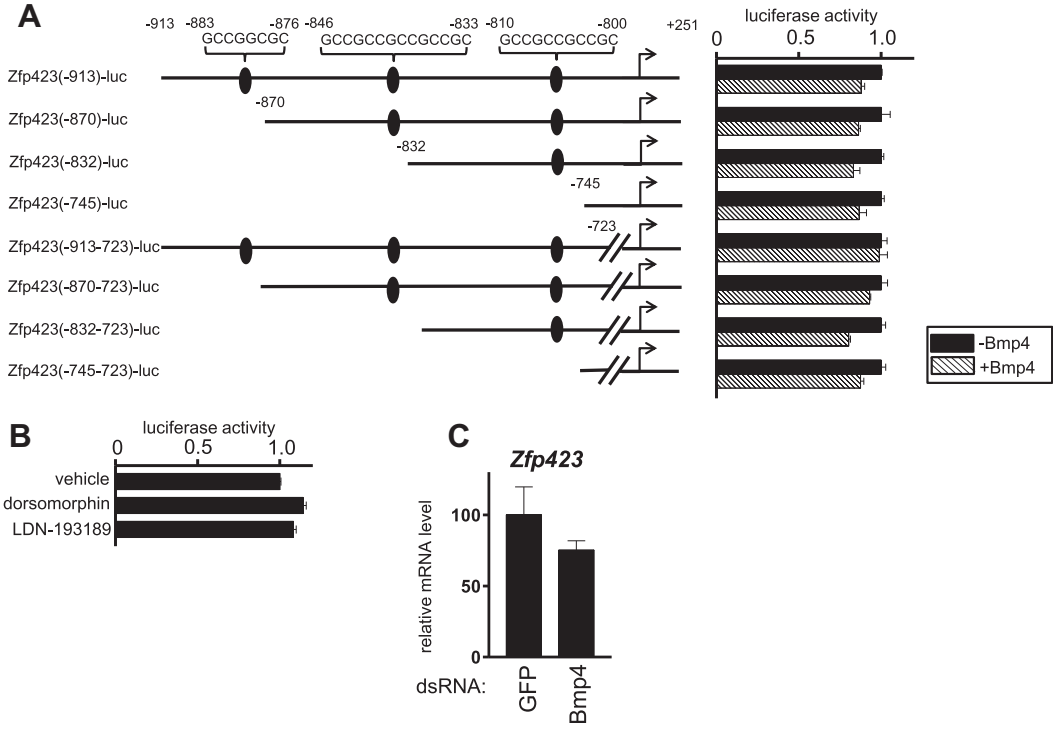

Fig. 8. Zfp423 transcriptional regulation is independent of Bmp activity (A) 3T3-L1 cells were transiently transfected with the indicated reporter gene and Renilla-luc and treated with or without Bmp4 (4 nM) for 16 h. Firefly luciferase activity was normalized to Renilla luciferase activity, and the luciferase activity in cell lysates in the absence of inhibitors and Bmp4 was set to 1. Data were expressed as the mean ± SE of triplicates from a representative experiment. (B) 3T3-L1 cells were transiently transfected with Zfp423(-913)-luc and Renilla-luc and treated with dorsomorphin (5 μM), LDN-193189 (100 nM) or DMSO as vehicle for 16 h. (C) 3T3-L1 cells were transfected with dsRNA for *Bmp4* or *GFP* on day −3. The gene transcript level of *Zfp423* on day 8 was measured by RT-qPCR and expressed as a ratio relative to *Hprt1* expression, with the level in 3T3-L1 cells treated with dsRNA for *GFP* set to 100. Data shown are the mean ± SE ($n = 4$).

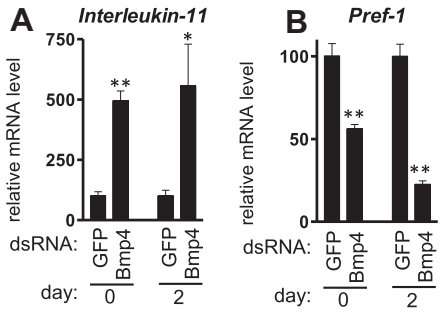

Fig. 9. Down-regulation of Bmp4 increases and decreases the expression of Interleukin-11 and Pref-1, respectively, in 3T3-L1 cells Increased expression of *Interleukin-11* (A) and decreased expression of *Pref-1* (B) in response to the down-regulation of *Bmp4* in 3T3-L1 cells. (A and B) 3T3-L1 cells were transfected with dsRNA for *Bmp4* or *GFP* on day −3. The gene transcript levels of *Interleukin-11* (A) and *Pref-1* (B) on day 0 and day 2 were measured by RT-qPCR and expressed as ratios relative to *Hprt1* expression, with the level in 3T3-L1 cells treated with dsRNA for *GFP* set to 100. Data shown are the mean ± SE ($n = 4$). * and ** $P < 0.05$ and 0.01, respectively, vs. GFP.

ferentiation inducers [2]. In contrast, little information is available on factors affecting preadipocytic properties. The present study indicates the importance of states prior to differentiation induction for adipocyte differentiation. The provided basic information potentially contributes to understanding the control of the number of adipocytes.

Treatment with Interleukin-11 inhibited the adipocyte differentiation of 3T3-L1 preadipocytes, irrespective of the down-regulation of Pref-1 expression [42]. In view of the well-defined role of Pref-1 as an inhibitor of adipocyte differentiation [35,37], these results suggest that Interleukin-11 negatively regulates adipogenesis in a Pref-1-independent manner. Bmp4 produced in preadipocytes may stimulate adipocyte differentiation through the repression of Interleukin-11 expression; the expression levels of *Interleukin-11* and *Pref-1* were increased and decreased, respectively, in 3T3-L1 cells with down-regulated Bmp4 expression.

The present study revealed that higher expression of Bmp4 is required for the progression of the adipogenic program in preadipocytes that are already committed to the adipogenic lineage. Previous studies indicated that Bmp4 stimulates the commitment of mesenchymal stem cells to the adipocyte lineage [5–7]. In conclusion, there are at least two roles of Bmp in adipocyte differentiation: a role in inducing the commitment of preadipocytes and a role in maintaining preadipocytic properties, as revealed in the present study.

Acknowledgements

We thank Dr. Peter ten Dijke for providing plasmid. This work was supported by Kakenhi from The Japan Society for the Promotion of Science.

References

[1] Rosen ED, Spiegelman BM. Adipocytes as regulators of energy balance and glucose homeostasis. Nature 2006;444:847–53.
[2] Tontonoz P, Spiegelman BM. Fat and beyond: the diverse biology of PPARγ. Annu Rev Biochem 2008;77:289–312.
[3] Chang H, Brown CW, Matzuk MM. Genetic analysis of the mammalian transforming growth factor-β superfamily. Endocr Rev 2002;23:787–823.
[4] Otto TC, Lane MD. Adipose development: from stem cell to adipocyte. Crit Rev Biochem Mol Biol 2005;40:229–42.
[5] Tang QQ, Otto TC, Lane MD. Commitment of C3H10T1/2 pluripotent stem cells to the adipocyte lineage. Proc Natl Acad Sci USA 2004;101:9607–11.
[6] Huang H, Song TJ, Li X, Hu L, He Q, Liu M, et al. BMP signaling pathway is required for commitment of C3H10T1/2 pluripotent stem cells to the adipocyte lineage. Proc Natl Acad Sci USA 2009;106:12670–5.
[7] Jin W, Takagi T, Kanesashi SN, Kurahashi T, Nomura T, Harada J, et al. Schnurri-2 controls BMP-dependent adipogenesis via interaction with Smad proteins. Dev Cell 2006;10:461–71.
[8] Bowers RR, Kim JW, Otto TC, Lane MD. Stable stem cell commitment to the adipocyte lineage by inhibition of DNA methylation: role of the BMP-4 gene. Proc Natl Acad Sci USA 2006;103:13022–7.
[9] Skillington J, Choy L, Derynck R. Bone morphogenetic protein and retinoic acid signaling cooperate to induce osteoblast differentiation of preadipocytes. J Cell Biol 2002;159:135–46.
[10] Rebbapragada A, Benchabane H, Wrana JL, Celeste AJ, Attisano L. Myostatin signals through a transforming growth factor β-like signaling pathway to block adipogenesis. Mol Cell Biol 2003;23:7230–42.
[11] Lane MD, Tang QQ, Jiang MS. Role of the CCAAT enhancer binding proteins (C/EBPs) in adipocyte differentiation. Biochem Biophys Res Commun 1999;266:677–83.
[12] Suenaga M, Matsui T, Funaba M. BMP Inhibition with dorsomorphin limits adipogenic potential of preadipocytes. J Vet Med Sci 2010;72:373–7.
[13] Hirai S, Matsumoto H, Hino N, Kawachi H, Matsui T, Yano H. Myostatin inhibits differentiation of bovine preadipocyte. Domest Anim Endocrinol 2007;32:1–14.
[14] Yu PB, Hong CC, Sachidanandan C, Babitt JL, Deng DY, Hoyng SA, et al. Dorsomorphin inhibits BMP signals required for embryogenesis and iron metabolism. Nat Chem Biol 2008;4:33–41.
[15] Yu PB, Deng DY, Lai CS, Hong CC, Cuny GD, Bouxsein ML, et al. BMP type I receptor inhibition reduces heterotopic ossification. Nat Med 2008;14:1363–9.
[16] Labarca C, Paigen K. A simple, rapid, and sensitive DNA assay procedure. Anal Biochem 1980;102:344–52.
[17] Funaba M, Murakami M. A sensitive detection of phospho-Smad1/5/8 and Smad2 in Western blot analyses. J Biochem Biophys Method 2008;70:816–9.
[18] Murakami M, Kawachi H, Ogawa K, Nishino Y, Funaba M. Receptor expression modulates the specificity of transforming growth factor-β signaling pathways. Genes Cells 2009;14:469–82.
[19] Feng XH, Derynck R. Specificity and versatility in TGF-β signaling through Smads. Annu Rev Cell Dev Biol 2005;21:659–93.
[20] Miyazono K, Kamiya Y, Morikawa M. Bone morphogenetic protein receptors and signal transduction. J Biochem 2010;147:35–51.
[21] Cuny GD, Yu PB, Laha JK, Xing X, Liu JF, Lai CS, et al. Structure-activity relationship study of bone morphogenetic protein (BMP) signaling inhibitors. Bioorg Med Chem Lett 2008;18:4388–92.
[22] Goumans MJ, Valdimarsdottir G, Itoh S, Lebrin F, Larsson J, Mummery C, et al. Activin receptor-like kinase (ALK)1 is an antagonistic mediator of lateral TGFβ/ALK5 signaling. Mol Cell 2003;12:817–28.
[23] Daly AC, Randall RA, Hill CS. Transforming growth factor β-induced Smad1/5 phosphorylation in epithelial cells is mediated by novel receptor complexes and is essential for anchorage-independent growth. Mol Cell Biol 2008;28:6889–902.
[24] Liu IM, Schilling SH, Knouse KA, Choy L, Derynck R, Wang XF. TGFβ-stimulated Smad1/5 phosphorylation requires the ALK5 L45 loop and mediates the pro-migratory TGFβ switch. EMBO J 2009;28:88–98.
[25] Wrighton KH, Lin X, Yu PB, Feng XH. Transforming growth factor β can stimulate Smad1 phosphorylation independently of bone morphogenic protein receptors. J Biol Chem 2009;284:9755–63.
[26] Korchynskyi O, ten Dijke P. Identification and functional characterization of distinct critically important bone morphogenetic protein-specific response elements in the Id1 promoter. J Biol Chem 2002;277:4883–91.
[27] Zhou G, Myers R, Li Y, Chen Y, Shen X, Fenyk-Melody J, et al. Role of AMP-activated protein kinase in mechanism of metformin action. J Clin Invest 2001;108:1167–74.
[28] Barak Y, Nelson MC, Ong ES, Jones YZ, Ruiz-Lozano P, Chien KR, et al. PPARγ is required for placental, cardiac, and adipose tissue development. Mol Cell 1999;4:585–95.
[29] Kubota N, Terauchi Y, Miki H, Tamemoto H, Yamauchi T, Komeda K, et al. PPARγ mediates high-fat diet-induced adipocyte hypertrophy and insulin resistance. Mol Cell 1999;4:597–609.
[30] Rosen ED, Sarraf P, Troy AE, Bradwin G, Moore K, Milstone DS, Spiegelman BM, Mortensen RM. PPARγ is required for the differentiation of adipose tissue in vivo and in vitro. Mol Cell 1999;4:611–7.
[31] Wu Z, Rosen ED, Brun R, Hauser S, Adelmant G, Troy AE, et al. Cross-regulation of C/EBPα and PPARγ controls the transcriptional pathway of adipogenesis and insulin sensitivity. Mol Cell 1999;3:151–8.
[32] Tang QQ, Zhang JW, Lane MD. Sequential gene promoter interactions by C/EBPβ, C/EBPα, and PPARγ during adipogenesis. Biochem Biophys Res Commun 2004;318:213–8.
[33] Gupta RK, Arany Z, Seale P, Mepani RJ, Ye L, Conroe HM, et al. Transcriptional control of preadipocyte determination by Zfp423. Nature 2010;464:619–23.
[34] Kim J, Johnson K, Chen HJ, Carroll S, Laughon A. Drosophila Mad binds to DNA and directly mediates activation of vestigial by Decapentaplegic. Nature 1997;388:304–8.
[35] Kusanagi K, Inoue H, Ishidou Y, Mishima HK, Kawabata M, Miyazono K. Characterization of a bone morphogenetic protein-responsive Smad-binding element. Mol Biol Cell 2000;11:555–65.
[36] Kawashima I, Ohsumi J, Mita-Honjo K, Shimoda-Takano K, Ishikawa H, Sakakibara S, et al. Molecular cloning of cDNA encoding adipogenesis inhibitory factor and identity with interleukin-11. FEBS Lett 1991;283:199–202.

[37] Smas CM, Sul HS. Pref-1, a protein containing EGF-like repeats, inhibits adipocyte differentiation. Cell 1993;73:725–34.
[38] Smas CM, Kachinskas D, Liu CM, Xie X, Dircks LK, Sul HS. Transcriptional control of the pref-1 gene in 3T3-L1 adipocyte differentiation. Sequence requirement for differentiation-dependent suppression. J Biol Chem 1998;273:31751–8.
[39] Smas CM, Chen L, Zhao L, Latasa MJ, Sul HS. Transcriptional repression of pref-1 by glucocorticoids promotes 3T3-L1 adipocyte differentiation. J Biol Chem 1999;274:12632–41.
[40] Garcés C, Ruiz-Hidalgo MJ, Bonvini E, Goldstein J, Laborda J. Adipocyte differentiation is modulated by secreted delta-like (dlk) variants and requires the expression of membrane-associated dlk. Differentiation 1999;64:103–14.
[41] Wang Y, Sul HS. Pref-1 regulates mesenchymal cell commitment and differentiation through Sox9. Cell Metab 2009;9:287–302.
[42] Boney CM, Fiedorek Jr FT, Paul SR, Gruppuso PA. Regulation of preadipocyte factor-1 gene expression during 3T3-L1 cell differentiation. Endocrinology 1996;137:2923–8.

Fish Sci (2013) 79:935–941
DOI 10.1007/s12562-013-0674-x

ORIGINAL ARTICLE

Biology

Genetic characterization of the progeny of a pair of the tetraploid silver crucian carp *Carassius auratus langsdorfii*

Jie Dong · Masaru Murakami · Takafumi Fujimoto · Etsuro Yamaha · Katsutoshi Arai

Received: 30 May 2013 / Accepted: 30 September 2013 / Published online: 19 October 2013

Abstract Silver crucian carp *Carassius auratus langsdorfii* comprises a diploid-polyploid complex in wild Japanese populations. Bisexually reproducing diploids are sympatrically distributed with gynogenetically developing triploids and tetraploids. Triploid and tetraploid males are very rare among Japanese silver crucian carp due to their gynogenetic reproduction. We examined the genetic characteristics of progeny that arose in a tank by natural spawning of a tetraploid silver crucian carp pair. The ploidy status of 120 samples randomly collected from these progeny was determined to be tetraploid by DNA content flow cytometry. DNA fingerprints from a random amplified polymorphic DNA assay indicated that almost all the progeny examined had genotypes identical to the maternal tetraploid female with no paternally derived fragments. Selected specimens' cytogenetic analyses revealed that the progeny examined had tetraploid chromosome numbers, categorized into 40 metacentric, 80 submetacentric, and 80 subtelocentric or telocentric chromosomes, which were arranged into quartets and six supernumerary microchromosomes. Fluorescence in situ hybridization signals were detected in four homologous chromosomes in all analyzed metaphases prepared from diploid goldfish specimens. Contrary, tetraploid silver crucian carp gave eight rDNA signals. These results suggest that gynogenetic development in eggs spawned by tetraploid females should be triggered by tetraploid males' homospecific sperm.

Keywords Silver crucian carp · Tetraploid · Gynogenesis · Flow cytometry · RAPD markers · FISH

J. Dong · T. Fujimoto · K. Arai (✉)
Faculty and Graduate School of Fisheries Sciences, Hokkaido University, Hakodate, Hokkaido, Japan
e-mail: araikt@fish.hokudai.ac.jp

M. Murakami
School of Veterinary Medicine, Azabu University, Sagamihara, Kanagawa, Japan

E. Yamaha
Nanae Fresh-Water Laboratory, Field Science Center for Northern Biosphere, Hokkaido University, Nanae, Hokkaido, Japan

Introduction

Silver crucian carp *C. auratus langsdorfii* comprises a diploid-polyploid complex in the wild populations of Japan. Bisexually reproducing diploids ($2n = 100$) are sympatrically distributed with gynogenetically developing triploids ($3n = 156$) and tetraploids ($4n = 206$) [1–3]. Frequencies of tetraploids are much lower than those of sympatric diploids and triploids [4, 5], and these tetraploids are considered to arise from triploids by accidental incorporation of a haploid sperm nucleus into a triploid egg [6–8]. The occurrence of relatively rare tetraploids from triploids, and the reproductive characteristics of such tetraploid progeny will provide good insights into mechanisms responsible for the origin, diversification and maintenance of such a diploid-polyploid complex in nature. Thus, the wild tetraploid Japanese silver crucian carp *C. auratus langsdorfii* has been considered excellent material to disclose the biological significance of polyploidy in fish reproduction and evolution.

Because unreduced eggs of both triploids and tetraploids develop by gynogenesis (sperm-dependent parthenogenesis) without any genetic contributions from males, the offspring are theoretically an all-female population due to no contribution by male-determinant Y chromosomes.

Although a high male incidence has been observed among Chinese silver crucian carp *C. auratus gibelio*, because these triploid forms undergo a mixture of allogynogenesis (gynogenesis triggered by heterospecific sperm from other species) and bisexual gonochoristic reproduction [9], both triploid and tetraploid males are very rare in the Japanese silver crucian carp *C. auratus langsdorfii* population [10, 11].

In 2003, we happened to discover a tetraploid male among samples from a rearing population in the Gunma Prefecture Fisheries Experiment Station. This male has been reared in the Nanae Fresh-Water Laboratory, Hokkaido University, Nanae, Hokkaido, since 2004. This male is kept in a tank along with a conspecific tetraploid female whose sampling site and year were not recorded. They reproduced in this tank by natural spawning, after which a large number of progeny appeared.

There are three possible genetic results for the progeny of a pair of tetraploids. (1) When some reduced diploid eggs are laid by a tetraploid female and then fertilized with diploid sperm from a tetraploid male, the resulting progeny are likely to be tetraploids with different genotypes. (2) Hexaploid progeny with different genotypes may result when unreduced tetraploid eggs accidentally incorporate a diploid sperm nucleus from a tetraploid male. (3) If unreduced tetraploid eggs of a tetraploid female initiate gynogenetic development due to the intrusion of diploid sperm from a tetraploid male, all of these progeny will grow to a second generation of gynogenetic tetraploids.

In the present study, 120 individuals were randomly selected from the large population of progeny arising from a pair of tetraploids and were assessed for their ploidy status by flow cytometry analysis. Then, using selected samples, the isogenic characteristics of these progeny were verified by random amplified polymorphic (RAPD) DNA-PCR fingerprints. Chromosomes of these progeny were also prepared and assessed by conventional karyotyping and rDNA detection using fluorescence in situ hybridization (FISH).

Materials and methods

Ethics

Research and handling of the animals were performed in line with the Guide for the Care and Use of Laboratory Animals at Hokkaido University.

Source of samples

A tetraploid male *C. a. langsdorfii* was found in a rearing population of the Gunma Prefectural Fisheries Station in 2003, and then transferred and kept at Azabu University. The rearing population of *C. a. langsdorfii* in the Gunma Prefectural Fisheries Station was originated from a wild population of the Jounuma Lake, Gunma Prefecture. The tetraploid male was transferred to the Nanae Freshwater Laboratory, Hokkaido University, Nanae, Hokkaido in 2004. No sampling and rearing record of the female *C. a. langsdorfii* tetraploid individual was available, but it has been reared together with the tetraploid male in the same tank. The tetraploid pair first reproduced in the tank in May, 2009 and a large number of progeny have appeared in the tank since then.

A total of 120 individuals were randomly sampled from these progeny. Due to their small body sizes (body length, 36–54 mm), sex could not be determined for each individual by naked-eye observation. Fin clips were collected for somatic cellular DNA content determinations and stored in 100 % ethanol at −30 °C for genomic DNA extraction. Samples of goldfish *Carassius auratus auratus* which were kept in the aquarium of the Environment Control Experiment Building, Faculty and Graduate School of Fisheries Sciences, Hokkaido University, Hakodate City, Hokkaido, were also used as a source of diploid control samples for these analyses.

Flow cytometry

Ploidy status of 120 individuals was determined by flow cytometry analysis using a previously described procedure [12]. Briefly, fin tissues were minced in DNA-extraction buffer (Cystain DNA 2 step, Partec GmbH, Münster, Germany) and then incubated at room temperature for 20 min. Samples were filtered through a 50-μm mesh filter (Cell TRICS disposable filter units, Partec GmbH), after which 5 volumes of staining solution (Cystain DNA 2 step, Partec GmbH) containing DAPI (4′,6-diamidino-2-phenylindole dihydrochloride) were added. DNA contents were then analyzed using a CyFlow ploidy analyzer (Partec GmbH). Ploidy status was determined by comparing the relative DNA content against standard goldfish diploid DNA content (2C).

DNA Preparation and RAPD-PCR Reactions

Total genomic DNA was isolated from fin-clip samples of 100 individuals by the phenol–chloroform method. RAPD amplification was performed as described previously [13]. From a total of 40 commercially available decamer random primers (Kits A and B, Operon Technologies, Alameda, CA, USA), three primers, OPA-07 (Kit A-7: 5′-GAAACG GGTG-3′), OPB-05 (Kit B-5: 5′-TGCGCCCTTC-3′), and OPB-07 (Kit B-7: 5′-GGTGACGCAG-3′), were selected on the basis of a preliminary screening for stable

amplification, reproducible fragment patterns, and the presence of polymorphisms between parents. The RAPD-PCR mixture contained 1.0 μl of a DNA template (100 ng/μl), 2.0 μl of 10 × PCR buffer (TaKaRa, Japan), 1.6 μl of a dNTP mixture (TaKaRa), 0.2 μl of rTaq polymerase (TaKaRa), 15.2 μl of DDW, and 1.0 μl of a random primer (20 μM). Amplification conditions were 3 min at 95 °C as an initial step, followed by 35 cycles of 95 °C for 30 s, 36 °C for 1 min for primer annealing, and 72 °C for 1 min for elongation. This was followed by a single final step of primer extension at 72 °C for 7 min. Approximately 9 μl of amplification products were separated by 1.5 % agarose gel electrophoresis in TBE buffer (89 mM Tris, 89 mM boric acid, 2.2 mM EDTA). Gels were stained with ethidium bromide and photographed on a UV trans-illuminator using a gel documentation system (Print-graph AE-6915H, Atto, Tokyo).

Chromosome preparation and karyotype analysis

Immature diploid goldfish and tetraploid silver crucian carp (total length: 40–65 mm; body weight: 1.0–3.0 g) were intraperitoneally injected with 50–150 μl of 0.001 % colchicine 3 h prior to sacrifice. Gill tissues were removed and minced finely with forceps and suspended in goldfish Ringer's solution (150 mM NaCl, 3.0 mM KCl, 3.5 mM $MgCl_2$, 5.0 mM $CaCl_2$, 10 mM HEPES, pH 7.5). After centrifugation at 100×*g* for 12 min, the cells were resuspended in 0.075 M KCl hypotonic solution for 40–60 min at room temperature. Then, the cells were fixed with chilled Carnoy's solution (methanol:acetic acid = 3:1) and stored at −20 °C. One droplet of a cell suspension was air-dried on a slide, which had been cleaned in advance with chilled 50 % ethanol. After Giemsa staining, karyotypes were analyzed on the basis of metaphase chromosomes, according to Levan et al. [14].

Fluorescence in situ hybridization

FISH was performed using the 5.8S + 28S rDNA probe according to the protocol described by Fujiwara et al. [15] with minor modifications. Briefly, human 5.8S + 28S rDNA was labeled with biotin-16-dUTP using a nick translation kit (Roche, Germany). Chromosome metaphase spread slides (pretreated with RNase) were denatured in 70 % formamide/2 × SSC (pH 7.0) at 70 °C for 2 min, dehydrated in cold 70 and 100 % ethanol for 10 min each, and then air dried. Then, 150–200 ng of labeled rDNA probe was denatured at 75 °C for 10 min and quickly placed on ice before hybridization with each chromosome slide. After washing in 50 % formamide/2 × SSC, 2 × SSC, 1 × SSC, and 4 × SSC, fluorescent signals were generated using an avidin–FITC (N-fluorescein isothiocyanate, Roche) conjugate. Finally, the slides were mounted in 100 μl of DABCO (1,4-Diazabicyclo-octane) antifade solution containing DAPI for counterstaining. The slides were observed under a Nikon ECLIPSE E800 microscope and images were captured with a Pixera Penguin 150CL-CU CCD camera (Pixera, San Jose, CA, USA).

Results

After testing all progenies ($n = 120$), a prominent tetraploid-range DNA content peak (Fig. 1b) was detected when compared with diploid goldfish as a control (Fig. 1a). RAPD-PCR was first performed for 100 (nos. 1–100) out of 120 tetraploid samples using OPA-07. No paternal contribution was detected by this primer, and the fingerprint pattern of progeny was identical to that of the maternal tetraploid female. Furthermore, no variations were detected among these progeny. Similar isogenic genotypes and all-

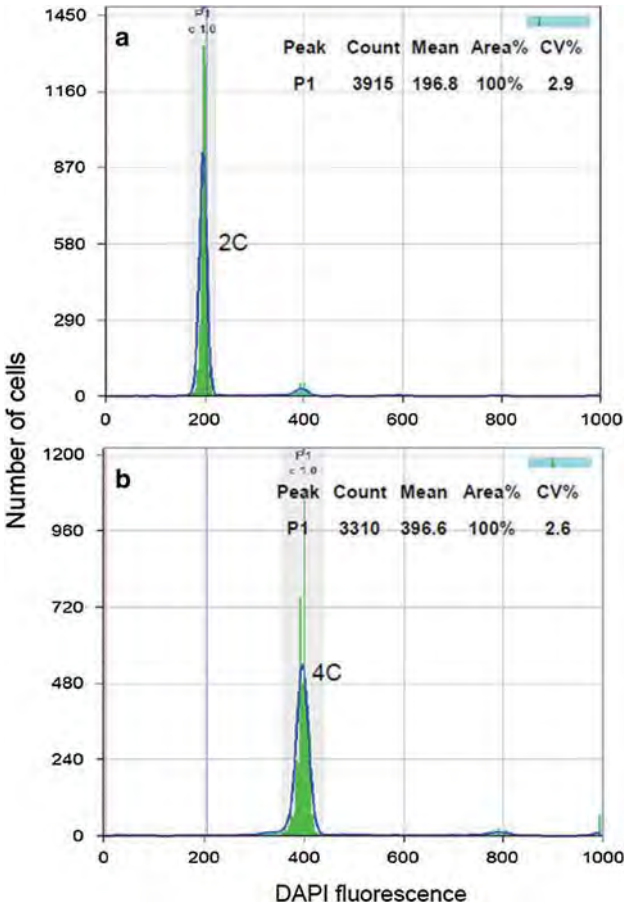

Fig. 1 Flow cytometry results for relative DNA contents in fin cells from control diploid goldfish *Carassius auratus auratus* 2C (**a**) and a tetraploid silver crucian carp *Carassius auratus langsdorfii* progeny 4C (**b**)

female inheritance by progeny were also verified in the same sample set (nos. 1–16) by RAPD-PCR using OPB-05 (Fig. 2).

Fingerprint pattern using OPB-07 primer exhibited no contribution of fragments specific to the father in all the samples examined ($n = 16$). Samples, except for sample #3, demonstrated DNA fingerprints identical to their mother, but a slight variation was found in electropherogram in one out of 16 progeny examined: one maternally derived fragment was faint or lacking when compared with other progeny (Fig. 2). However, this variant individual did not show any polymorphism in fingerprints amplified by other primers. These results indicated that almost all the second generation progeny of the tetraploid female were genetically isogenic and thus likely a gynogenetically generated clone without any contribution of paternal genome, and thus almost all the samples examined were likely genetically identical.

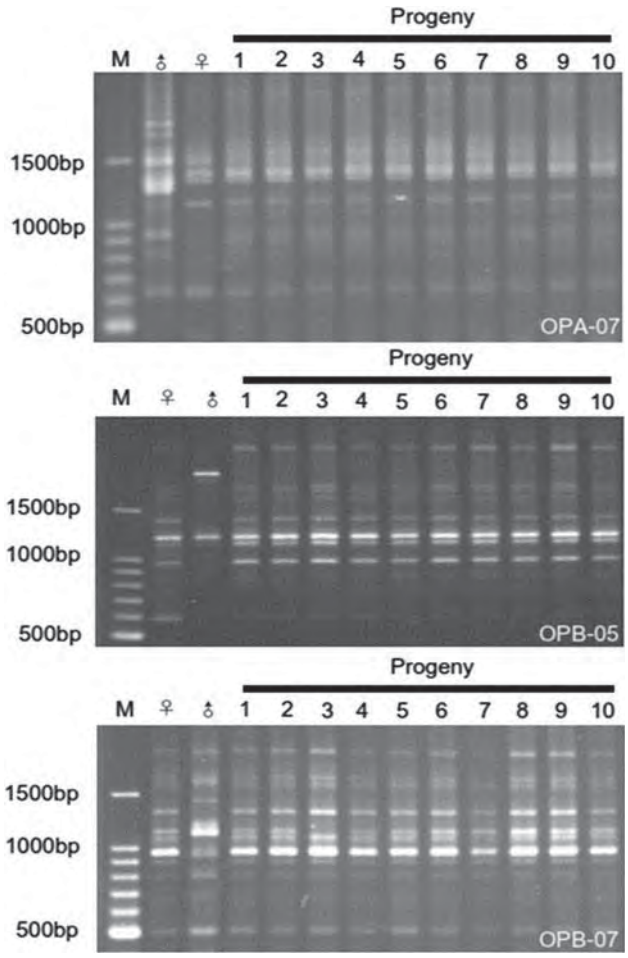

Fig. 2 Random amplified polymorphic DNA (RAPD)-PCR profiles using OPA-07 (*top*), OPB-05 (*middle*), and OPB-07 (*bottom*) primers for silver crucian carp *Carassius auratus langsdorfii*, tetraploid parents (♀ and ♂), and their progeny (nos. 1–10). *M* indicates molecular size markers

Table 1 Chromosome distributions in somatic cells of diploid goldfish *Carassius auratus auratus* and tetraploid silver crucian carp *Carassius auratus langsdorfii*

Fish	Sample no.	No. of cells with chromosomes							
		97	98	99	100	204	205	206	Total
Goldfish	1	0	0	0	12	–	–	–	12
	2	0	0	0	13	–	–	–	13
	3	1	0	0	11	–	–	–	12
Silver crucian carp	1	–	–	–	–	0	1	9	10
	2	–	–	–	–	1	0	10	11
	3	–	–	–	–	1	0	11	12

Table 1 shows the chromosome distributions determined for diploid goldfish and tetraploid silver crucian carp samples. Tetraploid progeny ($n = 3$) had a modal number of chromosomes of $4n = 206$ (Fig. 3c), whereas control goldfish ($n = 3$) had a modal number of $2n = 100$ (Fig. 3a). In goldfish, chromosomes were categorized into 20 metacentric (M), 40 submetacentric (SM), and 40 subtelocentric or telocentric (ST/T) chromosomes that were arranged into 10 M, 20 SM, and 20 ST/T pairs in their karyotypes (Fig. 3b). In tetraploid progeny, the most informative spreads gave karyotypes that were categorized into 40 M, 80 SM, 80 ST/T, and six supernumerary microchromosomes (m). Regular-sized chromosomes were arranged into 10 M, 20 SM, and 20 ST/T quartets in tetraploid karyotypes (Fig. 3d).

FISH signals using the 5.8S + 28S rDNA probe were detected in four chromosomes in all analyzed metaphases prepared from three goldfish samples (Fig. 4a). Tetraploid progeny had rDNA signals in eight chromosomes (Fig. 4b). However, the exact morphologies of rDNA bearing chromosomes and the exact locations of rDNA signals were difficult to identify.

Discussion

Tetraploid-range DNA contents and isogenic RAPD genotypes shown in these progeny clearly indicated the occurrence of gynogenetic development in tetraploid eggs that were spawned by a tetraploid female after fertilization by a tetraploid male sperm. These results indicated that sperm from the tetraploid male had triggered gynogenesis in unreduced tetraploid eggs spawned by the tetraploid female. In the Chinese silver crucian carp *C. auratus gibelio* both allogynogenetic and gonochoristic reproduction are involved [16]. In this species, gynogenesis is initiated only by fertilization with heterospecific sperm from other species (allogynogenesis), whereas

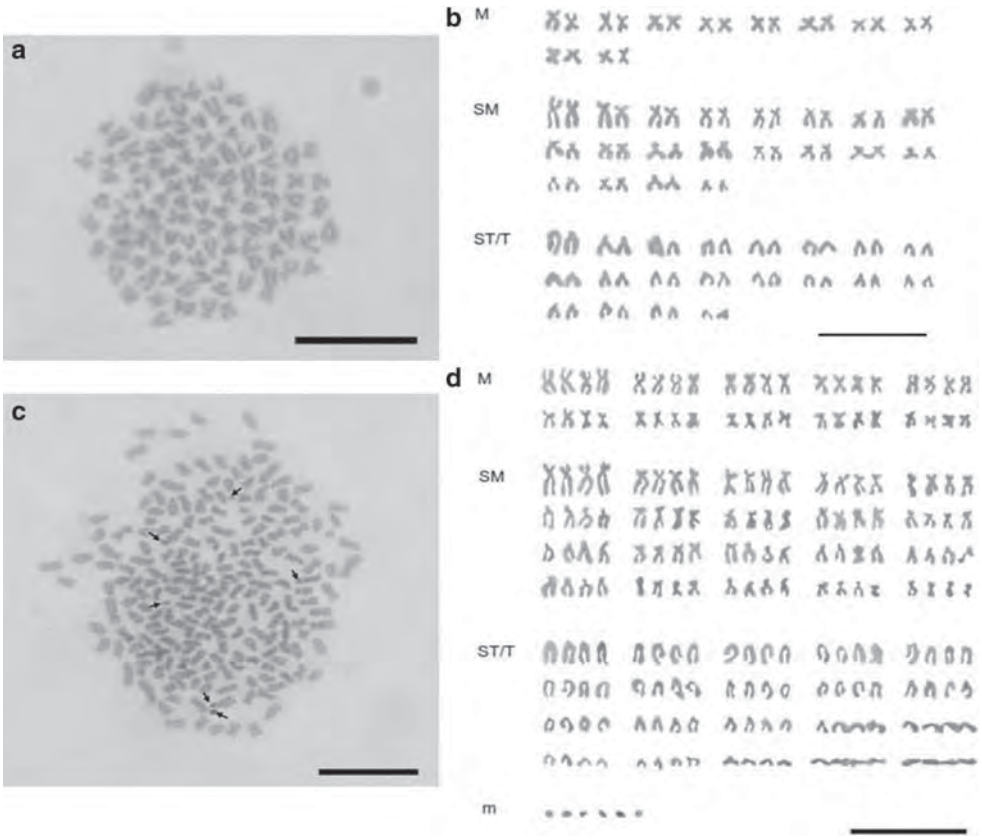

Fig. 3 Mitotic metaphase spread (**a**) and corresponding karyotype of goldfish *Carassius auratus auratus* with 100 chromosomes (**b**). Mitotic metaphase spread (**c**) and corresponding karyotype of silver crucian carp *Carassius auratus langsdorfii* (**d**) with 206 chromosomes. *Arrows* indicate microchromosomes. *Scale bars* 10 μm

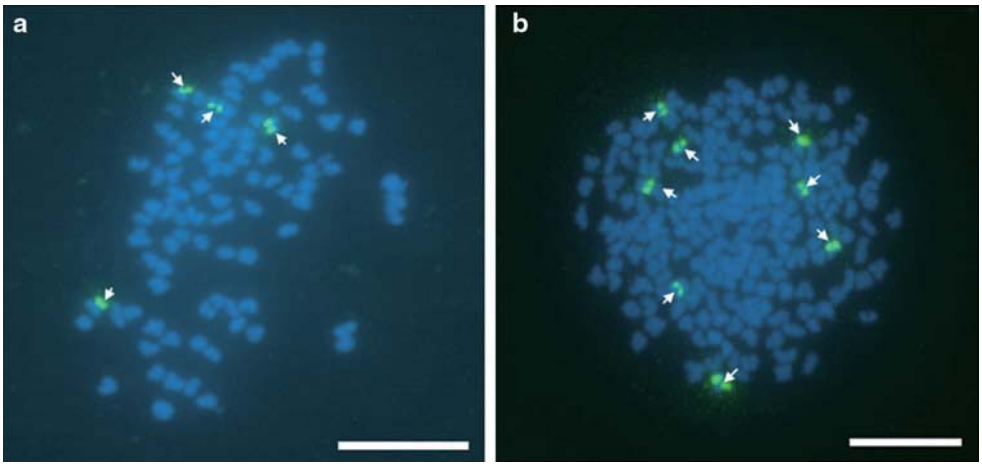

Fig. 4 Mitotic metaphase chromosomes identified after fluorescence in situ hybridization (FISH) probing with 5.8S + 28S rDNA sequences. *Arrows* indicate four fluorescent signals (*green*) in goldfish *Carassius auratus auratus* (**a**) and eight fluorescent signals (*green*) in tetraploid silver crucian carp *Carassius auratus langsdorfii* (**b**). All metaphase chromosomes were counterstained with 4′,6-diamidino-2-phenylindole dihydrochloride (DAPI). *Scale bars* 10 μm

normal bisexual fertilization occurs when eggs are fertilized with homospecific sperm (gonochorism) [16]. As shown in the present study, eggs from a tetraploid female initiated gynogenetic development even after fertilization with homospecific sperm from a tetralploid male. Among 120 individuals examined, no hexaploid individuals arose due to the incorporation of a sperm nucleus from the tetraploid male.

However, an exceptional progeny with a slight difference was detected by RAPD-PCR using OPB-07 in 16 samples examined. This result suggests that the tetraploid female presumably produced large numbers of unreduced clonal tetraploid eggs as well as a very small number of exceptional tetraploid eggs with genetic variation. Such variant eggs can be explained by unusual meiotic recombination during oogenesis of the tetraploid female. Genetic and cytogenetic

results showing the involvement of meiotic recombination by the formation of synapsed bivalents and partially paired trivalents have been reported in gynogenetic triploid silver crucian carp [17, 18]. A few tetraploid eggs may undergo paring and recombination between two homologous and/or homoeologous chromosomes, because they essentially have four sets of chromosomes with relatively higher similarities or affinities. The other possibility may be attributed to unstable reproducibility of RAPD-PCR itself, in which the purity of template DNA often affects amplification of fragments [19]. Therefore, further study is required to confirm the presence or absence of genetic variation among tetraploid eggs using more sensitive and reliable genetic markers such as a microsatellite DNA.

The karyotypes of the goldfish examined here were very similar to those previously reported for diploid *C. auratus* subsp. ($2n = 100$) and diploid Miyazaki race silver crucian carp *C. auratus langsdorfii* ($2n = 100$) [1], which had 20 M + 40 SM + 40 ST/T chromosomes. The karyotype of a tetraploid silver crucian carp *C. auratus langsdorfii* ($4n = 206$), obtained from the Kanto district was reported to be 44 M + 82 SM + 80 T [1], similar to our present results. They had 206 chromosomes, but six supernumerary chromosomes were not distinguished from 200 regular chromosomes. The presence of six microchromosomes found in the present study suggested that a gynogenetic tetraploid may have arisen from a triploid with $3n = 156$ chromosomes [1] by incorporation of haploid chromosomes.

An rDNA locus with 5.8S + 18S + 28S genes and that with 5S genes are located on different chromosomes in most taxa [20]. In triploid silver crucian carp *C. auratus gibelio*, 5S rDNA signals were detected in three STs [21]. In the present study, rDNA signals were detected in four chromosomes of diploid goldfish with $2n = 100$, whereas eight signals were detected in chromosomes of tetraploid silver crucian carp with $4n = 206$. These FISH results indicated that the progeny of silver crucian carp must have a tetraploid karyotype, including four sets of chromosomes. However, the exact morphologies of rDNA-bearing chromosomes have not been determined and additional molecular cytogenetic studies will be required in the near future.

Gynogenesis usually occurs by preventing the decondensation of a sperm nucleus due to a failure in the breakdown of the sperm nuclear envelope [22, 23] in fish species that spawn unreduced diploid or triploid eggs [13, 24–26]. Unreduced diploid eggs are generated by the mechanism of premeiotic endomitosis (chromosome doubling without cytokinesis) in the clonally reproducing diploid loach *Misgurnus anguillicaudatus* [13], whereas clonal triploid eggs are formed by apomixis (i.e., ameiotic division of oocytes by skipping the first meiotic division) in the silver crucian carp *C. auratus gibelio* [24, 25] and *C. auratus langsdorfii* [26], because the formation of a tripolar spindle may physically inhibit the first meiotic division.

The occurrence of a tripolar spindle is presumably related to the presence of three sets of chromosomes in gynogenetic triploid silver crucian carp. If so, then what would occur in unreduced tetraploid eggs that include four sets of chromosomes? This is an enigma that needs to be resolved. In tetraploid eggs with an even number of chromosome sets, normal synapsis and subsequent meiosis can be predicted, although tetraploid silver crucian carp produce unreduced tetraploid eggs that develop by gynogenesis.

In tetraploid silver crucian carp, the cytological mechanisms responsible for the formation of unreduced tetraploid eggs and the initiation of gynogenesis remain to be determined. Our tetraploid population is a reliable set of experimental animals for examining these problems. To identify these mechanisms, the presence or absence of multipolar and other unusual spindles must be investigated in the oocytes of tetraploid silver crucian carp, which can be induced to undergo final maturation by administering 17α-20β-dihydroxy-4-pregnene-3-one during in vitro culture [13, 26]. The configuration of meiotic chromosomes is also informative for determining the reproductive mode [13].

Furthermore, the second generation progeny of tetraploid silver crucian carp are reliable for generating sex-reversed tetraploid males, which are a genetic resource of diploid spermatozoa for further ploidy manipulations. A dimorphism of reproductive mode in the tetraploid silver crucian carp, showing gynogenetic unreduced oogenesis and reduced spermatogenesis, may provide an excellent model for reproductive biology in fishes.

References

1. Kobayasi H, Kawashima Y, Takeuchi N (1970) Comparative chromosome studies in the genus *Carassius*, especially with a finding of polyploidy in the ginbuna (*C. auratus langsdorfii*) (in Japanese with English abstract). Japanese J Ichthyol 17:153–160
2. Kobayasi H, Ochi H (1972) Chromosome studies of the hybrids, ginbuna *C. auratus langsdorfii* × kinbuna *C. auratus subsp* and ginbuna × loach *Misgurnus anguillicaudatus* (in Japanese with English abstract). Zool Mag 81:67–71
3. Kobayasi H, Nakano K, Nakamura M (1977) On the hybrids, 4n ginbuna (*Carassius auratus langsdorfii*) × kinbuna (*C. auratus subsp.*), and their chromosomes (in Japanese with English abstract). Bull Jap Soc Sci Fish 43:31–37
4. Onozato H, Torisawa M, Kusama M (1983) Distribution of the gynogenetic polyploid crucian carp *Carassius langsdorfii* in Hokkaido, Japan (in Japanese with English abstract). Jpn J Ichthyol 30:184–190
5. Maeda K, Nishimura D, Maemura H, Morishima K, Zhang Q, Umino T, Nakagawa H, Arai K (2003) Identification and distribution of gynogenetic clones in silver crucian carp *Carassius*

langsdorfii collected from the dokanbori moats of the imperial palace, Tokyo, Japan (in Japanese with English abstract). Nippon Suisan Gakkaishi 69:185–191
6. Takai A, Ojima Y (1983) Tetraploidy appeared in the offspring of triploid ginbuna, *Carassius auratus langsdorfii* (Cyprinidae, Pisces). Proc Japan Acad 59B:347–350
7. Dong S, Ohara K, Taniguchi N (1997) Introduction of sperm of common carp *Cyprinus carpio* into eggs of ginbuna *Carassius langsdorfii* by heat shock treatment and its confirmation by DNA markers (in Japanese with English abstract). Nippon Suisan Gakkaishi 63:201–206
8. Murakami M, Matsuda C, Fujitani H (2001) The maternal origins of the triploid ginbuna (*Carassius auratus langsdorfii*): phylogenetic relationship within the *C. auratus* taxa by partial mitochondrial D-loop sequencing. Genes Genet Syst 76:25–32
9. Jiang FF, Wang ZW, Zhou L, Jiang L, Zhang XJ, Apalikova OV, Brykov VA, Gui JF (2013) High male incidence and evolutionary implications of triploid form in northeast Asia. Mol Phylogenet Evol 66:350–359
10. Muramoto J (1975) A note on triploidy of the funa (Cyprinidae, Pisces). Proc Japan Acad 51B:583–587
11. Murakami M, Fujitani H (1997) Polyploid-specific repetitive DNA sequences from triploid ginbuna (Japanese silver crucian carp, *Carassius auratus langsdorfii*). Genes Genet Syst 72: 107–113
12. Morishima K, Horie S, Yamaha E, Arai K (2002) A cryptic clonal line of the loach *Misgurnus anguillicaudatus* (Teleostei: Cobitidae) evidenced by induced gynogenesis, interspecific hybridization, microsatellite genotyping and multilocus DNA fingerprinting. Zool Sci 19:565–575
13. Itono M, Morishima K, Fujimoto T, Bando E, Yamaha E, Arai K (2006) Premeiotic endomitosis produces diploid eggs in the natural clone loach, *Misgurnus anguillicaudatus* (Teleostei:Cobitidae). J Exp Zool 305A:513–523
14. Levan A, Fredga K, Sandberg AA (1964) Nomenclature for centromeric position on chromosomes. Hereditas 52:201–220
15. Fujiwara A, Abe S, Yamaha E, Yamazaki F, Yoshida MC (1998) Chromosomal localization and heterochromatin association of ribosomal DNA gene loci and silver-stained nucleolar organizer regions in salmonid fishes. Chromo Res 6:463–471
16. Zhou L, Wang Y, Gui JF (2000) Genetic evidence for gonochoristic reproduction in gynogenetic silver crucian carp (*Carassius auratus gibelio*) as revealed by RAPD assays. J Mol Evol 51:498–506
17. Kojima K, Matsumura K, Kawashima M, Kajishima T (1984) Studies on the gametogenesis in polyploidy ginbuna *Carassius auratus langsdorfii*. J Fac Sci Shinshu Univ 19:37–52
18. Zhang F, Oshiro T, Takashima F (1992) Chromosome synapsis and recombination during meiotic division in gynogenetic triploid ginbuna, *Carassius auratus langsdorfii*. Japan J Ichthyol 39:151–155
19. McClelland M, Welsh J (1994) DNA fingerprinting by arbitrarily primed PCR. PCR Methods Appl 4:s59–s65
20. Suzuki H, Sakurai S, Matsuda Y (1996) Rat rDNA spacer sequences and chromosomal assignment of the genes to the extreme terminal region of chromosome 19. Cytogenet Cell Genet 72:1–4
21. Zhu HP, Ma DM, Gui JF (2006) Triploid origin of the gibel carp as revealed by 5S rDNA localization and chromosome painting. Chromosome Res 14:767–776
22. Itono M, Okabayashi N, Morishima K, Fujimoto T, Yoshikawa H, Yamaha E, Arai K (2007) Cytological mechanisms of gynogenesis and sperm incorporation in unreduced diploid eggs of the clonal loach, *Misgurnus anguillicaudatus* (Teleostei: Cobitidae). J Exp Zool 307A:35–50
23. Yamashita M, Onozato H, Nakanishi T, Nagahama Y (1990) Breakdown of the sperm nuclear envelope is a prerequisite for male pronucleus formation: direct evidence from the gynogenetic crucian carp *Carassius auratus langsdorfii*. Dev Biol 137: 155–160
24. Cherfas NB (1966) Natural triploidy in females of the unisexual form of silver crucian carp (*Carassius auratus gibelio* Bloch). Genetika 5:16–24
25. Cherfas NB (1972) Results of a cytological analysis of unisexual and bisexual forms of silver crucian carp. In: Cherfas BI (ed) Genetics, selection, and hybridization of fish. Israel Program for Scientific Translations, Jerusalem, pp 79–90
26. Yamashita M, Jiang JQ, Onozato H, Nakanishi T, Nagahama Y (1993) A tripolar spindle formed at meiosis I assures the retention of the original ploidy in the gynogenetic triploid crucian carp, ginbuna *Carassius auratus langsdorfii*. Dev Growth Differ 35:631–636

日本食品微生物学会雑誌　Jpn. J. Food Microbiol., **30**(3), 160–164, 2013

＝Short Paper＝

Development of Duplex SYBR Green Real-Time PCR for Rapid and Simultaneous Detection of 16 Specific Genes of 16 Major Foodborne Bacteria

Natsuko IIDA*1, 3, Hiroshi FUKUSHIMA*2, Midori HIROI*1, Miya YAGI*1, Takashi KANDA*1, Masaru MURAKAMI*3, † and Kanji SUGIYAMA*1

(*1 Shizuoka Institute of Environment and Hygiene, Kita-ando, Aoi-ku, Shizuoka 420–8637)

(*2 Shimane Prefectural Livestock Technology Center, Kosi-cho, Izumo, Shimane 693–0031)

(*3 Azabu University School of Veterinary Medicine, Fuchinobe, Chuo-ku, Sagamihara 252–5201; † Corresponding author)

(Received: April 24, 2013)

(Accepted: June 17, 2013)

Key words: foodborne bacteria, duplex SYBR Green real-time PCR, simultaneous screening

Introduction

In foodborne outbreaks, public health administrators must respond promptly and effectively to prevent the spread of pathogens and the recurrence of food poisoning. To do this, it is necessary to identify the causative agents of outbreaks as soon as possible. Traditional culture methods that have been routinely used require several days to identify foodborne bacteria. Traditional culture methods are time-consuming and laborious, since the necessary culture conditions and nutrient media differ from bacteria to bacteria. Thus, simple and reasonable methods for simultaneously detecting various food-poisoning bacterial species are preferable.

Recently, specific gene sequences have been identified in various pathogenic bacteria, and reports on PCR methods targeting the gene sequences of foodborne or waterborne pathogens have been extensively studied[4, 7, 9]. In food poisoning tests, these PCR methods are useful for screening prior to culture. For instance, Fukushima *et al.* developed a method for simultaneously detecting 24 specific genes of foodborne bacteria using a relatively low-cost multiplex real-time PCR system[3]. However, the system is considered a little laborious and somewhat impractical to use in the field.

Here, we designed a modified duplex real-time PCR assay system for simultaneously detecting 16 specific genes of 16 common foodborne bacteria occurring mainly in Japan. The target foodborne pathogens were selected on the basis of data on foodborne outbreaks[5, 6] in Shizuoka Prefecture collected in the past 10 years. Of these, the following are considered the main causative pathogens of foodborne outbreaks: *Clostridium perfringens*, *Campylobacter jejuni*, enterohaemorrhagic *Escherichia coli* (EHEC), enteropathogenic *E. coli* (EPEC), enteroaggregative *E. coli* (EAEC), emetic toxin-producing *Bacillus cereus*, TDH-positive *Vibrio parahaemolyticus, Staphylococcus aureus*, and *Salmonella* spp. The aim of this study was to develop a simple, practical, labor-saving, and effective method for food poisoning examination in the field.

Materials and Methods

Bacterial strains

The 11 species of foodborne bacteria (*E. coli*, *Shigella* spp., *Salmonella* spp., *B. cereus*, *C. jejuni*, *C. perfringens*, *S. aureus*, *V. parahaemolyticus*, *Yersinia enterocolitica*, *Y. pseudotuberculosis*, and *Listeria monocytogenes*), including five groups of *E. coli* [EHEC, EPEC, EAEC, enteroinvasive *E. coli* (EIEC), and enterotoxigenic *E. coli* (ETEC)] and two groups of *B. cereus* (emetic toxin-producing *B. cereus* and enterotoxigenic *B. cereus*) were used as control for PCR analysis.

DNA extraction

DNA was extracted from bacterial cultures

e-mail: murakami@azabu-u.ac.jp

and stool samples with a QIAamp DNA Stool Mini kit (Qiagen) according to the manufacturer's instructions.

Primers

The 16 primer pairs were used to detect the above 11 species of foodborne bacteria. These primer pairs for 16 target genes were selected from previous reports (see Table 1 references). The primer sequence is listed in Table 1.

Duplex real-time PCR

Duplex SYBR Green real-time PCR was performed in 8 lines (12 wells per line) on a 96-well reaction plate using ABI7500 Real-Time PCR systems (Applied Biosystems). One line included a negative control (water), two lines included positive controls, and nine lines included template DNA samples from nine fecal samples. Real-time PCR was performed for a total volume of 20 μl. Each reaction well contained 10 μl of SYBR Premix DimerEraser (TaKaRa, Japan), 0.4 μl of ROX Reference Dye II (50×), 4.4 μl of PCR-grade H_2O, 0.8 μl of a 10 μM primer set for each of two target genes, and 2 μl of sample DNA in a 20 μl PCR mixture. The assay cycling profile was one cycle of 95℃ for 30 sec followed by 30 cycles of denaturation at 95℃ for 5 sec and annealing at 55℃ for 34 sec and then at 72℃ for 40 sec, and finally a dissociation stage of one cycle each at 95℃ for 15 sec, at 60℃ for 60 sec, and at 95℃ for 15 sec. The sizes and melting point temperatures (T_m's) of the PCR products are listed in Table 1.

Reaction specificity was determined on the basis of the T_m of the amplification products. The difference in Tm between two of the expected PCR products in a duplex reaction was set at more than 1.9℃.

Duplex real-time PCR analysis

Twelve foodborne-related outbreak cases that occurred in Shizuoka Prefecture from 2009 to 2012 were examined using duplex real-time PCR analysis. Fecal samples (≤200 mg) from diarrhea or symptomatic patients were treated with a QIAamp DNA Stool Mini kit.

Results and Discussion

We developed a modified real-time PCR screening system for eight duplex assays using a 96-well reaction plate to detect foodborne bacteria in feces and then assessed its usefulness. The present PCR system allows us to simultaneously analyze 16 specific genes of foodborne pathogens in up to nine fecal samples. There are many kinds of foodborne bacteria. In this study, we selected only 16 major foodborne bacteria and set a larger T_m distance in duplex PCR between the target gene's products in this study than in a previous study[3]. The Tm differences were sufficient to unequivocally distinguish between two given foodborne bacteria. The specificity of the present PCR assay was verified using three strains for each of the 16 target genes (a total of 48 strains). The detection limit, ranging from 10^3 to 10^6 CFU per gram of stool sample (CFU/g), was determined to be as follows: 10^3 CFU/g for *V. parahaemolyticus* and ETEC, 10^6 CFU/g for *S. aureus,* and 10^4 to 10^5 CFU/g for the other foodborne bacteria. This sensitivity was sufficient for practical screening.

The set of eight PCR duplex assays used in this study was evaluated to detect the causative bacteria in feces in 12 cases of foodborne-related outbreaks in Shizuoka Prefecture (Table 2). In all the 12 cases examined, the duplex PCR assay detected the causative bacteria from at least one of three fecal samples. Figure 1 shows the detection of a *C. jejuni*-specific gene using primer set B (Table 1) in case 3. In the duplex PCR assay with this primer set B, each PCR product showed a different Tm curve. *C. jejuni* was detected in six of seven stool specimens (S1–S7) from the symptomatic patients. Consistent with these molecular data, *C. jejuni* was isolated from six corresponding samples by the culture method (Table 2). The presence of causative agents presumed from the duplex PCR assay was thus confirmed from the results of bacterial culture. In case 3, *femB*-positive *S. aureus* and *astA*-positive *E. coli* (EAEC) were also simultaneously detected using primer set F from one of seven fecal specimens and primer set G from three of seven fecal specimens. Such occurrence of multiple foodborne bacterial pathogens was observed in 8 of 12 cases, which were demonstrated using the present duplex PCR assay system. In case 10, *Y. pseudotuberculosis* was rapidly and successfully detected in two patients by the PCR method, but not by the routine culture method. In cases 9 and 12, the number of positive results obtained by the PCR assay was less than that obtained by the conventional culture method. This might be due to the insufficient

Table 1. Eight primer sets of duplex SYBR Green real-time PCR with two primer pairs for two target genes used to simultaneously and rapidly screen various foodborne bacteria

Primer set		Species	Target gene	Primer name	Sequence (5′ → 3′)	Product size (bp)	T_m[b]	References
A	1[a]	*Clostridium perfringens*	*cpe*	GAP-11	GGTTCATTAATTGAAACTGGTG	154	75.9	3)
				GAP-12	AACGCCAATCATATAAATTACAGC			
	2	*Listeria monocytogenes*	*hly*	LM-hly-1	CGGAGGTTCCGCAAAAGATG	234	79.1	1)
				LM-hly-2	CCTCCAGAGTGATCGATGTT			
B	3[a]	*Campylobacter jejuni*	Specific	AB-F	CTGAATTTGATACCTTAAGTGCAGC	86	77.0	3)
				AB-R	AGGCACGCCTAAACCTATAGCT			
	4	EHEC	*stx2*	JMS2-F	CGACCCCTCTTGAACATA	108	80.4	3)
				JMS2-R	GATAGACATCAAGCCCTCGT			
C	5[a]	EHEC and EPEC	*eaeA*	eae-F2	CATTGATCAGGATTTTTCTGGTGATA	102	78.1	3)
				eae-R	CTCATGCGGAAATAGCCGTTA			
	6	EIEC and *Shigella* spp.	*virA*	virA-F	CTGCATTCTGGCAATCTCTTCACA	215	80.4	2)
				virA-R	TGATGAGCTAACTTCGTAAGCCCTCC			
D	7[a]	*Bacillus cereus*	*ces*	ces-TM-F	GATGTTTGCGACGATGCAA	65	78.5	3)
				ces-TM-R	CTTTCGGCGTGATACCCATT			
	8	ETEC	*lt*	LT-1	AGCAGGTTTCCCACCGGATCACCA	275	80.4	3)
				LT-2	GTGCTCAGATTCTGGGTCTC			
E	9[a]	*Vibrio parahaemolyticus*	*tdh*	Tdh199-F	GGTACTAAATGGCTGACATC	251	79.3	2)
				Tdh199-R	CCACTACCACTCTCATATGC			
	10	ETEC	*st*	ST-f	GCTAAACCAGTARGGTCTTCAAAA	147	76.6	8)
				ST-r	CCCGGTACARGCAGGATTACAACA			
F	11[a]	*Staphylococcus aureus*	*femB*	FemB-fw	AATTAACGAAATGGGCAGAAACA	93	81.2	3)
				FemB-rv	TGCGCAACACCCTGAACTT			
	12	*Yersinia enterocolitica* and *Y. pseudotuberculosis*	*yadA*	yadA-X-F	CCAGAACCAATTGCAATGCCT	100	78.7	2)
				yadA-X-R	CTTTAAACAGCTTGTTCCAGCCA			
G	13[a]	EAEC	*astA*	EAST-1-S	GCCATCAACACAGTATATCC	106	83.5	3)
				EAST-1-AS	GAGTGACGGCTTTGTAGTCC			
	14	EHEC	*stx1*	JMS1F	GTCACAGTAACAAACCGTAACA	95	79.6	3)
				JMS1R	TCGTTGACTACTTCTTATCTGGA			
H	15[a]	*Salmonella* spp.	*invA*	invA139	GTGAAATTATCGCCACGTTCGGGCAA	284	85.0	4)
				invA141	TCATCGCACCGTCAAAGGAACC			
	16	*B. cereus*	*nheB*	SG-F3	GCACTTATGGCAGTATTTGCAGC	152	79.6	2)
				SG-R3	GCATCTTTTAAGCCTTCTGGTC			

[a] Nine main foodborne bacteria
[b] Melting point temperatures value of PCR products

Table 2. Examination by duplex real-time PCR assay and bacterial culture in 12 foodborne-related outbreaks that occurred from 2009 to 2012 in Shizuoka Prefecture.

Case No.	Facility	Source of infection	Isolated bacteria	No. of examined samples	Positive detection	
					Conventional culture method	This study samples (Detected gene)
1	Hospital	Lunch	*C. perfringens* (TW9)	7	5	5 (*cpe*)
2	Restaurant	Supper	*C. jejuni*	3	1	1 (*C. jejuni* specific) 2 (*astA*)
3	Restaurant	Supper	*C. jejuni*	7	6	6 (*C. jejuni* specific) 1 (*femB*) 3 (*astA*)
4	Restaurant	Lunch	*C. perfringens* (TW12)	4	3	4 (*cpe*)
5	Hospital	Lunch	S. Nagoya	7	7	7 (*invA*) 2 (*femB*)
6	Hotel	Supper	*V. parahaemolyticus*	4	3	3 (*tdh*) 1 (*astA*)
7	Restaurant	Catering	*C. jejuni*	6	3	3 (*C. jejuni* specific)
8	Restaurant	Supper	*C. jejuni*	4	2	3 (*C. jejuni* specific) 1 (*astA*)
9	School	Unknown	*C. perfringens* (TW78)	9	8	6 (*cpe*) 1 (*astA*)
10	School	Unknown	*Y pseudotuberculosis* 5a	5	2	2 (*yadA*)
11	Caterer	Catering	S. Enteritidis	5	5	3 (*invA*) 2 (*astA*)
12	Caterer	Catering	*S. aureus*	8	8	4 (*femB*) 2 (*eaeA*)

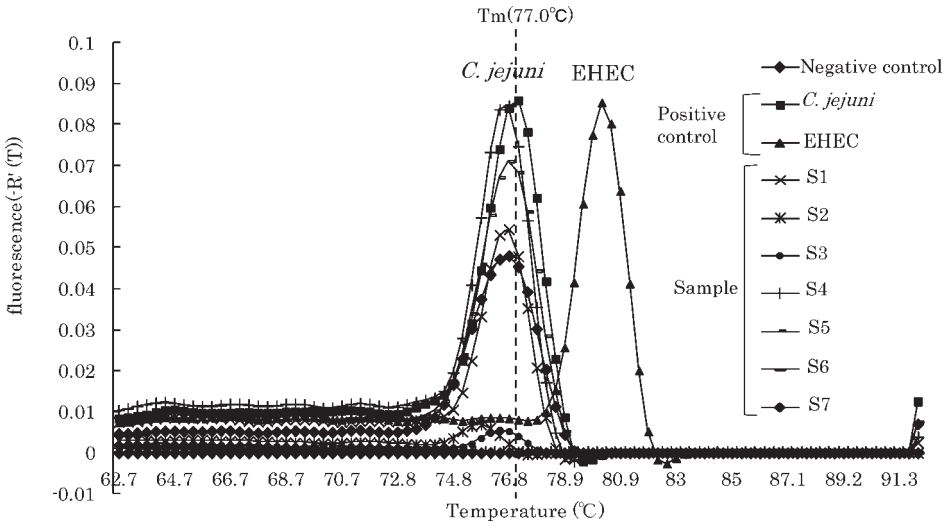

Fig. 1. Melting point temperature (T_m) curves for the products of duplex PCR using primer set B from seven samples in case 3 of the foodborne outbreak (see Table 2).
When a few target bacterial cells were present in the reaction well, T_m became lower than the expected value by approximately 1℃ . The T_m's of S2 and S3 were within allowable tolerance.

DNA extraction since *S. aureus* and *C. perfringens* are Gram-positive bacteria with a thick cell wall.

Analysis using the screening system (DNA extraction from feces and duplex real-time PCR reactions) was performed approximately 3 to 4 hours, faster than the conventional culture assay, where causative pathogens were isolated after 2 to 4 days. The results of the PCR assay were also essentially consistent with those of the culture method (Table 2). These data show that the proposed PCR method is useful for the rapid identification of the causative pathogens of foodborne outbreaks. Moreover, the system can rapidly, accurately, and safely detect various bacterial species, including *C. jejuni*, which require long culture times, as well as *C. perfringens* and ETEC,

which produce toxins.

The rapid and comprehensive presumption of food-poisoning pathogens, which can be obtained using the present simultaneous screening system by duplex real-time PCR assay, will enable public administrators to promptly and efficiently provide hygiene instructions in foodborne outbreaks.

In conclusion, the screening system described here enables the simultaneous analysis of 16 specific target genes of foodborne pathogens in up to nine stool specimens by using a set of eight duplex real-time PCR assays with a 96-well reaction plate. This PCR assay system is useful for detecting causative bacteria in fecal specimens obtained from symptomatic patients and is suitable for the rapid and presumptive diagnosis of food-poisoning pathogens in fecal specimens of foodborne outbreaks in Japan.

Acknowledgment

We thank the staff of health centers in Shizuoka Prefecture for performing the sample collection.

References

1) Bubert, A., Riebe, J., Schnitzler, N., Schönberg, A., Goebel, W. and Schubert, P.: Isolation of catalase-negative *Listeria monocytogenes* strains from listeriosis patients and their rapid identification by anti-p60 antibodies and/or PCR. J. Clin. Microbiol., **35**, 179–183 (1997).
2) Fukushima, H., Katsube, K., Tsunomori, Y., Kishi, R., Atsuta, J. and Akiba, Y.: Comprehensive and rapid real-time PCR analysis of 21 foodborne outbreaks. Int. J. Microbiol., Article ID 917623, 13 pages (2009).
3) Fukushima, H., Kawase, J., Etoh, Y., Sugama, K., Yashiro, S., Iida, N. and Yamaguchi, K.: Simultaneous screening of 24 target genes of foodborne pathogens in 35 foodborne outbreaks using multiplex real-time SYBR Green PCR analysis. Int. J. Microbiol., Article ID 864817, 17 pages (2010).
4) Fukushima, H., Tsunomori, Y. and Seki, R.: Duplex real-time SYBR Green PCR assays for detection of 17 species of food- or waterborne pathogens in stools. J. Clin. Microbiol., **41**, 5134–5146 (2003).
5) Health and Welfare Department, Shizuoka Prefecture: Food poisoning in Shizuoka Prefecture 2004 (in Japanese).
6) Health Department, Shizuoka Prefecture: Food poisoning in Shizuoka Prefecture 2009 (in Japanese).
7) Matsuki, T., Watanabe, K., Fujimoto, J., Takada, T. and Tanaka, R.: Use of 16S rRNA gene-targeted group-specific primers for real-time PCR analysis of predominant bacteria in human feces. Appl. Environ. Microbiol., **70**, 7220–7228 (2004).
8) Nguyen, T. V., Van, P. L., Huy, C. L., Gia, K. N. and Weintraub, A.: Detection and characterization of diarrheagenic *Escherichia coli* from young children in Hanoi, Vietnam. J. Clin. Microbiol., **43**, 755–760 (2005).
9) Ott, S. J., Musfeldt, M., Ullmann, U., Hampe, J. and Schreiber, S.: Quantification of intestinal bacterial populations by real-time PCR with a universal primer set and minor groove binder probes: a global approach to the enteric flora. J. Clin. Microbiol., **42**, 2566–2572 (2004).

Duplex SYBR Green real-time PCR法による食中毒起因菌16遺伝子の一斉迅速検査法の開発

飯田奈都子[*1,3]・福島　博[*2]・廣井みどり[*1]・八木美弥[*1]
神田　隆[*1]・村上　賢[*3,†]・杉山寛治[*1]

[*1]静岡県環境衛生科学研究所，[*2]島根県畜産技術センター，[*3]麻布大学獣医学部，[†]責任著者

細菌性食中毒検査の迅速化・省力化のため，duplex real-time PCR法を用いた食中毒起因菌のより実践的な一斉スクリーニング法を考案した．本法は，食中毒患者の糞便検体から抽出されたDNAを対象とし，Duplex SYBR Green real-time PCRの8反応系を同時に行い，発生頻度の高い食中毒起因菌の16遺伝子を一斉に検索する．菌種の同定は，融解曲線分析のT_m値との比較より，判定することが可能である．実際の食中毒事例の患者糞便検体に本法を導入したところ，培養法と同等の成績を約3～4時間で得ることができた．本法は，検査の効率化のみならず，食中毒事件へのより迅速な行政対応を可能にし，健康危機管理の一端を担う方法として活用が期待される．

Biochimica et Biophysica Acta 1830 (2013) 5027–5035

Contents lists available at ScienceDirect

Biochimica et Biophysica Acta

journal homepage: www.elsevier.com/locate/bbagen

Regulation of brown adipogenesis by the Tgf-β family: Involvement of Srebp1c in Tgf-β- and Activin-induced inhibition of adipogenesis

Hirofumi Yoshida [a], Yohei Kanamori [a], Hiroki Asano [a], Osamu Hashimoto [b], Masaru Murakami [c], Teruo Kawada [d], Tohru Matsui [a], Masayuki Funaba [a,*]

[a] Division of Applied Biosciences, Graduate School of Agriculture, Kyoto University, Kyoto 606-8502, Japan
[b] Laboratory of Experimental Animal Science, Kitasato University School of Veterinary Medicine, Towada 034-8628, Japan
[c] Laboratory of Molecular Biology, Azabu University School of Veterinary Medicine, Chuo-ku, Sagamihara 252-5201, Japan
[d] Division of Food Science and Biotechnology, Graduate School of Agriculture, Kyoto University, Kyoto 611-0011, Japan

ARTICLE INFO

Article history:
Received 13 February 2013
Received in revised form 12 June 2013
Accepted 30 June 2013
Available online 10 July 2013

Keywords:
Brown adipocyte
Tgf-β family
Tgf-β
Activin
Bmp

ABSTRACT

Background: Brown adipocytes generate heat through the expression of mitochondrial Ucp1. Compared with the information on the regulatory differentiation of white preadipocytes, the factors affecting brown adipogenesis are not as well understood. The present study examined the roles of the Tgf-β family members Bmp, Tgf-β and Activin during differentiation of HB2 brown preadipocytes.
Methods: Endogenous Bmp activity and effects of exogenous Tgf-β family members were examined. Role of Srebp1c in brown adipogenesis was further explored.
Results: Although Bmp7 has been suggested to be a potent stimulator of brown adipogenesis, it affected neither the expression of brown adipocyte-selective genes nor Ucp1 induction in response to a β adrenergic receptor agonist. Unlike in 3T3-L1 white preadipocytes, endogenous Bmp activity was not required for brown adipogenesis; treatment with inhibitors of the Bmp pathway did not affect differentiation of preadipocytes. Administration of Tgf-β1 or Activin A efficiently decreased the insulin-induced expression of brown adipocyte-selective genes. Tgf-β1 and Activin A decreased the expression of Pparγ2 and C/ebpα, suggesting the inhibition of adipogenesis. The Tgf-β- and Activin-induced inhibition of brown adipogenesis was mediated by the repression of Srebp1c expression; Tgf-β1 and Activin A blocked Srebp1c gene induction in response to the differentiation induction, and knock-down of Srebp1 expression inhibited brown adipogenesis.
Conclusion: Endogenous Bmp is dispensable for brown adipogenesis, and Srebp1c is indispensable, which is negatively regulated by Tgf-β and Activin.
General significance: Control of activity of the Tgf-β family is potentially useful for maintenance of energy homeostasis through manipulation of brown adipogenesis.

1. Introduction

There are two major types of adipocytes in mammals: white and brown. White adipocytes are specialized for the storage of excess energy, containing all of the enzymatic machinery necessary to build triacylglycerols from fatty acids synthesized de novo or from fatty acids imported from circulating lipoproteins [1]. In contrast, brown adipocytes dissipate chemical energy in the form of heat against cold exposure [2]. This thermogenic function of brown fat results from the expression of a series of genes related to a high mitochondrial content and the elevated cellular respiration that is largely uncoupled from ATP synthesis [3]. This uncoupling occurs through the mitochondrial uncoupling protein 1 (Ucp1), a mammalian brown adipocyte-specific protein that promotes proton leak across the inner mitochondrial membrane [2,4]. Recent findings that adult humans have functional brown adipocytes have initiated studies of the origin and regulatory differentiation of brown preadipocytes [5,6]. However, compared with the information known about white adipogenesis, knowledge of the regulation of brown adipogenesis is still limited.

Despite having a different physiological role from white adipocytes, brown adipocytes share many molecular components with white adipocytes [7–9]. Peroxisome proliferator-activated receptor (Ppar) γ and CCAAT-enhancer binding protein (C/ebp) α, transcription factors, potently regulate differentiation of preadipocytes into adipocytes; Pparγ-null mice exhibited extremely lower weight of white fat as well as brown fat [10], and C/ebpα was required for development of functional white and brown fat [11,12]. Pparγ and

* Corresponding author at: Division of Applied Biosciences, Graduate School of Agriculture, Kyoto University, Kitashirakawa Oiwakecho, Kyoto 606-8502, Japan. Tel.: +81 75 753 6055; fax: +81 75 753 6344.
E-mail address: mfunaba@kais.kyoto-u.ac.jp (M. Funaba).

0304-4165/$ – see front matter © 2013 Elsevier B.V. All rights reserved.
http://dx.doi.org/10.1016/j.bbagen.2013.06.036

C/ebpα stimulate the transcriptional activation of the large group of genes that produce the adipocyte phenotype [13]. In contrast, expression of genes related to mitochondrial biogenesis and oxidative metabolism highly expressed in brown adipocytes is mainly regulated by a transcriptional co-activator Pgc1α, a Pparγ-binding partner predominantly expressed in the brown fat [3].

Members of the transforming growth factor-β (Tgf-β) family potently regulate commitment, differentiation and maturation of mesenchymal cells [14]. This family also participates in the development of mature white adipocytes; treatment with Tgf-β or Activin A, representative members of the Tgf-β family, inhibited the transcriptional activity of C/ebpβ, the expression of Pparγ and lipid accumulation in 3T3-L1 white adipocytes, indicating inhibitory effects on adipogenesis [15,16]. Endogenous activity of bone morphogenetic protein (Bmp), another representative member of the Tgf-β family, in white preadipocytes was higher before differentiation induction, and this activity was indispensable for adipogenesis [17]. In contrast, exogenous Bmp regulates white adipogenesis in a cell context-dependent manner; treatment with Bmp2 decreased insulin-induced lipid accumulation in 3T3-F442A adipocytes [18], whereas Bmp7 stimulated differentiation of 3T3-L1 preadipocytes [19]. Furthermore, Bmp4 potentiated the commitment of pluripotent mesenchymal C3H10T1/2 cells to adipocyte-lineage cells [20,21].

Here, we explored the roles of the Tgf-β family in brown adipogenesis using HB2 preadipocytes [22]. Our results indicate that 1) both endogenous and exogenous Bmp do not affect brown adipogenesis, 2) Tgf-β and Activin inhibit differentiation of brown preadipocytes, and 3) Tgf-β and Activin block insulin-induced expression of sterol regulatory element-binding protein (Srebp) 1c, which is necessary for brown adipogenesis. The present results indicate the roles of Tgf-β and Activin as negative regulators of brown adipogenesis through the inhibition of differentiation into fat cells.

2. Materials and methods

2.1. Materials

The following reagents were purchased or provided: dorsomorphin (compound C: 6-[4-(2-piperidin-1-yl-ethoxy) phenyl]-3-pyridin-4-yl-pyrazolo[1,5-a] pyrimidine) was from Calbiochem (La Jolla, CA, USA); LDN-193189 was from Stemgent (San Diego, CA, USA); dexamethasone (Dex), 3-isobutyl-1-methylxanthine (IBMX), insulin, triiodothyronine (T_3) and isoproterenol were from Sigma (St. Louis, MO, USA); purified Tgf-β1 was from Becton Dickinson (Franklin Lakes, NJ, USA); recombinant Activin A, Bmp4 and Bmp7 were from R & D Systems (Minneapolis, MN, USA); troglitazone was from Daiichi-Sankyo (Tokyo, Japan); a rabbit polyclonal antibody against phospho-Smad1 (Ser463/Ser465)/Smad5 (Ser463/Ser465)/Smad8 (Ser426/Ser428) (#9511) and a rabbit polyclonal antibody against phospho-Smad2 (Ser465/Ser467) were from Cell Signaling Technology (Danvers, MA, USA); and a rabbit monoclonal antibody against Smad1 (ab33902), rabbit polyclonal antibodies against Pparγ2 (ab45278), Smad2 (ab63576) and Ucp1 (ab10983), and a mouse monoclonal antibody against β-actin (AC-15) were from Abcam (Cambridge, MA, USA).

2.2. Cell culture

HB2 brown preadipocytes, which were kindly provided by Dr. M. Saito (Tenshi University), were established from the stromal vascular fraction of the interscapular brown fat of mice deficient of a tumor-suppressor gene p53 [22]. Three cell lines immortalized brown preadipocytes have been reported; two were established from brown adipose tissue tumors induced by expression of SV40 T-antigen in transgenic mice [23,24], and one was immortalized the stromal vascular cells of the interscapular brown fat by infection with virus expressing SV40 T-antigen [25]. Genetic background and the cause of immortalization are clear in HB2 brown preadipocytes, as compared with brown preadipocyte lines transformed with SV40 T-antigen [23–25]. Thus, we used HB2 brown preadipocytes in this study.

HB2 cells were grown in growth medium (Dulbecco's modified Eagle's medium (DMEM) with heat-inactivated 10% FBS, 100 U/ml penicillin and 100 μg/ml streptomycin) at 37 °C in a humidified 5% CO_2 atmosphere. To examine the roles of endogenous Bmp activity, HB2 cells were differentiated with the differentiation protocol of 3T3-L1 cells [26]: two days after reaching confluence (day 0), the cells were cultured in the growth medium in the presence of differentiation inducers (Dex [0.25 μM], IBMX [0.5 mM] and insulin [10 μg/ml]) for 2 days, followed by culture with insulin (5 μg/ml) in the growth medium. In addition, T_3 (50 nM) was added to the medium; T_3 is frequently used during brown adipocyte differentiation in vitro [27–31]. To determine the minimal factors for brown adipogenesis, cells were cultured in the growth medium in the presence or absence of T_3 (50 nM) and insulin (20 nM). The Bmp inhibitors and Tgf-β family members were added at the following concentrations: dorsomorphin (5 μM), LDN-193189 (100 nM), Bmp (3.3 nM), Tgf-β1 (200 pM) and Activin A (4 nM). To examine the effects of cAMP stimulation, the cells were treated on day 8 with or without isoproterenol (10 μM) for 4 h. Oil Red O staining on day 6 or day 8 after the differentiation induction and the subsequent quantification of dye were performed as described previously [17].

2.3. Western blotting

Western blot analyses were performed as described previously [32]. The immunoreactive proteins were visualized using the ECL Advance Western blotting detection system (GE Healthcare, Buckinghamshire, UK) according to the manufacturer's protocol. After stripping the antibodies and the detection reagents, the membranes were reprobed with antibodies against Smad1, Smad2 or β-actin.

2.4. RT-quantitative PCR

RNA isolation and RT-quantitative PCR (qPCR) were performed as described previously [33,34]. The oligonucleotide primers for RT-qPCR are presented in Supplementary Table 1. The Ct value was determined, and the abundance of gene transcripts was analyzed using the $^{\Delta\Delta}$Ct method using 18S rRNA as the normalization gene.

2.5. siRNA transfection

To target the expression of Srebp1 and green fluorescent protein (GFP) as a control, the siRNAs of the respective genes were synthesized by Bonac Corp. (Kurume, Japan). Two oligonucleotides were used in combination to inhibit the expression of Srebp1, 5′-CCUACGA AGUGCACACAAAdTdT-3′ and 5′-UUUGUGUGCACUUCGUAGGdTdT-3′. The siRNA for GFP was described previously [34]. Overall, siRNA (60 pmol) was transfected in a 12-well plate using Lipofectamine RNAiMAX (Invitrogen) according to the manufacturer's protocol.

2.6. Statistical analyses

Data are expressed as the mean ± SEM. Data on gene expression were log-transformed to provide an approximation of a normal distribution before analysis. Data in Fig. 3 were analyzed by two-way ANOVA; the statistical model included effects of T_3, insulin and their interaction. As for the other data, differences between the control group and the tested group were examined using unpaired *t*-test. Differences of $P < 0.05$ were considered significant.

3. Results

3.1. Endogenous Bmp activity is not required for the onset of the adipogenic program in HB2 brown preadipocytes

We previously revealed that endogenous Bmp activity is higher prior to the induction of differentiation in 3T3-L1 white preadipocytes and that this activity is required for proper adipogenesis [17]. To examine the activity and role of endogenous Bmp during brown adipogenesis, HB2 brown preadipocytes were differentiated using the protocol for 3T3-L1 cells [26] supplemented with T_3, a procedure that has been reported to differentiate HB2 brown preadipocytes [35]. Endogenous Bmp activity was evaluated by phosphorylated Smad1/5/8 levels, as Bmp induces phosphorylation of Smad1/5/8 at the carboxyl-terminal serines after complex formation with the type I and type II receptors [36]. Time-course changes in the phosphorylation levels of Smad1/5/8 in HB2 cells were relatively constant throughout the differentiation process (Fig. 1A) and were lower than the phosphorylation levels in 3T3-L1 preadipocytes (data not shown). In addition, treatment with dorsomorphin or LDN-193189, kinase inhibitors for the Bmp type I receptors [37,38], did not affect lipid accumulation (Fig. 1B) or the expression of Pparγ2 and C/ebpα, regulators of brown and white adipogenesis [7–9,13], on day 8 (Fig. 1C). Brown adipocyte-specific Ucp1 is transcriptionally activated in response to β_3 adrenergic receptor activation [2]. Ucp1 expression was not affected by the inhibitors, irrespective of treatment with the β adrenergic receptor agonist isoproterenol (Fig. 1D). These results suggest that endogenous Bmp activity in HB2 brown preadipocytes is low and does not require the onset of the adipogenic program, indicating the differential role of endogenous Bmp in brown adipogenesis from that in white adipogenesis.

3.2. Neither Bmp4 nor Bmp7 affects brown adipogenesis-related gene expression in HB2 cells

Previously, exogenous Bmp7, but not Bmp2, 4, 5 and 6, stimulated differentiation of a brown preadipocyte cell line in the presence of T_3 and insulin [29]. We next explored whether the ability of exogenous Bmp7 could have a similar effect on the HB2 brown preadipocytes. Responsiveness to exogenous Bmp was first examined by evaluation of Smad phosphorylation levels. Smad1/5/8 was shown to be phosphorylated by treatment with Bmp4 or Bmp7 (Fig. 2A). Treatment with Bmp4 or Bmp7 significantly increased lipid accumulation on day 8 (Fig. 2B), but neither Bmp7 nor Bmp4 affected the expression of Pparγ2 (Fig. 2C). The expression of fatty acid-binding protein (Fabp) 4 and resistin, molecules expressed in mature adipocytes [39,40], was also unaffected by treatment with Bmp4 or Bmp7 (Fig. 2D–E). Furthermore, the Bmp treatments did not affect the basal or the induced levels of Ucp1 (Fig. 2F).

3.3. Insulin is essential for brown adipogenesis in HB2 cells

The lack of effects of endogenous and exogenous Bmp on brown adipogenesis may result from the presence of additional reagents other than the essential factors required for brown adipogenesis in the culture conditions; as the result, it is possible that the effects of Bmp are masked. Thus, we explored the essential factors that are necessary for brown adipogenesis.

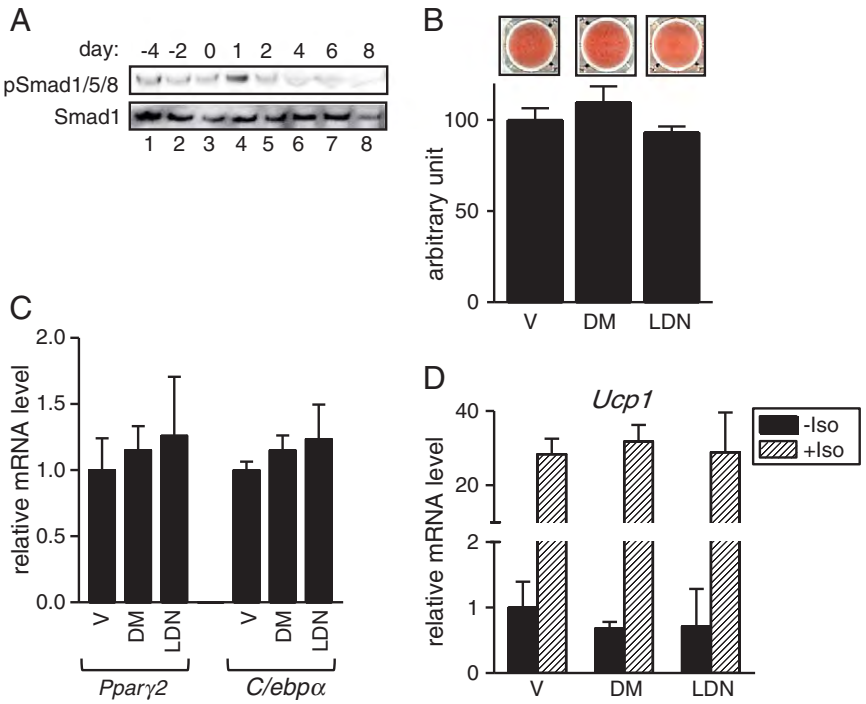

Fig. 1. Endogenous Bmp activity is lower and is dispensable for brown adipogenesis. (A) Phosphorylation status of Smad1/5/8 during differentiation of HB2 brown preadipocytes. HB2 cells were stimulated by differentiation inducers containing Dex (0.25 μM), IBMX (0.5 mM), insulin (10 μg/ml) and T_3 (50 nM) on day 0 for 2 days, followed by culture with insulin (5 μg/ml) and T_3 (50 nM). Samples containing 1 μg DNA were subjected to Western blotting to detect Smad1/5/8 phosphorylated at C-terminal serines (upper panel). The membranes were then re-blotted with an antibody against Smad1 (lower panel). (B−D) Effects of inhibition of Bmp activity on lipid accumulation (B) and expression of Pparγ2, C/ebpα (C) and Ucp1 (D). Dorsomorphin (DM: 5 μM), LDN-193189 (LDN: 100 nM) or DMSO as vehicle (V) was added to the culture medium from day −2 to day 0. (B) Lipid accumulation was examined on day 8 by Oil Red O staining (upper panel). After staining, the dye was extracted in 2-propanol, and the amount was quantified by measuring absorbance at 510 nm. The absorbance of the extracted dye from cells treated with vehicle was set at 100. Data are expressed as the mean ± SE (n = 4). (C) The gene transcript levels of Pparγ2 and C/ebpα on day 8 were measured by RT-qPCR and expressed as ratios to 18S rRNA, with the level in HB2 cells treated with vehicle set to 1. Data shown are the mean ± SE (n = 4). (D) HB2 cells on day 8 were treated with or without isoproterenol (Iso: 10 μM) for 4 h. The gene transcript level of Ucp1 was measured by RT-qPCR and expressed as a ratio to 18S rRNA, with the level in HB2 cells treated with or without isoproterenol set to 1. Data shown are the mean ± SE (n = 4).

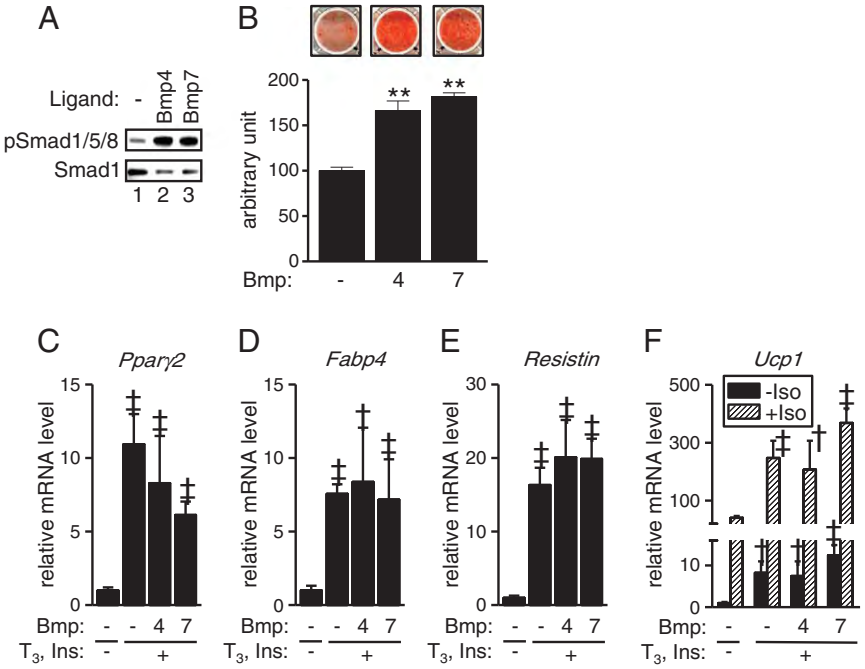

Fig. 2. Neither Bmp7 nor Bmp4 enhances expression of brown adipogenesis-related genes. (A) Smad phosphorylation in response to exogenous Bmp. HB2 cells were treated with Bmp4 (3.3 nM) or Bmp7 (3.3 nM) for 1 h. Phosphorylated Smad1/5/8 was examined by Western blotting, followed by re-blotting with an antibody against Smad1. (B–F) Effects of exogenous Bmp on lipid accumulation (B) and expression of genes related to brown adipogenesis (C–F) in HB2 cells. Bmp4 (3.3 nM) or Bmp7 (3.3 nM) was added to the culture medium supplemented with T_3 (50 nM) and insulin (Ins: 20 nM). (B) Lipid accumulation was examined on day 8 by Oil Red O staining (upper panel). After staining, the dye was extracted in 2-propanol, and the amount was quantified by measuring absorbance at 510 nm. The absorbance of the extracted dye from cells treated without Bmp was set at 100. Data are expressed as the mean ± SE (n = 4). **: $P < 0.01$ vs. cells treated without Bmp. (C–E) The gene transcript levels of Pparγ2 (C), Fabp4 (D) and Resistin (E) on day 8 were measured by RT-qPCR and expressed as ratios to 18S rRNA, with the level in HB2 cells treated with the growth medium alone set to 1. Data shown are the mean ± SE (n = 4). (F) HB2 cells on day 8 were treated with or without isoproterenol (Iso: 10 μM) for 4 h. The gene transcript level of Ucp1 was measured by RT-qPCR, and expressed as a ratio to 18S rRNA, with the level in HB2 cells treated with the growth medium alone set to 1. Data shown are the mean ± SE (n = 4). † and ‡: $P < 0.05$ and $P < 0.01$, respectively, vs. cells treated without Bmp, T_3 and insulin.

Irie et al. [22] showed that HB2 cells differentiated into brown adipocytes after 5 days in the presence of T_3 and insulin in the growth medium. We examined effects of T_3 or insulin or both on lipid accumulation (Fig. 3A), basal Ucp1 expression (Fig. 3B), expression of Pgc1α (Fig. 3C) and Cidea (Fig. 3D), genes expressed predominantly in brown fat and involved in the regulatory expression and activity of Ucp1 [3,41,42], and Pparγ2 expression (Fig. 3E) on day 8. Insulin increased lipid accumulation, whereas T_3 slightly but significantly decreased it (Fig. 3A and F). Expression of Ucp1, Pgc1α, Cidea and Pparγ2 was significantly increased by treatment with insulin alone (Fig. 3B–F). Insulin-induced expression of Ucp1 was also verified at the protein level; significant Ucp1 expression was detected in the presence of insulin (Fig. 3G, lane 2). The expression level of Ucp1 was further increased in the presence of troglitazone, a thiazolidinedione that activates the transcriptional activity of Pparγ [43] (Fig. 3G, lanes 4–6). Consistent with the expression at the mRNA level, isoproterenol treatment also enhanced the expression of Ucp1 induced by insulin and troglitazone (Fig. 3G, lanes 7–12). Unexpectedly, T_3 inhibited insulin-induced Ucp1 expression (Fig. 3G, lane 3), which contrasted with the evaluation at the mRNA level. All of these results indicate that insulin but not T_3 is a minimal factor for inducing differentiation in HB2 cells and that T_3 instead inhibits insulin-induced differentiation of brown preadipocytes. Previous studies showed that T_3 was required for optimal Ucp1 expression in primary cultures of brown adipocyte precursors [27,28,44]; thyroid hormones in FBS may be sufficient during brown adipogenesis of HB2 cells.

We further evaluated the effects of exogenous Bmp in insulin-mediated brown adipogenesis. Similar to the effects on the cultures in the presence of T_3 and insulin (Fig. 2B and F), both Bmp4 and Bmp7 potentiated an increase in lipid accumulation but did not increase basal and inducible Ucp1 expression in response to isoproterenol treatment on day 8 (Supplementary Fig. 1).

3.4. Tgf-β1 and Activin A inhibit brown adipogenesis in HB2 cells

Tgf-β and Activin A inhibit differentiation of 3T3-L1 white preadipocytes [15,16], suggesting that these growth factors may also inhibit brown adipogenesis. We showed that Smad2, a canonical signal mediator of Tgf-β and Activin [45], was phosphorylated by treatment with Tgf-β1 or Activin A (Fig. 4A), suggesting that HB2 cells are potentially target cells to Tgf-β and Activin. Furthermore, treatment with Tgf-β1 or Activin A for 8 days inhibited lipid accumulation (Fig. 4B), basal Ucp1 expression (Fig. 4C), and expression of the other brown adipocyte-selective genes such as Pgc1α, Cidea and Cox7a (Fig. 4C). In addition, the expression of Pparγ2, C/ebpα and Fabp4 was significantly decreased by treatment with Tgf-β1 or Activin A (Fig. 4D).

To characterize the inhibition of brown adipogenesis by Tgf-β and Activin, time-course changes in the expression of genes related to brown adipogenesis and effects of Tgf-β and Activin were evaluated. Gene transcript levels were increased after the insulin treatment within 2 days for Pparγ2 and within 4 days for Ucp1, Pgc1α and C/ebpα; Tgf-β1 and Activin A completely inhibited the gene induction (Fig. 5A–D). The blockage of insulin-induced expression of Ucp1 and Pparγ2 by Tgf-β1 and Activin A was also verified at the protein level (Fig. 6A). Furthermore, the isoproterenol-induced Ucp1 expression was blunted by Tgf-β1 or Activin A, which was verified at the mRNA level (Fig. 6B) and at the protein level (Fig. 6C). These results clearly indicate that Tgf-β and Activin function as inhibitors for the progression of brown adipogenesis.

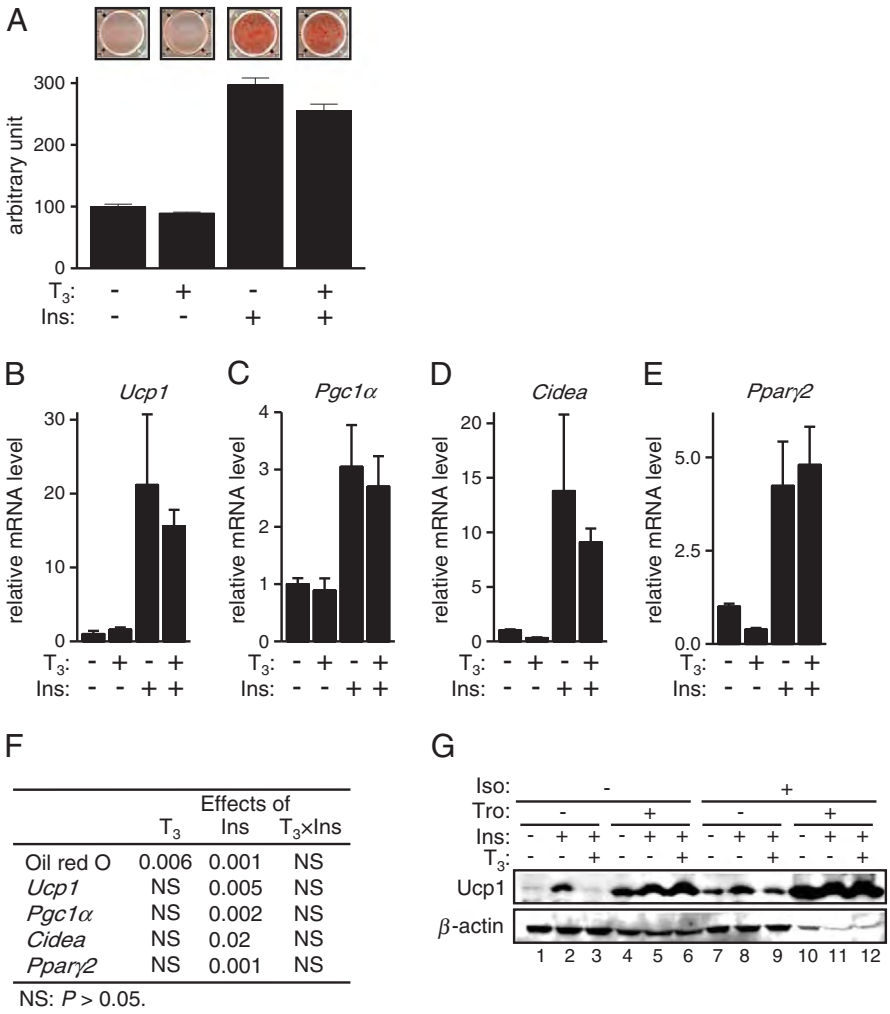

Fig. 3. Insulin is essential for brown adipogenesis. Effects of T_3 and insulin on lipid accumulation (A) and expression of genes related to brown adipogenesis (B–E and G). (A–E) T_3 (50 nM) or insulin (Ins: 20 nM) was added to the culture medium. (B) Lipid accumulation was examined on day 8 by Oil Red O staining (upper panel). After staining, the dye was extracted in 2-propanol, and the amount was quantified by measuring absorbance at 510 nm. The absorbance of the extracted dye from cells treated without T_3 and insulin was set at 100. Data are expressed as the mean ± SE (n = 4). (B–E) The gene transcript levels of Ucp1 (B), Pgc1α (C), Cidea (D) and Pparγ2 (E) on day 8 were measured by RT-qPCR and expressed as ratios to 18S rRNA, with the level in HB2 cells treated without T_3 and insulin set to 1. Data shown are the mean ± SE (n = 4). (F) Results of two-way ANOVA on data of lipid accumulation and gene expression are shown (G) T_3 (50 nM), insulin (20 nM) or troglitazone (Tro: 10 μM) was added to the culture medium for 8 days prior to treatment with or without isoproterenol (Iso: 10 μM) for 4 h. Ucp1 expression (upper panel) was examined by Western blotting, followed by re-blotting by an anti-β-actin antibody (lower panel).

However, when HB2 cells were differentiated under the conditions according to the modified protocol for 3T3-L1 cell differentiation as described above, the inhibitory activity of Tgf-β was less effective than that observed in HB2 cells differentiated with insulin alone; the decrease in lipid accumulation and expression of Ucp1, Cidea, Cox7a, Pparγ2 and C/ebpα were smaller compared with cells differentiated by insulin alone (Supplementary Fig. 2). In addition, no inhibitory effects of Activin A could be detected (Supplementary Fig. 2).

3.5. Srebp1c expression is responsible for brown adipogenesis, which is down-regulated by Tgf-β1 and Activin A

Given that Tgf-β and Activin blocked insulin-mediated induction of adipogenic genes such as Pparγ2 and C/ebpα, we concluded that these growth factors inhibit differentiation into fat cells. To explore how Tgf-β and Activin inhibit adipogenesis, we examined time-course changes in expression of several genes in more depth. We focused on genes that demonstrated modulation of expression levels within 2 days after insulin treatment, specifically those molecules with possible pro-adipogenic activity showing increases in expression and those molecules with putative inhibitory effects on adipogenesis showing decreases in expression. As the candidates with pro-adipogenic activity, we chose C/ebpβ, Krüeppel-like factor (Klf) 5, lysyl oxidase (Lox) and zinc finger protein 423 (Zfp423). Increased expression of C/ebpβ and Klf5 stimulated adipogenesis [46,47], and mesenchymal stem cells and fibroblasts were committed to the adipocyte-lineage cells by expression of Lox and Zfp423, respectively [21,48]. The transcript levels of these genes were not increased within 2 days after the insulin stimulation (Supplementary Fig. 3). We also examined expression of Foxo1, Klf2 and necdin as the putative genes involved in the inhibition of adipogenesis. Expression of Foxo1 and Klf2 inhibited adipocyte differentiation in 3T3-L1 cells [49,50]. Necdin expression was higher in brown preadipocytes that cannot differentiate, and knock-down of Necdin restored adipogenesis [51]. The expression of these genes was not downregulated within 2 days in response to insulin stimulation, although expression of Klf2 gradually tended to be decreased during the culture period (Supplementary Fig. 4). Thus, we conclude that these genes are not candidates that transmit the insulin signal through the regulation of their expression level in order to induce differentiation into brown adipocytes.

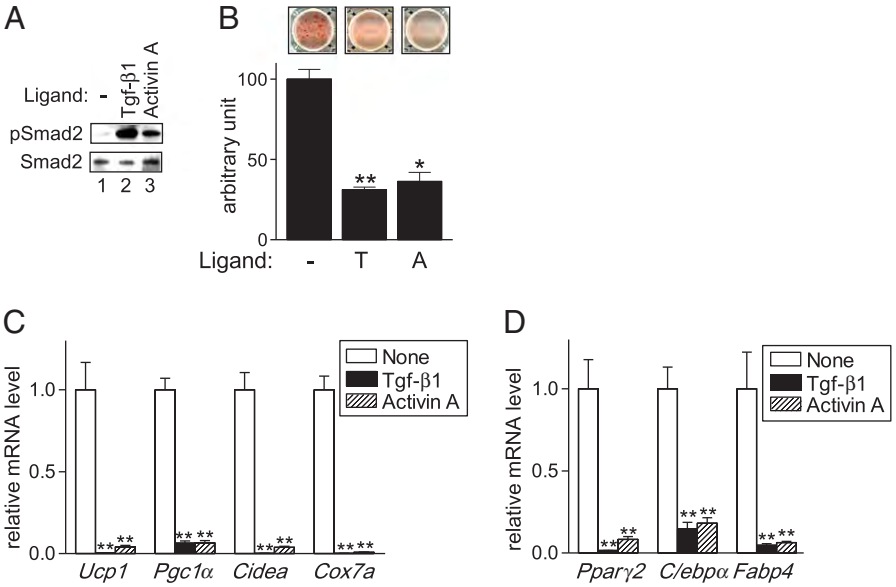

Fig. 4. Tgf-β1 and Activin A inhibit brown adipogenesis. (A) Smad phosphorylation in response to exogenous Tgf-β and Activin. HB2 cells were treated with Tgf-β1 (200 pM) or Activin A (4 nM) for 1 h. Phosphorylated Smad2 was examined by Western blotting, followed by re-blotting with an antibody against Smad2 (fourth panel). (B–D) Effects of Tgf-β1 and Activin A on insulin-mediated lipid accumulation (B) and expression of genes related to brown adipogenesis (C and D). Tgf-β1 (200 pM) or Activin A (4 nM) was added to the culture medium supplemented with insulin from day 0 to 8. (B) Lipid accumulation was examined on day 8 by Oil Red O staining (upper panel). After staining, the dye was extracted in 2-propanol, and the amount was quantified by measuring absorbance at 510 nm. The absorbance of the extracted dye from cells treated without ligand was set at 100. Data are expressed as the mean ± SE (n = 4). * and **: $P < 0.05$ and $P < 0.01$, respectively, vs. cells treated without Tgf-β1 and Activin A. (C and D) The gene transcript levels of Ucp1, Pgc1α, Cidea and Cox7a (C), and Pparγ2, C/ebpα and Fabp4 (D) on day 8 were measured by RT-qPCR and expressed as ratios to 18S rRNA, with the level in HB2 cells treated without Tgf-β1 and Activin A set to 1. Data shown are the mean ± SE (n = 4). **: $P < 0.01$ vs. cells treated without Tgf-β1 and Activin A.

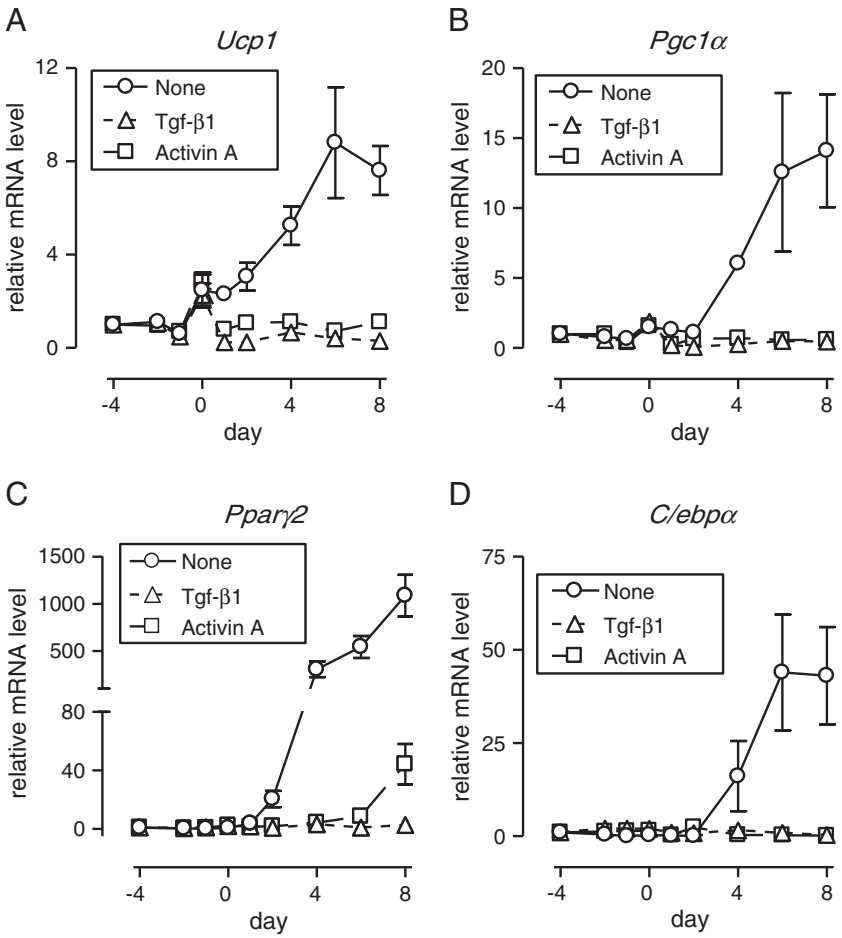

Fig. 5. Tgf-β1 and Activin A inhibit the onset of brown adipogenesis. Time-course changes in the expression of Ucp1 (A), Pgc1α (B), Pparγ2 (C) and C/ebpα (D) related to treatment with Tgf-β1 and Activin A. Tgf-β1 (200 pM) or Activin A (4 nM) was added to the culture medium supplemented with insulin (20 nM) from day 0 to 8. The gene transcript levels of Ucp1 (A), Pgc1α (B), Pparγ2 (C) and C/ebpa (D) were measured by RT-qPCR and expressed as ratios to 18S rRNA, with the level in HB2 cells on day −4 set to 1. Data shown are the mean ± SE (n = 4).

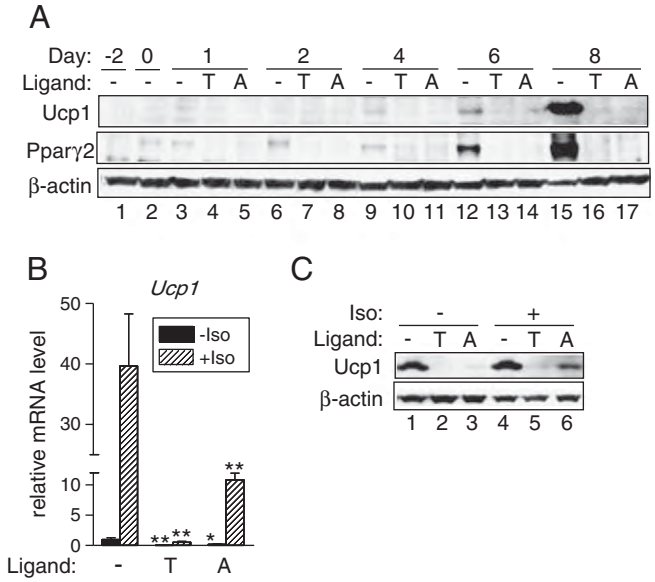

Fig. 6. Tgf-β1 and Activin A blunt responsiveness to β3 adrenergic receptor activation. Effects of Tgf-β1 and Activin A on expression of Ucp1 and Pparγ2. Tgf-β1 (200 pM) or Activin A (4 nM) was added to the culture medium supplemented with insulin from day 0 to 8. (A) Time-course changes in expression of Ucp1 (upper panel) and Pparγ2 (middle panel) were examined by Western blotting, followed by re-blotting with an anti-β-actin antibody (lower panel). (E and F) HB2 cells on day 8 were treated with or without isoproterenol (Iso: 10 μM) for 4 h. (B) The gene transcript level of Ucp1 was measured by RT-qPCR and expressed as a ratio to 18S rRNA, with the level in HB2 cells treated without Tgf-β1 and Activin A and isoproterenol set to 1. Data shown are the mean ± SE (n = 4). * and **: $P < 0.05$ and $P < 0.01$, respectively, vs. respective cells treated with or without isoproterenol and treated without Tgf-β1 and Activin A. (C) Ucp1 expression (upper panel) was examined by Western blotting, followed by re-blotting with an anti-β-actin antibody (lower panel).

We focused on the expression of Srebp1c because its expression is rapidly increased (<6 h) in response to insulin stimulation in 3T3-L1 cells [52] and hepatocytes [53] and because it stimulates adipogenesis [54]. Time-course changes in Srebp1 indicated that Srebp1c (Fig. 7A) but not Srebp1a (Fig. 7B) is increased within 2 days in response to the insulin stimulation. Treatment with Tgf-β1 or Activin A completely inhibited the insulin-induced Srebp1c expression but did not decrease the expression of Srebp1a (Fig. 7A and B).

We also examined insulin-induced genes (Insigs). In hepatocytes, insulin regulates Srebp activity at the mRNA and the post-translational levels; insulin-induced downregulation of Insig-2a expression enables the Srebp cleavage-activating protein/Srebp complex to travel to the Golgi where the transcription factor domain of Srebp is released by two membrane-bound proteases, site-1 protease and site-2 protease [55]. A significant expression of Insig-2a could not be detected in HB2 cells or brown fat (Supplementary Fig. 5A). In addition, the expression of Insig-1 and Insig-2b was not rapidly decreased in response to the insulin stimulation, and treatment with Tgf-β1 or Activin A did not increase the expression of any Insigs (Supplementary Fig. 5B and C). Thus, our results suggest that unlike hepatocytes, insulin may stimulate Srebp1c expression but not post-translational processing in brown preadipocytes, and Tgf-β and Activin negatively regulate Srebp1c expression at the mRNA level.

To understand the role of the induced Srebp1 in response to the insulin stimulation, HB2 preadipocytes were transfected with siRNA for Srebp1. The expression of Srebp1c was significantly down-regulated 4 days after the transfection as expected (Supplementary Fig. 6), but the decreased expression was also detected at 10 days after the transfection. The down-regulation of Srebp1c expression resulted in decreases in lipid accumulation and expression of genes related to brown adipogenesis on day 8 (Fig. 7C–F).

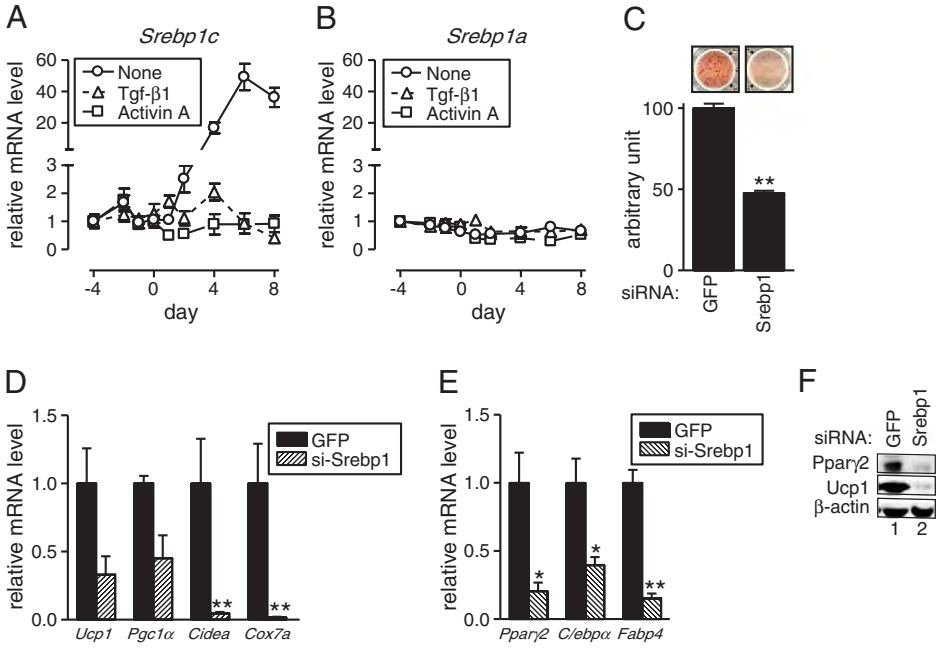

Fig. 7. Srebp1c induction is inhibited by Tgf-β1 and Activin A and is required for brown adipogenesis. (A and B) The gene transcript levels of Srebp1c (A) and Srebp1a (B) were measured by RT-qPCR and expressed as ratios to 18S rRNA, with the level in HB2 cells on day −4 set to 1. Data shown are the mean ± SE (n = 4). (C–F) Effects of knock-down of Srebp1 on insulin-mediated lipid accumulation (C) and expression of genes related to brown adipogenesis (D–F). HB2 cells were transfected with double-stranded RNAi for Srebp1 or GFP. (C) Lipid accumulation was examined on day 8 by Oil Red O staining (upper panel). After staining, the dye was extracted in 2-propanol, and the amount was quantified by measuring absorbance at 510 nm. The absorbance of the extracted dye from cells transfected with double-stranded RNAi for GFP was set at 100. Data are expressed as the mean ± SE (n = 4). **: $P < 0.01$ vs. cells treated with siRNA for GFP. (D and E) The gene transcript levels of Ucp1, Pgc1α, Cidea and Cox7a (D), and Pparγ2, C/ebpα and Fabp4 (E) on day 8 were measured by RT-qPCR and expressed as ratios to 18S rRNA, with the level in HB2 cells transfected with double-stranded RNAi for GFP set to 1. Data shown are the mean ± SE (n = 4). * and **: $P < 0.05$ and $P < 0.01$, respectively, vs. cells treated with siRNA for GFP. (F) Expression of Ucp1 (upper panel) and Pparγ2 (middle panel) on day 8 was examined by Western blotting, followed by re-blotting with an anti-β-actin antibody (lower panel).

4. Discussion

Although research on brown adipose tissue is advancing rapidly, the current information on factors affecting brown adipogenesis is not sufficient. Because members of the Tgf-β family potently regulate differentiation of mesenchymal cells to adipocytes, myocytes, osteoblasts and chondrocytes [14], we expected that these members would also play roles in the differentiation of brown preadipocytes. The present study illustrates that 1) endogenous Bmp activity is relatively constant during brown adipogenesis, 2) endogenous Bmp activity prior to differentiation stimulation is not required for brown adipogenesis, 3) unlike previous results [29], Bmp7 does not act as an inducer of brown adipogenesis, and 4) Tgf-β1 and Activin A act as inhibitors of adipogenesis, most likely through blocking the induction of Srebp1c. These results provide basic information on the regulation of brown adipogenesis by the Tgf-β family. Our results indicate that control of activity of the Tgf-β family is potentially useful for maintenance of energy homeostasis through manipulation of brown adipogenesis.

The role of Bmp in brown adipogenesis shown in this study is distinct from that shown in white adipogenesis [17]. Endogenous Bmp activity prior to onset of the adipogenic program was required for efficient differentiation of white preadipocytes [17], whereas it was not essential in brown preadipocytes. In vivo fate mapping revealed that brown adipocytes but not white adipocytes arise from precursors expressing Myf5, a myogenic molecule [56], indicating that cell lineage of brown adipocytes is distinct from that of white preadipocytes [56]. It is possible that the differences in the role of endogenous Bmp between brown preadipocytes and white preadipocytes are related to the differences of cell lineage.

The activity of Bmp7 during brown adipogenesis is also distinct from that in a different cell line of brown preadipocytes established by use of SV40 T-antigen [29]. Treatment with various Bmp isoforms during the differentiation of brown preadipocytes stimulated lipid accumulation, and Bmp7 selectively upregulated the expression of Ucp1, suggesting a role for Bmp7 as an inducer of brown adipogenesis [29]. In the present study, both Bmp4 and Bmp7 increased lipid accumulation of HB2 adipocytes, which is consistent with the study by Tseng et al. [29]. However, Bmp7 did not affect the basal expression of Ucp1 or the Ucp1 induction in response to β3 adrenergic receptor activation. Although the precise reason for the discrepant results is unclear, there may be differences in the stage of brown preadipocytes (i.e., the extent of commitment as preadipocytes) between HB2 cells and brown preadipocytes used by Tseng et al. [29]. In view of the role of Bmp as a molecule responsible for the commitment of mesenchymal stem cells to adipocyte-lineage cells [21] and osteoblast-lineage cells [57], the brown preadipocytes used by Tseng et al. [29] may be relatively closer to mesenchymal stem cells, as compared with HB2 brown preadipocytes. In fact, Schulz et al. [58] showed that Bmp7 treatment in $Sca1^+/CD45^-/Mac1^-$ stem cells promoted commitment to brown preadipocytes and subsequent brown adipogenesis. Although the reason should be clarified in future, the present results explicitly indicate that Bmp7 during brown adipogenesis is not required for the basal and the isoproterenol-induced expression of Ucp1 in brown adipocytes.

Previous studies revealed the role of Bmp in brown adipocyte development in vivo [29,59,60]; injection of Bmp7-treated mesenchymal stem cells developed a fat pad consisting of brown and white adipocytes [29]. In addition, injection of Bmp2 expressing cells into the skeletal muscle induced emergence of Ucp1-positive cells [59,60]. However, these results do not necessarily contradict from our data indicating dispensable role of Bmp7 in the basal and the induced expression of Ucp1; the in vivo results [29,59,60] could be explained by the role of Bmp as a stimulator of commitment of mesenchymal stem cells to brown preadipocytes.

There are two distinct types of brown adipocytes. There are brown adipocytes in classical brown fat and those in white fat called beige adipocytes or brite adipocytes; beige adipocytes resemble white adipocytes in that they have extremely low basal expression of Ucp1, but they express high Ucp1 similar to classical brown adipocytes in response to cyclic AMP stimulation [61]. Recently, the origin of classical brown adipocytes has been revealed to be different from that of beige adipocytes [61]. Mice lacking functional Smad3, a signal mediator of Tgf-β and Activin signals [45], produce beige adipocytes [62], suggesting that endogenous Tgf-β and Activin inhibit commitment to or differentiation of beige preadipocytes. These results, taken together with the results of the present study using brown preadipocytes originated from classical brown fat, indicate that the Tgf-β and Activin pathway negatively regulates brown adipogenesis, irrespective of brown adipocyte types.

Srebp1c is a membrane-bound and tissue-restricted transcription factor [63] that promotes white adipogenesis. Ectopic expression of Srebp1 has been shown to stimulate differentiation of non-adipogenic NIH-3T3 cells to adipocytes, whereas the expression of dominant-negative Srebp1 inhibited adipogenesis in 3T3-L1 cells [54]. Srebp1c acts as a positive regulator for white adipogenesis through upregulation of Pparγ expression and an increase in the synthesis of putative ligand(s) for Pparγ [64,65]. Despite the differences in the developmental origins of brown and white adipocytes [66], Pparγ expression is essential [10] and is part of a common transcriptional cascade that is shared between the development of brown adipocytes and white adipocytes [7–9]. Therefore, Srebp1c also regulates the process of conversion of preadipocytes to fat cells. In view of Srebp1c as a target molecule of Tgf-β and Activin, Tgf-β and Activin inhibit development of fat cells, resulting in inhibition of the gene induction related to the function of brown adipocytes.

Acknowledgements

We thank Dr. Masayuki Saito for providing cell line. This work was supported by a Grant-in-Aid for Scientific Research (23580368) from The Japan Society for the Promotion of Science.

Appendix A. Supplementary data

Supplementary data to this article can be found online at http://dx.doi.org/10.1016/j.bbagen.2013.06.036.

References

[1] E.D. Rosen, B.M. Spiegelman, Adipocytes as regulators of energy balance and glucose homeostasis, Nature 444 (2006) 847–853.
[2] B. Cannon, J. Nedergaard, Brown adipose tissue: function and physiological significance, Physiol. Rev. 84 (2004) 277–359.
[3] P. Seale, S. Kajimura, W. Yang, S. Chin, L.M. Rohas, M. Uldry, G. Tavernier, D. Langin, B.M. Spiegelman, Transcriptional control of brown fat determination by PRDM16, Cell Metab. 6 (2007) 38–54.
[4] S. Gesta, Y.H. Tseng, C.R. Kahn, Developmental origin of fat: tracking obesity to its source, Cell 131 (2007) 242–256.
[5] J. Nedergaard, T. Bengtsson, B. Cannon, Unexpected evidence for active brown adipose tissue in adult humans, Am. J. Physiol. Endocrinol. Metab. 293 (2007) E444–E452.
[6] B. Cannon, J. Nedergaard, Cell biology: neither brown nor white, Nature 488 (2012) 286–287.
[7] S. Kajimura, P. Seale, B.M. Spiegelman, Transcriptional control of brown fat development, Cell Metab. 11 (2010) 257–262.
[8] D. Richard, F. Picard, Brown fat biology and thermogenesis, Front. Biosci. 16 (2011) 1233–1260.
[9] J. Wu, P. Cohen, B.M. Spiegelman, Adaptive thermogenesis in adipocytes: is beige the new brown? Genes Dev. 27 (2013) 234–250.
[10] H. Koutnikova, T.A. Cock, M. Watanabe, S.M. Houten, M.F. Champy, A. Dierich, J. Auwerx, Compensation by the muscle limits the metabolic consequences of lipodystrophy in PPARγ hypomorphic mice, Proc. Natl. Acad. Sci. U. S. A. 100 (2003) 14457–14462.
[11] H.G. Linhart, K. Ishimura-Oka, F. DeMayo, T. Kibe, D. Repka, B. Poindexter, R.J. Bick, G.J. Darlington, C/EBPα is required for differentiation of white, but not brown, adipose tissue, Proc. Natl. Acad. Sci. U. S. A. 98 (2001) 12532–12537.
[12] M.C. Carmona, R. Iglesias, M.J. Obregón, G.J. Darlington, F. Villarroya, M. Giralt, Mitochondrial biogenesis and thyroid status maturation in brown fat require CCAAT/enhancer-binding protein α, J. Biol. Chem. 277 (2002) 21489–21498.

[13] Q.Q. Tang, M.D. Lane, Adipogenesis: from stem cell to adipocyte, Annu. Rev. Biochem. 81 (2012) 715–736.
[14] R. Derynck, E. Piek, R.A. Schneider, L. Choy, T. Alliston, TGF-β family signaling in mesenchymal differentiation, in: R. Derynck, K. Miyazono (Eds.), The TGF-β Family, Cold Spring Harbor Laboratory Press, Cold Spring Harbor, 2008, pp. 613–665.
[15] L. Choy, R. Derynck, Transforming growth factor-β inhibits adipocyte differentiation by Smad3 interacting with CCAAT/enhancer-binding protein (C/EBP) and repressing C/EBP transactivation function, J. Biol. Chem. 278 (2003) 9609–9619.
[16] S. Hirai, M. Yamanaka, H. Kawachi, T. Matsui, H. Yano, Activin A inhibits differentiation of 3T3-L1 preadipocyte, Mol. Cell. Endocrinol. 232 (2005) 21–26.
[17] M. Suenaga, T. Matsui, M. Funaba, BMP inhibition with dorsomorphin limits adipogenic potential of preadipocytes, J. Vet. Med. Sci. 72 (2010) 373–377.
[18] J. Skillington, L. Choy, R. Derynck, Bone morphogenetic protein and retinoic acid signaling cooperate to induce osteoblast differentiation of preadipocytes, J. Cell Biol. 159 (2002) 135–146.
[19] A. Rebbapragada, H. Benchabane, J.L. Wrana, A.J. Celeste, L. Attisano, Myostatin signals through a transforming growth factor β-like signaling pathway to block adipogenesis, Mol. Cell. Biol. 23 (2003) 7230–7242.
[20] Q.Q. Tang, T.C. Otto, M.D. Lane, Commitment of C3H10T1/2 pluripotent stem cells to the adipocyte lineage, Proc. Natl. Acad. Sci. U. S. A. 101 (2004) 9607–9611.
[21] H. Huang, T.J. Song, X. Li, L. Hu, Q. He, M. Liu, M.D. Lane, Q.Q. Tang, BMP signaling pathway is required for commitment of C3H10T1/2 pluripotent stem cells to the adipocyte lineage, Proc. Natl. Acad. Sci. U. S. A. 106 (2009) 12670–12675.
[22] Y. Irie, A. Asano, X. Cañas, H. Nikami, S. Aizawa, M. Saito, Immortal brown adipocytes from p53-knockout mice: differentiation and expression of uncoupling proteins, Biochem. Biophys. Res. Commun. 255 (1999) 221–225.
[23] U.C. Kozak, L.P. Kozak, Norepinephrine-dependent selection of brown adipocyte cell lines, Endocrinology 134 (1994) 906–913.
[24] S.R. Ross, L. Choy, R.A. Graves, N. Fox, V. Solevjeva, S. Klaus, D. Ricquier, B.M. Spiegelman, Hibernoma formation in transgenic mice and isolation of a brown adipocyte cell line expressing the uncoupling protein gene, Proc. Natl. Acad. Sci. U. S. A. 89 (1992) 7561–7565.
[25] M. Fasshauer, J. Klein, K. Ueki, K.M. Kriauciunas, M. Benito, M.F. White, C.R. Kahn, Essential role of insulin receptor substrate-2 in insulin stimulation of Glut4 translocation and glucose uptake in brown adipocytes, J. Biol. Chem. 275 (2000) 25494–25501.
[26] A.K. Student, R.Y. Hsu, M.D. Lane, Induction of fatty acid synthetase synthesis in differentiating 3T3-L1 preadipocytes, J. Biol. Chem. 255 (1980) 4745–4750.
[27] C. Guerra, C. Roncero, A. Porras, M. Fernández, M. Benito, Triiodothyronine induces the transcription of the uncoupling protein gene and stabilizes its mRNA in fetal rat brown adipocyte primary cultures, J. Biol. Chem. 271 (1996) 2076–2081.
[28] B. García, M.J. Obregón, Growth factor regulation of uncoupling protein-1 mRNA expression in brown adipocytes, Am. J. Physiol. Cell Physiol. 282 (2002) C105–C112.
[29] Y.H. Tseng, E. Kokkotou, T.J. Schulz, T.L. Huang, J.N. Winnay, C.M. Taniguchi, T.T. Tran, R. Suzuki, D.O. Espinoza, Y. Yamamoto, M.J. Ahrens, A.T. Dudley, A.W. Norris, R.N. Kulkarni, C.R. Kahn, New role of bone morphogenetic protein 7 in brown adipogenesis and energy expenditure, Nature 454 (2008) 1000–1004.
[30] J.Y. Lee, N. Takahashi, M. Yasubuchi, Y.I. Kim, H. Hashizaki, M.J. Kim, T. Sakamoto, T. Goto, T. Kawada, Triiodothyronine induces UCP-1 expression and mitochondrial biogenesis in human adipocytes, Am. J. Physiol. Cell Physiol. 302 (2012) C463–C472.
[31] H. Ohno, K. Shinoda, B.M. Spiegelman, S. Kajimura, PPARγ agonists induce a white-to-brown fat conversion through stabilization of PRDM16 protein, Cell Metab. 15 (2012) 395–404.
[32] M. Funaba, M. Murakami, A sensitive detection of phospho-Smad1/5/8 and Smad2 in Western blot analyses, J. Biochem. Biophys. Methods 70 (2008) 816–819.
[33] Y. Furutani, M. Murakami, M. Funaba, Differential responses to oxidative stress and calcium influx on expression of the transforming growth factor-β family in myoblasts and myotubes, Cell Biochem. Funct. 27 (2009) 578–582.
[34] M. Murakami, H. Kawachi, K. Ogawa, Y. Nishino, M. Funaba, Receptor expression modulates the specificity of transforming growth factor-β signaling pathways, Genes Cells 14 (2009) 469–482.
[35] N. Nakano, N. Miyazawa, T. Sakurai, T. Kizaki, K. Kimoto, K. Takahashi, H. Ishida, M. Takahashi, K. Suzuki, H. Ohno, Gliclazide inhibits proliferation but stimulates differentiation of white and brown adipocytes, J. Biochem. 142 (2007) 639–645.
[36] K. Miyazono, Y. Kamiya, M. Morikawa, Bone morphogenetic protein receptors and signal transduction, J. Biochem. 147 (2010) 35–51.
[37] G.D. Cuny, P.B. Yu, J.K. Laha, X. Xing, J.F. Liu, C.S. Lai, D.Y. Deng, C. Sachidanandan, K.D. Bloch, R.T. Peterson, Structure-activity relationship study of bone morphogenetic protein (BMP) signaling inhibitors, Bioorg. Med. Chem. Lett. 18 (2008) 4388–4392.
[38] P.B. Yu, C.C. Hong, C. Sachidanandan, J.L. Babitt, D.Y. Deng, S.A. Hoyng, H.Y. Lin, K.D. Bloch, R.T. Peterson, Dorsomorphin inhibits BMP signals required for embryogenesis and iron metabolism, Nat. Chem. Biol. 4 (2008) 33–41.
[39] C.R. Hunt, J.H. Ro, D.E. Dobson, H.Y. Min, B.M. Spiegelman, Adipocyte P2 gene: developmental expression and homology of 5′-flanking sequences among fat cell-specific genes, Proc. Natl. Acad. Sci. U. S. A. 83 (1986) 3786–3790.
[40] C.M. Steppan, S.T. Bailey, S. Bhat, E.J. Brown, R.R. Banerjee, C.M. Wright, H.R. Patel, R.S. Ahima, M.A. Lazar, The hormone resistin links obesity to diabetes, Nature 409 (2001) 307–312.
[41] P. Puigserver, Z. Wu, C.W. Park, R. Graves, M. Wright, B.M. Spiegelman, A cold-inducible coactivator of nuclear receptors linked to adaptive thermogenesis, Cell 92 (1998) 829–839.
[42] Z. Zhou, S. Yon Toh, Z. Chen, K. Guo, C.P. Ng, S. Ponniah, S.C. Lin, W. Hong, P. Li, Cidea-deficient mice have lean phenotype and are resistant to obesity, Nat. Genet. 35 (2003) 49–56.
[43] K.G. Lambe, J.D. Tugwood, A human peroxisome-proliferator-activated receptor-gamma is activated by inducers of adipogenesis, including thiazolidinedione drugs, Eur. J. Biochem. 239 (1996) 1–7.
[44] A. Hernández, M.J. Obregón, Triiodothyronine amplifies the adrenergic stimulation of uncoupling protein expression in rat brown adipocytes, Am. J. Physiol. Endocrinol. Metab. 278 (2000) E769–E777.
[45] X.H. Feng, R. Derynck, Specificity and versatility in TGF-β signaling through Smads, Annu. Rev. Cell Dev. Biol. 21 (2005) 659–693.
[46] W.C. Yeh, Z. Cao, M. Classon, S.L. McKnight, Cascade regulation of terminal adipocyte differentiation by three members of the C/EBP family of leucine zipper proteins, Genes Dev. 9 (1995) 168–181.
[47] Y. Oishi, I. Manabe, K. Tobe, K. Tsushima, T. Shindo, K. Fujiu, G. Nishimura, K. Maemura, T. Yamauchi, N. Kubota, R. Suzuki, T. Kitamura, S. Akira, T. Kadowaki, R. Nagai, Krüppel-like transcription factor KLF5 is a key regulator of adipocyte differentiation, Cell Metab. 1 (2005) 27–39.
[48] R.K. Gupta, Z. Arany, P. Seale, R.J. Mepani, L. Ye, H.M. Conroe, Y.A. Roby, H. Kulaga, R.R. Reed, B.M. Spiegelman, Transcriptional control of preadipocyte determination by Zfp423, Nature 464 (2010) 619–623.
[49] J. Nakae, T. Kitamura, Y. Kitamura, W.H. Biggs III, K.C. Arden, D. Accili, The forkhead transcription factor Foxo1 regulates adipocyte differentiation, Dev. Cell 4 (2003) 119–129.
[50] J. Wu, S.V. Srinivasan, J.C. Neumann, J.B. Lingrel, The KLF2 transcription factor does not affect the formation of preadipocytes but inhibits their differentiation into adipocytes, Biochemistry 44 (2005) 11098–11105.
[51] Y.H. Tseng, A.J. Butte, E. Kokkotou, V.K. Yechoor, C.M. Taniguchi, K.M. Kriauciunas, A.M. Cypess, M. Niinobe, K. Yoshikawa, M.E. Patti, C.R. Kahn, Prediction of preadipocyte differentiation by gene expression reveals role of insulin receptor substrates and necdin, Nat. Cell Biol. 7 (2005) 601–611.
[52] J.B. Kim, P. Sarraf, M. Wright, K.M. Yao, E. Mueller, G. Solanes, B.B. Lowell, B.M. Spiegelman, Nutritional and insulin regulation of fatty acid synthetase and leptin gene expression through ADD1/SREBP1, J. Clin. Invest. 101 (1998) 1–9.
[53] S. Li, M.S. Brown, J.L. Goldstein, Bifurcation of insulin signaling pathway in rat liver: mTORC1 required for stimulation of lipogenesis, but not inhibition of gluconeogenesis, Proc. Natl. Acad. Sci. U. S. A. 107 (2010) 3441–3446.
[54] J.B. Kim, B.M. Spiegelman, ADD1/SREBP1 promotes adipocyte differentiation and gene expression linked to fatty acid metabolism, Genes Dev. 10 (1996) 1096–1107.
[55] J.L. Goldstein, R.B. Rawson, M.S. Brown, Mutant mammalian cells as tools to delineate the sterol regulatory element-binding protein pathway for feedback regulation of lipid synthesis, Arch. Biochem. Biophys. 397 (2002) 139–148.
[56] P. Seale, B. Bjork, W. Yang, S. Kajimura, S. Chin, S. Kuang, A. Scimè, S. Devarakonda, H.M. Conroe, H. Erdjument-Bromage, P. Tempst, M.A. Rudnicki, D.R. Beier, B.M. Spiegelman, PRDM16 controls a brown fat/skeletal muscle switch, Nature 454 (2008) 961–967.
[57] T. Katagiri, A. Yamaguchi, T. Ikeda, S. Yoshiki, J.M. Wozney, V. Rosen, E.A. Wang, H. Tanaka, S. Omura, T. Suda, The non-osteogenic mouse pluripotent cell line, C3H10T1/2, is induced to differentiate into osteoblastic cells by recombinant human bone morphogenetic protein-2, Biochem. Biophys. Res. Commun. 172 (1990) 295–299.
[58] T.J. Schulz, T.L. Huang, T.T. Tran, H. Zhang, K.L. Townsend, J.L. Shadrach, M. Cerletti, L.E. McDougall, N. Giorgadze, T. Tchkonia, D. Schrier, D. Falb, J.L. Kirkland, A.J. Wagers, Y.H. Tseng, Identification of inducible brown adipocyte progenitors residing in skeletal muscle and white fat, Proc. Natl. Acad. Sci. U. S. A. 108 (2011) 143–148.
[59] E. Olmsted-Davis, F.H. Gannon, M. Ozen, M.M. Ittmann, Z. Gugala, J.A. Hipp, K.M. Moran, C.M. Fouletier-Dilling, S. Schumara-Martin, R.W. Lindsey, M.H. Heggeness, M.K. Brenner, A.R. Davis, Hypoxic adipocytes pattern early heterotopic bone formation, Am. J. Pathol. 170 (2007) 620–632.
[60] E.A. Salisbury, Z.W. Lazard, E.E. Ubogu, A.R. Davis, E.A. Olmsted-Davis, Transient brown adipocyte-like cells derive from peripheral nerve progenitors in response to bone morphogenetic protein 2, Stem Cells Transl. Med. 1 (2012) 874–885.
[61] J. Wu, P. Boström, L.M. Sparks, L. Ye, J.H. Choi, A.H. Giang, M. Khandekar, K.A. Virtanen, P. Nuutila, G. Schaart, K. Huang, H. Tu, W.D. van Marken Lichtenbelt, J. Hoeks, S. Enerbäck, P. Schrauwen, B.M. Spiegelman, Beige adipocytes are a distinct type of thermogenic fat cell in mouse and human, Cell 150 (2012) 366–376.
[62] H. Yadav, C. Quijano, A.K. Kamaraju, O. Gavrilova, R. Malek, W. Chen, P. Zerfas, D. Zhigang, E.C. Wright, C. Stuelten, P. Sun, S. Lonning, M. Skarulis, A.E. Sumner, T. Finkel, S.G. Rane, Protection from obesity and diabetes by blockade of TGF-β/Smad3 signaling, Cell Metab. 14 (2011) 67–79.
[63] J.D. Horton, J.L. Goldstein, M.S. Brown, SREBPs: activators of the complete program of cholesterol and fatty acid synthesis in the liver, J. Clin. Invest. 109 (2002) 1125–1131.
[64] J.B. Kim, H.M. Wright, M. Wright, B.M. Spiegelman, ADD1/SREBP1 activates PPARγ through the production of endogenous ligand, Proc. Natl. Acad. Sci. U. S. A. 95 (1998) 4333–4337.
[65] L. Fajas, K. Schoonjans, L. Gelman, J.B. Kim, J. Najib, G. Martin, J.C. Fruchart, M. Briggs, B.M. Spiegelman, J. Auwerx, Regulation of peroxisome proliferator-activated receptor γ expression by adipocyte differentiation and determination factor 1/sterol regulatory element binding protein 1: implications for adipocyte differentiation and metabolism, Mol. Cell. Biol. 19 (1999) 5495–5503.
[66] N. Petrovic, T.B. Walden, I.G. Shabalina, J.A. Timmons, B. Cannon, J. Nedergaard, Chronic peroxisome proliferator-activated receptor γ (PPARγ) activation of epididymally derived white adipocyte cultures reveals a population of thermogenically competent, UCP1-containing adipocytes molecularly distinct from classic brown adipocytes, J. Biol. Chem. 285 (2010) 7153–7164.

JCM
Journals.ASM.org

Genetic Characteristics of CTX-M-Type Extended-Spectrum-β-Lactamase (ESBL)-Producing *Enterobacteriaceae* Involved in Mastitis Cases on Japanese Dairy Farms, 2007 to 2011

Mamoru Ohnishi,[a] Alexandre T. Okatani,[b] Kazuki Harada,[c] Takuo Sawada,[d] Kenji Marumo,[e] Masaru Murakami,[f] Reiichiro Sato,[g] Hidetake Esaki,[h] Keiko Shimura,[h] Hajime Kato,[a] Naoki Uchida,[a] Toshio Takahashi[d]

Veterinary Clinical Laboratory, Nemuro District Agricultural Mutual Aid Association, Nakashibetsu, Hokkaido, Japan[a]; Laboratory of Veterinary Public Health II, School of Veterinary Medicine, Azabu University, Sagamihara, Kanagawa, Japan[b]; Department of Veterinary Internal Medicine, Tottori University, Tottori-shi, Tottori, Japan[c]; Laboratory of Veterinary Microbiology, School of Veterinary Medicine, Nippon Veterinary and Life Science University, Musashino, Tokyo, Japan[d]; Department of Microbiology and Immunology, Showa University School of Medicine, Shinagawa, Tokyo, Japan[e]; Laboratory of Molecular Biology, School of Veterinary Medicine, Azabu University, Sagamihara, Kanagawa, Japan[f]; Laboratory of Veterinary Obstetrics and Gynecology, School of Veterinary Medicine, Azabu University, Sagamihara, Kanagawa, Japan[g]; Research Institute for Animal Science in Biochemistry and Toxicology, Sagamihara, Kanagawa, Japan[h]

Sixty-five CTX-M-2/15/14 extended-spectrum-β-lactamase-producing *Enterobacteriaceae* were isolated from 258,888 mastitic milk samples from Japanese dairy farms between 2007 and 2011. CTX-M-2-producing *Klebsiella pneumoniae* and CTX-M-15-producing *Escherichia coli* were the predominant strains isolated. There was no predominant clonal type, and clonal diversity was found even in strains isolated from a single farm.

Since 2000, *Escherichia coli* and other *Enterobacteriaceae* species producing CTX-M-type extended-spectrum β-lactamases (ESBLs) (CTX-M) have been commonly isolated from community-acquired extraintestinal infections in humans and their companion animals (1, 2, 3, 4), from food-producing animals (3, 5, 6, 7, 8), and from retail meats, including chicken, beef, and pork (3), worldwide. The CTX-M-type genes are assumed to have been transferred separately to plasmids, including complex class 1 integrons and transposons (9), from chromosomes of different *Kluyvera* species (i.e., *Kluyvera ascorbata*, *K. georgiana*, and *K. cryocrescens*) that live in water, soil, and human and animal intestinal tracts; therefore, CTX-M has been divided into five clusters (CTX-M-1, CTX-M-2, CTX-M-8, CTX-M-9, and CTX-M-25) from base sequence homology (1, 9). CTX-M confers resistance against penicillins, oxyimino-cephalosporins, and monobactams (1, 4). Recently, the CTX-M-15-producing *E. coli* ST131 (O25:H4) clone has emerged as a multidrug-resistant pandemic strain affecting humans worldwide (4).

Bovine mastitis is the most common disease affecting dairy cattle (10). Both *E. coli* and *Klebsiella pneumoniae* often cause life-threatening clinical mastitis (5, 11). The incidence of bovine mastitis has been reported to be higher in Japan (30 to 35 cases per 100 cow-years at risk) (12) than in North America, Europe, and New Zealand (10 to 30 cases per 100 cow-years) (10). Only a few classes of antimicrobials are approved for the treatment of mastitis in Japan; however, large amounts of antimicrobials are used for mastitis treatment, creating selective pressure for drug-resistant organisms (13). In our previous report, we showed that Japanese dairy cattle might be a source of CTX-M-15/2/14- and CMY-2-producing *Enterobacteriaceae* (7). However, few studies have reported the prevalence of *Enterobacteriaceae* producing CTX-M in bovine mastitis (5). The aims of this study were to determine the genetic characteristics, antimicrobial susceptibility, and genetic relatedness of ESBL- and plasmid-mediated AmpC β-lactamase-producing *Enterobacteriaceae* isolated from bovine mastitis cases.

Screening of ESBLs. Bacterial cultures were carried out using standard procedures on a total of milk samples from 258,888 quarters obtained from 176,808 cows affected by (mainly clinical) mastitis on 1,000 dairy farms in the Nemuro Subprefecture of Hokkaido Prefecture, Japan, between February 2007 and April 2011 (14). *Streptococcus* spp. (mainly *Streptococcus uberis*) and *Enterococcus* spp., coagulase-negative staphylococci, *Staphylococcus aureus*, *E. coli*, and *Klebsiella* spp. were the organisms most commonly isolated from culture-positive samples.

Of the isolates, 28,900 were identified as Gram-negative bacilli and were submitted for susceptibility testing by disc diffusion according to the Clinical and Laboratory Standards Institute (CLSI) guidelines (15); 419 isolates were identified as being cefazolin resistant and oxidase negative. These strains were then submitted for CLSI combination disc ESBL confirmatory tests (15) and a chromogenic oxyimino-cephalosporins hydrolysis test (Cica-β-test I; Kanto Chemical, Tokyo, Japan) to detect ESBLs, plasmidic AmpC β-lactamases, and metallo-β-lactamases. Isolates with a positive ESBL confirmatory test and/or Cica-β-test were screened for metallo-β-lactamases using the sodium mercaptoacetic acid (SMA) double-disc synergy test (SMA test) using two Kirby-Bauer discs containing ceftazidime and one disc containing SMA (Eiken Chemical, Tokyo, Japan). The ESBL test-positive *Enterobacteriaceae* isolates were identified using the ID 32 E API system (Sysmex bioMérieux, Tokyo, Japan).

CTX-M genes and antimicrobial susceptibility. The ESBL- and/or Cica-β-test-positive and the SMA-test-negative isolates ($n = 65$) were analyzed by multiplex PCR for the presence of

Received 6 April 2013 Returned for modification 6 May 2013
Accepted 4 July 2013
Published ahead of print 10 July 2013
Address correspondence to Mamoru Ohnishi, monishi@kind.ocn.ne.jp.
Supplemental material for this article may be found at http://dx.doi.org/10.1128/JCM.00920-13.

doi:10.1128/JCM.00920-13

TABLE 1 Origins of CTX-M-2- and CTX-M-14 ESBL-producing *Enterobacteriaceae* isolates other than CTX-M-2-producing *K. pneumoniae* and *E. coli*

Isolate	Isolation date, farm, and cow	Bacterial species	CTX-M genotype	TEM or SHV genotype
MCKo1	July 2008, F, 20	*K. oxytoca*	CTX-M-2	OKP-A
MCKo2	Sept. 2008, H, 22	*K. oxytoca*	CTX-M-2	TEM-1
MCKo3	May 2009, O, 30	*K. oxytoca*	CTX-M-2	TEM-1
MCEa1	Sep. 2009, H, 36	*E. aerogenes*	CTX-M-2	Negative
MCKo4	Jan. 2010, M, 42	*K. oxytoca*	CTX-M-2	Negative
MCCk1	Apr. 2010, U, 47	*C. koseri*	CTX-M-2	Negative
MCCk2	Apr. 2010, V, 48	*C. koseri*	CTX-M-2	Negative
MCKo5	Aug. 2010, F, 50	*K. oxytoca*	CTX-M-2	SHV-1
MCKo6	Sept. 2010, F, 53	*K. oxytoca*	CTX-M-2	Negative
MCK45	Nov. 2010, Y, 57	*K. pneumoniae*	CTX-M-14	Negative
MCK46	Nov. 2010, Y, 57	*K. pneumoniae*	CTX-M-14	Negative

$bla_{\text{CTX-M}}$ genes (16) and plasmid-mediated AmpC β-lactamase genes (i.e., CMY, ACC, FOX, MOX, DHA, CIT, and EBC groups) (17). The CTX-M types of the CTX-M-positive isolates were identified by bidirectional sequencing using group-specific PCR primers for $bla_{\text{CTX-M-1 group}}$ (18), $bla_{\text{CTX-M-2 group}}$ and $bla_{\text{CTX-M-9 group}}$ (19). AmpC-positive isolates were analyzed using type-specific PCR primers (e.g., $bla_{\text{CMY-1}}$ and $bla_{\text{CMY-2}}$ genes), and bla_{TEM} and bla_{SHV} genes were analyzed and bidirectionally sequenced using

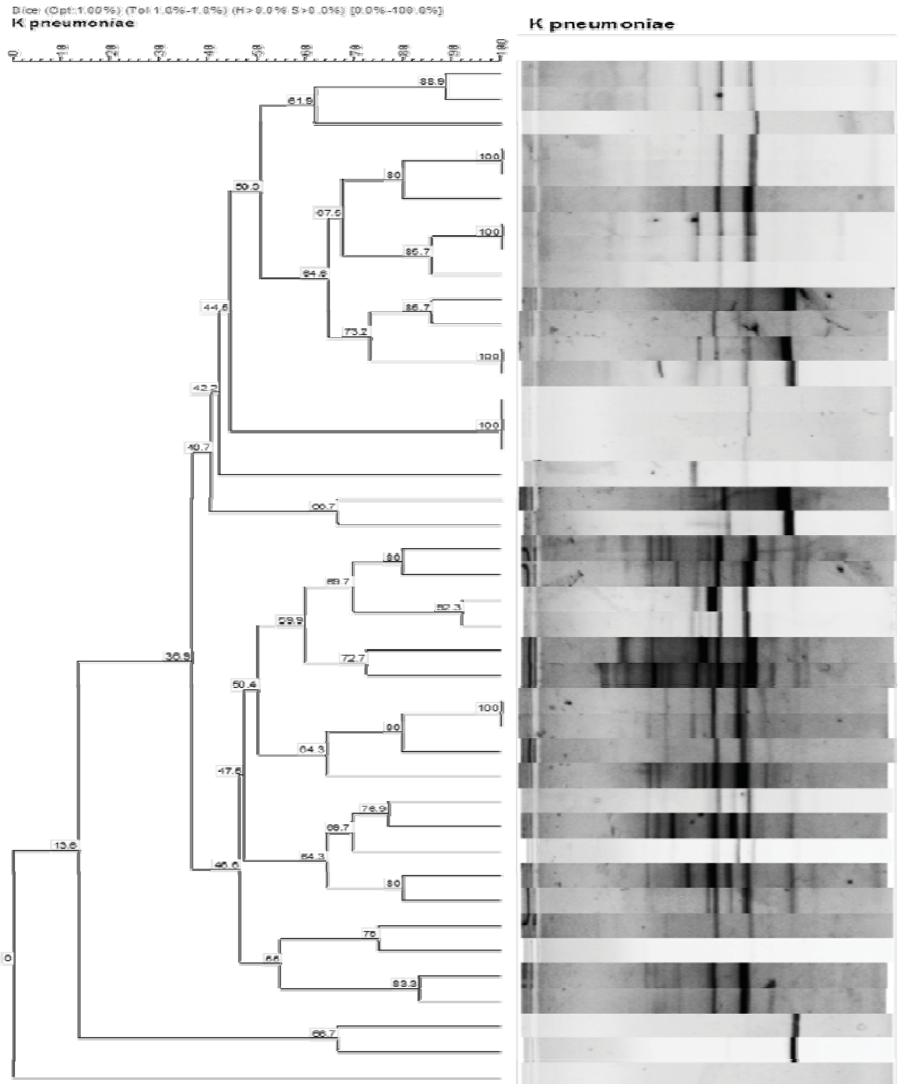

Isolate	Isolation date	Farm: Cow	RAPD Type	SHV, TEM
MCK10	Oct 07	H:11	R8	SHV-98, TEM-1
MCK12	Nov 07	J:14	R8	SHV-108
MCK15	Mar 08	F:16	R30	negative
MCK3A	Feb 07	B:2	R9	SHV-11
MCK3B	Feb 07	B:2	R9	SHV-11
MCK41	Apr 11	F:59	R24	OKP-A
MCK4B	May 07	C:3	R6	SHV-11
MCK4C	May 07	C:3	R6	SHV-11
MCK9	Oct 07	G:10	R7	SHV-11
MCK13	Jan 08	F:15	R15	SHV-11
MCK19	Jun 08	K:19	R2	SHV-98
MCK21	Aug 08	L:21	R1	SHV-11
MCK5	May 07	C:5	R1	SHV-11
MCK17	May 08	F:18	R25	OKP-A
MCK18	Jun 08	F:18	R25	OKP-A
MCK8	Sep 07	F:9	R25	SHV-1
MCK33	Feb 10	M:44	R27	negative
MCK27	July 09	Q:35	R3	SHV-28
MCK40	Oct 10	X:55	R29	negative
MCK24	Mar 09	F:28	R13	SHV-1
MCK7	Aug 07	F:8	R12	SHV-98
MCK36	July 10	L:49	R10	SHV-148
MCK39	Oct 10	W:54	R10	negative
MCK14	Jan 08	F:16	R14	SHV-92
MCK23	Jan 09	F:26	R11	SHV-11
MCK25	Jun 09	M:31	R4	SHV-148
MCK26	July 09	M:33	R4	SHV-148
MCK35	Mar 10	F:46	R5	SHV-148
MCK28	Sep 09	M:31	R32	SHV-148
MCK11	Oct 07	I:13	R17	OKP-A
MCK29	Sep 09	R:38	R18	OKP-A
MCK20	July 08	F:17	R21	OKP-A
MCK30	Nov 09	S:39	R20	OKP-A
MCK6	Aug 07	F:7	R19	SHV-52
MCK34	Mar 10	F:45	R23	SHV-83
MCK38	Sep 10	F:52	R16	SHV-1
MCK31	Dec 09	M:41	R22	OKP-A
MCK32	Feb 10	M:43	R22	OKP-A
MCK22	Oct 08	F:23	R26	SHV-11
MCK37	Aug 10	F:51	R28	SHV-28
MCK16	Mar 08	F:17	R31	OKP-A

FIG 1 RAPD-PCR of 41 *K. pneumoniae* isolates producing CTX-M-2. Cluster analysis was performed by the unweighted pair group method using arithmetic averages with a 1.0% band position tolerance window and 1.0% optimization. DNA relatedness was calculated based on the Dice coefficient. Thirty-two band patterns were typed using similarity cutoff values of approximately ≥85%.

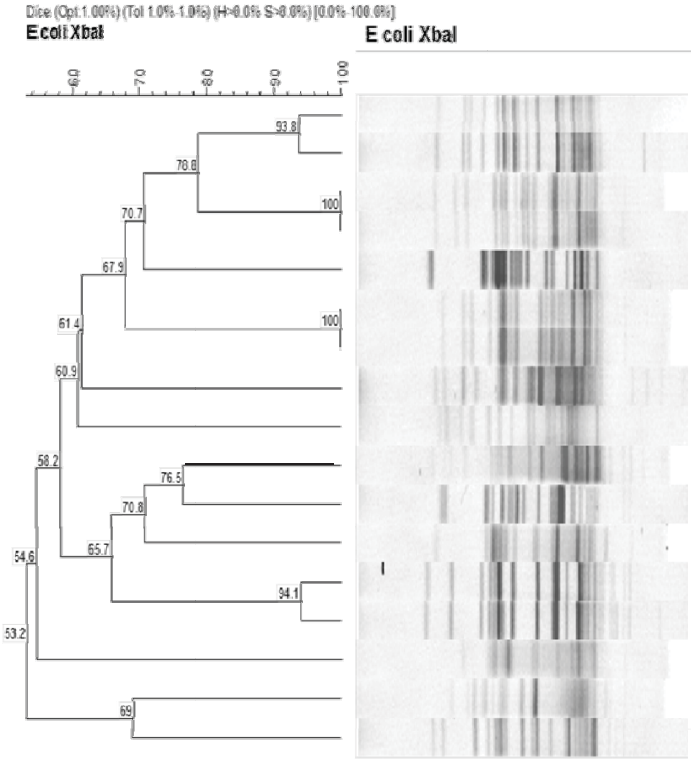

Isolate; Year; Farm: Cow	ST (STcomplex), Serotype	PFGE type	CTX-M	TEM, SHV
MCE4; Dec 08; M: 24	ST58 (155), OUT: HUT	V1	M-15	negative
MCE6; Mar 09; M: 27	ST58 (155), OUT: HUT	V2	M-15	negative
MCE3; Oct 07; D: 12	ST23 (23), OUT: HUT	W	M-14	TEM-1
MCE1; May 07; D: 4	ST23 (23), OUT: HUT	W	M-14	negative
MCE8; Jul 09; M: 32	ST101 (101), O159: H45	X	M-15	negative
FCE3; 07; M: Cow 2	ST1167 (−), OUT: H19	R	M-15	negative
FCE5; 07; M: Cow 4	ST1167(−), O28ac: HUT	R	M-15	negative
MCE13; Dec 10; Z: 58	ST1126 (−), OUT: HUT	AD	M-15	TEM-1
MCE5; Dec 08; M: 25	ST648 (−), O74: HUT	AC	M-15	negative
FCE16; 09; M: Calf 11	ST2325 (−), OUT: HUT	U	M-15	negative
MCE11; Nov 09; T: 40	ST1415(−), OUT: HUT	Y	M-15	TEM-1
MCE2; Aug 07; E: 6	ST1284 (−), OUT: HUT	O	M-15	negative
MCE9; Aug 09; P: 34	ST10 (10), OUT: H5	Z1	M-15	TEM-1
MCE10; Sep 09; P: 37	ST10 (10), OUT: H5	Z2	M-15	TEM-1
FCE4; 07; M: Cow 3	ST540 (−), OUT: HUT	D	M-15	negative
MCE12; Oct 10; M: 56	ST88(23), OUT: H6	AA	M-2	TEM-1
MCE7; Apr 09; N: 29	ST3499(−), OUT: HUT	AB	M-15	negative

FIG 2 PFGE patterns and cluster analysis of 13 CTX-M-producing *E. coli* isolates (MCE1 to 13) from mastitis cases, obtained using XbaI. Cluster analysis was performed by the unweighted pair group method using arithmetic averages with a 1.0% band position tolerance window and 1.0% optimization. DNA relatedness was calculated based on the Dice coefficient. Twelve band patterns were typed using similarity cutoff values of ≥90%. The *Salmonella* strain Braenderup CCUG50923 was used as a marker for assessing PFGE banding patterns. FCE3, -4, -5, and -16 were isolated from feces from cattle on farm M in our previous study (7).

previously described primers (19) (see Table S1 in the supplemental material). Comparison of nucleotide sequences and identification of each CTX-M, TEM, and SHV type were carried out using BLAST (http://blast.ncbi.nlm.nih.gov/Blast.cgi).

For these 65 isolates, the MICs of 23 antimicrobials were determined by the CLSI broth microdilution method (15, 20) using a custom-designed microtiter panel (Opt Panel MP; Kyokuto Pharmaceutical, Tokyo, Japan). The 23 drugs were ampicillin, cefazolin, cefuroxime, ceftazidime, ceftazidime/clavulanic acid, cefotaxime, cefotaxime/clavulanic acid, ceftriaxone, cefpodoxime, ceftiofur, cefquinome, cefepime, cefmetazole, moxalactam, imipenem, meropenem, aztreonam, gentamicin, amikacin, oxytetracycline, trimethoprim-sulfamethoxazole (SXT), enrofloxacin, and ciprofloxacin. Additional susceptibility tests for cefoxitin, kanamycin, chloramphenicol, and levofloxacin were performed by the CLSI disc diffusion method (15, 20). The breakpoints for veterinary pathogens were used for 12 antimicrobial agents (15), and the breakpoints for human *Enterobacteriaceae* isolates were used for the other 12 antimicrobial agents (20). *E. coli* ATCC 25922 and *Pseudomonas aeruginosa* ATCC 27853 were used as quality control strains.

Sixty-five of the 419 cefazolin-resistant isolates were identified as CTX-M-producing strains. Fifty-one isolates (78.5%), which included 41 *K. pneumoniae*, 6 *Klebsiella oxytoca*, 2 *Citrobacter koseri*, 1 *E. coli*, and 1 *Enterobacter aerogenes* isolate, harbored $bla_{\text{CTX-M-2}}$; 10 *E. coli* isolates (15.4%) harbored $bla_{\text{CTX-M-15}}$; and 4 isolates (6.2%; 2 *K. pneumoniae* and 2 *E. coli* isolates) harbored $bla_{\text{CTX-M-14}}$. No isolates contained the plasmidic AmpC gene (Table 1; Fig. 1 and 2).

Thirty-seven (90.2%) of 41 CTX-M-2-producing *K. pneumoniae* isolates also harbored genes encoding SHV-1/11/28/52/83/92/98/108/148, OKP-A, or TEM-1. Four (66.6%) of 6 CTX-M-2-producing *K. oxytoca* isolates also harbored $bla_{\text{TEM-1}}$, $bla_{\text{SHV-1}}$, or $bla_{\text{OKP-A}}$. Four (40.0%) of 10 CTX-M-15-producing *E. coli* isolates also harbored $bla_{\text{TEM-1}}$, but no *E. coli* isolates harbored bla_{SHV} (Table 1; Fig. 1 and 2). The gene sequences of the CTX-M-2/1/9, TEM, and SHV groups were 99 to 100% homologous with those of the CTX-M-2/15/14, TEM-1, and SHV subtypes which are available on GenBank.

The 65 CTX-M-producing *Enterobacteriaceae* were isolated from 61 quarters of 58 mastitis cases on 25 dairy farms in the Nemuro Subprefecture. Each of the 25 farms fed between 180 and 500 Holstein cattle with total mixed ration in free-stall barns or with grass-silage and concentrates fed separately in tie-stall barns; almost all used sawdust bedding. Their rolling yearly herd averages for milk production were 7,800 to 9,500 kg. The 58 affected cows had either subclinical or local to systemic clinical mastitis. Despite antimicrobial treatment, six cows were culled; and the remaining cows' clinical signs resolved 3 to 10 weeks after onset.

The isolation rate of strains producing CTX-M-2/15/14 in bovine mastitis was 0.22% of the 28,900 Gram-negative bacillus isolates from the milk samples from 258,888 quarters of 176,808 cows. The CTX-M-2/15-producing *K. pneumoniae* and *E. coli* strains were the most common ESBL producers causing bovine mastitis in this study. In France, CTX-M-1/14-producing *E. coli* and *K. pneumoniae* strains had an isolation rate of 0.4% (6 of 1,427 *E. coli* and *K. pneumoniae* isolates) from bovine mastitis cases (5). There were no significant ($P > 0.05$) differences between the iso-

TABLE 2 Antimicrobial susceptibilities of isolates producing CTX-M-type ESBL from mastitic cows

Antimicrobial agent[a]	Group 1							Group 2		Group 3	
	MIC range (μg/ml)	MIC_{50} (μg/ml)	MIC_{90} (μg/ml)	Breakpoint (μg/ml; mm)[b]	No. of isolates (%)			MIC range (μg/ml)	No. of resistant isolates (%) (B)[h]	MIC range (μg/ml)	No. of resistant isolates (%) (C)[h]
					Susceptible	Intermediate	Resistant (A)[h]				
Ampicillin[e]	>512	>512	>512	≥32	0	0	49 (100)	>512	10 (100)	>512	6 (100)
Cefazolin[e]	>256	>256	>256	≥32	0	0	49 (100)	>256	10 (100)	>256	6 (100)
Cefuroxime[e]	>256	>256	>256	≥32[c]	0	0	49 (100)	>256	10 (100)	>256	6 (100)
Ceftazidime	≤2 to 64	≤2	≤2	≥16[c]	45 (91.8)	3 (6.1)	1 (2.0)**[B]	16–64	10 (100)**[A,C]	≤2	0**[B]
CAZ/CLA	≤0.25 to >8	≤0.25	0.5					0.5 to >8		≤0.25 to 0.5	
Cefotaxime	≤16 to 256	64	128	≥4[c]	-[g]	4 (8.2)[g]	45 (91.8)	512 to >512	10 (100)	128 to >512	6 (100)
CTX/CLA	≤1 to >8	≤1	≤1					≤1 to 8		≤1	
Cefpodoxime	≤8 to >64	>64	>64	≥16	1 (2.0)	0	48 (98.0)	>64	10 (100)	>64	6 (100)
Ceftriaxone	64 to >512	512	>512	≥4[c]	0	0	49 (100)	>512	10 (100)	512 to >512	6 (100)
Ceftiofur[e]	64 to >512	>512	>512	≥8	0	0	49 (100)	>512	10 (100)	>512	6 (100)
Cefquinome[e]	16 to >128	128	>128	—[d]				>128		>128	
Cefepime	≤8 to 64	≤8	≤8	≥32[c]	43 (87.8)	3 (6.1)	3 (6.1)**[B,C]	>64	10 (100)**[A]	≤8 to >64	4 (66.6)**[A]
Cefmetazole	≤4 to >32	≤4	≤4	≥64[c]	47 (95.9)	0	2 (4.1)	≤4 to 32	0	≤4 to >32	1 (16.6)
Moxalactam	≤8 to >32	≤8	≤8	≥64[c]	48 (98.0)	0	1 (2.0)	≤8	0	≤8	0
Imipenem	≤1	≤1	≤1	≥16	49 (100)	0	0	≤1	0	≤1	0
Meropenem	≤2 to 4	≤2	≤2	≥4[c]	48 (98.0)	0	1 (2)	≤2	0	≤2	0
Aztreonam	≤8 to >64	≤8	16	≥16[c]	—[g]	43 (87.8)[g]	6 (12.2)**[B,]*[C]	64 to >64	10 (100)**[A,]*[C]	≤8 to 32	3 (50)*[A,B]
Gentamicin[e]	≤2 to >16	≤2	≤2	≥16	46 (93.9)	—[d]	3 (6.1)	≤2 to >16	1 (10.0)	≤2	0
Amikacin	≤4 to >16	≤4	≤4	≥64	48 (98.0)	1 (2.0)[g]		≤4 to 8	0	≤4	0
OTET[e]	≤4 to >16	≤4	>16	≥16	24 (49.0)	11 (22.4)	14 (28.6)*[B]	≤4 to >16	7 (70.0)*[A]	≥16	6 (100)
SXT[e]	≤0.5/9.5 to >4/76	≤0.5/9.5	4/76	≥4/76	42 (85.7)	—[d]	7 (14.3)**[B,]*[C]	4/76 to >4/76	7 (70.0)**[A]	≤0.5/9.5 to >4/76	3 (50)*[A]
Enrofloxacin[e]	≤0.25 to 2	≤0.25	2	≥2	45 (91.8)	2 (4.1)	2 (4.1)	≤0.25 to >2	1 (10.0)	≤0.25 to 0.5	0
Ciprofloxacin	≤0.5 to 2	≤0.5	≤0.5	≥4[c]	46 (93.9)	3 (6.1)	0*[B]	≤0.5 to >2	1 (10.0)*[A]	≤0.5 to 1	0
Cefoxitin[f]				≤14 mm[c]	48 (98.0)	1 (2.0)	0*[B,]**[C]	S to R	1 (10.0)*[A]	S to R	1 (16.6)**[A]
Kanamycin[e,f]				≤13 mm	38 (77.6)	1 (2.0)	10 (20.4)*[B, C]	S to R	5(50.0)*[A]	S to R	4 (66.6)*[A]
CHL[f]				≤13 mm	41 (83.7)	0	8 (16.3)	S to R	4 (40.0)	S to R	3 (50)
Levofloxacin[f]				≤13 mm[c]	49 (100)	0	0*[B]	S to R	1(10.0)*[A]	S	0

[a] Assessed by the broth microdilution or disk diffusion method for 41 *K. pneumoniae* and 6 *K. oxytoca* isolates producing CTX-M-2 and 2 *K. pneumoniae* isolates producing CTX-M-14 (group 1), 10 *E. coli* isolates producing CTX-M-15 (group 2), and other *Enterobacteriaceae* isolates producing CTX-M-2 or CTX-M-14 (group 3; CTX-M-2: *E. coli*, n = 1; *C. koseri*, n = 2; *E. aerogenes*, *n* = 1; *E. coli*, CTX-M-14, *n* = 2). Abbreviations: CAZ/CLA, ceftazidime/clavlanic acid; CTX, cefotaxime; OTET, oxytetracycline; SXT, trimethoprim/sulfamethoxazol; CHL, chloramphenicol.

[b] Breakpoint for resistance in accordance with CLSI document M31-A3 (2008) (15) for veterinary pathogens.

[c] Breakpoint for resistance in accordance with CLSI document M100-S21 (2011) (20) for isolates from human infections with *Enterobacteriaceae*.

[d] Breakpoint for resistance or intermediate is not defined in CLSI documents M31-A3 (2008) (15) and M100-S21 (2011) (20).

[e] Antimicrobial agent approved for cattle in Japan; the other 17 antimicrobials in this table are unapproved for cattle.

[f] Susceptibilities were tested by disc diffusion method according to CLSI documents M31-A3 (2008) (15) and M100-S21 (2011) (20).

[g] Isolates in the susceptible, intermediate, and resistant categories could not be differentiated.

[h] Significant differences were determined by the χ^2 test for comparison with the group indicated by the capital letter (A, B, or C): *, $P < 0.05$; **, $P < 0.01$.

lation rates found in our study and the French study (5) by the chi-square test using StatFlex version 6.0 (Artech Co., Ltd., Osaka, Japan). Among human and animal isolates in Western European countries and Japan, the most common CTX-M types were the CTX-M-1 cluster (CTX-M-1/15/55) and CTX-M-9 cluster (CTX-M-9/14/27) (2, 3, 4, 5, 6). Except for the dominance of CTX-M-2, our results are similar to these previous reports. The $bla_{\text{TEM-1}}$, $bla_{\text{SHV-1}}$, and $bla_{\text{SHV-11}}$ genes detected in the present study encode non-ESBL enzymes (21); however, it is not clear whether the SHV-28/52/83/92/98/108/148 and OKP-A are ESBLs, because the kinetic parameters of their purified enzymes were not determined.

Isolates producing CTX-M exhibited high resistance to oxyimino-cephalosporins; however, they exhibited high rates of susceptibility to cefmetazole, moxalactam, imipenem, meropenem, gentamicin, and amikacin. The isolates producing CTX-M-2 and CTX-M-14 showed high rates of susceptibility to ceftazidime and fluoroquinolones. In contrast, the CTX-M-15-producing *E. coli* strains showed significantly higher rates of resistance to ceftazidime, aztreonam, cefepime, SXT, oxytetracycline, ciprofloxacin, levofloxacin, cefoxitin, and kanamycin than CTX-M-2/14-producing *Klebsiella* spp. and/or other CTX-M-2/14-producing *Enterobacteriaceae* ($P < 0.05$) by the chi-square tests (Table 2). Our results are consistent with a previous study (1), and the CTX-M types other than CTX-M-15, CTX-M-16, and CTX-M-27 efficiently hydrolyze cefotaxime and ceftriaxone but not ceftazidime (1).

Molecular subtyping profiles. Random amplified polymorphic DNA (RAPD)-PCR analysis of the 41 CTX-M-2-producing *K. pneumoniae* isolates was performed using the oligonucleotide RAPD7 as previously described (22). Pulsed-field gel electrophoresis (PFGE) of a total of 13 CTX-M-producing *E. coli* isolates was conducted according to the PulseNet standardized laboratory protocol (23) using XbaI (Roche Applied Science, Mannheim, Germany) and the CHEF-DR III electrophoresis systems (Bio-Rad, Hercules, CA). Dendrograms of RAPD patterns and PFGE patterns were analyzed using BioNumerics software, version 5.1 (Applied Maths, Austin, TX). Four CTX-M-15-producing *E. coli* strains isolated from bovine feces on farm M in our previous study (7) were used for comparison with the *E. coli* isolates from mastitis cases.

Multilocus sequence typing (MLST) of the 13 CTX-M-producing *E. coli* isolates was conducted according to standard protocols using the *E. coli* database on the MLST website. (http://mlst.ucc.ie/mlst/dbs/Ecoli). The 13 *E. coli* isolates were serotyped according to O and H antigens using the pathogenic *E. coli* Seiken set 1 and set 2 antisera, respectively (Denka Seiken, Tokyo, Japan).

The 41 CTX-M-2-producing *K. pneumoniae* isolates from 15 farms revealed 32 RAPD types. More than half of the strains were isolated from 2 farms (F and M). The 18 isolates from farm F revealed 16 RAPD types. There was not a predominant RAPD type among the 41 isolates. However, two or three isolates each of *K. pneumoniae* (MCK17/18/8, MCK25/26, and MCK31/32), which were isolated from 2 different cows on same farm (F or M), showed closely related RAPD types (R25, R4, and R22, respectively) (Fig. 1).

The 13 *E. coli* isolates from 7 farms belonged to 10 STs and showed 12 PFGE types. Two isolates each of *E. coli* (MCE1/3, MCE4/6, and MCE9/10), which were isolated from 2 different cows on same farm (D, M, or P), had the same ST and closely related PFGE types (ST23/W, ST58/V1 and V2, and ST10/Z1 and Z2, respectively). There were not any closely related strains between the 5 mastitis and the 4 fecal *E. coli* CTX-M-15-producing isolates from farm M (Fig. 2). Most of the *E. coli* isolates had untypeable O and H antigens (OUT, HUT). Neither *E. coli* clone ST131 (O25:H4) nor enterohemorrhagic *E. coli* O157, O26, or O111 or other serotypes commonly isolated from human infections (8) were detected from the 13 isolates.

The genetic diversity in the 18 *K. pneumoniae* isolates obtained from bovine mastitis cases on farm F suggests that these were opportunistic infections originating from a wide variety of environmental sources (11). However, the presence of some strains of *K. pneumoniae* and *E. coli* showing closely related genotypes, which were isolated from the different cows on the same farm, suggests a contagious infection or an infection from an environmental point source (11). Similar to our results, *E. coli* clones ST10/23/58 producing CTX-M-14/1 have also been isolated from bovine mastitis in France (5). Consistent with this French study, we detected no *E. coli* clone ST131 (O25:H4) producing CTX-M-15/27. Thus, these results suggest that cattle, unlike humans, canines and felines, have little significance as a source of this clone (2, 4). In contrast, recently, two enterohemorrhagic *E. coli* strains (with serotypes O111:H8 and O26:H11) belonging to the B1 phylogenetic group and carrying $bla_{\text{CTX-M-15/9}}$ were isolated from diarrheic cattle in France (8).

In conclusion, the genes encoding CTX-M2/15/14 are present at a low frequency in *Enterobacteriaceae* isolates causing bovine mastitis on Japanese dairy farms. The ESBL producers were dominated by CTX-M-2-producing *K. pneumoniae* and CTX-M-15-producing *E. coli* strains which showed multidrug resistance to ceftazidime, aztreonam, and cefepime. There was not a predominant clonal type, and even the 18 *K. pneumoniae* strains isolated from a single farm showed clonal diversity by molecular subtyping.

REFERENCES

1. **Bonnet R.** 2004. Growing group of extended-spectrum β-lactamases: the CTX-M enzymes. Antimicrob. Agents Chemother. **48:**1–14.
2. **Harada K, Nakai Y, Kataoka Y.** 2012. Mechanisms of resistance to cephalosporin and emergence of O25b-ST131 clone harboring CTX-M-27 β-lactamase in extraintestinal pathogenic *Escherichia coli* from dogs and cats in Japan. Microbiol. Immunol. **56:**480–485.
3. **Overdevest I, Willemsen I, Rijnsburger M, Eustace A, Xu L, Hawkey P, Heck M, Savelkoul P, Vandenbroucke-Grauls C, van der Zwaluw K, Huijsdens X, Kluytmans J.** 2011. Extended-spectrum β-lactamase genes of *Escherichia coli* in chicken meat and humans, the Netherlands. Emerg. Infect. Dis. **17:**1216–1222.
4. **Peiranoa G, Pitou JDD.** 2010. Molecular epidemiology of *Escherichia coli* producing CTX-M β-lactamases: the worldwide emergence of clone ST131 O25:H4. Int. J. Antimicrob. Agents **35:**316–321.
5. **Dahmen S, Métayer V, Gay E, Madec JY, Haenni M.** 2013. Characterization of extended-spectrum beta-lactamase (ESBL)-carrying plasmids and clones of *Enterobacteriaceae* causing cattle mastitis in France. Vet. Microbiol. **162:**793–799.
6. **Madec JY, Poirel L, Saras E, Gourguechon A, Girlich D, Nordmann P, Haenni M.** 2012. Non-ST131 *Escherichia coli* from cattle harbouring human-like $bla_{\text{(CTX-M-15)}}$-carrying plasmids. J. Antimicrob. Chemother. **67:**578–581.
7. **Ohnishi M, Okatani AT, Esaki H, Harada K, Sawada T, Murakami M, Marumo K, Kato Y, Sato R, Shimura K, Hatanaka N, Takahashi T.** 2013. Herd Prevalence of *Enterobacteriaceae* producing CTX-M-type and CMY-2 β-lactamases among Japanese dairy farms. J. Appl. Microbiol. **115:**282–289.
8. **Valat C, Auvray F, Forest K, Metayer V, Gay E, Peytavin de Garam C, Madec JY, Haennia M.** 2012. Phylogenetic grouping and virulence po-

tential of extended-spectrum-β-lactamase-producing *Escherichia coli* strains in cattle. Appl. Environ. Microbiol. **78:**4677–4682.
9. **Cantón R, González-Alba JM, Galán JC.** 2012. CTX-M enzymes: origin and diffusion. Front. Microbiol. **3:**110.
10. **Contreras GA, Rodríguez JM.** 2011. Mastitis: comparative etiology and epidemiology. J. Mammary Gland Biol. Neoplasia **16:**339–356.
11. **Munoz MA, Welcome FL, Schukken YH, Zadoks RN.** 2007. Molecular epidemiology of two *Klebsiella pneumoniae* mastitis outbreaks on a dairy farm in New York State. J. Clin. Microbiol. **45:**3964–3971.
12. **Ministry of Agriculture, Forestry, and Fisheries (MAFF).** 2009. Statistical tables of livestock mutual relief, by agricultural disaster compensation system (2008). MAFF, Tokyo, Japan. (In Japanese.)
13. **Barlow J.** 2011. Mastitis therapy and antimicrobial susceptibility: a multi species review with a focus on antibiotic treatment of mastitis in dairy cattle. J. Mammary Gland Biol. Neoplasia **16:**383–407.
14. **National Mastitis Council.** 1999. Laboratory handbook on bovine mastitis. revised edition. National Mastitis Council, Madison, WI.
15. **Clinical and Laboratory Standards Institute (CLSI).** 2008. Performance standards for antimicrobial disk and dilution susceptibility tests for bacteria isolated from animals; approved standard, 3rd ed, M31-A3. CLSI, Wayne, PA.
16. **Xu L, Ensor V, Gossain S, Nye K, Hawkey P.** 2005. Rapid and simple detection of bla_{CTX-M} genes by multiplex PCR assay. J. Med. Microbiol. **54:**1183–1187.
17. **Pérez-Pérez FJ, Hanson ND.** 2002. Detection of plasmid-mediated AmpC β-lactamase genes in clinical isolates by using multiplex PCR. J. Clin. Microbiol. **40:**2153–2162.
18. **Mena A, Plasencia V, Garcia L, Hidalgo O, Avestarán JI, Alberti S, Borrell N, Pérez JL, Oliver A.** 2006. Characterization of a large outbreak by CTX-M-1-producing *Klebsiella pneumoniae* and mechanisms leading to *in vivo* carbapenem resistance development. J. Clin. Microbiol. **44:**2831–2837.
19. **Kojima A, Ishii Y, Ishihara K, Esaki H, Asai T, Oda C, Tamura Y, Takahashi T, Yamaguchi K.** 2005. Extended-spectrum-β-lactamase-producing *Escherichia coli* strains isolated from farm animals from 1999 to 2002: Report from the Japanese Veterinary Antimicrobial Resistance Monitoring Program. Antimicrob. Agents Chemother. **49:**3533–3537.
20. **Clinical and Laboratory Standards Institute (CLSI).** 2011. Performance standards for antimicrobial susceptibility testing, 21st informational supplement, M100-S21. CLSI, Wayne, PA.
21. **Paterson DL, Bonomo RA.** 2005. Extended-spectrum β-lactamases: a clinical update. Clin. Microbiol. Rev. **18:**657–686.
22. **Ben-Hamouda T, Foulon T, Ben-Cheikh-Masmoudi A, Fendri C, Belhadj O, Ben-Mahrez K.** 2003. Molecular epidemiology of an outbreak of multiresistant *Klebsiella pneumoniae* in a Tunisian neonatal ward. J. Med. Microbiol. **52:**427–433.
23. **Centers for Disease Control and Prevention (CDC).** 2004. One-day (24–28 h) standardized laboratory protocol for molecular subtyping of *Escherichia coli* O157:H7, nontyphoidal *Salmonella* serotypes, and *Shigella sonnei* by pulsed field gel electrophoresis (PFGE). Sections 5.1, 5.2, 5.4. CDC, Atlanta, GA.

Journal of Applied Microbiology

Journal of Applied Microbiology ISSN 1364-5072

ORIGINAL ARTICLE

Herd prevalence of *Enterobacteriaceae* producing CTX-M-type and CMY-2 β-lactamases among Japanese dairy farms

M. Ohnishi[1], A.T. Okatani[2], H. Esaki[3], K. Harada[4], T. Sawada[5], M. Murakami[6], K. Marumo[7], Y. Kato[2], R. Sato[8], K. Shimura[3], N. Hatanaka[2] and T. Takahashi[5]

1 Veterinary Clinical Laboratory, Nemuro District Agricultural Mutual Aid Association, Nakashibetsu, Hokkaido, Japan
2 Laboratory of Veterinary Public Health II, School of Veterinary Medicine, Azabu University, Sagamihara, Kanagawa, Japan
3 Department of Biotechnology, Research Institute for Animal Science in Biochemistry and Toxicology, Sagamihara, Kanagawa, Japan
4 Department of Veterinary Internal Medicine, Tottori University, Tottori-shi, Tottori, Japan
5 Laboratory of Veterinary Microbiology, School of Veterinary Medicine, Nippon Veterinary and Life Science University, Musashino, Tokyo, Japan
6 Laboratory of Molecular Biology, School of Veterinary Medicine, Azabu University, Sagamihara, Kanagawa, Japan
7 Department of Microbiology and Immunology, Showa University School of Medicine, Shinagawa, Tokyo, Japan
8 Laboratory of Gynecology and Obstetrics, School of Veterinary Medicine, Azabu University, Sagamihara, Kanagawa, Japan

Keywords
CMY-2 β-lactamase, CTX-M type ESBLs, dairy cattle, *Escherichia coli*, multilocus sequence typing, pulsed-field gel electrophoresis.

Correspondence
Mamoru Ohnishi, Veterinary Clinical Laboratory, Nemuro District Agricultural Mutual Aid Association, 11-5 Minami, 5 Nishi, Nakashibetsu-cho, Shibetsu-gun, Hokkaido 086-1105, Japan.
E-mail: monishi@kind.ocn.ne.jp

2013/0028: received 6 January 2013, revised 11 March 2013 and accepted 27 March 2013

doi:10.1111/jam.12211

Abstract

Aims: To determine the herd prevalence of *Enterobacteriaceae* producing CTX-M-type extended-spectrum β-lactamases (ESBLs) among 381 dairy farms in Japan.

Methods and Results: Between 2007 and 2009, we screened 897 faecal samples using BTB lactose agar plates containing cefotaxime (2 μg ml^{-1}). Positive isolates were tested using ESBL confirmatory tests, PCR and sequencing for CTX-M, AmpC, TEM and SHV. The incidence of *Enterobacteriaceae* producing CTX-M-15 (n = 7), CTX-M-2 (n = 12), CTX-M-14 (n = 3), CMY-2 (n = 2) or CTX-M-15/2/14 and CMY-2 (n = 4) in bovine faeces was 28/897 (3·1%) faecal samples. These genes had spread to *Escherichia coli* (n = 23) and three genera of *Enterobacteriaceae* (n = 5). Herd prevalence was found to be 20/381 (5·2%) dairy farms. The 23 *E. coli* isolates showed clonal diversity, as assessed by multilocus sequence typing and pulsed-field gel electrophoresis. The pandemic *E. coli* strain ST131 producing CTX-M-15 or CTX-M-27 was not detected.

Conclusions: Three clusters of CTX-M (CTX-M-15, CTX-M-2, CTX-M-14) had spread among Japanese dairy farms.

Significance and Impact of the Study: This is the first report on the prevalence of multidrug-resistant CTX-M-15–producing *E. coli* among Japanese dairy farms.

Introduction

Since 2000, *Escherichia coli* and other *Enterobacteriaceae* species producing CTX-M-type extended-spectrum β-lactamases (ESBLs) (CTX-M) have been commonly isolated from community-acquired extraintestinal infections in humans and their companion animals (Harada *et al.* 2012; Kuroda *et al.* 2012) and faeces of food-producing animals worldwide (Carattoli 2008). The $bla_{\text{CTX-M}}$-related genes were transferred separately to genetic mobilization units (i.e. plasmids) from chromosomes of different *Kluyvera* species (i.e. *K. ascorbata*, *K. georgiana*, *K. cryocrescens*) that live in water, soil, human and animal intestinal tract; and thereby, CTX-M has derived in five CTX-M clusters (CTX-M-1, CTX-M-2, CTX-M-8, CTX-M-9 and CTX-M-25) from base sequence homology. This has been facilitated by genetic mobilization units such as insertion sequences (i.e. IS*Ecp1* or IS*CR1*) (Bonnet 2004; Cantón *et al.* 2012). CTX-M confers resistance against penicillins, oxyimino-cephalosporins (i.e. cefuroxime, cefotaxime,

ceftriaxone, cefpodoxime, ceftazidime, ceftiofur, cefquinome) and monobactams (Bonnet 2004).

Plasmidic CMY-2, derived from the AmpC β-lactamase of *Citrobacter freundii*, became the dominant AmpC β-lactamase among *Enterobacteriaceae*, especially *Salmonella enterica*, in humans and animals throughout the world (Tamang *et al.* 2012). CMY-type β-lactamases are cephamycinases that confer resistance to cephamycins and oxyimino-cephalosporins. Recently, a high incidence of $bla_{\text{CTX-M}}$-positive *E. coli* was found in retail chicken meat. (Overdevest *et al.* 2011). However, few studies have reported the prevalence of *Enterobacteriaceae* producing CTX-M and CMY on dairy farms (Hartmann *et al.* 2012). The aims of the present study were to determine the herd prevalence of *Enterobacteriaceae* producing CTX-M and CMY among numerous dairy farms in Japan and to evaluate the genetic relatedness among *E. coli* isolates derived from dairy cattle by serotyping, multilocus sequence typing (MLST) and pulsed-field gel electrophoresis (PFGE).

Materials and methods

Faecal samples

A total of 897 faecal samples were obtained from each of 897 cattle affected by diarrhoea (caused by i.e. colibacillosis, rotavirus infection, cryptosporidiosis, coccidiosis, parasitic gastroenteritis) or dictyocauliasis; the 897 cattle consisted of 550 calves (<12 months old), 80 heifers ($\geq$12 months old to first parturition) and 267 cows. Faecal samples were submitted daily for clinical diagnostic tests to the clinical laboratory of the Nemuro District Agricultural Mutual Aid Association by nine-member veterinary clinics. The faecal samples were obtained from a total of 381 dairy farms localized in Nemuro Subprefecture of Hokkaido Prefecture, Japan; 475 samples were obtained from 244 dairy farms between May and December in 2007 and 422 samples from 214 dairy farms between July and December in 2009.

Screening, identification, PCR and sequence typing for ESBLs and AmpC producers

The faecal samples were cultured as the first screening for ESBL producers on the day they were submitted to the laboratory. Approximately, 50 μg faeces was streaked directly onto a BTB-lactose agar plate containing 2 μg ml^{-1} cefotaxime and 8 μg ml^{-1} vancomycin (Shiraki *et al.* 2004) and then incubated at 35°C for 40 h.

A total of 250 isolates were tested using the Clinical and Laboratory Standards Institute (CLSI) combination disc ESBL confirmatory tests (CLSI 2008) and a chromogenic oxyimino-cephalosporins hydrolysis test (Cica-β-test I; Kanto Chemical, Tokyo, Japan) to detect ESBLs, plasmidic AmpC β-lactamases and metallo-β-lactamases. All positive isolates were screened for metallo-β-lactamases by the sodium mercaptoacetic acid (SMA) double-disc synergy test using two Kirby–Bauer discs containing ceftazidime and one disc containing SMA (Eiken Chemical, Tokyo, Japan). *Enterobacteriaceae* isolates were identified using the ID 32 E API system (Sysmex bioMérieux, Tokyo, Japan).

All isolates that were positive for the ESBL confirmatory tests and/or the Cica-β-test were analysed by multiplex polymerase chain reaction (PCR) for the presence of $bla_{\text{CTX-M}}$ genes (Xu *et al.* 2007) and plasmid-mediated AmpC β-lactamase genes (i.e. CMY, ACC, FOX, MOX, DHA, CIT and EBC groups) (Pérez-Pérez and Hanson 2002). CTX-M-positive isolates were analysed by bidirectional sequencing using group-specific PCR primers for $bla_{\text{CTX-M-1 group}}$ (Mena *et al.* 2006), $bla_{\text{CTX-M-2 group}}$ and $bla_{\text{CTX-M-9 group}}$ (Kojima *et al.* 2005). The AmpC-positive isolates were analysed using type-specific PCR primers (Kojima *et al.* 2005). The bla_{TEM} and bla_{SHV} genes were analysed using primers (Kojima *et al.* 2005) and bidirectionally sequenced (Table S1).

Antimicrobial susceptibility testing

The minimum inhibitory concentrations (MICs) of 23 antimicrobial agents were determined for isolates positive for CTX-M and/or AmpC genes by broth microdilution using a customer-designed, commercially prepared microtiter panel (Opt Panel MP; Kyokuto Pharmaceutical, Tokyo, Japan), and additional susceptibility test for cefoxitin, kanamycin, chloramphenicol and levofloxacin was performed by disk diffusion according to the CLSI guidelines (CLSI 2008, 2011).

The breakpoints for veterinary pathogens were used for 12 antimicrobial agents (CLSI 2008), and the breakpoints for human *Enterobacteriaceae* isolates were used for the other 12 antimicrobial agents (CLSI 2011). *Escherichia coli* ATCC25922 and *Pseudomonas aeruginosa* ATCC27853 were used as quality-control strains.

Serotyping, MLST and PFGE of *Escherichia coli*

The 23 *E. coli* isolates were serotyped according to O and H antigens using the pathogenic *E. coli* antisera 'SEIKEN' Set 1 for 50 O antigens and Set 2 for 22 H antigens (Denka Seiken, Tokyo, Japan) according to the manufacturer's instructions.

We carried out the amplification and sequencing of seven housekeeping genes and determined the allelic profile and sequence types (STs) using the protocols and

database on the *E. coli* MLST website (http://mlst.ucc.ie/mlst/dbs/Ecoli).

Pulsed-field gel electrophoresis was conducted according the PulseNet standardized laboratory protocol (CDC 2004). The DNA restriction fragments digested with *Xba* I or *Bln* I (Roche Applied Science, Mannheim, Germany) were separated using the CHEF-DR III electrophoresis systems (Bio-Rad, Hercules, CA, USA). Dendrogram of the combined PFGE patterns of *Xba* I and *Bln* I was constructed using BioNumerics software version 5.1 (Applied Maths, Austin, TX, USA) with Dice coefficient and the unweighted pair group method, and the similarity of the average from the two experiments. PFGE types were distinguished at a cut-off of $\geq$90% similarity.

Results

Incidence and herd prevalence of CTX-M and CMY-2 producers

A total of 30 isolates were positive for the ESBL confirmatory tests and/or the Cica-β-test. However, no isolate was SMA test-positive. Twenty-eight CTX-M and/or CMY-2 producers (*E. coli*, n = 23; *Klebsiella pneumoniae*, n = 3; *C. freundii*, n = 1; *Enterobacter cloacae*, n = 1) were isolated from 28 faecal samples obtained from 17 calves, one heifer and 10 cows from 20 dairy farms between 2007 and 2009. The other two isolates identified as *Stenotrophomonas maltophilia* or *Burkholderia cepacia* were negative for CTX-M, AmpC, TEM and SHV genes.

Seven *E. coli* isolates (25·0%) harboured $bla_{\text{CTX-M-15}}$, 12 isolates (42·9%) (*E. coli*, n = 7; *K. pneumoniae*, n = 3; *E. cloacae*, n = 1; *C. freundii*, n = 1) harboured $bla_{\text{CTX-M-2}}$ and three *E. coli* isolates (10·7%) harboured $bla_{\text{CTX-M-14}}$. Two *E. coli* isolates (7·1%) harboured $bla_{\text{CMY-2}}$ and four *E. coli* isolates (14·3%) harboured $bla_{\text{CMY-2}}$ and $bla_{\text{CTX-M-2}}$ or $bla_{\text{CTX-M-15}}$ or $bla_{\text{CTX-M-14}}$. In addition to CTX-M and CMY-2, 12 *E. coli* isolates (42·9%) and one *C. freundii* isolate (3·6%) harboured $bla_{\text{TEM-1}}$ or $bla_{\text{SHV-11}}$ and one *K. pneumoniae* isolate (3·6%) harboured $bla_{\text{TEM-1}}$ and $bla_{\text{SHV-11}}$. Four (50%) of eight CTX-M-15–producing *E. coli* isolates also harboured $bla_{\text{TEM-1}}$ (Tables 1 and 2).

The incidence of *Enterobacteriaceae* producing CTX-M and/or CMY-2 in bovine faeces was 28 (3·1%) of the 897 faecal samples, and the incidence of *E. coli* producing these β-lactamases was 23 of 897 (2·6%). The incidence of *Enterobacteriaceae* was 17 (3·1%) of the 550 faecal samples from calves and 10 (3·7%) of the 267 faecal sam-

Table 1 ST and ST complex (multilocus sequence typing), pulsed-field gel electrophoresis (PFGE) and serotype of 23 β-lactamase–producing *Escherichia coli* isolates obtained from faeces

Isolate	Year, Farm, Cattle	CTX-M, CMY	TEM SHV	ST (ST complex)	PFGE type	O-, H-serotype
FE1	07, IA, Calf1	CTX-M-2	TEM-1	58 (155)	O	OUT*: HUT*
FE2	07, IB, Cow1	CTX-M-2		10 (10)	E	O8: H7
FE3	07, M, Cow2	CTX-M-15	TEM-1	1167 (–)†	K	OUT: H19
FE4	07, M, Cow3	CTX-M-15	TEM-1	540 (–)	U	OUT: HUT
FE5	07, M, Cow4	CTX-M-15		1167 (–)	K	O28ac: HUT
FE6	07, IC, Calf2	CTX-M-2		10 (10)	G	OUT: H51
FE7	07, IC, Calf3	CTX-M-2		10 (10)	G	OUT: HUT
FE8	07, ID, Calf4	CTX-M-14	TEM-1	69 (69)	L	O15: HUT
FE9	07, ID, Calf6	CTX-M-14	TEM-1	10 (10)	C	OUT: H9
FE10	07, IF, Cow5	CMY-2		1284 (–)	D	OUT: HUT
FE11	07, IG, Cow6	CTX-M-15, CMY-2	TEM-1	744 (–)	H	OUT: HUT
FE12	07, IH, Calf7	CTX-M-15		394 (394)	S	O44: H18
FE13	09, IJ, Heifer1	CTX-M-15		1266 (–)	R	OUT: H34
FE14	09, IL, Calf9	CMY-2	TEM-1	2438 (–)	A	OUT: H16
FE15	09, IM, Calf10	CTX-M-14	TEM-1	57 (350)	J	OUT: H6
FE16	09, M, Calf11	CTX-M-15	TEM-1	2325 (–)	M	OUT: HUT
FE17	09, IN, Calf12	CTX-M-2		2324 (–)	P	OUT: HUT
FE18	09, II, Calf13	CTX-M-2	SHV-11	2437 (–)	T	O164: HUT
FE19	09, IP, Cow9	CTX-M-2, CMY-2	SHV-11	44 (10)	I	OUT: HUT
FE20	09, IN, Calf14	CTX-M-14, CMY-2	TEM-1	88 (23)	B	OUT: HUT
FE21	09, IQ, Cow10	CTX-M-2		48 (10)	Q	O124: H4
FE22	09, IR, Calf16	CTX-M-2, CMY-2		46 (46)	N	OUT: HUT
FE23	09, IS, Calf17	CTX-M-15		744 (–)	F	OUT: HUT

*O-antigen untypable: H-antigen untypable.
†ST complex undefined.

Table 2 Origins of CTX-M, TEM and SHV type β-lactamase–producing *Enterobacteriaceae* isolates other than *Escherichia coli*

Isolate	Isolation year, Farm, Cattle	Bacterial species	CTX-M	TEM, SHV
FK1	07, IE, Calf5	*Klebsiella pneumoniae*	CTX-M-2	TEM-1, SHV-11
FK2	09, II, Calf8	*K. pneumoniae*	CTX-M-2	
FK3	09, IK, Cow7	*K. pneumoniae*	CTX-M-2	
FCf1	09, IO, Cow8	*Citrobacter freundii*	CTX-M-2	TEM-1
FEn1	09, II, Calf15	*Enterobacter cloacae*	CTX-M-2	

ples from cows; however, this difference was not significant ($P > 0{\cdot}05$, chi-square test). The herd prevalence of these *Enterobacteriaceae* was 20 (5·2%) of the 381 dairy farms. Four *E. coli* isolates from three cows and one calf on farm M harboured $bla_{\text{CTX-M-15}}$. (Tables 1 and 2).

Antimicrobial susceptibility and antimicrobial use

Isolates producing CTX-M exhibited high resistance to oxyimino-cephalosporins. However, isolates producing CTX-M-2 and CTX-M-14 were highly susceptible to ceftazidime, cefmetazole, moxalactam, carbapenems, gentamicin, amikacin and fluoroquinolones. MICs for ceftazidime, cefmetazole, enrofloxacin and ciprofloxacin were higher for the *E. coli* isolates producing CTX-M-15 and CMY-2 than for the isolates producing CTX-M-2 and CTX-M-14 (Table 3). Most of isolates producing CTX-M, especially CTX-M-15, exhibited resistance to kanamycin, oxytetracycline, chloramphenicol and trimethoprim-sulfamethoxazole (Table 3).

According to the clinical charts and the purchase volume of antimicrobial agents provided by the member veterinary clinics, subcutaneous injections of enrofloxacin (4 mg kg^{-1} body weight) were administered to one cow and one calf with diarrhoea once daily for 2–4 days. The other 26 calves, heifer and cows were not treated with oxyimino-cephalosporins or fluoroquinolones. Between 2006 and 2010, the member veterinary clinics used 2016 daily doses of ceftiofur and 1408 daily doses of enrofloxacin per year for approximately 130 000 cows and heifers of 1000 dairy farms in Nemuro Subprefecture. Daily doses were based on the weight of an adult cow. Neither cefquinome nor the other fluoroquinolones were used.

MLST, serotyping and PFGE of 23 *Escherichia coli* isolates

The 23 *E. coli* isolates were grouped into 18 STs (Table 1). The eight CTX-M-15–producing *E. coli* isolates belonged to six STs and were non-ST131. Four isolates belonged to ST10, and two isolates belonged to ST44 and ST48 [ST 10 complex (STC10)]. Five isolates belonged to ST46 (STC46), ST57 (STC350), ST58 (STC155), ST69 (STC69) and ST88 (STC 23) (Table 1). Most of the *E. coli* isolates were O-antigen untypable (OUT), but the serotypes of six isolates were O8:H7, O15:H-antigen untypable (HUT), O28ac:HUT, O44:H18, O124:H4 and O164:HUT (Table 1).

Pulsed-field gel electrophoresis analysis with *Xba* I and *Bln* I divided the 23 *E. coli* isolates into 21 genetic profiles. Nineteen of the genetic profiles consisted of a single strain. Isolates FE03 and FE05, isolated from two different cows from farm M, showed PFGE type K, ST1167 and $bla_{\text{CTX-M-15}}$; and FE06 and FE07, isolated from two different calves from farm IC, showed PFGE type G, ST10 and $bla_{\text{CTX-M-2}}$, but showed distinct serotypes. Conversely, isolates FE2 and FE9, isolated from two different cows from different farms, showed the ST10 but differed on PFGE type and serotype. The isolates FE11 and FE23, isolated from two different cows from different farms, showed ST744 but differed on PFGE type (Table 1, Fig 1).

Discussion

The incidence and herd prevalence of ESBL-positive *E. coli* among dairy farms in the present study were lower than those of French cattle (Hartmann *et al.* 2012). In agreement with Japanese studies of broiler chickens (Hiroi *et al.* 2012), three CTX-M clusters (CTX-M-15, CTX-M-2 and CTX-M-14) were detected in the present study. Among human and animal isolates in Western European countries, Japan, China, Taiwan and South Korea, the most common CTX-M types were the CTX-M-1 cluster (CTX-M-1, CTX-M-3, CTX-M-15, CTX-M-35, CTX-M-55) and CTX-M-9 cluster (CTX-M-9, CTX-M-14, CTX-M-27); however, CTX-M-15 predominated among human isolates in India (Carattoli 2008; Hawkey 2008; Suzuki *et al.* 2009; Overdevest *et al.* 2011; Harada *et al.* 2012; Kuroda *et al.* 2012; Tamang *et al.* 2012). Except for the dominance of CTX-M-2, our results are similar to these previous reports other than the Indian study.

Most of the CTX-M-15 producers also harboured $bla_{\text{TEM-1}}$ and were resistant to ceftazidime and

Table 3 Antimicrobial susceptibilities of 23 bovine faecal *Escherichia coli* isolates and five *Enterobacteriaceae* isolates other than *E. coli* that produce CTX-M type and/or CMY-2 β-lactamases, as assessed by broth microdilution or disk diffusion method

Antimicrobial agent	*E. coli* CTX-M-15 *n*=7	*E. coli* CTX-M-2 *n*=7	*E. coli* CTX-M-14 *n* = 3	*E. coli* CMY-2 and CTX-M- 2/15/14 *n* = 4	*E. coli* CMY-2 *n* = 2	*Klebsiella pneumoniae*, *n* = 3 *Citrobacter freundii*, *n* = 1 *Enterobacter cloacae*, *n* = 1; CTX-M-2	Breakpoint* μg ml^{-1}; mm
Ampicillin†	256 to >512	>512	>512	>512	>512	512 to >512	≥ 32
Cefazolin†	>256	>256	>256	>256	>256	>256	≥ 32
Cefuroxime†	64 to >256	>256	>256	>256	>256	>256	≥ 32‡
CAZ	16–64	4–32	≤ 2 to 4	32–64	16–64	≤ 2 to 32	≥ 16‡
CAZ/CLA	0·5 to >8	0·5	≤ 0·25 to 1	>8	8 to >8	≤ 0·25 to >8	
CTX	32 to >512	64 to >512	128–512	512 to >512	64 to >512	≤ 16 to >512	≥ 4‡
CTX/CLA	≤ 1 to 8	≤ 1 to 8	≤ 1	8 to >8	>8	≤ 1 to >8	
Cefpodoxime	64 to >64	>64	>64	>64	>64	>64	≥ 8
Ceftriaxone	64 to >512	>512	512 to >512	512 to >512	64 to >512	128 to >512	≥ 4‡
Ceftiofur†	64 to >512	512 to >512	>512	512 to >512	128 to >512	256 to >512	≥ 8
Cefquinome†	16 to >128	32 to >128	64 to >128	128 to >128	32 to >128	16 to >128	-§
Cefepime	8 to >64	≤ 8 to >64	16 to >64	64 to >64	≤ 8 to >64	≤ 8 to >64	≥ 32‡
Cefmetazole	≤ 4 to 32	≤ 4 to 32	≤ 4	32	32	≤ 4 to >32	≥ 64‡
Moxalactam	≤ 8	≤ 8 to 32	≤ 8	≤ 8 to 16	≤ 8	≤ 8 to >32	≥ 64‡
Imipenem	≤ 1	≤ 1	≤ 1	≤ 1	≤ 1	≤ 1	≥ 16
Meropenem	≤ 2	≤ 2 to 4	≤ 2	≤ 2	≤ 2	≤ 2	≥ 4‡
Aztreonam	≤ 8 to >64	16 to >64	≤ 8	64 to >64	≤ 8 to >64	≤ 8 to >64	≥ 16‡
Gentamicin†	≤ 2 to >16	≤ 2 to 4	≤ 2 to >16	≤ 2 to 16	>16	≤ 2	≥ 16
Amikacin	≤ 4 to 8	≤ 4 to 8	≤ 4	≤ 4 to >16	≤ 4	≤ 4 to 8	≥ 64
OTET†	>16	>16	≤ 4 to >16	>16	>16	8 to >16	≥ 16
SXT†	≤ 0·5/9·5 to >4/76	≤ 0·5/9·5 to >4/76	≤ 0·5/9·5 to >4/76	>4/76	>4/76	≤ 0·5/9·5 to >4/76	≥ 4/76
Enrofloxacin†	≤ 0·25 to >2	≤ 0·25	≤ 0·25	0·5 to >2	≥ 2	≤ 0·25	≥ 2
Ciprofloxacin	≤ 0·5 to >2	≤ 0·5	≤ 0·5	≤ 0·5 to >2	>2	≤ 0·5	≥ 4‡
Cefoxitin¶	S to R	S to R	S	R	R	S to R	≤ 14 mm‡
KAN†¶	S to R	S to R	S to R	S to R	R	S to R	≤ 13 mm
CHL¶	S to R	S to R	S to I	S to R	S or R	S to R	≤ 12 mm
LVX¶	S to R	S	S	S to R	S or R	S	≤ 13 mm‡

CAZ, ceftazidime; CLA, clavulanic acid; CTX, cefotaxime; OTET, oxytetracycline; SXT, trimethoprim-sulfamethoxazole; KAN, Kanamycin; CHL, chloramphenicol; LVX, levofloxacin.

*Breakpoint for resistance in accordance with CLSI document M31-A3 (2008) for veterinary pathogens.

†Antimicrobial agent approved for cattle in Japan; the other 17 antimicrobials in this table are unapproved for cattle.

‡Breakpoint for resistance in accordance with CLSI document M100-S21 (2011) for isolates from human infections with *Enterobacteriaceae*.

§Breakpoint for resistance is not defined in CLSI documents M31-A3 (2008) and M100-S21 (2011).

¶Susceptibilities were tested by disk diffusion method according to CLSI documents M31-A3 (2008) and M100-S21 (2011).

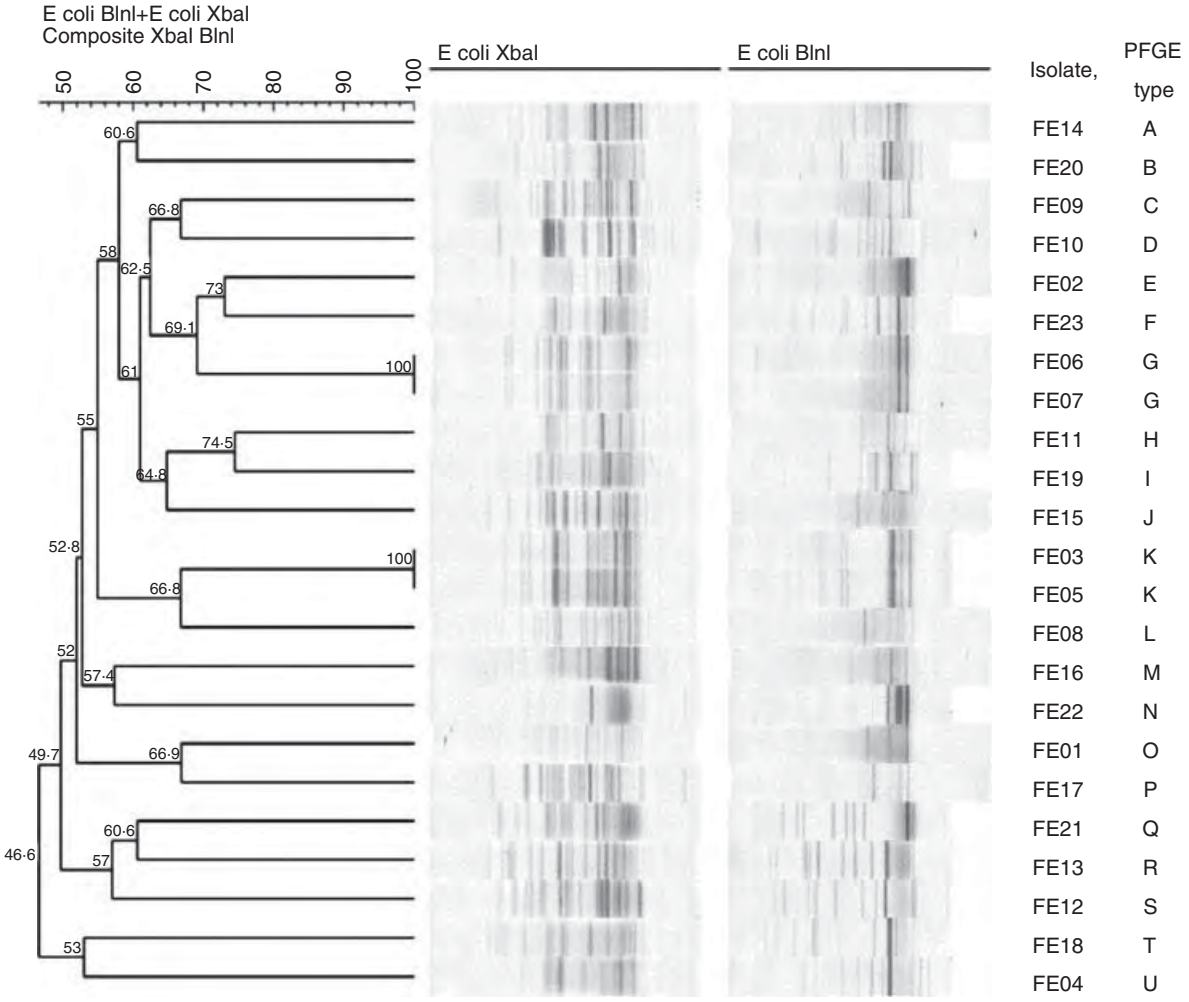

Figure 1 Pulsed-field gel electrophoresis (PFGE) types using *Xbl* 1 and *Bln*-I enzymes of 23 *Escherichia coli* isolates producing CTX-M and CMY-2 from faeces. PFGE analysis with *Xba* I and *Bln* I divided the 23 *E. coli* isolates into 21 genetic profiles. Nineteen of the genetic profiles consisted of a single strain. Dendrogram of the combined PFGE patterns of *Xba* I and *Bln* I was constructed with Dice coefficient and the unweighted pair group method, and the similarity of the average from the two experiments. PFGE types were distinguished at a cut-off of $\geq$90% similarity.

fluoroquinolones. CTX-M types other than CTX-M-15, CTX-M-16 and CTX-M-27 efficiently hydrolyse cefotaxime and ceftriaxone but not ceftazidime (Bonnet 2004). The $bla_{\text{TEM-1}}$ and $bla_{\text{SHV-11}}$ genes detected in the present study encode non-ESBL enzymes (Paterson and Bonomo 2005).

Annual ceftiofur and enrofloxacin use was low in the large dairy cattle population evaluated by our clinics, and their use does not appear to be a major risk factor for ESBL-producing *Enterobacteriaceae* infections. An earlier human study (Colodner *et al.* 2004) identified the previous use of fluoroquinolones, penicillins and second- and third-generation cephalosporins as risk factors for ESBL-producing *E. coli* and *K. pneumoniae* infections. Thus, the spread of $bla_{\text{CTX-M}}$ and $bla_{\text{CMY-2}}$ may be due in part to the frequent use of mastitis preparations consisting of first- and second-generation cephalosporins in member veterinary clinics in Nemuro Subprefecture and using waste milk mixed with cephalosporins to feed calves. Previous studies (Lowrance *et al.* 2007; Daniels *et al.* 2009) revealed that ceftiofur use had a transient effect on the selection of ceftiofur resistance in commensal *E. coli* at the individual calf level. However, most CTX-M-15 producers are resistant to both oxyimino-cephalosporins and fluoroquinolones.

Consistent with our findings, the *E. coli* clones ST10, ST44, ST48, ST57, ST58, ST69 and ST88, producing CTX-M-1, CTX-M-2, CTX-M-9, CTX-M-14, CTX-M-15, SHV-5 and SHV-12 were isolated from chicken caeca in the UK (Randall *et al.* 2011), and retail chicken meat in

the Netherlands (Overdevest *et al.* 2011). The clonal diversity of STs and PFGE types observed in our study among bovine *E. coli* strains harbouring the same type of bla_{CTX-M} is in agreement with a recent canine study (Tamang *et al.* 2012). Both PFGE and MLST were unable to differentiate isolates FCE03 and FCE05 and isolates FCE06 and FCE07, which differed according to serotype, indicating that the two clusters of two isolates each were closely related (Table 1, Fig 1). However, four ST10 isolates showed three distinct PFGE types, and two ST744 isolates showed two distinct PFGE types. It should be noted that PFGE showed a greater discriminatory ability than MLST in the present study, differentiating strains from different farms and strains of different serotypes. In general, housekeeping genes have low mutation rates, but PFGE is thought to easily detect mutations in *E. coli*.

In this study, we did not detect the CTX-M-15–producing *E. coli* ST131 (O25:H4), which is a worldwide pandemic multidrug-resistant strain that infects humans (Kuroda *et al.* 2012), nor epidemic *E. coli* strains ST38 (O86:H18) or ST131 (O25:H4), which produce the CTX-M-9 group of ESBLs that infect humans, canines and felines in Japan (Suzuki *et al.* 2009; Harada *et al.* 2012). Madec *et al.* (2012) revealed that $bla_{CTX-M-15}$–carrying plasmids from cattle-derived non-ST131 *E. coli* isolates were highly similar to those found in human-derived ST131 *E. coli* isolates.

Recently, a low incidence of bla_{CTX-M}-positive *E. coli* was reported in retail beef (Overdevest *et al.* 2011), suggesting that bovine bla_{CTX-M}-positive *E. coli* may pose a relatively low risk to public health.

In conclusion, the incidence of *E. coli* and three genera of *Enterobacteriaceae* producing CTX-M-15, CTX-M-2, CTX-M-14 or CMY-2 in bovine faeces was 3·1% of the 897 faecal samples. The herd prevalence was 5·2% of the 381 dairy farms in Nemuro Subprefecture, Japan. The 23 *E. coli* isolates showed clonal diversity, as assessed by MLST analysis and PFGE typing. The eight *E. coli* isolates producing CTX-M-15 belonged to six STs and were non-ST131; most were resistant to ceftazidime and fluoroquinolones. The present results indicate that dairy cattle are a potential reservoir of ESBL-producing bacteria. Thus, routine monitoring for CTX-M (especially CTX-M-15) and CMY-2 producers derived from faeces and mastitis milk and the prudent use of antimicrobial agents are necessary to prevent their clonal spread.

References

Bonnet, R. (2004) Growing group of extended-spectrum β-lactamases: the CTX-M enzymes. *Antimicrob Agents Chemother* **48**, 1–14.

Cantón, R., González-Alba, J.M. and Galán, J.C. (2012) CTX-M enzymes: origin and diffusion. *Front Microbial* **3**, doi: 10.3389/fmicb.2012.00110.

Carattoli, A. (2008) Animal reservoirs for extended spectrum β-lactamase producers. *Clin Microbiol Infect* **14**(Suppl 1), 117–123.

Centers for Disease Control and Prevention (CDC) (2004) *One-day (24-28 h) standardized laboratory protocol for molecular subtyping of Escherichia coli* O157:H7, non-typhoidal *Salmonella* serotypes, and *Shigella sonnei* by pulsed field gel electrophoresis (PFGE). Sections 5.1, 5.2, 5.4. Atlanta, GA: CDC.

Clinical and Laboratory Standards Institute (CLSI) (2008) *Performance Standards for Antimicrobial Disk and Dilution Susceptibility Tests for Bacteria Isolated from Animals; Approved Standard*, 3rd edn, M31–A3. Wayne, PA: CLSI.

Clinical and Laboratory Standards Institute (CLSI) (2011) *Performance Standards for Antimicrobial Susceptibility Testing, 21st Informational Supplement, M100–S21*. Wayne, PA: CLSI.

Colodner, R., Rock, W., Chazan, B., Keller, N., Guy, N., Sakran, W. and Raz, R. (2004) Risk factors for the development of extended-spectrum beta-lactamase-producing bacteria in nonhospitalized patient. *Eur J Clin Microbiol Infect Dis* **23**, 163–167.

Daniels, J.B., Call, D.R., Hancock, D., Sischo, W.M., Baker, K. and Besser, T.E. (2009) Role of ceftiofur in selection and dissemination of *bla* CMY-2-mediated cephalosporin resistance in *Salmonella enterica* and commensal *Escherichia coli* isolates from cattle. *Appl Environ Microbiol* **75**, 3648–3655.

Harada, K., Nakai, Y. and Kataoka, Y. (2012) Mechanisms of resistance to cephalosporin and emergence of O25b-ST131 clone harboring CTX-M-27 β-lactamase in extraintestinal pathogenic *Escherichia coli* from dogs and cats in Japan. *Microbiol Immunol* **56**, 480–485.

Hartmann, A., Locatelli, A., Amoureux, L., Depret, G., Jolivet, C., Gueneau, E. and Neuwirth, C. (2012) Occurrence of CTX-M producing *Escherichia coli* in soils, cattle, and farm environment in France (Burgundy region). *Front Microbial* **3**, doi: 10.3389/fmicb.2012.00083.

Hawkey, P.M. (2008) Prevalence and clonality of extended-spectrum β-lactamases in Asia. *Clin Microbiol Infect* **14** (Suppl 1), 117–123.

Hiroi, M., Yamazaki, F., Harada, T., Takahashi, N., Iida, N., Noda, Y., Yagi, M., Nishio, T. *et al.* (2012) Prevalence of extended-spectrum β-lactamase-producing *Escherichia coli* and *Klebsiella pneumoniae* in food-producing animals. *J Vet Med Sci* **74**, 189–195.

Kojima, A., Ishii, Y., Ishihara, K., Esaki, H., Asai, T., Oda, C., Tamura, Y., Takahashi, T. *et al.* (2005) Extended-spectrum-β-lactamase-producing *Escherichia coli* strains isolated from farm animals from 1999 to 2002: Report from the Japanese Veterinary Antimicrobial Resistance

Monitoring Program. *Antimicrob Agents Chemother* **49**, 3533–3537.

Kuroda, H., Yano, H., Hirakata, Y., Arai, K., Endo, S., Kanamori, H., Yamamoto, H., Ichimura, S. *et al.* (2012) Molecular characteristics of extended-spectrum β-lactamase-producing *Escherichia coli* in Japan: emergence of CTX-M-15-producing *E. coli* ST131. *Diagn Microbiol Infect Dis* **74**, 201–203.

Lowrance, T.C., Loneragan, G.H., Kunze, D.J., Platt, T.M., Ives, S.E., Scott, H.M., Norby, B., Echeverry, A. *et al.* (2007) Changes in antimicrobial susceptibility in a population of *Escherichia coli* isolated from feedlot cattle administered ceftiofur crystalline-free acid. *Am J Vet Res* **68**, 501–507.

Madec, J.Y., Poirel, L., Saras, E., Gourguechon, A., Girlich, D., Nordmann, P. and Haenni, M. (2012) Non-ST131 *Escherichia coli* from cattle harbouring human-like *bla* $_{(CTX-M-15)}$-carrying plasmids. *J Antimicrob Chemother* **67**, 578–581.

Mena, A., Plasencia, V., Garcia, L., Hidalgo, O., Avestarán, J.I., Alberti, S., Borrell, N., Pérez, J.L. *et al.* (2006) Characterization of a large outbreak by CTX-M-1-producing *Klebsiella pneumoniae* and mechanisms leading to *in vivo* carbapenem resistance development. *J Clin Microbiol* **44**, 2831–2837.

Overdevest, I., Willemsen, I., Rijnsburger, M., Eustace, A., Xu, L., Hawkey, P., Heck, M., Savelkoul, P. *et al.* (2011) Extended-spectrum β-lactamase genes of *Escherichia coli* in chicken meat and humans, the Netherlands. *Emerg Infect Dis* **17**, 1216–1222.

Paterson, D.L. and Bonomo, R.A. (2005) Extended-spectrum β-lactamases: a clinical update. *Clin Microbiol Rev* **18**, 657–686.

Pérez-Pérez, F.J. and Hanson, N.D. (2002) Detection of plasmid-mediated AmpC β-lactamase genes in clinical isolates by using multiplex PCR. *J Clin Microbiol* **40**, 2153–2162.

Randall, L.P., Clouting, C., Horton, R.A., Coldham, N.G., Wu, G., Clifton-Hadley, F.A., Davies, R.H. and Teale, C.J. (2011) Prevalence of *Escherichia coli* carrying extended-spectrum β-lactamases (CTX-M and TEM-52) from broiler chickens and turkeys in Great Britain between 2006 and 2009. *J Antimicrob Chemother* **66**, 86–95.

Shiraki, Y., Shibata, N., Doi, Y. and Arakawa, Y. (2004) *Escherichia coli* producing CTX-M-2 β-lactamase in cattle, Japan. *Emerg Infect Dis* **10**, 69–75.

Suzuki, S., Shibata, N., Yamane, K., Wachino, J., Ito, K. and Arakawa, Y. (2009) Change in the prevalence of extended-spectrum β-lactamase-producing *Escherichia coli* in Japan by clonal spread. *J Antimicrob Chemother* **63**, 72–79.

Tamang, M.D., Nam, H.-M., Jang, G.-C., Kim, S.-R., Chae, M.H., Jung, S.-C., Byun, J.-W., Park, Y.H. *et al.* (2012) Molecular characterization of extended-spectrum-β-lactamase-producing and plasmid-mediated AmpC β-lactamase-producing *Escherichia coli* isolated from stray dogs in South Korea. *Antimicrob Agents Chemother* **56**, 2705–2712.

Xu, L., Ensor, V., Gossain, S., Nye, K. and Hawkey, P. (2007) Rapid and simple detection of bla_{CTX-M} genes by multiplex PCR assay. *J Med Microbiol* **54**, 1183–1187.

Supporting Information

Additional Supporting Information may be found in the online version of this article:

Table S1 PCR primers used for detection and sequencing of CTX-M, CMY, AmpC, TEM, and SHV type β-lactamases.

NOTE *Bacteriology*

Correlation of Age with Distribution of Periodontitis-Related Bacteria in Japanese Dogs

Norihiko HIRAI[1)]**, Mitsuyuki SHIRAI[1)]**, Yukio KATO[2)]**, Masaru MURAKAMI[3)], Ryota NOMURA[4)], Yoshie YAMASAKI[5)], Soraaki TAKAHASHI[1)], Chihiro KONDO[1)], Michiyo MATSUMOTO-NAKANO[5)], Kazuhiko NAKANO[4)] and Fumitoshi ASAI[1)]*

[1)]*Department of Pharmacology, School of Veterinary Medicine, Azabu University, Sagamihara, Kanagawa 252–5201, Japan*
[2)]*Department of Veterinary Public Health II, School of Veterinary Medicine, Azabu University, Sagamihara, Kanagawa 252–5201, Japan*
[3)]*Department of Molecular Biology, School of Veterinary Medicine, Azabu University, Sagamihara, Kanagawa 252–5201, Japan*
[4)]*Department of Pediatric Dentistry, Osaka University Graduate School of Dentistry, Suita, Osaka 565–0871, Japan*
[5)]*Department of Pediatric Dentistry, Okayama University Graduate School of Medicine, Dentistry and Pharmaceutical Sciences, Okayama 700–8556, Japan*

(Received 24 January 2013/Accepted 26 February 2013/Published online in J-STAGE 12 March 2013)

ABSTRACT. We analyzed the distribution of 11 periodontitis-related bacterial species in dental plaque collected from 176 Japanese dogs divided into young (less than 2 years of age), middle-aged (2–7 years of age) and elderly (more than 8 years of age) groups using a polymerase chain reaction method. Clinical examination revealed that no dogs in the young group were affected by periodontitis, whereas the rates for gingivitis and periodontitis were high in the middle-aged and elderly groups. In addition, the total numbers of bacterial species in the middle-aged and elderly groups were significantly greater than in the young group. Our findings suggest that age is an important factor associated with the distribution of periodontitis-related bacteria and periodontal conditions in dogs.
KEY WORDS: age, canine, dental plaque, periodontitis, periodontitis-related bacteria.

doi: 10.1292/jvms.13-0041; *J. Vet. Med. Sci.* 75(7): 999–1001, 2013

Periodontal diseases are quite commonly identified in dogs. The diseases are composed of gingivitis, a reversible condition that features limited inflammation of gingival tissue, and periodontitis, which indicates destruction of periodontal tissues, such as the cementum, periodontal ligaments and supportive bone [8]. It has been summarized that the distribution frequency of gingivitis in dogs aged from 0 to 14 years old (average; approximately 6 years old) ranges from 95–100%, while that of periodontitis is from 50–70% [3].

Our previous study analyzed the distribution of 10 human periodontitis-related species in dogs and found that specific species, such as *Tannerella forsythia* and *Campylobacter rectus*, were frequently detected [5]. In addition, *Porphyromonas gulae*, a major pathogen of periodontitis in dogs [2], was also detected at a high frequency [5]. On the other hand, the detection rates of other species, including *Porphyromonas gingivalis*, *Treponema denticola*, *Capnocytophaga ochracea*, *Capnocytophaga sputigena*, *Prevotella intermedia*, *Prevotella nigrescens*, *Aggregatibacter actinomycetemcomitans* and *Eikenella corrodens*, were quite low [5]. In addition, several periodontopathic species were shown to be possibly transmitted between dogs and their owners, although the distribution of periodontopathic species in both is generally different [12].

In the present study, to investigate the influence of the age of dogs on the periodontal conditions and the distribution of the periodontitis-related species, 176 Japanese dogs were analyzed. On the basis of the age classifications of young (less than 2 years of age), middle-aged (2–7 years of age) and elderly (more than 8 years of age) dogs [6], the 176 dogs were classified into the young (n=39), middle-aged (n=62) and elderly (n=75) groups. The protocols used in this study were approved by Azabu University, Osaka University Graduate School of Dentistry and Okayama University Graduate School of Medicine, Dentistry and Pharmaceutical Sciences. The owners of the dogs also approved their participation in this study.

Periodontal condition was evaluated by measuring several parameters of a representative tooth (mandibular left canine), as previously described [13]. Briefly, periodontal pocket depth was measured to the nearest millimeter around the circumference of each tooth from the gingival margin to the deepest probing point, using a round-ended probe tip 0.4 mm in diameter, with the maximum value recorded. A periodontal pocket depth of 3 mm or less for large dogs, and 2 mm or less for medium and small dogs was regarded as healthy. In addition, no bleeding on probing, no pus discharge and no tooth mobility were regarded as healthy criteria. When deeper periodontal pockets and/or bleeding on probing were observed, the dogs were diagnosed with gingivitis or periodontitis. Periodontitis was diagnosed by pathological mobility due to obvious destruction of periodontal tissues, such as alveolar bone.

*CORRESPONDENCE TO: ASAI, F., Department of Pharmacology, School of Veterinary Medicine, Azabu University, 1–17–71 Fuchinobe, Chuo-ku, Sagamihara, Kanagawa 252–5201, Japan.
e-mail: asai@azabu-u.ac.jp
**These authors contributed equally to this work.

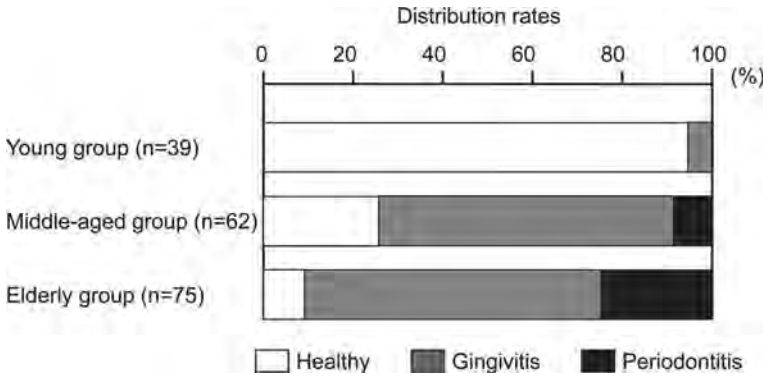

Fig. 1. Distribution rates of periodontal conditions in each age group.

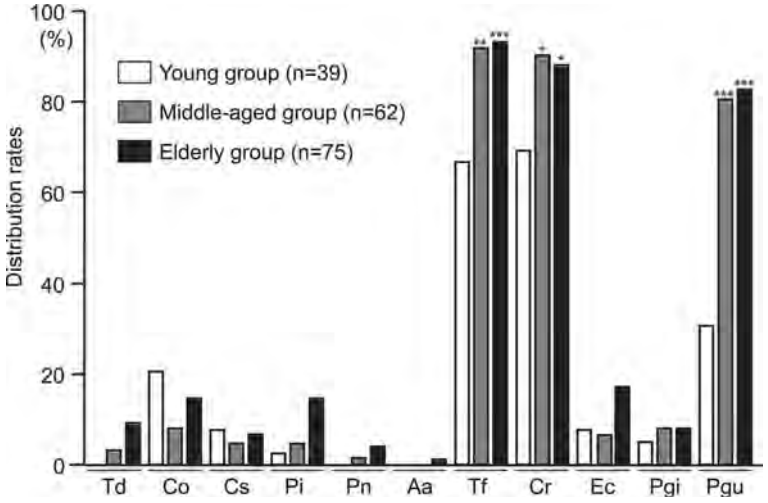

Fig. 2. Distribution rates of 11 periodontitis-related species in dental plaque specimens collected from each group. There were statistically significant differences in the group (**P*<0.05, ***P*<0.01, ****P*<0.001). Td; *T. denticola*, Co; *C. ochracea*, Cs; *C. sputigena*, Pi; *P. intermedia*, Pn; *P. nigrescens*, Aa; *A. actinomycetemcomitans*, Tf; *T. forsythia*, Cr; *C. rectus*, Ec; *E. corrodens*, Pgi; *P. gingivalis* and Pgu; *P. gulae.*

Figure 1 shows the distribution rates of dogs classified as healthy, with gingivitis and with periodontitis in each group. Fisher's protected least-significant difference test was utilized to compare the groups. None of the dogs in the young group were affected by periodontitis, whereas the distribution rate in the elderly group (24.0%) was significantly elevated compared to the young dogs ($P<0.001$). In addition, the distribution rate of gingivitis in the middle-aged and elderly groups (67.7% and 66.7%, respectively) was significantly greater than in the young group (5.1%) ($P<0.001$), while the distribution rate of dogs with a healthy periodontal condition was significantly higher in the young group (94.9%) than in the middle-aged and elderly groups (25.8% and 9.3%, respectively) ($P<0.001$). Harvey *et al*. [3] previously reported that the periodontal conditions in older dogs are worse than those in younger dogs in North America. Our present data suggested that age is also an important factor associated with the periodontal conditions in Japanese dogs.

Periodontitis-related species in dental plaque specimens were detected as previously described [5]. Briefly, oral specimens were collected from a specific location, the gingival margin of the mandibular left canine in the oral cavity, using swabs (Seed-Swab γ-1 or 2; Eiken Chemical Co., Ltd., Tokyo, Japan). Then, bacterial DNA was extracted using a Puregene Yeast/Bact. Kit B (QIAGEN Inc., Valencia, CA, U.S.A.). PCR was performed to identify bacterial DNA for the following 11 periodontopathic species, *T. denticola*, *C. ochracea*, *C. sputigena*, *P. intermedia*, *P. nigrescens*, *A. actinomycetemcomitans*, *T. forsythia*, *C. rectus*, *E. corrodens*, *P. gingivalis* and *P. gulae*, using bacterial DNA extracted from the specimens with species-specific sets of primers.

The distribution frequency of the 11 periodontitis-related species was statistically analyzed using Fisher's protected least-significant difference test to compare them among

the groups. The detection rates of *P. gulae*, *T. forsythia* and *C. rectus* were significantly higher in the middle-aged and elderly dogs than in the young dogs ($P<0.001$, $P<0.01$ and $P<0.05$, respectively) (Fig. 2). On the other hand, the distribution rates of other species were not significantly different among the groups. *P. gulae* is closely related to *P. gingivalis*, one of the major periodontitis pathogens in humans [1]. Furthermore, *T. forthysia* is a member of the red complex species, known to be associated with periodontitis severity in humans [4, 9], while *C. rectus* is also associated with the severity of periodontitis in humans [10, 11]. Thus, the presence of these three species indicated a poor periodontal condition. The total numbers of the 11 periodontitis-related species (mean ± standard error) in the middle-aged and elderly groups were 3.00 ± 0.12 and 3.40 ± 0.11, respectively, which were significantly greater than in the young group (2.10 ± 0.22) when analyzed using Bonferroni's method after analysis of variance (ANOVA) ($P<0.001$).

This is the first known study to analyze periodontal conditions and the presence of periodontitis-related species in Japanese dogs with a focus on age. It is generally accepted that age is an important factor for the development of periodontitis in humans [8]. The present findings demonstrate that age is also associated with the periodontal condition as well as the presence of periodontitis-related species in dogs. Unlike humans, prosthetic intervention is difficult in dogs, even if they lose their teeth; thus, periodontitis in these animals should be regarded as a life-threatening disease. Furthermore, periodontitis is thought to be associated with certain systemic diseases in dogs, such as cardiovascular diseases [7]. Therefore, it is important to consider the prevention of periodontitis for not only periodontal but also systemic health. In order to prevent periodontitis, it is important to keep in mind that age is an important factor related to periodontitis in dogs. Professional removal of dental plaque and calculus is important especially for elderly dogs, and thorough brushing instruction to their owners should be performed to prevent the onset of periodontitis.

ACKNOWLEDGMENTS. This study was supported by Grant-in-Aid for Scientific Research for Challenging Exploratory Research No. 23658256 from the Japan Society for Promotion of Science, and a research project grant awarded by the Azabu University.

REFERENCES

1. Amano, A. 2003. Molecular interaction of *Porphyromonas gingivalis* with host cells: implication for the microbial pathogenesis of periodontal disease. *J. Periodontol.* **74**: 90–96. [Medline] [CrossRef]
2. Hamada, N., Takahashi, Y., Watanabe, K., Kumada, H., Oishi, Y. and Umemoto, T. 2008. Molecular and antigenic similarities of the fimbrial major components between *Porphyromonas gulae* and *P. gingivalis*. *Vet. Microbiol.* **128**: 108–117. [Medline] [CrossRef]
3. Harvey, C. E., Shofer, F. S. and Laster, L. 1994. Association of age and body weight with periodontal disease in North American dogs. *J. Vet. Dent.* **11**: 94–105. [Medline]
4. Holt, S. C. and Ebersole, J. L. 2005. *Porphyromonas gingivalis, Treponema denticola*, and *Tannerella forsythia*: the "red complex", a prototype polybacterial pathogenic consortium in periodontitis. *Periodontol. 2000* **38**: 72–122. [Medline] [CrossRef]
5. Kato, Y., Shirai, M., Murakami, M., Mizusawa, T., Hagimoto, A., Wada, K., Nomura, R., Nakano, K., Ooshima, T. and Asai, F. 2011. Molecular detection of human periodontal pathogens in oral swab specimens from dogs in Japan. *J. Vet. Dent.* **28**: 84–89. [Medline]
6. Kyllar, M., Witter, K. and Tichy, F. 2010. Gingival stippling in dogs: clinical and structural characteristics. *Res. Vet. Sci.* **88**: 195–202. [Medline] [CrossRef]
7. Pavlica, Z., Petelin, M., Juntes, P., Erzen, D., Crossley, D. A. and Skaleric, U. 2008. Periodontal disease burden and pathological changes in organs of dogs. *J. Vet. Dent.* **25**: 97–105. [Medline]
8. Pihlstrom, B. L., Michalowicz, B. S. and Johnson, N. W. 2005. Periodontal diseases. *Lancet* **366**: 1809–1820. [Medline] [CrossRef]
9. Socransky, S. S., Haffajee, A. D., Cugini, M. A., Smith, C. and Kent, R. L. Jr. 1998. Microbial complexes in subgingival plaque. *J. Clin. Periodontol.* **25**: 134–144. [Medline] [CrossRef]
10. Suda, R., Kurihara, C., Kurihara, M., Sato, T., Lai, C. H. and Hasegawa, K. 2003. Determination of eight selected periodontal pathogens in the subgingival plaque of maxillary first molars in Japanese school children aged 8–11 years. *J. Periodontal Res.* **38**: 28–35. [Medline] [CrossRef]
11. Suda, R., Kobayashi, M., Nanba, R., Iwamaru, M., Hayashi, Y., Lai, C. H. and Hasegawa, K. 2004. Possible periodontal pathogens associated with clinical symptoms of periodontal disease in Japanese high school students. *J. Periodontol.* **75**: 1084–1089. [Medline] [CrossRef]
12. Yamasaki, Y., Nomura, R., Nakano, K., Naka, S., Matsumoto-Nakano, M., Asai, F. and Ooshima, T. 2012. Distribution of periodontopathic bacterial species in dogs and their owners. *Arch. Oral Biol.* **57**: 1183–1188. [Medline] [CrossRef]
13. Yamasaki, Y., Nomura, R., Nakano, K., Inaba, H., Kuboniwa, M., Hirai, N., Shirai, M., Kato, Y., Murakami, M., Naka, S., Iwai, S., Matsumoto-Nakano, M., Ooshima, T., Amano, A. and Asai, F. 2012. Distribution and molecular characterization of *Porphyromonas gulae* carrying a new *fimA* genotype. *Vet. Microbiol.* **161**: 196–205. [Medline] [CrossRef]

Biochem Genet (2013) 51:202–210
DOI 10.1007/s10528-012-9555-8

Expression of Activin Receptor-like Kinase 7 in Adipose Tissues

Masaru Murakami · Mitsuyuki Shirai · Ryo Ooishi · Asako Tsuburaya · Kumiko Asai · Osamu Hashimoto · Kenji Ogawa · Yoshii Nishino · Masayuki Funaba

Received: 2 December 2011 / Accepted: 11 September 2012 / Published online: 21 December 2012

Abstract The tissue distribution of activin receptor-like kinase 7 (*Alk7*) expression, the signaling ability of Alk7 variants, and Alk7 expression in response to β_3-adrenergic receptor activation were examined. Expression levels of *Alk7* varied greatly among tissues but were highest in white adipose tissue and brown adipose tissue. In addition to full-length Alk7 (*Alk7-v1*), *Alk7-v3*, an Alk7 variant, was expressed in adipose tissues, brain, and ovary. Nodal transmits signals via Alk7 in cooperation with its coreceptor, Cripto. Evaluation of the ability of Alk7 variants to confer Nodal signaling using luciferase-based reporter assays showed that Alk7-v3 does not transmit Nodal-Cripto-mediated signals. Expression of *Alk7* was down-

M. Murakami (✉) · R. Ooishi · A. Tsuburaya · K. Asai
Laboratory of Molecular Biology, School of Veterinary Medicine, Azabu University, Sagamihara 252-5201, Japan
e-mail: murakami@azabu-u.ac.jp

M. Shirai
Laboratory of Veterinary Pharmacology, School of Veterinary Medicine, Azabu University, Sagamihara 252-5201, Japan

O. Hashimoto
Laboratory of Experimental Animal Science, School of Veterinary Medicine, Kitasato University, Towada 034-8628, Japan

K. Ogawa
Chemical Genomics Research Group, ASI, Riken, Wako 351-0198, Japan

Y. Nishino
Department of Animal Medical Sciences, Faculty of Life Sciences, Kyoto Sangyo University, Kyoto 603-8555, Japan

M. Funaba (✉)
Division of Applied Biosciences, Kyoto University Graduate School of Agriculture, Kyoto 606-8502, Japan
e-mail: mfunaba@kais.kyoto-u.ac.jp

regulated in brown but not in white adipose tissue treated with CL316,243, a β_3-adrenergic receptor agonist. These results suggest involvement of Alk7 in modulation of metabolism in the adipose tissues in response to β_3-adrenergic receptor activation.

Keywords Alk7 · Tgf-β family · Variants · Adipose tissue

Introduction

Transforming growth factor-β (Tgf-β) family members, such as Tgf-βs, activins, and bone morphogenetic proteins, regulate a variety of cellular functions and play important roles in cell differentiation, adhesion, migration, and apoptosis. Tgf-β family members transmit signals through specific heteromeric complexes with type I receptors, called activin receptor-like kinases (Alks), and type II receptors; both complexes have intracellular serine/threonine kinase domains. Type II receptor kinases transphosphorylate and activate type I receptors and subsequently phosphorylate receptor-regulated (R)-Smad on carboxy-terminal serines; that is, Smad1, 5, and 8 are R-Smads regulated by bone morphogenetic proteins (BR-Smads) and Smad2 and 3 are R-Smads regulated by activin and Tgf-β (AR-Smads). Phosphorylated R-Smads form complexes with Smad4 and accumulate in the nucleus, where they interact with transcriptional factors to regulate target genes (Feng and Derynck 2005; Miyazono et al. 2010).

One of the type I receptors, *Alk7*, was initially cloned from rats as an orphan receptor (Lorentzon et al. 1996; Rydén et al. 1996; Tsuchida et al. 1996). Subsequently, Nodal, activin AB, activin B, Gdf-1, and Gdf-3, which are all members of the Tgf-β family, were identified as ligands of Alk7 (Reissmann et al. 2001; Tsuchida et al. 2004; Andersson et al. 2006, 2008). Unlike the other Alks, the expression pattern of *Alk7* was tissue-restricted; it was predominantly expressed in the central nervous system, as determined using Northern blotting, in situ hybridization, and RNase protection assays (Lorentzon et al. 1996; Rydén et al. 1996; Tsuchida et al. 1996). In addition, some reports have shown high levels of *Alk7* expression in rat kidneys (Rydén et al. 1996; Tsuchida et al. 1996), although other reports have observed no expression (Kang and Reddi 1996; Lorentzon et al. 1996). Furthermore, significant expression of *Alk7* was observed in pancreas, prostate, ovary, placenta, white adipose tissue, and brown adipose tissue (Kang and Reddi 1996; Rydén et al. 1996; Watanabe et al. 1999; Roberts et al. 2003; Carlsson et al. 2009). In particular, Carlsson et al. (2009) reported relatively higher expression of *Alk7* in human adipose tissues, although the expression was largely shown using data from the GEO database (http://www.ncbi.nlm.nih.gov/geo/). Currently, there are no well-controlled studies that quantitatively compare *Alk7* expression in different tissues.

In the human placenta, there are *Alk7* variants that are generated by alternative splicing (Roberts et al. 2003). In addition to the full-length Alk7 (*Alk7-v1*) consisting of 9 exons, three variants were identified that use an alternative first exon, Ia (*Alk7-v2*), lack exon III (*Alk7-v3*), or lack exons III and IV (*Alk7-v4*). As determined from the amino acid sequence, *Alk7-v2* is a variant of *Alk7* that is truncated at the extracellular domain including the signal peptide, and *Alk7-v3* and *Alk7-v4* are expected to yield

secreted forms of Alk7 (Roberts et al. 2003). The ability of these variants to confer signals is unknown. The present study demonstrates the tissue distribution of murine *Alk7*, the signaling capacity of the variant Alk7, and expression level of *Alk7* in white and brown adipose tissues of mice treated with CL316,243, a β_3-adrenergic receptor agonist (Yoshida et al. 1994).

Materials and Methods

Animals

Animal experiments were approved by the Azabu University Animal Experiment Committee. Of the 28 C57BL/6 mice used, tissue distribution of *Alk7* was examined in 14 mice aged 4–9 weeks, and 14 male mice aged 8 weeks were subcutaneously injected daily with 0.1 mg/kg CL316,243 ($n = 6$) or saline ($n = 8$) for 14 days.

RNA Isolation, RT-PCR, and Quantitative Real-Time RT-PCR

The isolation of total RNA from tissues, RT-PCR, and quantitative real-time RT-PCR (qRT-PCR) were performed as previously described (Murakami et al. 2007, 2009).

The relative expression level of *Alk7* was evaluated by qRT-PCR. The *Alk7* and β-*actin* mRNA levels were quantified by the standard curve method. The *Alk7* mRNA level was expressed relative to β-*actin* expression. The PCR primers to evaluate *Alk7* were 5′-tgggaaatagctcgaaggtg-3′ and 5′-gtaaggcaactggtactcctcaa-3′; these primers detect both *Alk7-v1* and *Alk7-v3*. The PCR primers for β-*actin* were previously described (Murakami et al. 2009).

Expression of *Alk7* variants was evaluated by RT-PCR. The PCR was performed using cDNA synthesized from 5 ng total RNA in a total volume of 25 μl containing 1× *Ex-Taq* buffer with 2.0 mM $MgCl_2$, 0.2 mM of each dNTP, 0.2 μM of each primer, and 1.25 U *Ex-Taq* HS DNA polymerase (Takara Bio, Otsu, Japan). The PCR primers were 5′-tctgggaccccgaagccttgcacc-3′ (F41) and 5′-ccagccctaagtcagctatggcac-3′ (R1111). The thermal cycling parameters consisted of an initial denaturation at 95 °C for 3 min; followed by 38 cycles for *Alk7* or 30 cycles for β-*actin* of denaturation at 95 °C for 30 s, annealing at 58 °C for 30 s, and extension at 72 °C for 45 s; with an additional final extension step of 72 °C for 5 min. PCR products were separated on 1.2 % agarose gels in 0.75× TAE and visualized with ethidium bromide. The band intensity was quantified by an ImageJ version 1.46p program (Rasband 2012). As a negative control, an RT-PCR without cDNA was carried out.

Cloning Analysis

Full-length *Alk7* was isolated from cDNA prepared from mouse brown adipose tissue. The cDNA was amplified by PCR using DNA polymerase PrimeStar (Takara Bio), which has high fidelity, and PCR primers 5′-ttGGATCCatgaccccagcgcgcggctccg-3′ and 5′-tttCTCGAGagctttacagtcttccttgacacaca-3′, with the indicated *Bam*HI and *Xho*I sites (capital letters). The thermal cycling parameters consisted of an initial

denaturation at 95 °C for 3 min; followed by 32 cycles of denaturation at 95 °C for 30 s, annealing at 60 °C for 5 s, and extension at 72 °C for 80 s; with a final extension at 72 °C for 5 min. The PCR products were purified using the Wizard SV Gel and PCR Clean-Up System (Promega, Madison, WI), digested with *Bam*HI and *Xho*I, cloned into an HA-tagged pcDNA vector (Inohara et al. 1998), and then transformed into *Escherichia coli* JM109. For 31 colonies, the nucleotide sequence of the insert was determined to identify the *Alk7* variant. Also, 511 independent colonies were examined to determine the *Alk7* variant by PCR amplification using primers of 5′-ccggaactaaatgctcaggtctt-3′ and R1111 and subsequent agarose electrophoresis.

Plasmids and Reporter Assay

CAGA-luc, an activin/Tgf-β-responsive reporter gene (Dennler et al. 1998), was kindly provided by Dr. P. ten Dijke. To prepare the *Nodal* and *Cripto* expression plasmids of *Alk7*, we amplified the coding regions of the genes using PCR and cloned them into an HA-tagged pcDNA vector (Inohara et al. 1998). All resulting constructs were verified by nucleotide sequencing.

Luciferase assays were conducted as previously described (Murakami et al. 2009). HepG2 cells were transiently transfected with the indicated expression vectors, reporter construct, and a plasmid expressing β-galactosidase (pCMV-βGal). The amount of DNA used in each experiment was supplemented with empty pcDNA3 so that equal amounts of DNA were transfected. Cells were harvested 40 h after transfection. Luciferase activity was normalized to β-galactosidase activity, and the luciferase activity in cells transfected with empty vector was set to 1.

Results and Discussion

The tissue distribution of *Alk7* was quantified by qRT-PCR (Fig. 1). Because β-actin was appropriate as a reference gene to compare expression levels among tissues (Ooishi et al. 2012), gene transcript levels of *Alk7* were calculated as the ratio to that of β-actin. As expected, significant expression of *Alk7* was detected in the brain. In addition, significant expression was detected in white and brown adipose tissues. Especially, expression in the adipose tissues was more than three-fold that in the brain; this is partly consistent with the results of Carlsson et al. (2009), which showed higher expression in white adipose tissue. Similar results were obtained on relatively higher expression in the adipose tissues, when it was corrected by expression of *Hprt1*, another gene frequently used as a reference gene (data not shown). It is possible, however, that the expression level of *Alk7* is higher in the specific brain area than in the adipose tissues. *Alk7* was expressed in neurons in the brain (Rydén et al. 1996), and the brain *Alk7* mRNA was localized to restricted areas of the hippocampus, telencephalon, the basal ganglia, the thalamus, the hypothalamus, and cerebellar cortex (Lorentzon et al. 1996; Rydén et al. 1996; Tsuchida et al. 1996).

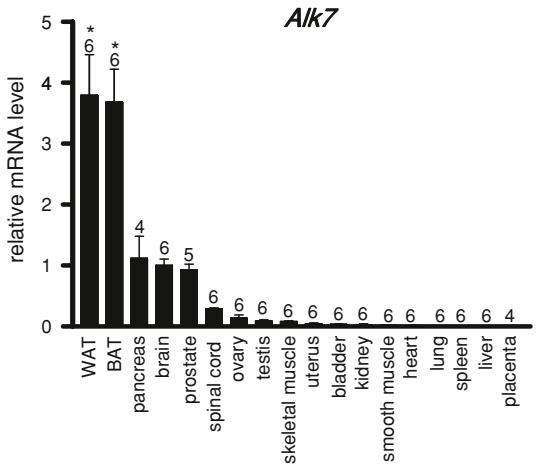

Fig. 1 Tissue distribution of Alk7. *Alk7* expression in 18 types of tissues was measured by qRT-PCR, as a ratio to β-*actin* expression. Data are shown as the mean ± SE. The number above each bar indicates the number of samples analyzed for that tissue. WAT, white adipose tissue. BAT, brown adipose tissue. Statistical differences between tissues were determined by one-way ANOVA, followed by Scheffe's test. *Significantly different from the other tissues at $P < 0.01$

Expression in the pancreas and prostate was comparable to that in the brain, which is consistent with previous results showing high expression in the rat pancreas (Watanabe et al. 1999) and prostate (Kang and Reddi 1996). Expression of *Alk7* in the kidney of adult mice was relatively weak; the gene transcript level was 0.03 of the expression in the brain. The findings in the previous studies are controversial. Significant expression of *Alk7* was detected in the kidney of adult rats (Tsuchida et al. 1996; Rydén et al. 1996), whereas no expression was detected in neonatal (Rydén et al. 1996) or fetal rats (Lorentzon et al. 1996). In addition to the effects of growth and developmental stage on expression of *Alk7* in the kidney, this may reflect species differences. There may also be species-specific differences in *Alk7* expression in the placenta. Abundant expression of *Alk7* could be detected in human placental tissue (Roberts et al. 2003). By contrast, expression of *Alk7* in mouse placenta was much lower, less than 0.01 of the expression in the brain.

Variants of *Alk7*, which are generated by alternative splicing, were isolated from human placenta (Roberts et al. 2003). At first, we explored expression of *Alk7* variants in brown adipose tissue. *Alk7* cDNAs were cloned by RT-PCR using primers targeting the translation initiation site and the final amino acid of full-length Alk7. Of the 31 independent colonies we analyzed, nucleotide sequencing indicated that plasmids from 20 independent colonies encoded full-length *Alk7* (*Alk7-v1*). Plasmids from 10 colonies encoded an *Alk7* variant corresponding to human *Alk7-v3* (Roberts et al. 2003), which lacks a part of the extracellular region, the whole transmembrane spanning region, and a portion of the kinase domain. In addition, a plasmid encoding a novel variant of *Alk7* lacking exons III and V was isolated from one colony; this variant was named *Alk7-v5*. We also examined expression of the *Alk7* variant corresponding to human *Alk7-v2* (Roberts et al. 2003) using a PCR primer set targeting exon Ia, but no significant band was detected (data not shown).

To compare expression levels among Alk7 variants, we performed PCR using primers that detect all three variants (*Alk7-v1*, *Alk7-v3,* and *Alk7-v5*). Bands corresponding to *Alk7-v1* and *Alk7-v3* but not *Alk7-v5* were clearly detected in brown and white adipose tissues, brain, and ovary; the ratio of *Alk7-v1* to *Alk7-v3* was not

greatly different among tissues (Fig. 2). In addition, analyses of 511 independent colonies of *E. coli* transformed with plasmid with amplified *Alk7* gene in brown adipose tissue indicated an *Alk7-v1* : *Alk7-v3* ratio of about 2.7:1, and no colony was detected for *Alk7-v5* (Fig. 2). We concluded that *Alk7-v5* is an artifact of PCR.

Given the significant expression of *Alk7-v3,* we evaluated the ability of Alk7-v3 to confer Nodal-induced transcriptional activation in HepG2 cells by a luciferase-based reporter assay using CAGA-luc, a representative reporter to evaluate Alk4-, 5-, and 7-mediated signaling (Dennler et al. 1998; Tojo et al. 2005). The expression of Cripto, a protein that acts as a coreceptor for Nodal signaling (Whitman 2001), was required for transcriptional activation of *CAGA-luc* by Nodal (Fig. 3). Expression of Alk7-v1 but not Alk7-v3 enhanced transcription of *CAGA-luc* induced by Nodal and Cripto. These results suggest that Alk7-v3 is not involved in canonical Alk7-mediated signaling. It is also possible that these variants regulate the pathway differently from the Tgf-β family members. Currently, the role of serine/threonine phosphorylation of extracellular molecules is not known; future studies are needed to clarify the biological activities of the soluble serine/threonine kinases Alk7-v3, especially in adipose tissues.

To gain insight on the role of Alk7 in adipose tissues, CL316,243, a β_3-adrenergic receptor agonist (Yoshida et al. 1994), was administered to C57BL/6 mice. It is known that the treatment induces emergence of brown adipocytes in white adipose tissue (Barbatelli et al. 2010) and activation of brown adipose tissue, as evidenced by up-regulation of *Ucp1* (Cinti et al. 2002), a brown adipocyte-specific gene (Cannon and Nedergaard 2004). Expression of *Alk7* was significantly lower in the interscapular brown adipose tissue treated with CL316,243 than in the control brown adipose tissue; to the contrary, *Alk7* expression in the inguinal white adipose tissue was comparable between groups (Fig. 4). Decrease in *Alk7* expression in brown adipose tissue may reflect down-regulation to reduce the signal transduction via Alk7, resulting from the prolonged activation of β_3-adrenergic receptor. Previous studies revealed that *Alk7* is expressed in fetal rat brown adipocytes (Lorentzon et al. 1996). Thus, the regulatory changes in *Alk7* expression in brown adipose tissue imply the involvement of Alk7 in β_3-adrenergic receptor-mediated modulation of brown adipocyte function.

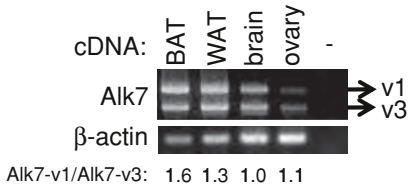

	Colonies	(%)
Alk7-v1	371	(72.6)
Alk7-v3	140	(27.4)
Total	511	(100)

Fig. 2 Expression of Alk7 variants. (*Left*) RT-PCR using primers that detect *Alk7-v1*, *Alk7-v3,* and *Alk7-v5* (i.e., F41 and R1111) in four tissues, brown adipose tissue (BAT), white adipose tissue (WAT), brain, and ovary. The PCR products were electrophoresed and stained by ethidium bromide. The band intensity was measured, and the ratio of *Alk7-v1* to *Alk7-v3* was calculated. A representative result is shown below each lane. (*Right*) *Escherichia coli* was transformed with plasmid ligated Alk7 amplified by PCR as a template of cDNA originated from brown adipose tissue. A total of 511 independent colonies was analyzed to identify the Alk7 variant

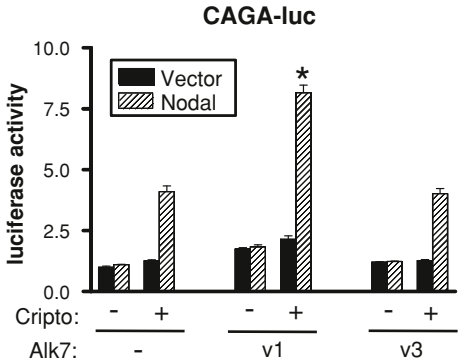

Fig. 3 Nodal-induced and Alk7-mediated transcription. HepG2 cells were transiently transfected with CAGA-luc and the indicated expression plasmids along with CMV-β-galactosidase to adjust for transfection efficiency. Luciferase activity was normalized to β-galactosidase activity, and the luciferase activity in cells transfected with empty vector was set to 1. Data are shown as the mean ± SE. Statistical differences between both Nodal and Cripto transfected groups were determined by one-way ANOVA, followed by Scheffe's test. *Significantly different from the other groups at $P < 0.01$

The present study examined comprehensive expression of *Alk7* in tissues and signaling of Alk7 variants. We show that (1) *Alk7* expression in mice is higher in the adipose tissues than in the brain, (2) the *Alk7-v3* variant is expressed in adipose tissues, brain, ovary, and possibly elsewhere, (3) only Alk7-v1 transmits Nodal-Cripto signaling, and (4) *Alk7* expression is down-regulated in activated brown

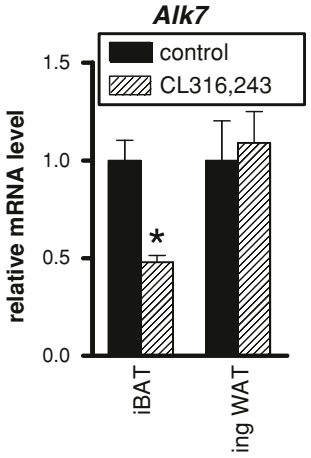

Fig. 4 Expression of Alk7 in brown and white adipose tissue treated with CL316,243. C57BL/6 mice were treated with CL316,243 ($n = 6$) or saline ($n = 8$) for 14 days. Interscapular brown adipose tissue (iBAT) and inguinal white adipose tissue (ing WAT) were collected, and expression of *Alk7* was examined by qRT-PCR. The expression was normalized to β-*actin* expression, and the expression in the control group in each fat depot was set to 1. Data are shown as the mean ± SE. Statistical differences between groups were determined by one-way ANOVA. *Significantly different from the other groups at $P < 0.01$

adipose tissue. Phenotypic analyses of Alk7-null mice and Nodal-null mice verified that Alk7 is not an essential mediator of Nodal signaling during mesoderm formation and left–right patterning (Brennan et al. 2001, 2002; Jörnvall et al. 2004). In addition, *Alk7*-null mice exhibited no histological abnormalities in the central nervous system, including cerebella, cortices, and hippocampi (Jörnvall et al. 2004). *Alk7*-null mice also exhibited an age-dependent syndrome involving progressive hyperinsulinemia, reduced insulin sensitivity, liver steatosis, impaired glucose tolerance, and pancreatic islet enlargement (Bertolino et al. 2008). In the study by Bertolino et al. (2008), the aberrant glucose/insulin metabolism was proposed to result from an Alk7 deficiency in the pancreas. In view of our data on the higher expression of *Alk7* in adipose tissues, however, the phenotypes of *Alk7*-null mice may result from impaired production of adipokines in white adipocytes and energy expenditure by brown adipocytes (Bertolino et al. 2008); these actually improve glucose metabolism through enhancing insulin sensitivity (Shimomura et al. 1999; Kubota et al. 2007; Seale et al. 2011). The present study suggests the necessity of further studies focusing on the role of Alk7 in adipose tissues.

Acknowledgments We thank Dr. Peter ten Dijke for providing plasmid. This work was supported by Kakenhi from The Japan Society for the Promotion of Science and a research project grant awarded by the Azabu University.

References

Andersson O, Reissmann E, Jörnvall H, Ibáñez CF (2006) Synergistic interaction between Gdf1 and Nodal during anterior axis development. Dev Biol 293:370–381

Andersson O, Korach-Andre M, Reissmann E, Ibáñez CF, Bertolino P (2008) Growth/differentiation factor 3 signals through ALK7 and regulates accumulation of adipose tissue and diet-induced obesity. Proc Natl Acad Sci USA 105:7252–7256

Barbatelli G, Murano I, Madsen L, Hao Q, Jimenez M, Kristiansen K, Giacobino JP, De Matteis R, Cinti S (2010) The emergence of cold-induced brown adipocytes in mouse white fat depots is determined predominantly by white to brown adipocyte transdifferentiation. Am J Physiol Endocrinol Metab 298:E1244–E1253

Bertolino P, Holmberg R, Reissmann E, Andersson O, Berggren PO, Ibáñez CF (2008) Activin B receptor ALK7 is a negative regulator of pancreatic β-cell function. Proc Natl Acad Sci USA 105:7246–7251

Brennan J, Lu CC, Norris DP, Rodriguez TA, Beddington RS, Robertson EJ (2001) Nodal signalling in the epiblast patterns the early mouse embryo. Nature 411:965–969

Brennan J, Norris DP, Robertson EJ (2002) Nodal activity in the node governs left-right asymmetry. Genes Dev 16:2339–2344

Cannon B, Nedergaard J (2004) Brown adipose tissue: function and physiological significance. Physiol Rev 84:277–359

Carlsson LM, Jacobson P, Walley A, Froguel P, Sjöström L, Svensson PA, Sjöholm K (2009) ALK7 expression is specific for adipose tissue, reduced in obesity and correlates to factors implicated in metabolic disease. Biochem Biophys Res Commun 382:309–314

Cinti S, Cancello R, Zingaretti MC, Ceresi E, De Matteis R, Giordano A, Himms-Hagen J, Ricquier D (2002) CL316,243 and cold stress induce heterogeneous expression of UCP1 mRNA and protein in rodent brown adipocytes. J Histochem Cytochem 50:21–31

Dennler S, Itoh S, Vivien D, ten Dijke P, Huet S, Gauthier JM (1998) Direct binding of Smad3 and Smad4 to critical TGFβ-inducible elements in the promoter of human plasminogen activator inhibitor-type 1 gene. EMBO J 17:3091–3100

Feng XH, Derynck R (2005) Specificity and versatility in TGF-b signaling through Smads. Annu Rev Cell Dev Biol 21:659–693

Inohara N, Koseki T, Chen S, Wu X, Núñez G (1998) CIDE, a novel family of cell death activators with homology to the 45 kDa subunit of the DNA fragmentation factor. EMBO J 17:2526–2533

Jörnvall H, Reissmann E, Andersson O, Mehrkash M, Ibáñez CF (2004) ALK7, a receptor for nodal, is dispensable for embryogenesis and left–right patterning in the mouse. Mol Cell Biol 24:9383–9389

Kang Y, Reddi AH (1996) Identification and cloning of a novel type I serine/threonine kinase receptor of the TGF-β/BMP superfamily in rat prostate. Biochem Mol Biol Int 40:993–1001

Kubota N, Yano W, Kubota T, Yamauchi T, Itoh S, Kumagai H, Kozono H, Takamoto I, Okamoto S, Shiuchi T, Suzuki R, Satoh H, Tsuchida A, Moroi M, Sugi K, Noda T, Ebinuma H, Ueta Y, Kondo T, Araki E, Ezaki O, Nagai R, Tobe K, Terauchi Y, Ueki K, Minokoshi Y, Kadowaki T (2007) Adiponectin stimulates AMP-activated protein kinase in the hypothalamus and increases food intake. Cell Metab 6:55–68

Lorentzon M, Hoffer B, Ebendal T, Olson L, Tomac A (1996) Habrec1, a novel serine/threonine kinase TGF-b type I-like receptor, has a specific cellular expression suggesting function in the developing organism and adult brain. Exp Neurol 142:351–360

Miyazono K, Kamiya Y, Morikawa M (2010) Bone morphogenetic protein receptors and signal transduction. J Biochem 147:35–51

Murakami M, Iwata Y, Funaba M (2007) Expression and transcriptional activity of alternative splice variants of Mitf exon 6. Mol Cell Biochem 303:251–257

Murakami M, Kawachi H, Ogawa K, Nishino Y, Funaba M (2009) Receptor expression modulates the specificity of transforming growth factor-b signaling pathways. Genes Cells 14:469–482

Ooishi R, Shirai M, Funaba M, Murakami M (2012) Microphthalmia-associated transcription factor is required for mature myotube formation. Biochim Biophys Acta 1820(2):76–83

Rasband WS (2012) ImageJ, 1997–2012. U.S. National Institutes of Health, Bethesda. http://imagej.nih.gov/ij/. Accessed June 2012

Reissmann E, Jörnvall H, Blokzijl A, Andersson O, Chang C, Minchiotti G, Persico MG, Ibáñez CF, Brivanlou AH (2001) The orphan receptor ALK7 and the Activin receptor ALK4 mediate signaling by Nodal proteins during vertebrate development. Genes Dev 15:2010–2022

Roberts HJ, Hu S, Qiu Q, Leung PC, Caniggia I, Gruslin A, Tsang B, Peng C (2003) Identification of novel isoforms of activin receptor-like kinase 7 (ALK7) generated by alternative splicing and expression of ALK7 and its ligand, Nodal, in human placenta. Biol Reprod 68:1719–1726

Rydén M, Imamura T, Jörnvall H, Belluardo N, Neveu I, Trupp M, Okadome T, ten Dijke P, Ibáñez CF (1996) A novel type I receptor serine-threonine kinase predominantly expressed in the adult central nervous system. J Biol Chem 271:30603–30609

Seale P, Conroe HM, Estall J, Kajimura S, Frontini A, Ishibashi J, Cohen P, Cinti S, Spiegelman BM (2011) Prdm16 determines the thermogenic program of subcutaneous white adipose tissue in mice. J Clin Invest 121:96–105

Shimomura I, Hammer RE, Ikemoto S, Brown MS, Goldstein JL (1999) Leptin reverses insulin resistance and diabetes mellitus in mice with congenital lipodystrophy. Nature 401:73–76

Tojo M, Hamashima Y, Hanyu A, Kajimoto T, Saitoh M, Miyazono K, Node M, Imamura T (2005) The ALK-5 inhibitor A-83-01 inhibits Smad signaling and epithelial-to-mesenchymal transition by transforming growth factor-β. Cancer Sci 96:791–800

Tsuchida K, Sawchenko PE, Nishikawa S, Vale WW (1996) Molecular cloning of a novel type I receptor serine/threonine kinase for the TGF-β superfamily from rat brain. Mol Cell Neurosci 7:467–478

Tsuchida K, Nakatani M, Yamakawa N, Hashimoto O, Hasegawa Y, Sugino H (2004) Activin isoforms signal through type I receptor serine/threonine kinase ALK7. Mol Cell Endocrinol 220:59–65

Watanabe R, Yamada Y, Ihara Y, Someya Y, Kubota A, Kagimoto S, Kuroe A, Iwakura T, Shen ZP, Inada A, Adachi T, Ban N, Miyawaki K, Sunaga Y, Tsuda K, Seino Y (1999) The MH1 domains of smad2 and smad3 are involved in the regulation of the ALK7 signals. Biochem Biophys Res Commun 254:707–712

Whitman M (2001) Nodal signaling in early vertebrate embryos: themes and variations. Dev Cell 1(5):605–617

Yoshida T, Sakane N, Wakabayashi Y, Umekawa T, Kondo M (1994) Anti-obesity and anti-diabetic effects of CL 316,243, a highly specific β_3-adrenoceptor agonist, in yellow KK mice. Life Sci 54:491–498

Medical Mycology February 2013, **51**, 144–149

informa
healthcare

Isolation of *Microsporum gallinae* from a fighting cock (*Gallus gallus domesticus*) in Japan

MICHIKO MURATA*, HIDEO TAKAHASHI†,‡, SANA TAKAHASHI§, YOKO TAKAHASHI#, HIROJI CHIBANA#, YOSHITERU MURATA‡,^, KAZUTOSHI SUGIYAMA +, TAKASHI KANESHIMA$, SAYAKA YAMAGUCHI¶, HITONA MIYASATO¶, MASARU MURAKAMI*, RUI KANO~, ATSUHIKO HASEGAWA~, HIROSHI UEZATO¶, ATSUSHI HOSOKAWA¶ & AYAKO SANO¥

**Department of Molecular Biology, Faculty of Veterynary Medicine, Azabu University, Kanagawa, Japan, †A-land Oyumino Animal Hospital, Chiba, Japan, ‡Committee of Infectious Diseases, Chiba Veterinary Medical Association, Chiba, Japan, §Faculty of Veterinary Medicine, Azabu University, Kanagawa, Japan, #Medical Mycology Research Center, Chiba University, Chiba, Japan, ^Murata Animal Hospital, Mobara, Chiba, Japan, + Sugiyama Veterinary Clinic, Shizuoka, Japan, $Ryukyu Animal Clinic Center, Tomigusuku, Okinawa, Japan, ¶Department of Dermatology, Faculty of Medicine, University of the Ryukyus, Okinawa, Japan, ~Department of Pathology, School of Veterinary Medicine, Nihon University, Fujisawa, Kanagawa, Japan, and ¥Department of Animal Sciences, Faculty of Agriculture, University of the Ryukyus, Okinawa, Japan*

A case of tinea corporis caused by *Microsporum gallinae* was found in 2011 in Okinawa, located in the southern part of Japan. The patient was a 96-year-old, otherwise healthy, Japanese man, who had been working as a breeder of fighting cocks for more than 70 years. He was bitten on his right forearm by one of the cocks and a few weeks later, two erythematous macules appeared on the right forearm, accompanied by a slight itchy sensation. While the first isolate of this dermatophyte was recovered from the region by Miyasato *et al*. in 2011, it was not obtained from the same fighting cock owned by the patient. However, frequent exchanges of fighting cocks and special domestic breeds of chickens related to fighting, mating, and/or bird fairs are common among the fans and breeders. We investigated 238 chickens and 71 fighting cocks in Okinawa and in the suburbs of Tokyo (Chiba, Tokyo, Ibaraki, and Sizuoka). One isolate of *M. gallinae* from a fighting cock in Chiba Prefecture in the Tokyo metropolitan area exhibited a different genotype, with a single base difference from the patient isolate based on the internal transcribed spacer 1-5.8s-ITS2 regions (ITS1-5.8S-ITS2) of the ribosomal RNA gene sequence. The isolation of *M. gallinae* from a fighting cock on the mainland of Japan is the first such finding in animals in our country.

Keywords *Microsporum gallinae*, fighting cock, *Gallus gallus domesticus*

Introduction

Microsporum gallinae is a dermatophyte that causes favus of the comb in chickens and related species [1–5]. White crusts or plaques containing fungal elements are associated with hyperkeratosis, and lesions may spread to the skin of the head and the neck with feather loss, although the feathers are not invaded. Chicks and roosters are more often infected than hens [1], especially fighting cocks or the oriental breed called 'Shamo' [6–9]. This fungal species also infects dogs [10–13], monkeys [14], cats [11,15], squirrels [13], mice, canary, pigeon, and turkey [1], and has been isolated from birds' nests [16]. In addition, *Microsporum gallinae* is zoonotic causing ringworm in humans [13,17–27] and severe infections in immunocompromised hosts [22,25]. These human cases involved patients who had had contact with infected animals, especially cocks [17,27]. Based on 44 reports, it would appear that the endemic areas of *M. gallinae* include European, Middle Eastern, and South American countries, in addition to the USA [28], Sweden, France, Germany, Czechoslovakia,

Received 19 March 2012; Received in final revised form 16 May 2012; Accepted 7 June 2012.

Correspondence: Ayako Sano, University of the Ryukyus, Faculty of Agriculture, Animal Sciences, Nakagusuku, Japan. E-mail: aya_grimalkin@yahoo.co.jp

DOI: 10.3109/13693786.2012.701766

Spain, Germany, Pakistan, Iran, Nigeria, Puerto Rico, Venezuela, and Japan [27].

In the first Japanese human case, infection may have been due to infected animals, i.e., cocks [17,27], although we could not isolate *M. gallinae* from the animal maintained by the patient. During a preliminary survey, we learned from a breeder that exchanges of birds and special breeds of chickens related to fighting, mating, and/or bird fairs are common among breeders throughout Japan. We conducted the present study to isolate *M. gallinae* from fowls in Japan.

Materials and methods

Animals

We examined 238 chickens and 71 fighting cocks in Japan in various prefectures, but the specific prefectures are not mentioned to comply with privacy policies of the funding agency. The research was supported by Grant-in-Aid for Scientific Research© by the Japan Society for the Promotion of Science (JSPS), No. 23580419 and approved by the ethics committee for animal welfare of the University of the Ryukyus.

Isolation

Eighteen-millimeter-wide transparent Scotch tape (Sumitomo 3A, Tokyo, Japan) was cut into strips approximately 10 cm in length and both 1-cm ends were folded for handling. The adhesive surface (approximately 6 cm in length) was placed on the comb and gently rubbed with both thumb and index fingers to collect scales. The tape was incubated at 42°C for 4 h to remove mites and then applied to the surface of BBL Mycosel Agar (Becton Dickinson [BD]; Sparks, MD, USA) plates supplemented with chloramphenicol (100 mg/liter, Wako Pure Chemical Industries, Ltd., Osaka, Japan) in duplicate, and incubated at 35°C for up to 28 days.

A white cottony colony with strawberry-colored pigmentation diffusing into the medium was transferred onto potato dextrose agar (Difco Potato Dextrose Agar; PDA, BD) slants and incubated at 25°C for further mycological and molecular biological analysis.

Mycological studies

Colonies grown on Sabouraud dextrose agar (SDA) containing 2% dextrose (Wako Pure Chemical Industries, Ltd.), 1% neopeptone (Difco, BD), and 1.5% Bacto Agar (Difco, BD) and PDA plates incubated at 25°C were observed for 21 days. The isolate was cultured on SDA and PDA blocks at 25°C for 28 days for light microscopic observation after staining with lactophenol cotton blue.

The present isolate was crossed with; (1) *Arthroderma grubyi* isolates IFM 48209, IFM 49901, and IFM 49902, (2) *M. gallinae* isolate IFM 56900 isolated from the first clinical case in Okinawa, Japan [27] and (3) *A. simii* isolates IFM 49897 and 49898, on salt-added 1/10 diluted Sabouraud dextrose agar plates at 25°C for 8 weeks [28]. In addition, *A. grubyi* isolates IFM 48209, IFM 49901, and IFM 49902 were crossed with each other to observe their sexual function.

Molecular biological identification

Sequences of the ITS1-5.8S-ITS2 region of the rRNA gene were obtained by routine methods [29]. Briefly, DNA was extracted with a DEXPAT kit (TaKaRa, Ohtsu, Japan) using a modified procedure. Approximately 100 µl of fungal cells from cultures incubated at 25°C for 1 month on PDA slants was placed in a sterilized microtube (1.5 ml) to which 0.5 ml of DEXPAT solution was added, and the mixture homogenized with a plastic pestle. The tube was incubated at 100°C for 10 min, and then centrifuged at 13,200 *g* for 10 min, and the supernatants were used as DNA samples. Although this type of kit is designed for extracting DNA from paraffin-embedded tissue samples, we routinely use it for the isolation of genes from fungal cultures because of its convenience [30].

We mixed 2.5 µl of DNA extract with Ready-To-Go PCR beads (Amersham Pharmacia Tokyo, Japan), 2.5 µl of 10 pM of the primers ITS-5 (5′- GGA AGT AAA AGT CGT AAC AAG G-3′) and ITS-4 (5′- TCC TCC GCT TAT TGA TAT GC-3′) [30], and 17.5 µl of distilled water. The reaction mixture was subjected to 1 cycle of denaturation at 95°C for 4 min, 30 cycles of amplification at 94°C for 1 min, 50°C for 1 min, and 72°C for 2 min, and a final extension cycle at 72°C for 10 min in a PCR Thermal Cycler MP (TaKaRa).

PCR products were visualized by electrophoresis on 1.0% agarose gels in 1 × TBE buffer (0.04 M Tris-boric acid, 0.001 M EDTA [pH 8.0]) followed by ethidium bromide staining. PCR samples were purified using a PCR purification kit (QIAquick, Qiagen Co. Ltd., Tokyo, Japan), and labeled with BigDye Terminator Ver. 1.1 (Applied Biosystems, Foster City, CA, USA) following the manufacturer's protocol. The labeled samples were directly sequenced on an ABI PRISM 3100 sequencer (Applied Biosystems) using the primers ITS-5, ITS-4, ITS-2 (5′- GCT GCG TTC TTC ATC GAT GC-3′), and ITS3 (5′- GCA TCG ATG AAG AAC GCA GC-3′) [30]. DNA sequences amplified by at least two primer pairs were aligned using GENETEX-MAC genetic information processing software (Software Development Co., Ltd., Tokyo, Japan). These procedures were performed twice on both the present isolate and *M. gallinae* IFM 56900 isolated

Table 1 The ITS rDNA sequences of *Microsporum gallinae* and related species in the GenBank database.

Species	Strain name	GenBank Accession no.	Country and host	Remarks
Arthroderma grubyi	CBS 244.66	AJ000613	USA Man, scalp	
	CBS 243.66	AJ000612*	USA, Montana ringworm infection in dog	Deposited by M. Elfar in July 1997
	IFM 48209	AB698453	France, man, skin lesion	
	IFM 49901	AB698454	USA, ATCC 14422 obtained by mating	
	IFM 49902	AB698455	Canada, ATCC 14423 obtained by mating	
Microsporum vanbreuseghemii	CBS 243.66	AJ970147**	USA, Montana ringworm infection in dog	Deposited by Y. Graser in November 2005
Microsporum gallinae	CHUS95902	EF581136	Spain	
	CBS 300.52	AJ000620	Unknown	
	ATCC 12108	EF631610	Puerto Rico, child's scalp	
	IFM 56900	AB455805	Japan, tinea corporis	
	IHEM 13565	FJ356083	Israel, chicken	
	IHEM 13563	FJ428241	Israel, monkey	
	IHEM 13564	FJ428242	Israel, unknown (maybe human)	
	IHEM 13373	FJ416304	Iran, unknown (maybe human)	
	778	JN134141	Iran, unknown (maybe human)	
	IFM 60027	AB698457	Israel, unknown (maybe human)	
	IFM 58803	AB667976	Japan, fighting cock. Present isolate	

* and ** derived from isolate CBS 243.66 showed one base difference. CBS, The Centraalbureau voor Schimmelcultures, The Netherlands. IFM, Medical Mycology Research Center, Chiba University, Japan. CHUS, University of Santiago, Spain. ATCC, American Type Culture Collection, USA. IHEM, BCCM/IHEM, Scientific Institute of Public Health Section Mycology and Aerobiology, Belgium.

from the first clinical case [27], to confirm differences in the sequences. Sequences were analyzed using a BLAST search (http:// www.ncbi.nlm.nih.gov/BLAST/Blast.cgi) and closely related sequences were obtained.

Seventeen nucleotide sequences from *M. gallinae* and its teleomorph species *A. grubyi* deposited in GenBank (Table 1) were aligned, together with the present nucleotide sequences, using the computer program ClustalX (Version 1.8) [31] followed by manual adjustments with a text editor. Phylogenetic analyses were performed with PAUP v4.0b10 [32] using a heuristic search for maximum parsimony trees. Base-pair composition and transition and/or transversion patterns of the dataset were estimated by PAUP v4.0b10. Bootstrap values were calculated over 1000 replicates to assess branch topology. Only one phylogenetic tree was obtained from the analysis and was drawn by Tree View PPC [33] (Roderic D. M. Page, Glasgow, Scotland, UK, 1998; http://taxonomy.zoology.gla.ac.uk/rod/treeview.html). Clades were supported by bootstrap values above 50.

Fig. 1 *Microsporum gallinae*-positive cock showing white scaling on the comb.

Results

One *M. gallinae* isolate was obtained from a 10-month-old male fighting cock from Chiba Prefecture. The comb of the cock was of the cushion type and showed white scaling (Fig. 1). The primary isolate appeared as a slightly yellowish white, cottony colony approximately 1.2 cm in diameter after incubation at 35°C for 2 weeks on a Mycosel agar plate, and showed slight strawberry-red pigment diffused into the medium (data not shown). A colony of the isolate grown on SDA at 25°C for 21 days was white and cottony, 5.7 cm in diameter, with slight strawberry-red pigment diffused into the medium. Those on PDA under the same culture conditions were pinkish-grey with a felt-like texture on the surface, 3.7 cm in diameter, and showed vibrant strawerry-red pigment diffused into the medium (Fig. 2).

Septate hyphae with small numbers of macroconidia consisting of 4–6 cells (4–7 × 12–18 μm) and ovoid to pyriform, single-celled microconidia (1–2 μm in diameter)

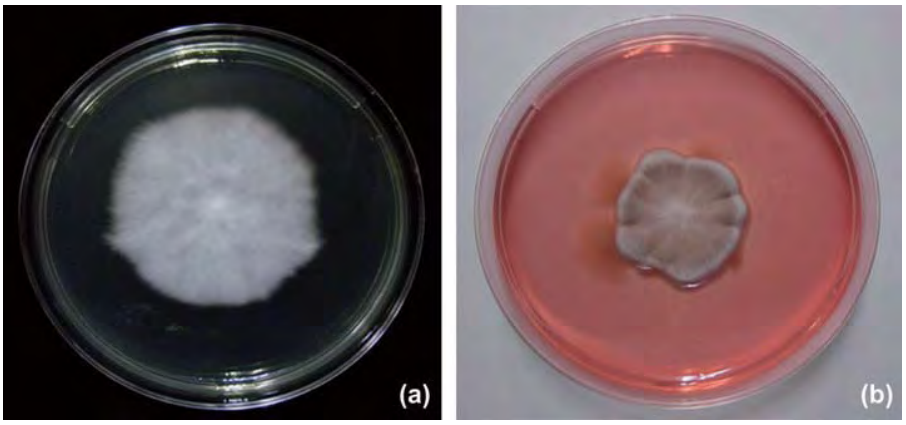

Fig. 2 Colony of isolate IFM 58803 on SDA (a) and PDA (b) cultured at 25°C for 21 days.

attached to the hyphae at right angles were observed on the SDA block incubnated at 25°C for 28 days. Hyphae were predominant on the PDA block with a few microconidia (Fig. 3).

Gymnothecia were not produced by any crosses. Crosses among *A. grubyi* were also negative.

The sequence of the ITS1-5.8S-ITS2 region of the rRNA gene obtained from the present isolate consisted of 597 base pairs, and showed 99% identity to GenBank database (http://www.ncbi.nlm.nih.gov/nuccore) accession number AB455805, derived from a clinical *M. gallinae* isolate (IFM 56900) in Japan [27]. The present isolate was deposited in the National BioResource Project culture collection at the Medical Mycology Research Center, Chiba University, 260-8673 Chiba, Japan as IFM 58803. The sequence of the ITS1-5.8S-ITS2 region of the rRNA gene was deposited in the GenBank database with accession number AB667976.

There were two genotype clusters of the ITS1-5.8S-ITS2 region of the rRNA gene based on the maximum parsimony tree (Fig. 4). One cluster mainly consisted of *M. gallinae* and the other comprised *A. grubyi*. The present sequence was located in the same cluster as those derived from a Japanese clinical isolate of *M. gallinae*.

Discussion

Recently, it has become clear that *M. gallinae* is not restricted to tropical and subtropical regions, but may be present in temperate areas, as revealed by records of infection and isolation in European countries [17,27]. Our isolation of *M. gallinae* from a fighting cock, following the human isolate reported by Miysasto *et al*. [27], indicates that Japan is one of the endemic areas.

Interestingly, the sequence of the ITS1-5.8S-ITS2 region of the rRNA gene derived from the present isolate was different from that of the human isolate in Okinawa prefecture, suggesting that at least two different genotypes of *M. gallinae* exist in Japan as confirmed by duplicate sequence analysis. In addition, phylogenetic analyses by the maximum parsimony method indicated that *M. gallinae* and *A. grubyi* were different species, although there are insufficient sequence data to confirm this at present. Furthermore, we could not correlate actual mating ability with genotype due to infertility of the tested *A. grubyi* isolates.

The immigration route of *M. gallinae* to Japan is unclear as only two isolates are known, i.e., from the clinical case in 2011 and the one described in this report.

Fig. 3 (a) Septate hyphae with a few macroconidia consisting of 4 to 6 cells, and (b) ovoid to pyriform single-celled microconidia attached to the hyphae at right angles on an SDA block cultured at 25°C for 28 days. Bars indicate 10 μm.

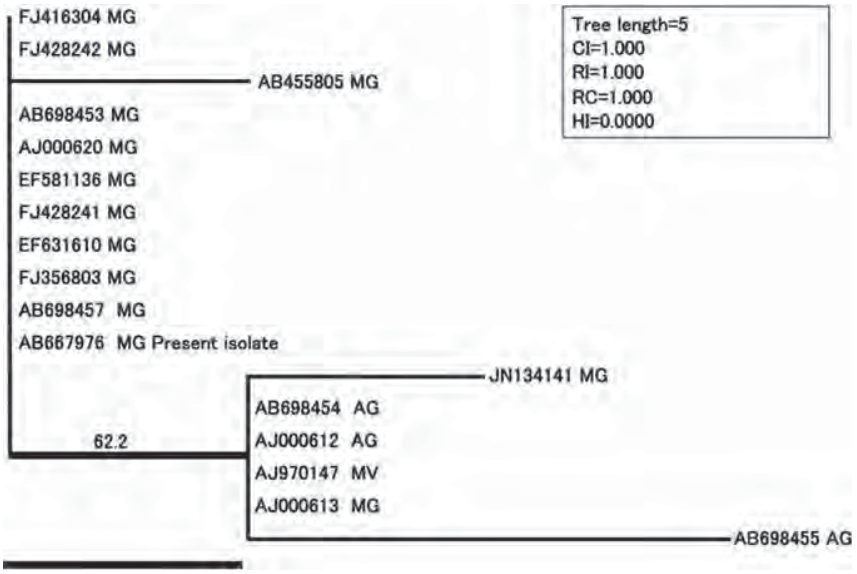

Fig. 4 The exclusive most-parsimonious tree obtained from heuristic searches based on ITS1-5.8S-ITS2 rRNA gene sequences using 546 bases. Bootstrap support value above 50% is indicated at the node. The bar indicates 1 base difference. Data are shown with accession numbers and fungal species as MG, *Microsporum gallinae*; AG, *Arthroderma grubyi*; and MV, *Microsporum vanbreuseghemii*. CI, consistency index. RI, retention index. RC, rescaled consistency index. HI, homoplasy index.

Neither human nor poultry infections had been reported prior to the first human case of *M. gallinae* infection. However, *M. gallinae* infection in fighting cocks is mild, and infections in humans closely resemble other dermatophytoses (such as *M. canis* infection). Therefore, many human cases and animal infections were likely ignored [27].

In conclusion, Japan is an endemic area of *M. gallinae* infection, based on a human case [27] and the present isolate from a fighting cock.

Acknowledgements

This study was supported in part by the Special Research Fund for Emerging and Re-emerging Infections of the Ministry of Health, Welfare and Labor (Grant No. H-21-Shinkou-004), and by a Grant-in-Aid for Scientific Research© by the Japan Society for the Promotion of Science (JSPS), No. 23580419. We express our thanks to Drs Takako Murano (Chiba Prefecture), Keiji Takahashi (Chiba Prefecture), Tadao Ikeda (Association Pasteur Japon), Eichiro Matayoshi (Okinawa Veterinary Medical Association), Taketoshi Kawamitsu (Okinawa Veterinary Medical Association), Takako Okubo (Ibaraki Prefecture), Masami Sudo (Ibaraki Prefecture), Tomo Inomata (Azabu University), Shigeyuki Mastui (Shizuoka Prefecture), Moriji Iketani (Shizuoka Prefecture), Yoshimi Imura (University of the Ryukyus), and Morihiko Hirakawa (University of the Ryukyus) for sample collection. We thank Ms Kyoko Yarita, Akiko Takayama and Yuki Hanami (Medical Mycology Research Center, Chiba University) for technical support.

Declaration of interest: The corresponding author, Ayako Sano declared the no conflict of interest submitted to the University of the Ryukyus No. H24-763.

References

1 Chermette R, Ferreiro L, Guillot J. Dermatophytoses in animals. *Mycopathologia* 2008; **166**: 385–405.
2 Megnin P. Nouvelle maladie, parasitaire de la peau chez un coq. *C R Seances Soc Biol* 1881; **33**: 404–406 [in French].
3 Londero AT, Fischman O, Ramos CD. *Trichophyton gallinae* in Brazil. *Sabouraudia* 1964; **3**: 233–234.
4 Londero AT, Ramos CD, Fischman O. Four epizooties of *Trichophyton gallinae* infection on chickens in Brazil. *Mykosen* 1969; **12**: 31–38.
5 Khosravi AR, Mahmoudi M. Dermatophytes isolated from domestic animals in Iran. *Mycoses* 2003; **46**: 222–225.
6 Fonseca E, Mendoza L. Favus in a fighting cock caused by *Microsporum gallinae*. *Avian Dis* 1984; **28**: 737–741.
7 Droual R, Bickford AA, Walker RL, Channing SE, McFadden C. Favus in a backyard flock of game chickens. *Avian Dis* 1991; **35**: 625–630.
8 Bradley FA, Bickford AA, Walker RL. Diagnosis of favus (avian dermatophytosis) in Oriental breed chickens. *Avian Dis* 1993; **37**: 1147–1150.
9 Bradley FA, Bickford AA, Walker RL. Efficacy of miconazole nitrate against favus in oriental breed chickens. *Avian Dis* 1995; **39**: 900–901.
10 Baudet E. Dermatomycosis in a dog produced by *Microsporum* (*Achorion*) *gallinae*. *J Am Vet Med Assoc* 1943; **102**: 383–384.
11 Dvorak J, Otcenasek M. Geophilic, zoophilic and anthropophilic dermatophytes. A review. *Mycopathol Mycol Appl* 1964; **23**: 294–296.
12 Komárek J, Wurst Z. Dermatophytes in clinically healthy dogs and cats. *Vet Med (Praha)* 1989; **34**: 59–63 [in Czech].

13 Georg LK, Ajello L, Friedman L, Brinkman SA. A new species of *Microsporum* pathogenic to man and animals. *Sabouraudia* 1962; **1**: 189–196.
14 Gordon MA, Little GN. *Trichophyton* (*Microsporum?) gallinae* ringworm in a monkey. *Sabouraudia* 1968; **6**: 207–212.
15 Korting HC, Zienicke H. Dermatophytoses as occupational dermatoses in industrialized countries. Report on two cases from Munich. *Mycoses* 1990; **33**: 86–89.
16 Goodenough AE, Stallwood B. Intraspecific variation and interspecific differences in the bacterial and fungal assemblages of blue tit (*Cyanistes caeruleus*) and great tit (*Parus major*) nests. *Microb Ecol* 2010; **59**: 221–232.
17 Sabouraud R. Maladies de Cuir Chevelu. III. In: *Les Maladies Cryptogamiques. Les Teignes*. Paris: Masson et Cie, 1910.
18 Georg LK, Torres G. A human case of *Trichophyton gallinae* infection; disease contracted from chickens. *AMA Arch Derm* 1956; **74**: 191–197.
19 Gip L. Isolation of *Trichophyton gallinae* from two patients with tinea cruris. *Acta Derm Venereol (Stockholm)* 1964; **44**: 251–254.
20 Dvorak J, Otcenasek M. The isolation of *Trichophyton Gallinae* (M'egnin) Silva et Benham 1952 from man. *J Invest Dermatol* 1964; **42**: 35–43.
21 de Albornoz MCB, Ramos Z, Vautrey RF. Tinea capitis by *Trichophyton gallinae*. *Dermatol Venezol* 1967; **1-2**: 52–59 [in Spanish].
22 Faruqui AH, Khan KA, Haroon TS. Scalp infection by *Trichophyton gallinae* (a case report from Pakistan). *Mykosen* 1984; **27**: 589–591.
23 del Palacio A, Pereiro-Miguens M, Gimeno C, *et al*. Widespread dermatophytosis due to *Microsporum* (*Trichophyton*) *gallinae* in a patient with AIDS – a case report from Spain. *Clin Exp Dermatol* 1992; **17**: 449–453.
24 Khosravi AR, Aghamirian MR, Mahmoudi M. Dermatophytoses in Iran. *Mycoses* 1994; **37**: 43–48.
25 Nweze EI. Etiology of dermatophytoses amongst children in northeastern Nigeria. *Med Mycol* 2001; **39**: 181–184.
26 Poblete-Gutiérrez P, Abuzahra F, Becker F, *et al*. Onychomycosis in a diabetic patient due to *Trichophyton gallinae*. *Mycoses* 2006; **49**: 254–257.
27 Miyasato H, Yamaguchi S, Taira K, *et al*. Tinea corporis caused by *Microsporum gallinae*: the first clinical case in Japan. *J Dermatol* 2011; **38**: 473–478.
28 Takahashi Y, Sano A, Takizawa K, *et al*. The epidemiology and mating behavior of *Arthroderma benhamiae* var. *erinacei* in household four-toed hedgehogs *(Atelerix albiventris)* in Japan. *Nihon* Ishinkin Gakkai Zasshi 2003; **44**: 31–38.
29 Murata Y, Sano A, Ueda Y, *et al*. Molecular epidemiology of canine histoplasmosis in Japan. *Med Mycol* 2007; **45**: 233–247.
30 White TJ, Bruns T, Lee S, Taylor JW. Amplification and direct sequencing of fungal ribosomal RNA genes for phylogenetics. In: Innis MH, Gelfand DH, Sninsky JJ, White TJ, (eds.), *PCR Protocols: A Guide to Methods and Applications*. San Diego, CA: Academic Press, 1990 : 315–322.
31 Jeanmougin F, Thompson JD, Gouy M, Higgins DG, Gibson TJ. Multiple sequence alignment with Clustal X. *Trends Biochem Sci* 1998; **23**: 403–405.
32 Swofford DL. *PAUP*. Phylogenetic Analysis Using Parsimony (*and other methods)* (version 4.0). Sunderland, MA: Sinauer Associates, 2001.
33 TreeView [homepage on the Internet]. Roderic D. M. Page, Glasgow, Scotland, UK, 1998. Available from: http://taxonomy.zoology.gla.ac.uk/rod/treeview.html

This paper was first published online on Early Online on 18 July 2012.

Veterinary Microbiology 161 (2012) 196–205

Contents lists available at SciVerse ScienceDirect

Veterinary Microbiology

journal homepage: www.elsevier.com/locate/vetmic

Distribution and molecular characterization of *Porphyromonas gulae* carrying a new *fimA* genotype

Yoshie Yamasaki [a,b], Ryota Nomura [a], Kazuhiko Nakano [a,*], Hiroaki Inaba [c], Masae Kuboniwa [d], Norihiko Hirai [e], Mitsuyuki Shirai [e], Yukio Kato [f], Masaru Murakami [g], Shuhei Naka [a], Soichi Iwai [h], Michiyo Matsumoto-Nakano [b], Takashi Ooshima [a], Atsuo Amano [d], Fumitoshi Asai [e]

[a] *Department of Pediatric Dentistry, Osaka University Graduate School of Dentistry, Suita, Osaka 565-0871, Japan*
[b] *Department of Pediatric Dentistry, Okayama University Graduate School of Medicine, Dentistry and Pharmaceutical Sciences, Okayama 700-8556, Japan*
[c] *Department of Oral Frontier Biology, Center for Oral Science, Osaka University Graduate School of Dentistry, Suita, Osaka 565-0871, Japan*
[d] *Department of Preventive Dentistry, Osaka University Graduate School of Dentistry, Suita, Osaka 565-0871, Japan*
[e] *Department of Pharmacology, School of Veterinary Medicine, Azabu University, Sagamihara, Kanagawa 252-5201, Japan*
[f] *Department of Veterinary Public Health II, School of Veterinary Medicine, Azabu University, Sagamihara, Kanagawa 252-5201, Japan*
[g] *Department of Molecular Biology, School of Veterinary Medicine, Azabu University, Sagamihara, Kanagawa 252-5201, Japan*
[h] *Department of Oral and Maxillofacial Surgey, Osaka University Graduate School of Dentistry, Suita, Osaka 565-0871, Japan*

ARTICLE INFO

Article history:
Received 14 May 2012
Received in revised form 14 July 2012
Accepted 16 July 2012

Keywords:
Fimbriae
Genotype
PCR
Periodontitis
Porphyromonas gulae
Risk marker

ABSTRACT

Porphyromonas gulae is a gram-negative black-pigmented anaerobe which is known to be a pathogen for periodontitis in dogs. Approximately 41 kDa filamentous appendages on the cell surface (FimA) encoded by the *fimA* gene are regarded as important factors associated with periodontitis. The *fimA* genotype was classified into two major types and strains in type B were shown to be more virulent than those in type A. In the present study, we characterized a strain with a novel *fimA* genotype and designated it as type C. The putative amino acid sequence was shown to be similar to the genotype IV *fimA* of *Porphyromonas gingivalis*, a major pathogen of human periodontitis. Analyses using an oral squamous cell carcinoma cell line derived from tongue primary lesions revealed that the type C strain inhibited proliferation and scratch closure more than genotype A and B strains. In addition, experiments using a mouse abscess model demonstrated that the type C strain could induce much higher systemic inflammation when compared with strains of the other genotypes. Furthermore, molecular analyses of oral swab specimens collected from dogs demonstrated that the detection frequencies of *P. gulae* and the genotype C in the periodontitis group were significantly higher than those in the periodontally healthy group. These results suggest that FimA of *P. gulae* is diverse with the virulence of genotype C strains the highest and that molecular identification of genotype C *P. gulae* could be a possible useful marker for identifying dogs at high risk of developing periodontitis.

1. Introduction

Periodontal diseases are initiated following gingivitis with localized inflammation without the destruction of the periodontal tissues (cementum, periodontal ligament and alveolar bone) (Pihlstrom et al., 2005). Without any intervention, this localized inflammation generally progresses to periodontitis, especially in elder subjects and

* Corresponding author at: Department of Pediatric Dentistry, Osaka University Graduate School of Dentistry, 1-8 Yamada-oka, Suita, Osaka 565-0871, Japan. Tel.: +81 6 6879 2963; fax: +81 6 6879 2965.
E-mail address: nakano@dent.osaka-u.ac.jp (K. Nakano).

0378-1135/$ – see front matter © 2012 Elsevier B.V. All rights reserved.
http://dx.doi.org/10.1016/j.vetmic.2012.07.026

those with systemic disorders. The symptoms of periodontitis are generally irreversible and include severe bleeding, pus discharge and mobility of the affected tooth and ultimately leads to tooth loss. The distribution of the periodontitis-related bacterial species has been investigated in the oral swab specimens taken from Japanese dogs and it was observed that *Porphyromonas gulae*, a gram-negative black-pigmented anaerobe, was one of the species frequently detected (Kato et al., 2011).

The cell surface 41 kDa fimbrillin (FimA), a subunit of fimbriae, was characterized in *P. gulae* and is known to be one of the major factors for periodontitis in dogs (Hamada et al., 2008). Furthermore, *P. gulae* invasion into gingival epithelial cells has also been demonstrated. In our recent study, FimA of *P. gulae* could be classified into two major genotypes, and analyses of the putative amino acid sequences of FimA in many clinical strains revealed that the type A FimA is specific for *P. gulae*, and the amino acid sequence of type B FimA is more closely related to that of genotype III FimA of *Porphyromonas gingivalis*, a major pathogen of human periodontitis (Nomura et al., 2012). On the other hand, there are several *P. gulae*-positive specimens which are negative for both types A and B, indicating the presence of *P. gulae* strains without FimA or those with additional *fimA* genotypes (Nomura et al., 2012).

In the present study, we successfully characterized a new genotype for *fimA* genes in *P. gulae* encoding a novel FimA and designated it as genotype C. The purpose of the present study was to compare the properties of each FimA genotype relative to its virulence potential in periodontitis. In addition, the distribution of the each group was analyzed focusing on the clinical conditions of the dogs sampled.

2. Materials and methods

2.1. Bacterial and cell culture conditions

Table 1 lists the *P. gulae* strains analyzed in the present study, among which all except for one strain (D049) were previously reported (Kato et al., 2011; Nomura et al., 2012). Strain D049 was isolated from an oral swab specimen from a dog and confirmed to be *P. gulae* by a molecular biological method described previously (Kato et al., 2011). In addition, 11 *P. gingivalis* strains listed in Table 1 were also used (Amano et al., 1999; Nakagawa et al., 2000, 2002). *P. gingivalis* and *P. gulae* strains were cultured in mhTS broth [Tripticase soy broth (Becton, Dickinson & Co, Franklin Lakes, NJ, USA) with hemin (50 mg/ml) and menadione (5 mg/ml)] under anaerobic conditions.

The SAS cells, an oral squamous cell carcinoma cell line, were obtained from Japanese Collection of Research Biosources (Tokyo, Japan). Cells were cultured in RPMI 1640 medium (Wako, Osaka, Japan) supplemented with 10% fetal bovine serum at 37 °C in 5% CO_2.

Table 1
P. gulae and *P. gingivalis* strains used in the present study.

Species	Name	*fimA* types	Length of *fimA* gene (bp)	Accession numbers of *fimA* gene	References
P. gulae	ATCC 51700[a]	A	1152	AB297918	Hamada et al. (2008)
	D024	A	1152	AB663087	Nomura et al. (2012)
	D025	A	1152	AB663088	Nomura et al. (2012)
	D028	A	1152	AB663089	Nomura et al. (2012)
	D034	A	1152	AB663090	Nomura et al. (2012)
	D035	A	1152	AB663091	Nomura et al. (2012)
	D036	A	1152	AB663092	Nomura et al. (2012)
	D042	A	1152	AB663093	Kato et al. (2011)
	D043	A	1152	AB663094	Kato et al. (2011)
	D060	A	1152	AB663095	Kato et al. (2011)
	D066	A	1152	AB663096	Kato et al. (2011)
	D067	A	1152	AB663097	Kato et al. (2011)
	D068	A	1152	AB663098	Kato et al. (2011)
	B43	B	972[b]	CS228034	Dreier et al. (2005)
	D040[a]	B	1161	AB663099	Kato et al. (2011)
	D044	B	1161	AB663100	Kato et al. (2011)
	D052	B	1161	AB663101	Kato et al. (2011)
	D053	B	1161	AB663102	Kato et al. (2011)
	D077	B	1161	AB663103	Nomura et al. (2012)
	D049[a]	C	1167	AB679295	This study
P. gingivalis	381	I	1044	D17794	Amano et al. (1999)
	ATCC 33277	I	1044	D17795	Amano et al. (1999)
	BH18/10	I	1044	D17796	Amano et al. (1999)
	HW24D1	II	1047	D17797	Amano et al. (1999)
	OMZ314[a]	II	1044	D17798	Amano et al. (1999)
	OMZ409	II	1047	D17799	Amano et al. (1999)
	ATCC 49417	II	1053	D17800	Amano et al. (1999)
	6/26	III	1062	D17801	Amano et al. (1999)
	HG564	IV	1083	D17802	Amano et al. (1999)
	HNA99	V	1104	AB027294	Nakagawa et al. (2000)
	HG1691	Ib	1044	AB058848	Nakagawa et al. (2002)

[a] Strains analyzed in the mouse abscess model.
[b] Only partial sequences corresponding to *fimA* of *P. gulae* are available.

2.2. Sequence of the fimA genes

The nucleotide alignment of the entire length of the *fimA* gene was determined by the method described previously with some modifications as follows (Nomura et al., 2012). PCR was performed with genomic DNA extracted from *P. gulae* D049 using six types of *P. gingivalis fimA* specific sets of primers listed in Table 2 (Amano et al., 1999; Nakagawa et al., 2000, 2002). Since the tested *P. gulae* strains showed positive reaction for *P. gingivalis* type IV *fimA*, we designed the primer sets (HG564-F and HG564-R) based on the adjacent sequence of HG564 (type IV). Next, PCR was performed using these primers to amplify the entire length of the *fimA* gene of *P. gulae*, which was separated by electrophoresis on a 0.7% agarose gel and the amplified DNA fragments were extracted from the gel using a QIAEX gel extraction kit (Qiagen, Düsseldorf, Germany). The DNA was then directly cloned into a pGEM-T Easy vector (Promega, Madison, WI, USA). The nucleotide sequence was determined by the dye-terminator reaction with a DNA sequencing system (373-18 DNA sequencer; Applied Biosystems, Foster City, CA, USA) and an ABI PRISM kit. Data analyses were performed using Gene Works software (IntelliGenetics, Mountain View, CA, USA). The putative amino acid sequences of the FimA of types A and B *P. gulae* strains and those of *P. gingivalis* strains with *fimA* genotypes I through V and Ib listed in Table 1 were compared using the neighbor-joining method to construct a phylogenetic tree using CLUSTAL W (DNA Databank of Japan) and Tree View software (http://taxonomy.zoologygla.ac.uk/rod/treeview.html). Since the sequence from D049 was distinct from those of other strains, we designated it as a novel genotype (type C).

2.3. Construction of a PCR method to classify fimA groups

We previously developed a molecular biological method to classify type A and type B *P. gulae* strains (Nomura et al., 2012). In the present study, the entire *fimA* sequence of D049 was compared to those of genotypes A and B to find specific regions for Type C. A primer set specific for genotype C (Pgufim-CF and Pgufim-CR; Table 2) was then constructed. The amplified fragment was estimated to be 631 bp. The specificities of these primers were tested by the program Amplify (Engels, 1993), based on information on the DNA sequences of *P. gulae* strains obtained in the present study as well as that of *P. gingivalis* in the GenBank database (http://www.ddbj.nig.ac.jp/). The specificity of the primers was also confirmed using the GenBank database. PCR amplification was performed in a total volume of 20 μl with 1 μl of template solution and Ex Taq polymerase (Takara Bio. Inc., Otsu, Japan) according to the supplier's instructions. The PCR amplification reaction was performed in a thermal cycler (iCycler; Bio-Rad, Hercules, CA, USA) with the following cycling parameters: an initial denaturation at 95 °C for 4 min and then 30 cycles consisting of 95 °C for 30 s, 60 °C for 30 s, and 72 °C for 30 s, with a final extension at 72 °C for 7 min. The PCR products were subjected to electrophoresis in a 1.5% agarose

Table 2
PCR primers used in the present study.

Specific primer set	Sequence (5′–3′)	References
Detection of *P. gulae*		
P. gulae 16S rRNA	TTG CTT GGT TGC ATG ATC GG GCT TAT TCT TAC GGT ACA TTC ACA	Kato et al. (2011)
Determination of *fimA* alignment		
HG564-F[a]	GAT TTG CTG CTC TTG CTA TGA CAG CTT GTA	This study
HG564-R[a]	TTT AGT CGT TTG ACG GGT CGA TTA CCA AGT	
Specification of *fimA* type		
Type A *fimA*		
Pgufim-AF[a]	TGA GAA TAT CAA ATG TGG TGC AGG CTC ACG	Nomura et al. (2012)
Pgufim-AR[a]	CTT GCC TGC CTT CAA AAC GAT TGC TTT TGG	
Type B *fimA*		
Pgufim-BF[a]	TAA GAT TGA AGT GAA GAT GAG CGA TTC TTA TGT	Nomura et al. (2012)
Pgufim-BR[a]	ATT TCC TCA GAA CTC AAA GGA GTA CCA TCA	
Type C *fimA*		
Pgufim-CF[a]	CGA TTA TGA CCT TGT CGG TAA GAG CTT GGA	This study
Pgufim-CR[a]	TGT GGC TTC GTT GTC GCA GAA TCC GGC ATG	
Type I *fimA*	CTG TGT GTT TAT GGC AAA CTT C AAC CCC GCT CCC TGT ATT CCG A	Amano et al. (1999)
Type II *fimA*	ACA ACT ATA CTT ATG ACA ATG G AAC CCC GCT CCC TGT ATT CCG A	Amano et al. (1999)
Type III *fimA*	ATT ACA CCT ACA CAG GTG AGG C AAC CCC GCT CCC TGT ATT CCG A	Amano et al. (1999)
Type IV *fimA*	CTA TTC AGG TGC TAT TAC CCA A AAC CCC GCT CCC TGT ATT CCG A	Amano et al. (1999)
Type V *fimA*	AAC AAC AGT CTC CTT GAC AGT G TAT TGG GGG TCG AAC GTT ACT GTC	Nakagawa et al. (2000)
Type Ib *fimA*	CAG CAG AGC CAA AAA CAA TCG TGT CAG ATA ATT AGC GTC TGC	Nakagawa et al. (2002)

[a] Names of primers are indicated.

gel–Tris–acetate–EDTA buffer. The gel was stained with 0.5 μg ethidium bromide per ml and photographed under UV illumination. A 100 bp DNA ladder (New England BioLabs, Beverly, MA, USA) was used as the molecular size standard. The sensitivity of the PCR assay was determined by using titrated cultures of D049.

2.4. In vitro assays using cultured cells

Infected or control SAS cells were incubated with the TetraColor ONE Cell Proliferation Assay System (SEIKAGAKU, Tokyo, Japan) according to the instructions provided by the manufacturer. Data were calculated as the relative ratio of infected/uninfected (no infection) animals and expressed as the means ± SD from three independent experiments. As for the scratch assays, confluent cell monolayers, grown on gelatin-coated 6 well dishes, were scraped using a plastic tip to form a scratch wound as described previously (Inaba et al., 2004). The exposed surfaces were then re-coated with gelatin dissolved in RPMI 1640 at 37 °C for 1 h. The SAS cells were mixed with bacterial strains at a MOI of 10 and 100 for 2 h and then incubated with metronidazole (200 mg/ml) and gentamicin (300 mg/ml) for 12 h. The rate of scratch closure was determined using ImageJ software as described previously (Rincon et al., 2003).

2.5. Mouse abscess model

All animal procedures and protocols were reviewed and approved by the Institutional Animal Care and Use Committee of Osaka University Graduate School of Dentistry prior to the experiments. The virulence of *P. gulae* D049 was evaluated using a mouse abscess model developed for evaluation of *P. gingivalis* strains with some modifications as follows (Nakano et al., 2004; Nomura et al., 2012). As a reference, *P. gulae* ATCC 51700 (type A), D040 (type B) and *P. gingivalis* OMZ314 (type II) were also analyzed. Fifty female BALB/c mice (5 weeks old), which were randomly divided into 5 groups, were maintained in horizontal-flow cabinets and provided with sterile food and water *ad libitum*. At 40 days of age, a single site approximately 1 cm lateral from the midline on the dorsal surface was depilated, and 0.1 ml of bacterial suspension, 1×10^9 colony-forming units (CFU) of a test strain or PBS (control group), was injected subcutaneously. For quantitative evaluation of the infectious inflammatory change, serum C-reactive protein (CRP) was measured. However, 90% of all mice in the group infected with D049 died by day 4. Therefore, the present experiment was terminated on that day although the original model evaluated inflammatory changes for 2 weeks. Blood specimens (0.1 ml) were collected from an orbital vein at 0, 1, 2 and 4 days after bacterial infection and then centrifuged at 3000 rpm for 10 min to separate the serum. CRP concentrations in sera were calorimetrically quantified using a commercial kit (MOUSE C-REACTIVE PROTEIN (CRP) ELISA TEST KIT; Life Diagnostics, Inc., West Chester, PA, USA) according to the supplier's instructions. The mice were also monitored for signs and symptoms of infection, *i.e.* ruffled hair, abscess formation and emergence of erosion, as described previously.

2.6. Distribution of *P. gulae fimA* genotypes in oral swab specimens

All study protocols were approved by the Animal Research Committee of Azabu University, the Ethics Committees of Osaka University Graduate School of Dentistry and Okayama University Graduate School of Medicine, Dentistry and Pharmaceutical Sciences. Prior to collection of the specimens, the owners of all dogs were informed of the protocols of the present study and gave approval for their participation. Oral swab specimens were collected from one specific location, the gingival margin of the mandibular left canine in the oral cavity of 139 dogs using swabs (Seed-Swab® γ-1, Eiken Chemical Co. Ltd., Tokyo, Japan, or 2), as described previously (Kato et al., 2011). The ages of the dogs ranged from 0 to 17 years and mean age was 7.72. These dogs came to the clinic for health examinations, vaccinations, coxarthropathy, external otitis, external disc disease, trauma, or diarrhea. All of the dogs were reported to be kept indoors.

The periodontal condition of each dog was evaluated by measuring several parameters of a representative tooth (mandibular left canine) as follows. The periodontal pocket depth was measured to the nearest millimeter around the circumference of each tooth from the gingival margin to the deepest probing point, using a round-ended probe tip 0.4 mm in diameter. The maximum values were recorded as the values for periodontal pocket depth of each tooth. The periodontal pocket depths of 3 mm or less for large dogs, 2 mm or less for medium and small dogs were regarded as healthy. In addition, other criteria, such as no bleeding on probing, no pus discharge and no tooth mobility were also observed in healthy subjects. When observing the deeper periodontal pockets and bleeding on probing, the dogs were diagnosed for gingivitis or periodontitis. Periodontitis was diagnosed by pathological mobility due to obvious destruction of periodontal tissues, such as alveolar bone. The bacterial DNA of each specimen was extracted and PCR was performed using *P. gulae*-specific sets of primers, as described above. The *fimA* genotype was determined for *P. gulae*-positive specimens using specific primer sets for types A, B and C (Table 2).

2.7. Statistical analyses

Statistical analyses were performed using the computational software package StatView 5.0 (SAS Institute Inc., Cary, NC, USA) and Prism 4 (GraphPad Software Inc., La Jolla, CA, USA). Intergroup differences in *in vitro* assays and animal experiments were estimated using Bonferroni's method after an analysis of variance (ANOVA). Fisher's protected least-significant difference test was utilized to compare the detection frequencies of each *fimA* genotype in each gingival condition. Odds ratio (OR) and 95% confidence interval (CI_{95}) values were calculated to determine any significant association regarding each *fimA* genotype in dogs with each periodontal condition. A *P* value of less than 0.05 was considered statistically significant.

Fig. 1. Comparison of the deduced amino acid sequences of FimAs encoded by type A, B and C *fimA* genes of *P. gulae*. Single and double dots indicate similar and highly similar amino acid residues, respectively. Dashes indicate the gaps when multiple alignments were performed. The arrow indicates the cleavage site estimated by the SignalP 3.0 Server (http://www.cbs.dtu.dk/services/SignalP/). The alignment was made using the CLUSTAL W program of the DNA Data Bank of Japan.

3. Results

3.1. Molecular biological properties of type C FimA

The entire length of the *fimA* gene of *P. gulae* strain D049 is 1167 bp, which was deposited in the DNA Database of Japan under accession no. AB679295. Fig. 1 shows the deduced amino acid sequence of strains ATCC 51700 (type A) and D077 (type B) as compared to that of D049 (type C). The FimA in D049 and that in *P. gulae* types A and B strains ranged from 49 to 50% identical, which was almost similar to those of types I, II, III, and Ib FimA in *P. gingivalis*. On the other hand, the identity of type C FimA with that in *P. gingivalis* HNA99 was 59%. In contrast, the FimA of D049 and that of *P. gingivalis* HG564 (type IV) showed 92% identity. Fig. 2 shows a phylogenetic tree comprised of the FimA of *P. gingivalis* types I through V and Ib as well as *P. gulae* types A, B and C. Type C FimA was shown to be the most closely related to genotype IV *P. gingivalis*.

3.2. Effects of P. gulae infection in SAS cells

P. gulae ATCC 51700 (type A) and D049 (type C) caused the cells to change into a contracted and rounded morphology, which was similar to that produced by *P. gingivalis* OMZ314 at a MOI 100 (Fig. 3A). In a proliferation assay, D049 (type C), but not types A and B strains, inhibited cell proliferation at a MOI 10 (Fig. 3B). In addition, D049 showed the maximum inhibition of cell proliferation and the other strains, except for D066 (type A), slowed proliferation at a MOI 100 (Fig. 3C). As for scratch closure assays, the migration rate of D049 was 42.4%, which was the lowest rate among the strains tested at a MOI 10 (Fig. 3D). The closure rate of D049-infected cells decreased to 31.4% at a MOI 100, although the rates for the other strains were shown to be similar to D049 or slightly decreased (data not shown).

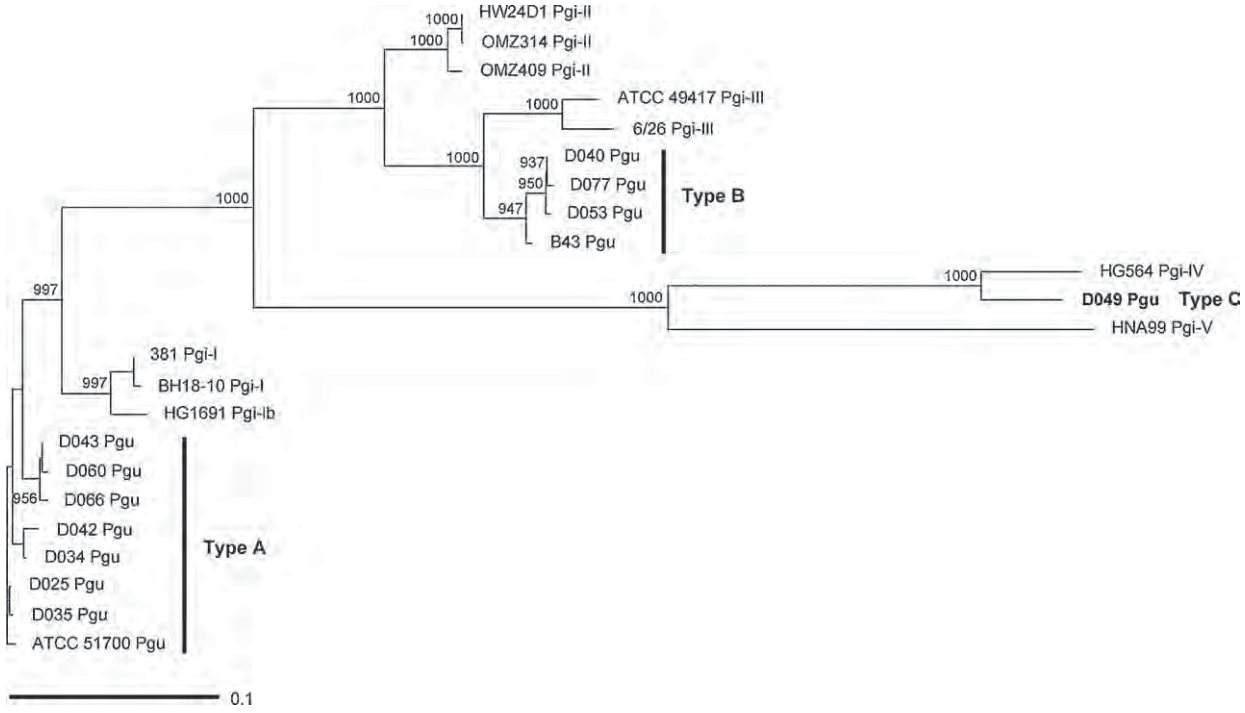

Fig. 2. Evolutionary relationship based on the synonymous site variation in the putative amino acid sequences of FimA encoded by *fimA* genes of *P. gulae* and *P. gingivalis*. The neighbor-joining method was used to construct the phylogenetic tree using CLUSTAL W (DNA Databank of Japan) and Tree View software (http://taxonomy.zoology.gla.ac.uk/rod/treeview.html). Pgu and Pgi indicate *P. gulae* and *P. gingivalis*, respectively. The roman numerals following Pgi indicate the *fimA* genotypes of *P. gingivalis*. The numbers shown in the tree are bootstrap values.

3.3. Mouse abscess model

Subcutaneous injections of D049 (type C) caused drastic weakened systemic conditions in the mice on Day 1 and the formation of erosions was observed on Day 2 although similar lesions were not observed in the mice injected with types A and B strains (Fig. 4). The serum CRP values in mice infected with D049 on Days 1 and 2 were significantly higher than those injected with the other strains (data not shown). On Day 4, 90% of all mice injected with D049 died.

3.4. Clinical specimens

139 specimens were divided into periodontally healthy ($n = 22$), gingivitis ($n = 94$) and periodontitis ($n = 23$) groups based on the clinical conditions of the dogs from which the specimens were isolated. The ages of the healthy group (mean 5.05) were significantly lower than those for the gingivitis (7.97) and periodontitis (10.57) groups ($P < 0.01$ and $P < 0.001$, respectively). Comparing the periodontitis and gingivitis groups, ages of the periodontitis group were significantly higher ($P < 0.05$).

The PCR system for identification of type C *fimA* was developed based on the specific nucleotide alignment of type C *fimA* as compared to those of types A and B *fimA* (Fig. 5A). The specificity of this PCR system was confirmed using the strains listed in Table 1, which demonstrated that primers designed for type C *fimA* genes of *P. gulae* did not generate positive bands from the *P. gingivalis* strains tested. In addition, the sensitivity was shown to be approximately 10–100 CFU per reaction (data not shown).

Fig. 5B shows representative results for the analyses of clinical specimens. *P. gulae* was detected in 110 out of 139 (79.1%) oral swab specimens (Table 3). The detection rate for *P. gulae* in the periodontitis group was 100%, which was significantly higher than that in healthy (63.6%) and gingivitis (77.7%) groups ($P < 0.001$ and $P < 0.05$, respectively). Single and multiples genotypes were identified in *P. gulae*-positive specimens and there were a few untypeable specimens in each group. The numbers of the specimens containing multiple genotypes were higher in the gingivitis and periodontitis groups than that of the periodontally healthy group ($P < 0.05$ and $P < 0.01$, respectively). The numbers of subjects with multiple genotypes or type B in the gingivitis and periodontitis groups and those of multiple types or type C in the periodontitis group were higher than those of the healthy group ($P < 0.01$ each).

The OR of *P. gulae* detection for periodontitis was 27.55 (CI_{95}; 1.48–514.10). In addition, those with multiple genotypes, multiple genotypes or single genotypes B and C were 8.23 (CI_{95}; 1.89–35.83), 8.44 (CI_{95}; 2.12–33.61) and 12.75 (CI_{95}; 3.06–53.19), respectively. Furthermore, the OR of multiple types or single type B detection for gingivitis was 4.50 (CI_{95}; 1.42–14.30).

4. Discussion

The present study characterizes a novel *fimA* genotype of *P. gulae*. We previously isolated many *P. gulae* strains

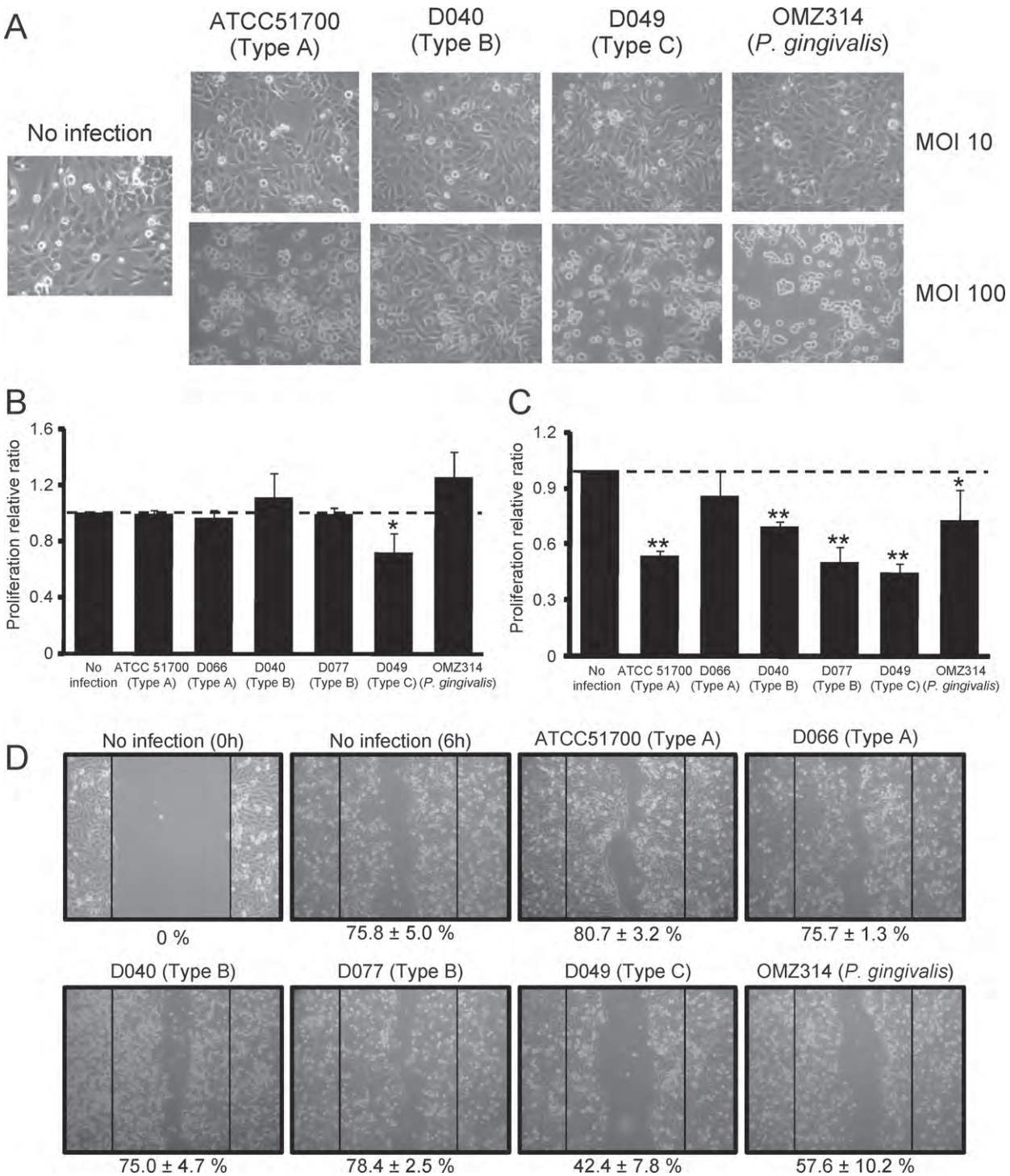

Fig. 3. Effects of *P. gulae* strains infection in cultured cells. (A) Light microscopy images showing morphology of the cells infected with *P. gulae* at a MOI of 10 and 100 for 24 h. Control cells were uninfected. (B and C) Cell proliferation assay measured by tetrazolium following infection with *P. gulae* strains at a MOI of 10 (B) and 100 (C). Data are expressed as relative ratio infected/uninfected (no infection) and are means ± SD from three independent experiments analyzed with a *t*-test ($^{*}P < 0.05$, $^{**}P < 0.01$). (D) *In vitro* scratch assay in the cells infected with *P. gulae* at a MOI of 10. Bars show the scratched wound regions at 0 h. The rates of wound closure are determined from assays and are means ± SD from three independent experiments.

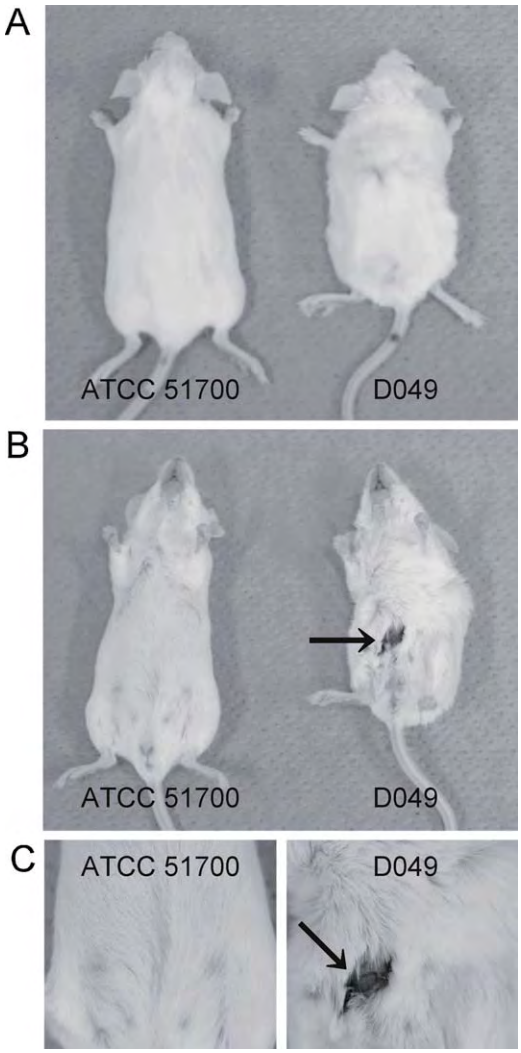

Fig. 4. Macroscopic observation of a representative mouse in the abscess model experiment. (A) Dorsal view, (B) ventral view and (C) magnification of the erosion area. Arrows indicate the areas of erosion.

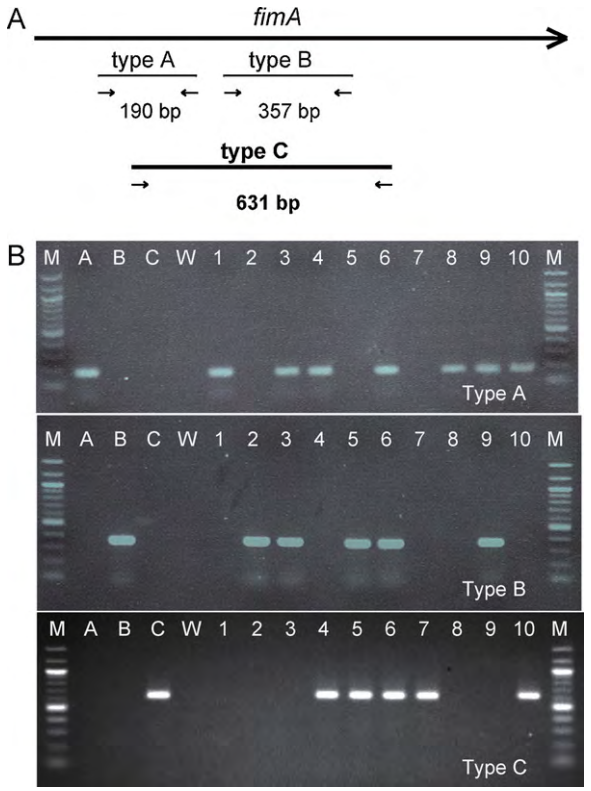

Fig. 5. Construction of the primers specific for type C of *P. gulae*. (A) The position of the primers for *fimA* genotypes A, B and C are illustrated, (B) analyses of clinical specimens for determination of *fimA* types. Lanes: M; molecular size marker (100-bp DNA ladder), A; ATCC 51700, B; D077, C; D049, W, sterile water. 1–10; clinical specimens.

from Japanese dogs, almost all of which were classified into types A or B *fimA* (Kato et al., 2011). Only a single strain (D049) was shown to be of a non-A and non-B FimA genotype, which is designated as type C in the present study. Type A FimA was shown to be *P. gulae*-specific and shares 73% amino acid homology with *P. gulae* type B and *P. gingivalis* type III FimA (Nomura et al., 2012). On the other hand, the present study revealed that the similarity of type C FimA and type IV FimA of *P. gingivalis* was very high. Relative to the virulence of *P. gingivalis*, types II/IV/Ib was shown to be more virulent than types I/III/V (Kuboniwa et al., 2010). Thus, we speculated that the virulence of type C would be the highest among all *fimA* types of *P. gulae*.

Initially, we used cultured cells to perform *in vitro* analyses. To begin the process of characterizing the response of SAS cells to infection with *P. gulae* strains, the infected cells were observed by microscopy and found to be altered in the morphology. Next, we analyzed the inhibition of cell proliferation, which demonstrated that the genotype C strain D049 caused the maximum inhibition of proliferation. It was reported that oral bacteria can inhibit cell migration (Inaba et al., 2004, 2005) and the *in vitro* scratch assay is effective in characterizing the properties of cell proliferation and migration (Liang et al., 2007). Thus, using the cell migration assay, we also demonstrated that D049 inhibited cell migration the most. These results support the proposal that type C fimbriae might be one of the important factors for the impairment of cellular function caused by *P. gulae*. However, further analyses, such as evaluation of multiple type C strains or strains with replacement of type C *fimA* with other genotype *fimA* genes and *vice versa* should be carried out to confirm this hypothesis.

A previous investigation using the mouse abscess model showed that strains with type B *fimA* caused more severe systemic inflammation than those with type A *fimA* (Nomura et al., 2012). The present study clearly showed that the properties inducing systemic inflammation by D049 (genotype C) were strongest compared to other *P. gulae* strains in the mouse model. When we developed a mouse model for evaluating the properties of *P. gingivalis* involved in inducing systemic inflammation, we found that strain OMZ314 (type II *fimA*) possessed the highest potential (Nakano et al., 2004). In fact, subcutaneous injection of OMZ314 resulted in the death of mice under

Table 3
Distribution frequency of *fimA* genotypes in *P. gulae*-positive specimens in periodontally healthy, as well as dogs with gingivitis and periodontitis.

	Healthy ($n = 22$)	Gingivitis ($n = 94$)	Periodontitis ($n = 23$)
Age [mean ± standard deviation (range)]	5.05 ± 4.29 (0–12)	7.97 ± 3.91 (1–17)**	10.57 ± 3.58 (2–16)***,#
P. gulae-positive	14 (63.6%)	73 (77.7%)	23 (100%)**#
Single type	9 (40.9%)	36 (38.3%)	10 (43.5%)
A	7 (31.8%)	20 (21.3%)	4 (17.4%)
B	1 (4.5%)	13 (13.8%)	2 (8.7%)
C	1 (4.5%)	3 (3.2%)	4 (17.4%)
Multiple types	3 (13.6%)	34 (36.2%)*	13 (56.5%)**
A and B	0 (0%)	4 (4.3%)	4 (17.4%)
A and C	1 (4.5%)	16 (17.0%)	8 (34.8%)
B and C	2 (9.1%)	4 (4.3%)	1 (4.3%)
A, B and C	0 (0%)	10 (10.6%)	0 (0%)
Untypeable	2 (9.1%)	3 (3.2%)	0 (0%)
Single A type or multiple types	10 (45.5%)	54 (57.4%)	17 (73.9%)
Single B type or multiple types	4 (18.2%)	47 (50.0%)**	15 (65.2%)**
Single C type or multiple types	4 (18.2%)	37 (39.4%)	17 (73.9%)**

* $P < 0.05$ against healthy group.
** $P < 0.01$ against healthy group.
*** $P < 0.001$ against healthy group.
\# $P < 0.05$ against gingivitis group.

the conditions tested. Since we attempted to develop a mouse model to evaluate systemic virulence over prolonged periods, we modified the mouse model so that all mice survived even in the group infected with OMZ314. Thus, it was very surprising that erosion was identified in almost all of the mice with subcutaneous injections of D049 even on Day 1, and dramatically weakened systemic conditions were observed in almost all of the mice leading to death by Day 4. Thus, we demonstrated that strain D049 could cause extremely severe systemic inflammation.

We are interested in applying the results obtained in the present study for clinical purposes. Therefore, we plan to develop a system for identifying high risk subjects for periodontitis. As a first step, the periodontal condition of the mandibular left canine was evaluated as a representative tooth for several reasons. First, it is relatively easy to visually inspect this region without general anesthesia. In addition, traction of the frenulum close to the mandibular canine can produce wide views of the area. For clinical evaluation, we can further simplify the criteria for diagnosis based on our current knowledge of periodontitis in humans. Periodontal pocket depth, bleeding on probing and tooth mobility were used as major criteria for diagnosis of gingivitis and periodontitis together with other evaluations such as pus discharge.

The distribution of *P. gulae* in the dogs in the periodontitis group was significantly higher than those of the healthy and gingivitis groups. The detection rates of *P. gulae* in Brazilian dogs with and without periodontitis were reported to be 92% and 56%, respectively (Senhorinho et al., 2011), which was almost similar to those of Japanese dogs analyzed in the present study. As for humans, the distribution rates of *P. gingivalis* in Japanese patients with periodontitis and periodontally healthy subjects were reported to be 87.1%, and 36.8%, respectively (Amano et al., 2000), indicating that the presence of *P. gingivalis* itself could be one possible risk marker for periodontitis. The predominant cultural subgingival flora in dogs shows great similarity to the subgingival bacteria from humans at the genus level, but distinct differences at the species level (Dahlén et al., 2012). In the present study, the statistical analyses indicated that *P. gulae* detection itself could be one possible risk factor for development of periodontitis. However, there are other species possibly associated with periodontitis. Further studies should focus on the analyses of the other species related to periodontitis in dogs.

It should be noted that there exist specimens which are negative for genotypes A, B and C *fimA* in *P. gulae*-positive specimens. This finding indicates the presence of *P. gulae* strains without FimA or those with additional *fimA* genotypes. Further studies are required to elucidate the *fimA* genotypes of these specimens. However, we speculate that the existence of unknown type(s) would not influence the results obtained in the present study since the number of such specimens are extremely low. Thus, we can design a system for identification of dogs at high risk for developing periodontitis without elucidating the details of the untypeable specimens.

Prediction of the risk for developing future periodontitis would be clinically beneficial. However, it was reported that the oral flora in health and periodontitis is highly diverse and that it contains high proportions of uncultured and potentially novel species (Riggio et al., 2011). It should be noted that the present study demonstrated that specific FimA genotypes of *P. gulae* could be one possible risk factor. Specifically, three factors, such as the presence of *P. gulae*, detection of multiple *fimA* genotypes with single type B or type C detection were suggested. The molecular biological analyses of the specimens taken from the dogs enable the identification of high risk dogs, who should be provided with intensive care for periodontitis. In addition, we propose that the dogs designated as risk subjects in healthy

and/or gingivitis groups should be carefully followed up for prevention of the onset of subsequent periodontitis. Further studies should also focus on large-scale analyses to identify the geographic specificity of the presence of the *fimA* genotypes. Such worldwide surveys could elucidate the validity of this method for identification of high risk subjects for periodontitis in dogs.

Acknowledgements

This study was supported by a Grant-in-Aid for Scientific Research for Challenging Exploratory Research No. 23658256 from the Japan Society for Promotion of Science, and was supported by the Promotion and Mutual Aid Corporation of Private Schools of Japan and a Grant-in-Aid for Matching Fund Subsidy for Private Universities. We also thank Prof. Howard K. Kuramitsu (State University of New York at Buffalo) for his editing this manuscript.

References

Amano, A., Kuboniwa, M., Nakagawa, I., Akiyama, S., Morisaki, I., Hamada, S., 2000. Prevalence of specific genotypes of *Porphyromonas gingivalis fimA* and periodontal health status. J. Dent. Res. 79, 1664–1668.

Amano, A., Nakagawa, I., Kataoka, K., Morisaki, I., Hamada, S., 1999. Distribution of *Porphyromonas gingivalis* strains with *fimA* genotypes in periodontitis patients. J. Clin. Microbiol. 37, 1426–1430.

Dahlén, G., Charalampakis, G., Abrahamsson, I., Bengtsson, L., Falsen, E., 2012. Predominant bacterial species in subgingival plaque in dogs. J. Periodontal Res. 47, 354–364.

Dreier, K.J., Hardham, J.M., Haworth, J.D., King, K.W., Krishnan, R., Mcgavin, D.R. 2005. Vaccine for periodontal disease. Patent: WO2005112993-A1/95.

Engels, W.R., 1993. Contributing software to the internet: the Amplify program. Trends Biochem. Sci. 18, 448–450.

Hamada, N., Takahashi, Y., Watanabe, K., Kumada, H., Oishi, Y., Umemoto, T., 2008. Molecular and antigenic similarities of the fimbrial major components between *Porphyromonas gulae* and *P. gingivalis*. Vet. Microbiol. 128, 108–117.

Inaba, H., Kawai, S., Nakayama, K., Okahashi, N., Amano, A., 2004. Effect of enamel matrix derivative on periodontal ligament cells *in vitro* is diminished by *Porphyromonas gingivalis*. J. Periodontol. 75, 858–865.

Inaba, H., Tagashira, M., Kanda, T., Ohno, T., Kawai, S., Amano, A., 2005. Apple- and hop polyphenols protect periodontal ligament cells stimulated with enamel matrix derivative from *Porphyromonas gingivalis*. J. Periodontol. 76, 2223–2229.

Kato, Y., Shirai, M., Murakami, M., Mizusawa, T., Hagimoto, A., Wada, K., Nomura, R., Nakano, K., Ooshima, T., Asai, F., 2011. Molecular detection of human periodontal pathogens in oral swab specimens from dogs in Japan. J. Vet. Dent. 28, 84–89.

Kuboniwa, M., Inaba, H., Amano, A., 2010. Genotyping to distinguish microbial pathogenicity in periodontitis. Periodontol. 2000 54, 136–159.

Liang, C.C., Park, A.Y., Guan, J.L., 2007. *In vitro* scratch assay: a convenient and inexpensive method for analysis of cell migration *in vitro*. Nat. Protoc. 2, 329–333.

Nakagawa, I., Amano, A., Kimura, R.K., Nakamura, T., Kawabata, S., Hamada, S., 2000. Distribution and molecular characterization of *Porphyromonas gingivalis* carrying a new type of *fimA* gene. J. Clin. Microbiol. 38, 1909–1914.

Nakagawa, I., Amano, A., Ohara-Nemoto, Y., Endoh, N., Morisaki, I., Kimura, S., Kawabata, S., Hamada, S., 2002. Identification of a new variant of *fimA* gene of *Porphyromonas gingivalis* and its distribution in adults and disabled populations with periodontitis. J. Periodontal Res. 37, 425–432.

Nakano, K., Kuboniwa, M., Nakagawa, I., Yamamura, T., Nomura, R., Okahashi, N., Ooshima, T., Amano, A., 2004. Comparison of inflammatory changes caused by *Porphyromonas gingivalis* with distinct *fimA* genotypes in a mouse abscess model. Oral Microbiol. Immunol. 19, 205–209.

Nomura, R., Shirai, M., Kato, Y., Murakami, M., Nakano, K., Hirai, N., Mizusawa, T., Naka, S., Yamasaki, Y., Matsumoto-Nakano, M., Ooshima, T., Asai, F., 2012. Diversity of Fimbrillin among *Porphyromonas gulae* clinical isolates from Japanese dogs. J. Vet. Med. Sci. 74, 885–891.

Pihlstrom, B.L., Michalowicz, B.S., Johnson, N.W., 2005. Periodontal diseases. Lancet 366, 1809–1820.

Riggio, M.P., Lennon, A., Taylor, D.J., Bennett, D., 2011. Molecular identification of bacteria associated with canine periodontal disease. Vet. Microbiol. 150, 394–400.

Rincon, J.C., Haase, H.R., Bartold, P.M., 2003. Effect of Emdogain on human periodontal fibroblasts in an *in vitro* wound-healing model. J. Periodontal Res. 38, 290–295.

Senhorinho, G.N., Nakano, V., Liu, C., Song, Y., Finegold, S.M., Avila-Campos, M.J., 2011. Detection of *Porphyromonas gulae* from subgingival biofilms of dogs with and without periodontitis. Anaerobe 17, 257–258.

Experimental and Toxicologic Pathology xxx (2011) xxx–xxx

Contents lists available at ScienceDirect

Experimental and Toxicologic Pathology

journal homepage: www.elsevier.de/etp

Short communication

Detection of Bcl-2 mRNA and its product in the glomerular podocytes of the normal rat kidney

Atsuko Haishima [a], Masaru Murakami [b], Teruo Ikeda [c], Kaoru Inoue [a], Junichi Kamiie [d], Kinji Shirota [a,d,*]

[a] Research Institute of Biosciences, Azabu University, Sagamihara, Kanagawa, Japan
[b] Laboratory of Molecular Biology, School of Veterinary Medicine, Azabu University, Sagamihara, Kanagawa, Japan
[c] Laboratory of Veterinary Immunology, School of Veterinary Medicine, Azabu University, Sagamihara, Kanagawa, Japan
[d] Laboratory of Veterinary Pathology, School of Veterinary Medicine, Azabu University, Sagamihara, Kanagawa, Japan

ARTICLE INFO

Article history:
Received 4 June 2010
Accepted 7 December 2010

Keywords:
Podocyte apoptosis
Bcl-2
Laser microdissection
Glomerulus
Kidney

ABSTRACT

Podocyte apoptosis underlies podocytepenia leading to glomerulosclerosis. An apoptosis inhibitory protein Bcl-2 is expressed in the podocytes in the early stage of nephrogenesis and downregulated in the maturing stage of human fetal kidneys. Recent studies reported changed localization and expression of Bcl-2 in the renal glomeruli under the pathologic conditions. This study aimed to confirm *in situ* localization of Bcl-2 mRNA and its product in the glomeruli, and to demonstrate the local expression of Bcl-2 mRNA in normal rat glomeruli. Paraffin sections of the kidneys from normal male Wistar rats were immunostained by anti-Bcl-2 monoclonal antibody. The localization of Bcl-2 mRNA in the glomeruli was evaluated by *in situ* hybridization. The glomeruli were dissected from frozen sections of the kidneys with the laser microdissection (LMD) system. Total RNA extracted from 10, 100 or 200 dissected glomeruli was used for reverse-transcription polymerase chain reaction (RT-PCR) and real-time PCR. Bcl-2 mRNA and its product were detected in the podocytes but barely in the mesangial cells. In RT-PCR, the specific-sized bands of Bcl-2 from 100 or 200 dissected glomeruli were clearly observed. Real-time PCR for Bcl-2 showed that cDNA from 100 or 200 dissected glomeruli became amplified at 36 or 33cycles, respectively. Bcl-2 is expressed in the glomerular podocytes of the normal rat kidney and quantitative analysis of Bcl-2 mRNA in the renal glomeruli is possible using the LMD technique.

1. Introduction

Apoptosis is a physiologic form of cell death, occurs in the individual cell in an endogenously programmed pattern (White, 1996; Tsujimoto and Shimizu, 2000). It can be triggered by a variety of physiologic stimuli, however the pathologic factors also affect the apoptotic pathways and then contribute to the induction or progression of many diseases (White, 1996; Shinoura et al., 1999; Yoshimura et al., 1999; Tsujimoto and Shimizu, 2000). Among the factors affecting apoptotic pathways, Bcl-2 is a protein encoded by *bcl-2* proto-oncogene and one of the molecular members of the cell survival factors in the Bcl-2 family (Yang and Korsmeyer, 1996; Tsujimoto and Shimizu, 2000). This protein is an important regulator of apoptosis, and can block programmed cell death. On the other hand, Bax, one of the Bcl-2 family molecules regulates the Bcl-2 protein activity and induces apoptosis. Therefore, the Bcl-2/Bax ratio is critical for the entry into apoptosis (White, 1996; Yang and Korsmeyer, 1996).

Recently, the importance of apoptosis has been emphasized in the progression of glomerular diseases (Sugiyama et al., 1997; Yoshimura et al., 1999; Barisoni and Mundel, 2003). In particular, podocyte apoptosis has been suggested to be an important cause of podocytepenia leading to glomeruloscrelosis (Yoshimura et al., 1999; Barisoni and Mundel, 2003). Podocytes are highly differentiated cells and lack proliferative activity under normal conditions. Their cellular foot processes are anchored to the outer surface of glomerular basement membrane (GBM) and keep structural integrity of the glomeruli. Adjacent foot processes are connected by a modified intercellular junction called as the slit diaphragm, which has a crucial role in selective filtration barrier in the glomeruli (Asanuma and Mundel, 2003). Therefore, detachment and loss of podocytes from the glomerular tufts consistently result in adhesion of denuded GBM to Bowman's capsule.

The changed localization of Bcl-2 or Bax proteins in the renal glomeruli has been observed both in experimental settings (Sugiyama et al., 1997; Wang et al., 2001) and in human glomerular diseases (Nakopoulou et al., 1996; Uda et al., 1998). In particular, the

* Corresponding author at: 1-17-71 Fuchinobe, Chuo-ku, Sagamihara, Kanagawa 252-2501, Japan. Tel.: +81 42 7692093; fax: +81 42 7692093.
E-mail address: shirota@azabu-u.ac.jp (K. Shirota).

0940-2993/$ – see front matter © 2010 Elsevier GmbH. All rights reserved.
doi:10.1016/j.etp.2010.12.006

expression of Bcl-2 increases in the proliferating cells in glomerulonephritis, suggesting that this protein is involved in pathologic cellular proliferation (Takemura et al., 1995; Sugiyama et al., 1997; Uda et al., 1998). On the other hand, a recent clinico-pathological study indicated that downregulation of Bcl-2 protein expression in the renal glomeruli was associated with indices of poor prognosis in human IgA nephritis (Qiu et al., 2004). Therefore, qualitative and quantitative analysis of the local expression of gene and product of Bcl-2 in the renal glomeruli will be very important to evaluate the role of the apoptosis-relating protein in the pathogenesis of glomerular injury and to access the influence of cellular stresses such as chemicals on the podocytes.

In the rat, the expression of Bcl-2 mRNA was detected in the podocytes of the renal glomeruli of puromycin aminonucleoside-treated and non-treated animals, and a focal increase of the signals was demonstrated by *in situ* hybridization (Wang et al., 2001). However, no significant change in glomerular Bcl-2 mRNA was revealed by reverse transcription-polymerase chain reaction (RT-PCR) using glomeruli isolated by the mesh-sieving method. Recently, we found a high expression of Bcl-2 protein in the glomerular podocytes of the normal rat kidney by immunohistochemistry using a monoclonal anti-human bcl-2 antibody.

For further confirmation of the localization of Bcl-2 in the podocytes, detection of its gene expression in the glomeruli might be required. We reported the utility of the laser microdissection (LMD) system for the analysis of the local gene expression in the renal glomeruli (Inoue et al., 2003) as well as in the ovarian follicles (Sakurada et al., 2006). In the present study, we confirmed the expression of Bcl-2 mRNA in the renal glomeruli dissected by LMD system. We also confirmed by *in situ* hybridization and immunohistochemistry the *in situ* localization of Bcl-2 mRNA and its product in the glomerular podocytes of the normal rat kidney.

2. Materials and methods

All procedures in this study were in accordance with the guidelines approved by the Animal Research Committee of Azabu University.

2.1. Kidney specimens and immunohistochemistry

Two 8-week-old normal male Wistar rats (Charles River Japan, Inc., Kanagawa) were euthanized by bleeding under anesthesia with intraperitoneal administration of pentobarbital sodium (60 mg/kg body weight), and their kidneys were collected. Parts of kidneys were fixed in 10% formalin (Masked Formalin, Japan Tanner Corp., Osaka) and embedded in paraffin after dehydration through a graded series of ethanol. Four-μm sections were cut and used for immunohistochemical detection of Bcl-2 by the streptavidin-biotin peroxidase method using a commercial kit (Histofine kit, Nichirei Corp., Tokyo). After deparaffinization and treatment in 3% H_2O_2 in methanol, the sections were incubated with normal rabbit serum and then with anti-human bcl-2 monoclonal antibody (Clone;124, pre-diluted, Nichirei Corp.). The immunoreaction was visualized by a diaminobenzidine-hydrogen peroxide solution, and the sections were counterstained with methyl green.

2.2. In situ hybridization

The Bcl-2 mRNA was localized by *in situ* hybridization (ISH). A 368 bp fragment of the rat Bcl-2 cDNA was amplified from reverse-transcribed total RNA of the rat kidney cortex using the following primers: upper, TAATACGACTCACTATAGGCGGGAGATCGTGATGAAGTA; lower, ATTTAGGTGACACTATAGAGAAGGGCGTCAGGTGC (Wang et al., 2001). The plasmid vector was inserted the Bcl-2 fragment and incubated with restriction enzyme. Sense and antisense RNA probes labeled with digoxigenin (DIG) were synthesized using T7 and SP6 RNA polymerase (MAXscript™ in vitro Transcription Kit, Ambion, USA), respectively. The ISH was performed under the standard protocols using an ISH kit (PanPath B. V., Amsterdam) on 4% paraformaldehyde (PFA)-fixed, paraffin-embedded tissues. The paraffin sections were dewaxed and air-dried and pretreated with 0.01 N HCl. After being washed in tris (hydroxymethyl) aminomethane-buffered saline (TBS), the sections were dehydrated by ethanol and air-dried. Hybridization was performed with a probe concentration of 0.6 μg/ml in a hybridization buffer (Nippon Gene Corp., Tokyo) at 50 °C overnight. After hybridization, the sections were washed with TBS, and then incubated with alkaline phosphatase-conjugated anti-digoxigenin (Fab fragment) (PanPath B. V., Amsterdam). After being washed in TBS, a mixture of nitroblue tetrazolium solution and 5-bromo, 4-chloro, 3-indolyphosphate solution was applied to the sections for color development.

Observation of the sections of immunohistochemistry and *in situ* hybridization was performed with a differential interference contrast microscope.

2.3. Laser microdissection

A part of the renal cortex specimens was quickly frozen in liquid nitrogen, cut into 7 μm sections by a cryostat microtome, and mounted on a glass slide cover with a 2.5 μm thin laser pressure catapulting membrane (PEN foil; Leica Microsystems, Wetzlar). They were fixed with 70% ethanol, gently washed twice with diethylpyrocarbonate (DEPC)-treated water, and thoroughly air-dried. Thereafter, the sections were stained with 0.05% toluidine blue (TB) solution, pH 4.1 (Wako Pure Chemical Industries, Ltd., Osaka), and then the TB solution was rinsed out with the DEPC-treated water, and the sections were air-dried. The renal glomeruli were randomly dissected from frozen sections with LMD systems (Leica Laser Microdissection System, Leica Microsystems). Ten, 100 or 200 glomeruli dissected from the frozen sections were collected immediately into a microcentrifuge tube cap filled with lysis buffer.

2.4. RT-PCR

To see specific size bands of Bcl-2 and glyceraldehyde-3-phosphate dehydrogenase (GAPDH) by electrophoresis, routine RT-PCR using the cDNA from dissected glomeruli was performed by Takara Thermal Cycler MP (Takara Shuzo, Kyoto). The total RNA was extracted from dissected glomeruli with RNeasy Mini Kit (Qiagen, Valencia, CA), and DNase digestion was performed with the RNase-free DNase set (Qiagen). First-strand cDNA was made from total RNA using Sensicript (Qiagen) with oligo (dT) 15primer (Promega, Madison, WI). The sequences of primers were as follows: upper, 5′-CGGGAGATCGTGATGAAGTA-3′; down, 5′-GGTAGCGACGAGAGAAGTCA-3′ (Wang et al., 2001) and the GAPDH primers as follows: upper, 5′-TCCCTCAAGATTGTCAGCAA-3′; lower, 5′-AGATCCACAACGGATACATT-3′ (Ando et al., 1995). The PCR was performed with Takara Taq™ (Takara Shuzo, Kyoto) under the following conditions: denature at 94 °C for 5 min; and then 40 cycles of denature at 94 °C for 1 min; annealing at 60 °C for 1 min; extension at 72 °C for 2 min; and finally extension at 72 °C for 7 min. Four μl of the PCR products were separated by electrophoresis in a 2% agarose gel and stained with ethidium bromide. The amplified products were verified to be a single band of 284 bp (Bcl-2) and 308 bp (GAPDH) in size.

2.5. Real-time PCR

The total RNA was extracted from dissected glomeruli with the RNeasy Mini Kit (Qiagen), and DNase digestion was performed with

Please cite this article in press as: Haishima A, et al. Detection of Bcl-2 mRNA and its product in the glomerular podocytes of the normal rat kidney. Exp Toxicol Pathol (2011), doi:10.1016/j.etp.2010.12.006

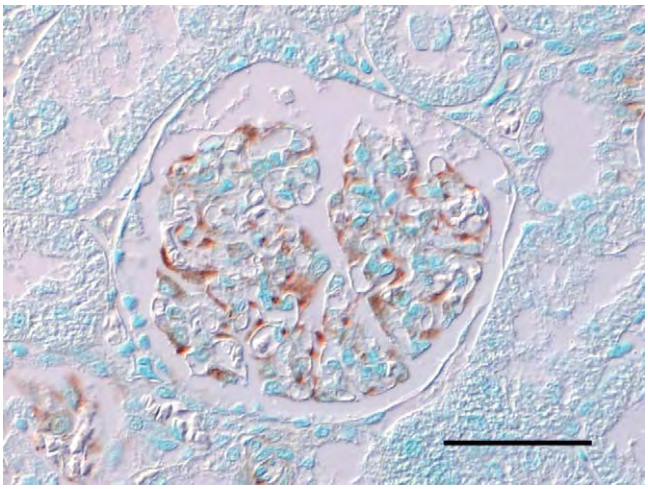

Fig. 1. Immunohistochemical staining of Bcl-2 in the renal glomerulus of the normal rat. Brown color indicates positive staining of Bcl-2 mostly in the podocytes. Bar = 50 μm.

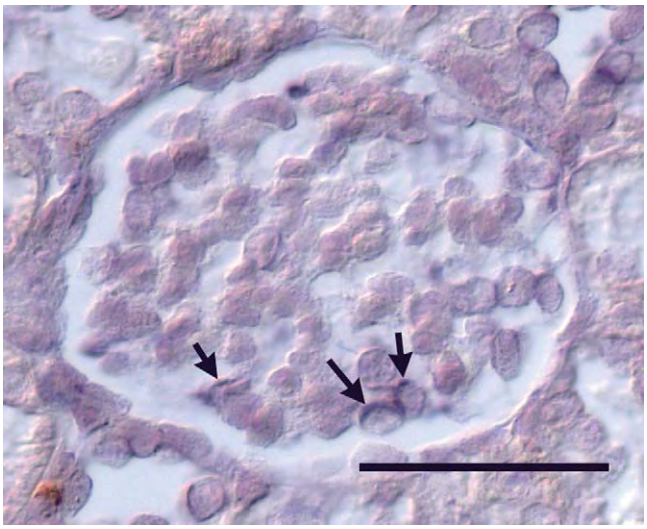

Fig. 2. *In situ* hybridization for Bcl-2 mRNA in the renal glomerulus of the normal rat. Arrows indicate positive signals in the podocytes. Bar = 50 μm.

the RNase-free DNase set (Qiagen). First-strand cDNA was made from total RNA using Sensicript (Qiagen) with oligo (dT) 15 primer (Promega). Real-time PCR was performed using the ABI Prism7700 Sequence Detection System (Applied Biosystems, Foster City, CA). For quantitative analysis of Bcl-2 expression, the TaqMan Bcl-2 (20X Pre-Developed TaqMan Assay Reagents, Applied Biosystems), and the TaqMan GAPDH (TaqMan Rodent GAPDH Control Reagents, Applied Biosystems) as an endogenous standard were amplified with each cDNA from dissected glomeruli using the universal PCR mastermix (Applied Biosystems). The reaction conditions were as follows: 2 min at 50 °C for warming up, samples were denatured at 95 °C for 10 min, then 40 cycles of 95 °C for 15 s and at 60 °C for 1 min.

3. Results

3.1. Immunohistochemistry and in situ hybridization

Immunohistochemistry clearly demonstrated that the Bcl-2 protein was localized in the podocytes but barely in the mesangial cells in the glomeruli (Fig. 1). Also, *in situ* hybridization revealed the limited localization of Bcl-2 mRNA in the glomerular podocytes (Fig. 2). Sense RNA probe used for negative control did not yielded any signals in the renal tissues.

3.2. Bcl-2 gene expression in the glomeruli

RT-PCR revealed that local expression of Bcl-2 mRNA was distinctly detected in 100 and 200 dissected glomeruli at 284 bp (specific size band of Bcl-2) but was not detected in 10 dissected glomeruli (Fig. 3). In real-time PCR, the cDNA of Bcl-2 and GAPDH derived from 200 dissected glomeruli began amplified at 33 and 28 cycles, respectively. It was also possible to detect exponential amplification of these cDNA from 100 dissected glomeruli that became amplified at over 36 (Bcl-2) and 30 (GAPDH) cycles. The cDNA of GAPDH from 10 dissected glomeruli was exponentially amplified, however that of Bcl-2 was not amplified (Fig. 4).

4. Discussion

We confirmed distinct *in situ* localization of Bcl-2 mRNA and its product in the glomerular podocytes of the normal rat kidney in this study. The localization of Bcl-2 mRNA in the rat glomerular podocytes was previously demonstrated by *in situ* hybridization (Wang et al., 2001) but we demonstrated local expression of Bcl-2 mRNA in the glomeruli by RT-PCR. Moreover, the real-time PCR for Bcl-2 revealed exponential amplification plots of cDNA, suggesting that quantitative evaluation of local Bcl-2 gene expression could be possible using dissected glomeruli by the LMD system. We did not precisely evaluate the difference in the results of PCR when cDNA from 10, 100 and 200 dissected glomeruli was amplified. However, the amplification plots of cDNA of the Bcl-2 indicated that 200 dissected glomeruli would be ideal for quantitative analysis of its local gene expression.

In human kidneys, Bcl-2 is not present in the podocytes in the maturing stage of nephrogenesis (Nagata et al., 1998) and also Bcl-2 mRNA was barely detectable in the normal human glomeruli (Qiu et al., 2004). There has been limited information on the role of Bcl-2 in the pathogenesis of glomerular injury. In human glomerular diseases such as lupus nephritis, IgA nephropathy, focal glomerulosclerosis and mesangial proliferative glomerulonephritis, increased expression of Bcl-2 in the glomeruli might contribute to the maintenance of hypercellularity by promoting cellular proliferation and by suppressing the function of Bax (Takemura et al., 1995; Uda et al., 1998). Nakopoulou et al. (1996) also reported

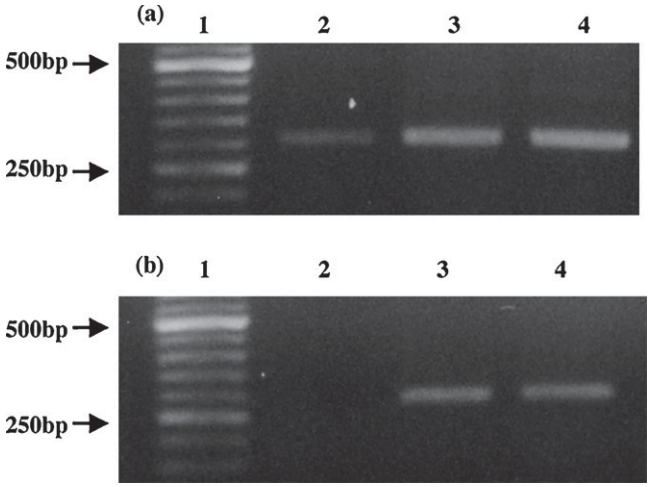

Fig. 3. The result of RT-PCR for GAPDH (a) and Bcl-2 (b) using total RNA from 10 (lane 2), 100 (lane 3) or 200 (lane 4) dissected glomeruli by laser microdissection system. Lane1: molecular weight marker.

Please cite this article in press as: Haishima A, et al. Detection of Bcl-2 mRNA and its product in the glomerular podocytes of the normal rat kidney. Exp Toxicol Pathol (2011), doi:10.1016/j.etp.2010.12.006

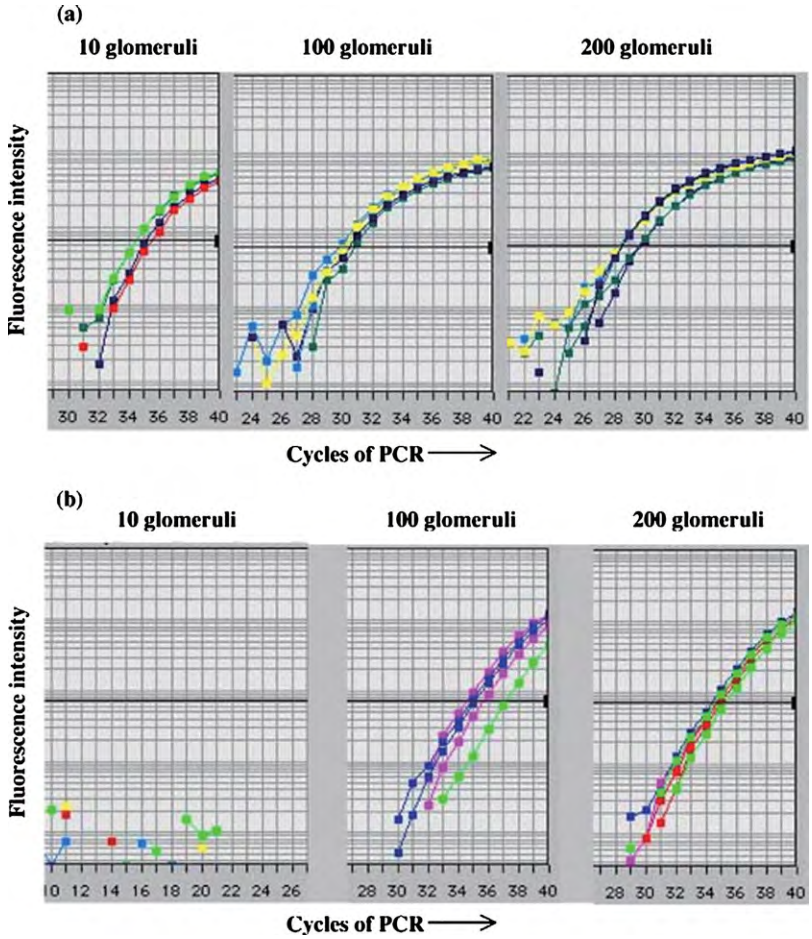

Fig. 4. Amplification curves of cDNA in real-time PCR of GAPDH (a) and Bcl-2 (b) using total RNA derived from 10, 100 or 200 dissected glomeruli. The amplification curves expressed by four different colors in each chart are of duplication samples from two normal rats.

restricted expression of Bcl-2 in the glomerular epithelial cells near intraglomerular fibrotic lesions and early adhesion and cellular crescents. In the rat model of focal segmental glomerulosclerosis, a focal increase in the expression of Bcl-2 mRNA in the renal glomeruli evaluated by *in situ* hybridization was suspected to be due to proliferated mesangial cells (Wang et al., 2001). More recently, Qiu et al. (2004) showed that Bcl-2 expression was upregulated in the early stage of IgA nephropathy and was downregulated in the advanced and end-stage of the disease. They revealed that Bcl-2 downregulation was closely associated with the development of progressive glomerular injury as well as being a clinical prognostic indicator of poor renal prognosis in human IgA nephropathy. These reports indicate that Bcl-2 may be closely associated with the pathogenesis of glomerulonephritis and that its role in glomerular injury might depend on the types of the injury and course of the diseases.

The podocytes are highly differentiated and growth-arrested cells (Nagata et al., 1998; Barisoni and Mundel, 2003). Therefore loss of these cells results in podocytepenia and underlies glomerulosclerosis, representing irreversible glomerular injury (Barisoni and Mundel, 2003) A recent experimental study has shown that Bcl-2 protects podocytes from apoptosis (Wada et al., 2005) Constant expression of Bcl-2 in the podocytes in the normal kidney as shown in this study may contribute to long-life of these cells as a cell survival factor. Therefore, quantitative analysis of local gene expression of Bcl-2 in the glomeruli under pathologic conditions caused by various factors such as immune mechanisms, chemical toxicity, ageing and others must be important for evaluating or monitoring podocyte injury and for understanding the pathogenesis of progressive glomerular injury.

References

Ando T, Okuda S, Tamaki K, Yoshitomi K, Fujishima M. Localization of transforming growth factor-β and latent transforming growth factor-β binding protein in rat kidney. Kidney Int 1995;47:733–9.
Asanuma K, Mundel P. The role of podocytes in glomerular pathobiology. Clin Exp Nephrol 2003;7:255–9.
Barisoni L, Mundel P. Podocyte biology and the emerging understanding of podocyte diseases. Am J Nephrol 2003;23:353–60.
Inoue K, Sakurada Y, Murakami M, Shirota M, Shirota K. Detection of gene expression of vascular endothelial growth factor and flk-1 in the renal glomeruli of the normal rat kidney using the laser microdissection system. Virchows Arch 2003;442:159–62.
Nagata M, Nakayama K, Terada Y, Hoshi S, Watanabe T. Cell cycle regulation and differentiation in the human podocyte lineage. Am J Pathol 1998;153:1511–20.
Nakopoulou L, Stefananki K, Papadakis J, Boletis J, Zeis PM, Kostakis A, et al. Expression of bcl-2 oncoprotein in various types of glomerulonephritis and renal allografts. Nephrol Dial Transplant 1996;11:997–1002.
Qiu LQ, Sinniah R, I-Hong Hsu S. Downregulation of Bcl-2 by podocytes is associated with progressive glomerular injury and clinical indices of poor renal prognosis in human IgA nephropathy. J Am Soc Nephrol 2004;15:79–90.
Sakurada Y, Shirota M, Inoue K, Shirota K. New approach to in situ quantification of ovarian gene expression in rat using a laser microdissection technique: relation between follicle types and regulation of Inhibin-α and cytochrome P450 aromatase genes in the rat ovary. Histochem Cell Biol 2006;126:735–41.
Shinoura N, Yoshida Y, Asai A, Kirino T, Hamada H. Relative level of expression of Bax and Bcl-XL determines the cellular fate of apoptosis/necrosis induced by the overexpression of Bax. Oncogene 1999;18:5703–13.
Sugiyama H, Kashihara N, Onbe T, Yamasaki Y, Wada J, Sekikawa T, et al. Bcl-2 expression and apoptosis in nephrotoxic nephritis. Exp Nephrol 1997;5:481–9.
Takemura T, Murakami K, Miyazato H, Yagi K, Yoshioka K. Expression of Fas antigen and Bcl-2 in human glomerulonephritis. Kidney Int 1995;48:1886–92.

Please cite this article in press as: Haishima A, et al. Detection of Bcl-2 mRNA and its product in the glomerular podocytes of the normal rat kidney. Exp Toxicol Pathol (2011), doi:10.1016/j.etp.2010.12.006

Tsujimoto Y, Shimizu S. Bcl-2 family: life or death switch. FEBS Lett 2000;466: 6–10.
Uda S, Yoshimura A, Sugenoya Y, Inui K, Taira T, Ideura T. Mesangial proliferative nephritis in man is associated with increased expression of cell survival factor, Bcl-2. Am J Nephrol 1998;18:291–5.
Wada T, Pippin JW, Marshall CB, Griffin SV, Shankland SJ. Dexamethasone prevents podocytes apoptosis induced by puromycin aminonucleoside: role of p53 and Bcl-2-related family proteins. J Am Soc Nephrol 2005;16:2615–25.
Wang W, Tzanidis A, Divjak M, Thomson NM, Stein-Oakley AN. Altered signaling and regulatory mechanisms of apoptosis in focal and segmental glomerulosclerosis. J Am Soc Nephrol 2001;12:1422–33.
White E. Life, death, and the pursuit of apoptosis. Genes Dev 1996;10:1–15.
Yang E, Korsmeyer SJ. Molecular thanatopsis: a discourse on the BCL2 family and cell death. Blood 1996;88:386–401.
Yoshimura A, Uda S, Inui K, Nemoto T, Sugenoya Y, Sharif S, et al. Expression of bcl-2 and bax in glomerular disease. Nephrol Dial Transplant 1999;14(Suppl. 1):55–7.

Please cite this article in press as: Haishima A, et al. Detection of Bcl-2 mRNA and its product in the glomerular podocytes of the normal rat kidney. Exp Toxicol Pathol (2011), doi:10.1016/j.etp.2010.12.006

FULL PAPER *Bacteriology*

Diversity of Fimbrillin among *Porphyromonas gulae* Clinical Isolates from Japanese Dogs

Ryota NOMURA[1)]**, Mitsuyuki SHIRAI[2)]**, Yukio KATO[3)]**, Masaru MURAKAMI[4)], Kazuhiko NAKANO[1)], Norihiko HIRAI[2)], Tetsuya MIZUSAWA[3)], Shuhei NAKA[1)], Yoshie YAMASAKI[1,5)], Michiyo MATSUMOTO-NAKANO[5)], Takashi OOSHIMA[1)] and Fumitoshi ASAI[2)]*

[1)]*Department of Pediatric Dentistry, Osaka University Graduate School of Dentistry, Suita, Osaka 565–0871, Japan*
[2)]*Department of Pharmacology, School of Veterinary Medicine, Azabu University, Sagamihara, Kanagawa 252–5201, Japan*
[3)]*Department of Veterinary Public Health II, School of Veterinary Medicine, Azabu University, Sagamihara, Kanagawa 252–5201, Japan*
[4)]*Department of Molecular Biology, School of Veterinary Medicine, Azabu University, Sagamihara, Kanagawa 252–5201, Japan*
[5)]*Department of Pediatric Dentistry, Okayama University Graduate School of Medicine, Dentistry and Pharmaceutical Sciences, Okayama 700–8556, Japan*

(Received 19 December 2011/Accepted 19 February 2012/Published online in J-STAGE 2 March 2012)

ABSTRACT. *Porphyromonas gulae*, a gram-negative black-pigmented anaerobe, is a pathogen for periodontitis in dogs. An approximately 41-kDa fimbrial subunit protein (FimA) encoded by *fimA* is regarded as associated with periodontitis. In the present study, the *fimA* genes of 17 *P. gulae* strains were sequenced, and classified into two major types. The generation of phylogenetic trees based on the deduced amino acid sequence of FimA of *P. gulae* strains along with sequences from several strains of *Porphyromonas gingivalis,* a major cause of human periodontitis, revealed that the two types of FimA (types A and B) of *P. gulae* were similar to type I FimA and types II and III FimA of *P. gingivalis*, respectively. A PCR system for classification was established based on differences in the nucleotide sequences of the *fimA* genes. Analysis of 115 *P. gulae*-positive oral swab specimens from dogs revealed that 42.6%, 22.6%, and 26.1% of them contained type A, type B, and both type A and B *fimA* genes, respectively. Experiments with a mouse abscess model demonstrated that the strains with type B *fimA* caused significantly greater systemic inflammation than those with type A. These results suggest that the FimA proteins of *P. gulae* are diverse with two major types and that strains with type B *fimA* could be more virulent.

KEY WORDS: fimbriae, genotype, periodontitis, *Porphyromonas gulae*, virulence.

doi: 10.1292/jvms.11-0564; *J. Vet. Med. Sci.* 74(7): 885–891, 2012

Periodontal diseases are characterized by gingivitis, a reversible condition involving gingival inflammation, and periodontitis, the irreversible destruction of periodontal tissues such as cementum, periodontal ligaments, and supportive bone [15]. In dogs, the prevalence of gingivitis is 95–100% and that of periodontitis, 50–70%, and the severity of periodontal disease tends to worsen with age, as in humans [8, 10].

Numerous periodontitis-related bacterial species have been reported in humans, with *Porphyromonas gingivalis*, a gram-negative black-pigmented anaerobe, considered a major species [15]. The 41-kDa cell surface protein fimbrillin (FimA), a subunit of fimbriae, is an important virulence factor of periodontitis, associated with adhesion to and invasion of gingival cells [4]. There are six genotypes of *fimA* encoding FimA (I through V and Ib), among which types II/IV/Ib and I/III/V are considered invasive and non-invasive, respectively [2, 3, 11–14, 17].

A previous analysis of 11 periodontitis-related bacterial species in oral swab specimens collected from 26 pet dogs in Japan showed that the isolation frequency of *P. gingivalis* was extremely low in dogs [9]. In contrast, *Porphyromonas gulae* was frequently detected in these specimens, accounting for approximately 70% of all *Porphyromonas* isolates. A recent study revealed the presence of a 41-kDa FimA, similar to that in *P. gingivalis*, in *P. gulae* [7]. In the present study, we performed molecular analyses of *fimA* in many clinical strains of *P. gulae* focusing on the association between the gene's diversity and virulence.

MATERIALS AND METHODS

Strains and culture conditions: Table 1 lists the *P. gulae* strains analyzed in the present study, 10 of which were isolated in Tokyo, Japan, previously [9]. The 7 new clinical strains were isolated from 7 dogs in Tokyo, Japan, by a method described previously [9]. Briefly, specimens collected from the gingival margin of the right fourth maxillary premolar using swabs (Seed-Swab^{R} γ-1 or 2, Eiken Chemical Co., Ltd., Tokyo, Japan) were directly streaked on culture plates (Tripticase Soy Agar, Becton, Dickinson & Co,

*CORRESPONDENCE TO: ASAI, F., Department of Pharmacology, School of Veterinary Medicine, Azabu University, 1–17–71 Fuchinobe, Chuo-ku, Sagamihara, Kanagawa 252–5201, Japan. e-mail: asai@azabu-u.ac.jp

**These authors were equally contributed.

Table 1. *P. gulae* and *P. gingivalis* strains used

Species	Strain	*fimA* types	Length of *fimA* gene (bp)	Accession Numbers	References
P. gulae	ATCC 51700[a,b)]	A	1152	AB297918	[7]
	D024	A	1152	AB663087	This study
	D025	A	1152	AB663088	This study
	D028	A	1152	AB663089	This study
	D034[a)]	A	1152	AB663090	This study
	D035[a)]	A	1152	AB663091	This study
	D036[a)]	A	1152	AB663092	This study
	D042	A	1152	AB663093	[9]
	D043	A	1152	AB663094	[9]
	D060	A	1152	AB663095	[9]
	D066	A	1152	AB663096	[9]
	D067	A	1152	AB663097	[9]
	D068	A	1152	AB663098	[9]
	B43	B	972[c)]	CS228034	[5]
	D040[a)]	B	1161	AB663099	[9]
	D044[a)]	B	1161	AB663100	[9]
	D052	B	1161	AB663101	[9]
	D053	B	1161	AB663102	[9]
	D077	B	1161	AB663103	This study
P. gingivalis	381	I	1044	D17794	[3]
	ATCC 33277[b)]	I	1044	D17795	[3]
	BH18/10	I	1044	D17796	[3]
	HW24D1	II	1047	D17797	[3]
	OMZ314[a)]	II	1044	D17798	[3]
	OMZ409	II	1047	D17799	[3]
	ATCC 49417	III	1053	D17800	[3]
	6/26	III	1062	D17801	[3]
	HG564	IV	1083	D17802	[3]
	HNA99	V	1104	AB027294	[11]
	HG1691	Ib	1044	AB058848	[12]

a) Strains analyzed in the mouse abscess model.
b) Type strains.
c) Only a partial sequence corresponding to the *fimA* of *P. gulae* is available.

Franklin Lakes, NJ, U.S.A.) supplemented with 5% horse defibrinated blood (TS) or TS with hemin (50 mg/m*l*) and menadion (5 mg/m*l*) (mhTS), and cultured under anaerobic conditions for 7 to 10 days. Four representative colonies selected at random from each plate were pure-cultured for 4 to 7 days. The strains were stored in TS broth with 10% glycerine at −80°C until use.

The isolated strains were confirmed as *P. gulae* based on molecular biological analyses described previously [9]. Briefly, genomic DNA of each strain was extracted using a commercial kit (Puregene Yeast/Bact. Kit B, QIAGEN Inc., Valencia, CA, U.S.A.), and a broad-ranging PCR was performed using TaKaRa Ex Taq (Takara Bio. Inc., Otsu, Shiga, Japan) with the primer fD1 and rP2 targeting the 16S rRNA gene (Table 2) [18]. PCR products were directly sequenced and the 16S rRNA sequences obtained were compared with those available in databases from the National Center for Biotechnology Information server (http://blast.ncbi.nlm.nih.gov/Blast.cgi). Identification at the species level was defined as a 16S rRNA sequence similarity of more than 99% with that of *P. gulae* type strain ATCC 51700.

The *P. gingivalis* strains with various *fimA* genotypes used in the present study are also listed in Table 1. *P. gingivalis* and *P. gulae* strains were cultured in mhTS broth under anaerobic conditions for 2 days when the extraction of genomic DNA and preparation of the bacterial suspension for animal experiments were performed.

Sequencing and characterization of fimA genes: The entire *fimA* gene was sequenced as follows. First, PCR was performed with genomic DNA extracted from *P. gulae* strains using the six *P. gingivalis fimA*-specific sets of primers listed in Table 2 [3, 11, 12]. Since the *P. gulae* strains tested showed positive reactions to the type I and III sets, we designed primers (33277-F and 33277-R; 6/26-F and 6/26R) based on the adjacent sequence of ATCC 33277 (*fimA* type I) and of 6/26 (*fimA* type III). PCR was performed using these primers to amplify the entire *fimA* gene of *P. gulae* by TaKaRa ExTaq under the following conditions: an intial denaturation at 95°C for 4 min and then 30 cycles at 94°C for 30 sec, 50°C for 30 sec, and 72°C for 30 sec with a final

Table 2. Primers used for PCR

Specific primer set	Sequence (5′ to 3′)	References
Amplification of 16S rRNA		
fD1[a)]	AGA GTT TGA TCC TGG CTC AG	[18]
rP2[a)]	ACG GCT ACC TTG TTA CGA CTT	
Detection of *P. gulae*		
P . gulae 16S rRNA	TTG CTT GGT TGC ATG ATC GG	[9]
	GCT TAT TCT TAC GGT ACA TTC ACA	
Determination of *fimA* sequence		
33277-F[a)]	TTC ATA CGT CGA CGA CTG CG	This study
33277-R[a)]	TTG AGG GTT GAT TAC CAA GT	
6/26-F[a)]	AAC TAC GAC GCT ATA TGC AA	This study
6/26-R[a)]	TAG ACA AAC TAT GAA AGT T	
Detection primers for *P. gulae fimA* types		
type A *fimA*		
Pgufim-AF[a)]	TGA GAA TAT CAA ATG TGG TGC AGG CTC ACG	This study
Pgufim-AR[a)]	CTT GCC TGC CTT CAA AAC GAT TGC TTT TGG	
type B *fimA*		
Pgufim-BF[a)]	TAA GAT TGA AGT GAA GAT GAG CGA TTC TTA TGT	This study
Pgufim-BR[a)]	ATT TCC TCA GAA CTC AAA GGA GTA CCA TCA	
Detection primers for *P. gingivalis fimA* types		
Type I *fimA*	CTG TGT GTT TAT GGC AAA CTT C	[3]
	AAC CCC GCT CCC TGT ATT CCG A	
Type II *fimA*	ACA ACT ATA CTT ATG ACA ATG G	[3]
	AAC CCC GCT CCC TGT ATT CCG A	
Type III *fimA*	ATT ACA CCT ACA CAG GTG AGG C	[3]
	AAC CCC GCT CCC TGT ATT CCG A	
Type IV *fimA*	CTA TTC AGG TGC TAT TAC CCA A	[3]
	AAC CCC GCT CCC TGT ATT CCG A	
Type V *fimA*	AAC AAC AGT CTC CTT GAC AGT G	[11]
	TAT TGG GGG TCG AAC GTT ACT GTC	
Type Ib *fimA*	CAG CAG AGC CAA AAA CAA TCG	[12]
	TGT CAG ATA ATT AGC GTC TGC	

a) Names of primers are indicated.

extension at 72°C for 7 min. Then, electrophoresis was done on a 0.7% agarose gel, and the amplified DNA fragments were extracted from the gel, using a QIAEX gel extraction kit (Qiagen, Düsseldorf, Germany). The DNA was directly cloned into a pGEM-T Easy vector (Promega, Madison, WI, U.S.A.), which was transformed into *Escherichia coli* XL-2. The plasmid containing the target gene was extracted using a FastGene Plasmid Mini Kit (NIPPON Genetics, Tokyo, Japan) and the nucleotide sequence was determined using a dye-terminator reaction with a DNA sequencing system (373–18 DNA sequencer; Applied Biosystems, Foster City, CA, U.S.A.) and an ABI PRISM kit. Data analyses were performed using Gene Works software (IntelliGenetics, Mountain View, CA, U.S.A.). The deduced amino acid sequences of the FimA proteins of all *P. gulae* strains tested and of *P. gingivalis* strains with *fimA* genotypes I through V and Ib listed in Table 1 were compared using the neighbor-joining method to construct a phylogenetic tree using CLUSTAL W (DNA Databank of Japan; http://clustalw.ddbj.nig.ac.jp/top-j.html) and Tree View software (http://taxonomy.zoology.gla.uk/rod/treeview.html).

Construction of a PCR method to classify fimA types: Table 2 lists the PCR primers used. Those for the classification of *fimA* type A and B were designed based on the *fimA* sequence of *P. gulae* determined in the present study. The specificity of these primers was tested with the program Amplify [6], based on information on the DNA sequence of *P. gulae* strains obtained in the present study as well as that of *P. gingivalis* in the GenBank database. The specificity of the primers was also confirmed using GenBank data. The amplification was performed in a total volume of 20 μl with 1 μl of template solution using TaKaRa Ex Taq. The PCR was performed in a thermal cycler (iCycler; Bio-Rad, Hercules, CA, U.S.A.) with the following parameters: an initial denaturation at 95°C for 4 min and then 30 cycles of 95°C for 30 sec, 60°C for 30 sec, and 72°C for 30 sec, with a final extension at 72°C for 7 min. The PCR products were subjected to electrophoresis in a 1.5% agarose gel-Tris-acetate-EDTA buffer. The sensitivity of the PCR assay was determined using serial dilutions of titrated *P. gulae* cultures in sterile distilled water.

Distribution of fimA types in P. gulae-positive oral swab

specimens: All study protocols were approved by the Animal Research Committee of Azabu University. Prior to collection of the specimens, the owners of all the dogs were informed of the contents of the present study and gave approval for their participation. Oral specimens were previously collected from one specific location, the gingival margin of the right fourth maxillary premolar, in 26 dogs using swabs (Seed-Swab^{R} γ-1 or 2) [9]. In the present study, 102 additional specimens were collected to give a total of 128. Mean age was 9.62 (2–16) years. These dogs came to the clinic for health checkups, vaccinations, coxarthropathy, external otitis, external disc disease, trauma, and diarrhea. All were reported to be kept indoors. First, bacterial DNA was extracted from each specimen and PCR was performed using *P. gulae*-specific sets of primers [9], as described above. Then, types of *fimA* were determined by a method established in the present study. For *P. gulae*-specific PCR positive but types A and B *fimA*-specific PCR negative specimens, the amplified *P. gulae*-specific PCR products were sequenced to confirm that they were indeed 16S rRNA gene sequences of *P. gulae*.

Mouse abscess model: All procedures and protocols involving animals were reviewed and approved by the Institutional Animal Care and Use Committee of Osaka University Graduate School of Dentistry prior to the experiments. The virulence of 6 *P. gulae* strains including ATCC 51700 as compared to *P. gingivalis* OMZ314 was evaluated using a mouse abscess model constructed for the evaluation of *P. gingivalis* strains with some modifications as follows [14]. Female BALB/c mice (5 weeks old) were maintained in horizontal-flow cabinets and provided with sterile food and water *ad libitum*. In all, 80 mice were randomly divided into 8 groups (6 *P. gulae*, 1 *P. gingivalis* and 1 phosphate-buffered saline (PBS) groups) to examine inflammatory changes caused by the infection. At 40 days of age, a single site approximately 1 cm lateral from the midline on the dorsal surface was depilated, and 0.1 m*l* of bacterial suspension (1×10^9 colony-forming units (CFU) of a test strain) or PBS (control group) was injected subcutaneously. For quantita-

```
                                          ↓
ATCC51700-A     1  MKKTKFFLLGLAALAMTACNKDNEAEPVVEGNATISVVLKTSNPNRAFGV    50
D067-A          1  ..................................................    50
D077-B          1  ........................I.........................    50

ATCC51700-A    51  ADDEAKVAKLTVMVYNGEQQEAIESAENATKIENIKCGAGSRTLVVMANT   100
D067-A         51  ..................................................   100
D077-B         51  ......................K.....I.V.....................   100

ATCC51700-A   101  GTMDLTGKTLADVKALTTELTAENQEAAGLIMTAEPKAIVLKAGKNYIGY   150
D067-A        101  ..................................................   150
D077-B        101  .G.E.A.....E..............T........VDVT.V..N..Y..   150

ATCC51700-A   151  NGAGEGNHIEND-PLEIKRVHARMAFTEIKVQMSAAYDNIYTFAPEKIYG   199
D067-A        151  ............-.....................................   199
D077-B        151  D.TQG..Q.SQGT.........I...K.E.K..DS.V.K.N.T..N..A   200

ATCC51700-A   200  LIAKKQSNLFGATLVNADANYLTGSLTTFNGAYTPANYANVPWLSRNYVA   249
D067-A        200  ..................................................   249
D077-B        201  .V...K.....TS.A.S.DA..................TH.A..G.G.T.   250

ATCC51700-A   250  PTANAPQGFYVLENDYSANGGTIHPTILCVYGKLQKN-GADLAGADLAAA   298
D067-A        250  ...................................-..............   298
D077-B        251  .SND.........SA.AQ.A.-LR......K...T.HD.TP.SSEEMT..   299

ATCC51700-A   299  QAANWV--DAEGKTYYPVLVNFNSNNYTYDNGYTPKNKIERNHKYDIKLT   346
D067-A        299  ......--..........................................   346
D077-B        300  FNVG.IVANNDPT.........E......TGDAVE.G..V....F..N..   349

ATCC51700-A   347  ITGPGTNNPENPITESAHLNVQCTVAEWVLVGQNATW                383
D067-A        347  ....................................                383
D077-B        350  ................N...N.V..A.KG.V..VI.                386
```

Fig. 1. Multiple alignments of deduced amino acid sequence of the FimA encoded by type A and B *fimA* genes of *P. gulae* compared to reference strain ATCC 51700. Only amino acid residues different from ATCC 51700 are presented. Identical amino acids are indicated by dots. The arrow indicates the cleavage site estimated by the SignalP 3.0 Server (http://www.cbs.dtu.dk/services/SignalP/).

tive evaluation of the infectious inflammatory change, serum C-reactive protein (CRP) was measured as follows. Blood specimens (0.1 m*l*) were collected from an orbital vein on days 0, 1, 2, 4, 7 and 14 after bacterial infection, and then centrifuged at 3,000 rpm. for 10 min to separate the serum. CRP concentrations in sera were colorimetrically quantified using a commercial kit (MOUSE C-REACTIVE PROTEIN (CRP) ELISA TEST KIT; Life Diagnostics, Inc., West Chester, PA, U.S.A.) according to the manufacturer's instructions. The mice were also monitored for signs and symptoms of infection, i.e. ruffled hair, abscess formation and emergence of erosion, as described previously [14]. Two weeks after infection, all mice were killed under ether anesthesia, and the spleens were extirpated and weighed. Spleen weight values were standardized by body weight.

Statistical analyses: Statistical analyses were performed using the computational software package Prism 4 (GraphPad Software Inc., La Jolla, CA, U.S.A.). Intergroup differences were estimated using Bonferoni's method after an analysis of variance (ANOVA). A *P* value of less than 0.05 was considered statistically significant.

RESULTS

Diversity of fimA sequences in clinical strains: The *fimA* genes of 17 *P. gulae* strains (deposited in the DNA Database of Japan under accession nos. AB663087-AB663103) were sequenced, and found to mainly fall into 2 *fimA* types. One type had a sequence of 1152 bp similar to ATCC 51700 and was designated type A. The length of the *fimA* gene in the other type, type B was 1161 bp. Figure 1 shows the deduced amino acid sequence of strains D067 (type A) and D077 (type B) as compared to that of *P. gulae* ATCC 51700 (type A). The FimA in D067 and that in *P. gulae* ATCC 51700 showed 100% identity. The FimA in D077 and that in *P. gulae* ATCC 51700 showed 73% identity. The phylogenetic tree showed that type A FimA of *P. gulae* was close to type I FimA of *P. gingivalis*(86–93% identity), whereas type B FimA of *P. gulae* was close to types II and III FimA of *P. gingivalis*(86–92% identity) (Fig. 2).

PCR system to identify fimA types of P. gulae: The primers used to identify type A and B *fimA* genes of *P. gulae* are listed in Table 2. Figure 3A illustrates the positions of those primers. The estimated size of the amplified fragments of *fimA* type A and B was 190 bp and 357 bp, respectively.

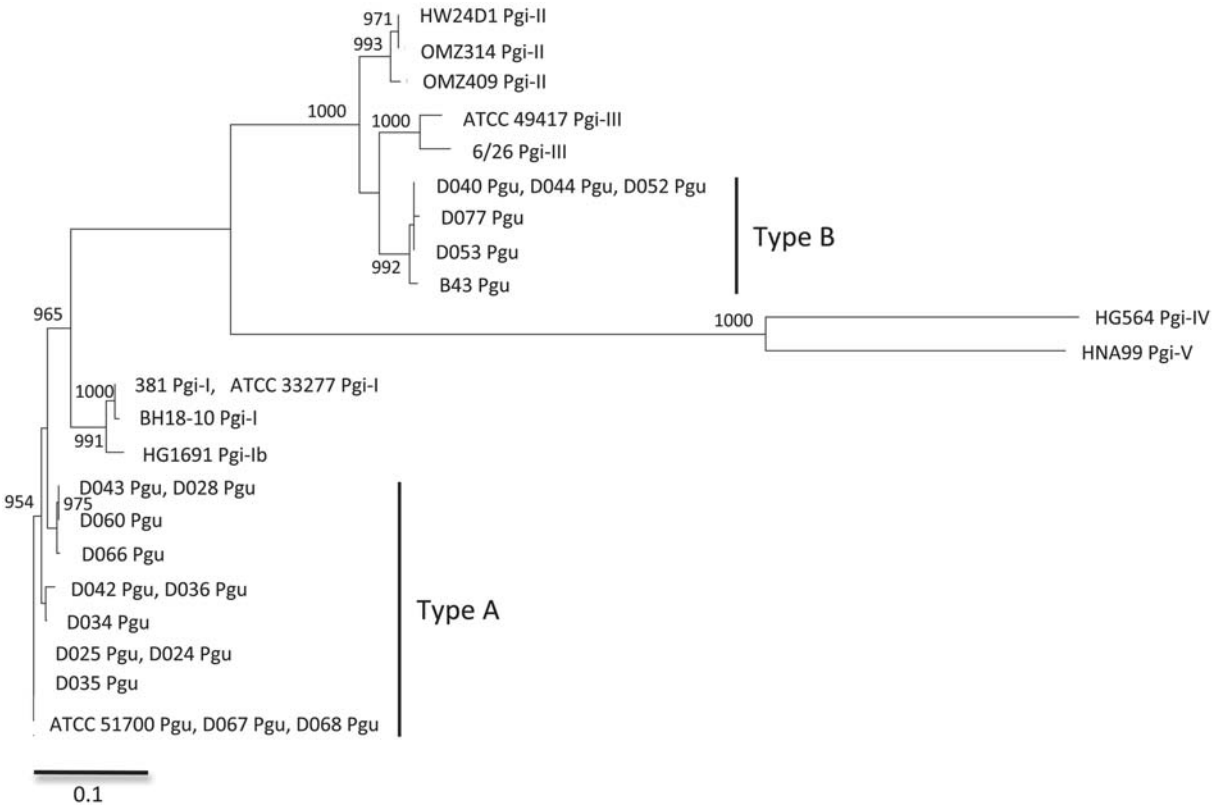

Fig. 2. Evolutionary relationship based on deduced amino acid sequences of FimA in *P. gulae* and *P. gingivalis*. The neighbor-joining method was used to construct a phylogenetic tree with CLUSTAL W (DNA Databank of Japan) and Tree View software. Pgu and Pgi indicate *P. gulae* and *P. gingivalis*, respectively. The roman numerals following Pgi give the *fimA* genotypes of *P. gingivalis*. The numbers shown in the tree are bootstrap values.

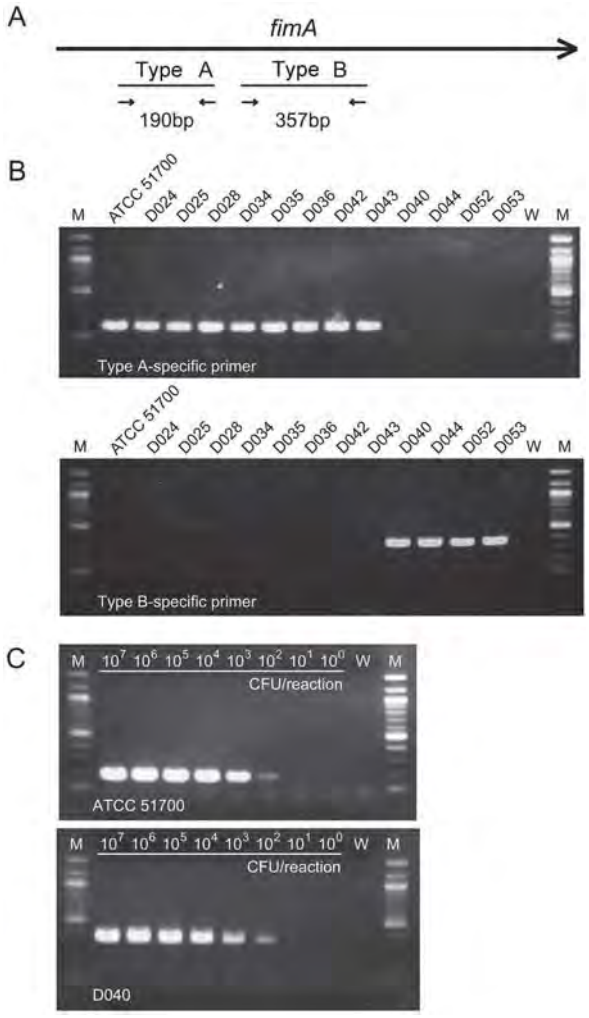

Fig. 3. Construction of the primers specific for type A and B *fimA* of *P. gulae*. (A) The position of the primers for each *fimA* type. (B) Specificity of the PCR method used in the present study. W, sterile water. M, molecular size marker (100-bp DNA ladder). (C) Sensitivity of the PCR method examined using titrated cultures of *P. gulae* strains ATCC 51700 (type A) and D040 (type B). W, sterile water. M, molecular size marker (100-bp DNA ladder).

The specificity of this PCR system was confirmed using the strains listed in Table 1, which demonstrated that primers designed for type A and B *fimA* genes of *P. gulae* did not generate positive bands from *P. gingivalis* strains tested. In addition, the sensitivity was shown to be approximately 100 CFU per reaction (Fig. 3B and 3C).

Prevalence of fimA types in clinical specimens: PCR analyses of 128 specimens using *P. gulae*-specific primers revealed that 115 were positive. PCR for typing of *fimA* of *P. gulae* showed that 49 (42.6%) and 26 (22.6%) specimens were positive for *fimA* type A and B, respectively. In addition, 30 specimens (26.1%) were positive for both *fimA* types. As for the remaining 10 specimens (8.7%), which were negative for *fimA* type A and B, the sequence of 16S rRNA gene fragments amplified by *P. gulae*-specific PCR had 100% homology with that of *P. gulae* type strain ATCC 51700.

Evaluation of virulence in the mouse abscess model: Table 3 summarizes the results of the experiment with the mouse abscess model. Subcutaneous injections of strains with type B *fimA*(D040 and D044) caused large abscesses to form similar to OMZ314. Serum CRP values at 2 days post-infection were significantly higher than for PBS ($P<0.05$), and the spleens extirpated at 14 days after infection were also significantly heavier ($P<0.05$). As for the mice inoculated with strains with type A *fimA*, the intensity of inflammation tended to be higher than that of PBS-inoculated mice, but the difference was not significant.

DISCUSSION

This is the 1st study to demonstrate the presence of 2 major *fimA* types of *P. gulae* using clinical isolates from dogs. The FimA of *P. gulae* was first demonstrated by Hamada *et al*. [7] who reported 96.8% identity between the FimA of ATCC 51700 and *P. gingivalis* ATCC 33277. Hamada *et al*. [7] analyzed one more strain, B43 [5], in a phylogenetic tree based on deduced amino acid sequences of FimA. They translated the *fimA* sequence of B43 into amino acids based on data in GenBank (accession number CS228034). The sequence was 16% incomplete, however, it belongs to *fimA* type B.

Analyses of *fimA* in *P. gulae* strains from our laboratory

Table 3. Infectious inflammation by *P. gulae* as compared with *P. gingivalis* OMZ314 evaluated with the mouse abscess model

Inoculated strains	*fimA* types	CRP values at 2 days after infection [μg/m*l* (mean ± SE)]	Symptom (no. of mice /total)	Spleen weight at 14 days after infection [mg/g body weight (mean ± SE)]
OMZ314	II	5.59 ± 0.35[b]	Abscess formation (9/10)	5.06 ± 0.27[a]
D044	B	11.63 ± 0.69[c]	Abscess formation (7/10)	5.33 ± 0.28[a]
D040	B	5.35 ± 0.25[a]	Abscess formation (10/10)	5.04 ± 0.30[a]
ATCC 51700	A	4.63 ± 0.36	Ruffled hair (10/10)	4.35 ± 0.14
D035	A	4.33 ± 0.23	Ruffled hair (4/10)	4.26 ± 0.18
D036	A	4.56 ± 0.53	Ruffled hair (4/10)	4.09 ± 0.10
D034	A	4.68 ± 0.51	Ruffled hair (6/10) Abscess formation (1/10)	3.67 ± 0.09
PBS	-	3.21 ± 0.35	None	3.79 ± 0.20

Statistically significant difference with the PBS group ([a]$P<0.05$, [b]$P<0.01$ and [c]$P<0.001$) by Bonferonni's method after ANOVA.

stock showed the prevalence of *fimA* type A and B to be 72.3% and 27.3%, respectively. Among the 115 *P. gulae*-positive oral swab specimens from dogs, approximately 70% had type A FimA and approximately 50% type B. Furthermore, there were several specimens positive for both *fimA* types. These results suggest that type A *fimA* could be more prevalent in dogs and that dogs carrying both strain with type A *fimA* and that with type B *fimA* are present. In addition, there are several *P. gulae*-positive specimens negative for type A and type B, indicating the presence of *P. gulae* strains without FimA. Alternatively, there might be additional *fimA* types. Further investigation of the *P. gulae* strains isolated from these specimens and determination of *fimA* sequences will be needed.

In *P. gingivalis*, the genotypic variation of *fimA* was suggested to be related to the severity of human periodontitis. *P. gingivalis* has been isolated from both periodontally healthy individuals and patients with periodontitis, though the distribution of *fimA* types was very different between the two groups [2]. In fact, strains with type II *fimA* were more virulent that those with type I *fimA* in a mouse abscess model [14]. Earlier studies obtained *P. gingivalis*-like isolates (likely *P. gulae*) from both healthy and diseased gingival pockets in dogs [1, 16]. In our previous study, *P. gulae* was detected in approximately 90% of oral swab specimens from Japanese dogs, which came to veterinary clinics for health checkups and vaccinations [9]. This evidence suggested the variation of *fimA* types in *P. gulae* to be associated with the virulence of periodontitis in dogs. The experiment using the mouse abscess model demonstrated that strains with type B *fimA* caused more severe systemic inflammation than those with type A. However, the mouse model may not necessarily reflect the virulence of periodontitis in dogs. Further studies should focus on elucidating the association between *fimA* type and periodontitis in dogs.

In summary, this is the first study to classify clinical isolates of *P. gulae* based on FimA. The distribution of the different *fimA* types in subjects with periodontitis should be analyzed further using large-scale studies.

ACKNOWLEDGMENTS. The authors thank Dr. Masae Kuboniwa, Department of Preventive Dentistry, Osaka University Graduate School of Dentistry, for culturing the *Porphyromonas* species. This study was supported by Grant-in-Aid for Scientific Research for Challenging Exploratory Research No. 23658256 from the Japan Society for Promotion of Science, and a research project grant awarded by the Azabu University.

REFERENCES

1. Allaker, R. P., de Rosayro, R., Young, K. A. and Hardie, J. M. 1997. Prevalence of *Porphyromonas* and *Prevotella* species in the dental plaque of dogs. *Vet. Rec.* **140**: 147–148. [Medline] [CrossRef]
2. Amano, A., Kuboniwa, M., Nakagawa, I., Akiyama, S., Morisaki, I. and Hamada, S. 2000. Prevalence of specific genotypes of *Porphyromonas gingivalis fimA* and periodontal health status. *J. Dent. Res.* **79**: 1664–1668. [Medline] [CrossRef]
3. Amano, A., Nakagawa, I., Kataoka, K., Morisaki, I. and Hamada, S. 1999. Distribution of *Porphyromonas gingivalis* strains with *fimA* genotypes in periodontitis patients. *J. Clin. Microbiol.* **37**: 1426–1430. [Medline]
4. Amano, A., Nakagawa, I., Okahashi, N. and Hamada, N. 2004. Variations of *Porphyromonas gingivalis* fimbriae in relation to microbial pathogenesis. *J. Periodontal Res.* **39**: 136–142. [Medline] [CrossRef]
5. Dreier, K. J., Hardham, J. M., Haworth, J. D., King, K. W., Krishnan, R. and Mcgavin, D. R. 2005. Vaccine for periodontal disease. Patent: WO2005112993-A1/ 95.
6. Engels, W. R. 1993. Contributing software to the internet: the Amplify program. *Trends Biochem. Sci.* **18**: 448–450. [Medline] [CrossRef]
7. Hamada, N., Takahashi, Y., Watanabe, K., Kumada, H., Oishi, Y. and Umemoto, T. 2008. Molecular and antigenic similarities of the fimbrial major components between *Porphyromonas gulae* and *P. gingivalis*. *Vet. Microbiol.* **128**: 108–117. [Medline] [CrossRef]
8. Harvey, C. E., Shofer, F. S. and Laster, L. 1994. Association of age and body weight with periodontal disease in North American dogs. *J. Vet. Dent.* **11**: 94–105. [Medline]
9. Kato, Y., Shirai, M., Murakami, M., Mizusawa, T., Hagimoto, A., Wada, K., Nomura, R., Nakano, K., Ooshima, T. and Asai, F. 2011. Molecular detection of human periodontal pathogens in oral swab specimens from dogs in Japan. *J. Vet. Dent.* **28**: 84–89. [Medline]
10. Meyle, J. and Gonzáles, J. R. 2001. Influences of systemic diseases on periodontitis in children and adolescents. *Periodontol. 2000* **26**: 92–112. [Medline] [CrossRef]
11. Nakagawa, I., Amano, A., Kimura, R. K., Nakamura, T., Kawabata, S. and Hamada, S. 2000. Distribution and molecular characterization of *Porphyromonas gingivalis* carrying a new type of *fimA* gene. *J. Clin. Microbiol.* **38**: 1909–1914. [Medline]
12. Nakagawa, I., Amano, A., Kuboniwa, M., Nakamura, T., Kawabata, S. and Hamada, S. 2002. Functional differences among FimA variants of *Porphyromonas gingivalis* and their effects on adhesion to and invasion of human epithelial cells. *Infect. Immun.* **70**: 277–285. [Medline] [CrossRef]
13. Nakagawa, I., Amano, A., Ohara-Nemoto, Y., Endoh, N., Morisaki, I., Kimura, S., Kawabata, S. and Hamada, S. 2002. Identification of a new variant of *fimA* gene of *Porphyromonas gingivalis* and its distribution in adults and disabled populations with periodontitis. *J. Periodontal Res.* **37**: 425–432. [Medline] [CrossRef]
14. Nakano, K., Kuboniwa, M., Nakagawa, I., Yamamura, T., Nomura, R., Okahashi, N., Ooshima, T. and Amano, A. 2004. Comparison of inflammatory changes caused by *Porphyromonas gingivalis* with distinct *fimA* genotypes in a mouse abscess model. *Oral Microbiol. Immunol.* **19**: 205–209. [Medline] [CrossRef]
15. Pihlstrom, B. L., Michalowicz, B. S. and Johnson, N. W. 2005. Periodontal diseases. *Lancet* **366**: 1809–1820. [Medline] [CrossRef]
16. Sarkiala, E. M., Asikainen, S. E., Kanervo, A., Junttila, J. and Jousimies-Somer, H. R. 1993. The efficacy of tinidazole in naturally occurring periodontitis in dogs: bacteriological and clinical results. *Vet. Microbiol.* **36**: 273–288. [Medline] [CrossRef]
17. Tamura, K., Nakano, K., Nomura, R., Miyake, S., Nakagawa, I., Amano, A. and Ooshima, T. 2005. Distribution of *Porphyromonas gingivalis fimA* genotypes in Japanese children and adolescents. *J. Periodontol.* **76**: 674–679. [Medline] [CrossRef]
18. Weisburg, W. G., Barns, S. M., Pelletier, D. A. and Lane, D. J. 1991. 16S ribosomal DNA amplification for phylogenetic study. *J. Bacteriol.* **173**: 697–703. [Medline]

NOTE *Pathology*

Deep Granulomatous Dermatitis of the Fin Caused by *Fusarium solani* in a False Killer Whale (*Pseudorca crassidens*)

Miyuu TANAKA[1)], Takeshi IZAWA[1)], Mitsuru KUWAMURA[1)], Tatsuko NAKAO[2)], Yuko MAEZONO[2)], Shu ITO[2)], Michiko MURATA[3)], Masaru MURAKAMI[3)], Ayako SANO[4)] and Jyoji YAMATE[1)]*

[1)]*Veterinary Pathology, Graduate School of Life and Environmental Science, Osaka Prefecture University, 1–58 Rinkuu ourai Kita, Izumisano, Osaka 598–8531, Japan*
[2)]*Adventureworld AWS Co. Ltd., Nishimurogun, Shirahama-cho, Katada, Wakayama 649–2201, Japan*
[3)]*School of Veterinary Medicine, Azabu University, 1–17–71 Fuchinobe, Sagamihara, Kanagawa 229–8501, Japan*
[4)]*Department of Subtropical Agro-Production Sciences, Faculty of Agriculture, University of the Ryukyus, 1 Senbaru, Nishihara, Okinawa 903–0213, Japan*

(Received 13 September 2011/Accepted 16 December 2011/Published online in J-STAGE 28 December 2011)

ABSTRACT. A 10-year-old female false killer whale (*Pseudorca crassidens*) developed skin lesions in the left breast fin. Histopathologically, the lesions consisted of multiple granulomas spread diffusely into the deep dermis and bone; characteristically, each granuloma had septate, branching fungal hyphae and chlamydospores surrounded by eosinophilic Splendore-Hoeppli materials. Macrophages, epithelioid cells and multinucleated giant cells in the granulomas reacted mainly to anti-SRA-E5 antibody against human macrophage scavenger receptor type I. *Fusarium solani* was isolated and its gene was detected from the skin samples. Mycotic skin lesions by *Fusarium* spp. reported so far in marine mammals were regarded as superficial dermatitis; therefore, the present case is very uncommon in that the lesions spread deeper into the skin.

KEY WORDS: deep granulomatous dermatitis, false killer whale, fungus, *Fusarium solani*, Splendore-Hoeppli.

doi: 10.1292/jvms.11-0421; *J. Vet. Med. Sci.* 74(6): 779–782, 2012

Fusarium spp. including *F. solani* and *F. oxysporum* are common soil saprophytes classified under the order of ascomycota hypocreales; they are important plant pathogens causing diseases such as crown rot, head blight, and scab in cereal grains [12–14]. *Fusarium* spp. possess virulent mycotoxins including trichothecene. The mycotoxins suppress both humoral and cellular immunity and may cause tissue injury [13]. Fusariosis has been reported with an increasing frequency as an opportunistic infection in humans and animals such as turtles, sharks, dolphins and pinnipeds [2, 5, 7, 11].

In humans, fusariosis tends to develop in patients who are immunocompromised due to HIV infection, leukemia or organ transplantation; the disseminated infection shows refractory fever, skin lesions at infected sites and sinopulmonary lesions. Fusarial skin lesions occur at any site, particularly with predominance in the extremities. The skin gross lesions are recognized as nodule, ulcer, mycetoma, and intertrigo; histologically, the lesions consist of necrosis, panniculitis or granuloma [6, 13]. In the lesions, hyaline acute-branching septate hyphae are seen, invading the dermis and occasionally extending into the blood vessels with thrombosis [4]. Recently, *Fusarium* keratitis associated with contamination of contact lens solution has been reported [3].

In marine mammals, *Fusarium* spp. are most likely opportunistic pathogens of the skin. Animals with compromised immune systems presumably due to stress or illness are most susceptible [7, 8]. Damage to the integument due to excessive chlorination of the water and high fluctuating pool temperatures may play important roles in skin mycosis of marine mammals [11]. *Fusarium*-induced dermatitis has been reported in a group of captive California sea lions, Atlantic white sided dolphins, harbor seals and a pygmy sperm whale [7, 11]; all cases were diagnosed as superficial dermatitis and the lesions developed as raised, firm, erythematous plaques or nodules in the face, trunk, and flippers. Hence, we describe pathological characteristics of deep granulomatous dermatitis with unique Splendore-Hoeppli phenomenon caused by *F. solani* in a false killer whale.

A 10-year-old female false killer whale (*Pseudorca crassidens*), that was captured and kept in an aquarium, developed dermatitis in the left breast fin and the skin lesions have gradually spread. Biopsies of skin lesions were performed by scrapings, and histopathologically, the lesion was diagnosed as granulomatous dermatitis caused by fungal infection. Two months later, the dolphin died suddenly. At necropsy, the skin lesions were grayish-red, raised nodules with occasional ulcers; on the cut surface, the lesions spread diffusely into the deep dermis (Fig. 1). Besides the skin lesions, severe accumulation of foamy fluid in the trachea and lung, ulcers in the esophagus and rumen, injured head skin and cerebral subdural hemor-

*CORRESPONDENCE TO: YAMATE, J., Veterinary Pathology, Graduate School of Life and Environmental Science, Osaka Prefecture University, 1–58 Rinkuu ourai Kita, Izumisano, Osaka 598–8531, Japan.
e-mail: yamate@vet.osakafu-u.ac.jp

rhage were observed. The tissue samples were fixed in 10% neutral buffered formalin and embedded in paraffin. Sections of 4 μm thick were cut and stained with hematoxylin and eosin (HE). Selected sections were also stained with periodic acid-Schiff (PAS) reaction and Grocott's methenamine silver nitrate stain (GMS). For immunohistochemistry, sections from skin lesions and ulcerated rumen lesions were incubated with a rabbit polyclonal antibody against *Candida* spp. or *Aspergillus* spp. (provided by Dr. M. Kubo, NIAH, Ibaraki, Japan, 1:100), mouse SRA-E5 (Trans Genic Inc., Kumamoto, Japan, 1:200) against human macrophage scavenger receptor type I protein, mouse AM-3K (Trans Genic Inc., 1:100) against human macrophage hemoglobin/haptoglobin complex receptor, rabbit anti-CD3 (Dako Corp., Glostrup, Denmark, 1:200), rabbit anti-CD20 (Thermo Fisher Scientific Inc., Fremont, CA, U.S.A., ready-to-use) and mouse anti-α-smooth muscle actin (α-SMA; Dako, 1:1,000) for 16 hr at 4°C. Bound antibodies were detected with horse radish peroxidase-conjugated anti-mouse or anti-rabbit secondary antibody (Histofine Simplestain MAX-PO; Nichirei, Tokyo, Japan) and 3,3'-diaminobenzidine tetrahydrochroride (DAB) (Vector Laboratories Inc., Burlingame, CA, U.S.A.) as chromogen.

Histopathologically, there were multiple granulomas in the fin lesions, and the granulomatous lesions expanded diffusely into the deep dermis (Fig. 2), partly bone tissues (Fig. 2; insert). Each granuloma consisted of fungal hyphae at the center surrounded by neutrophils, macrophages, epithelioid cells, multinucleated giant cells, lymphocytes and plasma cells; the fibrous connective tissues consisting of α-SMA-positive myofibroblasts enclosed and separated each of granuloma. Fragmented fungal hyphae were also observed within the cytoplasm of macrophages and multinucleated giant cells. Neither invasion of fungal hyphae into the blood vessels nor thrombus was found.

All fungal hyphae were septate, branching fungal hyphae irregular in diameter and thick-walled large spherical spores (chlamydospores) were also observed; the organisms were surrounded by intensely eosinophilic amorphous materials that often showed a clubbed or radiating appearance known as Splendore-Hoeppli phenomenon (Fig. 3). The hyphae were basophilic or amphophilic in HE-stained sections (Fig. 3), and stained red with PAS reaction (Fig. 4a) and brown-black with GMS stain (Fig. 4b). The Splendore-Hoeppli materials were intensely stained red with PAS reaction, but not by GMS stain. The hyphae were negative for antibodies against *Aspergillus* spp. and *Candida* spp. Immunohistochemically, main components of granulomas were SRA-E5 positive macrophages, epitheioid cells, multinucleated giant cells (Fig. 5a) and CD20 positive B lymphocytes (Fig. 6a). Fewer AM-3K positive macrophages (Fig. 5b) and CD3 positive T lymphocytes (Fig. 6b) were also observed. The multinucleated giant cells were negative for AM-3K (Fig. 5b). Esophagus and rumen developed erosion or mild ulcerative lesions, and fungal hyphae with slight infiltration of neutrophils were observed confined to the squamous epithelium. The hyphae were recognized by GMS stain and PAS reaction, and were immunopositive for *Candida* spp. and negative for *Aspergillus* spp. In the cerebrum, subdural and subpial hemorrhage corresponding to the gross finding and glial reactions in surrounding tissues were observed. Histological findings seen in other organs included severe pulmonary congestive edema and lymphopenia in the lymph nodes and spleen. *F. solani* were not detected in any visceral organs.

Samples of the kidney, spleen, heart, pancreas, lymph node, cerebrum, cerebellum and skin lesions were collected for fungal culture. These samples were inoculated onto potato dextrose agar (PDA, Difco, Detroit, MO, U.S.A.) plates at 35°C for 14 days. White floccose colonies were sprouted from the fin samples. Colonies on Sabouraud dextrose agar (SDA) containing 2% dextrose (Wako Chemical Co., Ltd., Osaka, Japan), 1% neopeptone (Difco) and 1.5% Bacto agar (Difco) and PDA showed white floccose colonies with pale red pigmentation into the media. Curved macroconidia consisted of 4 to 6 cells and chlamydospores were detected in the micro culture on PDA. DNA was extracted from the isolates and tissue samples. The internal transcribed spacer (ITS) 1-5.8S-ITS2 regions of ribosomal RNA gene sequences (ITS gene) consisted of 549 base pairs from both isolates obtained from the fin samples were 100% identical to the GenBank accession No. FN598930 derived from *F. solani* by BLAST (Basic Local Alignment Search Tool) searches. As a result, *F. solani* was identified only from the cultures of skin lesions. In addition, a partial sequence of ITS gene consisted of 226 base pairs obtained from a tissue sample by a nested PCR also showed 100% identity to No. FN598930.

Based on the pathological findings (characterized by multiple granulomas spread diffusely into the deep dermis and bones), as well as mycological studies and molecular analyses, the present skin lesion was diagnosed as deep granulomatous dermatitis caused by *F. solani*. *Fusarium*-induced dermatitis in marine mammals has been reported to be confined to the epidermis and sub-epidermal area (diagnosed as superficial dermatitis) [7, 11]. Interestingly, the present granulomas often involved Splendore-Hoeppli phenomenon around the fungal hyphae. The phenomenon is characterized by the presence of radiate, star-like, asteroid or club-shaped intensely eosinophilic materials around infectious or non-infectious agents [9]. Although the exact pathogenesis of the Splendore-Hoeppli phenomenon is not well understood, it has been thought to represent deposition of antigen-antibody complexes and cellular debris from inflammatory cells such as epithelioid cells and multinucleated giant cells. Development of Splendore-Hoeppli phenomenon has been reported in the occasional cases of fungal infections such as sporotrichosis, blastomycosis, zygomycosis, candidiasis and aspergillosis in humans and animals [9]. In a human fusariosis patient, the phenomenon was reported in association with mycetoma due to *F. moniliforme* [1]. To the best of our knowledge, the present case is the first report of *Fusarium* spp. infection in marine mammals accompanied with the Splendore-Hoeppli phenomenon.

The present study revealed that granulomas due to *F. solani* infection were composed mainly of SRA-E5-positive

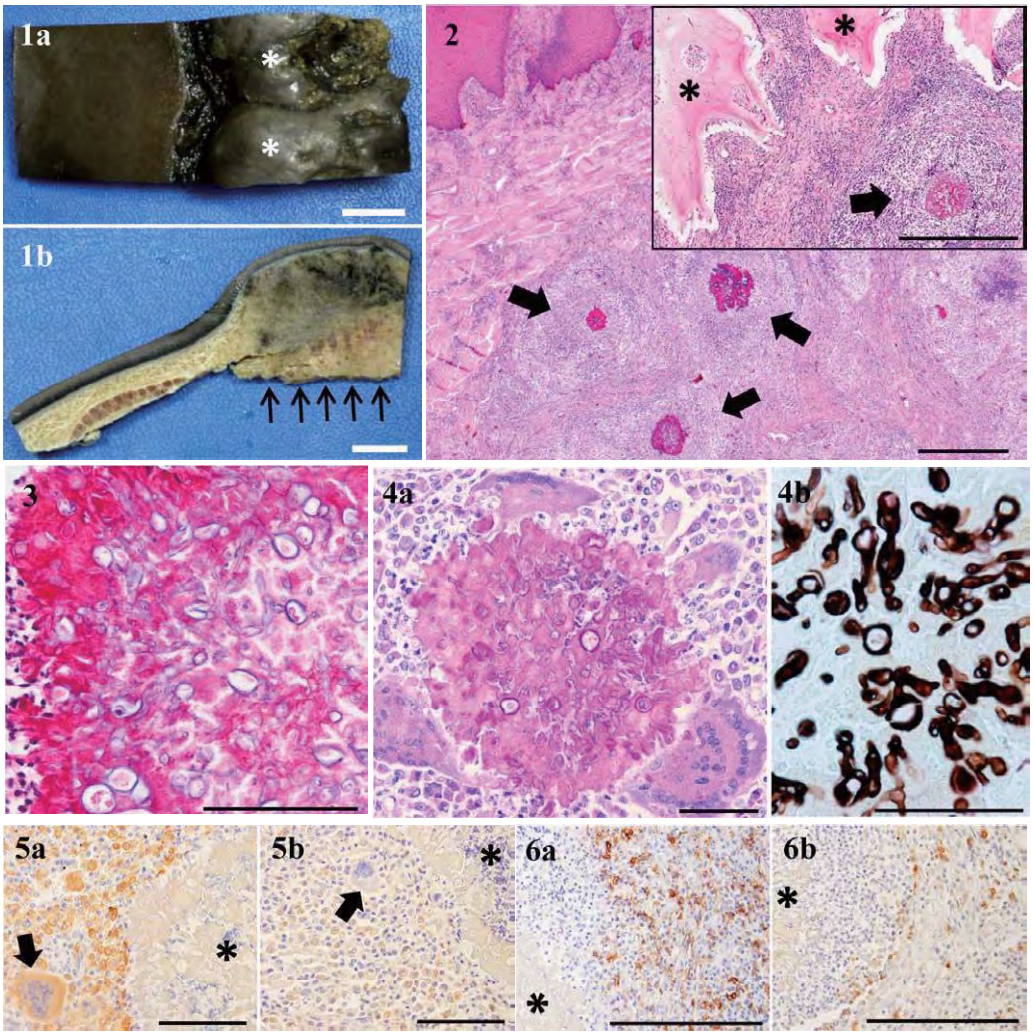

Fig. 1. Raised, nodular lesions (asterisks) with ulcer in the skin of the fin (1a). On the cut surface (1b), the lesions spread diffusely into the deep dermis (arrows). Bar=1 cm.

Fig. 2. Multiple granulomas (arrows) around clumps of fungal hyphae in the fin. Insert: the lesions spread diffusely into the deep skin, partly bone tissue (asterisks). HE. Bar=500 μm.

Fig. 3. The fungal hyphae are surrounded by intensely eosinophilic amorphous materials that sometimes show a clubbed or radiating appearance known as Splendore-Hoeppli phenomenon. HE. Bar=100 μm.

Fig. 4. The fungal hyphae are stained red with PAS reaction (4a) and brown-black with GMS (4b). Septate, branching fungal hyphae irregular in diameter and thick-walled large spherical spores (chlamydospores) are observed (4a and 4b). Bar=50 μm.

Fig. 5. Numerous SRA-E5-immunopositive macrophages, epitheliod cells and multinucleated giant cells (arrow) are seen in the granuloma (5a). Fewer AM-3K positive macrophages (5b) are also observed. Asterisks: the clumps of fungal hyphae. Bar=100 μm.

Fig. 6. In the granulomatous lesions, numerous CD20 positive lymphocytes (6a) and fewer CD3 positive lymphocytes (6b) are observed. Bar=200 μm.

macrophages, epithelioid cells and multinucleated giant cells; in contrast, AM-3K positive macrophages were very small in number. Similar immunohistochemical reactivities have been reported in human granulomatous diseases such as tuberculosis, sarcoidosis and foreign body reactions [10]. It is interesting to investigate different functions of macrophage populations participating in the granuloma formation, because macrophages are responsible for induction of T cells or B cells through antigen presentation in both cellular and humoral immunities.

The cerebral hemorrhage might have been due to accidental bruise on the head; judging from severe pulmonary congestive edema, under this condition the dolphin might have aspirated sea water and presumably died in a drown-

ing accident. Lymphopenia in the lymph nodes and spleen suggested decreased immunocompetence of the dolphin. Although the cause of immunosuppression of the present case was not determined, deeply spread mycotic granulomatous dermatitis caused by *F. solani* and candidiasis in the esophagus and rumen might have been related to decreased immunocompetence.

In conclusion, this is the first report of deep granulomatous dermatitis caused by *F. solani* in a False Killer Whale with a characteristic finding of Splendore-Hoeppli phenomenon.

REFERENCES

1. Ajello, L., Padhye, A. A., Chandler, F. W., McGinnis, M. R., Morganti, L. and Alberici, F. 1985. *Fusarium moniliforme*, a new mycetoma agent. Restudy of a European case. *Eur. J. Epidemiol.* **1**: 5–10. [Medline] [CrossRef]
2. Cabañes, F. J., Alonso, J. M., Castellá, G., Alegre, F., Domingo, M. and Pont, S. 1997. Cutaneous hyalohyphomycosis caused by *Fusarium solani* in a loggerhead sea turtle (*Caretta carreta* L.). *J. Clin. Microbiol.* **35**: 3343–3345. [Medline]
3. Chang, D. C., Grant, G. B., O'Donnell, K., Wannemuehler, K. A., Noble-Wang, J., Rao, C. Y., Jacobson, L. M., Crowell, C. S., Sneed, R. S., Lewis, F. M., Schaffzin, J. K., Kainer, M. A., Genese, C. A., Alfonso, E. C., Jones, D. B., Srinivasan, A., Fridkin, S. K. and Park, B. J. 2006. Multistate outbreak of *Fusarium* keratitis associated with use of a contact lens solution. *JAMA* **296**: 953–963. [Medline] [CrossRef]
4. Cocuroccia, B., Gaido, J., Gubinelli, E., Annessi, G. and Girolomoni, G. 2003. Localized cutaneous hyalohyphomycosis caused by a *Fusarium* species infection in a renal transplant patient. *J. Clin. Microbiol.* **41**: 905–907. [Medline] [CrossRef]
5. Crow, G. L., Brock, J. A. and Kaiser, S. 1995. *Fusarium solani* fungal infection of the lateral line canal system in captive scalloped hammerhead sharks (*Sphyrna lewini*) in Hawaii. *J. Wildl. Dis.* **31**: 562–565. [Medline]
6. Dignani, M. C. and Anaissie, E. 2004. Human fusariosis. *Clin. Microbiol. Infect.* **10**: 67–75. [Medline] [CrossRef]
7. Frasca, S. Jr., Dunn, J. L., Cooke, J. C. and Buck, J. D. 1996. Mycotic dermatitis in an Atlantic white-sided dolphin, a pygmy sperm whale, and two harbor seals. *J. Am. Vet. Med. Assoc.* **208**: 727–729. [Medline]
8. Higgins, R. 2000. Bacteria and fungi of marine mammals: a review. *Can. Vet. J.* **41**: 105–116. [Medline]
9. Hussein, M. R. 2008. Mucocutaneous Splendore-Hoeppli phenomenon. *J. Cutan. Pathol.* **35**: 979–988. [Medline] [CrossRef]
10. Komohara, Y., Hirahara, J., Horikawa, T., Kawamura, K., Kiyota, E., Sakashita, N., Araki, N. and Takeya, M. 2006. AM-3K, an anti-macrophage antibody, recognizes CD163, a molecule associated with an anti-inflammatory macrophage phenotype. *J. Histochem. Cytochem.* **54**: 763–771. [Medline] [CrossRef]
11. Montali, R. J., Bush, M., Strandberg, J. D., Janssen, D. L., Boness, D. J. and Whitla, J. C. 1981. Cyclic dermatitis associated with *Fusarium* sp infection in pinnipeds. *J. Am. Vet. Med. Assoc.* **179**: 1198–1202. [Medline]
12. Nelson, P. E., Dignani, M. C. and Anaissie, E. J. 1994. Taxonomy, biology, and clinical aspects of *Fusarium* species. *Clin. Microbiol. Rev.* **7**: 479–504. [Medline]
13. Nucci, M. and Anaissie, E. 2007. *Fusarium* infections in immunocompromised patients. *Clin. Microbiol. Rev.* **20**: 695–704. [Medline] [CrossRef]
14. Zhang, N., O'Donnell, K., Sutton, D. A., Nalim, F. A., Summerbell, R. C., Padhye, A. A. and Geiser, D. M. 2006. Members of the *Fusarium solani* species complex that cause infections in both humans and plants are common in the environment. *J. Clin. Microbiol.* **44**: 2186–2190. [Medline] [CrossRef]

NOTE *Anatomy*

Maternal Exposure to Low Doses of DES Altered mRNA Expression of Hepatic Microsomal Enz ymes in Male Rat Offspring

Osamu NISHIKAWA[1], Kazuyoshi ARISHIMA[1]*, Tetsuo KOBAYASHI[1], Mitsuyuki SHIRAI[2], Masaru MURAKAMI[3], Motoharu SAKAUE[1] and Masako YAMAMOTO[1]

[1]*Department of Anatomy II, School of Veterinary Medicine, Azabu University, 1–17–71 Fuchinobe, Chuo, Sagamihara, Kanagawa 252–5201, Japan*

[2]*Department of Veterinary Pharmacology, School of Veterinary Medicine, Azabu University, 1–17–71 Fuchinobe, Chuo, Sagamihara, Kanagawa 252–5201, Japan*

[3]*Department of Molecular Biology, School of Veterinary Medicine, Azabu University, 1–17–7 Fuchinobe, Chuo, Sagamihara, Kanagawa 252–5201, Japan*

(Received 17 December 2010/Accepted 16 September 2011/Published online in J-STAGE 30 September 2011)

ABSTRACT. Our previous studies demonstrated that prenatal diethylstilbestrol (DES) treatment disrupts steroidogenesis but induces high-level expression of androgen receptor (AR) mRNA to inhibit the disruption of spermatogenesis. This study examined which prenatal DES treatment influenced hepatic microsomal enzymes, CYP3A1, CYP2B1/2, CYP2C11, UGT2B1 (UDP-glucuronosyltransferase 2B1), and IGF-1 (insulin-like growth factor-1), in male rat offspring. DES treatment decreased the mRNA expression levels of CYP3A1 and CYP2B1/2, but did not alter the expression of CYP2C11. At 6 weeks, DES treatment increasd the mRNA expression levels of UGT2B1 and IGF-1. These results suggest that prenatal DES treatment alters two hepatic enzymes (CYP3A1 and CYP2B1/2) and IGF-1 mRNA expression levels to counteract the low level of testosterone, but this disrupted UGT2B1 mRNA expression reduces the testosterone level.
KEY WORDS: CYP, DES, IGF-1, liver, rat

doi: 10.1292/jvms.10-0564, *J. Vet. Med. Sci.* 74(2): 247–253, 2012

Diethylstilbestrol (DES), a synthetic non-steroidal estrogen, was widely used as one of the best medications for preventing threatened abortion in the late 1940s and 1950s. However, Kaplan [13] first reported that DES may have affected the normal development of the reproductive system in male offspring. Since then, many reports have appeared on the undesirable effects of DES on the reproductive systems of men and women [12] as well as experimental animals [1, 19]. Numerous studies have used prenatal or postnatal exposure to DES, mostly in high-dose ranges from 10 to 300 mg/kg, to induce gross adverse changes in the developing male reproductive system, e.g., testicular cancer, reduced testicular size and sperm production [10, 19, 20, 24].

We administered doses of DES much lower (1.5 μg/kg) than those previously applied [10, 11, 29] to pregnant rats at days 7–21 of gestation (in the second and third trimesters), and demonstrated that DES induced not only suppression of plasma testosterone levels in adolescent male offspring (6 weeks after birth), but also promoted follicular maturation in female offspring [36, 37]; in addition, maternal DES treatment disrupted steroidogenesis but increased the expression level of androgen receptor (AR) mRNA to inhibit the disruption of spermatogenesis to thereby counteract the low level of testosterone in testis [15].

* CORRESPONDENCE TO: ARISHIMA, K., Department of Anatomy II, Azabu University, School of Veterinary Medicine, 1–17–71 Fuchinobe, Chuo, Sagamihara, Kanagawa 252–5201, Japan.
e-mail: arishima@azabu-u.ac.jp

Secreted hormones exert their effects and are subsequently degraded in the liver to be excreted. Steroid hormones are maintained through a dynamic balance between steroidogenesis and inactivation to ensure their physiological functions. Hydroxylation by cytochrome P450 (CYP) enzymes and conjugation with glucuronide and sulfate are among the major hepatic pathways of steroid inactivation. The CYP3A subfamily catalyzes the 6β-hydroxylation of testosterone and metabolizes several drugs, and CYP3A1 is inducible by glucocorticoids, such as dexamethasone, and by pregnenolone-16α-carbonitrile [3, 21]. CYP 2B1/2 functions as a testosterone 16α- and 16β-hydroxylase and 17β-hydroxysteroid hydrogenase. CYP2C11 functions as a testosterone 2α- and 16α-hydroxylase. This enzyme is only expressed in male rat livers from 2 weeks of age and increases dramatically between 4 and 6 weeks of age to adult levels [30]; it represents the major constitutive CYP isoform in the male rat liver, accounting for up to 40% [23]. The expression of these transformation enzymes can be induced by many xenobiotics. The barbiturate phenobarbital and the environmental toxicant DDE [1,1-Dichloro-2,2-bis(*p*-chlorophenyl)ethylene] are among the well-characterized inducers for CYP 2B and 3A enzymes and selected conjugated enzymes [33, 34, 39]. Thus, xenobiotics, directly administered to an adult, induce degrading enzymes in the liver and are excreted. Maternally administered phenobarbital and DDE were demonstrated to induce CYP2B and 3A enzymes in the liver of a newborn [7, 39]. The mechanism involved remains unclear.

Uridine diphosphate-glucuronosyltransferase (UGT)

includes multiple isoforms that catalyze the glucuronidation of exogenous and endogenous compounds. The two families of UGT, UGT1 and UGT2, consist of more than 35 enzymes found in various species [14, 18]. Glucuronidation of steroids leads to termination of biological activity and elimination from the body. Among the isozymes, the UGT2B subfamily is more specific to steroid hormones [38].

We have investigated the effects of maternally administered DES on offspring, but have yet to evaluate the reaction of the offspring' s liver to DES. In this study, we aimed to elucidate the responsiveness of steroid-metabolizing enzymes in the liver of mature and immature male offspring of mothers who received low doses of DES during pregnancy.

Sprague-Dawley rats (Japan SLC, Hamamatsu, Japan) were given a commercial diet (CE-2, CLEA, Tokyo, Japan) and water, both *ad libitum*. Females were mated with males overnight and were examined the next morning for the presence of sperm in the vaginal smear. The day on which sperm was detected was counted as day 0 of gestation. Pregnant rats were housed individually and maintained in a 12/12 hr light-dark cycle at room temperature of 21 ± 2°C and humidity of 55 ± 5%. Pregnant rats were divided into three groups. The rats in each group were treated daily subcutaneously with DES (Sigma Chemical Co., St. Louis, MO, U.S.A.) at 0.5 or 1.5 μg/kg/day (DES 0.5 and DES 1.5 groups, respectively) dissolved in corn oil (tocopherol-stripped, ICN Biomedicals Inc., Aurora, OH, U.S.A.) or corn oil alone (Control group) on days 7–21 of gestation. The volume of a single dose ranged from 0.2–0.4 m*l*. Four days after birth, pups were controlled to 4 males and 4 females in each litter. There were 10 litters per group. The pups were kept with their natural mothers until weaning on day 21. Male rats at postnatal weeks 1, 3, 6, and 15 were autopsied under ether anesthesia to collect blood samples individually. The liver of each pup was removed and subjected to RNA extraction. The study was carried out in accordance with the Azabu University Animal Experiment Guidelines.

Livers at 15 weeks were fixed in 10% neutral buffered formalin, dehydrated in a graded series of ethanol, embedded in paraffin and sectioned at 5 μm. The sections were immunostained with rabbit anti-CYP3A1 serum (Enzo Life Sciences, Inc., Farmingdale, NY, U.S.A.) using the ABC method or stained hematoxylin-eosin. Total RNA from the liver of male offspring was extracted using Isogen (Nippon Gene Co., Toyama, Japan) according to the manufacturer' s protocol. The subsequent isolation involved chloroform extraction, isopropanol precipitation, and washing in 70% ethanol. The concentration of total RNA was determined by measuring the optical density at 260 and 280 nm. PCR amplification from reverse-transcribed cDNA was carried out with the following primers: CYP3A1, CYP2B1, CYP2C11, UGT2B1, IGF-1, and β-actin (Table 1). The reactions were performed according to the manufacturer' s instructions for the SuperScript One-step RT-PCR (Invitrogen, Carlsbad, CA, U.S.A.). A total volume of 50 μ*l* of the reaction mixture contained RNA, 200 nM of sense and antisense primers, tag Mix, and 1 X reaction mix. cDNA synthesis and pre-denaturation were performed with one cycle of 50°C for 30 min and 94°C for 2 min. Amplification was carried out in a thermal cycler (BIO-RAD, Hercules, CA, U.S.A.). Following PCR, the amplified DNA was separated by electrophoresis in a 2% agarose gel with an appropriate molecular weight marker (BIO-RAD). Gels were stained with ethidium bromide. The intensity of the ethidium bromide luminescence was measured using photographs and the intensity of the band was digitized using NIH Image software. The signal intensities were measured in three individual animals and two independent RT for each sample. Data were normalized for β-actin mRNA levels in each sample.

Levels of significance were analyzed by Fisher' s one-way analysis of variance. All values are expressed as the mean ± standard error of the mean (SEM). Differences are considered significant at $P<0.05$.

At 6 weeks of age, CYP3A1 mRNA expression levels were significantly lower in the DES 1.5 than in the other two groups, at 15 weeks of age, CYP3A1 mRNA expression levels were significantly lower in the DES 1.5 and 0.5 groups than in the Control group (Fig. 1). In all groups, livers did not show no histological changes (Fig. 2A–C). Positive signals for CYP3A1 were observed in many hepatocytes surrounding central vein in the Control group, but a small number of hepatocytes showed the signals in the both DES

Table 1. PCR primers for the detection of various gene expressions used in this study

Gene	Direction	Sequence (5' –3')	Product size (bp)
CYP3A1	Forward	ATCCGATATGGAGATCAC	580
	Reverse	GAAGAAGTCCTTGTCTGC	
CYP2B1/2	Forward	GAGTTCTTCTCTGGGTTCCTG	549
	Reverse	ACTGTGGGTCATGGAGAGCTG	
CYP2C11	Forward	TGCCCCCTTTTTACGAGGCT	367
	Reverse	GGAACAGATGACTCTGAATTCT	
UGT2B1	Forward	AATCACATGGTAGCCAAAGGA	288
	Reverse	GAGCAATAGGAACCCAATGACA	
IGF-1	Forward	GTGCTCCGCTGAAGCCTAC	126
	Reverse	AGGTCTTGTTTCCTGCACTTCC	
β-Actin	Forward	CAGCCTTCCTTCCTGGGTATG	246
	Reverse	TAGAGCCACCAATCCACACAG	

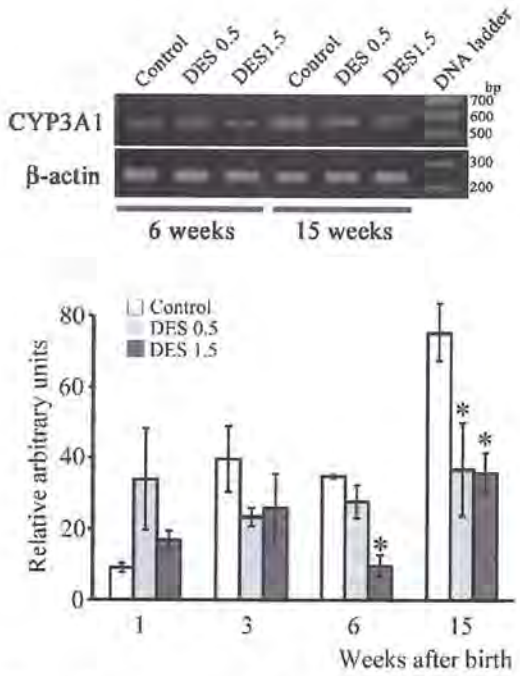

Fig. 1. The expression levels of hepatic CYP3A1 mRNA in offspring of mothers exposed to DES. Photographs show ethidium bromide-stained agarose gels of CYP3A1 at 6 and 15 weeks. The signal intensity of each cDNA was normalized for β-actin (internal control). Values are given as the mean ± SEM of 3 determinations. *: Significant difference from the Control ($P<0.05$).

groups (Fig. 2D–F). At 6 weeks of age, CYP2B1/2 mRNA expression levels were significantly lower in the DES 1.5 than in the other two groups (Fig. 3). At 1 and 3 weeks of age, CYP2C11 mRNA expression was not detected. At 6 and 15 weeks, CYP2C11 mRNA expression levels remained unchanged after DES administration (Fig. 3). At 6 weeks of age, UGT2B1 mRNA expression levels were significantly higher in the DES 1.5 than in the Control group (Fig. 4). At 15 weeks of age, UGT2B1 mRNA expression levels were significantly lower in the DES 1.5 and 0.5 groups than in the Control group (Fig. 4). At 1 week of age, IGF-1 mRNA expression was not detected. At 6 weeks of age, IGF-1 mRNA expression levels were significantly higher in the DES 1.5 and 0.5 groups than in the Control group (Fig. 5).

In our previous study [15], DES, administered during the fetal stage, reduced plasma LH level for three weeks after birth, the plasma testosterone levels of the DES1.5 (6 weeks old) and DES0.5 (15 weeks old) groups decreased, but the release of gonadotropins from the pituitary gland did not increase in response to this change. To compensate for the decreased testicular testosterone level due to DES, the AR (androgen receptor) mRNA expression level in the testicles increased, and the spermatogenesis in the testicles was rescued from the inhibitory effects of DES. However, the altered mRNA expression levels of enzymes associated with testicular steroidogenesis were found to be not directly correlated with the decreased plasma testosterone levels [15]. Therefore, we considered that the steroid metabolism in the liver, responsible for the maintenance and excretion of circulating hormones, might be altered by DES and contribute to the decreased plasma testosterone level. In this experiment, we investigated CYP3A1, CYP2B1/2, and CYP2C11 mRNA expression levels closely associated with steroid metabolism, the normal developmental changes in the mRNA expressions of these three hepatic cytochrome P450s were very similar to those in the previous report [40].

DDE induces hepatic CYP enzymes (CYP2B1, 3A1, and 2C11), which inactivate circulating androgens in the liver by their hydroxylating actions [39]. DDE could modulate the expression and activity levels of liver CYP enzymes in developing rats at early postnatal stages when DDE was given to pregnant dams during late gestation. For male rats, CYP2B1 and 3A1 increased in response to the DDE treatment at both infantile and adult stages, whereas CYP2A1, as a testosterone 7α-hydroxylase, increased only in the neonatal period and CYP2C11 decreased in the adult stage [39]. However, maternal treatment with DDE did not affect a newborn' s testosterone production, no direct evidence is available to show whether the circulating androgen levels are indeed affected by the DDE-induced alterations of testosterone hydroxylase activities. DES administered to a pregnant mother in our experiment, tended to decrease CYP3A1 and CYP2B1/2 mRNA expression levels and plasma testosterone levels at 6 weeks of age. These observations suggest that CYP3A1 and CYP2B-2/1 in the DES group were downregulated by circulating hormones to maintain the normal level of testosterone.

CYP2C11 is an enzyme specifically expressed only in male rats, a major isoform of the CYP family in the liver [30, 39]. In our study, CYP2C11 was not expressed for three weeks after birth as previously reported [30] and CYP2C11 expression was not altered in response to the decreased testosterone due to DES. Previous studies report gender-divergent mRNA expression patterns for both rat and mouse UGTs [4, 25]. Gonadectomy decreased mRNA expression of UGT2B1 in male mouse liver; testosterone treatment of gonadectomized mice increased this expression [5]. This report suggests that UGT2B1 mRNA expression in liver was regulated by testosterone. In our experiment, UGT2B1 mRNA increased in the liver of the DES1.5 group at 6 weeks after birth, but decreased in the liver of DES groups at 15 weeks; these changes did not parallel those of testosterone levels in our previous study [15]. These results suggest that maternal DES treatment might disrupt metabolic enzyme, UGT2B1, expressions in the liver of offspring to decrease the plasma testosterone level at 6 weeks of age.

Absence of IGF-1 leads to poor prenatal growth [31], and intrauterine growth restriction decreases serum IGF-1 [8]. Some studies demonstrated that GH plays a role in gonadal

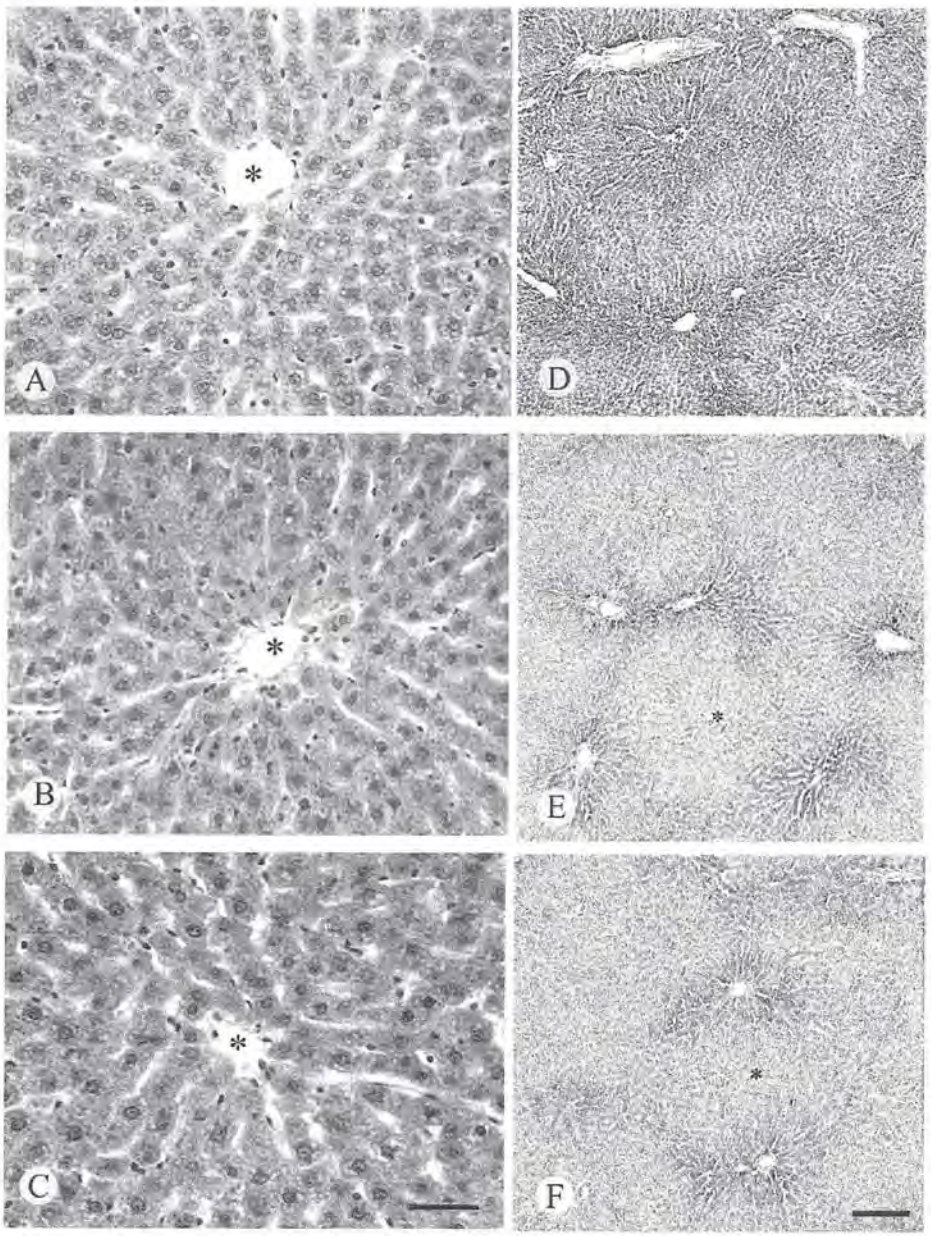

Fig. 2. Histomicrographs of the livers at 15 weeks. A-C: Sections of the livers stained with Hematoxylin and Eosin. There are no histological changes in livers of the DES 0.5 and DES 1.5 groups (B and C) to compared to the liver of Control group (A). Scale bar, 50 μm. D-F: Sections of the livers stained with anti-CYP3A1 serum. Many CYP3A1-positive hepatocytes are observed in surrounding the central veins (*) in Control group (D). In DES 0.5 and DES 1.5 groups (E and F), CYP3A1-positive hepatocytes are observed in small numbers. Scale bar, 200 μm.

steroidogenesis and gametogenesis [2], exerting endocrine activity either directly at gonadal sites or indirectly via IGF-1 [9]. IGF-1 and its receptor mRNAs are highly expressed in testicular Leydig cells [16]. IGF-1-deficient mouse model confirmed that liver is indeed the major source of circulating IGF-1 [26, 28, 32, 35], although testis locally produces IGF-1 [6, 17, 22]. Deficiency of liver-derived IGF-1 reduces the histological compartments of the prostate and decreases AR expression in prostate [27]. Because maternal DES treatment did not impair spermatogenesis despite the resulting low level of testosterone [15], we determined the level of liver-derived IGF-1. As a result, the IGF-1 level of

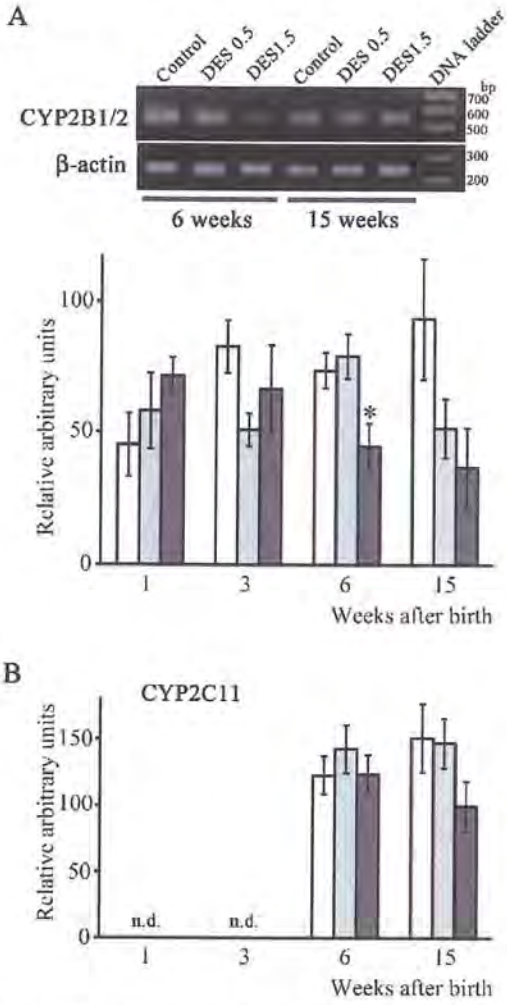

Fig. 3. The expression levels of hepatic CYP2B1/2 (A), and CYP2C11 (B) mRNA in offspring of mothers exposed to DES. Photographs show ethidium bromide-stained agarose gels of CYP2B1/2 at 6 and 15 weeks. The signal intensity of each cDNA was normalized for β-actin (internal control). Values are given as the mean ± SEM of 3 determinations. *: Significant difference from the Control (P<0.05). n.d.: Signals were not detected.

the DES group increased at 6 and 15 weeks of age, suggesting that the spermatogenesis in the DES group may have been maintained in part by IGF-1 from liver to compensate for the decreased plasma testosterone level due to DES.

In conclusion, maternal DES treatment decreased plasma testosterone, followed by the decreased expression levels of CYP3A1 and CYP2B1/2 to maintain the normal plasma testosterone level and the increased expression of IGF-1 to maintain the normal spermatogenesis, but DES treatment disrupted the expression level of UGT2B1, reducing the testosterone level at 6 weeks of age. We demonstrated the pos-

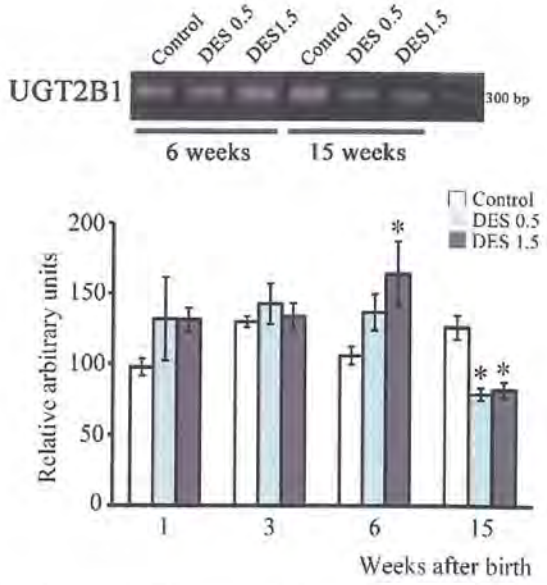

Fig. 4. The expression levels of hepatic UGT2B1 mRNA in offspring of mothers exposed to DES. Photographs show ethidium bromide-stained agarose gels at 6 and 15 weeks. Values are given as the mean ± SEM of 3 determinations. *: Significant difference from the Control (P<0.05).

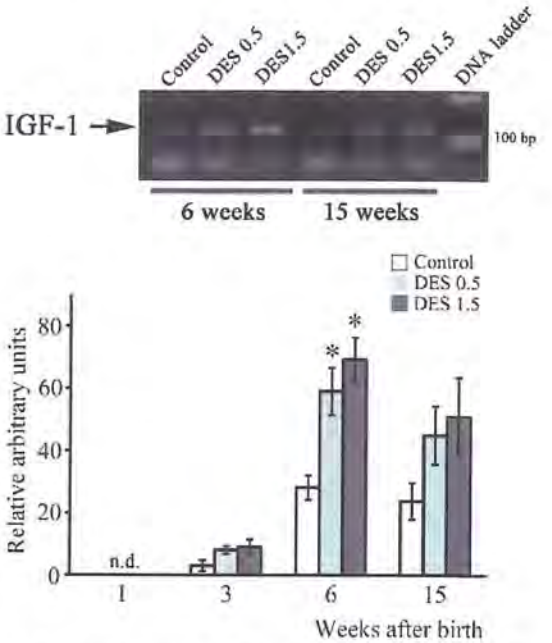

Fig. 5. The expression levels of hepatic IGF-1 mRNA in offspring of mothers exposed to DES. Photographs show ethidium bromide-stained agarose gels at 6 and 15 weeks. Values are given as the mean ± SEM of 3 determinations. *: Significant difference from the Control (P<0.05). n.d.: Signals were not detected.

sibility that prenatal DES treatment may disrupt the expression of the microsomal enzyme, UGT2B1, and this change induced in part the low levels of plasma testosterone. However, at 15 weeks of age, some changes in mRNA expression levels of metabolic enzymes and the growth factor do not explain the decreased levels of testosterone in the DES 0.5 group.

REFERENCES

1. Arai, Y., Mori, T., Suzuki, Y. and Bern, H. A. 1983. Long-term effects of perinatal exposure to sex steroid and diethylstilbestrol on the reproductive system of male mammals. *Int. Rev. Cytol.* **84**: 235–268.
2. Benahmed, M., Morera, A. M., Chauvin, M. C. and de Peretti, E. 1987. Somatomedin C/insulin-like growth factor I as a possible intratesticular regulator of Leydig cell activity. *Mol. Cell Endocrinol.* **50**: 69–77.
3. Black, S. D. and Coon, M. J. 1987. P-450 cytochromes: structure and function. *Adv. Enzymol. Relat. Areas. Mol. Biol.* **60**: 35–87.
4. Buckley, D. B. and Klaassen, C. D. 2007. Tissue- and gender-specific mRNA expression of UDP-Glucuronosyltransferase (UGTs) in mice. *Drug Metab. Dispos.* **35**: 121–127.
5. Buckley, D. B. and Klaassen, C. D. 2009. Mechanism of gender-divergent UDP-glucuronosyltransferase mRNA expression in mouse liver and kidney. *Drug Metab. Dispos.* **37**: 834–840.
6. Chuzel, F., Clark, A. M., Avallet, O. and Saez, J. M. 1996. Transcriptional regulation of the lutropin/human choriogonadotropin receptor and three enzymes of steroidogenesis by growth factors in cultured pig Leydig cells. *Eur. J. Biochem.* **239**: 8–16.
7. Ejiri, N., Kitayama, K. and Doi, K. 2005. Induction of cytochrome P450 isozymes by Phenobarbital in pregnant rat and fetal livers and placenta. *Exp. Mol. Pathol.* **78**: 150–155.
8. Fu, Q., Yu, X., Callaway, C. W., Lane, R. H. and McKnight, R. A. 2009. Epigenetics: intrauterine growth retardation (IUGR) modifies the histone code along the rat hepatic IGF-1 gene. *FASEB J.* **23**: 2438–2449.
9. Gelber, S. J., Hardy, M. P., Mendis-Handagama, S. M. and Casella, S. J. 1992. Effects of insulin-like growth factor-I on androgen production by highly purified pubertal and adult rat Leydig cells. *J. Androl.* **13**: 125–130.
10. Haavisto, T., Nurmela, K., Pohjanvirta, R., Huuskonen, H., El-Gehani, F. and Paranko, J. 2001. Prenatal testosterone and luteinizing hormone levels in male rats exposed during pregnancy to 2,3,7,8-tetrachlorodiabenzo-p-dioxin and diethylstilbestrol. *Mol. Cell. Endocrinol.* **178**: 169–179.
11. Haavisto, T. E., Adamsson, N. A., Myllmaki, S.A., Toppari, J. and Paranko, J. 2003. Effect of 4-tert-octylphenol, 4-tert-butylphenol, and diethylstilbestrol on prenatal testosterone surge in the rat. *Reprod. Toxicol.* **17**: 593–605.
12. Herbst, A. L. and Bern, H. A. 1981. Developmental Effects of Diethylstilbesrol (DES) in Pregnancy, Thieme-Stratton, New York.
13. Kaplan, N. M. 1959. Male pseudohermaphrodism: report of a case with observations on pathogenesis. *N. Engl. J. Med.* **261**: 641–644.
14. King, C. D., Rios, G. R. Green, M. D. and Tephly, T. R. 2000. UDP-glucuronosyltransferases. *Curr. Drug Metab.* **1**: 143–161.
15. Kobayashi, T., Shirai, M., Sakaue, M., Murakami, M., Ochiai, H., Arishima, K. and Yamamoto, M. 2009. Effects of maternal exposure to low doses of DES on testicular steroidogenesis and spermatogenesis in male rat offspring. *J. Reprod. Dev.* **55**: 629–637.
16. Lin, T. 1995. Regulation of Leydig cell function by insulin-like growth factor-I and binding proteins. *J. Androl.* **16**: 193–196.
17. Lin, T. 1996. Insulin-like growth factor-I regulation of the Leydig cell. pp. 477–492. *In*: The Leydig Cell (Payne, A. H., Hardy, M. P. and Russell LD, eds.), Cache River Press, Vienna.
18. Mackenzie, P. I., Owens, I. S., Burchell, B., Bock, K.W., Bairoch, A., Bélanger, A., Fournel-Gigleux, S., Green, M, Hum, D. W., Iyanagi, T., Lancet, D., Louisot, P., Magdalou, J., Chowdhury, J. R., Ritter, J. K., Schachter, H., Tephly, T. R., Tipton, K. F. and Nebert, D. W. 1997. The UDP glycosyltransferase gene superfamily: recommended nomenclature update based on evolutionary divergence. *Pharmacogenetics* **7**: 255–269.
19. McLachlan, J. A., Newbold, R. R. and Bullock, B. 1975. Reproductive tract lesions in male mice exposed prenatally to diethylstilbestrol. *Science* **190**: 991–992.
20. McKinnell, C., Atanassova, N., Williams, K., Fisher, J. S., Walker, M., Turner, K. J., Saunders, T. K. and Sharpe, R. M. 2001. Suppression of androgen action and the induction of gross abnormalities of the reproductive tract in male rats treated neonatally with diethylstilbestrol. *J. Androl.* **22**: 323–338.
21. Rich, K. J. and Boobis, A. R. 1997. Expression and inducibility of P450 enzymes during liver ontogeny. *Microsc. Res. Tech.* **39**: 424–435.
22. Saez, J. M. 1994. Leydig cells: endocrine, paracrine, and autocrine regulation. *Endocr. Rev.* **15**: 574–626.
23. Schenkman, J. B., Thummel, K. E. and Favreau, L. V. 1989. Physiological and pathophysiological alterations in rat hepatic cytochrome P-450. *Drug Metab. Rev.* **20**: 557–584.
24. Sharpe, R. M., Fisher, J. S., Millar, M. M., Jobling, S. and Sumpter, J. P. 1995. Gestational and lactational exposure of rats to xenoestrogens results in reduced testicular size and sperm production. *Environ. Health Perspect.* **103**: 1136–1143.
25. Shelby, M. K., Cherrington, N. J., Vansell, N. R. and Klaassen, C. D. 2003. Tissue mRNA expression of the rat UDP-glucuronosyltransferase gene family. *Drug Metab. Dispos.* **31**: 326–333.
26. Sjögren, K., Liu, J., Blad, K., Skrtic, S., Vidal, O., Wallenius, V., LeRoith, D., Törnell, J., Isaksson, O., Jansson, J.-O. and Ohisson, C. 1999. Liver-derived insulin-like growth factor I (IGF-I) is the principal source of IGF-I in blood but is not required for postnatal body growth in mice. *Proc. Natl. Acad. Sci. U.S.A.* **96**: 7088–7092.
27. Svensson, J., Kindblom, J., Shao, R., Movérare-Skrtic, S., Lagerquist, M. K., Andersson, N., Sjögren, K., Venken, K., Vanderschueren, D., Jansson, J. O., Isaksson, O. and Ohlsson, C. 2008. Liver-derived IFG1 enhances the androgenic response in prostate. *J. Endocrinol.* **199**: 489–497.
28. Ueki, I., Ooi, G. T., Tremblay, M. L., Hurst, K. R., Bach, L. A. and Boisclair, Y. R. 2000. Inactivation of the acid labile subunit gene in mice results in mild retardation of postnatal growth despite profound disruptions in the circulating insulin-like growth factor system. *Proc. Natl. Acad. Sci. U.S.A.* **97**: 6868–6873.
29. Warita, K., Sugawara, T., Yue, Z. P., Tsukahara, S., Mutoh, K., Hasegawa, Y., Kitagawa, H., Mori, C. and Hoshi, N. 2006. Progeression of the dose-related effects of estrogenic endocrine

disruptors, an important factor in declining fertility, differs between the hypothalamo-pituitary axis and reproductive organs of male mice. *J. Vet. Med. Sci.* **68**: 1257–1267.

30. Waxman, D. J., Dannan, G. A. and Guengerich, F. P. 1985. Regulation of rat hepatic cytochrome P450: age-dependent expression, hormonal imprinting, and xenobiotic inducibility of sex-specific isoenzymes. *Biochemistry* **24**: 4409–4417.
31. Woods, K. A., Camacho-Hübner, C., Savage M. O. and Clark, A. D. J. 1996. Intrauterine growth retardation and postnatal growth failure associated with deletion of the insulin-like growth factor I gene. *N. Engl. J. Med.* **33**: 1363–1367.
32. Wu, Y., Sun, H., Yakar, S. and LeRoith, D. 2009. Elevated levels of Insulin-like growth factor (IGF)-I in serum rescue the severe growth retardation of IGF-I null mice. *Endocrinology* **150**: 4395–4403.
33. Wyde, M. E., Bartolucci, E., Ueda, A., Zhang, H., Yan, B., Negishi, M and You, L. 2003. The environmental pollutant 1,1-dichloro-2,2-bis (p-chlorophenyl)ethylene induces rat hepatic cytochrome P450 2B and 3A expression through the constitutive androstane receptor and pregnane X receptor. *Mol. Pharmacol.* **64**: 474–481.
34. Wyde, M. E., Kirwan, S. E., Zhang, F., Laughter, A., Hoffman, H.B., Bartolucci-Page, E., Gaido, K. W., Yan B. and You, L. 2005. Di-n-butyl phthalate activates constitutive androstane receptor and pregnane X receptor and enhances the expression of steroid-metabolizing enzymes in the liver of rat fetuses. *Toxicol. Sci.* **86**: 281–290.
35. Yakar, S., Rosen, C. J., Beamer, W. G., Ackert-Bicknell, C. L., Wu, Y., Liu, J. L., Ooi, G. T., Setser, J., Frystyk, J., Boisclair, Y. R. and LeRoith, D. 2002. Circulating levels of IGF-I directly regulate bone growth and density. *J. Clin. Invest.* **110**: 771–781.
36. Yamamoto, M., Shirai, M., Sugita, K., Nagai, N., Miura, Y., Mogi, R., Yamamoto, K, Tamura, A. and Arishima, K. 2003. Effects of maternal exposure to diethylstilbestrol on the development of the reproductive system and thyroid function in male and female rat offspring. *J. Toxicol. Sci.* **28**: 385–394.
37. Yamamoto, M., Shirai, M., Tamura, A., Kobayashi, T., Kohara, S., Murakami, A. and Arishima, K. 2005. Effects of maternal exposure to a low dose of diethylstilbestrol on sexual dimorphic nucleus volume and male reproductive system in rat offspring. *J. Toxicol. Sci.* **30**: 7–18.
38. You, L. 2004. Steroid hormone biotransformation and xenobiotic induction of hepatic steroid metabolizing enzymes. *Chem. Biol. Interact.* **147**: 233–246.
39. You, L., Chan, S. K., Bruce, J. M., Archibeque-Engle, S., Casanova, M., Corton, J. C. and Heck, H. 1999. Modulation of testosterone-metabolizing hepatic cytochrome P-450 enzymes in developing Sprague-Dawley rats following in utero exposure to p,p' -DDE*Toxicol. Appl. Pharmacol.* **158**: 197–205.
40. de Zwart, L., Scholten, M., Monbaliu, J. G., Annaert, P. P., Van Houdt, J. M., Van den Wyngaert, I., De Schaepdrijver, L. M., Bailey, G. P., Coogan, T. P., Coussement, W. C. and Mannens, G. S. 2008. The ontogeny of drug metabolizing enzymes and transporters in the rat. *Reprod. Toxicol.* **26**: 220–230.

Biochimica et Biophysica Acta 1820 (2012) 76–83

Contents lists available at SciVerse ScienceDirect

Biochimica et Biophysica Acta

journal homepage: www.elsevier.com/locate/bbagen

Microphthalmia-associated transcription factor is required for mature myotube formation

Ryo Ooishi [a], Mitsuyuki Shirai [b], Masayuki Funaba [c,*], Masaru Murakami [a,**]

[a] Laboratory of Molecular Biology, Azabu University School of Veterinary Medicine, Sagamihara 252-5201, Japan
[b] Laboratory of Veterinary Pharmacology, Azabu University School of Veterinary Medicine, Sagamihara 252-5201, Japan
[c] Division of Applied Biosciences, Kyoto University Graduate School of Agriculture, Kyoto 606-8502, Japan

ARTICLE INFO

Article history:
Received 15 May 2011
Received in revised form 29 October 2011
Accepted 10 November 2011
Available online 20 November 2011

Keywords:
Mitf
Myogenesis
Integrin
p21
Myotube

ABSTRACT

Background: The roles of microphthalmia-associated transcription factor (Mitf) in the skeletal muscle and during myogenesis are unclear.
Methods: Expression of *Mitf* in mouse tissues and during myogenesis was evaluated. Effects of *Mitf* knockdown on myogenesis and gene expression related to myogenesis were subsequently explored. Furthermore, effects of *p21*, a cyclin-dependent kinase inhibitor, and *integrin α9* (*Itga9*) were examined.
Results: Mitf was highly expressed in the skeletal muscle; *Mitf-A* and *-J* were expressed. Mitf expression increased after differentiation stimulation in C2C12 myogenic cells. Down-regulation of *Mitf* expression by transfection of siRNA for common *Mitf* inhibited myotube formation, which was reproduced by *Mitf-A* knockdown. Morphometric analyses indicated that both multinucleated cell number and the proportion of myotubes with more than 6 nuclei were decreased in *Mitf*-knockdown cells, suggesting that Mitf is required for not only the formation of nascent myotubes but also their maturation. Searching for genes positively regulated by Mitf revealed *p21* and *Itga9*; decreasing *Mitf* expression inhibited up-regulation of *p21* expression after differentiation stimulation and blocked the induction of *Itga9* expression in response to differentiation. Knockdown of *p21* decreased the number of multinucleated cells, whereas *Itga9* knockdown did not affect the myotube number. Both *p21* knockdown and *Itga9* knockdown decreased the proportion of myotubes with more than 6 nuclei.
General significance: Mitf positively regulates skeletal muscle formation; Mitf is significantly expressed during myogenesis, and is required for efficient myotube formation through expression of p21 and Itga9.

1. Introduction

Skeletal muscle formation consists of a complex set of differentiation steps: commitment of mesenchymal stem cells to myoblast lineage cells, progression of differentiation with the expression of muscle-cell-specific proteins, and fusion of myoblasts into multinucleated myotubes. Mammalian myotube formation occurs in two phases [1,2]. In the first phase, differentiated myoblasts fuse together to form small myotubes; to accomplish this process, proliferating myoblasts exit cell cycle, and some myoblasts undergo apoptosis. In the second phase, additional myoblasts subsequently fuse with myotubes to form large myotubes. Although the roles of myogenic regulatory factors (MRFs), including Myf5, Myod, Myogenin and Mrf4, in myogenic differentiation are unquestionable [3–5], a number of factors, such as secreted proteins, membrane proteins and transcriptional regulators, are also involved in myogenesis [2].

Microphthalmia-associated transcription factor (Mitf) is a member of the basic helix–loop–helix leucine zipper (bHLH-LZ) family of transcription factors [6–8]. Expression levels of Mitf, evaluated by Western blotting and Northern blotting, vary among tissues; it is highly expressed in melanocytes, mast cells, osteoclasts, and the heart [9–11]. Thus, the roles of Mitf have been mainly examined in these cells [11–14], and Mitf activities in other tissues are largely unknown. Of the *Mitf* variants that are not the result of genetic mutation, nine *Mitf* isoforms have been identified in mice that differ in their transcriptional initiation site: *Mitf-A*, *-B*, *-C*, *-D*, *-E*, *-H*, *-J*, *-M* and *-mc*. The *Mitf* variants contain an isoform-specific first exon, while exons 2 to 9 of all *Mitf* isoforms examined to date are identical. *Mitf* isoforms are expressed in a cell type-specific manner, and their transcriptional activities are slightly but significantly different depending on the target gene [15–19]. In addition, two types of *Mitf* mRNAs with or without an 18-base insert (exon 6a) are generated by alternative use of the two acceptor sites located at the 5′ end of exon 6 in *Mitf-A*, *-H*, *-J*, *-M* and *-mc* [6,9,20,21]. In the present study, we show the relatively higher expression of *Mitf-A* in the skeletal muscle, and present the potential role of Mitf in the progression of myogenesis.

* Correspondence to: Tel.: +81 75 753 6055.
** Correspondence to: Tel.: +81 42 769 1624.
E-mail addresses: mfunaba@kais.kyoto-u.ac.jp (M. Funaba), murakami@azabu-u.ac.jp (M. Murakami).

0304-4165/$ – see front matter © 2011 Elsevier B.V. All rights reserved.
doi:10.1016/j.bbagen.2011.11.005

2. Materials and methods

2.1. Animals and cell culture

Nine C57BL/6 mice aged 7–8 wk were used to examine the tissue distribution of Mitf. The experiment was approved by Azabu University Animal Experiment Committee. C2C12 myoblasts were obtained from the American Type Culture Collection (Rockville, MD). Cells were cultured in growth medium, i.e., Dulbecco's modified Eagle's medium (DMEM) with heat-inactivated 10% fetal bovine serum (FBS), 100 U/ml penicillin and 100 μg/ml streptomycin, at 37 °C under a humidified 5% CO_2 atmosphere. To induce differentiation from myoblasts to myotubes, the medium was replaced at confluence (day 0) with differentiation medium consisting of DMEM with 2% horse serum supplementing the antibiotics. To isolate myotubes, cells on day 7 were trypsinized for a short time under a microscope until detachment of multinucleated cells (~2 min), followed by centrifugation to obtain a myotube-rich fraction.

2.2. RT-PCR, restriction fragment length polymorphism and quantitative RT-PCR

Total RNA isolation from tissues and cells, RT-PCR and restriction fragment length polymorphism (RFLP) were performed as described previously [21]. Quantitative RT-PCR (qRT-PCR) was carried out as described previously [22]. The used PCR primers in qRT-PCR are presented in Table 1. To compare tissue *Mitf* expression, the appropriate corrected gene was chosen using a mouse housekeeping gene primer set (TaKaRa, Otsu, Japan). The relative mRNA level was expressed as a ratio with *β-actin* to evaluate tissue distribution and *Gapdh* was used as a reference gene to examine regulatory expression in C2C12 cells.

2.3. Western blotting

To examine expression of Mitf in the skeletal muscle, thigh muscle and heart as a positive control were homogenized in RIPA buffer. After 30 min on ice, the debris was removed by centrifugation at 2500 ×*g* for 2 min at 4 °C. After centrifugation at 12,000 ×*g* for 5 min at 4 °C, the supernatant was recovered and the protein concentration was measured by the bicinchoninic acid method [23]. Fifty micrograms of the protein was loaded on 10% SDS-polyacrylamide gel. Western blotting was performed as described previously [24,25]. Expression of Mitf and myosin heavy chain (Myhc) was examined by use of mouse monoclonal antibodies against Mitf (X1405M; Exalpha Biologicals) and Myhc (MY-32; Sigma), respectively. There are two types of muscle fiber, i.e., fast-twitch and slow-twitch; fast-twitch muscle fibers express Myhc2a, Myhc2b and Myhc2x, whereas slow-twitch muscle fibers do Myhc1 [26]. According to the manufacturer's

Table 1
Oligonucleotide PCR primers for qRT-PCR.

	Oligonucleotide		GenBank accession number
	5′-primer	3′-primer	
Mitf			
Common *Mitf*	5′-GCCTTGCAAATGGCAAATAC-3′	5′-GCTGGACAGGAGTTGCTGAT-3′	
Mitf-A	5′-GAGGAGTTTCACGAAGAACC-3′	5′-GCTGGCGTAGCAAGATGCGTGA-3′	NM_001113198
Mitf-H	5′-GAGGAGTTTCACGAAGAACC-3′	5′-GCTGGCGTAGCAAGATGCGTGA-3′	NM_001178049
Mitf-J	5′-CCGTGTCTCTGGGCATCTGAAG-3′	5′-GCTGGCGTAGCAAGATGCGTGA-3′	AY632575
Mitf-M	5′-ATGCTGGAAATGCTAGAATACAG-3′	5′-CATACCTGGGCACTCACTCTC-3′	NM_008601
Myogenic regulatory factors			
Myf5	5′-GCCAGTTCTCCCCTTCTGAGTA-3′	5′-TGGTCCCCAAACTCATCCTCT-3′	NM_008656
Myod1	5′-GTGGCAGCGAGCACTA-3′	5′-GGGCCGCTGTAATCCATC-3′	NM_010866
Myogenin	5′-AGAAGCGCAGGCTCAAGAAA-3′	5′-ATCTCCACTTTAGGCAGCCG-3′	NM_031189
Mrf4	5′-GGGCCTCGTGATAACTGCT-3′	5′-AAGAAAGGCGCTGAAGACTG-3′	NM_008657
Myosin heavy chains			
Myhc2a	5′-AAAGCTCCAAGGACCCTCTT-3′	5′-AGCTCATGACTGCTGAACTCAC-3′	NM_001039545
Myhc2b	5′-CCGAGCAAGAGCTACTGGA-3′	5′-TGTTGATGAGGCTGGTGTTC-3′	NM_010855
Myhc2x	5′-TCGCTGGCTTTGAGATCTTT-3′	5′-CGAACATGTGGTGGTTGAAG-3′	NM_030679
Target candidates			
Adam12	5′-CAGAGCATCCCAGCCAAG-3′	5′-CAGGCTGAGGATCAGGTCTC-3′	NM_007400
Calpastatin	5′-CCTTCAGCTGGTGGAGAGAG-3′	5′-GCTGGTGTGAATGGTTTCTG-3′	NM_009817
Caveolin3	5′-CACAAGGCTCTGATCGCCTC-3′	5′-TCCGTGTGCTCTTCGGTCA-3′	NM_007617
Ccna2	5′-CTTGGCTGCACCAACAGTAA-3′	5′-CAAACTCAGTTCTCCCAAAAACA-3′	NM_009828
Cdh15	5′-TGACATTGCCAACTTCATCAG-3′	5′-GATGAGAGCTGTGTCGTAGGGAG-3′	NM_007662
Ctsb	5′-AAGCTGTGTGGCACTGTCCTG-3′	5′-GATCTATGTCCTCACCGAACGC-3′	NM_007798
Itga3	5′-CATCAACATGGAGAACAAGACC-3′	5′-CCAACCACAGCTCAATCTCA-3′	NM_013565
Itga4	5′-ACCAGACCTGCGAACAGC-3′	5′-CCCCCAGCCACTGGTTAT-3′	NM_010576
Itga5	5′-TACTCTGTGGCTGTGGGTGA-3′	5′-GCCATTAAGGACGGTGACAT-3′	NM_010577
Itga6	5′-GGTTGAGAGGCCATGAAAAG-3′	5′-TTCTTTTGTTCTACACGGACGA-3′	NM_008397
Itga9	5′-TGATGCCAACGTGTCCTTTA-3′	5′-GAAATGCCCATCTCCTCCT-3′	NM_133721
Itgb1	5′-ATGCAGGTTGCGGTTTGT-3′	5′-CATCCGTGGAAAACACCAG-3′	NM_010578
Myof	5′-CATTACTGGCTTCTAAGCTGTCG-3′	5′-AAATTTACTCCACCAGTCAACG-3′	NM_001099634
p21	5′-TGGGCCCGGAACATCTC-3′	5′-TGCGCTTGGAGTGATAGAAA-3′	NM_007669
p57	5′-CAGGACGAGAATCAAGAGCA-3′	5′-TGCGCTTGGCGAAGAAGT-3′	NM_009876
Ptger4	5′-TCCAGATGGTCATCTTACTCAT-3′	5′-TAACTGGTTAATGAACACTCGCA-3′	NM_001136079
Rb1	5′-GCTGCAAATACAGAGACACAAGCAG-3′	5′-CGGAGATATGCTAGACGGTACACTT-3′	NM_009029
v-Cam1	5′-TGATTGGGAGAGACAAAGCA-3′	5′-AACAACCGAATCCCCAACT-3′	NM_011693
Vcl	5′-GATAGCTGCTCTGACCTCTAA-3′	5′-TAGTGCCGTCGCCACTTGTTT-3′	NM_009502
Reference genes			
β-actin	5′-CTAAGGCCAACCGTGAAAAG-3′	5′-ACCAGAGGCATACAGGGACA-3′	X03672
Gapdh	5′-CGTGTTCCTACCCCCAATGT-3′	5′-TGTCATCATACTTGGCAGGTTTCT-3′	NM_008084

manual, this antibody for Myhc recognizes fast-type muscle fibers. After incubation of the membranes with ECL Advance reagent (GE Healthcare), the chemiluminescent signals were exposed to X-ray film. Subsequently, antibodies as well as the detection reagents were stripped and reprobed with anti-α-tubulin (ab11304; Abcam) or anti-β-actin antibody (AC-15; Abcam).

2.4. Immunohistochemistry

C2C12 cells were grown on glass chamber slides coated with type I collagen (Thermo Fisher Scientific) and were fixed with 3% paraformaldehyde in PBS for 30 min, followed by treatment with 1% Triton X-100 in PBS for 10 min. After washing with PBS, cells were incubated with 3% H_2O_2 to remove endogenous peroxidase. Subsequently, cells were treated with 1.5% normal goat serum in PBS for 20 min to block nonspecific reactions. Diluted mouse monoclonal antibody against Mitf (X1405M; Exalpha Biologicals) with 0.1% bovine serum albumin in PBS at 1:80 was used to identify Mitf expression at the protein level. After incubation with the primary antibody for 2 h at room temperature, Mitf-positive cells were visualized using VECTASTAIN Elite ABC kit (Vector Laboratories) and 3,3′-diaminobenzidine (DAB; Dojindo) according to the manufacturer's protocol.

2.5. siRNA transfection

To target the expression of common *Mitf*, *Mitf-A* or *Itga9* and *green fluorescent protein* (*GFP*) controls, oligonucleotides for the respective genes were synthesized by BONAC corporation (Kurume, Japan) as follows: 5′-GAAACUUGAUCGACCUCUACA-3′ and 5′-UAGAGGUCGAUCAAGUUUCCA-3′ for common *Mitf*, 5′-GGAGUCAUGCAGUCCGAAUTT-3′ and 5′-AUUCGGACUGCAUGACUCCTT-3′ for *Mitf-A*, 5′-CCUUAGUGCUCUUCCGAAAGA-3′ and 5′-UUUCGGAAGAGCACUAAGGUU-3′ for *Itga9*, and 5′-GGUUACGUCCAGGAGCGCATT-3′ and 5′-UGCGCUCCUGGACGUAGCCTT-3′ for *GFP*. The siRNA for *p21* was purchased (sc-29428; Santa Cruz Biotechnology). An equal amount of the oligonucleotide was mixed for each gene to prepare siRNA. Thirty picomoles of siRNA was transfected into C2C12 cells seeded at a density of 1.5×10^4 cells in 24-well plates every 48 h. siRNA was transfected using Lipofectamine RNAiMAX (Invitrogen) according to the manufacturer's protocol. Antibiotics were not supplemented to the culture media in siRNA transfection experiments.

2.6. Morphological analysis

Cells were fixed with methanol for 2 min and subsequently stained with Giemsa staining for 20 min. Cells with more than 3 nuclei were judged as myotubes. Eight views per treatment in an experiment were analyzed. Experiments were repeated two or three times, and similar results were obtained.

2.7. BrdU incorporation

Proliferation of C2C12 cells was measured by a BrdU cell proliferation assay (Cell Proliferation ELISA, BrdU (colorimetric); Roche) according to the manufacturer's protocol.

2.8. Statistical analysis

Data are presented as the mean ± SE. Comparisons between groups were conducted using Student's *t*-test. Results were considered significant at $P<0.05$.

3. Results

3.1. Expression of Mitf in tissues and during myogenesis

Tissue distribution of *Mitf* was quantified by qRT-PCR. First, the expressions of 12 genes, *Atp5f1*, *B2m*, *β-actin*, *Gapdh*, *Hprt1*, *Pgk1*, *Ppia*, *RpLp1*, *Rps18*, *Tbp*, *Tfrc*, and *Ywhaz*, were quantified for evaluation as appropriate corrected genes; quantitative PCR using cDNA prepared from equal amounts of total RNA revealed that *β-actin* expression was the most stable among the tested tissues, which were evaluated by "geNorm" (http://medgen.ugent.be/~jvdesomp/genorm/) (data not shown). Thus, the gene transcript level of *Mitf* was corrected for that of *β-actin* (Fig. 1A). Expression of *Mitf* was highest in the heart, as expected. Although Mitf is recognized as a tissue-restricted transcription factor [6–8], its expression was detected in a wide variety of tissues. In particular, expression in the skeletal muscle was relatively higher. Previous studies indicated *Mitf* expression in the skeletal muscle [9,27], but the role of Mitf is not known. Thus, we characterized the expression and function of Mitf in the skeletal muscle and during myogenesis in detail. Examining Mitf isoforms differing in transcriptional initiation site in the skeletal muscle indicated that more than 99% of *Mitf* was *Mitf-A*, and that *Mitf-H* and *-J* were also expressed significantly (Fig. 1B).

In a C2C12 myotube differentiation model, C2C12 myoblasts fuse to form multinucleated myotube cells upon serum starvation on day 0 [28]. To evaluate gene expression in C2C12 cells, we chose *Gapdh* instead of *β-actin* as a reference gene; qPCR using cDNA prepared from equal amount of total RNA indicated gradual decrease in *β-actin* expression with progression of myogenesis, whereas expression of *Gapdh* was relatively constant (Supplementary Fig. 1). Total *Mitf* expression level increased up to day 8 and then reached a plateau (Fig. 1C). Similar to the expression pattern in the skeletal muscle, *Mitf-A* was the main isoform (59–76% of total *Mitf*). In addition, *Mitf-J* but not *-H* was expressed. The expression pattern of *Mitf* isoform was constant during myogenesis; the ratio of *Mitf-A* to *Mitf-J* was 1.5 to 3.2:1. Expression of Mitf in the skeletal muscle and C2C12 cells was also verified at the protein level by Western blot analyses (Fig. 1D). In addition, consistent with the changes at the mRNA level, expression of Mitf protein was increased after differentiation stimulation (Fig. 1E). Furthermore, Mitf was exclusively localized in the nucleus of C2C12 cells (Fig. 1F). We also examined the ratio of gene transcripts of Mitf with exon 6a to that of Mitf without exon 6a by PCR-RFLP analyses; the ratios of *Mitf-A* and *Mitf-J* were relatively constant during myogenesis (Fig. 1G).

3.2. Disruption of Mitf expression inhibits myotube formation by blocking increased expression of p21 and Itga9 induction

To clarify the roles of Mitf in myogenesis, we evaluated effects of decreased expression of Mitf, which was achieved by transfection with siRNA for *Mitf* (Supplementary Fig. 2A, lanes 2 and 3, and B). Transfection of siRNA for common *Mitf* effectively decreased the emergence of multinucleated myotubes on day 6, as compared with *GFP* (Fig. 2A). Knockdown of *Mitf-A* also blocked the formation of thick myotubes (Fig. 2B, Supplementary Fig. 2C). Morphological analyses on day 6 indicated that the number of multinucleated cells, which were defined as cells with more than 3 nuclei, was significantly decreased by transfection of siRNA for *Mitf* (Fig. 2C). We also evaluated the differentiated myotubes in detail; knockdown of *Mitf* increased the proportion of myotubes with 3 to 5 nuclei, but decreased that of myotubes with more than 6 nuclei (Fig. 2D). Similar results were also obtained in C2C12 cells transfected with siRNA for *Mitf-A* (Supplementary Fig. 3). Furthermore, *Mitf* knockdown decreased the expression of Myhc, a myotube-specific protein [3–5], in C2C12 cells on day 8 (Fig. 2E, lanes 1 and 2). These results suggest that Mitf is required not only for myoblast–myoblast fusion but also for

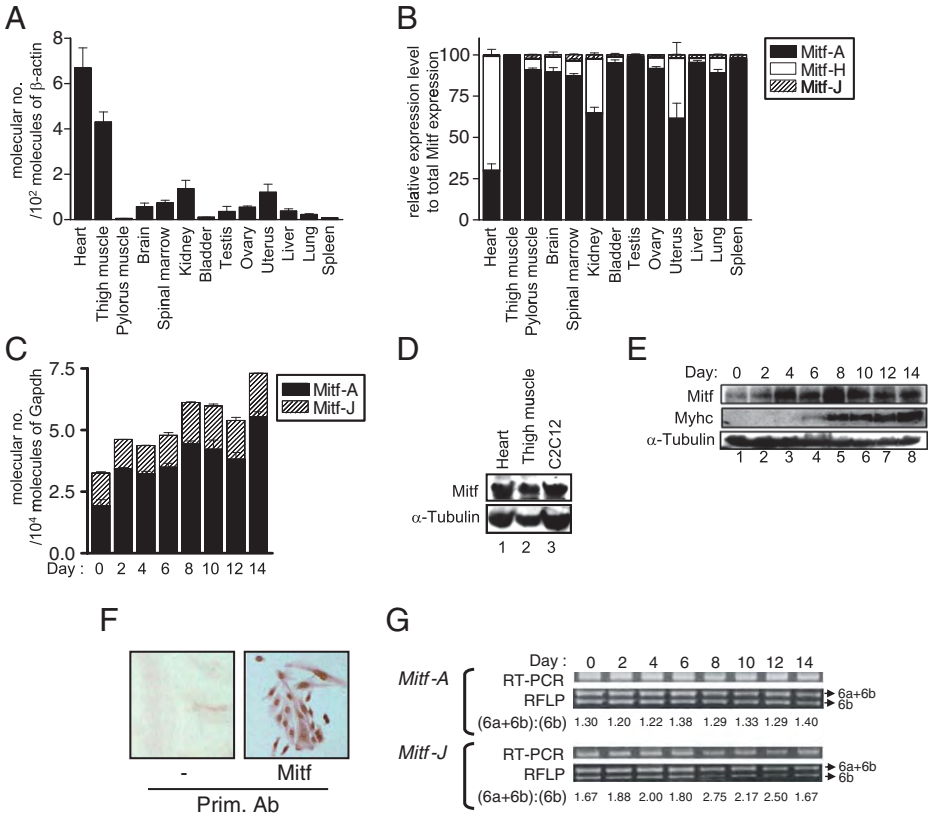

Fig. 1. Mitf expression is highly expressed in the skeletal muscle and increases with progression of myogenesis in C2C12 cells. (A) *Mitf* expression in various tissues was measured by qRT-PCR. *Mitf* expression was expressed as a ratio to *β-actin* expression. Data are shown as the mean ± SE. (B) Expression of *Mitf* isoform differing with transcriptional initiation site in the skeletal muscle was identified by qRT-PCR using isoform-specific 5′-primer and 3′-primer spanning the common *Mitf*. The percentage of the expression of each *Mitf* isoform to that of total *Mitf* was calculated. Data are shown as the mean ± SE. (C) C2C12 myoblasts were cultured to confluence (day 0) in growth medium, followed by culture in differentiation medium. Time-course changes in expression of *Mitf* isoform differing with transcriptional initiation site during myogenesis were examined in C2C12 cells. *Mitf* expression was expressed as a ratio to *Gapdh* expression. Data are shown as the mean ± SE (n = 2). (D) Expression of Mitf in the skeletal muscle. Protein extracted from heart, thigh muscle and C2C12 cells was subjected to Western blot analyses to examine Mitf expression at the protein level. A representative result of Western blot is shown. In the heart, Mitf-H as well as Mitf-A is mainly expressed shown in (B). Note that calculated molecular weight of Mitf-H and Mitf-A is 56.8 k and 58.6 k, respectively. (E) Time-course changes in expression of Mitf protein were examined during myogenesis of C2C12 cells. A representative result of Western blot is shown. (F) Immunolocalization of Mitf in C2C12 cells. C2C12 myoblasts were fixed and reacted with (*right*) or without (*left*) mouse monoclonal anti-Mitf antibody. Subsequently, cells were reacted with anti-mouse IgG antibody, and the antibody was visualized. A representative cell staining is shown. (G) The ratio of exon 6a-containing *Mitf* isoforms (exon 6a + 6b) to non-exon 6a-containing isoforms (exon 6b) was evaluated in C2C12 cells. PCR products of *Mitf-A* and *-J* were digested by *Hinf* I, and DNA fragments with or without exon 6a were separated by PAGE. A photograph of a representative gel stained with ethidium bromide is shown.

maturation of nascent myotubes. We also examined effects of forced Mitf expression on myotube formation; the expression did not enhance myogenesis (data not shown).

Molecular bases of decreased myotube formation by *Mitf* knockdown were then explored. Myogenesis is regulated through modulation of the expression and activity of MRFs [29,30]; however, gene transcript levels of *Myf5*, *Myod*, *Myogenin* and *Mrf4* were unchanged by *Mitf* knockdown, suggesting that impairment of myogenesis resulting from *Mitf* knockdown is not due to altered expression of MRFs (Fig. 3A–D).

Other than MRFs, several molecules related to cell attachment and fusion, such as *Adam12*, *Calpastatin*, *Caveolin3*, *Cdh15*, *Ctsb*, *Itga3*, *Itga4*, *Itga6*, *Itga9*, *Itgb1*, *Myof*, and *v-Cam1* are known to regulate myotube differentiation [2,31–34]. In addition, the cDNA microarray database (http://www.ncbi.nlm.nih.gov/geo/) indicated that the expressions of *Ccna2*, *Itga5*, *p21*, *p57*, *Ptger4*, *Rb1*, and *Vcl* increased with differentiation. In view of Mitf as a transcription factor, we expected that Mitf is involved in myogenesis through transcriptional activation of these myogenesis-regulating genes. Thus, the effects of decrease in *Mitf* expression on the expression level of these genes were explored. We found that gene transcript levels of *p21* and *Itga9* after differentiation stimulation were decreased by transfection of siRNA for common *Mitf*; expression of *p21* was increased in response to differentiation stimulation, and *Mitf* knockdown blocked the increased expression of *p21* (Fig. 3E). Significant expression of *Itga9* was detected after day 4, and the expression level was decreased by transfection of siRNA for *Mitf* (Fig. 3F). Decreased expression of *p21* and *Itga9* was also detected in *Mitf-A*-knockdown cells (Supplementary Fig. 4). Gene transcript levels of the other genes were unaffected by *Mitf* knockdown (Supplementary Fig. 5).

In a C2C12 myogenesis cell model, not all myoblasts not fuse into myotubes; co-existence of proliferating myoblasts and myotubes is detected after differentiation stimulation [35–37]. We separated the myotube-rich fraction by limited trypsinization to explore cells affected by *Mitf* knockdown. Although *Myhc2a* expression was not significantly different between the myotube fraction and the residual cell fraction in control cells (Fig. 4A), *Myhc2b* and *Myhc2x* were predominantly expressed in the myotube fraction as expected (Fig. 4B and C). Expression of *Myhc2x* in the myotube fraction was significantly lower in *Mitf*-knockdown cells than in control cells, whereas that of *Myhc2a* in the myotube fraction was higher in the *Mitf*-knockdown cells. The *Myhc2b* expression in the myotube fraction was comparable between in control cells and in *Mitf*-knockdown cells. Considering that *Myhc2x* was the major isoform of type 2 *Myhc* (>93%) (Fig. 4D), total expression of *Myhc* constituting of fast-twitch myofibers was largely limited to the myotube fraction, and was decreased by *Mitf* knockdown; the latter was consistent with the results on Myhc expression at the protein level (Fig. 2E).

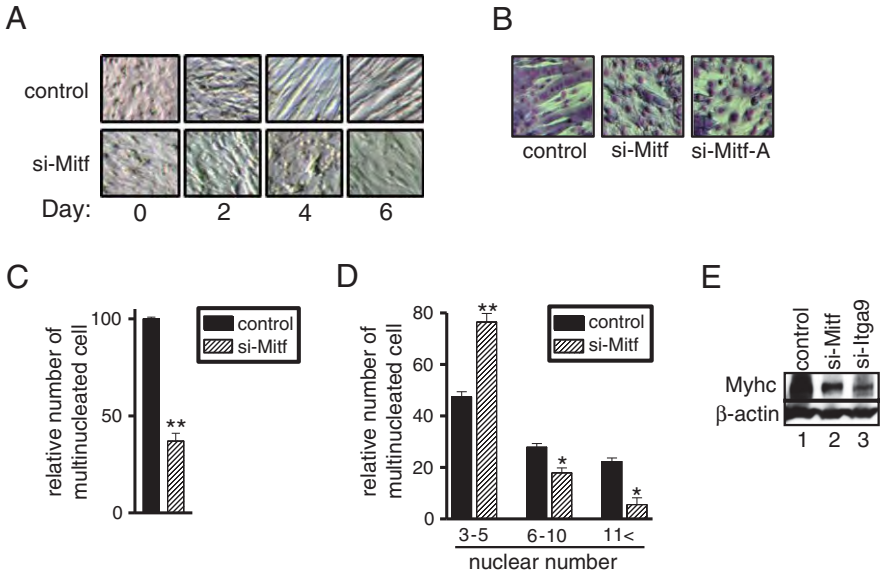

Fig. 2. Mitf expression is required for efficient myotube formation. C2C12 cells were transfected with siRNA for *GFP* as a control, common *Mitf* or *Mitf-A* every 2 days after day −2. (A) Effect of *Mitf* knockdown on myogenesis was evaluated. Representative phase-contrast images on days 0, 2, 4, and 6 are presented. (B) Role of Mitf-A was examined. Representative cells stained by Giemsa solution on day 6 are presented. (C and D) Myotube formation was evaluated in *Mitf*-knockdown C2C12 cells. Cells were transfected with siRNA for *GFP* as a control or *Mitf*, and morphology was evaluated on day 6. After staining with Giemsa solution, cell number and the number of nuclei were calculated. (C) Ratio of multinucleated cell number to total cell number was calculated, and the ratio of cells transfected with siRNA for *GFP* was set to 1. (D) Number of cells with 3 to 5, 6 to 10 or >11 nuclei was counted, and percentage to total multinucleated cells is shown. Data are shown as the mean ± SE (n = 6). * and **: $P<0.05$ and $P<0.01$, respectively, as compared to control. (E) Expression of Myhc in response to transfection of siRNA for *GFP* as a control, *Mitf* or *Itga9* in C2C12 cells on day 8 was examined by Western blot analyses. Subsequently, the membranes were reprobed with anti-β-actin antibody.

The extent of the decreased expression of *Mitf* resulting from knockdown of *Mitf* was comparable between the myotube fraction and the residual cell fraction, indicating effective inhibition of *Mitf* expression in both myoblasts and myotubes (Fig. 5A). Expression of *p21* was significantly higher in the myotube fraction than in the residual cell fraction (Fig. 5B). Knockdown of *Mitf* equally decreased the expression of between the two fractions. Expression of *Itga9* was also significantly higher in the myotube fraction (Fig. 5C). Similar to the expression of *p21*, *Mitf* knockdown down-regulated the expression of *Itga9* in both fractions.

Cell cycle exit in response to differentiation stimulation is a prerequisite for myotube formation [2]; p21, a cyclin-dependent kinase inhibitor inducing cell cycle exit, plays a role in post-mitotic myogenesis, although it also maintains anti-apoptotic states in differentiated myocytes [1]. To link the decreased *Mitf*-induced inhibition of myotube formation and blockage of *p21* induction, effects of the decreased *Mitf* expression on BrdU uptake were next examined; BrdU uptake was significantly increased by transfection of siRNA for *Mitf* on days 4–6 (Fig. 6A). Knockdown of *p21*, however, did not affect BrdU uptake (Fig. 6B). Similar to *Mitf* knockdown, decreased expression of p21

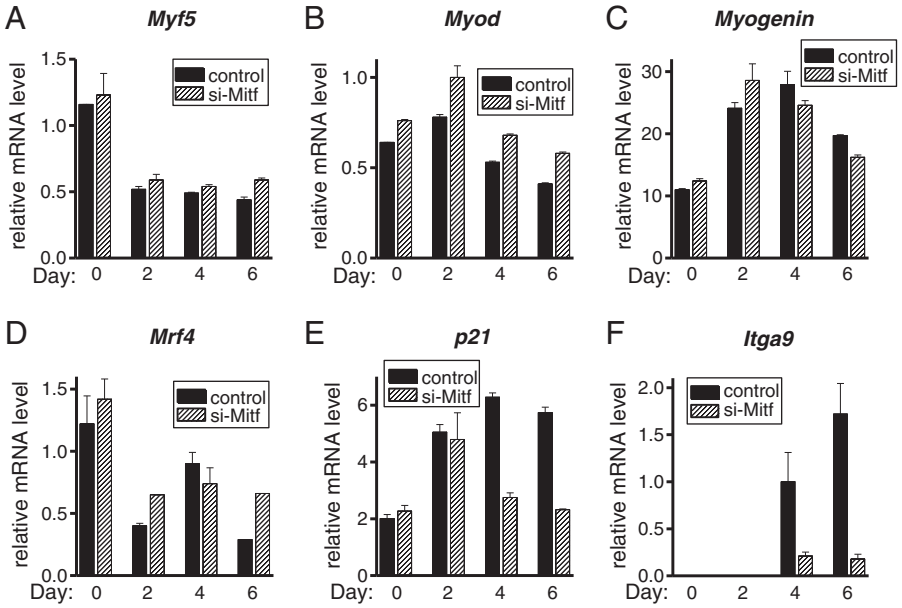

Fig. 3. p21 and Itga9 are targets of Mitf for progression of myogenesis. C2C12 cells were transfected with siRNA for *GFP* as a control or common *Mitf* every 2 days after day −2. Gene expression of *Myf5* (A), *Myod* (B), *Myogenin* (C), *Mrf4* (D), *p21* (E) and *Itga9* (F) was quantified by qRT-PCR. The expression was normalized to *Gapdh* expression. The expression in cells on day −2 was set to 1 for *Myf5*, *Myod*, *Myogenin*, *Mrf4* and *p21*, and that in cells transfected with siRNA for *GFP* on day 4 was set to 1 for *Itga9*. Data are shown as the mean ± SE (n = 2).

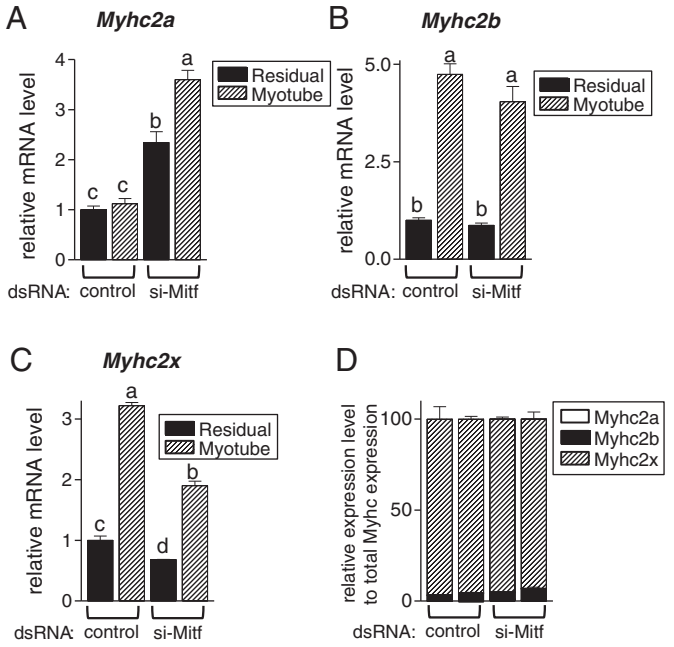

Fig. 4. Knockdown of Mitf in myoblasts and myotubes down-regulates expression of Myhc2x. C2C12 cells were transfected with siRNA for *GFP* as a control or common *Mitf* every 2 days after day −2. On day 7, multinucleated myotubes were separated from the residual cells by limited trypsinization. Expression of *Myhc2a* (A), *Myhc2b* (B) and *Myhc2x* (C) was quantified by qRT-PCR, and normalized to *Gapdh* expression. The expression in residual cells after limited trypsinization in the control group was set to 1. (D) The percentage of the expression of each *Myhc* isoform to that of total type II *Myhc* was calculated. Data are shown as the mean ± SE (n = 3). a, b, c, d: Means that do not have a common letter on the bar differ significantly ($P<0.05$).

inhibited emergence of maturated and thick myotubes (Fig. 6C). In addition, it significantly decreased the number of multinucleated cells (Fig. 6D), and increased and decreased the proportion of myotubes with 3 to 5 nuclei and those with more than 6 nuclei, respectively (Fig. 6E).

We next explored the effects of Itga9 knockdown on myotube formation. The morphology of cells transfected with siRNA for *Itga9* indicated that, compared to control cells, thinner myotubes were evident by *Itga9* knockdown, suggesting that Itga9 is required for myotube maturation (Fig. 7A), which was verified by morphometry. The multinucleated cell number itself was not affected by knockdown of *Itga9* (Fig. 7B), but the proportion of the number of myotubes with 3–5 nuclei in a cell to that of total myotubes was significantly increased, and that with more than 6 nuclei was decreased (Fig. 7C). Consistent with the results, knockdown of *Itga9* gene resulted in the decreased expression of Myhc (Fig. 2E, lanes 1 and 3).

4. Discussion

Here, we demonstrate that 1) an isoform of *Mitf* mRNA is abundant in the skeletal muscle, 2) *Mitf-A* expression increased with progression of myogenesis, 3) knockdown of *Mitf* mRNA disrupts myotube formation through inhibition of myoblast–myoblast fusion and subsequent myoblast–myotube fusion, but does not affect the expression of MRFs, and 4) expression of *p21*, a cyclin-dependent kinase inhibitor, and *Itga9* is regulated by Mitf in a stage-dependent manner for appropriate myogenesis. The present results indicate a novel role of a tissue-restricted transcription factor Mitf in the regulation of myogenesis, which is probably mediated by an MRF-independent pathway.

Mitf regulates myogenesis in multiple steps. Expression of *p21* and *Itga9* was modulated by decreased expression of *Mitf*; down-regulation of *p21* expression resulting from knockdown of *Mitf* mRNA was limited to post-differentiation, and significant *Itga9* expression was detected just after differentiation stimulation. Considering that significant expression of *Mitf* was detected prior to differentiation stimulation, the gene expression of *p21* and *Itga9* could not be regulated by Mitf alone, but in concert with Mitf and as yet unidentified factor(s). Transfection of siRNA for *Mitf* resulted in down-regulated expression of *Mitf* both in myoblasts and myotubes. Thus, the precise mechanism of how Mitf regulates not only *p21* in myoblasts and myotubes but also *Itga9* expression in myotubes remains unclear. Since Mitf binds to the E-box (CAnnTG) located in the 5′-untranslated region and activates transcription [6–8], Mitf may directly regulate transcription of *p21* and *Itga9*. Alternatively, it is possible that a factor regulated by Mitf in myoblasts acts as a regulator to induce *p21* or *Itga9* in myotubes.

A target gene of Mitf was *Itga9*. Among members of the integrin family, Itga3, 4, 6 and 9 have been suggested to regulate myogenesis [2,31,33,34]. Transcription of *Itga4* was activated through Mitf binding to the E-box located in the 5′-untranslated region in mast cells [38]. In the present study, however, *Itga4* mRNA was not decreased but rather increased by transfection of siRNA for *Mitf* in C2C12 cells (Supplementary Fig. 5H), suggesting that transcription by Mitf is regulated in a cell context-dependent manner. In addition, *Mitf* knockdown did not affect the expression level of *Itga3* and *6* (Supplementary Fig. 5G and J). In a study using a human mononucleated myogenic precursor cell culture system, addition of anti-INTEGRIN α9β1 antibody to the culture medium decreased the proportion of nuclei included in large myotubes (≥5 nuclei), whereas the proportion of nuclei incorporated in small myotubes (2–4 nuclei) was unchanged [33]. In the present study using a murine myogenesis model, transfection with siRNA for *Itga9* decreased the proportion of large myotubes (≥6 nuclei) and increased that of small myotubes (3–5 nuclei), but did not affect the number of multinucleated cells. Taking these results together, Itga9 is suggested to promote the

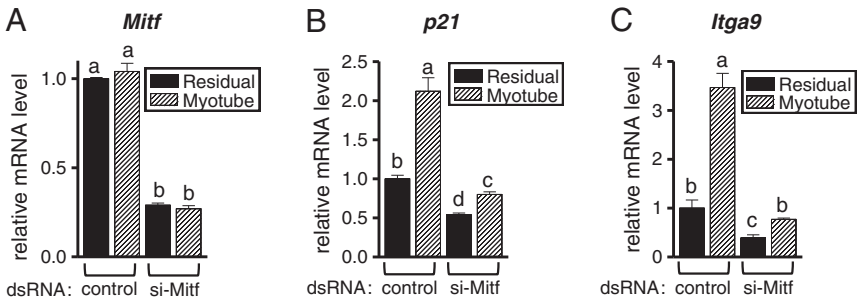

Fig. 5. Knockdown of Mitf in myoblasts and myotubes down-regulates expression of p21 and Itga9. C2C12 cells were transfected with siRNA for *GFP* as a control or common *Mitf* every 2 days after day −2. On day 7, multinucleated myotubes were separated from the residual cells by limited trypsinization. Expression of *Mitf* (A), *p21* (B), and *Itga9* (C) was quantified by qRT-PCR, and normalized to *Gapdh* expression. The expression in residual cells after limited trypsinization in the control group was set to 1. Data are shown as the mean ± SE (n = 3). a, b, c, d: Means that do not have a common letter on the bar differ significantly ($P<0.05$).

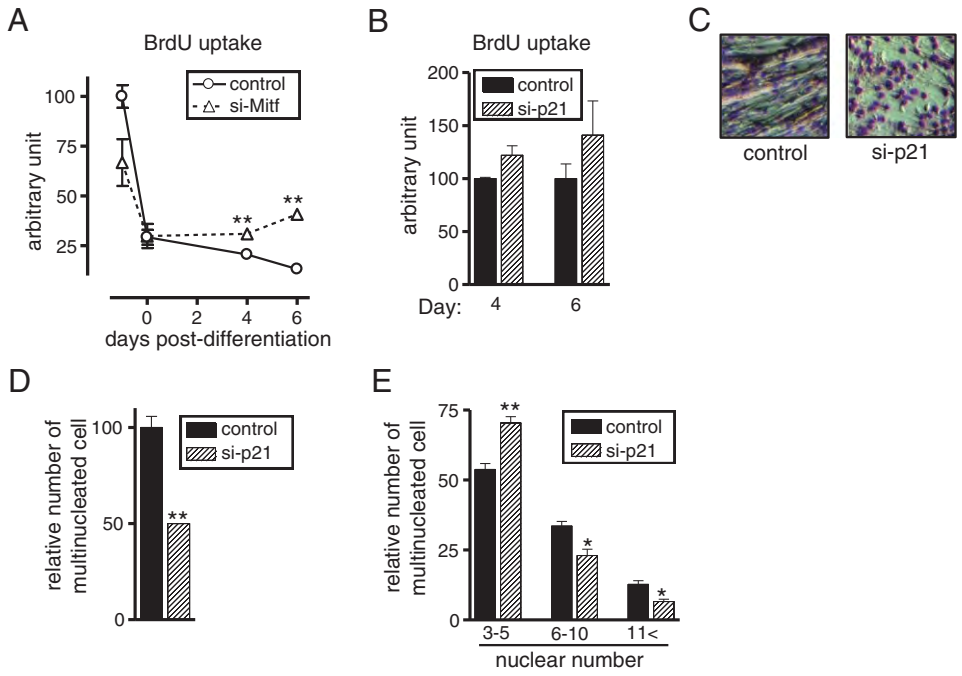

Fig. 6. p21 is involved in Mitf-mediated myogenesis. (A and B) Role of Mitf and p21 in BrdU uptake in C2C12 cells was evaluated. (A) Cells were transfected with siRNA for *GFP* as a control or common *Mitf* every 2 days after day −2, and BrdU uptake was examined on day −1, 0, 4 and 6. BrdU uptake in control cells on day −1 was set to 100. (B) Cells were transfected with siRNA for *GFP* or *p21* every 2 days after day 2, and BrdU uptake was examined on days 4 and 6. Data are shown as the mean ± SE (n = 3–4). **: $P<0.01$, as compared to control. (C–E) Role of p21 in myogenesis was evaluated. Cells were transfected with siRNA for *GFP* or *p21* every 2 days after day 2. (C) Representative cells stained by Giemsa solution on day 6 are shown. (D and E) Myotube formation was evaluated in *p21*-knockdown C2C12 cells. After staining cells with Giemsa solution on day 6, cell number and the number of nuclei were calculated. (D) Ratio of multinucleated cell number to total cell number was calculated, and the ratio of cells transfected with siRNA for *GFP* was set to 1. (E) Number of cells with 3 to 5, 6 to 10 or >11 nuclei was counted, and percentage to total multinucleated cells is shown. Data are shown as the mean ± SE (n = 4). * and **: $P<0.05$ and $P<0.01$, respectively, as compared to control.

growth of preformed myotubes rather than the formation of nascent myotubes during myogenesis.

Effects of knockdown of *Mitf* mRNA partly overlapped but were distinct from those of *Itga9* knockdown; the number of multinucleated cells was decreased by *Mitf* knockdown. This suggests that Mitf is involved in both myoblast–myoblast fusion and subsequent maturation of nascent myotubes. It is possible that Mitf regulates myoblast–myoblast fusion through the increase in p21 expression; regulatory expression of *p21* by Mitf has also been shown in melanocytes [39]. Cell cycle inhibition and apoptosis of myoblasts precede to myoblast–myoblast fusion, and both processes are necessary for the cell fusion [1]. p21 is principally involved as a molecule to establish post-mitotic and apoptosis-resistant states [1]; BrdU uptake was not detected in p21-positive myoblasts [40], and forced expression of p21 but not inactive p21 inhibited apoptosis of C2C12 myoblasts [41]. In fact, *p21* knockdown decreased the myotube number and increased proportion of small myotubes, suggesting that p21 expression is required for efficient myoblast–myoblast fusion.

Knockdown of *p21* did not increase BrdU uptake on days 4 and 6; it may be offset effects of the cell growth inhibition and the anti-apoptotic activity. In view of significant inhibition of BrdU uptake in *Mitf*-knockdown cells on days 4 and 6, Mitf regulates expression and activity of additional molecule(s) unidentified in this study.

Bharti et al. [19] revealed that *Mitf-A* and *-J* are expressed throughout eye development in both retina and pigment epithelium, whereas expression of *Mitf-D* and *-M* was limited to pigment epithelium. In addition, *Mitf-H* was preferentially found in pigment epithelium with temporal expression profile. Unlike the eye development, the proportion of expressed *Mitf* isoforms, i.e., *Mitf-A* and *Mitf-J* was almost constant during myogenesis of C2C12 cells, although total *Mitf*

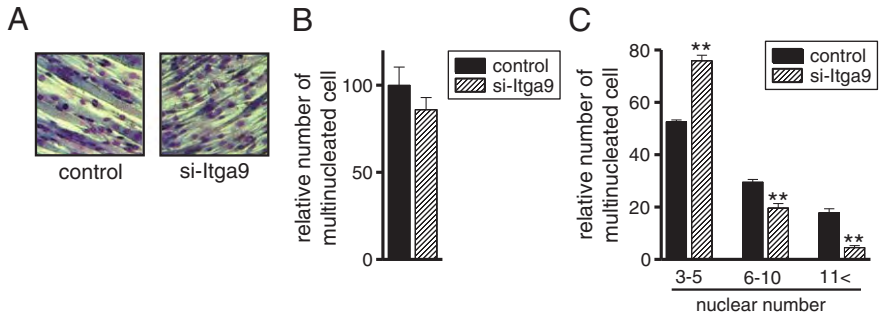

Fig. 7. Itga9 are involved in Mitf-mediated myogenesis. (A–C) Role of Itga9 in myogenesis was evaluated. Cells were transfected with siRNA for *GFP* or *Itga9* every 2 days after day −2. (A) Representative cells stained by Giemsa solution on day 6 are shown. (B and C) Myotube formation was evaluated in *Itga9*-knockdown C2C12 cells. After staining cells with Giemsa solution on day 6, cell number and the number of nuclei were calculated. (B) Ratio of multinucleated cell number to total cell number was calculated, and the ratio of cells transfected with siRNA for *GFP* was set to 1. (C) Number of cells with 3 to 5, 6 to 10 or >11 nuclei was counted, and percentage to total multinucleated cells is shown. Data are shown as the mean ± SE (n = 4). **: $P<0.01$, as compared to control.

expression was increased with progression of myogenesis (Fig. 1C). Thus, expression of *Mitf* isoforms is tissue-specific and stage-dependent. In view of different activity as transcription factors between the isoforms [15–18], regulation on the use of alternative promoter must be clarified in future studies.

Mitf encoded by the mutant *mi* allele deletes one of four consecutive arginines in the basic domain, and acts as a dominant-negative mutant [9,27,42]. The *mi*/*mi* mutant mice exhibited the pleiotropic effects of microphthalmia, depletion of pigment in both hair and eyes, and osteopetrosis resulting from defects of osteoclastogenesis [9,14]. In addition to these phenotype alterations, Katayama et al. [43] recently showed that masseter muscle development was disrupted in *mi*/*mi* mutant mice; they speculated that the disorder is a secondary event related to abnormal tooth formation related to osteoclast dysfunction; however, in view of the present results showing direct inhibition of myogenesis by decreased expression of *Mitf*, muscle development itself may be disturbed in *mi*/*mi* mice.

The present study indicates significant expression of *Mitf* in the skeletal muscle from re-evaluation of tissue distribution of *Mitf* by sensitive qRT-PCR analyses. Evaluation of Mitf activity clarifies its role as a positive regulator during myogenesis. Because Mitf is expressed also in other tissues with a variation of expression level, future studies should be directed to elucidate the role of Mitf in as yet uncharacterized tissues.

Supplementary materials related to this article can be found online at doi:10.1016/j.bbagen.2011.11.005.

Acknowledgements

This work was supported by Kakenhi from the Japan Society for the Promotion of Science, and a research project grant awarded by the Azabu University.

References

[1] K. Walsh, H. Perlman, Cell cycle exit upon myogenic differentiation, Curr. Opin. Genet. Dev. 7 (1997) 597–602.
[2] V. Horsley, G.K. Pavlath, Forming a multinucleated cell: molecules that regulate myoblast fusion, Cells Tissues Organs 176 (2004) 67–78.
[3] D.C. Ludolph, S.F. Konieczny, Transcription factor families: muscling in on the myogenic program, FASEB J. 9 (1995) 1595–1604.
[4] R.L. Perry, M.A. Rudnicki, Molecular mechanisms regulating myogenic determination and differentiation, Front. Biosci. 5 (2000) D750–D767.
[5] F. Lluís, E. Perdiguero, A.R. Nebreda, P. Muñoz-Cánoves, Regulation of skeletal muscle gene expression by p38 MAP kinases, Trends Cell Biol. 16 (2006) 36–44.
[6] K. Yasumoto, S. Amae, T. Udono, N. Fuse, K. Takeda, S. Shibahara, A big gene linked to small eyes encodes multiple Mitf isoforms: many promoters make light work, Pigment Cell Res. 11 (1998) 329–336.
[7] Y. Kitamura, E. Morii, T. Jippo, A. Ito, mi-transcription factor as a regulator of mast cell differentiation, Int. J. Hematol. 71 (2000) 197–202.
[8] H.R. Widlund, D.E. Fisher, Microphthalamia-associated transcription factor: a critical regulator of pigment cell development and survival, Oncogene 22 (2003) 3035–3041.
[9] E. Steingrímsson, K.J. Moore, M.L. Lamoreux, A.R. Ferré-D'Amaré, S.K. Burley, D.C. Zimring, L.C. Skow, C.A. Hodgkinson, H. Arnheiter, N.G. Copeland, N.A. Jenkins, Molecular basis of mouse microphthalmia (mi) mutations helps explain their developmental and phenotypic consequences, Nat. Genet. 8 (1994) 256–263.
[10] K.N. Weilbaecher, C.L. Hershey, C.M. Takemoto, M.A. Horstmann, T.J. Hemesath, A.H. Tashjian, D.E. Fisher, Age-resolving osteopetrosis: a rat model implicating microphthalmia and the related transcription factor TFE3, J. Exp. Med. 187 (1998) 775–785.
[11] S. Tshori, D. Gilon, R. Beeri, H. Nechushtan, D. Kaluzhny, E. Pikarsky, E. Razin, Transcription factor MITF regulates cardiac growth and hypertrophy, J. Clin. Invest. 116 (2006) 2673–2681.
[12] Y. Kitamura, E. Morii, T. Jippo, A. Ito, Regulation of mast cell phenotype by MITF, Int. Arch. Allergy Immunol. 127 (2002) 106–109.
[13] C.L. Hershey, D.E. Fisher, Mitf and Tfe3: members of a b-HLH-ZIP transcription factor family essential for osteoclast development and function, Bone 34 (2004) 689–696.
[14] E. Steingrímsson, N.G. Copeland, N.A. Jenkins, Melanocytes and the microphthalmia transcription factor network, Annu. Rev. Genet. 38 (2004) 365–411.
[15] S. Amae, N. Fuse, K. Yasumoto, S. Sato, I. Yajima, H. Yamamoto, T. Udono, Y.K. Durlu, M. Tamai, K. Takahashi, S. Shibahara, Identification of a novel isoform of microphthalmia-associated transcription factor that is enriched in retinal pigment epithelium, Biochem. Biophys. Res. Commun. 247 (1998) 710–715.
[16] C.M. Takemoto, Y.J. Yoon, D.E. Fisher, The identification and functional characterization of a novel mast cell isoform of the microphthalmia-associated transcription factor, J. Biol. Chem. 277 (2002) 30244–30252.
[17] M. Murakami, T. Ikeda, K. Ogawa, M. Funaba, Transcriptional activation of mouse mast cell protease-9 by microphthalmia-associated transcription factor, Biochem. Biophys. Res. Commun. 311 (2003) 4–10.
[18] M. Funaba, T. Ikeda, M. Murakami, K. Ogawa, M. Abe, Up-regulation of mouse mast cell protease-6 gene by transforming growth factor-β and activin in mast cell progenitors, Cell. Signal. 17 (2005) 121–128.
[19] K. Bharti, W. Liu, T. Csermely, S. Bertuzzi, H. Arnheiter, Alternative promoter use in eye development: the complex role and regulation of the transcription factor MITF, Development 135 (2008) 1169–1178.
[20] J.H. Hallsson, J. Favor, C. Hodgkinson, T. Glaser, M.L. Lamoreux, R. Magnúsdóttir, G.J. Gunnarsson, H.O. Sweet, N.G. Copeland, N.A. Jenkins, E. Steingrímsson, Genomic, transcriptional and mutational analysis of the mouse microphthalmia locus, Genetics 155 (2000) 291–300.
[21] M. Murakami, Y. Iwata, M. Funaba, Expression and transcriptional activity of alternative splice variants of Mitf exon 6, Mol. Cell. Biochem. 303 (2007) 251–257.
[22] M. Murakami, H. Kawachi, K. Ogawa, Y. Nishino, M. Funaba, Receptor expression modulates the specificity of transforming growth factor-β signaling pathways, Genes Cells 14 (2009) 469–482.
[23] P.K. Smith, R.I. Krohn, G.T. Hermanson, A.K. Mallia, F.H. Gartner, M.D. Provenzano, E.K. Fujimoto, N.M. Goeke, B.J. Olson, D.C. Klenk, Measurement of protein using bicinchoninic acid, Anal. Biochem. 150 (1985) 76–85.
[24] M. Funaba, M. Murakami, A sensitive detection of phospho-Smad1/5/8 and Smad2 in Western blot analyses, J. Biochem. Biophys. Methods 70 (2008) 816–819.
[25] M. Suenaga, T. Matsui, M. Funaba, BMP inhibition with dorsomorphin limits adipogenic potential of preadipocytes, J. Vet. Med. Sci. 72 (2010) 373–377.
[26] S. Schiaffino, C. Reggiani, Molecular diversity of myofibrillar proteins: gene regulation and functional significance, Physiol. Rev. 76 (1996) 371–423.
[27] C.A. Hodgkinson, K.J. Moore, A. Nakayama, E. Steingrímsson, N.G. Copeland, N.A. Jenkins, H. Arnheiter, Mutations at the mouse microphthalmia locus are associated with defects in a gene encoding a novel basic-helix–loop–helix-zipper protein, Cell 74 (1993) 395–404.
[28] D. Yaffe, O. Saxel, Serial passaging and differentiation of myogenic cells isolated from dystrophic mouse muscle, Nature 270 (1977) 725–727.
[29] F. Viñals, F. Ventura, Myogenin protein stability is decreased by BMP-2 through a mechanism implicating Id1, J. Biol. Chem. 279 (2004) 45766–45772.
[30] Y. Furutani, T. Umemoto, M. Murakami, T. Matsui, M. Funaba, Role of endogenous TGF-β family in myogenic differentiation of C2C12 cells, J. Cell. Biochem. 112 (2011) 614–624.
[31] S.K. Sastry, M. Lakonishok, D.A. Thomas, J. Muschler, A.F. Horwitz, Integrin α subunit ratios, cytoplasmic domains, and growth factor synergy regulate muscle proliferation and differentiation, J. Cell Biol. 133 (1996) 169–184.
[32] K.R. Doherty, A. Cave, D.B. Davis, A.J. Delmonte, A. Posey, J.U. Earley, M. Hadhazy, E.M. McNally, Normal myoblast fusion requires myoferlin, Development 132 (2005) 5565–5575.
[33] P. Lafuste, C. Sonnet, B. Chazaud, P.A. Dreyfus, R.K. Gherardi, U.M. Wewer, F.J. Authier, ADAM12 and α9β1 integrin are instrumental in human myogenic cell differentiation, Mol. Biol. Cell 16 (2005) 861–870.
[34] E. Brzóska, V. Bello, T. Darribère, J. Moraczewski, Integrin α3 subunit participates in myoblast adhesion and fusion in vitro, Differentiation 74 (2006) 105–118.
[35] M. Kitzmann, G. Carnac, M. Vandromme, M. Primig, N.J. Lamb, A. Fernandez, The muscle regulatory factors MyoD and Myf-5 undergo distinct cell cycle-specific expression in muscle cells, J. Cell Biol. 142 (1998) 1447–1459.
[36] N. Yoshida, S. Yoshida, K. Koishi, K. Masuda, Y. Nabeshima, Cell heterogeneity upon myogenic differentiation: down-regulation of MyoD and Myf-5 generates 'reserve cells', J. Cell Sci. 111 (1998) 769–779.
[37] M. Menconi, P. Gonnella, V. Petkova, S. Lecker, P.O. Hasselgren, Dexamethasone and corticosterone induce similar, but not identical, muscle wasting responses in cultured L6 and C2C12 myotubes, J. Cell. Biochem. 105 (2008) 353–364.
[38] D.K. Kim, E. Morii, H. Ogihara, K. Hashimoto, K. Oritani, Y.M. Lee, T. Jippo, S. Adachi, Y. Kanakura, Y. Kitamura, Impaired expression of integrin α-4 subunit in cultured mast cells derived from mutant mice of mi/mi genotype, Blood 92 (1998) 1973–1980.
[39] S. Carreira, J. Goodall, I. Aksan, S.A. La Rocca, M.D. Galibert, L. Denat, L. Larue, C.R. Goding, Mitf cooperates with Rb1 and activates p21Cip1 expression to regulate cell cycle progression, Nature 433 (2005) 764–769.
[40] V. Andrés, K. Walsh, Myogenin expression, cell cycle withdrawal, and phenotypic differentiation are temporally separable events that precede cell fusion upon myogenesis, J. Cell Biol. 132 (1996) 657–666.
[41] J. Wang, K. Walsh, Resistance to apoptosis conferred by Cdk inhibitors during myocyte differentiation, Science 273 (1996) 359–361.
[42] T.J. Hemesath, E. Steingrímsson, G. McGill, M.J. Hansen, J. Vaught, C.A. Hodgkinson, H. Arnheiter, N.G. Copeland, N.A. Jenkins, D.E. Fisher, Microphthalmia, a critical factor in melanocyte development, defines a discrete transcription factor family, Genes Dev. 8 (1994) 2770–2780.
[43] R. Katayama, A. Yamane, T. Fukui, Changes in the expression of myosins during postnatal development of masseter muscle in the microphthalmic mouse, Open Dent. J. 4 (2010) 1–7.

Biochimica et Biophysica Acta 1810 (2011) 1127–1135

Contents lists available at SciVerse ScienceDirect

Biochimica et Biophysica Acta

journal homepage: www.elsevier.com/locate/bbagen

Endogenous Bmp4 in myoblasts is required for myotube formation in C2C12 cells

Takenao Umemoto [a], Yuuma Furutani [a], Masaru Murakami [b], Tohru Matsui [a], Masayuki Funaba [a,*]

[a] Division of Applied Biosciences, Kyoto University Graduate School of Agriculture, Kyoto 606-8502, Japan
[b] Laboratory of Molecular Biology, Azabu University School of Veterinary Medicine, Sagamihara 229-5201, Japan

ARTICLE INFO

Article history:
Received 16 March 2011
Received in revised form 9 August 2011
Accepted 15 September 2011
Available online 22 September 2011

Keywords:
Bmp4
Myotube
Myogenesis
Myogenin

ABSTRACT

Background: Our previous study revealed the indispensable activity of endogenous bone morphogenetic protein (Bmp) prior to differentiation induction of C2C12 myoblasts for myogenesis. Here we investigated the Bmp isoform responsible for endogenous Bmp activity during differentiation and its role in myogenesis.
Methods: Gene expression of *Bmp4* during myogenesis was evaluated in C2C12 cells. Effects of inhibition of the Bmp pathway on myogenesis were examined. Cells expressing *Bmp4* and regulation of *Bmp4* expression in myoblasts were explored.
Results: The expression of *Bmp4* increased with the progression of myogenesis, although the extent of the increase after differentiation induction was smaller than that before the induction. Down-regulation of Bmp signal components including *Bmp4*, *Bmpr2*, and *Alk2/3* inhibited the emergence of positive cells for myosin heavy chain II. The treatments also decreased the Myogenin expression. Treatment with cytosine arabinoside decreased the expression of *Bmp4*. Also, *Bmp4* expression was also lower in isolated myotubes than in residual cells. Expression of *Rgm c* was higher in the myotube fraction. Transcription of *Bmp4* was repressed by the conditioned medium of mixed cells consisting of myoblasts and myotubes.
Conclusion: Bmp4 expressed in myoblasts has a positive role in myotube formation/maturation through myogenin expression. The presence of myotubes inhibits *Bmp4* expression in proliferating myoblasts through transcriptional regulation, although the expression is intrinsically increased with time of culture.
General significance: Taken previous results on involvement of Bmp in the commitment of osteoblasts and adipocytes with the present results together, Bmp may act as a general promoter of mesenchymal cell differentiation.

1. Introduction

Skeletal muscle is a highly specialized tissue composed of postmitotic, multinucleated muscle fibers, which contract to generate force and movement. Skeletal muscle is also critical to maintain metabolic health through glucose uptake and insulin sensitivity [1,2]. In addition, contracting skeletal muscle has been recently suggested to play a role as an endocrine organ producing various cytokines [3–5]. Skeletal muscle formation consists of a complex set of differentiation steps: commitment of mesenchymal stem cells to myoblast lineage cells, progression of differentiation with the expression of muscle-cell-specific proteins, and fusion of myoblasts into multinucleated myotubes. Myogenic differentiation is principally governed by activities of the MyoD family basic helix–loop–helix (bHLH) transcription factors, also known as myogenic regulatory factors (MRFs), i.e., Myod, Myf5, Myogenin and Mrf4. MRFs form a complex with E proteins, another class of bHLH transcription factors, such as E12 and E47, and stimulate the transcription of skeletal muscle-specific genes through binding to E-box (CANNTG) in the regulatory region [6–8]. To accomplish appropriate myogenesis, the activities of MRFs must be strictly regulated.

Bone morphogenetic proteins (Bmps), which were originally isolated as bone-inducing proteins [9], potently regulate various biological processes, including hematopoietic and neuronal development, iron metabolism, and vascular homeostasis [10]. The diverse effects of Bmp are mostly elicited through the phosphorylation and activation of Bmp-regulated Smad (BR-Smad), i.e., Smad1, Smad5 and Smad8, at the carboxyl-terminal serines [10]. Phosphorylated BR-Smad forms complexes with Smad4, which accumulate in the nucleus where they participate in transcriptional regulation of the target genes.

Previous studies revealed that Bmp acted as a negative regulator of myogenesis. Addition of Bmp to the culture medium of myogenic cells led to differentiation into osteoblast lineage cells [11–15]. This transdifferentiation was related to gene induction of the inhibitor of DNA binding 1 (Id1) [11]. Id1 heterodimerized with E proteins, which blocked the formation of active complex consisting of E proteins and Myod [16,17]. In addition, Id1 expression accelerated the degradation of myogenin [18]. As compared with the well-known effects of exogenous Bmp, information on the activity and role of endogenous Bmp is limited.

Recently, we revealed the importance of endogenous Bmp activity in undifferentiated myoblasts for myogenesis in a C2C12 myoblast

* Corresponding author at: Division of Applied Biosciences, Kyoto University Graduate School of Agriculture, Kitashirakawa Oiwakecho, Kyoto 606-8502, Japan. Tel.: +81 75 753 6055; fax: +81 75 753 6344.
E-mail address: mfunaba@kais.kyoto-u.ac.jp (M. Funaba).

0304-4165/$ – see front matter © 2011 Elsevier B.V. All rights reserved.
doi:10.1016/j.bbagen.2011.09.008

differentiation model [19]; in this model, mononucleated myoblasts are fused to multinucleated myotubes upon reduced serum or serum starvation [20]. Endogenous Bmp activity, which was monitored by the phosphorylation level of BR-Smad, was higher in the stage prior to differentiation induction, and inhibition of the Bmp pathway prior to differentiation induction down-regulated the expression of Myf5 and Myod, leading to impaired myotube formation [19]. The role of endogenous Bmp sharply contrasted to previous knowledge on the action of exogenously treated Bmp for myogenesis [11–15]; however, the level of phosphorylated BR-Smad remained after differentiation induction, although it was lower than before differentiation. This situation encouraged us to explore further the significance of endogenous Bmp activity during myotube differentiation. The present study reveals that *Bmp4* expression in proliferating myoblasts after differentiation induction is required for the progression of myogenesis to maintain *Myogenin* expression, and that the expression is negatively regulated by the presence of myotubes.

2. Materials and methods

2.1. Materials

The following reagents were purchased: recombinant Bmp4 was from R&D Systems (Minneapolis, MN, USA); cytosine arabinoside (cytosine-1-β-D(+)-arabinofuranocide) was from Wako (Tokyo, Japan); rabbit polyclonal antibody against Myogenin (ab11986), rabbit monoclonal antibody against Smad1 (ab33902) and β-actin (AC-15) were from Abcam (Cambridge, MA, USA); mouse monoclonal antibody against myosin heavy chain (MyHC) (MY-32) was from Sigma (St. Louis, MO, USA); rabbit polyclonal antibody against phospho-Smad1 (Ser463/Ser465) / Smad5 (Ser463/Ser465)/ Smad8 (Ser426/Ser428) (#9511) was from Cell Signaling Technology (Danvers, MA, USA); Alexa Fluoro 488 was from Invitrogen (Carlsbad, CA, USA).

2.2. Cell culture

C2C12 myoblasts were cultured in growth medium, i.e., Dulbecco's modified Eagle's medium (DMEM) with heat-inactivated 10% fetal bovine serum (FBS), 100 U/ml penicillin and 100 μg/ml streptomycin, at 37 °C under a humidified 5% CO_2 atmosphere. To induce differentiation from myoblasts to myotubes, the medium was replaced at confluence (day 0) with differentiation medium consisting of DMEM with 2% horse serum supplemented the antibiotics. Alternatively, the differentiation was induced by culture with serum-free DMEM supplemented the antibiotics to collect conditioned medium. To examine the effects of removing proliferating myoblasts, cytosine arabinoside was added to the culture medium at the final concentration of 10 μM or 20 μM for days 4 to 7 or days 11 to 14, and cells were recovered on day 7 or day 14, respectively. To isolate myotubes, cells on day 10 were trypsinized for a short time under the microscope until detachment of multinucleated cells (~2 min), followed by centrifugation to obtain a myotube-rich fraction. Collection of conditioned medium was done for days 4–6, days 6–8 and days 8–10. The conditioned medium was concentrated, and the solvent was changed to 20 mM HEPES (pH 7.5), 150 mM NaCl, 1 mM PMSF, 1% aprotinin by means of Centriprep-10 (Millipore, Bedford, MA), and protein concentrations were measured by the bicinchoninic acid method [21].

2.3. qRT-PCR

RNA isolation and qRT-PCR were carried out as previously described [22]. The following oligonucleotides were used as PCR primers: 5′-ACTCCCTTACGTCCATCGTG-3′ and 5′-CAGGACAGCCCCACTTAAAA-3′ for *Myogenin* (Genbank accession number: NM_031189.2), 5′-CAGCTACAAACCCAAGCAAG-3′ and 5′-AGGCATCCACGTTTGCTC-3′ for *Mrf4* (Genbank accession number: NM_008657.2), 5′-GCCTGGGCTTACCTCTCTATCAC-3′ and 5′-CTTCTCAGACTTCCGCAGGAA-3′ for *myosin heavy chain (Myhc) I* (Genbank accession number: BC158018), 5′-CCTGAGCAAGAAGCTGAGGA-3′ and 5′-GGTCATTCCACGCGTACAG-3′ for *Noggin* (Genbank accession number: NM_008711), 5′-ACCGCCCTACACCTAGTCTTC-3′ and 5′-CATACCCATCCATCCAGCTC-3′ for *repulsive guidance molecule (Rgm) a* (Genbank accession number: NM_177740.5), 5′-ACCTTTCGGTTCAAGTGACG-3′ and 5′-TCACAGCTTGGTACACCTTCTG-3′ for *Rgm b* (Genbank accession number: NM_178615.3), and 5′-GGCAATCATGGAGAAAGAGATG-3′ and 5′-TTTCTCTGGGTACTTCTGTGATGT-3′ for *Rgm c* (Genbank accession number: NM_027126.4). The other PCR primers used in this study were previously described [22,23]. The Ct value was determined, and the abundance of gene transcripts was calculated from the Ct value using *Hprt1* as the corrected gene.

2.4. Measurement of DNA content

To examine time-course changes in DNA content during myotube differentiation, recovered cells were resuspended in hypertonic buffer (200 mM phosphate buffer (pH 7.4), 2 M NaCl, 2 mM Na_3VO_4, 1 mM PMSF, 1% aprotinin), followed by lysis by ultrasonication. DNA content was measured by the method of Labarca and Paigen [24].

2.5. Double-stranded RNAi transfection

To target the expression of *Bmp4*, *Bmpr2*, *Alk2* or *Alk3* and green fluorescent protein (GFP) control, double-stranded (ds) RNAi of the respective genes was synthesized by Samchully Pharmaceuticals (Seoul, Korea). The coding sequences to inhibit the expression of *Bmp4*, four oligonucleotides, were designed: 5′-GUUGAAAAAUUAUCAGGAGAU-3′ (set 1), 5′-CUCCUGAUAAUUUUUCAACAC-3′ (set 1), and 5′-CAGACUAGUCCAUCACAAUGU-3′ (set 2), and 5′-AUUGUGAUGGACUAGUCUGGU-3′ (set 2). Two oligonucleotides of each set were mixed, and 1:1 mixtures of dsRNAi were prepared. The other dsRNAi used in this study were described previously [23]. Overall, 60 pmol dsRNAi in a 12-well plate was transfected using Lipofectamine RNAiMAX (Invitrogen), according to the manufacturer's protocol.

2.6. Immunofluorescence staining

Immunofluorescence staining for Myhc was performed as described previously [19]. Nuclei were also stained by 1 μg/ml 4′,6-diamidino-2-phenylindole (DAPI). The number of nuclei was calculated by Image J (http://rsbweb.nih.gov/ij/). Fusion index was calculated as a ratio of the number of nuclei incorporated in myotubes to the number of total nuclei [25].

2.7. Western blotting

To evaluate roles of endogenous Bmp activity in myogenin expression, dsRNAi for Bmp signal components was introduced in cells for 48 h. In addition, BR-Smad phosphorylation was evaluated in cells transfected with dsRNAi for *Bmp4* and treated with recombinant Bmp4. Western blotting was performed as described previously [19].

2.8. Reporter assays

The 5′-flanking regions of *Bmp4* (nucleotides (nt) −2372 to +115, relative to the transcriptional initiation site at +1) was isolated by PCR using mouse genomic DNA. The DNA fragment was cloned into a region upstream of the luciferase gene in pGL4-Basic (Promega, Madison, WI, USA) using the *Bgl* II and *Hind* III sites; it was verified by DNA sequencing. Luciferase-based reporter assays were conducted as described previously [23]. C2C12 myoblasts were seeded on 24-well plates, and transiently transfected with Bmp4-luc by use of Lipofectamine LTX reagent (Invitrogen). A *Renilla reniformis* luciferase vector

driven by thymidine kinase promoter (Promega) was co-transfected to serve as an internal control for transfection efficiency. At 24 h after the transfection, C2C12 cells on day −3, day 0, day 3 or day 6, which were recovered by use of cell dissociation buffer (Cell Dissociation Solution (1 ×) Non-enzymatic, Sigma) and resuspended in the growth medium for cells on day −3 or the differentiation medium for cells on day 0, day 3 and day 6, were added for 24 h. Alternatively, at 24 h after the transfection, 50 μg of protein prepared from the conditioned medium was added to the culture medium for 24 h. Firefly luciferase activity was normalized to *Renilla* luciferase activity, and the luciferase activity in the cell lysate cultured with growth medium and without addition of cells was set to 1.

2.9. Statistical analyses

Data are expressed as the mean ± SEM. Differences between treatments were examined by Student's *t*-test. Differences of $P<0.05$ were considered significant.

3. Results

3.1. Bmp4 expression increases with progression of myogenic differentiation

Changes in gene expression with myogenesis were examined (Fig. 1). Expression of MyoD family members, such as *Myf5* (Fig. 1A) and *Myod* (Fig. 1B), which are necessary for myotube differentiation [26], was highest on day 0. The expression level was decreased within 2 days after differentiation induction, and remained lower on day 14. Expression of *Myogenin* was extremely low prior to differentiation induction, and rapidly increased after differentiation induction. The expression of *Myogenin* reached a peak on day 2 (Fig. 1C). Expression of *Mrf4* peaked on day 8 (Fig. 1D). Expression of *Myhc I* (Fig. 1E) and *Myhc IIb* (Fig. 1F), which are myocyte (myotube)-specific genes, was increased in response to differentiation induction within 2 days for *Myhc I* and 4 days for *Myhc IIb*, and reached a peak on day 6–8 for *Myhc I* and on day 6–10 for *Myhc IIb*. We examined changes in the expression of several Bmp isoforms during myogenesis; expression of *Bmp2* and *Bmp7* was negligible ([22], data not shown). We also searched for the expression of the Bmp subfamily belonging to the Tgf-β family in a cDNA microarray database (http://www.ncbi.nlm.nih.gov/geo/) thoroughly, and found no significant expression of *Bmp2, Bmp5, Bmp6, Bmp7, Bmp8a, Bmp8b, Bmp9, Bmp10* and *Bmp15* (data not shown). Gdf5 elicits their signal via BR-Smad [13], but the expression of *Gdf5* could not be detected. Only *Bmp4* was significantly expressed in undifferentiated myoblasts. *Bmp4* expression was increased 7.8-fold for 2 days before the differentiation induction. The expression was still increased after the differentiation induction, but the extent of the increase was smaller, i.e., 3.1-fold increase for 14 days after the differentiation induction. As the results, the level on day 14 was more than 20-fold higher than that on day −2

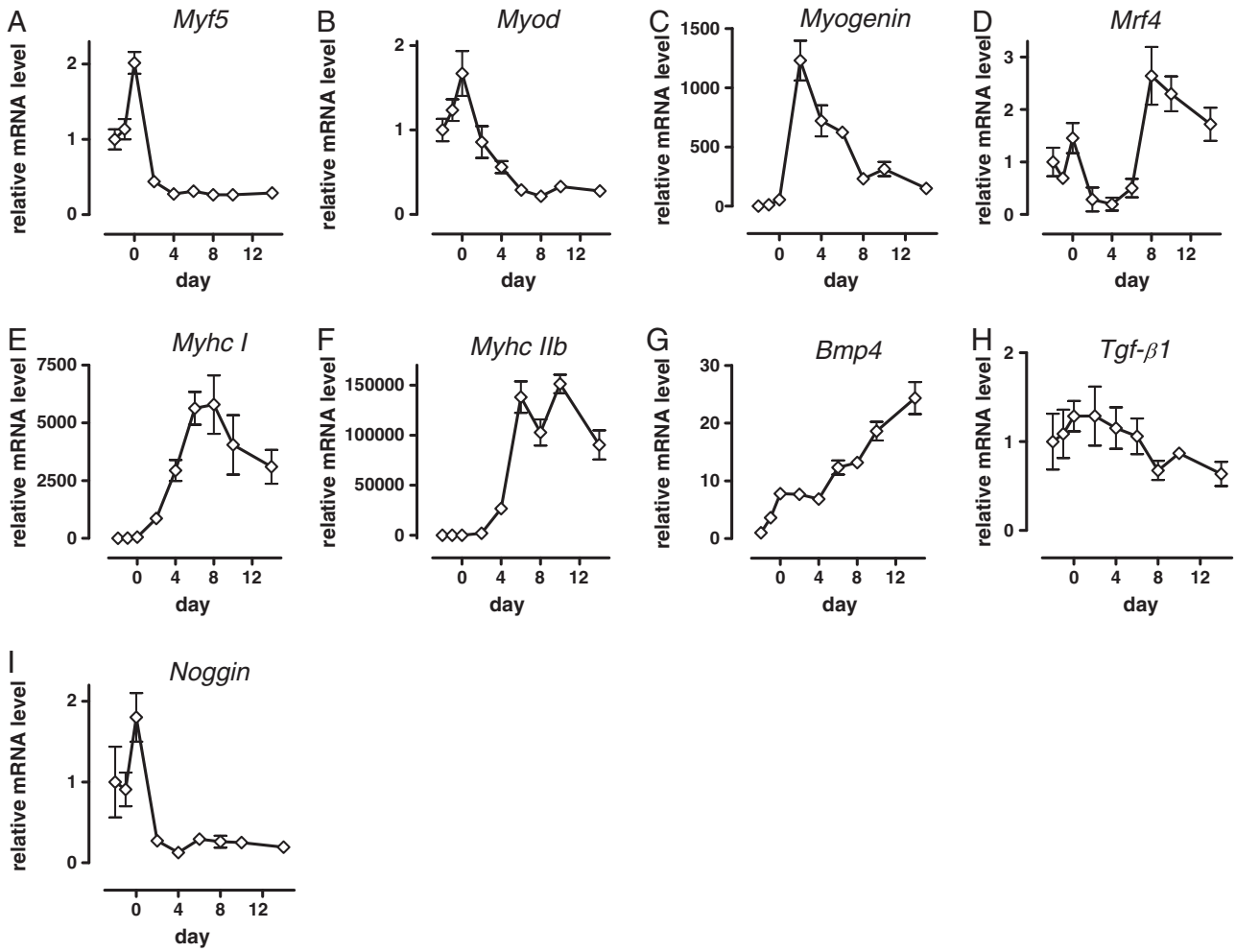

Fig. 1. Time-course changes in expression of molecules related to myogenesis, Bmp4, Tgf-β1 and Noggin in C2C12 cells. C2C12 myoblasts were cultured to reach confluence (day 0) in growth medium, followed by culture in differentiation medium. Expression of the indicated gene was quantified by qRT-PCR, and normalized to *Hprt1* expression. The expression on day −2 was set to 1. Data are shown as the mean ± SE ($n=4$).

(Fig. 1G). This expression pattern contrasted to that of the structurally related *Tgf-β* (Fig. 1H); *Tgf-β1* expression was relatively constant during myogenesis. Noggin acts as antagonists of the Bmp pathway [27]. *Noggin* expression was highest on day 0, and decreased after differentiation induction (Fig. 1I); the time-course changes in *Noggin* expression resembled to those in BR-Smad phosphorylation [19], suggesting the fine regulation of endogenous Bmp activity before the differentiation.

Cell morphology showed mononuclear myoblasts on day 0, the emergence of multinucleated myotubes within 4 days after differentiation induction, and an increase in the number of myotubes by day 14 (Fig. 2A); however, mononucleated cells were observed even on day 14, indicating that not all myoblasts fuse to and differentiate into myotubes (Fig. 2A). Cell number as well as DNA content also increased after differentiation induction (Fig. 2B and C). Cell growth during myogenic differentiation was basically consistent with the previous results, in which cell proliferation was observed on days 3–7 [28–30]. The present results indicate the co-existence of myoblasts and myotubes even by culture in differentiation medium for 14 days.

3.2. Bmp4 is required for efficient myotube formation

Effects of inhibition of the Bmp4 pathway were examined to elucidate the role of Bmp4 in myogenesis; we evaluated effects of transfection of dsRNAi for *Bmp4*, the type II receptor *Bmpr2*, and the type I receptors *Alk2* and *Alk3*. Alk6 is another type I receptor for Bmp, but the expression level in C2C12 cells was much lower (data not shown). Knockdown of genes for *Bmp4*, *Bmpr2* or *Alk2/3* induced the emergence of thin Myhc-positive cells (Fig. 3A). In fact, the fusion index, the ratio of the number of nuclei in Myhc-positive cells to the number of total nuclei, was decreased by down-regulation of components of the Bmp pathway (Fig. 3A–E). Down-regulation of the Bmp4 pathway also decreased gene transcript levels of *Myogenin* but not *Myf5* and *Myod* (Fig. 4). These results suggest that endogenous Bmp4 produced in proliferating myoblasts positively regulates myogenesis through *Myogenin* expression.

Although Bmp4 has been previously recognized only as a secreted growth factor, a recent study revealed a variant of Bmp4 localized in the nucleus [31]. We examined whether down-regulated *Myogenin* expression in *Bmp4*-knockdown C2C12 cells is recovered by simultaneous treatment with recombinant Bmp4. The used recombinant Bmp4 ranged over the recoverable concentrations on the decreased BR-Smad phosphorylation resulting from the *Bmp4* knockdown (Fig. 5A). The additional Bmp4 did not effectively recover *Bmp4* knockdown-induced down-regulation of *Myogenin* (Fig. 5B). We also examined effects of the higher concentrations of Bmp4, but could not detect up-regulation of *Myogenin* expression in any concentrations of Bmp4 (data not shown).

3.3. Expression of Bmp4 in myoblasts is modulated by the presence of myotubes

Co-existence of myoblasts and myotubes in a culture dish after differentiation induction suggests that increased expression of *Bmp4* with culture time does not necessarily reflect its expression in myotubes. Thus, we tried to identify cells expressing *Bmp4* predominantly by two approaches: *Bmp4* expression was examined in cells treated with cytosine arabinoside and in isolated myotubes. Cytosine arabinoside is incorporated into replicating DNA in the S-phase and damages DNA [30,32], leading to elimination of proliferating cells. Treatment with cytosine arabinoside for days 4–7 and days 11–14 efficiently decreased the expression of *Bmp4* but not *Tgf-β1* (Fig. 6A and B). Proliferating myoblasts express MRFs, such as *Myf5* and *Myod* [29], and the expression of these genes decreased as expected (Fig. 6C and D).

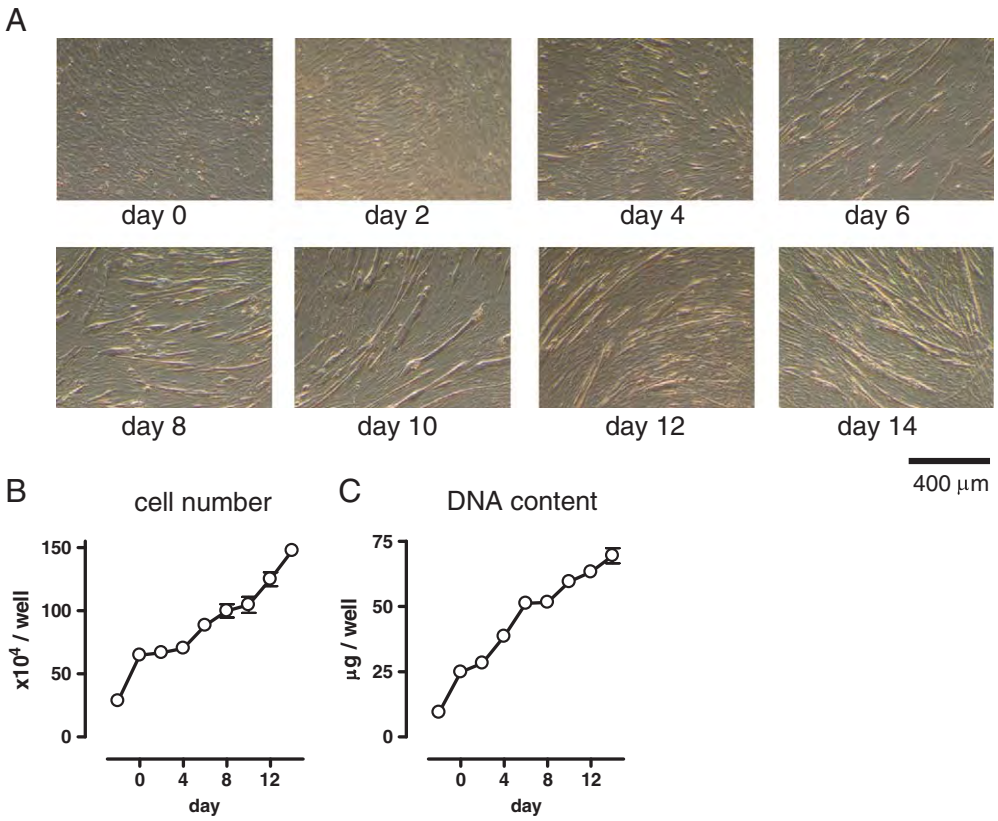

Fig. 2. Time-course changes in morphology, cell number and DNA content in C2C12 cells. C2C12 myoblasts were cultured to reach confluence (day 0) in growth medium, followed by culture in differentiation medium. (A) Representative morphology observed by phase-contrast microscope is shown. (B and C) Time-course changes in cell number (B) and DNA content (C) were examined. Data are shown as the mean ± SE ($n = 6$).

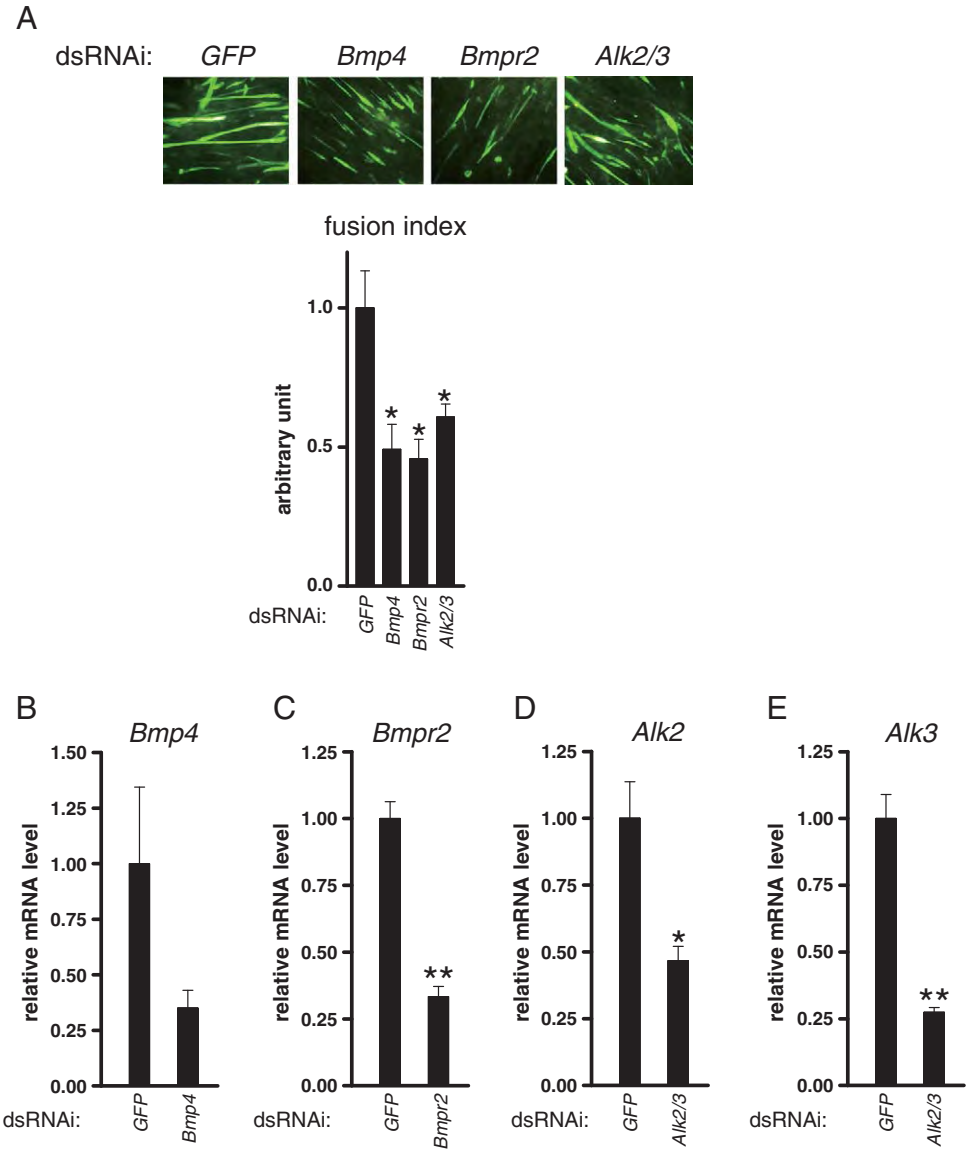

Fig. 3. Myotube differentiation in C2C12 cells down-regulated expression of the Bmp signal components. C2C12 myoblasts were cultured to reach confluence (day 0) in growth medium, followed by culture in differentiation medium. On day 2, cells were transfected with the indicated dsRNAi. (A) On day 8, myotube formation was examined by immunofluorescent analyses using anti-Myhc antibody. Representative immunostaining images are shown. Fusion index was calculated as a ratio of nuclei incorporated in myotubes relative to the total nuclei, and the index in cells treated with dsRNAi for *GFP* was set to 1 ($n=3$). (B–E) On day 6, the gene transcript level of *Bmp4* (B), *Bmpr2* (C), *Alk2* (D), and *Alk3* (E) was quantified by qRT-PCR. The gene expression was normalized to *Hprt1* expression. The expression in cells treated with dsRNAi for GFP was set to 1. Data are shown as the mean ± SE ($n=4$). * and **: $P<0.05$ and $P<0.01$, respectively, as compared to control (*GFP*).

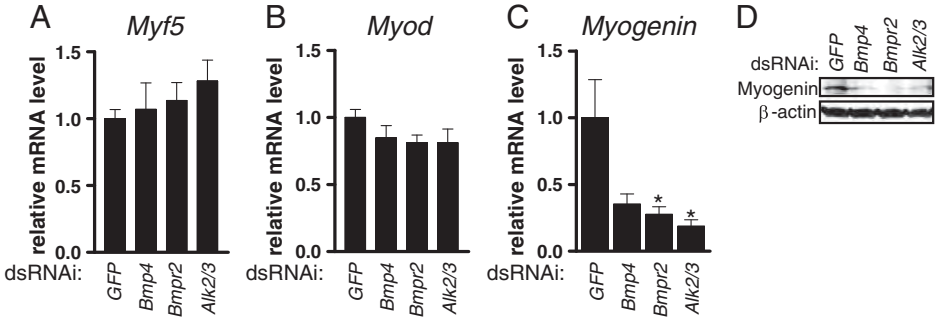

Fig. 4. Expression of MRFs in C2C12 cells down-regulated expression of the Bmp signal components. C2C12 myoblasts were cultured to reach confluence (day 0) in growth medium, followed by culture in differentiation medium. On day 4, cells were transfected with the indicated dsRNAi. On day 6, gene transcript level of *Myf5* (A), *Myod* (B), and *Myogenin* (C) was quantified by qRT-PCR. The gene expression was normalized to *Hprt1* expression. The expression in cells treated with dsRNAi for GFP was set to 1. Data are shown as the mean ± SE ($n=4$). *$P<0.05$, as compared to control (GFP). (D) On day 0, cells were transfected with the indicated dsRNAi. On day 2, Myogenin expression was examined by Western blot analyses. After stripping the antibodies and the detection reagents, the membranes were reprobed with anti-β-actin antibody.

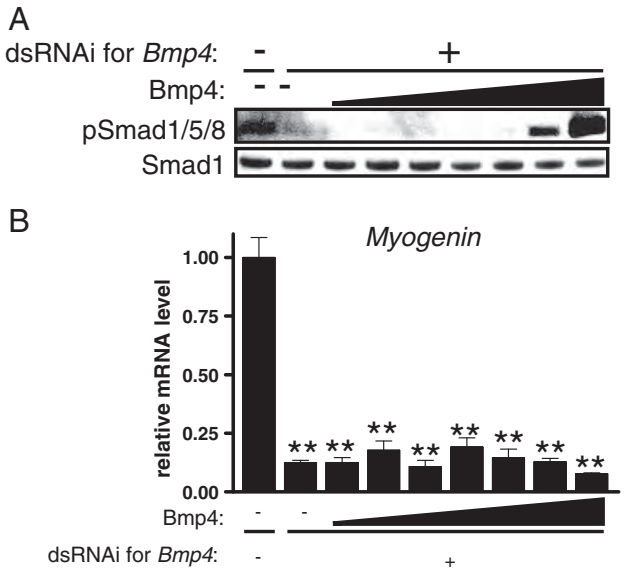

Fig. 5. Phosphorylation of BR-Smad and Myogenin expression in C2C12 cells down-regulated Bmp4 and treated with Bmp4. C2C12 myoblasts were cultured to reach confluence (day 0) in growth medium, followed by culture in differentiation medium. Cells were transfected with or without dsRNAi for Bmp4 on day 1. At 12 h after the transfection, cells were treated with various concentrations of Bmp4 (16 fM to 1.25 nM) for 36 h. (A) Phosphorylated Smad1/5/8 was evaluated by Western blot analyses. After stripping the antibodies and the detection reagents, the membranes were reprobed with anti-Smad1 antibody. (B) Gene transcript level of *Myogenin* was quantified by qRT-PCR. The gene expression was normalized to *Hprt1* expression. The expression in cells treated without dsRNAi for *Bmp4* was set to 1. Data are shown as the mean ± SE ($n=4$). $^{**}P<0.01$, as compared to expression in cells treated without dsRNAi for *Bmp4*.

We next separated the myotube-rich fraction by limited trypsinization. The expression level of *Bmp4* but not *Tgf-β1* was lower in isolated myotubes than in residual cells (Fig. 7A and B). Expectedly, *Myhc IIb* expression was predominantly detected in isolated myotubes (Fig. 7C), indicating the minimal presence of myotubes in the residual cell fraction. Consistent with previous results [29,33], *Myogenin* expression was also largely limited in the myotube fraction (Fig. 7D). Taking these results with results treated with cytosine arabinoside together, *Bmp4* is expressed in proliferating myoblasts in the presence of myotubes.

The expression of receptors for the Bmp pathway was also examined. Bmp receptors were comparatively expressed in both cell fractions (Fig. 7E–G). Members of the Rgm family: Rgm a; Rgm b, also known as Dragon; and Rgm c, also known as Hemojuvelin, are co-receptors of Bmp2 and Bmp4, and enhance Bmp signaling [34–36]. Expression of *Rgm c* was detected predominantly in the myotube fraction (Fig. 7H–J).

We next explored regulation of *Bmp4* expression in myoblasts. At first, effects of the presence of myoblasts or mixed cells consisting of myoblasts and myotubes on *Bmp4* transcription were examined. Reporter assays using *Bmp4* promoter indicated that the presence of proliferating myoblasts increased expression of Bmp4-luc (Fig. 8A). By contrast, the presence of cells after differentiation induction significantly decreased expression of Bmp4-luc. Addition of the conditioned medium prepared from cells on days 4–6, days 6–8 or days 8–10 also decreased Bmp4-luc (Fig. 8B). Consistent with the results, the conditioned medium significantly down-regulated *Bmp4* expression (Fig. 8C) but not *Tgf-β1* expression (Fig. 8D). These results suggest that Bmp4 expression in myoblasts is positively regulated in the presence of proliferating myoblasts and negatively regulated in the presence of myotubes at the transcription level.

4. Discussion

Myogenesis is a complex biological process, and is principally regulated by the expression and activity of MRFs [6–8,26]. The present study reveals that: (1) proliferating myoblasts express Bmp4; (2) Bmp4 expression in myoblasts is required for myotube formation/maturation through Myogenin expression in myotubes; and (3) possibly myotubes secrete factors down-regulating Bmp4 expression in myoblasts. Recently, we revealed that inhibition of endogenous Bmp activity prior to differentiation induction blocked myotube formation in C2C12 cells through down-regulation of Myf5 and Myod expression [19]. In

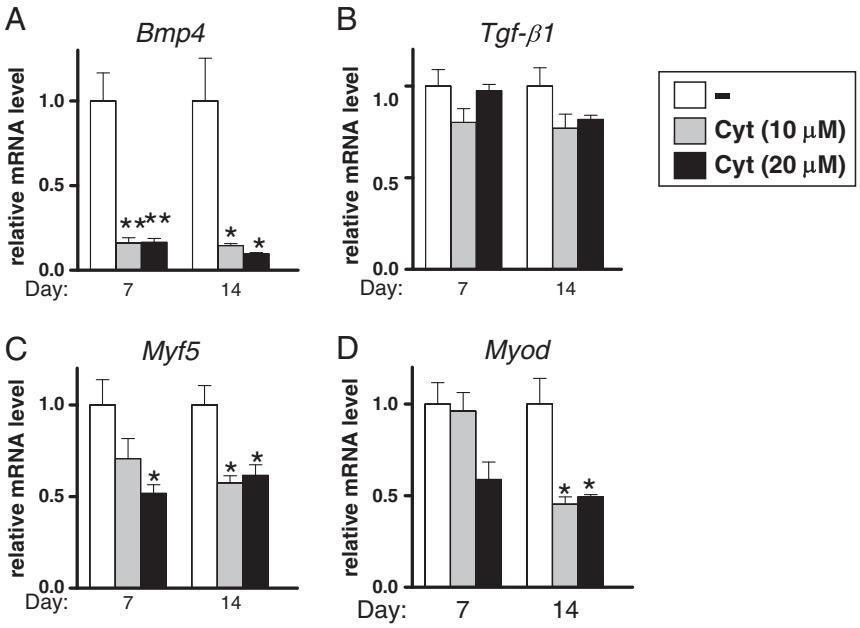

Fig. 6. Effects of cytosine arabinoside on expression of Bmp4, Tgf-β1, Myf5 and Myod in C2C12 cells. C2C12 myoblasts were cultured to reach confluence (day 0) in growth medium, followed by culture in differentiation medium. On days 4–7 and days 11–14, cytosine arabinoside (Cyt) at the indicated concentration was added to the differentiation medium. Gene expression of *Bmp4* (A), *Tgf-β1* (B), *Myf5* (C) and *Myod* (D) was quantified by qRT-PCR, and normalized to *Hprt1* expression. The expression in cells treated without cytosine arabinoside on each sampling day was set to 1. Data are shown as the mean ± SE ($n=4$). * and **: $P<0.05$ and $P<0.01$, respectively, as compared to expression in cells treated without cytosine arabinoside.

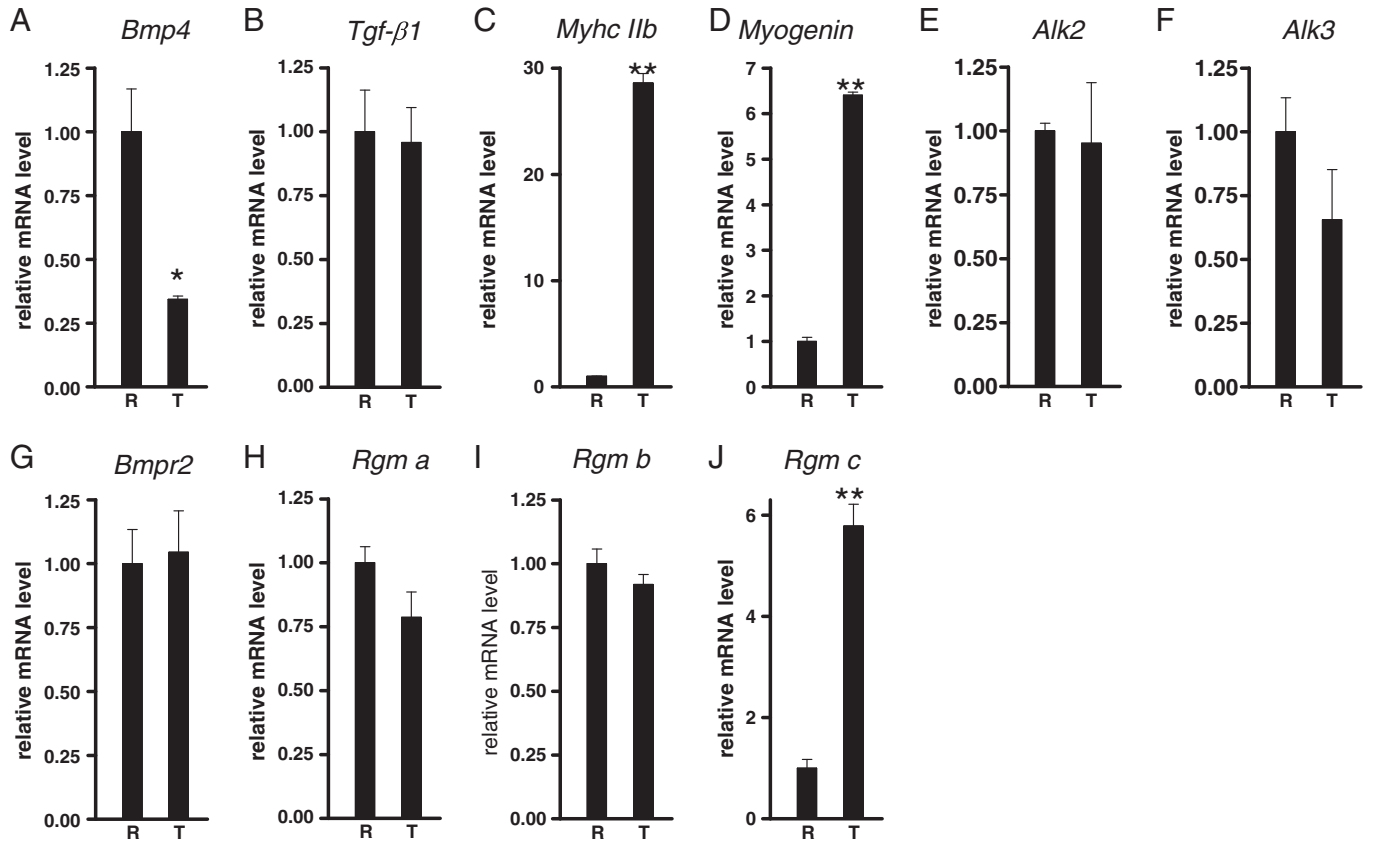

Fig. 7. Gene expression of Bmp4, Tgf-β1, Myhc IIb, Myogenin, Alk2, Alk3, Bmpr2, Rgm a, Rgm b and Rgm c in C2C12 cells after limited trypsinization. C2C12 myoblasts were cultured to reach confluence (day 0) in growth medium, followed by culture in differentiation medium. On day 10, multinucleated myotubes (T) were separated from the residual cells (R) by limited trypsinization. Expression of *Bmp4* (A), *Tgf-β1* (B), *Myhc IIb* (C), *Myogenin* (D), *Alk2* (E), *Alk3* (F), *Bmpr2* (G), *Rgm a* (H), *Rgm b* (I) and *Rgm c* (J) was quantified by qRT-PCR, and normalized to *Hprt1* expression. The expression in residual cells after limited trypsinization was set to 1. Data are shown as the mean ± SE ($n = 4$). * and **: $P < 0.05$ and $P < 0.01$, respectively, as compared to expression in the residual cells.

addition to the importance of Bmp activity in myoblasts before differentiation induction, the present results indicate the positive role of endogenous Bmp4 after differentiation induction in myogenesis. The role of Bmp4 produced in myoblasts as an accelerator of myogenesis and the inhibition of the Bmp4 expression by differentiated myotubes suggest the refined regulation of myogenesis through feedback loop mediated by Bmp4.

Bmps in fetal bovine serum in the culture medium were possibly responsible for the high endogenous Bmp activity prior to differentiation induction [19]. By contrast, Bmp4 produced in myoblasts was responsible for sustained endogenous Bmp activity after differentiation induction. Thus, differentiation induction changes the source of endogenous Bmp activity. Endogenous Bmp activity, however, plays a positive role in the progression of myogenesis, irrespectively of the differentiation stages.

Expression of *Rgm c*, which is a co-receptor of Bmp to enhance responsiveness to Bmp [36], was predominantly detected in myotubes. In C2C12 myotubes, soluble Rgm c was also produced by release from the cell membrane [37]; this molecular form of Rgm c inhibited the function of membrane-bound Rgm c [38]. However, the formation of soluble Rgm c was only partial, and was regulated by the iron status but not by the Bmp pathway [37]. Thus, we consider that myotubes efficiently receive Bmp4 produced by proliferating myoblasts through expressing Rgm c.

The present results suggest that effects of endogenous Bmp4 on myogenesis could not be explained by Bmp4 produced and secreted from myoblasts; knockdown of *Bmp4* inhibited myogenesis through down-regulation of *Myogenin* expression, but simultaneous administration of recombinant Bmp4 did not recover the expression of *Myogenin*. As described above, in addition to secreted form of Bmp4, there is a nuclear variant of Bmp4, which results from difference of translational initiation codon [31]. Since expression of this variant was detected in BALB/3T3 fibroblasts, C3H10T1/2 mesenchymal stem cells, and RCS chondrosarcoma cells, the two forms of Bmp4 would not be expressed in limited cells (Felin et al., 2010). Thus, it is possible that nuclear form of Bmp4 is required for the progression of myogenesis. In view of impaired myotube formation and decreased expression of *Myogenin* also in cells down-regulated Bmp receptors, both secreted form and nuclear form of Bmp4 may be indispensable for efficient myogenesis.

Expression of *Bmp4* in myoblasts was stimulated by the presence of proliferating myoblasts and inhibited by the presence of myotubes. These results partly explain remarkable increase with time in *Bmp4* expression before the differentiation and the slow increase after the differentiation; expression of *Bmp4* in myoblasts is intrinsically increased with progression of myogenesis, and factors being responsible for the increase should be clarified in future studies. Also, future studies should be directed to clarify soluble factor(s) produced in myotubes being responsible for the repression of *Bmp4* transcription in proliferating myoblasts.

The necessity of endogenous Bmp4 activity for myogenesis contrasts to the well-known effects of exogenous Bmp on myogenesis; Bmp4 addition to low serum-containing media in C2C12 myoblasts suppressed myogenesis, and induced transdifferentiation into osteoblast lineage cells [11–15]. Myoblasts responded to exogenous Bmp4, whereas myotubes responded to endogenous Bmp4; difference of the target cells

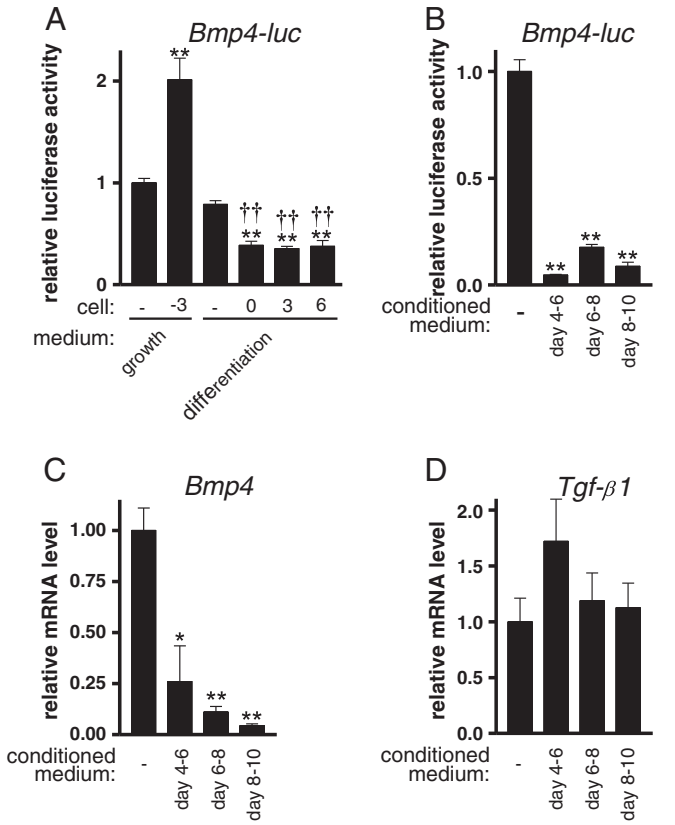

Fig. 8. Regulatory expression of Bmp4 in myoblasts by the presence of myotubes and by conditioned medium from myoblasts and myotubes. (A and B) C2C12 myoblasts were transiently transfected with Bmp4-luc and *Renilla*-luc. (A) At 24 h after the transfection, C2C12 cells on day −3, day 0, day 3 or day 6 were added for 24 h. (B) At 24 h after the transfection, 50 μg of protein prepared from the conditioned medium was added to the culture medium of the indicated culture period for 24 h. Firefly luciferase activity was normalized to *Renilla* luciferase activity, and the luciferase activity in the cell lysate cultured with growth medium and without addition of cells (A) and in those treated without the conditioned medium (B) was set to 1. Data are shown as the mean ± SE ($n=3$ or 4). (C and D) C2C12 myoblasts were cultured in the presence or absence of the conditioned medium for 48 h. Gene expression of *Bmp4* (C) and *Tgf-β1* (D) was quantified by qRT-PCR, and normalized to *Hprt1* expression. The expression in cells treated without the conditioned medium was set to 1. Data are shown as the mean ± SE ($n=3$). * and **: $P<0.05$ and $P<0.01$, respectively, as compared to expression in cells cultured with the same medium alone (A) and to expression in cells treated without the conditioned medium (B and C). ††: $P<0.01$, as compared to expression in cells treated with cells on day −3.

may be related to the disparate roles. Alternatively, as described above, the difference of molecular form between exogenous Bmp4, i.e., secreted Bmp4, and endogenous Bmp4, i.e., secreted and nuclear Bmp4, may be involved in the differential results. Furthermore, optimal Bmp activity is likely to be indispensable for myotube differentiation. Suppression of endogenous Bmp activity prior to differentiation induction inhibited myotube formation as described above [19], but increased Bmp activity by the addition of Bmp2 during this period also decreased the formation of multinucleated myotubes [19].

The present study revealed that the endogenous Bmp pathway unexpectedly regulates myogenesis positively. Myoblasts, osteoblasts and adipocytes are derived from common mesenchymal stem cells [39]. Involvement of Bmp in the commitment of osteoblasts and adipocytes is well known [39]. The present results in conjunction with our previous results [19] indicate that the differentiation and maturation of committed myoblast-lineage cells are positively regulated by endogenous Bmp at various differentiation stages. Thus, Bmp may act as a general promoter of mesenchymal cell differentiation and maturation, and contribute to the growth and development of the whole body.

Acknowledgments

This work was supported by Kakenhi from the Japan Society for the Promotion of Science, by a research project grant awarded by the Azabu University, and by Core Stage Backup Grants from Kyoto University.

References

[1] C.S. Stump, E.J. Henriksen, Y. Wei, J.R. Sowers, The metabolic syndrome: role of skeletal muscle metabolism, Ann. Med. 38 (2006) 389–402.
[2] S. Biressi, M. Molinaro, G. Cossu, Cellular heterogeneity during vertebrate skeletal muscle development, Dev. Biol. 308 (2007) 281–293.
[3] B.K. Pedersen, M.A. Febbraio, Muscle as an endocrine organ: focus on muscle-derived interleukin-6, Physiol. Rev. 88 (2008) 1379–1406.
[4] B.K. Pedersen, The diseasome of physical inactivity—and the role of myokines in muscle–fat cross talk, J. Physiol. 587 (2009) 5559–5568.
[5] K. Walsh, Adipokines, myokines and cardiovascular disease, Circ. J. 73 (2009) 13–18.
[6] D.C. Ludolph, S.F. Konieczny, Transcription factor families: muscling in on the myogenic program, FASEB J. 9 (1995) 1595–1604.
[7] R.L. Perry, M.A. Rudnicki, Molecular mechanisms regulating myogenic determination and differentiation, Front. Biosci. 5 (2000) D750–D767.
[8] F. Lluís, E. Perdiguero, A.R. Nebreda, P. Muñoz-Cánoves, Regulation of skeletal muscle gene expression by p38 MAP kinases, Trends Cell Biol. 16 (2006) 36–44.
[9] J.M. Wozney, V. Rosen, A.J. Celeste, L.M. Mitsock, M.J. Whitters, R.W. Kriz, R.M. Hewick, E.A. Wang, Novel regulators of bone formation: molecular clones and activities, Science 242 (1988) 1528–1534.
[10] K. Miyazono, Y. Kamiya, M. Morikawa, Bone morphogenetic protein receptors and signal transduction, J. Biochem. 147 (2010) 35–51.
[11] T. Katagiri, A. Yamaguchi, M. Komaki, E. Abe, N. Takahashi, T. Ikeda, V. Rosen, J.M. Wozney, A. Fujisawa-Sehara, T. Suda, Bone morphogenetic protein-2 converts the differentiation pathway of C2C12 myoblasts into the osteoblast lineage, J. Cell Biol. 127 (1994) 1755–1766.
[12] E. Chalaux, T. López-Rovira, J.L. Rosa, R. Bartrons, F. Ventura, JunB is involved in the inhibition of myogenic differentiation by bone morphogenetic protein-2, J. Biol. Chem. 273 (1998) 537–543.
[13] H. Aoki, M. Fujii, T. Imamura, K. Yagi, K. Takehara, M. Kato, K. Miyazono, Synergistic effects of different bone morphogenetic protein type I receptors on alkaline phosphatase induction, J. Cell Sci. 114 (2001) 1483–1489.
[14] S. Maeda, M. Hayashi, S. Komiya, T. Imamura, K. Miyazono, Endogenous TGF-β signaling suppresses maturation of osteoblastic mesenchymal cells, EMBO J. 23 (2004) 552–563.
[15] J. Nojima, K. Kanomata, Y. Takada, T. Fukuda, S. Kokabu, S. Ohte, T. Takada, T. Tsukui, T.S. Yamamoto, H. Sasanuma, K. Yoneyama, N. Ueno, Y. Okazaki, R. Kamijo, T. Yoda, T. Katagiri, Dual roles of smad proteins in the conversion from myoblasts to osteoblastic cells by bone morphogenetic proteins, J. Biol. Chem. 285 (2010) 15577–15586.
[16] R. Benezra, R.L. Davis, D. Lockshon, D.L. Turner, H. Weintraub, The protein Id: a negative regulator of helix–loop–helix DNA binding proteins, Cell 61 (1990) 49–59.
[17] X.H. Sun, N.G. Copeland, N.A. Jenkins, D. Baltimore, Id proteins Id1 and Id2 selectively inhibit DNA binding by one class of helix–loop–helix proteins, Mol. Cell. Biol. 11 (1991) 5603–5611.
[18] F. Viñals, F. Ventura, Myogenin protein stability is decreased by BMP-2 through a mechanism implicating Id1, J. Biol. Chem. 279 (2004) 45766–45772.
[19] Y. Furutani, T. Umemoto, M. Murakami, T. Matsui, M. Funaba, Role of endogenous TGF-β family in myogenic differentiation of C2C12 cells, J. Cell. Biochem. 112 (2011) 614–624.
[20] D. Yaffe, O. Saxel, Serial passaging and differentiation of myogenic cells isolated from dystrophic mouse muscle, Nature 270 (1977) 725–727.
[21] P.K. Smith, R.I. Krohn, G.T. Hermanson, A.K. Mallia, F.H. Gartner, M.D. Provenzano, E.K. Fujimoto, N.M. Goeke, B.J. Olson, D.C. Klenk, Measurement of protein using bicinchoninic acid, Anal. Biochem. 150 (1985) 76–85.
[22] Y. Furutani, M. Murakami, M. Funaba, Differential responses to oxidative stress and calcium influx on expression of the transforming growth factor-β family in myoblasts and myotubes, Cell Biochem. Funct. 27 (2009) 578–582.
[23] M. Murakami, H. Kawachi, K. Ogawa, Y. Nishino, M. Funaba, Receptor expression modulates the specificity of transforming growth factor-b signaling pathways, Genes Cells 14 (2009) 469–482.
[24] C. Labarca, K. Paigen, A simple, rapid, and sensitive DNA assay procedure, Anal. Biochem. 102 (1980) 344–352.
[25] D. Joulia, H. Bernardi, V. Garandel, F. Rabenoelina, B. Vernus, G. Cabello, Mechanisms involved in the inhibition of myoblast proliferation and differentiation by myostatin, Exp. Cell Res. 286 (2003) 263–275.
[26] H.H. Arnold, B. Winter, Muscle differentiation: more complexity to the network of myogenic regulators, Curr. Opin. Genet. Dev. 8 (1998) 539–544.
[27] C. Chang, Agonists and antagonists of the TGF-β family ligands, in: R. Derynck, K. Miyazono (Eds.), The TGF-β Family, Cold Spring Harbor Laboratory Press, Cold Spring Harbor, 2008, pp. 203–257.
[28] M. Kitzmann, G. Carnac, M. Vandromme, M. Primig, N.J. Lamb, A. Fernandez, The muscle regulatory factors MyoD and Myf-5 undergo distinct cell cycle-specific expression in muscle cells, J. Cell Biol. 142 (1998) 1447–1459.

[29] N. Yoshida, S. Yoshida, K. Koishi, K. Masuda, Y. Nabeshima, Cell heterogeneity upon myogenic differentiation: down-regulation of MyoD and Myf-5 generates 'reserve cells', J. Cell Sci. 111 (1998) 769–779.
[30] M. Menconi, P. Gonnella, V. Petkova, S. Lecker, P.O. Hasselgren, Dexamethasone and corticosterone induce similar, but not identical, muscle wasting responses in cultured L6 and C2C12 myotubes, J. Cell. Biochem. 105 (2008) 353–364.
[31] J.E. Felin, J.L. Mayo, T.J. Loos, J.D. Jensen, D.K. Sperry, S.L. Gaufin, C.A. Meinhart, J.B. Moss, L.C. Bridgewater, Nuclear variants of bone morphogenetic proteins, BMC Cell Biol. 11 (2010) 20.
[32] S.H. Cho, C.D. Toouli, G.H. Fujii, C. Crain, D. Parry, Chk1 is essential for tumor cell viability following activation of the replication checkpoint, Cell Cycle 4 (2005) 131–139.
[33] T.J. Brennan, E.N. Olson, Myogenin resides in the nucleus and acquires high affinity for a conserved enhancer element on heterodimerization, Genes Dev. 4 (1990) 582–595.
[34] T.A. Samad, A. Rebbapragada, E. Bell, Y. Zhang, Y. Sidis, S.J. Jeong, J.A. Campagna, S. Perusini, D.A. Fabrizio, A.L. Schneyer, H.Y. Lin, A.H. Brivanlou, L. Attisano, C.J. Woolf, DRAGON, a bone morphogenetic protein co-receptor, J. Biol. Chem. 280 (2005) 14122–14129.
[35] J.L. Babitt, Y. Zhang, T.A. Samad, Y. Xia, J. Tang, J.A. Campagna, A.L. Schneyer, C.J. Woolf, H.Y. Lin, Repulsive guidance molecule (RGMa), a DRAGON homologue, is a bone morphogenetic protein co-receptor, J. Biol. Chem. 280 (2005) 29820–29827.
[36] J.L. Babitt, F.W. Huang, D.M. Wrighting, Y. Xia, Y. Sidis, T.A. Samad, J.A. Campagna, R.T. Chung, A.L. Schneyer, C.J. Woolf, N.C. Andrews, H.Y. Lin, Bone morphogenetic protein signaling by hemojuvelin regulates hepcidin expression, Nat. Genet. 38 (2006) 531–539.
[37] A.S. Zhang, S.A. Anderson, K.R. Meyers, C. Hernandez, R.S. Eisenstein, C.A. Enns, Evidence that inhibition of hemojuvelin shedding in response to iron is mediated through neogenin, J. Biol. Chem. 282 (2007) 12547–12556.
[38] L. Lin, Y.P. Goldberg, T. Ganz, Competitive regulation of hepcidin mRNA by soluble and cell-associated hemojuvelin, Blood 106 (2005) 2884–2889.
[39] R. Derynck, R.J. Akhurst, Differentiation plasticity regulated by TGF-β family proteins in development and disease, Nat. Cell Biol. 9 (2007) 1000–1004.

International Journal of Systematic and Evolutionary Microbiology (2011), **61**, 2610–2615 **DOI** 10.1099/ijs.0.024521-0

Bifidobacterium kashiwanohense sp. nov., isolated from healthy infant faeces

Hidetoshi Morita,[1] Akiyo Nakano,[1] Hiromi Onoda,[1] Hidehiro Toh,[2] Kenshiro Oshima,[3] Hideto Takami,[4] Masaru Murakami,[1] Shinji Fukuda,[5, 6] Tatsuya Takizawa,[1] Tomomi Kuwahara,[7] Hiroshi Ohno,[5, 6] Soichi Tanabe[8] and Masahira Hattori[3]

Correspondence
Hidetoshi Morita
morita@azabu-u.ac.jp

[1]School of Veterinary Medicine, Azabu University, 1-17-71 Fuchinobe, Sagamihara, Kanagawa 229-8501, Japan

[2]Advanced Science Institute, RIKEN, 1-7-22 Suehiro, Tsurumi, Yokohama, Kanagawa 230-0045, Japan

[3]Graduate School of Frontier Sciences, The University of Tokyo, 5-1-5 Kashiwanoha, Kashiwa, Chiba 277-8562, Japan

[4]Microbial Genome Research Group, Japan Agency of Marine-Earth Science and Technology, 2-15 Natsushima, Yokosuka, Kanagawa 237-0061, Japan

[5]Laboratory for Epithelial Immunobiology, RIKEN Research Center for Allergy and Immunology, 1-7-22 Suehiro, Tsurumi, Yokohama, Kanagawa 230-0045, Japan

[6]Graduate School of Nanobioscience, Yokohama City University, 1-7-29 Suehiro, Tsurumi, Yokohama, Kanagawa 230-0045, Japan

[7]Department of Molecular Bacteriology, Institute of Health Biosciences, University of Tokushima, Graduate School, 3-18-15 Kuramoto-cho, Tokushima 770-8503, Japan

[8]Graduate School of Biosphere Science, Hiroshima University, 1-4-4 Kagamiyama, Higashi-Hiroshima, Hiroshima 739-8528, Japan

Strains HM2-1 and HM2-2^T were isolated from the faeces of a healthy infant and were characterized by determining their phenotypic and biochemical features and phylogenetic positions based on partial 16S rRNA gene sequence analysis. They were Gram-positive, obligately anaerobic, non-spore-forming, non-gas-producing, and catalase-negative non-motile rods. They did not grow at 15 or 45 °C in anaerobic bacterial culture medium, and their DNA G+C content was in the range 56–59 mol%. In enzyme activity tests, strains HM2-1 and HM2-2^T were positive for α/β-galactosidases and α/β-glucosidases but negative for β-glucuronidase and cystine arylamidase. An analysis of the cell-wall composition of strains HM2-1 and HM2-2^T revealed the presence of glutamic acid, alanine and lysine. The presence of fructose-6-phosphate phosphoketolase shows that isolates HM2-1 and HM2-2^T are members of the genus *Bifidobacterium*. These two isolates belong to the same species of the genus *Bifidobacterium*. Strain HM2-2^T was found to be related to *Bifidobacterium catenulatum* JCM 1194^T (97.4 % 16S rRNA gene sequence identity: 1480/1520 bp), *Bifidobacterium pseudocatenulatum* JCM 1200^T (97.2 %: 1472/1514 bp), *Bifidobacterium dentium* ATCC 27534^T (96.7 %: 1459/1509 bp) and *Bifidobacterium angulatum* ATCC 27535^T (96.5 %: 1462/1515 bp). The predominant cellular fatty acids of strains HM2-1 and HM2-2^T were 16 : 0 and 18 : 1ω9*c*, with proportions greater than 18 % of the total. Phylogenetic analyses involving phenotypic characterization, DNA–DNA hybridization and partial 16S rRNA gene sequencing proves that the strains represent a novel species of the genus *Bifidobacterium*, for which the name *Bifidobacterium kashiwanohense* sp. nov. is proposed. The type strain is HM2-2^T (=JCM 15439^T =DSM 21854^T).

The GenBank/EMBL/DDBJ accession numbers for the 16S rRNA and partial *hsp60* gene sequences of strain HM2-1 are AB491757 and AB578933, respectively. Those for strain HM2-2^T are AB425276.2 and AB491759.2, respectively.

Four supplementary figures are available with the online version of this paper.

The genus *Bifidobacterium* represents one of the bacterial groups within the class *Actinobacteria* and is prevalent within the gastrointestinal tracts of humans and animals (Mikkelsen *et al.*, 2003). At the time of writing, the genus *Bifidobacterium* is represented by over 30 species and subspecies, and the type strains of *Bifidobacterium adolescentis*, *B. angulatum*, *B. bifidum*, *B. breve*, *B. catenulatum*, *B. dentium*, *B. longum* subsp. *infantis*, *B. longum* subsp. *longum*, *B. pseudocatenulatum* and *B. scardovii* were isolated from human specimens (Scardovi, 1986; Hoyles *et al.*, 2002; Sakata *et al.*, 2002). The bifidobacteria have not been found to cause human diseases; instead, they are considered to be probiotic micro-organisms (Fuller, 1991; Ventura *et al.*, 2009; Whorwell *et al.*, 2006; Brenner *et al.*, 2009).

During our studies, two isolates, HM2-1 and HM2-2^T, from faeces of a healthy infant were not identified to the species level. Our results show that these isolates represent a novel *Bifidobacterium* species, for which the name *Bifidobacterium kashiwanohense* sp. nov. is proposed.

We isolated 51 strains of putative bifidobacteria inhabiting the faeces of a healthy infant (male; 1.5 years old) in 2008. Blood liver (BL) agar plates (Eiken Chemical) and anaerobic bacterial culture medium (ABCM broth; Eiken Chemical) were used for cell cultures. All 51 isolates were anaerobically cultured at 37 °C in ABCM broth and on BL agar plates for 24 and 72 h, respectively. Of the 51 isolates, *Bifidobacterium longum* subsp. *longum* (20 strains), *B. longum* subsp. *infantis* (2 strains), *B. bifidum* (6 strains) and *B. breve* (3 strains) were identified, whereas the other isolates (20 strains) were not identified to the species level. Of the 20 other isolates, the unidentified strains HM2-1 and HM2-2^T formed a subcluster in the genus *Bifidobacterium* in the taxonomic study. Strains HM2-1 and HM2-2^T were found to be Gram-positive, obligately anaerobic, non-spore-forming, non-gas-producing and catalase-negative non-motile rods. Table 1 shows the major characteristics of isolates HM2-1 and HM2-2^T, and the related strains *B. catenulatum* JCM 1194^T, *B. pseudocatenulatum* JCM 1200^T, *B. dentium* JCM 1195^T and *B. angulatum* JCM 7096^T. The results were recorded after 48 h at 37 °C. The isomer of lactic acid produced from D-glucose was determined by using an F-kit [D(−)-lactic acid/L(+)-lactic acid; Roche]. Other biochemical tests on motility, growth at a fixed temperature and gas production from D-glucose were performed using the methods described by Mitsuoka (1969). The optimal temperature for growth of strains HM2-1, HM2-2^T, JCM 7096^T and JCM 1194^T was 37 °C; no growth was observed at 15 or 45 °C in ABCM broth. Although all strains grew at pH 7.2 and pH 8.0, no growth was observed at pH 4.5. *B. pseudocatenulatum* JCM 1200^T grew weakly at 45 °C and pH 4.5. *B. dentium* JCM 1195^T grew at pH 4.5. Acid production from carbohydrates in ABCM broth is shown in Table 1. For the determination of phenotypic characteristics, API ZYM tests (bioMérieux) were performed in duplicate using the methods recommended by the manufacturer. Cells were collected from each ABCM culture by centrifugation at 12 000 r.p.m. for 5 min, inoculated onto the test strips and incubated for 4 h at 37 °C. Nineteen enzymic activities were estimated by the API ZYM tests, and strains HM2-1 and HM2-2^T showed 7 enzymic activities (Table 1). Enzyme activity tests were positive for α/β-galactosidases and α/β-glucosidases but negative for β-glucuronidase and cystine arylamidase. Isolates HM2-1 and HM2-2^T had fructose-6-phosphate phosphoketolase activity like the reference strains (Biavati & Mattarelli, 1991; Gavini *et al.*, 1991). An analysis of the cell-wall composition revealed the presence of glutamic acid, alanine and lysine by ultraperformance liquid chromatography according to the methods described by Komagata & Suzuki (1987). The ACQUITY UPLC System (Waters) was used in this study. Whole-cell fatty acid methyl

Table 1. Physiological characteristics of isolates HM2-1 and HM2-2^T and the type strains of closely related species of the genus *Bifidobacterium*

Strains: 1, HM2-1; 2, HM2-2^T; 3, *B. catenulatum* JCM 1194^T; 4, *B. pseudocatenulatum* JCM 1200^T; 5, *B. dentium* JCM 1195^T; 6, *B. angulatum* JCM 7096^T. +, Positive; –, negative; W, weakly positive. All strains were positive for the following characteristics: fermentation of glucose, fructose, mannose, maltose and sucrose; growth in ABCM broth at 37 °C, at intial pH 7.2 and 8.0, and under anaerobic conditions; no growth in ABCM broth at 15 °C under anaerobic conditions. All strains produced L-lactic acid and did not produce gas from D-glucose. All strains produced acid from D-xylose, D-ribose, L-arabinose, D-glucose, D-galactose, sucrose, maltose, lactose, melibiose, raffinose and salicin. None of the strains produced acid from glycerol or rhamnose. All strains possessed leucine arylamidase, α-galactosidase, β-galactosidase, α-glucosidase and β-glucosidase; none possessed alkaline phosphatase, esterase (C4), lipase (C14), valine arylamidase, trypsin, α-chymotrypsin, naphthol-AS-BI-phosphohydrolase, *N*-acetyl-β-glucosaminidase, α-mannosidase or α-fucosidase. DNA G+C contents were determined by HPLC.

Characteristic	1	2	3	4	5	6
Growth at:						
45 °C	−	−	−	W	−	−
Initial pH 4.5	−	−	−	W	+	−
Acid from:						
D-Mannose	+	W	−	+	+	−
Cellobiose	+	+	+	+	+	−
Trehalose	−	−	−	+	+	−
Melezitose	−	−	−	−	W	−
Dextrin	W	W	W	+	+	+
Starch	−	−	−	+	+	+
Inulin	−	W	−	−	−	+
D-Mannitol	−	−	−	−	+	−
D-Sorbitol	+	+	+	+	−	−
D-Fructose	+	+	+	+	W	+
API ZYM						
Esterase lipase (C8)	+	+	+	−	−	−
Cystine arylamidase	−	−	+	−	−	−
Acid phosphatase	+	+	+	+	+	−
β-Glucuronidase	−	−	−	−	+	−
DNA G+C content (mol%)	58.6	56.3	54.7	57.5	61.2	59.0

esters were obtained by saponification, methylation and extraction followed by analysis using a standardized Microbial Identification System (Microbial ID) (Tan *et al.*, 2010). The Sherlock standard library MOORE5 5.00 made it possible to standardize the bacterial fatty acid analysis (http://www.midi-inc.com) in Table 2.

The DNA G+C contents of strains HM2-1 and HM2-2^T were determined in three separate trials by high-performance liquid chromatography (Okamoto *et al.*, 2008). The DNA G+C contents of strains HM2-1 and HM2-2^T were 58.6 and 56.3 mol%, respectively. These differ from the values obtained for *B. catenulatum* JCM 1194^T and *B. dentium* JCM 1195^T, whose DNA G+C contents were 54.7 and 61.2 mol%, respectively (Scardovi & Crociani, 1974). However, the DNA G+C content of strains HM2-1 and HM2-2^T were similar to those of *B. pseudocatenulatum* JCM 1200^T (57.5 mol%) and *B. angulatum* JCM 7096^T (59.0 mol%) (Scardovi & Crociani, 1974; Scardovi *et al.*, 1979).

The 16S rRNA genes of strains HM2-1 and HM2-2^T were amplified by PCR using the universal primers 27F and 1492R (Weisburg *et al.*, 1991). The closest known relatives of the isolate were determined by performing database searches, and the sequences of closely related species were retrieved from public databases. Multiple alignments of the sequences were carried out using CLUSTAL W (Thompson *et al.*, 1994). We used the neighbour-joining method to reconstruct a phylogenetic tree (Saitou & Nei, 1987) and estimated the robustness of the individual branches by performing bootstrapping analysis with 1000 replicates (Felsenstein, 1985). Phylogenetic trees were also reconstructed using the maximum-likelihood (Cavalli-Sforza & Edwards, 1967) and maximum-parsimony (Kluge & Farris, 1969) methods with PHYLIP version 3.66. The partial 16S rRNA gene sequence of strain HM2-2^T was consistent with that of strain HM2-1. DNA–DNA hybridization was carried out using the microdilution-well technique, with photobiotin for DNA labelling (Ezaki *et al.*, 1989). Immobilized DNA in microdilution wells was incubated with a photobiotin-labelled DNA probe prepared from each strain at 48 °C for 3 h in hybridization buffer containing 50 % formamide, after 30 min of incubation at 37 °C in prehybridization buffer. The fluorescence intensity was measured with a MicroPlate reader (PerkinElmer) at a wavelength of 360 nm for excitation and 450 nm for emission. Values (%) of DNA–DNA hybridization were the mean of the two trials in this study. Strains HM2-1 and HM2-2^T shared high levels of DNA–DNA relatedness (92.1 %). We analysed the DNA profile by random amplified polymorphic DNA (RAPD) PCR performed using the random primers 103 (5′-GTGACGCCGC-3′), 127 (5′-ATCTGGCAGC-3′) and 173 (5′-CAGGCGGCGT-3′) (University of British Columbia) to compare strains HM2-1 and HM2-2^T. Their RAPD profiles (Supplementary Fig. S1 available in IJSEM Online) showed that they were different strains of the same species, supported by phenotypic and biochemical features and their phylogenetic position based on partial 16S rRNA gene sequence and DNA–DNA hybridization analyses.

Table 2. Cellular fatty acid contents (%) of isolates HM2-1 and HM2-2^T and the type strains of closely related species of the genus *Bifidobacterium*

Strains: 1, HM2-1; 2, HM2-2^T; 3, *B. catenulatum*; 4, *B. pseudocatenulatum*; 5, *B. dentium*; 6, *B. angulatum*. Data for reference strains were obtained from the standard Library MOORE5 5.00 of the Sherlock Microbial Identification System.

Fatty acid	1	2	3	4	5	6
10:0	1.6	2.1	0.7	1.2	0.7	1.5
12:0	3.8	8.1	1.3	2.9	1.2	2.7
11:0 DMA	0.6	0.8	0.7	0.5	0	0
14:0	6.8	15.9	5.3	10.5	5.1	8.4
14:0 DMA	2.7	3.3	3.5	2.7	2.9	2.1
16:1ω9*c*	3.4	6.3	2.2	2.2	1.8	2.6
16:1ω7*c*	0	0	1.8	3.9	1.1	2.6
16:0	30.3	26.8	25.7	13.7	25.8	18.1
16:0 DMA	0.9	0.7	0.5	0	0	0
16:1ω7*c* DMA	0	0	1.1	0.5	0	0.6
17:0 anteiso	0	0	0	0.7	0	0
18:2ω6,9*c*	0.8	1.1	0	0	0	0
18:1ω9*c*	18.1	19.4	18.3	33.6	22.8	33.5
18:0	6.1	2.5	3.3	2.3	6.9	3.7
18:1ω7*c* DMA	0	0	0.6	0	0	0
18:0 12-OH	0	0	1.5	0	0.6	0
18:1ω9*c* DMA	19.1	9.1	23.3	12.2	23.2	14.3
18:0 DMA	0	0	0	0	0.6	0

Two organisms are considered to represent the same species if their purified DNA exhibits greater than 70 % hybridization (Wayne *et al.*, 1987). DNA–DNA hybridization analysis was carried out comparing isolates HM2-1 and HM2-2^T and other related strains listed in Table 1 according to the method previously by Ezaki *et al.* (1989). DNA–DNA relatedness values between strain HM2-2^T and *B. catenulatum* JCM 1194^T were 8.1 %±1.6 % and 14.6 %±2.4 % using the probes for HM2-2^T and *B. catenulatum* JCM 1194^T, respectively. DNA–DNA relatedness values using the reference strains as DNA probes for strain HM2-2^T were as follows: HM2-2^T and *B. pseudocatenulatum* JCM 1200^T (6.5 %), HM2-2^T and *B. dentium* JCM 1195^T (5.7 %), and HM2-2^T and *B. angulatum* JCM 7096^T (6.8 %).

We reconstructed a phylogenetic tree based on a total of 44 partial 16S rRNA gene sequences, including those of members of the genus *Bifidobacterium* and related genera. The tree was rooted using *Actinomyces bovis* (Fig. 1). Strains HM2-1 and HM2-2^T had 16S rRNA gene sequences that were similar to those of *B. catenulatum*, *B. angulatum* and *B. dentium*. Levels of similarity for the partial 16S rRNA gene sequence of HM2-2^T in relation to *B. catenulatum* JCM 1194^T, *B. pseudocatenulatum* JCM 1200^T, *B. dentium* ATCC 27534^T and *B. angulatum*

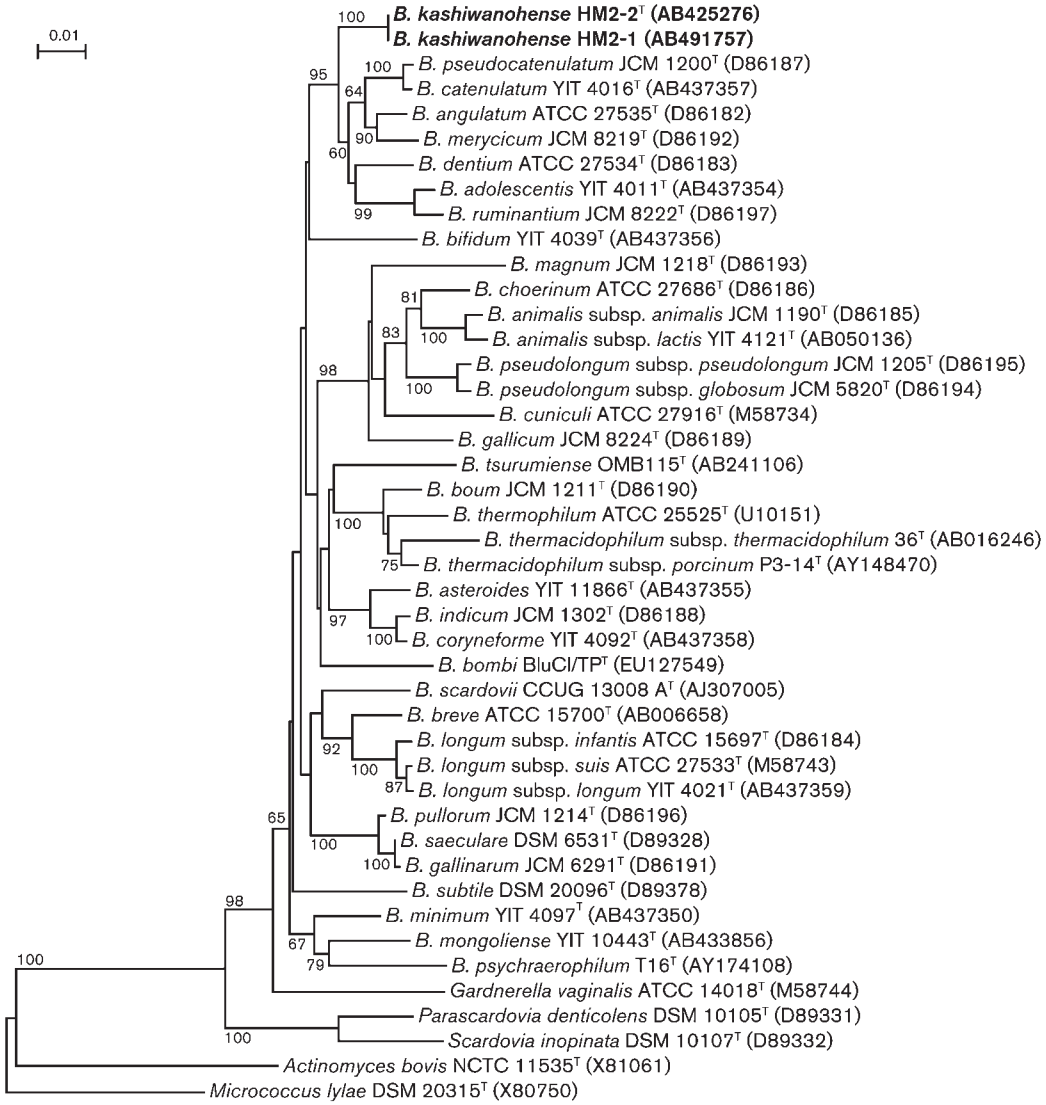

Fig. 1. Phylogenetic relationship between isolates HM2-1 and HM2-2^T, species of the genus *Bifidobacterium* and related genera, determined by 16S rRNA gene sequencing. The tree was reconstructed using the neighbour-joining method. *Actinomyces bovis* NCTC 11535^T was used as an outgroup. Bootstrap percentages (based on 1000 replicates) are shown at nodes; values lower than 50 % are not indicated. Accession numbers are given in parentheses. Bar, 10 % difference in nucleotide sequence.

ATCC 27535^T were 97.4 % (1480/1520 bp), 97.2 % (1472/1514 bp), 96.7 % (1459/1509 bp) and 96.5 % (1462/1515 bp), respectively. We obtained identical tree topologies in the maximum-parsimony and maximum-likelihood analyses (Supplementary Figs S2 and S3).

Heat-shock protein (*hsp60*; also known as *groEL*, *cpn60*, *groES* or *dnaK*) genes have also been adopted for taxonomic studies of bifidobacterial species (Jian *et al.*, 2001; Zhu *et al.*, 2003; Simpson *et al.*, 2004; Delcenserie *et al.*, 2005; Ventura *et al.*, 2005). The partial *hsp60* gene sequence of strain HM2-2^T was obtained by using the conditions and primers for PCR amplification described by Jian *et al.* (2001) and Okamoto *et al.* (2008). We reconstructed a phylogenetic tree based on a total of 40 sequences of *hsp60* genes, including those of members of the genus *Bifidobacterium* and related genera (Supplementary Fig. S4). Levels of similarity for the partial *hsp60* gene sequence of HM2-2^T in relation to *B. catenulatum* JCM 1194^T, *B. pseudocatenulatum* JCM 1200^T, *B. dentium* ATCC 27534^T and *B. angulatum* ATCC 27535^T were 96.1 % (567/590 bp), 90.8 % (536/590 bp), 92.0 % (544/591 bp) and 89.8 % (531/591 bp), respectively. The 16S rRNA and *hsp60* gene sequences were well related and useful for determining the phylogeny of strain HM2-2^T.

Detailed characteristics of the novel isolates are provided in the species description and in Table 1, and these characteristics were compared with those of the phylogenetic relatives

B. catenulatum JCM 1194^T, *B. pseudocatenulatum* JCM 1200^T, *B. angulatum* JCM 7096^T and *B. dentium* JCM 1195^T. The isolates were able to produce L(+)-lactic acid from D-glucose. Anaerobic conditions were essential for the growth of strains HM2-1 and HM2-2^T. These two isolates could be distinguished from *B. pseudocatenulatum* JCM 1200^T, *B. angulatum* JCM 7096^T and *B. dentium* JCM 1195^T by the pattern of acid production from D-mannose, cellobiose, trehalose, melezitose, dextrin, starch, inulin, D-mannitol, D-sorbitol and D-fructose. The cellular fatty acid profiles of strains HM2-1, HM2-2^T and the related genera *B. catenulatum*, *B. pseudocatenulatum*, *B. dentium* and *B. angulatum* are presented in Table 2. The predominant cellular fatty acids of strains HM2-1 and HM2-2^T were 16 : 0 and 18 : 1ω9*c*, with proportions greater than 18 % of the total.

Experimental data suggest that isolates HM2-1 and HM2-2^T can be assigned to the genus *Bifidobacterium* on the basis of their phylogenetic position; it can be concluded that these two isolates might be considered as representing a single novel species. Thus, these two isolates represent a novel species, for which we propose the name *Bifidobacterium kashiwanohense* sp. nov.

Description of *Bifidobacterium kashiwanohense* sp. nov.

Bifidobacterium kashiwanohense (ka.shi.wa.no.hen′se. N.L. neut. adj. *kashiwanohense* of Kashiwanoha in Japan, which is the name of the area, University of Tokyo, where this bacterium was originally isolated).

Cells are Gram-positive, non-motile, non-spore-forming rods measuring 1.0 × 1.3 μm. Colonies on BL agar after incubation under anaerobic conditions for 2 days at 37 °C are beige, smooth and approximately 1.0 mm in diameter. No growth is observed at 15 or 45 °C. Produces L(+)-lactic acid from D-glucose. Produces acid from D-xylose, D-ribose, D-mannose, cellobiose, D-sorbitol, L-arabinose, D-glucose, D-fructose, D-galactose, sucrose, maltose, lactose, melibiose, raffinose and salicin, and, to a weaker extent, from dextrin. Exhibits esterase lipase (C8), leucine arylamidase, acid phosphatase, α-galactosidase, β-galactosidase, α-glucosidase, β-glucosidase, and fructose-6-phosphate phosphoketolase activities. The cell wall contains glutamic acid, alanine and lysine. The DNA G+C content is 56–59 mol%.

The type strain is HM2-2^T (=JCM 15439^T =DSM 21854^T), isolated from faeces of a healthy infant (1.5 years old).

Acknowledgements

We wish to thank the Matching Fund Subsidy for financial support.

References

Biavati, B. & Mattarelli, P. (1991). *Bifidobacterium ruminantium* sp. nov. and *Bifidobacterium merycicum* sp. nov. from the rumens of cattle. *Int J Syst Bacteriol* **41**, 163–168.

Brenner, D. M., Moeller, M. J., Chey, W. D. & Schoenfeld, P. S. (2009). The utility of probiotics in the treatment of irritable bowel syndrome: a systematic review. *Am J Gastroenterol* **104**, 1033–1049, quiz 1050.

Cavalli-Sforza, L. L. & Edwards, A. W. F. (1967). Phylogenetic analysis. Models and estimation procedures. *Am J Hum Genet* **19**, 233–257.

Delcenserie, V., Bechoux, N., China, B., Daube, G. & Gavini, F. (2005). A PCR method for detection of bifidobacteria in raw milk and raw milk cheese: comparison with culture-based methods. *J Microbiol Methods* **61**, 55–67.

Ezaki, T., Hashimoto, Y. & Yabuuchi, E. (1989). Fluorometric deoxyribonucleic acid-deoxyribonucleic acid hybridization in micro-dilution wells as an alternative to membrane filter hybridization in which radioisotopes are used to determine genetic relatedness among bacterial strains. *Int J Syst Bacteriol* **39**, 224–229.

Felsenstein, J. (1985). Confidence limits on phylogenies: an approach using the bootstrap. *Evolution* **39**, 783–791.

Fuller, R. (1991). Probiotics in human medicine. *Gut* **32**, 439–442.

Gavini, F., Pourcher, A. M., Neut, C., Monget, D., Romond, C., Oger, C. & Izard, D. (1991). Phenotypic differentiation of bifidobacteria of human and animal origins. *Int J Syst Bacteriol* **41**, 548–557.

Hoyles, L., Inganäs, E., Falsen, E., Drancourt, M., Weiss, N., McCartney, A. L. & Collins, M. D. (2002). *Bifidobacterium scardovii* sp. nov., from human sources. *Int J Syst Evol Microbiol* **52**, 995–999.

Jian, W., Zhu, L. & Dong, X. (2001). New approach to phylogenetic analysis of the genus *Bifidobacterium* based on partial HSP60 gene sequences. *Int J Syst Evol Microbiol* **51**, 1633–1638.

Kluge, A. G. & Farris, F. S. (1969). Quantitative phyletics and the evolution of anurans. *Syst Zool* **18**, 1–32.

Komagata, K. & Suzuki, K. (1987). Lipid and cell wall analysis in bacterial systematics. *Methods Microbiol* **19**, 161–207.

Mikkelsen, L. L., Bendixen, C., Jakobsen, M. & Jensen, B. B. (2003). Enumeration of bifidobacteria in gastrointestinal samples from piglets. *Appl Environ Microbiol* **69**, 654–658.

Mitsuoka, T. (1969). [Comparative studies on lactobacilli from the faeces of man, swine and chickens]. *Zentralbl Bakteriol [Orig]* **210**, 32–51 (in German).

Okamoto, M., Benno, Y., Leung, K.-P. & Maeda, N. (2008). *Bifidobacterium tsurumiense* sp. nov., from hamster dental plaque. *Int J Syst Evol Microbiol* **58**, 144–148.

Saitou, N. & Nei, M. (1987). The neighbor-joining method: a new method for reconstructing phylogenetic trees. *Mol Biol Evol* **4**, 406–425.

Sakata, S., Kitahara, M., Sakamoto, M., Hayashi, H., Fukuyama, M. & Benno, Y. (2002). Unification of *Bifidobacterium infantis* and *Bifidobacterium suis* as *Bifidobacterium longum*. *Int J Syst Evol Microbiol* **52**, 1945–1951.

Scardovi, V. (1986). Genus *Bifidobacterium*. In *Bergey's Manual of Systematic Bacteriology*, **vol. 2**, pp. 1418–1434. Edited by P. H. A. Sneath, N. S. Mair, M. E. Sharpe & J. G. Holt. Baltimore: Williams & Wilkins.

Scardovi, V. & Crociani, F. (1974). *Bifidobacterium catenulatum*, *Bifidobacterium dentium*, and *Bifidobacterium angulatum*: three new species and their deoxyribonucleic acid homology relationships. *Int J Syst Bacteriol* **24**, 6–20.

Scardovi, V., Trovatelli, L. D., Biavati, B. & Zani, G. (1979). *Bifidobacterium cuniculi*, *Bifidobacterium choerinum*, *Bifidobacterium boum*, and *Bifidobacterium pseudocatenulatum*: four new species and their deoxyribonucleic acid homology relationships. *Int J Syst Bacteriol* **29**, 291–311.

Simpson, P. J., Ross, R. P., Fitzgerald, G. F. & Stanton, C. (2004). *Bifidobacterium psychraerophilum* sp. nov. and *Aeriscardovia aeriphila* gen. nov., sp. nov., isolated from a porcine caecum. *Int J Syst Evol Microbiol* **54**, 401–406.

Tan, Y., Wu, M., Liu, H., Dong, X., Guo, Z., Song, Z., Li, Y., Cui, Y., Song, Y. & other authors (2010). Cellular fatty acids as chemical markers for differentiation of *Yersinia pestis* and *Yersinia pseudotuberculosis*. *Lett Appl Microbiol* **50**, 104–111.

Thompson, J. D., Higgins, D. G. & Gibson, T. J. (1994). CLUSTAL W: improving the sensitivity of progressive multiple sequence alignment through sequence weighting, position-specific gap penalties and weight matrix choice. *Nucleic Acids Res* **22**, 4673–4680.

Ventura, M., Zink, R., Fitzgerald, G. F. & van Sinderen, D. (2005). Gene structure and transcriptional organization of the *dnaK* operon of *Bifidobacterium breve* UCC 2003 and application of the operon in bifidobacterial tracing. *Appl Environ Microbiol* **71**, 487–500.

Ventura, M., O'Flaherty, S., Claesson, M. J., Turroni, F., Klaenhammer, T. R., van Sinderen, D. & O'Toole, P. W. (2009). Genome-scale analyses of health-promoting bacteria: probiogenomics. *Nat Rev Microbiol* **7**, 61–71.

Wayne, L. G., Brenner, D. J., Colwell, R. R., Grimont, P. A. D., Kandler, O., Krichevsky, M. I., Moore, L. H., Moore, W. E. C., Murray, R. G. E. & other authors (1987). International Committee on Systematic Bacteriology. Report of the ad hoc committee on reconciliation of approaches to bacterial systematics. *Int J Syst Bacteriol* **37**, 463–464.

Weisburg, W. G., Barns, S. M., Pelletier, D. A. & Lane, D. J. (1991). 16S ribosomal DNA amplification for phylogenetic study. *J Bacteriol* **173**, 697–703.

Whorwell, P. J., Altringer, L., Morel, J., Bond, Y., Charbonneau, D., O'Mahony, L., Kiely, B., Shanahan, F. & Quigley, E. M. (2006). Efficacy of an encapsulated probiotic *Bifidobacterium infantis* 35624 in women with irritable bowel syndrome. *Am J Gastroenterol* **101**, 1581–1590.

Zhu, L., Li, W. & Dong, X. (2003). Species identification of genus *Bifidobacterium* based on partial HSP60 gene sequences and proposal of *Bifidobacterium thermacidophilum* subsp. *porcinum* subsp. nov. *Int J Syst Evol Microbiol* **53**, 1619–1623.

犬のてんかんの遺伝子解析

齋藤弥代子、十川剛（麻布大学　外科学第 2)、島倉秀勝、阪口雅弘（麻布大学微生物学第 1)

研究要旨

単一犬種における特発性てんかん罹患犬 10 頭と非罹患犬 22 頭のサンプルについて、イルミナ社の Chip array を用いて 17 万個の SNP を網羅的に解析したところ、特発性てんかん罹患犬群で変異の出現頻度の高い４つの SNP を認めた。特発性てんかん罹患犬群で変異の出現頻度が高かった SNP の幾つかは同一染色体上の一部の領域に存在し、高いオッズ比を示した。この領域には脳の機能に関わる遺伝子、ヒトのてんかんの原因となる遺伝子、さらに犬の症候性てんかんの関連遺伝子と同じ働きを持つ遺伝子が含まれていた。

研究目的

特発性てんかんは、人と同様に犬において最も一般的な神経疾患であるが、病因はほとんど分かっていない。遺伝的要因が疑われているが、関連遺伝子は 2 つしか明らかになっていない。人の本症において原因遺伝子が 20 ほど同定されていることを考えると、未同定の遺伝子変異がまだ多数存在すると考えられる。本疾患は原因が不明なため根治療法がなく、ほとんどの犬で、対症療法としてのてんかんを抑える薬の投与が生涯必要となる。本研究において、犬の特発性てんかんの原因遺伝子を同定し、病態機構を明らかにすることは、原因療法開発の糸口となり、獣医学の発展に大きく寄与できると考える。さらにその情報は、ヒトのてんかん医療に対しても有用性が高いと考える。

材料と方法

麻布大学附属動物病院神経科に来院し、特発性てんかんと診断された犬の血液サンプルの収集と臨床情報の収集を行った。

特発性てんかんの診断は、てんかん発作を 2 回以上起こしたことがあり、発作間欠期の神経学的検査と血液一般検査、さらに頭部 MRI にててんかん発作の原因となりうる異常がない場合とした。また、MRI を実施しない場合でも、初発のてんかん発作が１歳以上６歳未満であり、かつ、初発から 1 年以上にわたりてんかん発作以外の神経徴候を呈していなければ、一般的に特発性てんかんとして診断されるため((De Risio et al. BMC Veterinary Research (2015) 11:148)、それらを満たす場合も特発性てんかんとして本研究に含めた。遺伝子の保存と本研究使用に対する同意を飼い主から得た症例にて、血液一般検査時の残りの血液サンプルから、DNA 抽出を行った。発作時の徴候の詳細な問診とビデオ解析を行うとともに、可能な限り脳波検査も行い、それぞれの症例について、

発作型分類（発作の表現型の分類）を行った。

様々な犬種のサンプルが収集されたが、その中で、特発性てんかんが好発している単一犬種に着目し、罹患犬と非罹患犬の DNA を用いて、SNP アレイで網羅的な全ゲノム関連解析（GWAS）を行った。非罹患犬の DNA は遺伝子バンクに保管されている罹患犬種と同一犬種の検体を用いた。

GWAS によって絞った、てんかん発症と有意な関連性を示す SNP について、新たに検体を収集し確認実験を行った。新たな検体は、麻布大学附属動物病院神経科来院症例に加え、てんかんの診断や診療に長けた他の複数の施設からも収集した。確認実験では、ゲノム DNA をテンプレートとして、候補遺伝子に存在する SNP 領域の PCR を行った。

結果および考察

特発性てんかんと診断した計 143 頭から DNA サンプルが得られた。そのうち着目した一犬種からは、19 頭分のサンプルが得られた。

対象とした犬種の特発性てんかん罹患犬 10 頭と非罹患犬 22 頭のサンプルについて、イルミナ社の Chip array を用いて 17 万個の SNP を網羅的に解析したところ、特発性てんかん罹患犬群で変異の出現頻度の高い SNP を複数見出した（図 1、表１）。これらの幾つかは同一染色体上の一部の領域に存在し、高いオッズ比を示した。この領域には脳の機能に関わる遺伝子、ヒトのてんかんの原因となる遺伝子、さらに犬の症候性てんかんの関連遺伝子と同じ働きを持つ遺伝子が含まれていた。これら候補遺伝子の一つについては、犬の脳組織から抽出した mRNA を用いて RT-PCR を行い、犬で発現していることを確認した。

GWAS にててんかんとの関連性を持つ SNP が明らかになった犬種において、新規検体の収集を行った。新規罹患犬 9 頭と非罹患犬 13 頭の検体が収集された。検体数がさらに増えたのちに、発作型の解析と、ゲノム DNA をテンプレートとして、候補遺伝子に存在する SNP 領域の PCR を行うことによる確認実験を実施予定である。

本研究における特発性てんかん罹患犬 10 頭の発作型は、強直・間代発作 3 頭、焦点性運動発作 3 頭、行動発作 3 頭、自律神経発作 1 頭であった。血統書が入手できたのは 5 頭であり、同胎犬が 2 頭含まれていた。犬舎名の共通性を調べたところ、3 頭は一つの共通の犬舎名を持つ祖先を持っており、残り 2 頭も別の共通の犬舎名を持つ祖先を持っていた。

てんかん候補遺伝子を絞り込んだ犬種は、世界的にも一般的な犬種であり、表現型については、犬によく見られるタイプのてんかんであった。これに対し、現在までに報告のある犬のてんかんの関連遺伝子は、2 つとも比較的特殊な犬種における特殊なタイプのてんかんである。したがって、我々の成果をもとにしたこれからの研究は、より広く獣医療に貢献するものと考えられる。今後は症例数を増やして、発作型と遺伝子変異との関連性を調べる予定である。

遺伝子変異とてんかん発症の関連性を解析することと、原因遺伝子の機能解析とてんかん発症との関連の検討を行うことが、遺伝子同定のために実施すべき項目として残っている。

犬の特発性てんかんの候補遺伝子を絞り込んだが、同定までは至っていないため、研究を継続して、遺伝統計学的手法によって遺伝子変異とてんかん発症の関連性を解析し、さらに原因遺伝子の機能解析と発症との関連の検討を行う。そのために今後も研究を継続する。

図１．単一犬種における全ゲノム関連解析結果（マンハッタンプロット）

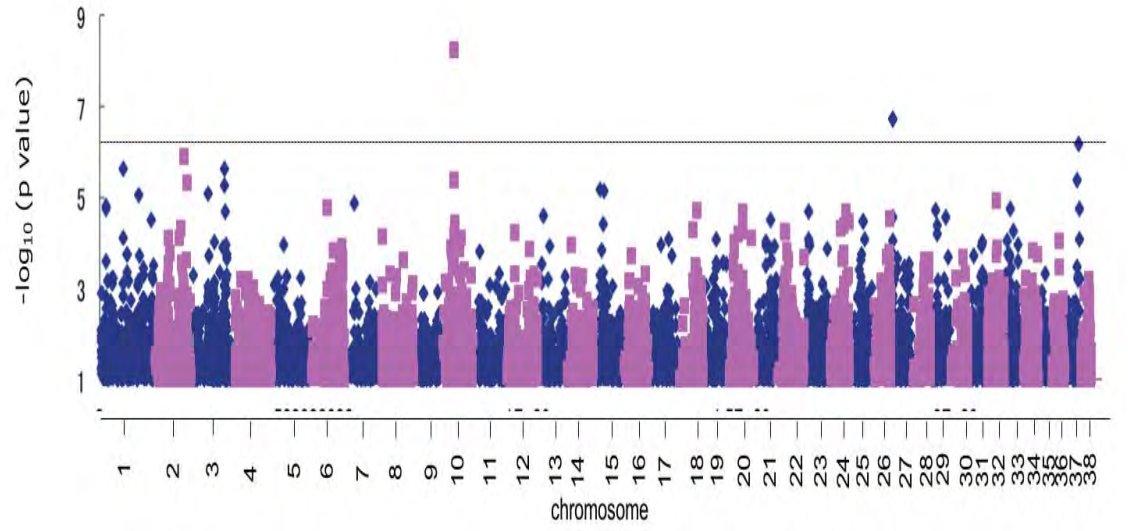

表１．罹患犬で高頻度に認められる SNP

順位	SNP (CanFam2.0)	染色体	F_A	F_U	CHISQ	OR	p値
1	BICF2S23126999	10	0.35	0.02273	13.46	23.15	5.67×10^{-9}
2	BICF2S23126865	10	0.35	0.02273	13.46	23.15	5.67×10^{-9}
3	BICF2G630137774	27	0.9	0.3636	15.88	15.75	1.88×10^{-7}
4	BICF2G630137812	27	0.9	0.3636	15.88	15.75	1.88×10^{-7}
5	BICF2G630133803	37	0.3	0.02273	10.85	18.43	6.67×10^{-7}
6	BICF2P1372847	2	0.25	0	11.93	NA	1.25×10^{-6}
7	BICF2P965671	1	0.4	0.06818	10.64	9.111	2.38×10^{-6}
8	BICF2P1172332	3	0.75	0.1818	19.28	13.5	2.39×10^{-6}
9	BICF2P413163	37	0.4	0.1136	6.966	5.2	4.01×10^{-6}
10	BICF2G630481165	10	0.35	0.02273	13.46	23.15	4.12×10^{-6}

研究発表

１. 論文発表

1) Ogawa M, Uchida K, Isobe K, Saito M, Harada T, Chambers JK, Nakayama H.: Globoid cell leukodystrophy (Krabbe's disease) in a Japanese domestic cat. Neuropathology 34,190-6, 2014.

2) Utsugi S, Saito M, Shelton D.: Resolution of polyneuropathy in a hypothyroid dog following thyroid supplementation. J Am Anim Hosp Assoc 50,345-9, 2014.

3) Kurihara Y, Suzuki T, Sakaue M, Murayama O, Miyazaki Y, Onuki A, Aoki T, Saito M, Fujii Y, Hisasue M, Tanaka K, Takizawa T.: Valproic acid, a histone deacetylase inhibitor, decreases proliferation of and induces specific neurogenic differentiation of canine adipose tissue-derived stem cells. J Vet Med Sci 76:15-23, 2014.

4) Tsuboi M, Uchida K, Ide T, Ogawa M, Inagaki T, Tamura S, Saito M, Chambers JK, Nakayama H.: Pathological features of polyneuropathy in three dogs. J Vet Med Sci 75,327-35, 2013.

5) Mizukami K, Kawamichi T, Koie H, Tamura S, Matsunaga S, Imamoto S, Saito M, Hasegawa D, Matsuki N, Tamahara S, Sato S, Yabuki A, Chang H, Yamato O.:Neuronal ceroid lipofuscinosis in border collie dogs in Japan: Clinical and molecular epidemiological study (2000-2011). ScientificWorldJournal Volume 2012 Article ID 383174, 7 pages, 2012.

6) 宇津木真一、齋藤弥代子：ミオキミア/ニューロミオトニアのヨークシャーテリアの1例. 日獣会誌、64, 56-60, 2011.

２. 学会発表

1) Nomura N, Saito M, Hasegawa D, Watanabe N. Uchida K, Okuno S, Nakai M, Orito K.: Clinical efficacy and safety of zonisamide monotherapy in dogs with newly diagnosed idiopathic epilepsy. 2015 ACVIM Forum, Indianapolis, June, 2015.

３. 知的財産の出願・登録状況

特許出願

1) 齋藤弥代子、横森稔「てんかん発作のモニタリングシステム及びモニタリング方法」, 特許公開 2014-21764(2014).

NEUROPATHOLOGY

Neuropathology 2014; **34**, 190–196 doi:10.1111/neup.12076

Case Report

Globoid cell leukodystrophy (Krabbe's disease) in a Japanese domestic cat

Mizue Ogawa,[1] Kazuyuki Uchida,[1] Kyoko Isobe,[3] Miyoko Saito,[2] Tomoyuki Harada,[1] James K. Chambers[1] and Hiroyuki Nakayama[1]

[1]Department of Veterinary Pathology, Graduate School of Agricultural and Life Sciences, The University of Tokyo, Tokyo, Departments of [2]Surgery II and [3]Veterinary Teaching Hospital, School of Veterinary Medicine, Azabu University, Kanagawa, Japan

A male Japanese domestic cat developed progressive limb paralysis from 4 months of age. The cat showed visual disorder, trismus and cognitive impairment and died at 9 months of age. At necropsy, significant discoloration of the white matter was observed throughout the brain and spinal cord. Histologically, severe myelin loss and gliosis were observed, especially in the internal capsule and cerebellum. In the lesions, severe infiltration of macrophages with broad cytoplasm filled with PAS-positive and non-metachromatic granules (globoid cells) was evident. On the basis of these findings, the case was diagnosed as feline globoid cell leukodystrophy (Krabbe's disease). Immunohistochemical observation indicated the involvement of oxidative stress and small HSP in the disease.

Key words: cat, central nervous system, globoid cell leukodystrophy, Krabbe's disease, macrophages.

INTRODUCTION

Globoid cell leukodystrophy (GLD; also known as Krabbe's disease) is an early-onset, rapidly progressive and fatal degenerative disease. The disease is pathologically characterized by almost complete myelin loss, reactive astrocytosis and the appearance of characteristic large round cells called globoid cells in the white matter of the CNS.[1] Diseases identical to GLD have been reported in several animal species:[2] dogs,[3,4] sheep,[5] rhesus monkeys[6,7] and cats.[8–10] GLD is defined by the deficiency of a lysosomal enzyme, galactocerebrosidase (GALC), resulting in the accumulation of a cytotoxic metabolite, psychosine.[1] GALC-deficient mice, such as Twitcher mice,[11,12] are being used as experimental GLD models.[13] Besides GALC, the deficiency of saposin A, [14] one of the sphingolipid activator proteins, also causes an identical disease to GLD in mice[15] and humans.[10] While GALC mutation was found in dogs[16] and rhesus monkeys.[17] To date, there have been only three reports of the disease in cats,[8–10] indicating that the disease is extremely rare in cats. These previous reports on feline GLD revealed histopathological features characterized by symmetrical myelin loss, astrocytosis and perivascular accumulation of large macrophages with intracytoplasmic deposits (globoid cells).

The present report describes histopathological, immunohistochemical and ultrastructural features of GLD in a young cat. In addition, immunohistochemistry for nitric oxide (NOS) and two types of small HSP (sHSP) was performed to assess the involvement of oxidative stress and/or sHSP, which are commonly upregulated in glial cells in patients with neurodegenerative diseases.[18]

CLINICAL SUMMARY

A male Japanese domestic cat had exhibited hind limb paresis since 4 months of age. Then the symptom progressed and clear tetraparesis developed. Although temporary recovery was achieved, loss of voluntary movement, trismus, and visual and cognitive impairment were observed during the last 2 months before death at 9 months of age. No significant findings were detected by X-ray examination or hematologic and biochemical analyses. The serum antibodies for feline immunodeficiency virus (FIV), feline leukemia virus (FeLV), feline coronavirus, feline parvovirus and *Toxoplasma* were all negative.

Correspondence: Kazuyuki Uchida, DVM, PhD, Department of Veterinary Pathology, Graduate School of Agricultural and Life Sciences, The University of Tokyo, 1-1-1 Yayoi, Bunkyo-ku, Tokyo 113-8657, Japan. Email: auchidak@mail.ecc.u-tokyo.ac.jp

Received 7 August 2013; revised 29 August 2013 and accepted 24 September 2013; published online 8 November 2013.

MATERIALS AND METHODS

Tissue samples including the brain, spinal cord and brachial plexus were fixed in 10% neutral-buffered formalin, processed routinely and embedded in paraffin wax. Paraffin sections 4 μm thick were stained with HE. Some selected sections were also subjected to PAS, toluidine blue (TB, pH 7.0), LFB, Sudan-black and von-Kossa staining. Immunohistochemistry was performed using the Envision polymer method. The primary antibodies used are listed in Table 1. Deparaffinized sections were first autoclaved at 120°C for 10 min in 10 mmol/L citrate buffer (pH 6.0) or Target retrieval solution (pH 9.0), for antigen retrieval. Then, the tissue sections were treated with 3% hydrogen peroxide (H_2O_2)-methanol at room temperature for 5 min and incubated in 8% skimmed milk–Tris-buffered saline with 0.2% Tween 20 (TBST) at 37°C for 1 h to avoid nonspecific reactions. The sections were then incubated at 4°C overnight with one of the primary antibodies. After washing three times in TBST, the sections were incubated with Envision horseradish peroxidase (HRP) mouse or rabbit polymer (Dako, Glostrup, Denmark) at 37°C for 40 min Then, the sections were washed with TBS and visualized with 0.05% 3-3'diaminobenzidine and 0.03% H_2O_2 in TBS. Counterstaining was performed with Mayer's hematoxylin.

For electron microscopic analysis, the formalin-fixed cerebellar white matter was fixed again in 2% glutaraldehyde in 0.1 mol/L phosphate buffer (PB) at 4°C for 2 h, and post-fixed in 1% OsO_4 at 4°C for 2 h. The samples were dehydrated in an ethanol series, replaced with QY-1 solution (Nisshin EM Corporation, Tokyo, Japan) and embedded in Quetol651 resin (Nisshin EM). Ultrathin sections were stained with uranyl acetate and lead citrate and examined with a Hitachi H-7500 transmission electron microscope (Hitachi High-Technologies, Tokyo, Japan).

PATHOLOGICAL FINDINGS

No marked gross lesions were detected in the CNS at necropsy, although discoloration of the white matter was observed on the cut surface of the formalin-fixed brain (Fig. 1) and spinal cord.

Histologically, thinning of the white matter was observed throughout the brain and spinal cord. LFB staining (Figs 2,3a) and immunostaining for myelin basic protein (MBP) revealed marked myelin loss in the white matter. Severe axonal degeneration characterized by swollen and fragmented axons (Fig. 3b) was also observed. Astrocytosis (Fig. 3c) and infiltration of ionized calcium-binding adapter molecule 1 (Iba-1)-positive cells (Fig. 3d) were frequently observed in the lesions. Oligodendrocyte transcription factor 2 (Olig2)-positive oligodendrocytes slightly decreased in number. These lesions were severe in the white matter of the internal capsule, cerebellum, medulla and spinal cord, but relatively less severe in the white matter of the cerebrum. In the deep white matter of the cerebellum, focal and symmetric necrosis was evident. In the necrotic areas, there were many calcified deposits forming psammoma bodies. The bodies were stained with LFB, PAS and von Kossa (Fig. 4).

Table 1 Primary antibodies used

Antibody	Type	Dilution	Source	Marker for	Antigen retrieval
GFAP	p	1:1000	Dako, Glostrup, Denmark	Astrocyte	None
NF	m	pre-diluted	Dako	Axon/neuron	None
pNF-H&M	m	1:1000	Millipore, MA, USA	–	None
MBP	p	1:200	Dako	Myelin	Citrate buffer, pH 6.0
Olig2	p	1:500	Millipore	Oligodendrocyte	Target retrieval solution (Dako), pH 9.0
CD3	p	1:50	Dako	T cell	Citrate buffer, pH 6.0
CD20	p	1:200	Thermo Scientific, CA, USA	B cell	None
Iba1	p	1:500	Wako Pure Chemical Industries, Osaka, Japan	Microglia/macrophage	Citrate buffer, pH 6.0
HLA-DR	m	1:100	Dako	Macrophage	Citrate buffer, pH 6.0
HSP27	p	1:100	Cell Signaling Technology, MA, USA	–	Citrate buffer, pH 6.0
αB-crystallin	m	1:1000	Santa Cruz Biotechnology, CA, USA	–	Citrate buffer, pH 6.0
iNOS	p	1:200	Calbiochem, CA, USA	–	Citrate buffer, pH 6.0
HO-1	p	1:100	ENZO Life Sciences, Plymouth Meeting, PA, USA	–	Citrate buffer, pH 6.0
SOD1	p	1:200	ENZO Life Sciences	–	Citrate buffer, pH 6.0
SOD2	p	1:200	ENZO Life Sciences	–	Citrate buffer, pH 6.0

HLA-DR, humanleukocyte antigen type DR; HO-1, heme oxygenase-1; Iba1, ionized calcium-binding adapter molecule 1; iNOS, inducible nitric oxide synthase; m, mouse monoclonal; MBP, myelin basic protein; NF, neurofilament; Olig2, oligodendrocyte transcription factor 2; p, rabbit polyclonal; SOD, superoxide dismutase.

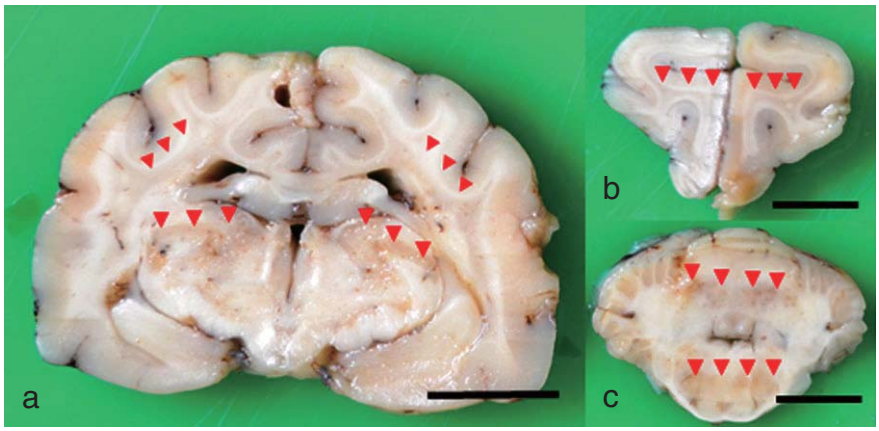

Fig. 1 Cut surfaces of the formalin-fixed brain. Severe discoloration throughout the white matter (arrowheads). (a) Cerebrum and thalamus, hypothalamus level. (b) Frontal lobe. (c) Cerebellum and ventral pons. Scale bar = 1 cm.

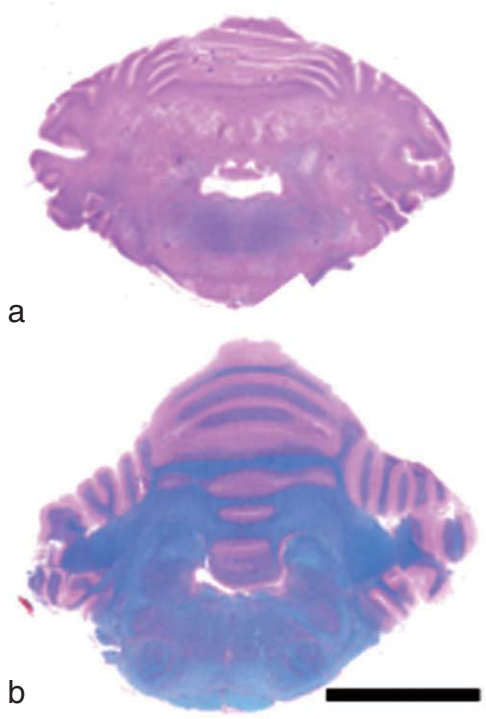

Fig. 2 The cerebellum. LFB-HE. (a) The present case. (b) A normal adult cat. Almost complete myelin loss is observed in the present case (a), compared with the control (b). Scale bar = 1 cm.

In the gray matter throughout the brain and spinal cord, prominent proliferation of gemistocytic astrocytes was observed. In the cerebellar cortex, there was moderate loss of granule cells and Purkinje cells with proliferation of Bergmann's glia. Neurofilament- and phosphorylated neurofilament-positive torpedoes were frequently observed in the granular cell layer (Fig. 5).

A large number of macrophages with broad cytoplasm and single or multiple eccentric nuclei (globoid cells) were observed in the lesions of the brain white matter, especially in the perivascular area (Fig. 6a). In the thoracic and lumbar cord, where myelin and axons were completely lost, there were a few globoid cells. Immunohistochemically, these globoid cells were strongly positive for Iba-1 (Fig. 6a, insertion) and HLA type DR (HLA-DR). The globoid cells had fine granular or filamentous deposits in their cytoplasm, which were PAS-positive (Fig. 6b), Sudan-black-negative and non-metachromatic by TB staining (Fig. 6c). Ultrastructural examination indicated the detailed features of the cytoplasmic deposits: variably sized, and straight and curved tubular structures (Fig. 6d). In the same area, mild perivascular infiltration of CD3-positive lymphocytes was also observed, whereas there was no infiltration of CD20-positive cells.

The results of immunohistochemistry also demonstrated that the cytoplasm of the globoid cells and of the few reactive astrocytes was positive for inducible nitric oxide (iNOS) (Fig. 7). Superoxide dismutase (SOD)1 expression was seen in reactive astrocytes and degenerated axons. Granules strongly positive for SOD2 were observed in cytoplasm of globoid cells, excluded by cytoplasmic deposit. Reactive astrocytes were occasionally positive for heme oxygenase-1 (HO-1).

On the other hand, reactive astrocytes were mostly positive for αB-crystallin in a broad area of the CNS. HSP27-positive astrocytes were rarely observed.

In the peripheral nerves including the brachial plexus, trigeminal nerve and dorsal and ventral roots of the spinal cord, various levels of myelin loss and axonal degeneration were observed, while there were no globoid cells in the lesions. No significant lesions were observed in the visceral organs.

DISCUSSION

Considering the severe myelin loss throughout the CNS and the appearance of characteristic globoid cells with intracellular PAS-positive and non-metachromatic deposits, the present case was diagnosed as feline GLD. In

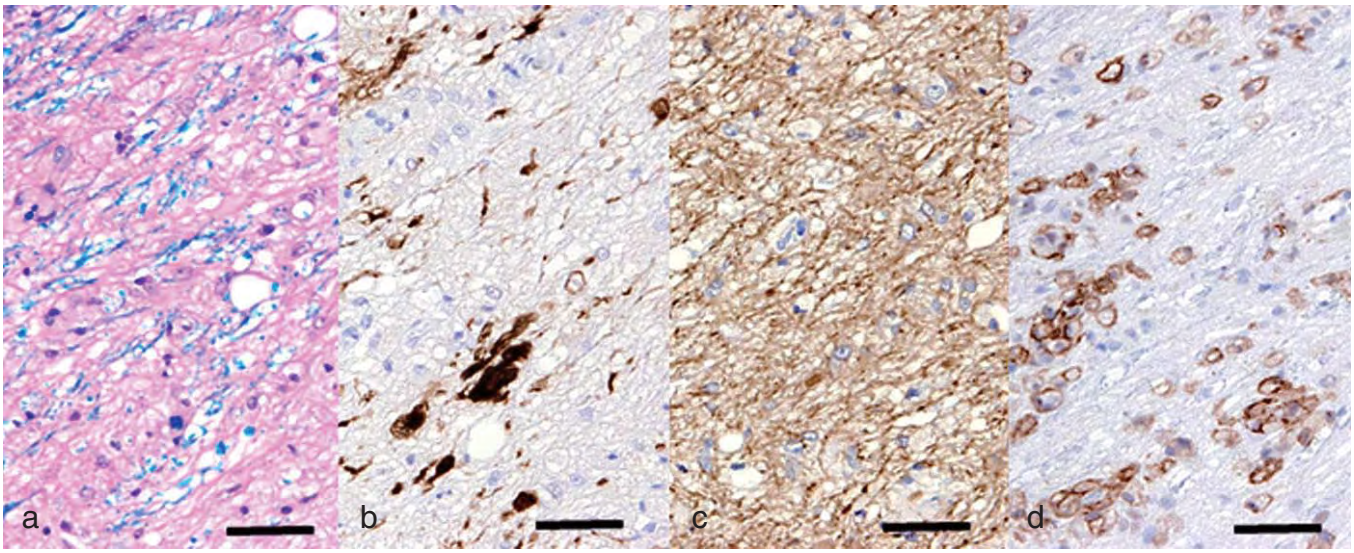

Fig. 3 A lesion of the cerebellar white matter. (a) LFB-HE. Immunostain for (b) neurofilament, (c) GFAP and (d) Iba-1. In addition to myelin loss (a), severe axonal degeneration/loss (b) and astrogliosis (c) are observed in the area with macrophage infiltration (d). Scale bar = 50 µm.

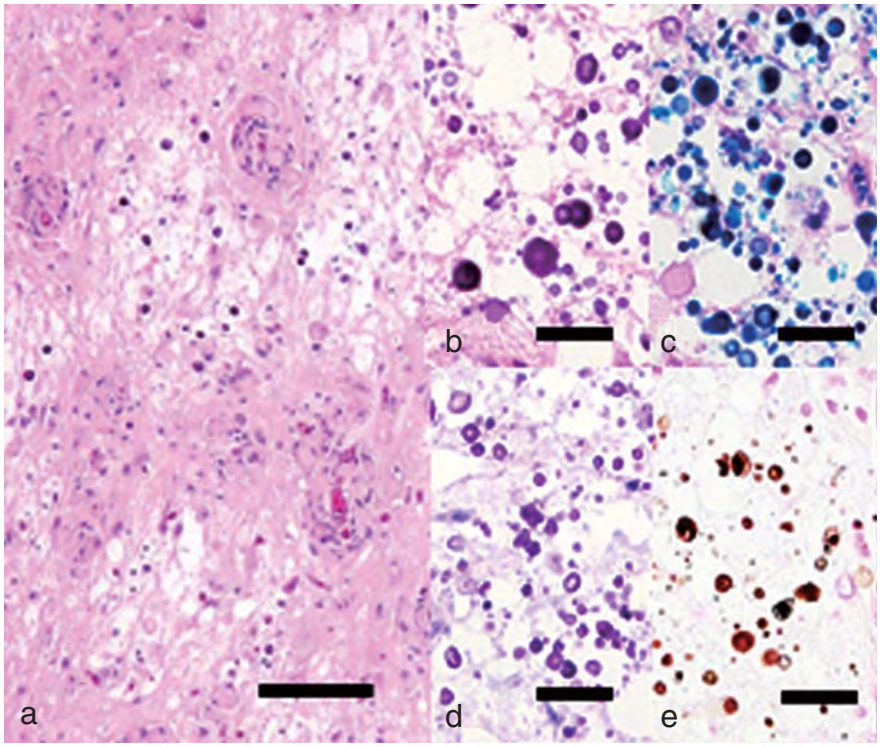

Fig. 4 Psammoma body in the cerebellar white matter. (b)–(e) are higher magnifications of (a): (a) and (b) HE, (c) LFB-HE, (d) PAS, and (e) von Kossa. The eosinophilic deposits were positive for LFB, PAS and von Kossa stains. Scale bar = 100 µm (a) and 25 µm (b–e).

addition, the formation of torpedoes observed in the present case is also common in human GLD.[19]

As far as we know, there have been three reports on spontaneous GLD in cats[8–10] and the distribution of the lesions and histological findings in the present case resemble those of GLD in humans[20] and in cats,[9] indicating that the present feline case is included in the same disease category. This is the first report of GLD in a Japanese domestic cat. In addition, despite the exact age of the cat being unknown, the present case may be relatively old compared with the previous feline GLD cases, probably because of effective care.

Psammoma body-like calcium deposits probably contained decayed products of myelin because they

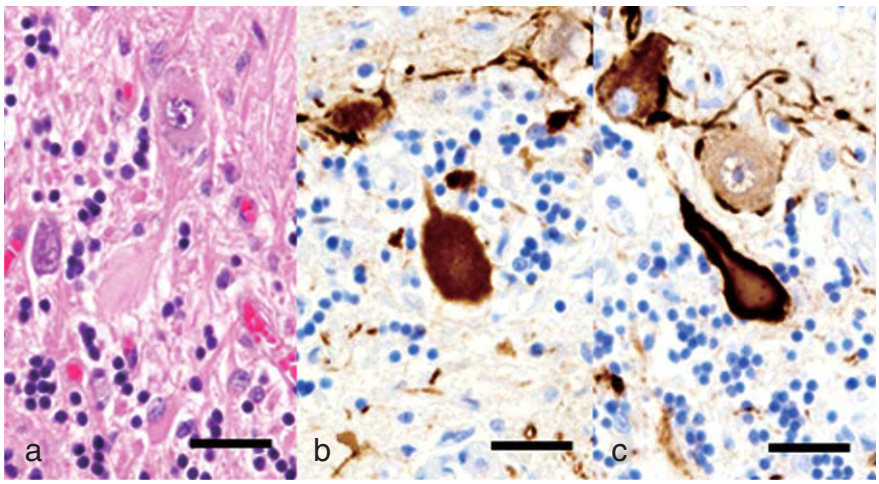

Fig. 5 A torpedo in the cerebellum. (a) HE. Immunostain for (b) neurofilament and (c) phosphorylated neurofilament. Neurofilament- and phospho-neurofilament-positive torpedoes were frequently observed. Scale bar = 25 μm.

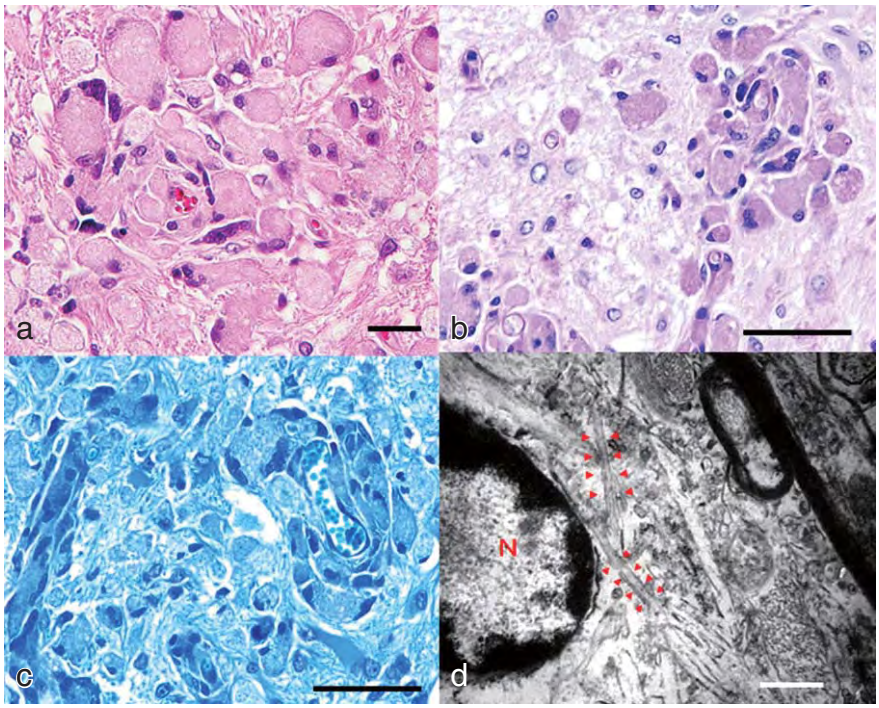

Fig. 6 Globoid cells in the cerebellar white matter. (a) HE, (b) PAS, (c) toluidine blue (TB) and (d) ultrastructural observation of a globoid cell. Globoid cells were round-shaped macrophages with broad cytoplasm (a). The deposits in the cytoplasm of a globoid cell were PAS-positive (b) and non-metachromatic with TB stain (c). Ultrastructurally, fine tubular structures with a diameter of 30–100 nm were accumulated in the cytoplasm of a globoid cell (d). Scale bar = 25 μm (a), 50 μm (b, c) and 500 nm (d).

were LFB-positive. A slight decrease of olig2-positive oligodendrocytes in spite of the severe myelin loss suggests that feline GLD may be a disease mostly caused by the dysfunction of myelination, maybe due to psychosine accumulation, rather than by the degeneration of mature myelin. Biochemical analysis or analysis of GALC or the saposin A gene was not performed because all tissues were unfortunately formalin-fixed at nectropsy because of the suspicion of infectious diseases. To determine whether this feline disease is exactly the same as human GLD, gene analysis should be performed.

The infiltration of CD3-positive T cells into the lesions in the present case indicates the involvement of immunological responses in the pathogenicity of the feline disease, like in human GLD.[19] However, the infiltration was not very severe in view of the longer survival and/or because of steroid treatment.

The production of reactive oxygen species (ROS) was observed in Twitcher mice, a GLD model, as a secondary event following psychosine toxicity.[21] The expression of iNOS, which results in ROS production, was reported to be distributed mostly in GFAP-positive astrocytes in human GLD,[21] and in both astrocytes and globoid cells of GLD of rhesus macaques,[7] as well as in the present case. On the other hand, in the present case, SOD2, a mitochondrial antioxidant enzyme, was strongly expressed by globoid cells themselves. SOD1[17] and HO-1,[23] the molecules usually induced by ROS, were also expressed by reactive

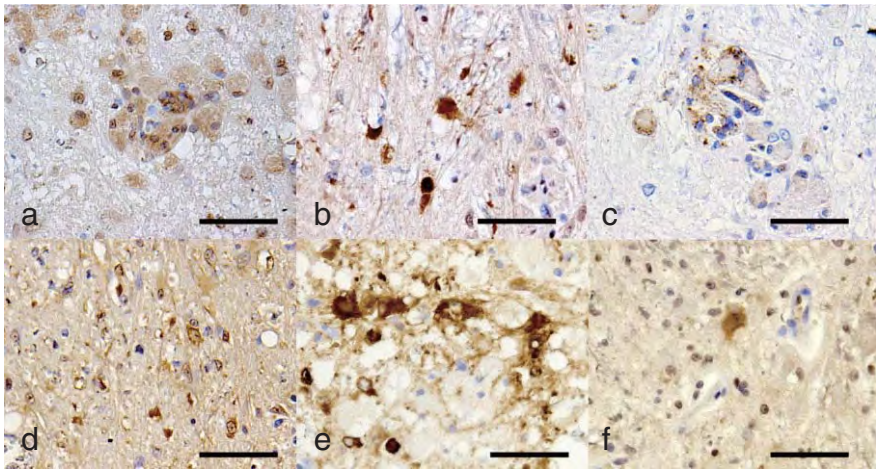

Fig. 7 The cerebellum. Immunohistochemistry for inducible nitric oxide (iNOS), SOD, heme oxygenase-1 (HO-1) and sHSPs. (a) iNOS, (b) SOD1, (c) SOD2, (d) HO-1, (e) αB-crystallin and (f) HSP27. Positive staining for iNOS and SOD2 was observed in the cytoplasm of globoid cells, not including filamentous deposit (a, c). SOD1 (b) and HO-1 (d) expression was occasionally observed in reactive astrocytes. αB-crystallin expression was observed in reactive astrocytes (e), whereas only few astrocytes were positive for HSP27 (f). Scale bar = 50 μm.

astrocytes. Although it is interesting that the iNOS expression patterns vary among animals, it may be a common accelerating factor for disease progression, not an exclusive factor for the pathogenesis. The induction of the antioxidant enzymes may be a physiological consequence in the recovery of neuronal tissue following oxidative damage.

Increased expressions of αB-crystallin and HSP27 were reported in Rosenthal fibers of Alexander's disease and in GFAP-positive gliosis lesions of human neurodegenerative diseases,[18] but the roles of these molecules in the pathogenicity of such neurodegenerative diseases are still controversial. The strong expressions of the molecules in the CNS of the present case suggest involvement of the molecules in disease progression also in feline GLD.

REFERENCES

1. Suzuki K. Globoid cell leukodystrophy (Krabbe's disease): update. *J Child Neurol* 2003; **18** (9): 595–603.
2. Wenger DA. Murine, canine and non-human primate models of Krabbe disease. *Mol Med Today* 2000; **6** (11): 449–451.
3. Fletcher JL, Williamson P, Horan D, Taylor RM. Clinical signs and neuropathologic abnormalities in working Australian Kelpies with globoid cell leukodystrophy (Krabbe disease). *J Am Vet Med Assoc* 2010; **237** (6): 682–688.
4. McGraw RA, Carmichael KP. Molecular basis of globoid cell leukodystrophy in Irish setters. *Vet J* 2006; **171** (2): 370–372.
5. Pritchard DH, Napthine DV, Sinclair AJ. Globoid cell leucodystrophy in polled Dorset sheep. *Vet Pathol* 1980; **17** (4): 399–405.
6. Baskin GB, Ratterree M, Davison BB *et al*. Genetic galactocerebrosidase deficiency (globoid cell leukodystrophy, Krabbe's disease) in rhesus monkeys (Macaca mulatta). *Lab Anim Sci* 1998; **48** (5): 476–482.
7. Borda JT, Alvarez X, Mohan M *et al*. Clinical and immunopathologic alterations in rhesus macaques affected with globoid cell leukodystrophy. *Am J Pathol* 2008; **172** (1): 98–111.
8. Johnson K. Globoid leukodystrophy in the cat. *J Am Vet Med Assoc* 1970; **157**: 2057–2064.
9. Salvadori C, Modenato M, Corlazzoli D, Arispici M, Cantile C. Clinicopathological features of globoid cell leucodystrophy in cats. *J Comp Pathol* 2005; **132** (4): 350–356.
10. Sigurdson CJ, Basaraba RJ, Mazzaferro EM, Gould DH. Globoid cell-like leukodystrophy in a domestic longhaired cat. *Vet Pathol* 2002; **39** (4): 494–496.
11. Lee WC, Tsoi YK, Dickey CA, DeLucia MW, Dickson DW, Eckman CB. Suppression of galactosylceramidase (GALC) expression in the twitcher mouse model of globoid cell leukodystrophy (GLD) is caused by nonsense-mediated mRNA decay (NMD). *Neurobiol Dis* 2006; **23** (2): 273–280.
12. Sakai N, Inui K, Tatsumi N, Fukushima H *et al*. Molecular cloning and expression of cDNA for murine galactocerebrosidase and mutation analysis of the twitcher mouse, a model of Krabbe's disease. *J Neurochem* 1996; **66** (3): 1118–1124.
13. Potter GB, Santos M, Davisson MT *et al*. Missense mutation in mouse GALC mimics human gene defect and offers new insights into Krabbe disease. *Hum Mol Genet* 2013; **22** (17): 3397–3414.
14. Spiegel R, Bach G, Sury V *et al*. A mutation in the saposin A coding region of the prosaposin gene in an infant presenting as Krabbe disease: first report of saposin A deficiency in humans. *Mol Genet Metab* 2005; **84** (2): 160–166.

15. Matsuda J, Vanier MT, Saito Y, Tohyama J, Suzuki K, Suzuki K. A mutation in the saposin A domain of the sphingolipid activator protein (prosaposin) gene results in a late-onset, chronic form of globoid cell leukodystrophy in the mouse. *Hum Mol Genet* 2001; **10** (11): 1191–1199.
16. Victoria T, Rafi MA, Wenger DA. Cloning of the canine GALC cDNA and idntification of the mutation causing globoid cell leukodystrophy in West Highland White and Cairn terriers. *Genomics* 1996; **33** (3): 457–462.
17. Andersen JK. Oxidative stress in neurodegeneration: cause or consequence? *Nat Med* 2004; **10**: S18–S25.
18. Van Rijk A, Bloemendal H. Alpha-B-crystallin in neuropathology. *Ophthalmologica* 2000; **214** (1): 7–12.
19. Itoh M, Hayashi M, Fujioka Y, Nagashima K, Morimatsu Y, Matsuyama H. Immunohistological study of globoid cell leukodystrophy. *Brain Dev* 2002; **24** (5): 284–290.
20. Percy AK, Odrezin GT, Knowles PD, Rouah E, Armstrong DD. Globoid cell leukodystrophy: comparison of neuropathology with magnetic resonance imaging. *Acta Neuropathol* 1994; **88** (1): 26–32.
21. Hawkins-Salsbury JA, Qin EY, Reddy AS, Vogler CA, Sands MS. Oxidative stress as a therapeutic target in globoid cell leukodystrophy. *Exp Neurol* 2012; **237** (2): 444–452.
22. Giri S, Jatana M, Rattan R, Won JES, Singh I, Singh AK. Galactosylsphingosine (psychosine)-induced expression of cytokine-mediated inducible nitric oxide synthases via AP-1 and C/EBP: implications for Krabbe disease. *FASEB J* 2002; **16** (7): 661–672.
23. Schipper HM, Song W, Zukor H *et al*. Heme oxygenase-1 and neurodegeneration: expanding frontiers of engagement. *J Neurochem* 2009; **110** (2): 469–485.

Resolution of Polyneuropathy in a Hypothyroid Dog Following Thyroid Supplementation

Shinichi Utsugi, DVM, Miyoko Saito, DVM, PhD, G. Diane Shelton, DVM, PhD, DACVIM

ABSTRACT

An 8 yr old male golden retriever was evaluated because of chronic, progressive, multiple neurologic signs. Physical examination showed marked obesity and facial swelling with a "tragic facial expression." Neurologic evaluation revealed the dog had multiple cranial nerve deficits and lower motor neuron signs in the pelvic limbs. Serum biochemical analysis and thyroid function tests were consistent with hypothyroidism. A biopsy from the common peroneal nerve revealed a loss of myelinated fibers, inappropriately thin myelinated fibers, and resolving subperineurial edema. The diagnosis of polyneuropathy associated with hypothyroidism was made. Levothyroxine therapy was initiated. Response to levothyroxine treatment was slow, with most neurologic abnormalities persisting for >6 wk. However, the dog made a full neurologic recovery within 6 mo. Although the occurrence of polyneuropathy in dogs resulting from hypothyroidism has been controversial, the study authors demonstrated that hypothyroid polyneuropathy can occur in dogs as documented in humans. This is the first report describing long-term follow-up information together with detailed pathological features of hypothyroid polyneuropathy in a dog. In hypothyroid polyneuropathy, the response to thyroid replacement may be slow, but a recovery can be expected if treatment is initiated before peripheral nerve fiber loss becomes severe. (*J Am Anim Hosp Assoc* 2014; 50:345–349. DOI 10.5326/JAAHA-MS-6035)

Introduction

Hypothyroidism is the most common hormonal disease in dogs.[1] Because thyroid hormone has a wide variety of physiologic effects, this disease can cause a broad range of problems in many organs. Reportedly, various neurologic signs resulting from either central or peripheral nervous system involvement, such as vestibular dysfunction; facial paralysis; and reduced spinal reflexes, ataxia, and paresis, are associated with hypothyroidism. However, a causal relationship with hypothyroidism has been proven in only a limited number of cases.[2–7]

The occurrence of hypothyroid polyneuropathy in dogs has been controversial, and pathological findings have been mentioned briefly in only rare cases.[2,3,5] In a recent study in which hypothyroidism was experimentally induced in dogs, peripheral neuropathy was not evident clinically, electrophysiologically, or histopathologically.[8] Based on that study, it was suggested that canine peripheral nerves may be relatively resistant to chronic thyroid hormone deficiency.[8]

In humans, it is known that hypothyroidism is an uncommon cause of peripheral neuropathy, such as carpal tunnel syndrome and some types of polyneuropathies.[9] Although the pathogenesis of peripheral neuropathy due to hypothyroidism remains to be fully elucidated, it is generally understood that hypothyroidism can cause mucous deposits and fluid retention resulting in nerve damage through a compression mechanism.[9]

In this report, an older golden retriever with chronic, progressive, multiple neurologic signs was diagnosed with hypothyroid polyneuropathy after complete diagnostic investigations. To the authors' knowledge, this is the first report describing long-term follow-up information together with detailed pathological features of hypothyroid polyneuropathy of a dog.

From the Department of Surgery II, School of Veterinary Medicine, Azabu University, Kanagawa, Japan (S.U., M.S.); and Department of Pathology, University of California, San Diego, La Jolla, CA (G.D.S.).

Correspondence: msaito@azabu-u.ac.jp (M.S.)

ATP, adenosine triphosphate; PO, *per os*; T_4, thyroxine

Case Report

An 8 yr old male golden retriever weighing 47.5 kg was referred to the Azabu University Veterinary Teaching Hospital for evaluation of head tilt, ptosis, pelvic limb ataxia, and exercise intolerance. Clinical signs began 1 mo prior to evaluation and had progressively worsened. The owner also noticed that the dog was less active and appeared somewhat depressed, although appetite and water consumption was normal. The dog's vaccination status was current. On physical examination, the dog had a rectal temperature of 38.2°C, pulse rate of 96 beats/min, and respiratory rate of 24 breaths/min. The dog was obese (body condition score 5 out of 5) and appeared to be moderately swollen in the face with a "tragic facial expression." Mild otitis externa of both ears was noted. Neurologic examination revealed ataxia of both pelvic limbs, but conscious proprioception and hopping reactions were normal in all limbs. Patellar and withdrawal reflexes were diminished in the right pelvic limb. There was a right-sided head tilt together with a right-sided ptosis. Pain sensation was considered normal in all limbs. The remaining neurologic examinations did not show any abnormalities. The complete blood cell count and serum biochemical analysis (after fasting for 12 hr) were performed. Results of the complete blood cell count were unremarkable. Serum biochemical analysis revealed hypercholesterolemia (46.1 mmol/L; reference range, 2.77–8.13 mmol/L) and hypertriglyceridemia (13.97 mmol/L; reference range, 0.19–1.15 mmol/L), with no other abnormalities. Hypothyroidism was suspected, and thyroid function tests were performed. They revealed low serum thyroxine (T_4) $<$5.13 nmol/L; (0.3 μg/dL; reference range, 18.8–61.54 nmol/L; 1.1–3.6 μg/dL), low serum free T_4 [(3.86 pmol/L; 0.3 ng/dL; reference range, 11.58–33.46 pmol/L; 0.9–2.6 ng/dL)], and an increased serum level of thyroid-stimulating hormone (1.6 ng/mL; reference range, 0.08–0.32 ng/mL). Thoracic radiographs were interpreted as normal.

On the basis of thyroid function test results, a diagnosis of hypothyroidism was made. Differential diagnoses for neurologic signs included a brain stem tumor, encephalitis, and polyneuropathy due to variable causes, including hypothyroidism and possibly otitis media and/or interna. Levothyroxine Na[a] (0.02 mg/kg *per os* [PO] *q* 12 hr) was initiated.

Seven days after the first presentation, the dog was reevaluated at the hospital. The dog was more active, but did not show any changes in other clinical signs. Serum T_4 levels were measured and were high (130.77 nmol/L). Serum biochemical analysis revealed some improvement of hypercholesterolemia (33.39 mmol/L) and hypertriglyceridemia (2.05 mmol/L). The dose of levothyroxine Na was decreased to 0.01 mg/kg PO *q* 12 hr.

At that time, the owner decided to have the dog undergo further diagnostic testing rather than adopting a "wait and see" approach for whether levothyroxine treatment would have a positive effect on neurologic signs. The dog was anesthetized and MRI of the head and spine was performed 9 days after initial presentation. T1-weighted, T2-weighted, and fluid-attenuated inversion recovery scans were performed in the transverse and sagittal planes. Additionally, gadoteridol[b] at 0.2 mL/kg was administered IV, and a postcontrast transverse T1-weighted sequence was obtained. MRI showed no abnormality. Following MRI, cerebrospinal fluid was obtained from the cerebellomedullary cistern. No abnormalities were detected on cytologic analysis including cell counts and protein concentrations. Serologic evaluation for canine distemper virus immunoglobulin G antibodies in the cerebrospinal fluid and serum were negative. Polymerase chain reaction examination of nasal, oral, and conjunctival epithelium, stool, and digital pads was performed and were negative for the canine distemper virus. *Toxoplasma gondii* and *Neospora caninum* immunoglobulin G antibodies were both negative in the serum. Serum T_4 was measured before anesthesia and was considered still slightly high (94.36 nmol/L). A dose reduction of levothyroxine Na to 0.005 mg/kg PO *q* 12 hr was instructed. Hypercholesterolemia (19.89 mmol/L) and hypertriglyceridemia (1.36 mmol/L) were further improved.

Five weeks after initial presentation, the dog was reevaluated at the hospital. The body weight decreased to 43.5 kg. Ataxia, exercise intolerance, and facial swelling were resolved, but other neurologic signs including diminished patellar and withdrawal reflexes, head tilt, and ptosis did not show any apparent improvement. Serum creatine kinase was measured and was within normal limits (46.0 IU/L; reference range, 40–151 IU/L). The dog was placed under general anesthesia for evaluation of lower motor neuron dysfunction. Electromyography was within normal limits. Motor nerve conduction velocity in the right tibial nerve was within the reference range, but was polyphasic with a decreased amplitude of the compound muscle action potential (0.9 mV; reference range, 23.3 ± 2.3 mV).[10]

Biopsy specimens were obtained from the right common peroneal nerve and were fixed in neutral-buffered 10% formalin. Nerve specimens were plastic embedded and evaluated in 1 μm sections (**Figure 1**). Subjectively, there was a mild (medium-size fascicle) to moderate (smaller fascicle) loss of myelinated fibers without obvious axonal degeneration (Figure 1A). Occasional large and small caliber fibers showed inappropriately thin myelin sheaths for the axon diameter (Figure 1B). Numerous collagen bundles consistent with resolving subperineurial edema were evident in all fascicles (Figure 1A). To determine quantitatively if fiber loss was selective to specific nerve fiber diameters, axonal size frequency distribution was determined for the golden retriever

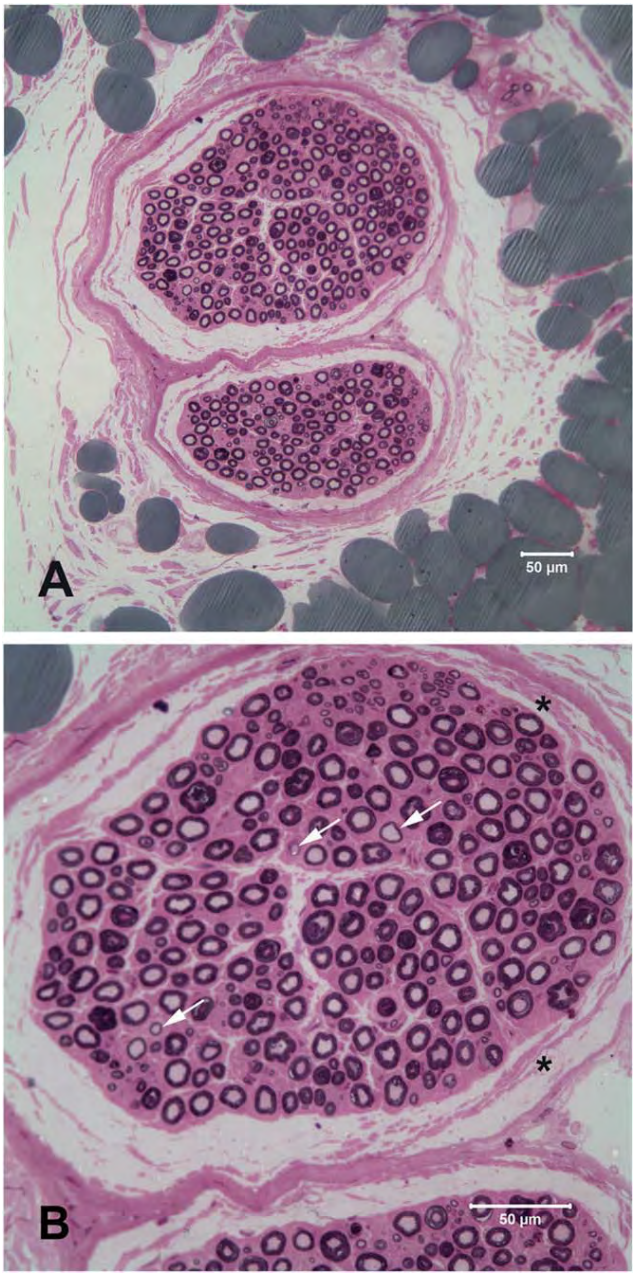

FIGURE 1 A: *Low-power, resin-embedded, toluidine blue-stained 1 µm section from the peroneal nerve biopsy showing two nerve fascicles. Resolving subperineurial edema is present in both fascicles. Although axonal degeneration was not noted, nerve fiber loss was suspected indicating previous degeneration.* B: *Higher-power image of the larger nerve fascicle highlighting edema (*) and nerve fibers with inappropriately thin myelin sheaths for the axon diameter* (arrows). *Bar represents 50 µm.*

of this report and compared with three large-breed dogs without neurologic abnormalities that were used as controls for another study (**Figure 2**).[11] Compared with the control group,

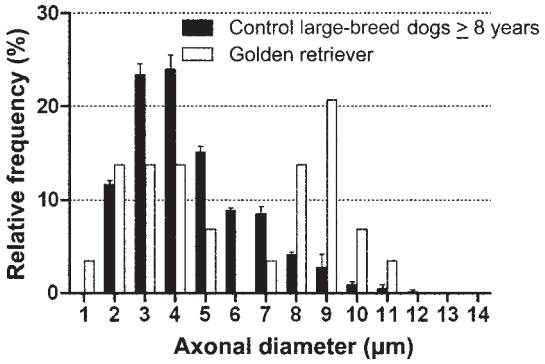

FIGURE 2 *Histogram showing axonal size frequency distribution of myelinated nerve fibers from the peroneal nerve of the dog of this report compared with peroneal nerves from three large-breed control dogs ≥8 yr of age and no neurologic dysfunction. Loss of myelinated fibers in the 3–7 µm range was demonstrated in the hypothyroid dog. Bars, standard error of the mean for control dogs.*

nerve fiber loss was limited to those with axon diameters in the 3–7 µm range.

Serum T_4 was again reassessed and was within the normal range (40.85 nmol/L). Serum biochemical analysis revealed further improvement in hypercholesterolemia (10.46 mmol/L) and hypertriglyceridemia (0.59 mmol/L). Although the neurologic signs remained, biochemical abnormalities showed marked improvement and the levothyroxine Na dosage was not changed (i.e., 0.005 mg/kg PO *q* 12 hr).

Six weeks after the initial presentation, the withdrawal reflex normalized but other neurologic abnormalities including diminished patellar reflex, head tilt, and ptosis persisted. The dog was again reevaluated at 6 mo following the initial presentation. The owner reported that the dog showed steady improvement and became completely normal. The body weight increased to 45.9 kg. The head tilt and ptosis resolved, and the patellar reflexes normalized. There were no abnormalities noted on neurologic examination at this time.

Discussion

The polyneuropathy documented in this report is most likely a result of hypothyroidism because the dog had clinical and biochemical abnormalities consistent with hypothyroidism, other causes of neurologic signs such as intracranial disorders were ruled out, and lastly, complete recovery of neurologic abnormalities was achieved following supplementation with levothyroxine Na alone.

In a recent study in which hypothyroidism was experimentally induced in young adult beagles, peripheral neuropathy

was not evident 18 mo following induction.[8] However, older dogs and dogs with a larger body size (like the dog described herein) were not studied. Peripheral neuropathy associated with hypothyroidism may target only some dogs, and the authors speculate that age and body size may play a role in disease development.

The pathophysiology of hypothyroidism-induced peripheral neuropathy in adults has not been clarified; however, mucinous deposits around peripheral nerves (i.e., mechanical compression and entrapment of nerves by localized myxedema) is considered to be the main cause of hypothyroidism-associated mononeuropathy and multiple mononeuropathy.[9] In diffuse polyneuropathy associated with hypothyroidism, direct metabolic changes due to a decreased thyroid hormone level in either Schwann cells or neurons may be considered.[9,12] For example, it has been demonstrated in rat studies that thyroidectomy results in slowed axonal transport.[13] Because thyroid hormone acts on mitochondria directly and increases adenosine triphosphate (ATP) production and ATPase activity by promoting cellular respiration, reduced thyroid hormone levels induce ATP deficiency and reduce ATPase activity levels in nerve cell bodies. That results in reduced Na^+/potassium pump activity and impairment of axonal transport.[13]

Motor nerve conduction velocity was not decreased in the dog described herein. That finding is not unexpected given that the largest caliber fastest conducting nerve fibers were not decreased (Figure 2). However, a markedly decreased amplitude of the compound muscle action potential and temporal dispersion were noted. Those findings may reflect loss of 3–7 μm nerve fibers and the presence of the inappropriately thin myelinated fibers identified by peripheral nerve biopsy in the dog of this report. Regarding electrophysiological abnormalities of spontaneously occurring hypothyroidism in dogs, variable changes (including reduced motor-nerve conduction velocity and electromyographic abnormalities, such as fibrillation potentials, positive sharp waves, and complex repetitive discharges) have been reported.[2,3] Abnormalities on electromyography were not noted in the dog in this report. Although muscle biopsies were not performed, the absence of both muscle atrophy and hypertrophy clinically together with the depressed spinal reflexes suggest that hypothyroid myopathy was unlikely.

There is only limited information concerning pathological changes in peripheral nerves in dogs with hypothyroidism. Peripheral nerve biopsy abnormalities included myelin irregularities, intercalated internodes, internodal globules, and axonal necrosis.[2,3,5] Neurogenic atrophy was often seen on muscle biopsy of dogs showing clinical signs of polyneuropathy.[2,3] Segmental demyelination and marked myelinated fiber loss accompanied by axonal degeneration were noted on histopathological examination of peripheral nerves in two dogs with signs of polyneuropathy and reduced T_4 levels.[14] However, both dogs were diagnosed with neoplasia and thyroid-stimulating hormone concentration was not measured. Therefore, it cannot be ruled out that polyneuropathy in those cases was a paraneoplastic syndrome or the cause of reduced T_4 levels was euthyroid sickness.

Pathological changes in peripheral nerves in the dog described herein included myelinated fiber loss accompanied by resolving subperineurial edema. To the authors' knowledge, edematous changes within nerves in dogs with this disease have not been previously reported, but are consistent with pathological findings in human hypothyroid polyneuropathy.[15] Although the cause of edema was not investigated in this case, epi- and perineurial infiltration by edematous protein assumed to be a metachromatic mucoid material, probably mucopolysaccharide-protein complexes, has also been observed in humans.[15] Perineurial deposition of that substance has not been reported in hypothyroid dogs, but subcutaneous hyaluronic acid deposition manifesting as skin myxedema has been described.[16] Hyaluronic acid is a mucopolysaccharide and its deposition may cause edema because it is markedly hygroscopic. Furthermore, myelinated fiber loss apparent in the current case is a common pathological finding in human hypothyroid neuropathy.[9] In this dog, edematous deposition resulting in compression of nerve fibers may have occurred due to hypothyroidism.

In canine hypothyroid polyneuropathy, both spinal and cranial nerves may be impaired.[5] However, there are reports in which various cranial nerve abnormalities were induced by cerebral infarction due to the cerebral artery atherosclerosis.[17,18] Because a necropsy was not performed in this dog, it cannot be definitively concluded that the cranial nerve abnormalities were part of a polyneuropathy and not a central manifestation. However, the neurologic history of this dog (i.e., chronic onset and progression) was not suggestive of a vascular disorder. Furthermore, abnormalities such as necrotic lesions were not noted on MRI. Cranial nerve signs slowly improved and resolved along with spinal nerve signs following only hormone replacement therapy.

Most dogs with hypothyroid myopathy rapidly respond to thyroid replacement therapy, and clinical normalization is obtained within 2–8 wk.[2,3] In contrast, the response of peripheral neuropathy to thyroid replacement therapy is not clear and it is said that responses to treatment may be poor.[19] The dog in this report required 6 wk to observe the first improvement of neurologic signs after initiation of thyroid replacement. The remaining signs slowly improved, and the dog was neurologically normal on

follow up at 6 mo. It has been pointed out that relatively early impairments caused by hypothyroidism are mainly metabolic functional abnormalities, rather than structural changes in peripheral nerves.[20] Hence, early recovery by thyroid replacement can be expected at this stage. In contrast, when either apparent structural changes of nerves occur or there is nerve fiber loss resulting from axonal degeneration, a prolonged time may be required to recover or recovery may be incomplete. Therefore, establishing an early and accurate diagnosis and initiating appropriate treatment are necessary when hypothyroid neuropathy is suspected.

Conclusion

The study authors demonstrated that hypothyroid polyneuropathy can occur in dogs as described in humans. Pathological changes in peripheral nerves included myelinated fiber loss accompanied by subperineurial edema. The dog made a full recovery with only thyroid supplementation. However, response to the treatment was slow and most neurologic abnormalities persisted for >6 wk. When apparent structural changes of nerves occur, a prolonged time may be required to recover or recovery may be incomplete. Therefore, establishing an early and accurate diagnosis and initiating appropriate treatment are both necessary when hypothyroid neuropathy is suspected.

This research was partially supported by a research project grant awarded by the Azabu University.

FOOTNOTES

[a] Soloxine; Virbac, Fort Worth, TX

[b] ProHance; Eisai, Tokyo, Japan

REFERENCES

1. Ferguson DC. Testing for hypothyroidism in dogs. *Vet Clin North Am Small Anim Pract* 2007;37(4):647–69, v.
2. Indrieri RJ, Whalen LR, Cardinet GH, et al. Neuromuscular abnormalities associated with hypothyroidism and lymphocytic thyroiditis in three dogs. *J Am Vet Med Assoc* 1987;190(5):544–8.
3. Jaggy A, Oliver JE, Ferguson DC, et al. Neurological manifestations of hypothyroidism: a retrospective study of 29 dogs. *J Vet Intern Med* 1994;8(5):328–36.
4. Higgins MA, Rossmeisl JH Jr, Panciera DL. Hypothyroid-associated central vestibular disease in 10 dogs: 1999–2005. *J Vet Intern Med* 2006;20(6):1363–9.
5. Dewey CW, Shelton GD, Bailey CS. Neuromuscular dysfunction in five dogs with acquired myasthenia gravis and presumptive hypothyroidism. *Prog Vet Neurol* 1995;6(4):117–23.
6. Bichsel P, Jacobs G, Oliver JE Jr. Neurologic manifestations associated with hypothyroidism in four dogs. *J Am Vet Med Assoc* 1988;192(12):1745–7.
7. Bruchim Y, Kushnir A, Shamir MH. L-thyroxine responsive cricopharyngeal achalasia associated with hypothyroidism in a dog. *J Small Anim Pract* 2005;46(11):553–4.
8. Rossmeisl JH Jr. Resistance of the peripheral nervous system to the effects of chronic canine hypothyroidism. *J Vet Intern Med* 2010; 24(4):875–81.
9. Pollard JD. Neuropathy in diseases of the thyroid and pituitary glands. In: Dyck PJ, Thomas PK, eds. *Peripheral neuropathy.* 4th ed. Philadelphia (PA): Elsevier Saunders; 2005:2039–49.
10. Walker TL, Redding RW, Braund KG. Motor nerve conduction velocity and latency in the dog. *Am J Vet Res* 1979;40(10):1433–9.
11. Shelton GD, Johnson GC, O'Brien DP, et al. Degenerative myelopathy associated with a missense mutation in the superoxide dismutase 1 (SOD1) gene progresses to peripheral neuropathy in Pembroke Welsh corgis and boxers. *J Neurol Sci* 2012;318(1-2):55–64.
12. Shirabe T, Tawara S, Terao A, et al. Myxoedematous polyneuropathy: a light and electron microscopic study of the peripheral nerve and muscle. *J Neurol Neurosurg Psychiatry* 1975;38(3):241–7.
13. Sidenius P, Nagel P, Larsen JR, et al. Axonal transport of slow component a in sciatic nerves of hypo- and hyperthyroid rats. *J Neurochem* 1987;49(6):1790–5.
14. Dyer KR, Duncan ID, Hammang JP, et al. Peripheral neuropathy in two dogs: correlation between clinical, electrophysiological and pathological findings. *J Small Anim Pract* 1986;27:133–46.
15. Ropper AH, Samuels MA. Diseases of the peripheral nerves. In: Ropper AH, Samuels MA, eds. *Adams and Victor's principles of neurology.* 9th ed. New York: McGraw-Hill Medical; 2009:1251–325.
16. Doliger S, Delverdier M, Moré J, et al. Histochemical study of cutaneous mucins in hypothyroid dogs. *Vet Pathol* 1995;32(6):628–34.
17. Patterson JS, Rusley MS, Zachary JF. Neurologic manifestations of cerebrovascular atherosclerosis associated with primary hypothyroidism in a dog. *J Am Vet Med Assoc* 1985;186(5):499–503.
18. Blois SL, Poma R, Stalker MJ, et al. A case of primary hypothyroidism causing central nervous system atherosclerosis in a dog. *Can Vet J* 2008;49(8):789–92.
19. Platt SR. Neuromuscular complications in endocrine and metabolic disorders. *Vet Clin North Am Small Anim Pract* 2002;32(1):125–46.
20. Quattrini A, Nemni R, Marchettini P, et al. Effect of hypothyroidism on rat peripheral nervous system. *Neuroreport* 1993;4(5):499–502.

FULL PAPER *Surgery*

Valproic Acid, a Histone Deacetylase Inhibitor, Decreases Proliferation of and Induces Specific Neurogenic Differentiation of Canine Adipose Tissue-Derived Stem Cells

Yasuhiro KURIHARA[1)], Takehito SUZUKI[1)], Motoharu SAKAUE[1)], Ohoshi MURAYAMA[2)], Yoko MIYAZAKI[1)], Atsushi ONUKI[1)], Takuma AOKI[1)], Miyoko SAITO[1)], Yoko FUJII[1)], Masaharu HISASUE[1)], Kazuaki TANAKA[1)] and Tatsuya TAKIZAWA[1)*]

[1)]*Graduate School of Veterinary Medicine, Azabu University, Fuchinobe, Chuo-ku, Sagamihara 252–5201, Japan*
[2)]*School of Life and Environmental Science, Azabu University, Fuchinobe, Chuo-ku, Sagamihara 252–5201, Japan*

(Received 30 April 2013/Accepted 7 August 2013/Published online in J-STAGE 27 August 2013)

ABSTRACT. Adipose tissue-derived stem cells (ADSCs) isolated from adult tissue have pluripotent differentiation and self-renewal capability. The tissue source of ADSCs can be obtained in large quantities and with low risks, thus highlighting the advantages of ADSCs in clinical applications. Valproic acid (VPA) is a widely used antiepileptic drug, which has recently been reported to affect ADSC differentiation in mice and rats; however, few studies have been performed on dogs. We aimed to examine the *in vitro* effect of VPA on canine ADSCs. Three days of pretreatment with VPA decreased the proliferation of ADSCs in a dose-dependent manner; VPA concentrations of 4 mM and above inhibited the proliferation of ADSCs. In parallel, VPA increased *p16* and *p21* mRNA expression, suggesting that VPA attenuated the proliferative activity of ADSCs by activating p16 and p21. Furthermore, the effects of VPA on adipogenic, osteogenic or neurogenic differentiation were investigated morphologically. VPA pretreatment markedly promoted neurogenic differentiation, but suppressed the accumulation of lipid droplets and calcium depositions. These modifications of ADSCs by VPA were associated with a particular gene expression profile, viz., an increase in neuronal markers, that is, *NSE*, *TUBB3* and *MAP2*, a decrease in the adipogenic marker, *LPL*, but no changes in osteogenic markers, as estimated by reverse transcription-PCR analysis. These results suggested that VPA is a specific inducer of neurogenic differentiation of canine ADSCs and is a useful tool for studying the interaction between chromatin structure and cell fate determination.

KEY WORDS: adipose tissue-derived stem cell, cell proliferation, histone deacetylase inhibitor, pluripotency, valproic acid.

doi: 10.1292/jvms.13-0219; *J. Vet. Med. Sci.* 76(1): 15–23, 2014

Spinal cord injury (SCI) often occurs in dogs, due to motor vehicle accidents or intervertebral disease (IVDD). Most canine patients suffer from sustained incontinence and loss of walking ability, and the prognosis of severe SCI cases is poor. Unfortunately, no effective drug or surgical therapy has been established for severe SCI cases, and there is a need for new therapeutic approaches. One possibility is stem cell transplantation therapy, which is used as a radical cure treatment for refractory SCI [2, 14, 25, 26].

Adipose tissue-derived stem cells (ADSCs) are isolated from the stromal vascular fraction of adipose tissues [8, 24, 39]. ADSCs, similar to pluripotent adult mesenchymal stem cells, can differentiate into mesenchymal lineage cells, such as adipocytes, osteocytes, chondrocytes and myocytes [36, 38]. ADSCs have characteristics similar to those of bone marrow-derived mesenchymal stem cells (BMSCs), including gene expression and differentiation potential [1, 3, 5, 17, 19, 22, 33, 35, 37, 39]. Unlike BMSCs, however, the tissue source of ADSCs can be obtained in large quantities and with low risks [11]. Therefore, it is reasonable that ADSCs will be the preferred adult stem cells for future clinical applications [24]. Moreover, the dog has been found to be a good animal model of human disease [32], and thus, the study of canine ADSCs is particularly useful. Stem cells derived from bone marrow and from olfactory ensheathing glia (OEG) have been studied for spinal cord regenerative therapy in dogs [6, 14, 16, 25, 26, 31]. However, only a few studies have been performed on the differentiation of canine ADSCs, except for a comparative study showing that BMSCs and ADSCs could be differentiated into neurospheres and neuron-like cells in dogs [2].

Valproic acid (VPA), a widely used antiepileptic and anticonvulsant drug, is an inhibitor of class 1 histone deacetylases (HDACs) [7, 27]. Histone acetylation correlates with gene activation [12, 13], and modification of histone N-terminal tails through acetylation or deacetylation can alter the interaction between histones and DNA, affecting the regulation of gene expression [9, 12, 13, 18, 34]. Therefore, HDAC inhibitors have been a useful tool for studying the association between chromatin modification and cell lineage specification. VPA has been found to promote differentiation of hippocampal neural progenitors into neurons, but inhibit their glial differentiation in adult rats [12].

In the present study, we have investigated the effects of VPA on the proliferation and differentiation of canine ADSCs isolated from subcutaneous adipose tissue in the

*CORRESPONDENCE TO: TAKIZAWA, T., Graduate School of Veterinary Medicine, Azabu University, Fuchinobe, Chuo-ku, Sagamihara 252–5201, Japan.
e-mail: takizawa@azabu-u.ac.jp

Table 1. Primers used in RT-PCR and real-time PCR

Gene		Primer sequence (5′–3′)	Product length (bp)
p16	Forward	CGATCCAGGTCATGATGATGG	145
	Reverse	ACCACCAGCGTGTCCAGGAA	
p21	Forward	CATCCCTCATGGCAGCAAG	208
	Reverse	AGGCAGGGAGACCTTGGACA	
PPARγ2	Forward	ACACGATGCTGGCGTCCTTGATG	119
	Reverse	TGGCTCCATGAAGTCACCAAAGG	
FABP4	Forward	ATCAGTGTAAACGGGGATGTG	117
	Reverse	GACTTTTCTGTCATCCGCAGTA	
LPL	Forward	ACACATTCACAAGAGGGTCACC	134
	Reverse	CTCTGCAATCACACGGATGGC	
BMP2	Forward	CACTAACCACGCCATTGTTCA	163
	Reverse	ACAACCCTCCACAACCATGTC	
Dlx5	Forward	TGCTCTCCTACCTCGGCTTC	224
	Reverse	TTGCCATTCACCATCCTCAC	
COL1A1	Forward	GTAGACACCACCCTCAAGAGC	119
	Reverse	TTCCAGTCGGAGTGGCACATC	
NSE	Forward	GACCAACCCAAAGCGTATTGA	180
	Reverse	GCAATGAACGTGTCCTCAGTC	
TUBB3	Forward	AGCCAAGTTCTGGGAAGTCA	238
	Reverse	CCCACTCTGACCAAAGATGAA	
MAP2	Forward	AGAGGAGGTGTCTGCAAGGA	161
	Reverse	GTGATGGAGGTGGAGAAGGA	
NEFH	Forward	CTCAAAGGCACCAAGGACTC	244
	Reverse	CAAAGCCAATCCGACATTCT	
GFAP	Forward	AGATCCACGATGAGGAGGTG	104
	Reverse	TCTTAGGGCTGCTGTGAGGT	
GAPDH	Forward	GCTGAACGGGAAGCTCACTG	221
	Reverse	CGTCGAAGGTGGAAGAGTGG	

inguinal region.

MATERIALS AND METHODS

Animals: Subcutaneous adipose tissue was obtained from the inguinal region of 8 healthy laboratory beagles (age, 1–2 years) (Kitayama Labes, Ina, Japan). All animals were anesthetized with propofol, before tissue samples were obtained. After intubation, anesthesia was maintained with isoflurane (2.0%) in oxygen. At the end of each experiment, the animals were euthanized by additional doses of anesthesia (pentobarbital, 100 mg/kg). The protocol of this study was approved by the Committee for Animal Experimentation at Azabu University.

Isolation and culture of canine ADSCs: Adipose tissue samples were processed for ADSC isolation as described previously [23, 24] with a slight modification. Briefly, the adipose tissue removed was extensively washed with sterile phosphate-buffered saline (PBS) containing penicillin (100 U/m*l*) and streptomycin (0.25 μg/m*l*) in order to remove contaminating blood cells and local anesthetics. The tissue was minced into small pieces and then incubated in a solution containing 0.05% collagenase type IA (Sigma-Aldrich, St. Louis, MO, U.S.A.) at 37°C for 1 hr with vigorous shaking. The top lipid layer was removed, and the remaining liquid portion was centrifuged at 200 × *g* for 10 min. The pellet was resuspended in Dulbecco's modified Eagle's medium (DMEM, Nissui, Tokyo, Japan) supplemented with 10% newborn bovine serum (NBS, Invitrogen, Carlsbad, CA, U.S.A.) and spread in 100-mm collagen type I-coated dishes (Iwaki, Tokyo, Japan) at a density of 1×10^6 cells per dish. Cells were maintained in growth medium (DMEM supplemented with 10% NBS, penicillin [100 U/m*l*] and streptomycin [0.25 μg/m*l*]) at 37°C and 5% CO_2. After 24 hr, the unattached cells were removed by washing with PBS. Canine ADSCs from passages 1–3 were used, and no difference was observed in ADSCs between these passages.

Measurement of proliferation potential: The effects of VPA or valpromide (VPM; Wako Pure Chemical Ind., Osaka, Japan), an analogue of VPA with no HDAC inhibi-

tory activity, on ADSC proliferation were measured using a 3-(4, 5-dimethyl-thiazol-2-yl)-2, 3-diphenyltetrazolium bromide (MTT) assay kit (Roche Applied Science, Basel, Switzerland) according to the manufacturer's instructions. Briefly, canine ADSCs were plated in 96-well plates at a density of 1×10^4 per well and cultured in growth medium for 48 hr. VPA or VPM (0–8 mM) was then added to the medium, and cultures were incubated for 3 days. Subsequently, 10 μl of MTT stock solution was added, and the plates were further incubated for 4 hr at 37°C. Diluted HCl (100 μl) was then added to solubilize the formazan crystals, and the absorbance of each well at 570 *n*m was measured with a microplate reader LS-PLATE manager 2004 (Wako Pure Chemical Ind.); the average of measurements of 6 wells per sample has been presented.

In vitro differentiation assay: *In vitro* assay of cell differentiation into adipogenic, osteogenic and neurogenic lineages was performed as described previously [4, 29, 39] with a slight modification. Briefly, ADSCs were seeded into 35-mm dishes at a density of 1×10^5 cells per dish. The cells were incubated on glass coverslips in growth medium containing 4 mM VPA for 3 days and then transferred to adipogenic induction medium (DMEM supplemented with 10% FBS, 1 μM dexamethasone, 10 μM insulin and 0.5 mM isobutylmethylxanthine) or to osteogenic induction medium (DMEM supplemented with 10% FBS, 0.1 μM dexamethasone, 50 μM L-ascorbate-2-phosphte and 10 mM glycerophosphate) for 14 days [39] and then to neurogenic induction medium (DMEM supplemented with100 μM dibutyryl cyclic adenosine monophosphate and 125 μM isobutylmethylxanthine) for 2 hr [23, 24]. Intracellular lipid accumulation, as an indicator of adipogenic differentiation, was visualized by oil red O staining. Osteogenic differentiation was confirmed by positive staining with alizarin red S, a specific marker for calcium deposition. Neurogenic differentiation was assessed by immunofluorescence staining for βIII-tubulin or neuron-specific enolase (NSE). Reagents for this induction medium were purchased from Wako Pure Chemical Ind.

Immunofluorescence staining: Immunocytochemical analyses of HDAC1, acetylation of histone H3 (ace H3), βIII-tubulin and NSE were performed. ADSCs were incubated in growth medium for 3 days as described above. Some cultures were processed for neurogenic induction. At the end of incubation, the cells were fixed in PBS containing 3.7% formaldehyde for 15 min at 4°C. After PBS washes, the cells were permeabilized with 0.2% Triton X-100 for 10 min at room temperature. The cells were then incubated with an anti-HDAC1 antibody (sc-7872, Santa Cruz Biotechnology, Santa Cruz, CA, U.S.A.), an anti-histone H3 (acetyl K9) antibody (Novus Biologicals, Littleton, CO, U.S.A.), an anti-βIII-tubulin antibody (ab78078, Abcam, Cambridge, U.K.) or an anti-NSE antibody (PA1-46203, Thermo Scientific, Billerica, MA, U.S.A.) for 1 hr at room temperature. After further PBS washes, cells were incubated with secondary antibody (Cy3-conjugated goat anti-rabbit IgG or FITC-conjugated goat anti-mouse IgG, Jackson ImmunoResearch, West Grove, PA, U.S.A.) for 30 min at room temperature. The cells were then washed with PBS and counterstained with 4′, 6-diamidino-2-phenyl-indole (DAPI) for nuclear staining before fluorescence microscopic observation.

Reverse transcription-PCR and real-time PCR: Total RNA was extracted using ISOGEN (NIPPON GENE, Tokyo, Japan) and reverse-transcribed to single-strand cDNA using oligo-dT primer and Superscript III reverse transcriptase (Invitrogen) according to the manufacturer's instructions. PCR was performed using *Taq* DNA polymerase (KAPA Biosystems, Woburn, MA, U.S.A.) and using specific primers, and each cycle consisted of the following steps: denaturation for 10 sec at 98°C, annealing for 30 sec at 53–65°C and a 30-sec elongation at 72°C (Table 1). Reaction products were electrophoresed on a 2.0% agarose gel and visualized with ethidium bromide. Real-time PCR of the mRNAs for *p16*, *p21* and *GAPDH* was performed using an ABI PRISM 7500 Sequence Detection System (Applied Biosystems Japan, Tokyo, Japan) according to the manufacturer's instructions. Analysis of the results was carried out using ABI PRISM 7500 Dissociation Curve Software v 1.0 (Applied Biosystems Japan). The relative amount of mRNA was normalized to that of *GAPDH*.

Statistical analysis: Results are expressed as the mean ± standard error. Multiple comparisons were done with the Turkey–Kramer test after one-way analysis of variance. A p-value<0.05 was considered statistically significant.

RESULTS

VPA induces acetylation of histone H3 and decreased cell proliferation: To confirm the effect of VPA on HDAC1 and acetylation of histone H3, we examined the expression of HDAC1 and acetylation of histone H3 by immunofluorescence staining. Minimal HDAC1 and acetylation of histone H3 were observed in the control ADSCs. VPA flattened the morphology of ADSCs and increased the expression of HDAC1 and the acetylation of histone H3 in ADSCs after 3 days of treatment (Fig. 1A and 1B). In contrast, VPM did not cause any morphological changes or significant changes in HDAC1 and histone H3 staining in ADSCs.

Moreover, VPA treatment significantly decreased the proliferation of ADSCs in a dose-dependent manner: about 20% (2 mM VPA), 40% (4 mM VPA) and 80% (8 mM VPA) of the control group (Fig. 1C). However, VPM treatment did not substantially affect ADSC proliferation. No dead cells were observed in any VPA-treated groups by phase-contrast microscopy.

VPA induces upregulation of cyclin-dependent kinase inhibitors: To assess the effect of VPA on the expression of cyclin-dependent kinase (CDK) inhibitors, we examined the expression of these genes by real time-PCR. The expression levels of *p16* mRNA significantly increased in the ADSCs treated with 4 mM VPA (4.6 fold vs. control); however, *p16* mRNA expression levels did not change in the cells treated with 8 mM VPA (2.1 fold vs. control; Fig. 2A). *p21* mRNA expression levels significantly increased in the cells treated with 8 mM VPA (Fig. 2B). The expression levels of *p21* mRNA were approximately 2.6 fold (4 mM VPA) and 3.0 fold (8 mM VPA) of that of the control group.

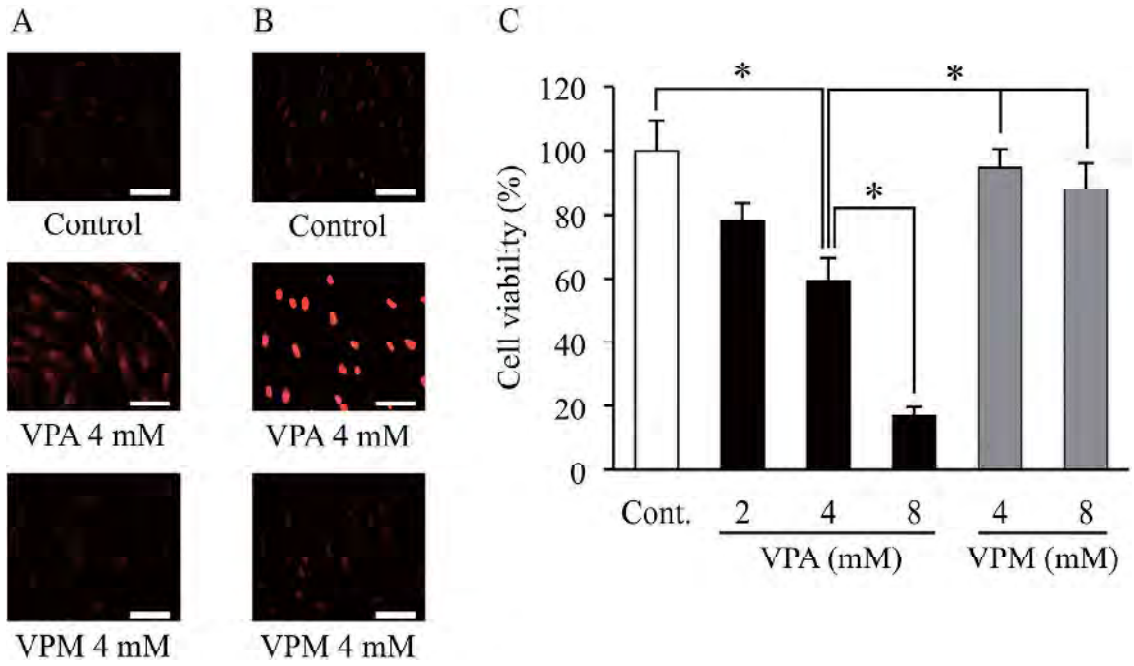

Fig. 1. Effects of valproic acid on histone deacetylase 1 expression, histone H3 acetylation and cell proliferation. Canine adipose tissue-derived stem cells (ADSCs) were treated with valproic acid (VPA) or valpromide (VPM). (A) ADSCs were then processed for immunofluorescence staining with an anti-histone deacetylase 1 (HDAC1) or an anti-histone H3 (acetyl K9) antibody and a secondary antibody (Cy3-conjugated goat anti-rabbit IgG). Red fluorescence indicates positive staining for HDAC1 (A) and acetylation of histone H3 (B). Scale bar, 50 μm. (C) Cell proliferation was measured by MTT assay and expressed as percentage of the negative control (DMSO). Data represent the means ± S.E. (% of control) of 4 independent experiments; each measurement was the average for 6 wells. *P<0.05, significant difference among the indicated groups.

VPA suppresses adipogenic and osteogenic differentiation: To assess the effect of VPA on the pluripotency of ADSCs, we investigated whether VPA treatment alters the differentiation of ADSCs into adipogenic and osteogenic lineages using an *in vitro* differentiation assay. Oil red O staining revealed that ADSCs that differentiated into the adipogenic lineage accumulated lipid droplets in the cytosol, as compared to undifferentiated cells, which did not accumulate lipid droplets (Fig. 3A). VPA pretreatment followed by adipogenic induction significantly suppressed the accumulation of lipid droplets. RT-PCR analysis showed that the mRNA expression levels of adipogenic markers, peroxisome proliferator-activated receptor γ2 (*PPARγ2*), fatty acid binding protein 4 (*FABP4*) and lipoprotein lipase (*LPL*) were elevated by adipogenic induction (Fig. 3B). On the other hand, VPA pretreatment followed by adipogenic induction significantly reduced the *LPL* mRNA expression level, in parallel with the decreased accumulation of lipid droplets. Alizarin red S staining revealed that ADSCs differentiated into osteogenic lineage cells with accumulated calcium deposition, as compared with the undifferentiated cells, which demonstrated no calcium deposition (Fig. 4). VPA pretreatment followed by osteogenic induction significantly reduced calcium deposition (Fig. 4A). mRNA expression levels of osteogenic markers, viz., bone morphogenetic protein 2 (*BMP2*) and distal-less homeobox 5 (*DLX5*), were also elevated by osteogenic induction, but were not significantly affected by VPA pretreatment (Fig. 4B).

VPA promotes neurogenic differentiation: We further examined the effect of VPA on the neurogenic lineage induction of ADSCs. βIII-tubulin immunofluorescence staining revealed that ADSCs that differentiated into neurogenic cells had typical neuron-like cell protrusions and higher βIII-tubulin levels than undifferentiated cells. βIII-tubulin-positive cells also stained for NSE. VPA pretreatment followed by neurogenic induction significantly enhanced the level of βIII-tubulin-positive cells with approximately 90% of ADSCs showing βIII-tubulin expression (Fig. 5A).

mRNA levels of neurogenic markers, viz., *NSE*, *TUBB3* and microtubule-associated protein 2 (*MAP2*), were also elevated by neurogenic induction, but mRNA expression of the glial cell marker, *GFAP,* was not observed in any groups (Fig. 5B). Pretreatment with VPA followed by neurogenic induction increased the expression of *NSE*, *TUBB3* and *MAP2* and of neurofilament heavy polypeptide (*NEFH*), as compared to that in the neurogenic induction group. VPA pretreatment increased the number of βIII-tubulin-positive cells, even without neurogenic induction. Furthermore, VPA elevated the mRNA expression levels of neurogenic markers in ADSCs with and without neurogenic induction.

DISCUSSION

Here, we demonstrated that VPA flattened the morphol-

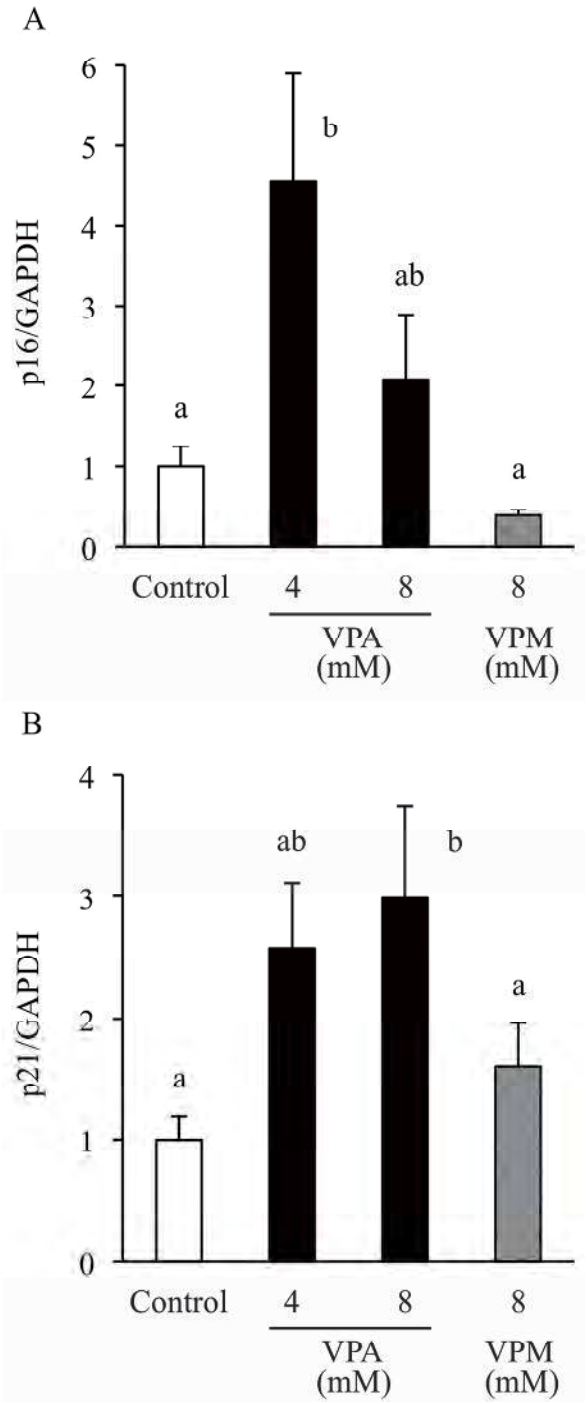

Fig. 2. Effects of valproic acid on cyclin-dependent kinase inhibitor expression. Adipose tissue-derived stem cells (ADSCs) were treated with valproic acid (VPA) or valpromide (VPM). Total RNA was extracted from ADSCs after 3 days of treatment with VPA (4 or 8 mM) or VPM (8 mM). The relative expression of the cyclin-dependent kinase (CDK) inhibitors *p16*(A) and *p21*(B) was quantified by real time-PCR. Glyceraldehyde-3-phosphate dehydrogenase (*GAPDH*) was used as an internal standard. Data are the means ± S.E. of 4–7 independent experiments. a, b: bars with different letters at the top differ significantly; a vs. b, $P<0.05$.

ogy of canine ADSCs and markedly induced their expression of HDAC1 and acetylation of histone H3. In contrast, VPM, an analogue of VPA with no HDAC inhibitory activity, did not cause any morphological changes and had no significant effects on HDAC1 and histone H3, indicating that the H3 acetylation was increased by VPA. These observations support the findings of Lee *et al.* [20]. Thus, our results clearly indicated that VPA induced H3 acetylation by reducing HDAC1 activity in canine ADSCs.

VPA, but not VPM, induced a significant and dose-dependent decrease in the proliferation of ADSCs, suggesting that VPA suppresses ADSC proliferation through acetylation of histone H3. p21 and p16, well-known CDK inhibitors, regulate cell cycle arrest. VPA induces expression of these CDK inhibitors in human ADSCs and mesenchymal stem cells [20, 30]. We found that VPA significantly induced mRNA expression levels of *p16* at 4 mM and of *p21* at 8 mM without inducing cell death. *p21* is also a well-known HDAC-inhibitor responsive gene that is upregulated by hyperacetylation of histones H3 and H4 [10, 20, 28]. In addition, using immunofluorescence, we showed that H3 acetylation was markedly increased by VPA and that *p21* mRNA was significantly increased by 8 mM VPA; thus, cell viability was further reduced by 8 mM VPA treatment, again supporting the findings of Lee *et al.* [20] who reported that VPA causes cell cycle arrest through increased *p21* expression in the absence of *p16* mRNA expression in human ADSCs. Therefore, the inhibitory effect of VPA on proliferation of canine ADSCs was due to cell cycle arrest, although the underlying mechanism needs to be further examined.

Furthermore, VPA promoted differentiation of approximately 90% of ADSCs into a neuronal cell lineage after 3 days of treatment. The differentiated cells have neuron-like morphology and significantly expressed βIII-tubulin protein. Pretreatment with VPA followed by neurogenic induction also promoted mRNA expression of the neuronal markers *NSE*, *TUBB3*, *MAP2* and *NEFH* as compared to the pretreatment without VPA, suggesting that promotional effects of VPA on neuronal differentiation of ADSCs were induced by upregulation of these genes. Previous reports have shown that VPA promotes differentiation of neural stem cells into neurons in adult rats [12, 15]. To our knowledge, the present study is the first report that VPA promotes neuronal differentiation of ADSCs.

Interestingly, VPA pretreatment in the absence of neurogenic induction caused moderate differentiation into neuron-like cells and also increased mRNA expression levels of neurogenic markers in ADSCs. Thus, our data indicated that VPA could induce neurogenic differentiation in the absence of neurogenic induction. We also demonstrated that VPA increased the acetylation of histone H3 that has been correlated with gene activation [12, 13]; thus, VPA caused gene expression in part through H3 acetylation. In addition, we showed that the neuron-like differentiated cells all stained positively for βIII-tubulin. Using NG108-15 cells, Liu *et al.* [21] recently reported that neuronal differentiation could modulate gene transcription, translation and post-translational modulation of Ca^{2+} channels to change the Ca^{2+} ion

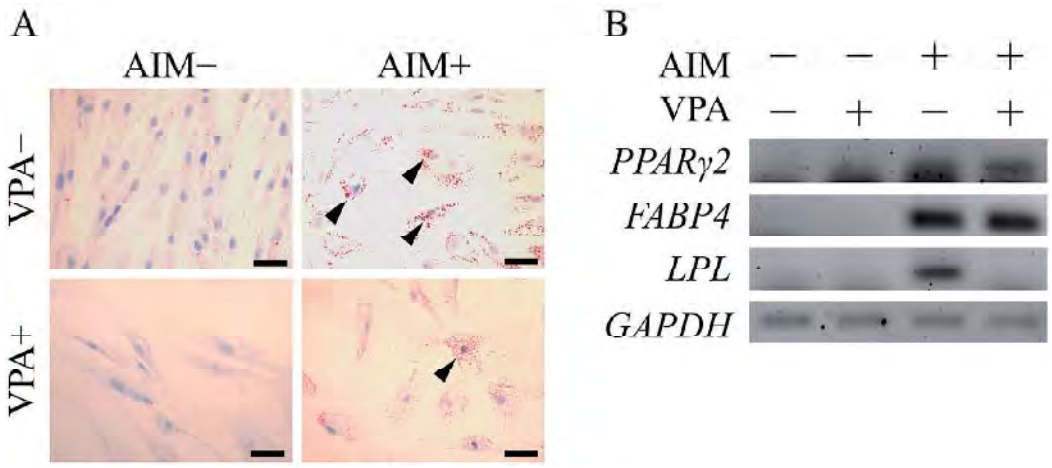

Fig. 3. Valproic acid suppresses accumulation of lipid droplets. Adipose tissue-derived stem cells (ADSCs) were pretreated with valproic acid (VPA) for 3 days followed by adipogenic induction for 14 days. (A) Adipogenic differentiation was visualized by oil red O staining after 14 days of induction with adipogenic medium. Arrowheads show cells that accumulated lipid droplets. Scale bar, 50 μm. (B) RT-PCR analysis of adipogenic markers, *PPARγ2*, *FABP4* and *LPL*, was performed using total RNA extracted from ADSCs after 14 days of adipogenic induction. AIM, adipogenic induction medium.

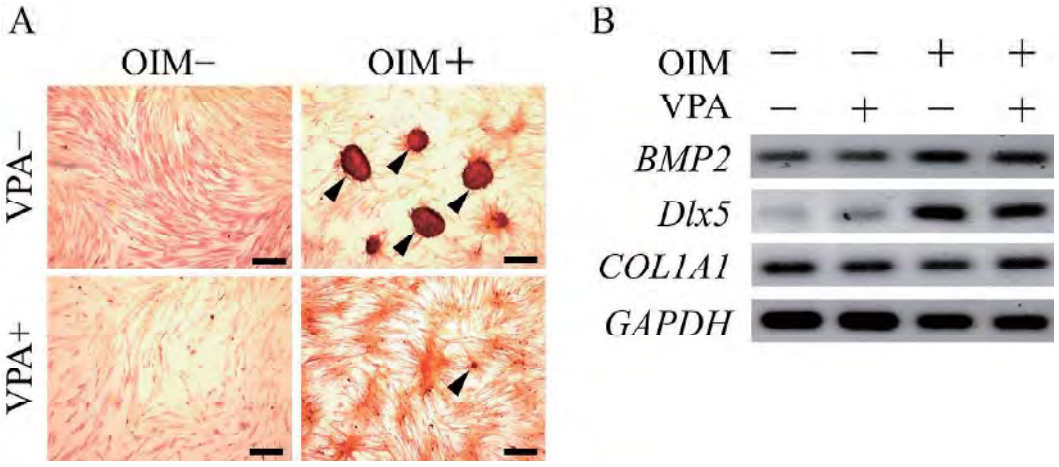

Fig. 4. Valproic acid suppresses calcium deposition. Adipose tissue-derived stem cells (ADSCs) were pretreated with valproic acid (VPA) for 3 days followed by osteogenic induction for 14 days. (A) Osteogenic differentiation was evaluated by alizarin red S staining after 14 days of induction with osteogenic medium. Arrowheads show cells that accumulated calcium in the cytosol. Scale bar, 200 μm. (B) RT-PCR analysis of osteogenic markers, *BMP2*, *Dlx5* and *COL1A1*, was performed using total RNA extracted from ADSCs after 14 days of osteogenic induction. OIM, osteogenic induction medium.

currents; our results suggested that neuronal differentiation could modulate *TUBB3* transcription and translation. In the present study, VPA promoted ADSCs differentiation into neuronal cells in the absence of neurogenic induction factors and induced acetylation of histone H3, indicating that VPA is a useful tool for studying the interaction between chromatin structure and cell fate determination. Further studies are needed to examine the molecular mechanism underlying the neurogenic differentiation induced by VPA using canine ADSCs.

In contrast, VPA suppressed the late stage of differentiation into adipogenic and osteogenic lineage cells. Two of the 3 adipogenic marker genes examined showed no reduction after VPA pretreatment; however, lipid accumulation appeared to be suppressed, suggesting that the VPA inhibits accumulation of lipid droplets rather than an inhibiting the whole adipogenic differentiation process.

Similarly, osteogenic marker genes showed no changes

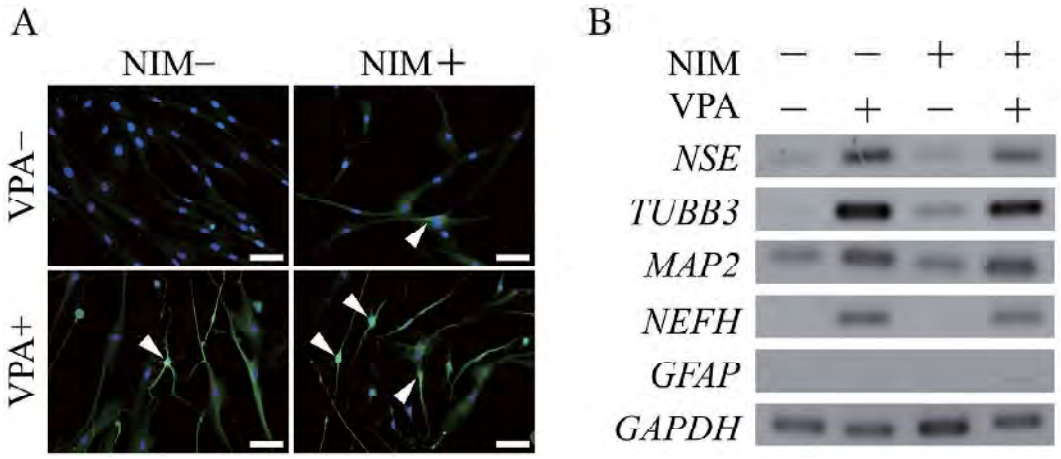

Fig. 5. Valproic acid promotes neurogenic differentiation. Adipose tissue-derived stem cells (ADSCs) were pretreated with valproic acid (VPA) for 3 days followed by neurogenic induction. (A) Neurogenic differentiation was assessed by immunofluorescence staining using an anti-βIII-tubulin antibody and a secondary antibody (FITC-conjugated goat anti-mouse IgG) after 2 hr of induction with neurogenic medium. Arrowheads show cells that expressed βIII-tubulin. Scale bar, 50 μm. (B) RT-PCR analysis of the neurogenic markers, *NSE*, *TUBB3*, *MAP2* and *NEFH* and the glial marker, *GFAP,* was performed using total RNA extracted from ADSCs after 2 hr of neurogenic induction. NIM, neurogenic induction medium.

after VPA treatment, but accumulation of calcium deposition by osteogenic induction was significantly reduced, suggesting that VPA inhibits calcium deposition rather than inhibiting the osteogenic differentiation process as a whole. The mechanism underlying the differential effects of VPA on the pluripotent capacity of ADSCs remains unclear. A previous report has shown that VPA decreases adipogenic and neurogenic differentiation, but increases osteogenic differentiation in human ADSCs [20]. The reason for VPA acting as a stimulator for differentiation of canine ADSCs and as a suppressor for that of human ADSCs is not immediately clear. Therefore, chromatin structure and cell fate determination need to be further examined in relation to the pluripotency of ADSCs, including this difference between humans and dogs.

In conclusion, pretreatment with VPA dose-dependently decreased proliferation of canine ADSCs. In parallel with its inhibitory effects, VPA increased *p16* and *p21* mRNA expression, implying induction of cell cycle arrest through activation of p16 and p21. In addition, pretreatment with VPA followed by adipogenic, osteogenic or neurogenic induction markedly promoted *in vitro* neurogenic differentiation, but suppressed accumulation of lipid droplets and calcium deposition. These *in vitro* modifications of ADSCs by pretreatment with VPA were associated with changes in expression of relevant markers. These results suggested that VPA is a specific inducer of neurogenic differentiation of canine ADSCs and is a useful tool for studying the interaction between chromatin structure and cell fate determination.

ACKNOWLEDGMENTS. This work was supported in part by the Science Research Promotion Fund of The Promotion and Mutual Aid Corporation for Private Schools of Japan. This work was also supported in part by the MEXT Program for the Strategic Research Foundation at Private Universities, 2011–2015.

REFERENCES

1. Case, J., Horvath, T. L., Howell, J. C., Yoder, M. C., March, K. L. and Srour, E. F. 2005. Clonal multilineage differentiation of murine common pluripotent stem cells isolated from skeletal muscle and adipose stromal cells. *Ann. N. Y. Acad. Sci.* **1044**: 183–200. [Medline] [CrossRef]
2. Chung, C. S., Fujita, N., Kawahara, N., Yui, S., Nam, E. and Nishimura, R. 2013. A comparison of neurosphere differentiation potential of canine bone marrow-derived mesenchymal stem cells and adipose-derived mesenchymal stem cells. *J. Vet. Med. Sci.* **75**: 879–886. [Medline] [CrossRef]
3. De Ugarte, D. A., Morizono, K., Elbarbary, A., Alfonso, Z., Zuk, P. A., Zhu, M., Dragoo, J. L., Ashjian, P., Thomas, B., Benhaim, P., Chen, I., Fraser, J. and Hedrick, M. H. 2003. Comparison of multi-lineage cells from human adipose tissue and bone marrow. *Cells Tissues Organs* **174**: 101–109. [Medline] [CrossRef]
4. Deng, W., Obrocka, M., Fischer, I. and Prockop, D. J. 2001. *In vitro* differentiation of human marrow stromal cells into early progenitors of neural cells by conditions that increase intracellular cyclic AMP. *Biochem. Biophys. Res. Commun.* **282**: 148–152. [Medline] [CrossRef]
5. Dicker, A., Le Blanc, K., Astrom, G., van Harmelen, V., Gotherstrom, C., Blomqvist, L., Arner, P. and Ryden, M. 2005. Functional studies of mesenchymal stem cells derived from adult human adipose tissue. *Exp. Cell Res.* **308**: 283–290. [Medline] [CrossRef]
6. Edamura, K., Kuriyama, K., Kato, K., Nakano, R., Teshima, K., Asano, K., Sato, T. and Tanaka, S. 2012. Proliferation capacity, neuronal differentiation potency and microstructures after the differentiation of canine bone marrow stromal cells into neurons. *J. Vet. Med. Sci.* **74**: 923–927. [Medline] [CrossRef]
7. Göttlicher, M., Minucci, S., Zhu, P., Krämer, O. H., Schimpf, A., Giavara, S., Sleeman, J. P., Coco, F. L., Nervi, C., Pelicci, P.

G. and Heinzel, T. 2001. Valproic acid defines a novel class of HDAC inhibitors inducing differentiation of transformed cells. *EMBO J.* **20**: 6969–6978. [Medline] [CrossRef]
8. Gronthos, S., Franklin, D. M., Leddy, H. A., Robey, P. G., Storms, R. W. and Gimble, J. M. 2001. Surface protein characterization of human adipose tissue-derived stromal cells. *J. Cell. Physiol.* **189**: 54–63. [Medline] [CrossRef]
9. Grunstein, M. 1997. Histone acetylation in chromatin structure and transcription. *Nature* **389**: 349–352. [Medline] [CrossRef]
10. Han, J. W., Ahn, S. H., Kim, Y. K., Bae, G. U., Yoon, J. W., Hong, S., Lee, H. Y., Lee, Y. W. and Lee, H. W. 2001. Activation of p21 (WAF1 / Cip1) transcription through Sp1 sites by histone deacetylase inhibitor apicidin: involvement of protein kinase C. *J. Biol. Chem.* **276**: 42084–42090. [Medline] [CrossRef]
11. Housman, T. S., Lawrence, N., Mellen, B. G., George, M. N., Filippo, J. S., Cerveny, K. A., DeMarco, M., Feldman, S. R. and Fleischer, A. B. 2002. The safety of liposuction: results of a national survey. *Dermatol. Surg.* **28**: 971–978. [Medline] [CrossRef]
12. Hsieh, J., Nakashima, K., Kuwabara, T., Mejia, E. and Gage, F. H. 2004. Histone deacetylase inhibition-mediated neuronal differentiation of multipotent adult neural progenitor cells. *Proc. Natl. Acad. Sci. U.S.A.* **101**: 16659–16664. [Medline] [CrossRef]
13. Jenuwein, T. and Allis, C. D. 2001. Translating the histone code. *Science* **293**: 1074–1080. [Medline] [CrossRef]
14. Jung, D. I., Ha, J., Kang, B. T., Kim, J. W., Quan, F. S., Lee, J. H., Woo, E. J. and Park, H. M. 2009. A comparison of autologous and allogenic bone marrow-derived mesenchymal stem cell transplantation in canine spinal cord injury. *J. Neurol. Sci.* **285**: 67–77. [Medline] [CrossRef]
15. Jung, G. A., Yoon, J. Y., Moon, B. S., Yang, D. H., Kim, H. Y., Lee, S. H., Bryja, V., Arenas, E. and Choi, K. Y. 2008. Valproic acid induces differentiation and inhibition of proliferation in neural progenitor cells via the beta-catenin-Ras-ERK-p21Cip/WAF1 pathway. *BioMed. Cen. Cell Biol.* **9**: 66.
16. Kamishina, H., Cheeseman, J. A. and Clemmons, R. M. 2008. Nestin-positive spheres derived from canine bone marrow stromal cells generate cells with early neuronal and glial phenotypic characteristics. *In Vitro Cell Dev. Biol. Anim.* **44**: 140–144. [Medline] [CrossRef]
17. Kern, S., Eichler, H., Stoeve, J., Kluter, H. and Bieback, K. 2006. Comparative analysis of mesenchymal stem cells from bone marrow, umbilical cord blood, or adipose tissue. *Stem Cells (Dayton, Ohio)* **24**: 1294–1301. [Medline] [CrossRef]
18. Kuo, M. H. and Allis, C. D. 1998. Roles of histone acetyltransferases and deacetylase in gene regulation. *BioEssays* **20**: 615–626. [Medline] [CrossRef]
19. Lee, R. H., Kim, B., Choi, I., Kim, H., Choi, H. S., Suh, K., Bae, Y. C. and Jung, J. S. 2004. Characterization and expression analysis of mesenchymal stem cells from human bone marrow and adipose tissue. *Cell. Physiol. Biochem.* **14**: 311–324. [Medline] [CrossRef]
20. Lee, S., Park, J. R., Seo, M. S., Roh, K. H., Park, S. B., Hwang, J. W., Sun, B., Seo, K., Lee, Y. S., Kang, S. K., Jung, J. W. and Kang, K. S. 2009. Histone deacetylase inhibitors decrease proliferation potential and multi-lineage differentiation capability of human mesenchymal stem cells. *Cell Prolif.* **42**: 711–720. [Medline] [CrossRef]
21. Liu, J., Tu, H., Zhang, D. and Li, Y.L. 2012. Changes of calcium channel mRNA, protein and current in NG108-15 cells after cell differentiation. *Biochem. Biophys. Res. Commun.* **423**: 55–59. [Medline] [CrossRef]
22. Liu, T. M., Martina, M., Hutmacher, D. W., Hui, J. H., Lee, E. H. and Lim, B. 2007. Identification of common pathways mediating differentiation of bone marrow- and adipose tissue-derived human mesenchymal stem cells into three mesenchymal lineages. *Stem Cells* **25**: 750–760. [Medline] [CrossRef]
23. Ning, H., Lin, G., Lue, T. F. and Lin, C. S. 2006. Neuron-like differentiation of adipose tissue-derived stromal cells and vascular smooth muscle cells. *Differentiation* **74**: 510–518. [Medline] [CrossRef]
24. Ning, H., Guiting, L., Fandel, T., Banie, L., Lue, T. F. and Lin, C.S. 2008. Insulin growth factor signaling mediates neuron-like differentiation of adipose tissue-derived stem cells. *Differentiation* **76**: 488–494. [Medline] [CrossRef]
25. Nishida, H., Nakayama, M., Tanaka, H., Kitamura, M., Hatoya, S., Sugiura, K., Suzuki, Y., Ide, C. and Inaba, T. 2011. Evaluation of transplantation of autologous bone marrow stromal cells into the cerebrospinal fluid for treatment of chronic spinal cord injury in dogs. *Am. J. Vet. Res.* **72**: 1118–1123. [Medline] [CrossRef]
26. Olby, N. 2010. The pathogenesis and treatment of acute spinal cord injuries in dogs. *Vet. Clin. North Am. Small Anim. Pract.* **40**: 791–807. [Medline] [CrossRef]
27. Phiel, C. J., Zhang, F., Huang, E. Y., Guenther, M. G., Lazar, M. A. and Klein, P. S. 2001. Histone deacetylase is a direct target of valproic acid, a potent anticonvulsant, mood stabilizer, and teratogen. *J. Biol. Chem.* **276**: 36734–36741. [Medline] [CrossRef]
28. Richon, V. M., Sandhoff, T. W., Rifkind, R. A. and Marks, P. A. 2000. Histone deacetylase inhibitor selectively induces p21WAF1 expression and gene-associated histone acetylation. *Proc. Natl. Acad. Sci. U.S.A.* **97**: 10014–10019. [Medline] [CrossRef]
29. Sago, K., Tamahara, S., Tomihari, M., Matsuki, N., Asahara, Y., Takei, A., Bonkobara, M., Washizu, T. and Ono, K. 2008. In vitro differentiation of canine celiac adipose tissue-derived stromal cells into neuronal cells. *J. Vet. Med. Sci.* **70**: 353–357. [Medline] [CrossRef]
30. Shibata, K. R., Aoyama, T., Shima, Y., Fukiage, K., Otsuka, S., Furu, M., Kohno, Y., Ito, K., Fujibayashi, S., Neo, M., Nakayama, T., Nakamura, T. and Toguchida, J. 2007. Expression of the p16INK4A gene is associated closely with senescence of human mesenchymal stem cells and is potentially silenced by DNA methylation during in vitro expansion. *Stem Cells* **25**: 2371–2382. [Medline] [CrossRef]
31. Skinner, A. P., Pachnicke, S., Lakatos, A., Franklin, R. J. and Jeffery, N. D. 2005. Nasal and frontal sinus mucosa of the adult dog contain numerous olfactory sensory neurons and ensheathing glia. *Res. Vet. Sci.* **78**: 9–15. [Medline] [CrossRef]
32. Starkey, M. P., Scase, T. J., Mellersh, C. S. and Murphy, S. 2005. Dogs really are man's best friend—canine genomics has applications in veterinary and human medicine! *Brief Funct. Genomic Proteomic.* **4**: 112–128. [Medline] [CrossRef]
33. Strem, B. M., Hicok, K. C., Zhu, M., Wulur, I., Alfonso, Z., Schreiber, R. E., Fraser, J. K. and Hedrick, M. H. 2005. Multipotential differentiation of adipose tissue-derived stem cells. *Keio J. Med.* **54**: 132–141. [Medline] [CrossRef]
34. Struhl, K. 1998. Histone acetylation and transcriptional regulatory mechanisms. *Genes Dev.* **12**: 599–606. [Medline] [CrossRef]
35. Wagner, W., Wein, F., Seckinger, A., Frankhauser, M., Wirkner, U., Krause, U., Blake, J., Schwager, C., Eckstein, V., Ansorge, W. and Ho, A. D. 2005. Comparative characteristics of mesenchymal stem cells from human bone marrow, adipose tissue, and umbilical cord blood. *Exp. Hematol.* **33**: 1402–1416. [Medline] [CrossRef]
36. Wu, P., Sato, K., Yukawa, S., Hikasa, Y. and Kagota, K. 2001. Differentiation of stromal-vascular cells isolated from canine

adipose tissues in primary culture. *J. Vet. Med. Sci.* **63**: 17–23. [Medline] [CrossRef]
37. Yoshimura, H., Muneta, T., Nimura, A., Yokoyama, A., Koga, H. and Sekiya, I. 2007. Comparison of rat mesenchymal stem cells derived from bone marrow, synovium, periosteum, adipose tissue, and muscle. *Cell Tissue Res.* **327**: 449–462. [Medline] [CrossRef]
38. Zuk, P. A., Zhu, M., Ashjian, P., DeUgarte, D. A., Huang, J. I., Mizuno, H., Alfonso, Z. C., Benhaim, P. and Hedrick, M. H. 2002. Human adipose tissue is a source of multipotent stem cells. *Mol. Biol. Cell* **13**: 4279–4295. [Medline] [CrossRef]
39. Zuk, P. A., Zhu, M., Mizuno, H., Huang, J., Futrell, J. W., Katz, A. J., Benhaim, P., Lorenz, H. P. and Hedrick, M. H. 2001. Multilineage cells from human adipose tissue: implications for cell-based therapies. *Tissue Eng.* **7**: 211–228. [Medline] [CrossRef]

FULL PAPER *Pathology*

Pathological Features of Polyneuropathy in Three Dogs

Masaya TSUBOI[1)], Kazuyuki UCHIDA[1)]*, Tetsuya IDE[1)], Mizue OGAWA[1)], Takehiko INAGAKI[2)], Shinji TAMURA[3)], Miyoko SAITO[4)], James K. CHAMBERS[1)] and Hiroyuki NAKAYAMA[1)]

[1)]*Department of Veterinary Pathology, Graduate School of Agricultural and Life Sciences, The University of Tokyo, 1–1–1 Yayoi, Bunkyo-ku, Tokyo 113–8657, Japan*

[2)]*Department of Neurology, Japan Animal Referral Medical Center, 2–5–8 Kuji, Takatsu-ku, Kawasaki-shi, Kanagawa 213–0032, Japan*

[3)]*Tamura Animal Clinic, 7–16 Saeki-ku, Hiroshima-shi, Hiroshima 731-5100, Japan*

[4)] *Department of Surgery II, School of Veterinary Medicine, Azabu University, 1–17–71 Fuchinobe, Chuo-ku, Sagamihara-shi, Kanagawa 229–8501, Japan*

(Received 16 May 2012/Accepted 18 October 2012/Published online in J-STAGE 1 November 2012)

ABSTRACT. Canine polyneuropathy is a neurological disorder characterized by a dysfunction of multiple peripheral nerves. The etiology of the disease is diverse; it may occur in cases of infectious, immune-mediated, or hereditary conditions or in association with endocrinopathy, neoplasm, or chemical intoxication. It is often difficult to determine the etiology through clinical symptoms. The aim of this study is to investigate pathological differences among three canine polyneuropathy cases with each presumably having a different etiology. Cases included a 13-month-old female border collie (Dog No.1), a 21-month-old male chihuahua (Dog No.2) and an 11-year-old male beagle (Dog No.3). Clinical examinations revealed hindlimb ataxia and sensory loss in Dog No.1, forelimb paralysis and vertebral pain in Dog No.2, and paddling-gait and hypothyroidism in Dog No.3. Histopathologically, axonal swelling and pale myelin were observed in Dog No.1. Giant axons mimicking giant axonal neuropathy were obvious in Dog No.2. Dog No.3 showed atrophic axons and severe interstitial edema. Distributions of peripheral nerve lesions coincided with respective clinical symptoms. According to their clinical and pathological features, Dogs No.1 and No.2 were suspected of hereditary polyneuropathy, while Dog No.3 seemed to have hypothyroidism-associated polyneuropathy. As each case demonstrated unique pathological features, different pathogeneses of peripheral nerve dysfunction were suggested.

KEY WORDS: canine, congenital, hypothyroidism, polyneuropathy.

doi: 10.1292/jvms.12-0224; *J. Vet. Med. Sci.* 75(3): 327–335, 2013

Polyneuropathy in dogs is a neurological disorder characterized by a dysfunction of multiple peripheral nerves. Initial symptoms of the disease are a lack of coordination and instability, and often progress to decreased reflexes and muscle tone, paralysis, and sensory deficits [45]. Electromyographic evidence of denervation and decreased nerve conduction velocity has been observed in affected nerves [45]. Somatic nerve dysfunctions are most predominant, and autonomic nerves may also be affected. As autonomic dysfunction may lead to laryngeal or pharyngeal paralysis, aspiration pneumonia is frequently diagnosed as a cause of death in canine polyneuropathy cases [6, 16, 26, 32, 46].

Several etiologies of polyneuropathy in dogs have been previously proposed. In some cases, the disease occurs in association with *Neospora caninum* infection [10] or some immune-mediated diseases, such as systemic lupus erythematosus [11]. Primary autoimmune diseases against peripheral nerve myelin may also lead to the disease [1, 51]. Some seem to occur in specific breeds, indicating that hereditary, familial or breed-associated factors are related to the etiology of the disease [17]. It may also be associated with endocrinopathy including diabetes mellitus [27, 34, 47] and hypothyroidism [25, 49], intoxication of n-hexane [37] or acrylamide [20], administration of cisplatin [36] or vincristine [21], or paraneoplastic syndromes in cases of insulinoma [3, 5], multicentric lymphoma [5], or disseminated carcinoma [5]. It is often difficult to distinguish the etiology of this disease through clinical symptoms.

The distribution of lesions (*i.e.* motor or sensory, distal or proximal, anterior or posterior and symmetric or asymmetric) is useful for etiology-based classification of polyneuropathy [7, 8, 10]. In the human-inherited polyneuropathy, Charcot-Marie-Tooth (CMT) disease, classification is established according to lesion distribution, age onset, progression speed and pathological features [18], and a number of genetic mutations have been identified in respective subtypes [7, 43]. In contrast, little information on genetic factors has been accumulated in canine-inherited polyneuropathy [8]. So far, canine-inherited polyneuropathy has been reported in 22 breeds, but underlying genetic defects are not yet confirmed in most breeds [8, 17].

The aim of this study is to investigate pathological differences among three cases of canine polyneuropathy with each presumably having a different etiology. Possible pathogenesis and respective etiologies of each case are discussed.

*CORRESPONDENCE TO: UCHIDA, K., Department of Veterinary Pathology, Graduate School of Agricultural and Life Sciences, The University of Tokyo, 1–1–1 Yayoi, Bunkyo-ku, Tokyo 113–8657, Japan.
e-mail:auchidak@mail.ecc.u-tokyo.ac.jp

MATERIALS AND METHODS

Cases: Three dogs were examined; Dog No.1 was a 13-month-old female border collie, Dog No.2 was a 21-month-old male chihuahua and Dog No.3 was an 11-year-old male beagle. Clinical features of these cases are summarized in Table 1.

Dog No.1 showed progressive hind limb ataxia at the age of 3 months, and started chewing her front paw. Ataxia then spread to all 4 limbs. Spinal reflexes were normal to reduced in the hind limbs. Superficial sensation was not detected in sciatic and femoral areas of both sides of the distal hind limbs and in the radial area of both sides of the distal front limbs. Magnetic resonance imaging (MRI) of the spinal cord and cerebrospinal fluid (CSF) examination showed no specific findings. Ataxia gradually progressed, and the dog developed megaesophagus at the age of 12 months. The dog suddenly died 1 month after the onset of megaesophagus.

Dog No.2 was presented to the veterinary hospital 2 months prior to his death with a chief complaint of crying when held in his owner's arms. One month after the initial symptom, the dog exhibited salivation and a pitter-patter gait. Further clinical examination revealed a reduced bilateral palpebral reflex, persistent prolapse of the penis, and vertebral pain induced by manual compression. MRI and computerized tomography (CT) of the entire body showed no specific findings. Thyroid hormone levels were normal, and anti-acetylcholine receptor antibody was not detected in the serum. Tandem mass spectrometry used for the diagnosis of inherited metabolic disorders was conducted, but no specific information was obtained. Although the dog was treated with corticosteroids and vitamin supplements, symptoms did not improve. The forelimbs gradually became paralyzed, and atrophy of the forelimb muscle was marked. Finally, the dog exhibited epileptiform seizures and died of respiratory failure.

Dog No.3 began to show a characteristic paddling gait at the age of 3, wherein the distal palmar and plantar aspects of the feet flip forward at the impact to the ground. The dog also sank on these limbs during the impact. Two years after the onset of the first symptom, the dog presented to the veterinary hospital with a chief complaint of a wobbling gait. The dog exhibited bradycardia at the initial visit, and neurological examination revealed a reduced postural reaction. MRI showed no specific findings. Biochemical examination at the age of 7 revealed low thyroxine (T4) and free T4 (fT4) concentrations (T4: 0.79 μg/d*l*, relative to normal values of>2.0 μg/d*l*, and fT4: 0.08 *n*g/d*l*, relative to normal values of>0.6 *n*g/d*l*). Thus, the dog was diagnosed with hypothyroidism. The dog was treated with thyroid hormone, but symptoms gradually developed. The dog began to present difficulty in walking at the age of 9. Using sensory nerve action potential examination, the dog was further diagnosed with sensory nerve predominant segmental demyelinative neuropathy at the age of 10, and was treated with an immune suppressor and prednisolone. The treatment, however, had no effect. Finally, the dog died of aspiration pneumonia at the age of 11.

Antemortem biopsy and teased nerve fiber test: Antemortem biopsy and a teased nerve fiber test were conducted only in Dog No.1. Peripheral nerves (including the right common peroneal nerve and right caudal cutaneous antebrachial nerve) and the skin of the dorsal part of the right front paw were taken for biopsy.

Postmortem examination: Tissue samples were taken from the brain, spinal cord and nerve roots of the 3 dogs. Other main organs including the heart, lungs, liver, spleen, kidneys, alimentary tract, pituitary gland, thyroid glands, adrenal glands, ovaries and uterus were taken only from Dog No.1, because autopsies of the other dogs were performed at the veterinary hospitals. The trigeminal ganglion, stellate ganglion, brachial plexus, femoral obturator nerve, vagus nerve, biceps femoris muscle, temporal muscle and lingual muscle were also taken from Dog No.1. Sciatic and tibial nerves were taken from Dog No.3. All tissue samples were fixed in 10% neutral buffered formalin, processed routinely, embedded in paraffin wax, and sectioned at 4 μm. Sections were double-stained with luxol-fast blue (LFB) and hematoxylin-eosin (HE).

Immunohistochemistry: Primary antibodies used were mouse monoclonal anti-neurofilament (NF, pre-diluted, Dako, Glostrup, Denmark), rabbit polyclonal anti-peripheral myelin protein 22 (PMP22, 1:400, Sigma, St. Louis, MO, U.S.A.), rabbit polyclonal anti-periaxin (PRX, 1:250, Sigma) and rabbit polyclonal anti-Myelin protein zero (MPZ, 1:100, Abcam, Cambridge, UK). Immunohistochemistry was performed using Envision polymer reagent (Dako). Antigen retrieval was performed by heating sections in an autoclave at 121°C for 10 min in 10 mM citrate buffer (pH6.0), except for NF immunohistochemistry. Sections were next incubated in 3% hydrogen peroxide (H_2O_2)-methanol at room temperature for 5 min to block endogenous peroxidase, in 8% skim milk-tris buffered saline (TBS) at 37°C for 40 min to avoid nonspecific reactions, and then with primary antibody at 4°C overnight. Sections were further incubated with

Table 1. Canine polyneuropathy cases examined

Case	Breed	Gender	Onset	Death	Major clinical signs
Dog No.1	Border collie	Female	3m	1y1m	Hind limb ataxia, pain sensability loss, megaesophagus, chewing front paws, and aspiration pneumonia
Dog No.2	Chihuahua	Male	1y7m	1y9m	Salivation, bilateral eyelid reflex reduction, continuous penis prolapse, ataxia, forelimb paralysis, and vertebral pain
Dog No.3	Beagle	Male	3y	11y	Paddling-gait, bradycardia, hypothyroidism, walking difficulty, and aspiration pneumonia

Envision horseradish peroxidase (HRP)-labeled mouse or rabbit polymer reagent (Dako) at 37°C for 60 min. Reaction products were visualized with 3.3'-diaminobenzidine (DAB, Dojindo, Kumamoto, Japan) and 0.03% H_2O_2 in TBS. Sections were counterstained with Mayer's hematoxylin. As a control, sections from dogs showing no clinical/pathological signs of polyneuropathy were used.

Quantitative analysis: NF-stained transverse sections of the lumber nerve root were used for quantitative analysis. Microscopic pictures of 2 randomly selected-areas of dorsal and ventral nerve roots were taken with a Nikon Digital Camera DXM1200F (Nikon, Tokyo, Japan) at a magnification of × 200 with ACT-1 software (Nikon). The smallest diameters of respective NF-positive axons were then computed using Mac-Biophotonics ImageJ software. More than 1,000 fibers in each nerve root were measured.

RESULTS

Antemortem biopsy and the teased nerve fiber test: Antemortem peripheral nerve biopsy was conducted only in Dog No.1. The right common peroneal nerve, right caudal cutaneous antebrachial nerve, and peripheral nerves from the dorsal skin of the right front paw showed severe degeneration and denervation with both sensory and motor involvement (Data not shown). The teased nerve fiber test was also conducted only in Dog No.1. Neither Wallarian-like axonal degeneration nor regenerative changes were observed in the teased nerve fiber test (Data not shown).

Gross findings on necropsy: Details were available only in Dog No.1. Severe emaciation, multiple ulcerations on the bilateral hind limb paws, swelling of systemic lymph nodes, and aspiration pneumonia were observed. There were no specific findings in the gross appearance of the brain and spinal cord of all three cases.

Histopathological findings on necropsy: Major pathological lesions were located at nerve roots and/or distal peripheral nerves in all cases (Fig. 1A, 1B and 1C). Histopathological lesions and their distributions in peripheral nerves were different among cases (Table 2).

In Dog No.1, lesions were predominant at lumbar and sacral ventral nerve roots, and the major lesion was axonal swelling (Fig. 1D). Myelin stained with LFB was paler than usual at the central area of nerve roots. Axonal loss was not evident in any nerve roots of Dog No.1. Lesions in Dog No.2 were located mainly in cervical and thoracic nerve roots. Almost all axons were lost and lesions were replaced by dense fibrous connective tissues (Fig. 1G and 1H). Lesions were asymmetric and randomly distributed. At the lumber level, axonal and myelin loss was milder than that at the cervical level, but multiple axonal swellings were observed at the unilateral sensory nerve root at L4 (Fig. 1E). Such swollen axons were roughly distorted and were huge (10 to 30 μm as the shortest diameter). In Dog No.3, lesions were found at the cervical and lumber level of motor and sensory nerve roots, where diffuse axonal atrophy was evident. Severe endoneurial edema and mild fibrous connective tissue proliferation were associated with lesions (Fig. 1F). Lesions were more severe in sensory nerve roots than those in motor nerve roots. Inflammatory cell infiltration was not observed in any cases.

Distal peripheral nerves were also examined in Dogs No.1 and No.3. In Dog No.1, lesions of the femoral obturator nerve and brachial plexus were more severe than those of nerve roots. Severe axonal swelling, mild axonal loss, pale myelin and mild proliferation of collagen fibers were also observed (Fig. 1I). In Dog No.3, sural and tibial nerves showed a severe decrease in axons and loss of myelin. Most lesions were replaced with fibrous connective tissues (Fig. 1J).

Minor lesions were observed in the central nervous system (CNS), such as focal neuronal loss in the cerebral cortex of Dog No.2 and diffuse spheroid formation in the spinal cord of Dog No.3 (Data not shown).

Quantitative analysis: The axonal diameter of nerve roots was analyzed using NF-immunostained specimens (Fig. 2). In control cases, the shape of the histogram for the motor nerve root showed a "bimodal" pattern, which indicates the presence of large caliber fibers ranging from 6 to 8 μm, and small caliber fibers ranging from 1 to 3 μm (Fig. 2G, 2H and 2I). In contrast, the number of large caliber fibers in the sensory nerve root was fewer than that in the motor nerve root (Fig. 2J, 2K and 2L). Therefore, the shape of the histogram showed a "triangular" pattern.

In Dog No.1, a bimodal pattern in motor nerve roots was still evident, but the distribution of the axonal diameter tended to shift to the right (larger area) (Fig. 2G). The distribution in the sensory nerve root showed a slight left shift (Fig. 2J). In Dog No.2, distribution in both motor and sensory nerves shifted to the left, and giant axons more than 15 μm were often observed in the sensory nerve root (Fig. 2H and 2K). In Dog No.3, the axonal distribution of both motor and sensory nerve roots markedly shifted to the left, and the regular "bimodal" pattern of the motor nerve root changed to a "triangular" pattern (Fig. 2I and 2L).

Immunohistochemistry for myelin components: Among 3 peripheral myelin components examined, PMP22 and PRX were strongly positive in the axonal surroundings. MPZ expression was limited to Dog No.1, and non-specific MPZ expressions were observed in the axons of Dogs No.2 and No.3 (data not shown).

DISCUSSION

Severe degenerative changes were broadly distributed in the peripheral nervous system (PNS) of the three present cases, while significant pathological changes were not observed in the CNS. Thus, the present cases were diagnosed as canine polyneuropathy. Interestingly, the distributions and pathological features of lesions were different among the cases. This fact indicates different pathogeneses in the respective cases.

According to clinical histories and pathological findings, Dogs No.1 and No.2 were suspected of hereditary polyneuropathy. Both dogs were young at the onset of the disease and took long-standing courses until death. Such features are

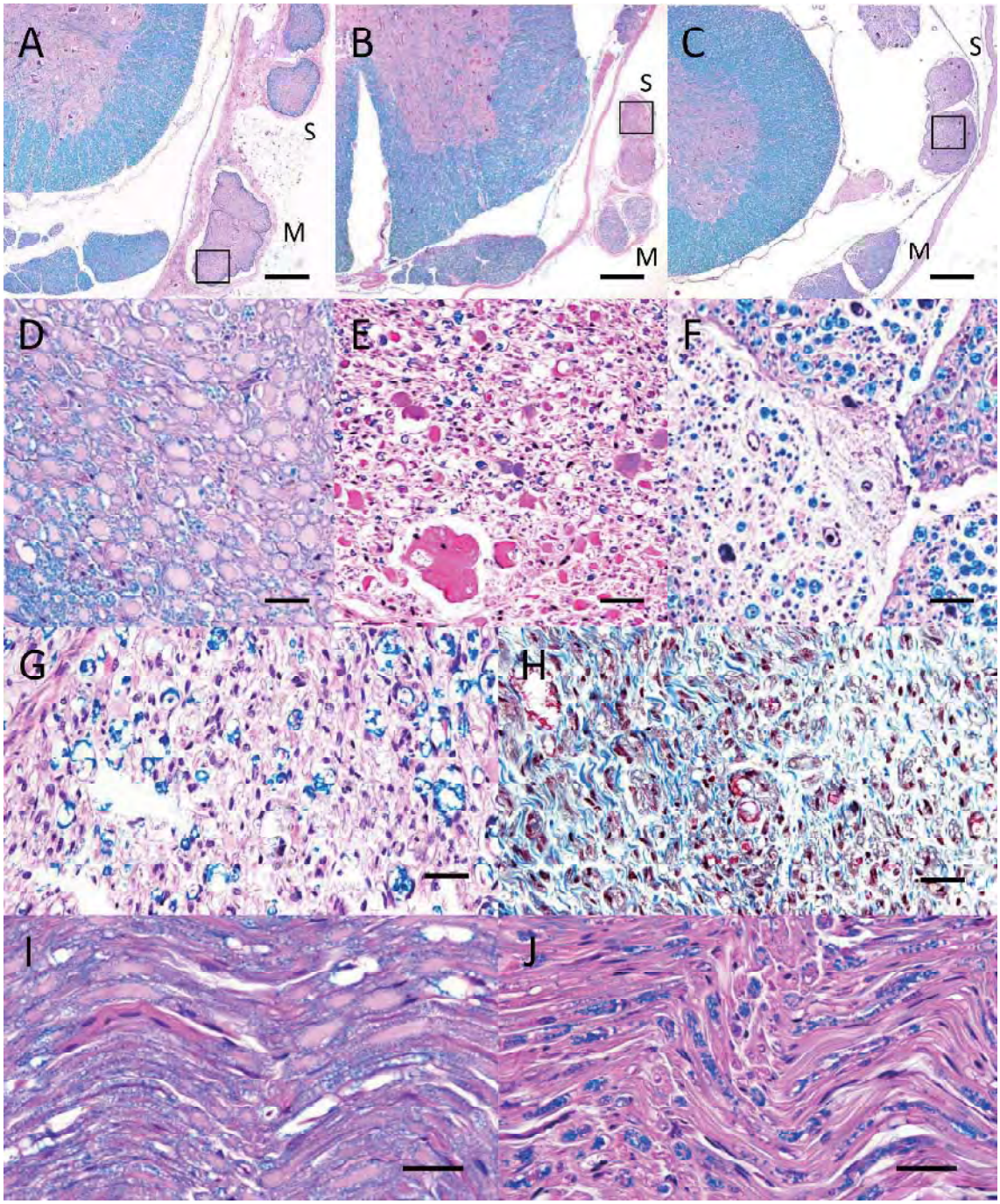

Fig. 1. (A-C): Low magnification of the lumber cord and associated nerve roots of Dogs No.1 (A), No.2 (B) and No.3 (C). LFB-HE stain. Bar=500 μm. In all cases, lesions were located in sensory (S) and/or motor (M) nerve roots. (D-F): Higher magnification of the boxes shown in (A-C). LFB-HE stain. Bar=20 μm. (D) Axons in Dog No.1 were severely swollen, and surrounding myelin was pale stained with LFB. (E) Dog No.2 had giant axons, and surrounding myelin was lost. (F) Axons in Dog No.3 were small in diameter, and severe edema was observed in the interstitium. (G, H): High magnification of the cervical sensory nerve root in Dog No.2. LFB-HE stain (G) and Masson's trichrome stain (H). Bar=20 μm. Severe edema and mild fibrous connective tissue proliferation were associated with severe axonal loss. (I, J): High magnification of distal peripheral nerves of Dogs No.1 (I) and No.3 (J). LFB-HE stain. Bar=20 μm. (I) Femoral obturator nerve in Dog No.1 had more severe degeneration in both axons and myelin than that in nerve roots. (J) Axons and myelin in the tibial nerve of Dog No.3 were severely lost, and most lesions were replaced with connective tissue.

Table 2. Histological lesions in the cervical, thoracic, lumber and sacral nerve roots

	Dog No.1		Dog No.2		Dog No.3	
	Motor	Sensory	Motor	Sensory	Motor	Sensory
Cervical						
Axonal swelling	−	+	−	−	−	−
Axonal loss	−	−	+++	+++	++	+++
Myelin loss	+	+	+++	+++	++	++
Edema	−	−	+	-	++	++
Fibrosis	+	−	+++	++	++	++
Thoracic						
Axonal swelling	++	−	−	−	ND	ND
Axonal loss	−	−	++	+	ND	ND
Myelin loss	+	−	+++	+++	ND	ND
Edema	−	−	++	++	ND	ND
Fibrosis	+	−	++	+	ND	ND
Lumbar						
Axonal swelling	+++	−	−	+++	−	−
Axonal loss	−	−	+	+	−	++
Myelin loss	++	+	++	++	−	++
Edema	−	−	+	+	+	+++
Fibrosis	−	−	+	+	++	++
Sacral						
Axonal swelling	+++	−	−	−	ND	ND
Axonal loss	−	−	−	−	ND	ND
Myelin loss	++	++	−	−	ND	ND
Edema	−	−	−	−	ND	ND
Fibrosis	−	−	−	−	ND	ND

−: None, +: Faint, ++: Mild, +++: Moderate, and ND: No data.

characteristic of inherited polyneuropathy [17]. Other causes such as chemical or drug intoxication were rejected, because of their clinical histories. Infectious or autoimmune diseases were also rejected, because inflammatory cell infiltration was not associated with the present cases. Endocrinopathy was not detected through the antemortem blood test, and neoplasm hardly occurs at their ages. Therefore, breed-associated congenital factors are the most likely etiology in the 2 dogs.

Breed-associated polyneuropathy in border collies has been previously reported in the United Kingdom [50], Belgium [48], and North America [22]. Although there was no information concerning the familial history of the present border collie dog (Dog No.1), clinical signs were almost consistent with those of previous cases [22, 48, 50]: the onset of disease occurred at 2 to 5 months old, and erosion in the hind footpad was observed. Pathological findings of the antemortem biopsy (*i.e.* severe degeneration and denervation) were also similar to those of previous reports [22, 48, 50]. Taking these similarities into account, it is likely that Dog No.1 suffered border collie polyneuropathy.

In spite of clinical and antemortem pathological similarities, postmortem pathological features in Dog No.1 were quite different from those of previous reports. Axonal swelling and pale myelin seen in the present case have never been mentioned in previous reports. This intriguing phenomenon may be explained by a difference in examined regions between past and present cases; pathological features previously described are confined to the distal end of peripheral nerves, and more proximal regions, as in the present case, were not examined in previous reports.

The disorder in the border collie was previously called "sensory neuropathy", because initial symptoms were predominantly located at sensory nerves [48, 50]. Harkin *et al.* [22] proposed the name "sensory and motor neuropathy", because motor nerves were also involved in his case. Lesions of the present case support Harkin's opinion, because both motor and sensory nerves were impaired.

Giant axons observed in the dorsal lumber root of Dog No.2 were variable in size and had an irregular shape. They seemed to be different from the axonal swelling observed in Dog No.1, but were similar to lesions observed in "giant axonal neuropathy" (GAN) in humans [31] and German shepherds [13, 14, 19]. However, the distribution of giant axons in Dog No.2 was different from that in previous GAN cases. While the distribution of giant axons in GAN has been reported in both central and peripheral nervous systems [13, 14, 19], these CNS lesions were not found in Dog No.2. Moreover, hind limbs were mostly affected in GAN cases, while forelimbs were mostly affected in Dog No.2. Combining these differences, we suggest that the present case of Dog No.2 is a unique congenital polyneuropathy newly emerged in the chihuahua.

Although peripheral nerves were mostly impaired in Dog No.2, a minor lesion was also observed in the CNS; there was focal neuron loss at the cerebral cortex. This pathologic

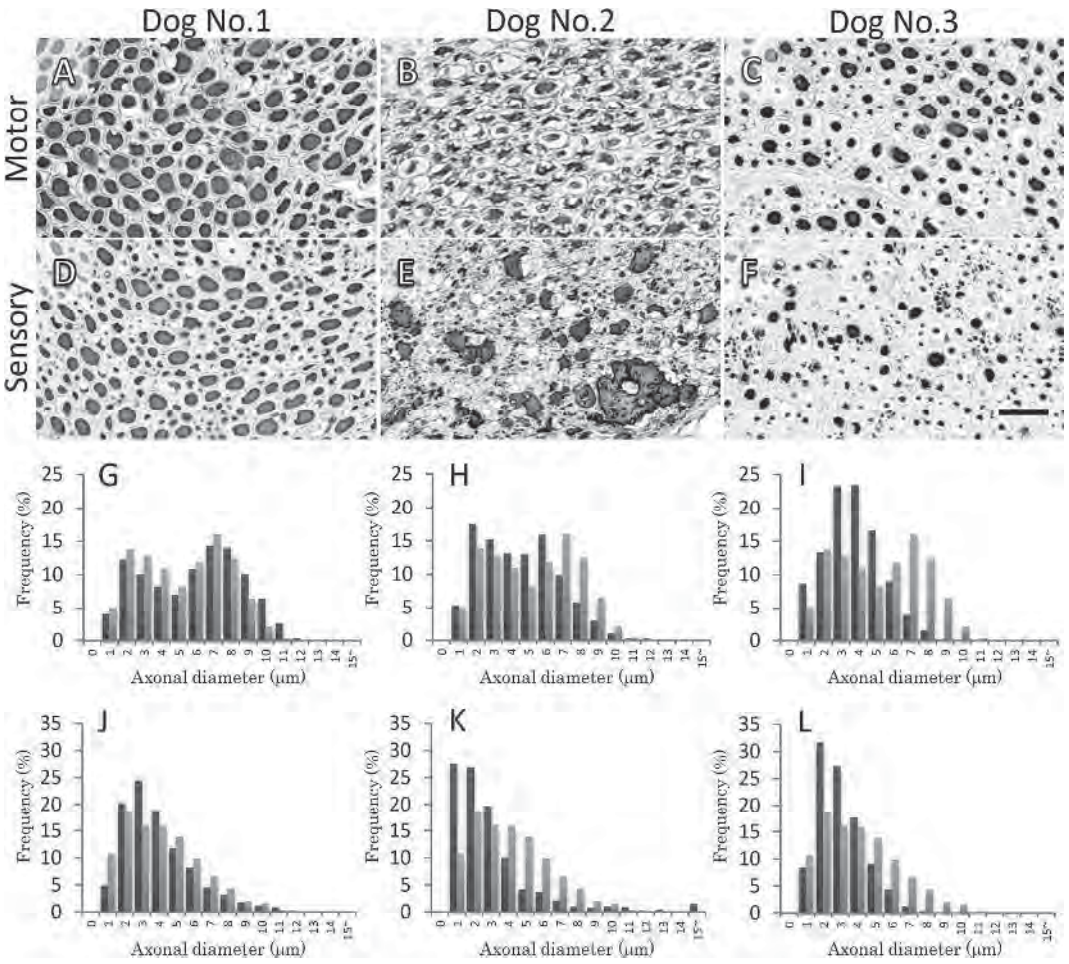

Fig. 2. (A-F): Transverse sections of lumber motor (A-C) and sensory (D-F) nerve roots. Anti-neurofilament immunohistochemistry. Bar=20 μm. Axonal diameters were measured using Mac-Biophotonics ImageJ software. (G-L): Axonal diameter distributions of motor (G-I) and sensory (J-L) nerve roots of Dogs No.1 (G and J; shown in dark bars), No.2 (H and K; shown in dark bars), No.3 (I and L; shown in dark bars), and control dogs (G-L; shown in light bars), respectively.

feature correlates with antemortem epileptic symptoms. On another hand, there were some discrepancies between clinical and pathological appearances in Dog No.2; the dog clinically showed palpebral reflex reduction, but a pathological lesion related to the reflex was not observed in the CNS. The neural circuit of the palpebral reflex consists of the trigeminal nerve, mesencephalon and facial nerve, but the CNS part of this neural circuit was not impaired in this dog. Thus, we suspect that the clinical symptom seemed to be attributed to cranial nerve dysfunction. Nevertheless, we could not evaluate pathological changes in these cranial nerves, because we failed to investigate them on necropsy.

In human CMT disease, more than 30 genes have been identified as causal genes [7, 43]. Some of those genes encode constructive proteins of peripheral myelin sheaths. MPZ, for example, is an integral membrane glycoprotein and is a major component of peripheral nerve myelin [39]. MPZ guides the wrapping process in Schwann cells and ultimately compacts adjacent lamellae [39]. More than 120 mutations in the *MPZ* gene have been identified in CMT type 1B, which is demyelinative neuropathy [23], or in CMT types 2I and 2J, which are axonal neuropathies [2, 28]. Likewise, PRX and PMP22 protein construct peripheral myelin sheaths, and genetic failures in these proteins are the causes of CMT type 1A and type 4F, respectively [30, 41]. Altered amino acid sequences of these constructive proteins lead to a failure to interact properly with other myelin components, and results in myelin disruption.

On another hand, the genetic background of canine hereditary polyneuropathy remains unclear in most breeds. Recently, Drögemüller *et al.* [12] identified a deletion in the N-myc downstream regulated gene 1 (*NDRG1*) gene in greyhound polyneuropathy. It was recognized as the first genetically characterized canine model of human CMT disease, as the *NDRG1* mutation had been identified in human CMT disease type 4D. It may offer an opportunity to gain further

insight into the pathobiology and therapy of human *NDRG1* associated CMT disease.

We probatively tried to investigate the genetic causes of the 2 present cases that were suspected of hereditary polyneuropathies. Using immunohistochemical methods, we evaluated PMP22, PRX and MPZ protein expressions in intact peripheral nerves. Among them, PMP22 and PRX were expressed normally in the peripheral myelin sheath in all cases. Therefore, genes encoding these proteins do not seem to be responsible for the onset of the disease. MPZ expression in the myelin sheath was observed only in Dog No.1, and only faint axonal expression was observed in Dogs No.2 and No.3. Faint axonal expression was also observed in several samples from control cases. Therefore, we concluded that differences in expression may be due to respective fixation conditions, not *MPZ* gene mutations.

Contrary to Dogs No.1 and No.2, Dog No.3 was suspected to have acquired neuropathy with an association of hypothyroidism. Clinical signs of tetraparesis and postural reaction dysfunction in Dog No.3 were consistent with those of previous reports of canine hypothyroid polyneuropathy [4, 24, 25, 42, 49]. Even though hypothyroidism is a common endocrinopathy of dogs and has been blamed for generalized peripheral neuropathy, there is currently insufficient objective evidence to prove a causal relationship between hypothyroidism and acquired polyneuropathy in dogs [11]. Previously, Rossmeisl [42] experimentally induced chronic hypothyroidism in dogs using radioactive iodine administration, and evaluated clinical and electrophysiologic effects on multiple peripheral nerves. The previous report succeeded in replicating the hypothyroid condition, but failed to detect any adverse clinical or electrophysiologic peripheral neuropathic changes. Another report of experimentally induced hypothyroidism in the rat showed similar results [40]. Thus, it is likely that other factors may be required for the development of hypothyroid polyneuropathy.

The pathological features of hypothyroid polyneuropathy have not been identified in dogs. In humans [33, 35, 38, 44], it has been reported that demyelination and interstitial edema may be associated with axonal atrophy in a long-standing course of hypothyroidism. The bimodal pattern is lost in the histogram of peripheral nerve axons in human hypothyroid neuropathy [44]. These features are very similar to those in Dog No.3.

There are some hypotheses that explain the pathomechanism of human hypothyroid polyneuropathy. Altered Schwann cell metabolism may cause mucinous deposition, which results in nerve entrapment and demyelination [9, 15, 29]. Severe metabolic defects in neurons may also disturb axonal transport and lead to axonal atrophy [9, 15, 29]. Vascular nerve damage secondary to hypothyroid-induced alternations in the blood-nerve barrier may also cause demyelination [9, 15, 29]. Considering these pathologic similarities, hypothyroid polyneuropathy in dogs may have the same pathogenesis as that of humans.

In conclusion, the present paper describes the pathological features of three canine cases of polyneuropathy. All 3 cases exhibited unique pathologic features, and the respective etiologies seemed different from each other. The cases of the border collie and chihuahua were suspected of inherited polyneuropathy, with each perhaps having different genetic factors, while the case of the beagle was presumably associated with hypothyroidism. This paper presents new aspects of the respective polyneuropathies. In the case of the border collie, the pathologic appearance of peripheral nerves showed quite different features from that of previous reports. The case of the chihuahua indicates a newly-emerged hereditary polyneuropathy, the features of which partly resemble GAN in German shepherd dogs. The case of the beagle presented a novel pathologic feature of canine hypothyroid polyneuropathy for the first time. Further studies are required to confirm respective pathogeneses of canine polyneuropathy.

REFERENCES

1. Alaedini, A., Sander, H. W., Hays, A. P. and Latov, N. 2003. Antiganglioside antibodies in multifocal acquired sensory and motor neuropathy. *Arch. Neurol.* **60**: 42–46. [Medline] [CrossRef]
2. Auer-Grumbach, M., Strasser-Fuchs, S., Robl, T., Windpassinger, C. and Wagner, K. 2003. Late onset Charcot-Marie-Tooth 2 syndrome caused by two novel mutations in the MPZ gene. *Neurology* **61**: 1435–1437. [Medline] [CrossRef]
3. Bergman, P. J., Bruyette, D. S., Coyne, B. E., Shelton, G. D., Ogilvie, G. K., Munana, K. R. and Richter, K. P. 1994. Canine clinical peripheral neuropathy associated with pancreatic-islet cell-carcinoma. *Prog. Vet. Neurol.* **5**: 57–62.
4. Bichsel, P., Jacobs, G. and Oliver, J. E. Jr. 1988. Neurologic manifestations associated with hypothyroidism in four dogs. *J. Am. Vet. Med. Assoc.* **192**: 1745–1747. [Medline]
5. Braund, K. G., Mcguire, J. A., Amling, K. A. and Henderson, R. A. 1987. Peripheral neuropathy associated with malignant neoplasms in dogs. *Vet. Pathol.* **24**: 16–21. [Medline]
6. Braund, K. G., Steinberg, H. S., Shores, A., Steiss, J. E., Mehta, J. R., Toiviokinnucan, M. and Amling, K. A. 1989. Laryngeal paralysis in immature and mature dogs as one sign of a more diffuse polyneuropathy. *J. Am. Vet. Med. Assoc.* **194**: 1735–1740. [Medline]
7. Burns, T. M. and Mauermann, M. L. 2011. The evaluation of polyneuropathies. *Neurology* **76**: S6–S13. [Medline] [CrossRef]
8. Coates, J. R. and O'Brien, D. P. 2004. Inherited peripheral neuropathies in dogs and cats. *Vet. Clin. North Am. Small Anim. Pract.* **34**: 1361–1401. [Medline] [CrossRef]
9. Cruz, M. W., Tendrich, M., Vaisman, M. and Novis, S. A. 1996. Electroneuromyography and neuromuscular findings in 16 primary hypothyroidism patients. *Arq. Neuropsiquiatr.* **54**: 12–18. [Medline] [CrossRef]
10. Cuddon, P., Lin, D. S., Bowman, D. D., Lindsay, D. S., Miller, T. K., Duncan, I. D., Delahunta, A., Cummings, J., Suter, M., Cooper, B., King, J. M. and Dubey, J. P. 1992. *Neospora caninum* infection in English Springer Spaniel littermates. Diagnostic evaluation and organism isolation. *J. Vet. Intern. Med.* **6**: 325–332. [Medline] [CrossRef]
11. Cuddon, P. A. 2002. Acquired canine peripheral neuropathies. *Vet. Clin. North Am. Small Anim. Pract.* **32**: 207–249. [Medline] [CrossRef]
12. Drögemüller, C., Becker, D., Kessler, B., Kemter, E., Tetens, J., Jurina, K., Jäderlund, K. H., Flagstad, A., Perloski, M., Lindblad-Toh, K. and Matiasek, K. 2010. A deletion in the N-myc

downstream regulated gene 1 (NDRG1) gene in Greyhounds with polyneuropathy. *PLoS ONE* **5**: e11258. [Medline] [CrossRef]
13. Duncan, I. D. and Griffiths, I. R. 1979. Peripheral nervous system in a case of canine giant axonal neuropathy. *Neuropathol. Appl. Neurobiol.* **5**: 25–39. [Medline] [CrossRef]
14. Duncan, I. D. and Griffiths, I. R. 1981. Canine giant axonal neuropathy; some aspects of its clinical, pathological and comparative features. *J. Small Anim. Pract.* **22**: 491–501. [Medline] [CrossRef]
15. El-Salem, K. and Ammari, F. 2006. Neurophysiological changes in neurologically asymptomatic hypothyroid patients: a prospective cohort study. *J. Clin. Neurophysiol.* **23**: 568–572. [Medline] [CrossRef]
16. Gabriel, A., Poncelet, L., Van Ham, L., Clercx, C., Braund, K. G., Bhatti, S., Detilleux, J. and Peeters, D. 2006. Laryngeal paralysis-polyneuropathy complex in young related Pyrenean mountain dogs. *J. Small Anim. Pract.* **47**: 144–149. [Medline] [CrossRef]
17. Granger, N. 2011. Canine inherited motor and sensory neuropathies: An updated classification in 22 breeds and comparison to Charcot-Marie-Tooth disease. *Vet. J.* **188**: 274–285. [Medline] [CrossRef]
18. Grant, I. A. and Benstead, T. J. 2005. Differential diagnosis of polyneuropathy. pp. 1163–1180. *In*: Peripheral Neuropathy, 4th ed. (Dyck, P. J. and Thomas, P. K. eds.), Elsevier, Philadelphia.
19. Griffiths, I. R. and Duncan, I. D. 1979. The central nervous system in canine giant axonal neuropathy. *Acta Neuropathol.* **46**: 169–172. [Medline] [CrossRef]
20. Gupta, R. P. and Abou-Donia, M. B. 1996. Alterations in the neutral proteinase activities of central and peripheral nervous systems of acrylamide-, carbon disulfide-, or 2,5-hexanedione-treated rats. *Mol. Chem. Neuropathol.* **29**: 53–66. [Medline] [CrossRef]
21. Hamilton, T. A., Cook, J. R. Jr., Braund, K. G., Morrison, W. B. and Mehta, J. R. 1991. Vincristine-induced peripheral neuropathy in a dog. *J. Am. Vet. Med. Assoc.* **198**: 635–638. [Medline]
22. Harkin, K. R., Cash, W. C. and Shelton, G. D. 2005. Sensory and motor neuropathy in a Border Collie. *J. Am. Vet. Med. Assoc.* **227**: 1263–1265. [Medline] [CrossRef]
23. Hayasaka, K., Himoro, M., Sato, W., Takada, G., Uyemura, K., Shimizu, N., Bird, T. D., Conneally, P. M. and Chance, P. F. 1993. Charcot-Marie-Tooth neuropathy type 1B is associated with mutations of the myelin P0 gene. *Nat. Genet.* **5**: 31–34. [Medline] [CrossRef]
24. Indrieri, R. J., Whalen, L. R., Cardinet, G. H. and Holliday, T. A. 1987. Neuromuscular abnormalities associated with hypothyroidism and lymphocytic thyroiditis in three dogs. *J. Am. Vet. Med. Assoc.* **190**: 544–548. [Medline]
25. Jaggy, A., Oliver, J. E., Ferguson, D. C., Mahaffey, E. A. and Glausjun, T. 1994. Neurological manifestations of hypothyroidism: a retrospective study of 29 dogs. *J. Vet. Intern. Med.* **8**: 328–336. [Medline] [CrossRef]
26. Jeffery, N. D., Talbot, C. E., Smith, P. M. and Bacon, N. J. 2006. Acquired idiopathic laryngeal paralysis as a prominent feature of generalised neuromuscular disease in 39 dogs. *Vet. Rec.* **158**: 17–21. [Medline] [CrossRef]
27. Johnson, C. A., Kittleson, M. D. and Indrieri, R. J. 1983. Peripheral neuropathy and hypotension in a diabetic dog. *J. Am. Vet. Med. Assoc.* **183**: 1007–1009. [Medline]
28. Kabzińska, D., Korwin-Piotrowska, T., Dreschler, H., Drac, H., Hausmanowa-Petrusewicz, I. and Kochański, A. 2007. Late-onset Charcot-Marie-Tooth type 2 disease with hearing impairment associated with a novel Pro105Thr mutation in the MPZ gene. *Am. J. Med. Genet. A.* **143A**: 2196–2199. [Medline] [CrossRef]
29. Khedr, E. M., El Toony, L. F., Tarkhan, M. N. and Abdella, G. 2000. Peripheral and central nervous system alterations in hypothyroidism: electrophysiological findings. *Neuropsychobiology* **41**: 88–94. [Medline] [CrossRef]
30. Kijima, K., Numakura, C., Shirahata, E., Sawaishi, Y., Shimohata, M., Igarashi, S., Tanaka, T. and Hayasaka, K. 2004. Periaxin mutation causes early-onset but slow-progressive Charcot-Marie-Tooth disease. *J. Hum. Genet.* **49**: 376–379. [Medline] [CrossRef]
31. Koch, T., Schultz, P., Williams, R. and Lampert, P. 1977. Giant axonal neuropathy: a childhood disorder of microfilaments. *Ann. Neurol.* **1**: 438–451. [Medline] [CrossRef]
32. MacPhail, C. M. and Monnet, E. 2001. Outcome of and postoperative complications in dogs undergoing surgical treatment of laryngeal paralysis: 140 cases (1985–1998). *J. Am. Vet. Med. Assoc.* **218**: 1949–1956. [Medline] [CrossRef]
33. Meier, C. and Bischoff, A. 1977. Polyneuropathy in hypothyroidism. Clinical and nerve biopsy study of 4 cases. *J. Neurol.* **215**: 103–114. [Medline] [CrossRef]
34. Misselbrook, N. G. 1987. Peripheral neuropathy in diabetic bitch. *Vet. Rec.* **121**: 287. [Medline] [CrossRef]
35. Nemni, R., Bottacchi, E., Fazio, R., Mamoli, A., Corbo, M., Camerlingo, M., Galardi, G., Erenbourg, L. and Canal, N. 1987. Polyneuropathy in hypothyroidism: clinical, electrophysiological and morphological findings in four cases. *J. Neurol. Neurosurg. Psychiatry* **50**: 1454–1460. [Medline] [CrossRef]
36. Ongerboer de Visser, B. W. and Tiessens, G. 1985. Polyneuropathy induced by cisplatin. *Prog. Exp. Tumor Res.* **29**: 190–196. [Medline]
37. Paulson, G. W. and Waylonis, G. W. 1976. Polyneuropathy due to n-hexane. *Arch. Intern. Med.* **136**: 880–882. [Medline] [CrossRef]
38. Pollard, J. D., McLeod, J. G., Honnibal, T. G. and Verheijden, M. A. 1982. Hypothyroid polyneuropathy. Clinical, electrophysiological and nerve biopsy findings in two cases. *J. Neurol. Sci.* **53**: 461–471. [Medline] [CrossRef]
39. Quarles, R. H., Macklin, W. B. and Morell, P. 2006. Myelin formation, structure, and biochemistry, in basic neurochemistry: molecular, cellular and medical aspects. pp. 51–71., *In*: Basic Neurochemistry: Molecular, Cellular, and Medical Aspects, 7th ed. (Siegel, G. J., Albers, R. W., Brady, S. T. and Price, D. eds.), Academic Press Elsevier, New York.
40. Quattrini, A., Nemni, R., Marchettini, P., Fazio, R., Iannaccone, S., Corbo, M. and Canal, N. 1993. Effect of hypothyroidism on rat peripheral nervous system. *Neuroreport* **4**: 499–502. [Medline] [CrossRef]
41. Rosen, S. A., Wang, H., Cornblath, D. R., Uematsu, S. and Hurko, O. 1989. Compression syndromes due to hypertrophic nerve roots in hereditary motor sensory neuropathy type I. *Neurology* **39**: 1173–1177. [Medline] [CrossRef]
42. Rossmeisl, J. H. Jr. 2010. Resistance of the peripheral nervous system to the effects of chronic canine hypothyroidism. *J. Vet. Intern. Med.* **24**: 875–881. [Medline] [CrossRef]
43. Saporta, A. S. D., Sottile, S. L., Miller, L. J., Feely, S. M. E., Siskind, C. E. and Shy, M. E. 2011. Charcot-Marie-Tooth disease subtypes and genetic testing strategies. *Ann. Neurol.* **69**: 22–33. [Medline] [CrossRef]
44. Shirabe, T., Tawara, S., Terao, A. and Araki, S. 1975. Myxedematous polyneuropathy: a light and electron microscopic study of peripheral nerve and muscle. *J. Neurol. Neurosurg. Psychiatry* **38**: 241–247. [Medline] [CrossRef]

45. Taylor, S. M. 2009. Disorders of peripheral nerves and the neuromuscular junction. pp. 1055–1056. *In*: Small Animal Internal Medicine, 4th ed. (Nelson, R. W. and Couto, C. G. eds.), Elsevier, Philadelphia.
46. Thieman, K. M., Krahwinkel, D. J., Sims, M. H. and Shelton, G. D. 2010. Histopathological Confirmation of polyneuropathy in 11 dogs with laryngeal paralysis. *J. Am. Anim. Hosp. Assoc.* **46**: 161–167. [Medline]
47. Towell, T. L. and Shell, L. C. 1994. Endocrinopathies that affect peripheral nerves of cats and dogs. *Compend. Contin. Educ. Pract. Vet.* **16**: 157–161.
48. Vermeersch, K., Van Ham, L., Braund, K. G., Bhatti, S., Tshamala, M., Chiers, K. and Schrauwen, E. 2005. Sensory neuropathy in two Border collie puppies. *J. Small Anim. Pract.* **46**: 295–299. [Medline] [CrossRef]
49. Vitale, C. L. and Olby, N. J. 2007. Neurologic dysfunction in hypothyroid, hyperlipidemic Labrador Retrievers. *J. Vet. Intern. Med.* **21**: 1316–1322. [Medline] [CrossRef]
50. Wheeler, S. J. 1987. Sensory Neuropathy in a Border Collie Puppy. *J. Small Anim. Pract.* **28**: 281–289. [CrossRef]
51. Yuki, N., Ang, C. W., Koga, M., Jacobs, B. C., van Doorn, P. A., Hirata, K. and van der Meché, F. G. 2000. Clinical features and response to treatment in Guillain-Barré syndrome associated with antibodies to GM1b ganglioside. *Ann. Neurol.* **47**: 314–321. [Medline] [CrossRef]

The Scientific World Journal
Volume 2012, Article ID 383174, 7 pages
doi:10.1100/2012/383174

The ScientificWorldJOURNAL

Research Article

Neuronal Ceroid Lipofuscinosis in Border Collie Dogs in Japan: Clinical and Molecular Epidemiological Study (2000–2011)

Keijiro Mizukami,[1] Takuji Kawamichi,[2] Hiroshi Koie,[3] Shinji Tamura,[4] Satoru Matsunaga,[5] Shigeki Imamoto,[6] Miyoko Saito,[7] Daisuke Hasegawa,[8] Naoaki Matsuki,[9] Satoshi Tamahara,[9] Shigenobu Sato,[10] Akira Yabuki,[1] Hye-Sook Chang,[1] and Osamu Yamato[1]

[1]*Laboratory of Clinical Pathology, Department of Veterinary Medicine, Kagoshima University, 1-21-24 Korimoto, Kagoshima, Kagoshima 890-0065, Japan*
[2]*Japan Border Collie Health Network, 1-14-8 Manabigaoka, Tarumi-ku, Hyogo, Kobe 655-0004, Japan*
[3]*Department of Veterinary Medicine, College of Bioresource Sciences, Nihon University, 1866 Kameino, Kanagawa, Fujisawa 252-0880, Japan*
[4]*Tamura Animal Clinic, 7-16 Yoshimien, Saeki-ku, Hiroshima, Hiroshima 731-5132, Japan*
[5]*Japan Animal Referral Medical Center, 2-5-8 Kuji, Takatsu-ku, Kanagawa, Kawasaki 213-0032, Japan*
[6]*Shinjo Animal Hospital, 104-1 Katsuragi, Nara, Katsuragi 639-2144, Japan*
[7]*Laboratory of Veterinary Surgery II, School of Veterinary Medicine, Azabu University, 1-17-71 Fuchinobe, Kanagawa, Sagamihara 229-8501, Japan*
[8]*Department of Veterinary Science, Nippon Veterinary and Life Science University, 1-7-1 Kyounan-chou, Tokyo, Musashino 180-8602, Japan*
[9]*Department of Veterinary Clinical Pathobiology, Graduate School of Agricultural and Life Sciences, The University of Tokyo, 1-1-1 Yayoi, Tokyo, Bunkyo-ku 113-8657, Japan*
[10]*Sato Animal Hospital, 6-38-20 Goinishi, Chiba, Ichihara 290-0038, Japan*

Correspondence should be addressed to Osamu Yamato, osam@vet.kagoshima-u.ac.jp

Received 12 April 2012; Accepted 3 May 2012

Academic Editors: M. F. Landoni and E. J. Thompson

Neuronal ceroid lipofuscinosis (NCL) is an inherited, neurodegenerative lysosomal disease that causes premature death. The present study describes the clinical and molecular epidemiologic findings of NCL in Border Collies in Japan for 12 years, between 2000 and 2011. The number of affected dogs was surveyed, and their clinical characteristics were analyzed. In 4 kennels with affected dogs, the dogs were genotyped. The genetic relationships of all affected dogs and carriers identified were analyzed. The survey revealed 27 affected dogs, but there was a decreasing trend at the end of the study period. The clinical characteristics of these affected dogs were updated in detail. The genotyping survey demonstrated a high mutant allele frequency in examined kennels (34.8%). The pedigree analysis demonstrated that all affected dogs and carriers in Japan are related to some presumptive carriers imported from Oceania and having a common ancestor. The current high prevalence in Japan might be due to an overuse of these carriers by breeders without any knowledge of the disease. For NCL control and prevention, it is necessary to examine all breeding dogs, especially in kennels with a high prevalence. Such endeavors will reduce NCL prevalence and may already be contributing to the recent decreasing trend in Japan.

1. Introduction

Neuronal ceroid lipofuscinosis (NCL) is a rare group of inherited, neurodegenerative lysosomal storage diseases characterized histopathologically by the abnormal accumulation of ceroid- or lipofuscin-like autofluorescent lipopigments in neurons, retinal cells, and other visceral cells throughout the body [1–4]. NCL shares certain clinical features in both human beings and animals, including behavioral abnormalities, such as personality changes and

aggressiveness, mental retardation and/or dementia; motor disturbances, such as ataxia and incoordination; visual problems leading to central and/or retinal blindness; premature death, but these differ in degree based on the causative gene, of which there are currently at least 8, all recessively inherited [4]. NCL has been described in several domestic species and occurs most commonly in dogs [1, 2, 5].

NCL in Border Collies was first identified in Australia in the 1980s [6–8], and a sporadic case with the disease was also reported in the USA in the 1990s [9]. A diagnosis of the first case in Japan was made in a Border Collie that was born in 2000 [10]. The pathogenic mutation was reported in 2005 to be a nonsense mutation (c.619C>T) in exon 4 in the canine *CLN5* gene [11], which enabled a DNA-based genotyping of affected dogs and carriers. Recently, several types of rapid genotyping assays for this mutation were developed, and the carrier frequency (8.1%) in Japan was determined by a genotyping survey using these assays, suggesting the mutant allele frequency of NCL in Border Collies is high enough in Japan that measures to control and prevent the disease would be warranted [5].

The present study describes the clinical and molecular epidemiologic findings of NCL in Border Collies in Japan for 12 years, between 2000 and 2011. This study also discusses the control and prevention of the disease based on the results of these analyses.

2. Materials and Methods

2.1. Dogs Affected with NCL. The number of affected dogs was surveyed based on the records in our laboratory, which have been exclusively supporting the diagnosis of the disease in Japan. Among 27 affected dogs identified in the present study, NCL was diagnosed definitively in 25 dogs by a genetic test [5] using their specimens containing DNA, but in the remaining 2 dogs that died without any specimens before the genetic test got available, NCL was strongly suspected based on their typical clinical history and blood relationship with molecularly defined affected littermates and/or carrier parents. The clinical characteristics were analyzed and summarized using information about all of the affected dogs, which was gleaned from interviews and questionnaires of their owners and veterinarians. Some of the affected dogs were examined using the following prediagnostic tests: magnetic resonance image (MRI) scan in 7 dogs, including a previously reported dog [10]; computed tomography (CT) scan in 2 dogs; ophthalmologic examination in 3 dogs. The findings of these examinations were also analyzed and summarized.

2.2. Genotyping Survey. Border Collies belonging to 4 special kennels (A, B, C, and D), which generated one or more affected dogs, were surveyed between 2008 and 2010 using a genetic test with the breeders' cooperation. The number of dogs examined was 82, including 23, 20, 29, and 10 in kennels A, B, C, and D, respectively. Whole blood or saliva specimens were collected from these dogs using the Flinders Technology Associates filter paper (FTA card, Whatman International). Genotyping was performed as reported previously [5].

2.3. Pedigree Analysis. Pedigree analysis was performed to elucidate the genetic relationships of affected and carrier dogs identified in Japan and to deduce the pathway of transmission and distribution of the mutant allele. The genetic relationships among affected and carrier dogs found in the present study were analyzed using the pedigree papers issued by the Japan Kennel Club (http://www.jkc.or.jp/) and the Kennel Club of Japan (http://www.kcj.gr.jp/). The pedigree information of carrier dogs identified in the previous random survey in Japan [5] was analyzed and added to the results of the present study. The pedigree information of the dogs was used under the informed consent of their owners. The ancestry in Oceania was traced using pedigree information of carrier dogs provided by the New South Wales Border Collie Club (http://www.mybcsite.com/bccnswwebfiles/bccnswframe.htm), which was also disclosed via the website of the Japan Border Collie Health Network (http://www.jbchn.net/cl_carrier.htm), a volunteer breeders' association for the healthy breeding of Border Collies. Pedigree information published in the Border Collie Database (http://db.kennel.dk/) was used to supplement the information about the ancestor dogs in Oceania.

All animals were cared for and were used in the experiments in accordance with the guidelines for proper conduct of animal experiments issued by the Science Council of Japan (http://www.scj.go.jp/en/animal/index.html). All experimental procedures using animals and their specimens were performed in accordance with the guidelines regulating animal use at Kagoshima University.

3. Results

3.1. The Number and Clinical Characteristics of Border Collies with NCL. The survey revealed that there were 27 affected dogs (13 males and 14 females) in the 12 years from 2000 to 2011 in Japan (Table 1). The first case, born in 2000, was diagnosed with NCL histopathologically [10], which was confirmed molecularly using the stored liver specimen. Since this case, several affected dogs from a single or a few litters were diagnosed nearly every year up until recently in Japan. However, currently there seems to be a decreasing trend based on the observation that only 1 affected dog was identified since 2009.

The clinical features of the affected dogs are summarized and listed in Table 2. They were divided into 3 stages, that is, early (15–20 months of age), middle (19–23 months of age), and late-to-terminal stages (22–32 months of age). The overlaps in age between adjacent stages were due to individual variability in the onset and progression rate of the disease. The features at the early stage were mainly behavioral problems that most owners of the dogs did not regard as pathological changes. The features at the middle stage included serious behavioral abnormalities, visual impairments, and slight motor disorders, which prompted

Table 1: Number of Border Collies with neuronal ceroid lipofuscinosis and the number of litters that included affected dogs during the 12 years between 2000 and 2011 in Japan.

Year of birth	Number of affected dogs (male and female)	Number of litters
2000	2 (2, 0)	1
2001	6 (3, 3)	3
2002	0 (0, 0)	0
2003	4 (3, 1)	3
2004	4 (1, 3)	2
2005	2 (1, 1)	2
2006	1 (0, 1)	1
2007	2 (1, 1)	2
2008	5 (2, 3)	4
2009	1 (0, 1)	1
2010–present*	0 (0, 0)	0
Total	27 (13, 14)	19

*June 2012.

Table 2: Summary of clinical features in Border Collies with neuronal ceroid lipofuscinosis*.

Stage (months of age)	Clinical signs
Early (15–20)	Altered characteristics; disregard for owner's commands; loss of interest in play and other dogs; morbid fear of noise, humans, and unspecified things; hallucination; disorientation; biting; averse to going up and down stairs (especially down)
Middle (19–23)	Fly-biting behavior; continuous shaking of the head; sudden halts during walks; uncooperativeness with other dogs; head tilt; chomping without food; tooth grinding; leg jerking; visual impairments (fear of darkness, unawareness of things such as food, and frequently hitting obstacles); aggressiveness; excitation; staggering; falling; toileting accidents; myoclonus; myoclonic seizure
Late to terminal (22–32)	Wandering; hair-pulling disorder; circadian rhythm disorder; acoustic and cutaneous hyperesthesia; cognitive and emotional impairments; blindness; dysmetria; gait deficiency; convulsive seizure; face and mouth tic; chewing difficulty; lethargy; stupor; death (mean age 26.7 months, ranging from 23 to 32 months)†

*Data summarized from the information of 27 affected dogs.
†Data from 17 affected dogs that died naturally without euthanasia.

the owners to consult veterinarians. The features at the late-to-terminal stage included serious motor, visual, psychointellectual, and vital dysfunctions due to a wide spectrum of brain dysfunctions. The mean life span of the 23 affected dogs examined was 26.4 months of age. Of these, 17 died naturally at a mean age of 26.7 months, ranging from 23 to 32 months. The other 6 dogs were euthanized at the terminal stage an average of 25.6 months. Although there were few specific changes before 15 months of age, some of the owners had an impression that their dogs had unusual characteristics and behaviors and low learning ability in the puppy and juvenile years. There was no abnormal change on general clinicopathological examinations. No abnormal vacuoles in the cytoplasm of leukocytes were observed in blood smear examinations.

3.2. MRI, CT, and Ophthalmologic Examinations. MRI, CT, and ophthalmologic examinations were performed in affected dogs in the middle-to-late stage (at approximately 2 years of age). The common findings of MR and CT images were ventricular enlargement and well-demarcated cerebral sulci (Figure 1). Dilation of cerebellar fissures was also observed at a sagittal section of the MRI scan (Figure 1(c)). No other organic lesion was detected in MRI and CT scans. In the affected dogs examined ophthalmologically, slight narrowing of blood vessels in the retina was commonly observed in ophthalmoscopy (Figure 2(a)), but this ophthalmoscopic finding was evaluated within the normal range by veterinary ophthalmologists. An examination using a slit lamp detected no abnormal finding, such as clouding of the cornea and lens (Figure 2(b)).

3.3. Genotyping Survey. The results of the genotyping survey in the 4 specific kennels are shown in Table 3. The frequencies of carriers (32.9%), affected dogs (18.3%), and the mutant allele (34.8%) were markedly high in the 4 kennels.

3.4. Pedigree Analysis. The pedigree analysis was performed mainly using the pedigree information of the 27 affected dogs and 58 carriers identified so far in Japan (Figure 3). These dogs were related to at least 13 possible carriers imported from Oceania to Japan in the middle 1990s, which ultimately revealed an ancestry from a male dog born in 1944 in Australia through 9 carriers reported by the New South Wales Border Collie Club. As a result, this analysis revealed that all dogs carrying the mutant allele in Japan share a blood relationship and a single common ancestor in Australia.

The pedigree analysis also revealed that breeding was repeated using a small number of carriers and their offspring in the 4 kennels surveyed in the present study. The breeders of these kennels were not aware of NCL in Border Collies before the genotyping survey. As a result, these kennels had markedly high frequencies of the mutant allele.

4. Discussion

The present study revealed 27 Border Collies (13 males and 14 females) with NCL in Japan during 2000–2011 (Table 1), although there might have been additional affected dogs elsewhere that had no opportunity to be diagnosed. Since the first affected dog, born in 2000, was diagnosed in 2002 [10], several affected dogs from a single or a few litters have been diagnosed nearly every year up until recently, but currently there seems to be a decline in the frequency of NCL. The decreasing trend may be due to the publication of the pathogenic mutation in 2005 [11], the subsequent

Table 3: Results of the genotyping survey carried out in 4 kennels that generated affected dogs*.

Kennel	Number of			Frequency (%)		
	Dogs examined	Carriers	Affected dogs	Carriers	Affected dogs	Mutant allele
A	23	9	8	39.1	34.8	54.3
B	20	11	2	55.0	10.0	37.5
C	29	6	2	20.7	6.7	17.2
D	10	1	3	10.0	30.0	35.0
Total	82	27	15	32.9	18.3	34.8

*These genotyping surveys were carried out between 2008 and 2010.

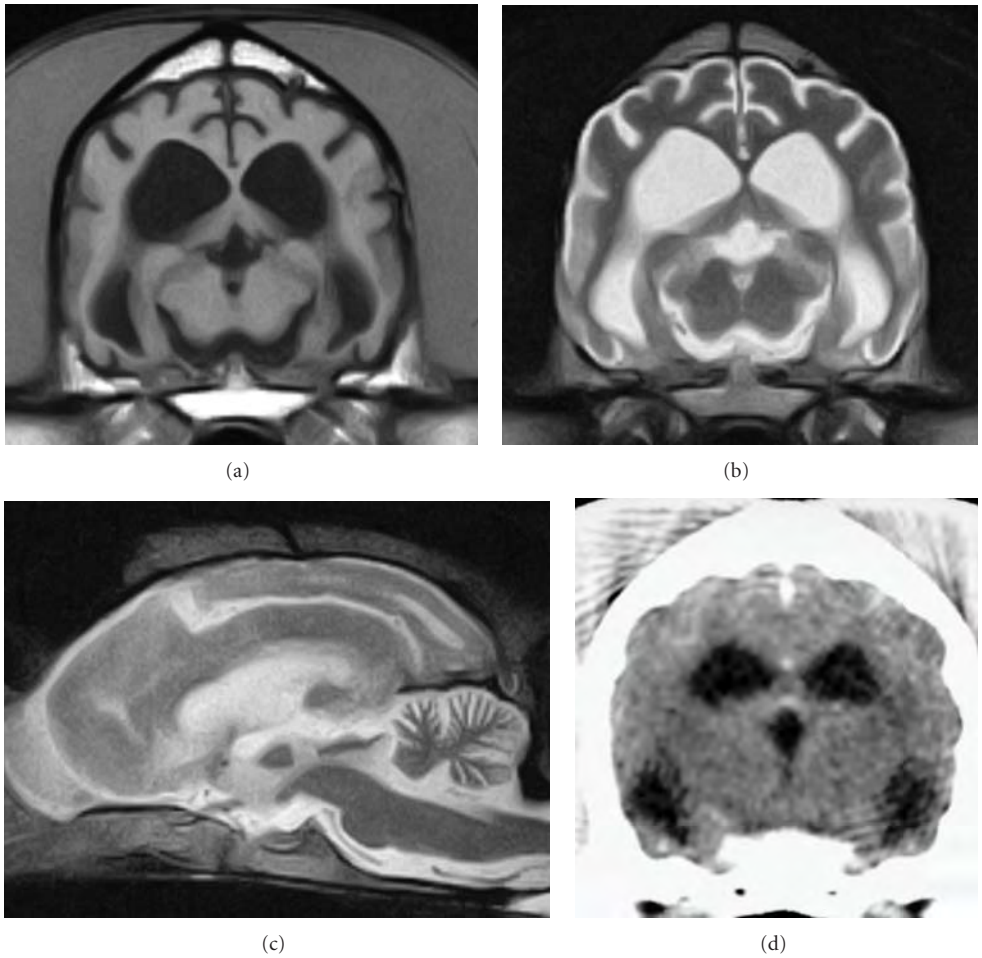

Figure 1: Representative magnetic resonance (MR) and computed tomography (CT) images of the brain of Border Collies with neuronal ceroid lipofuscinosis. MR images were obtained using a 0.3-tesla system (AIRIS2-comfort, Hitachi Medical Corporation) in a 24-month-old dog under general anesthesia. CT images were obtained using a multislice CT system (ECLOS, Hitachi Medical Corporation) in another 24-month-old dog under general anesthesia. (a) MR T1-weighted image (TR/TE = 500/20 ms) of a transverse section at the level of the thalamus, (b) MR T2-weighted image (TR/TE = 4,000/120 ms) of a transverse section at the level of the thalamus, (c) MR T2-weighted image of a sagittal section, and (d) CT image of a transverse section at the level of the thalamus. These images show enlarged ventricles and dilated cerebral and cerebellar sulci, suggesting forebrain atrophy.

development of a variety of genetic testing methods [5], and genotyping surveys in a random population of breeding Border Collies [5] and in a few specific kennels that generated affected dog(s) (present study). These events may have contributed to the prevention and control of the disease through the education of related breeders and fanciers of Border Collies.

Based on information from the owners and veterinarians of the affected dogs, their characteristic clinical features were determined (Table 2), although there were individual differences in the onset and progression rate of the disease and the symptoms, as reported previously [6]. Mild clinical signs, such as behavioral problems, begin at 15 months of age at the earliest, but the onset is usually a few months later

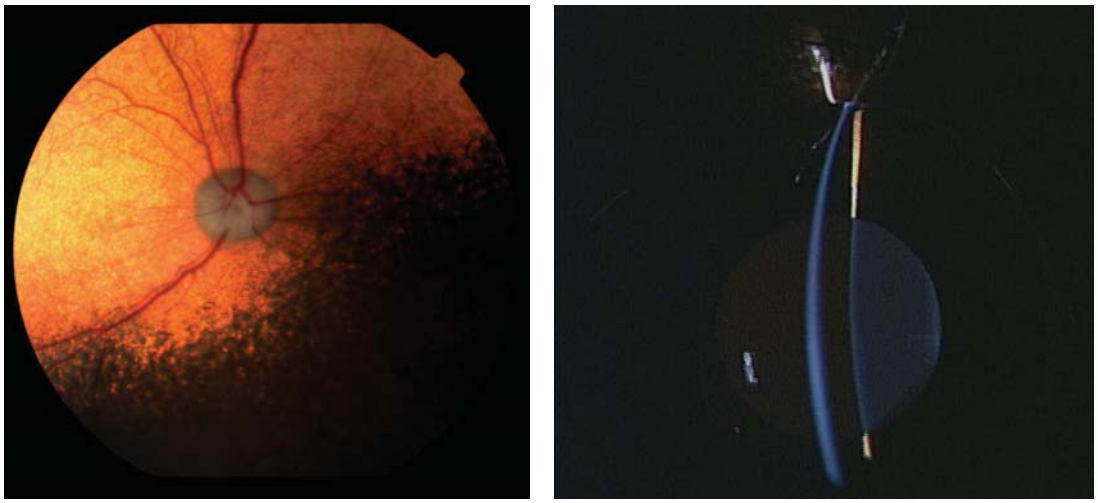

(a) (b)

Figure 2: Photographs of ophthalmoscopic and slit-lamp examinations of the right eye in a 21-month-old Border Collie with neuronal ceroid lipofuscinosis. (a) Slight narrowing of blood vessels in the retina is observed, but (b) there is no abnormal finding in the slit-lamp examination.

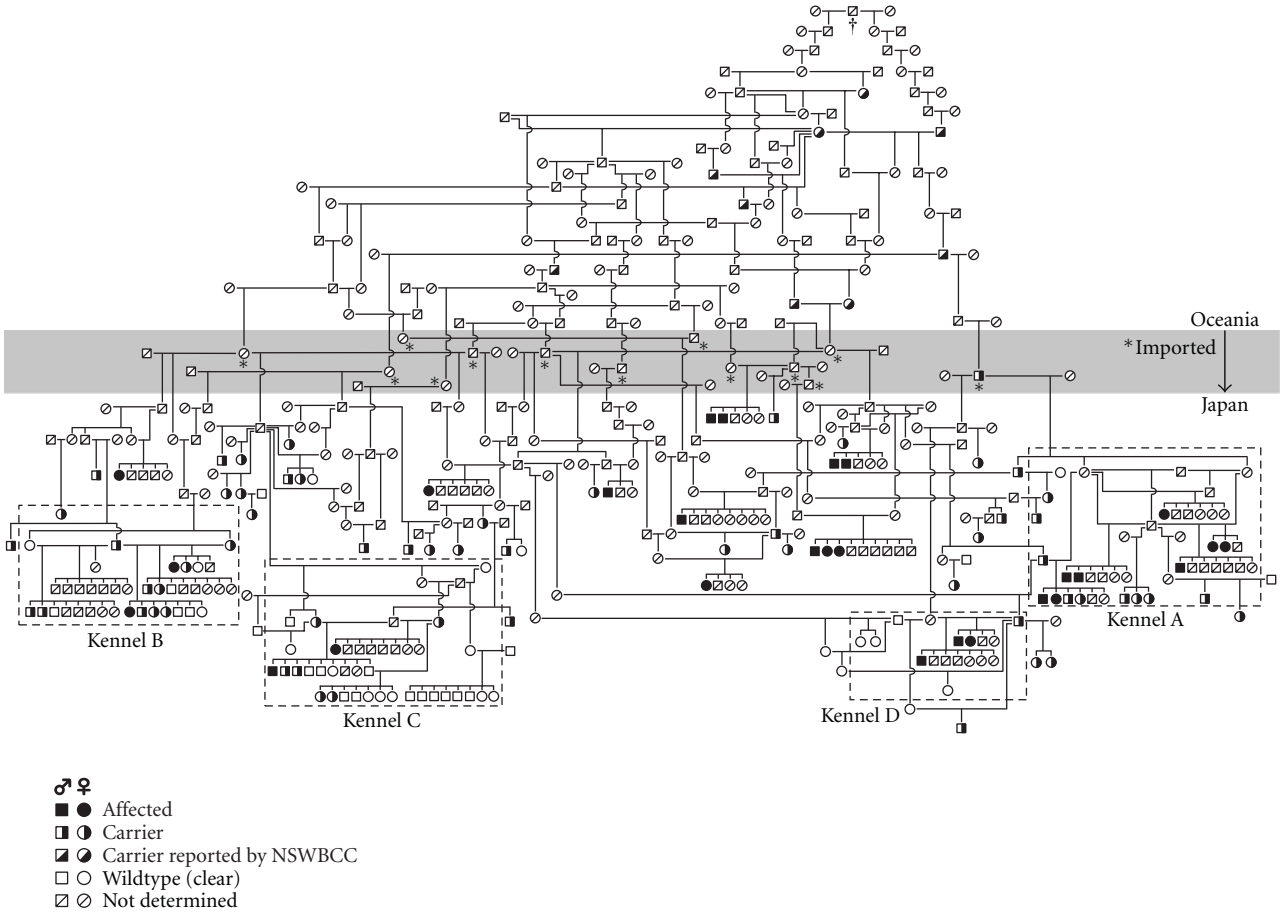

Figure 3: Genetic relationship of affected and carrier dogs identified in Japan between 2000 and 2011. The analysis was carried out using pedigree papers issued by the Japan Kennel Club and the Kennel Club of Japan and information reported by the New South Wales Border Collie Club (NSWBCC) and the Border Collie Database. The gray area indicates a border between Oceania and Japan. Dogs imported from Oceania to Japan were marked with an asterisk (*). All dogs carrying the mutant allele shared a common ancestor (†) born in 1944 in Australia. Areas surrounded by a dashed line indicate the 4 kennels surveyed using a genotyping test.

(approximately 18 months of age) at the early stage. The earliest age of onset in the present study is consistent with that in a previous report [8]. Clinical signs observed at the early stage (15–20 months of age) are mainly mild behavioral abnormalities that the owners, without any knowledge of NCL, hardly regard as pathological. Visual disorders become unambiguous and behavioral abnormalities increase in severity at the middle stage (19–23 months of age). Serious clinical signs, such as convulsive seizure and motor disorders, appear at the late-to-terminal stage (older than 22 months of age). The mean life span of affected dogs was 26.7 months of age in the present study. The life span was 26.4 months of age in the dogs that died naturally, ranging from 23 to 32 months of age. This is longer than the 23.1-month life span of affected Border Collies in a previous report in Australia [7]. The difference could be attributed to the fact that many Japanese pet owners feel that euthanasia is inhumane and do not want to kill animals before they die naturally.

The characteristic clinical features determined in the present study are similar to those in previous reports [6, 7]. However, a previously reported clinical sign, mania [7], was not observed in the present study. In addition, some affected dogs had unusual characteristics and behaviors and low learning ability in the puppy and juvenile years, which was not reported previously. These clinical characteristics, updated in detail, will be of further help for the diagnosis of NCL in Border Collies.

In the MRI examination, ventricular enlargement and dilated cerebral and cerebellar sulci were common findings in affected dogs (Figure 1). The CT examination also demonstrated ventricular enlargement. These characteristic findings suggest atrophy of the forebrain, which was similarly observed in previous MRI [10] and CT examinations [9]. The changes suggesting brain atrophy developed as early as the middle stage, when affected dogs were usually referred to animal hospitals. Similar changes have been observed in other types of NCL [12, 13] and other lysosomal storage diseases, such as GM1 gangliosidosis [14] and GM2 gangliosidosis [15–17] in dogs and cats. The brain atrophy usually develops as a specific and severe change even at the middle stage in NCL but as a secondary and mild change in the late-to-terminal stage in other lysosomal diseases. Therefore, the atrophic changes would be useful as an adjunct to the diagnosis of NCL. No other organic lesion was detected in MRI scans in Border Collies with NCL, although hyperintensity in T2-weighted images of the cerebral white matter is observed in GM1 and GM2 gangliosidoses in dogs and cats [14, 16–19]. Meningeal thickening, reported in Chihuahuas with NCL [13], was not observed in Border Collies with NCL.

Visual impairments appeared to various degrees in all affected dogs, especially at the middle stage (Table 2). Previous reports have not described any abnormal changes on ophthalmoscopic examination [7, 10]. In the present study, the affected dogs examined had slight narrowing of blood vessels in the retina (Figure 2(a)), but this ophthalmoscopic finding was considered within the normal range by veterinary ophthalmologists (Figure 2). In humans with NCL, there is a pronounced loss of photoreceptors in the end stage of the disease, but in NCL in English Setters only minimal structural damage is observed in the retina [20]. In Border Collies with NCL, inclusions with variable ultrastructure are common in all cells of the retina, but the pigment accumulation does not damage the retinal architecture [8]. The retinal lesions in the Border Collies are similar to those in the English Setters but are much less severe than in juvenile NCL in humans. The narrowing of retinal blood vessels observed in affected Border Collies may be an indication of mild retinal degeneration, but this feature cannot be used as a valuable diagnostic for NCL.

Based on data of the pedigree analysis, affected dogs and carriers identified in Japan share a blood relationship and a single common ancestor born in 1944 in Australia via some presumptive carriers in Oceania (Figure 3). Although it is impossible to demonstrate whether this ancestor was a founder of NCL in Border Collies, there is a possibility that the mutant allele was transmitted from Oceania to Japan in this way mainly in the middle of the 1990s, when the causative mutation had not been identified yet. The recent increase in prevalence of the disease in Japan is likely due to an overuse of imported carriers and their offspring as breeding dogs without any knowledge of the disease. Hereafter, dogs that will be bred should be genotyped beforehand.

The pedigree analysis also suggests that breeding has been repeated using a small number of carriers and their offspring in the 4 kennels that generated affected dogs (Figure 3). There was a trend toward inbreeding in these kennels. In addition, the breeders of the kennels were not aware of the disease until they were informed of the generation of affected dogs in their kennels. These issues may have caused the high frequencies of carriers (32.9%) and the mutant allele (34.8%) in the 4 kennels (Table 3), compared to the carrier (8.1%) and mutant allele frequencies (4.1%) in the random population of Border Collies [5]. Fifteen (55.6%) of the 27 affected dogs identified so far in Japan were generated in these 4 kennels. It is thought that affected dogs are generated in a small proportion of kennels, which have a high frequency of the mutant allele. Therefore, it is important for prevention of the disease to rapidly genotype all breeding dogs in kennels that have had an opportunity to generate affected dogs. This type of examination helps the kennels not only stop generating additional affected dogs but also stop spreading carriers to other kennels. In addition, a genotyping test using specimens from a random population of breeding Border Collies should be continued [5] to detect sporadic carriers and prevent them from being used as breeding dogs. These approaches would gradually decrease the number of dogs carrying the mutant allele. These active and continuous preventive measures may be necessary to eliminate NCL in Border Collies.

Acknowledgments

The authors are grateful to Ms. Kasukawa (the first affected dog's owner), all other affected dogs' owners, and all veterinarians associated with the dogs for providing their

specimens and information about them. The authors are also grateful to all members of the Japan Border Collie Health Network for their help with the collection of information about affected and carrier Border Collies. This study was supported financially by grants (nos. 14560258, 1680210, 20380173, 20-08112, and 21658109, O. Yamato) from the Ministry of Education, Culture, Sports, Science and Technology of Japan.

References

[1] R. D. Jolly, D. N. Palmer, R. H. Studdert et al., "Canine ceroid-ipofuscinoses: a review and classification," *Journal of Small Animal Practice*, vol. 35, no. 6, pp. 299–306, 1994.

[2] R. D. Jolly and D. N. Palmer, "The neuronal ceroid-lipofuscinoses (Batten disease): comparative aspects," *Neuropathology and Applied Neurobiology*, vol. 21, no. 1, pp. 50–60, 1995.

[3] S. L. Hofmann and L. Petronen, "The neuronal ceroid lipofuscinoses," in *The Metabolic and Molecular Bases of Inherited Disease*, C. Scriver, A. Beaudet, W. Sly, and D. Valle, Eds., pp. 3877–3894, McGraw-Hill, New York, NY, USA, 8th edition, 2001.

[4] A. Jalanko and T. Braulke, "Neuronal ceroid lipofuscinoses," *Biochimica et Biophysica Acta*, vol. 1793, no. 4, pp. 697–709, 2009.

[5] K. Mizukami, H.-S. Chang, A. Yabuki et al., "Novel rapid genotyping assays for neuronal ceroid lipofuscinosis in Border Collie dogs and high frequency of the mutant allele in Japan," *Journal of Veterinary Diagnostic Investigation*, vol. 23, no. 6, pp. 1131–1139, 2011.

[6] R. M. Taylor and B. R. H. Farrow, "Ceroid-lipofuscinosis in Border Collie dogs," *Acta Neuropathologica*, vol. 75, no. 6, pp. 627–631, 1988.

[7] V. P. Studdert and R. W. Mitten, "Clinical features of ceroid lipofuscinosis in Border Collie dogs," *Australian Veterinary Journal*, vol. 68, no. 4, pp. 137–140, 1991.

[8] R. M. Taylor and B. R. H. Farrow, "Ceroid lipofuscinosis in the Border Collie dog: retinal lesions in an animal model of juvenile Batten disease," *American Journal of Medical Genetics*, vol. 42, no. 4, pp. 622–627, 1992.

[9] J. N. Franks, C. W. Dewey, M. A. Walker, and R. W. Storts, "Computed tomographic findings of ceroid lipofuscinosis in a dog," *Journal of the American Animal Hospital Association*, vol. 35, no. 5, pp. 430–435, 1999.

[10] H. Koie, H. Shibuya, T. Sato et al., "Magnetic resonance imaging of neuronal ceroid lipofuscinosis in a Border Collie," *Journal of Veterinary Medical Science*, vol. 66, no. 11, pp. 1453–1456, 2004.

[11] S. A. Melville, C. L. Wilson, C. S. Chiang, V. P. Studdert, F. Lingaas, and A. N. Wilton, "A mutation in canine CLN5 causes neuronal ceroid lipofuscinosis in Border Collie dogs," *Genomics*, vol. 86, no. 3, pp. 287–294, 2005.

[12] M. Kuwamura, R. Hattori, J. Yamate, T. Kotani, and K. Sasai, "Neuronal ceroid-lipofuscinosis and hydrocephalus in a chihuahua," *Journal of Small Animal Practice*, vol. 44, no. 5, pp. 227–230, 2003.

[13] Y. Nakamoto, O. Yamato, K. Uchida et al., "Neuronal ceroid-lipofuscinosis in longhaired chihuahuas: clinical, pathologic, and MRI findings," *Journal of the American Animal Hospital Association*, vol. 47, no. 4, pp. e64–e70, 2011.

[14] D. Hasegawa, O. Yamato, Y. Nakamoto et al., "Serial MRI features of canine GM1 gangliosidosis: a possible imaging biomarker for diagnosis and progression of the disease," *The Scientific World Journal*, vol. 2012, Article ID 250197, 2012.

[15] N. Matsuki, O. Yamato, M. Kusuda, Y. Maede, H. Tsujimoto, and K. Ono, "Magnetic resonance imaging of GM2-gangliosidosis in a golden retriever," *Canadian Veterinary Journal*, vol. 46, no. 3, pp. 275–278, 2005.

[16] D. Hasegawa, O. Yamato, M. Kobayashi et al., "Clinical and molecular analysis of GM2 gangliosidosis in two apparent littermate kittens of the Japanese domestic cat," *Journal of Feline Medicine and Surgery*, vol. 9, no. 3, pp. 232–237, 2007.

[17] S. Tamura, Y. Tamura, K. Uchida et al., "GM2 Gangliosidosis variant 0 (Sandhoff-like disease) in a family of toy poodles," *Journal of Veterinary Internal Medicine*, vol. 24, no. 5, pp. 1013–1019, 2010.

[18] E. M. Kaye, J. Alroy, S. S. Raghavan et al., "Dysmyelinogenesis in animal model of GM1 gangliosidosis," *Pediatric Neurology*, vol. 8, no. 4, pp. 255–261, 1992.

[19] R. A. Kroll, M. A. Pagel, S. Roman-Goldstein, A. J. Barkovich, A. N. D'Agostino, and E. A. Neuwelt, "White matter changes associated with feline G(M2) gangliosidosis (Sandhoff disease): correlation of MR findings with pathologic and ultrastructural abnormalities," *American Journal of Neuroradiology*, vol. 16, no. 6, pp. 1219–1226, 1995.

[20] N. Koppang, "The English setter with ceroid-lipofuscinosis: a suitable model for the juvenile type of ceroid-lipofuscinosis in humans," *American Journal of Medical Genetics*, vol. 5, pp. 117–125, 1988.

短　報

ミオキミア／ニューロミオトニアのヨークシャーテリアの１例

宇津木真一　　齋藤弥代子†　　久末正晴

麻布大学獣医学部（〒229–8501　相模原市淵野辺1–17–71）

（2010年2月8日受付・2010年9月24日受理）

要　　約

８歳齢の雌のヨークシャーテリアが呼吸促迫および四肢の硬直を主徴とする発作を主訴に来院した．身体一般および神経学的検査で，体幹部および四肢の筋肉に律動的で波状のミオキミアに特徴的な動きが観察された．筋電図ではミオキミア放電を認めた．脳脊髄液検査は単核細胞増多を示したが，脳のMRIでは明らかな異常を認めなかった．これらの所見から炎症性脳疾患を伴うミオキミア／ニューロミオトニアと診断し，抗生剤とゾニサミド，プロカインアミドの投与を行った．初診から５カ月後の脳脊髄液検査は，正常に復していた．現在11カ月が経過し，ゾニサミドとプロカインアミドの投薬を継続中だが，呼吸促迫および四肢の硬直を示すニューロミオトニアは認められておらず，ミオキミアは頻度と程度が顕著に改善されている．――キーワード：犬，ミオキミア，ニューロミオトニア．

日獣会誌　64，56～60（2011）

筋の不随意的反復性収縮に伴い直上の皮膚が波打ち，まるで皮膚の下を虫がうごめくように見える臨床徴候は，ミオキミア（myokymia：MK）と呼ばれる［1–4］．また，運動や興奮により誘発される発作性の全身性筋硬直を特徴とする持続的筋収縮は，ニューロミオトニア（neuromyotonia：NMT）と呼ばれている［1–6］．MKとNMTはともに末梢神経軸索の興奮性の亢進により生じ，同一症例にてMKとNMTがともに認められることが多いため，同一の異常が背景にあると考えられている［2, 4, 6, 7］．獣医療におけるMK/NMTの報告は非常に少なく，８例の犬と１例の猫での報告があるのみである［6–9］．またわれわれの知るかぎり本邦における報告はない．今回，われわれは炎症性脳疾患に伴いMK/NMTを呈したヨークシャーテリア（YT）に遭遇し，診断と治療を行う機会を得たので，その臨床像を報告する．

症　　例

８歳齢，体重2.4kg，雌のYTが約２年前から月に１，２回発作を起こし，悪化傾向にあるとの主訴で麻布大学附属動物病院神経科（以下当院）に紹介来院した．発作はおもに車での外出や来客，トリミング時に発現し，呼吸速迫から始まり四肢が硬直し，その後後肢が虚脱し起立不能に陥り重症時には横臥へと進行，それらが約２～５時間持続しこの間は呼びかけに反応するとのことだった．発作が長時間に及ぶと全身を繰り返し大きくピクッとさせる（ミオクローヌス（MC）様）徴候に移行することがあるとのことだった．この発作以外にほぼ毎日間欠的に皮膚がピクピク動き頻繁にその部分を噛む動作が認められていた．この皮膚徴候の発現は前述の発作とほぼ同時期の発症であった．身体一般検査では四肢の近位筋の肥大が認められた．さらに体幹部および四肢の筋に，律動的で波状のあたかも皮膚の下を小さな虫がうごめいているかのようなMKに特徴的な動きが観察され，特に上腕と大腿外側面の筋で顕著であった．その他の身体一般検査と神経学的検査に異常は認めなかった．全血球算定と生化学的検査ではCKの軽度上昇（177IU/*l*）以外異常を呈さなかったが，総胆汁酸は空腹時25.1 μmol/*l*，食後２時間91.5μmol/*l*と高値を示した（表）．腹部単純X線で小肝を認めたが超音波検査では肝実質に異常はなく門脈体循環シャントを疑う所見も認めなかった．続いて全身麻酔下で神経系の精査を行ったが，全身麻酔中もさまざまな四肢や体幹の筋で前述と同様の波状の細かい動きが時折観察された．頭部MRIにおいて明らかな異常は認めなかった．大槽からの脳脊髄液（CSF）検査では，単核細胞増多症（総有核細胞数49/μ*l*（基準値０～5/μ*l*），大単核球と小単核球各50％）を呈した．蛋白は21.8mg/d*l*（基準値＜25mg/d*l*），糖は71mg/d*l*とともに正常であった．CSFあるいは血液にて，犬ジステンパー，*Toxoplasma gondii*，*Neospora caninum*の

† 連絡責任者：齋藤弥代子（麻布大学獣医学部外科学第二研究室）
〒229–8501　相模原市淵野辺1–17–71　☎042–754–7111　FAX 042–769–1639　E-mail : msaito@azabu-u.ac.jp

表　大学初診時血液検査結果

項　目	結　果	項　目	結　果	項　目	結　果
WBC（$\times 10^2/\mu l$）	118.0	TP（g/d*l*）	7.9	Ca（mg/d*l*）	11.8
RBC（$\times 10^4/\mu l$）	700.0	Alb（g/d*l*）	4.2	IP（mg/d*l*）	2.7
PCV（%）	48.6	Glu（mg/d*l*）	116.0	LDH（IU/*l*）	68.0
Hgb（g/d*l*）	16.6	AST（IU/*l*）	26.0	CK（IU/*l*）	177.0
MCV（fl）	69.3	ALT（IU/*l*）	38.0	Na（mmol/*l*）	143.0
MCH（pg）	23.8	ALP（IU/*l*）	337.0	K（mmol/*l*）	4.1
MCHC（g/d*l*）	34.3	Tbil（mg/d*l*）	0.4	Cl（mmol/*l*）	103.0
PLT（$\times 10^4/\mu l$）	54.6	Tchol（mg/d*l*）	269.0		
		BUN（mg/d*l*）	15.0	総胆汁酸（空腹時）（μmol/*l*）	25.1
		Cre（mg/d*l*）	0.4	総胆汁酸（食後２時間）（μmol/*l*）	91.5

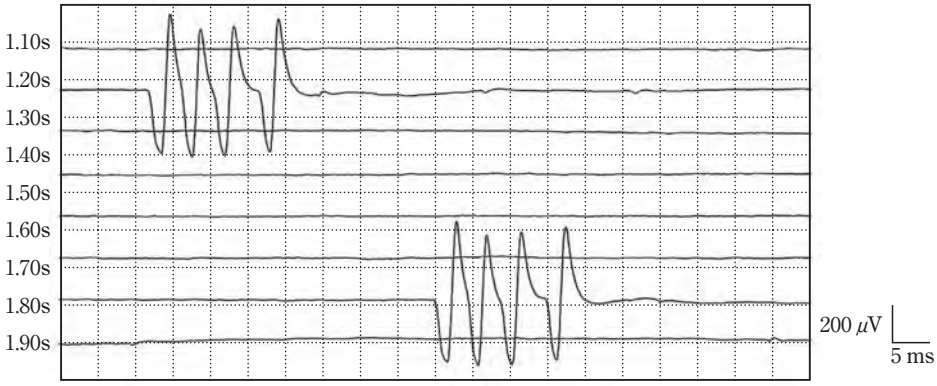

図１　左橈側手根屈筋の針筋電図検査で記録されたミオキミア放電の一部．
単一運動単位電位が短持続（約20ms）の群をなして発射し，約0.5秒の静止期の後，同一の群放電の反復が認められた．

IgG測定，犬ジステンパー抗原PCR検査，細菌・真菌培養を行ったが，いずれも異常は認めなかった．脳波検査では左前頭・側頭葉優位に突発性発射（棘波）を多数認めた．針筋電図検査（EMG）では，左側橈側手根屈筋から単一運動単位電位が130～250Hzの頻度で短持続の群をなして発射し，短い静止期の後，同一の群放電が反復するという，ミオキミア放電に一致する所見が認められた（図1）．また，左上腕三頭筋からは複合反復放電が得られたがその他の四肢，体幹，顔面の筋は異常を呈さなかった．EMG時にMK様の動きが視認された筋はなかったが，左側橈側手根屈筋においては筋がピクピクと動く感触を触知することは可能であった．以上を総合して，本症例における筋の波状の動きはMKであり，発作性の筋硬直はNMTの可能性が高いと判断した．CSF所見と臨床所見から髄膜脳炎を始めとする炎症性脳疾患が疑われたため，感染性疾患の検査結果を待つ間クリンダマイシン（ダラシンカプセル，ファイザー㈱，東京）10mg/kg１日２回およびドキシサイクリン（ビブラマイシン錠，ファイザー㈱，東京）5mg/kg１日２回の経口投与を開始した．後日出た検査結果は感染性髄膜脳炎を示唆するものではなく特定の免疫介在性脳炎を裏付ける所見にも乏しかったため，原因不明の髄膜脳炎として飼い主との相談の下合計２カ月間上記２種の抗生剤投与を継続した．初診から５日目に筋硬直から開始し全身をピクッとする発作が半日持続したと連絡を受けた．そこでゾニサミド（ZNS）（エクセグラン散20％，大日本住友製薬㈱，大阪）5mg/kg１日２回の投与開始を紹介元獣医師へ指示した．その後３カ月間MKは改善なく持続したがNMTとMC様徴候は認めなかった．しかし初診から110日目にNMTが再発し，さらに117日目の当院再診時にも院内で呼吸速迫および軽度の四肢硬直を示すNMTを認めその際発熱（39.5℃）も確認された．安静と冷却処置を施したところ発作は急速に終息し平熱に復した．同日からプロカインアミド（PA）（アミサリン錠，第一三共㈱，東京）17mg/kg１日３回の経口投与を開始した．同日行ったZNS血中濃度測定結果は7.6μg/d*l*（トラフ値）と低値を示し，粉末状ZNSの投与不良が判明したため10mg/kg１日２回への増量と錠剤への変更を指示した．145日目に再度CSF検査を行ったところ細胞数は4/μlと正常に復していた．NMTは終息していたがMKは改善がなかったため，PAを26mg/kg１日３回へ増量し，その後MKの頻度と程度が顕著に減少した．現在初診から11カ月が経過しZNSとPA投薬を継続中だが，NMTとMC様徴候は認めら

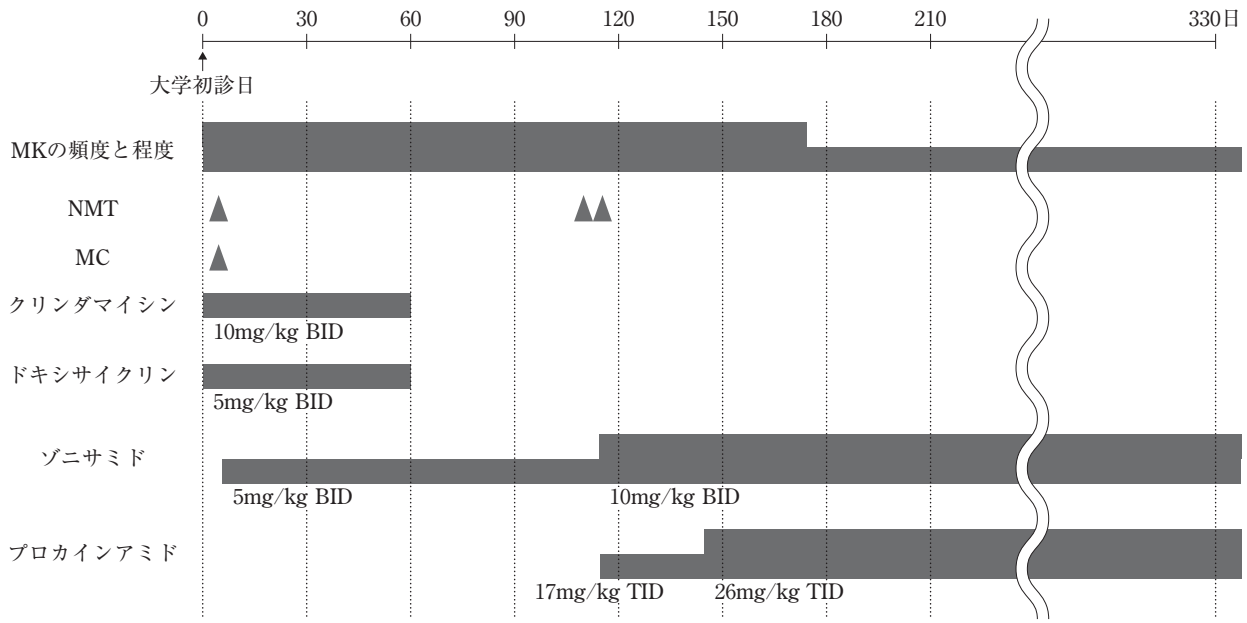

図2　治療およびMK/NMT，MC徴候の経過
（MK：ミオキミア，NMT：ニューロミオトニア，MC：ミオクローヌス様の発作）

れていない．さらに飼い主の報告や院内での観察では，MKの律動的で波状の筋の動きが程度と頻度ともに初診時よりも明らかに減少した状態が継続している（図2）．

考　　察

本症例では体幹部および四肢の筋に律動的で波状の虫が這っているような動きが観察され，この動きは全身麻酔中も消失しなかった．これらは犬猫における過去のMKの報告と同一である［6, 8］．MKにおけるEMGでは，単一運動単位が5～400Hzの頻度で数秒間群をなして発射し短い静止期の後に同じ群放電を繰り返すミオキミア放電が認められるが［4, 6, 10］，われわれの症例でも同様のEMG所見が認められた．NMTは発作性の全身性筋硬直を特徴とする持続的筋収縮であるが，ストレスや興奮がNMTの引き金になる，発作中は意識が保たれる，高体温を示すなどの共通点が示されている［6–9］．さらにNMTはわれわれの症例を含めすべての犬猫でMKと併発している．NMTにおけるEMGはニューロミオトニー放電と呼ばれMKと同様突発性に生じる運動単位発射であるが，ミオキミア放電よりも持続時間が長く非律動性で典型例では電位の振幅が漸減する［7, 10］．われわれの症例のEMGでは，ニューロミオトニー放電は観察されなかった．MK/NMTはともに末梢神経軸索の興奮性の亢進によって生じるが，この亢進は電位依存性カリウムチャネル（VGKC）機能不全が原因とされる［11］．人の先天性MKではVGKC遺伝子変異が報告されている［12］．後天性の場合は，各種免疫介在性疾患との併発を始め感染症との併発あるいは腫瘍随伴症候群としての発症が知られ，患者血清中に抗VGKC抗体が検出されることが多い［1–3, 5, 13, 14］．しかし獣医学領域では，MK/NMTの発症機序や併発誘因疾患についてはまったく解明されていない．MK/NMTを呈した1頭の猫での抗VGKC抗体測定の報告があるが陰性であった［6］．われわれの症例では炎症性中枢疾患に一致するCSF有核細胞数増多が認められたが，顔面MKの犬1頭においても原因不明のCSF有核細胞数増多が報告されている［9］．人では，NMTを呈した抗VGKC抗体陽性辺縁系脳炎の報告があるが［15］，一般的に本脳炎におけるNMTはまれであり，本脳炎とNMTとの関連性は不明と結論付けられている［15, 16］．われわれの症例では，人の抗VGKC抗体陽性辺縁系脳炎に類似したMRI所見や臨床所見は観察されなかった．われわれの症例におけるCSF有核細胞数増多の原因は不明であるが，炎症性脳疾患とMK/NMTが同一の免疫学的機序により発症した，あるいは炎症性脳疾患が先行感染としてMK/NMT発症に関与した可能性があるかもしれない．本症例ではさらに総胆汁酸の高値を認めたが飼い主の希望によりそれ以上の精査を行うことができなかった．過去の報告をみると，MK/NMTの犬において肝酵素の軽度上昇を認めるものがあるがMK/NMTとの関連性は言及されていない［6］．人ではB型肝炎とデルタ肝炎が併発したMKの報告が1例あるが，MKと肝炎との関連は不明とされている［17］．人におけるMK/NMTの治療は併発誘因疾患の治療が主体をなす．MK/NMTに対する治療として，カルバマゼピン，フェニトインなどの抗けいれん薬が人では使用され［3］，特に抗VGKC抗体陽性例において高い効果が認められている［18–20］．これらの薬剤の作用機序として，Na^+チャネ

ルからのNa^+の細胞内流入抑制による膜の安定化作用が考えられている［21］．犬ではカルバマゼピンやフェニトインは薬物代謝が速く血中濃度を維持できないため通常使用されない［22］．同様の作用機序を持つPA投与の効果がMK/NMTを呈した1頭のYTで報告されている［8］．その他免疫抑制量のプレドニゾロンやジアゼパム使用の報告があるがMK/NMTに効果は認められていない［6, 7］．本症例の長時間のNMTに続発したMC様徴候をわれわれが直接観察する機会はなかったが，MC徴候は必ずNMT発現時に認められたため，NMTの一徴候として生じた可能性が考えられる．しかし鑑別のために行った脳波上でてんかん性異常波を多数確認したため，MC様徴候は炎症性脳疾患により生じたてんかん発作である可能性も考慮すべきと考えた．そのためNa^+チャネル不活性化による膜の安定化作用を有し理論上MK/NMTにも効果がある可能性のある抗てんかん薬，ZNS投与をまず試みた．ZNS投与のコンプライアンスは良好とはいえなかったがZNS開始から3カ月間NMTの制御が可能であった．その後NMTが再燃したためZNS増量とともにPA投与を開始した．以降NMTは認めておらずMKにおいても頻度や程度の改善が認められた．MK/NMTはまれな疾患であるが罹患動物のQOLを著しく落とし死亡例も報告されていることから見過ごしてはいけない疾患である．未解明な点が非常に多く今後は世界レベルでの症例の蓄積を行い獣医療における本疾患の発症機序，臨床像，さらに適切な治療法を明らかにする必要があると考えられた．

最後に，症例をご紹介頂いた八王子市ノア動物病院に深謝する．なお，本研究は科研費（20580359）の助成を一部受けたものである．

引　用　文　献

［1］ Gutmann L, Gutmann L : Myokymia and neuromyotonia 2004, J Neurol, 251, 138–142 (2004)
［2］ Gutmann L, Libell D, Gutmann L : When is myokymia neuromyotonia?, Muscle Nerve, 24, 151–153 (2001)
［3］ Vincent A : Understanding neuromyotonia, Muscle Nerve, 23, 655–657 (2000)
［4］ Dewey CW : A Practical Guide to Canine and Feline Neurology, 2nd, 482–485, Blackwell Publishing, Iowa (2008)
［5］ Gutmann L : facial and limb myokymia, Muscle Nerve, 14, 1043–1049 (1991)
［6］ Van Ham L, Bhatti S, Polis I, Fatzer R, Braund K, Thoonen H : Continuous muscle fibre activity in six dogs with episodic myokymia, stiffness and collapse, Vet Rec, 155, 769–774 (2004)
［7］ Galano HR, Olby NJ, Howard JF Jr, Shelton GD : Myokymia and neuromyotonia in a cat, J Am Vet Med Assoc, 227, 1608–1612 (2005)
［8］ Reading MJ, McKerrell RE : Suspected myokymia in a Yorkshire terrier, Vet Rec, 132, 587–588 (1993)
［9］ Walmsley GL, Smith PM, Herrtage ME, Jeffery ND : Facial myokymia in a puppy, Vet Rec, 158, 411–412 (2006)
［10］ 幸原伸夫，木村　淳：刺入時電位と安静時電位，神経伝導検査と筋電図を学ぶ人のために，166–188，医学書院，東京（2003）
［11］ Sinha S, Newsom-Davis J, Mills K, Byrne N, Lang B, Vincent A : Autoimmune aetiology for acquired neuromyotonia, Lancet, 338, 75–77 (1991)
［12］ Browne DL, Gancher ST, Nutt JG, Brunt ER, Litt M : Episodic ataxia/myokymia syndrome is associated with point mutations in the human potassium channel gene, KCNA1, Nat Genet, 8, 136–140 (1994)
［13］ Grant R, Graus F : Paraneoplastic movement disorders, Mov Disord, 24, 1715–1724 (2009)
［14］ Basiri K, Fatehi F : Isaacs syndrome associated with chronic hepatitis B infection : a case report, Neurol Neurochir Pol, 43, 388–390 (2009)
［15］ Vincent A, Buckley C, Schott JM, Baker I, Dewar BK, Detert N, Clover L, Parkinson A, Bien CG, Omer S, Lang B, Rossor MN, Palace J : Potassium channel antibody–associated encephalopathy : a potentially immunotherapy–responsive form of limbic encephalitis, Brain, 127, 701–712 (2004)
［16］ 高堂裕平，下畑享良，徳永　純，河内　泉，田中惠子，西澤正豊：不眠と手指振戦を合併した抗VGKC抗体陽性辺縁系脳炎の1例，臨床神経学，48，338–342（2008）
［17］ Cargnel A, Davoli C, Vigano P, Caccia MR, Zanetti AR, Zuckerman AJ : Seventh cranial nerve paralysis with myokymia during acute co–infection with hepatitis B and delta viruses, J Med Virol, 25, 245–247 (1988)
［18］ Ishii A, Hayashi A, Ohkoshi N, Oguni E, Maeda M, Ueda Y, Ishii K, Arasaki K, Mizusawa H, Shoji S : Clinical evaluation of plasma exchange and high dose intravenous immunoglobulin in a patient with Isaacs' syndrome, J Neurol Neurosurg Psychiatry, 57, 840–842 (1994)
［19］ 園田至人，有村公良：Isaacs症候群と抗カリウムチャネル抗体，Clinical Neuroscience，16，84–87（1998）
［20］ Ramseyer JC : Isaacs' syndrome, West J Med, 123, 130 (1975)
［21］ Bowman WC, Rand MJ : Textbook of pharmacology, 2nd ed, 31, Blackwell Scientific, Oxford (1980)
［22］ Frey HH : Anticonvulsant drugs used in the treatment of epilepsy, Probl Vet Med, 1, 558–577 (1989)

Generalized Myokymia and Neuromyotonia in a Yorkshire Terrier

Shinichi UTSUGI *, Miyoko SAITO† and Masaharu HISASUE

** School of Veterinary Medicine, Azabu University, 1–17–71 Fuchinobe, Sagamihara, 229–8501, Japan*

SUMMARY

An eight-year-old female Yorkshire terrier presented with episodes of hyperpnea and stiffness of the limbs. A physical and neurological examination revealed rhythmic, undulating movement across the muscles of the trunk and limbs. This movement was characteristic of myokymia. An electromyogram demonstrated myokymicdischarges. The cisternal cerebrospinal fluid (CSF) showed mononuclear pleocytosis, which was indicative of inflammatory central nervous system disease. The MRI of the brain was unremarkable. A clinical diagnosis of myokymia/neuromyotonia with inflammatory brain disease was made, and the dog was treated with antibiotics, zonisamide and procainamide. A follow-up CSF analysis performed 5 months after the initial examination was normal. At present, 11 months after the diagnosis, the dog is still being treated with zonisamide and procainamide. No episodes of hyperpnea or stiffness of the limbs have been observed, and the myokymia has decreased markedly in frequency and severity. —— Key words : dog, myokymia, neuromyotonia.

† *Correspondence to : Miyoko SAITO (Department of Veterinary Surgery Ⅱ, Azabu University)*
1–17–71 Fuchinobe, Sagamihara, 229–8501, Japan
TEL 042–754–7111 FAX 042–769–1639 E-mail : msaito@azabu-u.ac.jp

J. Jpn. Vet. Med. Assoc., 64, 56～60 (2011)

犬のアレルギー疾患の遺伝子解析

１．犬のアトピー性皮膚炎の診断方法の開発

２．犬のアトピー性皮膚炎に疾患原因遺伝子の同定

川原井晋平（麻布大学小動物臨床）

研究要旨

犬のアトピー性皮膚炎は、最も一般的な犬の皮膚疾患で、人のそれと非常によく似た病態を示す。小動物臨床においても罹患率が高く、適切な検査、治療管理、病態解析が望まれている。犬のアトピー性皮膚炎の疾患原因遺伝子を解明するために、適切なアトピー性皮膚炎の診断法や検査法の確立が必要である。犬のアトピー性皮膚炎の診断法のゴールデンスタンダードとして皮内試験を確立し､症例の選択において精度の高い診断を行えるようになった。また、犬のアトピー性皮膚炎に疾患原因遺伝子の解析のための基礎的な研究の１つとして犬の CD14 遺伝子のクローニングを行った。

１．犬のアトピー性皮膚炎の診断方法の開発

研究目的

犬のアトピー性皮膚炎の原因アレルゲンを同定するためのアレルギー検査は主に皮内反応検査と血清抗原特異的 IgE 検査が実施されている。血液検査を外注する血清抗原特異的 IgE 検査は簡便であるが、受託機関において多様な方法で実施されており、検査機関において結果が異なることが課題となっている。そこで、質の高い犬のアトピー性皮膚炎罹患症例のゲノム DNA を採取するため、皮内反応検査を麻布大学において確立することを目的とした。さらに適切な診断と治療を飼い主に提供することが症例の収集には重要である。そこで、犬のアトピー性皮膚炎の症状を維持するシャンプー療法の提案と、抗原特異的な犬のアトピー性皮膚炎の治療法についても麻布大学にて確立することを目的とした。

材料と方法

麻布大学附属動物病院に来院したアトピー性皮膚炎が疑われる症例 29 頭を対象とし､皮内反応検査（IDT）と IgE test を実施した。IDT は国産抗原液として鳥居薬品（株）製を 1:100～1:10000(w/v)の濃度と、輸入抗原液として Greer 社製を 1:50000（w/v）の濃度で用い、紅斑のある膨疹形成を陽性とした｡IgE test はヒト高親和性 IgE レセプターα鎖を用いた ELISA 法を用いて 150LU 以上を陽性として外部機関で測定した。それぞれの関連性を Fisher's exact test を用いて統計解析した。

麻布大学附属動物病院に来院した犬アレルギー性皮膚炎の 6 症例に対し、週 1 回のシャンプー療法を実施し、メチシリン耐性ブドウ球菌の常在化の改善について検証した。コナヒョウヒダニに対するアトピー性皮膚炎が疑われる症例 2 頭を対象とし、国産抗原液を用いた減感作療法を実施した。

結果および考察

IgE test と輸入抗原液を用いた IDT の間に有意差を認めた(P<0.01)。1:100(w/v)と 1:10000(w/v)の国産抗原液は、IgE test および輸入抗原液との間に有意差が認められた(P<0.05)。以上より、国産抗原液の犬アトピー性皮膚炎の診断における有用性が明らかとなった(表 1)。

痒みのスコア、メチシリン耐性ブドウ球菌の常在箇所がシャンプー療法前と比較して有意に減少した(P<0.05)(図１)。減感作療法を実施後、2 頭の臨床症状が改善した(図２)。これらの結果からシャンプー療法及び減感作療法は犬のアレルギー性皮膚炎の治療法として有用であることが示唆された。

表 1　IDT と IgE test の比較結果

国産抗原液×100

	Serum Allergen test negative (<250)	Serum Allergen test weak positive (250～399)	Serum Allergen test positive (400～999)	Serum Allergen test strong positive (1000≦)
IDST positive	9	1	2	5
IDST negative	12	0	0	0

国産抗原液x10000

	Serum Allergen test negative (<250)	Serum Allergen test weak positive (250～399)	Serum Allergen test positive (400～999)	Serum Allergen test strong positive (1000≦)
IDST positive	3	1	2	2
IDST negative	16	0	0	1

輸入抗原液x50000

	Serum Allergen test negative (<250)	Serum Allergen test weak positive (250～399)	Serum Allergen test positive (400～999)	Serum Allergen test strong positive (1000≦)
IDST positive	0	1	2	4
IDST negative	14	0	0	1

図１　シャンプー療法実施前後の各臨床スコアと菌検出頻度の変化

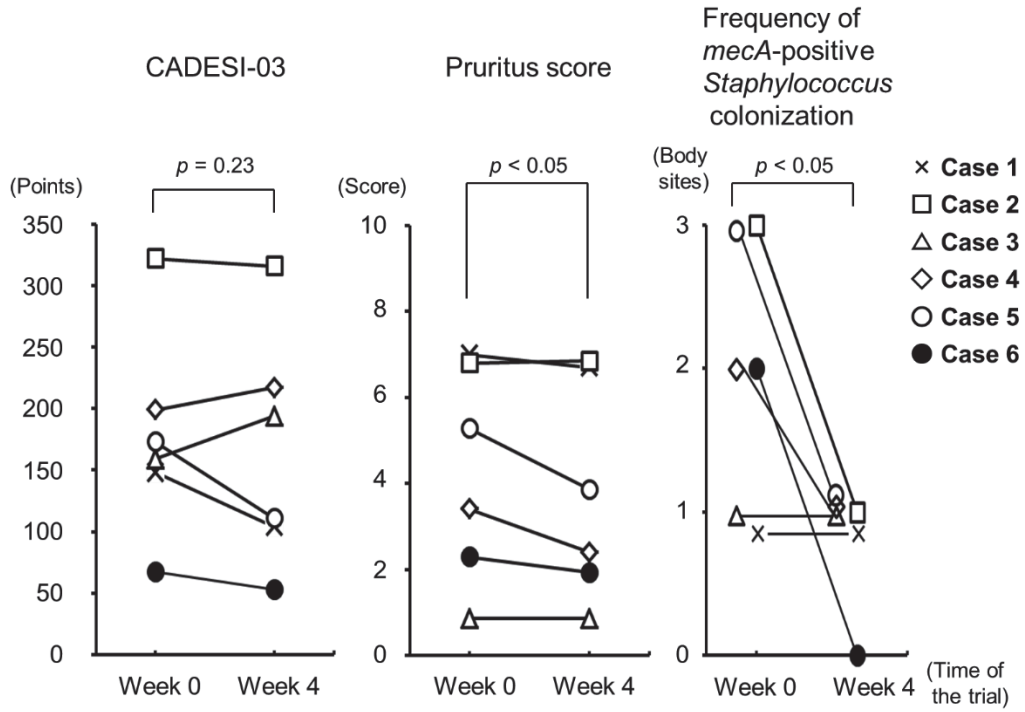

図２　各２症例の減感作治療前後の臨床症状の変化

症例１

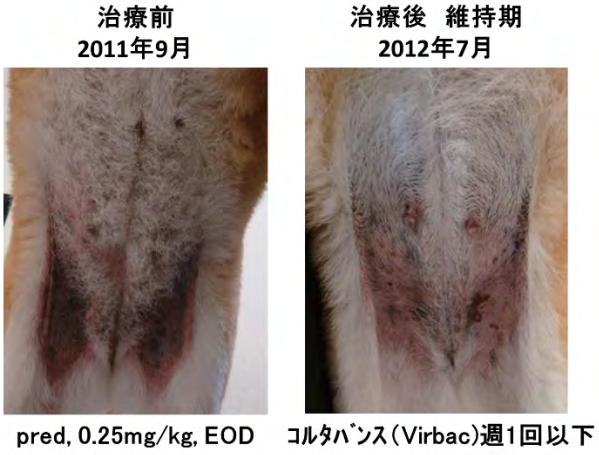

症例２

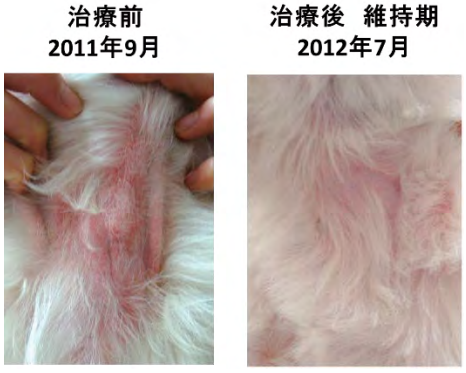

2. アトピー性皮膚炎に疾患原因遺伝子の同定

研究目的

CD14 は単球の細胞表面に主に発現するグラム陰性菌の細胞壁構成タンパクでリポポリサッカライド（LPS）の認識に関わる分子である。CD14 のプロモーター領域の変異は喘息、アトピー性皮膚炎、鼻腔ポリープとの関係性が人で明らかとなっている。犬の CD14 の遺伝子はまだクローニングされていない。犬のアトピー性皮膚炎に疾患原因遺伝子の解析のための基礎的な研究の１つとして犬の CD14 の遺伝子はクローニングを行うことを目的とした。

材料と方法

ビーグル犬から cDNA を合成し、CD14 のクローニングを 5'-race および 3'-race 法を用いて実施した。麻布大学皮膚科に来院する血餅検体を述べ 500 検体以上収集した。

結果と考察

CD14 の遺伝子配列は、Pubmed に掲載されている情報と異なっていた（図３）。犬の CD14 は 290 個のアミノ酸からなり、牛と 75%、羊と 76%、人と 72%、ヤギと 68%の相同性であった。血餅より精製したゲノム DNA を用いて今後、遺伝子多型の解析を進めることが可能になった。

図３

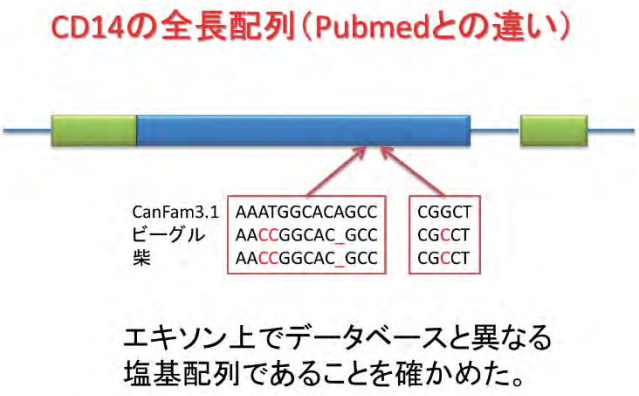

研究発表

1. 論文発表

1) Kawarai S, Fujimoto A, Nozawa G, Kanemaki N, Madarame H, Shida T, Kiuchi A.: Evaluation of weekly bathing in allergic dogs with methicillin-resistant Staphylococcal colonization. Jpn J Vet Res in press.

2) Kawarai S, Hisasue M, Matsuura S, Ito T, Inoue Y, Neo S, Fujii Y, Madarame H, Shirota, K, Tsuchiya R.: Canine pemphigus foliaceus with concurrent immune mediated thrombocytopenia. J Am Anim Hosp Assoc 51:56-63, 2015

3) Kawarai S, Matsuura M, Yamamoto S, Kiuchi A, Kanemaki N, Madarame H, Sirota K.: A case of cutaneous sterile pyogranuloma/granuloma syndrome in a Maltese. J Am Anim Hosp Assoc

50:278-283, 2014

4) Kanemaki N, Tchedre KT, Imayasu M, Kawarai S, Sakaguchi M, Meguro A, Mizuki N.: Identification of S1 RNA Binding Domain-1 SRBD1 as a Major Gene Determining Japanese Shiba-Inu Dog Glaucoma. PLoS One 8:e74372, 2013
5) Kaburaki Y, Fujimura T, Kurata K, Matsuda K, Toda M, Yasueda H, Chida K, Kawarai S, Sakaguchi M.: Induction of Th1 immune responses to Japanese cedar pollen allergen in mice immunized with Cry j 1 conjugated with CpG oligodeoxynucleotide. Comp Immunol Microbiol Infect Dis 34,157-61, 2011
6) Kawarai S, Sato K, Horiguchi A, Kurata K, Kiuchi A, Tsujimoto H, Sakaguchi M.: Potential immunological adjuvant of 'K'-type CpG-oligodeoxynucleotides enhanced the cell proliferation and IL-6 mRNA expression in canine B cells. J Vet Med Sci 73,177-184, 2011

2. 学会発表

1) 川原井晋平：皮膚感染症の検査と解釈・維持の仕方，日本獣医内科学アカデミー第 10 回記念学術大会、横浜、2 月 2014 年
2) Kawarai S, Fujimoto A, Nozawa G, Kanemaki N, Madarame H, Shida T, Kiuchi A.: Decreasing methicillin-resistant Staphylococcal colonization in allergic dog skin by shampoo. The Asian Meeting of Animal Medicine Specialties, Bogor, Indonesia, Dec, 2013
3) 村上弘正、細川聖矢、川原井晋平、斑目広郎: 減感作療法を実施した犬アトピー性皮膚炎の 2 例. 日本小動物獣医学会東北地区大会、郡山、10 月 2013 年 1
4) 飯野瑞貴、西本優子、藤本あゆみ、野澤源太、川原井晋平、信田卓男、木内明男： 犬のアレルギー性皮膚炎の症状維持におけるマイクロバブルを用いたシャンプー療法の有効性の検討. 日本動物看護学会関西地区第 5 回例会. 大阪、3 月 2012 年
5) 細川聖矢、川原井晋平、津久井利広、久末正晴、印牧信行、斑目広郎、土屋亮、小方宗次:国産コナヒョウヒダニ抗原液の有用性に関する再考. 第 154 回日本獣医学会学術集会、岩手、9 月 2012 年
6) 松浦祐介、高橋亮二、川原井晋平、山口忠義、斑目広郎、代田欣二： 犬における無菌性肉芽腫性皮膚炎の一例. 関東・東京合同地区獣医師大会、神奈川、9 月 2011 年
7) Kawarai S, Takahashi R, Madarame H, Shirota K.: A case of granulomatous dermatitis in a dog. The Asian Meeting of Animal Medicine Specialties. Thailand, May, 2011

Japanese Journal of Veterinary Research 64(2): 000–000, 2016

NOTE

Evaluation of weekly bathing in allergic dogs with methicillin-resistant *Staphylococcal* colonization

Shinpei Kawarai[1,*], Ayumi Fujimoto[2], Genta Nozawa[3], Nobuyuki Kanemaki[1], Hiroo Madarame[1], Takuo Shida[4] and Akio Kiuchi[3]

[1]Veterinary Teaching Hospital Laboratory of Small Animal Clinics; Department of Veterinary Medicine
[2]Laboratory of Internal Medicine II;
[3]Laboratory of Microbiology I; and
[4]Laboratory of Veterinary Radiology, Azabu University, 1–17–71, Fuchinobe, Chuo-ku, Sagamihara, Kanagawa 252–5201, Japan

Received for publication, 00000 00, 0000; accepted, 00000 00, 0000

Abstract

We evaluated the efficacy of weekly bathing in reducing methicillin-resistant *Staphylococcus* (MRS) colonization in canine allergic dermatitis in a pilot clinical trial. Six dogs with allergic dermatitis controlled by prescription medications were treated with weekly bathing for 1 month. The Canine Atopic Dermatitis Extent and Severity Index version 3 (CADESI-03) and pruritus scores and frequency of *mecA*-positive *Staphylococcus* spp. isolated from three body sites between weeks 0 and 4 were compared. There was no significant difference in CADESI-03 scores with bathing, whereas the pruritus scores were significantly reduced ($p < 0.05$). Furthermore, MRS frequency was decreased in four of the six dogs ($p < 0.05$). In conclusion, weekly bathing should be considered for reducing MRS colonization in canine allergic dermatitis.

Key Words: allergic dermatitis, bathing, *mecA*

Staphylococcus spp. are part of the commensal flora of canine skin. In dogs with allergic skin conditions, such as canine atopic dermatitis (CAD) and adverse food reactions (AFR), *Staphylococcus* spp. are common causative pathogens isolated from skin lesion[6,7,13]. During antibiotic therapy, *Staphylococcus* spp. frequently acquire genes that provide resistance to antimicrobial agents; one example is *mecA* found in methicillin-resistant *Staphylococcus* spp. (MRS)[1]. These resistance genes in pathogenic *Staphylococcus* spp. constitute a risk for horizontal gene transfer to commensals and transients[2,4], which is particularly problematic for methicillin-

*Corresponding author: Shinpei Kawarai, Veterinary Teaching Hospital, Azabu University, 1–17–71 Fuchinobe, Chuo, Sagamihara, Kanagawa 252–5201, Japan
Phone: +81–(0)42–754–7111. Fax: +81–(0)42–850–2506. E-mail: kawarai@azabu-u.ac.jp
doi: 10.14943/jjvr.64.2.★★

resistant *Staphylococcus pseudointermedius* in dogs because of the risk of colonization or *mecA* gene transfer to owners[3,6]. In this clinical pilot study, we evaluated the efficacy of weekly bathing in decreasing MRS colonization in the skin of allergic dogs.

Six dogs with chronic, recurrent, and pruritic skin symptoms that were diagnosed with CAD and/or concurrent AFR based on Favrot's criteria for canine atopic dermatitis, serum allergen-specific immunoglobulin E (IgE) test, and food elimination and provocation trials were enrolled (Table 1)[5,9]. The allergic skin conditions of all dogs were under control by prescription medications and food avoidance. All six dogs were routinely bathed by their owners at a frequency of once a week or once every other week. All dogs had a history of superficial pyoderma due to *Staphylococcus* spp., in which *mecA*-positive *Staphylococcus* spp. was isolated from the skin surface. After informed consent was obtained, owners were instructed to declare any unusual events regarding their dogs such as the living environment and diet during the study period. The trial was conducted between September 2010 and December 2011. This trial was approved by the ethical committee for clinical trials at the Veterinary Teaching Hospital of Azabu University in Sagamihara, Kanagawa Prefecture, Japan.

The trial participants were bathed by veterinary technicians (VTs) once a week for 1 month. VTs photographed the dogs before their weekly baths. The Canine Atopic Dermatitis Extent and Severity Index version 3 (CADESI-03), which has a maximum score of 1,240, was used to evaluate skin symptoms[8]. Pruritus was assessed daily by the owners on a scale of 0–10 (0 = no pruritus; 10 = severe pruritus), and weekly average scores were calculated. To evaluate changes in clinical scores, the scores at the start (week 0) and end (week 4) of the trial were compared.

The swab samples were collected from the skin surface before the baths. Three swab samples were collected from three different affected body sites that showed signs such as erythema and atopic dermatitis. At each site, an area of 5 cm^2 was swabbed and cultured for bacteria on blood agar. Five, morphologically similar colonies representing the majority from each agar plate were selected. The expression of *mecA* of gram-positive cocci was detected by polymerase chain reaction (PCR), as described by Sasaki *et al*[12]. The bacterial species of *mecA*-positive gram-positive cocci were identified by sequencing *16S rRNA* with species-specific primers using the Microseq 500 PCR kit (Applied Biosystems; Foster City, U.S.A.), according to the manufacturer's protocols[12]. The frequencies of *mecA* in isolated *Staphylococcus* spp. from each body site at week 0 and 4 were compared. Changes in clinical scores were not available to the microbiologists until the end of the trial.

Changes in outcome measures between weeks 0 and 4 were compared using statistical analysis. Wilcoxon rank sum test was used for clinical scores, and Mann-Whitney *U* test was used for frequency of *mecA*-positive *Staphylococcus* colonization using the Microsoft Excel program with the Statcel software add-in (version 4; OMS Publishing, Japan). Data were presented as means ± standard deviation, and p values of <0.05 were considered statistically significant for all analyses performed.

The changes in the frequency of *mecA*-positive *Staphylococcus* colonization, CADESI-03 and pruritus scores are presented in Fig. 1. Table 2 shows the PCR analysis for *mecA*. The frequency of *mecA*-positive *Staphylococcus* spp. isolated from all three body sites decreased in four dogs (cases 2, 4, 5, and 6). Specifically, the frequency at week 4 was significantly lower than that at week 0 (0.8 ± 0.4 versus 2.0 ± 0.9, respectively; $p < 0.05$). At week 0, *mecA*-positive *Staphylococcus* spp. were isolated from 12 out of a total of 18 body sites (eleven *S. pseudointermedius* and one *S. aureus*). In contrast, *mecA*-positive *Staphylococcus* spp. were isolated from five body sites (four *S. pseudointermedius* and one *S. epidermis*) at the end of the trial at week 4. There was no significant difference in the CADESI-03

Table 1. Profile, skin symptoms, skin lesions, identified allergens, and prescribed medications and shampoos of six allergic dogs enrolled in the trial

Case No.	Breeds	Sex[1)]	Age (year)	1st onset (year)	Seasonality of symptoms	Major Skin symptoms	Major Skin lesions	Results of serum allergen specific Immunoglobulin E test	Results of food provocation test	Prescribed medications[2)]	Prescribed shampoos[3)]
1	Shiba Inu	SF	10	5	All year	Erythema, Scales, Lichenification, Hyperpigmentation, Alopecia	Muzzle, Periocular, Feet, Axillae, Ventral abdomen, Prianal	*D. farinae, D. pteronyssinus*	Not determined	Clemastine fumarate, Glycyrrhizinate, Ointment	Chlorhexidine
2	Yorkshire Terrier	SF	6	1	All year	Erythema, Excoriation, Papule, Scales, Lichenification, Hyperpigmentation, Alopecia	Muzzle, Ear, Periocular, Feet, Axillae, Dorsal trunk, Ventral abdomen	*D. farinae, D. pteronyssinus*	Chicken	Clemastine fumarate, Ointment	Chlorhexidine
3	Toy Manchester Terrier	SF	9	2	Autumn, Winter	Erythema, Scales, Alopecia	Axillae, Dorsal trunk, Ventral abdomen	*A. siro*	Not determined	Prednisolone, Ointment	Chlorhexidine
4	Shiba Inu	NM	10	1	All year	Scales, Lichenification, Hyperpigmentation, Alopecia	Muzzle, Periocular, Feet, Axillae, Ventral abdomen	*D. pteronyssinus*	Chicken, Sardine, Sprout, Potato, Rice, Wheat	Prednisolone, Clemastine fumarate, Glycyrrhizinate, Ointment	Miconazole nitrate and Chlorhexidine
5	Brussels Griffon	NM	8	4	All year	Erythema, Excoriation, Papule, Scales, Lichenification, Hyperpigmentation, Alopecia, Fistula	Muzzle, Face, Dorsal trunk, Ventral abdomen, Interdigital skin	*A. siro*	Japanese sweets	Ointment	Chlorhexidine
6	Labrador Retriever	F	8	2	All year	Erythema, Papule, Lichenification, Hyperpigmentation, Alopecia, Fistula	Muzzle, Face, Ear, Axillae, Ventral abdomen, Interdigital skin	*A. fumigatus*	Chicken, Potato	Prednisolone, Thyroxin, Ointment	Chlorhexidine

1) F, female; SF, Spayed female; NM, Neutered male
2) Ointment, Hand-mixed topical corticosteroid (0.12% betamethasone valeratel and 0.3% heparinoidm)
3) Chlorhexidine, Nolvasan, Fort dodge animal health, IA; Miconazole nitrate and Chlorhexidine, Malaseb, Fort dodge animal health, IA

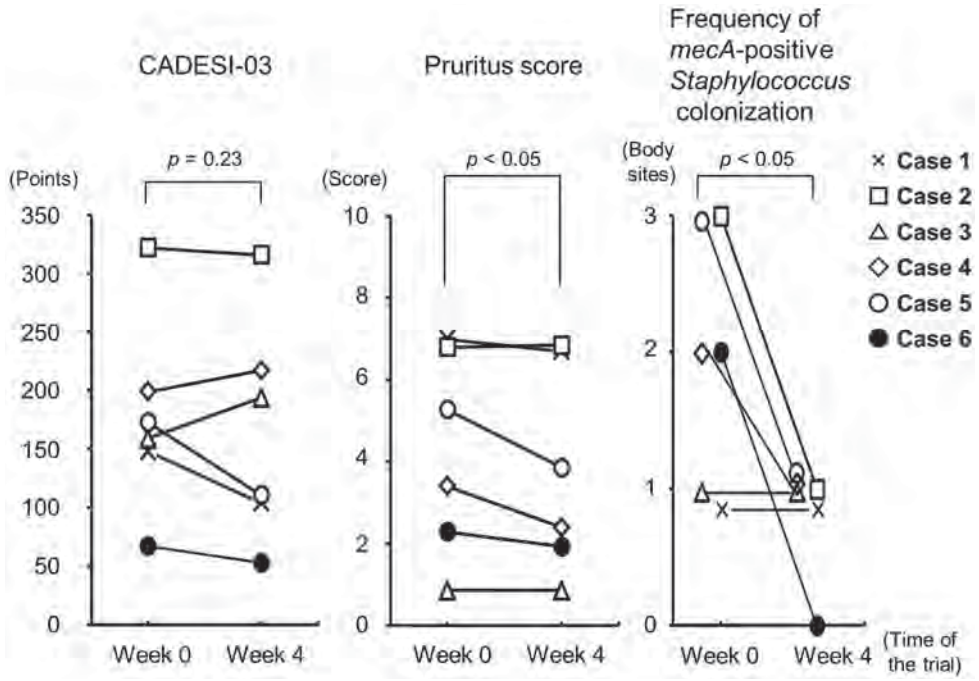

Fig. 1. Changes in the clinical scores and frequency of *mecA*-positive *Staphylococcus* colonization in six dogs enrolled in the trial.

score between week 0 (178 ± 83) and week 4 (166 ± 95); however, two of the six participant dogs (cases 1 and 5) exhibited decreases of ≥25% in CADESI-03 scores compared with those at week 0. The pruritus score was significantly lower at week 4 than at week 0 (3.8 ± 2.5 versus 4.3 ± 2.5, respectively; $p < 0.05$). Cases 4 and 5 showed decreases of ≥25% in pruritus scores at week 4 compared with those at week 0.

In this trial, we were successful in maintaining allergic dermatitis under control using weekly bathing without antibiotics. Four weeks after the trial, the pruritus scores and MRS colonization on the skin surface decreased. Previous studies showed that transient infectious as well as resident non-infectious *Staphylococcus* spp. were present in the skin of atopic canines[6,11,14]. While aggressive antibiotic therapy can be useful for the elimination of pathogenic *Staphylococcus* spp. from skin lesions, long term antibiotic use are likely to increase the risk for disruption of the skin and other organ-resident floras[14]. In addition, the risk of both pathogenic and non-pathogenic *Staphylococcus* spp. to acquire antibiotic resistance genes are increased with this approach[1–3,6,10,14], as demonstrated by the colonization of healthy dogs by *mecA*-positive *S. pseudointermedius*[10]. In this study, *S. epidermis*, a typically non-pathogenic spp. that was isolated from case 3 at week 4 was found to have *mecA*. The roles of *S. epidermis* as a reservoir and transmitter of linezolid resistance genes were previously described[2]. Restoration of commensal skin flora and prevention of drug resistance are considered as logical goals to control allergies in dogs[14]. Thus, weekly bathing following clinical cure with antibiotics should be useful in preventing the risk for development of multidrug resistance in not only skin microflora but also in other organs.

In the present study, we performed weekly bathing only for enrolled dogs that were being bathed two to four times a month by their owners before the trial. The environment and housekeeping conditions differed between the dogs. For example, the elderly owners may have had trouble in efficiently bathing their dogs, and one major reason for the success of this trial could be because of the experienced VTs who

Table 2. Summary of *Staphylococcus* spp. and their *mecA* status in six dogs enrolled in the trial

		At week 0			At week 4		
Case No.	Body sites where swab samples were collected	The results of the culture	The results of *mecA*	Isolated *Staphylococcus* spp. by PCR	The results of the culture	The results of *mecA*	Isolated *Staphylococcus* spp. by PCR
1	Right axillae	Positive	Positive	*S. peudointermedius*	Positive	Positive	*S. peudointermedius*
	Ventral abdomen	Negative			Negative		
	Right feet	Negative			Negative		
2	Right axillae	Positive	Positive	*S. peudointermedius*	Negative		
	Right ear	Positive	Positive	*S. peudointermedius*	Positive	Positve	*S. peudointermedius*
	Dorsal trunk	Positive	Positive	*S. peudointermedius*	Negative		
3	Left Axillae	Negative			Negative		
	Dorsal trunk	Positive	Postitive	*S. peudointermedius*	Negative		
	Ventral abdomen	Negative			Positive	Positive	*S. epidermidis*
4	Muzzle	Positive	Postitive	*S. peudointermedius*	Positive	Postitive	*S. peudointermedius*
	Right Axillae	Positive	Postitive	*S. peudointermedius*	Negative		
	Ventral abdomen	Negative			Negative		
5	Right Interdigital skin	Positive	Postitive	*S. peudointermedius*	Negative		
	Dorsal trunk	Positive	Postitive	*S. peudointermedius*	Negative		
	Ventral abdomen	Positive	Postitive	*S. aureus*	Positive	Postitive	*S. peudointermedius*
6	Right Interdigital skin	Positive	Postitive	*S. peudointermedius*	Negative		
	Muzzle	Positive	Postitive	*S. peudintermedius*	Negative		
	Right Axillae	Negative			Negative		

bathed the dogs in not a specific but a certain manner. Furthermore, worsening condition of the ventral abdominal lesions and increased CADESI-03 score were observed in case 3 at week 4. The ventral abdominal skin is comparatively thin in the breed phenotype of case 3. Therefore, it may be preferable to tailor the frequency of bathing in each dog based on breed characteristics to avoid excessive washing.

A limitation of the present trial was treatment necessity, and it was not possible to obtain permission from the owners for their animals to be bathed with only tap water as a control group participating in this trial. Further clinical trials with this control group are needed based on this pilot study. In conclusion, we propose weekly bathing as useful in controlling canine allergic dermatitis by preventing recurrent MRS skin infections.

This study was partially supported by the Young Scientist Research Training Award (2012) funded by the Azabu University Research Service Division, by Grant-in-Aid for Young Scientists (B) by the Japan Society for the Promotion of Science (JSPS) (23780330), and by MEXT-Supported Program for the Strategic Research Foundation at Private Universities (2011–2015).

References

1) Beck, K. M., Waisglass, S. E., Dick, H.L. and Weese, J. S. 2012. Prevalence of meticillin-resistant *Staphylococcus pseudintermedius* (MRSP) from skin and carriage sites of dogs after treatment of their meticillin-resistant or meticillin-sensitive staphylococcal pyoderma. *Vet. Dermatol*., **23**: 369–375, e66–67.
2) Cafini, F., Nguyen le T. T., Higashide, M., Román, F., Prieto, J. and Morikawa, K. 2016. Horizontal gene transmission of the cfr gene to MRSA and *Enterococcus*: role of *Staphylococcus epidermidis* as a reservoir and alternative pathway for the spread of linezolid

resistance. *J. Antimicrob. Chemother*., **71**: 587–592.
3) Davis, J. A., Jackson, C. R., Fedorka-Cray, P. J., Barrett, J. B., Brousse, J. H., Gustafson, J. and Kucher, M. 2014. Carriage of methicillin-resistant staphylococci by healthy companion animals in the US. *Lett. Appl. Microbiol.*, **59**: 1–8.
4) Hanssen, A. M., Kjeldsen, G., Sollid, J. U. 2004. Local variants of Staphylococcal cassette chromosome mec in sporadic methicillin-resistant *Staphylococcus aureus* and methicillin-resistant coagulase-negative Staphylococci: evidence of horizontal gene transfer? *Antimicrob. Agents Chemother*., **48**: 285–296.
5) Kawarai, S., Ishihara, J., Masuda, K., Yasuda, N., Ohmori, K., Sakaguchi, M., Asami, Y. and Tsujimoto, H. 2010. Clinical efficacy of a novel elimination diet composed of a mixture of amino acids and potatoes in dogs with non-seasonal pruritic dermatitis. *J. Vet. Med. Sci.*, **72**: 1413–1421.
6) Lloyd, D. 2013. Chapter 4, Bacterial skin diseases. In: *Muller and Kirk's small animal dermatology*, 7 th ed., pp. 184–186, Miller, W. H., Jr, Griffin, C. E. and Campbell, K. L., eds., Elsevier Mosby, St. Louis, Missouri.
7) McEwan, N. A., Mellor, D. and Kalna, G. 2006. Adherence by *Staphylococcus intermedius* to canine corneocytes: a preliminary study comparing noninflamed and inflamed atopic canine skin. *Vet. Dermatol.*, **17**: 151–154.
8) Olivry, T., Marsella, R., Iwasaki, T. and Mueller, R. 2007. International task force on canine atopic dermatitis. Validation of CADESI-03, a severity scale for clinical trials enrolling dogs with atopic dermatitis. *Vet. Dermatol.*, **18**: 78–86.
9) Olivry, T., DeBoer, D. J., Favrot, C., Jackson, H. A., Mueller, R. S., Nuttall, T. and Prélaud, P. 2010. International task force on canine atopic dermatitis. Treatment of canine atopic dermatitis: clinical practice guidelines from the international task force on canine atopic dermatitis. *Vet. Dermatol.*, **21**: 233–248.
10) Priyantha, R., Gaunt, M. C. and Rubin, J. E. 2016. Antimicrobial susceptibility of *Staphylococcus pseudintermedius* colonizing healthy dogs in Saskatoon, Canada. *Can. Vet. J.,* **57**: 65–69.
11) Rodrigues Hoffmann, A., Patterson, A. P., Diesel, A., Lawhon, S. D., Ly, H. J., Elkins Stephenson, C., Mansell, J., Steiner, J. M., Dowd, S. E., Olivry, T. and Suchodolski, J. S. 2014. The skin microbiome in healthy and allergic dogs. *PLoS. One*, **9**: e83197.
12) Sasaki, T., Kikuchi, K., Tanaka, Y., Takahashi, N., Kamata, S. and Hiramatsu, K. 2007. Methicillin-resistant *Staphylococcus pseudointermedius* in a veterinary teaching hospital. *J. Clin. Microbiol.*, **45**: 1118–1125.
13) Simou, C., Thoday, K. L., Forsythe, P. J. and Hill, P. B. 2005. Adherence of *Staphylococcus intermedius* to corneocytes of healthy and atopic dogs: effect of pyoderma, pruritus score, treatment and gender. *Vet. Dermatol.*, **16**: 385–391.
14) Weese, J. S. 2013. The canine and feline skin microbiome in health and disease. *Vet. Dermatol.*, **24**: 137–145.

Canine Pemphigus Foliaceus with Concurrent Immune-Mediated Thrombocytopenia

Shinpei Kawarai, PhD, DVM, Masaharu Hisasue, PhD, DVM, Shinobu Matsuura, PhD, DVM, Tetsuro Ito, DVM, Yukari Inoue, DVM, Sakurako Neo, PhD, DVM, DACVP, Yoko Fujii, PhD, DVM, DACVIM (Cardiology), Hiroo Madarame, PhD, DVM, DJCVP, Kinji Shirota, PhD, DVM, DJCVP, Ryo Tsuchiya, PhD, DVM

ABSTRACT

A 3 yr old wirehaired fox terrier was presented to his primary care veterinarian with fever, thrombocytopenia, and generalized crusting dermatitis. The skin lesion had progressed for at least 18 days, and thrombocytopenia had developed 3 days before presentation. Histopathology and direct immunofluorescence studies of the skin were consistent with pemphigus foliaceus (PF). Immunofluorescence revealed immunoglobulin G deposition around the keratinocytes in the stratum spinosum. A diagnosis of immune-mediated thrombocytopenia (IMT) was confirmed by the presence of platelet surface-associated immunoglobulin using flow cytometry. Systemic immunosuppressive therapy with cyclosporine and azathioprine was effective, and the dog survived for >2 years from the initial presentation. IMT is rarely associated with PF. This appears to be the first detailed report of a definitive diagnosis of concurrent PF and IMT in a dog. The authors' findings indicate that canine PF could be complicated by hematologic immune-mediated diseases such as IMT. (*J Am Anim Hosp Assoc* 2015; 51:56–63. DOI 10.5326/JAAHA-MS-6044)

Introduction

Canine pemphigus foliaceus (PF) is the most common autoimmune pustular skin disease in dogs characterized by pustules, crusting, erosions, and alopecia of the head, face, nasal planum, pinnae, and footpads.[1–3] When generalized, skin lesions spread over the entire body, and symptoms include fever, lethargy, and limb edema. Histopathologically, acantholytic keratinocytes are found within intraepidermal-to-subcorneal neutrophilic and eosinophilic pustules. Direct immunofluorescence (IF) has shown that antikeratinocyte autoantibodies are deposited in vivo in the subcorneal layers, especially the stratum spinosum and granulosum.[1–9] Indirect IF using canine PF sera revealed the presence of circulating antikeratinocyte immunoglobulin (Ig) G in vitro.[10] Recently, several different epidermal staining patterns were identified by indirect IF using healthy canine footpad epithelium as a substrate.[11] Comparisons of IF staining patterns of desmosomal and nondesmosomal adhesion molecules of keratinocytes with those of canine PF sera showed that desmocolin-1 was the major autoantigen of canine PF.[11,12] Although circulating antikeratinocyte autoantibodies are considered to cause acantholysis only on the epidermis, canine PF reportedly occurs either concurrently with or following hypothyroidism, leishmaniasis, and systemic lupus erythematosus (SLE).[3,13–15] Dysregulated antibody production based on polyclonal B cell activation, cross-reacting antigens, and the innocent bystander reaction due to adsorption of circulating immune complexes onto keratinocytes are thought to cause these autoimmune disorders.[3,13–15]

From Laboratory of Small Animal Clinics, Veterinary Teaching Hospital (S.K., T.I., H.M.) and Laboratory of Veterinary Internal Medicine II (M.H., Y.I., S.N., R.T.), Laboratory of Veterinary Surgery I (Y.F.), and Laboratory of Veterinary Pathology (K.S.), Department of Veterinary Medicine, Azabu University, Fuchinobe, Chuo-ku, Sagamihara, Kanagawa, Japan; and Center for Advanced Biomedical Research, Boston University School of Medicine, Boston, MA (S.M.).

Correspondence: hisasue@azabu-u.ac.jp (M.H.)

CRP, C-reactive protein; IF, immunofluorescence; Ig, immunoglobulin; IMT, immune-mediated thrombocytopenia; IV, intravenous injection; PF, pemphigus foliaceus; PO, *per os*; PSA, platelet surface-associated; RF, rheumatoid factor; SLE, systemic lupus erythematosus

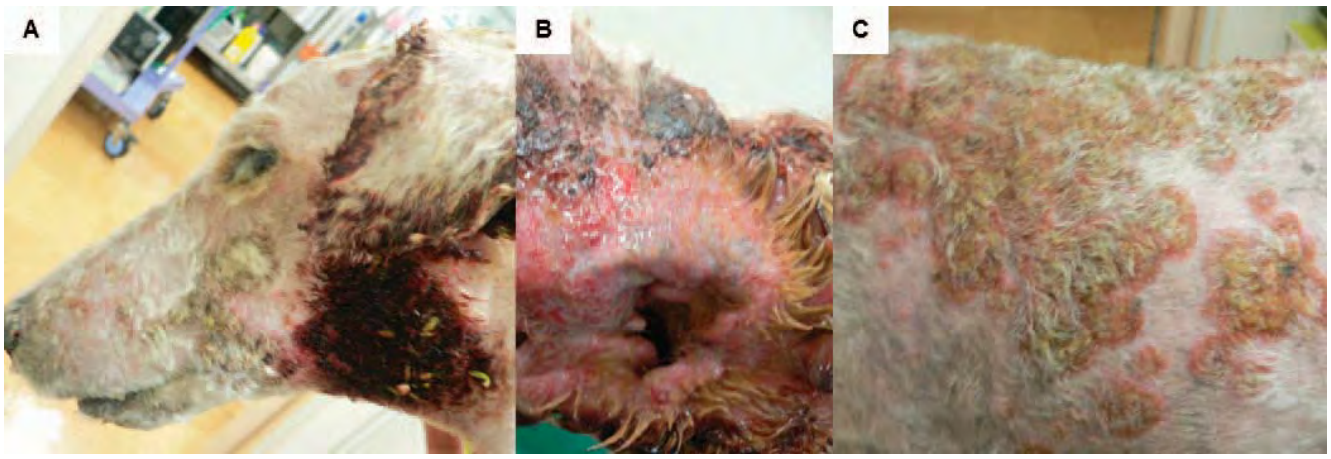

FIGURE 1 *Appearance of the wirehaired fox terrier at the time of presentation.* A, B: *Note the generalized dermatitis with pustules, crusts, erosions, and alopecia, on the face (*A*), ear (*B*), and trunk (*C*) at the primary care hospital. The dog's hair was clipped by the primary care veterinarian.*

Thrombocytopenia in dogs is often immune mediated.[16] The pathogenesis of canine immune-mediated thrombocytopenia (IMT) involves platelet surface-associated (PSA) Ig binding, which leads to the increased removal of antibody-coated platelets by macrophages through phagocytosis in the reticuloendothelial system.[16] Canine IMT is difficult to diagnose because it occurs not only primarily without obvious underlying causes, but also secondarily to various systemic diseases including infectious, neoplasias, adverse reactions to drugs (e.g., sulfonamide, cephalosporin, cyclophosphamide, etc.), and systemic autoimmune diseases such as SLE.[16–20] Typically, IMT is diagnosed by excluding other causes of thrombocytopenia, such as disseminated intravascular coagulation and deficient platelet production by bone marrow.[16–20] Kristensen et al. (1994) established a direct assay for measuring PSA-Ig using flow cytometry, which can be used to diagnose canine IMT.[16,17,19] Tsuchiya et al. (2010) recently improved the accuracy of the assay using established artificial positive-control platelets.[21] The authors of this study routinely use this assay when canine IMT is suspected in their hospital.

The purpose of this article is to describe a rare association of PF with concurrent IMT. Diagnosis was made based on histopathological findings, immunohistochemical detection of IgG deposition around keratinocytes, and flow cytometric detection of PSA-Ig.

Case Report

A 3 yr, 10 mo old male wirehaired fox terrier was presented to his primary care veterinarian with pruritus and generalized dermatitis. The owner noticed that the dog's skin lesions had worsen 6 days before presentation. At the time of examination, the dog was pyrexic (39.7°C) and the skin lesions were bilateral, symmetrical, and manifested as pustules, crusting, and erosions. The pustules initially appeared on the ventral trunk, in the ear canal, and on the pinnae. Multifocal crusting and erosion then progressed over the entire body to cover the nasal planum, top of the head, muzzle, dorsal and ventral trunk, feet, and paw pads over the next 18 days (**Figures 1A, B, and C**). Prior to referral, commercially-available rapid drug sensitivity testing (Monoris Inc., Tokyo, Japan) was performed without bacterial identification from swabs collected from underneath a crust on the ventral trunk. Although the crusting dermatitis did not respond to a systemic antibiotic (cephalexin[a], 25 mg/kg per os [PO] *q* 12 h) selected by the drug sensitivity test, the fever was reduced with a single dose of diclofenac sodium[b] (1.25 mg PO). Because leukocytosis, anemia, and thrombocytopenia were diagnosed after the administration of cephalexin and diclofenac sodium, the dog was referred to the study authors' hospital for further examination, diagnosis, and treatment.

Twelve days after the initial presentation at the primary care hospital (day 1), the dog had lost 10% of its body weight (new body weight was 9 kg). Body temperature, pulse, and respiratory rates were 37.9°C, 120 beats/min, and 25 breaths/min, respectively. A physical examination revealed lameness; swelling of all limbs in the synovial joints of the carpus, stifle, and hock; conjunctivitis; and peripheral lymphadenopathies on the superficial cervical and popliteal lymph nodes. A grade 2/6 systolic heart murmur, loudest over the left thorax, was audible during cardiac auscultation. The skin showed generalized erythema, pustules, crusting, and erosions.

Those lesions were distributed symmetrically on the dog's face (including the muzzle, nasal planum from the top of the muzzle to the front of the glabella, the periocular region, ear canal and pinnae), ventral and dorsal trunk, feet, and paw pads. The oral mucosa and mucocutaneous junctions, such as the eyelids and anus, were free of lesions. Impression smears were obtained from the erosive skin lesions under the crusting. Cytology findings showed eosinophilic, pyogranulomatous inflammation comprising numerous degenerate and nondegenerate neutrophils, many eosinophils and macrophages, and a few small lymphocytes. A few oval and intensely basophilic acantholytic keratinocytes with a centrally placed nucleus were individually surrounded by abundant neutrophils. Infectious organisms such as bacteria and *Malassezia* spp. were unremarkable in smears. Swabs collected from pustules in the axillary area were examined for bacterial and fungal cultures at Hoken Kagaku Laboratory (Kanagawa, Japan) using sheep blood agar and Sabouraud agar, respectively. Sarcoptic mange and *Demodex canis* were not detected in skin scrapings or plucked hairs.

Considering the diagnosis of hematologic abnormalities by the primary care veterinarian and based on the physical exam findings conducted at the authors' hospital, immunologic tests, diagnostic imaging, arthrocentesis, fine-needle aspiration of lymph nodes, skin biopsy, and a histopathological examination were performed.

Table 1 shows the hematologic and serum biochemical findings. Complete blood cell counts showed a slightly elevated white blood cell count (1.76×10^9/L; reference range, 0.6–1.7 10^9/L), a low red blood cell count (4.3×10^{12}/L; reference range, 5.5–8.5 10^{12}/L), a packed cell volume of 0.29 (reference range, 0.37–0.55), and a remarkably low platelet count (PLT; 70×10^9/L; reference range, 200–500 10^9/L). The ratio and cell counts of reticulocytes were 0.0032 proportion of red blood cells and 13.76×10^9/L, respectively (the range of reticulocyte counts in regenerative response to mild anemia (a packed cell volume of 0.26–0.38) are $100–150 \times 10^9$/L). A slightly low serum iron concentration (16.11 μmol/L; reference range, 16.83–21.84 μmol/L) and low unsaturated iron binding capacity (6.80 μmol/L, reference range; 22.73–60.86 μmol/L) indicated that chronic inflammation caused the mild nonregenerative anemia. Blood coagulation tests showed an elevated plasma fibrinogen (13.35 μmol/L; reference range, 2.59–9.88 μmol/L), a normal prothrombin time (8.1 s; reference range, 6.8–8.6 s), a slightly prolonged activated partial prothrombin time (28.1 s; reference range, 13.1–26.9 s), and a normal fibrinogen-fibrin degradation product (<2.5 mg/L; reference range, 0–2.5 mg/L). The blood coagulation test results excluded disseminated intravascular coagulation. The serum biochemical analysis showed moderately low total protein (47 g/L; reference range, 51–77 g/L) and albumin (18 g/L; reference range, 25–40 g/L) with high alkaline phosphatase (68.17 μkat/L; reference range, 0.6–4.33 μkat/L), and bilirubin (16.93 μmol/L; reference range, <5.13 μmol/L). C-reactive protein (CRP) was measured using a laser nephelometric immunoassay[c] to evaluate the degree of systemic inflammation. Examination of globulin protein fraction by serum protein electrophoresis was performed because hypoalbuminemia was observed. CRP was obviously elevated at 114.29 nmol/L (reference, <9.52 nmol/L) and serum protein electrophoresis revealed elevated α_2-globulin level.[22]

TABLE 1

Complete Blood Cell Count and Serum Biochemical Profile Results at the Time of Initial Presentation

Variable	Value	Reference range
WBC ($\times 10^9$/L)	1.76	(0.6–1.7)
Red blood cell count ($\times 10^{12}$/L)	4.3	(5.5–8.5)
Hemoglobin (g/L)	96	(120–180)
Packed cell volume	0.29	(0.37–0.55)
Mean corpuscular volume (fL)	67	(66–77)
Mean corpuscular hemoglobin (pg/cell)	22.3	(19.9–24.5)
Mean corpuscular hemoglobin concentration (g/L)	333	(320–360)
Platelet count ($\times 10^9$/L)	70	(200–500)
Total protein (g/L)	47	(51–77)
Albumin (g/L)	18	(25–40)
Blood urea nitrogen (mmol/L)	7.43	(3.28–10.42)
Creatinine (μmol/L)	35.36	(44.2–132.6)
Phosphorus (mmol/L)	1.39	(0.71–1.78)
Calcium, total (mmol/L)	2.2	(2.15–2.85)
Alanine aminotransferase (μkat/L)	0.25	(0.3–1.19)
Alkaline phosphatase (μkat/L)	68.17	(0.6–4.33)
Total cholesterol (mmol/L)	5.26	(2.77–8.13)
Triglycerides (mmol/L)	1.34	(0.19–1.15)
Total bilirubin (μmol/L)	16.93	(0.0–5.13)
Glucose (mmol/L)	4.11	(3.83–6.77)
Sodium (mmol/L)	152.4	(142–152)
Potassium (mmol/L)	4.48	(3.7–5.3)
Chloride (mmol/L)	118.6	(105–117)

To determine the cause of the hypoalbuminemia, diagnostic imaging was performed, focusing on possible renal and hepatic abnormalities. Thoracic and abdominal radiography revealed no apparent abnormalities. An abdominal ultrasound showed hepatic venous congestion and mild hyperechogenicity of the liver parenchyma and renal cortex. The dog underwent a cardiac work-up to determine the cause of its heart murmur and hepatic venous congestion. Echocardiography revealed mild pulmonary

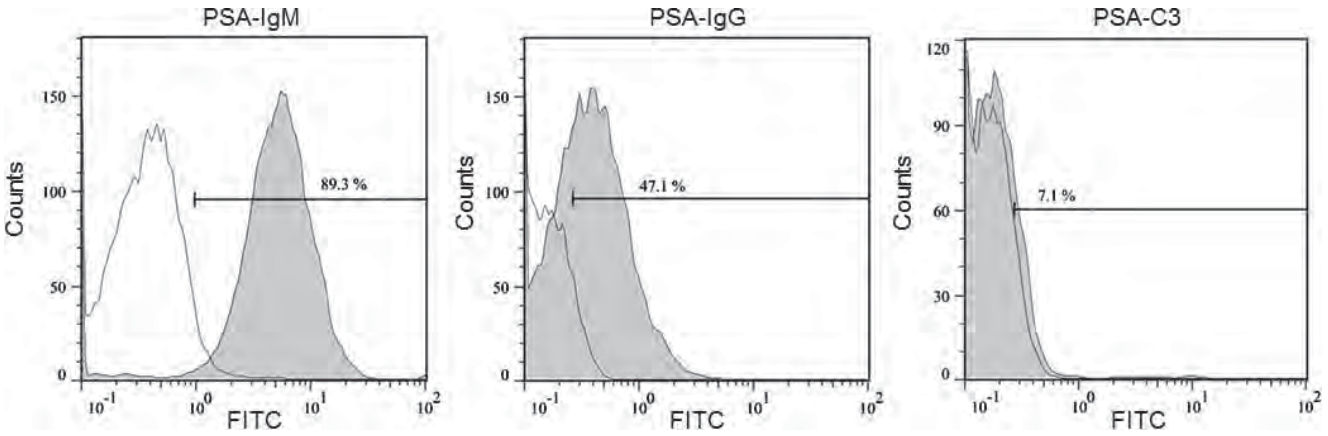

FIGURE 2 *Flow cytometric analysis of platelet surface-associated (PSA) immunoglobulin (Ig) M, -IgG, and complement 3 (-C3). Platelets from sick (*filled curve*) and healthy control (*open curve*) dogs stained with anti-canine IgM, IgG, and C3 antibodies conjugated with fluorescein isothiocyanate. Numbers in the graphs indicate binding percentage (%) of PSA-IgM, -IgG, and -C3 on platelets obtained from sick dog. Reference lines for PSA-IgM, -IgG, and -C3 positive platelets from healthy control are set at 5%.*

hypertension on the basis of increased tricuspid regurgitation velocity (3.41 m/s, reference range <3.0 m/s; estimated pressure gradient across the tricuspid valve, 46 mm Hg). The dog's systolic blood pressure was 120 mmHg, which was considered normal for dogs. Urinalysis revealed a specific gravity of 1.045, a protein content of 1.8 g/L, and a protein/creatinine ratio of 1.5, indicated mild proteinurea (reference ranges, 1.020–1.050, <0.5 g/L, and <0.5, respectively). The findings of proteinurea and a hyperechoic renal cortex indicated protein-losing nephropathy. The leakage of antithrombin III from the kidneys is considered a possible cause of pulmonary thromboembolism, which leads to pulmonary hypertension; however, further work-up was not performed.

To exclude lymphoma, a fine-needle aspirate of the lymph nodes was obtained, which showed mild-to-moderate reactive lymphoid hyperplasia with mild neutrophilic infiltration. the authors performed arthrocentesis because idiopathic polyarthritis was suspected on the basis of the history of fever, physical findings of lameness, and increased serum CRP level. A gross examination of joint fluid showed turbidity and decreased viscosity. A cytologic examination identified low-to-moderate cellularity and mild inflammation consisting of large mononuclear cells (94%), small mononuclear cells (5%), and neutrophils (1%). Those findings were consistent with polyarthropathy associated with chronic inflammation.

At that point, a mild anemia, polyarthropathy (possibly due to chronic inflammation), thrombocytopenia, hypoalbuminemia (probably due to protein-losing nephropathy), and pulmonary hypertension were identified. Based on those findings, the authors' differential diagnoses included PF, pemphigus erythematous, panepidermal pustular pemphigus, cutaneous lymphoma, erythema multiforme, cutaneous vasculitis, IMT, and SLE. An additional skin biopsy and immunologic tests were conducted to reach a definitive diagnosis.

A commercial laboratory (Monoris Inc, Tokyo, Japan) performed a direct Coombs' test and measured serum antinuclear antibodies and rheumatoid factor (RF) to determine the presence of SLE. The direct Coombs' test (37°C and 4°C) and antinuclear antibodies were negative, but RF was positive (titer was 320; reference value; 0). Nine days after the initial presentation, flow cytometry for PSA-IgM, -IgG, and -C3 was performed as described by Tsuchiya et al (2010) for the diagnosis of canine IMT.[21] The gates for positive events were set based on healthy control samples at 0–5%. Values >10% were judged positive. The results showed apparently positive anti-canine IgM (89.3%) and anti-canine IgG (47.1%) antibodies, but negative anti-canine C3 (7%) antibody compared with the healthy control (**Figure 2**).

Skin biopsies obtained using a 4 mm biopsy punch from the crusting skin lesions on the dog's head, neck, and dorsal trunk were examined by routine histopathology. Those findings revealed severe crusting of the superficial epidermis and large intraepidermal to subcorneal pustules (**Figure 3A**) that mainly comprised neutrophils and eosinophils, and some included acantholytic keratinocytes (**Figure 3B**). The pustules involved the hair follicles and extended into the follicular infundibula. Neutrophilic and eosinophilic inflammation was seen in the pustules. Primarily neutrophils and then mononuclear cells infiltrated the superficial-to-middle dermis. Direct IF using anti-canine IgG antibodies[d] (1:800) identified IgG deposition throughout the superficial-to-middle epidermis layer, particularly in the stratum spinosum (**Figure 3C**). Canine PF and

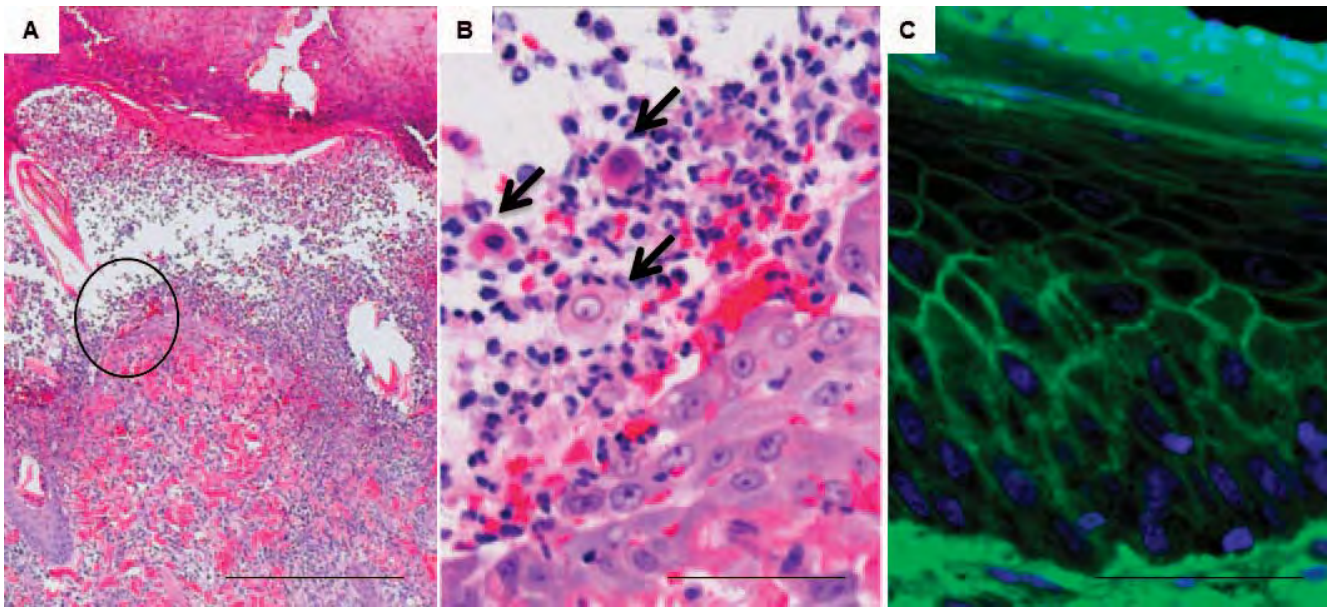

FIGURE 3 A: *Histopathological features of the superficial pustules.* B: *High-power magnification of the area circled in* A. *The pustules are comprised of neutrophils with some acantholytic keratinocytes (*arrows*).* C: *Direct immunofluorescence shows immunoglobulin G deposition from the superficial to middle epidermal layers, especially the stratum spinosum. Hematoxylin and eosin stainining (*A *and* B*) and Immunofluorescence staining with anti-dog IgG (*green*) and antinuclear stain, DAPI (*blue*) (*C*). Bar = 400 μm (*A*), 100 μm (*B*), and 100 μm (*C*).*

IMT were diagnosed based on those histopathological and immunologic findings.

The dog was hospitalized for 7 days and received fluid therapy with acetate Ringer's solution (3 mL/kg/hr) supplemented with low molecular weight heparin (dalteparin sodium[e], 75 U/kg/day) and monoammonium glycyrrhizinate[f] (1 mg/kg intravenous injection [IV] *q* 12 hr). Cefazolin sodium hydrate[g] (25 mg/kg IV *q* 8 hr) and enrofloxacin[h] (5 mg/kg BW *q* 24 hr) were administered to prevent bacterial growth, and ursodeoxycholic acid[i] (10 mg/kg PO *q* 12 hr) was administered as liver function support. Hand-mixed topical corticosteroid (0.12% betamethasone valerate[j] and 0.3% heparinoid[k]) and 0.5% vitamin A oil[l] was applied to reduce the inflammation and as a moisturizer. After cutaneous lymphoma had been excluded by frozen-section histopathology by day 3 from the first presentation at the authors' institution, cyclosporine[m] (5.5 mg/kg PO *q* 24 hr) was started. A bacterial culture and sensitivity tests were performed on day 7. *Escherichia coli* and *Staphylococcus* spp. with methicillin resistance (i.e., penicillin, oxacillin, cephalexin, cefazolin, imipenem, lincomycin, enrofloxacin, minocycline, gentamicin, and sulfamethoxazole-trimethoprim) were isolated on the basis of the Clinical Laboratory Standard Institute guidelines.[23] Based on the culture, the previously prescribed antibiotics were substituted with fosfomycin calcium hydrate[n] (25 mg/kg PO *q* 12 hr). The results of fungal cultures were negative on day 17.

Follow-up examination on day 22 after initial therapy revealed a 50% improvement in the skin lesions. The physical findings, PLT (359×10^9/L), and CRP (46.67 nmol/L) were also improved. Because of persistent erythema and pruritus on the skin lesion and hyperthermia (39.8°C), azathioprine[o] (2 mg/kg PO *q* 24 hr) was coadministered with cyclosporine. On day 36, the red blood cell count and packed cell volume had recovered (5.14×10^{12}/L and 0.37, respectively) and CRP had decreased to 11.43 nmol/L. Cyclosporine was discontinued immediately. On day 64, 90% of the skin lesions were improved and were completely resolved by day 120 (**Figure 4**). The dog's physical condition and complete blood cell count had also improved. The azathioprine dosage was gradually tapered to 0.8 mg/kg PO *q* 48 hr. On day 309 from the time of referral, PSA-IgM, -IgG, and -C3 were re-evaluated by flow cytometry. The results were negative for IgM (7%), IgG (5.1%), and C3 (3.6%). The skin symptoms were controlled by azathioprine monotherapy until day 785.

Discussion

To the author's knowledge, this is the first report to describe a dog definitively diagnosed with concurrent PF and IMT. Some forms of immune-mediated skin disease have been considered as possible causes of IMT and an epidemiological survey by Grindem et al. (1991) found that IMT in pemphigus complex is very rare.[16,18] The

FIGURE 4 *Appearance of the wirehaired terrier following treatment with azathioprine 120 days after initially being presented to the authors' hospital.*

following forms of histological types of pemphigus are recognized in dogs and cats: PF, pemphigus erythematosus, panepidermal pustular pemphigus, pemphigus vulgaris, and paraneoplastic pemphigus.[1–9] The most common form of pemphigus complex is PF, of which symptoms are commonly less severe than in other forms, such as pemphigus vulgaris.[1–4] Although Grindem et al. (1991) did not specify the forms of pemphigus, recent retrospective studies have not reported those diseases to occur simultaneously.[7,8,19,20] Therefore, the presence of PF and IMT seems to be rare.

The present findings of PSA-Ig analysis reflect immunological signs of canine PF in addition to known physiological and hematological abnormalities. In canine PF, symptoms are generally localized to the skin. Although systemic symptoms, including anorexia, depression, fever, and weight loss are rare, they become obvious when erosive skin lesions progress over the entire body.[3] Various hematologic abnormalities, such as moderate to severe leukocytosis and neutrophilia, mild nonregenerative anemia, thrombocytopenia, mildly to moderately elevated α_2-, β_2-, and γ-globulins, and mild hypoalbuminemia have also been reported.[7,8,14,15] Those features are usually associated with the severity of skin symptoms; however, the results of routine blood tests, diagnostic imaging, and urinalysis have received relatively little focus because they are not considered to support a specific diagnosis.[3] Focusing on thrombocytopenia among systemic symptoms, IMT was diagnosed on the basis of PSA-Ig levels measured using flow cytometry. Therefore, if dogs with PF have obvious systemic signs, systemic work-ups and immunological tests should be conducted to identify complicating factors and associated diseases.

A diagnosis of canine IMT is difficult because it is usually only concluded by excluding other potential causes of thrombocytopenia.[16–20] Dogs with IMT develop an increased risk of spontaneous hemorrhage when PLT fall below $10–30 \times 10^9$/L, whereas O'Marra et al. (2011) reported that signs of bleeding were absent in 19% of 73 dogs showing platelet counts $<50 \times 10^9$/L.[16–20,24] Those asymptomatic dogs with moderate thrombocytopenia are not thoroughly evaluated in routine clinical practice because an invasive bone marrow examination is needed to exclude nonimmune-mediated thrombocytopenia. The authors of the current study diagnosed IMT in a dog by measuring PSA-Ig using flow cytometry at the time of the initial presentation at their hospital. Furthermore, the positive PSA-IgM and -IgG findings became negative when the thrombocytopenia was improved by immunosuppressive therapy with azathioprine. The study authors thus considered that the PSA-Ig level correlated with disease status and was useful for the diagnosis and evaluation of treatment in dogs with IMT.

Vaughan et al. (2010) reported that complicated cases of canine PF concurrent with allergic skin disease and other systemic diseases are significantly associated with the presence of eosinophil infiltration in intraepidermal pustules.[8] In the present case, eosinophil infiltration was detected in the pustules, and the dog presented with pruritus at onset and a history of recurrent pyoderma. Concurrent IMT was also diagnosed. Those finding are consistent with those of Vaughan et al. (2010).[8] One case, positive for eosinophil infiltration, was provisionally diagnosed with drug hypersensitivity against ampicillin, amoxicillin, enrofloxacin, and metronidazole.[8] Because PF and IMT, as observed in the present case, are clinical symptoms in drug hypersensitivity, it was possible that those symptoms persisted at the initial presentation to the authors' hospital.[2,6,8,16] If canine PF is accompanied with eosinophilic infiltration, it may be necessary to examine underlying diseases.

Skin lesions had been evident in the case described herein since the first examination at the primary care veterinary hospital. However, the PLT (194×10^9/L; reference range, $200–500 \times 10^9$/L) at that time were essentially normal and gradually decreased thereafter. The possible causes of secondary IMT include infectious diseases, neoplasia, adverse reactions to drugs, and systemic autoimmune diseases such as SLE. In the current case, PF and adverse drug reaction were considered as the possible etiologies. IMT may also arise in association with circulating antikeratinocyte autoantibodies.[3] Secondary IMT develops following SLE in some dogs, suggesting that immune complexes bound to platelets by complement-mediated immune adherence or nonspecific interactions cause IMT concurrent with SLE.[16] The current case had IgG antibodies on the epidermis, had IgM and IgG antibodies on the platelet-cell surface, and was RF positive. Those findings indicate

that in this case, PF may have been the cause of hematologic immune-mediated diseases such as IMT. The other possible cause of IMT was an adverse drug reaction. Prior to referral, IMT occurred after administration of cephalexin, which is a known cause of secondary IMT. In the present case, cefazolin sodium hydrate, which belongs to the same drug class as cephalexin, had been administered IV for 3 days before administration of cyclosporine. Because the symptoms did not worsen after cefazolin administration without any immunosuppressant drug, the possibility of an adverse drug reaction was considered low. Epidemiological studies are warranted to determine the prevalence and association of IMT with PF in dogs.

Conclusion

Canine PF is autoimmune pustular disease with symptoms that are generally localized to the skin. Although a low incidence of thrombocytopenia associated with pemphigus complex is reported, the study authors confirmed the diagnosis of concurrent PF and IMT based on histology findings, direct IF, and the presence of PSA-Ig. The dermatologic and hematologic signs were treated with immunosuppressive therapy using cyclosporine and azathioprine, and the dog has survived for >2 yr since the day of first presentation at the authors' animal hospital. Positive findings for PSA-IgM and IgG became negative when thrombocytopenia was improved after immunosuppressive therapy. Those findings indicate that IMT can develop with canine PF; thus, systemic evaluation should include precise hematologic assessment.

The authors would like to thank Dr. Takao Otsuki (Heiwa Animal Hospital, Japan) for referring patients, Dr. Yoko Kakinuma for the technical assistance with the histological sections, Dr. Ryoji Takahashi and Dr. Shinsuke Fujimoto for supporting patient care at the clinic, and Jonathan Bloch for proofreading the manuscript. The authors declare that there are no conflicts of interest associated with the present report. This study was supported by the Grant-in-Aid for Matching Fund Subsidy for Private University and by the Science Research Promotion Fund of The Mutual Aid Corporation for Private Schools of Japan.

FOOTNOTES

[a] Larixin; Toyama chemical, Tokyo, Japan

[b] Voltaren; Novartis Pharma, Tokyo, Japan

[c] Canine CRP measurement system CRP-2; Arrows Co. Ltd, Osaka, Japan

[d] Fluorescein-conjugated goat affinity purified antibody to dog IgG (whole molecule); MP bio Japan K.K., Tokyo, Japan

[e] Hepagumin α; Sawai Pharma, Osaka, Japan

[f] Stronger neo-minophagen C, Eisai, Tokyo, Japan

[g] Cefamezin α; Astellas, Tokyo, Japan

[h] Baytril; Bayer Health Care, Tokyo, Japan

[i] URSO; Mitsubishi Tanabe Pharma Co., Osaka, Japan

[j] Rinderon-V Ointment; Shionogi Co. Ltd., Osaka, Japan

[k] Hirudoid Soft Ointment; Maruho, Osaka, Japan

[l] Sahne Oint; Eisai, Tokyo, Japan

[m] Atopica; Novartis Animal Health, Tokyo, Japan

[n] FOSMICIN; Meiji Seika Pharma Co. Ltd., Tokyo, Japan

[o] Imuran, GlaxoSmithKline, Tokyo, Japan

REFERENCES

1. Werner LL, Brown KA, Halliwell RE. Diagnosis of autoimmune skin disease in the dog: correlation between histopathologic, direct immunofluorescent and clinical findings. *Vet Immunol Immunopathol* 1983;5(1):47–64.
2. Scott DW, Miller WH, Griffin CE, eds. Immune-Mediated Disorders. In: Miller and Kirk's Small Animal Dermatology. 6th ed. Philadelphia (PA): WB Saunders; 2001:667–779.
3. Olivry T. A review of autoimmune skin diseases in domestic animals: I - superficial pemphigus. *Vet Dermatol* 2006;17(5):291–305.
4. Scott DW, Lewis RM. Pemphigus and pemphigoid in dog and man: comparative aspects. *J Am Acad Dermatol* 1981;5(2):148–67.
5. Gross TL, Ihrke PJ, Walder EJ, Affolter VK, eds. Pustular diseases of the epidermis. In: *Skin diseases of the dog and cat: clinical and histopathologic diagnosis*. 2nd ed. Oxford (UK): Blackwell Publishing; 2005:4–26.
6. Rosenkrantz WS. Pemphigus: current therapy. *Vet Dermatol* 2004;15(2):90–8.
7. Mueller RS, Krebs I, Power HT, et al. Pemphigus foliaceus in 91 dogs. *J Am Anim Hosp Assoc* 2006;42(3):189–96.
8. Vaughan DF, Clay Hodgin E, Hosgood GL, et al. Clinical and histopathological features of pemphigus foliaceus with and without eosinophilic infiltrates: a retrospective evaluation of 40 dogs. *Vet Dermatol* 2010;21(2):166–74.
9. Olivry T, Linder KE. Dermatoses affecting desmosomes in animals: a mechanistic review of acantholytic blistering skin diseases. *Vet Dermatol* 2009;20(5–6):313–26.
10. Olivry T, Dunston SM, Walker RH, et al. Investigations on the nature and pathogenicity of circulating antikeratinocyte antibodies in dogs with pemphigus foliaceus. *Vet Dermatol* 2009;20(1):42–50.
11. Bizikova P, Linder KE, Olivry T. Immunomapping of desmosomal and nondesmosomal adhesion molecules in healthy canine footpad, haired skin and buccal mucosal epithelia: comparison with canine pemphigus foliaceus serum immunoglobulin G staining patterns. *Vet Dermatol* 2011;22(2):132–42.
12. Bizikova P, Dean GA, Hashimoto T, Olivry T. Cloning and establishment of canine desmocollin-1 as a major autoantigen in canine pemphigus foliaceus. *Vet Immunol Immunopathol* 2012. In press.
13. Ginel PJ, Mozos E, Fernandez A, et al. Canine pemphigus foliaceus associated with leishmaniasis. *Vet Rec* 1993;133(21):526–7.
14. Foster AP, Sturgess CP, Gould DJ, et al. Pemphigus foliaceus in association with systemic lupus erythematosus, and subsequent lymphoma in a cocker spaniel. *J Small Anim Pract* 2000;41(6):266–70.
15. Werner LL, Bloomberg MS, Calderwood et al. Progressive polysystemic immune-mediated disease in a dog. *Vet Immunol Immunopathol* 1985;8(1–2):183–92.
16. Scott MA, Jutkowitz LA. Immune-Mediated Thrombocytopenia. In: *Veterinary Hematology*. 6th ed. Philadelphia (PA): WB Saunders; 2011:586–604.

17. Kristensen AT, Weiss DJ, Klausner JS, Laber J, Christie DJ. Comparison of microscopic and flow cytometric detection of platelet antibody in dogs suspected of having immune-mediated thrombocytopenia. *Am J Vet Res* 1994;55(8):1111–4.
18. Grindem CB, Breitschwerdt EB, Corbett WT, Jans HE. Epidemiologic survey of thrombocytopenia in dogs: a report on 987 cases. *Vet Clin Pathol* 1991;20(2):38–43.
19. Dircks BH, Schuberth HJ, Mischke R. Underlying diseases and clinicopathologic variables of thrombocytopenic dogs with and without platelet-bound antibodies detected by use of a flow cytometric assay: 83 cases (2004–2006). *J Am Vet Med Assoc* 2009;235(8):960–6.
20. Botsch V, Küchenhoff H, Hartmann K, Hirschberger J. Retrospective study of 871 dogs with thrombocytopenia. *Vet Rec* 2009;164(21):647–51.
21. Tsuchiya R, Komatsu T, Ishikawa T, et al. Preparation of positive control platelets for detection of canine platelet surface-associated IgG, IgM and complement (C3) by flow cytometry. *J Vet Med Sci* 2010;72(8):1063–6.
22. Onishi T, Inokuma H, Ohno K, et al. C-reactive protein concentration in normal and diseased dogs measured by laser nephelometric immunoassay. *J Jpn Vet Med Assoc* 2000;53:595–601 [in Japanese].
23. Clinical Laboratory Standards Institute. Performance standards for antimicrobial susceptibility testing; seventeenth informational supplement. In: *CLSI document M100-S17*. Pennsylvania (PA): Clinical and Laboratory Standards Institute; 2007.
24. O'Marra SK, Delaforcade AM, Shaw SP. Treatment and predictors of outcome in dogs with immune-mediated thrombocytopenia. *J Am Vet Med Assoc* 2011;238(3):346–52.

A Case of Cutaneous Sterile Pyogranuloma/ Granuloma Syndrome in a Maltese

Shinpei Kawarai, PhD, DVM, Shinobu Matsuura, PhD, DVM, Saburo Yamamoto, PhD, Akio Kiuchi, PhD, DVM, Nobuyuki Kanemaki, PhD, DVM, DAiCVO, Hiroo Madarame, PhD, DVM, DJCVP, Kinji Shirota, PhD, DVM, DJCVP

ABSTRACT

Cutaneous sterile pyogranuloma/granuloma syndrome (SPGS) is a locally restricted multinodular dermatitis. Affected dogs are typically healthy, but a few show systemic signs. Herein, a case of a dog presenting with generalized ulcerative dermatitis with systemic signs of mild anemia and an increased C-reactive protein level is described. Cutaneous SPGS was diagnosed by histopathology, negative staining causative organisms, and polymerase chain reaction for *Mycobacterium* spp. Successful treatment was achieved by immunosuppressive drugs, including prednisolone and azathioprine, administered for at least 20 mo. Recurrences of skin lesions were observed when prednisolone and/or azathioprine were discontinued. Long-term management with immunosuppressive agents may be required if the affected dog exhibits severe symptoms of cutaneous SPGS.

(*J Am Anim Hosp Assoc* 2014; 50:278–283. DOI 10.5326/JAAHA-MS-6009)

Introduction

Cutaneous sterile pyogranuloma/granuloma syndrome (SPGS) is a skin disease that is uncommon in dogs and extremely rare in cats.[1–4] In the literature, SPGS is also termed idiopathic periadnexal multinodular granulomatous dermatitis.[2] No age or gender predisposition is reported; however, boxers, golden retrievers, collies, Great Danes, and Weimaraners may be predisposed, and male dogs seem to be affected at a higher frequency.[1–5] Characteristic skin lesions are usually observed on the bridge of the nose, muzzle, periocular region, pinnae, and paws.[1–5] These lesions comprise dermal papules and nodules, which are multiple, well demarcated, firm, painless, and nonpruritic.[1–5] They may become alopecic and ulcerated and may get secondarily infected, particularly on the paws.[1–5] Although systemic signs such as lymphadenopathy and hypercalcemia have been reported in dogs and cats, the affected animals are typically healthy.[1–7]

The diagnosis of cutaneous SPGS is challenging and can be made only after ruling out other granulomatous and pyogranulomatous skin diseases.[1–4] According to Santoro et al. (2008), the etiology of granulomatous and pyogranulomatous skin diseases can be divided into two major groups. The first group is infectious diseases caused by protozoans, mycobacteria, pathologic dimorphic fungi, etc. and noninfectious diseases with a known etiology such as a foreign body, hair, sebum, etc. The second group includes unknown etiologies, such as idiopathic "sterile" dermatitis.[4] Histopathologically, those criteria were also based on visible infectious and known etiological agents and etiologic agents not detectable by analytical methods and possible immune-mediated (idiopathic) mechanisms. Some organisms such as *Mycobacterium* spp. and *Leishmania* spp. are not easily detected by histopathology; therefore, polymerase chain reaction (PCR) analysis is required.[4,7,8] A diagnosis of cutaneous SPGS can be made after

From the Veterinary Teaching Hospital Laboratory of Small Animal Clinics (S.K., N.K., H.M.), Department of Veterinary Medicine Laboratory of Veterinary Pathology (K.S.), and Laboratory of Microbiology I (A.K.), Azabu University, Sagamihara, Kanagawa, Japan; Whitaker Cardiovascular Institute, Boston University School of Medicine, Boston, MA (S.M.); and Central Laboratory, Japan BCG Laboratory, Kiyose, Tokyo, Japan (S.Y.).

Correspondence: kawarai@azabu-u.ac.jp (S.K.)

CRP, C-reactive protein; Ig, immunoglobulin; PCR, polymerase chain reaction; PO, *per os*; SPGS, sterile pyogranuloma/granuloma syndrome

ruling out noninfectious granulomas of unknown etiologies, such as reactive histiocytosis, juvenile sterile granulomatous dermatitis and lymphadenitis, cutaneous xanthoma, and canine sarcoidosis.[1–4]

Herein, the successful long-term treatment of a dog presenting with cutaneous SPGS characterized by generalized ulcerative dermatitis, systemic signs of mild anemia, and an increased C-reactive protein (CRP) level is described. Cutaneous SPGS was diagnosed by histopathology, negative staining, and PCR for *Mycobacterium* spp.

Case Report

An indoor 3 yr old castrated male Maltese weighing 4.2 kg was referred to the Veterinary Teaching Hospital, Azabu University, with generalized ulcerative dermatitis. Initially, the skin lesions occurred on the dog's head, identified by mild scales. The lesions progressed to crusting and multifocal ulcers, which spread to the head, dorsal and ventral trunk, and limbs over a period of 8 mo. Prior to being referred, the dog was administered systemic antibacterial and antifungal drugs [30 mg/kg cephalexin *per os* (PO) *q* 12 hr and 6 mg/kg ketoconazole PO *q* 12 hr, respectively] for 4 wk; however, the dog was unresponsive. Physical and dermatological examinations, bacterial culture with antimicrobial susceptibility testing, fungal culture, blood tests, diagnostic imaging, urinalysis, arthrocentesis, skin biopsy, and histopathological examinations were subsequently performed at the time of referral.

On physical examination, the dog presented with severe pain, mild pruritus of the skin, and a body temperature of 39°C. Bilateral lymphadenopathy of the superficial cervical and popliteal lymph nodes was observed. Skin lesions comprised alopecia and erythema with epidermal detachment and multifocal ulcers with crusting. Although haired skin on the top of the muzzle remained, demarcated alopecic skin lesions were observed on the dog's face, including the periocular, periauricular regions, and the planum nasale from the top of the muzzle to the head. Other affected areas were the dorsal trunk, extending from the neck to the front of the tail; the ventral trunk extending from the anterior chest; and the axilla to the inguinal region, limbs, paws, and perianal region (**Figure 1**). Impression smears were obtained from the ulcerative skin lesions of the dorsal and ventral regions and stained by the Wright's-Giemsa method. Cytology revealed a pyogranulomatous inflammation comprising macrophages and nondegenerate neutrophils; however, acantholytic keratinocytes, bacteria such as cocci and bacilli, and *Malassezia* spp. were not apparent. Infection with *Demodex canis* was ruled out by skin scraping and hair plucking, and sarcoptic mange was ruled out by only mild pruritus of the skin.

Hematologic analysis revealed results within reference ranges, except for a slight decrease in the red blood cell count (3.92×10^{12}/L; reference range, 5.5–8.5 $\times$ 10^{12}/L) and packed cell volume (0.31%; reference range,) and a remarkable increase in CRP level (142.86 nmol/L; reference range 0.37–0.55, $<$ 9.52 nmol/L) as described in **Table 1**. After severe inflammation was suspected in the dog, CRP level was monitored using a laser nephelometric immunoassay system[a] for dogs.[9] Serum protein electrophoresis revealed an increased α_2-globulin fraction level, but did not indicate gammopathy.

Differential diagnoses from the findings at the first visit were both aerobic and anaerobic bacteria, including *Nocardia* and *Actinomyces* spp.; deep and intermediate fungi; dermatophytosis; pemphigus foliaceus; pemphigus vulgaris; erythematosus paraneoplastic pemphigus; discoid lupus erythematosus; systemic lupus erythematosus; cutaneous lymphoma; erythema multiforme; cutaneous vasculitis; toxic epidermal necrolysis; hepatocutaneous syndrome; and idiopathic ulcerative dermatosis.

Antimicrobial susceptibility testing was conducted at Hoken Kagaku Laboratory (Kanagawa, Japan) using the Clinical Laboratory Standards Institute method. Aerobic bacterial culture from a swab of a dorsal ulcerative skin lesion using sheep blood agar was negative. Although the association of anaerobic bacteria could not be ruled out, anaerobic culture was not performed because the ulcerative lesion was aerobically exposed on the superficial epidermis. Fungal culture performed and analyzed at Hoken Kagaku Laboratory from the same skin lesion was negative. Sabouraud agar, which is used for detection of dermatophytes, yeast-like organisms, and *Cryptococcus* spp., was used for the culture. Because specific bacterial and fungal features were not identified by the impression smears, macerated tissue culture and specialized culture were not performed.

Thoracic and abdominal radiographs and ultrasonography did not reveal any apparent abnormalities. Dermatoses associated with systemic diseases such as paraneoplastic pemphigus and hepatocutaneous syndrome was ruled out because none of findings indicated either a tumor mass or a remarkable abnormality of the liver parenchyma. To examine the possibility of systemic lupus erythematosus, urinalysis (Table 1), and arthrocentesis of synovial fluid from the left knee joint were performed. Urine test strips were positive for protein (2+) and negative to occasionally positive leukocytes, nitrate, urobilinogen, blood, ketones, bilirubin, and glucose. Zero to occasional red blood cells, white blood cells, and transitional cells were seen, but no crystals or casts were detected by urinary sediment examination. The synovial fluid was clear, colorless, and extremely viscous. Cytology revealed a few large and small mononuclear inflammatory cells, which was not suggestive of arthropathy.

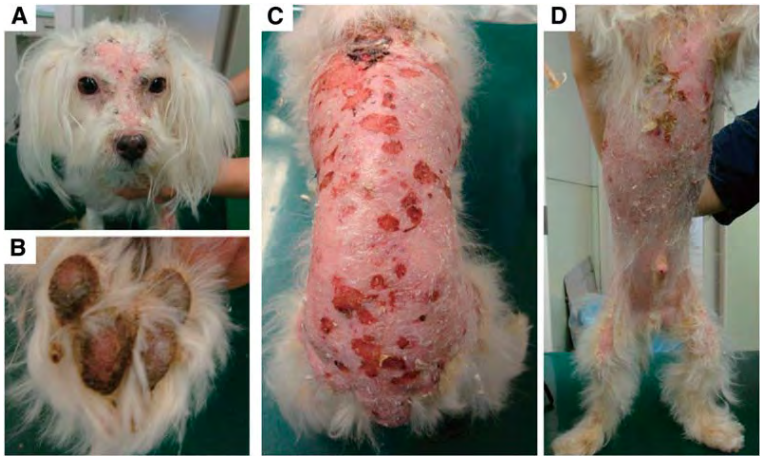

FIGURE 1 *Photographs of the dog's head (*A*), right paw (*B*), dorsal region (*C*), and ventral region (*D*) on day 1 showing alopecia and erythematous dermatitis with ulcerative plaques.*

Specimens were collected using a 4 mm punch biopsy from skin lesions on the dog's head and dorsal trunk. Histopathology revealed a nodular to diffuse dermatitis characterized by intense lymphohistiocytic infiltration and fibrosis involving the superficial dermis and subcutis (**Figure 2**). The adnexa, such as the hair follicles and sebaceous glands, were obscured by fibrosis. Deposition of autoantibodies in the tissue was not detected by immunofluorescence using fluorescein isothiocyanate-labeled anti-dog immunoglobulin (Ig) G antibodies[b] (diluted 1:800). Based on the histopathological evaluation, pemphigus foliaceus, pemphigus vulgaris, and systemic and discoid lupus erythematosus, cutaneous lymphoma, erythema multiforme, cutaneous vasculitis, toxic epidermal necrolysis, and idiopathic ulcerative dermatosis were ruled out. Histopathological analysis revealed the presence of nodular granuloma, which suggested a deep pyoderma and fungal infection by an antibiotic-resistant microorganism, atypical mycobacteriosis (canine leproid granuloma syndrome), and cutaneous SPGS. Cutaneous leishmaniasis was ruled out because it is not endogenous to Japan and the dog has never been outside Japan. Periodic acid-Schiff, Ziehl-Neelsen, Grocott's methenamine silver, and gram staining were used, but failed to detect any etiologic agent in the tissue specimens.

Using the primers described by Cornegliani et al. (2005), PCR was performed to detect *Mycobacterium* spp.[8] DNA extraction from paraffin-embedded tissues was conducted using a commercial kit[c]. Five microliters of the extracted DNA solution were used for the nested PCR amplification of a 16S rRNA fragment with a DNA polymerase[d] using a gradient thermal cycler[e]. The external primers (FO16S, 5′-GATAAGCCTGGGAAACTGGGTC-3′; RO16S, 5′-TTCTCCACCTACCGTCAATCCG-3′) were used to amplify a 344-base pair fragment and the internal primers (F116S, 5′-CATGTCTTGTGGTGGAAAGCG-3′; RI16S, 5′-TACCGTC AATCCGAGAGAACCC-3′) were used to amplify a 288-base pair fragment. The first and second PCR amplification consisted of one cycle at 98°C for 3 min, followed by 35 cycles of denaturation (98°C for 30 sec), annealing (65.7°C for 30 sec), and extension (72°C for 30 sec). The PCR products were separated by 2% agarose gel electrophoresis, stained with ethidium bromide, and visualized using an UV transilluminator[f]. DNA was extracted from a BCG vaccine strain[g] and used as a positive control. The PCR results were negative, and mycobacteriosis was ruled out in the present case.

Clinical findings (age of onset and breed), histopathological findings, and diagnostic imaging results ruled out the other noninfectious granulomas of unknown etiologies; therefore, a diagnosis of cutaneous SPGS was considered most suitable for the present case. Consequently, prednisolone[h] (1 mg/kg PO *q* 12 hr) and fosfomycin Ca hydrate[i] (25 mg/kg PO *q* 12 hr) therapy was initiated. In addition, as a supportive therapy, famotidine[j] (1 mg/kg PO *q* 12 hr) and ursodeoxycholic acid[k] (10 mg/kg PO *q* 12 hr) was administered for protection against the adverse effects of prednisolone. The treatment of skin barrier restoration included 0.5% vitamin A oil[l] and a topical corticosteroid preparation comprising 0.12% betamethasone valerate[m] and 0.3% heparinoid[n]. One wk after the initiation of therapy (day 7), the ulcerative dermatitis improved and CRP level decreased (4.76 nmol/L). After 1 mo (28 days), the dog was free of grossly visible ulcerative skin lesions (**Figures 3A–C**) and the packed cell volume increased to 43%. Subsequently, the dose of prednisolone was tapered by 0.5 mg/kg BW at 2 wk intervals and administration of azathioprine[o] (1 mg/kg PO *q* 24 hr) was initiated. After decreasing the dose of prednisolone to 0.5 mg/kg *q* 48 hr (day 82), it was

TABLE 1

Complete Blood Cell Count, Serum Biochemical Profile, and Urinalysis Results on the Day of Referral

Analyte	Value	Reference range
WBC ($\times 10^9$/L)	1.66	(0.6–1.7)
Red blood cell count ($\times 10^{12}$/L)	3.92	(5.5–8.5)
Hemoglobin (g/L)	99	(120–180)
Packed cell volume	0.31	(0.37–0.55)
Mean corpuscular volume (fl)	77.8	(66–77)
Mean corpuscular hemoglobin (pg/cell)	25.3	(19.9–24.5)
Mean corpuscular hemoglobin concentration (g/L)	325	(320–360)
Platelet count ($\times 10^9$/L)	388	(200–500)
Total protein (g/L)	61	(51–77)
Albumin (g/L)	27	(25–40)
Blood urea nitrogen (mmol/L)	18.6	(6.57–20.9)
Creatinine (μmol/L)	26.5	(44.2–132.6)
Phosphorus (mmol/L)	1.2	(0.7–1.8)
Ca, total (mmol/L)	2.4	(2.2–2.9)
Alanine aminotransferase (μkat/L)	0.2	(0.3–1.2)
Alkaline phosphatase (μkat/L)	4.3	(0.6–4.3)
Total cholesterol (mmol/L)	5.1	(2.8–8.1)
Triglycerides (mmol/L)	0.6	(0.2–1.2)
Total bilirubin (μmol/L)	0	(0.0–5.1)
Glucose (mmol/L)	5.7	(3.8–6.8)
Na (mmol/L)	142	(142–152)
Potassium (mmol/L)	4.49	(3.7–5.3)
Chloride (mmol/L)	106.8	(105–117)
Urine specific gravity	1.074	(1.020–1.050)
Urine pH	7.0	(5.5–7.5)
Urine protein/creatinine ratio	0.22	(< 0.5)

further decreased to *q* 72 hr for 2 mo (day 110). Following the cessation of prednisolone on day 138, mild skin lesions with crusting and erosion were observed on the dorsum of the neck on day 166 (**Figures 3D, E**). Those relapses were treated with prednisolone, and the dosage of azathioprine was decreased to 1 mg/kg *q* 48 hr. Maintenance doses of prednisolone (0.5 mg/kg *q* 48 hr) and azathioprine (1 mg/kg *q* 48 hr) were selected on day 197; however, the owner had administered a single dose of prednisolone (0.5 mg/kg) 1–2 times/wk according to the owner's judgment, although the dog received azathioprine as scheduled. At a 3 mo routine follow-up examination (day 278), the dog exhibited mild skin lesions of erythema and crusting on the limbs and dorsal and ventral trunk. A fungal culture using a dermatophyte test agar medium was negative. The owner was reminded to continue prednisolone. The skin symptoms did not become aggravated and remained unchanged for at least 9 mo. However, on day 537 during a routine follow-up examination, the owner

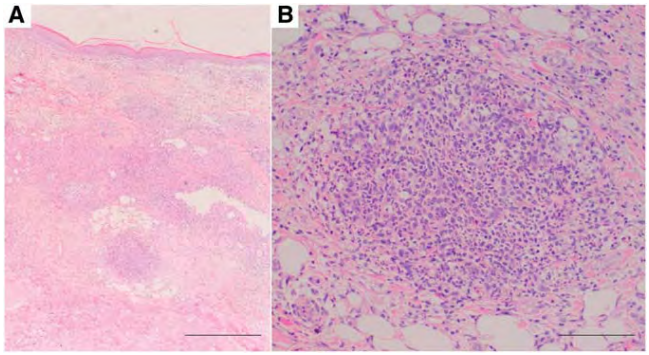

FIGURE 2 A: *Nodular to diffuse dermatitis characterized by intense lymphohistiocytic infiltration and fibrosis throughout the superficial dermis and subcutis.* B: *A nodular lesion mainly comprised of macrophages and neutrophils in the subcutis. Hematoxylin and eosin stain, bar represents 500 μm* (A) *and 100 μm* (B).

reported an apparent recurrence of pruritus and crusting on the dog's face and back within 2 wk after discontinuing prednisolone and azathioprine. The recurrent lesions were treated with prednisolone and azathioprine that were prescribed by the referring veterinarian. No hair regrowth was observed during the course of the treatment (day 624).

Discussion

At the time of referral, the study authors considered a diagnosis of pustular skin disease; however, based on the histopathological findings of granulomatous dermatitis, that diagnosis was changed to granulomatous and pyogranulomatous skin disease. Based on the criteria described by Santoro et al. (2008), a diagnosis of cutaneous SPGS was made.[4]

The etiology and pathogenesis of cutaneous SPGS is unknown.[1–8] The absence of infectious agents and foreign materials together with a good response to systemic glucocorticoids suggested the involvement of immune-mediated mechanisms.[1–7] In the present case, neither causative organisms nor foreign bodies were detected by culture, impression smears, special histopathological staining, or PCR for *Mycobacterium* spp. Because *Leishmania* spp. is not endogenous to Japan, diagnoses were only made for *Mycobacterium* spp.[4,8] Although potentially infectious bacteria, such as antimicrobial-resistant bacteria, anaerobic bacteria, and bacteria requiring special culture methods, were not ruled out, the authors attempted to limit the possibility of infection using fosfomycin. Fosfomycin is a broad-spectrum antibiotic for gram-positive and gram-negative bacteria and is well distributed in tissues with clinically relevant concentrations in the serum, kidneys, bladder wall, prostate, lungs, inflamed tissues, bone, cerebrospinal fluid, abscess fluid, and heart valves.[10] The efficacy of

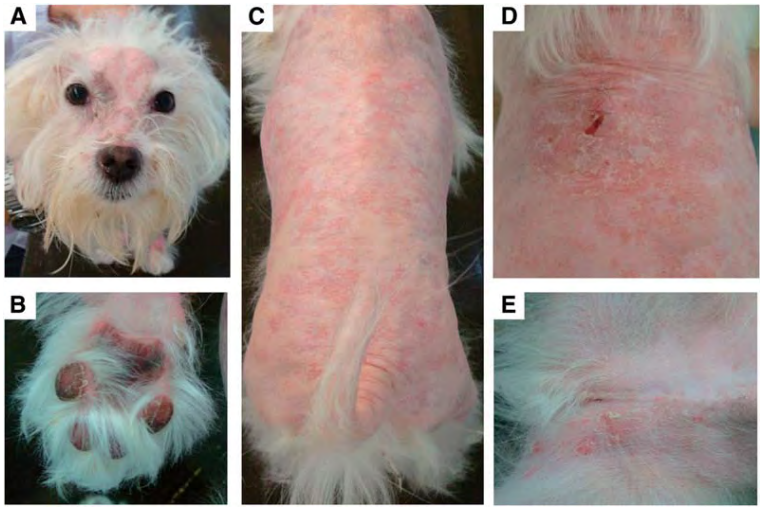

FIGURE 3 *Photographs of the head (*A*), right paw (*B*), dorsal region (*C*), ventral neck (*D*), and ventral abdomen (*E*) indicating that the erythematous dermatitis and ulcerative plaques improved by day 28; however, no hair regrowth was observed (*A, B, and C*). A recurrence of skin lesions was observed on day 166 after discontinuation of prednisolone (*D, E*).*

fosfomycin against cephalexin-resistant *Staphylococcus* spp. isolated from a patient with pyoderma and otitis externa has been reported in Japan.[11] In the present case, systemic inflammation was indicated by fever, an increased CRP level, and lymphadenopathy. The dog was also treated with immunosuppressive drugs, including prednisolone and azathioprine, although recurrences of skin lesions were observed when both drugs were discontinued. Those findings suggested that systemic inflammation, which was treated with prednisolone and azathioprine, was associated with the pathogenesis in the present case.

Hair regrowth was not observed even after successful treatment with prednisolone and azathioprine, possibly due to the presence of extensive fibrosis involving the superficial dermis and subcutis at the site of adnexa. The dermal papilla and the bulge region, where arrector pili muscles insert into hair follicles, are considered to contain stem cells capable of hair and skin regeneration.[12,13] The presence of fibrosis suggested severe inflammation that possibly destroyed the hair follicles and sebaceous glands at the affected sites.

In the present case, lymphohistiocytic infiltrations were observed by histopathology; however, deposition of the IgG antibody was not detected using immunofluorescence. It has been proposed that cutaneous SPGS is associated with immune dysfunction in response to chronic antigenic stimulation.[1] The absence of IgG autoantibodies suggested that the pathogenesis of the diseases was not associated with humoral-mediated immunity (as observed in pemphigus complex) but with cell-mediated immunity, in which effecter cells comprise macrophages and lymphocytes, as observed in the present case. The examination of surface cluster of differentiation antigens and major histocompatibility complex molecules on infiltrated cells could provide clues to elucidate the immune mechanisms involved in cutaneous SPGS.

Conclusion

Cutaneous SPGS is an uncommon skin disease in dogs.[1–4] The affected animals are typically healthy, but a few exhibit systemic signs.[1–7] This report documented a case of SPGS diagnosed by histopathological findings of a nodular to diffuse granulomatous dermatitis with intense lymphohistiocytic infiltration, negative staining for causative organisms, and PCR for *Mycobacterium* spp. The dog presented with generalized ulcerative dermatitis and systemic signs of mild anemia and an increased CRP level. Successful treatment was achieved by administration of immunosuppressive drugs (prednisolone and azathioprine) for at least 20 mo. Recurrence of skin lesions after cessation of prednisolone and/or azathioprine was observed, suggesting that long-term management using immunosuppressive drugs may be required if the dog exhibits severe systemic signs of cutaneous SPGS.

The authors would like to thank Tadayoshi Yamaguchi (Ann Animal Hospital) for providing the initial information, Yoko Kakinuma (Research Institute of Biosciences, Azabu University) for technical assistance with the histologic sections, Takahiro Hamada (Kurume University) for his advice regarding the present case, Dr. Ryoji Takahashi and Dr. Yusuke Matsuura (Veterinary Teaching Hospital, Azabu University) for supporting patient care, and Jonathan Bloch

(Service Employees International Union Training and Education Funds, Renton, WA) for proofreading the manuscript. This report was partially supported by a project grant (Young Scientist Research Training Award, 2010 and 2011) funded by the Azabu University Research Service Division and Grant-in-Aid for Young Scientists (B) by the Japan Society for the Promotion of Science (23780330). The authors declare that there are no conflicts of interest associated with the present report.

FOOTNOTES

[a] Canine CRP measurement system CRP-2; Arrows Co. Ltd., Osaka, Japan

[b] Fluorescein-conjugated goat affinity purified antibody to dog IgG (whole molecule); MP Bio Japan K.K., Tokyo, Japan

[c] DEXPAT; Takara Bio Inc., Siga, Japan

[d] MightyAmp DNA Polymerase Ver. 2; Takara Bio Inc., Siga, Japan

[e] MJ Mini; Bio-Rad Laboratories, Hercules, CA

[f] DigDoc-It Imaging System; UVP, CA

[g] BCG vaccine strain; Japan BCG Laboratory, Tokyo, Japan

[h] Prednisolone; Sanwa Kagaku Kenkyusho Co. Ltd., Aichi, Japan

[i] FOSMICIN; Meiji Seika Pharma Co. Ltd., Tokyo, Japan

[j] Gaster; Astellas, Tokyo, Japan

[k] URSO; Mitsubishi Tanabe Pharma Co., Osaka, Japan

[l] Sahne Oint; Eisai, Tokyo, Japan

[m] Rinderon-V Ointment; Shionogi Co. Ltd., Osaka, Japan

[n] Hirudoid Soft Ointment; Maruho, Osaka, Japan

[o] Imuran; Glaxo Smith Kline, Tokyo, Japan

REFERENCES

1. Scott DW, Miller WH, Griffin CE, eds. Miscellaneous skin diseases. In: *Muller and Kirk's Small Animal Dermatology*. 6th ed. Philadelphia (PA): WB Saunders; 2001:1136–40.
2. Torres SMF. Sterile nodular dermatitis in dogs. *Vet Clin North Am Small Anim Pract* 1999;29(6):1311–23.
3. Gross TL, Ihrke PJ, Walder EJ, et al., eds. Noninfectious nodular and diffuse granulomatous and pyogranulomatous diseases of the dermis. In: *Skin diseases of dog and cat: Clinical and histopathologic diagnosis*. 2nd ed. Oxford, UK: Blackwell Publishing; 2005:320–3.
4. Santoro D, Prisco M, Ciaramella P. Cutaneous sterile granulomas/pyogranulomas, leishmaniasis and mycobacterial infections. *J Small Anim Pract* 2008;49(11):552–61.
5. Panich R, Scott DW, Miller WH. Canine cutaneous sterile granulomas/pyogranulomas syndrome: a retrospective analysis of 29 cases (1976 to 1988). *J Am Anim Hosp Assoc* 1991;27:519–28.
6. Barrett SJ, Sheafor SE, Hillier A, et al. Challenging cases in internal medicine: what's your diagnosis? *Vet Med* 1998;93:35–44.
7. Santoro D, Spaterna A, Mechelli L, et al. Cutaneous sterile pyogranuloma/granuloma syndrome in a dog. *Can Vet J* 2008;49(12):1204–7.
8. Cornegliani L, Fondevila D, Vercelli A, et al. PCR technique detection of *Leishmania* spp. but not *Mycobacterium* spp. in canine cutaneous 'sterile' pyogranuloma/granuloma syndrome. *Vet Dermatol* 2005;16(4):233–8.
9. Onishi T, Inokuma H, Ohno K, et al. C reactive protein concentration in normal and diseased dogs measured by laser nephelometric immunoassay. *J Jpn Vet Med Assoc* 2000;53:595–601 [in Japanese with English summary].
10. Michalopoulos AS, Livaditis IG, Gougoutas V. The revival of fosfomycin. *Int J Infect Dis* 2011;15(11):e732–9.
11. Yakuyama T, Namikawa K, Ichikawa Y, et al. Antimicrobial drug susceptibility of *Staphylococcus* clinical isolate from canine pyoderma and external otitis. *Jpn J Vet Dermatol* 2008;14(3):135–7.
12. Mercati F, Pascucci L, Ceccarelli P, et al. Expression of mesenchymal stem cell marker CD90 on dermal sheath cells of the anagen hair follicle in canine species. *Eur J Histochem* 2009;53(3):159–66.
13. Mercati F, Pascucci L, Gargiulo AM, et al. Immunohistochemical evaluation of intermediate filament nestin in dog hair follicles. *Histol Histopathol* 2008;23(9):1035–41.

FULL PAPER *Int ernal Medicine*

Potential Immunological Adjuvant of 'K' -Type CpG-Oligodeoxynucleotides Enhanced the Cell Proliferation and IL-6 mRNA Transcription in Canine B Cells

Shinpei KAWARAI[1,3], Kaoru SATO[1], Anna HORIGUCHI[1], Keigo KURATA[2], Akio KIUCHI[1], Hajime TSUJIMOTO[3] and Masahiro SAKAGUCHI[1]*

[1]*Department of Veterinary Microbiology, School of Veterinary Medicine, Azabu University, 1–17–71 Fuchinobe, Chuo-ku, Sagamihara, Kanagawa 252–5201,* [2]*Institute of Tokyo Environmental Allergy, Suwanbiru 8F, 2–2–4 Yushima, Bunkyo-ku, Tokyo 113–0034 and* [3]*Department of Veterinary Internal Medicine, Graduate School of Agricultural and Life Sciences, The University of Tokyo, 1–1–1Yayoi, Bunkyo-ku, Tokyo 113–8657, Japan*

(Received 2 July 2010/Accepted 8 September 2010/Published online in J-STAGE 22 September 2010)

ABSTRACT. CpG oligodeoxynucleotides (CpG-ODNs) are ligands for toll-like receptor 9 (TLR9), signaling of which plays a role in innate immunity by inducing T helper 1 (TH1)-cell responses and pro-inflammatory cytokine production. The activation of TLR9 signaling is considered to be effective for the therapy of cancer, infectious diseases, and allergies and preclinical studies using CpG-ODNs have been performed in dogs and humans. In order to investigate the precise mechanisms responsible for the effect of CpG-ODNs in dogs, we examined their role in cell proliferation and cytokine gene expression in canine B cells. Canine B cells were collected by a magnetic cell isolation method using anti-CD21 antibody. Flow cytometric analysis for the intracellular CD79α revealed the purity of canine B cells to be as high as 90.2 ± 2.1%. Transcription of TLR2, TLR4, and TLR9 mRNA on canine $CD21^+$ cells was confirmed by reverse-transcript polymerase chain reaction (RT-PCR). CpG-ODNs induced dose-dependent proliferation of canine $CD21^+$ cells ($P<0.05$ compared with control-ODNs) detected by BrdU incorporation. Quantification of IL-6, IL-10, and IL-12p40 mRNA transcription on canine $CD21^+$ cells revealed that CpG-ODNs enhanced IL-6 mRNA transcription but not IL-10 and IL-12p40 mRNA transcription ($P<0.05$ compared with control-ODNs). These responses to CpG-ODNs in the canine B cells indicated that CpG-ODNs would be useful as an immunological adjuvant for vaccine in dogs.

KEY WORDS: adjuvant, B cells, canine, CpG-oligodeoxynucleotides, IL-6.

J. Vet. Med. Sci. 73(2): 177–184, 2011

Activation of immune cells by bacterial DNA was first discovered through induction of interferon (IFN) secretion and tumor inhibition by the DNA fraction of *Mycobacterium bovis* strain BCG [30]. These effects depend on a hexamer-palindromic sequence with 5' -Cytosine-phosphodiester-Guanin (CpG)-3' motifs in the bacterial DNA [30]. CpG motifs are recognized by the cells expressing toll-like receptor 9 (TLR9), a pattern-recognition receptor (PRR) [9]. Signaling through the TLR9 pathway leads to innate immune responses from B cells and plasmacytoid dendritic cells (pDCs) [16, 18]. These cells induce the production of T helper 1 (TH1)-cell biased cytokines such as IFN-γ and interleukin (IL)-12 and pro-inflammatory cytokines such as IL-1, IL-6, IL-18, and tumor necrosis factor (TNF) and differentiate into plasma cells and/or professional antigen presenting cells (APCs) [16, 18, 30]. Because synthetic oligodeoxynucleotides containing unmethylated CpG motifs (CpG-ODNs) are useful as anti-allergic and otherwise immunoprotective agents and as vaccine adjuvants, TLR9 signaling has been used in cancer, infectious disease, and allergy therapy [13, 16, 18, 30].

Examination of homology of TLR9 amino acid sequences shows that the nucleotide binding domains of leucine-rich repeats (LRRs) are heterogenous among species [7, 9], such that the optimal sequence motifs of CpG-ODNs for stimulating human cells (GTCGTT) can differ from those for mouse cells (GACGTT) [1, 2, 6]. For therapeutic uses of CpG-ODNs in humans, at least three structurally distinct classes of CpG-ODNs have been developed: 'D' -type ODNs (also known as CpG-A), 'K' -type ODNs (also known as CpG-B), and 'C' -type ODNs[6, 20, 22, 31]. 'D' -type ODNs are constructed using a mixed phosphodiester (PO) and phosphorothionate (PS) backbone and contain a single CpG motif in palindromic sequence, the 3' end of which flanks poly-G tail. 'K' -type ODNs encode multiple CpG motifs and consist of only PS backbone. 'D' -type ODNs have potent ability to induce IFN-α secretion from pDCs, but have little stimulatory activity on B cells. In contrast, 'K' -type ODNs are strong stimulators for B cells, but only weakly induce IFN-α secretion from pDC. 'C' -type ODNs are intermediate in structure and activity between the 'K' - and 'D' -type ODNs [5, 24, 32]. Due to the diversity of immune responses to CpG-ODNs among species and immune cells, it is necessary to selectively employ the optimal sequence motifs of CpG-ODNs.

Whereas 'K' -type ODNs have a preferential effect on B cells, it is possible that when 'K' -type ODNs are artificially loaded on cationic microparticles or conjugated to cationic lipids, 'K' -type ODNs gain immune effects similar to those of 'D' -type ODNs [4, 10, 14]. Using 'K' -type ODNs, preclinical studies have already been performed in humans [13,

* CORRESPONDENCE TO: SAKAGUCHI, M., Department of Veterinary Microbiology, School of Veterinary Medicine, Azabu University, 1–17–71 Fuchinobe, Chuo-ku, Sagamihara, Kanagawa 252–5201, Japan.
e-mail: sakagum@azabu-u.ac.jp

16, 18]. In dogs, 'K' -type ODNs have also been studied *in vivo* as a potential vaccine adjuvant for rabies virus [28] and a potential cancer immunotherapy agent for malignant melanoma [25].

Selection of optimal CpG-ODN types for clinical trials must be preceded by extensive study of effects of various CpG motifs. However, few such studies of dogs have been reported. Wernette *et al.* [33] and Ren *et al.* [28] found that 'K' -type ODNs induced proliferation of canine spleen cells, lymph node cells, or both; however there are no reports that have shown the direct effects of CpG-ODNs on canine B cells. In our previous study, it was shown that 'D' -type ODNs induced canine PBMCs to secrete IFN-γ and to express IL-12p40 mRNA [21]. Im Hof *et al.* [12] examined the effects of novel synthetic agonists of TLR9, which are referred to as immune modulatory oligonucleotides (IMOs), on the proliferation and TH1 immune responses of T- and B-cells in canine PBMCs; however the effect of IMOs on immune cells needed co-stimulation by lipopolysaccharide (LPS) and/or concanavalin A.

For the purpose of developing an effective immunological adjuvant in dogs, we examined the direct effects of 'K' -type ODNs on the cell proliferation and induction of IL-6, IL-10, and IL-12p40 mRNA transcription in canine B cells. We focused on these cytokines because enhancements of the cytokine production by CpG-ODNs have previously reported in human and murine B cells [1, 6, 8, 17, 23, 24, 32]; both of the IL-6 and IL-10 are known to a B-cell growth and differentiation factor [8, 15, 26, 29]; and IL-12 has been shown to promote shifting the B-cell phenotype to TH1 in cooperation with CpG-ODN [23]. In the present study, we tried to make clear whether B cells could be identified as primary target cells for CpG-ODNs in dogs.

MATERIALS AND METHODS

Dogs: Six 2–7-year-old healthy beagle dogs (2 males, 3 females, and 1 neutered female) were kept according to the "Guidelines of Animal Welfare for Experimental Animals" issued by Azabu University. All dogs have been annually vaccinated against canine rabies virus every year and milbemycin oxime was administered monthly for prevention of heartworm diseases.

Reagents: All synthetic phosphorothioate oligodeoxynucleotides (ODNs) were purchased from Hokkaido System Science (Hokkaido, Tokyo, Japan). LPS contamination in ODNs was below the detection limit of 5 endotoxin units/mg ODN as determined by the manufacturer using the kinetic colorimetric method. Sequences of 'K' -type ODNs, 2006 [TCGTCGTTTTGTCGTTTTGTCGTT, molecular weight (MW)=7,697] and 1018 (TGACTGTGAACGTTCGAGATG, MW=7,150) used in this study were described in previous reports that showed effects of 'K' -type ODNs on human B cells and canine splenocytes [6, 24, 33]. Those of the negative control used in the present study were 2137, the GpC variant of 2006 (TGCTGC TTTTGTGCTTTTGTGCTT, MW=7,697) and 1040, the mutant CpG variant of 1018 (TGACTGTGAACCTTAGAGATGA, MW=7,134), respectively. LPS from *E.coli* (O55:B5, Sigma-Aldrich, St. Louis, MO, U.S.A.), which is known to be a TLR4 signaling-mediated mitogen for murine B cells, was used as a positive control.

Isolation of canine CD21-positive cells from venous blood: PBMCs were isolated from the venous blood of dogs by density gradient centrifugation using Lymphoprep (specific gravity 1.077) (AXIS-SHILD, Oslo, Norway) as directed by the manufacturer. The canine B cells were isolated from the PBMCs by positive selection using the magnetic cell isolation method (MACS, Miltenyi Biotec, Bergisch Gladbach, Germany). After blocking with canine sera at 4°C for 30 min, the cells were incubated with R-phycoerythrin (RPE)-conjugated mouse anti-canine CD21 antibody (clone CA2.1D6) (AbD Serotec, Oxford, U.K.) at 4°C for 10 min, and then reacted with anti-PE microbeads (Miltenyi Biotec) at 4°C for 10 min. The CD21-positive ($CD21^+$) cells were collected using L/S column (Miltenyi Biotec) and cell viability (>95%) was determined by 0.5% trypan blue exclusion. The purity of canine B cells was assessed by morphology using Wright-Giemsa staining and flow cytometric analysis. The isolated canine $CD21^+$ cells were suspended in RPMI1640 medium containing 10% fetal bovine serum (FBS) and cultivated at 37°C in a humidified atmosphere with 5% CO_2.

Flow cytometry: Intracellular staining of CD79α was performed on $CD21^+$ cells soon after isolation by MACS, using a commercial kit (IntraStain, DAKO, Copenhagen, Denmark) according to the manufacturer' s instructions. Briefly, the $CD21^+$ cells were fixed with 100 μl of IntraStain reagent A. Then the cells were permeabilized with 100 μl of IntraStain reagent B and simultaneously stained with antibodies for 15 min at RT in the dark. Mouse anti-human CD79αcy antibody (clone HM-57, DAKO) or the isotype control of mouse IgG1 antibody (AbD Serotec) was used at the concentration of 1 μg per 150 μl. The anti-human CD79αcy monoclonal antibody was previously shown to cross-react with canine B cells by immunohistochemistry and flow cytometry [3]. Prior to the staining of the cells, these antibodies were labeled with Alexa 488 using Zenon® Alexa Fluor® 488 mouse IgG labeling kit (Invitrogen, Carlsbad, CA, U.S.A.) according to the manufacturer' s instructions. The fluorescence of RPE and Alexa 488 on the stained cells (1.0×10^4 cells) was analyzed by flow cytometry (Epics XL ADC system) (Beckman Coulter, Fullerton, CA, U.S.A.) using Expo32 software (Beckman Coulter).

Stimulation of the cells: Canine $CD21^+$ cells that were approximately 90% positive for CD79α by flow cytometric analysis were used. For the proliferation assay, the cells ($1–2 \times 10^5$ cells) were seeded in 96-well flat-bottom plates in a volume of 100 μl medium/well and stimulated with 8 μg/ml of each of 2006, 1018, 2137, 1040, and LPS for 68 hr. To examine the dose-dependent effects of CpG-ODNs, a titrated dose range of 2006 and 2137 at 0.9, 2.7, 8, and 24 μg/ml was used. For the quantification of cytokine gene expression, the cells (4×10^5 cells) were cultivated in 5 ml

polystyrene round-bottom tubes (Becton Dickinson, Franklin Lakes, NJ, U.S.A.) in a volume of 500 μl per tube and stimulated with 24 $\mu g/ml$ of 2006, 2137, and LPS for 2 , 4 and 6 hr. Cells cultivated in a similar manner but without stimulators were also used as negative controls.

Proliferation assay: A 5-bromo-2' -deoxyuridine (BrdU)-based cell proliferation ELISA kit (Roche Diagnostics, Tokyo, Japan) was used for the measurement of proliferation activity of the cells according to the manufacturer' s protocol. Forty-eight hours from the start of cultivation, BrdU labeling reagent was added at 10 μl per well. The cells were incubated with the BrdU for an additional 20 hr (total 68 hr). After centrifugation, the plate was dried at 60°C for 1 hr. BrdU-labeled DNA in the cells was fixed and denatured by incubation with FixDenat solution for 30 min at RT. After washing, the BrdU-labeled DNA was stained with peroxidase-conjugated anti-BrdU antibody for 90 min at RT. The plate was washed again, and TMB substrate solution was added. The reaction was stopped by adding 1 M H_2SO_4 solution. Absorbance was measured at 450 nm using a microplate reader (Multiskan JX, Thermo Labsystems, Helsinki, Finland). Stimulation index (SI) was calculated by dividing absorbance of the stimulated cells by that of the cells cultured without stimulators.

Reverse transcriptase (RT) assay: Total RNA was extracted from the cells using RNeasy plus micro kit, which was designed to purify total RNA from less than 5×10^5 of cells and remove genomic DNA in the same procedure (Qiagen, Tokyo, Japan). The cells were lysed with buffer RLT plus, then homogenized by QIAshredder homogenizer (Qiagen), and stored at –80°C until use. First strand cDNA was generated from 50 and 25 *ng* of the total RNA by reverse transcription (RT) using the SuperScript® VILO cDNA synthesis kit (Invitrogen, Rockville, MD, U.S.A.).

Reverse transcriptase polymerase chain reaction: Using the primers listed in Table 1, cDNA was amplified with a TAKARA Ex Taq hot start version (TAKARA, Shiga, Japan) using a thermal cycler (iCycler, Bio-Rad Laboratories, Hercules, CA, U.S.A.). The PCR amplification consisted of 35 cycles of denaturation (98°C, 10 sec), annealing [60°C for TLR2, TLR4, and TLR9, and 62°C for Glyceraldehydes-3-phosphate dehydrogenase (GAPDH), 30 sec], and extension (72°C, 30 sec). Absence of contamination by genomic DNA in total RNA was confirmed by amplification of non-RT controls (data not shown). The PCR products were analyzed by ethidium bromide-electrophoresis in a 2% agarose gel and visualized using UV transilluminator (BioDoc-It® Imaging System, UVP, Upland, CA, U.S.A.).

Quantitative polymerase chain reaction: Taqman gene expression assay (Applied Biosystems, Foster, CA, U.S.A.) was used for measurement of IL-6, IL-10, and IL-12p40 mRNA transcription. Eukaryotic 18S ribosomal RNA was used as an internal control. The assay ID of primer probe-mix of each gene is shown in Table 2. The PCR amplification was carried out using Taqman universal PCR master mix (Applied Biosystems) on ABI 7500 amplification system (Applied Biosystems) according to the manufacturer' s instructions. Data were analyzed by the comparative threshold cycle (CT) method described in the previous report [21]. Fold change in expression was calculated by dividing the value of the stimulated cells by that of the non-stimulated cells. Statistically significant differences were not observed between CT values of the internal control in the cells before and after the cultivation with stimulator (Dunnet test) (data not shown).

Statistical analysis: Kruskal-Wallis ANOVA was applied for comparison of data among groups using the different stimulators in the cell proliferation assay. Post hoc analysis (Turkey-Kramer HSD test) was performed to determine the groups showing significant differences in cell proliferation.

Table 1. Canine oligonucleotide primers for reverse transcriptase-polymerase chain reaction

Target	Primer type	Olig onucleotides (5' –3')	Amplicon size (bp)	Seaquence reference
TLR2	Forward	GGAGAACCTTCTGGTCAGAAGC	310	In this study
	Reverse	GGTGTTCATTATCTTCCGCAGC		NM_001005264
TLR4	Forward	GCTTCTCGCTTGGCTTGCAAAAGG	419	In this study
	Reverse	CCCATTCCAGGTAAGT GTTCCTGC		NM_001002950
TLR9	Forward	GGTGCTGGACCTGAGTGAGAACTTCC	510	In this study
	Reverse	GGTCCAAGGTGAAGTTGAGGGTCC		NM_001002998
GAPDH	Forward	CTCATGACCACAGTCCATGC	412	Ohmori *et al.* (2004) [27]
	Reverse	TGAGCTTGACAAAGTGGTCA		AB_038240

Table 2. Canine oligonucleotide primer probe-mix for quantitative-polymerase chain reaction

Target	Assay ID in Taqman gene expression assay	Amplicon size (bp)	Seaquence reference
IL-6	Cf02624282_m1	105	NM_001003301.1
IL-10	Cf02624265_m1	89	NM_001003077.1
IL-12p40	Cf02623323_m1	96	NM_001003292.1
18s rRNA*	Hs99999901_s1	187	X03205

*The primers and probe are constructed at high homology region on nucleotide sequence between dog and human 18s rRNA.

Multivariate ANOVA (MANOVA) was used to analyze the dose-dependent effect of 2006 on cell proliferation. Wilcoxon rank-sum test was performed to compare the ratio of fold change in the cytokine mRNA transcription between the cells stimulated with 2006 and 2137. *P*-values lower than 0.05 were considered significant. All statistical tests were performed using JMP software version 8 (SAS Institute, Cary, NC, U.S.A.).

RESULTS

Isolation of canine B cells from whole blood: Between 10^7 and 2×10^7 canine PBMC were obtained from 10 ml of whole blood. The mean (± SD) of canine $CD21^+$ cells isolated from 1×10^7 canine PBMC by MACS was $4.5 \pm 2.0 \times 10^5$ cells (n=5 individual dogs). The uniform population of canine $CD21^+$ cells was verified by the dot plots of forward scatter (FSC) vs. side scatter (SSC) produced by flow cytometric analysis (Fig. 1a). Wright-Giemsa staining showed that in contrast to the canine PBMC, which were composed of a variety of cell types such as band neutrophil, monocyte, and lymphocyte, the isolated canine $CD21^+$ cells were composed of a uniform population showing morphology characteristic of lymphocytes (Fig. 1b). Differential leukocyte counts evaluated from the preparation of canine $CD21^+$ cells showed the following mean (± SD) percentages for the different leukocyte types: 0.7 ± 0.8% band neutrophils, 0.2 ± 0.3% segmented neutrophils, 0.1 ± 0.1% eosinophils, 0% basophils, 3.0 ± 2.7% monocytes, and 96.0 ± 3.2% lymphocytes (n=5). Flow cytometric analysis using anti-CD79α antibody showed that the purity of canine B cells in the canine $CD21^+$ cells was as high as 90.2 ± 2.1% (n=5) (Fig. 1a).

Transcription of TLR2, TLR4, and TLR9 mRNA in canine B cells: In order to evaluate the ability of canine B cells to recognize the LPS and CpG-ODNs, the transcriptions of TLR2, TLR4 and TLR9 mRNA on canine $CD21^+$ cells were examined. RT-PCR analysis showed that the isolated $CD21^+$ cells expressed all of three TLRs. The intensities of the amplified bands of TLR2, TLR4 and TLR9 on agarose gel were as high as those of GAPDH (Fig. 2).

Proliferation of canine B cells induced by CpG-ODNs: To extend the study of the effects of 'K' -type ODNs in dogs, BrdU incorporation in the DNA of proliferating canine $CD21^+$ cells was assessed in cells stimulated with 2006, 2137, 1018, 1040, and LPS. The SI values for the proliferation were significantly different among groups ($P<0.05$) (Fig.3a). To determine whether the enhanced proliferative

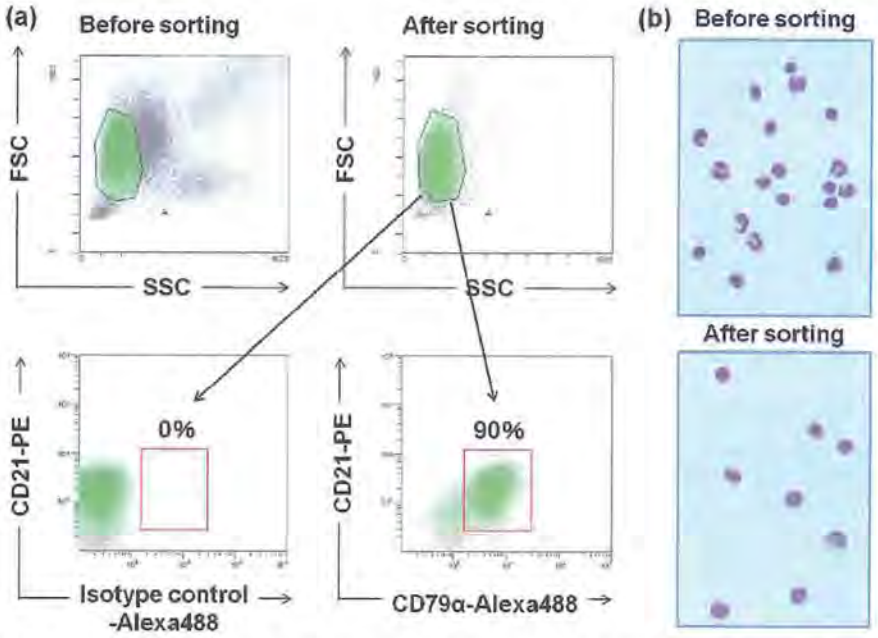

Fig. 1. Isolation of canine B cells. (a) The cells are shown in the dot plots of forward scatter (FSC) vs. side scatter (SSC) before and after the isolation by MACS using anti-CD21 antibody. Gates shown in the dot plots indicate a lymphocyte region. The isolated canine $CD21^+$ cells stained with anti-CD79α antibody or isotype control labeled with Alexa 488 are shown in dot plots of fluorescent intensity for CD21-RPE vs. CD79α-Alexa 488. The figures shown in the dot plots indicate the percentage of CD21 and CD79α double-positive cells in the square. The percentage of isotype control was set at smaller than 3% and 1.0×10^6 cells are shown in the dot plots. (b) Light microscopic observations of the cytocentrifuged preparations stained with Wright-Giemsa solution (magnification, × 400). The cells are shown before and after the isolation by MACS. Data were representative of two independent experiments from 5 individual dogs.

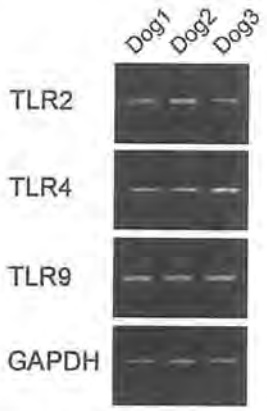

Fig. 2. Transcription of TLR2, TLR4, and TLR9 mRNA on canine CD21$^+$ cells. Total RNA was extracted from canine CD21$^+$ cells and subjected to RT-PCR analysis using the specific primers for TLR2, TLR4, TLR9 and GAPDH. The data shown here are representative of the results in three individual dogs (Dogs 1–3).

responses were CpG-motif dependent, the SI values of 'K' -type ODNs were compared with those of control-ODNs. As compared with the response to the negative controls of 2137 and 1040, 'K' -type ODNs 2006 and 1018 induced significantly greater proliferation of canine CD21$^+$ cells, 2.1-fold (P<0.05) and 1.5-fold (P<0.05), respectively (Fig. 3a). Furthermore, the response to 2006 was significantly higher than that to 1018 (1.3-fold, P<0.05) (Fig. 3a). Based on the ability to induce high-level cell proliferation, 2006 was used for the following assays. Dose-dependent proliferation was observed in response to 2006 (P<0.05) and the dose-response curve peaked at the concentration of 2.7 μg/ml (Fig. 3b).

Cytokine gene expression in canine B cells induced by CpG-ODNs: To determine the effects of 'K' -type ODNs on the production of cytokines in dogs, the transcription levels of IL-6, IL-10, and IL-12p40 mRNA on canine PBMC and isolated canine CD21$^+$ cells were measured by qPCR. After 4 hr of stimulation of canine PBMC and CD21$^+$ cells with 2006 and 2137, IL-6 mRNA transcription in canine CD21$^+$ cells stimulated with 2006 was 9.3-folds higher than that in the cells subjected to 2137 (P<0.05) (Fig. 4a). Although the enhanced IL-10 and IL-12p40 mRNA transcription were not observed, time course-dependent increase was observed in the transcription of IL-6 mRNA in the canine CD21$^+$ cells after stimulation with 2006 (P<0.05) (Fig. 4b).

DISCUSSION

We revealed that 'K' -type ODNs affected the proliferation of, and IL-6 gene expression in, canine B cells isolated from PBMCs. IL-6, which was originally identified as B cell stimulating factor 2 (BSF2), has been shown to have various biological activities such as stimulation of the growth of B cells and differentiation of naïve B cells into antibody-secreting plasma cells [15]. It has been reported that over expression of IL-6 gene in transgenic mice induces polyclonal increase in IgG1 in serum and generation of massive plasmacytosis in thymus, lymph node, and spleen [29]. Klinman *et al.* [17] revealed that CpG-induced IgM production was regulated by IL-6. Ren *et al.* [28] reported that the CpG-ODN called YW07 induced antigen-specfic IgG antibody responses in dogs with immunization against the rabies virus. It may be that 'K' -type ODN-induced B-cell proliferation is associated with IL-6 secreted by B cells in an autocrine manner. 'K' -type ODNs might have the potential to induce IL-6 mediated-antigen response in canine B cells.

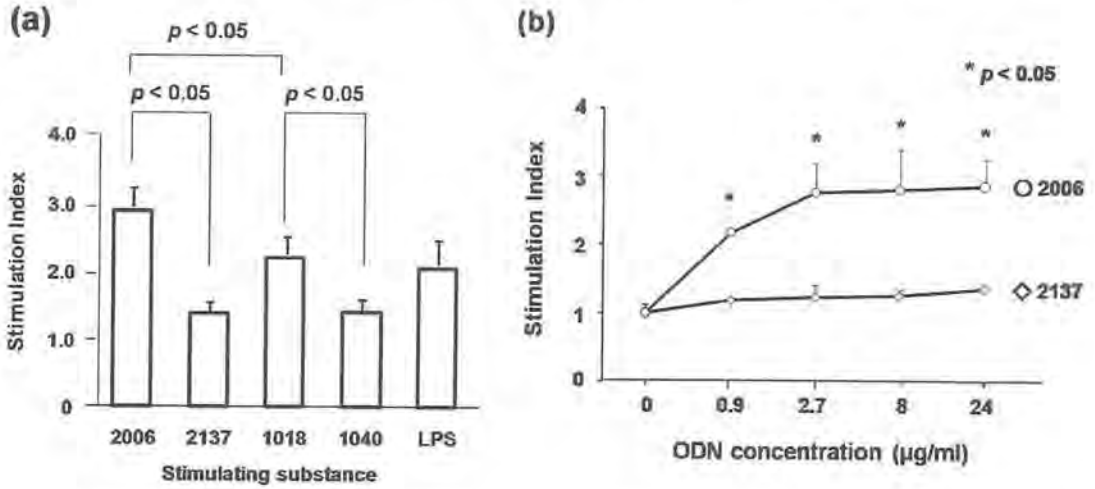

Fig. 3. Cell proliferation responses of canine CD21$^+$ cells to CpG-ODNs. (a) Stimulation index of cell proliferation for the responses to 2006, 2137, 1018, 1040, and LPS. (b) Stimulation index of cell proliferation for the responses to 2006 and 2137. Each bar represents mean ± SD of stimulation index. The P-values were shown in figures. These experiments were performed on 5 individual dogs in duplicate.

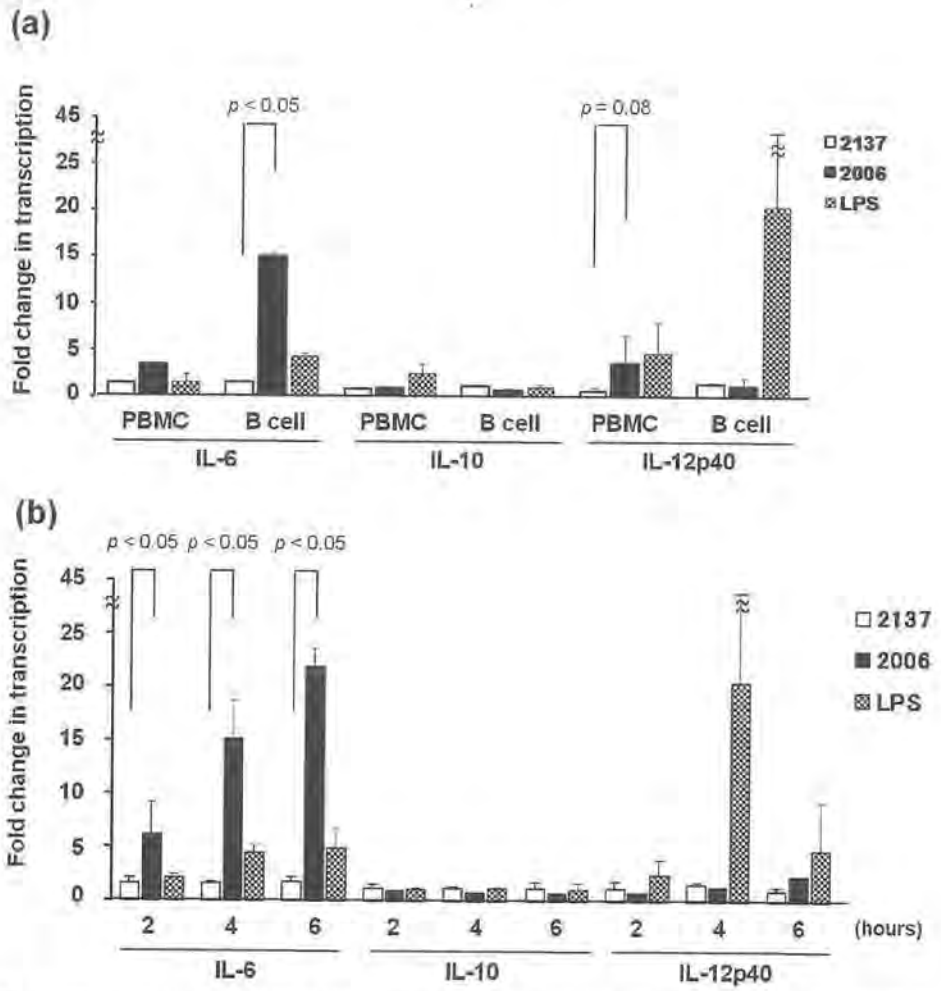

Fig. 4. Transcription of the IL-6, IL-10, and IL-12p40 mRNA induced by CpG-ODNs. (a) Fold change in cytokine mRNA transcription on canine CD21$^+$ cells and PBMC for the responses to 2006, 2137, and LPS after 4 hr cultivation. (b) Fold change in cytokine mRNA transcription on canine CD21$^+$ cells for the responses to 2006, 2137, and LPS after 2, 4, and 6 hr of cultivation. Each bar represents mean ± SD of fold change in transcription. The *P*-values compared 2006 with 2137 are shown in figures. These experiments were performed on 3 to 4 individual dogs.

Further researches are needed to examine the antibody response of canine B cells stimulated by 'K' -type ODNs.

The proliferation of canine CD21$^+$ cells in response to 2006 was shown to be significantly higher than in response to 1018. Both 2006 and 1018 have often been used as typical 'K' -type ODNs which potently activate human B cells. 2006 and 1018 have different immune stimulatory CpG motifs; 2006 contains TCGTCG at the 5' end and multiple GTCGTT motifs with no palindromes while 1018 contains the palindromic motif of AACGTTCG [24]. It has been reported that the optimal CpG motifs for activating human B cells contain $(TCG)_n$ [6]. The 'C' -type ODN called C274, which is generated by substitution of TCGTCG for 5' base flanking AACGTTCG in 1018, resulting in the sequence 5' -TCGTCGAACGTTCGAGATGAT-3' , induces more proliferation, maturation, and cytokine production in human B cells than 1018 [24]. In the present study, canine CD21$^+$ cells responded little to control ODN 2137, while a dose-dependent response to 2006 was shown. These results could indicate that effects of 2006 were CpG-specific and the motif of $(TCG)_n$ was suitable for the activation of canine B cells.

We previously showed that 'D' -type ODNs induced the production and mRNA transcription of IL-12p40 from canine PBMCs [21]. In the present study, although the significant difference was not reached (P=0.08), the transcription of IL-12p40 mRNA in canine PBMCs was enhanced after 4-hr stimulation with 'K' -type ODNs (5.2-fold higher than control-ODNs) (Fig. 4a). In human PBMCs, B cells and pDCs highly express TLR9 and are directly reactive to

CpG-ODNs, whereas T cells, NK cells, and monocytes express much lower level of TLR9 than B cells and pDCs and they do not respond to CpG-ODNs [2, 11]. In our study, the proliferation of canine $CD21^+$ cells by (K' -type ODNs was observed; however that of non-$CD21^+$ cells, which consisted largely of T cells and monocytes, was not (data not shown). In contrast to the cellular patterns of TLR9 expression in human PBMCs, murine monocytes have been known responding to CpG-ODNs [18]. Comparison of the cell sensitivity to CpG-ODNs among the human, mouse and dog suggest that canine T cells may be less sensitive to CpG-ODNs. Since 'K' -type ODNs could not induce the IL-12p40 mRNA transcription in canine $CD21^+$ cells, it might be considered that the cellular source of the IL-12 mRNA transcription in canine PBMCs was not B and T cells but monocytes or pDCs.

B cells are considered an attractive target for immunotherapy due to their relative abundance in peripheral blood, ability to produce antibodies and present antigens to naïve T cells, and potential for expansion and long-lived humoral immunity. Accordingly, human clinical trials using 'K' -type ODNs have been performed for the therapy of cancers such as non-Hodgkins lymphoma and colorectal cancer, infectious diseases such as hepatitis B, and allergies such as asthma and allergic rhinitis [13, 16, 18, 30]. In the present study, we demonstrated that 'K' -type ODNs acted as an immunological B cell adjuvant in vitro. Further studies of biological activities of CpG-ODNs in immune cells are needed to extend the usefulness of CpG-ODNs as immunological adjuvants in dogs.

ACKNOWLEDGMENTS. We thank Dr. Shinobu Matsuura and Jonathan Bloch for their review and constructive comment on the manuscript. This work was supported by a Grant-in Aid for Scientific Research from the Ministry of Health, Labour and Welfare of Japan, by the Promotion and Mutual Aid Corporation for Private Schools of Japan, and by Grant-in-Aid for Matching Fund Subsidy for Private Universities.

REFERENCES

1. Bauer, M., Heeg, K., Wagner, H. and Lipford, G. B. 1999. DNA activates human immune cells through a CpG sequence-dependent manner. *Immunology* **97**: 699–705.
2. Bauer, S., Kirschning, C. J., Hacker, H., Redecke, V., Hausmann, S., Akira, S., Wagner, H. and Lipford, G. B. 2001. Human TLR9 confers responsiveness to bacterial DNA via species-specific CpG motif recognition. *Proc. Natl. Acad. Sci. U. S. A.* **98**: 9237–9242.
3. Faldyna, M., Samankova, P., Leva, L., Cerny, J., Oujezdska, J., Rehakova, Z. and Sinkora, J. 2007. Cross-reactive anti-human monoclonal antibodies as a tool for B-cell identification in dogs and pigs. *Vet. Immunol. Immunopathol.* **119**: 56–62.
4. Fearon, K., Marshall, J. D., Abbate, C., Subramanian, S., Yee, P., Gregorio, J., Teshima, G., Ott, G., Tuck, S., Van Nest, G. and Coffman, R. L. 2003. A minimal human immunostimulatory CpG motif that potently induces IFN-gamma and IFN-alpha production. *Eur. J. Immunol.* **33**: 2114–2122.
5. Hartmann, G., Battiany, J., Poeck, H., Wagner, M., Kerkmann, M., Lubenow, N., Rothenfusser, S. and Endres, S. 2003. Rational design of new CpG oligonucleotides that combine B cell activation with high IFN-alpha induction in plasmacytoid dendritic cells. *Eur. J. Immunol.* **33**: 1633–1641.
6. Hartmann, G. and Krieg, A. M. 2000. Mechanism and function of a newly identified CpG DNA motif in human primary B cells. *J. Immunol.* **164**: 944–953.
7. Hashimoto, M., Asahina, Y., Sano, J., Kano, R., Moritomo, T. and Hasegawa, A. 2005. Cloning of canine toll-like receptor 9 and its expression in dog tissues. *Vet. Immunol. Immunopathol.* **106**: 159–163.
8. He, B., Qiao, X. and Cerutti, A. 2004. CpG DNA induces IgG class switch DNA recombination by activating human B cells through an innate pathway that requires TLR9 and cooperates with IL-10. *J. Immunol.* **173**: 4479–4491.
9. Hemmi, H., Takeuchi, O., Kawai, T., Kaisho, T., Sato, S., Sanjo, H., Matsumoto, M., Hoshino, K., Wagner, H., Takeda, K. and Akira, S. 2000. A Toll-like receptor recognizes bacterial DNA. *Nature* **408**: 740–745.
10. Honda, K., Ohba, Y., Yanal, H., Negishi, H., Mizutani, T., Takaoka, A., Taya, C. and Taniguchi, T. 2005. Spatiotemporal regulation of MyD88-IRF-7 signalling for robust type-I interferon induction. *Nature* **434**: 1035–1040.
11. Hornung, V., Rothenfusser, S., Britsch, S., Krug, A., Jahrsdorfer, B., Giese, T., Endres, S. and Hartmann, G. 2002. Quantitative expression of toll-like receptor 1–10 mRNA in cellular subsets of human peripheral blood mononuclear cells and sensitivity to CpG oligodeoxynucleotides. *J. Immunol.* **168**: 4531–4537.
12. Im Hof, M., Williamson, L., Summerfield, A., Balmer, V., Dutoit, V., Kandimalla, E. R., Yu, D., Zurbriggen, A., Doherr, M. G., Peel, J. and Roosje, P. J. 2008. Effect of synthetic agonists of toll-like receptor 9 on canine lymphocyte proliferation and cytokine production in vitro. *Vet. Immunol. Immunopathol.* **124**: 120–131.
13. Kanzler, H., Barrat, F. J., Hessel, E. M. and Coffman, R. L. 2007. Therapeutic targeting of innate immunity with Toll-like receptor agonists and antagonists. *Nat. Med.* **13**: 552–559.
14. Kerkmann, M., Costal, L. T., Richter, C., Rothenfusser, S., Battiany, J., Hornung, V., Johnson, J., Englert, S., Ketterer, T., Heckl, W., Thalhammer, S., Endres, S. and Hartmann, G. 2005. Spontaneous formation of nucleic acid-based nanoparticles is responsible for high interferon-α induction by CpG-A in plasmacytoid dendric cells. *J. Biol. Chem.* **280**: 8086–8093.
15. Kishimoto, T. 2005. Interleukin-6: from basic science to medicine—40 years in immunology. *Annu. Rev. Immunol.* **23**: 1–21.
16. Klinman, D. M. 2004. Immunotherapeutic uses of CpG oligodeoxynucleotides. *Nat. Rev. Immunol.* **4**: 249–258.
17. Klinman, D. M., Yi, A. K., Beaucage, S. L., Conover, J. and Krieg, A. M. 1996. CpG motifs present in bacteria DNA rapidly induce lymphocytes to secrete interleukin 6, interleukin 12, and interferon gamma. *Proc. Natl. Acad. Sci. U.S.A.* **93**: 2879–2883.
18. Krieg, A. M. 2006. Therapeutic potential of Toll-like receptor 9 activation. *Nat. Rev. Drug Discov.* **5**: 471–484.
19. Krieg, A. M., Yi, A. K., Matson, S., Waldschmidt, T. J., Bishop, G. A., Teasdale, R., Koretzky, G. A. and Klinman, D. M. 1995. CpG motifs in bacterial DNA trigger direct B-cell activation. *Nature* **374**: 546–549.
20. Krug, A., Rothenfusser, S., Hornung, V., Jahrsdorfer, B., Blackwell, S., Ballas, Z. K., Endres, S., Krieg, A. M. and Hartmann, G. 2001. Identification of CpG oligonucleotide

sequences with high induction of IFN-alpha/beta in plasmacytoid dendritic cells. *Eur. J. Immunol.* **31**: 2154–2163.
21. Kurata, K., Iwata, A., Masuda, K., Sakaguchi, M., Ohno, K. and Tsujimoto, H. 2004. Identification of CpG oligodeoxynucleotide sequences that induce IFN-gamma production in canine peripheral blood mononuclear cells. *Vet. Immunol. Immunopathol.* **102**: 441–450.
22. Liang, H., Nishioka, Y., Reich, C. F., Pisetsky, D. S. and Lipsky, P. E. 1996. Activation of human B cells by phosphorothioate oligodeoxynucleotides. *J. Clin. Invest.* **98**: 1119–1129.
23. Liu, N., Ohnishi, N., Ni, L., Akira, S. and Bacon, K. B. 2003. CpG directly induce T-bet expression and inhibits IgG1 and IgE switching in B cells. *Nat. Immunol.* **4**: 687–693.
24. Marshall, J. D., Fearon, K. L., Abbate, C., Subramanian, S. Yee, P., Gregorio, J., Coffman, R. L. and Van Nest, G. 2003. Identification of a novel CpG DNA class and motif that optimally stimulate B cell and plasmacytoid dendritic cell functions. *J. Leukoc. Biol.* **73**: 781–792.
25. Milner, R. J., Salute, M., Crawford, C., Abbot, J. R. and Farese, J. 2006. The immune response to disialoganglioside GD3 vaccination in normal dogs: a melanoma surface antigen vaccine. *Vet. Immunol. Immunopathol.* **114**: 273–284.
26. Moore, K. W., de Waal Malefyt, R., Coffman, R. L. and O' Garra, A. 2001. Interleukin-10 and the Interleukin-10 receptor. *Ann. Rev. Immunol.* **19**: 683–765.
27. Ohmori, K., Maeda, S., Okayama, T., Masuda, K., Ohno, K. and Tsujimoto, H. 2004. Molecular cloning of canine activation-induced cytidine deaminase (AID) cDNA and its expression in normal tissues. *J. Vet. Med. Sci.* **66**: 739–741.
28. Ren, J., Sun, L., Yang, L., Wang, H., Wan, M., Zhang, P., Yu, H., Guo, Y., Yu, Y. and Wang, L. 2010. A novel canine favored CpG oligodeoxynucleotide capable of enhancing the efficacy of an inactivated aluminum-adjuvanted rabies vaccine of dog use. *Vaccine* **28**: 2458–2464.
29. Suematsu, S., Matsuda, T., Aozasa, K., Akira, S., Nakano, N., Ohno, S., Miyazaki, J., Yamamura, K., Hirano, T. and Kishimoto T. 1989. IgG1 plasmacytosis in interleukin 6 transgenic mice. *Proc. Natl. Acad. Sci. U.S.A.* **86**: 7547–7551.
30. Tokunaga, T., Yamamoto, T. and Yamamoto, S. 1999. How BCG led to the discovery of immunostimulatory DNA. *Jpn. J. Infect. Dis.* **52**: 1–11.
31. Verthelyi, D., Ishii, K. J., Gursel, M., Takeshita, F. and Klinman, D. M. 2001. Human peripheral blood cells differentially recognize and respond to two distinct CpG motifs. *J. Immunol.* **166**: 2372–2377.
32. Vollmer, J., Weeratna, R., Payette, P., Jurk, M., Schetter, C., Laucht, M., Wader, T., Tluk, S., Liu, M., Davis, H. L. and Krieg, A. M. 2004. Characterization of three CpG oligodeoxynucleotide classes with distinct immunostimulatory activities. *Eur. J. Immunol.* **34**: 251–262.
33. Wernette, C. M., Smith, B. F., Barksdale, Z. L., Hecker, R. and Baker, H. J. 2002. CpG oligodeoxynucleotides stimulate canine and feline immune cell proliferation. *Vet. Immunol. Immunopathol.* **84**: 223–236.

学会発表要旨

演者名	S. Kawarai, A. Fujimoto, G. Nozawa, N. Kanemaki, H. Madarame, T. Shida, A. Kiuchi
演題名	Decreasing methicillin-resistant Staphylococcal colonization in allergic dog skin by shampoo
学会名	The Asian Meeting of Animal Medicine Specialties
場所、開催日	Bogor,Indonesia, Dec, 2013

We evaluated the effects of shampoo against methicillin-resistant Staphylococcus (MRS) colonization in dogs with allergic dermatitis in a pilot clinical trial. Six allergic dogs were referred to our hospital for weekly shampoo for 1 month. Diagnosis of canine atopic dermatitis (CAD) and adverse food reactions were made based on Favrot's criteria for CAD, serum allergen-specific immunoglobulin E (IgE) tests and food elimination and/or provocation trials. The Canine Atopic Dermatitis Extent and Severity Index (CADESI-03) by veterinarians, pruritus score by owners, and isolation frequencies of *mecA*-positive *Staphylococcus* spp. from skin surface of the three body site between weeks 0 and 4 were compared. Polymerase chain reaction was used for evaluation of *mecA* gene. There was no significant difference in CADESI-03; however, the pruritus scores showed the significance ($p < 0.05$, Wilcoxon signed-rank test). The frequencies of MRS isolated from the skin surface also decreased in 4 of the 6 dogs ($p < 0.05$, Mann-Whitney U test). MRS is usually colonized and associated with recurrent pyoderma in allergic dog skin. Decrease of MRS by the shampoo presents useful for control of allergic dog skin.

学会発表要旨

演者名	村上弘正、細川聖矢、川原井晋平、斑目広郎
演題名	減感作療法を実施した犬アトピー性皮膚炎の 2 例
学会名	日本小動物獣医学会東北地区大会
場所、開催日	郡山市、2013 年 10 月

【目的】減感作療法は犬アトピー性皮膚炎に対する根本的治療法のひとつである。段階的に濃度を濃く調整した抗原液を定期的に皮下投与することで、抗原に対する過敏反応を減少させる。一般的に初回抗原液の濃度は、感作抗原毎に Protein Nitrogen Unit（PNU）を用いた一定の希釈倍率により定められているが、抗原に対する感作は個々の症例において異なることが考えられる。今回、初回に投与する抗原濃度を皮内反応によって決定し、重篤な副作用がなく減感作療法を実施できた犬の 2 例について報告する。

【材料と方法】症例 1 は 10 歳 1 カ月齢の雌の柴犬で、瘙痒と顔面（口唇・眼周囲)、下腹部、四肢端、陰部から肛門、尾根部にかけて紅斑、色素沈着、苔癬化を呈していた。Favrot（2010）の診断基準をもとに犬アトピー性皮膚炎と診断した。皮内反応検査によりコナヒョウヒダニに対して陽性反応を示したことから、検査陰性となる抗原液の濃度から減感作療法を実施した。症例 2 は 3 歳 9 カ月齢の去勢雄のペキニーズで、体幹に瘙痒を認め、頸部、腋下、腹部、背部体幹、四肢端に脂漏と丘疹を認めていた。除去食試験に反応して臨床症状の改善が認められ、Favrot（2010）の診断基準をもとに犬アトピー性皮膚炎と食物有害反応の併発と診断した。皮内反応検査を実施してコナヒョウヒダニに対する犬アトピー性皮膚炎と診断し、検査陰性となる抗原液の濃度から減感作療法を実施した。

【結果および考察】症例 1 は実施 2 カ月後に、2 日に 1 回処方を行っていたプレドニゾロン（0.5 ㎎/㎏）の休薬が可能となった。実施 4 カ月半後に抗原液の維持量に達し、以降 1 年間、1 カ月に 1 回の投薬とした。現在、外用副腎皮質ホルモン剤（コルタバンス、Virbac、大阪）を症状悪化時のみに少量使用するだけで良好に症状が維持できている。症例 2 は、減感作療法をフマル酸クレマスチン（タベジール錠、ノバルティスファーマ、東京）と併用して実施した。実施 6 カ月後に抗原液が維持量に達し、以降 8 カ月、1 カ月に 1 回の投薬を行った。現在、食物有害反応の発症に注意しながら、抗ヒスタミン剤の内服および外用副腎皮質ホルモン剤（コルタバンス）を少量使用するだけで症状が良好に維持できている。皮内検査を指標に、初回抗原濃度を症例に合わせて決定し、減感作療法を実施できた。今後、症例数を増やして、副作用の少ない効率的な治療方法を検討していく必要がある。

学会発表要旨

演者名	飯野瑞貴、西本優子、藤本あゆみ、野澤源太、川原井晋平、信田卓男、木内明男
演題名	犬のアレルギー性皮膚炎の症状維持におけるマイクロバブルを用いたシャンプー療法の有効性の検討
学会名	日本動物看護学会関西地区第 5 回例会
場所、開催日	大阪、2012 年 3 月

【目的】犬のアレルギー性皮膚炎は、根治困難な疾患であり日常的な症状の維持が重要である。その増悪因子として薬剤感受性ブドウ球菌の存在が知られている。シャンプー療法は被毛に付着したアレルゲンの除去および感染症の予防に有効である。マイクロバブルを用いたシャンプー療法によって臨床症状の維持が可能であるか、有効性を検討した。

【材料と方法】麻布大学附属動物病院に来院したアレルギー性皮膚炎と診断された犬 3 頭。週 1 回、シャワーヘッド型マイクロバブルを用いてシャンプー療法を実施した。試験前と試験 4 週後に獣医師による皮膚重症度スコア、飼い主による痒みのスコア、皮膚から培養した菌種の同定および薬剤感受性、看護師による被毛の観察を行った。

【結果および考察】獣医師による皮膚重症度スコアに変化は認められなかったが、飼い主による痒みのスコアは 3 例中 2 例において改善した。細菌培養検査では、3 症例中 2 例において試験 4 週後の検査結果が陰性となった。看護師がみた皮膚と被毛の状態については、試験前と比べて、全症例で皮膚の発赤が減少し、発毛が認められた。以上から犬のアレルギー性皮膚炎における臨床症状の維持にマイクロバブルを用いたシャンプー療法は有効であると考えられた。今回は対象症例が 3 頭だったため、今後対象症例を増やして検討していくことが必要である。

学会発表要旨

演者名	細川聖矢、川原井晋平、津久井利広、久末正晴、印牧信行、斑目広郎、土屋亮、小方宗次
演題名	国産コナヒョウヒダニ抗原液の有用性に関する再考.
学会名	第 154 回日本獣医学会学術集会.
場所、開催日	岩手、2012 年 9 月

【目的】犬のアトピー性皮膚炎の原因アレルゲンを同定するためのアレルギー検査は主に皮内反応検査と血清抗原特異的 IgE 検査が実施されている。血液検査を外注する血清抗原特異的 IgE 検査は簡便であるが、受託機関において多様な方法で実施されており、検査機関において結果が異なることが課題となっている。そこで、質の高い犬のアトピー性皮膚炎罹患症例のゲノム DNA を採取するため、皮内反応検査を麻布大学にて立ち上げを行った。

【材料と方法】 麻布大学附属動物病院に来院した CAD が疑われる症例 29 頭を対象とし、IDT と IgE test を実施した。IDT は国産抗原液として鳥居薬品（株）製を 1:100～1:10000(w/v)の濃度と、輸入抗原液として Greer 社製を 1:50000（w/v）の濃度で用い、紅斑のある膨疹形成を陽性とした。IgE test はヒト高親和性 IgE レセプターα鎖を用いた ELISA 法を用いて 150LU 以上を陽性として外部機関で測定した。それぞれの関連性を Fisher's exact test を用いて統計解析した。

【結果および考察】 IgE test と輸入抗原液を用いた IDT の間に有意差を認めた（$P<0.01$）。1:100（w/v）と 1:10000（w/v）の国産抗原液は、IgE test および輸入抗原液との間に有意差が認められた（$P<0.05$）。以上より、国産抗原液の犬アトピー性皮膚炎の診断における有用性が明らかとなった。

学会発表要旨

演者名	Kawarai S, Takahashi R, Madarame H, Shirota K.
演題名	A case of granulomatous dermatitis in a dog.
学会名	The Asian Meeting of Animal Medicine Specialties.
場所、開催日	Thailand , May, 2011.

Cutaneous sterile pyogranuloma /granuloma syndrome (SPGS) is a locally restricted multinodular dermatitis. Affected dogs are typically healthy, but a few show systemic signs. Herein, a case of a dog presenting with generalized ulcerative dermatitis with systemic signs of mild anemia and an increased C-reactive protein level is described. Cutaneous SPGS was diagnosed by histopathology, negative staining causative organisms, and polymerase chain reaction for Mycobacterium spp. Successful treatment was achieved by immunosuppressive drugs, including prednisolone and azathioprine, administered for at least 20 mo. Recurrences of skin lesions were observed when prednisolone and/or azathioprine were discontinued. Long-term management with immunosuppressive agents may be required if the affected dog exhibits severe symptoms of cutaneous SPGS.

犬のアトピー性皮膚炎の遺伝子解析

村上裕信（麻布大学衛生学第 2)、佐々木慎二(社団法人畜産技術協会附属動物遺伝研究所)、岡本憲明、島倉秀勝、阪口雅弘（麻布大学微生物学第 1)

研究要旨

犬のアトピー性皮膚炎(cAD)は環境や食物中に含まれる抗原への過敏反応であり、人のアトピー性皮膚炎と病態が類似しているだけでなく、疾病と遺伝的背景が密接に関与していることが疑われている。そこで、cAD に関連する遺伝子を網羅的に探索するために、cAD を発症した犬の血液サンプルを収集し、さらに収集したサンプルの血清からダニに対する特異的 IgE を検出した。その結果、cAD であり、IgE 陽性の柴犬 29 頭と、cAD 未発症で IgE が検出されなかった柴犬 19 頭を収集できたため、これらの DNA サンプルを用いて DNA アレイを行い、cAD に関連する遺伝子があるのかを解析した。cAD 発症犬では第 29 番および 8 番染色体の限局した領域に一塩基多型(SNP)が認められ、そのうちひとつは第 29 番染色体にコードされている機能不明な RBM12B 遺伝子のエクソン上の SNP であることが明らかとなった。本研究ではアレルギーに関連する遺伝子上または近傍の SNP は認められなかったが、第 29 番染色体上に cAD に関連する遺伝子領域が有ることが示唆された。

目的

犬のアトピー性皮膚炎(cAD)は環境や食物中に含まれる抗原への過敏反応であり、人のアトピー性皮膚炎と病態が類似している。また、cAD は家族性素因だけでなく犬種により発生率が異なることから、人と同様、疾病と遺伝的背景が密接に関与していることが疑われる。このことから、cAD 発症に寄与する遺伝子を同定することにより、cAD の治療に寄与するだけでなく人のアトピー性皮膚炎に関連する遺伝子である可能性が考えられ、治療の基礎的な知見となるため、cAD に関連する遺伝子領域を網羅的に解析した。

材料と方法

柴犬、フレンチブルドック、ミニチュアダックスフント、トイプードルのいずれかの犬種であり、同じ地域で室内飼育されている犬に限定して血液サンプルの収集を行った。cAD の診断については、Favrot の診断基準(Veterinary Dermatology, 2009)に準じた 7 項目(3 歳以下で発症、ステロイド投薬で痒みが治まる、損傷の伴わない痒み、前肢に病変がある、耳介に病変がある、耳の辺縁には病変がない、腰背部に病変がない)のうち 5 項目が当てはまった場合に cAD と診断した。また、cAD を発症していない健常犬は 7 歳以上で cAD を疑う症状がなく、過去においても症状がない個体とした。これらの診断は同じ獣医師によって行うことにより、診断基準を統一した。これらの cAD 発症犬お

よび未発症犬から採血を行い、血液サンプルから血清分離および DNA 抽出を行った。これらのサンプルは、血清を用いた ELISA によりダニアレルゲン特異的 IgE の検出、DNA は DNA アレイにより、SNP 解析を行った。

結果および考察

cAD 好発犬種である柴犬、フレンチブルドック、ミニチュアダックスフント、トイプードルの血液サンプルの収集を行い、cAD 発症犬は、柴犬 45 頭、ミニチュアダックスフント 33 頭、トイプードル 30 頭、フレンチブルドック 20 頭の計 128 頭から DNA サンプルを得られた。また、健常犬は柴犬 20 頭、ミニチュアダックスフント 41 頭、トイプードル 16 頭、フレンチブルドック 2 頭の計 79 頭から DNA サンプルを得ることができた。さらに、cAD 発症犬においてダニアレルゲン特異的 IgE 抗体検査を行ったところ、柴犬では 72.5%と他の犬種より高い抗体保有率(フレンチブルドック:55.6%, ミニチュアダックスフント:50.0%, トイプードル:20%)であった。これらのサンプルを用いて、cAD の原因遺伝子を網羅的に探索するため、柴犬のサンプルを用いてダニアレルゲン特異的 IgE 陽性の cAD 発症犬 29 頭と IgE 陰性で cAD 未発症犬 19 頭において DNA アレイを用いた SNP の網羅的遺伝子解析を行った。その結果、cAD 陽性群で認められた SNP の上位 5 つ(図 1)が第 29 番染色体に存在し、上位 6〜20 が第 8 番染色体に存在していた(表 1)。この第 29 番染色体の 5 つの SNP のうち 2 つの SNP は遺伝子がコードされている領域のものであり、 第 29 番染色体 41,618,514 番塩基の SNP は詳細な機能が不明な RBM12B 遺伝子のエクソンに、41,640,547 番塩基の SNP は線毛構造に関与する TMEM67 のイントロンに位置していた。その他の 3 つの SNP は遺伝子がコードされていない領域に位置していたが、これら 5 つの SNP は約 600kbp 内に集中して存在していた。また、第 8 番染色体の 11 の SNP(塩基番号: 4,976,006、 4,989,539、 4,990,277、 4,992,651、 5,007,184、 5,021,922、 5,041,692、 5,066,269、 5,072,825、 5,083,229、 5,099,699)は細胞死に関与する IPTK1 遺伝子上のイントロン領域に位置しており、他の 4 つの SNP(塩基番号: 4,926,998、 4,939,363、 4,940,129、 4,954,751)は遺伝子がコードされていない領域に位置していた。これらの第 8 番染色体上の 15 の SNP は約 90kbp 内に密集して位置していた。これらの SNP の近傍にはアレルギーに関与する遺伝子は認められなかったが、第 29 番染色体の SNP の近傍には RBM12B 同様に機能が不明な遺伝子である LOC100685605 などが位置していた。以上のことから第 8 および 29 番染色体上に cAD に関連する SNP が認められ、特に第 29 番染色体には cAD 発症犬で高頻度に 5 つの SNP が限局して認められたことから、cAD に関連する遺伝子が第 29 番染色体に存在することが示唆された。また、この第 29 番染色体の SNP は cAD 発症犬で高頻度に認められることから、cAD 発症予測に有用である可能性も考えられる。

図 1　cAD 発症犬のゲノムワイド関連解析

A. Q-Q プロット

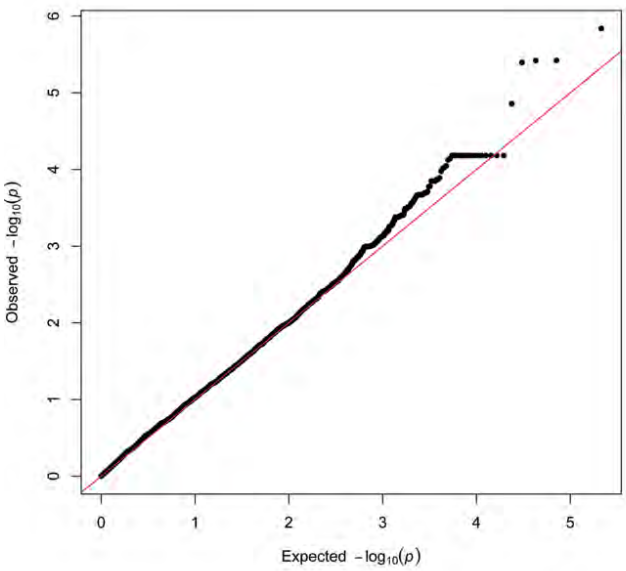

B. マンハッタンプロット

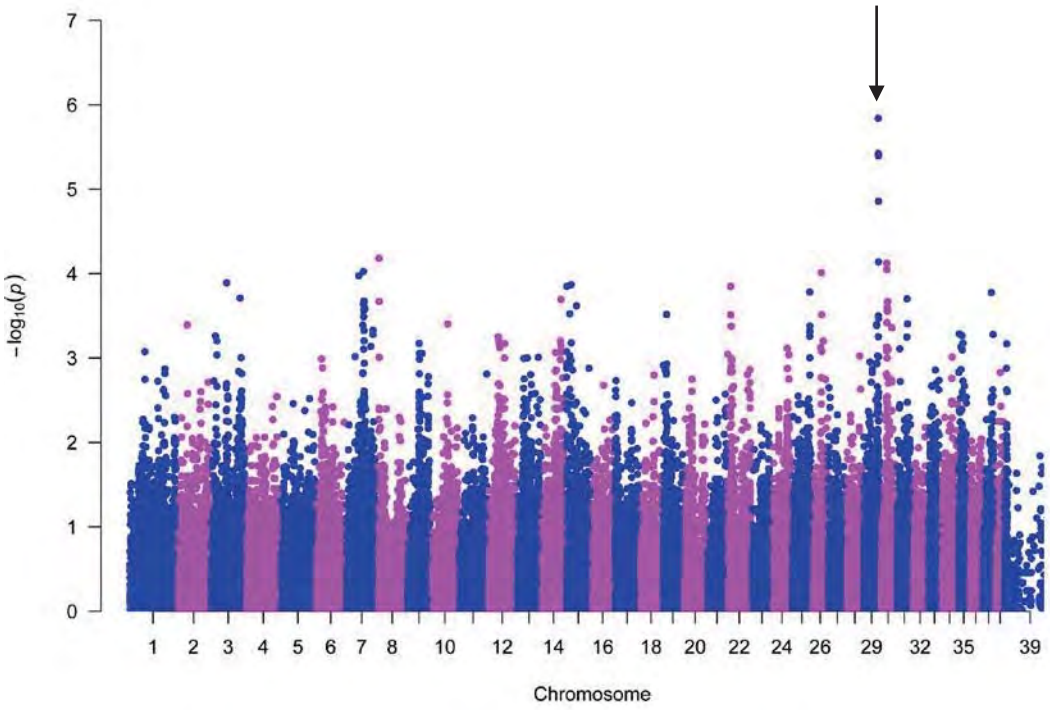

表 1 cAD 発症犬で高頻度に認められる SNP

順位	染色体	位置	P 値	頻度	
				Case	Control
1	29	41126533	1.45282E-06	0.7931	0.2941
2	29	41618514	3.78361E-06	0.5000	0.02941
3	29	41300904	3.80005E-06	0.7931	0.3235
4	29	41640547	4.03532E-06	0.7414	0.2647
5	29	41703308	1.39326E-05	0.6552	0.1765
6	8	4926998	6.58203E-05	0.1379	0.4706
7	8	4939363	6.58203E-05	0.1379	0.4706
8	8	4940129	6.58203E-05	0.1379	0.4706
9	8	4954751	6.58203E-05	0.1379	0.4706
10	8	4976006	6.58203E-05	0.1379	0.4706
11	8	4989539	6.58203E-05	0.1379	0.4706
12	8	4990277	6.58203E-05	0.1379	0.4706
13	8	4992651	6.58203E-05	0.1379	0.4706
14	8	5007184	6.58203E-05	0.1379	0.4706
15	8	5021922	6.58203E-05	0.1379	0.4706
16	8	5041692	6.58203E-05	0.1379	0.4706
17	8	5066269	6.58203E-05	0.1379	0.4706
18	8	5072825	6.58203E-05	0.1379	0.4706
19	8	5083229	6.58203E-05	0.1379	0.4706
20	8	5099699	6.58203E-05	0.1379	0.4706

研究発表

1.発表論文

1) Yuan Y, Kitamura-Muramatsu Y, Saito S, Ishizaki H, Nakano M, Haga S, Matoba K, Ohno A, Murakami H, Takeshima SN, Aida Y. Detection of the BLV provirus from nasal secretion and saliva samples using BLV-CoCoMo-qPCR-2: Comparison with blood samples from the same cattle. Virus Res 210:248-54,2015.

2) 村上裕信、間陽子: HIV-1 アクセサリー蛋白質 Vpr と宿主因子. 臨床免疫・アレルギー科. 63:484-488,2015.

3) Aida Y, Murakami H, Takahashi M, Takeshima S.: Mechanisms of pathogenesis induced by bovine leukemia virus (BLV) as a model for human T-cell leukemia virus (HTLV)" Front. Microbiol 4:328, 2013.

2.学会発表

1) 村上裕信、二階堂紗恵、佐藤礼一郎、塚本健司： 牛白血病ウイルス G4 遺伝子欠損株のウイルス産生量. 第 63 回日本ウイルス学術集会、福岡、11 月 2015 年

2) 鈴木千裕、戸髙晴菜、二階堂紗恵、佐藤礼一郎、塚本健司、村上裕信: BLV 感染性分子クローンを用いたウイルス産生量とゲノム変異の解析. 第 63 回日本ウイルス学術集会、福岡、11 月 2015 年

3) 村上裕信、萩原恭二、鈴木健裕、堂前直、間陽子: プロテオミクス法により同定した新規 Vpr 結合因子 PRMT5/7 によるウイルス複製制御機構. 第 27 回日本エイズ学術集会、11 月 2013 年

4) 村上裕信、萩原恭二、鈴木健裕、堂前直、間陽子: 新規 Vpr 結合因子のプロテオミクス法による同定およびウイルス産生への影響. 第 61 回日本ウイルス学会学術集会、神戸、11 月 2013 年

Virus Research 210 (2015) 248–254

Contents lists available at ScienceDirect

Virus Research

journal homepage: www.elsevier.com/locate/virusres

Detection of the BLV provirus from nasal secretion and saliva samples using BLV-CoCoMo-qPCR-2: Comparison with blood samples from the same cattle

Yuan Yuan[a,1], Yuri Kitamura-Muramatsu[a,1], Susumu Saito[a,*], Hiroshi Ishizaki[b], Miwa Nakano[b], Satoshi Haga[b], Kazuhiro Matoba[b], Ayumu Ohno[c], Hironobu Murakami[d], Shin-nosuke Takeshima[c], Yoko Aida[c,**]

[a] RIKEN GENESIS CO., LTD., RIKEN Yokohama Institute, East Research Building 3F, 1-7-22 Suehiro-cho, Tsurumi-ku, Yokohama, Kanagawa 230-0045, Japan
[b] NARO Institute of Livestock and Grassland Science, 768 Senbonmatsu, Nasushiobara, Tochigi 329-2793, Japan
[c] Viral Infectious Diseases Unit, RIKEN, 2-1 Hirosawa, Wako, Saitama 351-0198, Japan
[d] School of Veterinary Medicine, Azabu University, 1-17-71 Fuchinobe, Chuo-ku, Sagamihara, Kanagawa 252-5201, Japan

ARTICLE INFO

Article history:
Received 30 April 2015
Received in revised form 12 August 2015
Accepted 12 August 2015
Available online 20 August 2015

Keywords:
Proviral load
BLV-CoCoMo-qPCR-2
Nasal secretion
Saliva
Blood

ABSTRACT

Bovine leukemia virus (BLV) induces enzootic bovine leukosis, which is the most common neoplastic disease in cattle. Sero-epidemiological studies show that BLV infection occurs worldwide. Direct contact between infected and uninfected cattle is thought to be one of the risk factors for BLV transmission. Contact transmission occurs via a mixture of natural sources, blood, and exudates. To confirm that BLV provirus is detectable in these samples, matched blood, nasal secretion, and saliva samples were collected from 50 cattle, and genomic DNA was extracted. BLV-CoCoMo-qPCR-2, an assay developed for the highly sensitive detection of BLV, was then used to measure the proviral load in blood ($n = 50$), nasal secretions ($n = 48$), and saliva ($n = 47$) samples. The results showed that 35 blood samples, 14 nasal secretion samples, and 6 saliva samples were positive for the BLV provirus. Matched blood samples from cattle that were positive for the BLV provirus (either in nasal secretion or saliva samples) were also positive in their blood. The proviral load in the positive blood samples was >14,000 (copies/1×10^5 cells). Thus, even though the proviral load in the nasal secretion and saliva samples was much lower (<380 copies/1×10^5 cells) than that in the peripheral blood, prolonged direct contact between infected and healthy cattle may be considered as a risk factor for BLV transmission.

1. Introduction

Bovine leukemia virus (BLV), which is closely related to human T-cell leukemia virus types 1 and 2 (HTLV-1 and HTLV-2), is the etiologic agent of enzootic bovine leucosis (EBL), a disease characterized by a very extended course that often involves persistent lymphocytosis (PL) and culminates in B-cell lymphosarcoma (Aida et al., 2013). Sero-epidemiological studies show that BLV infection is a global phenomenon (Kobayashi et al., 2010; Kurdi et al., 1999; Monti and Frankena, 2005; Schoepf et al., 1997; VanLeeuwen et al., 2006; Wang, 1991; Zaghawa et al., 2002). The world organization for animal health lists EBL as a disease that can have a significant impact on international trade (Rodriguez et al., 2011).

Although BLV uses both horizontal and vertical transmission routes, horizontal transmission is one of the major routes of transmission in most settings (Hopkins and DiGiacomo, 1997). Horizontal transmission occurs through hematophagous insects (Bech-Nielsen et al., 1978; Buxton et al., 1985), prolonged direct contact between infected and uninfected cattle (Kono et al., 1983), and iatrogenic procedures such as dehorning (DiGiacomo et al., 1985), ear tattooing, and the use of infected needles and plastic sleeves (Hopkins and DiGiacomo, 1997; Hopkins et al., 1988). The virus is transmitted to cattle primarily through direct exposure to infected blood, saliva, semen, and milk (Hopkins and DiGiacomo, 1997).

After infecting cattle, BLV integrates into the genomic DNA of host lymphocytes as a provirus (Kettmann et al., 1982), leading to lifelong infection despite the induction of virus-neutralizing anti-

* Corresponding author. Fax: +81 45 521 8786.
** Corresponding author. Fax: +81 48 462 4399.
E-mail addresses: susumu.saito@rikengenesis.jp (S. Saito), aida@riken.jp (Y. Aida).
[1] These authors contributed equally to this work.

http://dx.doi.org/10.1016/j.virusres.2015.08.013
0168-1702/

bodies (Tajima et al., 2003). In addition to conventional serological tests such as agar gel immunodiffusion (Aida et al., 1989; Kurdi et al., 1999) and enzyme-linked immunosorbent assay (ELISA) (Beier et al., 2004; Kurdi et al., 1999; Trono et al., 2001), diagnostic BLV polymerase chain reaction (PCR) techniques are often used to detect the integrated BLV proviral genome within the host DNA (Lew et al., 2004; Nagy et al., 2003; Rola and Kuzmak, 2002; Tajima et al., 1998). In 2010, a new quantitative real-time PCR method (BLV-CoCoMo-qPCR) was developed, which is based on the use of Coordination of Common Motifs (CoCoMo) primers to measure the proviral load of both known and novel BLV variants in BLV-infected animals (Jimba et al., 2010, 2012; Miyasaka et al., 2013; Panei et al., 2013). The BLV-CoCoMo-qPCR technique amplifies a single-copy host gene, the bovine leukocyte antigen *BoLA-DRA* gene, in parallel with viral genomic DNA; this technique effectively normalizes the level of viral genomic DNA. Recently, a modified version of BLV-CoCoMo-qPCR, BLV-CoCoMo-qPCR-2 (which uses optimized degenerate primers), was developed (Polat et al., 2015; Takeshima et al., 2015).

Studies based on nucleotide and amino acid sequence comparisons demonstrate that different BLV variants occur in different geographical regions. Recent phylogenetic studies of the BLV *env* gene from strains isolated across the globe demonstrate that the virus can be classified into eight genotypes (Ababneh et al., 2012; Balic et al., 2012; Matsumura et al., 2011; Moratorio et al., 2010; Polat et al., 2015; Rodriguez et al., 2009; Rola-Luszczak et al., 2013).

Currently, genomic DNA can be isolated from a variety of sources, including whole blood, milk, semen, saliva, and nasal secretions (Foley et al., 2011; Mitsouras and Faulhaber, 2009). Therefore, to confirm whether BLV provirus is detected from these specimens, we collected matched blood, nasal secretion, and saliva samples from 50 animals and extracted the genomic DNA. We then used the BLV-CoCoMo-qPCR-2 to determine the absolute copy number of BLV provirus in nasal secretion and saliva samples, and compared the results with those from matched blood samples. Moreover, we sequenced the partial BLV gp51 *env* gene region to confirm the BLV genotype.

2. Materials and methods

2.1. Samples

Matched blood, nasal secretion, and saliva samples were obtained from 50 cattle (34 Japanese black, six Holstein-Friesian, and ten crossbred) in Japan. Blood samples used for PCR amplification and lymphocyte counts were collected from the neck vein using an ethylenediaminetetraacetic acid (EDTA) vacuum blood collection tube. Serum (used to detect anti-BLV antibodies) was obtained from blood collected from the same cattle using a vacuum blood collection tube. Nasal and saliva samples were collected using the Performagene Livestock PG-100 collection device (DNA Genotek Inc., Ontario, Canada) with minimum restraint. Samples were collected carefully to avoid contamination with blood. All experiments were conducted in accordance with the Guidelines for Laboratory Animal Welfare and Animal Experiment Control set out by the NARO Institute of Livestock and Grassland Science (permit numbers: NILGS-13053101 and NILGS-14112050).

2.2. Genomic DNA extraction

DNA was obtained from blood samples (300 μL) using the Wizard Genomic DNA Purification Kit (Promega K. K., Tokyo, Japan) and dissolved in 100 μL of DNA Rehydration Solution, according to the manufacturer's instructions (Promega K. K.). DNA was extracted from nasal and saliva samples (500 μL) using DNA Genotek purification protocol PD-PR-083 (DNA Genotek Inc.) and dissolved in 20 μL of TE buffer (10 mM Tris–HCl [pH 8.0] and 1 mM EDTA [pH 8.0]).

2.3. DNA quantity and quality

The quantity and quality of the DNA (A260/A280 ratio) were assessed using a NanoDrop ND-1000 Spectrophotometer (Thermo Fisher Scientific K. K., Kanagawa, Japan), according to the manufacturer's instructions. Furthermore, to test whether the quality of the extracted DNA was suitable for PCR amplification, and to examine the efficiency of amplification (threshold cycle value), DNA from a subset of the paired samples was subjected to real-time PCR to amplify a single-copy bovine gene: *BoLA-DRA* (DDBJ: D37956). A 151 bp fragment of the *BoLA*-DRA gene was amplified in a total volume of 20 μL comprising 1×TaqMan Gene Expression Master Mix containing 50 nM forward primer (5′-CCCAGAGTATGAAGCTCCAGCCC-3′), 50 nM reverse primer (5′-CCCTCGGCGTTCAACGGTGT-3′), 150 nM FAM-DRA probe (5′-FAM-TGTGTGCCCTGGGC-NFQ-MGB-3′), and 150 ng of template DNA. PCR was performed using the ABI 7500 Fast Dx Real-time PCR system according to the following program: Uracil-DNA Glycosylase (UDG) enzyme activation at 50 °C for 2 min, followed by AmpliTaq Gold Ultra Pure (UP) enzyme activation at 95 °Cfor 10 min, followed by 60 cycles of 15 s at 95 °C and 1 min at 60 °C.

2.4. Detection of anti-BLV antibodies in serum samples

Anti-BLV antibodies were detected using ELISA kits according to the manufacturer's instructions (JNC Inc., Tokyo, Japan).

2.5. Measurement of the BLV proviral load using BLV-CoCoMo-qPCR-2

The BLV proviral load was measured by BLV-CoCoMo-qPCR-2, as previously described (Polat et al., 2015; Takeshima et al., 2015), using 150 ng of template DNA. Briefly, the BLV long terminal repeat (LTR) region was amplified using the degenerate primer pair, CoCoMo-FRW and CoCoMo-REV. The *BoLA-DRA* gene (internal control) was amplified using the protocol described in "DNA quantity and quality" above.

2.6. PCR amplification and sequencing of BLV env gp51

Nested PCR was performed as described below (the nucleotide number (nt) indicates the position of the FLK-BLV subclone, pBLV913 [DDBJ: EF600696], within the nucleotide sequence). The first round of amplification (the full-length BLV gp51 *env* gene [913 bp]) was performed using the following primers (Moratorio et al., 2010): forward, 5′-ATGCCYAAAGAACGACGG-3′ (nt 4826–4843), and reverse, 5′-CGACGGGACTAGGTCTGACCC-3′ (nt 5738–5718). The second round of amplification (the partial BLV gp51 *env* gene [598 bp]) was carried out using the following primers (Asfaw et al., 2005): forward, 5′-TCTGTGCCAAGTCTCCCAGATA-3′ (nt 5037–5058), and reverse, 5′-AACAACAACCTCTGGGAAGGGT-3′ (nt 5634–5613). All reagents (except the primers) were contained within the PrimerSTAR GXL DNA Polymerase mix (Takara Bio Inc. Shiga, Japan). The final reaction mixture (25 μL/sample) used for the first round of amplification contained 100 ng of sample DNA, each primer (0.2 μM), 200 μM dNTPs, and 0.625 U PrimerSTAR GXL DNA Polymerase. The PCR conditions were as follows: 30 cycles of denaturation at 98 °C for 15 s, followed by annealing at 60 °C for 20 s, and extension at 68 °C for 1 min. The PCR product (1 μL for blood samples and 5 μL for nasal and saliva samples) from the first round of amplification was then used in a second round of amplification

Table 1
Detection of the BLV provirus using BLV-CoCoMo-qPCR-2 extracted from blood, nasal, and saliva sample.

Cattle	Breed	Age (years)	WBC (/μL)	LYMPH (/uL) (%)	ELISA[a]	Proviral load (copies/1 × 10^5 cells)[b]		
						Blood	Nasal	Saliva
896	Japanese black	2.0	5730	3080 (53.8)	–	0.00	0.00	0.00
922	Japanese black	1.8	7150	3670 (51.3)	–	0.00	0.00	0.00
926	Japanese black	1.8	8290	4080 (49.2)	–	0.00	0.00	0.00
916	Japanese black	1.8	6790	3430 (50.5)	–	0.00	0.00	0.00
917	Japanese black	1.8	7950	4480 (56.4)	–	0.00	0.00	0.00
797	Holstein	3.3	6030	3380 (56.1)	–	0.00	0.00	0.00
550	Holstein	5.9	5840	2850 (48.8)	–	0.00	0.00	0.00
832	Japanese black	2.8	9680	4850 (50.1)	–	0.00	0.00	0.00
836	Japanese black	2.8	10030	5250 (52.3)	–	0.00	0.00	0.00
842	Japanese black	2.8	10790	7800 (72.3)	–	0.00	0.00	0.00
958	Japanese black	1.9	12530	8380 (66.9)	–	0.00	0.00	0.00
959	Japanese black	1.8	6810	3720 (54.6)	–	0.00	0.00	N/A
960	Japanese black	1.8	6940	3410 (49.1)	–	0.00	0.00	0.00
881	Crossbred	2.2	8440	4400 (52.1)	–	2.00	0.00	0.00
927	Japanese black	1.8	9810	5510 (56.2)	–	2.77	0.00	0.00
961	Japanese black	1.7	8110	5370 (66.2)	–	4.92	0.00	0.00
837	Japanese black	2.8	11830	7060 (59.7)	–	30.93	0.00	0.00
586	Japanese black	5.6	7760	4190 (54.0)	+	0.00	0.00	0.00
554	Holstein	5.8	9030	3910 (43.3)	+	0.00	N/A	0.00
78	Crossbred	13.3	5840	2350 (40.2)	+	1.04	0.00	0.00
801	Japanese black	4.1	7960	3770 (47.4)	+	2.92	0.00	0.00
112	Crossbred	12.3	5760	3270 (56.8)	+	11.30	0.00	0.00
874	Crossbred	2.3	6070	2680 (44.2)	+	17.09	0.00	0.00
451	Holstein	8.1	6840	2750 (40.2)	+	120.33	0.00	N/A
869	Japanese black	2.5	7950	3410 (42.9)	+	227.49	0.00	0.00
914	Japanese black	1.8	8490	4580 (53.9)	+	555.17	0.00	0.00
532	Holstein	6.1	5900	3120 (52.9)	+	934.45	0.00	N/A
866	Japanese black	2.5	6530	3590 (55.0)	+	2489.92	0.00	0.00
681	Japanese black	4.6	6720	3320 (49.4)	+	3229.27	0.00	0.00
511	Holstein	6.3	7720	4010 (51.9)	+	13451.40	0.00	0.00
839	Japanese black	2.8	9110	5090 (55.9)	+	14448.86	0.10	0.00
829	Japanese black	2.8	12110	7380 (60.9)	+	18724.23	0.00	0.19
943	Japanese black	1.6	10490	6980 (66.5)	+	20911.28	22.15	0.00
920	Japanese black	1.8	10020	7280 (72.7)	+	22256.03	2.75	0.00
635	Crossbred	5.2	10330	4510 (43.7)	+	25606.87	N/A	0.00
677	Japanese black	4.6	13000	8210 (63.2)	+	27211.34	6.66	0.00
522	Japanese black	6.2	8090	3690 (45.6)	+	27211.50	0.00	0.00
688	Japanese black	4.5	16390	7380 (45.0)	+	29161.25	0.00	0.00
938	Japanese black	1.7	14410	11440 (79.4)	+	29294.26	16.48	2.56
674	Japanese black	4.6	8080	4150 (51.4)	+	29443.66	24.19	1.09
118	Crossbred	12.2	12560	9600 (76.4)	+	33240.22	22.48	0.00
82	Crossbred	13.3	9000	5700 (63.3)	+	35778.32	4.86	0.00
856	Japanese black	2.7	15840	11040 (69.7)	+	44995.08	25.79	2.11
571	Japanese black	5.8	13210	8180 (61.9)	+	45742.17	13.09	5.06
425	Crossbred	7.3	10220	6770 (66.2)	+	51469.03	1.34	0.00
207	Crossbred	10.3	12280	8720 (71.0)	+	51898.17	0.00	0.00
838	Japanese black	2.8	21610	15690 (72.6)	+	52951.79	0.00	0.00
774	Japanese black	3.5	16250	12030 (74.0)	+	54684.07	2.71	0.00
676	Japanese black	4.6	16720	12390 (74.1)	+	58062.62	8.53	0.00
216	Crossbred	10.1	20400	14340 (70.3)	+	62601.38	1.87	379.70

N/A, not analyzed.

[a] ELISA was performed using an anti-BLV ELISA kit according to the manufactcture's instructions (JNC Inc., Tokyo, Japan). +, positive for anti-BLV antibodies; –, negative for anti-BLV antibodies.

[b] The proviral load (expressed as the copy number per 10^5 cells) was evaluated by BLV-CoCoMo-qPCR as previously described (Jimba et al., 2010). The copy number of the single copy of the bovine leukocyte antigen *BoLA-DRA* gene was used to evaluate the cell number in the blood, nasal secretion and saliva.

Table 2
The comparison between the results of BLV-CoCoMo-qPCR-2 and ELISA.

		ELISA		Total
		Positive	Negative	
BLV-CoCoMo-qPCR-2	Positive	31	4	35
	Negative	2	13	15
Total		33	17	50
		Sensitivity (%) (95% CI)	Specificity (%) (95% CI)	
		93.9 (79.8–99.3)	76.5 (50.1–93.2)	

CI, confidence interval.

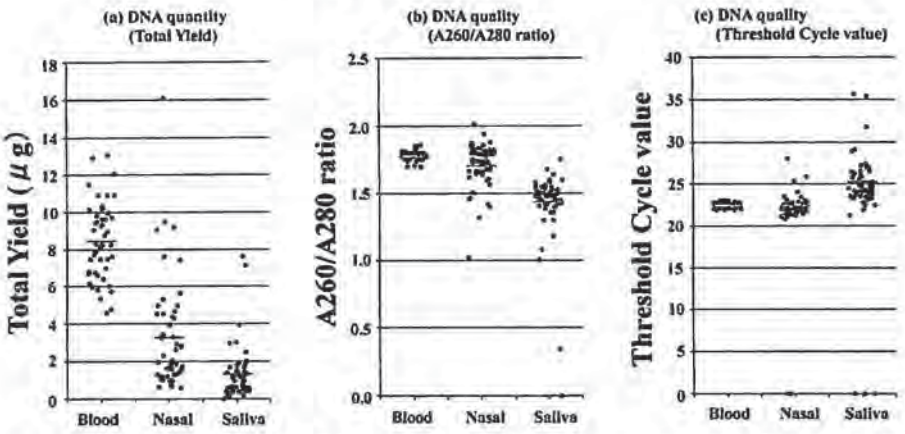

Fig. 1. Scatter plot showing the quantity (a) and quality (b and c) of DNA in samples obtained from 50 cattle. Matched blood, nasal, and saliva samples were obtained, and DNA was extracted and purified as described in the "Methods". The average total yield of DNA (blood, 8.46 μg; nasal, 3.30 μg; and saliva, 1.33 μg), the A260/A280 ratio (blood, 1.78; nasal, 1.70; and saliva, 1.44), and the threshold cycle value (blood, 22.49; nasal, 22.46; and saliva, 25.35) are indicated by red lines. (For interpretation of the references to color in this figure legend, the reader is referred to the web version of this article.)

Table 3
The sensitivity and specificity of BLV-CoCoMo-qPCR-2 for nasal secretion (a), and saliva (b).

(a) Nasal secretion

		Blood		Total[a]
		BLV provirus positive	BLV provirus negative	
Nasal secretion	BLV provirus positive	14	0	14
	BLV provirus negative	20	14	34
Total[a]		34	14	48
		Sensitivity (%) (95% CI)	Specificity (%) (95% CI)	
		41.2 (24.7–59.3)	100 (76.8–100)	

(b) Saliva

		Blood		Total[b]
		BLV provirus positive	BLV provirus negative	
Saliva	BLV provirus positive	6	0	6
	BLV provirus negative	27	14	41
Total[b]		33	14	47
		Sensitivity (%) (95% CI)	Specificity (%) (95% CI)	
		18.2 (7.0–35.5)	100 (76.8–100)	

CI, confidence interval.
[a] Two nasal secretion samples were not amplified the *BoLA-DRA* gene. These samples were discarded. A total of 48 sample was analyzed.
[b] Three saliva samples were not amplified the *BoLA-DRA* gene. These samples were discarded. A total of 47 sample was analyzed.

under the same conditions. Amplicons were purified using a Wizard SV Gel and PCR Clean-Up System (Promega K. K.). Both strands of the purified amplicon were sequenced using the second round amplification primers, a Big Dye Terminator v3.1Cycle Sequencing Kit (Life Technologies, Tokyo, Japan), and a 3730 DNA Sequencer (Life Technologies).

3. Results

DNA was extracted from matched blood, nasal secretion, and saliva samples collected from 50 cattle (34 Japanese black, six Holstein-Friesian, and ten crossbred). DNA was obtained from all 50 blood and nasal secretion samples, and from 49 saliva samples. Scatter plots showing DNA quantity (a) and quality (b and c) are shown in Fig. 1. The average DNA yield from 300 μL of blood, 500 μL of nasal secretions, and 500 μL of saliva was 8.46 μg, 3.30 μg, and 1.33 μg, respectively. The quality of the DNA (average A260/A280 ratio) obtained from blood, nasal secretions, and saliva was 1.78, 1.70, and 1.44, respectively.

All DNA samples were subjected to PCR to amplify the *BoLA-DRA* gene, and the efficiency of amplification was tested as a measure of DNA sample quality. The *BoLA-DRA* gene was amplified from all 50 blood samples. However, two nasal secretion samples (animals 554 and 635) and three saliva samples (animals 451, 532, and 959) failed; therefore, these samples were discarded. The average threshold cycle value (Ct value) obtained for the blood, nasal secretion, and saliva samples was 22.49, 22.46, and 25.35, respectively.

We next used BLV-CoCoMo-qPCR-2 to detect the BLV provirus in DNA extracted from 50 blood, 48 nasal secretion, and 47 saliva samples (Table 1). Of these, 35 blood samples, 14 nasal secretion samples, and six saliva samples were positive for the BLV provirus. Only five cattle (animals 938, 674, 856, 571, and 216) harbored the BLV provirus in genomic DNA extracted from matched blood, nasal secretion, and saliva samples. However, the provirus was detected

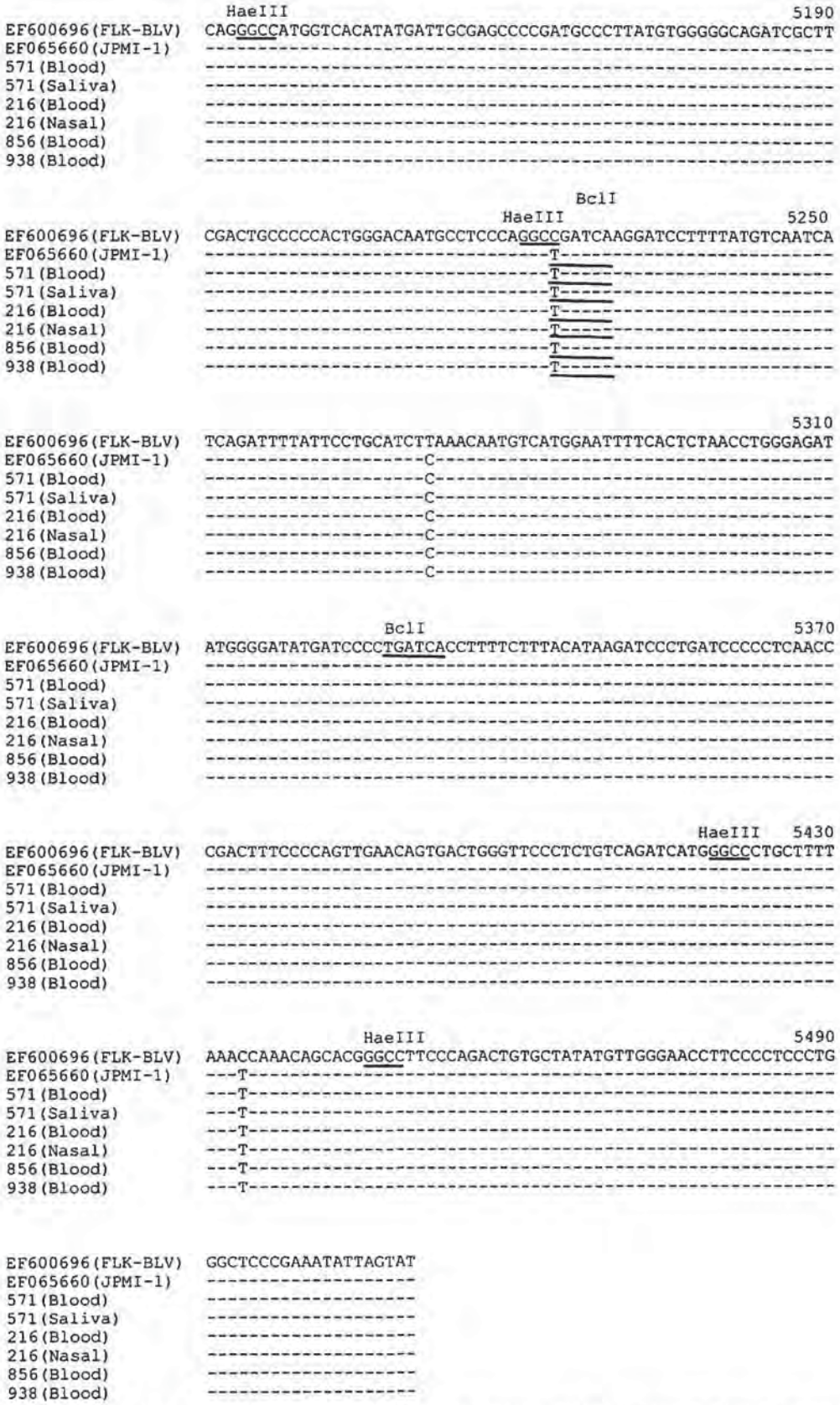

Fig. 2. DNA sequence alignment of the partial BLV gp51 *env* gene region. The reference sequence, EF600696 (FLK-BLV), is shown at the top. The nucleotide number is indicated on the right-hand side of the figure. The sequences of the BLV isolates identified in this study were aligned with that of a previously sequenced BLV variant, EF065660 (JPMI-1). Dashes represent nucleotides that match the reference sequence. When compared with the reference strain, nucleotide substitutions were observed at positions 5224 (C to T), 5272 (T to C), and 5434 (C to T). The cleavage sites for the restriction enzymes *Hae* III and *Bcl* I are underlined.

in matched blood samples and nasal secretion samples from nine animals (animals 839, 943, 920, 677, 118, 82, 425, 774, and 676), and in matched blood and saliva samples from one animal (animal 829). Interestingly, the proviral load in blood samples from these cattle was >14,000 copies/1 × 10^5 cells.

We next compared the specificity and sensitivity of the PCR for the BLV provirus with that of an ELISA designed to detect anti-BLV antibodies in the blood (Table 2). A total of 13/50 cattle (26%) were negative for both the BLV provirus (according to BLV-CoCoMo-qPCR-2) and anti-BLV antibodies (according to a conventional ELISA). Furthermore, 31/50 cattle (62%) were positive for both the BLV provirus and anti-BLV antibodies. Of the 17 cattle that were negative for antibodies, 13 were also negative for the BLV provirus (specificity: 76.5%; 95% CI: 50.1–93.2%), and of the 33 cattle that were positive for antibodies, 31 were also positive for the BLV provirus (sensitivity: 93.9%; 95% CI: 79.8–99.3%).

Table 3 shows the specificity and sensitivity of BLV-CoCoMo-qPCR-2 for nasal secretion (a), saliva (b). 41.2% (95% CI: 24.7–59.3%) of the nasal secretion samples were positive among a total of 34 blood samples. 18.2% (95% CI: 7.0–35.5%) of the saliva samples were also positive among a total of 33 blood samples. Finally, we sequenced a partial BLV gp51 *env* gene region to confirm whether PCR products detected from nasal secretion and saliva samples by BLV-CoCoMo-qPCR-2, really derived from BLV, and these results are identical to those from blood samples from the same animal. Samples from four of the five animals (nos. 216, 571, 856, and 938) that were positive for the BLV provirus in matched blood, nasal secretion, and saliva samples were sequenced. Results were obtained for four blood samples, one saliva sample (animal 571), and one nasal secretion sample (animal 216) (Fig. 2). The nucleotide sequences obtained from the saliva (animal 571) and nasal secretion (animal 216) samples were identical to those obtained from blood samples from the same animals. These sequences were aligned with that of a previously sequenced BLV variant, EF065660 (JPMI-1; also isolated in Japan), and with corresponding sequences from reference strain EF600696 (FLK-BLV) (Fig. 2). The sequences of all BLV strains isolated in the present study were identical to that of strain EF065660 (JPMI-1). When these sequences were aligned with reference strain EF600696 (FLK-BLV), we identified three nucleotide substitutions: one at position 5224 (C to T), one at position 5272 (T to C), and one at position 5434 (C to T). The substitution at position 5224 of the reference sequence led to the exchange of a *Hae III* site (GGCC) for a *Bcl* I site (TGATCA). Both EF065660 (JPMI-1) and EF600696 (FLK-BLV) belong to genotype 1 (Balic et al., 2012; Matsumura et al., 2011; Moratorio et al., 2010; Polat et al., 2015). The sequencing results showed that the isolates identified in the present study also belonged to genotype 1.

4. Discussion

Here, we collected matched blood, nasal secretion, and saliva samples from 50 cattle and extracted genomic DNA. Whole blood is the preferred source of high quality genomic DNA and provides sufficient quantity for genetic research. Genomic DNA can be isolated from a variety of animal-derived samples, including whole blood, milk, semen, saliva, and nasal secretions (Foley et al., 2011; Mitsouras and Faulhaber, 2009). The Performagene Livestock PG-100 collection device (DNA Genotek Inc) is designed to facilitate the reliable extraction of genomic DNA from nasal secretion samples. We used this device to extract genomic DNA from nasal secretion and saliva samples, and compared it with DNA extracted from blood samples in terms of quantity and quality. The average yield from blood, nasal, and saliva samples was sufficient to detect BLV provirus using the BLV-CoCoMo-qPCR-2 assay. The average A260/A280 ratio for DNA obtained from saliva was lower than that for DNA obtained from blood and nasal secretion samples. Moreover, the average Ct value for saliva samples was higher than that for nasal secretion and blood samples. These results suggest that the quality of the DNA obtained from saliva may be lower than that of DNA obtained from nasal secretion or blood samples.

The present results clearly show that 14 nasal secretion samples, 6 saliva samples, and 35 blood samples were positive for the BLV provirus. The proviral load in the nasal secretion and saliva samples was much lower (<380 copies/1 × 10^5 cells) than that in peripheral blood. Importantly, BLV-positive nasal secretion or saliva samples were detected when the proviral load in the blood samples was >14,000 copies/1 ×1 0^5 cells. Detection of BLV in nasal secretions has already been performed (Lucas et al., 1993; Roberts et al., 1982). However, the absolute copy number of BLV provirus in nasal secretions remains to be evaluated. Therefore, this is the first study to compare the BLV proviral load in nasal secretion, saliva, and blood samples from the same cattle. Although a previous study experimentally infected sheep with BLV by exposing them to infected blood, nasal secretions, and saliva, the results showed that neither saliva nor nasal secretions facilitated BLV transmission (Gatei et al., 1989). Because the proviral load in nasal and saliva secretions is much lower than that in peripheral blood, more precise studies are needed to confirm the mechanism underlying contact-mediated transmission of BLV via saliva and nasal secretions. Subsequently, we performed a sequence analysis of the partial BLV gp51 *env* gene. The BLV strains analyzed in this study were identical to strain EF065660 (JPMI-1), which was isolated in Japan (Matsumura et al., 2011) and belongs to genotype 1 (Moratorio et al., 2010; Matsumura et al., 2011; Balic et al., 2012; Polat et al., 2015). This genotype is the major BLV genotype found in Japan (Asfaw et al., 2005; Mekata et al., 2015). Lymphocytes in the blood of cattle showing an increased BLV proviral load may play a central role in transmission via nasal secretions and saliva.

Horizontal transmission of BLV appears to occur via the transfer of BLV-infected cells, possibly via blood-sucking insects (Gillet et al., 2007; Rodriguez et al., 2011). Because cell-free infection by BLV viruses is very inefficient, most probably due to virion instability, efficient transmission requires cell–cell contact (Johnston et al., 1996; Voneche et al., 1992). Studies show that, in Japan, BLV transmission is more common during the summer. However, BLV transmission can occur in narrow pens under insect-free conditions (Kono et al., 1983). We suspect that BLV-infected cells might be present in nasal secretions and saliva; therefore, BLV might infect healthy cattle after transfer of infected cells between animals (via licking, sneezing, or rubbing of noses, for example). Therefore, more in-depth studies are needed to confirm the mechanism of BLV transmission through direct contact between animals.

Conflict of interest

The authors have no conflicts of interest to declare.

Acknowledgments

The authors wish to thank Mr. Masato Kamiyama and Ms. Yuki Matsumoto for technical support and helpful feedback. We also thank Mr. Takashi Shimokihara (KYODO INTERNATIONAL INC., Kanagawa, Japan) for providing invaluable methodological knowledge. We are grateful to the Support Unit at the Bio-material Analysis, RIKEN BSI Research Resources Center, for help with sequence analysis. This work was supported by A-STEP (Adaptable & Seamless Technology Transfer Program through Target-driven R&D), by a grant from the Program for the Promotion of Basic and Applied Research for Innovations in Bio-oriented Industry, and by

a grant from Integration research for agriculture and interdisciplinary fields in Japan.

References

Ababneh, M.M., Al-Rukibat, R.K., Hananeh, W.M., Nasar, A.T., Al-Zghoul, M.B., 2012. Detection and molecular characterization of *Bovine leukemia viruses* from Jordan. Arch. Virol. 157 (12), 2343–2348.

Aida, Y., Miyasaka, M., Okada, K., Onuma, M., Kogure, S., Suzuki, M., Minoprio, P., Levy, D., Ikawa, Y., 1989. Further phenotypic characterization of target cells for *Bovine leukemia virus* experimental infection in sheep. Am. J. Vet. Res. 50 (11), 1946–1951.

Asfaw, Y., Tsuduku, S., Konishi, M., Murakami, K., Tsuboi, T., Wu, D., Sentsui, H., 2005. Distribution and superinfection of *Bovine leukemia virus* genotypes in Japan. Arch. Virol. 150 (3), 493–505.

Balic, D., Lojkic, I., Periskic, M., Bedekovic, T., Jungic, A., Lemo, N., Roic, B., Cac, Z., Barbic, L., Madic, J., 2012. Identification of a new genotype of *Bovine leukemia virus*. Arch. Virol. 157 (7), 1281–1290.

Bech-Nielsen, S., Piper, C.E., Ferrer, J.F., 1978. Natural mode of transmission of the *Bovine leukemia virus*: role of bloodsucking insects. Am. J. Vet. Res. 39 (7), 1089–1092.

Beier, D., Riebe, R., Blankenstein, P., Starick, E., Bondzio, A., Marquardt, O., 2004. Establishment of a new *Bovine leukosis virus* producing cell line. J. Virol. Methods 121 (2), 239–246.

Buxton, B.A., Hinkle, N.C., Schultz, R.D., 1985. Role of insects in the transmission of *Bovine leukosis virus*: potential for transmission by stable flies, horn flies, and tabanids. Am. J. Vet. Res. 46 (1), 123–126.

DiGiacomo, R.F., Darlington, R.L., Evermann, J.F., 1985. Natural transmission of *Bovine leukemia virus* in dairy calves by dehorning. Can. J. Comp. Med. 49 (3), 340–342.

Foley, C., O'Farrelly, C., Meade, K.G., 2011. Technical note: comparative analyses of the quality and yield of genomic DNA from invasive and noninvasive, automated and manual extraction methods. J. Dairy Sci. 94 (6), 3159–3165.

Gatei, M.H., McLennan, M.W., Lavin, M.F., Daniel, R.C., 1989. Experimental infection of sheep with *Bovine leukemia virus*: infectivity of blood, nasal and saliva secretions. Zentralb. Veterinarmed. B 36 (9), 652–660.

Gillet, N., Florins, A., Boxus, M., Burteau, C., Nigro, A., Vandermeers, F., Balon, H., Bouzar, A.B., Defoiche, J., Burny, A., Reichert, M., Kettmann, R., Willems, L., 2007. Mechanisms of leukemogenesis induced by *Bovine leukemia virus*: prospects for novel anti-retroviral therapies in human. Retrovirology 4, 18.

Hopkins, S.G., DiGiacomo, R.F., 1997. Natural transmission of *Bovine leukemia virus* in dairy and beef cattle. Vet. Clin. North Am. Food Anim. Pract. 13 (1), 107–128.

Hopkins, S.G., Evermann, J.F., DiGiacomo, R.F., Parish, S.M., Ferrer, J.F., Smith, S., Bangert, R.L., 1988. Experimental transmission of *Bovine leukosis virus* by simulated rectal palpation. Vet. Rec. 122 (16), 389–391.

Jimba, M., Takeshima, S.N., Matoba, K., Endoh, D., Aida, Y., 2010. BLV-CoCoMo-qPCR: quantitation of *Bovine leukemia virus* proviral load using the CoCoMo algorithm. Retrovirology 7, 91.

Jimba, M., Takeshima, S.N., Murakami, H., Kohara, J., Kobayashi, N., Matsuhashi, T., Ohmori, T., Nunoya, T., Aida, Y., 2012. BLV-CoCoMo-qPCR: a useful tool for evaluating *Bovine leukemia virus* infection status. BMC Vet. Res. 8, 167.

Johnston, E.R., Powers, M.A., Kidd, L.C., Radke, K., 1996. Peripheral blood mononuclear cells from sheep infected with a variant of *Bovine leukemia virus* synthesize envelope glycoproteins but fail to induce syncytia in culture. J. Virol. 70 (9), 6296–6303.

Kettmann, R., Deschamps, J., Cleuter, Y., Couez, D., Burny, A., Marbaix, G., 1982. Leukemogenesis by *Bovine leukemia virus*: proviral DNA integration and lack of RNA expression of viral long terminal repeat and 3' proximate cellular sequences. Proc. Natl. Acad. Sci. U. S. A. 79 (8), 2465–2469.

Kobayashi, S., Tsutsui, T., Yamamoto, T., Hayama, Y., Kameyama, K., Konishi, M., Murakami, K., 2010. Risk factors associated with within-herd transmission of *Bovine leukemia virus* on dairy farms in Japan. BMC Vet. Res. 6, 1.

Kono, Y., Sentsui, H., Arai, K., Ishida, H., Irishio, W., 1983. Contact transmission of *Bovine leukemia virus* under insect-free conditions. Jpn. J. Vet. Sci. 45 (6), 799–802.

Kurdi, A., Blankenstein, P., Marquardt, O., Ebner, D., 1999. Serologic and virologic investigations on the presence of BLV infection in a dairy herd in Syria. Berl. Munch. Tierarztl. Wochenschr. 112 (1), 18–23.

Lew, A.E., Bock, R.E., Molloy, J.B., Minchin, C.M., Robinson, S.J., Steer, P., 2004. Sensitive and specific detection of proviral *Bovine leukemia virus* by 5' Taq nuclease PCR using a 3' minor groove binder fluorogenic probe. J. Virol. Methods 115 (2), 167–175.

Lucas, M.H., Roberts, D.H., Banks, J., 1993. Shedding of *Bovine leukosis virus* in nasal secretions of infected animals. Vet. Rec. 132 (11), 276–278.

Matsumura, K., Inoue, E., Osawa, Y., Okazaki, K., 2011. Molecular epidemiology of *Bovine leukemia virus* associated with enzootic bovine leukosis in Japan. Virus Res. 155 (1), 343–348.

Mekata, H., Sekiguchi, S., Konnai, S., Kirino, Y., Horii, Y., Norimine, J., 2015. Horizontal transmission and phylogenetic analysis of bovine leukemia virus Bovine leukemia virus in two districts of Miyazaki. JapanJ. Vet. Med. Sci. http://doi.org/10.1292/jvms.14-0624

Mitsouras, K., Faulhaber, E.A., 2009. Saliva as an alternative source of high yield canine genomic DNA for genotyping studies. BMC Res. Notes 2, 219.

Miyasaka, T., Takeshima, S.N., Jimba, M., Matsumoto, Y., Kobayashi, N., Matsuhashi, T., Sentsui, H., Aida, Y., 2013. Identification of bovine leukocyte antigen class II haplotypes associated with variations in *Bovine leukemia virus* proviral load in Japanese Black cattle. Tissue Antigens 81 (2), 72–82.

Monti, G.E., Frankena, K., 2005. Survival analysis on aggregate data to assess time to sero-conversion after experimental infection with *Bovine leukemia virus*. Prev. Vet. Med. 68 (2–4), 241–262.

Moratorio, G., Obal, G., Dubra, A., Correa, A., Bianchi, S., Buschiazzo, A., Cristina, J., Pritsch, O., 2010. Phylogenetic analysis of *Bovine leukemia viruses* isolated in South America reveals diversification in seven distinct genotypes. Arch. Virol. 155 (4), 481–489.

Nagy, D.W., Tyler, J.W., Kleiboeker, S.B., Stoker, A., 2003. Use of a polymerase chain reaction assay to detect *Bovine leukosis virus* in dairy cattle. J. Am. Vet. Med. Assoc. 222 (7), 983–985.

Panei, C.J., Takeshima, S.N., Omori, T., Nunoya, T., Davis, W.C., Ishizaki, H., Matoba, K., Aida, Y., 2013. Estimation of *Bovine leukemia virus* (BLV) proviral load harbored by lymphocyte subpopulations in BLV-infected cattle at the subclinical stage of enzootic bovine leucosis using BLV-CoCoMo-qPCR. BMC Vet. Res. 9, 95.

Polat, M., Ohno, A., Takeshima, S.N., Kim, J., Kikuya, M., Matsumoto, Y., Mingala, C.N., Onuma, M., Aida, Y., 2015. Detection and molecular characterization of *Bovine leukemia virus* in Philippine cattle. Arch. Virol. 160 (1), 285–296.

Roberts, D.H., Lucas, M.H., Wibberley, G., Bushnell, S., 1982. Detection of *Bovine leukosis virus* in bronchoalveolar lung washings and nasal secretions. Vet. Rec. 111 (22), 501–503.

Rodriguez, S.M., Florins, A., Gillet, N., de Brogniez, A., Sanchez-Alcaraz, M.T., Boxus, M., Boulanger, F., Gutierrez, G., Trono, K., Alvarez, I., Vagnoni, L., Willems, L., 2011. Preventive and therapeutic strategies for *Bovine leukemia virus*: lessons for HTLV. Viruses 3 (7), 1210–1248.

Rodriguez, S.M., Golemba, M.D., Campos, R.H., Trono, K., Jones, L.R., 2009. *Bovine leukemia virus* can be classified into seven genotypes: evidence for the existence of two novel clades. J. Gen. Virol. 90 (11), 2788–2797.

Rola-Luszczak, M., Pluta, A., Olech, M., Donnik, I., Petropavlovskiy, M., Gerilovych, A., Vinogradova, I., Choudhury, B., Kuzmak, J., 2013. The molecular characterization of *Bovine leukaemia virus* isolates from Eastern Europe and Siberia and its impact on phylogeny. PloS one 8 (3), e58705.

Rola, M., Kuzmak, J., 2002. The detection of *Bovine leukemia virus* proviral DNA by PCR-ELISA. J. Virol. Methods 99 (1–2), 33–40.

Schoepf, K.C., Kapaga, A.M., Msami, H.M., Hyera, J.M., 1997. Serological evidence of the occurrence of enzootic bovine leukosis (EBL) virus infection in cattle in Tanzania. Trop. Anim. Health Prod. 29 (1), 15–19.

Tajima, S., Ikawa, Y., Aida, Y., 1998. Complete *Bovine leukemia virus* (BLV) provirus is conserved in BLV-infected cattle throughout the course of B-cell lymphosarcoma development. J. Virol. 72 (9), 7569–7576.

Tajima, S., Takahashi, M., Takeshima, S.N., Konnai, S., Yin, S.A., Watarai, S., Tanaka, Y., Onuma, M., Okada, K., Aida, Y., 2003. A mutant form of the tax protein of *Bovine leukemia virus* (BLV), with enhanced transactivation activity, increases expression and propagation of BLV in vitro but not in vivo. J. Virol. 77 (3), 1894–1903.

Takeshima, S.N., Kitamura-Muramatsu, Y., Yuan, Y., Polat, M., Saito, S., Aida, Y., 2015. BLV-CoCoMo-qPCR-2: improvements to the BLV-CoCoMo-qPCR assay for *Bovine leukemia virus* by reducing primer degeneracy and constructing an optimal standard curve. Arch. Virol. 160 (5), 1325–1332.

Trono, K.G., Perez-Filgueira, D.M., Duffy, S., Borca, M.V., Carrillo, C., 2001. Seroprevalence of *Bovine leukemia virus* in dairy cattle in Argentina: comparison of sensitivity and specificity of different detection methods. Vet. Microbiol. 83 (3), 235–248.

VanLeeuwen, J.A., Tiwari, A., Plaizier, J.C., Whiting, T.L., 2006. Seroprevalences of antibodies against *Bovine leukemia virus*, bovine viral diarrhea virus, *Mycobacterium avium* subspecies paratuberculosis, and *Neospora caninum* in beef and dairy cattle in Manitoba. Can. Vet. J. 47 (8), 783–786.

Voneche, V., Portetelle, D., Kettmann, R., Willems, L., Limbach, K., Paoletti, E., Ruysschaert, J.M., Burny, A., Brasseur, R., 1992. Fusogenic segments of *Bovine leukemia virus* and simian immunodeficiency virus are interchangeable and mediate fusion by means of oblique insertion in the lipid bilayer of their target cells. Proc. Natl. Acad. Sci. U. S. A. 89 (9), 3810–3814.

Wang, C.T., 1991. *Bovine leukemia virus* infection in Taiwan: epidemiological study. J. Vet. Med. Sci. 53 (3), 395–398.

Zaghawa, A., Beier, D., Abd El-Rahim, I.H., Karim, I., El-ballal, S., Conraths, F.J., Marquardt, O., 2002. An outbreak of enzootic bovine leukosis in upper Egypt: clinical, laboratory and molecular-epidemiological studies. J. Vet. Med. B 49 (3), 123–129.

frontiers in
MICROBIOLOGY

REVIEW ARTICLE
published: 08 November 2013
doi: 10.3389/fmicb.2013.00328

Mechanisms of pathogenesis induced by bovine leukemia virus as a model for human T-cell leukemia virus

Yoko Aida[1], Hironobu Murakami[1,2], Masahiko Takahashi[3] and Shin-Nosuke Takeshima[1]*

[1] Viral Infectious Diseases Unit, RIKEN, Wako, Saitama, Japan
[2] Laboratory of Animal Health II, Azabu University, Sagamihara, Kanagawa, Japan
[3] Division of Virology, Niigata University Graduate School of Medical and Dental Sciences, Niigata, Japan

Edited by:
Akio Adachi, The University of Tokushima Graduate School, Japan

Reviewed by:
Toshiki Watanabe, The University of Tokyo, Japan
Takeo Ohsugi, Kumamoto University, Japan

***Correspondence:**
Yoko Aida, Viral Infectious Diseases Unit, RIKEN, 2-1 Hirosawa, Wako, Saitama 351-0198, Japan
e-mail: aida@riken.jp

Bovine leukemia virus (BLV) and human T-cell leukemia virus type 1 (HTLV-1) make up a unique retrovirus family. Both viruses induce chronic lymphoproliferative diseases with BLV affecting the B-cell lineage and HTLV-1 affecting the T-cell lineage. The pathologies of BLV- and HTLV-induced infections are notably similar, with an absence of chronic viraemia and a long latency period. These viruses encode at least two regulatory proteins, namely, Tax and Rex, in the pX region located between the *env* gene and the 3′ long terminal repeat. The Tax protein is a key contributor to the oncogenic potential of the virus, and is also the key protein involved in viral replication. However, BLV infection is not sufficient for leukemogenesis, and additional events such as gene mutations must take place. In this review, we first summarize the similarities between the two viruses in terms of genomic organization, virology, and pathology. We then describe the current knowledge of the BLV model, which may also be relevant for the understanding of leukemogenesis caused by HTLV-1. In addition, we address our improved understanding of Tax functions through the newly identified BLV Tax mutants, which have a substitution between amino acids 240 and 265.

Keywords: BLV, HTLV-1, EBL, B-cell lymphoma, Tax, leukemogensis, transactivation, apoptosis

INTRODUCTION

Bovine leukosis was first reported in 1871 as the presence of slightly yellow nodules in the enlarged spleen of cattle (Leisering, 1871). Spleen disruption consecutive to tumor formation is one of the most important clinical manifestations of bovine leukemia. Bovine leukosis is classified into two types, sporadic bovine leukosis (SBL) and enzootic bovine leukosis (EBL), which are characterized by T- and B-cell leukosis, respectively (Gillet et al., 2007). The occurrence of EBL in cattle is much higher than that of SBL (Theilen and Dungworth, 1965; Onuma et al., 1979). Bovine leukemia virus (BLV), which belongs to the *Retroviridae* family and *Deltaretrovirus* genus, is the etiologic agent of EBL, although it remains unknown what causes SBL (Gillet et al., 2007). The natural hosts of BLV are domestic cattle and water buffaloes; however, experimental infection with BLV in sheep can lead to the development of lymphoma (Djilali and Parodi, 1989). Interestingly, BLV is consistently associated with leukemia only in cattle and sheep, even though it can infect many cell lines (Graves and Ferrer, 1976) and can be experimentally transmitted to rabbits (Wyatt et al., 1989; Onuma et al., 1990), rats (Altanerova et al., 1989), chickens (Altanerova et al., 1990), pigs, goats, and sheep (Mammerickx et al., 1981). Most BLV-infected cattle are asymptomatic, but approximately one-third of them suffer from persistent lymphocytosis (PL) characterized by non-malignant polyclonal B-cell expansion and 1–5% of them develop B-cell leukemia/lymphoma after a long latency period (Gillet et al., 2007). On the other hand, sheep that are experimentally inoculated with BLV develop B-cell tumors at a higher frequency and with a shorter latency period than those observed in naturally infected cattle (Ferrer et al., 1978; Burny et al., 1979; Kenyon et al., 1981; Aida et al., 1989). Interestingly, the transformed B-lymphocytes in cattle are $CD5^+$ IgM^+ B-cells (Aida et al., 1993), whereas in sheep they are $CD5^-$ IgM^+ B-cells (Murakami et al., 1994a,b), suggesting that the mechanisms of leukemogenesis induced by BLV may differ (Graves and Ferrer, 1976; Djilali and Parodi, 1989).

BLV is closely related to human T-cell leukemia virus type 1 (HTLV-1), which is the causative agent of adult T-cell leukemia (ATL) and a chronic neurological disorder known as tropical spastic paraparesis or HTLV-1-associated myelopathy HAM/TSP (Gessain et al., 1985; Osame et al., 1986; Gillet et al., 2007). Therefore, studies on BLV may facilitate our understanding of the mechanism of leukemogenesis induced by HTLV-1.

BLV AND HTLV-1

All retroviruses are encoded by *gag*, *pro*, *pol*, and *env* essential genes, which are necessary for the production of infectious virions, and are flanked by two identical long terminal repeats (LTRs; **Figure 1**). The *gag*, *pro*, *pol*, and *env* genes encode the internal structural proteins of the virion, the viral protease, the reverse transcriptase, and the envelope glycoproteins of the virion, respectively. The genome sequences of BLV and HTLV-1 are different, but have a unique sequence called the pX situated between the *env* gene and the 3′LTR and encoded by the regulatory gene (**Figure 1**). The pX sequence is not of host cell origin; that is, it is not an oncogene. It has been reported that both viruses have an ability to immortalize primary cells *in vitro* (Grassmann et al., 1989; Willems

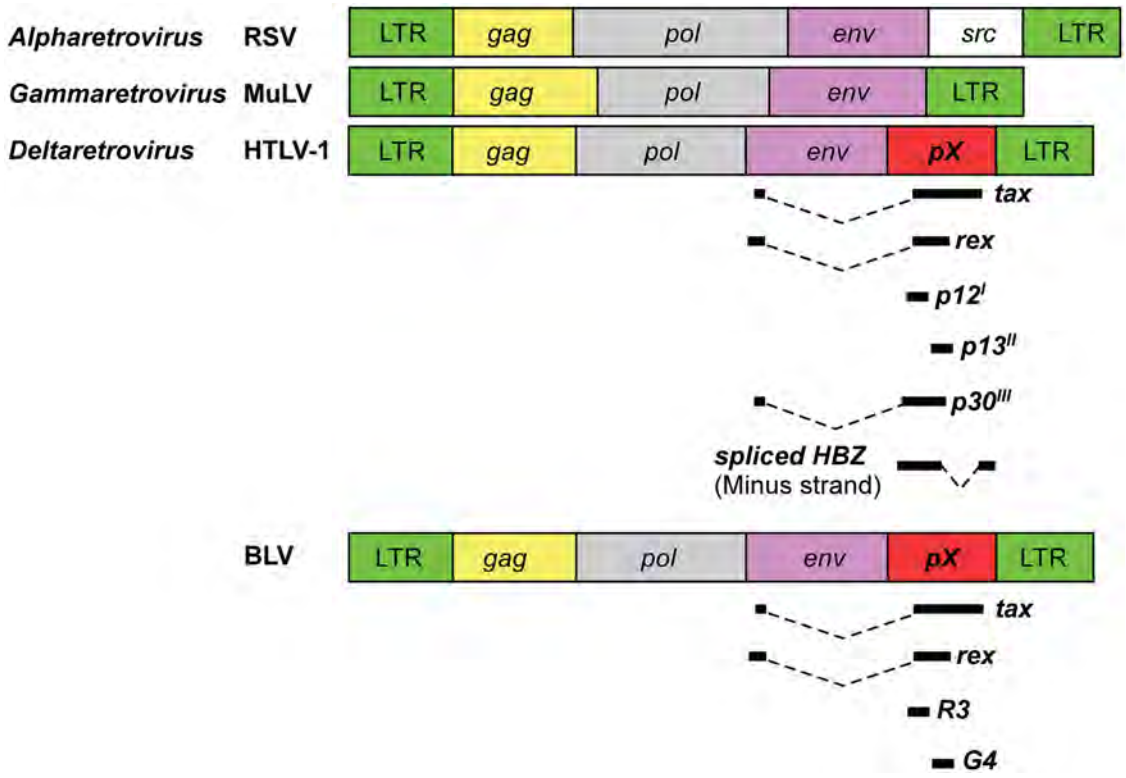

FIGURE 1 | Schematic representation of genome organization of retroviruses. HTLV-1 and BLV encode unique regulatory and accessory proteins in the pX region. RSV, Rous sarcoma virus; MuLV, murine leukemia virus.

et al., 1990). Because their structure and properties differ from any other class of retroviruses, BLV and HTLV-1 viruses were classified into a new group of retroviruses (Gillet et al., 2007). In both viruses the regulatory proteins Tax and Rex are encoded in the pX region. The R3 and G4 proteins are encoded in the BLV pX region, while $p12^{I}$, $p13^{II}$, and $p30^{II}$ are encoded in the HTLV-1 pX region (Sagata et al., 1984b; Franchini et al., 2003; **Figure 1**). Interestingly, the HTLV-1 genome codes for HBZ, a unique gene encoded by the minus strand chain (Gaudray et al., 2002; **Figure 1**). The major functions of the viral proteins encoded in the BLV and HTLV-1 pX regions are summarized in **Table 1**. The Tax protein has been extensively studied, and it is believed to play a critical role in leukemogenesis induced by BLV and HTLV-1 (Katoh et al., 1989; Tanaka et al., 1990; Willems et al., 1990). The Rex protein is responsible for nuclear export of viral RNA and promotes cytoplasmic accumulation and translation of viral messenger mRNA in BLV- and HTLV-1-infected cells (Felber et al., 1989). BLV R3 and G4 proteins contribute to the maintenance of high viral load (Willems et al., 1994; Florins et al., 2007). The G4 protein is particularly relevant to leukemogenesis, since it can immortalize primary rat embryo fibroblasts (REFs; Lefebvre et al., 2002). HTLV-1 $p12^{I}$ is similar to the R3 protein, in that it contributes to the maintenance of infectivity (Collins et al., 1998), and both proteins are located in the nucleus and cellular membranes (Gillet et al., 2007). On the other hand, HTLV-1 $p13^{II}$ protein resembles the G4 protein, since both proteins bind to farnesyl pyrophosphate synthetase, which farnesylates Ras (Lefebvre et al., 2002), and the $p13^{II}$ protein promotes Ras-dependent apoptosis (Hiraragi et al., 2005). HTLV-1 $p30^{II}$ protein regulates gene transcription through its interaction with the cAMP responsive element (CRE) binding protein (CREB)/p300 (Zhang et al., 2001). The HBZ protein plays a critical role in the leukemogenesis of HTLV-1, and HBZ knockdown inhibits the proliferation of ATL cells (Satou et al., 2006). However, since the BLV genome does not code for HBZ, it is assumed that the Tax protein plays a central role in the leukemogenesis of BLV.

The infection route of BLV and HTLV is by horizontal and vertical transmission. BLV is transmitted via direct contact (Kono et al., 1983), milk, and insect bites (Ferrer and Piper, 1978), while HTLV-1 is transmitted via milk and sexual intercourse (Bangham, 2003). Moreover, the artificial transmission of BLV is caused by iatrogenic procedures such as dehorning, ear tattooing, and reuse of needles (Hopkins and DiGiacomo, 1997), whereas the artificial transmission of HTLV-1 is caused by blood transfusion and needle sharing among drug abusers (Robert-Guroff et al., 1986). Since cell contact is required for the efficient transmission of both BLV and HTLV-1, cell-free infection by these viruses is believed to be very inefficient, most probably due to virion instability (Voneche et al., 1992; Johnston et al., 1996; Igakura et al., 2003).

As shown in **Figure 2**, an infection with BLV is characterized by three progressive stages of disease, including an asymptomatic

Table 1 | Viral proteins are encoded in BLV and HTLV-1 pX regions.

Virus	Viral protein	Major reported functions	Reference
BLV	Tax	Transcriptional activator of viral expression	Derse (1987), Willems et al. (1987), Katoh et al. (1989)
		Oncogenic potential	Willems et al. (1990)
		Activation of NF-kappa B (NF-κB) pathway	Szynal et al. (2003), Klener et al. (2006)
	Rex	Nuclear export of viral mRNAs	Felber et al. (1989)
	G4	The maintenance of high viral load	Willems et al. (1994), Florins et al. (2007)
		Oncogenic potential	Kerkhofs et al. (1998), Lefebvre et al. (2002)
	R3	The maintenance of high viral load	Willems et al. (1994), Florins et al. (2007)
HTLV-1	Tax	Transcriptional activator of viral expression	Kashanchi and Brady (2005)
		Oncogenic potential	Matsuoka and Jeang (2011)
		Induction of DNA damage, cellular senescence and apoptosis	Chlichlia and Khazaie (2010)
		Functional regulation of many cellular proteins by direct binding	Boxus et al. (2008)
	HBZ	Inhibition of HTLV-1 transcription	Lemasson et al. (2007)
		Suppression of the classical pathway of NF-κB	Zhao et al. (2009)
		Enhancement of TGF-β signaling	Zhao et al. (2011)
		Oncogenic potential	Satou et al. (2006, 2011)
	Rex	Nuclear export of viral mRNAs	Felber et al. (1989)
	$p12^{I}$	Maintenance of viral infectivity	Collins et al. (1998)
		Activation of nuclear factor of activated T-cells (NFAT) pathway	Ding et al. (2002)
	$p13^{II}$	Suppression of viral replication	Andresen et al. (2011)
		Interaction with farnesyl pyrophosphate synthetase	Lefebvre et al. (2002)
		Activation of Ras-mediated apoptosis	Hiraragi et al. (2005)
	$p30^{II}$	Suppression of viral replication	Nicot et al. (2004)
		Regulation of gene transcription by binding with p300	Zhang et al. (2001)
		Enhancement of Myc transforming potential	Zhang et al. (2001)

stage, PL, and lymphoma. Most BLV-infected cattle are asymptomatic, but approximately one-third of them suffer from PL characterized by a permanent and relatively stable increase in the number of B-lymphocytes in the peripheral blood. PL is considered to be a benign form of the disease resulting from the accumulation of untransformed B-lymphocytes. Finally, 1–5% of BLV-infected cattle develop B-lymphoma in various lymph nodes after a long latency period (Schwartz and Levy, 1994; Florins et al., 2008). Although BLV can also infect $CD4^+$ T-cells, $CD8^+$ T-cells, γ/δ T-cells, monocytes, and granulocytes in cattle (Williams et al., 1988; Stott et al., 1991; Schwartz et al., 1994; Mirsky et al., 1996; Wu et al., 1996; Panei et al., 2013), a large number of the tumor cells are derived from $CD5^+$ IgM^+ B-cell subpopulations (Schwartz and Levy, 1994). Interestingly, the full-length BLV proviral genome is maintained in each animal throughout the course of the disease (Tajima et al., 1998a). In addition, previous studies have shown that both large and small deletions of proviral genomes may be very rare events in BLV-infected cattle. Thus, the proviral loads were significantly increased at the PL stage compared with the aleukemic stage and were further increased at the lymphoma stage (Jimba et al., 2010, 2012; **Figure 2B**). These findings clearly demonstrated that the BLV proviral copy number increases with increasing severity of the disease. On the other hand, unlike BLV, HTLV-1 is associated with ATL and with the chronic neurological disorder, HAM/TSP, and induces not only a malignant tumor but also an inflammatory disease (Gessain et al., 1985; Osame et al., 1986). Although the pathogenesis of HTLV-1 is slightly different from BLV, HTLV-1, like BLV, can infect many cells in addition to T-cells, including B-cells and monocytes (Koyanagi et al., 1993; Schwartz and Levy, 1994). In contrast to BLV, defective HTLV-1 proviral genomes have been found in more than half of all examined patients with ATL (Konishi et al., 1984; Korber et al., 1991; Ohshima et al., 1991; Tsukasaki et al., 1997).

MECHANISM OF LEUKEMOGENESIS BY BLV

Animal retroviruses, which belong to the *Alpharetrovirus* and *Gammaretrovirus* genera, induce tumors by one of two mechanisms: either by activation of the "viral oncogene" or by "insertional activation" of a cellular gene such as a proto-oncogene (Weiss et al., 1985; **Figure 1**). By contrast, BLV lacks a known oncogene (Sagata et al., 1984a,b) and does not integrate into preferred sites in their host cell genomes, which related to the disruption of the host gene but not to the suppression of viral gene expression (Murakami et al., 2011b).

Most studies of BLV-induced leukemogenesis have focused on the Tax protein because it is believed to be a potent transcriptional

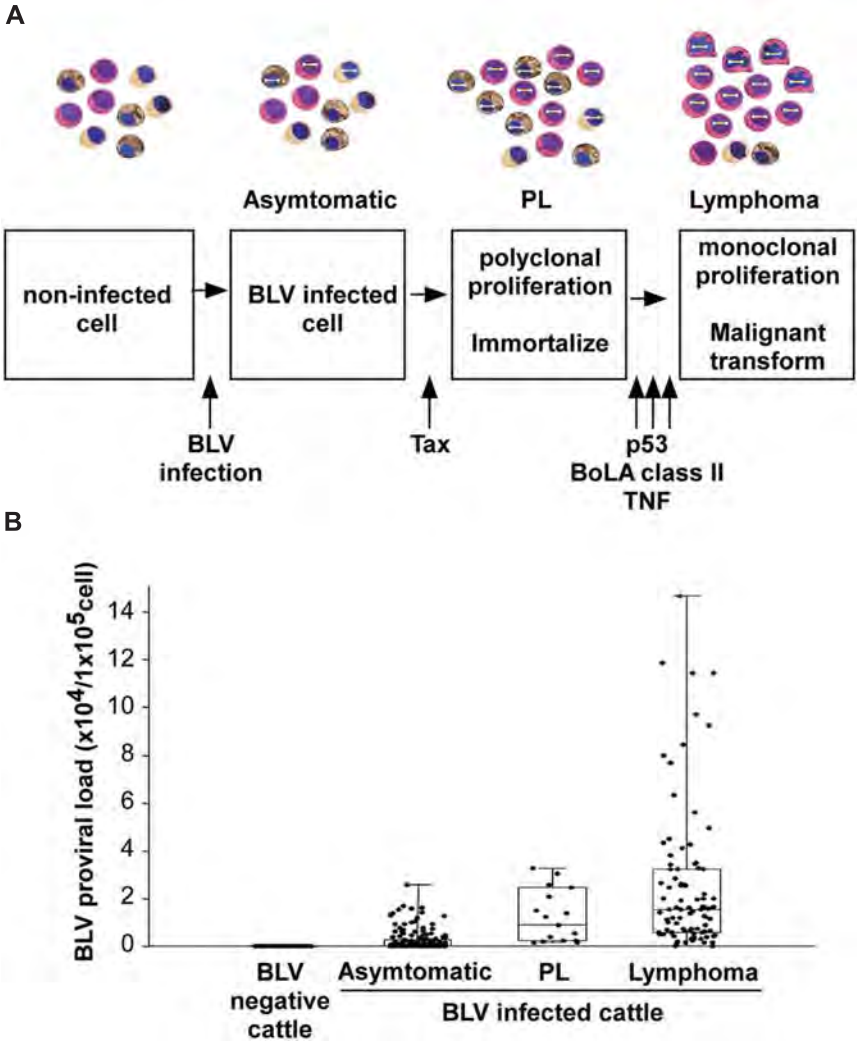

FIGURE 2 | BLV-induced leukemogenesis is a multistep process. (A) An infection with BLV is characterized by three progressive stages of disease: asymptomatic stage, persistent lymphocytosis (PL), and lymphoma. BLV infects to cells non-specifically. Among them, BLV Tax protein immortalizes a part of BLV-infected cells, probably only $CD5^+$ IgM^+ B-cells, and induces polyclonal proliferation of the cells. However, the Tax protein does not have the ability to transform the cells. For lymphoma to develop, a malignant transformation needs to occur with the help of host factors, such as p53 mutation, TNF-α activities or bovine leukocyte antigen (BoLA) class II phosphorylation. **(B)** The provirus load increases with disease progression.

activator of viral gene expression. In addition to its function as a transcriptional activator, Tax induces immortalization of primary REFs (Willems et al., 1990, 1998). Furthermore, Tax cooperates with the Harvey rat sarcoma viral oncoprotein (Ha-ras) for the induction of full transformation of primary REF (Willems et al., 1990). Importantly, the Tax transformed cells induce tumors in nude mice. The ability of the Tax protein to induce immortalization may be the first step in the BLV-mediated transformation process. Moreover, after the infection of cattle and during the latency period, the expression of BLV becomes blocked at the transcriptional level (Kettmann et al., 1982; Lagarias and Radke, 1989). Such repression appears to be very important for the escape of BLV from the host's immunosurveillance system, and later only a certain small proportion of infected animals rapidly develop a terminal disease (Gillet et al., 2007). Indeed, transcription of the BLV genome in fresh tumor cells or in fresh peripheral blood mononuclear cells (PBMCs) from infected individuals is almost undetectable by conventional techniques (Kettmann et al., 1982; Tajima et al., 2003b; Tajima and Aida, 2005). *In situ* hybridization has revealed the expression of viral RNA at low levels in many cells, and at a high level in only a few cells within PBMCs freshly isolated from BLV-infected asymptomatic animals (Lagarias and Radke, 1989). Thus, BLV infection is probably not sufficient for leukemogenesis and some additional events such as gene mutations might be involved in the leukemogenic process (**Figure 2A**). Taken together, Tax may induce immortalization of only $CD5^+$ IgM^+ B-cells among BLV-infected B-cells, $CD4^+$ T-cells, $CD8^+$ T-cells, γ/δ T-cells, monocytes, and granulocytes in cattle, thereby conferring a selective transformation advantage to the infected $CD5^+$ IgM^+ B-cells by a second event.

A mutation in the p53 tumor suppressor gene is one of several genetic changes known to be involved in the development of lymphoma (**Figure 2A**). The protein encoded by the p53 tumor suppressor gene plays a critical role in transducing a signal from the damaged DNA to genes that control cell cycle and apoptosis. Approximately half of the solid tumors induced by BLV in cattle (Dequiedt et al., 1995; Ishiguro et al., 1997; Zhuang et al., 1997; Tajima et al., 1998b) and three of four bovine B-cell lymphoma lines (Komori et al., 1996) were shown to harbor missense mutations in p53. By contrast, very few mutations were found in B-cells from cows with PL and none of the uninfected cattle harbored a mutated p53 gene. These observations indicate that p53 mutations frequently occur at the final stage of lymphoma in cattle. A previous study of the molecular mechanism of mutations at codons 206, 207, 241, and 242, which were identified in lymphoma, showed that these mutations may potentially alter the wild-type function of the bovine p53 protein, including the conformation and transactivator and growth suppressor activities, and then cause lymphoma (Tajima et al., 1998b). These four mutations were clearly divided into two functionally distinct groups: (i) the mutant forms with substitutions at codons 241 and 242, which were mapped within an evolutionarily conserved region and corresponded to the human "hot-spot" mutations, and had completely lost the capacity for transactivation and growth suppression while gaining transdominant repression activity in p53-null SAOS-2 cells; and (ii) the mutations at codons 206 and 207, which were located outside the evolutionarily conserved regions and partially retained the capacity for transactivation and growth suppression. Collectively, these naturally occurring mutations may potentially alter the wild-type function, and in addition, out of the four missense mutations, at least two mutations may be sufficient to cause lymphoma. However, since the other two mutations may be insufficient to induce lymphoma, it is possible that other cancer-related genes may contribute to lymphoma in concert with the p53 mutations.

A major factor involved in the clinical progression of BLV-infected animals is the bovine leukocyte antigen (BoLA; **Figure 2A**), which plays a crucial role in determining immune responsiveness (Lewin and Bernoco, 1986; Lewin et al., 1988; Zanotti et al., 1996; Takeshima and Aida, 2006). Several studies have shown that genetic variations in *BoLA-DRB3*, which is a functionally important and the most polymorphic BoLA class II locus in cattle, influence resistance and susceptibility to a wide variety of infectious diseases, including lymphoma (Aida, 2001) and PL (Xu et al., 1993; Sulimova et al., 1995; Starkenburg et al., 1997; Juliarena et al., 2008), and affect BLV proviral load (Miyasaka et al., 2013). For example, the presence of the amino acids Glu–Arg (ER) at positions 70–71 of the BoLA-DRβ chain was associated with resistance to PL in BLV-infected cattle (Xu et al., 1993). Furthermore, the *BoLA-DRB3* alleles encoding Glu, Arg, and Val at positions 74, 77, and 78, respectively, of the BoLA-DRβ chain might be associated with resistance to tumor development (Aida, 2001). In a related study, Nagaoka et al. (1999) and Konnai et al. (2003) found that the ovine leukocyte antigen (*OLA*)-*DRB1* alleles encoding the Arg–Lys (RK) and the Ser–Arg (SR) motifs at positions 70–71 of the OLA-DRβ chain are associated with resistance (RK motif) and susceptibility (SR motif) to the development of lymphoma after experimental infection of sheep with BLV. The sheep with alleles encoding the RK motif produced neutralizing antibodies against BLV and interferon-γ, eliminated BLV completely, and did not develop lymphoma (Konnai et al., 2003). The susceptibility to the monoclonal expansion of BLV-infected B-lymphocytes is thus associated with specific alleles of BoLA system.

A polymorphism in the promoter region of the tumor necrosis factor (TNF)-α gene is one of several genetic changes involved in the development of lymphoma (**Figure 2A**). A previous study found that, in sheep experimentally infected with BLV, the frequency of the TNF-α-824G allele, which has been associated with low transcription activity of the promoter/predicted enhancer region of the bovine TNF-α gene, was higher in animals with lymphoma than in asymptomatic carrier animals. In addition, a tendency was observed for increased BLV-provirus load in cattle homozygous for the TNF-α-824G/G allele compared to cattle homozygous for the TNF-α-824A/A or TNF-α-824A/G alleles. These data suggest that the observed polymorphism in the promoter region of the TNF-α gene could at least in part contribute to the progression of lymphoma in BLV infection (Konnai et al., 2006).

The BLV studies have also focused on understanding the process of signal transduction such as B-cell receptor (BCR) signaling (Alber et al., 1993), since many signal transduction factors have been implicated in leukemogenesis of B-cells in humans (Murakami et al., 2011a). For example, the immunoreceptor tyrosine-based activation (ITAM) motifs present in the transmembrane gp30 proteins of the BLV envelope are important for the incorporation of envelope proteins into the virion (Inabe et al., 1999) and are required for infectivity *in vivo* (Willems et al., 1995). In addition to the viral signaling motif, the spleen tyrosine kinase (Syk) mRNA expression was significantly increased in PL samples, whereas it was decreased in tumor samples, suggesting that Syk mRNA expression dynamics is closely related to the progression of BLV-induced disease (Murakami et al., 2011a).

BLV Tax FUNCTION

As mentioned above, the Tax gene is a key contributor to the oncogenic potential, as well as a key protein involved in the replication of the virus. **Table 1** summarizes the functions of the Tax protein. The Tax open reading frame is mainly encoded in the pX region, and its translation occurs upstream of the *pol* stop codon. The Tax protein is modified by phosphorylation of two serine residues and is detected as a 34–38 kDa product (Chen et al., 1989; Willems et al., 1998). In addition, the Tax protein has T- and B-cell epitopes corresponding to regions 110–130/131–150 and 261–280, respectively (Sakakibara et al., 1998). One of the best characterized functions of Tax is the activation of viral transcription. The Tax protein acts on a triplicate 21 bp enhancer motif known as the Tax-responsive element (TxRE) in the U3 region of the 5′LTR, and it stimulates transactivation of the viral genome (Derse, 1987; Willems et al., 1987; Katoh et al., 1989). The TxRE consists of a cyclic AMP-response element (CRE)-like sequence, and it has been suggested that Tax binds to this element

indirectly through cellular factors, such as the members of the CREB/activating transcription factor (ATF) family of basic leucine zipper proteins that have been shown to bind to the CRE-like sequence (Adam et al., 1994, 1996; Boros et al., 1995). Furthermore, the Tax protein modulates the expression of cellular genes that are involved in the regulation of cell growth (Tajima and Aida, 2002). In addition to its function in the regulation of cellular and viral transcription, the Tax protein can induce immortalization of primary REF and cooperates with Ha-Ras oncogene to fully transform the primary cells (Willems et al., 1990). On the other hand, the transactivation and transformation of Tax may be independently induced by each mechanism, since phosphorylation of Tax is required for its transformation but not for its activation (Willems et al., 1998). Moreover, the expression of Tax in primary ovine B-cells, which depends on CD154 and interleukin-4, affects B-cell proliferation, cell cycle phase distribution, and survival, leading to cytokine-independent growth (Szynal et al., 2003). This immortalization process is also associated with increased B cell leukemia/lymphoma 2 (Bcl-2) protein levels, nuclear factor kappa B (NF-κB) accumulation, and a series of intracellular pathways that remain to be characterized (Klener et al., 2006). In addition, Tax inhibits base-excision DNA repair of oxidative damage, thereby potentially increasing the accumulation of ambient mutations in cellular DNA (Philpott and Buehring, 1999).

NEGATIVE REGULATION OF BLV Tax BY THE REGION BETWEEN RESIDUES 240–265

Our studies (Tajima and Aida, 2000) demonstrated new functions of the region between amino acids 240 and 265 of BLV Tax. As shown in **Figure 3**, a series of mutants with at least one amino acid substitution between amino acids 240 and 265 of BLV Tax were identified, including TaxD247G and TaxS240P, which exhibit an enhanced ability to stimulate and reduce viral LTR-directed transcription respectively, compared to the wild-type protein (Tajima and Aida, 2000). Transient expression analysis revealed that the TaxD247G mutant increased the production of viral protein and particles from a defective recombinant proviral BLV clone to a greater extent than the wild-type Tax (TaxWT). Conversely, the TaxS240P mutant was unable to induce the release of viral particles. The microarray data in human HeLa cells and its validation of differentially expressed genes at the RNA and protein levels in bovine 23CLN cells revealed several alterations in genes involved in many cellular functions such as transcription, signal transduction, cell growth, apoptosis, and the immune response (Arainga et al., 2012). In both of human HeLa cells and bovine 23CLN cells, the TaxD247G mutant induced higher gene expression compared with TaxWT and TaxS240P and many of these genes were expressed at the lowest level in the TaxS240P-transfected cells. In particular, our results showed that Tax activates the proteins which are involved in activator protein 1 (AP-1) signaling pathway [FBJ osteosarcoma

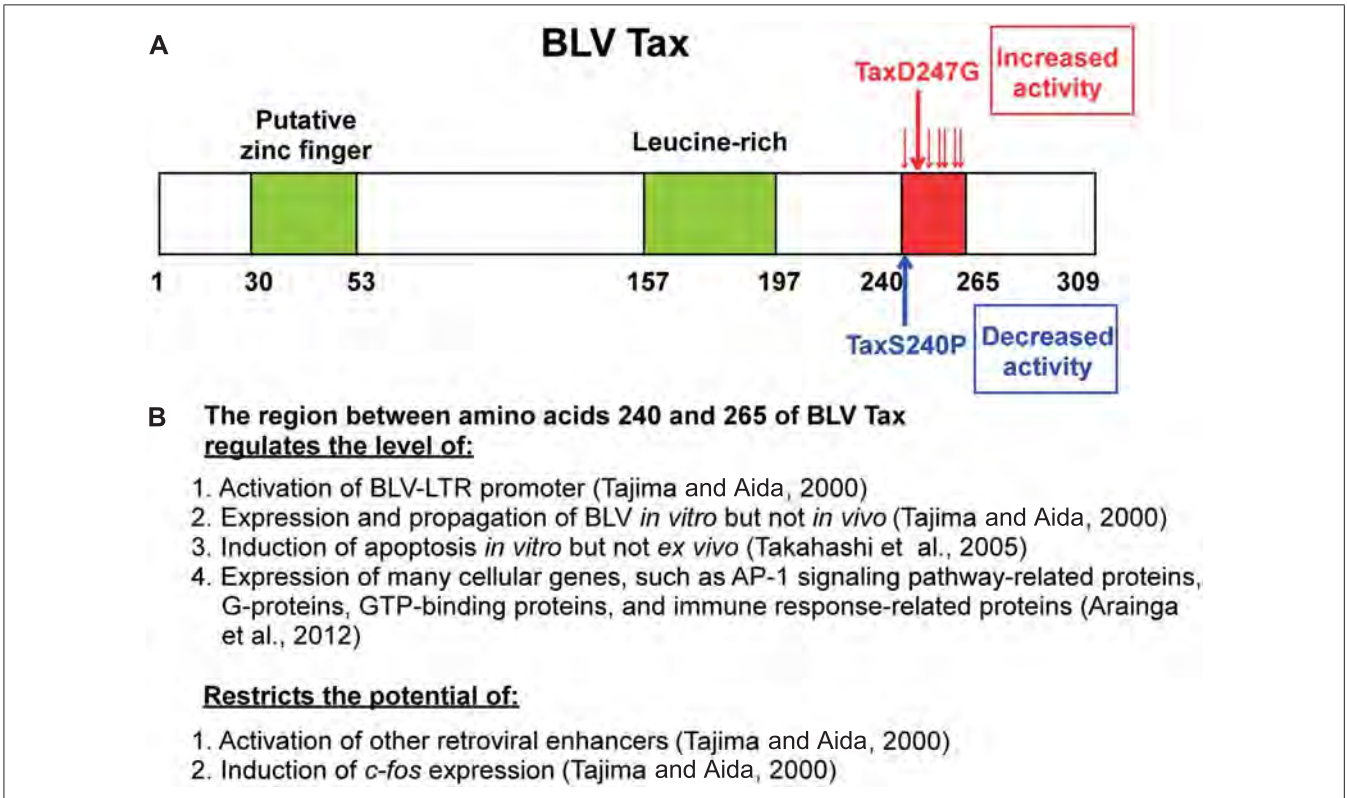

FIGURE 3 | Schematic representations of BLV Tax protein mutants and function. (A) Missense mutations between amino acids 240 and 265 containing D247G and S240P influence the transactivation activity of the BLV Tax protein. A putative zinc finger structure (amino acids 30–53) and a leucine-rich activation domain (amino acids 157–197) are also indicated. **(B)** Multiple functions of the region between amino acids 240 and 265.

oncogene (FOS), jun proto-oncogene (JUN), etc.] via interactions with other transcriptional pathways (G-protein, GTP-binding proteins, etc.). Likewise, the TaxD247G mutant induced apoptosis in transfected cells more effectively than the TaxWT (Takahashi et al., 2005). These results suggest that the region between amino acids 240 and 265 of the Tax protein might act as a negative regulatory domain, and missense mutations in this region might lead to enhanced transactivation activity of Tax, expression of many cellular genes and induction of apoptosis. Our results raise the possibility that the target sequence specificity of retroviral enhancers of Tax might be limited by this region because TaxD247G, but not TaxS240P, was found to activate other retroviral enhancers such as HTLV-1, HIV-1, and mouse mammary tumor virus (MMTV) and Moloney murine leukemia virus (M-MuLV), and *c-fos*, which are not activated by TaxWT (Tajima and Aida, 2000; **Figure 3B**). The microarray data also raised the possibility that BLV Tax regulates the innate immune response (**Figure 3B**): the largest group of downregulated genes was related to the immune response, and the majority of these genes belonged to the interferon family of antiviral factors, such as interferon-induced protein with tetratricopeptide repeats 1 (IFIT1; Arainga et al., 2012). Interferons are major components of the innate immune system, and are recognized for their antiviral function in addition to their antiproliferative and immunomodulatory effects on cells (Hu et al., 1993). It is likely that BLV Tax downregulates the innate immune response, thereby increasing the production of viral protein.

An infectious molecular clone of BLV encoding the TaxD247G was examined for the viral expression and propagation, as well as for the induction of apoptosis in a sheep model (Tajima et al., 2003a; Takahashi et al., 2004, 2005). Interestingly, the infectious molecular clone of BLV encoding the TaxD247G produced more viral particles and was transmitted at an elevated rate *in vitro*, but with no significant differences in the proviral load and the expression of viral RNA between sheep experimentally injected with BLVs encoding the TaxWT or the mutant TaxD247G proteins (Tajima et al., 2003a). These findings suggest the presence of a dominant host defense mechanism regulating BLV–LTR-directed transcription by Tax that may play an important role in viral silencing *in vivo* (**Figure 4**). Likewise, although the transient expression of TaxD247G induced apoptosis in transfected cells *in vitro* more effectively than TaxWT, higher level of protection against apoptosis was observed in PBMCs isolated from sheep infected with TaxD247G-encoded BLV compared to TaxWT-encoded BLV (Takahashi et al., 2005; **Figure 4**). These findings demonstrate that TaxD247G has an increased potential to induce apoptosis, which could be beneficial for BLV propagation like other viruses (Wurzer et al., 2003; Richard and Tulasne, 2012). One possible explanation for our results might be that TaxD247G-induced apoptosis is modulated by a dominant mechanism *ex vivo*, so the function might be suppressed.

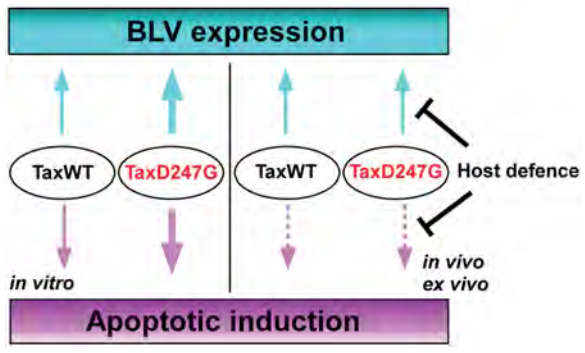

FIGURE 4 | Proposed mechanism for the regulation of BLV expression and apoptosis induction in TaxD247G-encoded BLV-infected sheep.

CONCLUSION

BLV is the etiologic agent of EBL, which is the most common neoplastic disease in cattle. It infects cattle worldwide, thereby imposing a severe economic burden on the dairy cattle industry. In this review, we evaluated existing information on the mechanism of BLV-induced leukemogenesis. We propose that, since BLV Tax induces immortalization of only $CD5^+$ IgM^+ B-cells within BLV-infected B-cells, $CD4^+$ T-cells, $CD8^+$ T-cells, γ/δ T-cells, monocytes, and granulocytes in cattle, it may confer a selective transformation advantage to the infected $CD5^+$ IgM^+ B-cells by a second event, such as p53 mutation, polymorphisms of BoLA, or the promoter region of the TNF-α gene. We also propose new functions of the region between amino acids 240 and 265 of BLV Tax (**Figure 3**). Namely, the transactivation activity and target sequence specificity of BLV Tax might be limited or negatively regulated by this region. The most interesting point regarding the ability of TaxD247G to enhance BLV expression and apoptotic induction *in vitro* is that it might be suppressed *in vivo* or *ex vivo*. Thus, we hypothesize that there could be dominant mechanisms controlling the functions of TaxD247G *ex vivo* and *in vivo*, as shown in **Figure 4**. For HTLV-1, it has been reported that $CD8^+$ cell-mediated cytotoxic T-lymphocytes (CTLs) target Tax-expressing cells, thereby reducing the number of infected cells (Hanon et al., 2000). Likewise, BLV-infected cells expressing Tax may be exposed to the host defense system, and BLV may evolve in a manner that promotes the shielding of their potential abilities. Therefore, a strong transactivation activity of BLV Tax might not be advantageous for the propagation of BLV *in vivo*. Taken together, the findings discussed in this review suggest that there might be a dominant mechanism involved in the induction of apoptosis and expression of HTLV-1 *in vivo*. To address our hypothesis, it seems necessary to evaluate whether possible host responses against BLV infection, such as the induction of CTLs, genetic, and epigenetic alterations in apoptosis-regulatory genes, and DNA and chromatin modifications of BLV promoter for the suppression of viral expression, could be enhanced in animals infected with TaxD247G-encoded BLV. Thus, future investigations of the relationship between apoptosis and viral expression using BLV containing the mutant D247G Tax as a model will broaden our understanding of the replication and propagation of HTLV-1, and leukemia progression.

ACKNOWLEDGMENTS

The studies on BLV were supported by Grants-in-Aid for Scientific Research (A, B, and C) from the Japan Society for the Promotion of

Science (JSPS), and by a grant from the Program for the Promotion of Basic and Applied Research for Innovations in Bio-oriented Industry.

REFERENCES

Adam, E., Kerkhofs, P., Mammerickx, M., Burny, A., Kettmann, R., and Willems, L. (1996). The CREB, ATF-1, and ATF-2 transcription factors from bovine leukemia virus-infected B lymphocytes activate viral expression. *J. Virol.* 70, 1990–1999.

Adam, E., Kerkhofs, P., Mammerickx, M., Kettmann, R., Burny, A., Droogmans, L., et al. (1994). Involvement of the cyclic AMP-responsive element binding protein in bovine leukemia virus expression *in vivo*. *J. Virol.* 68, 5845–5853.

Aida, Y. (2001). Influence of host genetic differences on leukemogenesis induced by bovine leukemia virus. *AIDS Res. Hum. Retroviruses* 17, S12.

Aida, Y., Miyasaka, M., Okada, K., Onuma, M., Kogure, S., Suzuki, M., et al. (1989). Further phenotypic characterization of target cells for bovine leukemia virus experimental infection in sheep. *Am. J. Vet. Res.* 50, 1946–1951.

Aida, Y., Okada, K., and Amanuma, H. (1993). Phenotype and ontogeny of cells carrying a tumor-associated antigen that is expressed on bovine leukemia virus-induced lymphosarcoma. *Cancer Res.* 53, 429–437.

Alber, G., Kim, K. M., Weiser, P., Riesterer, C., Carsetti, R., and Reth, M. (1993). Molecular mimicry of the antigen receptor signalling motif by transmembrane proteins of the Epstein–Barr virus and the bovine leukaemia virus. *Curr. Biol.* 3, 333–339. doi: 10.1016/0960-9822(93)90196-U

Altanerova, V., Ban, J., Kettmann, R., and Altaner, C. (1990). Induction of leukemia in chicken by bovine leukemia virus due to insertional mutagenesis. *Arch. Geschwulstforsch.* 60, 89–96.

Altanerova, V., Portetelle, D., Kettmann, R., and Altaner, C. (1989). Infection of rats with bovine leukaemia virus: establishment of a virus-producing rat cell line. *J. Gen. Virol.* 70(Pt 7), 1929–1932. doi: 10.1099/0022-1317-70-7-1929

Andresen, V., Pise-Masison, C. A., Sinha-Datta, U., Bellon, M., Valeri, V., Washington Parks, R., et al. (2011). Suppression of HTLV-1 replication by Tax-mediated rerouting of the p13 viral protein to nuclear speckles. *Blood* 118, 1549–1559. doi: 10.1182/blood-2010-06-293340

Arainga, M., Takeda, E., and Aida, Y. (2012). Identification of bovine leukemia virus tax function associated with host cell transcription, signaling, stress response and immune response pathway by microarray-based gene expression analysis. *BMC Genomics* 13:121. doi: 10.1186/1471-2164-13-121

Bangham, C. R. (2003). Human T-lymphotropic virus type 1 (HTLV-1): persistence and immune control. *Int. J. Hematol.* 78, 297–303. doi: 10.1007/BF02983553

Boros, I. M., Tie, F., and Giam, C. Z. (1995). Interaction of bovine leukemia virus transactivator Tax with bZip proteins. *Virology* 214, 207–214. doi: 10.1006/viro.1995.9939

Boxus, M., Twizere, J. C., Legros, S., Dewulf, J. F., Kettmann, R., and Willems, L. (2008). The HTLV-1 Tax interactome. *Retrovirology* 5, 76. doi: 10.1186/1742-4690-5-76

Burny, A., Bex, F., Bruck, C., Cleuter, Y., Dekegel, D., Ghysdael, J., et al. (1979). Biochemical and epidemiological studies on bovine leukemia virus (BLV). *Haematol. Blood Transfus.* 23, 445–452.

Chen, G., Willems, L., Portetelle, D., Willard-Gallo, K. E., Burny, A., Gheysen, D., et al. (1989). Synthesis of functional bovine leukemia virus (BLV) p34tax protein by recombinant baculoviruses. *Virology* 173, 343–347. doi: 10.1016/0042-6822(89)90254-7

Chlichlia, K., and Khazaie, K. (2010). HTLV-1 Tax: linking transformation, DNA damage and apoptotic T-cell death. *Chem. Biol. Interact.* 188, 359–365. doi: 10.1016/j.cbi.2010.06.005

Collins, N. D., Newbound, G. C., Albrecht, B., Beard, J. L., Ratner, L., and Lairmore, M. D. (1998). Selective ablation of human T-cell lymphotropic virus type 1 p12I reduces viral infectivity *in vivo*. *Blood* 91, 4701–4707.

Dequiedt, F., Kettmann, R., Burny, A., and Willems, L. (1995). Mutations in the p53 tumor-suppressor gene are frequently associated with bovine leukemia virus-induced leukemogenesis in cattle but not in sheep. *Virology* 209, 676–683. doi: 10.1006/viro.1995.1303

Derse, D. (1987). Bovine leukemia virus transcription is controlled by a virus-encoded trans-acting factor and by *cis*-acting response elements. *J. Virol.* 61, 2462–2471.

Ding, W., Albrecht, B., Kelley, R. E., Muthusamy, N., Kim, S. J., Altschuld, R. A., et al. (2002). Human T-cell lymphotropic virus type 1 p12(I) expression increases cytoplasmic calcium to enhance the activation of nuclear factor of activated T cells. *J. Virol.* 76, 10374–10382. doi: 10.1128/JVI.76.20.10374-10382.2002

Djilali, S., and Parodi, A. L. (1989). The BLV-induced leukemia–lymphosarcoma complex in sheep. *Vet. Immunol. Immunopathol.* 22, 233–244. doi: 10.1016/0165-2427(89)90010-X

Felber, B. K., Derse, D., Athanassopoulos, A., Campbell, M., and Pavlakis, G. N. (1989). Cross-activation of the Rex proteins of HTLV-I and BLV and of the Rev protein of HIV-1 and nonreciprocal interactions with their RNA responsive elements. *New Biol.* 1, 318–328.

Ferrer, J. F., Marshak, R. R., Abt, D. A., and Kenyon, S. J. (1978). Persistent lymphocytosis in cattle: its cause, nature and relation to lymphosarcoma. *Ann. Rech. Vet.* 9, 851–857.

Ferrer, J. F., and Piper, C. E. (1978). An evaluation of the role of milk in the natural transmission of BLV. *Ann. Rech. Vet.* 9, 803–807.

Florins, A., Boxus, M., Vandermeers, F., Verlaeten, O., Bouzar, A. B., Defoiche, J., et al. (2008). Emphasis on cell turnover in two hosts infected by bovine leukemia virus: a rationale for host susceptibility to disease. *Vet. Immunol. Immunopathol.* 125, 1–7. doi: 10.1016/j.vetimm.2008.04.007

Florins, A., Gillet, N., Boxus, M., Kerkhofs, P., Kettmann, R., and Willems, L. (2007). Even attenuated bovine leukemia virus proviruses can be pathogenic in sheep. *J. Virol.* 81, 10195–10200. doi: 10.1128/JVI.01058-07

Franchini, G., Fukumoto, R., and Fullen, J. R. (2003). T-cell control by human T-cell leukemia/lymphoma virus type 1. *Int. J. Hematol.* 78, 280–296. doi: 10.1007/BF02983552

Gaudray, G., Gachon, F., Basbous, J., Biard-Piechaczyk, M., Devaux, C., and Mesnard, J. M. (2002). The complementary strand of the human T-cell leukemia virus type 1 RNA genome encodes a bZIP transcription factor that down-regulates viral transcription. *J. Virol.* 76, 12813–12822. doi: 10.1128/JVI.76.24.12813-12822.2002

Gessain, A., Barin, F., Vernant, J. C., Gout, O., Maurs, L., Calender, A., et al. (1985). Antibodies to human T-lymphotropic virus type-I in patients with tropical spastic paraparesis. *Lancet* 2, 407–410. doi: 10.1016/S0140-6736(85)92734-5

Gillet, N., Florins, A., Boxus, M., Burteau, C., Nigro, A., Vandermeers, F., et al. (2007). Mechanisms of leukemogenesis induced by bovine leukemia virus: prospects for novel anti-retroviral therapies in human. *Retrovirology* 4, 18. doi: 10.1186/1742-4690-4-18

Grassmann, R., Dengler, C., Muller-Fleckenstein, I., Fleckenstein, B., Mcguire, K., Dokhelar, M. C., et al. (1989). Transformation to continuous growth of primary human T lymphocytes by human T-cell leukemia virus type I X-region genes transduced by a Herpesvirus saimiri vector. *Proc. Natl. Acad. Sci. U.S.A.* 86, 3351–3355. doi: 10.1073/pnas.86.9.3351

Graves, D. C., and Ferrer, J. F. (1976). *In vitro* transmission and propagation of the bovine leukemia virus in monolayer cell cultures. *Cancer Res.* 36, 4152–4159.

Hanon, E., Hall, S., Taylor, G. P., Saito, M., Davis, R., Tanaka, Y., et al. (2000). Abundant tax protein expression in CD4+ T cells infected with human T-cell lymphotropic virus type I (HTLV-I) is prevented by cytotoxic T lymphocytes. *Blood* 95, 1386–1392.

Hiraragi, H., Michael, B., Nair, A., Silic-Benussi, M., Ciminale, V., and Lairmore, M. (2005). Human T-lymphotropic virus type 1 mitochondrion-localizing protein p13II sensitizes Jurkat T cells to Ras-mediated apoptosis. *J. Virol.* 79, 9449–9457. doi: 10.1128/JVI.79.15.9449-9457.2005

Hopkins, S. G., and DiGiacomo, R. F. (1997). Natural transmission of bovine leukemia virus in dairy and beef cattle. *Vet. Clin. North Am. Food Anim. Pract.* 13, 107–128.

Hu, R., Gan, Y., Liu, J., Miller, D., and Zoon, K. C. (1993). Evidence for multiple binding sites for several components of human lymphoblastoid interferon-alpha. *J. Biol. Chem.* 268, 12591–12595.

Igakura, T., Stinchcombe, J. C., Goon, P. K., Taylor, G. P., Weber, J. N., Griffiths, G. M., et al. (2003). Spread of HTLV-I between lymphocytes by virus-induced polarization of the cytoskeleton. *Science* 299, 1713–1716. doi: 10.1126/science.1080115

Inabe, K., Nishizawa, M., Tajima, S., Ikuta, K., and Aida, Y. (1999). The YXXL sequences of a transmembrane protein of bovine leukemia virus are required for viral entry and incorporation of viral envelope protein into virions. *J. Virol.* 73, 1293–1301.

Ishiguro, N., Furuoka, H., Matsui, T., Horiuchi, M., Shinagawa, M., Asahina, M., et al. (1997). p53 mutation as a potential cellular factor for tumor development

in enzootic bovine leukosis. *Vet. Immunol. Immunopathol.* 55, 351–358. doi: 10.1016/S0165-2427(96)05721-2

Jimba, M., Takeshima, S. N., Matoba, K., Endoh, D., and Aida, Y. (2010). BLV-CoCoMo-qPCR: quantitation of bovine leukemia virus proviral load using the CoCoMo algorithm. *Retrovirology* 7, 91. doi: 10.1186/1742-4690-7-91

Jimba, M., Takeshima, S. N., Murakami, H., Kohara, J., Kobayashi, N., Matsuhashi, T., et al. (2012). BLV-CoCoMo-qPCR: a useful tool for evaluating bovine leukemia virus infection status. *BMC Vet. Res.* 8:167. doi: 10.1186/1746-6148-8-167

Johnston, E. R., Powers, M. A., Kidd, L. C., and Radke, K. (1996). Peripheral blood mononuclear cells from sheep infected with a variant of bovine leukemia virus synthesize envelope glycoproteins but fail to induce syncytia in culture. *J. Virol.* 70, 6296–6303.

Juliarena, M. A., Poli, M., Sala, L., Ceriani, C., Gutierrez, S., Dolcini, G., et al. (2008). Association of BLV infection profiles with alleles of the BoLA-DRB3.2 *gene. Anim. Genet.* 39, 432–438. doi: 10.1111/j.1365-2052.2008.01750.x

Kashanchi, F., and Brady, J. N. (2005). Transcriptional and post-transcriptional gene regulation of HTLV-1. *Oncogene* 24, 5938–5951. doi: 10.1038/sj.onc.1208973

Katoh, I., Yoshinaka, Y., and Ikawa, Y. (1989). Bovine leukemia virus trans-activator p38tax activates heterologous promoters with a common sequence known as a cAMP-responsive element or the binding site of a cellular transcription factor ATF. *EMBO J.* 8, 497–503.

Kenyon, S. J., Ferrer, J. F., Mcfeely, R. A., and Graves, D. C. (1981). Induction of lymphosarcoma in sheep by bovine leukemia virus. *J. Natl. Cancer Inst.* 67, 1157–1163.

Kerkhofs, P., Heremans, H., Burny, A., Kettmann, R., and Willems, L. (1998). *In vitro* and *in vivo* oncogenic potential of bovine leukemia virus G4 protein. *J. Virol.* 72, 2554–2559.

Kettmann, R., Deschamps, J., Cleuter, Y., Couez, D., Burny, A., and Marbaix, G. (1982). Leukemogenesis by bovine leukemia virus: proviral DNA integration and lack of RNA expression of viral long terminal repeat and 3′ proximate cellular sequences. *Proc. Natl. Acad. Sci. U.S.A.* 79, 2465–2469. doi: 10.1073/pnas.79.8.2465

Klener, P., Szynal, M., Cleuter, Y., Merimi, M., Duvillier, H., Lallemand, F., et al. (2006). Insights into gene expression changes impacting B-cell transformation: cross-species microarray analysis of bovine leukemia virus tax-responsive genes in ovine B cells. *J. Virol.* 80, 1922–1938. doi: 10.1128/JVI.80.4.1922-1938.2006

Komori, H., Ishiguro, N., Horiuchi, M., Shinagawa, M., and Aida, Y. (1996). Predominant p53 mutations in enzootic bovine leukemic cell lines. *Vet. Immunol. Immunopathol.* 52, 53–63. doi: 10.1016/0165-2427(95)05538-X

Konishi, H., Kobayashi, N., and Hatanaka, M. (1984). Defective human T-cell leukemia virus in adult T-cell leukemia patients. *Mol. Biol. Med.* 2, 273–283.

Konnai, S., Takeshima, S. N., Tajima, S., Yin, S. A., Okada, K., Onuma, M., et al. (2003). The influence of ovine MHC class II DRB1 alleles on immune response in bovine leukemia virus infection. *Microbiol. Immunol.* 47, 223–232.

Konnai, S., Usui, T., Ikeda, M., Kohara, J., Hirata, T., Okada, K., et al. (2006). Tumor necrosis factor-alpha genetic polymorphism may contribute to progression of bovine leukemia virus-infection. *Microbes Infect.* 8, 2163–2171. doi: 10.1016/j.micinf.2006.04.017

Kono, Y., Sentsui, H., Arai, K., Ishida, H., and Irishio, W. (1983). Contact transmission of bovine leukemia virus under insect-free conditions. *J. Vet. Med. Sci.* 45, 799–802.

Korber, B., Okayama, A., Donnelly, R., Tachibana, N., and Essex, M. (1991). Polymerase chain reaction analysis of defective human T-cell leukemia virus type I proviral genomes in leukemic cells of patients with adult T-cell leukemia. *J. Virol.* 65, 5471–5476.

Koyanagi, Y., Itoyama, Y., Nakamura, N., Takamatsu, K., Kira, J., Iwamasa, T., et al. (1993). *In vivo* infection of human T-cell leukemia virus type I in non-T cells. *Virology* 196, 25–33. doi: 10.1006/viro.1993.1451

Lagarias, D. M., and Radke, K. (1989). Transcriptional activation of bovine leukemia virus in blood cells from experimentally infected, asymptomatic sheep with latent infections. *J. Virol.* 63, 2099–2107.

Lefebvre, L., Vanderplasschen, A., Ciminale, V., Heremans, H., Dangoisse, O., Jauniaux, J. C., et al. (2002). Oncoviral bovine leukemia virus G4 and human T-cell leukemia virus type 1 p13(II) accessory proteins interact with farnesyl pyrophosphate synthetase. *J. Virol.* 76, 1400–1414. doi: 10.1128/JVI.76.3.1400-1414.2002

Leisering, A. (1871). Hypertrophy der Malpigischen Korperchen der Milz. *Bericht uber das Veterinarwesen im Konigreich Sachsen* 16, 15–16.

Lemasson, I., Lewis, M. R., Polakowski, N., Hivin, P., Cavanagh, M. H., Thebault, S., et al. (2007). Human T-cell leukemia virus type 1 (HTLV-1) bZIP protein interacts with the cellular transcription factor CREB to inhibit HTLV-1 transcription. *J. Virol.* 81, 1543–1553. doi: 10.1128/JVI.00480-06

Lewin, H. A., and Bernoco, D. (1986). Evidence for BoLA-linked resistance and susceptibility to subclinical progression of bovine leukaemia virus infection. *Anim. Genet.* 17, 197–207. doi: 10.1111/j.1365-2052.1986.tb03191.x

Lewin, H. A., Wu, M. C., Stewart, J. A., and Nolan, T. J. (1988). Association between BoLA and subclinical bovine leukemia virus infection in a herd of Holstein–Friesian cows. *Immunogenetics* 27, 338–344. doi: 10.1007/BF00395129

Mammerickx, M., Portetelle, D., and Burny, A. (1981). Experimental cross-transmissions of bovine leukemia virus (BLV) between several animal species. *Zbl. Vet. Med. B* 28, 69–81. doi: 10.1111/j.1439-0450.1981.tb01740.x

Matsuoka, M., and Jeang, K. T. (2011). Human T-cell leukemia virus type 1 (HTLV-1) and leukemic transformation: viral infectivity, Tax, HBZ and therapy. *Oncogene* 30, 1379–1389. doi: 10.1038/onc.2010.537

Mirsky, M. L., Olmstead, C. A., Da, Y., and Lewin, H. A. (1996). The prevalence of proviral bovine leukemia virus in peripheral blood mononuclear cells at two subclinical stages of infection. *J. Virol.* 70, 2178–2183.

Miyasaka, T., Takeshima, S. N., Jimba, M., Matsumoto, Y., Kobayashi, N., Matsuhashi, T., et al. (2013). Identification of bovine leukocyte antigen class II haplotypes associated with variations in bovine leukemia virus proviral load in Japanese Black cattle. *Tissue Antigens* 81, 72–82. doi: 10.1111/tan.12041

Murakami, H., Kuroiwa, T., Suzuki, K., Miura, Y., and Sentsui, H. (2011a). Analysis of Syk expression in bovine lymphoma and persistent lymphocytosis induced by bovine leukemia virus. *J. Vet. Med. Sci.* 73, 41–45. doi: 10.1292/jvms.10-0225

Murakami, H., Yamada, T., Suzuki, M., Nakahara, Y., Suzuki, K., and Sentsui, H. (2011b). Bovine leukemia virus integration site selection in cattle that develop leukemia. *Virus Res.* 156, 107–112. doi: 10.1016/j.virusres.2011.01.004

Murakami, K., Aida, Y., Kageyama, R., Numakunai, S., Ohshima, K., Okada, K., et al. (1994a). Immunopathologic study and characterization of the phenotype of transformed cells in sheep with bovine leukemia virus-induced lymphosarcoma. *Am. J. Vet. Res.* 55, 72–80.

Murakami, K., Okada, K., Ikawa, Y., and Aida, Y. (1994b). Bovine leukemia virus induces $CD5^-$ B cell lymphoma in sheep despite temporarily increasing $CD5^+$ B cells in asymptomatic stage. *Virology* 202, 458–465. doi: 10.1006/viro.1994.1362

Nagaoka, Y., Kabeya, H., Onuma, M., Kasai, N., Okada, K., and Aida, Y. (1999). Ovine MHC class II DRB1 alleles associated with resistance or susceptibility to development of bovine leukemia virus-induced ovine lymphoma. *Cancer Res.* 59, 975–981.

Nicot, C., Dundr, M., Johnson, J. M., Fullen, J. R., Alonzo, N., Fukumoto, R., et al. (2004). HTLV-1-encoded p30II is a post-transcriptional negative regulator of viral replication. *Nat. Med.* 10, 197–201. doi: 10.1038/nm984

Ohshima, K., Kikuchi, M., Masuda, Y., Kobari, S., Sumiyoshi, Y., Eguchi, F., et al. (1991). Defective provirus form of human T-cell leukemia virus type I in adult T-cell leukemia/lymphoma: clinicopathological features. *Cancer Res.* 51, 4639–4642.

Onuma, M., Honma, T., Mikami, T., Ichijo, S., and Konishi, T. (1979). Studies on the sporadic and enzootic forms of bovine leukosis. *J. Comp. Pathol.* 89, 159–167. doi: 10.1016/0021-9975(79)90055-0

Onuma, M., Wada, M., Yasutomi, Y., Yamamoto, M., Okada, H. M., and Kawakami, Y. (1990). Suppression of immunological responses in rabbits experimentally infected with bovine leukemia virus. *Vet. Microbiol.* 25, 131–141. doi: 10.1016/0378-1135(90)90072-4

Osame, M., Usuku, K., Izumo, S., Ijichi, N., Amitani, H., Igata, A., et al. (1986). HTLV-I associated myelopathy, a new clinical entity. *Lancet* 1, 1031–1032. doi: 10.1016/S0140-6736(86)91298-5

Panei, C. J., Takeshima, S. N., Omori, T., Nunoya, T., Davis, W. C., Ishizaki, H., et al. (2013). Estimation of bovine leukemia virus (BLV) proviral load harbored by lymphocyte subpopulations in BLV-infected cattle at the subclinical stage of enzootic bovine leucosis using BLV-CoCoMo-qPCR. *BMC Vet. Res.* 9:95. doi: 10.1186/1746-6148-9-95

Philpott, S. M., and Buehring, G. C. (1999). Defective DNA repair in cells with human T-cell leukemia/bovine leukemia viruses: role of tax gene. *J. Natl. Cancer Inst.* 91, 933–942. doi: 10.1093/jnci/91.11.933

Richard, A., and Tulasne, D. (2012). Caspase cleavage of viral proteins, another way for viruses to make the best of apoptosis. *Cell Death Dis.* 3, e277. doi: 10.1038/cddis.2012.18

Robert-Guroff, M., Weiss, S. H., Giron, J. A., Jennings, A. M., Ginzburg, H. M., Margolis, I. B., et al. (1986). Prevalence of antibodies to HTLV-I, -II, and -III in intravenous drug abusers from an AIDS endemic region. *JAMA* 255, 3133–3137. doi: 10.1001/jama.1986.03370220095034

Sagata, N., Yasunaga, T., Ogawa, Y., Tsuzuku-Kawamura, J., and Ikawa, Y. (1984a). Bovine leukemia virus: unique structural features of its long terminal repeats and its evolutionary relationship to human T-cell leukemia virus. *Proc. Natl. Acad. Sci. U.S.A.* 81, 4741–4745. doi: 10.1073/pnas.81.15.4741

Sagata, N., Yasunaga, T., Ohishi, K., Tsuzuku-Kawamura, J., Onuma, M., and Ikawa, Y. (1984b). Comparison of the entire genomes of bovine leukemia virus and human T-cell leukemia virus and characterization of their unidentified open reading frames. *EMBO J.* 3, 3231–3237.

Sakakibara, N., Kabeya, H., Ohashi, K., Sugimoto, C., and Onuma, M. (1998). Epitope mapping of bovine leukemia virus transactivator protein tax. *J. Vet. Med. Sci.* 60, 599–605. doi: 10.1292/jvms.60.599

Satou, Y., Yasunaga, J., Yoshida, M., and Matsuoka, M. (2006). HTLV-I basic leucine zipper factor gene mRNA supports proliferation of adult T cell leukemia cells. *Proc. Natl. Acad. Sci. U.S.A.* 103, 720–725. doi: 10.1073/pnas.05076 31103

Satou, Y., Yasunaga, J., Zhao, T., Yoshida, M., Miyazato, P., Takai, K., et al. (2011). HTLV-1 bZIP factor induces T-cell lymphoma and systemic inflammation *in vivo*. *PLoS Pathog.* 7:e1001274. doi: 10.1371/journal.ppat.1001274

Schwartz, I., Bensaid, A., Polack, B., Perrin, B., Berthelemy, M., and Levy, D. (1994). *In vivo* leukocyte tropism of bovine leukemia virus in sheep and cattle. *J. Virol.* 68, 4589–4596.

Schwartz, I., and Levy, D. (1994). Pathobiology of bovine leukemia virus. *Vet. Res.* 25, 521–536.

Starkenburg, R. J., Hansen, L. B., Kehrli, M. E. Jr., and Chester-Jones, H. (1997). Frequencies and effects of alternative DRB3.2 alleles of bovine lymphocyte antigen for Holsteins in milk selection and control lines. *J. Dairy Sci.* 80, 3411–3419. doi: 10.3168/jds.S0022-0302(97)76316-1

Stott, M. L., Thurmond, M. C., Dunn, S. J., Osburn, B. I., and Stott, J. L. (1991). Integrated bovine leukosis proviral DNA in T helper and T cytotoxic/suppressor lymphocytes. *J. Gen. Virol.* 72(Pt 2), 307–315. doi: 10.1099/0022-1317-72-2-307

Sulimova, G. E., Udina, I. G., Shaikhaev, G. O., and Zakharov, I. A. (1995). DNA polymorphism of the BoLA-DRB3 gene in cattle in connection with resistance and susceptibility to leukemia. *Genetika* 31, 1294–1299.

Szynal, M., Cleuter, Y., Beskorwayne, T., Bagnis, C., Van Lint, C., Kerkhofs, P., et al. (2003). Disruption of B-cell homeostatic control mediated by the BLV-Tax oncoprotein: association with the upregulation of Bcl-2 and signaling through NF-kappaB. *Oncogene* 22, 4531–4542. doi: 10.1038/sj.onc.1206546

Tajima, S., and Aida, Y. (2000). The region between amino acids 245 and 265 of the bovine leukemia virus (BLV) tax protein restricts transactivation not only via the BLV enhancer but also via other retrovirus enhancers. *J. Virol.* 74, 10939–10949. doi: 10.1128/JVI.74.23.10939-10949.2000

Tajima, S., and Aida, Y. (2002). Mutant tax protein from bovine leukemia virus with enhanced ability to activate the expression of c-fos. *J. Virol.* 76, 2557–2562. doi: 10.1128/jvi.76.5.2557-2562.2002

Tajima, S., and Aida, Y. (2005). Induction of expression of bovine leukemia virus (BLV) in blood taken from BLV-infected cows without removal of plasma. *Microbes Infect.* 7, 1211–1216. doi: 10.1016/j.micinf.2005.04.010

Tajima, S., Ikawa, Y., and Aida, Y. (1998a). Complete bovine leukemia virus (BLV) provirus is conserved in BLV-infected cattle throughout the course of B-cell lymphosarcoma development. *J. Virol.* 72, 7569–7576.

Tajima, S., Zhuang, W. Z., Kato, M. V., Okada, K., Ikawa, Y., and Aida, Y. (1998b). Function and conformation of wild-type p53 protein are influenced by mutations in bovine leukemia virus-induced B-cell lymphosarcoma. *Virology* 243, 735–746. doi: 10.1006/viro.1998.9051

Tajima, S., Takahashi, M., Takeshima, S. N., Konnai, S., Yin, S. A., Watarai, S., et al. (2003a). A mutant form of the tax protein of bovine leukemia virus (BLV), with enhanced transactivation activity, increases expression and propagation of BLV *in vitro* but not *in vivo*. *J. Virol.* 77, 1894–1903. doi: 10.1128/JVI.77.3.1894-1903.2003

Tajima, S., Tsukamoto, M., and Aida, Y. (2003b). Latency of viral expression *in vivo* is not related to CpG methylation in the U3 region and part of the R region of the long terminal repeat of bovine leukemia virus. *J. Virol.* 77, 4423–4430. doi: 10.1128/JVI.77.7.4423-4430.2003

Takahashi, M., Tajima, S., Okada, K., Davis, W. C., and Aida, Y. (2005). Involvement of bovine leukemia virus in induction and inhibition of apoptosis. *Microbes Infect.* 7, 19–28. doi: 10.1016/j.micinf.2004.09.014

Takahashi, M., Tajima, S., Takeshima, S. N., Konnai, S., Yin, S. A., Okada, K., et al. (2004). Ex vivo survival of peripheral blood mononuclear cells in sheep induced by bovine leukemia virus (BLV) mainly occurs in $CD5^{-}$ B cells that express BLV. *Microbes Infect.* 6, 584–595. doi: 10.1016/j.micinf.2004.02.014

Takeshima, S-N., and Aida, Y. (2006). Structure, function and disease susceptibility of the bovine major histocompatibility complex. *Anim. Sci. J.* 77, 138–150. doi: 10.1111/j.1740-0929.2006.00332.x

Tanaka, A., Takahashi, C., Yamaoka, S., Nosaka, T., Maki, M., and Hatanaka, M. (1990). Oncogenic transformation by the tax gene of human T-cell leukemia virus type I *in vitro*. *Proc. Natl. Acad. Sci. U.S.A.* 87, 1071–1075. doi: 10.1073/pnas.87.3.1071

Theilen, G. H., and Dungworth, D. L. (1965). Bovine lymphosarcoma in California. 3. The calf form. *Am. J. Vet. Res.* 26, 696–709.

Tsukasaki, K., Tsushima, H., Yamamura, M., Hata, T., Murata, K., Maeda, T., et al. (1997). Integration patterns of HTLV-I provirus in relation to the clinical course of ATL: frequent clonal change at crisis from indolent disease. *Blood* 89, 948–956.

Voneche, V., Portetelle, D., Kettmann, R., Willems, L., Limbach, K., Paoletti, E., et al. (1992). Fusogenic segments of bovine leukemia virus and simian immunodeficiency virus are interchangeable and mediate fusion by means of oblique insertion in the lipid bilayer of their target cells. *Proc. Natl. Acad. Sci. U.S.A.* 89, 3810–3814. doi: 10.1073/pnas.89.9.3810

Weiss, R., Teich, N., Varmus, H., and Coffin, J. (1985). *RNA Tumor Viruses*. New York: Cold Spring Harbor Laboratory.

Willems, L., Gatot, J. S., Mammerickx, M., Portetelle, D., Burny, A., Kerkhofs, P., et al. (1995). The YXXL signalling motifs of the bovine leukemia virus transmembrane protein are required for *in vivo* infection and maintenance of high viral loads. *J. Virol.* 69, 4137–4141.

Willems, L., Gegonne, A., Chen, G., Burny, A., Kettmann, R., and Ghysdael, J. (1987). The bovine leukemia virus p34 is a transactivator protein. *EMBO J.* 6, 3385–3389.

Willems, L., Grimonpont, C., Kerkhofs, P., Capiau, C., Gheysen, D., Conrath, K., et al. (1998). Phosphorylation of bovine leukemia virus Tax protein is required for *in vitro* transformation but not for transactivation. *Oncogene* 16, 2165–2176. doi: 10.1038/sj.onc.1201765

Willems, L., Heremans, H., Chen, G., Portetelle, D., Billiau, A., Burny, A., et al. (1990). Cooperation between bovine leukaemia virus transactivator protein and Ha-ras oncogene product in cellular transformation. *EMBO J.* 9, 1577–1581.

Willems, L., Kerkhofs, P., Dequiedt, F., Portetelle, D., Mammerickx, M., Burny, A., et al. (1994). Attenuation of bovine leukemia virus by deletion of R3 and G4 open reading frames. *Proc. Natl. Acad. Sci. U.S.A.* 91, 11532–11536. doi: 10.1073/pnas.91.24.11532

Williams, D. L., Barta, O., and Amborski, G. F. (1988). Molecular studies of T-lymphocytes from cattle infected with bovine leukemia virus. *Vet. Immunol. Immunopathol.* 19, 307–323. doi: 10.1016/0165-2427(88)90117-1

Wu, D., Takahashi, K., Murakami, K., Tani, K., Koguchi, A., Asahina, M., et al. (1996). B-1a, B-1b and conventional B cell lymphoma from enzootic bovine leukosis. *Vet. Immunol. Immunopathol.* 55, 63–72. doi: 10.1016/S0165-2427(96)05631-0

Wurzer, W. J., Planz, O., Ehrhardt, C., Giner, M., Silberzahn, T., Pleschka, S., et al. (2003). Caspase 3 activation is essential for efficient influenza virus propagation. *EMBO J.* 22, 2717–2728. doi: 10.1093/emboj/cdg279

Wyatt, C. R., Wingett, D., White, J. S., Buck, C. D., Knowles, D., Reeves, R., et al. (1989). Persistent infection of rabbits with bovine leukemia virus associated with development of immune dysfunction. *J. Virol.* 63, 4498–4506.

Xu, A., Van Eijk, M. J., Park, C., and Lewin, H. A. (1993). Polymorphism in BoLA-DRB3 exon 2 correlates with resistance to persistent lymphocytosis caused by bovine leukemia virus. *J. Immunol.* 151, 6977–6985.

Zanotti, M., Poli, G., Ponti, W., Polli, M., Rocchi, M., Bolzani, E., et al. (1996). Association of BoLA class II haplotypes with subclinical progression of bovine leukaemia virus infection in Holstein–Friesian cattle. *Anim. Genet.* 27, 337–341.

Zhang, W., Nisbet, J. W., Albrecht, B., Ding, W., Kashanchi, F., Bartoe, J. T., et al. (2001). Human T-lymphotropic virus type 1 p30(II) regulates gene transcription by binding CREB binding protein/p300. *J. Virol.* 75, 9885–9895. doi: 10.1128/JVI.75.20.9885-9895.2001

Zhao, T., Satou, Y., Sugata, K., Miyazato, P., Green, P. L., Imamura, T., et al. (2011). HTLV-1 bZIP factor enhances TGF-beta signaling through p300 coactivator. *Blood* 118, 1865–1876. doi: 10.1182/blood-2010-12-326199

Zhao, T., Yasunaga, J., Satou, Y., Nakao, M., Takahashi, M., Fujii, M., et al. (2009). Human T-cell leukemia virus type 1 bZIP factor selectively suppresses the classical pathway of NF-kappaB. *Blood* 113, 2755–2764. doi: 10.1182/blood-2008-06-161729

Zhuang, W., Tajima, S., Okada, K., Ikawa, Y., and Aida, Y. (1997). Point mutation of p53 tumor suppressor gene in bovine leukemia virus-induced lymphosarcoma. *Leukemia* 11(Suppl 3), 344–346.

Conflict of Interest Statement: The authors declare that the research was conducted in the absence of any commercial or financial relationships that could be construed as a potential conflict of interest.

Received: 30 July 2013; accepted: 17 October 2013; published online: 08 November 2013.

*Citation: Aida Y, Murakami H, Takahashi M and Takeshima S-N (2013) Mechanisms of pathogenesis induced by bovine leukemia virus as a model for human T-cell leukemia virus. Front. Microbiol. **4**:328. doi: 10.3389/fmicb.2013.00328*

This article was submitted to Virology, a section of the journal Frontiers in Microbiology.

犬の IL-13 遺伝子の解析

１．犬 IL-13 遺伝子の遺伝子多型探索
２．犬 IL-13 遺伝子上の遺伝子多型の頻度調査
３．犬 IL-13 遺伝子の多型とアトピー性皮膚炎との相関解析

滝沢達也（麻布大学動物工学）、田中和明（麻布大学動物工学）

１．犬 IL-13 遺伝子の遺伝子多型探索

研究要旨

IL-13 は、主に Th2 細胞によって産生されるサイトカインで、アレルギー性疾患や自己免疫疾患の関連因子として注目されている。本研究では、イヌ *IL-13* 遺伝子に存在する多型を見つけるために、全エクソン・イントロンを含む約 4.8ｋｂの塩基配列を 15 犬種合計 34 個体で決定した。配列を相互に比較した結果、14 カ所の一塩基多型（SNP）と、１つの縦列反復多型を検出した。このうち 6 つの多型は、dbSNP に登録されていない新規のものであった。検出した多型のうち rs22147008 は、IL-13 の 63 番目のアミノ酸をトレオニンからアラニンに変更する。ウマ、ヒト、チンパンジー、カニクイザル、ウシ、ブタ、ラットおよびマウスのアミノ酸配列を比較すると 63 番目は全ての種でトレオニンであり、アラニンへの置換は進化学的に例外であることが示された。さらに、Polyphen-2 を用いたシミュレーションでもタンパク質の高次構造に大きなダメージを与えることが示唆された。ゆえに rs22147008 多型は、イヌにおいて IL-13 が関与する疾病に影響をおよぼす変異の重要な候補であることが示された。また、5´隣接領域に 9 カ所の多型が検出されたことから、IL-13 の発現に影響する多型の候補を見つけることができた。

研究目的

IL-13 は、主に Th2 細胞によって産生されるサイトカインで、Ｂ細胞による IgE 生産を促進し、IL-1 や IL-6 といった炎症誘発性サイトカインの生産を抑制することでマクロファージの活性を低下させる。IL-13 は喘息などのアレルギー性疾患や潰瘍性大腸炎などの自己免疫疾患の関連因子として注目されている。さらに IL-13 を欠損したマウスモデルでは、DMBA/TPA 誘発皮膚腫瘍の発生率が高まる事が報告されている。ヒトでは、IL-13 の 5’隣接領域-1112 C>T 多型(rs1800925)および、コーデング領域の NM_002188.2(IL13):c.431A>G 多型（rs20541）が、喘息またはアトピー性皮膚炎のリスク因子として報告されている。rs20541 多型はヒト IL-13 前駆体タンパク質の 144 番目（IL-13 では 110 番目）の残基をアルギニンからグルタミンに置換させる。グル

タミンに置換しているタイプではTh2機能が野生型よりも増強されると報告がある。このような背景から、イヌにおいても *IL-13* 遺伝子上に、IL-13の制御に変更を加える変異が見つかる可能性がある。そこで、日本犬を含む15犬種を用いて *IL-13* 遺伝子の配列を決定し多型を検索した。

材料と方法

IL-13 遺伝子の配列決定は、コリー(1個体)、ボーダーコリー（1個体)、シェットランドシープドッグ(1個体）、ラブラドールレトリーバー（1個体)、ゴールデンレトリーバー（3個体)、セッター（2個体)、ジャーマンシェパード（3個体)、ミニチュアダックスフント（3個体)、ビーグル（3個体)、ポメラニアン(2個体)、シーズー（2個体)、シベリアンハスキー（2個体)、柴犬（2個体)、秋田犬（3個体)、甲斐犬（5個体）の15犬種34個体を用いた。イヌ11番染色体のリファレンスゲノム(NC_006593.3)において、g.20956959からg.20961751までの約4.8kbの配列を対象に、表１に示した3組のプライマーセットを用いて *IL-13* 遺伝子のDNA断片を増幅した。この区間は、イヌ *IL-13* 遺伝子の全てのエクソンとイントロンおよび、推定転写開始点から5´側に1.5kb上流と停止コドンから3´側下流1.1ｋｂを含んでいる。これらのDNA断片を精製した後、BigDye Terminator v3.1 Cycle Sequencing KitおよびABI 3130 シークエンサー(Thermo Fisher Scientific, Waltham, Massachusetts, USA）を用いて塩基配列を決定した。得られた配列は、リファレンスゲノム配列（犬種はボクサー）と相互に比較し多型を検出した。

結果および考察

34個体の配列およびリファレンスゲノム配列を比較した結果、表２に示した14か所の1塩基多型（SNP）と、AGGTGGGCAの9塩基を単位とする縦列反復多型が1か所で見つかった。このうち6つの多型は、dbSNPに登録されていない新規のものであった。これらの多型の中で、rs22147008は、IL-13前駆体タンパク質の81番目のアミノ酸をトレオニンからアラニンに変更する非同義置換であった。この位置は、18個のアミノ酸からなるシグナルペプチドを除去したIL-13では、63番目の残基に位置づけられる。このアミノ酸置換（以後IL-13　p.63 Thr>Alaと表記）の進化学的位置づけを行うために、ウマ、ヒト、チンパンジー、カニクイザル、ウシ、ブタ、ラットおよびマウスのIL-13のアミノ酸配列と比較した（図１)。p.63 Thr>Ala多型は、IL-13の構造上重要なαヘリックスCの中央に位置する事が明らかとなった。また、比較に用いた全ての種においてトレオニンに固定されていた。ゆえに、IL-13番目のアミノ酸残基がトレオニンである事がIL-13の機能に重要であると考えられた。さらに、Polyphen-2（http://genetics.bwh.harvard.edu/pph2/）を用いたシミュレーションからp.63 Thr>Ala多型は、タンパク質の高次構造に大きなダメージを与えることが予測された。

以上の事から、rs22147008 多型は、IL-13 の機能に大きな変更を加える事が強く示唆された。ゆえにこの多型は、イヌにおいて IL-13 シグナルの異常が関与する疾患に対する重要な候補変異である事が示された。また、本研究で発見した *IL-13* 遺伝子の 5´ 隣接領域における縦列反復多型の中には、NFAT 1 や SP1 を含む複数の転写因子と潜在的に結合するモチーフが含まれていた。プロモータ内での反復配列多型が、遺伝子の転写活性に影響を及ぼす例が多く知られていることから、5´ 隣接領域内の多型も同時に調査する必要がある。

表1. イヌ*IL-13*遺伝子の増幅に用いたプライマーの塩基配列

		プライマーの塩基配列	アニーリング温度	産物の大きさ(bp)	注釈
領域1	F側	TACAGCCAAGTGACAGCACA	63	1655	5´隣接領域からエクソン1
	R側	AATGAGCTCCTTGAGGGTTG			
領域2	F側	GGTGGGAGGCGTCATCATTT	63	1695	エクソン1からエクソン3
	R側	TGCTTTCAGCATCCTCTGGG			
領域3	F側	CCATGCAGACCAGTGAAGGT	63	1810	イントロン2から3´隣接領域
	R側	GGACAAAGGAAGGCAAAGTG			

表2. イヌ*IL13*遺伝子上で見つかった多型. 染色体上の位置はイヌ11番染色体のリファレンスゲノム(NC_006593.3)に従っている.

染色体上の位置	機能的位置	mRNA上の位置	多型	dbSNPでのID	アミノ酸置換
20957075	5´隣接領域		AGGTGGGCA:[1]>[2]	新規	
20957380	5´隣接領域		G>C	新規	
20957425	5´隣接領域		A>G	新規	
20957580	5´隣接領域		G>A	rs8973297	
20957626	5´隣接領域		T>C	rs8973298	
20957831	5´隣接領域		A>C	新規	
20957836	5´隣接領域		G>C	新規	
20958170	5´隣接領域		T>C	rs8973300	
20958378	5´隣接領域		G>A	rs8973301	
20958774	イントロン1		T>C	rs852551792	
20958830	イントロン1		C>A	rs851187807	
20958940	イントロン1		G>C	新規	
20960082	エクソン3	292	A>G	rs22147008	Thr > Ala(IL13前駆体の81番目/IL13の63番目)
20960989	エクソン4	847	G>C	rs22133662	非コード
20961598	3´隣接領域		T>C	rs22098236	

図１ IL-13 のアミノ酸配列の比較．アミノ酸残基のポジジョンはシグナルペプチドが除去されている。

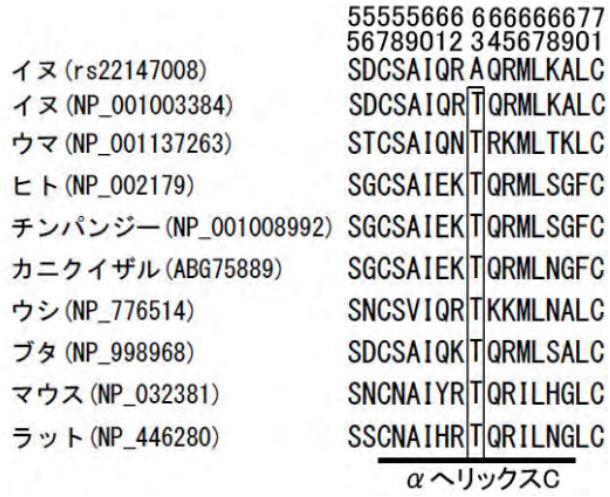

２．犬 IL-13 遺伝子上の遺伝子多型の頻度調査

研究要旨

イヌ *IL-13* 遺伝子において、転写調整に影響を与える可能性のある 5´隣接領域に存在する g 20957075 AGGTGGGCA：[1] > [2]、g. 20957831 A>C、 rs8973298 および、rs8973300 の 4 カ所と IL-13 の非同義置換 rs22147008 の対立遺伝頻度を、20 犬種を対象に調査した。調査結果は、表２に示した。５つの座位は、9 犬種から 20 犬種において対立遺伝子の多型が認められた。一部の品種でアレルの固定が認められたものの、本研究の対象とした５つの座位は、いずれも広範囲の犬種で対立遺伝子の多様性が存在したことから、家畜犬に広く分布するコモン多型であることが明らかとなった。5 つの座位のうち g. 20957831 A>C を除く４つの多型部位では、品種間で対立遺伝子頻度に大きな差が認められ、メジャーアレルとマイナーアレルの関係が逆転する現象も認められた。20 犬種における対立遺伝頻度の傾向を明らかにしたことで、イヌ *IL-13* 遺伝子多型を対象とする相関解析を実施するための基礎情報を得ることができた。

研究目的

前項の研究でイヌ *IL-13* 遺伝子において 15 カ所の多型を検出した。この中で、5´隣接領域に存在する g 20957075 AGGTGGGCA：[1] > [2]、g. 20957831 A>C、 rs8973298 および、rs8973300 の 4 カ所の多型は、IL-13 の転写調節に関与する可能性のある複数の転写因子の結合モチーフを含んでいた。また、rs22147008 は、IL-13 の構造上重要と考えられる位置でのアミノ酸配列を生じさせる。ゆえに、IL-13 が寄与する疾患との相関する可能性がある。しかし、これらの多型における対立遺伝子頻度に関する情報は、これまで全く知られていない。一般に、イヌの繁殖は品種ごとに独立して行われていることから、遺伝子浮動の影響を受けやすく、品種ごとに対立遺伝子頻度が大きく異なる事が予想され

る。本研究では、*IL-13*遺伝多型と疾患との関連を調査する前段階として、犬種別の対立遺伝子頻度を明らかにすることを目的とした。

材料と方法

ゴールデンレトリーバー、ラブラドールレトリーバー、ビーグル、シェットランドシープドッグ、マルチーズ、・コーギーヨークシャーテリア、トイプードル、ミニチュアダックスフント、チワワ、ジャーマンシェパード、シーズー、ポメラリアン、パピヨン、ウェルッシュ・コーギー、パグ、ミニチュアピンシャー、シベリアンハスキー、柴犬、甲斐犬および秋田犬の 20 犬種において、見かけ上健康な成犬を選択し、1 犬種あたり 8 から 35 個体の DNA 試料を解析した。g 20957075 AGGTGGGCA : [1] > [2]、g.20957831 A>C、rs8973298、rs8973300 および、rs22147008 の多型部位を含む DNA 断片を表 1 に示した 5 組のプライマーセットを用いて PCR 増幅した。このうち g 20957075 AGGTGGGCA: [1] > [2] 多型は、PCR 産物をアガロースゲル電気泳動する事で、増幅断片長多型として遺伝子型を判定した。残りの 4 カ所に SNP に対しては、表 1 に示した制限酵素を用いて DNA 断片を処理した後に、アガロースゲル電気泳動を行い、制限酵素切断断片長多型として遺伝子型を判定した。

結果および考察

イヌ *IL-13* 遺伝子に存在する 5 つの多型座位に対する対立遺伝子頻度を表 2 に示した。rs8973300 では、調査した 20 犬種全てから多型が検出された。また、g 20957075 AGGTGGGCA : [1] > [2] と rs8973298 でも、シベリアンハスキーを除く 19 犬種で多型が認められた。これに対して、rs22147008 と g.20957831 A>C では、多型認められた犬種は、それぞれ 14 犬種と 9 犬種であり、残りの犬種ではマイナーアレルが全く検出されなかった。g.20957831 A>C では、調査した 20 犬種において常に A 型がメジャーアレルであった。これに対して、残りの 4 つの多型では、犬種によってメジャーアレルとマイナーアレルの関係が逆転することがあった。

一部の品種でアレルの固定が認められたものの本研究の調査対象とした 5 つの多型は、いずれも広範囲の犬種に分布していることから、個々の品種が確立した後に新しく生じた変異ではなく、家畜犬に広く分布するコモン多型であることが明らかとなった。また、アレルが固定されていた品種間に明確な関連性は認められないことから遺伝子浮動によって生じた現象であると考えられた。

前項の研究で、IL-13 タンパク質の構造に大きな影響をおよぼすと考えられた rs22147008 の G 型について、頻度 10%未満の品種が 20 犬種中 10 犬種と最も多く、結果としてホモ接合体は極めて少数であった。このため、疾病との相関解析を進めるにあたり、rs22147008 の G 型ホモ接合の個体を見つけることが困難な品種が多く存在する事が示された。しかし、ミニュチュアダックスフント、チワワ、ポメラニアンおよび、パグでは、G

型の頻度が約 50%前後の高い値を示し、ハーディワインベルグ平衡の期待値に近い割合で G 型ホモ接合体が認められた。ゆえに rs22147008 の G 型ホモ接合が先天的に明確な異常表現型もつことはないと考えられた。rs22147008 の G 型と疾病との関係を相関解析には、集団内でホモ接合の個体がえやすいこれらの品種を用いると効率的であることが示された。

以上のように、日本国内で飼育されている 20 犬種における対立遺伝頻度の傾向を明らかにしたことで、イヌ IL-13 遺伝子多型を対象とする相関解析を実施するための基礎情報を得ることができた。

表1. イヌ*IL-13*遺伝子上の多型座位の遺伝子型判定方法

プライマーの塩基配列		アニーリング温度	制限酵素	断片長
	g.20957075 AGGTGGGCA:[1]>[2]	65℃	不要	
F側	TCTGGCGAGCAGAGAAGGT			[1]型113bp
R側	CTTGCTCAGGCTCCCTTTGT			[2]型122bp
	rs8973298	55℃	*Tsp*45I	
F側	ACCTGGCCCATTAAGGGTTT			C型226bp
R側	ATCCACCTGATTCCCTGTTGG			T型103bpと113bp
	g.20957831 A>C	52℃	*Hpy*188I	
F側	TTTTAAGATCTTACTTATTCATCAG			A型24bpと175bp
R側	TTGGATACAAACTCAAACAGG			C型199bp
	rs8973300	66℃	*Msp*I	
F側	TCAGAGCATGGTTTGCTGAGA			C型97bpと153bp
R側	TTGTGGAAAATCCAGCGTCG			T型250bp
	rs22147008	65℃	*Apa*Iもしくは	
F側	TCTCAAACCCCACCTCCTGT			A型230bp
R側	AGGACAGAGGGCCTTACCC		*Psp*OMI	G型62bpと168bp

表2. イヌ*IL-13*遺伝子の多型における対立遺伝子頻度

		g.20957075 AGGTGGGCA:[1]>[2]		rs8973298		g.20957831 A>C		rs8973300		rs22147008	
犬種	個体数	1回	2回	T	C	A	C	T	C	A	G
ゴールデンレトリーバー	15	0.07	0.93	0.50	0.50	1.00	0.00	0.63	0.37	0.73	0.27
ラブラドールレトリーバー	20	0.40	0.60	0.55	0.45	1.00	0.00	0.48	0.53	0.95	0.05
ビーグル	35	0.43	0.57	0.29	0.71	0.97	0.03	0.36	0.64	0.77	0.23
シェトランドシープドッグ	15	0.47	0.58	0.20	0.80	0.88	0.13	0.20	0.80	1.00	0.00
マルチーズ	16	0.09	0.91	0.83	0.13	1.00	0.00	0.75	0.25	0.94	0.06
ヨークシャーテリア	8	0.19	0.81	0.25	0.75	1.00	0.00	0.50	0.50	0.68	0.31
トイプードル	28	0.61	0.39	0.13	0.88	0.89	0.11	0.14	0.86	0.86	0.14
ミニチュアダックスフント	23	0.24	0.76	0.21	0.79	0.91	0.09	0.28	0.72	0.48	0.52
チワワ	21	0.19	0.81	0.07	0.93	1.00	0.00	0.45	0.55	0.50	0.50
ジャーマンシェパード	29	0.48	0.52	0.55	0.45	0.91	0.09	0.52	0.48	1.00	0.00
シーズー	18	0.28	0.72	0.00	1.00	1.00	0.00	0.94	0.06	1.00	0.00
ポメラリアン	14	0.25	0.75	0.14	0.86	1.00	0.00	0.21	0.79	0.54	0.46
パピヨン	14	0.32	0.68	0.25	0.75	1.00	0.00	0.50	0.50	0.86	0.14
ウェルシュ・コーギー	8	0.75	0.25	0.00	1.00	0.75	0.25	0.06	0.94	0.75	0.25
パグ	9	0.28	0.72	0.22	0.88	1.00	0.00	0.39	0.61	0.28	0.72
ミニチュアピンシャー	8	0.25	0.75	0.25	0.75	1.00	0.00	0.56	0.44	1.00	0.00
シベリアンハスキー	20	0.00	1.00	1.00	0.00	1.00	0.00	0.90	0.10	0.95	0.05
柴犬	27	0.13	0.87	0.54	0.46	0.80	0.20	0.56	0.44	0.89	0.11
甲斐犬	34	0.28	0.72	0.32	0.68	0.62	0.38	0.41	0.59	1.00	0.00
秋田犬	29	0.07	0.93	0.26	0.74	0.81	0.19	0.22	0.78	1.00	0.00

３． 犬 IL-13 遺伝子の多型とアトピー性皮膚炎との相関解析

研究要旨

アトピー性皮膚炎を発症した柴犬 10 個体と、アトピー性皮膚炎の兆候が認められない柴犬 33 個体に対して前項に示した５つの多型座位の遺伝子型判定を行った。患畜群と非患畜群における遺伝子型頻度に基づいて、Mantel-Haenszel 法によるカイ二乗検定を用いて、症例対照研究を行った。5 座位のうち rs8973298 のマイナーアレルである C 型ホモ接合（CC 型）の出現頻度が、患畜群において非患畜群に比べて有意に高かった。この時、CC 型をアトピー性皮膚炎に対するリスク型と想定したオッズ比は、4.833（95％信頼区間 1.018-23.455，Fisher の正確確率検定による p 値＝0.070）であった。ゆえに、rs8973298 の CC 遺伝子型は、柴犬においてアトピー性皮膚炎の発症リスクを高める事が示唆された。

研究目的

ヒトでは、*IL-13* 遺伝子の 5’隣接領域 SNP(rs1800925)とコーデング領域の SNP(rs20541)が、アトピー性皮膚炎のリスク因子として報告されている。前項の２つの研究によって、イヌ *IL-13* 遺伝子に、これらヒト SNP と類似する多型が存在する事が示された。そこで、犬の遺伝性疾患における原因遺伝子解析のための遺伝子（DNA）バンク拠点形成プロジェクトで収集されたアトピー性皮膚炎を発症犬の DNA 試料を用いて、症例対照研究を行い、*IL-13* 遺伝子多型の寄与を解析した。

材料と方法

本プロジェクト研究で収集されたアトピー性皮膚炎を発症した柴犬 10 個体と、アトピー性皮膚炎の兆候が認められない柴犬 33 個体に対して前項に示した５つの多型座位の遺伝子型判定を行った。患畜群と非患畜群の遺伝子型頻度比較には Mantel-Haenszel 法によるカイ二乗検定および Fisher の正確確率検定を用いた。

結果および考察

アトピー性皮膚炎の患畜と非患畜における 5 座位の遺伝子型頻度を表 1 にまとめた。g 20957075 AGGTGGGCA：[1]>[2]、g.20957831 A>C、rs22147008 では、それぞれの座位のマイナーアレルである、[1]型、C 型、G 型ホモ接合体が片方もしくは両方の群に含まれていなかった。このため、これら 3 座位では、マイナーアレルのホモ接合に対する相関は解析できなかった。これに対して rs8973298 と rs8973300 では、マイナーアレルのホモ接合体も認められた。これらの座位のうち、rs8973298 のマイナーアレルである C 型ホモ接合（CC 型）の出現頻度が、患畜群において非患畜群に比べて有意に高かった（Mantel-Haenszel 法によるカイ二乗検定での p 値＝0.05）。この時、CC 型をアトピー性皮膚炎発症のリスク型と想定したオッズ比は 4.833（95%信頼区間 1.018-23.455，Fisher の正確確率検定による p

値＝0.070）であった。ゆえに、rs8973298 の CC 遺伝子型は、柴犬においてアトピー性皮膚炎の発症リスクを高める事が示唆された。今後、他の犬種でも、同様の相関が認められるかどうかを解析する必要がある。また、機能的な推定では、IL-13 に対して、最も大きな変化をもたらすと考えられる rs22147008 について G 型ホモ接合が存在する品種で相関解析を行う事が今後の課題として残された。

表1. 柴犬を対象とした*IL-13*遺伝子多型とアトピー性皮膚炎との症例対照研究

		アトピー性皮膚炎	
多型座位	遺伝子型	患畜	非患畜
g.20957075 AGGTGGGCA:[1]>[2]	[1][1]	0	1
	[1][2]	2	6
	[2][2]	8	26
	[1]型アレル頻度	0.10	0.12
rs8973298	CC	4	4
	TC	3	21
	TT	3	8
	C型アレル頻度	0.55	0.44
g.20957831 A>C	CC	0	0
	AC	3	12
	AA	7	21
	C型アレル頻度	0.15	0.18
rs8973300	CC	3	4
	TC	4	21
	TT	3	8
	C型アレル頻度	0.50	0.44
rs22147008	AA	9	26
	AG	1	7
	GG	0	0
	G型アレル頻度	0.05	0.11

研究発表

1. 論文発表

1) Okubo T, Hayashi D, Yaguchi T, Fujita Y, Sakaue M, Suzuki T, Tsukamoto A, Murayama O, Lynch J, Miyazaki Y, Tanaka K, Takizawa T.: Differentiation of rat adipose tissue-derived stem cells into neuron-like cells by valproic acid, a histone deacetylase inhibitor. Exp Anim [Epub ahead of print] , PMID: 26411320,2015.

2) Kurihara Y, Suzuki T, Sakaue M, Murayama O, Miyazaki Y, Onuki A, Aoki T, Saito M, Fujii Y, Hisasue M, Tanaka K, Takizawa T. Valproic acid, a histone deacetylase inhibitor, decreases proliferation of and induces specific neurogenic differentiation of canine adipose tissue-derived stem cells. *J Vet Med Sci* 76:15-23, 2014.

3) Watanabe M, Tanaka K, Takizawa T, Segawa K, Neo S, Tsuchiya R, Murata M,

Murakami M, Hisasue M.:Characterization of a canine tetranucleotide microsatellite marker located in the first intron of the tumor necrosis factor alpha gene. *J Vet Med Sci* 76,119-22. 2014.

4) Ishii Y, Takizawa T, Iwasaki H, Fujita Y, Murakami M, Groppe JC, Tanaka K.: Nucleotide polymorphisms in the canine Noggin gene and their distribution among dog (*Canis lupus familiaris*) breeds. *Biochem Genet* 50, 12-8,2012.

2. 学会発表

1) 田中和明、 滝沢達也、 山本未咲、 岡本憲明、島倉秀勝、 阪口雅弘：イヌ *IL-13* 遺伝の多型と柴犬におけるアトピー性皮膚炎との関連調査. 日本畜産学会第 121 回大会, 東京都武蔵野市　3 月　2016

2) 佐藤美紀、宮崎陽子、青木卓磨、藤田幸弘、圓尾拓也、齊藤弥代子、藤井洋子、久末正晴、田中和明、滝沢達也:イヌ脂肪組織幹細胞(ASC)の細胞増殖と神経分化に及ぼすバルプロ酸と低酸素の影響.　第 87 回日本生化学会、京都 10 月 2014

3) 渡辺征, 田中和明, 滝沢達也, 瀬川和仁, 根尾櫻子, 土屋亮, 村田倫子,村上賢, 久末正晴 : イヌ腫瘍壊死因子(TNFA)遺伝子の第 1 イントロンに存在する 4 塩基反復マイクロサテライトの特徴. 第 156 回日本獣医学会、岐阜、9 月 2013

4) 栗原康弘、中岡優希、藤井祐輝、藤田雄大、山本未咲、宮崎陽子、田中和明、滝沢達也：イヌ脂肪組織由来間葉系幹細胞の神経分化に及ぼすヒストン脱アセチル化酵素阻害剤の影響. 第 154 回日本獣医学会学術集会、岩手、9 月 2012 年

5) 栗原康弘、中岡優希、藤井祐輝、藤田雄大、宮崎陽子、田中和明、滝沢達也：イヌ脂肪組織由来間葉系幹細胞の細胞増殖および多分化能に及ぼすヒストン脱アセチル化酵素阻害剤の影響.　第 152 回日本獣医学会学術集会、堺、9 月 2011 年

Exp. Anim. 65(1), 45–51, 2016

—Original—

Differentiation of rat adipose tissue-derived stem cells into neuron-like cells by valproic acid, a histone deacetylase inhibitor

Takumi OKUBO[1)], Daiki HAYASHI[1)], Takayuki YAGUCHI[1)], Yudai FUJITA[1)], Motoharu SAKAUE[1)], Takehito SUZUKI[1)], Atsushi TSUKAMOTO[1)], Ohoshi MURAYAMA[2)], Jonathan LYNCH[2)], Yoko MIYAZAKI[1)], Kazuaki TANAKA[1)], and Tatsuya TAKIZAWA[1)]

[1)]*Graduate School of Veterinary Medicine, Azabu University, Fuchinobe, Chuo-ku, Sagamihara, Kanagawa 252–5201, Japan*
[2)]*School of Life and Environmental Science, Azabu University, Fuchinobe, Chuo-ku, Sagamihara, Kanagawa 252–5201, Japan*

Abstract: Valproic acid (VPA) is a widely used antiepileptic drug, which has recently been reported to modulate the neuronal differentiation of adipose tissue-derived stem cells (ASCs) in humans and dogs. However, controversy exists as to whether VPA really acts as an inducer of neuronal differentiation of ASCs. The present study aimed to elucidate the effect of VPA in neuronal differentiation of rat ASCs. One or three days of pretreatment with VPA (2 mM) followed by neuronal induction enhanced the ratio of immature neuron marker βIII-tubulin-positive cells in a time-dependent manner, where the majority of cells also had a positive signal for neurofilament medium polypeptide (NEFM), a mature neuron marker. RT-PCR analysis revealed increases in the mRNA expression of microtubule-associated protein 2 (*MAP2*) and *NEFM* mature neuron markers, even without neuronal induction. Three-days pretreatment of VPA increased acetylation of histone H3 of ASCs as revealed by immunofluorescence staining. Chromatin immunoprecipitation assay also showed that the status of histone acetylation at H3K9 correlated with the gene expression of *TUBB3* in ASCs by VPA. These results indicate that VPA significantly promotes the differentiation of rat ASCs into neuron-like cells through acetylation of histone H3, which suggests that VPA may serve as a useful tool for producing transplantable cells for future applications in clinical treatments.

Key words: adipose tissue-derived stem cells, histone deacetylase inhibitor, neuronal differentiation, neuron marker, rats

Introduction

Adipose tissue-derived stem cells (ASCs) are mesenchymal stem cells that are isolated from the stromal vascular fraction of adipose tissues [3, 14, 19]. In a similar way to bone marrow-derived mesenchymal stem cells (BMSCs), ASCs can differentiate into not only mesenchymal lineage cells [17, 18], but also into neurogenic lineage cells [16, 18]. However, unlike BMSCs, ASCs can easily be obtained in large quantities and with minimum risk from invasive surgery [5]. Therefore, it is reasonable to conclude that ASCs will be the preferred adult stem cells for future clinical applications [14].

Valproic acid (VPA), well known as an antiepileptic and anticonvulsant drug, is an inhibitor of class I histone deacetylase (HDACs) [2, 15]. The acetylation of histone

(Received 16 April 2015 / Accepted 16 August 2015 / Published online in J-STAGE 25 September 2015)
Address corresponding: T. Takizawa, Graduate School of Veterinary Medicine, Azabu University, Fuchinobe, Chuo-ku, Sagamihara, Kanagawa 252–5201, Japan

N-terminal tails is thought not only to alter the interaction between histone and DNA, but also to bind acetylated histone to bromodomain proteins and transcription activators [8], thus inducing the expression of genes on the loci [4, 6, 7, 10]. We have previously shown that VPA induces neuronal differentiation of canine ASCs [11], a result that suggests a safer and more direct method for preparing the cell source for future applications. However, Lee *et al*. [12] showed that the pretreatment of VPA diminished efficiency of neuronal differentiation of human ASCs. Thus there is debate over the role of VPA as an inducer of neuronal differentiation of ASCs. To address this, we examined the effect of VPA on neuronal differentiation of ASCs isolated from adipose tissue in rats in the present study. The results indicate that VPA induced differentiation of rat ASCs into neuron-like cells through acetylation of histone H3.

Materials and Methods

Isolation and culture of rat ASCs

ASCs were isolated as previously described [11]. Briefly, 10 to 12-week-old male Wistar rats (Charles River Japan, Yokohama, Japan) were euthanatized by decapitation under light anesthesia. Subcutaneous adipose tissue was excised from the inguinal regions and extensively washed with a washing buffer of sterile phosphate-buffered saline (PBS) containing penicillin (100 U/ml) and streptomycin (100 μg/ml) to remove contaminating blood cells and local anesthetics. The tissue was minced into small pieces and then incubated in washing buffer with added 0.05% collagenase type 1A (Sigma-Aldrich, St. Louis, MO, USA) at 37°C for 1 h with vigorous shaking. The top lipid layer was removed, and the remaining liquid portion was centrifuged at 200 × *g* for 10 min. The pellet was resuspended in a growth medium of Dulbecco's modified Eagle's medium (DMEM, Nissui, Tokyo, Japan) supplemented with 10% newborn bovine serum (NBS, Invitrogen, Carlsbad, CA, USA) and antibiotics above described, and then spread in 100-mm collagen type 1-coated dishes (Iwaki, Tokyo, Japan) at a density of 1×10^6 cells per dish. Cells were maintained in growth medium at 37°C and 5% CO_2. After 24 h, the unattached cells were removed by rinsing with washing buffer. ASCs were identified by confirming multilineage potentials to adipogenic, osteogenic and neurogenic cells (data not shown). Twice-passaged ASCs were used in the present study. All animal experiments in the present study were carried out according to the guidelines of the Committee for Animal Experimentation at Azabu University.

In vitro neuronal differentiation assay

In vitro assay of neuronal differentiation was carried out as previously described [1] with a minor modification. Briefly, ASCs were seeded on non-coating glass coverslips in 35-mm dishes at a density of 1×10^4 cells per dish. ASCs were incubated for one or three days in growth medium containing 2 mM of VPA. After pretreatment with and without VPA, vehicle dimethylsulfoxide (DMSO), the medium was changed to a neuronal induction medium (NIM) of DMEM supplemented with 100 μM dibutyryl cyclic adenosine monophosphate (dbcAMP, Wako Pure Chemical Ind., Osaka, Japan) and 125 μM isobutylmethylxanthine (IBMX, Wako Pure Chemical Ind.) for 2 h [1, 11]. Control for NIM was NIM minus dbcAMP and IBMX. After pretreatment of VPA followed by NIM, the cells were fixed in PBS containing 3.7% formaldehyde for 15 min at room temperature. Similarly incubated ASCs on non-coating 35-mm dishes were removed by a cell-scraper and the removed-cells were immersed in ISOGEN (Nippon Gene, Tokyo, Japan) and stored at –80°C until further analysis. Neuronal differentiation was determined by immunofluorescence staining for βIII-tubulin and neurofilament medium polypeptide (NEFM) and by RT-PCR analysis for expression of genes, βIII-tubulin (*TUBB3*), *NEFM*, microtubule-associated protein 2 (*MAP2*), glial fibrillary acidic protein (*GFAP*) and housekeeping gene hypoxanthine-guanine phosphoribosyl-transferase (*HPRT*).

Immunofluorescence staining

Immunocytochemical analyses for βIII-tubulin, NEFM and acetylation of histone H3 were performed. Formaldehyde-fixed ASCs were rinsed with PBS three times. The cells were then permeated with 0.2% Triton X-100 in PBS for 10 min at room temperature, and then incubated with, an anti-βIII-tubulin antibody (1:200; Abcam, ab74978, Cambridge, UK), an anti-NEFM antibody (1:400; Proteus BioSciences, Inc., 40-1259, Ramona, CA, USA) and an anti-acetylated histone H3 (K9) antibody (1:100; Novus Biologicals, NB21-1081SS, Littleton, CO, USA) for 1 h at room temperature. After being washed with PBS, the cells were incubated with secondary antibody (Cy3-conjugated goat anti-rabbit IgG, 1:1600 or FITC-conjugated goat anti-mouse IgG, 1:200,

Jackson ImmunoResearch, West Grove, PA) for 30 min at room temperature. The cells were then rinsed with PBS and counterstained with 4', 6-diamidino-2-phenylindole (DAPI) for nuclear staining before fluorescence microscopic observation. The percentage of βIII-tubulin-positive cells was determined based on the total number of counting cells. At least 300 cells were evaluated per culture.

Reverse transcription-PCR

Total RNA was extracted using ISOGEN and reverse-transcribed for single-strand cDNA, using oligo (dT) primer and Superscript III reverse transcriptase (Invitrogen) according to the manufacture's instruction. PCR was performed using *Taq* DNA polymerase (KAPA Biosystems, Woburn, MA, USA) and specific primers, and each cycle consisted of the following steps: denaturation at 98°C for 10 s, annealing at 57°C to 65°C for 30 s, and elongation at 72°C for 30 s (Table 1). Reaction products were electrophoresed on a 2.0% agarose gel and visualized with ethidium bromide.

Effect of VPA on the acetylation of histone H3

To confirm the effect of VPA on the acetylation of histone H3, ASCs were incubated for three days using a similar method to that described above, in growth medium containing 2 mM VPA or valpromide (VPM), an analogue of VPA without HDAC inhibitory activity. After treatment with these reagents, the cells were fixed with formaldehyde in a similar method to that described above. The effect of VPA on the acetylation of histone H3 was examined by immunofluorescence staining for acetylated-histone H3.

Chromatin Immunoprecipitation assay

Tissue samples were treated with chromatin immunoprecipitation (ChIP) reagents (Nippon Gene), following the manufacturer's instructions with minor modifications. Cells were harvested and mixed with formaldehyde at a final concentration of 1.0% for 5 min at room temperature to cross-link protein to DNA. Cells were then suspended in lysis buffer (Protease Inhibitors, Pierce, Rockford, IL, USA) and incubated on ice for 10 min. DNA cross-linked with protein was sonicated into fragments of 200–1,000 bp by an Ultrasonic Homogenizer (Taitec, Koshigaya, Japan). Samples were subsequently incubated at 4°C with Dynabeads (Invitrogen) to obtain the soluble chromatin fraction. Dynabeads were previously incubated with 4 μg rabbit anti-histone H3 (acetyl K9) antibody (Novus Biologicals, Littleton) or ChIP rabbit IgG control antibody (Santa Cruz Biotechnology, Santa Cruz, CA, USA) for 16 h overnight at 4°C. The chromatin-antibody complexes were eluted with ChIP direct elution buffer. Protein-DNA cross-links were reversed with 5 M NaCl for 12 h incubation at 65°C. Proteinase K treatment and phenol-chloroform extraction were carried out, and the DNA was then precipitated in ethanol, and used as a template for PCR. PCR amplification was carried out with primers specific for promoter region of *TUBB3*. Primer sequences were shown as follows, forward; 5'- ACTCCATACCCCCTCTTTGC-3', reverse; 5'-AGTCCATGGCTCCACAAAAG-3'. Input DNA and DNA immunoprecipitated by anti-IgG served as positive and negative control, respectively.

Statistical analysis

Results are expressed as means ± standard error. Multiple comparisons were performed with the Turkey-Kramer test after one-way analysis of variance (ANOVA). A *P* value of less than 0.05 was considered statistically significant.

Table 1. Primer sequences used in RT-PCR

Gene		Primer sequence (5'-3')	Anealing temperature	Product length (bp)
TUBB3	Forward	5'-GGCCTCCTCTCACAAGTATGT-3'	58°C	167
	Reverse	5'-CGCCCTCTGTATAGTGC-3'		
NEFM	Forward	5'-AGGCTGAGTCCCCAGTGAAA-3'	58°C	220
	Reverse	5'-TCCACCTCCCCATTGATAGC-3'		
MAP2	Forward	5'-ACCTTCCTCCATCCTCCCTC-3'	57°C	151
	Reverse	5'-AGTAGGTGTTGAGGTGCCGC-3'		
GFAP	Forward	5'-ACATCGAGATCGCCACCTAC-3'	58°C	228
	Reverse	5'-GCACACCTCACATCACATCC-3'		
HPRT	Forward	5'-AATGTCTGTTGCTGCGTC-3'	55°C	92
	Reverse	5'-TGTCTGTCTACAAGGGAAG-3'		

Results

VPA promotes neuronal differentiation in a time-dependent manner

Using immunocytochemistry and RT-PCR analysis, neuronal differentiation was determined in ASCs with and without VPA pretreatment for 1 or 3 days, followed by treatment with and without NIM for 2 h. Regardless of the duration of VPA treatment, differentiated ASCs showed neuron-like morphology with several branching neurite-like cell processes, in which most of the cells had positive signals of an immature neuron marker βIII-tubulin and a mature neuron marker NEFM. Three-days treatment with VPA significantly enhanced the positive signal of βIII-tubulin and NEFM with and even without NIM treatment. The majority of βIII-tubulin positive cells also expressed NEFM, and both immunofluorescence intensities were reduced without VPA pretreatment (Fig. 1A). Neuronal induction significantly increased the ratio of βIII-tubulin-positive cells from 15.7 ± 1.4% without VPA to 85.6 ± 1.9% with three-days treatment of VPA (Fig. 1B). Three-days treatment of VPA also significantly increased the ratio of βIII-tubulin-positive cells from 35.4 ± 1.2% without NIM to 85.6 ± 1.9% with NIM. Without NIM groups, VPA significantly increased the ratio of βIII-tubulin-positive cells in a time-dependent manner (Fig. 1B).

mRNA expressions of immature neuron marker *TUBB3* were observed in all groups with and without pretreatment of VPA, but mRNA expression of the glial cell marker *GFAP* was not detected in any groups (Fig. 1C). Furthermore, three-days treatment of VPA markedly elevated not only the mRNA expression levels of immature neuron marker *TUBB3*, but also mature neuron markers *MAP2* and *NEFM* in ASCs with and without NIM. One-day treatment of VPA also induced the expression of these mature neuron markers (data not shown). In addition, NIM treatment without VPA did not significantly enhance the expressions of these neuron markers when compared to those observed in the groups with VPA.

VPA induces acetylation of histone H3

To confirm the effect of VPA on acetylation of histone H3, we examined the acetylated histone H3 by immunofluorescence staining. Minimal acetylation of histone H3 were observed in the control ASCs. Three-days pretreatment of VPA gave morphological changes of the ASCs such as flattened and expanded shapes, and increased their acetylation of histone H3 (Fig. 2A). In contrast, VPM, an analogue of VPA without HDAC inhibitory activity, did not cause any morphological changes or significant changes in acetylation-positive signal of histone H3 in ASCs.

VPA increases H3K9 acetylation levels at the proximal promoter region of TUBB3

The state of the histone tails of ASCs pretreated with VPA for three days was analyzed by ChIP assay using antibody to acetylated lysine 9 on histone H3 (anti-AcH3K9). The acetylated state of histone H3 tails associated with the proximal region of *TUBB3* increased in ASCs pretreated by VPA compared to those in the ASCs without VPA (Fig. 2B), indicating that the increase of histone acetylation of H3K9 correlated with the expression of the *TUBB3* gene of ASCs pretreated with VPA.

Discussion

In this study we demonstrated that VPA promoted the differentiation of approximately 86% of ASCs into βIII-tubulin-positive neuron-like cells after three-days treatment followed by neuronal induction. The differentiated cells showed neuron-like morphology with branching neurite-like cell protrusions, and were significantly immunostained to an immature neuron marker βIII-tubulin, and a mature neuron marker NEFM. Pretreatment with VPA followed by neuronal induction also significantly enhanced mRNA expressions of *TUBB3, MAP2* and *NEFM,* compared to the groups without VPA. We also demonstrated that VPA induced differentiation of ASCs into neuron-like cells in a time-dependent manner. The present study is in agreement with our previous study demonstrating that VPA promotes neuronal differentiation of canine ASCs [11], and further indicates that VPA not only promotes neuronal differentiation but can also promote more mature neuron-like cells. The present data also show that VPA enhances expression of neuron markers, whereas no effect was observed for glial marker. This suggests that VPA induces the differentiation of ASCs into neuron-like cells by neuronal induction, although further confirmation by means of a detailed study is required.

In the present study, we used a well-known neuronal differentiation medium including IBMX and dbcAMP.

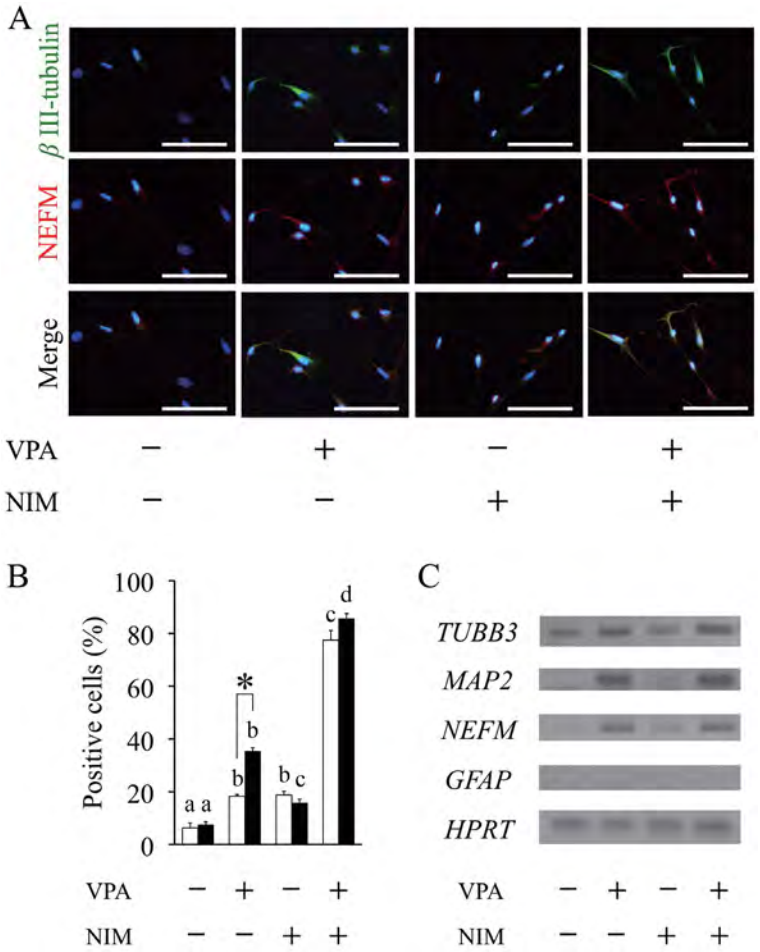

Fig. 1. Valproic acid promotes neuronal differentiation. Adipose tissue-derived stem cells (ASCs) were pretreated with valproic acid (VPA) for 1 or 3 days followed by neuronal induction medium (NIM) for 2 h. (A) Neuronal differentiation was assessed by immunocytochemistry using anti-βIII-tubulin antibody (green) and anti-NEFM antibody (Red) after fixing at the end of incubation in 3-days VPA treatment group. Nuclei were counterstained with DAPI (blue). Scale bar, 100 μm. (B) The percentage of βIII-tubulin-positive cells was determined based on the total number of counting cells in 1 or 3 days VPA treatment. At least 300 cells were evaluated per culture. Data are the means ± S.E. of 4 independent experiments. Open and solid bars represent 1 or 3 days VPA treatment, respectively. a, b, c, d: bars with different letters at the top differ significantly among same duration group, asterisk indicates significantly different compared to one-day treatment group, $P<0.05$. (C) RT-PCR analysis of neuronal markers *TUBB3*, *MAP2* and *NEFM*, the glial marker *GFAP* and house keeping gene *HPRT* was performed using total RNA extracted from ASCs after 3-days VPA treatment followed by 2 h of neuronal induction.

We showed that VPA increased the neuronal morphological changes and neuron markers expression even without neuronal induction treatment, thus indicating that VPA can induce neuronal differentiation in the absence of neuronal induction. We also demonstrated that VPA increased the acetylation of histone H3K9 on the proximal region of *TUBB3* in rat ASCs, leading to the neuronal differentiation. Present results suggest that the promotional effect of VPA on neuronal differentiation occurs through inducing the acetylation of histone H3.

The investigation demonstrated that VPA flattened and expanded the shape of rat ASCs and markedly induced their acetylation of histone H3. These observations are in accordance with the findings of Lee *et al.* [12] and Kurihara *et al*. [11]. Lee *et al*. [12], however, showed that VPA diminished the efficiency of neuronal differentiation of human ASCs. The study showed that one-day pretreatment of VPA (1, 10 mM) followed by neuronal

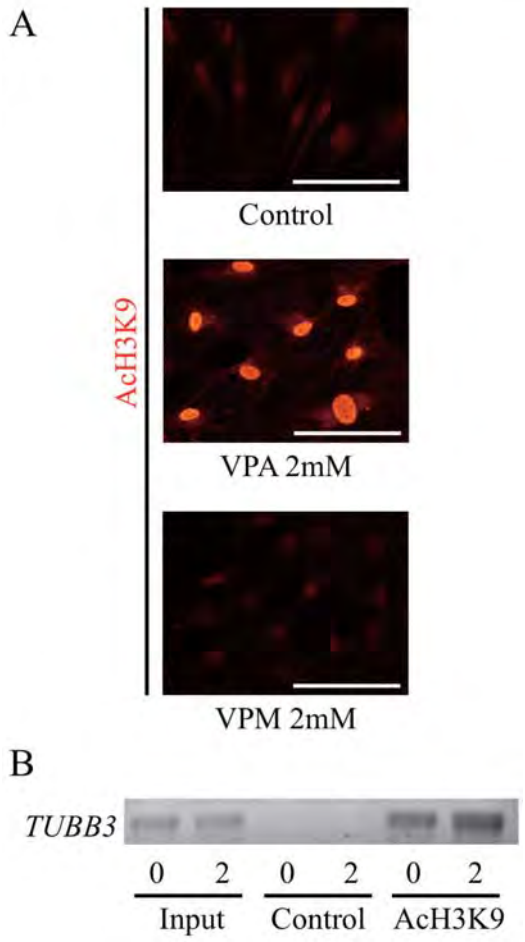

Fig. 2. Effects of valproic acid on histone H3 acetylation. (A) Adipose tissue-derived stem cells (ASCs) from rats were incubated with valproic acid (VPA) or valpromide (VPM), an analogue of VPA without histone deacetylase inhibitory activity, for 3 days. Control group was treated with solvent, DMSO. ASCs were immunostained with an anti-acetylated histone H3 (K9) antibody (Red). Acetylated histone H3 (K9) antibody was visualized with Cy3-conjugated goat anti-rabbit IgG. Scale bar, 100 μm. (B) VPA increased acetylation levels at the proximal region of *TUBB3*. The state of the histone tails of ASCs pretreated with VPA for 3 days was analyzed by ChIP assay using antibody to acetylated lysine 9 on histone H3 (anti-AcH3K9). Typical electrophoresis of PCR analysis of *TUBB3* was shown.

induction decreased neurite formation and expression of βIII-tubulin in human ASCs [12]. On the other hand, the study of Kurihara *et al*. [11] showed that VPA induced neuronal differentiation of canine ASCs with three-days pretreatment of VPA (4 mM) followed by neuronal induction [11]. Differing treatment regimens of VPA were implemented in these studies and this can partially explain the different effect on neuronal differentiation of ASCs. In the present study, we examined the time-course effects of VPA on the neuronal differentiation of ASCs by immunocytochemistry and RT-PCR analysis. This investigation clearly demonstrated that VPA induced differentiation of ASCs into neuron-like cells, not only as a result of three-days treatment, but also from a one-day course of treatment. Together with the previous study [11], the present results demonstrate that VPA is highly effective in neuronal differentiation of ASCs at least for rats and dogs, when VPA treatment is applied over one and three days. Taken together with the present study, an appropriate treatment of VPA promotes the differentiation of rat ASCs into neuron-like cells, although species difference should be examined in future.

It is well known that the differential potential of neural stem cells (NSCs) into neurons depends on the stages occurring during brain development; early stage NSCs prefer to differentiate into neurons, whereas late stage NSCs into astrocytes [13]. VPA has also been shown to promote the differentiation of adult hippocampal neural progenitors into neurons, but inhibited their glial differentiation in adult neural progenitor cells [6, 9]. These reports offer another explanation that the different effect of VPA on neuronal differentiation depends on the stages of ASCs similarly observed in NSCs during brain development.

In conclusion, the results have shown that, through the acetylation of histone H3, VPA significantly promotes the differentiation of rat ASCs into neuron-like cells, with expression of mature neuron markers. The findings suggest that VPA may prove to be a useful tool for producing transplantable cells for future applications in clinical treatments.

Acknowledgment

This work was supported in part by the Science Research Promotion Fund of The Promotion and Mutual Aid Corporation for Private Schools of Japan. This work was also supported in part by the MEXT Program for the Strategic Research Foundation at Private Universities, 2011–2015.

References

1. Deng, W., Obrocka, M., Fischer, I., and Prockop, D.J. 2001. In vitro differentiation of human marrow stromal cells into

early progenitors of neural cells by conditions that increase intracellular cyclic AMP. *Biochem. Biophys. Res. Commun.* 282: 148–152. [Medline] [CrossRef]

2. Göttlicher, M., Minucci, S., Zhu, P., Krämer, O.H., Schimpf, A., Giavara, S., Sleeman, J.P., Lo Coco, F., Nervi, C., Pelicci, P.G., and Heinzel, T. 2001. Valproic acid defines a novel class of HDAC inhibitors inducing differentiation of transformed cells. *EMBO J.* 20: 6969–6978. [Medline] [CrossRef]
3. Gronthos, S., Franklin, D.M., Leddy, H.A., Robey, P.G., Storms, R.W., and Gimble, J.M. 2001. Surface protein characterization of human adipose tissue-derived stromal cells. *J. Cell. Physiol.* 189: 54–63. [Medline] [CrossRef]
4. Grunstein, M. 1997. Histone acetylation in chromatin structure and transcription. *Nature* 389: 349–352. [Medline] [CrossRef]
5. Housman, T.S., Lawrence, N., Mellen, B.G., George, M.N., Filippo, J.S., Cerveny, K.A., DeMarco, M., Feldman, S.R., and Fleischer, A.B. 2002. The safety of liposuction: results of a national survey. *Dermatol. Surg.* 28: 971–978. [Medline]
6. Hsieh, J., Nakashima, K., Kuwabara, T., Mejia, E., and Gage, F.H. 2004. Histone deacetylase inhibition-mediated neuronal differentiation of multipotent adult neural progenitor cells. *Proc. Natl. Acad. Sci. USA* 101: 16659–16664. [Medline] [CrossRef]
7. Jenuwein, T. and Allis, C.D. 2001. Translating the histone code. *Science* 293: 1074–1080. [Medline] [CrossRef]
8. Josling, G.A., Selvarajah, S.A., Petter, M., and Duffy, M.F. 2012. The role of bromodomain proteins in regulating gene expression. *Genes Basel* 3: 320–343. [Medline] [CrossRef]
9. Jung, G.A., Yoon, J.Y., Moon, B.S., Yang, D.H., Kim, H.Y., Lee, S.H., Bryja, V., Arenas, E., and Choi, K.Y. 2008. Valproic acid induces differentiation and inhibition of proliferation in neural progenitor cells via the beta-catenin-Ras-ERK-p21Cip/WAF1 pathway. *BMC Cell Biol.* 9: 66. [Medline] [CrossRef]
10. Kuo, M.H. and Allis, C.D. 1998. Roles of histone acetyltransferases and deacetylases in gene regulation. *BioEssays* 20: 615–626. [Medline] [CrossRef]
11. Kurihara, Y., Suzuki, T., Sakaue, M., Murayama, O., Miyazaki, Y., Onuki, A., Aoki, T., Saito, M., Fujii, Y., Hisasue, M., Tanaka, K., and Takizawa, T. 2014. Valproic acid, a histone deacetylase inhibitor, decreases proliferation of and induces specific neurogenic differentiation of canine adipose tissue-derived stem cells. *J. Vet. Med. Sci.* 76: 15–23. [Medline] [CrossRef]
12. Lee, S., Park, J.R., Seo, M.S., Roh, K.H., Park, S.B., Hwang, J.W., Sun, B., Seo, K., Lee, Y.S., Kang, S.K., Jung, J.W., and Kang, K.S. 2009. Histone deacetylase inhibitors decrease proliferation potential and multilineage differentiation capability of human mesenchymal stem cells. *Cell Prolif.* 42: 711–720. [Medline] [CrossRef]
13. Namihira, M., Nakashima, K., and Taga, T. 2004. Developmental stage dependent regulation of DNA methylation and chromatin modification in a immature astrocyte specific gene promoter. *FEBS Lett.* 572: 184–188. [Medline] [CrossRef]
14. Ning, H., Lin, G., Fandel, T., Banie, L., Lue, T.F., and Lin, C.S. 2008. Insulin growth factor signaling mediates neuron-like differentiation of adipose-tissue-derived stem cells. *Differentiation* 76: 488–494. [Medline] [CrossRef]
15. Phiel, C.J., Zhang, F., Huang, E.Y., Guenther, M.G., Lazar, M.A., and Klein, P.S. 2001. Histone deacetylase is a direct target of valproic acid, a potent anticonvulsant, mood stabilizer, and teratogen. *J. Biol. Chem.* 276: 36734–36741. [Medline] [CrossRef]
16. Safford, K.M., Hicok, K.C., Safford, S.D., Halvorsen, Y.D., Wilkison, W.O., Gimble, J.M., and Rice, H.E. 2002. Neurogenic differentiation of murine and human adipose-derived stromal cells. *Biochem. Biophys. Res. Commun.* 294: 371–379. [Medline] [CrossRef]
17. Wu, P., Sato, K., Yukawa, S., Hikasa, Y., and Kagota, K. 2001. Differentiation of stromal-vascular cells isolated from canine adipose tissues in primary culture. *J. Vet. Med. Sci.* 63: 17–23. [Medline] [CrossRef]
18. Zuk, P.A., Zhu, M., Ashjian, P., De Ugarte, D.A., Huang, J.I., Mizuno, H., Alfonso, Z.C., Fraser, J.K., Benhaim, P., and Hedrick, M.H. 2002. Human adipose tissue is a source of multipotent stem cells. *Mol. Biol. Cell* 13: 4279–4295. [Medline] [CrossRef]
19. Zuk, P.A., Zhu, M., Mizuno, H., Huang, J., Futrell, J.W., Katz, A.J., Benhaim, P., Lorenz, H.P., and Hedrick, M.H. 2001. Multilineage cells from human adipose tissue: implications for cell-based therapies. *Tissue Eng.* 7: 211–228. [Medline] [CrossRef]

FULL PAPER *Surgery*

Valproic Acid, a Histone Deacetylase Inhibitor, Decreases Proliferation of and Induces Specific Neurogenic Differentiation of Canine Adipose Tissue-Derived Stem Cells

Yasuhiro KURIHARA[1)], Takehito SUZUKI[1)], Motoharu SAKAUE[1)], Ohoshi MURAYAMA[2)], Yoko MIYAZAKI[1)], Atsushi ONUKI[1)], Takuma AOKI[1)], Miyoko SAITO[1)], Yoko FUJII[1)], Masaharu HISASUE[1)], Kazuaki TANAKA[1)] and Tatsuya TAKIZAWA[1)*]

[1)]*Graduate School of Veterinary Medicine, Azabu University, Fuchinobe, Chuo-ku, Sagamihara 252–5201, Japan*
[2)]*School of Life and Environmental Science, Azabu University, Fuchinobe, Chuo-ku, Sagamihara 252–5201, Japan*

(Received 30 April 2013/Accepted 7 August 2013/Published online in J-STAGE 27 August 2013)

ABSTRACT. Adipose tissue-derived stem cells (ADSCs) isolated from adult tissue have pluripotent differentiation and self-renewal capability. The tissue source of ADSCs can be obtained in large quantities and with low risks, thus highlighting the advantages of ADSCs in clinical applications. Valproic acid (VPA) is a widely used antiepileptic drug, which has recently been reported to affect ADSC differentiation in mice and rats; however, few studies have been performed on dogs. We aimed to examine the *in vitro* effect of VPA on canine ADSCs. Three days of pretreatment with VPA decreased the proliferation of ADSCs in a dose-dependent manner; VPA concentrations of 4 mM and above inhibited the proliferation of ADSCs. In parallel, VPA increased *p16* and *p21* mRNA expression, suggesting that VPA attenuated the proliferative activity of ADSCs by activating p16 and p21. Furthermore, the effects of VPA on adipogenic, osteogenic or neurogenic differentiation were investigated morphologically. VPA pretreatment markedly promoted neurogenic differentiation, but suppressed the accumulation of lipid droplets and calcium depositions. These modifications of ADSCs by VPA were associated with a particular gene expression profile, viz., an increase in neuronal markers, that is, *NSE*, *TUBB3* and *MAP2*, a decrease in the adipogenic marker, *LPL*, but no changes in osteogenic markers, as estimated by reverse transcription-PCR analysis. These results suggested that VPA is a specific inducer of neurogenic differentiation of canine ADSCs and is a useful tool for studying the interaction between chromatin structure and cell fate determination.

KEY WORDS: adipose tissue-derived stem cell, cell proliferation, histone deacetylase inhibitor, pluripotency, valproic acid.

doi: 10.1292/jvms.13-0219; *J. Vet. Med. Sci.* 76(1): 15–23, 2014

Spinal cord injury (SCI) often occurs in dogs, due to motor vehicle accidents or intervertebral disease (IVDD). Most canine patients suffer from sustained incontinence and loss of walking ability, and the prognosis of severe SCI cases is poor. Unfortunately, no effective drug or surgical therapy has been established for severe SCI cases, and there is a need for new therapeutic approaches. One possibility is stem cell transplantation therapy, which is used as a radical cure treatment for refractory SCI [2, 14, 25, 26].

Adipose tissue-derived stem cells (ADSCs) are isolated from the stromal vascular fraction of adipose tissues [8, 24, 39]. ADSCs, similar to pluripotent adult mesenchymal stem cells, can differentiate into mesenchymal lineage cells, such as adipocytes, osteocytes, chondrocytes and myocytes [36, 38]. ADSCs have characteristics similar to those of bone marrow-derived mesenchymal stem cells (BMSCs), including gene expression and differentiation potential [1, 3, 5, 17, 19, 22, 33, 35, 37, 39]. Unlike BMSCs, however, the tissue source of ADSCs can be obtained in large quantities and with low risks [11]. Therefore, it is reasonable that ADSCs will be the preferred adult stem cells for future clinical applications [24]. Moreover, the dog has been found to be a good animal model of human disease [32], and thus, the study of canine ADSCs is particularly useful. Stem cells derived from bone marrow and from olfactory ensheathing glia (OEG) have been studied for spinal cord regenerative therapy in dogs [6, 14, 16, 25, 26, 31]. However, only a few studies have been performed on the differentiation of canine ADSCs, except for a comparative study showing that BMSCs and ADSCs could be differentiated into neurospheres and neuron-like cells in dogs [2].

Valproic acid (VPA), a widely used antiepileptic and anticonvulsant drug, is an inhibitor of class 1 histone deacetylases (HDACs) [7, 27]. Histone acetylation correlates with gene activation [12, 13], and modification of histone N-terminal tails through acetylation or deacetylation can alter the interaction between histones and DNA, affecting the regulation of gene expression [9, 12, 13, 18, 34]. Therefore, HDAC inhibitors have been a useful tool for studying the association between chromatin modification and cell lineage specification. VPA has been found to promote differentiation of hippocampal neural progenitors into neurons, but inhibit their glial differentiation in adult rats [12].

In the present study, we have investigated the effects of VPA on the proliferation and differentiation of canine ADSCs isolated from subcutaneous adipose tissue in the

*CORRESPONDENCE TO: TAKIZAWA, T., Graduate School of Veterinary Medicine, Azabu University, Fuchinobe, Chuo-ku, Sagamihara 252–5201, Japan.
e-mail: takizawa@azabu-u.ac.jp

Table 1. Primers used in RT-PCR and real-time PCR

Gene		Primer sequence (5′–3′)	Product length (bp)
p16	Forward	CGATCCAGGTCATGATGATGG	145
	Reverse	ACCACCAGCGTGTCCAGGAA	
p21	Forward	CATCCCTCATGGCAGCAAG	208
	Reverse	AGGCAGGGAGACCTTGGACA	
PPARγ2	Forward	ACACGATGCTGGCGTCCTTGATG	119
	Reverse	TGGCTCCATGAAGTCACCAAAGG	
FABP4	Forward	ATCAGTGTAAACGGGGATGTG	117
	Reverse	GACTTTTCTGTCATCCGCAGTA	
LPL	Forward	ACACATTCACAAGAGGGTCACC	134
	Reverse	CTCTGCAATCACACGGATGGC	
BMP2	Forward	CACTAACCACGCCATTGTTCA	163
	Reverse	ACAACCCTCCACAACCATGTC	
Dlx5	Forward	TGCTCTCCTACCTCGGCTTC	224
	Reverse	TTGCCATTCACCATCCTCAC	
COL1A1	Forward	GTAGACACCACCCTCAAGAGC	119
	Reverse	TTCCAGTCGGAGTGGCACATC	
NSE	Forward	GACCAACCCAAAGCGTATTGA	180
	Reverse	GCAATGAACGTGTCCTCAGTC	
TUBB3	Forward	AGCCAAGTTCTGGGAAGTCA	238
	Reverse	CCCACTCTGACCAAAGATGAA	
MAP2	Forward	AGAGGAGGTGTCTGCAAGGA	161
	Reverse	GTGATGGAGGTGGAGAAGGA	
NEFH	Forward	CTCAAAGGCACCAAGGACTC	244
	Reverse	CAAAGCCAATCCGACATTCT	
GFAP	Forward	AGATCCACGATGAGGAGGTG	104
	Reverse	TCTTAGGGCTGCTGTGAGGT	
GAPDH	Forward	GCTGAACGGGAAGCTCACTG	221
	Reverse	CGTCGAAGGTGGAAGAGTGG	

inguinal region.

MATERIALS AND METHODS

Animals: Subcutaneous adipose tissue was obtained from the inguinal region of 8 healthy laboratory beagles (age, 1–2 years) (Kitayama Labes, Ina, Japan). All animals were anesthetized with propofol, before tissue samples were obtained. After intubation, anesthesia was maintained with isoflurane (2.0%) in oxygen. At the end of each experiment, the animals were euthanized by additional doses of anesthesia (pentobarbital, 100 mg/kg). The protocol of this study was approved by the Committee for Animal Experimentation at Azabu University.

Isolation and culture of canine ADSCs: Adipose tissue samples were processed for ADSC isolation as described previously [23, 24] with a slight modification. Briefly, the adipose tissue removed was extensively washed with sterile phosphate-buffered saline (PBS) containing penicillin (100 U/m*l*) and streptomycin (0.25 μg/m*l*) in order to remove contaminating blood cells and local anesthetics. The tissue was minced into small pieces and then incubated in a solution containing 0.05% collagenase type IA (Sigma-Aldrich, St. Louis, MO, U.S.A.) at 37°C for 1 hr with vigorous shaking. The top lipid layer was removed, and the remaining liquid portion was centrifuged at 200 × *g* for 10 min. The pellet was resuspended in Dulbecco's modified Eagle's medium (DMEM, Nissui, Tokyo, Japan) supplemented with 10% newborn bovine serum (NBS, Invitrogen, Carlsbad, CA, U.S.A.) and spread in 100-mm collagen type I-coated dishes (Iwaki, Tokyo, Japan) at a density of 1×10^6 cells per dish. Cells were maintained in growth medium (DMEM supplemented with 10% NBS, penicillin [100 U/m*l*] and streptomycin [0.25 μg/m*l*]) at 37°C and 5% CO_2. After 24 hr, the unattached cells were removed by washing with PBS. Canine ADSCs from passages 1–3 were used, and no difference was observed in ADSCs between these passages.

Measurement of proliferation potential: The effects of VPA or valpromide (VPM; Wako Pure Chemical Ind., Osaka, Japan), an analogue of VPA with no HDAC inhibi-

tory activity, on ADSC proliferation were measured using a 3-(4, 5-dimethyl-thiazol-2-yl)-2, 3-diphenyltetrazolium bromide (MTT) assay kit (Roche Applied Science, Basel, Switzerland) according to the manufacturer's instructions. Briefly, canine ADSCs were plated in 96-well plates at a density of 1×10^4 per well and cultured in growth medium for 48 hr. VPA or VPM (0–8 mM) was then added to the medium, and cultures were incubated for 3 days. Subsequently, 10 μl of MTT stock solution was added, and the plates were further incubated for 4 hr at 37°C. Diluted HCl (100 μl) was then added to solubilize the formazan crystals, and the absorbance of each well at 570 *n*m was measured with a microplate reader LS-PLATE manager 2004 (Wako Pure Chemical Ind.); the average of measurements of 6 wells per sample has been presented.

In vitro differentiation assay: *In vitro* assay of cell differentiation into adipogenic, osteogenic and neurogenic lineages was performed as described previously [4, 29, 39] with a slight modification. Briefly, ADSCs were seeded into 35-mm dishes at a density of 1×10^5 cells per dish. The cells were incubated on glass coverslips in growth medium containing 4 mM VPA for 3 days and then transferred to adipogenic induction medium (DMEM supplemented with 10% FBS, 1 μM dexamethasone, 10 μM insulin and 0.5 mM isobutylmethylxanthine) or to osteogenic induction medium (DMEM supplemented with 10% FBS, 0.1 μM dexamethasone, 50 μM L-ascorbate-2-phosphte and 10 mM glycerophosphate) for 14 days [39] and then to neurogenic induction medium (DMEM supplemented with100 μM dibutyryl cyclic adenosine monophosphate and 125 μM isobutylmethylxanthine) for 2 hr [23, 24]. Intracellular lipid accumulation, as an indicator of adipogenic differentiation, was visualized by oil red O staining. Osteogenic differentiation was confirmed by positive staining with alizarin red S, a specific marker for calcium deposition. Neurogenic differentiation was assessed by immunofluorescence staining for βIII-tubulin or neuron-specific enolase (NSE). Reagents for this induction medium were purchased from Wako Pure Chemical Ind.

Immunofluorescence staining: Immunocytochemical analyses of HDAC1, acetylation of histone H3 (ace H3), βIII-tubulin and NSE were performed. ADSCs were incubated in growth medium for 3 days as described above. Some cultures were processed for neurogenic induction. At the end of incubation, the cells were fixed in PBS containing 3.7% formaldehyde for 15 min at 4°C. After PBS washes, the cells were permeabilized with 0.2% Triton X-100 for 10 min at room temperature. The cells were then incubated with an anti-HDAC1 antibody (sc-7872, Santa Cruz Biotechnology, Santa Cruz, CA, U.S.A.), an anti-histone H3 (acetyl K9) antibody (Novus Biologicals, Littleton, CO, U.S.A.), an anti-βIII-tubulin antibody (ab78078, Abcam, Cambridge, U.K.) or an anti-NSE antibody (PA1-46203, Thermo Scientific, Billerica, MA, U.S.A.) for 1 hr at room temperature. After further PBS washes, cells were incubated with secondary antibody (Cy3-conjugated goat anti-rabbit IgG or FITC-conjugated goat anti-mouse IgG, Jackson ImmunoResearch, West Grove, PA, U.S.A.) for 30 min at room temperature. The cells were then washed with PBS and counterstained with 4′, 6-diamidino-2-phenyl-indole (DAPI) for nuclear staining before fluorescence microscopic observation.

Reverse transcription-PCR and real-time PCR: Total RNA was extracted using ISOGEN (NIPPON GENE, Tokyo, Japan) and reverse-transcribed to single-strand cDNA using oligo-dT primer and Superscript III reverse transcriptase (Invitrogen) according to the manufacturer's instructions. PCR was performed using *Taq* DNA polymerase (KAPA Biosystems, Woburn, MA, U.S.A.) and using specific primers, and each cycle consisted of the following steps: denaturation for 10 sec at 98°C, annealing for 30 sec at 53–65°C and a 30-sec elongation at 72°C (Table 1). Reaction products were electrophoresed on a 2.0% agarose gel and visualized with ethidium bromide. Real-time PCR of the mRNAs for *p16*, *p21* and *GAPDH* was performed using an ABI PRISM 7500 Sequence Detection System (Applied Biosystems Japan, Tokyo, Japan) according to the manufacturer's instructions. Analysis of the results was carried out using ABI PRISM 7500 Dissociation Curve Software v 1.0 (Applied Biosystems Japan). The relative amount of mRNA was normalized to that of *GAPDH*.

Statistical analysis: Results are expressed as the mean ± standard error. Multiple comparisons were done with the Turkey–Kramer test after one-way analysis of variance. A p-value<0.05 was considered statistically significant.

RESULTS

VPA induces acetylation of histone H3 and decreased cell proliferation: To confirm the effect of VPA on HDAC1 and acetylation of histone H3, we examined the expression of HDAC1 and acetylation of histone H3 by immunofluorescence staining. Minimal HDAC1 and acetylation of histone H3 were observed in the control ADSCs. VPA flattened the morphology of ADSCs and increased the expression of HDAC1 and the acetylation of histone H3 in ADSCs after 3 days of treatment (Fig. 1A and 1B). In contrast, VPM did not cause any morphological changes or significant changes in HDAC1 and histone H3 staining in ADSCs.

Moreover, VPA treatment significantly decreased the proliferation of ADSCs in a dose-dependent manner: about 20% (2 mM VPA), 40% (4 mM VPA) and 80% (8 mM VPA) of the control group (Fig. 1C). However, VPM treatment did not substantially affect ADSC proliferation. No dead cells were observed in any VPA-treated groups by phase-contrast microscopy.

VPA induces upregulation of cyclin-dependent kinase inhibitors: To assess the effect of VPA on the expression of cyclin-dependent kinase (CDK) inhibitors, we examined the expression of these genes by real time-PCR. The expression levels of *p16* mRNA significantly increased in the ADSCs treated with 4 mM VPA (4.6 fold vs. control); however, *p16* mRNA expression levels did not change in the cells treated with 8 mM VPA (2.1 fold vs. control; Fig. 2A). *p21* mRNA expression levels significantly increased in the cells treated with 8 mM VPA (Fig. 2B). The expression levels of *p21* mRNA were approximately 2.6 fold (4 mM VPA) and 3.0 fold (8 mM VPA) of that of the control group.

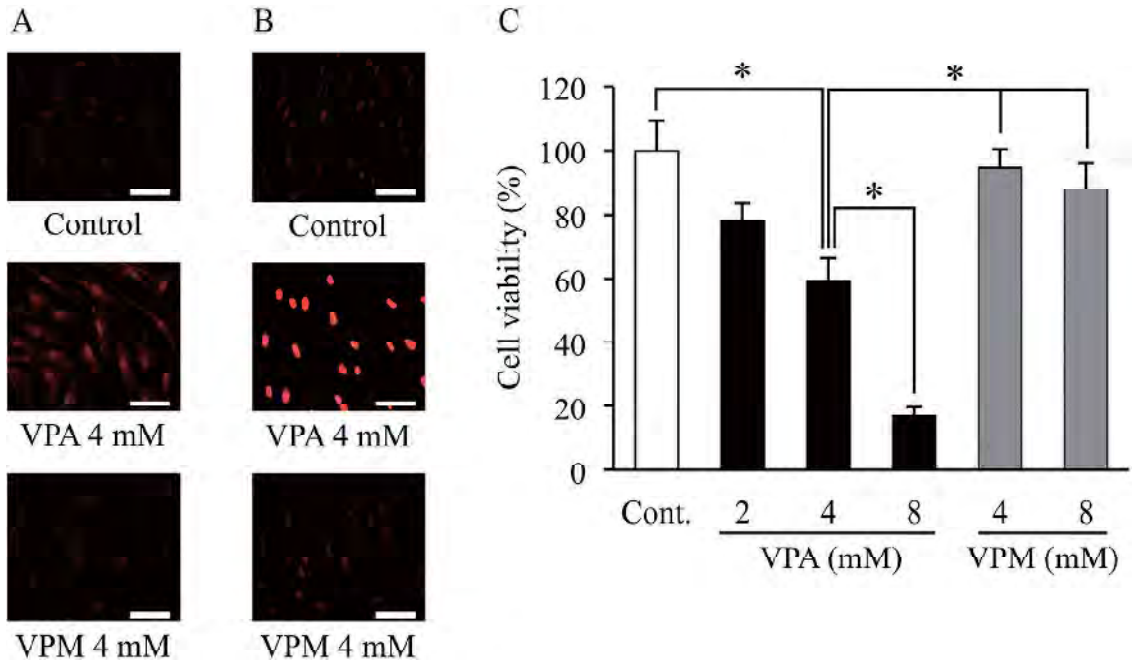

Fig. 1. Effects of valproic acid on histone deacetylase 1 expression, histone H3 acetylation and cell proliferation. Canine adipose tissue-derived stem cells (ADSCs) were treated with valproic acid (VPA) or valpromide (VPM). (A) ADSCs were then processed for immunofluorescence staining with an anti-histone deacetylase 1 (HDAC1) or an anti-histone H3 (acetyl K9) antibody and a secondary antibody (Cy3-conjugated goat anti-rabbit IgG). Red fluorescence indicates positive staining for HDAC1 (A) and acetylation of histone H3 (B). Scale bar, 50 μm. (C) Cell proliferation was measured by MTT assay and expressed as percentage of the negative control (DMSO). Data represent the means ± S.E. (% of control) of 4 independent experiments; each measurement was the average for 6 wells. *P<0.05, significant difference among the indicated groups.

VPA suppresses adipogenic and osteogenic differentiation: To assess the effect of VPA on the pluripotency of ADSCs, we investigated whether VPA treatment alters the differentiation of ADSCs into adipogenic and osteogenic lineages using an *in vitro* differentiation assay. Oil red O staining revealed that ADSCs that differentiated into the adipogenic lineage accumulated lipid droplets in the cytosol, as compared to undifferentiated cells, which did not accumulate lipid droplets (Fig. 3A). VPA pretreatment followed by adipogenic induction significantly suppressed the accumulation of lipid droplets. RT-PCR analysis showed that the mRNA expression levels of adipogenic markers, peroxisome proliferator-activated receptor γ2 (*PPARγ2*), fatty acid binding protein 4 (*FABP4*) and lipoprotein lipase (*LPL*) were elevated by adipogenic induction (Fig. 3B). On the other hand, VPA pretreatment followed by adipogenic induction significantly reduced the *LPL* mRNA expression level, in parallel with the decreased accumulation of lipid droplets. Alizarin red S staining revealed that ADSCs differentiated into osteogenic lineage cells with accumulated calcium deposition, as compared with the undifferentiated cells, which demonstrated no calcium deposition (Fig. 4). VPA pretreatment followed by osteogenic induction significantly reduced calcium deposition (Fig. 4A). mRNA expression levels of osteogenic markers, viz., bone morphogenetic protein 2 (*BMP2*) and distal-less homeobox 5 (*DLX5*), were also elevated by osteogenic induction, but were not significantly affected by VPA pretreatment (Fig. 4B).

VPA promotes neurogenic differentiation: We further examined the effect of VPA on the neurogenic lineage induction of ADSCs. βIII-tubulin immunofluorescence staining revealed that ADSCs that differentiated into neurogenic cells had typical neuron-like cell protrusions and higher βIII-tubulin levels than undifferentiated cells. βIII-tubulin-positive cells also stained for NSE. VPA pretreatment followed by neurogenic induction significantly enhanced the level of βIII-tubulin-positive cells with approximately 90% of ADSCs showing βIII-tubulin expression (Fig. 5A).

mRNA levels of neurogenic markers, viz., *NSE*, *TUBB3* and microtubule-associated protein 2 (*MAP2*), were also elevated by neurogenic induction, but mRNA expression of the glial cell marker, *GFAP,* was not observed in any groups (Fig. 5B). Pretreatment with VPA followed by neurogenic induction increased the expression of *NSE*, *TUBB3* and *MAP2* and of neurofilament heavy polypeptide (*NEFH*), as compared to that in the neurogenic induction group. VPA pretreatment increased the number of βIII-tubulin-positive cells, even without neurogenic induction. Furthermore, VPA elevated the mRNA expression levels of neurogenic markers in ADSCs with and without neurogenic induction.

DISCUSSION

Here, we demonstrated that VPA flattened the morphol-

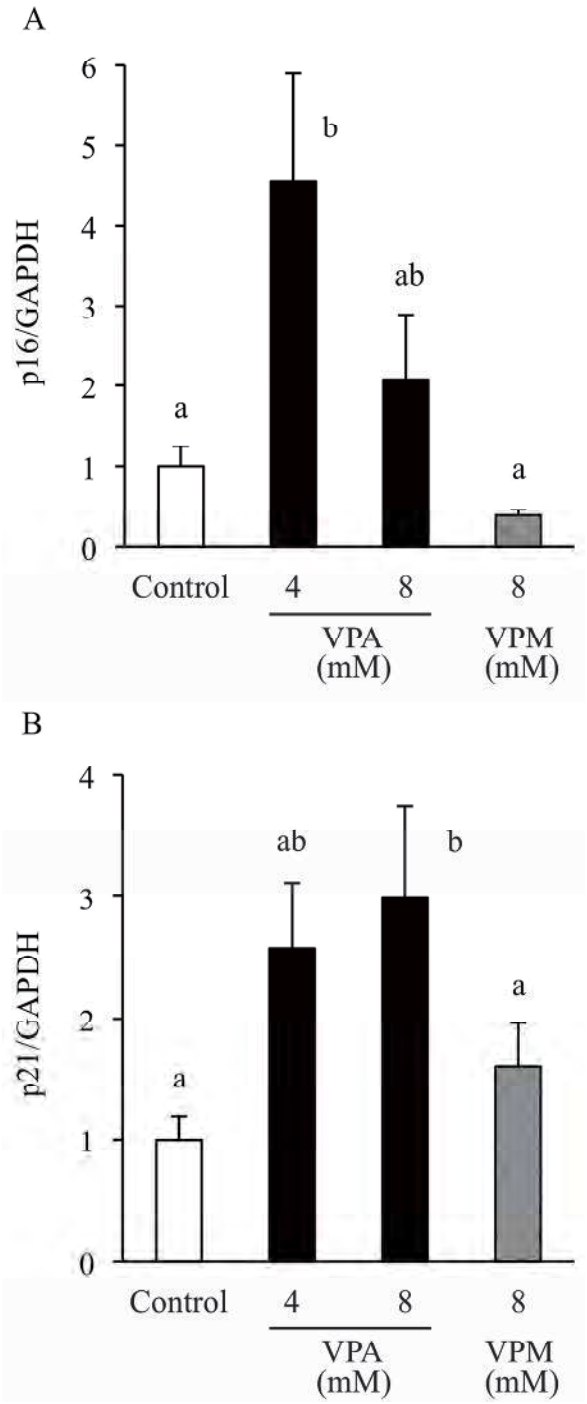

Fig. 2. Effects of valproic acid on cyclin-dependent kinase inhibitor expression. Adipose tissue-derived stem cells (ADSCs) were treated with valproic acid (VPA) or valpromide (VPM). Total RNA was extracted from ADSCs after 3 days of treatment with VPA (4 or 8 mM) or VPM (8 mM). The relative expression of the cyclin-dependent kinase (CDK) inhibitors *p16*(A) and *p21*(B) was quantified by real time-PCR. Glyceraldehyde-3-phosphate dehydrogenase (*GAPDH*) was used as an internal standard. Data are the means ± S.E. of 4–7 independent experiments. a, b: bars with different letters at the top differ significantly; a vs. b, $P<0.05$.

ogy of canine ADSCs and markedly induced their expression of HDAC1 and acetylation of histone H3. In contrast, VPM, an analogue of VPA with no HDAC inhibitory activity, did not cause any morphological changes and had no significant effects on HDAC1 and histone H3, indicating that the H3 acetylation was increased by VPA. These observations support the findings of Lee *et al.* [20]. Thus, our results clearly indicated that VPA induced H3 acetylation by reducing HDAC1 activity in canine ADSCs.

VPA, but not VPM, induced a significant and dose-dependent decrease in the proliferation of ADSCs, suggesting that VPA suppresses ADSC proliferation through acetylation of histone H3. p21 and p16, well-known CDK inhibitors, regulate cell cycle arrest. VPA induces expression of these CDK inhibitors in human ADSCs and mesenchymal stem cells [20, 30]. We found that VPA significantly induced mRNA expression levels of *p16* at 4 mM and of *p21* at 8 mM without inducing cell death. *p21* is also a well-known HDAC-inhibitor responsive gene that is upregulated by hyperacetylation of histones H3 and H4 [10, 20, 28]. In addition, using immunofluorescence, we showed that H3 acetylation was markedly increased by VPA and that *p21* mRNA was significantly increased by 8 mM VPA; thus, cell viability was further reduced by 8 mM VPA treatment, again supporting the findings of Lee *et al.* [20] who reported that VPA causes cell cycle arrest through increased *p21* expression in the absence of *p16* mRNA expression in human ADSCs. Therefore, the inhibitory effect of VPA on proliferation of canine ADSCs was due to cell cycle arrest, although the underlying mechanism needs to be further examined.

Furthermore, VPA promoted differentiation of approximately 90% of ADSCs into a neuronal cell lineage after 3 days of treatment. The differentiated cells have neuron-like morphology and significantly expressed βIII-tubulin protein. Pretreatment with VPA followed by neurogenic induction also promoted mRNA expression of the neuronal markers *NSE*, *TUBB3*, *MAP2* and *NEFH* as compared to the pretreatment without VPA, suggesting that promotional effects of VPA on neuronal differentiation of ADSCs were induced by upregulation of these genes. Previous reports have shown that VPA promotes differentiation of neural stem cells into neurons in adult rats [12, 15]. To our knowledge, the present study is the first report that VPA promotes neuronal differentiation of ADSCs.

Interestingly, VPA pretreatment in the absence of neurogenic induction caused moderate differentiation into neuron-like cells and also increased mRNA expression levels of neurogenic markers in ADSCs. Thus, our data indicated that VPA could induce neurogenic differentiation in the absence of neurogenic induction. We also demonstrated that VPA increased the acetylation of histone H3 that has been correlated with gene activation [12, 13]; thus, VPA caused gene expression in part through H3 acetylation. In addition, we showed that the neuron-like differentiated cells all stained positively for βIII-tubulin. Using NG108-15 cells, Liu *et al.* [21] recently reported that neuronal differentiation could modulate gene transcription, translation and post-translational modulation of Ca^{2+} channels to change the Ca^{2+} ion

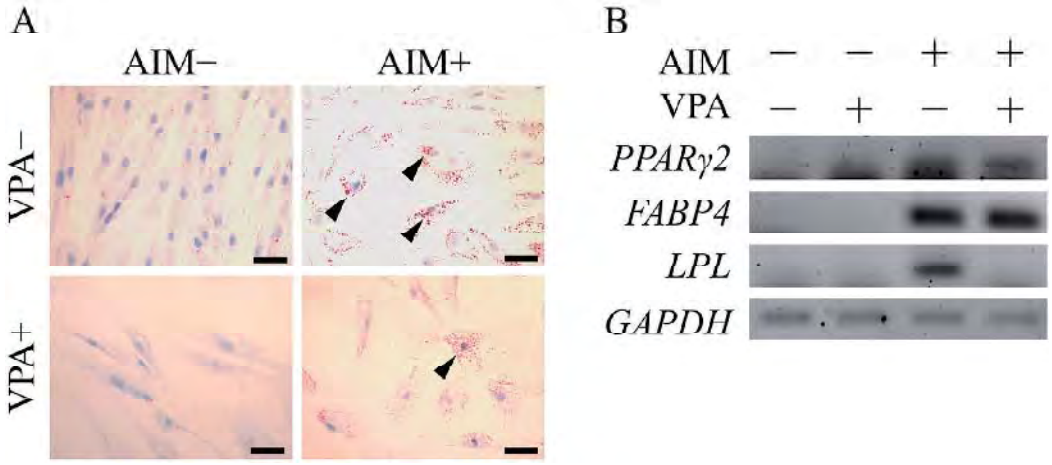

Fig. 3. Valproic acid suppresses accumulation of lipid droplets. Adipose tissue-derived stem cells (ADSCs) were pretreated with valproic acid (VPA) for 3 days followed by adipogenic induction for 14 days. (A) Adipogenic differentiation was visualized by oil red O staining after 14 days of induction with adipogenic medium. Arrowheads show cells that accumulated lipid droplets. Scale bar, 50 μm. (B) RT-PCR analysis of adipogenic markers, *PPARγ2*, *FABP4* and *LPL*, was performed using total RNA extracted from ADSCs after 14 days of adipogenic induction. AIM, adipogenic induction medium.

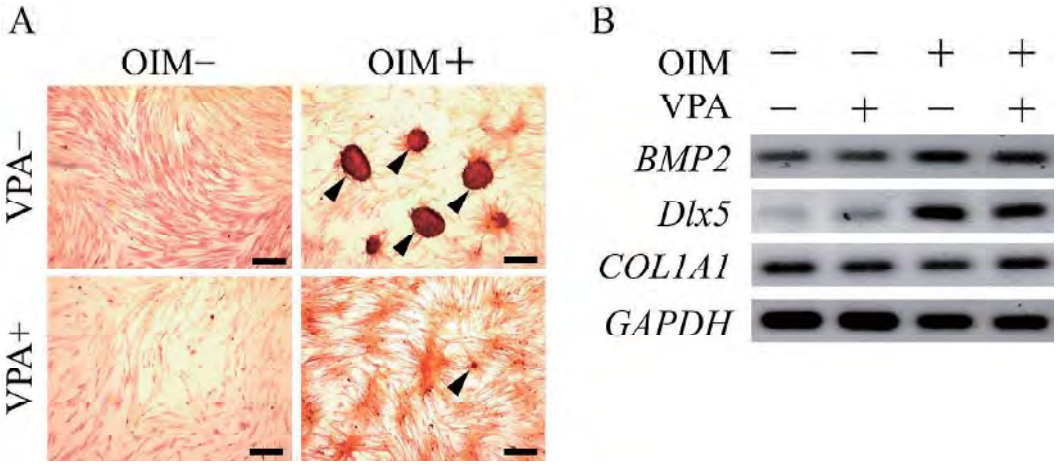

Fig. 4. Valproic acid suppresses calcium deposition. Adipose tissue-derived stem cells (ADSCs) were pretreated with valproic acid (VPA) for 3 days followed by osteogenic induction for 14 days. (A) Osteogenic differentiation was evaluated by alizarin red S staining after 14 days of induction with osteogenic medium. Arrowheads show cells that accumulated calcium in the cytosol. Scale bar, 200 μm. (B) RT-PCR analysis of osteogenic markers, *BMP2*, *Dlx5* and *COL1A1*, was performed using total RNA extracted from ADSCs after 14 days of osteogenic induction. OIM, osteogenic induction medium.

currents; our results suggested that neuronal differentiation could modulate *TUBB3* transcription and translation. In the present study, VPA promoted ADSCs differentiation into neuronal cells in the absence of neurogenic induction factors and induced acetylation of histone H3, indicating that VPA is a useful tool for studying the interaction between chromatin structure and cell fate determination. Further studies are needed to examine the molecular mechanism underlying the neurogenic differentiation induced by VPA using canine ADSCs.

In contrast, VPA suppressed the late stage of differentiation into adipogenic and osteogenic lineage cells. Two of the 3 adipogenic marker genes examined showed no reduction after VPA pretreatment; however, lipid accumulation appeared to be suppressed, suggesting that the VPA inhibits accumulation of lipid droplets rather than an inhibiting the whole adipogenic differentiation process.

Similarly, osteogenic marker genes showed no changes

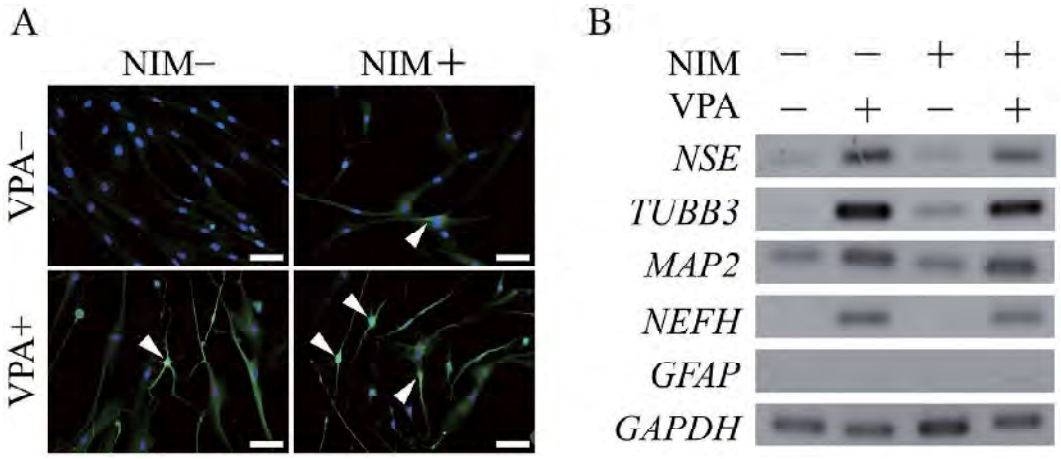

Fig. 5. Valproic acid promotes neurogenic differentiation. Adipose tissue-derived stem cells (ADSCs) were pretreated with valproic acid (VPA) for 3 days followed by neurogenic induction. (A) Neurogenic differentiation was assessed by immunofluorescence staining using an anti-βIII-tubulin antibody and a secondary antibody (FITC-conjugated goat anti-mouse IgG) after 2 hr of induction with neurogenic medium. Arrowheads show cells that expressed βIII-tubulin. Scale bar, 50 μm. (B) RT-PCR analysis of the neurogenic markers, *NSE*, *TUBB3*, *MAP2* and *NEFH* and the glial marker, *GFAP,* was performed using total RNA extracted from ADSCs after 2 hr of neurogenic induction. NIM, neurogenic induction medium.

after VPA treatment, but accumulation of calcium deposition by osteogenic induction was significantly reduced, suggesting that VPA inhibits calcium deposition rather than inhibiting the osteogenic differentiation process as a whole. The mechanism underlying the differential effects of VPA on the pluripotent capacity of ADSCs remains unclear. A previous report has shown that VPA decreases adipogenic and neurogenic differentiation, but increases osteogenic differentiation in human ADSCs [20]. The reason for VPA acting as a stimulator for differentiation of canine ADSCs and as a suppressor for that of human ADSCs is not immediately clear. Therefore, chromatin structure and cell fate determination need to be further examined in relation to the pluripotency of ADSCs, including this difference between humans and dogs.

In conclusion, pretreatment with VPA dose-dependently decreased proliferation of canine ADSCs. In parallel with its inhibitory effects, VPA increased *p16* and *p21* mRNA expression, implying induction of cell cycle arrest through activation of p16 and p21. In addition, pretreatment with VPA followed by adipogenic, osteogenic or neurogenic induction markedly promoted *in vitro* neurogenic differentiation, but suppressed accumulation of lipid droplets and calcium deposition. These *in vitro* modifications of ADSCs by pretreatment with VPA were associated with changes in expression of relevant markers. These results suggested that VPA is a specific inducer of neurogenic differentiation of canine ADSCs and is a useful tool for studying the interaction between chromatin structure and cell fate determination.

ACKNOWLEDGMENTS. This work was supported in part by the Science Research Promotion Fund of The Promotion and Mutual Aid Corporation for Private Schools of Japan. This work was also supported in part by the MEXT Program for the Strategic Research Foundation at Private Universities, 2011–2015.

REFERENCES

1. Case, J., Horvath, T. L., Howell, J. C., Yoder, M. C., March, K. L. and Srour, E. F. 2005. Clonal multilineage differentiation of murine common pluripotent stem cells isolated from skeletal muscle and adipose stromal cells. *Ann. N. Y. Acad. Sci.* **1044**: 183–200. [Medline] [CrossRef]
2. Chung, C. S., Fujita, N., Kawahara, N., Yui, S., Nam, E. and Nishimura, R. 2013. A comparison of neurosphere differentiation potential of canine bone marrow-derived mesenchymal stem cells and adipose-derived mesenchymal stem cells. *J. Vet. Med. Sci.* **75**: 879–886. [Medline] [CrossRef]
3. De Ugarte, D. A., Morizono, K., Elbarbary, A., Alfonso, Z., Zuk, P. A., Zhu, M., Dragoo, J. L., Ashjian, P., Thomas, B., Benhaim, P., Chen, I., Fraser, J. and Hedrick, M. H. 2003. Comparison of multi-lineage cells from human adipose tissue and bone marrow. *Cells Tissues Organs* **174**: 101–109. [Medline] [CrossRef]
4. Deng, W., Obrocka, M., Fischer, I. and Prockop, D. J. 2001. *In vitro* differentiation of human marrow stromal cells into early progenitors of neural cells by conditions that increase intracellular cyclic AMP. *Biochem. Biophys. Res. Commun.* **282**: 148–152. [Medline] [CrossRef]
5. Dicker, A., Le Blanc, K., Astrom, G., van Harmelen, V., Gotherstrom, C., Blomqvist, L., Arner, P. and Ryden, M. 2005. Functional studies of mesenchymal stem cells derived from adult human adipose tissue. *Exp. Cell Res.* **308**: 283–290. [Medline] [CrossRef]
6. Edamura, K., Kuriyama, K., Kato, K., Nakano, R., Teshima, K., Asano, K., Sato, T. and Tanaka, S. 2012. Proliferation capacity, neuronal differentiation potency and microstructures after the differentiation of canine bone marrow stromal cells into neurons. *J. Vet. Med. Sci.* **74**: 923–927. [Medline] [CrossRef]
7. Göttlicher, M., Minucci, S., Zhu, P., Krämer, O. H., Schimpf, A., Giavara, S., Sleeman, J. P., Coco, F. L., Nervi, C., Pelicci, P.

G. and Heinzel, T. 2001. Valproic acid defines a novel class of HDAC inhibitors inducing differentiation of transformed cells. *EMBO J.* **20**: 6969–6978. [Medline] [CrossRef]
8. Gronthos, S., Franklin, D. M., Leddy, H. A., Robey, P. G., Storms, R. W. and Gimble, J. M. 2001. Surface protein characterization of human adipose tissue-derived stromal cells. *J. Cell. Physiol.* **189**: 54–63. [Medline] [CrossRef]
9. Grunstein, M. 1997. Histone acetylation in chromatin structure and transcription. *Nature* **389**: 349–352. [Medline] [CrossRef]
10. Han, J. W., Ahn, S. H., Kim, Y. K., Bae, G. U., Yoon, J. W., Hong, S., Lee, H. Y., Lee, Y. W. and Lee, H. W. 2001. Activation of p21 (WAF1 / Cip1) transcription through Sp1 sites by histone deacetylase inhibitor apicidin: involvement of protein kinase C. *J. Biol. Chem.* **276**: 42084–42090. [Medline] [CrossRef]
11. Housman, T. S., Lawrence, N., Mellen, B. G., George, M. N., Filippo, J. S., Cerveny, K. A., DeMarco, M., Feldman, S. R. and Fleischer, A. B. 2002. The safety of liposuction: results of a national survey. *Dermatol. Surg.* **28**: 971–978. [Medline] [CrossRef]
12. Hsieh, J., Nakashima, K., Kuwabara, T., Mejia, E. and Gage, F. H. 2004. Histone deacetylase inhibition-mediated neuronal differentiation of multipotent adult neural progenitor cells. *Proc. Natl. Acad. Sci. U.S.A.* **101**: 16659–16664. [Medline] [CrossRef]
13. Jenuwein, T. and Allis, C. D. 2001. Translating the histone code. *Science* **293**: 1074–1080. [Medline] [CrossRef]
14. Jung, D. I., Ha, J., Kang, B. T., Kim, J. W., Quan, F. S., Lee, J. H., Woo, E. J. and Park, H. M. 2009. A comparison of autologous and allogenic bone marrow-derived mesenchymal stem cell transplantation in canine spinal cord injury. *J. Neurol. Sci.* **285**: 67–77. [Medline] [CrossRef]
15. Jung, G. A., Yoon, J. Y., Moon, B. S., Yang, D. H., Kim, H. Y., Lee, S. H., Bryja, V., Arenas, E. and Choi, K. Y. 2008. Valproic acid induces differentiation and inhibition of proliferation in neural progenitor cells via the beta-catenin-Ras-ERK-p21Cip/WAF1 pathway. *BioMed. Cen. Cell Biol.* **9**: 66.
16. Kamishina, H., Cheeseman, J. A. and Clemmons, R. M. 2008. Nestin-positive spheres derived from canine bone marrow stromal cells generate cells with early neuronal and glial phenotypic characteristics. *In Vitro Cell Dev. Biol. Anim.* **44**: 140–144. [Medline] [CrossRef]
17. Kern, S., Eichler, H., Stoeve, J., Kluter, H. and Bieback, K. 2006. Comparative analysis of mesenchymal stem cells from bone marrow, umbilical cord blood, or adipose tissue. *Stem Cells (Dayton, Ohio)* **24**: 1294–1301. [Medline] [CrossRef]
18. Kuo, M. H. and Allis, C. D. 1998. Roles of histone acetyltransferases and deacetylase in gene regulation. *BioEssays* **20**: 615–626. [Medline] [CrossRef]
19. Lee, R. H., Kim, B., Choi, I., Kim, H., Choi, H. S., Suh, K., Bae, Y. C. and Jung, J. S. 2004. Characterization and expression analysis of mesenchymal stem cells from human bone marrow and adipose tissue. *Cell. Physiol. Biochem.* **14**: 311–324. [Medline] [CrossRef]
20. Lee, S., Park, J. R., Seo, M. S., Roh, K. H., Park, S. B., Hwang, J. W., Sun, B., Seo, K., Lee, Y. S., Kang, S. K., Jung, J. W. and Kang, K. S. 2009. Histone deacetylase inhibitors decrease proliferation potential and multi-lineage differentiation capability of human mesenchymal stem cells. *Cell Prolif.* **42**: 711–720. [Medline] [CrossRef]
21. Liu, J., Tu, H., Zhang, D. and Li, Y.L. 2012. Changes of calcium channel mRNA, protein and current in NG108-15 cells after cell differentiation. *Biochem. Biophys. Res. Commun.* **423**: 55–59. [Medline] [CrossRef]
22. Liu, T. M., Martina, M., Hutmacher, D. W., Hui, J. H., Lee, E. H. and Lim, B. 2007. Identification of common pathways mediating differentiation of bone marrow- and adipose tissue-derived human mesenchymal stem cells into three mesenchymal lineages. *Stem Cells* **25**: 750–760. [Medline] [CrossRef]
23. Ning, H., Lin, G., Lue, T. F. and Lin, C. S. 2006. Neuron-like differentiation of adipose tissue-derived stromal cells and vascular smooth muscle cells. *Differentiation* **74**: 510–518. [Medline] [CrossRef]
24. Ning, H., Guiting, L., Fandel, T., Banie, L., Lue, T. F. and Lin, C.S. 2008. Insulin growth factor signaling mediates neuron-like differentiation of adipose tissue-derived stem cells. *Differentiation* **76**: 488–494. [Medline] [CrossRef]
25. Nishida, H., Nakayama, M., Tanaka, H., Kitamura, M., Hatoya, S., Sugiura, K., Suzuki, Y., Ide, C. and Inaba, T. 2011. Evaluation of transplantation of autologous bone marrow stromal cells into the cerebrospinal fluid for treatment of chronic spinal cord injury in dogs. *Am. J. Vet. Res.* **72**: 1118–1123. [Medline] [CrossRef]
26. Olby, N. 2010. The pathogenesis and treatment of acute spinal cord injuries in dogs. *Vet. Clin. North Am. Small Anim. Pract.* **40**: 791–807. [Medline] [CrossRef]
27. Phiel, C. J., Zhang, F., Huang, E. Y., Guenther, M. G., Lazar, M. A. and Klein, P. S. 2001. Histone deacetylase is a direct target of valproic acid, a potent anticonvulsant, mood stabilizer, and teratogen. *J. Biol. Chem.* **276**: 36734–36741. [Medline] [CrossRef]
28. Richon, V. M., Sandhoff, T. W., Rifkind, R. A. and Marks, P. A. 2000. Histone deacetylase inhibitor selectively induces p21WAF1 expression and gene-associated histone acetylation. *Proc. Natl. Acad. Sci. U.S.A.* **97**: 10014–10019. [Medline] [CrossRef]
29. Sago, K., Tamahara, S., Tomihari, M., Matsuki, N., Asahara, Y., Takei, A., Bonkobara, M., Washizu, T. and Ono, K. 2008. In vitro differentiation of canine celiac adipose tissue-derived stromal cells into neuronal cells. *J. Vet. Med. Sci.* **70**: 353–357. [Medline] [CrossRef]
30. Shibata, K. R., Aoyama, T., Shima, Y., Fukiage, K., Otsuka, S., Furu, M., Kohno, Y., Ito, K., Fujibayashi, S., Neo, M., Nakayama, T., Nakamura, T. and Toguchida, J. 2007. Expression of the p16INK4A gene is associated closely with senescence of human mesenchymal stem cells and is potentially silenced by DNA methylation during in vitro expansion. *Stem Cells* **25**: 2371–2382. [Medline] [CrossRef]
31. Skinner, A. P., Pachnicke, S., Lakatos, A., Franklin, R. J. and Jeffery, N. D. 2005. Nasal and frontal sinus mucosa of the adult dog contain numerous olfactory sensory neurons and ensheathing glia. *Res. Vet. Sci.* **78**: 9–15. [Medline] [CrossRef]
32. Starkey, M. P., Scase, T. J., Mellersh, C. S. and Murphy, S. 2005. Dogs really are man's best friend—canine genomics has applications in veterinary and human medicine! *Brief Funct. Genomic Proteomic.* **4**: 112–128. [Medline] [CrossRef]
33. Strem, B. M., Hicok, K. C., Zhu, M., Wulur, I., Alfonso, Z., Schreiber, R. E., Fraser, J. K. and Hedrick, M. H. 2005. Multipotential differentiation of adipose tissue-derived stem cells. *Keio J. Med.* **54**: 132–141. [Medline] [CrossRef]
34. Struhl, K. 1998. Histone acetylation and transcriptional regulatory mechanisms. *Genes Dev.* **12**: 599–606. [Medline] [CrossRef]
35. Wagner, W., Wein, F., Seckinger, A., Frankhauser, M., Wirkner, U., Krause, U., Blake, J., Schwager, C., Eckstein, V., Ansorge, W. and Ho, A. D. 2005. Comparative characteristics of mesenchymal stem cells from human bone marrow, adipose tissue, and umbilical cord blood. *Exp. Hematol.* **33**: 1402–1416. [Medline] [CrossRef]
36. Wu, P., Sato, K., Yukawa, S., Hikasa, Y. and Kagota, K. 2001. Differentiation of stromal-vascular cells isolated from canine

adipose tissues in primary culture. *J. Vet. Med. Sci.* **63**: 17–23. [Medline] [CrossRef]
37. Yoshimura, H., Muneta, T., Nimura, A., Yokoyama, A., Koga, H. and Sekiya, I. 2007. Comparison of rat mesenchymal stem cells derived from bone marrow, synovium, periosteum, adipose tissue, and muscle. *Cell Tissue Res.* **327**: 449–462. [Medline] [CrossRef]
38. Zuk, P. A., Zhu, M., Ashjian, P., DeUgarte, D. A., Huang, J. I., Mizuno, H., Alfonso, Z. C., Benhaim, P. and Hedrick, M. H. 2002. Human adipose tissue is a source of multipotent stem cells. *Mol. Biol. Cell* **13**: 4279–4295. [Medline] [CrossRef]
39. Zuk, P. A., Zhu, M., Mizuno, H., Huang, J., Futrell, J. W., Katz, A. J., Benhaim, P., Lorenz, H. P. and Hedrick, M. H. 2001. Multilineage cells from human adipose tissue: implications for cell-based therapies. *Tissue Eng.* **7**: 211–228. [Medline] [CrossRef]

Biochem Genet (2012) 50:12–18
DOI 10.1007/s10528-011-9453-5

Nucleotide Polymorphisms in the Canine *Noggin* Gene and Their Distribution Among Dog (*Canis lupus familiaris*) Breeds

Yuji Ishii · Tatsuya Takizawa · Hiroshi Iwasaki · Yukihiro Fujita · Masaru Murakami · Jay C. Groppe · Kazuaki Tanaka

Received: 17 March 2010 / Accepted: 28 April 2011 / Published online: 1 September 2011

Abstract Noggin (NOG) is an important regulator for the signaling of bone morphogenetic proteins. In this study, we sequenced the complete coding sequence of the canine *NOG* gene and characterized the nucleotide polymorphisms. The sequence length varied from 717 to 729 bp, depending on the number of a 6-bp tandem repeat unit (GGCGCG), an insertion that has not been observed in other mammalian *NOG* genes investigated to date. It results in extensions of $(Gly–Ala)_{3–5}$ in the putative NOG protein. To survey the distribution of these tandem repeat polymorphisms, we analyzed 126 individuals in seven dog breeds. We identified only three alleles: $(GGCGCG)_3$, $(GGCGCG)_4$, and $(GGCGCG)_5$. Although the allele frequencies were remarkably different among the breeds, the three alleles were present in all seven of the breeds and did not show any deviation from Hardy–Weinberg equilibrium.

Electronic supplementary material The online version of this article (doi: 10.1007/s10528-011-9453-5) contains supplementary material, which is available to authorized users.

Y. Ishii · T. Takizawa · H. Iwasaki · K. Tanaka (✉)
Laboratory of Animal Biotechnology, School of Veterinary Medicine, Azabu University, Chuou-ku, Sagamihara 252-5201, Japan
e-mail: tanakak@azabu-u.ac.jp

Y. Fujita
Laboratory of Veterinary Surgery 2, School of Veterinary Medicine, Azabu University, Chuou-ku, Sagamihara 252-5201, Japan

M. Murakami
Laboratory of Molecular Biology, School of Veterinary Medicine, Azabu University, Chuou-ku, Sagamihara 252-5201, Japan

J. C. Groppe
Department of Biomedical Sciences, Baylor College of Dentistry, TAMHSC, Dallas, TX 75246, USA

Keywords Noggin · Dog · *Canis lupus familiaris* · Polymorphisms · VNTR

Introduction

Noggin (NOG) is a member of the bone morphogenetic protein (BMP) family and a major extracellular antagonist of the BMP. NOG regulates dorsal induction and joint formation in embryonic development by blocking BMP signaling (Smith and Harland 1992; Zimmerman et al. 1996; Brunet et al. 1998; McMahon et al. 1998; Canalis et al. 2003). NOG also controls bone regeneration and homeostasis in adults (Canalis et al. 2003; Canalis 2009). The coding sequences of mammalian NOG genes are contained in a single exon and are highly conserved among species (Valenzuela et al. 1995). Nucleotide and amino acid sequence similarities are more than 90% among humans, mice, and other mammals (Valenzuela et al. 1995). In humans, several point mutations in the *NOG* gene have been linked to congenital skeletal malformations, for example, proximal symphalangism or multiple synostoses syndrome (Gong et al. 1999; Marcelino et al. 2001; Hirshoren et al. 2008). Therefore, the *NOG* gene is a potential candidate for involvement in congenital skeletal malformations in domesticated dogs. Partial DNA sequences at this locus have been defined by the Canine Genome Project (NW_876332; *Canis familiaris* chromosome 9 genomic contig). To the best of our knowledge, no nucleotide polymorphisms have been described in the canine *NOG* gene. In the present study, we first determined the DNA sequence of the complete coding sequence of the canine *NOG* gene, to scan for all the possible nucleotide polymorphisms encoded at this locus. We subsequently surveyed the allelic distribution of the variable number of tandem repeats (VNTRs) that were identified in the canine *NOG* gene.

Materials and Methods

Tissue and nail samples from non-sibling dogs were collected at veterinary hospitals and dog-grooming shops in Japan; 127 samples were obtained from 24 long-haired Miniature Dachshunds, 25 long-haired Chihuahuas, 23 Miniature Poodles, 19 Shih Tzus, 13 Papillons, 12 Malteses, 10 Yorkshire Terriers, and 1 Beagle. Genomic DNA was extracted from tissue or nails by a standard phenol–chloroform extraction method (Sambrook et al. 1989) or using the QuickGene DNA tissue kit (Fuji Film, Tokyo, Japan).

Amplification and Sequencing of Canine *NOG* Coding Sequence

Four animals from three breeds were selected for DNA sequence determination of the complete coding sequence for the canine *NOG* gene (one Beagle, two Miniature Dachshunds, and one Chihuahua). Primers for polymerase chain reaction (PCR) and sequencing were designed from dog genome draft sequences (chromosome 9, NW_876332); rat (NM_012990), mouse (NM_008711), and human (NM_005450) *NOG* gene sequences (Table 1). The primer sets of Can*NOG*-F1 and Can*NOG*-R1

Table 1 Primers for canine *NOG* gene

Primer	Sequence (5′ to 3′)	Position on NW_876332[a]
Can*NOG*-F1	TGGTGATGGAGCTGAAAGTG	13273923–13273942
Can*NOG*-R1	ACCACAGCCACATCTGTAACTTC	13274986–13275008
Can*NOG*-F2	ACCCGGACCCTATCTTTGAC	13274685–13274704
Can*NOG*-R2	TTTCTGGCTACAGAGACCTAGCT	13275418–13275440
Can*NOG*-S1[b]	GAAGTTACAGATGTGGCTGTGGT	Reverse complement of R1
Can*NOG*-S2[b]	GTCAAAGATAGGGTCCGGGT	Reverse complement of F2

[a] *Canis familiaris* chromosome 9 genomic contig, whole genome shotgun sequence

[b] Primers used only for sequencing

produce about 1.1 kbp DNA products, whereas the primer sets of Can*NOG*-F2 and Can*NOG*-R2 produce about 700 bp. The two products overlapped with one another in the canine *NOG* coding sequence.

The PCR was performed according to the manufacturer's instructions for PrimeStar HS DNA polymerase with GC buffer (Takara Biotechnology, Shiga, Japan). The program included first denaturation at 98°C for 2 min; 35 cycles of denaturation at 98°C for 20 s, annealing at 55°C for 5 s, and extension at 72°C for 60 s; and final extension at 72°C for 3 min. The amplified products of each reaction were cloned into the plasmid pCR-Blunt II-TOPO using the Zero Blunt TOPO PCR Cloning kit (Invitrogen, Carlsbad, USA). At least five clones were isolated from each individual and sequenced using the Big Dye Terminator version 3.1 Cycle Sequencing Kit and ABI 3100 sequencer (Applied Biosystems, Foster City, USA) with M13 universal primers and additional sequencing primers (Table 1).

Detection of the VNTR Polymorphisms in the *NOG* Coding Sequence

In order to survey the distribution of the VNTR alleles in dog breeds, we analyzed 126 animals from seven breeds (Table 2). The 300 bp DNA products of the canine *NOG* gene, including the 6-bp tandem repeats (GGCGCG), were PCR-amplified

Table 2 Genotype and allele frequency of $(GGCGCG)_n$ VNTR in canine *NOG* gene among seven dog breeds

Breed (number of animals sampled)	Genotype						Allele frequency		
	3	4	5	3/4	3/5	4/5	3	4	5
Miniature Dachshund, long hair (24)	1	7	0	7	7	2	0.333	0.479	0.188
Chihuahua, long hair (25)	3	0	6	5	7	4	0.360	0.180	0.460
Miniature poodle (23)	2	2	2	5	6	6	0.326	0.326	0.348
Shih Tzu (19)	9	0	2	3	4	1	0.658	0.105	0.237
Papillon (13)	5	0	0	2	4	2	0.615	0.154	0.231
Maltese (12)	2	1	0	0	6	3	0.417	0.208	0.375
Yorkshire Terrier (10)	8	0	0	1	1	0	0.900	0.050	0.050

using primer sets of Can*NOG*-F2 and Can*NOG*-R1 and then purified with the High Pure PCR Product Purification Kit (Roche Applied Science, Mannheim, Germany). Purified DNAs were sequenced directly with the primer Can*NOG*-F2 as described above. Heterozygous individuals that had a different number of tandem repeats were genotyped from their electropherograms.

Results and Discussion

In four domestic dogs, we sequenced the entire coding region of the *NOG* gene. which included an unidentified region of 91 nucleotides in NW_876332. These nucleotide sequences were entered into the DDBJ, EMBL, and GenBank nucleotide databases with accession numbers AB544074–AB544077. After multiple alignment of canine sequences with human *NOG* (NM_005450) and mouse *Nog* (NM_008711), we found that the coding sequence of the canine *NOG* gene is longer than that of humans and mice. The coding sequence of the human and mouse genes is consistently 699 bp in length. The coding sequence in the four dogs showed three polymorphisms, of 717, 723, and 729 bp, caused by inserted sequences of 18, 24, and 30 bp, respectively. These inserted sequences in the canine *NOG* gene were constructed by different numbers of the 6-bp tandem repeats (GGCGCG) unit (Fig. 1). These GGCGCG tandem repeats immediately preceded the inserted sequences. Thus, these sequence-length polymorphisms are the result of the duplicated insertion of this repeat unit. The insertions of tandem repeats were aligned with the reading frame of the *NOG* gene and found to encode a Gly–Ala repeat

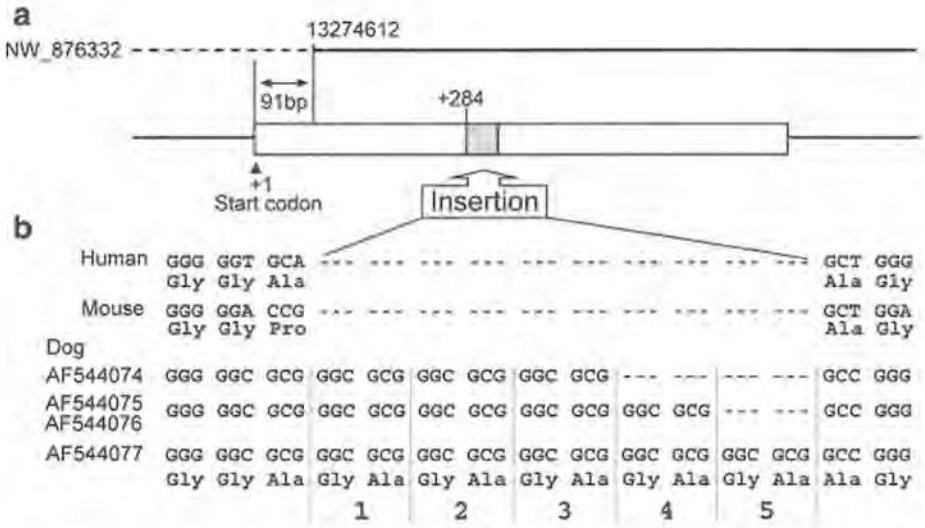

Fig. 1 The coding region of the canine *NOG* gene and polymorphisms detected in this study. **a** Structure of the coding region of the canine *NOG* gene. The solid upper line indicates the partial sequence of canine chromosome 9 (NW_876332), and the broken line represents the undeciphered region in NW_876332. The start codon of canine *NOG* was located in the unidentified region, −91 bp from position 13274612 on NW_876332. The *white blocks* of the diagram represent the canine *NOG* coding sequence, and the *shaded block* indicates the region of the inserted sequence. **b** The nucleotide and amino acid sequences around the canine-specific insertion. The repeating units are ruled off by vertical lines. The numbers at the *bottom* indicate the number of repetitions. Repetition of GGCGCG was translated into the amino acids Gly–Ala

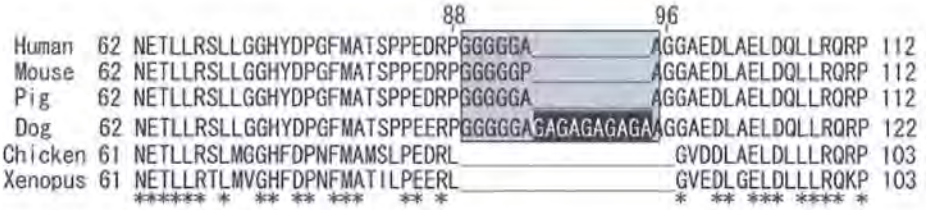

Fig. 2 Comparison of partial amino acid sequences of vertebrate Noggin. *Asterisks* indicate the conserved amino acids among the six species. The *gray box* encloses the polyglycine loop (Gly–Gly–Gly–Gly–Gly–Ala–Ala) insertion, which is present only in mammalian Noggin (Groppe et al. 2002). The *highlighted letters* indicate extension of the Gly–Ala repeat in the canine Noggin. The Gly–Ala repeat is connected to the polyglycine loop. Citation of sequences: human NM_005450, mouse NM_008711, pig NM_001143691, dog AF544077, chicken NM_204123, and *Xenopus* NM_00185644

(Fig. 1). These $(Gly–Ala)_{3–5}$ insertions are located in the polyglycine loop which is present only in mammalian Noggin (Fig. 2). The polyglycine loop is the most flexible part of the mammalian Noggin protein, as a complex with the BMP ligand (Groppe et al. 2002). Excluding these inserted-sequence regions, the coding sequence of the canine *NOG* gene displayed 96.7% sequence similarity with the nucleotides of human *NOG* and 94.0% with mouse *Nog*. No other polymorphic sites were found among the four canine *NOG* sequences, except the above-mentioned inserted sequences.

We sequenced part of the *NOG* gene, including the tandem repeat $(GGCGCG)_n$, in 126 dogs from seven breeds, and identified three alleles, $(GGCGCG)_3$, $(GGCGCG)_4$, and $(GGCGCG)_5$, among these individuals (Table 2). The genotypic and allelic frequencies of these VNTR alleles did not deviate from Hardy–Weinberg equilibrium among the seven breeds. Although the three alleles of the VNTR were present in all the dog breeds analyzed in this study, distributions varied widely among the breeds. $(GGCGCG)_4$ had the highest frequency in the Miniature Dachshund, whereas $(GGCGCG)_3$ was extremely high in the Shih Tzu, Papillon, and Yorkshire Terrier (Table 2). Since the three *NOG* VNTR alleles were distributed widely among various dog breeds, these sequence-length polymorphisms arose long before the modern dog breeds were established several hundred years ago.

Because we collected DNA samples from visibly healthy dogs, each VNTR allele in the canine *NOG* gene did not appear to be linked to fatal outcomes and severe pathological phenotypes in young dogs. Considering the important role of *NOG* in bone regeneration and homeostasis in adults (Canalis 2009), however, the three canine *NOG* variations theoretically could be associated with susceptibility to bone or joint disorders in the lifetime of the domestic dog. Nevertheless, the polymorphisms are most likely silent with respect to function given that (1) the additional residues encoded by the repeats were inserted in the most flexible portion of the Noggin protein, (2) the segment is well removed from the ligand-binding interface, (3) the loop is expanded in other mammals with no apparent loss of function, and (4) the inserted residues are small and functionally inert in the context of a disordered loop (Supplementary Fig. 1). In contrast, polymorphisms resulting in insertion of tracts of polyglutamine in transcription factors can have a toxic

gain-of-function effect in neurodegenerative disorders, triggering conformational changes that disrupt gene regulation (Riley and Orr, 2006) or culminate in formation of amyloid-like fibrils (Robertson et al. 2011). Indeed, insertion of glutamine repeats in Runx-2 protein, a transcription factor that regulates osteoblast differentiation, can have dramatic effects on canine skeletal morphogenesis (Fondon and Garner 2004). Introduction of amide-containing side-chains, with two functional groups capable of hydrogen bonding, can enhance interactions within multiprotein transcriptional complexes, leading to upregulation of target genes involved in skeletogenesis. Therefore, although polymorphisms within domestic dog breeds can have pronounced effects on development, the structural context and nature of the side-chain of the inserted residues appears to dictate whether the effect is functionally silent, accumulating over evolutionarily large time spans, or pronounced, capable of generating rapid diversity of form.

Acknowledgment This work was partly supported by a research project grant awarded by the Azabu University to K. Tanaka.

References

Brunet LJ, McMahon JA, McMahon AP, Harland RM (1998) Noggin, cartilage morphogenesis, and joint formation in the mammalian skeleton. Science 280:1455–1457

Canalis E (2009) Growth factor control of bone mass. J Cell Biochem 108:769–777

Canalis E, Economides AN, Gazzerro E (2003) Bone morphogenetic proteins, their antagonists, and the skeleton. Endocr Rev 24:218–235

Fondon JW, Garner HR (2004) Molecular origins of rapid and continuous morphological evolution. Proc Natl Acad Sci USA 101:18058–18063

Gong Y, Krakow D, Marcelino J, Wilkin D, Chitayat D, Babul-Hirji R, Hudgins L, Cremers CW, Cremers FP, Brunner HG, Reinker K, Rimoin DL, Cohn DH, Goodman FR, Reardon W, Patton M, Francomano CA, Warman ML (1999) Heterozygous mutations in the gene encoding noggin affect human joint morphogenesis. Nature Genet 21:302–304

Groppe J, Greenwald J, Wiater E, Rodriguez-Leon J, Economides AN, Kwiatkowski W, Affolter M, Vale WW, Belmonte JC, Choe S (2002) Structural basis of BMP signalling inhibition by the cystine knot protein Noggin. Nature 420:636–642

Hirshoren N, Gross M, Banin E, Sosna J, Bargal R, Raas-Rothschild A (2008) P35S mutation in the *NOG* gene associated with Teunissen-Cremers syndrome and features of multiple *NOG* joint-fusion syndromes. Eur J Med Genet 51:351–357

Marcelino J, Sciortino CM, Romero MF, Ulatowski LM, Ballock RT, Economides AN, Eimon PM, Harland RM, Warman ML (2001) Human disease-causing *NOG* missense mutations: effects on noggin secretion, dimer formation, and bone morphogenetic protein binding. PNAS 98:11353–11358

McMahon JA, Takada S, Zimmerman LB, Fan CM, Harland RM, McMahon AP (1998) Noggin-mediated antagonism of BMP signaling is required for growth and patterning of the neural tube and somite. Genes Dev 12:1438–1452

Riley BE, Orr HT (2006) Polyglutamine neurodegenerative diseases and regulation of transcription: assembling the puzzle. Genes Dev 20:2183–2192

Robertson AL, Bate MA, Androulakis SG, Bottomly SP, Buckle AM (2011) PolyQ: a database describing the sequence and domain context of polyglutamine repeats in proteins. Nucleic Acids Res 39(Database issue):D272–D276

Sambrook J, Fritsch EF, Maniatis T (1989) Molecular cloning: a laboratory manual, 2nd edn. Cold Spring Harbor Laboratory Press, New York

Smith WC, Harland RM (1992) Expression cloning of noggin, a new dorsalizing factor localized to the Spemann organizer in *Xenopus* embryos. Cell 70:829–840

Valenzuela DM, Economides AN, Rojas E, Lamb TM, Nunez L, Jones P, Lp NY, Espinosa R 3rd, Brannan CI, Gilbert DJ, Copeland NG, Jenkins NA, Le Beau MM, Harland RM, Yancopoulos GD (1995) Identification of mammalian noggin and its expression in the adult nervous system. J Neurosci 15:6077–6084

Zimmerman LB, De Jesus-Escobar JM, Harland RM (1996) The Spemann organizer signal noggin binds and inactivates bone morphogenetic protein 4. Cell 86:599–606

学会発表要旨

演者名	田中和明, 滝沢達也, 山本未咲, 岡本憲明, 島倉秀勝, 阪口雅弘
演題名	イヌ *IL-13*遺伝の多型と柴犬におけるアトピー性皮膚炎との関連調査.
学会名	日本畜産学会第 121 回大会
場所、開催日	東京都武蔵野市　3 月　2016 年

【目的】

IL13 は、IgE 生産調節に重要なサイトカインである．本研究では、イヌ IL13 遺伝子の多型検索と疾病との相関解析を行った．

【実験方法】

15 犬種 34 個体の *IL13* 遺伝子の塩基配列を決定した．また IL13 遺伝子上の rs22147008(p.63 Thr>Ala)と rs8973298(5´隣接領域)について、アトピー性皮膚炎を発症した柴犬 10 個体と、皮膚炎が認められない柴犬 33 個体を用いた症例対照解析を行った．

【結果】

NC_006593 を基準として、g.20957075 AGGTGGGCA:[1]>[2]縦列反復多型と 15 カ所の SNP を検出した．柴犬を用いた症例対照解析では、rs22147008 では G 型対立遺伝子頻度は、症例群で 0.05、対照群で 0.11 であり有意な差は認められなかった．また G 型対立遺伝子を持つ個体は全てヘテロ接合体であった．rs8973298 の遺伝子型は、患畜群では CC 型 4 個体、CT 型 3 個体、TT 型 3 個体であったのに対して、非患畜群では CC 型 4 個体、CT 型 21 個体、TT 型 8 個体であった．患畜群と非患畜群の遺伝子型頻度は、ピアソン方法によるカイ二乗値が 3.939（p=0.047）で有意に異なっていた．この時、C 型対立遺伝子のホモ接合（CC 型）を、アトピー性皮膚炎のリスク型と想定するとオッズ比が 4.833（95%信頼区間 1.018～23.455）であった．これにより、柴犬では rs8973298 の C のホモ接合型は、アトピー性皮膚炎の発症リスクを高めることが示唆された．

私立大学戦略的研究基盤形成支援事業

中間報告会・進捗状況評価書

外部評価委員

東京大学大学院農学生命科学研究科教授

辻本　元先生

北海道大学大学院獣医学研究科教授

稲葉　睦先生

酪農学園大学教授

北村　浩先生

開催日　平成２６年６月２８日（土）

麻布大学　研究プロジェクト進捗状況評価書

東京大学大学院農学生命科学研究科
辻本　元

私立大学戦略的研究基盤形成支援事業による研究プロジェクト「犬の遺伝性疾患における原因遺伝子解析のための遺伝子(DNA)バンク拠点形成」の進捗状況に関して、研究進捗状況報告書および 2014 年 6 月 28 日に開催された研究者によるプレゼンテーションを通して、その内容を評価する機会を得たので報告させていただく。

(1) 研究プロジェクトの基本的理念について

臨床獣医学においては、2000 年以降になって急速に進歩した分野の一つとして、病理発生に関する分子生物学的研究がある。2003 年にイヌの全ゲノムが発表されたことが当該分野研究の発展を強力に推進することとなった。米国や欧州の数カ国においてイヌの DNA バンク作りが始められているように、ヒトと同様のレベルでゲノム解析が可能となったイヌの DNA サンプルは、病気の診断、治療、および予防に関する研究にとってきわめて貴重な研究資源となる。

イヌ DNA バンク作りに関しては、日本の国家的プロジェクトとして進めるべきものと思われるが、現時点においては本研究プロジェクトがその拠点となって将来のより大型のバンクの核になることを期待する。このような観点から、本研究プロジェクトの年限（平成 23~27 年度）の後の展開について、あらかじめプラニングしておく必要がある。

(2) 研究プロジェクトの体制構築について

サンプル収集、症例個体情報収集、およびその管理について、簡易性および汎用性を兼ね備えたシステムを構築しておられ、これまでの努力を高く評価することができる。ヒトの遺伝子(DNA)バンク形成のノウハウを積極的に導入していることも、多数サンプルの保存管理の効率化に役立っているものと考えられる。

平成 23 年度から現在までの体制構築により、イヌ遺伝子(DNA)バンクの基本的な体制はすでに整っている。今後のサンプル数増加を考慮し、施設、設備、人員、および保存管理システムの充実を図るべきである。

(3) 遺伝子(DNA)バンクへのサンプル収集について

サンプル収集に関しては、麻布大学附属動物病院に受診した症例から得られたものが

中心となっているが、連携の他大学との協力をさらに進めることが本プロジェクト成功の鍵となる。また、最近では大学附属動物病院と同等あるいはそれよりも症例数の多い二次獣医療機関や総合的開業動物病院が増えており、それら診療機関からのサンプル収集に関する検討も望まれる。

(4) 遺伝子(DNA)バンクに収集されたサンプルを利用した研究について

6 月 28 日開催の研究者によるプレゼンテーションでは、各分野にわたって DNA バンクに収集されたサンプルを利用した研究成果が発表された。課題によってその進捗状況はさまざまであったが、「犬の社会性を司る遺伝子の探索」(菊水健史先生)に関する研究発表では、とくに優れた成果が報告されていた。本遺伝子(DNA)バンクへのサンプル収集を促進するためには、それによって得られた研究成果と本バンクとのつながりを明確にし、ホームページ等でアナウンスすることが望まれる。

本研究プロジェクトでは、研究代表者の阪口雅弘先生のリーダーシップのもとに精力的に研究が進められており、当初計画のプロジェクトによる成果の多くがすでに報告されている。今後、将来に向けた長期的なビジョンを持って本プロジェクトが遂行されることを強く望む。

麻布大学　研究プロジェクト進捗状況評価書

北海道大学大学院獣医学研究科
稲　葉　　睦

１．はじめに

「犬の遺伝性疾患における原因遺伝子解析のための遺伝子(DNA)バンク拠点形成」について、「研究進捗状況報告書」ならびに研究成果発表会（６月２８日開催）における口頭発表・質疑応答をもとに、１）進捗状況・研究成果等、２）研究費の効率性・妥当性、３）目的達成の可能性、４）研究の発展性の観点から評価を行い、以下のとおり報告する。

２．進捗状況・研究成果等

１）DNA 試料の集積：ほぼ計画通りに試料の収集・保存が進んでいる。ただし、犬の疾患（特定遺伝性疾患を含めて）の遺伝的背景を今後網羅的に解析する場合と、特定疾患の解析に重点を置く場合とでは（あるいは両者)、試料の収集対象／方法が自ずと異なるから、この点を明確にした工夫が必要かもしれない。計画時の疾患試料が不足して進行が遅れているものについては特に何らかの対処が必要であろう。

２）対象疾患：約１０の特定疾患を対象に、それぞれほぼ工程表に沿った DNA の解析が進められている。DNA 収集にあたっては、適切・充分で信頼性の高い臨床データ／検査データの集積・照合が不可欠であるが、この点についてやや不鮮明であった。充分に考慮のこととは思うが、本プロジェクトにおける最も重要な要素と言って過言ではなく、可能な限り一定内容／基準でのデータベースの構築と利用が望まれる。

また、これら対象疾患の遺伝様式や単一遺伝子疾患／多因子疾患の別が必ずしも明確でない疾患があったように思われる。つまりターゲットが疾患の「原因遺伝子」なのか、「リスクファクター（感受性遺伝子)」なのか、あるいは不明なのか、これをクリアに把握して研究にあたるべきであろう。

３）原因遺伝子異常の解析：緑内障、白内障、アロペシア X 等、いくつかの疾患について原因遺伝子異常の候補となる変異が見出され、成果は論文２編と６件の学会発表等にて公表されており、現段階ではほぼ順調に経過しているといえる。ただし、現状では何れの場合も遺伝子変異と発症・病態の因果関係は必ずしも明確ではない。今後、「遺伝子型⇄病態表現型関連の明確化」と「遺伝子産物機能の解明→発症機構解明」が進展することを期待したい。例えば攻撃性／社会認知などについては、雑種系統の解析が研究の効率化に有用と思われ、バンク構築の全体計画にも一考を要すかもしれない。今後、参加研究者間、特に基礎系と臨床系研究者間の議論、連携を一層強化して今後の解析にあたることが望まれる。

３．研究費の効率性・妥当性

・この種の研究では、試料とデータベースの収集／維持管理、DNA 解析に相当な経費を要する。年間 30,000 千円の経費と内訳は妥当であり、約１０疾患を対象とした解析を実施していることに鑑みれば効率性は良いと評価できよう。むしろ、今後、機能解

析を並行して充分に実施するための資金獲得が要求されるであろう。

４．研究の発展性

・本プロジェクトは、臨床獣医学に止まらず、基礎獣医学・動物医科学、生命科学、医学、社会科学等、多様な分野への影響が大である。すなわち、犬疾患発症の診断法開発や予防・制御はもちろん、原因遺伝子／関連遺伝子の機能解明を通しての基礎生命科学への貢献、ヒト疾患モデル動物の開発／治療法の開発など、多様な発展性と科学としての大きな価値を有する。それだけに、バンクの構築から当面のターゲット疾患原因遺伝子の明確な同定に至る計画が確実な信頼性をもって達成されることを期待するものである。

５．総評

・本プロジェクトは、日本では最初の比較的大規模な犬のバイオバンク計画であり、その意義は大きい。現時点の進捗状況は、DNA 試料の収集・保存、それを用いての特定疾患原因遺伝子の解析ともに、ほぼ年度計画工程表に準じている。上記指摘を含め、必要に応じて新たな参加・連携研究者を動員するなどにより所定の目的を達成でき、また獣医学、医学、生命科学等に大きな波及効果をもたらすことが期待できる。
・本プロジェクトの継続にあたっては、遺伝子解析研究の確実な進展はもとより、DNA バンクの効果的・適正な利用等についても充分な考慮が行われることが望ましい。

麻布大学　研究プロジェクト進捗状況評価書

酪農学園大学教授

北村　浩

私立大学戦略的研究基盤形成支援事業「犬の遺伝性疾患における原因遺伝子解析のための遺伝子（DNA）バンクの拠点形成」研究プロジェクトの進捗状況を以下のように評価する。

1）イヌ DNA バンクに関して

本プロジェクトの最大の目標は有用なイヌ DNA バンクの創成である。本プロジェクトではこれまでに 9,000 検体程度の DNA が採取された。当初予定された検体の約半数に止まったが、国内で初めてイヌ DNA 臨床サンプルの DNA バンク化に着手し、1 万検体近くのサンプルと情報を蓄積できたことは評価に値する。また、プロジェクト遂行に当たり、他大学とサンプルや情報を共有する計画が進んでいることも評価できる。

一方で、本プロジェクト成果の価値は集積できた検体数に大きく依存していることから、より一層、収集サンプル数を増やす努力が必要である。今回、サンプルの内訳をみると、圧倒的に眼疾患に偏っていた。このことは参画した研究者間の温度差を反映している。眼疾患サンプルの充実をバンクの特色として生かすか、より広範囲な情報を集積するかは判断の分かれるところであろう。ただ、国家的展望に立った拠点形成という点を鑑みると、現在協力校に含まれていない大学も含め、他大学からのサンプル受け入れを強化すると共に、インフォームドコンセントを洗練化するなどサンプル収集の工夫が必要かもしれない。

DNA バンクにおいて、DNA サンプルに付随する情報資源の充実は、サンプル自体の充実と両輪をなす。DNA バンクのサンプル情報には詳細な臨床データに加え、普遍性・客観性が求められる。登録用の電子ファイルを作成し、それを基にデータベースの情報を更新する仕組みが出来上がったことは評価できる。一方で DNA バンクの普及を視野に入れると情報をブラウズする機能も工夫する必要がある。また海外の既に公開されているプロジェクトデータと如何に情報互換性を持たせるか、そして臨床獣医師が真に求める情報として公開できるかが今後の大きな課題と言えよう。

情報シーズを価値の高い資源に成長させるには、“旬な時期”に情報を一般公開することも大切と考える。同様のプロジェクトがまだ少ない現段階で、段階的にでも成果を公開し、データベース利用者を増やすことが、本 DNA バンクの認知度を高め、成果の波及性を高めることに繋がると考える。

２）研究課題・研究体制について

臨床分野の研究者の弱点を補強する形で基礎分野の研究者が参画できている点は評価できる。バンク自体の基盤を強化するには、データベースやブラウザ作成に実績のある研究者を加えることが望ましい。また、本プロジェクトに参画した多くの研究者が、DNA 配列を基に病態メカニズムに迫ろうと考えているが、より確定的なデータを得、インパクトのある形で成果を公開するには国内外の競争力のある異分野の研究者との共同研究は避けられないだろう。

３）疾患関連遺伝子や関連 SNP の評価について

本プロジェクトでは殆どの研究者が得られた DNA サンプルを基に、ゲノミクスの手法を用いて、疾患の原因候補遺伝子・候補 SNP の同定に成功した。十分に検体数が確保できない疾患もある中、柔軟に対応し、一定の成果は得られていた。

ヒト疾患関連遺伝子のオルソログのマイクロアレイ解析を行い、原因 SNP を推測しているケースが複数みられた。しかしこれはあくまで“注目した遺伝子の SNP が原因で疾患が起こる”という前提での議論であり、その仮説が真である保証は無い。特に有意差の無いデータを基にした推測や、同義置換を原因と予想する報告もあり、今後の cause-and-effect の検証は極めて慎重に行うべきである。

候補遺伝子・候補 SNP の同定から、それが引き起こす病態メカニズムの解析に移行している研究課題が殆どであった。その中で、基礎分野の研究者を新たにメンバーに加える課題があった。メカニズム解析のノウハウを持つ研究者を柔軟に加えていくことは理にかなっている。柴犬の行動学的解析の成果も幅広い共同研究が展開できており、インパクトの高い研究成果に繋がることが予想された。一方で、他の課題については、競争力のある研究チームとの共同研究を前向きに検討する必要性がある。

本プロジェクトの多くの課題はヒトの疾患遺伝子や自らが過去に研究してきた遺伝子についての“決め打ち”に終始していた。イヌ DNA バンクの独自性を考えると、探索的な data-driven study も検討すべきだと考える。

４）研究成果の波及性・普及性に関して

緑内障に関する成果などが国際誌に掲載されたのは評価できるが、全体的な視野に立つと、論文実績の点では、質・量共に費用対効果が大きいとは言い難い。しかし評価会で発表された成果の中には柴犬のゲノム研究などインパクトが大きく、論文発表が近い内容もあり、次の１年の成果が期待できる。また、DNA バンクというシーズの創成は論文実績に反映されにくい側面もあるので、長い目で運用実績を見ていく必要がある。例えば被引用論文数などシーズがどれだけ基礎研究・臨床研究に貢献したかを示す指標も必要であろう。